

# THE JOURNAL OF PHYSICAL CHEMISTRY

(Registered in U. S. Patent Office)

---

---

## SAMUEL COLVILLE LIND

Born June 15, 1879

Editor of the "Journal of Physical Chemistry", 1933-1951

President of the American Chemical Society, 1940

AMERICAN CHEMICAL SOCIETY  
WASHINGTON, D. C.

---

---

# THE JOURNAL OF PHYSICAL CHEMISTRY

(Registered in U. S. Patent Office)

W. ALBERT NOYES, JR., EDITOR

ALLEN D. BLISS

ASSISTANT EDITORS

A. B. F. DUNCAN

## EDITORIAL BOARD

C. E. H. BAWN

G. D. HALSEY, JR.

R. G. W. NORRISH

R. W. DODSON

S. C. LIND

A. R. UBBELOHDE

PAUL M. DOTY

H. W. MELVILLE

E. R. VAN ARTSDALEN

JOHN D. FERRY

EDGAR F. WESTRUM, JR.

Published monthly by the American Chemical Society at 20th and Northampton Sts., Easton, Pa.

Second-class mail privileges authorized at Easton, Pa. This publication is authorized to be mailed at the special rates of postage prescribed by Section 132.122.

The *Journal of Physical Chemistry* is devoted to the publication of selected symposia in the broad field of physical chemistry and to other contributed papers.

Manuscripts originating in the British Isles, Europe and Africa should be sent to F. C. Tompkins, The Faraday Society, 6 Gray's Inn Square, London W. C. 1, England.

Manuscripts originating elsewhere should be sent to W. Albert Noyes, Jr., Department of Chemistry, University of Rochester, Rochester 20, N. Y.

Correspondence regarding accepted copy, proofs and reprints should be directed to Assistant Editor, Allen D. Bliss, Department of Chemistry, Simmons College, 300 The Fenway, Boston 15, Mass.

Business Office: Alden H. Emery, Executive Secretary, American Chemical Society, 1155 Sixteenth St., N. W., Washington 6, D. C.

Advertising Office: Reinhold Publishing Corporation, 430 Park Avenue, New York 22, N. Y.

Articles must be submitted in duplicate, typed and double spaced. They should have at the beginning a brief Abstract, in no case exceeding 300 words. Original drawings should accompany the manuscript. Lettering at the sides of graphs (black on white or blue) may be pencilled in and will be typeset. Figures and tables should be held to a minimum consistent with adequate presentation of information. Photographs will not be printed on glossy paper except by special arrangement. All footnotes and references to the literature should be numbered consecutively and placed in the manuscript at the proper places. Initials of authors referred to in citations should be given. Nomenclature should conform to that used in *Chemical Abstracts*, mathematical characters marked for italic, Greek letters carefully made or annotated, and subscripts and superscripts clearly shown. Articles should be written as briefly as possible consistent with clarity and should avoid historical background unnecessary for specialists.

Notes describe fragmentary or incomplete studies but do not otherwise differ fundamentally from articles and are subjected to the same editorial appraisal as are articles. In their preparation particular attention should be paid to brevity and conciseness. Material included in Notes must be definitive and may not be republished subsequently.

Communications to the Editor are designed to afford prompt preliminary publication of observations or discoveries whose value to science is so great that immediate publication is

imperative. The appearance of related work from other laboratories is in itself not considered sufficient justification for the publication of a Communication, which must in addition meet special requirements of timeliness and significance. Their total length may in no case exceed 500 words or their equivalent. They differ from Articles and Notes in that their subject matter may be republished.

Symposium papers should be sent in all cases to Secretaries of Divisions sponsoring the symposium, who will be responsible for their transmittal to the Editor. The Secretary of the Division by agreement with the Editor will specify a time after which symposium papers cannot be accepted. The Editor reserves the right to refuse to publish symposium articles, for valid scientific reasons. Each symposium paper may not exceed four printed pages (about sixteen double spaced typewritten pages) in length except by prior arrangement with the Editor.

Remittances and orders for subscriptions and for single copies, notices of changes of address and new professional connections, and claims for missing numbers should be sent to the American Chemical Society, 1155 Sixteenth St., N. W., Washington 6, D. C. Changes of address for the *Journal of Physical Chemistry* must be received on or before the 30th of the preceding month.

Claims for missing numbers will not be allowed (1) if received more than sixty days from date of issue (because of delivery hazards, no claims can be honored from subscribers in Central Europe, Asia, or Pacific Islands other than Hawaii), (2) if loss was due to failure of notice of change of address to be received before the date specified in the preceding paragraph, or (3) if the reason for the claim is "missing from files."

Subscription Rates (1959): members of American Chemical Society, \$8.00 for 1 year; to non-members, \$16.00 for 1 year. Postage free to countries in the Pan American Union; Canada, \$0.40; all other countries, \$1.20. Single copies, current volume, \$1.35; foreign postage, \$0.15; Canadian postage \$0.05. Back volumes (Vol. 56-59) \$15.00 per volume; (starting with Vol. 60) \$18.00 per volume; foreign postage, per volume \$1.20, Canadian, \$0.15; Pan-American Union, \$0.25. Single copies: back issues, \$1.75; for current year, \$1.35; postage, single copies: foreign, \$0.15; Canadian, \$0.05; Pan-American Union, \$0.05.

The American Chemical Society and the Editors of the *Journal of Physical Chemistry* assume no responsibility for the statements and opinions advanced by contributors to THIS JOURNAL.

The American Chemical Society also publishes *Journal of the American Chemical Society*, *Chemical Abstracts*, *Industrial and Engineering Chemistry*, *Chemical and Engineering News*, *Analytical Chemistry*, *Journal of Agricultural and Food Chemistry*, *Journal of Organic Chemistry* and *Journal of Chemical and Engineering Data*. Rates on request.

## CONTENTS

### Testimonial Number in Honor of Samuel Colville Lind

|                                                                                                                                                                                                                            |     |
|----------------------------------------------------------------------------------------------------------------------------------------------------------------------------------------------------------------------------|-----|
| Ellison H. Taylor: Samuel Colville Lind. Born June 15, 1879.....                                                                                                                                                           | 773 |
| Russell R. Williams, Jr.: Chemical Effects of Low Energy Electrons.....                                                                                                                                                    | 776 |
| Robert C. Brasted and Chikara Hirayama: An Examination of the Absorption Spectra of Some Cobalt(III)-Amine Complexes. Effect of Ligand and Solvents in Absorption.....                                                     | 780 |
| James S. Johnson, George Scatchard and Kurt A. Kraus: The Use of Interference Optics in Equilibrium Ultracentrifugations of Charged Systems.....                                                                           | 787 |
| Robert Livingston and V. Subba Rao: A Further Study of the Photochemical Autooxidation of Anthracenes.....                                                                                                                 | 794 |
| Leon M. Dorfman and Kenneth E. Wilzbach: Tritium Labelling of Organic Compounds by Means of Electric Discharge.....                                                                                                        | 799 |
| Adolphe Chapiro: Determination of Free Radical Yields in the Radiolysis of Mixtures by the Polymerization Method.....                                                                                                      | 801 |
| Nathaniel F. Barr and Robert H. Schuler: The Dependence of Radical and Molecular Yields on Linear Energy Transfer in the Radiation Decomposition of 0.8 N Sulfuric Acid Solutions.....                                     | 808 |
| Harold A. Dewhurst: Radiation Chemistry of Organic Compounds. IV. Cyclohexane.....                                                                                                                                         | 813 |
| I. M. Kolthoff and B. van't Riet: Studies on Formation and Aging of Precipitates. XLVI. Precipitation of Lead Sulfate at Room Temperature.....                                                                             | 817 |
| Thomas J. Sworski: Reduction of Dichromate Ion by Thallous Ion Induced by $\gamma$ -Radiation.....                                                                                                                         | 823 |
| R. Barker, W. H. Hamill and R. R. Williams, Jr.: Ion-Molecule Reactions of 1,3-Butadiene, of Acetylene and of Acetylene-Methane Mixtures.....                                                                              | 825 |
| George Glockler: Carbon-Halogen Bond Energies and Bond Distances.....                                                                                                                                                      | 828 |
| Marc Lefort and Xavier Tarrago: Radiolysis of Water by Particles of High Linear Energy Transfer. The Primary Chemical Yields in Aqueous Acid Solutions of Ferrous Sulfate, and in Mixtures of Thallous and Ceric Ions..... | 833 |
| Hiroshi Matsuo and Malcolm Dole: Irradiation of Polyethylene. IV. Oxidation Effects.....                                                                                                                                   | 837 |
| A. Serewicz and W. Albert Noyes, Jr.: The Photolysis of Ammonia in the Presence of Nitric Oxide.....                                                                                                                       | 843 |
| F. Scott Mathews and William N. Lipscomb: The Structure of Silver Cyclooctatetraene Nitrate.....                                                                                                                           | 845 |
| Gideon Czapski and Gabriel Stein: The Oxidation of Ferrous Ions in Aqueous Solution by Atomic Hydrogen.....                                                                                                                | 850 |
| G. E. Adams, J. H. Baxendale and R. D. Sedgwick: Some Radical and Molecular Yields in the $\gamma$ -Irradiation of Some Organic Liquids.....                                                                               | 854 |
| Peter Riesz and Edwin J. Hart: Absolute Rate Constants for H Atom Reactions in Aqueous Solutions.....                                                                                                                      | 858 |
| P. G. Clay, G. R. A. Johnson and J. Weiss: The Action of $^{60}\text{Co}$ $\gamma$ -Radiation on Aqueous Solutions of Acetylene.....                                                                                       | 862 |
| Conrad N. Trumbore and Edwin J. Hart: $\alpha$ -Ray Oxidation of Ferrous Sulfate in 0.4 M Sulfuric Acid Solutions. The Effect of 0 to 0.4 M Oxygen.....                                                                    | 867 |
| J. G. Burr and J. D. Strong: The Radiolysis of Organic Solutions. II. The Benzophenone-Propanol-2 System.....                                                                                                              | 873 |
| Roswell F. Pottie and William H. Hamill: Persistent Ion-Molecule Collision Complexes of Alkyl Halides.....                                                                                                                 | 877 |
| Adolf E. de Vries and Augustine O. Allen: Radiolysis of Liquid <i>n</i> -Pentane.....                                                                                                                                      | 879 |
| J. Belloni, M. Haissinsky and Halim N. Salama: On the Adsorption of Some Fission Products on Various Surfaces.....                                                                                                         | 881 |
| J. Weiss and N. Miller: The Reduction of Ceric Ions by $\text{Po}^{210}$ $\alpha$ -Particles.....                                                                                                                          | 888 |
| C. Surasiti and E. B. Sandell: Kinetics of the Ruthenium-catalyzed Arsenic(III)-Cerium(IV) Reaction.....                                                                                                                   | 890 |
| J. W. Boyle, S. Weiner and C. J. Hohanadel: Kinetics of the Radiation-induced Reaction of Fe(III) with Sn(II).....                                                                                                         | 892 |
| T. J. Hartwick and W. S. Guentner: On the Use of Aqueous Sodium Formate as a Chemical Dosimeter.....                                                                                                                       | 896 |
| Milton Burton and K. C. Kurien: Effects of Solute Concentration in Radiolysis of Water.....                                                                                                                                | 899 |
| H. T. J. Chilton and G. Porter: Radiation Chemical Processes in Rigid Solutions.....                                                                                                                                       | 904 |
| E. Collinson, F. S. Dainton and H. A. Gillis: The Radiation Induced Polymerization of Isobutene: A Liquid Phase Ionic Reaction.....                                                                                        | 909 |
| P. S. Rudolph and C. E. Melton: Mass Spectrometric Studies of Ionic Intermediates in the $\alpha$ -Particle Radiolysis of the $\text{C}_2$ Hydrocarbons. I. Acetylene.....                                                 | 916 |
| G. E. Boyd and J. W. Cobble: Recoil Reactions with High Intensity Slow Neutron Sources. III. The Radiation Decomposition of Crystalline $\text{KBrO}_3$ .....                                                              | 919 |
| Robert H. Schuler: Radical Production in Hydrocarbons by Heavy Particle Radiations.....                                                                                                                                    | 925 |
| Nathaniel F. Barr and Augustine O. Allen: Hydrogen Atoms in the Radiolysis of Water.....                                                                                                                                   | 928 |
| Hugo Fricke, Wendell Landmann, Charles Leone and James Vincent: Application of Optical Rotation Measurements in Studying the Structural Degradation of $\gamma$ -Irradiated Ovalbumin.....                                 | 932 |
| Charles R. Maxwell and Dorothy C. Peterson: The Effect of $\alpha$ -Radiation on Aqueous Glycine.....                                                                                                                      | 935 |
| Sheldon Datz and William T. Smith, Jr.: The Molecular Composition of Sodium Iodide Vapor from Molecular Weight Measurements.....                                                                                           | 938 |
| Henry A. Bent and Bryce Crawford, Jr.: Infrared Studies of Propellant Flames.....                                                                                                                                          | 941 |
| Edward L. Yuan, John I. Slaughter, William B. Koerner and Farrington Daniels: Kinetics of the Decomposition of Nitric Oxide in the Range 700-1800°.....                                                                    | 952 |
| P. Harteck and S. Dondes: The Kinetic Radiation Equilibrium of Air.....                                                                                                                                                    | 956 |
| G. Blyholder and P. H. Emmett: Fischer-Tropsch Synthesis Mechanism Studies. The Addition of Radioactive Ketene to the Synthesis Gas.....                                                                                   | 962 |
| Harold W. Kohn and Ellison H. Taylor: The Hydrogen-Deuterium Exchange Activity and Radiation Behavior of Some Silica Catalysts.....                                                                                        | 966 |
| A. Charlesby, W. H. T. Davison and D. G. Lloyd: Intensity and Concentration Dependence of Some Radiation-induced Reactions in Anthracene Solutions.....                                                                    | 970 |
| P. Balestic and M. Magat: A Note on the Radiation-Induced Synthesis of Lauth's Violet.....                                                                                                                                 | 976 |

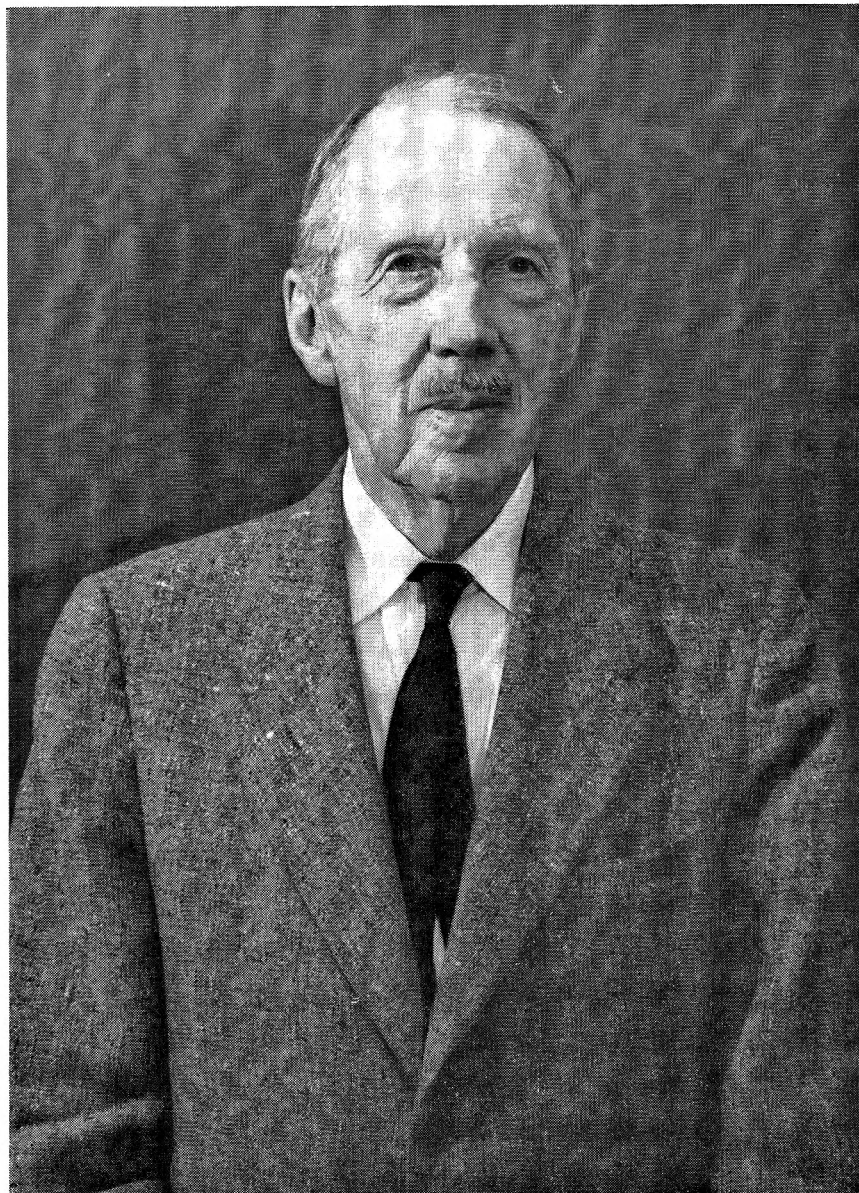
#### NOTES

|                                                                                                                       |     |
|-----------------------------------------------------------------------------------------------------------------------|-----|
| M. A. Bredig: Dimeric Bismuth(I) Ion. $(\text{Bi}_2)^{2+}$ in Molten Bismuth Trihalide-Bismuth Systems.....           | 978 |
| A. Henglein, J. Langhoff and G. Schmidt: Tetranitromethane as a Radical Scavenger in Radiation: Chemical Studies..... | 980 |
| Leon M. Dorfman and P. C. Noble: Reactions of Gaseous Ions. Ammonium Ion Formation in Ionized Ammonia.....            | 980 |
| <hr/>                                                                                                                 |     |
| I. A. Ammar and Soheir Darwish: Overpotential on Activated Pt Cathodes in NaOH Solutions.....                         | 983 |
| Wladimir Philippoff and Frederick H. Gaskins: The Experimental Check of Theories of the Viscosities of Solutions..... | 985 |
| Robert A. Wires, Leland A. Watermeier and Roger A. Strehlow: The Dry Carbon Monoxide-Oxygen Flame.....                | 989 |

|                                                                                                                                                                    |      |
|--------------------------------------------------------------------------------------------------------------------------------------------------------------------|------|
| Frank R. Meeks, Ram Gopal and O. K. Rice: Critical Phenomena In the Cyclohexane–Aniline System: Effect of Water at Definite Activity.....                          | 992  |
| D. M. Alexander: A Calorimetric Measurement of the Heats of Solution of the Inert Gases in Water.....                                                              | 994  |
| W. I. Higuchi, M. A. Schwartz, E. G. Rippie and T. Higuchi: A Thermometric Method for Thermodynamics Studies and Molecular Weight Determinations in Solutions..... | 996  |
| Y. Marcus: The Anion-exchange of Metal Complexes. III. The Cadmium–Chloride System.....                                                                            | 1000 |
| George Blyholder and Henry Eyring: Kinetics of Graphite Oxidation. II.....                                                                                         | 1004 |
| P. Balk and G. C. Benson: Calorimetric Determination of the Surface Enthalpy of Potassium Chloride.....                                                            | 1009 |
| J. B. Hudson, W. B. Hillig and R. M. Strong: The Solidification Kinetics of Benzene.....                                                                           | 1012 |
| Joan M. Forrest, Robert L. Burwell, Jr., and Benjamin K. C. Shim: Isotopic Exchange between Ethers and Deuterium on Metallic Catalysts.....                        | 1017 |

#### NOTES

|                                                                                                                        |      |
|------------------------------------------------------------------------------------------------------------------------|------|
| D. M. Alexander: The Solubility of Benzene in Water.....                                                               | 1021 |
| H. O. Pollak and H. L. Frisch: The Time Lag in Diffusion. III.....                                                     | 1022 |
| A. E. Westwell and E. W. Anacker: Adsorption of Cetylpyridinium Chloride on Glass.....                                 | 1022 |
| O. Redlich and D. L. Peterson: A Useful Adsorption Isotherm.....                                                       | 1024 |
| Rex E. Lovrien and Charles Tanford: Rapid Flow Titration and the Rate of the Acid Expansion of Bovine Serum Albumin..  | 1025 |
| D. A. I. Goring and Carol Chepeswick Bryson: A Photoelectric Method for Observing Sedimentation at Low Concentration.. | 1026 |



**SAMUEL COLVILLE LIND**

President of the American Chemical Society, 1940  
Editor of the "Journal of Physical Chemistry," 1933-1951

---

---

# THE JOURNAL OF PHYSICAL CHEMISTRY

(Registered in U. S. Patent Office) (© Copyright, 1959, by the American Chemical Society)

VOLUME 63

JUNE 24, 1959

NUMBER 6

---

---

## SAMUEL COLVILLE LIND

Born June 15, 1879

Samuel Colville Lind was almost eight years old when the *Zeitschrift für physikalische Chemie* was founded by Ostwald in Leipzig. Since the latter event is often considered to mark the birth of Physical Chemistry as a separate discipline, he is some ten per cent. older than the subject of his career. He was born on June 15, 1879, to Thomas Christian Lind and Ida Colville Lind, the latter a native of McMinnville, Tennessee, the former a native of Sweden. Thomas Lind, a mate on one of his father's ships at nineteen, left the sea in New York to join the Union Army in the Civil War. After the war he was sent by his employers, the Pennsylvania Oil Company, to find whether the gas bubbles rising from the Barren Fork of the Collins River at McMinnville were a sign of petroleum. When test drilling failed to disclose any, he abandoned the oil business in disgust, read law in McMinnville, married a local girl and settled down to practice law in that small, Middle Tennessee county seat, where his oldest child, Samuel Colville, was born and grew up.

After graduating from high school, Lind was sent to Washington and Lee University at the instigation of an alumnus, the superintendent of the McMinnville High School. It would have been natural for him to study law, but his father advised against it because the prospects for young lawyers in the South seemed to be declining. He elected a general course in college, studying primarily classics for three years. As a senior, he found that he needed six points in science or mathematics for graduation, and only for that reason elected the elementary course in chemistry.

This course determined Lind's future career. It was taught by Jas. L. Howe, Professor of Chemistry at Washington and Lee from 1894 to 1937 and an active chemist (platinum metals, especially ruthenium) until 1955 when he died at the age of 96. He presented the subject so attractively that Lind returned for a fifth year in order to prepare himself

for advanced work. Since the Massachusetts Institute of Technology had then the outstanding undergraduate course in chemistry in this country, Lind went there in 1900, received an S.B. degree in 1902 and returned in 1903 as an assistant, teaching Advanced Analysis under I. P. Talbot.

In 1904 M.I.T. granted Lind a Dalton Traveling Fellowship, which he used to go to Ostwald's laboratory in Leipzig for a Ph.D. By that time Ostwald had almost disengaged himself from lecturing and research, and the choice of thesis professors in Physical Chemistry lay between Luther, the electrochemist, and Bodenstein, the kineticist. The former was the favorite with the graduate students, perhaps because Bodenstein's problems, in gas kinetics, were more difficult experimentally and perhaps partly because Bodenstein, being independently wealthy, was somewhat more aloof. Lind approached Luther for a thesis problem but found that he could accommodate no more students that year. Turning, therefore, to Bodenstein, he was assigned the kinetics of the thermal reaction of bromine with hydrogen. Quite in contrast to the simple, second-order kinetics shown by hydrogen and iodine, the results for bromine and hydrogen could only be fitted by an equation with two numerical constants, a square root dependence on bromine and a function of hydrogen and bromine concentrations in the denominator. This new kinetic equation remained unexplained for thirteen years, being finally interpreted independently by Christiansen, Polanyi and Herzfeld by an atomic chain mechanism. After receiving the Ph.D. for this work in 1905, Lind was offered an appointment as assistant at Leipzig, but the salary was too small for subsistence, and his mother, fearing his expatriation, declined to assist him. He, therefore, returned to America in 1906 and accepted an instructorship at the University of Michigan. Here he taught General and Physical Chemistry and conducted research in analysis and in solution kinetics.

Michigan then had a plan by which a faculty member could take a year off with salary after only five at the university, by teaching summers without pay. Lind did this and in 1910 left for a year in Marie Curie's laboratory in Paris. Radioactivity was the newest thing in chemistry, and he wished to learn about it at the source.

Although Madame Curie was largely occupied in writing her "Traité de Radioactivité" in 1910, she continued to deliver her lectures on radioactivity, and the Chef de Laboratoire, André Debierne, with William Duane, introduced Lind to experimental radioactivity. Duane, from the University of Colorado, had been instrumental in obtaining money from the Carnegie Foundation for the Curie laboratory and was at that time concluding his second stay there. Lind's research was on the  $\alpha$ -ray induced combination of hydrogen and bromine and the decomposition of hydrogen bromide, the latter in the liquid and in aqueous solution as well as in the gas. He moved to the new Institut für Radiumforschung in Vienna for the last part of his leave, working with Stefan Meyer and Victor F. Hess (now at Fordham), the discoverer (1912) of cosmic rays. Here Lind carried out the first research in which the amount of ionization and the amount of chemical change were directly compared, namely, the ozonization of oxygen by  $\alpha$ -rays.

Lind returned to Ann Arbor as assistant professor, with the intention of initiating chemical work with  $\alpha$ -particles in this country. He recalculated previous results by Cameron and Ramsay, by Usher, by Debierne, and by himself, and showed that there was a close equivalence between the amount of chemical reaction and the number of gaseous ions formed by the  $\alpha$ -particles. He was unable, however, to obtain support for experimental work in this field (radium at that time cost over \$100,000 per gram), and in 1913 he accepted a position with the Bureau of Mines at Denver, Colorado, where a group under R. B. Moore was building a plant to isolate about eight grams of radium from carnotite. This undertaking was sponsored jointly by the Bureau of Mines and the newly-formed National Radium Institute, a creation of H. A. Kelly and J. Douglas, of Baltimore and New York, respectively, who intended to use the radium in experimental therapy. Lind, of course, took part in the chemical developments necessary to the process, but, as the expert in radioactivity, his principal efforts were devoted to radioactive measurements and to the handling of the material in the final stages of purification. He was, for instance, responsible for the division of each batch of final product into two equal parts for shipment to the two sponsoring hospitals. As a result of these operations he carries about a tenth of a microgram of radium in his system, apparently not to his detriment, at least in comparison to ordinary persons.

By the end of the production operations, about half a gram (of a total of 8.9) was in excess of the contract requirements, and Lind was able to employ it in studies of chemical changes. It was loaned to him when he left the Bureau of Mines, accompanying him to his subsequent posts, even to the present, where it is in use by Lind and his colleagues

at the Oak Ridge National Laboratory. Some thirty-five research papers have described work done with this sample of radium.

While in Denver, he married Marie Holliday, an Omaha girl, whose charm and graciousness have complemented his own in all of his subsequent life. They have one son, Thomas Colville Lind, and three grandchildren. The boy is his grandfather's favorite fishing companion on his visits to Oak Ridge.

The Bureau of Mines station at Denver was moved first to Golden, Colorado, in 1916 and then in 1920 to Reno, Nevada, as the Rare and Precious Metals Experiment Station, with Lind in charge. In 1923 he moved to Washington, D. C., succeeding R. B. Moore as chief chemist of the Bureau of Mines. Finally, in 1925, he left to become associate director of the Fixed Nitrogen Laboratory of the Department of Agriculture. In 1926 Lind was called from Washington to become Director of the School of Chemistry of the University of Minnesota, returning thus to academic life after thirteen years in Government service. After nine further years he was made Dean of the Institute of Technology, where he continued until his retirement in 1947.

Lind wished to return to Tennessee after retirement, and, therefore, sought a position with the Union Carbide Corporation, which operates the atomic energy facilities in Oak Ridge for the Atomic Energy Commission. He was made a technical consultant to C. E. Center, at that time the general superintendent for Union Carbide in Oak Ridge. Although Lind's headquarters were at the Gaseous Diffusion Plant, most of his attention soon came to be directed to the Oak Ridge National Laboratory, where the largest part of the research in Oak Ridge is conducted, and since 1951 he has been in almost full-time residence there. From 1951 to 1954 he was acting director of the Chemistry Division of the Laboratory and since then he has been a consultant to the Laboratory, as well as to the vice-president. He is (with two associates) revising and enlarging his ACS Monograph, "The Chemical Effects of Alpha Particles and Electrons" to make it a comprehensive treatise on experimental results in radiation chemistry. The original edition was the second monograph to be published by the American Chemical Society and, with its revision in 1928, has been the standard reference on the subject. He also continues to direct research in experimental radiation chemistry of gases.

Lind's connection with scientific publications started with *Chemical Abstracts*, for which he was an abstracter from 1908 through 1911 and 1915 through 1921, and an assistant editor (in charge of "Subatomic Phenomena and Radiochemistry") from 1922 through 1929. He has been an associate editor of the *Journal of the American Chemical Society* and a member of the Board of Editors of the American Chemical Society Series of Chemical Monographs. In 1933 he assumed the editorship of the *Journal of Physical Chemistry* from its founder, W. D. Bancroft. He edited it from Minnesota until 1947, when he moved the editorial of-

fices to Oak Ridge. He continued as editor until 1951.

Numerous prizes, offices and other honors have accrued to Lind. He was president of the Electrochemical Society in 1927 and vice-president (Section C—Chemistry) of the American Association for the Advancement of Science in 1930. He was president of the American Chemical Society in 1940. He received the Nichols Medal of the New York Section of the American Chemical Society in 1926 in recognition of his work on chemical activation by  $\alpha$ -particles, and the Priestley Medal of the American Chemical Society at the Diamond Jubilee Meeting of the Society in 1951 in New York. He was elected to the National Academy of Sciences in 1930 and for some years after returning to Tennessee was the only member residing in that state.

The positions and honors which Lind has received testify to his distinction as a scientist and his ability as a teacher and administrator. Since his scientific work so typifies the spirit of physical chemistry, it may be permissible to attempt a brief recapitulation. Growing up, scientifically, in the middle of the development of physical chemistry, he has quite naturally remained an experimental physical chemist throughout his career. Well over a hundred papers have resulted from his research, the largest part of them dealing with reactions under  $\alpha$ -particle radiation or in the electric discharge. His principal collaborators have been D. C. Bardwell, G. Glockler, R. S. Livingston and C. H. Shiflett. In addition, he has authored several papers on related subjects, numerous reviews, and another book, "The Electrochemistry of Gases," with George Glockler. His primary concern has been careful measurement and simple transformation of the results into terms (rate equations, M/N ratios, etc.) that can be used in compilation and in theoretical speculations. Whenever needed, he has supplied new techniques or ingenious improvements. The thin-walled  $\alpha$ -ray bulb (developed with Duane, following earlier experiments with thin capillaries by Rutherford) and the Lind electroscope are tributes to his skill and ingenuity. His thesis, under Bodenstein, stands as one of the classics of chemical kinetics, and repetition with newer information and apparatus has merely confirmed the results which he obtained fifty-four years ago.

Lind has been equally careful and ingenious in drawing conclusions from his experimental results. Sometimes, as in his thesis, these have been simply crystallizations of the data into empirical equations, but these have withstood time and re-examination. Sometimes, his results have revealed new phenomena such as the catalysis of radiation effects by inert gases, or the effect of recoils in  $\alpha$ -ray reactions. He has hunted such discoveries, as well as contradictions and anomalies, out of his own work and that of others with almost unerring aim. He suggested in 1911, from evidence in his experiments, the existence of indirect action of radiation upon a solute, a concept that is central to most radiation chemical work with solutions and to most of radiobiology.

The thread of all his work has been the importance of ionization in radiation-induced reactions.

This concept was not original with him, but he recognized its probable soundness and its usefulness as a working hypothesis. He provided the first careful measurements designed to test it (the ozonization of oxygen), and a whole series of experiments to explore the effect of chemical variation. He correlated these results in terms of molecules reacting per ion-pair formed in the gas (M/N) and observed regularities in behavior, from simple reactions for which M/N was a small number to cases of obvious chain reaction ( $H_2 + Cl_2$ ) for which M/N was very large. Directed by such observations and by physical evidence for clustering of molecules about gaseous ions, Lind put forward in 1923 a "cluster hypothesis" for radiation-induced reactions, in which the chemical action took place within a cluster of molecules as a result of the energy liberated by neutralization of oppositely charged ions. The concreteness of this hypothesis and its success in accounting for numerous results led it to be widely used, among others by Mund, by Rideal, and by Brewer and Westhaver. A few critical experiments were suggested, by Lind and by others, but were not feasible because of the short molecular or ionic free path in gases at pressures where chemical reactions could be followed. Rapid developments in kinetics during the next few years brought the role of atoms and radicals in thermal and photochemical reactions to attention, and in 1936 J. O. Hirschfelder, H. Eyring and H. S. Taylor showed that two  $\alpha$ -ray reactions could be explained without invoking clustering. This marked a turning point in the theory of radiation chemistry, since it showed that no special behavior different from that demonstrated for other types of activation needed to be assumed. Although Lind was undoubtedly attached to the cluster hypothesis, he recognized the merits of the (by then) more conventional explanation and retained the cluster hypothesis only for cases where the newer mechanism did not seem to work.

Mainly because gas reactions were little studied during the war, when radiation chemistry achieved its present, greatly enlarged status, the role of ions, except as fleeting, initial products began to be neglected. More recently, experiments in mass spectrometers at higher than usual pressure have begun to show the wide occurrence and large probability of ion-molecule reactions, and the most recent research in gas-phase radiation chemistry has shown that ion-molecule reactions are probably highly important. Thus, the essence of Lind's approach, the importance of ions as reacting species, and the importance of measuring the ions (because they alone of the activated primary species can be quantitatively measured, even now) is again proving fruitful.

Although Lind was not unaware of the revolution in physics which has occurred during his lifetime, and of its impact upon chemistry, he has remained essentially an experimental physical chemist, devoted to the experimental discovery of regularities in chemical behavior. A few incidental remarks in his papers suggest that he could as well have approached chemistry from the theoretical viewpoint. Thus, the electronic picture he suggested in 1923



for coloration and thermoluminescence is remarkably sensible in present-day terms, and the discussions of nuclear physics, photochemistry and other topics in some of his reviews reveal a most lucid grasp of modern theoretical developments. The quick, penetrating intelligence which shows throughout his writing and appears daily in his conversation about science, world affairs, or people, could have brought him success in any field. Since he elected to apply his talents to physical

chemistry, he is now, as he has been for more than fifty years, one of the foremost physical chemists of his time.

It remains only to wish Lind a happy eightieth birthday and continued happiness and success. The papers in this Jubilee Issue are but an insignificant token of the esteem and affection in which he is held by his colleagues.

OAK RIDGE NATIONAL LABORATORY  
OAK RIDGE, TENNESSEE

ELLISON H. TAYLOR

## CHEMICAL EFFECTS OF LOW ENERGY ELECTRONS<sup>1</sup>

BY RUSSELL R. WILLIAMS, JR.

*Haverford College, Haverford, Pa.*

*Received October 15, 1958*

A new technique has been developed for the study of chemical decomposition of gases by low energy electrons. Ultraviolet light falling on a silver surface generates photoelectrons which are accelerated in the gas by application of an electric field. The electron yields of products formed by irradiation of methane and ethane have been examined as a function of applied potential and the behavior of the systems suggests that an important primary process is non-ionizing excitation by electron impact.

It has been presumed for some time that radiolysis by high energy electrons produces chemical reaction by excitation<sup>2</sup> as well as by ionization although most of the mechanisms proposed have emphasized the importance of ionization as the primary process, relegating excitation to an undetermined role. This report describes the first results of a new attempt to investigate the chemical effects of electrons of such low energies that ionization will be impossible or inefficient.

The prior literature reveals several instances in which chemical decomposition by electron excitation appears to occur. Essex and his collaborators<sup>3</sup> found that the ion-pair yield in the alpha radiolysis of gaseous ethane was increased by the application of an electric field in a manner which led them to conclude that electron excitation was responsible for the increase. In like manner Meisels, Hamill and Williams<sup>4</sup> found that the ion pair yield in the X-radiolysis of methane in argon was increased by application of an electric field. Kiser and Johnston<sup>5</sup> have analyzed the products and determined electron yields in Geiger-Müller discharge in ethanol-argon and 2-propanol-argon mixtures. They find, respectively, 285 and 56 molecules decomposed per electron collected. They conclude that the magnitude of these yields indicates a primary process of excitation rather than ionization. Mechanisms of decomposition in electric discharge have been proposed<sup>6</sup> which depend heavily on excitation as a primary process.

In the present investigation low energy electrons are introduced into a gas *via* the photoelectric effect from a metal surface. The electrons then are caused to drift through the gas by application of an adjustable electric field. Chemical decomposition is determined as a function of applied potential per unit gas pressure.

### Experimental

**Apparatus.**—The reaction chamber consists of a cylindrical silver cathode 12 mm. in diameter  $\times$  120 mm. in length centered in a cylindrical anode 29 mm. in diameter  $\times$  120 mm. in length constructed from 18 mesh bronze screen. Thus the electrode spacing is 8.5 mm. with a maximum variation of *ca.*  $\pm$  1 mm. This electrode assembly is encased in a Vycor 7910 jacket with appropriate gas and electrical connections as shown in Fig. 1. Some care must be exercised to avoid discharge points on the electrodes and leads.

The reaction chamber is inserted within the coil of a Hanovia SC2537 mercury resonance lamp formed from 10 mm. quartz tubing shaped in the form of a four turn helix with inside diameter 50 mm. and length 100 mm. The radiation from the lamp passes through the Vycor jacket, through the screen anode and falls on the surface of the silver cathode as shown in Fig. 1.

Power for the mercury resonance lamp is furnished by a 5000 volt transformer operated from a variable transformer in the primary. The electrode potentials for the reaction chamber are furnished by the d.c. supply of a Geiger-Müller counting circuit and a d.c. microammeter is placed between the cathode and ground to permit measurement of the photoelectron currents, which ranged from 2 to 100 microamp.

Preliminary tests on several metals resulted in the selection of silver for its relatively high photoelectron efficiency. After pretreatment of the silver by high voltage, high frequency discharge in hydrogen at *ca.* 1 mm. pressure the vacuum photoelectron current, collected with an applied potential <50 volts, was *ca.* 10 microamp. The current varied slowly with time and with the nature of the experimental procedure.

The reaction chamber was permanently connected through a stopcock to a typical vacuum system for gas handling and to a gas collecting apparatus. The latter consisted of a McLeod gauge modified to have a calibrated volume connected by a stopcock to the top of the closed arm. By successive strokes of the mercury in the McLeod the gaseous products were collected in the calibrated volume or in a sample holder for analysis.

(1) Work supported by a special grant from the Board of Managers of Haverford College.

(2) In the present context the use of the term excitation will be confined to processes which do not result in positive ion formation in the initial act or in any subsequent unimolecular process.

(3) *E.g.*, N. T. Williams and H. Essex, *J. Chem. Phys.*, **17**, 995 (1949).

(4) G. G. Meisels, W. H. Hamill and R. R. Williams, Jr., *THE JOURNAL*, **61**, 1456 (1957).

(5) R. W. Kiser and W. H. Johnston, *J. Am. Chem. Soc.*, **78**, 707 (1956); **79**, 811 (1957).

(6) *E.g.*, M. Burton and J. L. Magee, *J. Chem. Phys.*, **23**, 2194, 2195 (1955).

Considerable care was taken to avoid entrance of mercury vapor into the reaction chamber. A trap immediately outside the chamber was always cooled in Dry Ice-acetone or in liquid nitrogen when the chamber was exposed to the vacuum system. Furthermore, the presence of silver in the chamber should drastically lower the vapor pressure of mercury through formation of the silver amalgam. The trap outside of the reaction chamber also was used to separate reactants from products after irradiation.

**Reagents.**—Reagents used were: methane, Phillips research grade, >99.6 mole %; ethane, Phillips research grade, >99.75 mole %; argon, Matheson, >99.9 mole %.

**Procedure.**—A typical experiment with methane or methane and argon proceeded as follows. The reagents were cooled in their reservoirs to liquid nitrogen temperatures and then admitted to the reaction chamber, the desired pressure being obtained by allowing the reservoir to warm slowly from liquid nitrogen temperature. This procedure was used to reduce the possibility of introducing small amounts of contaminants which might be condensable on liquid nitrogen. A Dry Ice-acetone bath was placed around the trap next to the reaction chamber during sample introduction and the ultraviolet lamp was turned on for warm-up. After sample introduction the electric field was applied for a measured period of time and the photoelectron current observed during the irradiation. The lamp primary, and therefore its intensity, was adjusted during the run to maintain a constant photocurrent. It was shown that the rate of reactions is simply proportional to the light intensity.

After completion of the exposure liquid nitrogen was placed around the trap next to the reaction chamber and the sample was passed slowly through the trap. Non-condensables were discarded and the condensable products (ethane, etc.) were warmed to room temperature and collected in the modified McLeod where their  $PV$  product was measured. The amount of product collected was typically 10–40 cc.  $\times$  mm. at room temperature, and the reaction chamber volume was ca. 250 cc. Therefore the extent of decomposition was usually less than one per cent., except where larger samples were collected for mass spectrometric analysis. Comparison of the amount of product collected with the total charge passed through the system permitted calculation of the electron yield,  $Y = \text{moles of product/faradays of charge}$ .

The procedure for ethane was similar except that ethane was condensed on liquid nitrogen and the non-condensable products (hydrogen and methane) were collected.

## Results

**Ethane.**—Blank runs (ultraviolet irradiation with no field applied) demonstrated a small but significant rate of reaction which might be either a mercury photosensitized reaction or a photolyzable impurity in the sample. Several attempts to purify the ethane by distillation failed to reduce the blank. However, the rate of this reaction was very consistent even after complete disassembly of the chamber for replacement of electrodes, and the rate was approximately proportional to the pressure of ethane. These observations favor the impurity hypothesis. The correction for the blank was as high as 20% in one or two experiments at very low fields, but otherwise always less than 10%.

The electron yield,  $Y$ , in the decomposition of ethane was examined principally at two pressures as a function of applied voltage. The products collected in these experiments were non-condensable on liquid nitrogen. Mass spectrometric analysis of several samples showed that the hydrogen-methane ratio was ca. 5:1. The observed yields are plotted versus  $V/P$  in volts/mm. gas pressure in Fig. 2. (The field strength is approximately uniform at 1.18 volts/cm. at 1 volt applied potential.) The upper limit of the measurements was determined by the onset of intermittent discharges in the

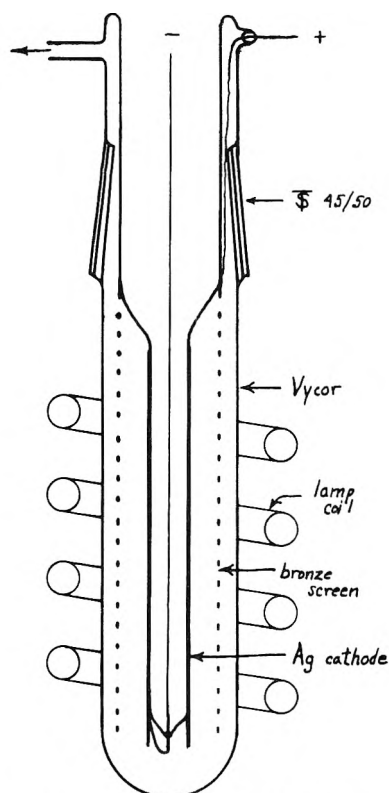


Fig. 1.—Apparatus for photoelectron experiments.

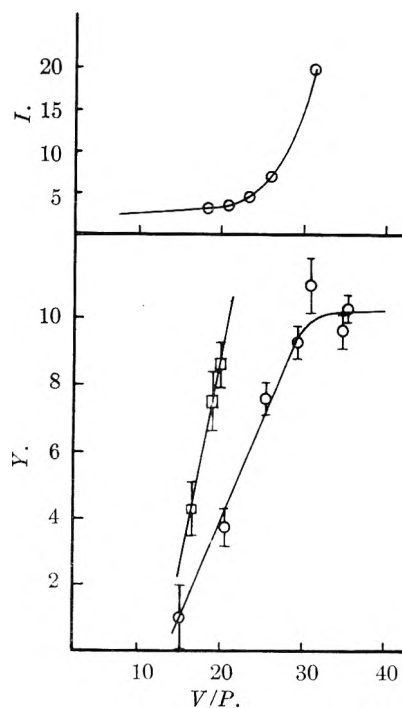


Fig. 2.—Decomposition of ethane: O, 38 mm.; □, 79 mm.

chamber at high potentials and no results are reported in which this occurred. The lines drawn through the data are merely to show the apparent trends of the points and have no immediate theoretical origin. It is seen that, within the precision of the data, the lower points fall on straight lines having a common intercept and with slopes approximately proportional to the gas pressure.

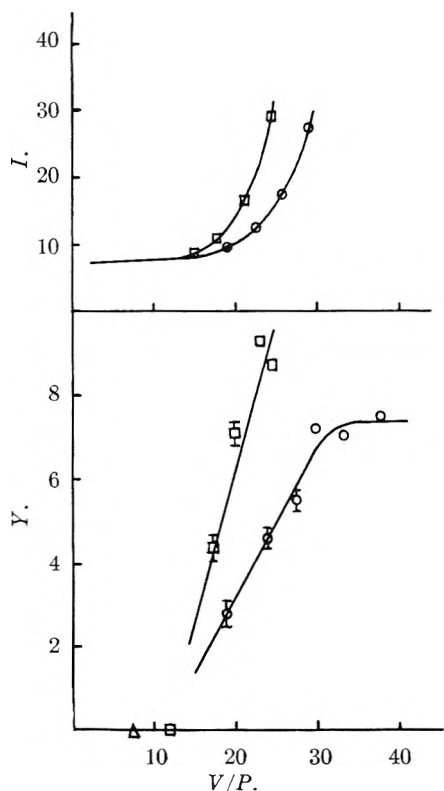


Fig. 3.—Decomposition of methane:  $\circ$ , 30 mm.;  $\square$ , 66 mm.,  $\triangle$ , 82 mm.

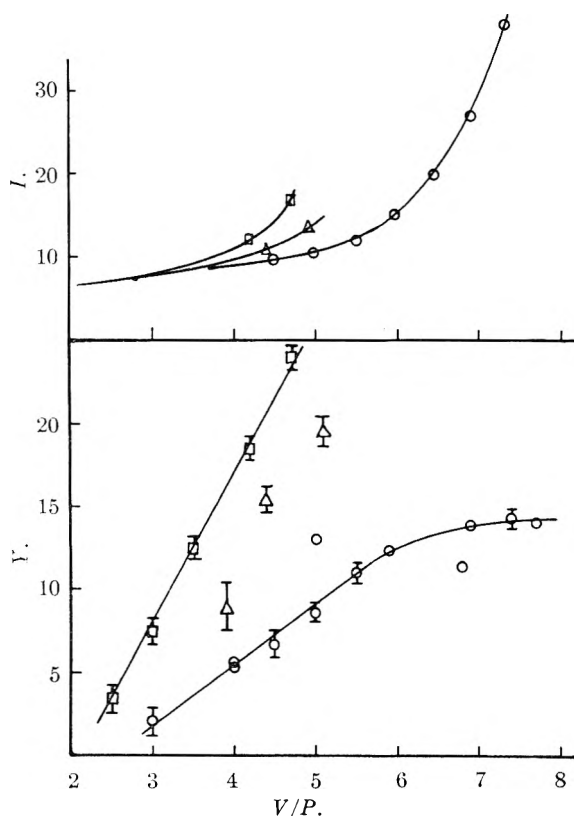


Fig. 4.—Decomposition of methane in argon:  $\circ$ , 10 mm.  $\text{CH}_4$ , 190 mm. Ar;  $\square$ , 10 mm.  $\text{CH}_4$ , 400 mm. Ar;  $\triangle$ , 20 mm.  $\text{CH}_4$ , 390 mm. Ar.

Figure 2 also shows the current-voltage curve at the lowest ethane pressure. The scale of current

here does not correspond quantitatively to the decomposition experiments and such curves are given only to show their shapes.

**Methane.**—Blank runs with methane showed that the sample contained a very small amount of condensable impurity but, in contrast to the ethane, there was no evidence of reaction upon ultraviolet irradiation. The collected impurity was shown to be a constant proportion of the methane and therefore accurate correction was possible. Again the correction was as large as 20% only for a few experiments at very low rates and was ordinarily much less than 10%.

The electron yield in the decomposition of methane was examined principally at two pressures as a function of applied voltage and the results are shown in Fig. 3. The products collected in these experiments are condensable on liquid nitrogen and mass spectrometric analysis<sup>7</sup> of two runs showed the following principal products: ethane, 72%; propane, 19%; *n*-butane, 2%; isopentane, 4%. Exceptionally long runs were required to obtain sufficient product for analysis and it may be that this analysis does not accurately represent the initial product distribution. As with ethane the lower yields appear to be a linear function of  $V/P$  with a common intercept and a slope proportional to the pressure. Curves of photocurrent *vs.*  $V/P$  are given for both pressures of methane.

**Methane in Argon.**—Blank runs with methane in argon showed that no condensable impurity was obtained from the argon and only that attributable to the methane was observed.

The addition of small amounts of methane to argon has a strong effect on the current *versus*  $V/P$  curves. The current in the flat portion of the curve ( $V/P < 3$ ) is less by 25–50 than in pure argon and the “plateau” is longer than in pure argon.

The yields of condensable products as a function of applied voltage were determined for three mixtures as shown in Fig. 4 and the corresponding photocurrent curves were obtained. The yield curves are of the same general form as those obtained for pure ethane and pure methane, but the yields are higher and the reaction occurs at lower values of  $V/P$ . The data at 10 mm.  $\text{CH}_4$ , 190 mm. Ar include two points which do not fit the presumed curve. The low yield at  $V/P = 6.8$  is a result of an unusually long exposure which was subsequently shown to result in diminished yield. There is no evident reason for the high yield at  $V/P = 5$ . Mass spectrometric analysis<sup>7</sup> of two runs showed a product composition essentially the same as that observed in irradiation of pure methane.

#### Discussion

The chief point of interest in the present study is the assessment of the significance of excitation as opposed to ionization in the primary process. While there are practically no positive ions formed at low  $V/P$ , the sharp rise of the current at higher  $V/P$ , *e.g.*,  $V/P > 20$  for ethane at 38 mm., indicates significant ionization by electron impact to form positive ions and additional electrons. The positive ions thus formed could lead to product formation through ion-molecule reactions and/or charge neutralization at the cathode. The onset of

such ionization cannot be clearly defined since the electron swarm acquires a broad distribution of energies as it drifts through the gas under the influence of an applied field.<sup>8</sup> In the cases of methane and ethane the onset of chemical reaction with increasing  $V/P$  occurs at values of  $V/P$  comparable with those at which ionization sets in. In the argon-methane system there appears to be a significant difference between these subjective "thresholds" but because of the breadth of the electron energy distribution this is a nearly worthless test.

Two characteristics of the yield curves strongly suggest that excitation is an important primary process in these systems. First, the shapes of the chemical yield curves are clearly different from those for electron multiplication, *i.e.*, positive ion formation, which are approximately exponential. Secondly, the values of the chemical yield are so large as to defy explanation by any ordinary ionic mechanism. In radiolysis the ion-pair yield for production of non-condensable gas from ethane is 1.5<sup>3</sup> and for decomposition of methane it is 2.2.<sup>9</sup>

The behavior of these systems may be analyzed in further detail as follows. The dependence of the number of electrons collected at the anode,  $n$ , on the number leaving the cathode,  $n_0$ , the distance between electrodes,  $l$ , and the gas pressure,  $P$  is well known to be<sup>8</sup>

$$n = n_0 \exp(\alpha_i Pl) \quad (1)$$

in a parallel plate system at constant  $X/P$  (field strength per unit gas pressure). The coefficient  $\alpha_i$  represents the number of new electrons created per unit distance per unit gas pressure. It is found that  $\alpha_i$  is a smooth function of  $X/P$  alone, to be discussed below.

In a manner analogous to that used in deduction of equation 1, we now write an expression for the rate of formation of product molecules as a function of  $P$  and  $l$ , assuming that a fixed number of product molecules is formed as an ultimate consequence of each productive electron impact. Let  $N$  be the number of product molecules and  $\alpha_p$  the number of product molecules created per unit distance per unit pressure. The latter property may be expected to be a function of  $X/P$ .

$$dN = \alpha_p n d(Pl)$$

Substituting for  $n$  by equation 1 and integrating yields

$$N = (\alpha_p/\alpha_i) n_0 [\exp(\alpha_i Pl) - 1] \quad (2)$$

This equation indicates that the electron yield,  $Y = N/n$ , at constant  $X/P$  should depend on  $P$  and  $l$  as

$$N/n = (\alpha_p/\alpha_i) [1 - \exp(-\alpha_i Pl)] \quad (3)$$

At small values of the exponent,  $N/n \approx \alpha_p Pl$  and the yield is approximately proportional to the gas pressure.

It is more interesting to examine the behavior of  $\alpha_p/\alpha_i$  with changing  $V/P$  (proportional to  $X/P$ ). For this purpose it is appropriate to replace  $\exp(\alpha_i Pl)$  by  $n/n_0$  and rearrange equation 2 to the form

(8) See L. B. Loeb, "Fundamental Processes in Electrical Discharge in Gases," esp. Ch. VIII, John Wiley and Sons, Inc., New York, N. Y., 1939.

(9) S. C. Lind and D. C. Bardwell, *J. Am. Chem. Soc.*, **48**, 2335 (1926). Only about 25% of the product is condensable.

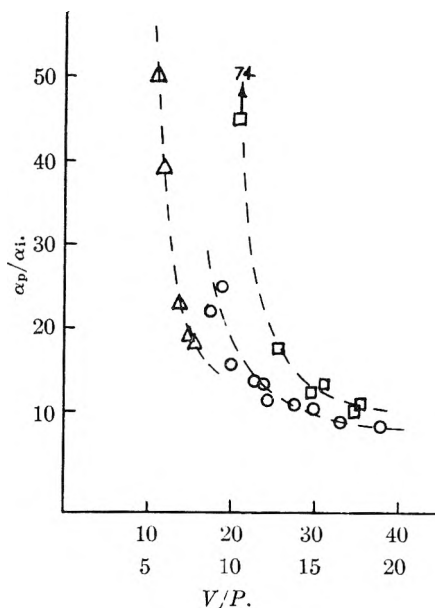


Fig. 5.— $\alpha_p/\alpha_i$  vs.  $V/P$ : O, CH<sub>4</sub>; □, C<sub>2</sub>H<sub>6</sub> (top abscissa for both); △, Ar + CH<sub>4</sub> (bottom abscissa).

$$N/(n - n_0) = \alpha_p/\alpha_i \quad (4)$$

As suggested by this equation  $N/(n - n_0)$  has been plotted versus  $V/P$  in Fig. 5 for the three systems. (The quantity  $N/(n - n_0)$  is also the yield of product molecules per positive ion, which is to be contrasted with the ion pair yields in radiolysis.) The lack of any true "plateau" in the ionization curves makes it difficult to make an objective determination of  $n_0$  (from  $I_0$ ) and this introduces a large uncertainty into values of  $\alpha_p/\alpha_i$  at low values of  $n - n_0$ . In spite of this difficulty it is clear that  $\alpha_p/\alpha_i$  decreases with increasing  $V/P$ . Therefore the formation of products cannot be a simple consequence of a single ionization process. Since dissociative excitation may be expected to occur at energies below that required for ionization the evidence indicates that excitation is an important process in the formation of products.

The dependence of  $\alpha_i$  on  $X/P$  has been experimentally determined for a few simple gases, but no manageable theoretical expression is available for description of this behavior, largely due to difficulties in describing the electron energy distribution. There is, however, a simple equation derived by Townsend but now known to be inadequate,<sup>8</sup> which approximates the observed behavior. This is of the form

$$\alpha_i = A \exp[-BE_i/(X/P)]$$

where  $E_i$  is the ionization energy. If the dependence of  $\alpha_p$  on  $X/P$  were of the same form, but with  $E_i$  replaced by  $E_p < E_i$ , then the ratio  $\alpha_p/\alpha_i$  would vary with  $V/P$  ( $X/P$ ) as shown in Fig. 5. In fact a plot of  $\log(\alpha_p/\alpha_i)$  vs.  $1/(V/P)$  is nearly linear, but unfortunately the theory is inadequate to justify such a quantitative interpretation.

In the argon-methane system reaction occurs at much lower  $V/P$  than in the case of pure methane. This can be understood from examination of curves of mean electron energy,  $\bar{\epsilon}$ , vs.  $X/P$  for various gases.<sup>10</sup> These show that for argon  $\bar{\epsilon}$  rises rapidly

with increasing  $X/P$ , reaching *ca.* 12 e.v. at 2 volts/cm./mm. This corresponds to the energy of the first excited state of argon. Evidently the loss of energy by elastic collision is very inefficient and the energy of the electrons increases readily until inelastic collision is possible. On the other hand, a polyatomic molecule can undergo inelastic collisions at much lower energies. The data show that  $\bar{\epsilon}$  increases much more slowly with  $X/P$  and the increase continues to much higher values of  $X/P$  than in the case of a monoatomic gas. Consequently much higher values of  $X/P$  will be required to produce an appreciable number of electrons of the high energy required for chemical decomposition.

In the argon-methane mixtures the possibility exists that either component could be the seat of the primary excitation. If it were argon it then would be necessary to postulate a process such as  $A^* + CH_4 = CH_3 + H + A$  to initiate reaction. The higher yields of methane decomposition in the presence of argon and the increase in yield with increas-

(10) B. Rossi and H. Staub, "Ionization Chambers and Counters," Ch. 1, N. N. E. S., Div. 5, Vol. 2, McGraw-Hill Book Co., New York, N. Y., 1949.

ing proportion of methane tempt one to adopt this view. However, the decision should not be made on this basis, for the electron energy distribution is certainly a function of gas composition and is undoubtedly a strong factor in determining the observed yields.

Little can be said at present about the nature of the products of these reactions other than to note that they correspond, qualitatively, to those obtained in radiolysis reactions. It is difficult to conceive of a radical reaction which could produce a product such as isopentane from methane at room temperature. The possibility remains that ionic reactions may contribute some small part of the total product yield and may be primarily responsible for such a product. Further investigation to examine this and other aspects of the problem has been initiated.

**Acknowledgment.**—The author wishes to acknowledge the several valuable suggestions and comments received from Prof. W. H. Hamill of the University of Notre Dame during the conduct of this work

## AN EXAMINATION OF THE ABSORPTION SPECTRA OF SOME COBALT(III)-AMINE COMPLEXES. EFFECT OF LIGAND AND SOLVENTS IN ABSORPTION

BY ROBERT C. BRASTED AND CHIKARA HIRAYAMA

*Contribution from the School of Chemistry, University of Minnesota, Minneapolis, Minn.*

*Received October 24, 1958*

There are numerous reports in the literature with regard to the absorption spectra of coordination compounds of cobalt(III). Practically all of these reports are concerned with the absorption spectra in aqueous solutions. There are some inconsistencies in the data in regard to the absorption characteristics of some of the cobalt compounds. In some cases the positions of maxima are not clearly defined in aqueous solutions, whereas some of these maxima become clearly defined in non-aqueous solvents. A study was initiated to coordinate some of the absorption spectra of some of the cobalt(III) amine complexes, compare and contrast reported spectra from other sources, and to make a study of the absorption spectra in alcohols as well as in aqueous solutions. Certain of the spectra are interpreted in terms of crystal field theory.

### Experimental

**Preparation of Compounds.**—The compounds were prepared by well-established methods.<sup>1-8</sup> Most of these com-

pounds were assayed by analyzing for cobalt, and the analyses in each case showed satisfactory agreement with the theoretical percentage of cobalt. The diaquo complexes were prepared only in solution, by hydrolysis of the corresponding dichloro complexes.

**Method of Analysis for Cobalt.**—The analyses for cobalt were done by the electrolytic method.<sup>9</sup> In the analysis of the ethylenediamine and propylenediamine complexes, it was first necessary to treat the sample with concentrated sulfuric acid and ignite to remove the amine. The residue was then dissolved by treatment with nitric acid and a 30%  $H_2O_2$  solution. The nitric acid subsequently was removed by evaporation to fumes after adding sulfuric acid.

**Determination of Absorption Spectra.**—The absorption spectra in the various solvents were determined at room temperature by use of a Cary recording spectrophotometer. Fused quartz cells of two- and ten-cm. lengths were used.

Certain of the complexes isomerize as soon as they are dissolved, *e.g.*, *cis*-dichloro complexes of the tetramine, bis(ethylenediamine) and bis(propylenediamine). Some are unstable in aqueous solutions in which they undergo rapid aquation, such as the chloro complexes. Still others are unstable to heat, such as the nitritopentammine cobalt(III) chloride. Therefore, the solids of the more readily soluble compounds were weighed into volumetric flasks and the solutions were made immediately before determining the spectrum. In this way, it was possible to determine the spectra of these compounds within 15 to 20 minutes after the solutions were made. In those instances in which the compounds were only slightly soluble (as the nitritopentamminecobalt(III) chloride in methanol) a solution was made by shaking a large excess of the solid with the solvent followed by rapid filtration and then obtaining the spectrum. The

(1) H. F. Walton, "Inorganic Preparations," Prentice-Hall, Inc., New York, N. Y., 1948, p. 91.

(2) A. Werner, *Ber.*, **40**, 4821 (1907).

(3) S. M. Jorgensen, *Z. anorg. Chem.*, **14**, 416 (1897).

(4) S. M. Jorgensen, *J. prakt. Chem.*, **42**, 211 (1890).

(5) W. C. Fernelius, "Inorganic Syntheses," Vol. II, John Wiley and Sons, Inc., New York, N. Y., 1946, p. 222.

(6) W. C. Fernelius, *ibid.*, Vol. II, p. 222.

(7) A. Werner and A. Fröhlich, *Ber.*, **40**, 2228 (1907).

(8) J. C. Bailar, Jr., "Inorganic Syntheses," Vol. IV, John Wiley and Sons, Inc., New York, N. Y., 1953, p. 176.

(9) I. M. Kolthoff and E. B. Sandell, "Textbook of Quantitative Inorganic Analysis," 3rd Ed., The Macmillan Co., New York, N. Y., 1953, p. 410.

TABLE I  
OPTICAL ABSORPTION OF COBALT(III) AMMINES AND AMINES IN DIFFERENT SOLVENTS

| Compound                                                                                | Wave length of maxima (m $\mu$ ) |                |          |                |         |                |          |                |
|-----------------------------------------------------------------------------------------|----------------------------------|----------------|----------|----------------|---------|----------------|----------|----------------|
|                                                                                         | Water                            | log $\epsilon$ | Methanol | log $\epsilon$ | Ethanol | log $\epsilon$ | Propanol | log $\epsilon$ |
| 1,2-[Co(NH <sub>3</sub> ) <sub>4</sub> Cl <sub>2</sub> ]Cl                              | 540                              | 1.64           | ca. 560  |                |         |                |          |                |
| 1,6-[Co(NH <sub>3</sub> ) <sub>4</sub> Cl <sub>2</sub> ]Cl                              | 630                              | 1.49           | 627.5    | 1.58           |         |                |          |                |
|                                                                                         | 465                              | 1.37           | 468      | 1.31           |         |                |          |                |
|                                                                                         | 366                              | 1.62           | 384      | 1.71           |         |                |          |                |
|                                                                                         | 253                              | ..             | 256      | ..             |         |                |          |                |
| 1,2-[Co(en) <sub>2</sub> Cl <sub>2</sub> ]Cl                                            | 530                              | 1.89           | 540      | 1.93           | 540     | 1.98           |          |                |
|                                                                                         | 380                              | 1.84           | ..       | ..             | ..      | ..             |          |                |
| 1,6-[Co(en) <sub>2</sub> Cl <sub>2</sub> ]Cl                                            | 620                              | 1.53           | 608      | 1.55           | 610     | 1.68           |          |                |
|                                                                                         | ..                               |                | 442      | 1.38           | 450     | 1.42           |          |                |
|                                                                                         | ..                               |                | 390      | 1.63           | 390     | 1.67           |          |                |
|                                                                                         | 304                              | 3.11           | 305      | 3.05           | 305     | ..             |          |                |
|                                                                                         | 247                              | 4.45           | 250      | 4.44           | 252     | ..             |          |                |
| 1,2-[Co(pn) <sub>2</sub> Cl <sub>2</sub> ]Cl                                            | 529                              | 1.81           | 540      | 1.83           | 540     | 1.87           | 540      | 1.90           |
|                                                                                         | 382                              | 1.84           | ..       | ..             | ..      | ..             | ..       | ..             |
|                                                                                         | 244                              | 4.26           | 246      | 4.20           | 247     | 4.25           | 249      | 4.26           |
| 1,6-[Co(pn) <sub>2</sub> Cl <sub>2</sub> ]Cl                                            | 615                              | 1.55           | 605      | 1.57           | 608     | 1.60           | 608      | 1.60           |
|                                                                                         | ..                               | ..             | 450      | 1.43           | 450     | 1.45           | 454      | 1.40           |
|                                                                                         | ca. 394                          | 1.6            | 384      | 1.67           | 386     | 1.71           | 385      | 1.70           |
|                                                                                         | 307                              | 3.15           | 307      | 3.09           | 306     | 3.12           | 306      | 3.06           |
|                                                                                         | 246                              | 4.44           | 251      | 4.38           | 252     | 4.36           | 252-253  | 4.2            |
| 1,2-[Co(en) <sub>2</sub> (NO <sub>2</sub> ) <sub>2</sub> ]NO <sub>3</sub>               | 447                              | 1.98           | 434      | 2.30           |         |                |          |                |
|                                                                                         | 335                              | 3.06           | 333.5    | 3.07           |         |                |          |                |
| 1,6-[Co(en) <sub>2</sub> (NO <sub>2</sub> ) <sub>2</sub> ]NO <sub>3</sub>               | 433                              | 2.28           | 416      | 2.51           | ..      |                |          |                |
|                                                                                         | 338                              | 3.55           | 340      | 3.50           | 342     | 3.51           |          |                |
|                                                                                         | 247.5                            | 4.31           | 250      | 4.06           | 251     | 4.10           |          |                |
| [Co(NH <sub>3</sub> ) <sub>5</sub> NO <sub>2</sub> ]Cl <sub>2</sub>                     | 457.5                            | 2.34           | 450      | 2.17           |         |                |          |                |
|                                                                                         | 325                              | 3.23           | 330      | 3.24           | 330     |                |          |                |
|                                                                                         | 239                              | 4.05           | 240      | 4.04           | 242     |                |          |                |
| [Co(NH <sub>3</sub> ) <sub>5</sub> ONO]Cl <sub>2</sub>                                  | 486                              | ..             | ..       |                |         |                |          |                |
|                                                                                         | ca. 330                          | ..             | ..       |                |         |                |          |                |
|                                                                                         | 220                              | ..             | 223      |                |         |                |          |                |
| [Co(NH <sub>3</sub> ) <sub>5</sub> Cl]Cl <sub>2</sub>                                   | 535                              |                | 532      |                |         |                |          |                |
|                                                                                         | 362                              |                | 364      |                |         |                |          |                |
|                                                                                         | 228                              |                | 231      |                |         |                |          |                |
| 1,2-[Co(NH <sub>3</sub> ) <sub>4</sub> (H <sub>2</sub> O)Cl]Cl <sub>2</sub>             | ..                               |                | 530      |                |         |                |          |                |
|                                                                                         | ..                               |                | 360      |                |         |                |          |                |
|                                                                                         | ..                               |                | 240.5    |                |         |                |          |                |
| 1,2-[Co(NH <sub>3</sub> ) <sub>4</sub> (H <sub>2</sub> O) <sub>2</sub> ]Cl <sub>3</sub> | 513                              |                |          |                |         |                |          |                |
|                                                                                         | 360                              |                |          |                |         |                |          |                |
| [Co(en) <sub>2</sub> (H <sub>2</sub> O) <sub>2</sub> ]Cl <sub>3</sub>                   | 502                              |                |          |                |         |                |          |                |
|                                                                                         | 364                              |                |          |                |         |                |          |                |
| [Co(pn) <sub>2</sub> (H <sub>2</sub> O) <sub>2</sub> ]Cl <sub>3</sub>                   | 498                              |                |          |                |         |                |          |                |
|                                                                                         | 362                              |                |          |                |         |                |          |                |
| [Co(NH <sub>3</sub> ) <sub>6</sub> ] <sup>+3</sup>                                      | 474 (ref. 10)                    |                |          |                |         |                |          |                |
|                                                                                         | 349 (ref. 10)                    |                |          |                |         |                |          |                |
| [Co(en) <sub>3</sub> ] <sup>+3</sup>                                                    | 465 (ref. 10)                    |                |          |                |         |                |          |                |
|                                                                                         | 349 (ref. 10)                    |                |          |                |         |                |          |                |

concentrations of these solutions were not determined in most instances. However, since we are chiefly interested in the positions of the maxima rather than the intensity of the bands, this procedure was quite satisfactory.

In instances in which the compounds aquate readily, such as the dichloro complexes, the spectra were determined in two (or more) different parts. This process was accomplished by weighing two (or more) different portions of the solid in volumetric flasks, making the solutions immediately before measurement, and carrying out the measurement for any one solution over a short wave length region. In this way the spectrum was measured before it could be significantly affected by aquation.

The nitro complexes are slightly soluble in alcohols, but

they are stable in both aqueous and alcoholic solutions. Therefore, these alcoholic solutions were made by shaking the solvent with an excess of the solid over a period of a half-hour to several hours, filtering and measuring the spectrum. The concentrations of most of these solutions were estimated by evaporating a known volume of the solution to redness in a platinum dish and determining the weight of the residue. The nitro complexes are stable up to 80° (the temperature at which the alcohol was evaporated) so that the concentration could be estimated to about  $\pm 15\%$ .

Since the absorption increases greatly in the deeper ultra-violet region, it was necessary to make dilutions of ten- to a hundred-fold. This dilution was especially necessary in the region of 2500 Å., where the absorption coefficient was

in the order of 10–20,000 as compared to approximately 75 in the visible.

Ordinary distilled water was used to make the aqueous solution. The methanol, ethanol and 1-propanol were redistilled after drying with sodium.

The molar absorption coefficient is defined by the expression  $\log I_0/I = \epsilon cl$ .

### Experimental Results

The positions of the maxima and  $\log \epsilon$  values are shown in Table I. The detailed results are described for the individual compounds.

**cis-Dichloro-(ethylenediamine)-cobalt(III) Chloride.**—The data of Table I show this compound to have two distinct maxima, at 530 and 380  $m\mu$ , in aqueous solutions, but only one distinct maximum in the alcohol solutions. This compound isomerizes readily to the *trans* form, and the rate of isomerization is markedly affected by ultraviolet light. Linhard and Weigel<sup>10</sup> show a definite shoulder on the absorption curve at around 560  $m\mu$ , with a distinct maximum at 625 and calculated bands at 392 and 312  $m\mu$ . Basolo<sup>11</sup> reports a diffuse fourth band at 240  $m\mu$ . The present work gives no indication of a shoulder in 560  $m\mu$  region. A plateau at about 240  $m\mu$  is indicated in aqueous solution. The alcoholic solution, however, shows a continued increase in absorption.

**trans-Dichlorobis-(ethylenediamine)-cobalt(III) Chloride.**—Basolo<sup>11</sup> reports four maxima for a 95–99% methanol–water solution of this compound, these appearing at 252, 385, 450 and 625  $m\mu$ . Linhard and Weigel<sup>10</sup> report only two maxima in aqueous solution, although three others are calculated. In the present investigation, three distinct maxima are found in aqueous solution, while in the alcohols there are five. The 450 and 390  $m\mu$  bands are broad, permitting only  $\pm 2 m\mu$  estimate of the peaks. These two bands are overlapped by their neighboring bands in the shorter wave length region to such a degree in aqueous solution that the peak does not rise to its expected maximum. The band at 305  $m\mu$  appears as a definite maximum with the peak slightly displaced to shorter wave length in the aqueous solution. In dilute solutions this band does not appear to have a maximum in the alcoholic solutions, but, instead, appears as a plateau in this region.

**cis-Dichlorotetramminecobalt(III) Chloride.**—The spectrum of this compound was obtained only in the visible region. The compound is unstable in aqueous solution. A maximum in aqueous solution is found at 540  $m\mu$ . The spectrum of this compound in methanol could not be obtained due to its slight solubility and very rapid isomerization to the *trans* form. When an excess of the *cis* compound was shaken with methanol, the purple solution rapidly changed to green and subsequently exhibited a yellow turbidity. It was apparent that the compound reacted with methanol, resulting in the formation of the insoluble solid. This reaction with methanol also was noticed with the *trans* complex. The concentrations of the complexes whose spectra are recorded in Table I are: *cis*-complex in water =  $8.6 \times 10^{-4} M$ ; *trans*-complex in water =  $8.5 \times 10^{-4} M$ ; and *trans*-complex in methanol =  $3.7 \times 10^{-4} M$ .

**trans-Dichlorotetramminecobalt(III) Chloride.**—The present work shows four maxima for this compound. Tsuchida and Kashimoto<sup>12</sup> report only three of these bands at 666, 475 and 312  $m\mu$ . Linhard and Weigel<sup>10</sup> report bands at 629 and 253  $m\mu$ , with additional bands calculated at 475, 401 and 304  $m\mu$ . In the present investigation the maxima in aqueous solution appear at 630, 366, 465 and 253  $m\mu$ .

**cis-Dichlorobis-(propylenediamine)-cobalt(III) Chloride.**—The aqueous solution of this compound has three maxima at 529, 382 and 244  $m\mu$  (see Fig. 1 and Table I). The shape of the absorption curve of this compound suggests at least four bands similar to the analogous ethylenediamine complex, with an additional apparent band in the neighborhood of 600  $m\mu$  where a slight hump appears. The first band appears at 540  $m\mu$  in methanol, ethanol and propanol solutions. However, the absorption increases rapidly as the wave length diminishes, such that the band in the 380  $m\mu$  region does not show a clear maximum.

**trans-Dichlorobis-(propylenediamine)-cobalt(III) Chloride.**—As with the ethylenediamine analog, there are five maxima in the alcohol solutions and only three well-defined maxima in the aqueous solution (see Fig. 2 and Table I). The ultraviolet spectra are practically the same as those for the ethylenediamine complex. In the 395  $m\mu$  region in water the maximum is ill-defined. It is estimated that this maximum in the aqueous solution is located at 394  $m\mu$ . Due to the overlapping of bands in the region between 450 and 380  $m\mu$  the maxima in this region are determined to an accuracy no better than  $\pm 2$  to 3  $m\mu$ . The band at 307  $m\mu$  appears at practically the same position for all four solvents. The 250  $m\mu$  band appears at shortest wave length in water and at longest wave length in propanol. Basolo<sup>11</sup> reports only four bands in 95–99% methanol–water solution, these being at 610, 450, 380 and 255  $m\mu$ . As was the case for the ethylenediamine analog, he does not report the 307  $m\mu$  band.

**Nitropentamminecobalt(III) Chloride.**—The first maximum for this compound appears at a longer wave length in the aqueous solution than for a corresponding alcoholic solution. The maxima in the ultraviolet region appear at shorter wave lengths in the aqueous solution than in the alcohols. Tsuchida and Kashimoto<sup>12</sup> report only two bands at 455 and 323  $m\mu$  in aqueous solution, and they claim that the third band is absent. Linhard and Weigel<sup>13</sup> report a third distinct band at 238.6  $m\mu$ , in agreement with our results.

**Nitritopentamminecobalt(III) Chloride.**—This compound was not sufficiently soluble in the alcoholic solvents to be able to obtain the absorption characteristics with the exception of the third band in a very dilute saturated solution of the complex in methanol. The band at 202  $m\mu$  appears as a flat band with slight maximum at 220 and 223  $m\mu$  in water and methanol, respectively. In aqueous solutions there are bands at 485 and 330  $m\mu$ . Tsuchida and Kashimoto<sup>12</sup> report just two bands at 486 and 330  $m\mu$ . Linhard and Weigel<sup>13</sup> report bands at 491, 361.5 and a shoulder in the region of 263  $m\mu$ . There is a discrepancy in the position of the second band between Linhard and Weigel, on one hand, and Tsuchida and Kashimoto and the present investigators. Linhard and Weigel observed a distinctly peaked band at 361.5  $m\mu$ , whereas the band (this work) at 330  $m\mu$  is somewhat overlapped. It is, however, definitely not in the region of 360  $m\mu$ . There is also a discrepancy in the position of the third band. A much shorter wave length is therein indicated for this band.

It was noticed that the nitrito and nitro complexes decomposed in aqueous solutions after being stored at 35°. This decomposition takes place at a slower rate at room temperature. A blackish-brown precipitate is formed. The decomposition appeared to be prevented in acid solutions. The precipitate is cobalt(III) hydroxide,<sup>14</sup> which is formed by the photodecomposition of the complex.

**cis-Chloroaquatetramminecobalt(III) Chloride.**—The spectrum of this compound was obtained only in methanol solution. Three maxima were obtained at 530, 360 and 240.5  $m\mu$ . Shimura<sup>15</sup> reports bands at 529 and 363  $m\mu$  in aqueous solution.

**trans-Dinitrobis-(ethylenediamine)-cobalt(III) Nitrate.**—The first band in the ethanolic solution was overlapped by the second band such that the maximum was obscured. However, the first band in water appears at a longer wave length than in methanol. The second and third bands showed maxima at shorter wave lengths in water than in the alcohols. Basolo<sup>11</sup> reports maxima in 95–99% methanol–water solution at 433, 347 and 250  $m\mu$ .

**cis-Dinitrobis-(ethylenediamine)-cobalt(III) Nitrate.**—This compound has only two absorption maxima between 700 and 230  $m\mu$ . Both maxima appear at longer wave lengths in the aqueous solution as compared to those in methanol. Basolo<sup>11</sup> reports three maxima for this compound in methanol–water solution at 438, 325 and 240  $m\mu$ .

### Discussion

**Bands I and II.**—In the past five years the crystal field theory has been used very successfully in the interpretation of magnetic, spectroscopic and

(10) M. Linhard and M. Weigel, *Z. anorg. allgem. Chem.*, **271**, 101 (1952).

(11) F. Basolo, *J. Am. Chem. Soc.*, **72**, 4393 (1950).

(12) R. Tsuchida and S. Kashimoto, *Bull. Chem. Soc. Japan*, **11**, 785 (1936).

(13) M. Linhard and M. Weigel, *Z. anorg. allgem. Chem.*, **267**, 113 (1951).

(14) M. Linhard and M. Weigel, *ibid.*, **266**, 49 (1951).

(15) Y. Shimura, *Bull. Chem. Soc. Japan*, **25**, 49 (1952).

stereochemical data of discrete transition metal complexes.<sup>16</sup> In the case of complexes of octahedral symmetry, the first two bands are due to electronic transitions within the central metal ion. However, in the case of a complex of tetragonal symmetry the first band is further split into two components, the magnitude of the splitting depending upon the relative magnitude of crystal field contribution of the ligands. It has been shown by Orgel<sup>17</sup> that the magnitude of the crystal field effect on the d-electrons of the central ion is in the increasing order of the spectrochemical series, *i.e.*, the order  $I^- > Br^- > Cl^- > F^- > H_2O > C_2O_4^{2-} > pyridine > NH_3 > en > NO_2^- > CN^-$ , where *en* is ethylenediamine. The greater crystal field produced by one ligand compared to another, on a d-electron of the central ion in a complex of identical symmetry, will manifest itself in the shifting of the first maximum to shorter wave lengths. The results of Linhard and Weigel<sup>10</sup> show this shift for the ammine and ethylenediamine complexes of cobalt(III). The results in Table I for the aqueous solutions agree with those of Linhard and Weigel. However, whereas some of the peaks are not observed in aqueous solutions, these peaks are actually observed in the alcoholic solutions in the present investigation.

In the case of cobalt(III) complexes of octahedral symmetry (hexamminecobalt(III), hexaquo cobalt(III), etc.) a calculation<sup>17</sup> based on a simple perturbation theory shows that the band separation should be about  $10,500\text{ cm.}^{-1}$ . However, it is found that the actual band separations are  $8,500$  and  $8,000\text{ cm.}^{-1}$  for hexamminecobalt(III) and tris-(ethylenediamine)-cobalt(III) complexes,<sup>10</sup> respectively. The band separation between the same first-order electron configuration is related to the intermixing of molecular orbitals,<sup>18</sup> which gives a measure of covalency. As the crystal field effect of the ligand increases (increasing order in the spectrochemical series) the band separation in the octahedral complexes decreases. Thus the separation is greater in the hexammine than it is in the tris-(ethylenediamine) complexes, and the hexacyano complex is even smaller at  $6600\text{ cm.}^{-1}$ .<sup>18</sup> The decrease in band separation is, to a reasonable approximation, in the order of increasing covalency.

The effect of changing the symmetry of the crystal field results in different orders of splitting of the electronic energy levels. The splitting of the first band is increased as the difference in the crystal field effect of the incoming ligand and that of the other ligand becomes greater.<sup>17</sup> Thus a change from the octahedral symmetry of the hexammine to the tetragonal symmetry of the chloropentamine predicts a further splitting of the first band. Linhard and Weigel<sup>14</sup> have shown that the splitting of the halopentamine first band is greatest for the iodopentamine and that there is no splitting of the fluoropentamine first band. The broad first band of chloropentaminecobalt(III) is attributed to a splitting of this band. The nitro and nitritopen-

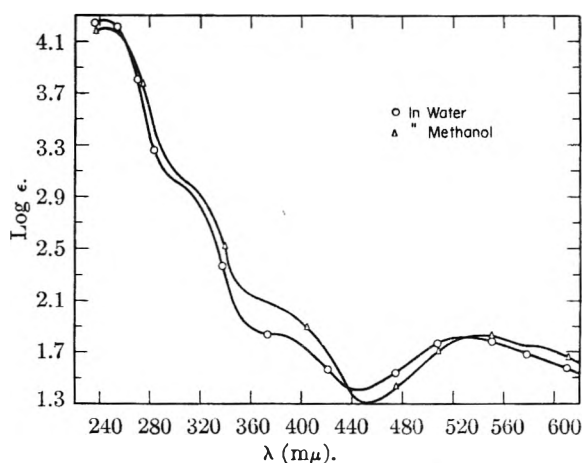


Fig. 1.—Absorption of *cis*-[Co(pn)<sub>2</sub>Cl<sub>2</sub>]Cl.

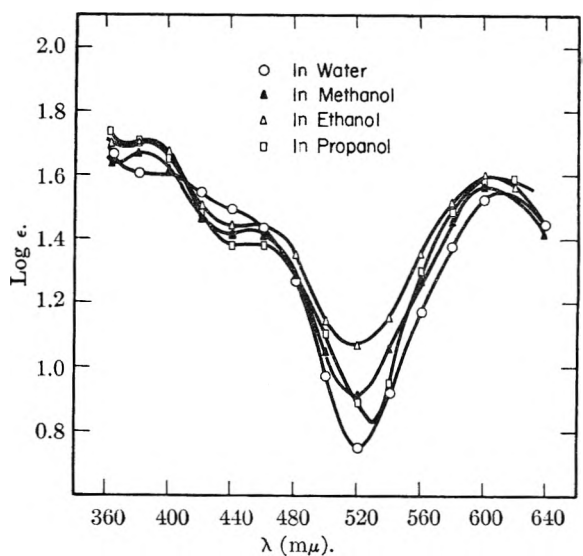


Fig. 2.—Absorption of *trans*-[Co(pn)<sub>2</sub>Cl<sub>2</sub>]Cl.

taminecobalt(III) complexes do not show evidence of splitting in the first band since these ligands lie very close to ammonia in the spectrochemical series.

Since the nitro ligand produces a greater crystal field than either the ammonia or amine ligands, the position of the first band for the latter ligands is more bathochromic than for the nitro complexes. Shimura<sup>15</sup> has determined the order of the spectrochemical series and has placed the nitrito ligand before ammonia. The earlier position of the nitrito ligand is manifested in the slightly longer wave length of the first band of nitritopentamine as compared to that of the hexammine complex.

In disubstituted complexes, the crystal field theory predicts that the splitting of the longest wave length transition would be much more marked in the *trans* complexes than in the *cis*.<sup>19</sup> As predicted by the theory the intensity of the first band of the *trans*-dihalo complexes is greater than that of the *cis*-complexes show greater intensity than the *trans* complexes. Basolo, Ballhausen and Bjerum<sup>20</sup> report similar observations. These latter

(16) See, for example, L. E. Orgel, *J. Chem. Soc.*, 4756 (1953), and papers by Orgel and by Nyholm in "Proceedings of the Tenth Solvay Conference in Chemistry," R. Stoops, Ed., Brussels, 1956.

(17) L. E. Orgel, *J. Chem. Soc.*, 4756 (1953).

(18) C. K. Jorgensen, *Acta Chem. Scand.*, 10, 500 (1956).

(19) L. E. Orgel, *J. Chem. Phys.*, 23, 1004 (1955).



investigators also reported a splitting of the first band of the *cis* isomer of  $[\text{Co}(\text{en})_2(\text{NO}_2)\text{Cl}]^+$ , in contrast to the *trans* isomer. They explained the splitting in the *cis* complex as being due to the much smaller contribution of the chloride, compared to one-half ethylenediamine and the nitro groups. The ultimate result is ascribed to a greater tetragonal symmetry in the *cis* complex. The *cis*-chloroaquatetramminecobalt(III) chloride does not show any splitting of the first band due to the small crystal field contributions of the chloride ion and water as compared to the chloronitrotetrammine complex.

The *trans*-dinitrobis-(ethylenediamine)-cobalt(III) does not show any splitting in the first band. Basolo<sup>11</sup> and Linhard and Weigel<sup>21</sup> also have shown no splitting in the *trans*-dinitrotetramminecobalt(III) complexes. It is seen from Table I that the first band of the *trans*-dinitro complex has the greatest hypsochromic shift. Both the *cis* and *trans* complexes exhibit a first band whose maximum is more hypsochromic than the tris-(ethylenediamine)-cobalt(III) complex. These relative band positions can be explained easily on the basis of the nitro groups exhibiting a greater crystal field effect than ethylenediamine. For this reason it would be expected that the *trans*-dinitro-(ethylenediamine)-cobalt(III) would have a more hypsochromic first band than the corresponding *cis* complex. The lack of splitting in the *trans* isomer may be attributed to the comparatively similar crystal field contributions of the ethylenediamine and nitro ligands.

The replacement of a propylenediamine by two chloro groups to form the dichlorobis-(propylenediamine)-cobalt(III) complex results in the appearance of the first band at a shorter wave length than the ethylenediaminecobalt(III) complex. Assuming that the dihalo complexes follow the same order as the pure amine complexes in their relative first band positions (as the trend seems to indicate from the spectra for other diacidoamine complexes), the propylenediamine ligand would be placed in a later position than ethylenediamine in the spectrochemical series.

In examining the frequency difference ( $\nu_{II} - \nu_{Ia}$ ) (see Table II) it is seen that the magnitude of this difference increases in the order of complexes of ethylenediamine < propylenediamine < ammonia. In every case the difference in the *trans*-dichloro complex is greater than that in the monochloro and ammine complex. If the decreasing magnitude of ( $\nu_{II} - \nu_{Ia}$ ) is a measure of increasing covalency, then this order follows that of increasing stability of the complexes since the stability of ammine complexes increases in the order ammonia, propylenediamine, ethylenediamine.<sup>22</sup> In this case, it would appear that the spectrochemical series does not give the order of increasing stability of the ligand.

The values of ( $\nu_{II} - \nu_{Ib}$ ) for the *trans*-dichloro complexes show a fairly wide variation for the different complexes in the different solvents; how-

ever, the difference ( $\Delta\nu_a - \Delta\nu_b$ ) remains quite constant. This value represents the splitting in the first band of the *trans*-dichloro complexes. From the constancy of this value, it seems that the effect of the chloro ligand on the symmetry of the field due to ammonia, ethylenediamine and propylenediamine is of the same magnitude.

**Bands III and IV.**—The results obtained in the present investigation are in general agreement with those previously reported (*vide infra*). The only disagreement is in the absorption of nitropentamminecobalt(III) chloride. The present results for the positions of bands I and III agree with those of Tsuchida and Kashimoto,<sup>12</sup> these being at 486 and 330  $m\mu$ , respectively. Linhard and Weigel<sup>21</sup> report band III at 361.5  $m\mu$ . There is also a disagreement in the position of band IV between that of the latter workers and that obtained by the present investigators. There is, however, general agreement in that the charge-transfer band III of this compound is more bathochromic than that of the corresponding nitro complex. It is thus indicated that there is greater photosensitivity in the nitrito complex. The greater photosensitivity of the nitro and nitrito complexes is shown by the comparatively rapid decomposition of these complexes in aqueous solution in the presence of light.

**Effect of Solvents on Absorption.**—The most prominent effect of solvent on the absorption is seen in the shifting of the maxima (see Table II). There is a difference in the direction of the shift for the longer wave length bands depending on whether the solvent is water or an alcohol and on the type of complex concerned. The position of band IV, the most hypsochromic band, is always at the shortest wave length for the aqueous solution, increasing in the order: water < methanol < ethanol < propanol. It is to be noted that the diacido complexes show this band at longer wave lengths than the monoacido complexes. The hexammine and tris-(ethylenediamine) complexes do not show either bands III or IV down to 200  $m\mu$ .<sup>23</sup> The *cis*-diacido complexes always have their respective bands at shorter wave length than those of the corresponding *trans* complexes.

The most significant shift of the maxima with solvent is observed in the visible bands. The maxima of the first band of *cis*-dichlorobis-(ethylenediamine)-cobalt(III), *cis*-dichlorotetramminecobalt(III) and *cis*-dichlorobis-(propylenediamine)-cobalt(III) complexes all appear at shorter wave lengths in water than in the alcohols. The position of the band in the alcohols remains constant. On the other hand, *cis*-dinitrobis-(ethylenediamine)-cobalt(III) has the maximum for this band at longer wave length in the aqueous solution. All of the *trans* complexes, nitropentamine, and chloropentamminecobalt(III) chloride also have their first band at longer wave length in the aqueous solution. It is noted, on the other hand, that the magnitude of the shift in the *trans*-dinitrobis-(ethylenediamine)-cobalt(III) nitrate is greater than that of the corresponding *cis*-complex.

The charge-transfer band, III, in *trans*-dichlorobis-(ethylenediamine)-cobalt(III) and the corre-

(20) F. Basolo, C. J. Ballhausen and J. Bjerrum, *Acta Chemica Scand.*, **9**, 810 (1955).

(21) M. Linhard and M. Weigel, *Z. anorg. allgem. Chem.*, **278**, 287 (1955).

(22) G. Schwarzenbach, *Helv. Chim. Acta*, **36**, 2344 (1952).

(23) M. Linhard, *Z. Elektrochem.*, **60**, 224 (1944).

TABLE II  
 FREQUENCY DIFFERENCES IN MAXIMA (FREQUENCY IN CM.<sup>-1</sup> × 10<sup>3</sup>)<sup>c</sup>

| Compound                                                                            | Solvent  | $\nu_{II} - \nu_{Ia}$ | $\nu_{II} - \nu_{Ib}$ | $\Delta\nu_a - \Delta\nu_b$ | $\nu_{IV} - \nu_{III}$ |
|-------------------------------------------------------------------------------------|----------|-----------------------|-----------------------|-----------------------------|------------------------|
| <i>trans</i> -[Co(NH <sub>3</sub> ) <sub>4</sub> Cl <sub>2</sub> ]Cl                | Water    | 11.45                 | 5.85                  | 5.60                        | 9.2 <sup>a</sup>       |
|                                                                                     |          | (9.0) <sup>b</sup>    |                       |                             | (6.5) <sup>b</sup>     |
| <i>trans</i> -[Co(NH <sub>3</sub> ) <sub>4</sub> Cl <sub>2</sub> ]Cl                | Methanol | 10.1                  | 4.65                  | 5.5                         | ...                    |
| <i>cis</i> -[Co(en) <sub>2</sub> Cl <sub>2</sub> ]Cl                                | Water    | ...                   | 7.45                  | ..                          | (9.7) <sup>b</sup>     |
| <i>trans</i> -[Co(en) <sub>2</sub> Cl <sub>2</sub> ]Cl                              | Water    | (9.8) <sup>b</sup>    | (3.4) <sup>b</sup>    | ..                          | 7.6                    |
|                                                                                     |          |                       |                       |                             | (7.8) <sup>b</sup>     |
| <i>trans</i> -[Co(en) <sub>2</sub> Cl <sub>2</sub> ]Cl                              | Methanol | 9.11                  | 3.61                  | 5.5                         | 7.2                    |
| <i>trans</i> -[Co(en) <sub>2</sub> Cl <sub>2</sub> ]Cl                              | Ethanol  | 9.2                   | 3.4                   | 5.8                         | 6.9                    |
| <i>cis</i> -[Co(pn) <sub>2</sub> Cl <sub>2</sub> ]Cl                                | Water    | ...                   | 7.3                   | ..                          | ...                    |
| <i>trans</i> -[Co(pn) <sub>2</sub> Cl <sub>2</sub> ]Cl                              | Water    | 9.7                   | ..                    | ..                          | 8.0                    |
| <i>trans</i> -[Co(pn) <sub>2</sub> Cl <sub>2</sub> ]Cl                              | Methanol | 9.5                   | 3.9                   | 5.7                         | 7.2                    |
| <i>trans</i> -[Co(pn) <sub>2</sub> Cl <sub>2</sub> ]Cl                              | Ethanol  | 9.5                   | 3.70                  | 5.8                         | 7.0                    |
| <i>trans</i> -[Co(pn) <sub>2</sub> Cl <sub>2</sub> ]Cl                              | Propanol | 9.6                   | 4.0                   | 5.6                         | ca. 7.0                |
| <i>trans</i> -[Co(en) <sub>2</sub> (NO <sub>2</sub> ) <sub>2</sub> ]NO <sub>3</sub> | Water    | ...                   | ..                    | ..                          | 10.8                   |
| <i>trans</i> -[Co(en) <sub>2</sub> (NO <sub>2</sub> ) <sub>2</sub> ]NO <sub>3</sub> | Methanol | ...                   | ..                    | ..                          | 10.6                   |
| <i>trans</i> -[Co(en) <sub>2</sub> (NO <sub>2</sub> ) <sub>2</sub> ]NO <sub>3</sub> | Ethanol  | ...                   | ..                    | ..                          | 10.6                   |
| <i>trans</i> -[Co(NH <sub>3</sub> ) <sub>4</sub> Cl <sub>2</sub> ]Cl                | Water    | 11.45                 | 5.85                  | 5.60                        | 9.2 <sup>a</sup>       |
|                                                                                     |          | (9.0) <sup>b</sup>    |                       |                             | (6.5) <sup>b</sup>     |
| <i>trans</i> -[Co(NH <sub>3</sub> ) <sub>4</sub> Cl <sub>2</sub> ]Cl                | Methanol | 10.1                  | 4.65                  | 5.5                         | ...                    |
| <i>cis</i> -[Co(en) <sub>2</sub> Cl <sub>2</sub> ]Cl                                | Water    | ...                   | 7.45                  | ..                          | (9.7) <sup>b</sup>     |
| <i>trans</i> -[Co(en) <sub>2</sub> Cl <sub>2</sub> ]Cl                              | Water    | (9.8) <sup>b</sup>    | (3.4) <sup>b</sup>    | ..                          | 7.6                    |
|                                                                                     |          |                       |                       |                             | (7.8) <sup>b</sup>     |
| <i>trans</i> -[Co(en) <sub>2</sub> Cl <sub>2</sub> ]Cl                              | Methanol | 9.11                  | 3.61                  | 5.5                         | 7.2                    |
| <i>trans</i> -[Co(en) <sub>2</sub> Cl <sub>2</sub> ]Cl                              | Ethanol  | 9.2                   | 3.4                   | 5.8                         | 6.9                    |
| <i>cis</i> -[Co(pn) <sub>2</sub> Cl <sub>2</sub> ]Cl                                | Water    | ...                   | 7.3                   | ..                          | ...                    |
| <i>trans</i> -[Co(pn) <sub>2</sub> Cl <sub>2</sub> ]Cl                              | Water    | 9.7                   | ..                    | ..                          | 8.0                    |
| <i>trans</i> -[Co(pn) <sub>2</sub> Cl <sub>2</sub> ]Cl                              | Methanol | 9.5                   | 3.9                   | 5.7                         | 7.2                    |
| <i>trans</i> -[Co(pn) <sub>2</sub> Cl <sub>2</sub> ]Cl                              | Ethanol  | 9.5                   | 3.70                  | 5.8                         | 7.0                    |
| <i>trans</i> -[Co(pn) <sub>2</sub> Cl <sub>2</sub> ]Cl                              | Propanol | 9.6                   | 4.0                   | 5.6                         | ca. 7.0                |
| <i>trans</i> -[Co(en) <sub>2</sub> (NO <sub>2</sub> ) <sub>2</sub> ]NO <sub>3</sub> | Water    | ...                   | ..                    | ..                          | 10.8                   |
| <i>trans</i> -[Co(en) <sub>2</sub> (NO <sub>2</sub> ) <sub>2</sub> ]NO <sub>3</sub> | Methanol | ...                   | ..                    | ..                          | 10.6                   |
| <i>trans</i> -[Co(en) <sub>2</sub> (NO <sub>2</sub> ) <sub>2</sub> ]NO <sub>3</sub> | Ethanol  | ...                   | ..                    | ..                          | 10.6                   |
| [Co(NH <sub>3</sub> ) <sub>5</sub> NO <sub>2</sub> ]Cl <sub>2</sub>                 | Water    | ...                   | ..                    | ..                          | 11.1                   |
| [Co(NH <sub>3</sub> ) <sub>6</sub> NO <sub>2</sub> ]Cl <sub>2</sub>                 | Methanol | ...                   | ..                    | ..                          | 11.3                   |
| [Co(NH <sub>3</sub> ) <sub>5</sub> NO <sub>2</sub> ]Cl <sub>2</sub>                 | Ethanol  | ...                   | ..                    | ..                          | 11.1                   |
| [Co(NH <sub>3</sub> ) <sub>5</sub> Cl]Cl <sub>2</sub>                               | Water    | ...                   | ..                    | ..                          | ca. 15                 |
| [Co(NH <sub>3</sub> ) <sub>5</sub> Cl]Cl <sub>2</sub>                               | Water    | 8.9                   | ..                    | ..                          | 7.5 <sup>b</sup>       |
| [Co(NH <sub>3</sub> ) <sub>5</sub> Cl]Cl <sub>2</sub>                               | Methanol | 8.7                   | ..                    | ..                          | ...                    |
| [Co(NH <sub>3</sub> ) <sub>6</sub> ] <sup>+3</sup>                                  | Water    | 8.5 <sup>a</sup>      | ..                    | ..                          | ...                    |
| [Co(en) <sub>3</sub> ] <sup>+3</sup>                                                | Water    | 8.0 <sup>b</sup>      | ..                    | ..                          | ...                    |

<sup>a</sup> Calculated from  $\nu_{III}$  value of Linhard and Weigel.<sup>10</sup> <sup>b</sup> Values of Linhard and Weigel.<sup>10</sup> <sup>c</sup>  $\nu_{II}$  = frequency of second band;  $\nu_{Ia}$  = band Ia;  $\nu_{Ib}$  = band Ib;  $\nu_{IV}$  = band IV;  $\nu_{III}$  = band III;  $\Delta\nu_a = \nu_{II} - \nu_{Ia}$ ;  $\Delta\nu_b = \nu_{II} - \nu_{Ib}$ .

sponding propylenediamine complex appear at practically the same wave length in all solvents for both these complexes. This charge-transfer band is overlapped heavily in *trans*-dichlorotetramminecobalt(III) and appears as just a slight shoulder in the region of 300 m $\mu$ . It already has been shown (*vide supra*) that the corresponding *cis*-complexes only show a slight shoulder in this region.

The nitrocomplexes show a different behavior in their first charge-transfer band. This band in *cis*-dinitrobis-(ethylenediamine)-cobalt(III) appears at a slightly longer wave length in the aqueous solution. The bands for the *trans* isomer as well as the nitropentamminecobalt(III) chloride are both more hypsochromic in the aqueous solution than in the alcohols. This band is at a longer wave length in ethanol than in methanol for the *trans* isomer. Tsuchida and co-workers<sup>24</sup> studied the effect of solvent on the absorption of some cobalt(III) and

chromium(III) ammine and acidoammine complexes. These investigators report bathochromic shifts for the first two bands of all compounds with a solvent change from alcohol, to water, to acetic acid. The characteristic bands showed a hypsochromic shift. These workers apparently studied only monoacido and *trans*-diacido isomers where the acido ligand was thiocyanate. In general, the observations of Tsuchida and co-workers are in agreement with our results. However, if the second band of the nitro complexes is defined as the characteristic ligand band by these workers, then there is disagreement in our results since there is a difference in the direction of the shift between the *cis*- and *trans*-dinitro complexes.

Band Ib, the second band due to splitting, in the *trans*-dichloro complexes is somewhat obscured by the flatness of the absorption in this region. The shapes of the absorption curves seem, however, to indicate a hypsochromic shift for this band in water. This shift is fairly well defined in *trans*-dichloro-

(24) N. Nakamoto, M. Kobayashi and R. Tsuchida, *J. Chem. Phys.*, **22**, 957 (1954).

tetramminecobalt(III) chloride. On the other hand band III, which is also somewhat obscured due to overlapping, shows a bathochromic shift in water relative to the alcohols. The band Ib has been attributed<sup>10</sup> to the acido-cobalt bond. In the *cis*-dichlorotetrammine (and amine) complexes the first band was ascribed by these workers to the Ib (splitting) component. In the dinitrobis-(ethylenediamine)-cobalt(III) and the monoacido-pentammine the first band is not split to any noticeable extent unless the monoacido ligand has a very marked difference in crystal field effect from that of the ammine. In agreement with Tsuchida<sup>24</sup> the hypsochromic shift in *cis*-dichlorotetrammine and amine complexes can be attributed to the characteristic band originating from the effect of the chloro ligand on the crystal field of the ammine.

It is seen in the *trans*-diacido complexes that the frequency difference between bands IV and III (indicated by  $\nu_{IV} - \nu_{III}$  in Table II) decreases as the solvent goes from water to the less polar solvents. This decrease is greater in the *trans*-dichloro complexes than in the dinitro, although the value of  $(\nu_{IV} - \nu_{III})$  is higher for the nitro complexes. Linhard and Weigel<sup>10</sup> have shown that band III for *cis*- and *trans*-dichlorobis-(ethylenediamine)-cobalt(III) appear in identical positions in their aqueous solutions. From general observations we would expect the *cis* isomer to show band IV at a shorter wave length than the corresponding *trans* isomer. If this be the case, it can be seen that  $(\nu_{IV} - \nu_{III})$  for the *cis* isomer would also be greater than that for the *trans* isomer.

A number of investigators have reported on the effect of solvent on the absorption spectra of complex organic molecules.<sup>25,26</sup> However, there has been very little work of this type done on solutions of inorganic complexes. In the case of square planar Cu(II) complexes, Calvin and co-workers<sup>27</sup> have shown that the shifting of the band in the visible and near infrared is due to solvation of the complex with the resultant formation of an octahedral complex. The formation of the complex results in a hypsochromic shift of the bands. Similar effects have been observed for some square planar Ni(II) complexes.<sup>28</sup> Schlafer and Skoludek<sup>29</sup> have observed that the 730 m $\mu$  band of CrCl<sub>2</sub> is shifted to a longer wave length in solutions of increasing acidity and also as the solvent goes from water to methanol to ethanol. In the alcoholic solutions, the hypsochromic shift is attributed to the formation of octahedral complexes of the form [Cr<sup>II</sup>-

(alc)<sub>6</sub>]<sup>++</sup>. Tsuchida and co-workers,<sup>24</sup> on the other hand, applied McConnell's theory<sup>25</sup> and attribute the hypsochromic shift to  $\pi \rightarrow \pi$  transitions, while the bathochromic shift, characteristic of the acido ligand bands, is designated as  $\sigma \rightarrow \pi$  transitions.

From the shifting of the absorption bands, it is seen that although the effect is small, the solvent has a definite perturbing influence on the crystal field around the central ion. It would seem at first sight that the effect of the solvent on octahedral complexes is primarily electrostatic rather than any effect on the symmetry of the complex. The interaction of the solvent on the field due to amine ligands causes a hypsochromic shift. According to McConnell's theory, which applies to non-charge-transfer processes, this effect could be interpreted as an interaction and excitation of a  $\pi$ -electron of the ligand on the field due to the solvent molecule. On the other hand, the bathochromic shift of the characteristic Ib band in the *cis*-dichloro complexes would be due to interaction of a  $\sigma$ -electron of the solute with a  $\pi$ -electron of a solvent.

The opposite influences of the solvent on the intensities, depending on the type of shift, is perhaps manifested in some way in the absorption characteristics of the *cis*- and *trans*-complexes. *cis*-Dichlorobis-(ethylenediamine)-cobalt(III) and the corresponding propylenediamine complex both show distinct maxima for band II at 380 m $\mu$  in aqueous solution, whereas the alcoholic solutions only indicate a shoulder in this region. The *trans*-dichloro complexes, on the other hand, have distinct maxima for band II and Ib in alcoholic solutions, while the aqueous solution does not show distinct maxima in this region. In the latter solutions, band II appears as a plateau.

The charge-transfer band IV is affected to a greater extent as the polarity of the solvent increases. Linhard and Weigel<sup>14</sup> attribute this band to the formation of an excited complex resulting from a charge-transfer process within the complex ion. Rabinowitch,<sup>30</sup> on the other hand, has indicated that the charge-transfer bands are shifted to longer wave lengths when an association complex is formed. The bathochromic shift as a result of ion-pair formation in aqueous solution has been shown in a number of cases.<sup>30,31</sup> Thus the bathochromic shift of band IV with decreasing polarity of the solvent may be attributed to the formation of ion-pairs between the complex ion and the negative ion in solution. Association would be expected to be least in aqueous solution and greatest in propanol.

**Acknowledgment.**—The authors wish to thank Mr. Robert Rinehart for measurement of some of the absorption spectra.

(25) H. McConnell, *J. Chem. Phys.*, **20**, 700 (1952).

(26) J. Ferguson, *ibid.*, **24**, 1263 (1956).

(27) R. L. Belford, M. Calvin and G. Belford, *ibid.*, **26**, 1165 (1957).

(28) L. Sacconi, P. Paoletti and G. Del Re, *J. Am. Chem. Soc.*, **79**, 4062 (1957).

(29) H. C. Schlafer and H. Skoludek, *Z. physik. Chem.*, **11**, 277 (1957).

(30) E. Rabinowitch, *Rev. Modern Phys.*, **14**, 112 (1942).

(31) H. Taube and F. A. Posey, *J. Am. Chem. Soc.*, **75**, 1463 (1953).

# THE USE OF INTERFERENCE OPTICS IN EQUILIBRIUM ULTRACENTRIFUGATIONS OF CHARGED SYSTEMS<sup>1</sup>

BY JAMES S. JOHNSON, GEORGE SCATCHARD<sup>1a</sup> AND KURT A. KRAUS

*Contribution from the Oak Ridge National Laboratory, Chemistry Division, Oak Ridge, Tennessee*

*Received November 3, 1958*

The use of interference optics for concentration measurements is discussed for equilibrium ultracentrifugations of charged solutes in supporting electrolytes. A procedure suitable for machine computation is presented. Experimental tests on three "known" systems ( $\text{Na}_2\text{MoO}_4$  in 1 *M*  $\text{NaClO}_4$ ,  $\text{BiOClO}_4$  in 1 *M*  $\text{NaClO}_4$ , and  $\text{BaCl}_2$  in 1 *M*  $\text{HCl}$ ) are presented together with pertinent apparent volume and refractive index increment measurements. The results show that interference optics is much more accurate than schlieren optics and that use of wedged centerpieces allows simultaneous ultracentrifugation of several solutions without significant loss of accuracy. The importance of activity coefficient derivatives in the evaluation of degrees of polymerization and of charges by ultracentrifugation is demonstrated with a discussion of the  $\text{BaCl}_2$ - $\text{HCl}$  system, and the feasibility of studying complexing reactions (average charge determination) is discussed.

Procedures<sup>2,3</sup> have been described for interpretation of equilibrium ultracentrifugation of charged solutes in the presence of slightly sedimenting supporting electrolytes. These discussions dealt primarily with results obtained by schlieren optics, with which the concentration of solutes in the centrifugal field is followed by measurement of the refractive index gradient  $dn/dx$  as a function of radius  $x$ . In recent years interference optical systems, which give differences in refractive index, have come into use,<sup>4</sup> and it is the purpose of this note to discuss the interpretation of results obtained with this system.

With interference optics, a double compartment cell is used: one (solution compartment) contains solvent, the solute whose molecular weight is to be determined, and supporting electrolyte; the other one (background or solvent compartment) contains solvent and supporting electrolyte, usually at approximately the same concentration as in the solution compartment. Both compartments are sector shaped, *i.e.*, the side walls lie along radii, and both cover the same range of radius. Monochromatic light passes through both compartments and is recombined to give interference fringes. With the ultracentrifuge which we use (manufactured by Spinco Division, Beckman Instruments), these fringes are horizontal when the refractive index difference between the two compartments  $n^*$  is independent of the radius. Essentially this pattern is observed at the start of centrifugation. As sedimentation proceeds and the refractive indices of the solution and background begin to vary with  $x$ , the fringes will curve. Between any two adjacent fringes in the horizontal (radial) direction, there will be a difference in  $n^*$  equal to  $\lambda/h$ , where  $\lambda$  is the wave length of light used and  $h$  is the thickness of the solution in the direction of observation. If the difference  $n^*$  between the refractive index of solution and background can be established at one

radius (*e.g.*, by following the movement of fringes from the start of centrifugation, or by an integration procedure), the values of  $n^*$  are known for the other radii. Some complications stemming from details of construction and from the use of a multiple-cell rotor will be discussed later.

**1. Uncharged Solutes.**—If the solute is uncharged, the values of  $n^*$  may be converted to concentrations ( $c$ ), if the refractive index increment  $k = \partial n/\partial c$  is known. The slope  $S = d \ln c/d(x^2)$  can then be obtained. The molecular weight  $M$  may be computed by the equation

$$M = \frac{2RT}{(1 - \bar{v}\rho)\omega^2} S \quad (1)$$

where  $R$  is the gas constant;  $T$ , the absolute temperature;  $\bar{v}$ , the partial specific volume;  $\rho$ , the density of the solution; and  $\omega$ , the angular velocity. Activity coefficients,  $\bar{v}$ , and  $\rho$  are assumed constant in equation 1. Frequently,  $k$  will be essentially constant, and with sufficient accuracy,  $S$  will be given by  $d \ln n^*/d(x^2)$ . If an integration procedure is used to establish concentrations (hence  $n^*$ ) at one radius, the condition which must be satisfied for sector shaped cells is given by the equation<sup>5</sup>

$$\int_{\alpha}^{\omega} cx \, dx = (c_0/2)(x\omega^2 - x\alpha^2) \quad (2)$$

$c_0$  being the initial concentration, the index  $\omega$  indicating the maximum radius of the solution, and  $\alpha$  indicating the radius at the meniscus. If  $k$  is constant, values of  $n^*$  may be substituted for  $c$  in equation 2. The equation follows from the fact that the total amount of solute in the cell at equilibrium is the same as at the start of centrifugation.

**2. Charged Solutes.**—Sedimentation of ionized solutes depends on the charge<sup>6</sup> as well as on molecular weight. The effect of charge varies with concentration of the solute and of supporting electrolyte, and by varying their concentration ratio, that molecular weight and charge can be selected which best satisfies all results. In principle, the variation of concentrations in a single centrifugation is sufficient for simultaneous charge and molecular weight determination, but in practice more experiments frequently are required.

Equations for computing molecular weights from centrifugation results as a function of assumed

(1) This document is based on work performed for the U. S. Atomic Energy Commission at the Oak Ridge National Laboratory, Oak Ridge, Tennessee, operated by Union Carbide Corporation.

(1a) Department of Chemistry, Massachusetts Institute of Technology, Cambridge, Massachusetts; Consultant, Chemistry Division Oak Ridge National Laboratory.

(2) J. S. Johnson, K. A. Kraus and G. Scatchard, *THIS JOURNAL*, **58**, 1034 (1954).

(3) J. S. Johnson, K. A. Kraus and R. W. Holmberg, *J. Am. Chem. Soc.*, **78**, 26 (1956).

(4) See *e.g.*, J. W. Beams, N. Snidow, A. Robeson and H. M. Dixon, *III. Rev. Sci. Inst.*, **25**, 295 (1954).

(5) T. Svedberg and K. O. Pedersen, "The Ultracentrifuge," The Clarendon Press, Oxford, England, 1940, p. 312.

(6) O. Lamm, *Arkiv. Kemi. Mineral. Geol.*, **17A**, No. 25 (1944).

charge were developed for an idealized system,<sup>2</sup> which will also be used for the present discussion: a polymeric component  $PX_z$ , which is ionized in solution as  $P^{-z} + zX^-$ ; a supporting electrolyte  $BX$ ; and solvent. In the assumed system, the partial specific volumes and solution density are constant. Charge per monomer unit  $z'$  (primes refer to quantities expressed in terms of monomer) is also constant. The discussion will be limited to a monodisperse polymeric solute.

In such a charged system the supporting electrolyte does not sediment independently of the polymeric solute; *i.e.*,  $BX$  is distributed differently in the background and solution compartments. To minimize this difficulty and to make derivation of the equations more convenient, the components are redefined in a manner used by Scatchard<sup>7</sup> for interpretation of osmotic pressure measurements on similar systems, and also employed in light scattering work.<sup>8</sup>

The polymer component (2) is redefined as  $(PX_z - (z/2)BX)$  or  $(PX_{z/2}B_{-z/2})$ ; the concentration  $c_2$  of this component is the same as that of  $PX_z$ , but its activity is  $a_2 = c_P c_X^{z/2} c_B^{-z/2} g_P g_X^{z/2} g_B^{-z/2} = c_P c_X^{z/2} c_B^{-z/2} G_2$ , where  $g$  indicates activity coefficients of ions and  $G$  the appropriate activity coefficient products. The equilibrium condition for component (2) is given by

$$d \ln a_2 = d \ln c_P c_X^{z/2} c_B^{-z/2} + d \ln G_2 = \\ d \ln c_2 + (z/2) d \ln \frac{1 + \eta}{1 - \eta} \\ + d \ln G_2 = A_2 d(x^2) \quad (3)$$

where

$$\eta = \frac{zc_2}{2c_3} = \frac{z'c_2'}{2c_3}, \quad A_i = \frac{M_i(1 - \bar{v}_i \rho)\omega^2}{2RT}$$

The subscript  $i$  indicates the component in question. Contrary to our earlier procedure,<sup>2</sup> activity coefficient terms will be left in the expressions. Sufficient information to evaluate them usually is not available, and they are assumed independent of radius (*i.e.*,  $d \ln G_i/d(x^2) = 0$ ).

The activity of the supporting electrolyte, component (3), is given by the product  $a_3 = c_B c_X g_B g_X = c_B c_X G_3$ , but its concentration in presence of component 2 is  $c_3 = c_B + (z/2)c_2 = c_X - (z/2)c_2$ . With this definition of components, it was shown<sup>2</sup> that, at centrifugation equilibrium

$$d \ln a_3 = d \ln a_{bg} = 2 d \ln c_3 + \\ d \ln (1 - \eta^2) + d \ln G_3 = 2 d \ln c_{bg} + \\ d \ln G_{bg} = A_3 d(x^2) = A_{bg} d(x^2) \quad (4)$$

where the subscript  $bg$  indicates  $BX$  in the background compartment. The quantity  $\eta$  usually is small enough compared to unity to allow neglect of the term  $d \ln(1 - \eta^2)$  in equation 4. Thus, with components defined in this way, the distribution of  $BX$  in the background compartment approximates the distribution of component (3) in the solution compartment, *i.e.*, ratios of concentration of component (3) at two radii will be nearly the same as the ratios of  $c_{bg}$ .

The refractive index difference between solution and background is given by the equation

(7) G. Scatchard, *J. Am. Chem. Soc.*, **68**, 2315 (1946).

(8) J. T. Edsall, H. Edelhoch, R. Lontie and P. R. Morrison, *ibid.*, **72**, 4641 (1950).

$$n^* = k_2'c_2' + k_3(c_3 - c_{bg}) \quad (5)$$

in which  $k_2' = \partial n / \partial c_2' = \partial n / \partial c'_{PX_z} - (z'/2)(\partial n / \partial c_{BX})$  and  $k_3 = \partial n / \partial c_{BX}$ . Usually the initial concentrations of  $BX$  in the two compartments are approximately the same. Then the difference in the initial concentrations of component (3) ( $c_{30}$ ) and of  $BX$  in the background compartment ( $c_{bg0}$ ) is given by the equation

$$c_{30} - c_{bg0} = (z'/2)c_{20}' \quad (6)$$

Further, at equilibrium the difference between  $c_3$  and  $c_{bg}$  is approximately equal to  $(z'/2)c'_{20}$  at all radii. Values of  $c_2'$  necessary for computation of molecular weights would be given to good accuracy by  $n^*/k_2'$  only if solutions are made up so that  $c_{30} = c_{bg0}$ . However, usually  $z'$  is not known beforehand and iterative experiments would be required. The error incurred by neglect of the difference between  $c_3$  and  $c_{bg}$  is usually small if interpretation is based on refractive index gradients, but must be considered with interference optics, and a computational procedure to eliminate it is desirable.

The greater precision attainable with interference optics makes it desirable to eliminate some other approximations made in the interpretation of data obtained with a schlieren optical system. To do so makes the arithmetic rather burdensome, and a procedure adaptable to machine computation was developed. To reiterate, the problem is the computation of the degree of polymerization  $N$  implied by the results of a centrifugation for a series of values of  $z'$  covering the expected range. After comparison, those values of  $z'$  and  $N$  best satisfying all results can be selected. It is assumed, for the present, that the menisci in the solution and solvent compartments are at the same radius.

**3. Computational Procedure.** (a) **Input Information.**—The centrifugation results are recorded as photographs of fringes stemming from recombination of light passing through the solution and solvent compartments. On the same photograph are reference fringes, resulting from slots in the counterbalance, which enable alignment of the plate. The horizontal (radial) positions of maxima (or minima) of darkness are determined with a comparator and corrected for cell distortion. With knowledge of the radial magnification of the optical system, and of the radius at one point on the photograph, computation yields a list of radii for which there is a known and constant difference in  $n^*$  between adjacent points.

Additional input information required are the partial specific volumes and refractive index increments of polymeric solute and of supporting electrolyte, molecular weights of the supporting electrolyte and of the monomer unit of the polymeric solute, density of the solution, speed of rotation and temperature, and the difference in  $n^*$  corresponding to one fringe interval ( $\lambda/h$ ).

(b) **Integration Procedure.**—If refractive index increments  $k_i$  are constant

$$n_0^*(x_\omega^2 - x_\alpha^2) = (k_2'c_{20}' + k_3c_{30} - k_3c_{bg0})(\omega^2 - \alpha^2) = \\ = \int_\alpha^\omega n^* d(x^2) = n_\alpha^*(x_\omega^2 - x_\alpha^2) + \\ \int_\alpha^\omega (n^* - n_\alpha^*) d(x^2) \quad (7)$$

where  $n_0^*$  is the initial value of  $n^*$  and  $n_\alpha^*$  is the equilibrium value of  $n^*$  at the meniscus.

The value of  $(n^* - n_\alpha^*)$  for any radius may be obtained from the number of fringe intervals between  $x_\alpha$  and  $x$ . The integral  $\int_\alpha^\omega (n^* - n_\alpha^*)d(x^2)$  can therefore be evaluated by standard methods, for example by the trapezoidal rule. Since the change in  $n^*$  per fringe interval is constant, Simpson's rule may also be used, with  $(x_\omega^2 - x^2)$  as the varying quantity. In the latter case, an estimate of the contribution to the integral by elements at the limiting radii may be made by a trapezoidal computation. With the integral evaluated,  $n_\alpha^*$  and therefore  $n^*$  at any fringe position may be computed.

(c) **Computation of  $c_{bg}$ .**—Values of  $c_{bg}$  at various radii are needed in subsequent steps of the computation. From equation 4

$$dc_{bg} = (A_3/2)c_{bg} d(x^2) - \frac{c_{bg}}{2} d \ln G_{bg} \quad (8)$$

and

$$\int_\alpha^\omega c_{bg} d(x^2) = c_{bg0} (x_\omega^2 - x_\alpha^2) = (2/A_3) \left[ \int_\alpha^\omega dc_{bg} + \int_\alpha^\omega (c_{bg}/2) d \ln G_{bg} \right] = (2/A_3) \left[ (c_{bg\omega} - c_{bg\alpha}) + \int_\alpha^\omega (c_{bg}/2) d \ln G_{bg} \right] \quad (9)$$

$$c_{bg\alpha} = c_{bg\omega} (G_{bg\omega}/G_{bg\alpha})^{1/2} \exp\{(A_3/2)(x_\alpha^2 - x_\omega^2)\} \quad (10)$$

$$c_{bg\omega} = \frac{A_3 [c_{bg0} (x_\omega^2 - x_\alpha^2) - (1/A_3) \int_\alpha^\omega c_{bg} d \ln G_{bg}]}{2[1 - (G_{bg\omega}/G_{bg\alpha})^{1/2} \exp\{(A_3/2)(x_\alpha^2 - x_\omega^2)\}]} \quad (11)$$

Once  $c_{bg\omega}$  is known,  $c_{bg}$  at other values of  $x$  may be computed.

(d) **Computation of  $c_2'$  ( $z' = 0$ ).**—For  $z'$  assumed equal to 0,  $c_3 = c_{BX}$  in the solution compartment, and  $c_2'$  may be computed by a modified form of equation 5

$$c_2' = \frac{n^* - k_3 c_{bg} \{ [(c_{30}/c_{bg0})G^{1/2}] - 1 \}}{(k_2')^2} \quad (12)$$

where

$$G = (G_{30}G_{bg})/(G_{bg0}G_3)$$

Equation 12 follows from the fact that  $d \ln (1 - \eta^2)/d(x^2) = 0$ , and

$$\frac{c_{BX0} \left( \frac{G_{BX0}}{G_{bg0}} \right)^{1/2}}{c_{bg0}} = \frac{c_{30}}{c_{bg0}} \left( \frac{G_{30}}{G_{bg0}} \right)^{1/2} = \frac{c_3}{c_{bg}} \left( \frac{G_3}{G_{bg}} \right)^{1/2}$$

when  $z' = 0$  (see also footnote 10).

(e) **Computation of  $c_2'$  ( $z' \neq 0$ ).**—For computations of  $c_2'$  with assumed polymer charge other than zero, it is convenient to make use of a quadratic equation in  $\eta$ . After substitution of  $2\eta c_3/z'$  for  $c_2'$

$$c_3 = (n^* + k_3 c_{bg}) / \left( \frac{2k_2\eta}{z'} + k_3 \right) \quad (13)$$

With the approximation that the initial value of the activity of component (3) and of the background solute occur at the same radius at equilibrium, we obtain from equation 4

$$\frac{a_3}{a_{30}} = \frac{a_{bg}}{a_{bg0}} = \frac{c_3^2(1 - \eta^2)G_3}{c_{30}^2(1 - \eta_0^2)G_{30}} = \frac{c_{bg}^2 G_{bg}}{c_{bg0}^2 G_{bg0}} \quad (14)$$

From equation 6

$$c_{bg0}/c_{30} = 1 - \eta_0 \quad (15)$$

Combination of these equations yields

$$(1 - \eta^2)(1 - \eta_0^2)(n^* + k_3 c_{bg})^2 = c_{bg}^2 (1 - \eta_0^2)[(2k_2' \eta/z') + k_3]^2 G \quad (16)$$

This equation must be modified to allow for some complications resulting from details of construction of the equipment, as well as departures from assumed experimental conditions which are inconvenient to control.

(i) The initial concentration of  $c_{BX}$  in solution and background compartment may not be precisely the same. The assumption that they are was not made in the equations involving refractive index (5 and progeny) but is made in equation 15. Correction may be made by adding a term  $\Delta = (c_{bg0} - c_{BX0})/c_{30}$ , to the right side of this equation.<sup>9</sup>

(ii) In equations 7 and 14, use of the initial background concentration ( $c_{bg0}$ ) involves the assumption that the menisci in solution and solvent compartments occur at the same radius. In practice, this is seldom precisely the case; indeed, it is well to fill the background compartment more completely than the other, so that the fringe pattern will cover as much of the polymer solution as possible. The value needed for  $c_{bg0}$  in the equations is that concentration which would have to be introduced into the compartment to give the actual distribution of  $c_{bg}$ , if the menisci in the solution and background compartments were located at the same radius. Once  $c_{bg\omega}$  has been computed for the actual limits of the background solution, the required value of  $c_{bg0}$  may be computed by substituting  $x_\alpha^2$  and  $x_\omega^2$  for the solution compartment into equation 11.

(iii) In the mask at the upper collimating lens of the Spinco optical system, the slits are frequently located unsymmetrically, *i.e.*, the slit for the solution compartment is centered along the optical axis, while that for the background compartment is off center. As a result, light going through a given radius of the solution compartment interferes with light from a slightly different radius of the background. The difference  $\epsilon$  will vary with radius, but for present purposes it is sufficient to use an average value; thus light from the solution compartment, radius  $x$ , will be assumed to recombine with light passing through the background compartment at  $x^\pm = x + \epsilon$ , where  $\epsilon \approx 0.0123$  cm. for centrifugations reported here. Three modifications of the procedure are incurred by this.

(a) The light will be cut off in the background compartment between the solution compartment radii  $x_\omega - \epsilon$  and  $x_\omega$ , and to cover the full range of the polymer solution in the integration (equation 7), a short extrapolation is necessary.

(b) The concentration  $c_{bg0}$  in equation 7 must be replaced by  $c_{bg0}^\pm$  computed for the limits  $x_\alpha^\pm$  and  $x_\omega^\pm$  (the limits of the polymer solution  $+\epsilon$ ) in the manner described in (ii).

(c) The value of  $c_{bg}$  in the refractive index equation 5 and progeny must be replaced by  $c_{bg}^\pm$ , the

(9) If  $\Delta$  is defined a little differently,  $((c_{bg})_{x30} - c_{BX0})/c_{30}$ , where  $(c_{bg})_{x30}$  is the value of the background concentration at the radius for which  $a_3 = c_3^2(1 - \eta^2)G_3 = a_{30} = c_{30}^2(1 - \eta_0^2)G_{30}$ , the approximation that the initial activity of both component (3) and the background solute occur at the same radius (equation 14) would be eliminated. The difference between the two definitions of  $\Delta$  usually may be neglected for practical purposes.

concentration of background solute at a radius greater by  $\epsilon$  than the corresponding solution radius. Note that  $c_{bg}$  in equation 14 is not changed—values computed for the same radius as that in question for the solution are used.

(iv) With the multicell (Analytical G) rotor now available from Spinco, simultaneous centrifugation of five solutions is possible. The fringe patterns for the five cells are separated by wedging of the centerpieces, and consequently there is a slightly different length of light path for the two compartments. Although the difference in thickness of the column of solution (at most about 0.007 cm. out of 1.2 cm.) is the same at all radii, the difference in light path varies somewhat with radius, since the total concentration of solute varies. Correction is made by multiplying  $c_{bg}^{\pm}$  by a factor  $h_2/h_1$ , where  $h_1$  is the thickness of the solution compartment, and  $h_2$  the thickness of the background compartment. (The value for  $\Delta n^*$ /fringe interval is computed for the solution compartment, *i.e.*,  $\lambda/h_1$ ). Note that only the terms  $c_{bg}^{\pm}$  which arise from equations involving refractive index are multiplied by  $h_2/h_1$ ; however, the correction also must be made in computing the value of the integral, equation 7, *i.e.*,  $(h_2/h_1)c_{bgo}^{\pm}$  is substituted for  $c_{bgo}^{\pm}$ .

With these modifications equation 16 becomes

$$(1 - \eta^2)(1 - \eta_0 + \Delta)^2(n^* + k_3(h_2/h_1)c_{bg}^{\pm})^2 = c_{bg}^2(1 - \eta_0^2)[(2k_2'\eta/z') + k_3]^2G \quad (16a)$$

or rearranged as a quadratic in  $\eta$

$$\begin{aligned} &[(1 - \eta_0 + \Delta)^2(n^* + k_3(h_2/h_1)c_{bg}^{\pm})^2 + c_{bg}^2(1 - \eta_0^2) \\ & (4k_2'^2/z_2'^2)G]\eta^2 + [c_{bg}^2(1 - \eta_0^2)G \\ & 4k_2'k_3/z_2'\eta + c_{bg}^2(1 - \eta_0^2)k_3^2G - (1 - \eta_0 + \Delta)^2 \\ & (n^* + k_3(h_2/h_1)c_{bg}^{\pm})^2] = 0 \quad (16b) \end{aligned}$$

When  $\eta$  is evaluated,  $c_3$  and  $c_2'$  are given by the equations

$$c_3 = \frac{n^* + k_3(h_2/h_1)c_{bg}^{\pm}}{2(k_2'\eta/z') + k_3} \quad (17)$$

$$c_2' = 2c_3\eta/z' \quad (18)$$

With the values of  $c_2'$  computed at the radii of fringe positions, the value of  $N$  implied for the  $z'$  in question<sup>10</sup> may be computed with the equation

$$N = \frac{d \ln c_2'/d(x^2) + d \ln G_2/d(x^2)}{A_2' - (z'/2) \frac{d \ln (1 + \eta)/(1 - \eta)}{d(x^2)}} \quad (19)$$

which is obtained by substituting  $Nz'$  for  $z$  and  $NA_2'$  for  $A_2$  in equation 3.

The above procedure has been coded for the Oak Ridge National Laboratory digital computer, the ORACLE, with activity coefficients assumed constant, and tests are presented for centrifugations of known systems.

Computations are most satisfactorily effected by

(10) In the computation of  $c_2'$  for  $z' = 0$ , equation 12 is modified somewhat by allowance for the complications discussed above.

$$c_2' = \frac{n^* - k_3c_{bg}^{\pm} \left[ \frac{c_{30}}{c_{bg}^{\pm}} \left( \frac{G_{30}G_{bg}^{\pm}}{G_{bg}^{\pm}G_{30}} \right)^{1/2} - \frac{h_2}{h_1} \right]}{k_2'} \quad (12a)$$

A small approximation is involved since

$$\frac{c_3}{c_{bg}^{\pm}} = \frac{c_{30}}{c_{bg}^{\pm}} \left( \frac{G_{30}G_{bg}^{\pm}}{G_{bg}^{\pm}G_{30}} \right)^{1/2} \exp \left\{ (A_3/2) [(x^2 - x_0^2) - (x_0^2 - x_0^2)] \right\}$$

In equation 12a, the exponential term is taken as unity.

machine, but where this course is not feasible an equation derived by making certain approximations may be useful. It has given values of  $N$  within 3% of those obtained by the more complete procedure in the few cases so far tried, in spite of the fact that allowance is not made for the factors discussed in Sec. 3e. Taking the logarithm of both sides of 5, followed by differentiation, yields, for constant activity coefficients

$$\frac{d \ln n^*}{d(x^2)} - \frac{d \ln c_2'}{d(x^2)} = \frac{(k_3/k_2')[(c_3 - c_{bg})/c_2'] [d \ln (c_3 - c_{bg})/d(x^2) - d \ln c_2'/d(x^2)]}{1 + (k_3/k_2')(c_3 - c_{bg})/c_2'} \quad (20)$$

If the approximations are made that the original concentrations of  $c_2'$ ,  $c_3$  and  $c_{bg}$  occur at the same radius, that  $\eta^2$  is negligible in comparison with unity, and that  $d \ln c_3/d(x^2)$  is small compared with  $d \ln c_2'/d(x^2)$ , the equation

$$d \ln n^*/d(x^2) - d \ln c_2'/d(x^2) = S - \mathcal{S} = \frac{(A_3/2) - NA_2'/(1 + Nz'\eta)}{(2k_2'/z'k_3) + 1} \quad (21)$$

is obtained. After a table of  $n^*$  as a function of  $x$  has been computed from the fringe positions, one may compute  $N$  for assumed values of  $z'$  by iteration with equation 21 and an approximate form of 19.<sup>3</sup>

$$N = \frac{(d \ln c_2'/d(x^2))/A_2'}{1 - \frac{z'\eta}{A_2'} \left[ \frac{d \ln c_2'}{d(x^2)} - \frac{d \ln c_3}{d(x^2)} \right]} \quad (19a)$$

### Experimental

Centrifugations were carried out with a Spinco Model E Ultracentrifuge, equipped with a Rayleigh interference optical system, and with an Analytical G (five-cell) rotor. Most of the centrifugation technique is standard or has been described earlier<sup>3,11</sup> and for the most part only changes resulting from the use of interference optics will be discussed.

It has already been mentioned that the data are recorded as photographs of fringe patterns, resulting from refractive index differences between solution and solvent compartments. Reference fringes from gaps in the counterbalance permit alignment of the plates. Progress of centrifugation is followed, and attainment of equilibrium established, by examination of the plates with a comparator capable of measurements in both vertical and horizontal directions. For an arbitrary vertical setting relative to the reference fringes, the horizontal position of the fringes is determined. When there is no significant change in position from day to day, equilibrium is considered established.

Cell distortion is evidenced in centrifugations with water in both compartments by departures of the fringes from the horizontal. Normally water centrifugations are carried out both before and after centrifugation of solutions. The distortion indicated by these runs is reproducible to about  $\pm 0.1$  fringe interval. Distortion of as much as 1.5 fringe intervals has been found, but the extent for a given cell does not seem to change rapidly with time, nor does it seem very sensitive to speeds of rotation in our usual range of operation, from 14,000 to 30,000 r.p.m. In reading plates for interpretation, correction is effected by altering the vertical setting of the comparator to compensate for departures from the horizontal with water. An average of the distortion found in the water centrifugations before and after the run is used.

Because of the acidity of some of the solutions studied, cell centerpieces of pure epoxy resin were used, rather than the usual aluminum filled type. Normally the cells were not disassembled between centrifugations, but were rinsed, shaken overnight filled with water, rinsed again and dried. Values of the thickness  $h$  of the column of solution were obtained by subtracting the thickness of the quartz windows

(11) J. S. Johnson, K. A. Kraus and T. F. Young, *J. Am. Chem. Soc.*, **76**, 1436 (1954).

(assumed not to compress) from the distances between their outer faces in the assembled cells. A Baird interference filter assembly was used for isolation of the 546 m $\mu$  Hg line, and photographs were made on Eastman Spectroscopic IID plates. Temperature, controlled by equipment now standard with the machine, was  $25.0 \pm ca. 0.1^\circ$ .

Refractive index increments were determined with a Brice-Phoenix Differential Refractometer. Densities were measured pycnometrically.

Sodium perchlorate solutions were prepared by neutralization of HClO<sub>4</sub> with NaOH; concentrations were established by density measurements.<sup>12</sup> Concentrated bismuth stock solutions were prepared by dissolving Bi<sub>2</sub>O<sub>3</sub> in HClO<sub>4</sub> solutions, and characterized by bismuth and perchlorate (precipitation of tetraphenylarsonium perchlorate) analyses. All chemicals used in these and other preparations were C.P. or reagent grade. The composition of the Na<sub>2</sub>MoO<sub>4</sub>·2H<sub>2</sub>O used in preparation of solutions was checked by precipitation of PbMoO<sub>4</sub>.

### Results and Discussion

In order to test the performance of the equipment and to see how far some real systems depart from the assumptions made in the derivation of equations, we have carried out studies of three solutes having known molecular weights: Na<sub>2</sub>MoO<sub>4</sub> in 1 M NaClO<sub>4</sub>, BiOClO<sub>4</sub> in 1 M NaClO<sub>4</sub>, and BaCl<sub>2</sub> in 1 M HCl. The centrifugation results, corrected for cell distortion, are presented in Fig. 1 as deviation plots of  $\log n^* - (S/2.303)x^2$ . The points are computed from the value of  $n^*$  at individual fringe positions, and  $S$  is an average slope,  $d \ln n^*/d(x^2)$ , computed for all the points. Since these solutes are monodisperse, graphs of  $\log c' vs. x^2$  should be linear, except for charge and activity coefficient effects. The graphs of  $\log n^* vs. x^2$ , are close enough to linear for the deviation plot in Fig. 1 to be a use-

TABLE I

CENTRIFUGATION CONDITIONS, REFRACTIVE INDEX AND VOLUME DATA

| Molarity component 2                                     | $k_2'$ for $z' = 0$ (546 m $\mu$ ) | Apparent specific vol., cc. | Centrifugation conditions <sup>a</sup> | S       |
|----------------------------------------------------------|------------------------------------|-----------------------------|----------------------------------------|---------|
| Na <sub>2</sub> MoO <sub>4</sub> -1 M NaClO <sub>4</sub> |                                    |                             |                                        |         |
| 0.1029                                                   | 0.0334                             | 0.168                       |                                        |         |
| .1003                                                    | .0336                              | .177                        |                                        |         |
| .0558                                                    | .0336                              | .166                        | A1                                     | 0.00607 |
|                                                          |                                    |                             | A2                                     | .00608  |
|                                                          |                                    |                             | A3                                     | .00603  |
|                                                          |                                    |                             | A4                                     | .00597  |
|                                                          |                                    |                             | A5                                     | .00631  |
| .0535                                                    | .0336                              | .170                        |                                        |         |
| .0497                                                    | .0335                              | .167                        |                                        |         |
| .0255                                                    | .0336                              | .156                        |                                        |         |
| .0249                                                    | .0336                              | .159                        |                                        |         |
|                                                          | .0335 <sup>b</sup>                 | .165 <sup>b</sup>           |                                        |         |
| BiOClO <sub>4</sub> -1 M NaClO <sub>4</sub>              |                                    |                             |                                        |         |
| 0.1004                                                   | 0.0300                             | 0.155                       | B3                                     | 0.02598 |
| .0602                                                    | .0299                              | .153                        | B1                                     | .02488  |
| .0200                                                    | .0314                              | .151                        | B5                                     | .03012  |
| .0080                                                    |                                    |                             | B5                                     | .03508  |
|                                                          | .0300 <sup>b</sup>                 | .154 <sup>b</sup>           |                                        |         |
| BaCl <sub>2</sub> -1 M HCl                               |                                    |                             |                                        |         |
| 0.1009                                                   | 0.0295                             | 0.143                       | A4                                     | 0.00794 |
| .0575                                                    | .0295                              | .143                        | A5                                     | .00885  |
| .0350                                                    | .0297                              | .138                        | A1                                     | .00832  |
|                                                          | .0295 <sup>b</sup>                 | .143 <sup>b</sup>           |                                        |         |

<sup>a</sup> Letters: speed of rotation: A, ca. 27,690 r.p.m.; B, ca. 14,290 r.p.m. Numbers: cell number. <sup>b</sup> Used in computations.

(12) H. E. Wirth and F. N. Collier, *ibid.*, **72**, 5292 (1950).

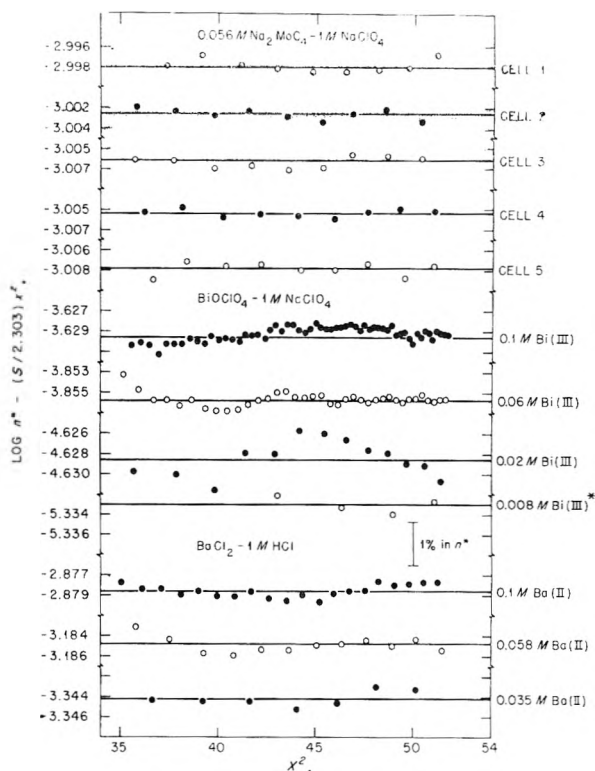


Fig. 1.—Deviation plot of ultracentrifugation results, interference optical system (values of  $S$  listed in Table I). (Each fringe position is represented by a point.) One point at  $x^2 \approx 39.3$ , not shown, from centrifugation of 0.008 M BiOClO<sub>4</sub>, was about 5% in  $n^*$  below the average line for the other points.

ful test of precision, although in principle  $d \log n^*/d(x^2)$  is only approximately constant. Most of the points scatter less than  $\pm 0.5\%$  in  $n^*$ . The precision is much better than with schlieren optics. (See e.g., the comparable graph in ref. 3, Fig. 1). Values of  $S$  and the experimental conditions are summarized in Table I.

1. Volumes and Refractive Index Increments.—The results of refractive index and apparent specific volume measurements of sodium molybdate, barium chloride and bismuth oxyperchlorate in the supporting electrolytes are summarized in Table I. In the case of Na<sub>2</sub>MoO<sub>4</sub>, values are given for several solutions for which centrifugations are not reported. Within the accuracy of our measurements, no dependence of specific volumes or refractive index increments on concentration was observed, and average values were used in the centrifuge computations. Since the precision of these measurements depends on the concentration of solute, the averages were weighted with factors proportional to concentration. Further, (averaged) apparent specific volumes were taken as the partial specific volumes. For BiOClO<sub>4</sub> in 1 M NaClO<sub>4</sub>, the present value of the volume agrees with that reported earlier.<sup>13</sup>

Literature values were used for partial specific volumes and refractive index increments of the supporting electrolytes. For NaClO<sub>4</sub>,  $k_3 = 0.0074$ <sup>14</sup>

(13) R. W. Holmberg, K. A. Kraus and J. S. Johnson, *ibid.*, **78**, 5506 (1956).

(14) H. Kohner, *Z. physik. Chem.*, **B1**, 427 (1928). These measure-



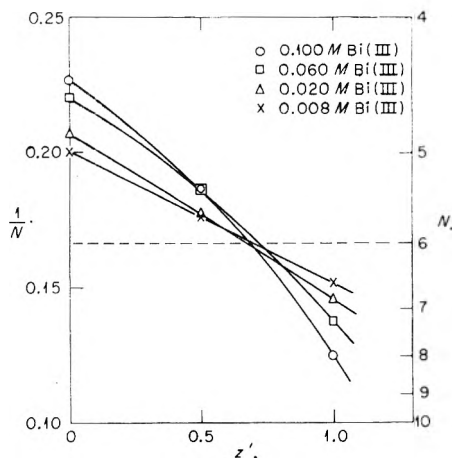


Fig. 2.—Degree of polymerization  $N$  of  $\text{BiOClO}_4$  in  $1 M$   $\text{NaClO}_4$ , as a function of charge  $z'$ .

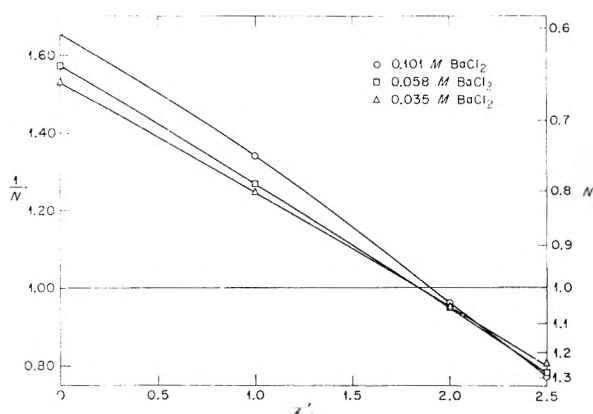


Fig. 3.—Degree of polymerization  $N$  of  $\text{BaCl}_2$  in  $1 M$   $\text{HCl}$  computed as a function of charge  $z'$ .

and  $\bar{v} = 0.373$  cc.<sup>12</sup> were used and for  $\text{HCl}$ ,  $k_3 = 0.0083$ <sup>15</sup> and  $\bar{v} = 0.533$  cc.<sup>16</sup>

TABLE II  
REPRODUCIBILITY OF MEASUREMENTS

(5-cell rotor, wedged cells,  $0.056 M \text{Na}_2\text{MoO}_4$ - $1 M \text{NaClO}_4$ )

| Cell | $h_1(\text{cm.})^a$ | $h_2(\text{cm.})^b$ | $N_{z'=2}$ |
|------|---------------------|---------------------|------------|
| 1    | 1.202               | 1.195               | 1.07       |
| 2    | 1.201               | 1.197               | 1.06       |
| 3    | 1.198               | 1.198               | 1.05       |
| 4    | 1.193               | 1.197               | 1.03       |
| 5    | 1.196               | 1.203               | 1.06       |

Theoretical degree of polymerization  $N_{z'=2} = 1.00$ .

<sup>a</sup> Thickness of "solution" compartment. <sup>b</sup> Thickness of "background" compartment.

2.  $\text{Na}_2\text{MoO}_4$  in  $1 M \text{NaClO}_4$ .—Reproducibility of the experiments and adequacy of the procedure used to diminish effect of cell distortion were tested by centrifugation of identical solutions of  $0.056 M \text{Na}_2\text{MoO}_4$ - $1 M \text{NaClO}_4$  in the five cells of the "Analytical G" rotor. The values of  $N$  computed for the known charge,  $z' = 2$ , are given in Table II. The values fall within  $\pm 0.02$  of  $N = 1.05$ . (If computed for  $z' = 0$ ,  $N$  is about 0.5.) A spread of only

ments were for Na-D light, but there is little change of  $\partial n/\partial c$  for this salt with wave length.

(15) O. R. Howell, *J. Chem. Soc.*, 2039 (1927). The value given is  $\partial n/\partial c$  for  $1 M \text{HCl}$ , interpolated for  $546 \text{ m}\mu$  for measurements at other wave lengths.

(16) H. E. Wirth, *J. Am. Chem. Soc.*, **62**, 1128 (1940).

4% in  $N$  for such a light solute indicates a substantial improvement in precision over schlieren optics, with which a coherent result would be difficult to obtain, with cells of the same thickness. About 2% of the variation of the mean from  $N = 1$  may be attributed to neglect of the contribution to  $n^*$  of pressure differences between the two compartments.<sup>11</sup> The rest lies easily within the range either of possible experimental errors or of activity coefficient effects (see below).

3.  $\text{BiOClO}_4$  in  $1 M \text{NaClO}_4$ .—A system more of the type we have ordinarily studied is hydrolyzed  $\text{Bi(III)}$  in  $\text{NaClO}_4$ . Earlier investigations<sup>13</sup> with the schlieren optical system indicated a degree of polymerization of 5-6 and some complexing of perchlorate ions by the polymer. Since then, X-ray scattering measurements on concentrated  $\text{BiOClO}_4$  solutions, carried out in this Laboratory,<sup>17</sup> have strongly suggested that the Bi atoms are arranged octahedrally, which would indicate a hexamer. Olin,<sup>18</sup> on the basis of e.m.f. measurements carried out in Sillén's laboratory, also favors this species.

We have centrifuged  $\text{BiOClO}_4$  solutions of (initial) concentrations 0.008 to  $0.100 M$  in  $1 M \text{NaClO}_4$  supporting electrolyte. To prevent precipitation the solutions contained also  $0.01$  to  $0.02 M \text{HClO}_4$  in excess of the composition  $\text{BiOClO}_4$ . Under these conditions the hydroxyl number is two, and—except for perchlorate complexing—the predominant species is  $(\text{BiO})_N^{+N}$ .<sup>13</sup>

The results of the centrifugations are summarized as plots of  $1/N$  vs.  $z'$  (Fig. 2). Previously, similar results have been presented as  $N$  vs.  $z'$  graphs<sup>3</sup>; the reciprocal  $1/N$  is used here, since the graphs are more linear. The curves for all concentrations approach one another most closely for  $N = 6$  (within a spread of about 2% in  $N$ ). The corresponding value of  $z'$  indicates that about two perchlorates are complexed per polymeric aggregate and that hence the average formula of the species is  $\text{Bi}_6\text{O}_6(\text{ClO}_4)_2^{+4}$ .

4.  $\text{BaCl}_2$  in  $\text{HCl}$ .—Three solutions of  $\text{BaCl}_2$  (initial concentrations 0.035 to  $0.100 M$ ) were centrifuged in  $1 M \text{HCl}$  supporting electrolyte. The results are presented in Fig. 3 as graphs of  $1/N$  computed as a function of assumed charge  $z'$ . The curves should, of course, cross at  $N = 1$  and  $z' = 2$ . The values of  $N$  computed for  $z' = 2$  are about 5% high. The discrepancy is not far outside of probable experimental uncertainties for such a low molecular weight solute. However, we shall examine how far it might result from activity coefficient effects since in this case data on the pertinent three-component systems are available.<sup>19</sup> The activity coefficients enter principally in two ways, as  $d \ln G_2/d(x^2)$  in the sedimentation equation of the component of interest and as a correction for the differences in the sedimentation of the supporting electrolyte in the solution and background compartments ( $d \ln \gamma_{\pm \text{HCl}}/dx^2$ ).

Estimates of activity coefficients were made with the equations

(17) H. Levy, M. D. Danford, P. Agron and M. A. Bredig, unpublished results.

(18) A. Olin, *Acta Chem. Scand.*, **11**, 1445 (1957).

(19) H. S. Harned and R. Gary, *J. Am. Chem. Soc.*, **76**, 5924 (1954).

$$2 \log \gamma_A = - \frac{1.018\mu^{1/2}}{1 + 1.5\mu^{1/2}} + b_{AAA}m_A + b_{AB}m_B + d_{AAA}m_A^2 + 2d_{AAB}m_Am_B + d_{ABB}m_B^2 \quad (22)$$

and

$$3 \log \gamma_B = - \frac{3.054\mu^{1/2}}{1 + 1.5\mu^{1/2}} + b_{AB}m_A + b_{BB}m_B + d_{AAB}m_A^2 + 2d_{ABB}m_Am_B + d_{BBB}m_B^2 \quad (23)$$

where  $b$  and  $d$  are constants or interaction coefficients<sup>20</sup>; A and B indicate HCl or BaCl<sub>2</sub>, respectively;  $\mu$  is the ionic strength ( $\Sigma m_i z_i^2/2$ ) and  $m$  the molality. The coefficients in these equations were evaluated from tables<sup>21</sup> of  $\gamma_{\pm\text{HCl}}$  and osmotic coefficients,  $\phi$ , of BaCl<sub>2</sub>, and the constant  $\alpha_{12}$  for HCl in BaCl<sub>2</sub>.<sup>19</sup> The values of  $\gamma_{\pm\text{HCl}}$  and  $\phi_{\text{BaCl}_2}$  in water were represented by equations having a Debye-Hückel term, in addition to terms linear and quadratic in molality<sup>22</sup>;  $\alpha_{12}$  was assumed to vary linearly with  $\mu$ .

Correction for  $d \ln G_2/d(x^2)$  was found to lower  $N$  (computed for  $z' = 2$ ) by ca. 3% for 0.035  $M$  BaCl<sub>2</sub>; by ca. 4% for 0.058  $M$  BaCl<sub>2</sub>; and by ca. 6% for 0.1  $M$  BaCl<sub>2</sub>. Corrections for the effect of differences in  $d \ln \gamma_{\pm\text{HCl}}/d(x^2)$  between solution and background compartments were smaller. The  $N$  for 0.1  $M$  BaCl<sub>2</sub> was raised by about 1%; corrections for the other two solutions could not be estimated accurately enough for application but appeared to be less.

In addition, corrections for the effect of differences in pressure on the two compartments<sup>11</sup> were estimated to decrease  $N$  by about 2% in all cases. The net effect of these corrections lowers the computed values of  $N$  from ca. 1.05 to 0.97 for 0.1  $M$  BaCl<sub>2</sub>, to 0.99 for .058  $M$  BaCl<sub>2</sub>, and to 1.00 for 0.035  $M$  BaCl<sub>2</sub>. It appears that in this case, differences between known and observed values of  $N$  are indeed of approximately the magnitude expected from activity coefficient variations.

**5. General Discussion.**—We may conclude from the coherence of the results in the three examples that considerably more accurate estimates of the degree of aggregation of charged solutes may be obtained with interference optics than with schlieren optics. Further, with proper corrections, use of wedged centerpieces allows simultaneous centrifugation of five solutions with no significant loss in accuracy. In equilibrium ultracentrifugations with deep cells,<sup>23</sup> this permits a substantial

(20) The values of the coefficients of equations 22 and 23 are:  $b_{AA} = 0.210$ ,  $d_{AAA} = 0.012$  (from  $\gamma_{\pm\text{HCl}}$  in water);  $b_{BB} = 0.2241$ ,  $d_{BBB} = 0.0468$  (from  $\phi_{\text{BaCl}_2}$  in water);  $b_{AB} = 0.2478$ ,  $d_{AAB} = 0.0327$ ;  $d_{ABB} = 0.0882$ .

(21) R. A. Robinson and R. H. Stokes, "Electrolyte Solutions," Butterworths Scientific Publications, London, 1955, p. 476, 471. Original source: HCl, H. S. Harned and R. W. Ehlers, *J. Am. Chem. Soc.*, **55**, 2179 (1933); BaCl<sub>2</sub>, R. A. Robinson, *Trans. Faraday Soc.*, **36**, 735 (1940).

(22) G. Scatchard and L. F. Epstein, *Chem. Revs.*, **30**, 211 (1942).

(23) Recently, techniques have been described for equilibrium ultracentrifugations with columns of solution shallow in the radial direction (K. E. Van Holde and R. L. Baldwin, *This Journal*, **62**, 734 (1958)). By this device, much less time is required to attain equilibrium.

reduction in the time required for a single set of results, particularly since with digital computers the time needed for computations is greatly decreased.

It has been stated earlier and reiterated in the examples that determination of the degree of aggregation implies simultaneous estimation of the charge of the ions. In many cases this implies that through equilibrium ultracentrifugation some information regarding complexing reactions of the solutes with ions of the supporting electrolyte may be obtained. Thus, we concluded that the Bi(III)-hexamer ( $\text{Bi}_6\text{O}_6^{+6}$ ) is to some extent complexed by perchlorate ions. Further, equilibrium centrifugations gave the expected result that Ba(II) is not complexed by chloride ions in the medium studied and that the molybdate ions are not complexed by sodium ions. In an earlier study<sup>24</sup> of considerably less precision, since it was carried out with schlieren optics, we pointed out that In(III) in bromide solutions appeared to be considerably less complexed than some have stated.

One method of estimating  $z'$  involves determination of an intersection of the curves of  $N$  vs. assumed charge  $z'$  (see Figs. 2 and 3). With light solutes in light supporting electrolytes these curves are too nearly parallel for this to be a sensitive procedure. In such cases it is sometimes better to determine  $z'$  at the point where such curves cross the proper value of  $N$ . For this to be effective the activity coefficient derivatives, particularly the derivative  $d \ln G_2/d(x^2)$ , should be small. Often it is more effective to centrifuge in a relatively high molecular weight supporting electrolyte since then the curves of  $N$  vs.  $z'$  will be steep and more sensitive to the concentration ratio  $c'_2/c_3$ .

If one deals with a monodisperse solute, the charge  $z$  obtained should equal the average charge of all species ( $z = \Sigma z_i F_i$  where  $z_i$  is the charge of the species  $i$  and  $F_i = m_i/\Sigma m_i$  is the fraction of the solute as species  $i$ ). In principle, knowledge of the average charge as a function of ligand concentration permits computation of complex constants; however, at present it appears that such an objective is not practical. Experimental difficulties, as well as expected variations in activity coefficient terms, make estimates of  $z'$  too uncertain for evaluation of complex constants. In the BaCl<sub>2</sub> and Na<sub>2</sub>MoO<sub>4</sub> experiments, without activity coefficient corrections,  $z'$  would be estimated with an accuracy of approximately 0.2 in charge units. These experiments were carried out at moderate ionic strength, in the region where most activity coefficient vs. concentration curves have a minimum. It is difficult to predict at present if results useful in the study of complex reactions may be obtained at substantially higher ionic strength, where activity coefficient derivatives should be larger and more difficult to estimate.

**Acknowledgment.**—We are indebted to Miss Neva E. Harrison for technical assistance.

(24) J. S. Johnson and K. A. Kraus, *J. Am. Chem. Soc.*, **79**, 2034 (1957).

แผนกห้องสมุด กรมวิทยาศาสตร์  
กระทรวงอุตสาหกรรม

# A FURTHER STUDY OF THE PHOTOCHEMICAL AUTOÖXIDATION OF ANTHRACENES<sup>1</sup>

BY ROBERT LIVINGSTON AND V. SUBBA RAO

*Contribution from the Division of Physical Chemistry, Institute of Technology,  
University of Minnesota, Minneapolis, Minn.*

*Received November 10, 1958*

The quantum yields of the photoautooxidation of anthracene and diphenylanthracene were measured in several solvents. The results of these measurements demonstrate that the fluorescent state as well as the triplet state of the hydrocarbon can react with O<sub>2</sub> to form an intermediate, leading to the formation of a peroxide. In strongly fluorescent solutions (*e.g.*, diphenylanthracene in benzene), the interaction of the fluorescent state with O<sub>2</sub> is the principal step. For weakly fluorescent solutions, the triplet state plays the dominant role. Diphenylanthracene sensitizes the oxidation of anthracene. This process was studied by illuminating a solution, containing both substances, with light which was absorbed by diphenylanthracene only. An analysis of these measurements indicates that the Kautsky mechanism, which involves molecular oxygen in a singlet state as a reaction intermediate, is not compatible with our results.

The photochemical autooxidation of anthracene and its derivatives has been studied quantitatively and extensively by Bowen and his co-workers.<sup>2,3</sup> They determined the quantum yields of fluorescence, dimerization and autooxidation of several anthracenes in a variety of solvents and over a wide range of hydrocarbon concentrations. However, their measurements were limited to oxygen concentrations corresponding to solutions saturated with pure O<sub>2</sub>, air or pure N<sub>2</sub>, each at 1 atm. The present experiments include the results of measurements of the oxidation of diphenylanthracene in benzene at oxygen concentrations ranging from  $1.00 \times 10^{-2}$  to  $2.5 \times 10^{-4}$  M and of anthracene in bromobenzene at concentrations from  $8 \times 10^{-3}$  to  $8 \times 10^{-5}$  M. In addition, the effect of the addition of small amounts of quinone upon the rate of autooxidation of anthracene was studied. The photochemical autooxidation of anthracene sensitized by diphenylanthracene also was investigated.

E. J. Bowen<sup>3a</sup> has demonstrated that, under certain conditions, the oxidation of anthracene is the consequence of a reaction between an oxygen molecule and a molecule of the hydrocarbon in its lowest triplet state; he has suggested that the photochemical autooxidations of all anthracenes proceed, always, by way of this step. Our results show that the interaction of an oxygen molecule with one of the hydrocarbon in either its triplet or fluorescent state can induce the formation of the peroxide. In strongly fluorescent solutions (*e.g.*, diphenylanthracene in benzene) the important intermediate is the fluorescent state, while in practically non-fluorescent solutions of anthracene in bromobenzene the dominant step is the interaction of an oxygen molecule with one of anthracene in its triplet state.

The publication of the results of measurements of the half-life of the triplet state of anthracene and of the rate constant for its bimolecular reaction with oxygen<sup>4,5</sup> offers the opportunity for an additional

test of the reliability of the proposed mechanism of these reactions.

## Experimental

**Materials.**—Benzene and carbon disulfide were high-grade commercial samples and were used without further purification. Bromobenzene was twice distilled under nitrogen. Quinone was sublimed shortly before it was used. The final purification of anthracene and diphenylanthracene was accomplished chromatographically or activated alumina.

**Flash-photolytic Measurements.**—A few preliminary measurements of the half-life of the triplet state of diphenylanthracene and of the quenching of the triplet of anthracene by quinone were made, using the apparatus and technique described by Livingston and Tanner.<sup>5</sup>

**Measurements of Photochemical Autooxidation.**—A modification of the method of Bowen and Tanner<sup>2</sup> was used to measure the rates of photochemical autooxidation. Two 3.00-ml. samples, containing identical concentrations of anthracene or diphenylanthracene, were exposed simultaneously to the complete radiation (filtered only by a 5-cm. layer of a 2% CuSO<sub>4</sub> solution) from a GE AH5 mercury arc. One sample, which was free from quenchers and was in equilibrium with air at 1 atm., was used as the reference solution. The ratio of the change in anthracene concentration in this solution to that in the other solution, which contained a quencher or was in equilibrium with a different, known concentration of oxygen, was a measure of the effect of the variable upon the rate (*i.e.*, the quantum yield) of photooxidation.

The reaction cells were Pyrex cylinders, about 4.0 cm. in diameter and 10.0 cm. long. At each end, the cylinders were fitted with projecting axially-centered tubes, 0.6 cm. in diameter and 5 cm. long. One such tube was sealed; the other ended, for the reference cell, in a male  $\frac{1}{8}$  joint, which could be closed by the external member of the joint without danger of contaminating the contents of the cylinder with (silicone) lubricating grease. Cells which were used with air or oxygen at pressures other than 1 atm. had, in place of the seal, a constriction followed by a  $\frac{1}{8}$  joint, by which they could be connected to an ordinary vacuum line. To fill the cylinder with gas at a known pressure, it was clamped in a vertical position and connected to the vacuum line. The 3.00-ml. sample was pipetted into the small, closed-end tube. The solution was then frozen with liquid nitrogen and the cylinder evacuated. The solution was degassed by successive freezing, pumping and thawing; after which, with the solution frozen and the cylinder at room temperature, gas was admitted to the desired pressure. The cylinder was then sealed at the constriction and separated from the vacuum line. Since the volume of the solution was less than 2.5% of that of the gas in the reaction vessel, the oxygen was seriously depleted only in those few experiments where its initial partial pressure was less than 1 mm. (see Table I).

The two cylinders were supported side by side on a set of three horizontal, rubber-covered rollers and were rotated

(1) This work was in part supported by grants from the National Science Foundation (NSF-G 1449) and from the Graduate School of the University of Minnesota, for which the authors are grateful.

(2) E. J. Bowen and D. W. Tanner, *Trans. Faraday Soc.*, **51**, 475 (1955).

(3) (a) E. J. Bowen, *Disc. Faraday Soc.*, **14**, 143 (1953); (b) E. J. Bowen, *Trans. Faraday Soc.*, **50**, 97 (1954).

(4) G. Porter and M. W. Windsor, *Disc. Faraday Soc.*, **17**, 178 (1954); *Proc. Roy. Soc. (London)*, **245A**, 238 (1958).

(5) R. Livingston and D. W. Tanner, *Trans. Faraday Soc.*, **54**, 765 (1958).

about their axes at about 150 r.p.m. The rotation of the cylinders spread the solutions on their inner walls as thin, continuously renewed films. Bowen and Tanner demonstrated,<sup>2</sup> and it was confirmed under our experimental conditions, that the oxygen in the solution was maintained in equilibrium with the gas phase by this procedure. A series of calibrating experiments showed that the rate of oxidation was sensibly independent of what cylinder was used and of which position on the rollers it occupied.

The solutions were analyzed spectrophotometrically, before and after irradiation. Since the solutions were much too concentrated to be analyzed spectrophotometrically in a cell of normal thickness, samples were diluted with the aid of a calibrated micro-dilution pipet. The resulting solution was further diluted to 10 ml. and its optical density determined with a Cary spectrophotometer using matched 2.00-cm. silica cells. For the solutions used in these experiments, the complete analysis (dilution + measurement of optical density) was reproducible to better than 0.5%. In a few cases, the decrease in anthracene concentration was checked using Bowen and Tanner's analysis for anthracene peroxide; however, in our hands this method proved to be less precise than the spectrophotometric measurements.

### Experimental Results

**The Photooxidation of Anthracene in Bromobenzene.**—The results of measurements of the rate of disappearance of anthracene, in bromobenzene containing various concentrations of oxygen, are summarized in Table I. Measurements were made of the change of concentration of anthracene in pairs of reaction vessels, as is described in the preceding section of this paper. In each pair of vessels, the concentration of anthracene was initially the same and the vessels were exposed simultaneously to light of the same intensity for the same length of time. The solubility of oxygen in bromobenzene is not known. The tabulated concentrations of oxygen were calculated upon the arbitrary assumption that bromobenzene saturated with air at 1 atm. contains  $2.0 \times 10^{-3} M$  oxygen, which is approximately the solubility of oxygen in benzene.

In contrast to the report of Bowen and Tanner,<sup>2</sup> we observed an appreciable photodimerization of anthracene in bromobenzene. The rate of disappearance of anthracene from an illuminated, oxygen-free solution was about one-fourth that observed in the reference solution, but the standard analytical method<sup>2</sup> fails to indicate the presence of any peroxide in such an anaerobic solution. Direct evidence for dimerization was obtained.

A  $3 \times 10^{-2} M$  deoxygenated solution was illuminated for an hour. The resulting crystalline precipitate was filtered, washed and dissolved in benzene. This solution was transparent for light of wave lengths greater than 3000 Å., but showed an absorption maximum at 2830 Å. Its absorption spectrum was similar to that reported for the anthracene dimer by Noland.<sup>5</sup>

It is apparent from the data listed in the first five columns of Table I that the rate of the photochemical reaction of anthracene in bromobenzene is practically independent of the oxygen concentration, in the range from  $8.2 \times 10^{-3}$  to  $8.3 \times 10^{-6} M$ . At lower concentrations, the rate of peroxide formation decreases rapidly.

The values in column six have been (approximately) corrected for the effect upon the rate of the differently changing concentrations of anthracene. The rates of both dimerization and peroxide

TABLE I

EFFECT OF OXYGEN CONCENTRATION UPON THE RATE OF FORMATION OF ANTHRACENE PEROXIDE IN BROMOBENZENE

| [A] × 10 <sup>2</sup> | P <sub>O<sub>2</sub></sub> , mm. | [O <sub>2</sub> ] × 10 <sup>4</sup> | Δ[A] × 10 <sup>4</sup> (air sat.) | Ratio of rates |      |                  |
|-----------------------|----------------------------------|-------------------------------------|-----------------------------------|----------------|------|------------------|
|                       |                                  |                                     |                                   | Obsd.          | Cor. | Calcd.           |
| 1.00                  | 625.5                            | 82.0                                | 1.40                              | 0.93           | 0.93 | 1.03             |
| 1.00                  | 97.6                             | 12.8                                | 2.64                              | 1.03           | 1.03 | 0.99             |
| 1.00                  | 6.0                              | .79                                 | 2.09                              | 0.97           | 0.97 | .98              |
| 1.00                  | 2.4                              | .31                                 | 1.96                              | .91            | .91  | .96              |
| 0.36                  | 1.7                              | .22                                 | 1.58                              | 1.00           | 1.00 | .96              |
| 0.36                  | 0.6                              | .083                                | 0.93                              | 0.91           | 0.91 | .96              |
| 1.05                  | 0.2 <sup>c</sup>                 | .026 <sup>c</sup>                   | 4.51                              | .33            | .27  | .69 <sup>c</sup> |
| 1.03                  | 0 <sup>a</sup>                   | 0                                   | 4.56                              | .26            | .22  | .22              |
| 1.03                  | 0 <sup>b</sup>                   | 0                                   | 4.47                              | .24            | .20  | .22              |
| 1.03                  | 0 <sup>b</sup>                   | 0                                   | 4.60                              | .26            | .22  | .22              |

<sup>a</sup> Oxygen removed by successive freezing, pumping and melting. Vessel finally filled with purified N<sub>2</sub>. <sup>b</sup> Oxygen removed as stated above. Vessel sealed off while evacuated. <sup>c</sup> The total number of moles oxygen present is several-fold less than the number of moles of anthracene consumed. An approximate calculation indicates that the average concentration of oxygen was  $1.6 \times 10^{-6} M$ . In calculating a value for the ratio of the rates, a constant value of [O<sub>2</sub>] =  $1.5 \times 10^{-6} M$  was used.

formation increase with increasing concentration of the hydrocarbon. For the peroxide formation in bromobenzene, the rate is, within the limits of precision, directly proportional to the anthracene concentration, at least to 0.02 *M*. In the last four experiments listed in Table I, the disappearance of anthracene was much faster in the reference vessel than in the other vessel. To correct approximately for this difference, the observed ratio of the rates has been multiplied by the ratio of the average concentrations in the reference and reaction vessels, respectively.

**The Photooxidation of Diphenylanthracene in Benzene.**—The photochemical properties of 9,10-diphenylanthracene in benzene differ markedly from those of anthracene in bromobenzene. Diphenylanthracene is not detectably photodimerized.<sup>2</sup> Its fluorescence has a high yield (about 0.8 in benzene) and is not measurably self-quenched. In view of these differences, it is not surprising that, unlike anthracene in bromobenzene, its rate of photooxidation is strongly dependent upon the concentration of oxygen. Evidence for this dependence is summarized in Table II.

Since for these experiments the decrease in the concentration of hydrocarbon was quite different in the reference and reaction vessels, the observed ratio of the rates were corrected, approximately, by multiplying the observed values by the ratio of the average concentrations of the hydrocarbon in the reference and reaction vessels. The corrected values are given in column six.

Carbon disulfide efficiently quenches the fluorescence of the anthracenes<sup>3</sup> but has little effect upon the half-life of the triplet state of anthracene.<sup>5</sup> In terms of a possible mechanism for these reactions (which is discussed in a later section of this paper) it is to be expected that the photooxidation of diphenylanthracene should be practically independent of oxygen concentration (except at very low concentrations) in solutions containing carbon

TABLE II

THE EFFECT OF OXYGEN CONCENTRATION UPON THE RATE OF FORMATION OF DIPHENYLANTHRACENE PEROXIDE IN BENZENE

| [A $\phi_2$ ]<br>$\times 10^2$ | P <sub>O<sub>2</sub></sub> ,<br>mm. | [O <sub>2</sub> ] $\times 10^3$ | $\frac{\Delta[A\phi_2]}{\times 10^3}$<br>(in air) | Ratio of the rates |      |        |
|--------------------------------|-------------------------------------|---------------------------------|---------------------------------------------------|--------------------|------|--------|
|                                |                                     |                                 |                                                   | Obsd.              | Cor. | Calcd. |
| 1.03                           | 1049.0                              | 10.05                           | 1.59                                              | 2.27               | 2.51 | 2.38   |
| 1.02                           | 652.1                               | 6.24                            | 1.64                                              | 2.11               | 2.28 | 2.01   |
| 1.04                           | 619.3                               | 5.93                            | 1.84                                              | 2.02               | 2.24 | 1.96   |
| 1.05                           | 314.8                               | 3.01                            | 2.32                                              | 1.28               | 1.36 | 1.46   |
| 1.05                           | 205.7                               | 1.97                            | 1.95                                              | 1.32               | 1.36 | 1.17   |
| 1.07                           | 140.0                               | 1.34                            | 2.39                                              | 1.03               | 1.06 | 0.96   |
| 0.98 <sup>a</sup>              | 58.6                                | 0.56                            | 1.35 <sup>a</sup>                                 | 0.52               | 0.50 | .63    |
| 1.03                           | 58.5                                | .56                             | 1.69                                              | .53                | .49  | .63    |
| 1.04                           | 26.1                                | .25                             | 1.86                                              | .33                | .32  | .47    |

<sup>a</sup> The intensity of the incident light was reduced about 2.5-fold by the use of a neutral filter (screen) and the time of illumination was increased to compensate partially for this change.

disulfide. The data of Table III confirm this prediction.

TABLE III

THE EFFECT OF OXYGEN CONCENTRATION UPON THE RATE OF FORMATION OF DIPHENYLANTHRACENE PEROXIDE IN BENZENE CONTAINING CARBON DISULFIDE

| Vol. %<br>of CS <sub>2</sub> | [A $\phi_2$ ]<br>$\times 10^2$ | P <sub>O<sub>2</sub></sub> ,<br>mm. | $\frac{\Delta[A\phi_2]}{\times 10^2}$<br>(in air) | Ratio of the<br>rates<br>(obsd.) |
|------------------------------|--------------------------------|-------------------------------------|---------------------------------------------------|----------------------------------|
| 1                            | 1.02                           | 602.0                               | 3.20                                              | 1.14                             |
| 1                            | 1.02                           | 10.7                                | 3.15                                              | 0.98                             |
| 1                            | 1.02                           | 4.9                                 | 3.02                                              | 1.00                             |
| 9                            | 1.06                           | 642.0                               | 3.65                                              | 1.01                             |
| 9                            | 1.02                           | 9.9                                 | 3.14                                              | 1.00                             |
| 9                            | 1.02                           | 4.2                                 | 3.38                                              | 0.88                             |

**Effect of Quinone upon the Photooxidation of Anthracene.**—Using the apparatus and technique of Livingston and Tanner<sup>6</sup> we have shown that *p*-benzoquinone quenches the triplet state of anthracene about as efficiently as oxygen. In bromobenzene, the bimolecular quenching constant is approximately  $1.6 \times 10^9 M^{-1} \text{sec}^{-1}$ . A similar value has been reported<sup>7</sup> for the quenching of the triplet state of chlorophyll *a* by quinone. Schenck observed<sup>8</sup> that quinone inhibits photoautooxidations sensitized by a number of dyes and pigments and interprets this effect as the consequence of the quenching of the triplet state by quinone. As is illustrated by the data of Table IV, quinone has a similar retarding effect upon the photochemical autooxidation of anthracene in bromobenzene. However, it should be remembered that the observed rate of disappearance of anthracene is the sum of the rates of photooxidation and dimerization.

**The Photooxidation of Anthracene Sensitized by Diphenylanthracene.**—It has been demonstrated by Bowen and Tanner<sup>2</sup> that in solutions containing both anthracene and diphenylanthracene either substance can sensitize the photooxidation of the other. Most of their measurements were made with systems in which each substance absorbed an appreciable fraction of the incident light. This fact

renders any quantitative analysis of their results difficult. To avoid this difficulty, we illuminated solutions (in benzene) of anthracene and diphenylanthracene with light from a mercury arc after it had passed through 2 cm. of a concentrated solution of anthracene in toluene. Since the anthracene in the filter was rapidly dimerized and oxidized, it was renewed before each measurement. Under these conditions, pure anthracene in benzene did not react detectably. In mixtures, both anthracene and diphenylanthracene were consumed.

The reaction mixtures were analyzed spectrophotometrically. The concentration of diphenylanthracene was calculated from the optical density measured at 3930 Å., at which wave length the absorption of anthracene is negligible. Optical densities were also measured at shorter wave lengths, corresponding to three maxima and two minima of the anthracene absorption spectrum. Knowing the diphenylanthracene concentration and the extinction coefficients of each hydrocarbon, a value for the anthracene concentration can be calculated from the measurements at each of the five wave lengths. The concentration was taken as the average of five such determinations. We found this to be a more reliable and reproducible way of measuring the anthracene concentration in the mixture than the use of the iodimetric method<sup>2</sup> of analysis for anthracene peroxide.

In each experiment two tubes were exposed side by side. They both contained diphenylanthracene at the same concentration but one had, in addition, a known concentration of anthracene. All solutions were saturated with air.

The results of such measurements are presented in Table V. The values of  $\Delta[A]/\Delta[A\phi_2]$  which are listed in column three are the ratios of the changes in the concentrations of anthracene and diphenylanthracene, respectively, based upon the analysis of the solution contained in the reaction cell. The ratios  $\Delta[A\phi_2]^0/\Delta[A\phi_2]$ , listed in column five, were obtained by dividing the decrease in the concentration of diphenylanthracene in the reference cell by the corresponding decrease which occurred in the reaction (*i.e.*, mixture-containing) vessel.

It is noteworthy that the values of  $\Delta[A\phi_2]^0/\Delta[A\phi_2]$  are all close to unity; in fact, their average is  $0.98 \pm 0.06$ . For the range of concentrations investigated, these data demonstrate that the addition of anthracene to a diphenylanthracene solution has little, if any, effect on the rate of disappearance of diphenylanthracene, although the anthracene itself is photooxidized.

## Discussion

The following generalized mechanism is consistent with the measurements of the maximum yield of fluorescence, the quenching of fluorescence,<sup>3</sup> the natural life and quenching of the triplet state,<sup>4,5</sup> the photodimerization,<sup>2,3</sup> the photoautooxidation<sup>2,3</sup> and the photosensitized oxidation of the anthracenes. The roles played by the fluorescent and lowest triplet states ( $\text{H}^*$  and  $\text{H}'$ , respectively) are well established and are represented by the first seven steps of the mechanism. The third intermediate,  $\text{X}$ , has not been detected directly and its

(7) E. Fujimori and R. Livingston, *Nature*, **180**, 1036 (1957).

(8) G. Schenck and K. Kinkel, *Naturwissenschaften*, **38**, 355 (1951); G. Schenck and K. H. Ritter, *ibid.*, **41**, 334 (1954).

TABLE IV  
EFFECT OF QUINONE UPON THE PHOTOOXIDATION OF ANTHRACENE IN BROMOBENZENE

| [Q]/[O <sub>2</sub> ] | [O <sub>2</sub> ] × 10 <sup>6</sup> | [A] × 10 <sup>2</sup> | Rate |        | Ratio = R <sub>Ref</sub> /R <sub>Q</sub> |      | Calcd. |
|-----------------------|-------------------------------------|-----------------------|------|--------|------------------------------------------|------|--------|
|                       |                                     |                       | Ref. | With Q | Obsd.                                    | Cor. |        |
| 1.0                   | 9.60                                | 3.20                  | 1.14 | 0.72   | 1.58                                     | 1.61 | 1.51   |
| 2.1                   | 9.60                                | 1.63                  | 0.67 | .32    | 1.97                                     | 2.05 | 1.90   |
| 2.1                   | 9.60                                | 3.18                  | 1.10 | .56    | 1.96                                     | 2.05 | 1.87   |
| 3.1                   | 9.60                                | 3.22                  | 1.20 | .57    | 2.14                                     | 2.21 | 2.15   |
| 5.2                   | 9.60                                | 3.15                  | 1.19 | .41    | 2.90                                     | 3.03 | 2.52   |
| 5.2                   | 9.60                                | 3.25                  | 1.21 | .48    | 2.52                                     | 2.61 | 2.52   |
| 6.9                   | 2.88                                | 3.27                  | 0.78 | .36    | 2.16                                     | 2.16 | 2.72   |
| 9.5                   | 2.11                                | 3.20                  | .68  | .22    | 3.09                                     | 3.09 | 2.95   |
| 10.4                  | 1.92                                | 2.84                  | .44  | .19    | 2.32                                     | 2.33 | 3.05   |
| 10.4                  | 1.92                                | 3.14                  | .50  | .20    | 2.50                                     | 2.56 | 3.05   |

TABLE V  
THE PHOTOOXIDATION OF ANTHRACENE SENSITIZED BY  
DIPHENYLANTHRACENE IN BENZENE

| [φ <sub>2</sub> A]<br>× 10 <sup>2</sup> | [A]/[Aφ <sub>2</sub> ] | Δ[A]/Δ[Aφ <sub>2</sub> ] |        | Δ[Aφ <sub>2</sub> ] <sup>0</sup> /Δ[Aφ <sub>7</sub> ] |        |
|-----------------------------------------|------------------------|--------------------------|--------|-------------------------------------------------------|--------|
|                                         |                        | Obsd.                    | Calcd. | Obsd.                                                 | Calcd. |
| 1.05                                    | 1.42                   | 0.17                     | 0.30   | 0.94                                                  | 1.00   |
| 1.11                                    | 1.44                   | .36                      | .32    | ...                                                   | ...    |
| 0.34                                    | 2.44                   | .46                      | .51    | ...                                                   | ...    |
| 1.06                                    | 3.02                   | .42                      | .62    | 1.03                                                  | 1.01   |
| 1.09                                    | 3.36                   | .54                      | .70    | 0.90                                                  | 1.01   |
| 1.12                                    | 3.75                   | .86                      | .76    | .91                                                   | 1.01   |
| 0.66                                    | 4.03                   | .75                      | .80    | 1.02                                                  | 0.98   |
| 1.22                                    | 4.96                   | 1.31                     | 1.00   | ...                                                   | ...    |
| 1.08                                    | 5.36                   | 1.53                     | 1.08   | ...                                                   | ...    |
| 1.09                                    | 5.78                   | 1.44                     | 1.16   | 1.11                                                  | 1.02   |
| 0.87                                    | 5.82                   | 1.05                     | 1.16   | 1.02                                                  | 1.00   |
| .14                                     | 6.33                   | 2.15                     | 1.25   | 0.95                                                  | 0.92   |
| .27                                     | 7.52                   | 1.51                     | 1.47   | ...                                                   | ...    |
| .68                                     | 7.78                   | 1.72                     | 1.55   | 1.02                                                  | 0.98   |
| .65                                     | 8.15                   | 1.62                     | 1.58   | ...                                                   | ...    |
| .34                                     | 15.08                  | 2.13                     | 2.64   | ...                                                   | ...    |
| .34                                     | 15.30                  | 2.51                     | 2.68   | 0.91                                                  | .88    |

nature is in dispute. It has been postulated that it is either a reactive, labile moleoxide, O<sub>2</sub>H',<sup>2,9</sup> or else an oxygen molecule in a metastable singlet state.<sup>2,10</sup> An alternative mechanism, involving a labile reactive dimer of the hydrocarbon,<sup>11</sup> can be rejected in terms of kinetic evidence<sup>2</sup> and of the measured properties<sup>4,5</sup> of the triplet state.

The kinetics of the autooxidations are consistent with either of the postulated descriptions of the intermediate X. However, we believe that the measurements of the photochemical oxidation of anthracene sensitized by diphenylanthracene are incompatible with the view that X is a metastable, singlet state of O<sub>2</sub>.

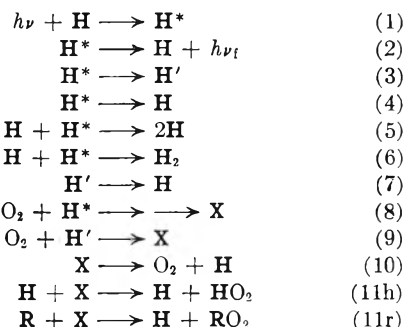
In the following scheme, the dimer and stable peroxide of the anthracene are indicated by H<sub>2</sub> and HO<sub>2</sub>, respectively. R represents the second hydrocarbon, whose oxidation is sensitized by H; in the present case, H is diphenylanthracene and R is anthracene.

The following set of consistent values for the several rate constants, for anthracene in benzene and in bromobenzene and diphenylanthracene in benzene, have been fitted to the available data.

(9) H. Koblitz and W. Schumacher, *Z. physik. Chem.*, **B35**, 11 (1935); **B37**, 462 (1937); A. Schönberg, *Ann. Chem.*, **518**, 300 (1935).

(10) H. Kautsky, *et al.*, *Ber.*, **66**, 1588 (1933); H. Kautsky, *Biochem. Z.*, **291**, 271 (1937).

(11) C. Dufraisse and M. Gérard, *Compt. rend.*, **201**, 428 (1935); C. Dufraisse, *Bull. soc. chim.*, **6**, 422 (1939).



Values of  $k_2$  were calculated by Bowen<sup>3b</sup> from the integrated extinction coefficients. Values of  $k_3 + k_4$  were derived by combining  $k_2$  with the maximum<sup>3b</sup> quantum yields of fluorescence. The ratio,  $k_3/(k_3 + k_4)$ , was estimated from the limiting, maximum yields of photooxidation.<sup>2</sup> The sum,  $k_5 + k_6$ , was obtained from the self-quenching constant for fluorescence<sup>2,3b</sup> and  $k_2$ . The maximum yield of dimerization<sup>2</sup> was used to calculate  $k_6/(k_5 + k_6)$ . The value of  $k_7$  was obtained directly by flash-photolytic measurements.<sup>4,5</sup>  $k_8$  was derived from the Stern-Volmer quenching constant for oxygen<sup>3b</sup>;  $k_9$ , from flash photolytic studies.<sup>4,5</sup> The ratio,  $k_{10}/k_{11}$ , was obtained from the variation of the yield of photooxidation with the concentration of the hydrocarbon.<sup>1</sup>

TABLE VI  
SUMMARY OF THE VALUES OF THE RATE CONSTANTS

| Hydrocarbon solvent                              | Anthracene Benzene   | Anthracene Bromobenzene | Diphenylanthracene Benzene |
|--------------------------------------------------|----------------------|-------------------------|----------------------------|
| $k_2$ , sec. <sup>-1</sup>                       | $7.4 \times 10^7$    | $7.4 \times 10^7$       | $1.5 \times 10^8$          |
| $k_3 + k_4$ , sec. <sup>-1</sup>                 | $2.4 \times 10^8$    | $4.0 \times 10^8$       | $3.2 \times 10^7$          |
| $k_3/(k_3 + k_4)$                                | 0.67                 | 0.90                    | 0.5                        |
| $k_5 + k_6$ , M <sup>-1</sup> sec. <sup>-1</sup> | $5 \times 10^9$      | $8 \times 10^9$         | $<1 \times 10^7$           |
| $k_6/(k_5 + k_6)$                                | 0.20                 | ~1                      | ...                        |
| $k_7$ , sec. <sup>-1</sup>                       | $2.0 \times 10^3$    | $2.0 \times 10^3$       | $\sim 2 \times 10^3$       |
| $k_8$ , M <sup>-1</sup> sec. <sup>-1</sup>       | $4.0 \times 10^{10}$ | $3 \times 10^{10}$      | $3.2 \times 10^{10}$       |
| $k_9$ , M <sup>-1</sup> sec. <sup>-1</sup>       | $4.0 \times 10^9$    | $2.0 \times 10^9$       | $\sim 4 \times 10^9$       |
| $k_{10}/k_{11}$                                  | 0.57                 | 0.12                    | 0.045                      |

Making the usual steady-state approximations, the following expressions may be derived for the quantum yields of dimerization, autooxidation (in the absence of a second hydrocarbon) and sensitized oxidation.

$$\varphi_{A_2} = \frac{k_6[\text{H}]}{k_2 + k_3 + k_1 + (k_5 + k_6)[\text{H}] + k_8[\text{O}_2]} = \frac{k_6}{\text{Den.}} [\text{H}] \quad (1)$$

$$\varphi_{\text{AO}_2} = \frac{[\text{H}][\text{O}_2]}{\text{Den. } (k_{11}/k_{11,\text{H}} + [\text{H}])} \left( k_8 + \frac{k_3}{k_7/k_9 + [\text{O}_2]} \right) \quad (2)$$

$$\varphi_{\text{RO}_2} = \frac{[\text{R}][\text{O}_2]}{\text{Den. } (k_{10}/k_{11,\text{R}} + [\text{H}]k_{11,\text{H}}/k_{11,\text{R}} + [\text{R}])} \left( k_8 + \frac{k_3}{k_7/k_9 + [\text{O}_2]} \right) \quad (3)$$

The quantum yield for the disappearance of anthracene, as in bromobenzene where both dimerization and oxidation are appreciable

$$\varphi_{-\text{H}} = \varphi_{\text{H}_2} + \varphi_{\text{HO}_2}$$

is given by the sum of equations 1 and 2. This equation was used to calculate the values of the ratios of the yield at various oxygen concentration to the yield in air-saturated solutions. These values are listed in the last column of Table I, under the title of

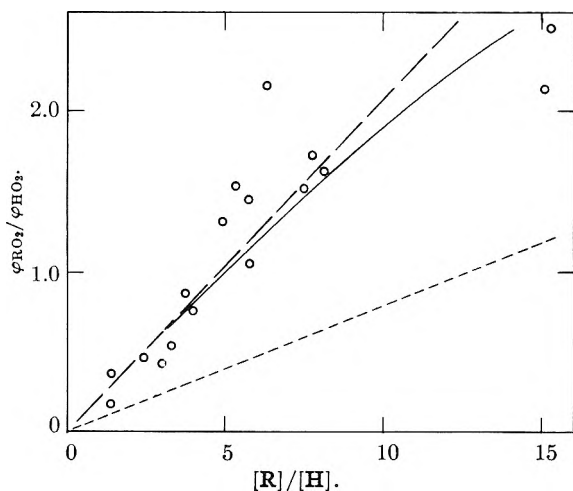
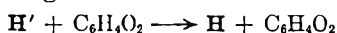


Fig. 1.—Ratio of the quantum yields of sensitized and direct autooxidation.

Ratio of rates, calcd. Since the intensities of the absorbed light were the same in the vessels being compared, the ratio of the rates equals the ratio of yields. In general, the agreement between the observed and calculated values appears to be within the limits of experimental error.

The calculated values for the ratios of the rates of autooxidation of diphenylanthracene in benzene were obtained by the use of equation 2 and the appropriate values of the several rate constants; since, in this case, the dimerization may be neglected. Here again, the agreement between observed and calculated values appears to be within the limits of experimental error. In these strongly fluorescent solutions, step 8 makes the chief contribution to the oxidation, whereas step 9 was the dominant one in the preceding example. The addition of carbon disulfide to benzene solutions of diphenylanthracene strongly quenches their fluorescence. As a result, the mean life of the fluorescent state, which equals  $(k_2 + k_3 + k_4)^{-1}$ , is greatly reduced; step 8 becomes negligible compared to step 9, and the yield is independent of the oxygen concentration, for all except very small values.

To allow for the retarding effect of quinone on the oxidation of anthracene, the following step must be added to the general mechanism.



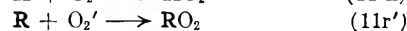
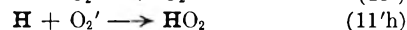
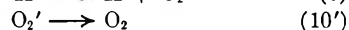
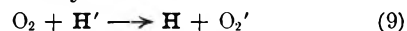
The rate constant for this reaction was evaluated, directly by the flash-photolytic method, as  $1.6 \times 10^{10} \text{ M}^{-1} \text{ sec}^{-1}$ . It is possible that quinone also quenches the fluorescence of anthracene but, if it does, its bimolecular rate constant cannot exceed  $4 \times 10^{10} \text{ M}^{-1} \text{ sec}^{-1}$ . The highest concentration of quinone used was  $2 \times 10^{-4} \text{ M}$ . Therefore, the product  $4 \times 10^{10} [\text{C}_6\text{H}_4\text{O}_2] \text{ sec}^{-1}$  can be safely neglected relative to the sum  $k_2 + k_3 + k_4 = 4.7 \times 10^9 \text{ sec}^{-1}$ . Introducing the term  $1.6 \times 10^{10} [\text{C}_6\text{H}_4\text{O}_2] \text{ sec}^{-1}$  into the sum of equation 1 and 2, the ratio of the rates of disappearance of anthracene, with and without added quinone, were calculated and are given in the last column of Table IV. In general, the agreement between the calculated and observed values is surprisingly good. For the last three values, corresponding to  $[\text{O}_2] = 2 \times 10^{-5} \text{ M}$ , the somewhat larger deviation can be attributed to the uncertainty in the measurement of the relatively low rates.

In studying the autooxidation of mixtures of two hydrocarbons, it is convenient to measure the ratio of the rate of oxidation of the substrate R to that of the sensitizer H. Values of this ratio,  $\Delta[\text{R}]/\Delta[\text{H}] = \varphi_{\text{RO}_2}/\varphi_{\text{HO}_2}$ , are listed in the third column of Table V. In these experiments, anthracene was the substrate and diphenylanthracene, the sensitizer. It follows from the general mechanism that, at the steady state

$$\frac{\varphi_{\text{RO}_2}}{\varphi_{\text{HO}_2}} = \frac{k_{11\text{R}}[\text{R}]}{k_{11\text{H}}[\text{H}]} \quad (4)$$

As a test of this equation, the experimental values of  $\varphi_{\text{RO}_2}/\varphi_{\text{HO}_2}$  have been plotted as a function of  $[\text{R}]/[\text{H}]$ . As is evident from Fig. 1, the data can be represented by a straight line passing through the origin with a slope of 0.21.

If it be assumed that the intermediate, X, is an  $\text{O}_2$  molecule in a metastable, singlet state,  $\text{O}_2'$ , the last four steps of the generalized mechanism should be replaced by the reactions

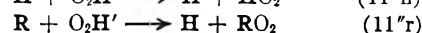
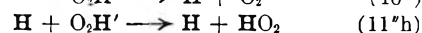
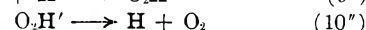
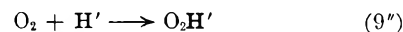


The specific reaction rates,  $k_i$ , of steps 10' and 11R' must be the same regardless of whether  $\text{O}_2'$  was formed by step 9' or the analogous reaction involving  $\text{R}'$ . Therefore, it should be possible to evaluate the ratio  $k'_{11\text{R}}/k'_{11\text{H}}$  from the results of separate measurements of  $k'_{10}/k'_{11\text{H}}$  in solutions containing only H or only R (but using the same solvent). Taking the values from Table VI

$$\frac{k'_{11\text{R}}}{k'_{11\text{H}}} = \left( \frac{k'_{10}}{k'_{11,\text{H}}} \right)_{\text{H}} \left( \frac{k'_{10}}{k'_{11,\text{R}}} \right)_{\text{R}} = \frac{0.045}{0.57} = 0.079$$

The dotted line on Fig. 1 which has this slope obviously does not fit the experimental data. It follows that the "Kautsky"<sup>10</sup> or singlet-oxygen mechanism is incompatible with our data.

The alternative hypothesis, that the intermediate is a labile moleoxide,  $\text{O}_2\text{H}'$ , leads to the reaction steps



There is no obvious reason why the specific reaction rates of the spontaneous decompositions of  $O_2H'$  and  $O_2R'$  should be identical. It is, therefore, impossible, in terms of this mechanism, to evaluate  $k''_{11R}/k''_{11H}$  from the results of measurements made with solutions containing the two hydrocarbons separately. Although it cannot properly be said that the present results confirm the moleoxide mechanism, they are consistent with it.

An additional test of the mechanism can be made by comparing calculated and observed (column 5 of Table V) values of  $\varphi_{HO_2}^0/\varphi_{HO_2}$  (*i.e.*, yields of diphenylperoxide in the absence and presence of anthracene). The mechanism leads to the equation

$$\frac{\varphi_{HO_2}^0}{\varphi_{HO_2}} = 1 + \frac{(k''_{11R}/k''_{10})[R]}{1 + (k''_{11H}/k''_{10})[H]} \quad (5)$$

For the range of concentrations used in the experiments, values calculated with the aid of this equation range from 1.04 to 1.19 and show a marked dependence upon  $[R]$ . In contrast, the observed values are not appreciably affected by a variation of either  $[R]$  or  $[R]/[H]$  and their average is  $0.98 \pm 0.06$ . This discrepancy, while not very great, is probably too large to be attributed to experimental error.

The mechanism may be brought into agreement

with the data by modifying step 11''R. It is possible that an encounter between a molecule of diphenylanthracene moleoxide and one of anthracene may sometimes result in the formation of the stable diphenylanthracene peroxide, rather than anthracene peroxide. Taking this possibility into account and letting  $\alpha$  indicate the fraction of such encounters which produce the peroxide of the sensitizer, we should replace equation 5 with the expression

$$\frac{\varphi_{HO_2}^0}{\varphi_{HO_2}} = \left(1 + \frac{(k''_{11R}/k''_{11H})[R]}{(k''_{10}/k''_{11H}) + [H]}\right) \left(1 + \alpha \frac{k''_{11R}[R]}{k''_{11H}[H]}\right)^{-1} \quad (6)$$

This equation is in agreement with the experimental data if it is assumed that  $\alpha = 0.07$ . Values calculated with the aid of this equation are listed in the last column of Table V.

To be consistent with this modification of the mechanism, we should substitute the following expression for equation 4

$$\frac{\varphi_{RO_2}}{\varphi_{HO_2}} = \frac{(1 - \alpha)(k''_{11R}/k''_{11H})[R]/[H]}{1 + \alpha(k''_{11R}/k''_{11H})[R]/[H]} \quad (7)$$

The full line curve of Fig. 1 and the calculated values given in column 4 of Table V were obtained by the use of this equation. Either equation 4 or 7 is in satisfactory agreement with the data.

## TRITIUM LABELING OF ORGANIC COMPOUNDS BY MEANS OF ELECTRIC DISCHARGE<sup>1</sup>

BY LEON M. DORFMAN AND KENNETH E. WILZBACH

*Argonne National Laboratory, Lemont, Illinois*

*Received November 14, 1958*

Tritium labeling of solid organic compounds by means of electric discharge in tritium in the 10 mm. pressure region is shown to be a feasible technique. Details of experiments with *p*-dichlorobenzene, naphthalene and palmitic acid are presented. Some advantages of the discharge method are pointed out, and results are compared with those obtained by the gas exposure technique for labeling.

### Introduction

In the labeling technique involving exposure of organic compounds to tritium gas,<sup>2</sup> the tritium has two obvious and quite separate functions. It is, of course, the radioactive label which is to be introduced into the compound by exchange. This requires millicurie amounts of tritium. It serves also as an internal source of radiation which effects the exchange. This requires curie amounts of tritium and, usually, exposure times of several days to obtain a sufficiently high level of labeling.

It seemed logical to try to replace this second function and eliminate the need for curie amounts of tritium by using an electric discharge in tritium at a pressure of 5 to 15 mm. The discharge would be expected to initiate exchange by means of ionization, excitation and dissociation of the tritium molecules in contact with a solid organic compound. This technique has been tested with three different compounds and seems to be effective enough to be of general interest. It has some advantage over the

exposure technique in that the amount of tritium required is reduced by an order of magnitude, hence the handling techniques and precautions which must be taken are considerably simplified. In addition the exposure time required is reduced from days to minutes. A possible disadvantage, which has not yet been fully assessed, is that the extent of formation of labeled decomposition products may be greater.

Recently Wolfgang, Pratt and Rowland investigated<sup>3</sup> the labeling of organic compounds by a discharge in tritium in the 50  $\mu$  pressure region on the assumption that accelerated tritium ions were the active transients required for labeling. The substantially more promising results of the present experiments must be due, in part, to the greater amount of tritium available at the higher pressure.

### Experimental

The discharge was carried out in a cylindrical Pyrex cell, volume approximately 35 cc., with electrodes 20 mm. apart. The cell is shown in Fig. 1. The compound to be labeled was placed in the lower, cup-shaped electrode. The source

(1) Based on work performed under the auspices of the U. S. Atomic Energy Commission.

(2) K. E. Wilzbach, *J. Am. Chem. Soc.*, **79**, 1013 (1957).

(3) R. Wolfgang, T. Pratt and F. S. Rowland, *J. Am. Chem. Soc.*, **78**, 5132 (1956).



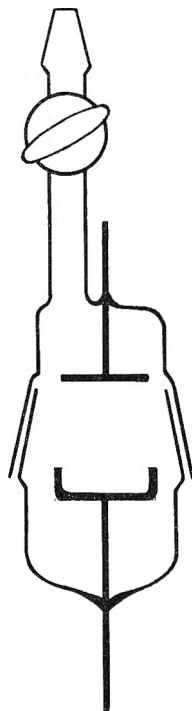


Fig. 1.—Discharge cell.

of the discharge was simply a Tesla coil leak tester which was connected to one electrode of the cell, the other electrode of the cell being grounded. The discharge was normally run for 3 to 10 min. at approximately 100 microamp. current and somewhat less than 1000 volts, although no attempt was made to control this in these rather simple experiments.

Three compounds were used: *p*-dichlorobenzene, naphthalene and palmitic acid<sup>4</sup>; the first two were selected for their relatively high vapor pressure so that products could be analyzed by vapor fractometry.

The procedure used with naphthalene and *p*-dichlorobenzene follows: a weighed quantity (approximately 0.5 g.) was placed in the lower electrode and the cell degassed. During the degassing, as well as the subsequent discharge period, the cup was cooled by conduction by keeping the tungsten lead from this electrode immersed in liquid nitrogen. This was considered advisable to keep the volatile compound in the condensed phase, and is not at all necessary with compounds of low vapor pressure. After the cell was degassed, tritium (which has been passed through a trap immersed in liquid nitrogen) was introduced and the discharge run. The tritium had an isotopic purity of approximately 90%, but contained almost an equal volume of helium-3. In running the discharge, arcing to the rim of the lower electrode occasionally occurred, but this could generally be avoided by keeping the setting on the Tesla coil turned down.

After the discharge the cell was degassed through a U-tube immersed in liquid nitrogen to condense volatile decomposition products. The bulk of the organic compound then was distilled over into the same U-tube and benzene was added. The solution now was injected into a vapor fractometer containing an ion-chamber connected in series with the thermistors, thus permitting analysis of both chemical and radioactive products. The technique has been described.<sup>5</sup>

The palmitic acid was subjected to a tritium discharge in the same way, except that the lower electrode was not cooled. After the discharge the cell was degassed and flushed twice with air, and the palmitic acid was removed and assayed for tritium in a liquid scintillation counter. The acid also was assayed after several purifications were carried

out by recrystallization, chromatography on Norite and, in the second of two runs, conversion to the *p*-bromophenacyl ester.

In addition to the labeling experiments, two discharge runs were carried out with naphthalene in deuterium to obtain an estimate of the amount of hydrogen lost from the gas phase as well as the amount formed from the organic compound. The same discharge procedure was followed. The gas was analyzed before and after the discharge.

### Results and Discussion

In each case, incorporation of tritium into the parent compound to the mc./g. level was obtained by the procedure described. Labeled decomposition products of the *p*-dichlorobenzene and naphthalene were identified. The results are shown in the following tabulations.

Table I shows the activity levels obtained for the three compounds subjected to the discharge technique. The table indicates as well the sample weight used, the pressure of gas (tritium-helium) in the discharge and the duration of the discharge. It is clear that useful activity levels are readily obtained, and it is important, further, to draw attention to the fact that these levels are produced in a significant quantity of material. The results thus suggest that the technique might be of general use for preparation of labeled compounds, but the broad applicability of the method must, of course, be investigated more fully.

TABLE I  
LABELING BY ELECTRIC DISCHARGE IN TRITIUM

| Compound                  | Quantity, g. | Gas pressure, mm. | Discharge time, min. | Activity, mc./g. Crude product | Pure product |
|---------------------------|--------------|-------------------|----------------------|--------------------------------|--------------|
| <i>p</i> -Dichlorobenzene | 0.490        | 7                 | 3                    | 65                             | 20           |
| Naphthalene               | .585         | 5                 | 5                    | ..                             | 4.1          |
|                           | .518         | 13                | 5                    | 52                             | 4.5          |
| Palmitic acid             | .254         | 9                 | 6                    | 42 <sup>a</sup>                | 3.4          |
|                           | .350         | 13                | 5                    | 32 <sup>a</sup>                | 3.7          |

<sup>a</sup> Possibly high due to incomplete removal of tritium in the initial degassing in which the sample was swept with air.

For comparison purposes, analogous data, obtained for these three compounds by the gas exposure method, are presented in Table II. In Table III are shown the results of the radio-assay, by vapor fractometry, of the labeled by-products formed in both the electric discharge and the gas exposure techniques. These data, which give relative values for the tritium content of the by-products in the naphthalene and *p*-dichlorobenzene labeling, indicate a somewhat greater extent and variety of formation of these labeled products in the discharge technique. With these relatively simple compounds increased formation of labelled by-products did not increase the difficulty of purification. In the labeling of more complex compounds it may prove to be a more critical factor. It should, however, be pointed out that in these experiments no attempt was made to select optimum conditions (with respect to pressure, discharge voltage, cell design, etc.) so as to minimize the decomposition.

The results of the two discharge experiments with deuterium are shown in Table IV. The depletion of deuterium from the gas phase amounts to 16%. The quantity of hydrogen formed from the

(4) The experiment with palmitic acid was performed at the Miami Valley Laboratories of the Procter and Gamble Co. on the occasion of a consulting visit of one of us (LMD) to that laboratory. We are indebted to Procter and Gamble for permission to report these results here.

(5) P. Riesz and K. E. Wilzbach, *THIS JOURNAL*, **62**, 6 (1958).

TABLE II  
LABELING BY EXPOSURE TO TRITIUM GAS

| Compound                  | Quantity, g. | Tritium, curies | Exposure time, days | Activity, mc./g. |      |
|---------------------------|--------------|-----------------|---------------------|------------------|------|
|                           |              |                 |                     | Crude            | Pure |
| <i>p</i> -Dichlorobenzene | 0.525        | 1.5             | 3                   | 44               | 32   |
| Naphthalene               | 1.0          | 3.4             | 0.8                 | 28               | 7.2  |
| Palmitic acid             | 20           | 10.4            | 11                  | 41               | 15   |

TABLE III  
LABELED BY-PRODUCTS FORMED IN THE ELECTRIC DISCHARGE AND GAS EXPOSURE TECHNIQUES

| By-product                    | Relative tritium content, parent compd. = 100 |              |
|-------------------------------|-----------------------------------------------|--------------|
|                               | Discharge                                     | Gas exposure |
| From dichlorobenzene:         |                                               |              |
| Chlorobenzene                 | 68                                            | 26           |
| Benzene                       | 87                                            | 1            |
| Hydrocarbons, <C <sub>6</sub> | 39                                            | ..           |
| Other <sup>a</sup>            | ..                                            | 8            |
| From naphthalene:             |                                               |              |
| Tetrahydronaphthalene         | 17                                            | 23           |
| <i>trans</i> -Decalin         | 9                                             | ..           |
| Alkylbenzenes <sup>b</sup>    | 57                                            | ..           |
| Benzene                       | 28                                            | 3            |
| Hydrocarbons, <C <sub>6</sub> | 71                                            | 3            |

<sup>a</sup> Unidentified product less volatile than dichlorobenzene.  
<sup>b</sup> Including toluene, ethylbenzene and butylbenzene.

naphthalene is considerably lower, amounting to 2 micromoles. On this basis the decomposition of the organic compound can be estimated to be certainly less than 0.1%, a conclusion which is consistent with the failure to observe chemical decomposition products by conventional analysis in the vapor fractometer. It seems reasonable to assume, since chemical decomposition was undetectable by vapor fractometry and since a reservoir of tritium

remains after the discharge times used, that even higher levels could be attained by prolonging the discharge.

TABLE IV  
DISCHARGE IN DEUTERIUM-NAPHTHALENE

| Wt. C <sub>10</sub> H <sub>8</sub> , g. | Discharge time, min. | Pressure, mm. |       | Final gas composition <sup>a</sup> |      |                |
|-----------------------------------------|----------------------|---------------|-------|------------------------------------|------|----------------|
|                                         |                      | Initial       | Final | D <sub>2</sub>                     | HD   | H <sub>2</sub> |
| 0.535                                   | 5                    | 12.2          | 11.0  | 81.7                               | 16.6 | 1.6            |
| 0.501                                   | 5                    | 14.1          | 13.2  | 83.1                               | 12.7 | 1.6            |

<sup>a</sup> Initial composition: D<sub>2</sub> = 99%, HD = 1%.

It appears, from a consideration of the fact that the discharge has effectively produced labeling at pressures as high as 13 mm., at which pressure the mean free path in the gas is less than  $5 \times 10^{-4}$  cm., that the process does not likely depend solely upon accelerated tritium ions. The complexities of a Tesla discharge, however, are so great that this conclusion cannot be reached with certainty from the present experiments. A definitive answer to this question will have to come from experiments with a steady-state glow discharge, along with a determination of the labeling yields in such a discharge.

Labeling would be expected to occur as a result of the primary processes of ionization, excitation and dissociation of the tritium molecules in the gas phase. Following this, hydrogen abstraction from the organic compound and subsequent combination with tritium atoms, or abstraction by the organic free radical of a tritium atom from the gaseous molecule would lead to a labeled compound. Ionization and excitation of the compound by the discharge also may be involved. The data obtained furnish no basis for any more extensive discussion of mechanism.

## DETERMINATION OF FREE RADICAL YIELDS IN THE RADIOLYSIS OF MIXTURES BY THE POLYMERIZATION METHOD

By ADOLPHE CHAPIRO

*Laboratoire de Chimie Physique de la Faculté des Sciences de Paris, Paris, France*

*Received November 14, 1958*

Radiation initiated solution polymerization of vinyl monomers can be used as a method for investigating the radiolysis of binary mixtures. In such systems the monomer is one of the components of the mixture and at the same time acts as a free radical scavenger. The rate of free radical production in the system can be derived from polymerization rates provided the rate constants for chain propagation and termination are known. A number of systems have been examined. In the most simple case the rate of free radical production is a linear function of chemical composition of the mixture. This situation applies to styrene solutions in aromatic hydrocarbons and to methyl methacrylate and vinyl acetate solutions in methyl and ethyl acetate. Other systems however exhibit "protection" and sensitization effects. These results are discussed on the basis of current theories for the kinetics of energy transfer processes. Free radical yields are derived from all available data and the results are compared with yields obtained by other methods.

### I. Introduction

The interest of radiation chemists has been focussed in recent years on the radiolysis of binary mixtures. In such systems energy transfer processes often are observed which lead to non-linear relationships between product yields and the chemical composition of the mixture. Observations along these lines were made by measuring gas evolution in the radiolysis of a number of mixtures,<sup>1-3</sup> dis-

appearance of diphenylpicrylhydrazyl (DPPH),<sup>4-6</sup> reaction with mercaptans<sup>7</sup> and polymer degrada-

- (1) J. P. Manion and M. Burton, *THIS JOURNAL*, **56**, 560 (1952).
- (2) S. Gordon and M. Burton, *Faraday Soc. Disc.*, **12**, 88 (1952).
- (3) W. N. Patrick and M. Burton, *THIS JOURNAL*, **58**, 421 (1954).
- (4) L. Bouby and A. Chapiro, *J. chim. phys.*, **52**, 645 (1955).
- (5) L. Bouby, Thesis, University of Paris, 1957.
- (6) M. Magat, L. Bouby, A. Chapiro and N. Gislou, *Z. Elektrochem.*, **62**, 307 (1958).
- (7) T. D. Nevitt, W. A. Wilson and H. S. Seelig, 131st A.C.S. Meeting, Miami, April 1957.

tion in solution.<sup>8</sup> Direct evidence for the existence of energy transfer processes in irradiated liquids was gained from studies on radiation induced luminescence in various solutions.<sup>9-10</sup>

Another method for investigating the radiolysis of binary mixtures is based on kinetic studies of radiation-initiated polymerizations of vinyl monomers in solution.<sup>11-16</sup> In such systems the vinyl monomer is one of the components of the mixture and at the same time acts as a free radical scavenger. The rate of polymerization is directly related to the rate of free radical production in the mixture and hence the primary free radical yields can be determined. Since the process involved here is a chain reaction, the ratio of rate constants for chain propagation and termination must be accurately known and furthermore only mixtures in which the reaction follows normal kinetic behavior can be investigated by this method. These requirements are best fulfilled for styrene, methyl methacrylate and vinyl acetate solutions in substances which also dissolve the corresponding polymer, since it is well established that anomalous kinetic features occur when polymerization takes place in heterogeneous media.<sup>11</sup> Several attempts already have been made to determine free radical yields by this method. In earlier work<sup>11-14</sup> it was assumed that a simple additivity rule was governing free radical yields in binary mixtures. This assumption was however found to hold only in a few special cases and more often energy transfer processes were operative.<sup>15-16</sup> The present article is an attempt to correlate all available data in this field and to examine the validity of this method and also its limitations. Experimental material is collected from both earlier publications and unpublished work from this Laboratory.

## II. Basic Kinetic Equations

When a vinyl monomer is radiation polymerized in solution at ordinary temperatures, the reaction is initiated usually by free radicals  $R\cdot$  originating from the radiolysis of both the monomer  $M$  and the solvent  $S$ . The propagation step proceeds in the conventional manner and, provided the radiation dose-rate is not too high and the monomer concentration is large enough to trap all primary radicals, termination occurs exclusively by the bimolecular interaction of two growing chains. This leads to the conventional kinetic scheme of free radical polymerizations

(8) A. Henglein, C. Schneider and W. Schnabel, *Z. physik. Chem.* **12**, 339 (1957).

(9) (a) P. J. Berry and M. Burton, *J. Chem. Phys.*, **23**, 1969 (1955); (b) P. J. Berry, S. Lipsky and M. Burton, *Trans. Faraday Soc.*, **52**, 311 (1956).

(10) F. H. Brown, M. Furst and H. P. Kallmann, *J. chim. phys.*, **55**, 689 (1958).

(11) A. Chapiro, *ibid.*, **47**, 747, 764 (1950).

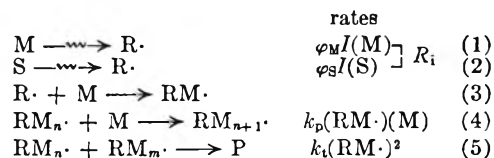
(12) Y. Landler, Thesis, University of Paris, 1952.

(13) C. Cousin, Thesis, University of Paris, 1953.

(14) W. H. Seitzer and A. V. Tobolsky, *J. Am. Chem. Soc.*, **77**, 2687 (1955).

(15) A. Chapiro, M. Magat, A. Prevot-Bernas and J. Sebban, *J. chim. phys.*, **52**, 689 (1955).

(16) (a) T. S. Nikitina and Kh. S. Badgasarian, "Sbornik Rabot po Radiazionnoi Khimii," Academy of Sciences USSR, Moscow, 1955, p. 183; (b) S. S. Medvedev, *J. chim. phys.*, **52**, 677 (1955).



At the stationary state

$$R_i = k_t(RM\cdot)^2$$

and the over-all rate is given by the rate of chain propagation

$$R = \frac{-d(M)}{dt} = k_p(RM\cdot)(M) = \frac{k_p}{k_t^{1/2}} (R_i)^{1/2}(M) \quad (6)$$

If the concentration of monomer is lower than a critical value, some of the primary radicals  $R\cdot$  escape scavenging by the monomer and either recombine or react with growing chains. In such event the reaction rate is lower than expected on the basis of equation 6.<sup>17</sup>

The rate of free radical production is equal to the rate of chain initiation  $R_i$  and can be derived immediately from equation 6

$$R_i = \frac{k_t}{k_p^2} \times \frac{R^2}{(M)^2} \quad (7)$$

It is seen that  $R_i$  is proportional to the square of the measured over-all polymerization rate.

In order to compare the results of different investigators obtained with a given system under different experimental conditions (temperature and dose rate), it is convenient to consider relative reaction rates with respect to rate of polymerization of the pure monomer  $R_0$ . It immediately follows from the equations above that

$$R/R_0 = (R_i/R_{i0})^{1/2}(M)/(M_0) \quad (8)$$

and

$$R_i/R_{i0} = (R/R_0)^2(M_0)^2/(M)^2 \quad (9)$$

Here  $R_0$ ,  $R_{i0}$  and  $(M_0)$  pertain to polymerization in bulk and  $R$ ,  $R_i$  and  $(M)$  to polymerization in solution.

If free radicals are produced independently from the monomer and from the solvent (*i.e.*, if energy transfer is not operative), the simple additivity rule applies to the system and the over-all rate of initiation is

$$R_i = [\varphi_M(M) + \varphi_S(S)]I \quad (10)$$

This equation can be modified to

$$R_i = \varphi_M(M)I \left[ 1 + \frac{\varphi_S(S)}{\varphi_M(M)} \right] \quad (11)$$

$\varphi_M$  can be derived from the rate of polymerization of the pure monomer; hence  $\varphi_S$  can be calculated according to equation 11.

In the more general case equation 10 is not applicable and if  $R_i$  is plotted *versus*  $(M)$  a non-linear relationship usually is observed.

It should be noted that when the chemical composition of the mixture is modified while the samples are irradiated in the same radiation field, the absorbed dose can be noticeably different in each set of experiments. It follows that only the exposure dose remains constant in such experiments and

(17) A. Chapiro, M. Magat, J. Sebban and P. Wahl, "Internat. Symp. Macromol. chem. Milan-Turin," 1954, Suppl. La Ricerca Scientifica, 1955, p. 73.

hence the symbol  $I$  is used to designate exposure dose-rate, expressed in roentgens per second. The reduced rates of free radical production  $\varphi_M(M)$  and  $\varphi_S(S)$  are expressed in moles of free radicals formed per roentgen per second.  $G_R$  values can be derived from the corresponding values of  $\varphi$  according to the equation

$$G_R^M = \frac{\varphi_M(M) \times 6.02 \times 10^{23} \times 100}{1000 d_M e_M} \quad (12)$$

Here  $d_M$  is the specific gravity of  $M$  and  $e_M$  is the amount of energy (in electron volts) absorbed per roentgen in one gram of  $M$ . A similar equation applies to values of  $G_R^S$ . In the following, all the  $G_R$  values are calculated on the basis of  $G(\text{Fe}^{3+}) = 15.5$  for the yield of oxidation of ferrous sulfate in 0.8  $N$  sulfuric acid solutions.

### III. Experimental Results

Various types of radiations have been used in the past for initiating vinyl polymerizations in solution. These include  $\gamma$ -rays<sup>11,16,18-21</sup>  $\beta$ -particles<sup>14</sup> and mixed radiation from a nuclear reactor.<sup>12,13</sup> Most of the work was carried out with either styrene or methyl methacrylate although a few data are available as well for other monomers. A number of binary mixtures show linear relationships between rates of initiation and chemical composition. These often correspond to compounds having similar chemical structure. Mixtures of other types usually exhibit energy transfer processes.

**1. Mixtures Showing a Simple Dilution Effect.**—This group of mixtures includes styrene solutions in various aromatic hydrocarbons and methyl methacrylate or vinyl acetate in methyl and ethyl acetate solutions.

**A. Styrene Solutions in Aromatic Hydrocarbons.**—The radiation polymerization of styrene in benzene, toluene, ethylbenzene and xylene was studied by the author with a 0.4 curie radium source at a single dose rate.<sup>11</sup> Sebban<sup>18</sup> initiated the polymerization of styrene in toluene solutions with cobalt-60  $\gamma$ -rays over a very broad range of dose rates. The  $\beta$ -ray initiated reaction in both benzene and toluene was reported by Seitzer and Tobolsky.<sup>14</sup> Finally Cousin<sup>13</sup> investigated the polymerization of styrene solutions in benzene in the nuclear reactor Zoé at Chatillon, France.

Linear plots are obtained from most experimental data when plotting the rate of initiation *versus* composition of the mixture. For very dilute solutions, rates are lower than expected, in accordance with the discussion above.<sup>17</sup> In the case of toluene, the agreement reached between all results is excellent and the ratio  $\varphi_S/\varphi_M$  is found to be 1.5. Assuming a  $G_R$  value of 0.69 for pure styrene, which best fits with all experimental data,<sup>22</sup> the  $G_R$  value derived for toluene is 1.15. This value is in very close agreement with the  $G_R$  value determined for this compound by the DPPH method *in vacuo*, *i.e.*,

(18) J. Sebban, unpublished results; see also references 15 and 17.

(19) K. Hayashi, unpublished results, 1957.

(20) I. Mita, unpublished results, 1957.

(21) P. Cordier, unpublished results, 1957.

(22) A. Chapiro, "Radiation Chemistry of Polymeric Systems," Interscience Publishers, New York, N. Y., to be published. See also A. Chapiro and M. Magat in "Actions chimiques et biologiques des radiations ionisantes," 3ème série, Masson et Cie., Paris, 1958.

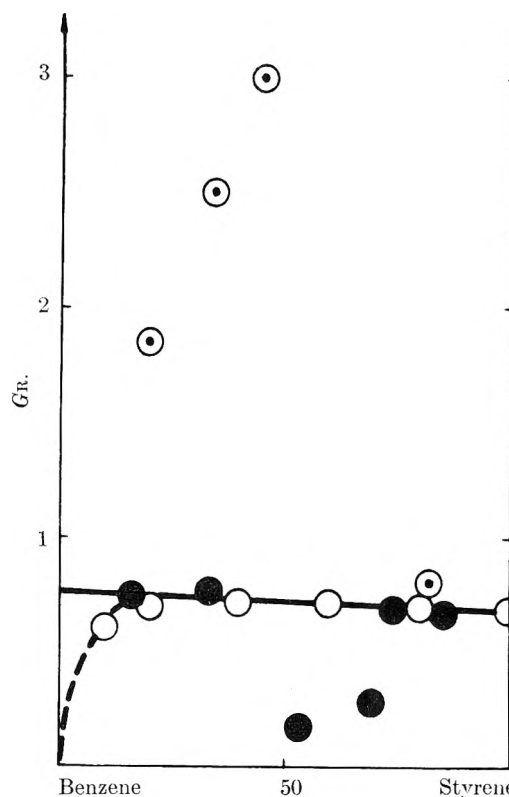


Fig. 1.—Free radical yields in mixtures of styrene with benzene derived from data of the following sources: O, A. Chapiro<sup>11</sup>; ●, C. Cousin<sup>13</sup>; ○, W. H. Seitzer and A. V. Tobolsky.<sup>14</sup>

$G(-\text{DPPH}) = 1.1^{23}$ ; it is noticeably lower than the  $G_R$  value found with iodine,  $G(-\text{I}) = 2.36^{24}$  (see Table I).

TABLE I

RELATIVE RATES OF FREE RADICAL PRODUCTION AND  $G_R$  VALUES OF AROMATIC HYDROCARBONS DERIVED FROM THE SOLUTION POLYMERIZATION OF STYRENE AND FROM SCAVENGER DATA

| Compound     | Polymerization        |       | DPPH |       | Iodine |                   |
|--------------|-----------------------|-------|------|-------|--------|-------------------|
|              | $\varphi_S/\varphi_M$ | $G_R$ | Ref. | $G_R$ | Ref.   | $G_R$             |
| Styrene      | ..                    | 0.69  | 22   | 0.6   | 25     |                   |
| Benzene      | 0.95                  | 0.74  | 11   | 0.6   | 26     | 0.66              |
|              | 1.0                   | 0.78  | 13   | 0.74  | 4      | 0.78 <sup>a</sup> |
|              | 3.1                   | 2.3   | 14   | 0.75  | 25, 27 |                   |
| Toluene      | 1.45                  | 1.1   | 11   | 1.1   | 23     | 2.41              |
|              | 1.55                  | 1.2   | 14   |       |        |                   |
| Xylene       | 4.5                   | 2.8   | 11   |       |        | 2.5               |
| Ethylbenzene | 6.5                   | 4.0   | 11   |       |        | 2.8               |

<sup>a</sup>  $G(-\text{Fe}^{+3})$  determined by the ferric ion method.

In the case of benzene solutions, both the results of Cousin and the earlier results of the author lead to values of  $\varphi_S/\varphi_M$  very close to unity, whereas the data derived from  $\beta$ -ray experiments are much more scattered and correspond to a higher value. The various results are shown in Fig. 1. The  $G_R$  value for benzene derived from the straight line determined by most results is  $G_R^{\text{benzene}} = 0.76$ . This value agrees well with  $G_R$  values for benzene ob-

(23) N. Gislou, unpublished results, 1957-1958.

(24) E. N. Weber, P. F. Forsyth and R. H. Schuler, *Radiation Research*, **3**, 63 (1955).

tained by scavenger studies. The available data on  $G_R$  values of aromatic hydrocarbons are summarized in Table I.

**B. Methyl Methacrylate Solutions.**—The  $\gamma$ -ray initiated polymerization of methyl methacrylate in ethyl acetate solutions was reported by Nikitina and Bagdasarian.<sup>16</sup> These authors found a linear relationship when plotting over-all rates of polymerization *versus* monomer concentration. Such a relationship demonstrates that the simple additivity rule applies to this system and that the over-all rate of free radical production remains constant over the entire range of concentrations. It follows that

$$\varphi_M = \varphi_S$$

and hence that the  $G_R$  value of ethyl acetate is close to that of methyl methacrylate. A similar result was found by Sebban<sup>18</sup> for methyl methacrylate solutions in methyl acetate. The rate of polymeri-

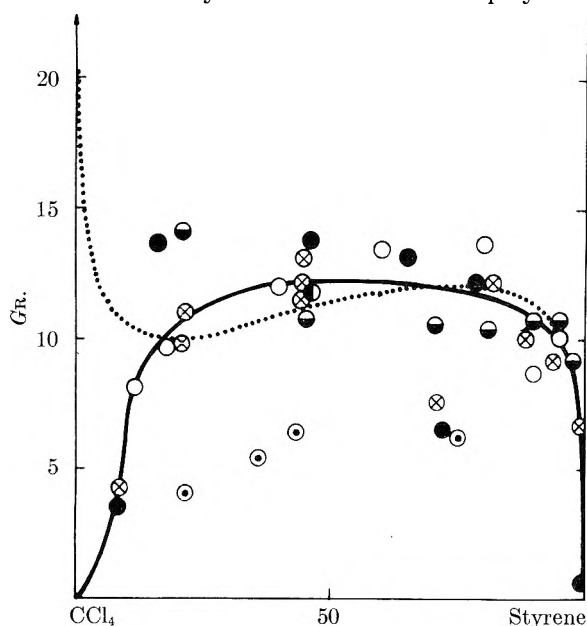


Fig. 2.—Free radical yields in mixtures of styrene with carbon tetrachloride derived from data of the following sources:  $\circ$ , A. Chapiro<sup>11</sup>;  $\otimes$ , Y. Landler<sup>12</sup>;  $\bullet$ , C. Cousin<sup>13</sup>;  $\odot$ , W. H. Seitzer and A. V. Tobolsky<sup>14</sup>;  $\bullet$ , T. S. Nikitina and Kh. S. Bagdasarian<sup>16</sup>;  $\bullet$ , P. Cordier.<sup>21</sup> The dotted line is based on  $G_R$ -values determined by the DPPH method in mixtures of benzene with carbon tetrachloride.<sup>6</sup>

zation of methyl methacrylate in acetone was reported by Seitzer and Tobolsky.<sup>14</sup> Although the results obtained by these authors are very scattered, a straight line can be drawn through most experimental points when plotting rates of initiation *versus* monomer concentration. The value of  $\varphi_S/\varphi_M$  derived from these data is 0.72 which leads to a  $G_R$  value of acetone in reasonable agreement with results obtained by other methods (see Table II).

In order to calculate  $G_R$  values from the results above, it is necessary to know the absolute yield of free radical production in the monomer. The  $G_R$  value of methyl methacrylate was determined directly by Krongauz and Bagdasarian<sup>25</sup> using the

(25) V. A. Krongauz and Kh. S. Bagdasarian, quoted by S. S. Medvedev, Proceedings of the first (UNESCO) International Conference "Radioisotopes in Scientific Research" Pergamon Press, London, 1958, Vol. I, p. 757.

DPPH method. These authors found  $G(-\text{DPPH}) = 5.5$  in the pure monomer. This value is roughly two times lower than the  $G_R$  value derived from polymerization rate data, *i.e.*,  $G_R = 11-12$ .<sup>22</sup> The reason for this discrepancy is not known.

It should be noted that the DPPH method *in vacuo* usually leads to lower  $G_R$  values than other methods in the case of oxygenated compounds.<sup>29,30</sup> On the other hand  $G_R$  values obtained with DPPH in aerated solutions correspond to the higher values.<sup>4</sup>

**C. Vinyl Acetate Solutions.**—Various mixtures of vinyl acetate and ethyl acetate were irradiated by Nikitina and Bagdasarian<sup>16</sup> in the presence of DPPH.  $G_R$  values were not derived from these experiments. It was found however that the rates of disappearance of DPPH were equal in pure vinyl acetate, in pure ethyl acetate and in an equimolecular mixture of these two compounds. It can be concluded from this result that  $\varphi_S/\varphi_M = 1$  in this system. The absolute yield of DPPH consumption in ethyl acetate was reported by Krongauz and Bagdasarian to be 7.<sup>27</sup> Here again this value is one-half the  $G_R$  value of vinyl acetate derived from kinetic data.<sup>22</sup>

$G_R$  values for these various compounds derived either from polymerization studies or by other methods are listed in Table II.

TABLE II

RELATIVE RATES OF FREE RADICAL PRODUCTION AND  $G_R$  VALUES OF OXYGENATED COMPOUNDS DERIVED FROM SOLUTION POLYMERIZATION IN METHYL METHACRYLATE AND VINYL ACETATE AND FROM OTHER METHODS

| Compound            | —Polymerization—      |       | DPPH and other methods |      |
|---------------------|-----------------------|-------|------------------------|------|
|                     | $\varphi_S/\varphi_M$ | $G_R$ | $G_R$                  | Ref. |
| Methyl methacrylate | ..                    | 11.5  | 5.5                    | 25   |
| Methyl acetate      | 0.95                  | 10.9  | 6.8                    | 4    |
|                     |                       |       | 5.5                    | 29   |
|                     |                       |       | 10.5 <sup>a</sup>      | 30   |
| Ethyl acetate       | 1                     | 11.5  | 7                      | 27   |
| Acetone             | 0.72                  | 9.4   | 5.6                    | 29   |
|                     |                       |       | 11.8                   | 28   |
| Vinyl acetate       | ..                    | 14    |                        | 22   |
| Ethyl acetate       | 1 <sup>b</sup>        | 14    | 7                      | 27   |

<sup>a</sup> Derived from an analysis of products of radiolysis.

<sup>b</sup> Determined by the DPPH method.

## 2. Mixtures Exhibiting Energy Transfer.—

In the earlier work on radiation-initiated polymerization in solution it was noticed for a number of systems that the ratio  $\varphi_S/\varphi_M$  did not remain constant but steadily changed with monomer concentration.<sup>11</sup> When the rate of initiation calculated from these data was plotted *versus* monomer concentration, non-linear curves were obtained.<sup>15</sup> A quantitative treatment of these effects was proposed by Nikitina and Bagdasarian<sup>16</sup> on the basis of

(26) W. Wild, *Faraday Soc. Disc.*, **12**, 127 (1952).

(27) V. A. Krongauz and Kh. S. Bagdasarian, "Deistvie ioniziruyushchikh izluchenii na neorganicheskie i organicheskie sistemy," Academy of Sciences, USSR, 1958, p. 205.

(28) E. A. Cherniak, E. Collinson, F. S. Dainton and G. M. Meaburn, *Proc. Chem. Soc.*, 54 (1958). See also R. A. Back, *et al.*, Second United Nations International Conference on the Peaceful Uses of Atomic Energy, Geneva 1958, 15/P/1516.

(29) W. Wild, *J. chim. phys.*, **52**, 653 (1955).

(30) P. Ausloos and C. Trumbore, to be published.

an energy transfer process. A similar scheme was developed further by Bouby.<sup>5,6</sup> In the following, several monomer-solvent mixtures are considered in which these effects are particularly pronounced.

#### A. Styrene Solutions in Carbon Tetrachloride.

—Radiation polymerization of styrene solutions in carbon tetrachloride was studied by a number of investigators using  $\gamma$ -rays,<sup>11,16,21</sup>  $\beta$ -particles<sup>14</sup> and mixed radiation from a nuclear reactor.<sup>12,13</sup> In order to compare these various results, the rate of radiation polymerization of pure styrene was used as a chemical dosimeter. Relative rates of polymerization in solution with respect to the reaction in bulk were calculated from experimental data and from these the relative rates of initiation were derived (see equation 8).  $G_R$  values for the mixtures are plotted in Fig. 2. The experimental points show considerable scatter partly because  $G_R$  values are proportional to the square of measured polymerization rates. Average deviations from the solid line are of the order of 20%. The general agreement between results obtained with  $\gamma$ -rays and reactor radiation is satisfactory, whereas  $\beta$ -ray experiments definitely show a different trend. The reason for this discrepancy is not clear. It can be seen that the addition of small amounts of carbon tetrachloride to styrene leads to a very important sensitization of the reaction. A similar effect was observed in mixtures of benzene with carbon tetrachloride. The dotted line in Fig. 2 shows  $G_R$  values obtained by the DPPH method for carbon tetrachloride benzene mixtures *in vacuo*.<sup>6</sup> When comparing the two curves it appears that the results are almost identical for both systems over most of the range of concentrations studied. However, in solutions containing more than 80% carbon tetrachloride, the two curves are distinctly separated. In this range of concentrations, benzene strongly "protects" carbon tetrachloride, as shown by the experiments with DPPH, whereas in styrene solutions this effect, if it does take place, is hidden by a sudden drop in rate of initiation owing to incomplete scavenging of primary radicals by the monomer.

It is of interest that Bagdasarian<sup>31</sup> obtained an identical relationship between over-all rate of polymerization and monomer concentration when using either  $\gamma$ -rays or ultraviolet light for initiating the reaction. This observation demonstrates that the processes occurring in this reaction involve only transfer of excitation energy and that transfer of charge is unimportant. On the other hand, the good agreement reached between the results of the various investigators who worked at different reaction temperatures (between 15 and 40°) and with both  $\gamma$ -rays and mixed radiation from the nuclear reactor, demonstrates that these excitation transfer processes only depend to a small extent on temperature and on type of radiation.

**B. Styrene Solutions in Chloroform.**—The results obtained with styrene solutions in chloroform are very similar to those found in carbon tetrachloride. The former mixture was studied using  $\gamma$ -rays,<sup>11</sup>  $\beta$ -particles<sup>14</sup> and reactor radiation.<sup>13</sup> The results are shown in Fig. 3. Here again the poly-

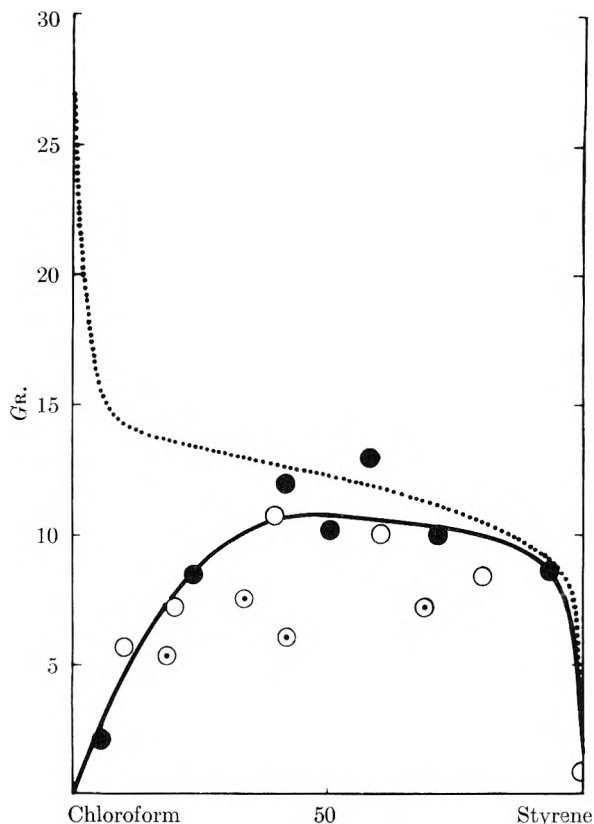


Fig. 3.—Free radical yields in mixtures of styrene with chloroform derived from data of the following sources:  $\circ$ , A. Chapiro<sup>11</sup>;  $\bullet$ , C. Cousin<sup>13</sup>;  $\odot$ , W. H. Seitzer and A. V. Tobolsky.<sup>14</sup> The dotted line is based on  $G_R$ -values determined by the DPPH method in mixtures of benzene with chloroform.<sup>4,6</sup>

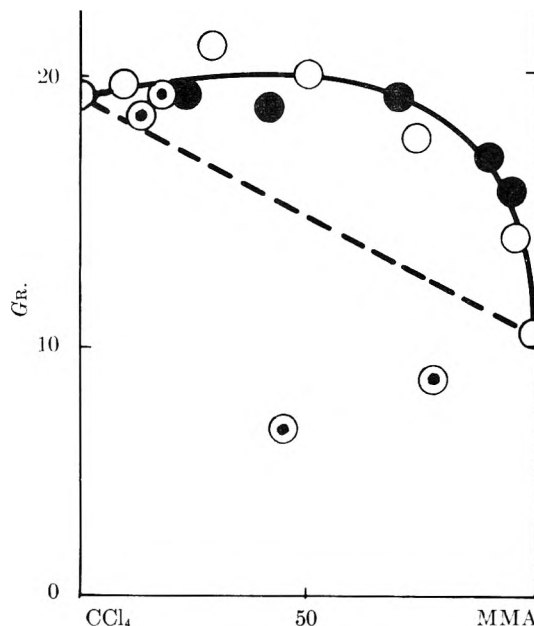


Fig. 4.—Free radical yields in mixtures of methyl methacrylate with carbon tetrachloride derived from data of the following sources:  $\circ$ , W. H. Seitzer and A. V. Tobolsky<sup>19</sup>;  $\bullet$ , T. S. Nikitina and Kh. S. Bagdasarian<sup>16</sup>;  $\odot$ , K. Hayashi.<sup>14</sup>

merization data show a similar trend to the data obtained by the DPPH method for chloroform-benzene mixtures.<sup>4,6</sup> This is shown by the dotted curve. In both systems the addition of small

(31) Kh. S. Bagdasarian, Thesis, Institut Karpov Moscow, 1950. See also ref. 16b and 25.

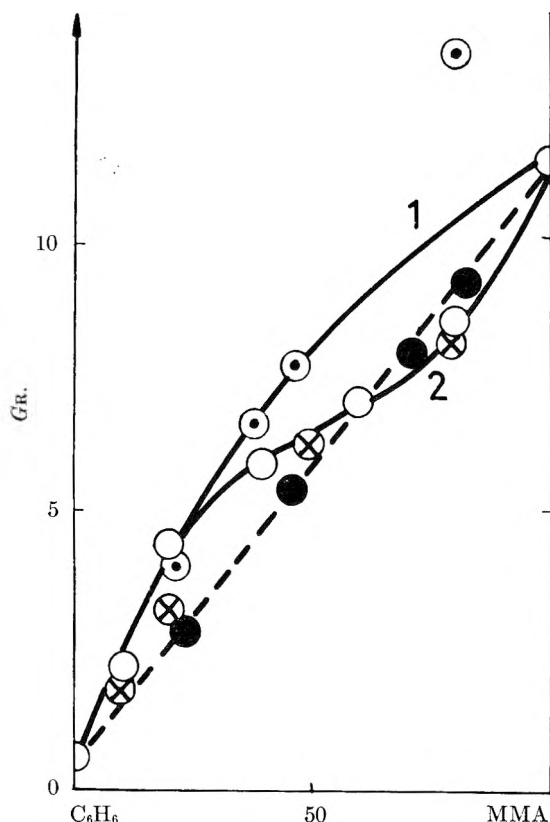


Fig. 5.—Free radical yields in mixtures of methyl methacrylate with benzene derived from data of the following sources:  $\circ$ , A. Chapiro<sup>11</sup>;  $\square$ , W. H. Seitzer and A. V. Tobolsky<sup>14</sup>;  $\bullet$ , T. S. Nikitina and Kh. S. Bagdasarian<sup>16</sup>;  $\otimes$ , I. Mita.<sup>20</sup>

amounts of chloroform to the aromatic hydrocarbon leads to a strong sensitization. The deviation occurs at lower concentrations of monomer than in carbon tetrachloride solutions. In addition the dotted curve shows that small amounts of benzene very efficiently "protect" chloroform.

**C. Methyl Methacrylate Solutions in Carbon Tetrachloride.**—Carbon tetrachloride strongly sensitizes the polymerization of methyl methacrylate. The reaction was initiated both with  $\gamma$ -rays<sup>16,19</sup> and with  $\beta$ -particles<sup>14</sup>; the latter results are very scattered.  $G_R$  values for this system are plotted in Fig. 4 using the higher  $G_R$  value for methyl methacrylate, *i.e.*,  $G_R^{\text{MMA}} = 11.5$ <sup>22</sup>. The  $G_R$  value thus obtained for pure carbon tetrachloride is 19, a value which is reasonably close to the result obtained by the DPPH method *in vacuo*, *i.e.*,  $G_R^{\text{CCl}_4} = 18$ – $20$ .<sup>5,6,23</sup> It should further be noticed that even in very dilute solutions the monomer acts as a very efficient free radical scavenger in this system.

The curve in Fig. 4 shows a flat maximum at approximately 80%  $\text{CCl}_4$ . A very similar curve was obtained when plotting  $G_R$  values for mixtures of chloroform and methyl acetate determined by the DPPH method.<sup>4</sup> Here again the agreement reached by the two methods is very good.

**D. Methyl Methacrylate Solutions in Benzene.**—The radiation initiated polymerization of methyl methacrylate in benzene solution proceeds at a lower rate than in bulk over the entire range of concentrations. This reaction was studied with

$\gamma$ -rays<sup>11,16,20</sup> and with  $\beta$ -particles.<sup>14</sup> Figure 5 shows a plot of  $G_R$  values derived from all available data. It should be noted that the accuracy in deriving rates of initiation from polymerization data is very poor when  $G_R^S$  is lower than  $G_R^M$ ; *i.e.*, when  $\varphi_S/\varphi_M < 1$ . It follows that it is difficult to conclude definitely from the data whether energy transfer actually takes place in this system or not. It can be seen from the plot in Fig. 5 that the data of Nikitina and Bagdasarian<sup>16</sup> lead to an almost linear relationship between  $G_R$  and concentration; the data of Seitzer and Tobolsky<sup>14</sup> are consistent with a sensitizing effect (curve 1), whereas the earlier data of the author<sup>11</sup> as well as the more recent experiments of Mita<sup>20</sup> indicate sensitization for low monomer concentrations and "protection" in concentrated monomer solutions (curve 2). It is noteworthy that a curve of type 1 was obtained for free radical yields in mixtures of benzene with methyl acetate by the DPPH method *in vacuo* whereas a curve of type 2 was found in aerated solutions.<sup>32</sup>

**E. Other Systems.**—A number of data are available on radiation-initiated solution polymerization of several other systems. The results are usually too scattered or involve too complicated processes to make it possible to derive any quantitative information on radical yields of the added substance. In a few special cases however more systematic work has been carried out. A brief survey of the data is presented below.

(a) **Styrene Solutions.**—Butylamine, dibutylamine, benzylamine and aniline all significantly sensitize the  $\gamma$ -ray initiated polymerization of styrene.<sup>11</sup> The effect is less pronounced with aniline than with aliphatic amines. The experimental data do not fit with the simple energy transfer theory developed by Nikitina and Bagdasarian.<sup>16</sup> This situation presumably results from the fact that amines inhibit vinyl polymerization. The results obtained by adding small amounts of amine to the monomer suggest that energy transfer takes place in the radiolysis of these mixtures leading to very strong sensitization. Quantitative data on the influence of amines on polymerization rates are still scarce and the mechanism of this inhibition is not definitely established. Hence  $G_R$  values for amines cannot be derived from these data.

Inhibition seems to be operative as well when ethyl iodide<sup>14</sup> and carbon disulfide<sup>11</sup> are added to styrene. The radiolysis of these substances leads to the formation of iodine and sulfur, respectively; the latter are known to act as efficient polymerization inhibitors. It is interesting to notice that protection is observed when carbon disulfide is dissolved in chloroform whereas some sensitization occurs in carbon disulfide-benzene mixtures.<sup>5</sup>

Diphenylmethane, unlike other aromatic hydrocarbons, strongly sensitizes the radiation polymerization of styrene; the same applies to the addition of small amounts of hydroquinone to styrene.<sup>33</sup>

Benzoyl peroxide produces an important increase in the rate of styrene polymerization,<sup>33</sup>

(32) L. Bouby and A. Chapiro, *J. chim. phys.*, **54**, 341 (1957).

(33) A. Chapiro, unpublished results.

whereas *t*-butyl peroxide does not show any pronounced effect.<sup>14</sup> This observation can be interpreted on the basis of more recent work on the radiolysis of peroxide solutions in various solvents. Thus Krongauz and Bagdasarian found that when benzoyl peroxide was irradiated in benzene solution a very rapid decomposition ensued which led to an apparent  $G(-Bz_2O_2)$  of the order of 1700.<sup>27</sup> It was demonstrated that the reaction did not proceed through a chain mechanism and hence a very efficient energy transfer process was assumed to occur in this system. No energy transfer was observed in cyclohexane and ethyl acetate solutions but the decomposition of benzoyl peroxide occurred through a chain reaction in these two solvents. The addition of small amounts of methyl methacrylate prevented chain propagation and reduced the over-all  $G(-Bz_2O_2)$ . On the other hand, *t*-butyl peroxide, when dissolved in either benzene, cyclohexane or methyl acetate, decomposed exclusively by a straightforward reaction apparently without energy transfer. The observed  $G$ -value was  $G(-\text{peroxide}) = 17$ .<sup>34</sup> The  $G_R$  value for decomposition of benzoyl peroxide was found to be 40.<sup>27</sup> If one assumes that the behavior of these peroxides is similar in styrene and in benzene solutions, it becomes clear why only benzoyl peroxide sensitizes the radiation polymerization of styrene.

Experiments were carried out as well with solutions of styrene in ether,<sup>11</sup> nitrobenzene, propionitrile,<sup>33</sup> bromoform<sup>12</sup> and dioxane.<sup>14</sup> In all cases the reaction rate increased with dilution.

Protection seemed to be operative in styrene solutions in cyclohexane and in *n*-heptane. In contrast, strong sensitization occurred in various alcohols and in acetone.<sup>11</sup> In these mixtures, however, polymer precipitation during the reaction leads to anomalous kinetic behavior.

The radiation polymerization of styrene dissolved in binary mixtures of carbon tetrachloride and benzene also was investigated.<sup>14</sup> The rate was found to be higher in the mixtures than in either solvent alone.

(b) **Methyl Methacrylate Solutions.**—Only little information is available on the influence of other additives on the radiation polymerization of methyl methacrylate. Experiments were carried out by Seitzer and Tobolsky<sup>14</sup> with ethyl bromide, ethyl iodide and dioxane. The results indicate a sensitizing effect in most cases. Methyl methacrylate dissolved in binary mixtures of carbon tetra-

chloride and benzene was found to polymerize faster than in carbon tetrachloride alone. On the other hand, the addition of water to methyl methacrylate solutions in dioxane increased the polymerization rate whereas water had no significant effect on the rate of polymerization in acetone solutions. The higher rates observed in dioxane-water mixtures were assumed to arise as a result of the tighter coiling of growing chains in the poor solvent which would be expected to slow down the termination step.

(c) **Vinyl Acetate Solutions.**—The radiation polymerization of vinyl acetate was found to be strongly inhibited by the addition of small amounts of benzene.<sup>16</sup> It is difficult to draw any conclusion on the existence of energy transfer from this result since benzene is known to inhibit polymerization of vinyl acetate when initiated by conventional means, presumably by a deactivating copolymerization mechanism.<sup>35</sup> A few experiments were conducted with diphenylpicrylhydrazyl in mixtures of vinyl acetate and benzene.<sup>16</sup> The rate of disappearance of DPPH indicated that sensitization takes place in a similar manner as in mixtures of benzene with methyl methacrylate and methyl acetate. On the other hand, carbon tetrachloride, which strongly sensitizes radiation polymerization of both styrene and methyl methacrylate, does not produce any measurable increase in the polymerization rate of vinyl acetate.<sup>16</sup>

#### IV. General Conclusions

The various data presented herein show how radiation polymerization can be applied to the study of the radiolysis of binary mixtures. The advantages of this method are primarily that conventional analytical techniques can be used for determining primary yields and that no foreign compound is added to the system since one of the two components acts as a scavenger. On the other hand, the method is necessarily limited to mixtures in which the polymerization kinetics are not complicated by secondary effects such as polymer precipitation, inhibition, etc. Furthermore, the rate constants of chain propagation and termination must be accurately known for the monomer used. Finally it should be stressed that since the reaction rate measured experimentally is proportional to the square root of free radical yield, this method is generally less sensitive than the direct determination of free radicals by other scavenger methods.

(34) V. A. Krongauz and Kh. S. Bagdasarian, *Zh. fiz. Khim. U.S.S.R.*, **32**, 717 (1958).

(35) W. H. Stockmayer and L. H. Peebles, *J. Am. Chem. Soc.*, **75**, 2279 (1953).



# THE DEPENDENCE OF RADICAL AND MOLECULAR YIELDS ON LINEAR ENERGY TRANSFER IN THE RADIATION DECOMPOSITION OF 0.8 N SULFURIC ACID SOLUTIONS<sup>1</sup>

BY NATHANIEL F. BARR AND ROBERT H. SCHULER<sup>2</sup>

*Contribution from the Department of Chemistry, Brookhaven National Laboratory, Upton, N. Y.*

*Received November 19, 1958*

Absolute radiation yields for oxidation of ferrous ion in deaerated solution and for the reduction of ceric ion in aerated and deaerated 0.8 N sulfuric acid solutions have been determined for a number of different radiations having energy loss parameters from 0.02 to 25 e.v./Å. These data have been combined with the results of previous measurements on the oxidation of ferrous ion in aerated solution to obtain values for the individual radical and molecular yields characteristic of the various radiations. A quantitative description of the dependence of these radical and molecular yields on linear energy transfer is given.

In a continuation of studies<sup>3-5</sup> on the effect of linear energy transfer (LET)<sup>6</sup> on radiation chemical reactions in aqueous systems, further measurements have been made on the oxidation of ferrous ion and the reduction of ceric ion in 0.8 N sulfuric acid solution for a variety of different radiations. This work was undertaken in order to determine the quantitative details of the variation of the yields of primary chemical products with increase in the density of energy release by the ionizing particle. Various early studies concerning this subject have been reviewed in the summary papers by Allen<sup>7</sup> and Hart.<sup>8</sup> More recent studies of hydrogen production from aerated ferrous sulfate solutions<sup>4</sup> and of oxidation of ferrous ion in the presence of cupric ion<sup>9,10</sup> have provided additional preliminary information for radiations of high LET. In the present work the determination of the primary yields is based on knowledge of the mechanisms for the radiation induced oxidation of ferrous ion and reduction of ceric ion in both aerated and deaerated 0.8 N sulfuric acid solution. These systems have been investigated to a very considerable extent with  $\gamma$ -radiation and appear to be reasonably well understood at the present time. It is possible to express the yields for each of these reactions in terms of the absolute yields for the formation of radical and molecular products arising from the primary decomposition of water ( $G_H$ ,  $G_{OH}$ ,  $G_{H_2O_2}$  and  $G_{H_2}$ , expressed here as molecules per 100 e.v. of absorbed energy).

Recent studies of the oxidation of ferrous sulfate in the absence of dissolved oxygen<sup>11</sup> have shown

(1) Research performed under the auspices of the U. S. Atomic Energy Commission.

(2) Radiation Research Laboratories, Mellon Institute, Pittsburgh, Pennsylvania.

(3) R. H. Schuler and A. O. Allen, *J. Am. Chem. Soc.*, **77**, 507 (1955).

(4) R. H. Schuler and A. O. Allen, *ibid.*, **79**, 1565 (1957).

(5) R. H. Schuler and N. F. Barr, *ibid.*, **78**, 5756 (1956).

(6) LET =  $-dE/dz$ , the energy transferred per unit length of track of the ionizing particle; cf. R. E. Zirkle, "Radiation Biology," A. Hollaender, ed., McGraw-Hill Book Co., New York, N. Y., 1954, p. 315.

(7) A. O. Allen, *Radiation Research*, **1**, 85 (1954).

(8) E. J. Hart, *ibid.*, **1**, 53 (1954); *Ann. Rev. Phys. Chem.*, **5**, 139 (1954).

(9) E. J. Hart, W. J. Ramler and R. S. Rocklin, *Radiation Research*, **4**, 378 (1956).

(10) D. M. Donaldson and N. Miller, *Trans. Faraday Soc.*, **52**, 652 (1956).

(11) N. F. Barr and C. G. King, *J. Am. Chem. Soc.*, **76**, 5565 (1954); **78**, 303 (1956).

that the measured yield is consistent with the observed molecular hydrogen yield if the hydrogen atoms are assumed to oxidize a single ferrous ion. This stoichiometry is further confirmed by the extensive work of Rothschild and Allen<sup>12</sup> and by the present study. Thus the yield of ferric ion from deaerated ferrous sulfate solution is given as

$$G(\text{Fe}^{+++})_{\text{deaerated}} = G_{OH} + 2G_{H_2O_2} + G_H \quad (1)$$

In aqueous solutions containing dissolved oxygen, a fraction of the hydrogen atoms which would otherwise combine to form molecular hydrogen<sup>13</sup> is scavenged by the oxygen. This leads to a different and somewhat enhanced hydrogen atom yield from aerated solutions which is designated in the present work by the symbol  $G'_H$ .

$$G'_H = G_H + \Delta \quad (2)$$

Since in the presence of oxygen the hydrogen atoms react to form  $\text{HO}_2\cdot$  radicals, each of which ultimately oxidizes three ferrous ions, the yield is given by

$$G(\text{Fe}^{+++})_{\text{aerated}} = 2G_{H_2O_2} + G_{OH} + 3G'_H \quad (3)$$

The term  $\Delta$  is of small importance in the case of  $\gamma$ -irradiations since the molecular products represent only a minor fraction of the over-all decomposition. Scavenging effects such as represented by this difference do, however, increase very markedly in heavy particle irradiations and must be considered in combining the results obtained from different systems.

The magnitude of  $\Delta$  may be estimated by a comparison of the yield for reduction of ceric ion in aerated and deaerated solution. In this system hydrogen atoms and hydrogen peroxide both reduce ceric ion while hydroxyl radicals oxidize cerous ion present. The yield for reduction of ceric ion is therefore given by

$$G(\text{Ce}^{+++})_{\text{deaerated}} = 2G_{H_2O_2} + G_H - G_{OH} \quad (4)$$

in the absence of dissolved oxygen. In the presence of dissolved oxygen the hydrogen atoms first react to form  $\text{HO}_2\cdot$  radicals each of which subsequently reduces a ceric ion. The yield is therefore given by

$$G(\text{Ce}^{+++})_{\text{aerated}} = 2G_{H_2O_2} + G'_H - G_{OH} \quad (5)$$

The difference between observations in the aerated

(12) W. Rothschild and A. O. Allen, *Radiation Research*, **8**, 101 (1958).

(13) In the following we neglect the small perturbation this produces in the yields of other primary products.

and deaerated systems provides us directly with a measure of  $\Delta$ . The value of this quantity can then be combined with measurements on the oxidation of iron in aerated and deaerated solutions to give the hydrogen atom and net water decomposition yields. The hydroxyl radical yields can be similarly calculated from equations 1 and 4 and the molecular hydrogen and hydrogen peroxide yields can be obtained from equations of material balance.

$$G_{\text{H}_2\text{O}} = G_{\text{H}} + 2G_{\text{H}_2} = G_{\text{OH}} + 2G_{\text{H}_2\text{O}_2} \quad (6)$$

### Experimental

**Solutions.**—Iron solutions contained 10 mM ferrous ammonium sulfate, 1 mM sodium chloride and 0.8 N sulfuric acid and were initially free of any significant concentration of ferric ion. Ceric ion solutions of approximately 100  $\mu\text{M}$  concentration were prepared by diluting a stock 0.1 M ceric sulfate solution with 0.8 N sulfuric acid. Since the presence of organic impurities in the water may result in abnormally high radiation yields, particularly in studies of the reduction of ceric ion, only water prepared by redistillation from acid dichromate and basic permanganate was used. Deaerated samples were prepared in a manner similar to that described by Johnson and Allen.<sup>14</sup>

**Sample Irradiation.**—Gamma irradiations were carried out in a 100 curie cylindrical  $\text{Co}^{60}$   $\gamma$ -ray source at a dose rate of approximately  $3 \times 10^{16}$  e.v. cc.<sup>-1</sup> min.<sup>-1</sup>. Yields were obtained by comparison of the observed rates of reaction to the rate of oxidation of ferrous sulfate in the Fricke dosimeter under the same irradiation conditions. The yield of oxidation was taken as 15.45.<sup>15</sup>

Fast-electron irradiations were carried out using the focused electron beam from the Brookhaven 2 Mev. Van de Graaff generator. Beam currents were approximately 10<sup>-8</sup> amp. All glass, thin window irradiation cells with stirrers similar to those employed in earlier studies were used here. The absolute dose delivered to the sample was determined by the charge-input method with corrections applied in a manner similar to that described in the previous work on the Fricke dosimeter.<sup>15</sup>

Heavy-particle irradiations were conducted at the Brookhaven 60-inch cyclotron with both helium ion and deuteron beams. These experiments were in general similar to the previous work on aerated ferrous sulfate solutions.<sup>4</sup> The radiation doses were calculated from the measured particle energy and the integrated current, with corrections made for the window displacement current as previously described.<sup>16</sup> Current densities were 0.05 to  $2 \times 10^{-9}$  ampere/cm.<sup>2</sup>. Experiments at lower energies than the maximum available at the cyclotron (20 Mev. for deuterons and 40 Mev. for helium ions) were carried out by degrading the energies of the particles with aluminum absorbers of known thickness.

Studies of the effect of the recoil radiations from the nuclear reaction  $\text{B}^{10}(\text{n}, \alpha)\text{Li}^7$  on ceric sulfate solutions were carried out in the thermal neutron facility of the Brookhaven reactor used for previous studies of ferrous sulfate oxidation.<sup>5</sup> Both ceric sulfate and ferrous sulfate solutions containing added boric acid were irradiated for 6 to 8 hours at the neutron flux of approximately  $6.5 \times 10^8$  n./cm.<sup>2</sup>. The absolute yield for ceric sulfate reduction was determined relative to the previously measured value of the oxidation of ferrous ion,  $G(\text{Fe}^{+++}) = 4.22$ .<sup>5</sup> Solutions of ceric ion and ferrous sulfate which did not contain boric acid were simultaneously irradiated in order that the  $\gamma$ -ray background in the neutron facility might be corrected for.

**Sample Analysis.**—The irradiation cells used in the electron and cyclotron beam experiments had one centimeter Pyrex optical absorption cells attached and permitted transmission measurements to be made during the course of the irradiations without exposing the solutions to air. Ferric ion was determined at 325  $\mu$  where the transparency of the cells was greater than at the 305  $\mu$  wave length normally used for this measurement. The extinction coefficient in 0.8 N sulfuric acid at 23.7° was found to be 1624 at 325  $\mu$

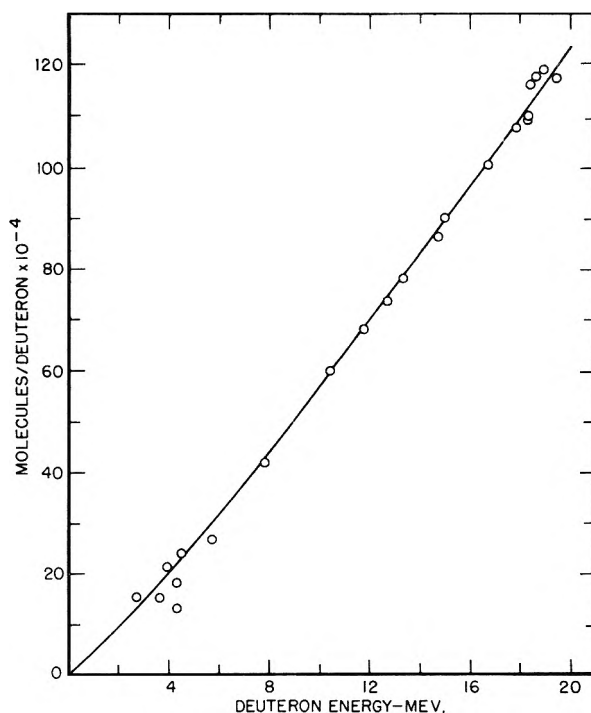


Fig. 1.—Number of ferric ions produced per deuteron ( $G_0 E_0$ ) as a function of deuteron energy.

compared to a value of 2174 at 305  $\mu$ . Ceric ion concentration was also determined at 325  $\mu$  where the extinction coefficient was measured to be 5585 relative to a value of 2174 for ferric ion at 305  $\mu$ . This measurement was made by adding an excess of ferrous sulfate to a ceric sulfate solution and takes into account the significant absorption of cerous ion at 305  $\mu$  ( $B_{305} = 21$ ). The wave length used here is slightly longer than that of the maximum in the ceric ion absorption spectrum (320  $\mu$ ) where the extinction coefficient was found to be 5650. Analysis of solutions irradiated in the  $\text{Co}^{60}$  facility and in the thermal neutron column were made using conventional spectrophotometric techniques.

### Results

#### Oxidation of Ferrous Ion in Deaerated Solution.

—In the  $\gamma$ -ray irradiation of ferrous sulfate solutions in the absence of oxygen it is known that a competition for the hydrogen atoms produced by the radiation exists between ferrous ion and any ferric ion present.<sup>12</sup> Ten millimolar ferrous sulfate solutions were used in the present measurements in order to permit observations to be made at low fractional conversions of the ferrous ion and thus reduce the effects of this competition. For all radiations used in this work the production of ferric ion in deaerated solution was found to be proportional to the dose. Five series of determinations of ferrous ion oxidation in deaerated solution were made with 2 Mev. electrons and gave an absolute yield of  $8.22 \pm 0.12$ . This observation can be compared to the value of 8.07 calculated from equations 1, 2, 3 and 6 using the yields observed for the oxidation of iron and for molecular hydrogen production in the aerated system, *i.e.*

$$G(\text{Fe}^{+++})_{\text{deaerated}} = \frac{1}{2}G(\text{Fe}^{+++})_{\text{aerated}} + G_{\text{H}_2} - \frac{1}{2}\Delta \quad (7)$$

where  $G(\text{Fe}^{+++})_{\text{aerated}} = 15.45$ ,  $G_{\text{H}_2} = 0.40$  (for sulfuric acid solutions)<sup>17,18</sup> and  $\Delta = 0.04$ . It will be

(14) E. R. Johnson and A. O. Allen, *J. Am. Chem. Soc.*, **74**, 4147 (1952).

(15) R. H. Schuler and A. O. Allen, *J. Chem. Phys.*, **24**, 56 (1956).

(16) R. H. Schuler and A. O. Allen, *Rev. Sci. Instr.*, **26**, 1128 (1955).

(17) H. A. Schwarz, J. P. Losce, Jr., and A. O. Allen, *J. Am. Chem. Soc.*, **76**, 4693 (1954).

TABLE I  
OXIDATION OF Fe<sup>II</sup> IN DEAERATED SOLUTION BY VARIOUS RADIATIONS

| Radiation                                                            | Ferrous sulfate<br>concn.,<br>$M \times 10^3$ | $G(\text{Fe}^{+++})_{\text{deaerated}}$ | $\frac{G(\text{Fe}^{+++})_{\text{aerated}}}{G(\text{Fe}^{+++})_{\text{deaerated}}}$ |  | Ref.         |
|----------------------------------------------------------------------|-----------------------------------------------|-----------------------------------------|-------------------------------------------------------------------------------------|--|--------------|
|                                                                      |                                               |                                         |                                                                                     |  |              |
| Co <sup>60</sup> $\gamma$ -rays                                      | 10                                            | 8.17 <sup>a</sup>                       | 1.89                                                                                |  | 11           |
| Co <sup>60</sup> $\gamma$ -rays                                      | 10                                            | 8.22 <sup>a</sup>                       | 1.88                                                                                |  | 12           |
| Co <sup>60</sup> $\gamma$ -rays                                      | 1                                             | 7.97 <sup>a</sup>                       | 1.91                                                                                |  | 12           |
| Co <sup>60</sup> $\gamma$ -rays                                      | 1 <sup>b</sup>                                | 8.05 <sup>a</sup>                       | 1.92                                                                                |  | 12           |
| 2 Mev. electrons                                                     | 10                                            | 8.22                                    | 1.88                                                                                |  | Present work |
| 18 Mev. deuterons                                                    | 10                                            | 6.21                                    | 1.84                                                                                |  | Present work |
| 32 Mev. helium ions                                                  | 10                                            | 4.93                                    | 1.65                                                                                |  | Present work |
| Tritium recoils from Li <sup>6</sup> (n, $\alpha$ )T <sup>3</sup>    | 10                                            | 4.52                                    | 1.51                                                                                |  | 5            |
| Recoil radiations from B <sup>10</sup> (n, $\alpha$ )Li <sup>7</sup> | 10                                            | 3.91                                    | 1.12                                                                                |  | 5            |

<sup>a</sup> Relative to 15.45 for aerated ferrous sulfate; all others are absolute determinations. <sup>b</sup> No added chloride; all other results for samples containing 1 mM NaCl.

noted that the term  $\Delta$  raises the ratio of the yield in the aerated system to that in the deaerated system by a slight amount (0.02) over the value of 1.90 expected when only the molecular hydrogen is taken into account.<sup>11,16</sup> Various recently observed values for this ratio are given in Table I.

The yield for reduction of ceric ion in the presence of thallos ion is, from the work of Sworski,<sup>19</sup> also equal to  $2G_{\text{H}_2\text{O}_2} + G_{\text{H}} + G_{\text{OH}}$  (cf. equation 1) and has been found to be 7.92. Thus it is seen that in the case of  $\gamma$ -irradiations the measurements appear to be generally consistent with a common set of primary products which interact with the solutes according to the stoichiometry indicated in the above equations.

The results obtained with deuteron beams are summarized in Fig. 1 where the number of ferric ions produced per deuteron ( $G_0E_0/100$ ) is plotted as a function of the deuteron energy. The radiation yield which is the ratio of the ordinate to the abscissa of the points in Fig. 1 decreases from a value of 6.25 at 20 Mev. to a value of about 5 at 5 Mev. Due to the relative constancy of the yields for the deaerated solutions the dependence illustrated in this figure has much less curvature than the similar curve previously given for aerated solutions. The thin target or differential yield,  $G_i = d(G_0E_0)/dE_0$ , is 6.9 at 15 Mev. The ratio of this thin target yield to that for aerated solutions ( $G_i = 13.0$  for 15 Mev. deuterons) is 1.88. One determination of hydrogen production by 18.9 Mev. deuterons showed a yield equal to one-half that of ferrous ion oxidation and no detectable oxygen in agreement with the expected stoichiometric relation.

A total of 15 experiments were performed with helium ions at initial energies between 30.2 and 33.5 Mev. Determinations of the absolute yield for ferrous sulfate oxidation gave values which varied from 4.81 to 5.05 with a mean value of 4.93 at 32.0 Mev.

We have previously reported a value of 3.91 for the oxidation of 10 mM ferrous ion in deaerated solution by the recoil radiation from the (n, $\alpha$ ) reaction in boron.<sup>5</sup>

**Reduction of Ceric Ion.**—The results of the ceric reduction experiments with beams of both cyclotron deuterons and helium ions and also Van de Graaff electrons were highly reproducible. The reduction

of ceric ion by  $\gamma$ -radiation was, however, much less reproducible. Satisfactory results could be obtained in the case of  $\gamma$ -irradiations only by using large ( $\sim 100$  cc.) containers which had been carefully cleaned and preirradiated and by using solutions initially containing a small amount of cerous ion ( $\sim 100 \mu\text{M}$  Ce<sup>+++</sup>). When this was done, it was found that the amount of reduction was proportional to dose with a high degree of precision. Under other experimental conditions the observed yields scattered to a much greater extent and were always higher. From the relative rates of ceric reduction and ferrous oxidation in the Co<sup>60</sup> source,  $G(\text{Ce}^{+++})$  is found to be  $2.33 \pm 0.03$  for Co<sup>60</sup>  $\gamma$ -radiation. Except for the recent work of Sworski<sup>16</sup> where a yield of 2.39 was obtained, other determinations have given considerably higher values and probably reflect some of the difficulties mentioned above in the  $\gamma$ -ray radiolysis of cerium solutions. It will be noted that twice the yield for hydrogen peroxide production from air-saturated sulfuric acid is also given by  $2G_{\text{H}_2\text{O}_2} + G_{\text{H}}' - G_{\text{OH}}$  and has been measured to be  $2(1.17) = 2.34$ .<sup>20</sup>

The results of six experiments with 2 Mev. electrons gave an absolute yield for ceric reduction of  $2.32 \pm 0.02$ . A single irradiation also was carried out on a deaerated solution which was broken open immediately after the irradiation and the experiment rerun with fresh aerated solution. This direct comparison of the yield in aerated and deaerated solution gave a difference of 2%, in agreement with the effect expected from the results of Ghormley and Hochanadel on the effect of dissolved air on molecular hydrogen production.<sup>18</sup>

An over-all summary of the results of 20 experiments with deuterons and 21 experiments with helium ions is given in Table II. Since only a slight variation of yield with energy is observed here it did not seem warranted to undertake a more extensive investigation of the functional dependence of the yield without a significant increase in the accuracy of the determinations. It will be noted that the difference in yields for aerated and deaerated systems is quite large, being 0.14 for 18 Mev. deuterons and 0.19 for 33 Mev. helium ions.

In a typical experiment with the recoil radiations from the boron (n, $\alpha$ ) reaction, seven samples of 90  $\mu\text{M}$  ceric ion containing 0.120  $M$  boric acid, two samples of 1 mM ferric ion containing 1.050  $M$  boric

(18) J. A. Ghormley and C. J. Hochanadel, *Radiation Research*, **3**, 227 (1955).

(19) T. J. Sworski, *ibid.*, **4**, 483 (1956).

(20) T. J. Sworski, *J. Am. Chem. Soc.*, **76**, 4687 (1954).

acid and two samples each of ceric ion and ferrous ion containing no added boric acid were radiated for six hours in the neutron facility. The absorbance changes in the ceric solutions ranged from 0.400 to 0.420 with a mean of 0.411. The radiation yield calculated by comparison to the amount of ferrous sulfate oxidation observed (absorbance change = 0.302) after correcting for the  $\gamma$ -ray background and for the difference in boric acid concentration was found to be 2.92. In these experiments the reduction of ceric ion by the  $\gamma$ -radiation was always slightly greater than that estimated from the ferrous sulfate solutions and again appears to reflect the difficulties mentioned above with respect to the use of small irradiation cells. Fortunately because the yields for light and heavy particles are about the same, the correction applied here for the  $\gamma$ -ray background represents a much smaller fraction of the effect than in the case of observations on ferrous sulfate solutions so that this difference does not affect the results significantly. A total of 18 determinations of the yield of ceric reduction were made in four sets and gave an over-all absolute yield of 2.94 with standard deviation of  $\pm 0.12$ .

TABLE II  
REDUCTION OF  $\text{Ce}^{\text{IV}}$  BY VARIOUS RADIATIONS

| Radiation                                                          | $G(\text{Ce}^{+++})_{\text{aerated}}$ | $\frac{G(\text{Ce}^{+++})_{\text{aerated}}}{G(\text{Ce}^{+++})_{\text{deaerated}}}$ |
|--------------------------------------------------------------------|---------------------------------------|-------------------------------------------------------------------------------------|
| $\text{Co}^{60}$ $\gamma$ -rays                                    | $2.33 \pm 0.03$                       | ...                                                                                 |
| 2 Mev. electrons                                                   | $2.32 \pm .02$                        | 1.02                                                                                |
| 18 Mev. deuterons                                                  | $2.84 \pm .05$                        | 1.052                                                                               |
| 10 Mev. deuterons                                                  | $2.80 \pm .04$                        | 1.075                                                                               |
| 33 Mev. helium ions                                                | $2.92 \pm .04$                        | 1.070                                                                               |
| 11 Mev. helium ions                                                | $2.90 \pm .06$                        | ...                                                                                 |
| Recoil radiations from $\text{B}^{10}(\text{n},\alpha)\text{Li}^7$ | $2.94 \pm .12$                        | ...                                                                                 |

The constancy of the ceric ion reduction yield over the range of heavy-particle energies studied suggests that this system might be useful in the estimation of the energy deposited in an aqueous system from a mixed  $\gamma$ -ray-neutron field especially where there exists at least some approximate knowledge of the relative energy contribution due to  $\gamma$ -radiation and recoil protons.

### Discussion

The various yields for the reduction of ceric ion and for the oxidation of ferrous ion in both aerated and deaerated solutions are given in Fig. 2 as a function of the reciprocal of the initial energy loss parameter,  $(-dE/dx)_0$ , characteristic of the radiation. It is seen that, as expected from previous qualitative considerations of the molecular and radical products,<sup>6,21</sup> the yield for oxidation of ferrous ion decreases and for reduction of ceric ion increases as the LET of the particle increases. Kinetic consideration of these data should be based on the instantaneous or differential yields, *i.e.*,  $G_i = d(G_0 - E_0)/dE_0$ . Since the observed yields change only slowly with LET the instantaneous values for the particular radiation will be similar to the integrated yields given in Fig. 2.

The hydrogen atom and net water decomposition yield can be calculated from equations 1, 2, 3 and 6 to be

(21) T. J. Hardwick, *Disc. Faraday Soc.*, **12**, 203 (1952).

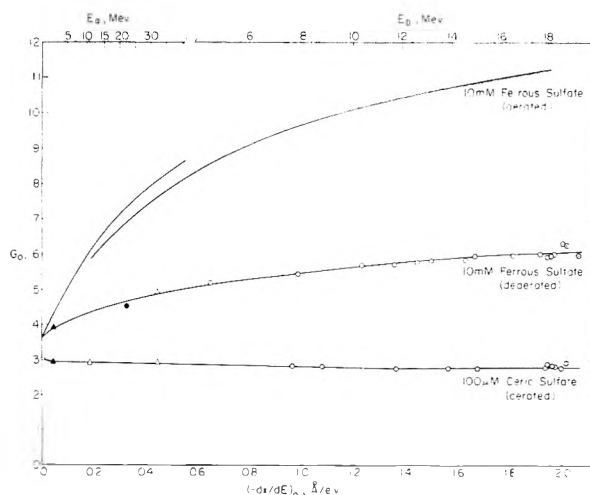


Fig. 2.—Yields ( $G_0$ ) for oxidation of ferrous ion and reduction of ceric ion as a function of the reciprocal of the energy loss parameter  $(-dE/dx)_0$ ; O, deuterons;  $\Delta$ , helium ions;  $\blacktriangle$ ,  $\text{B}(\text{n},\alpha)\text{Li}$  recoil radiations;  $\bullet$ , tritium component of  $\text{Li}(\text{n},\alpha)\text{T}$  recoil radiations. Curve for aerated ferrous sulfate taken from ref. 4. Limiting values of 15.45 for aerated ferrous sulfate, 8.22 for deaerated ferrous sulfate and 2.32 for aerated ceric sulfate were obtained with fast electrons.

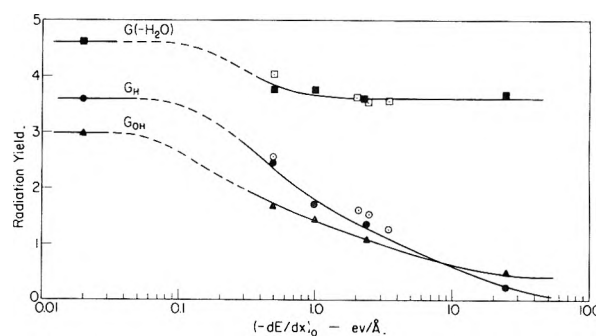


Fig. 3.—Dependence of yields for hydrogen atom and hydroxyl radical production and net water decomposition on LET for deaerated 0.8 N sulfuric acid solutions. Curves and closed symbols are taken from Fig. 2, open symbols represent values calculated from measurements of the molecular hydrogen yield from air-saturated ferrous sulfate solutions (*cf.* ref. 4).

$$G_{\text{H}} = \frac{1}{2}[G(\text{Fe}^{+++})_{\text{aerated}} - G(\text{Fe}^{+++})_{\text{deaerated}}] - \frac{1}{2}\Delta \quad (8)$$

$$G(-\text{H}_2\text{O}) = G(\text{Fe}^{+++})_{\text{deaerated}} - G_{\text{H}} \quad (9)$$

Since  $\Delta$  is always small, the hydrogen atom yield is approximately equal to one-half the difference between the yields observed for ferrous sulfate oxidation in the aerated and deaerated systems. In Fig. 2 the curves representing these yields appear to be approaching a common value of 3.6 for particles of very high LET. This indicates that the hydrogen atom yield goes to zero. Similarly the net water decomposition yield calculated from equations 8 and 9 appears to be constant at a value of 3.6 for radiations of energy loss parameters above 1 e.v./ $\text{\AA}$ . The molecular hydrogen yield for fission recoils has been found to have a value in agreement with this limit.<sup>22</sup> For all LET's less than the rather considerable value of 100 e.v./ $\text{\AA}$ . there should be a detectable atom yield.

(22) J. W. Boyle, C. J. Hochanadel, T. J. Sworski, J. A. Ghormley and W. F. Kieffer, *Proc. Int. Conf. Peaceful Uses Atomic Energy*, **7**, 576 (1955).

As indicated above, the term  $\Delta$  has a significant value for particles of intermediate LET and must be included in any precise calculation of the hydrogen atom and net water decomposition yields. As an example, we may consider the data for the 33 Mev. helium ions where  $\Delta$  is estimated from the effect of oxygen on the ceric reduction yields to be 0.19. The inclusion of this term in the calculations on the net water decomposition yield increases the derived value from 3.3 to 3.6. Taking this into account the net water decomposition yields calculated from the curves of Fig. 2 are given in Fig. 3. The hydrogen atom yields which are indicated in Fig. 3 for deaerated solutions are 0.2 to 0.3 unit higher in air-saturated solutions. The molecular hydrogen yield is, of course, one half the difference between  $G(-H_2O)$  and the hydrogen atom yield. Values of 0.63 for 18 Mev. deuterons and 1.01 for 35 Mev. helium ions determined in this way may be compared with experimental molecular hydrogen yields of 0.75 and 1.01 from air-saturated ferrous sulfate solutions.<sup>4</sup> Hart, Ramler and Rocklin<sup>9</sup> have similarly combined measurements on the ferrous sulfate and ferrous sulfate-cupric sulfate systems to obtain an estimate of the molecular hydrogen and net water decomposition yields for protons and deuterons having LET's between 0.5 and 5 e.v./Å. Their values for these quantities are in general 10-30% lower than those given by the present studies but are, however, for solutions 10 mM in cupric sulfate at which concentration the molecular hydrogen yield is expected to be appreciably depressed<sup>23</sup> due to the scavenging of hydrogen atoms by cupric ion. For heavy-particle irradiations the concentrations of radicals along the track are very high and scavenger effects become in general considerably more pronounced than in the case of electron irradiations. This is illustrated by observations on the effect of oxygen and ferrous ion concentration on ferrous sulfate oxidation,<sup>4,5,24</sup> by the present studies on the effect of oxygen on ceric ion reduction and by other recent studies of heavy particle bombardments of the ferrous sulfate-cupric sulfate<sup>25</sup> and potassium nitrite<sup>26</sup> systems.

From equations 1 and 4 the hydroxyl radical yield is given by

$$G_{OH} = \frac{1}{2}[G(Fe^{+++})_{de-aerated} - G(Ce^{+++})_{de-aerated}] \quad (10)$$

It would seem from analogy with the results on hydrogen atom production that this yield might well also be expected to go to zero. If this is so then

(23) H. A. Schwarz, *J. Am. Chem. Soc.*, **77**, 4960 (1955).

(24) R. H. Schuler, *Radiation Research*, **8**, 388 (1958).

(25) N. Miller, private communication.

(26) H. A. Schwarz, private communication.

the yields for ceric sulfate reduction and for ferrous sulfate oxidation should approach a common value for radiations of infinite LET. Results from the boron ( $n, \alpha$ ) experiments indicate that a significant difference exists for particles of ion density 25 e.v./Å. What appears to be a yield of hydroxyl radicals may, however, actually be due, as suggested by Donaldson and Miller,<sup>10</sup> to the diffusion of  $HO_2$  radicals out of the track as a result of intratrack reactions between hydroxyl radicals and the molecular peroxide.



Inspection will show that such a reaction will not directly affect the stoichiometry involved in the net effects on ferrous sulfate and ceric sulfate. The occurrence of reaction I however interferes with the recombination of hydroxyl radicals thus lowering the observed yield for ceric ion reduction. We estimate from the difference between 3.6 and the measured value of 2.9 for boron ( $n, \alpha$ ) radiations that the yield for reaction I must be between 0.25 and 0.35. This value of course depends on an unmeasured correction which must be applied for the yield of free hydroxyl radicals which actually escape from the track. This estimate is in excellent agreement with the value of 0.25 for polonium  $\alpha$ -radiation determined by Donaldson and Miller from measurements of oxygen production in the ferrous sulfate-copper sulfate system.<sup>10</sup> It would seem from the trend of the curves in Fig. 3 that this reaction must become important for all radiations of LET greater than 1 e.v./Å. The interpretation of other systems in terms of the primary yields given in this paper must be slightly modified taking into account the occurrence of such reactions within the track, *e.g.*, reaction I would materially affect the stoichiometry involved in the ferrous sulfate-copper sulfate system since the  $HO_2$  radical reduces a single ferric ion whereas the initial reactants oxidize three ferrous ions.

It will be noted in Fig. 3 that the yield of water decomposition appears to be independent of LET for particles having energy loss parameters greater than 1 e.v./Å. In this region the molecular yields continue to increase and radical yields to decrease to a rather considerable extent. It would seem that the reformation of water by the combination of hydrogen atoms and hydroxyl radicals does not increase in a manner analogous to that of the other molecular products.

**Acknowledgment.**—The authors wish to thank Drs. A. O. Allen and H. A. Schwarz for many valuable discussions during the course of this investigation.

## RADIATION CHEMISTRY OF ORGANIC COMPOUNDS.

## IV. CYCLOHEXANE

BY HAROLD A. DEWHURST

*General Electric Research Laboratory, Schenectady, New York**Received November 25, 1958*

The major products formed in the 800 kvp, electron radiolysis of cyclohexane are hydrogen, cyclohexene and dicyclohexyl. Minor amounts of products result from fragmentation and isomerization of the ring system. The initial yields are,  $G(\text{C}_6\text{H}_{10}) = 2.5$  and  $G(\text{dicyclohexyl}) = 2.0$  and were unchanged by irradiation either in 10 atmospheres of hydrogen or at liquid nitrogen temperature. In the presence of solutes, oxygen, iodine and benzene, the cyclohexene yield decreased to a limiting value of  $G = 0.7$ . The results are discussed in terms of a mechanism which involves the decomposition of excited cyclohexane molecules. The results show that of the excited molecules that decompose approximately 15% give products directly by an unspecified molecular process.

The gaseous products from the radiolysis of cyclohexane liquid are mainly hydrogen and small amounts of  $\text{C}_2$  hydrocarbons.<sup>1,2</sup> Recently it has been shown that the liquid products are cyclohexene, dicyclohexyl and small amounts of products which result from ring fragmentation.<sup>3</sup> Because of the relative simplicity of product formation, cyclohexane is a particularly interesting molecule for radiation chemical investigation. Previous studies with cyclohexane have been concerned mainly with the gaseous products. For example, the hydrogen yield has been shown to be independent of linear energy transfer<sup>4</sup> and temperature.<sup>5</sup> However, in the presence of solutes, notably benzene<sup>2</sup> and iodine,<sup>6,7</sup> the hydrogen yield decreased. The formation of liquid products under these conditions has not been investigated and is essential for a complete understanding of the radiation chemistry. The present report is primarily concerned with the effect of solutes and temperature on liquid product formation.

## Experimental

**Materials.**—The following samples of cyclohexane were used as received: (a) Eastman Kodak, spectro grade; (b) Phillips, research grade; and (c) API grade, which contained  $0.010 \pm 0.006$  mole % impurity. Gas chromatograms of the spectro grade material showed a large impurity peak ( $\sim 0.8$  mole %) which was probably methylcyclopentane. Chromatograms of the Phillips and API material did not show any impurity peaks. The same product yields were obtained with all three samples of cyclohexane.

The following solutes were used: cyclohexene (Phillips pure grade); benzene (Phillips research grade);  $\text{I}_2$  (Malinckrodt);  $\text{O}_2$  (Matheson); and hydrogen (Matheson electrolytic grade).

**Irradiation.**—The samples contained in a 2" diameter aluminum dish were irradiated at room temperature with the 800 kvp. electron beam from a resonant transformer unit.<sup>8</sup> Unless otherwise specified all samples were prepared for irradiation in a  $\text{N}_2$  dry box. The electron beam dose rate determined by ionization chamber measurements and based on 93 ergs/g./r. was  $8.7 \times 10^{20}$  e.v./g./min. This value was in agreement with energy absorption calculations based on the hydrogen yield from cyclohexane liquid utilizing  $G(\text{H}_2) = 5.5$ .

A specially designed high-pressure cell<sup>9</sup> was used for irradiations in high pressure (10 atmospheres) of oxygen and hydrogen.

**Product Analysis.**—Conventional high-vacuum techniques were used for the preparation and analysis of samples.<sup>8</sup> Infrared spectra were obtained with a Perkin-Elmer (model 21) spectrometer. The cyclohexene concentration was determined at  $718 \text{ cm.}^{-1}$  using a molar extinction coefficient of 45.4 determined in separate experiments. The concentration of cyclohexanone was determined at  $1717 \text{ cm.}^{-1}$  using the molar extinction coefficient of 304 reported by Cross and Rolfe.<sup>10</sup> A Perkin-Elmer vapor refractometer was used for the gas-liquid partition chromatography. Most of the analyses were performed with either a 1- or 2-meter didecyl phthalate column. The refractometer was calibrated with known solutions of cyclohexene and dicyclohexyl in cyclohexane. In most cases the cyclohexene concentration was determined by both IR spectrophotometry and gas chromatography, and the agreement was always good.

## Results and Discussion

**Gas Products.**—The gaseous products volatile at  $-120^\circ$  consisted largely of  $\text{H}_2$  with small amounts of methane and  $\text{C}_2$  hydrocarbons, mainly ethylene. The volatile gas had the following composition:  $\text{H}_2 = 96\%$ ,  $\text{CH}_4 < 0.4\%$ ,  $\text{C}_2\text{H}_6 < 0.3\%$  and  $\text{C}_2\text{H}_4 = 3.1\%$  in fair agreement with the data of Manion and Burton.<sup>2</sup>

**Liquid Products.**—The gas chromatograms showed this product distribution

linear  $\text{C}_6$  hydrocarbon (hexene)  
methylcyclopentane  
cyclohexene  
intermediate cyclohexanes  
dicyclohexyl  
cyclohexylcyclohexene (?)

The cyclohexene and dicyclohexyl accounted for approximately 90% of the liquid products.

The formation of cyclohexene as a function of the energy absorbed is shown in Fig. 1. Each point represents the average of at least two separate determinations. The initial slope of the curve was used to calculate the initial yield of cyclohexene,  $G(\text{C}_6\text{H}_{10})_i = 2.5$ . The cyclohexene yield gradually decreased with increase in energy absorbed toward a limiting concentration.

The formation of dicyclohexyl as a function of the energy absorbed is shown in Fig. 2, where each point represents the average of at least two separate determinations. From the initial slope the initial yield was calculated,  $G(\text{dicyclohexyl})_i = 2.0$ . The reproducibility of the cyclohexene and

(1) C. S. Schoepfle and C. H. Fellows, *Ind. Eng. Chem.*, **23**, 1396 (1931).

(2) J. P. Manion and M. Burton, *This Journal*, **56**, 560 (1952).

(3) H. A. Dewhurst, *J. Chem. Phys.*, **24**, 1254 (1956).

(4) R. H. Schuler and A. O. Allen, *J. Am. Chem. Soc.*, **77**, 507 (1955).

(5) M. Hamashima, M. P. Reddy and M. Burton, *This Journal*, **62**, 246 (1958).

(6) R. H. Schuler, *ibid.*, **61**, 1472 (1957).

(7) M. Burton, J. Chang, S. Lipsky and M. P. Reddy, *Rad. Research*, **8**, 203 (1958).

(8) H. A. Dewhurst, *This Journal*, **61**, 1466 (1957).

(9) E. J. Lawton and J. S. Balwit, private communication.

(10) L. H. Cross and A. C. Rolfe, *Trans. Faraday Soc.*, **47**, 354 (1951).

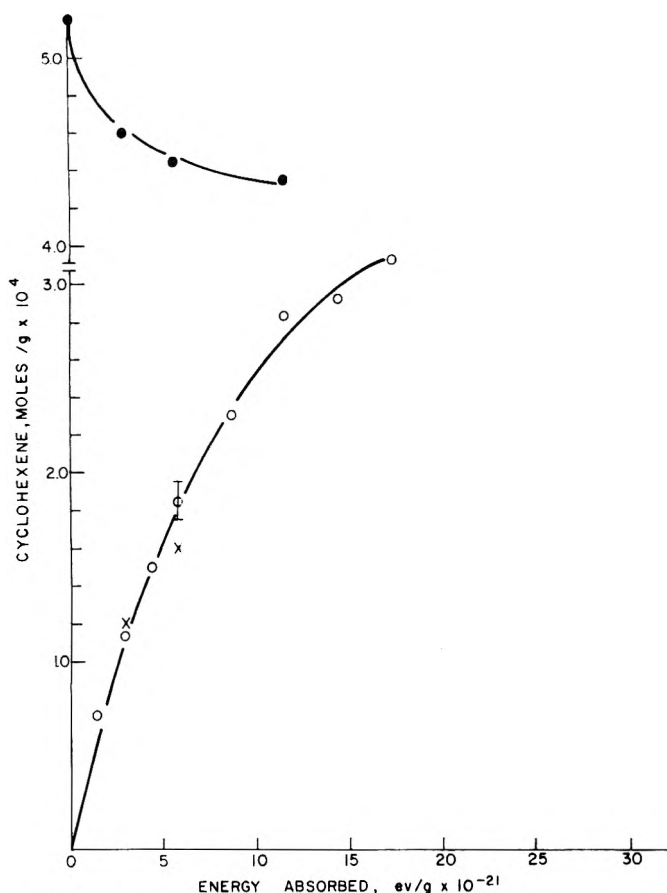


Fig. 1.—Formation of cyclohexene at room temperature (O) and liquid nitrogen temperature (X). Filled circles, added cyclohexene =  $5.2 \times 10^{-4}$  mole/g.

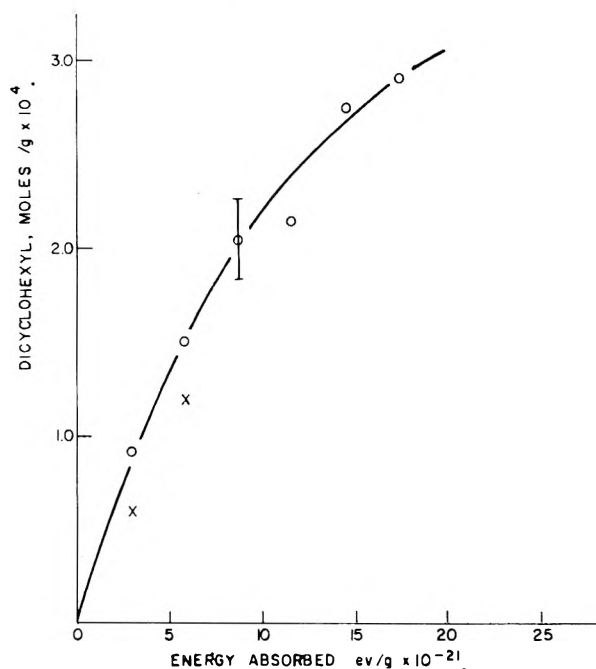


Fig. 2.—Formation of dicyclohexyl at room temperature (O) and liquid nitrogen temperature (X).

dicyclohexyl results is indicated by the vertical lines in Figs. 1 and 2.

It is of considerable interest to note that the

initial yield ratio  $G(\text{C}_6\text{H}_{10})/G(\text{C}_{12}\text{H}_{22}) = 1.25$  is more than double the ratio of rate constants for disproportionation and combination of cyclohexyl radicals ( $k_{\text{disp}}/k_{\text{comb}} = 0.5$ ) measured by Gunning, *et al.*,<sup>11</sup> in the gas phase. This discrepancy suggests that if Gunning's ratio can be accepted for the liquid phase, then a simple interpretation of product formation based entirely on disproportionation and combination of cyclohexyl radicals is not valid.

The formation of the other product groups (Fig. 3) was found to be a linear function of the energy absorbed. For the purpose of estimating  $G$ -values it was assumed that area per cent. of the peaks on the chromatogram was directly proportional to mole per cent. On this basis the yield of hexene product was  $G(\text{hexene}) \cong 0.2$ ,  $G(\text{methylcyclopentane}) \cong 0.3$  and  $G(\text{intermediate cyclohexanes}) \cong 0.3$ . The latter products were not well characterized but had retention times similar to the  $n$ -alkyl (ethyl to hexyl) substituted cyclohexanes.

Infrared examination of the irradiated liquid showed, in addition to a strong cyclohexene band at  $718 \text{ cm.}^{-1}$ , weak absorption bands at  $972$  and  $1379 \text{ cm.}^{-1}$  characteristic of *trans*-vinylene unsaturation and methyl groups, respectively. The *trans*-vinylene band has been assigned to the hexene product and the methyl band to the methylcyclopentane product.

To determine whether any significant amount of products higher than dimer were formed a residue determination was done. The irradiated sample ( $2.9 \times 10^{21}$  e.v./g.), evaporated to constant weight in a vacuum desiccator, did not contain any measurable amount of product higher than dimer. The infrared spectrum ( $0.025$  mm. micro cell) of the residue, essentially dimer, was found to contain a negligible amount of unsaturation.

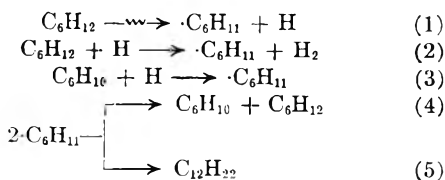
The above results are at variance with the product yields reported by Nixon and Thorpe.<sup>12</sup> The differences have been attributed to the effect of dose rate. Similar differences, attributed to dose rate dependent reactions, have been found with cobalt-60  $\gamma$ -rays.<sup>13</sup>

**Effects of Products.**—The effect of adding  $5.2 \times 10^{-4}$  mole/g. cyclohexene is shown in Fig. 1 (filled circles). The cyclohexene concentration decreased rapidly toward the limiting concentration. Under these conditions the initial yield for cyclohexene disappearance was  $G(-\text{C}_6\text{H}_{10}) = 2.3$ , the hydrogen yield was  $G(\text{H}_2) = 2.9$  and the dicyclohexyl yield was unchanged. The decrease in the hydrogen yield,  $\Delta G(\text{H}_2) = 2.4$ , is in good agreement with the yield for cyclohexene disappearance and suggests that cyclohexene is reacting either with H-atoms or their precursor. These results are consistent with the reactions.

(11) P. W. Beck, D. V. Kniebes and H. E. Gunning, *J. Chem. Phys.*, **22**, 672 (1954).

(12) A. C. Nixon and R. E. Thorpe, *ibid.*, **28**, 1004 (1958).

(13) H. A. Dewhurst and R. H. Schuler, *J. Am. Chem. Soc.*, **81**, in press (1959).



This reaction sequence predicts no change in the number of cyclohexyl radicals formed and, therefore, no change in dimer yield in agreement with experiment.

The irradiation of cyclohexane at room temperature in the presence of 10 atmospheres of added hydrogen (concentration approximately  $10^{-4}$  mole/g.) did not change the yield of any of the reaction products measured by infrared and gas chromatography. Under these conditions, therefore, hydrogen does not enter into any significant back reaction at room temperature.

**Effect of Solutes.**—In the presence of  $10^{-4}$  mole/g. of benzene, both the cyclohexene and dicyclohexyl yields were markedly decreased. The methylcyclopentane and  $\text{C}_6$  hydrocarbon products were apparently unchanged. For a total dose of  $5.8 \times 10^{21}$  e.v./g. the benzene disappearance corresponded to a yield of  $G(-\text{C}_6\text{H}_6) = 1.2$  as measured by gas chromatography and by the change in infrared absorption at  $672 \text{ cm}^{-1}$ . Under these conditions the cyclohexene yield was  $G(\text{C}_6\text{H}_{10}) = 1.2$ , and the dicyclohexyl yield was  $G(\text{C}_{12}\text{H}_{22}) = 0.8$ . The infrared absorption spectrum showed a new band at  $724 \text{ cm}^{-1}$  which is in the region for monosubstituted benzene absorption. These results show that the disappearance of one benzene molecule results in a corresponding decrease in the yields of cyclohexene and dicyclohexyl. If these products are formed by disproportionation and combination of cyclohexyl radicals (reactions 4 and 5), then each benzene must remove either two cyclohexyl radicals or their precursor.

Oxygen was found to have a profound effect on the radiolysis of cyclohexane. The effects observed were essentially independent of oxygen pressure between one and 10 atmospheres ( $10^{-4}$  mole/g.) and directly proportional to the total energy absorbed up to  $5.8 \times 10^{21}$  e.v./g. The gas chromatograms showed the formation of two major oxidation products in approximately equal amounts which were identified as cyclohexanol and cyclohexanone. Infrared examination of radio-oxidized cyclohexane showed the presence of both hydroxyl and carbonyl groups and served to confirm the gas chromatography assignments.

The cyclohexene yield in the presence of oxygen was  $G = 0.7$ , less than one-third the value in the absence of oxygen. Under the same conditions the yield of dicyclohexyl product was negligible ( $G < 0.1$ ). The combined yield of oxidation product determined by gas chromatography was  $G(\text{cyclohexanol} + \text{cyclohexanone}) = 7.2$ . The carbonyl yield determined by infrared absorption was  $G(\text{cyclohexanone}) = 3.5$  and by difference the cyclohexanol yield was  $G(\text{cyclohexanol}) = 3.7$ .

The carbonyl yield determined by infrared and the total yield of cyclohexanone and cyclohexanol determined by gas chromatography was found to be independent of dose rate over a 10-fold range.

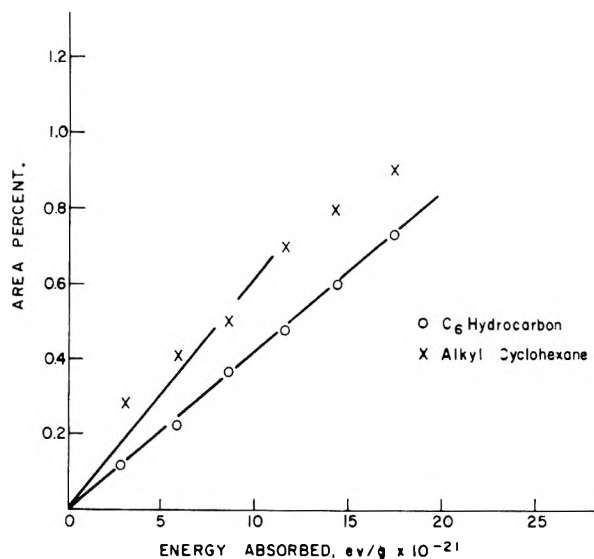
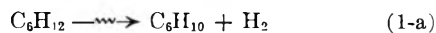


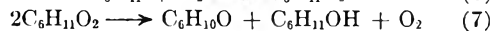
Fig. 3.—Formation of linear  $\text{C}_6$  hydrocarbons (hexene) and alkyl cyclohexanes at room temperature.

Treatment of the irradiated solution with sodium sulfite did not change the amount of cyclohexanol formed.<sup>14</sup> This suggested that cyclohexyl hydroperoxide, known to be stable above room temperature,<sup>15</sup> was not a major product. Bakh<sup>16</sup> has reported that hydroperoxide is the major oxidation product ( $G = 1.2$ ) along with carbonyl ( $G = 0.6$ ) and a small amount of acid ( $G = 0.2$ ). The total yield of oxidized product reported by Bakh is considerably smaller (factor of three) than the present results.

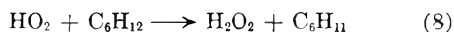
The oxygen results show that the residual cyclohexene yield is independent of the oxygen concentration which suggests that it may be formed by a molecular process



The major oxidation products can be accounted for by the sequence which was proposed recently



by Russell.<sup>17</sup> In the absence of any complicating chain reactions the product yields lead to  $G(\text{cyclohexyl radicals}) = 7.2$ . In the absence of oxygen a similar calculation based on product yields gave  $G(\text{cyclohexyl radicals}) = 7.6$ . Oxygen appears, therefore, to be a useful solute for radical counting. In view of the good agreement for the yield of cyclohexyl radicals obtained in the presence and absence of oxygen, it is proposed that the H-atoms formed in reaction 1 either abstract as in reaction 2 or, more likely in the presence of oxygen, they form  $\text{HO}_2$  radicals which react as



Cyclohexane samples saturated with iodine ( $\sim 0.04 M$ ) were irradiated in a special water-cooled cell equipped with a magnetic stirrer to ensure that

(14) The author is indebted to G. A. Russell for this suggestion.

(15) A. Farkas and E. Passaglia, *J. Am. Chem. Soc.*, **72**, 3333 (1950).

(16) N. Bakh, *Inter. Conf. Peace. Use At. Energy*, **7**, 538 (1956), United Nations, N. Y.

(17) G. A. Russell, *J. Am. Chem. Soc.*, **79**, 3871 (1957).



saturation with iodine was maintained. The chromatograms showed the presence of the following products: cyclohexene, hexyl iodide, cyclohexyl iodide and a small amount of dicyclohexyl. The cyclohexene yield under these conditions was  $G(\text{C}_6\text{H}_{10}) = 0.8$ . The yield of hexyl iodide was  $G = 0.3$ , while the cyclohexyl iodide yield was  $G = 4.0$  and the dicyclohexyl yield  $G = 0.3$ . Fessenden and Schuler<sup>18</sup> have reported that at low-iodine concentrations the yield for formation of alkyl iodide was  $G = 5.6$  which increased to about  $G = 7.5$  in saturated iodine solutions. In the present work the yield of observable alkyl iodide was  $G = 4.3$ , which is much lower than the value reported by Fessenden and Schuler. However, since the latter authors did not specify the nature of the alkyl iodides formed, a rigorous comparison is not possible at present.

The yield of cyclohexyl radicals deduced from the iodine experiments would be  $G(\text{cyclohexyl radicals}) = 4.0$ , a value appreciably smaller than that deduced from the oxygen and vacuum experiments. These results are consistent with the above mechanism, if it is assumed that the H-atoms react with iodine, thereby eliminating reaction 2 and effectively decreasing the yield of cyclohexyl radicals by one-half. Schuler<sup>19</sup> has cautioned against the use of iodine as a radical counter at concentrations greater than  $10^{-3} M$ . In the liquid butane system, however, the yields of  $\text{C}_1$  to  $\text{C}_4$  radicals were independent of iodine concentrations from  $10^{-3} M$  to above  $10^{-2}$ .<sup>20</sup> It is concluded therefore that the yield of cyclohexyl iodide is a measure of the cyclohexyl radical yield from reaction 1. Since it is postulated that reaction 2 is eliminated by iodine, then the total yield of cyclohexyl radicals would be 8 (in absence of iodine) in approximate agreement with the results obtained in the presence and absence of oxygen.

The residual yield of cyclohexene in the presence of iodine is consistent with the suggested molecular reaction (1a). This conclusion is contrary to that of Burton, *et al.*,<sup>7</sup> who have suggested that iodine

(18) R. W. Fessenden and R. H. Schuler, *THIS JOURNAL*, **79**, 273 (1957).

(19) R. H. Schuler, *THIS JOURNAL*, **62**, 37 (1958).

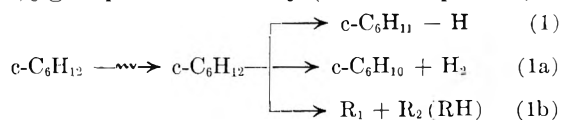
(20) C. E. McCauley and R. H. Schuler, *J. Am. Chem. Soc.*, **79**, 4008 (1957).

acts to suppress the molecular formation of cyclohexene.

**Effect of Temperature.**—The effect of temperature on the radiolysis of cyclohexane was examined at room temperature and at liquid nitrogen temperature. There was little effect of temperature on the cyclohexene formation (Fig. 1, crosses) and only a small effect, if any, on the formation of dicyclohexyl (Fig. 2, crosses). The formation of methylcyclopentane and the  $\text{C}_6$  hydrocarbon product also appeared to be independent of temperature. These results are consistent with the recent results of Burton, *et al.*,<sup>5</sup> showing that the hydrogen yield is independent of temperature.

### Conclusion

The major products formed in the radiolysis of liquid cyclohexane result from C-H bond cleavage without rupture of the ring. A minor amount of product results from fragmentation and isomerization of the ring system. These results are qualitatively consistent with mass spectrometric studies of cyclohexane which show high stability for the parent molecule-ion. The role of molecule-ion reactions in the condensed phase is, at the present time, largely a matter of speculation. The present results are consistent with a mechanism which involves the formation and decomposition of excited cyclohexane molecules. Reaction 1b is included to represent the small amounts of products which result from ring fragmentation and isomerization reactions. The present results show that of the excited molecules that decompose approximately 15% give products directly (molecular process).



**Acknowledgments.**—The author is indebted to J. S. Balwit for the electron irradiations and to E. H. Winslow for considerable assistance with the gas chromatography. The author is indebted to the referee for calling attention to the paper by Burton and Meshitsuka, *Radiation Research*, **9**, 152 (1958), to be cited in support of the production and scavenging of H-atoms.

# STUDIES ON FORMATION AND AGING OF PRECIPITATES. XLVI. PRECIPITATION OF LEAD SULFATE AT ROOM TEMPERATURE<sup>1,2</sup>

BY I. M. KOLTHOFF AND B. VAN'T RIET

*Contribution from the School of Chemistry of the University of Minnesota, Minneapolis, Minn.*

*Received December 27, 1958*

Lead sulfate crystals were precipitated by rapid mixing of solutions of lead perchlorate and alkali sulfates or sulfuric acid of varying concentrations in polyethylene beakers. Except with potassium sulfate sharp maxima in particle size were found at intermediate supersaturations. In equimolar lead perchlorate-sulfate suspensions the maximum occurred at the following concentrations of lead sulfate:  $6.4 \times 10^{-3} M$  with sodium,  $6.2 \times 10^{-3} M$  with lithium,  $6.6 \times 10^{-3} M$  with ammonium sulfate,  $7.0 \times 10^{-3} M$  with sodium bisulfate, and  $6.9 \times 10^{-3} M$  with sulfuric acid. At lead sulfate concentrations greater than those at the maximum the particle size and the relative degree of perfection decreased rapidly, while the specific surface determined by the radioactive method increased sharply. Specific surfaces of highly imperfect crystals were determined by the radioactive method in a medium of 60–90% ethanol. The same results in exchange experiments were found using radioactive sulfate ( $S^{35}O_4$ ) and lead ( $Pb^{210}$ ). A plot of the log of the induction period  $t$  versus the log of the molar concentration  $c_i$  of lead sulfate was found to be composed of three straight lines, indicating that the usual relation:  $\log t = \text{constant} - x c_i^n$ , does not hold for lead sulfate. At the high supersaturations used in the present study the nucleation reaction rate increases greatly toward the end of the induction period, a result which is in contrast to a homogeneous nucleation reaction as the only source of formation of nuclei.

In recent years many studies have been made of the kinetics of precipitation of slightly soluble salts at relatively low supersaturations. O'Rourke and Johnson<sup>3</sup> reviewed the theories of nucleation and crystal growth under these conditions. Their conclusion is that nucleation occurs as a homogeneous reaction in relatively weakly supersaturated solutions. Systematic studies on solutions of very high degree of supersaturation are lacking in the literature. Christiansen and Nielsen<sup>4</sup> determined induction periods in highly supersaturated solutions of barium sulfate and of silver chromate, but their interpretation assuming homogeneous nucleation is not supported by other experimental evidence, as was shown in a recent study by Nielsen.<sup>5</sup> Results on the precipitation of lead sulfate described in the present paper are also contrary to homogeneous nucleation at relatively large supersaturations.

The solubility of lead sulfate is more than ten times greater than that of barium sulfate and a wide range of supersaturations can be studied in the precipitation of lead sulfate. In our study supersaturated solutions of lead sulfate were prepared by rapid mixing under conditions of rapid stirring of equimolar solutions of sulfates and lead perchlorate. Under standardized and reproducible conditions of precipitation the effect of concentration and of the specific nature of the reactants on the characteristics of the precipitates was studied. The habit of crystalline fresh precipitates was observed microscopically and the approximate size estimated from these observations. Specific surfaces were determined by a modification of the method of Paneth<sup>6</sup> using exchange with the radioactive isotopes  $Pb^{210}$  and  $S^{35}O_4$ . Also, the apparent degree of perfection was determined by measuring the apparent rate of exchange of aqueous sus-

pensions of the precipitates with solutions containing radioactive lead or sulfate.

Induction periods were determined in two different ways. In one method the time elapsed before appearance of a precipitate was determined. The other method is novel and based on the fact that the dye wool violet is strongly coprecipitated with lead sulfate. Wool violet was added to the supersaturated solutions of lead sulfate at various periods of time after mixing of the reactants. When the dye was added during the induction period a maximum amount of dye was found in the crystals. This amount decreased when the dye was added after the induction period. Only surface adsorption was observed when the dye was added after complete formation of the crystalline precipitate. Thus the curve giving the amount of wool violet in a given weight of lead sulfate plotted vs. time of addition after mixing gives a measure of the induction period and of the time of completion of crystallization.

## Experimental

**Chemicals.**—Merck Analytical Reagent grade potassium, sodium and ammonium sulfates were used to prepare 0.05  $M$  stock solutions in twice distilled water. These were filtered through fine glass filters before use in precipitation experiments. "Chemically pure" lithium sulfate of Riedel de Haen and anhydrous sodium perchlorate of G. F. Smith Co. were used to make stock solutions 0.10 and 2.00  $M$ , respectively, in these reagents.

Lead perchlorate was prepared according to the directions of Hershenson, *et al.*<sup>7</sup> Reagent grade yellow lead oxide of General Chem. Co. was used to neutralize 70% Baker Analytical Reagent grade perchloric acid. After filtration through a fine glass filter the solution appeared to be strongly buffered at pH ca. 5.0. Perchloric acid was added to lower the pH to 3.0 and then the solution was diluted to a concentration of 1  $M$  in lead. Unless otherwise stated all reactant solutions were acidified to a pH of 3.0 with perchloric acid.

**Radioactive Materials.**— $Pb^{210}$  (Ra-D) was separated from deposits in old radon bulbs in which this lead isotope accumulates. The deposits were dissolved in a mixture of dilute nitric and hydrofluoric acid. After adjusting the pH to 2 with dilute sodium hydroxide, Ra-E and Ra-F were removed by extracting twice with 0.005% dithizone in carbon tetrachloride. Extraction of lead is insignificant at this pH. The aqueous layer containing Ra-D was adjusted to pH 10.5 with 1  $N$  ammonia. After addition of citrizon the lead dithizonate was extracted at this pH in carbon

(1) From a Doctor's Thesis, submitted by Bartholomeus van't Riet to the Graduate School of the University of Minnesota, 1957. Presented before the 134th A.C.S. Meeting, September, 1958, Chicago, Ill.

(2) This investigation was supported by a grant from the Office of Ordnance Research.

(3) J. D. O'Rourke and R. A. Johnson, *Anal. Chem.*, **27**, 1699 (1955).

(4) J. A. Christiansen and A. E. Nielsen, *Acta Chim. Scand.*, **5**, 673 (1951).

(5) A. E. Nielsen, *J. Colloid Sci.*, **10**, 576 (1955).

(6) F. Paneth, *Z. Elektrochem.*, **28**, 113 (1922).

(7) H. M. Hershenson, M. E. Smith and D. N. Hume, *J. Am. Chem. Soc.*, **75**, 507 (1953).

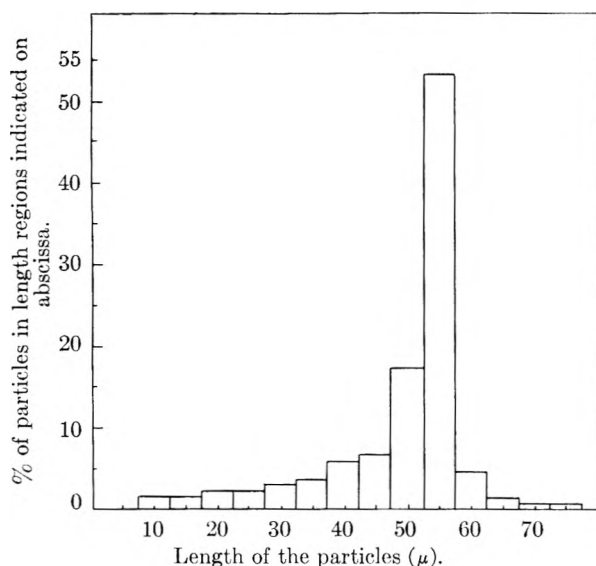


Fig. 1.—Size distribution of lead sulfate crystals.

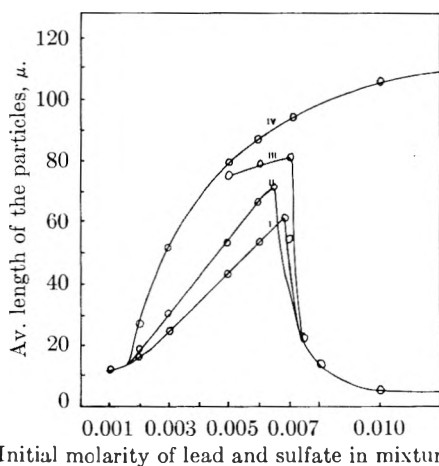


Fig. 2.—Relation between particle size and concentration in mixtures of solutions of lead perchlorate and of various sulfate: I,  $H_2SO_4$ ; II,  $Na_2SO_4$ ; III,  $NaHSO_4$ ; IV,  $K_2SO_4$ .

tetrachloride, from which the lead was extracted again with aqueous 0.1 *N* perchloric acid. The extractions were done a short time before each experiment.

$Pb^{210}$  has a half-life of 22 years; it decays to  $Bi^{210}$ . The  $\beta$ -particles given off are too soft to be measured with an ordinary Geiger counter. The daughter element  $Bi^{210}$  decays with a half-life of 5 days to  $Po^{210}$ ;  $\beta$ -particles of high energy are emitted which can be measured with a Geiger counter. In exchange experiments using  $Pb^{210}$  the quantity of this isotope can be measured by determination of the equilibrium concentration of  $Bi^{211}$  in the sample. This build-up requires a waiting period of 15 days at least. Correction was made for non-attainment of equilibrium.

Radioactive  $S^{35}$  was obtained from Oak Ridge in the form of  $H_2S^{35}O_4$  in 0.4 ml. of 0.89 *N* hydrochloric acid (no inactive sulfur). The half-life of  $S^{35}$  is 87.1 days ( $\beta$ -decay). The energy of the  $\beta$ -particles is 0.167 Mev., and sufficiently high to be measured with the Geiger counter. The activity of the solution was 10 mcuries on arrival. The solution was diluted 10,000-fold with twice distilled water. The low concentration of sulfuric acid in the stock solution eliminated the possibility of precipitation of lead sulfate on addition of the radioactive solution to saturated solutions of lead sulfate, even if they contained a large excess of lead ions.

**Microscopic and Radioactive Measurements.**—Precipitates were observed under a Spencer microscope and photographs were made using a Bausch and Lomb eyepiece camera. Length measurements on crystals were made, using a Leitz micrometer eyepiece which was calibrated with a grating on a slide.

Radioactivity of solutions was measured after evaporation by exposure to infrared radiation of a neutralized aliquot portion. Counting was done using a thin mica window Geiger counter TCG2-1B-84 connected to a conventional scaler unit.

**Method of Precipitation.**—In order to get reproducible precipitates the reactant solutions must be mixed rapidly. Generally 50 ml. of each solution (*pH* 3.0) was used to give the reported concentrations in the mixtures. Either the sulfate or the lead solution was poured within one second into the other reactant solution from graduates of 50 ml. content. Rapid mixing was carried out in a 450-ml. polyethylene beaker in which a perpendicularly bent silicone coated glass rod was stirred at a rate of 500 r.p.m. In experiments in which the concentrations of lead and sulfate exceeded 0.05 *M* in the mixture the sulfate solution was poured within one-half of a second into the lead solution from a 50-ml. beaker, or *vice versa*. With rapid mixing no difference in the properties of the crystals was observed between "direct" and "reverse" precipitation.

Generally the experiments were carried out at  $25 \pm 0.1^\circ$ . Crystal growth was allowed to proceed in stirred mixtures of the reactants. When the concentration of the reactants was greater than  $2.5 \times 10^{-3}$  *M* the precipitation was virtually complete within 5 minutes and the precipitate then was examined under the microscope.

Under the specified experimental conditions deviations from mean particle length were found to be small. As an example, a size distribution curve is illustrated in Fig. 1. The precipitate was formed from a mixture  $5 \times 10^{-3}$  *M* in sodium sulfate and  $5 \times 10^{-3}$  *M* in lead perchlorate under the specified conditions.

Appreciable deviations from mean size were observed if precipitation occurred in non-stirred solutions, or when glass beakers, or even silicone coated glass beakers were used. Precipitates in glass beakers contained agglomerates of very small crystals, which prohibited a precise count.

**Change of Supersaturation During Crystal Growth.**—The following methods were used.

(a) At a given time after mixing the supersaturation was suddenly decreased to saturation conditions by addition of a complexing agent, *e.g.*, E.D.T.A., acetate or by dilution with 0.001 *N* perchloric acid solution.

(b) At a given time after mixing the supersaturation was suddenly increased to a value at which a different crystal habit is observed upon direct mixing.

**Effect of *pH*.**—Because appreciable hydrolysis to basic lead salt occurs in unacidified lead perchlorate solutions, the effect of *pH* on particle size was studied in mixtures of solutions of lead perchlorate and sodium sulfate. Pronounced variations in size were observed with mixtures of *pH* higher than 3.2. Unless stated otherwise the *pH* of the mixtures was 3.0.

## Results

**Particle Length as a Function of the Concentration of the Reactants.**—Mixtures of solutions of lead perchlorate and of sulfuric acid or alkali sulfate were made in concentrations varying from 0.001 to 0.1 *M* lead and sulfate in the mixtures. After precipitation from stirred solutions the length of the crystals was measured. Some of the results are presented graphically in Fig. 2.

Under the same conditions the curves in Fig. 2 obtained with lithium and ammonium sulfate, sodium bisulfate and sulfuric acid were very similar to those found with sodium sulfate. At a concentration of  $1.25 \times 10^{-3}$  *M* rhombohedra were observed (Fig. 3A). Increasing the concentration to  $2.5 \times 10^{-3}$  *M* (Fig. 3B) and  $5 \times 10^{-3}$  *M* (Fig. 3C) resulted in a deformation of the rhombohedra to rectangular crosses with preferred growth in one direction, while an increase to  $6 \times 10^{-3}$  *M* with sodium sulfate as a precipitant produced crystals composed of obtuse angle crosses which reached a maximum length at a concentration of  $6.4 \times 10^{-3}$  *M* (Fig. 3D). The length decreased sharply with increasing con-

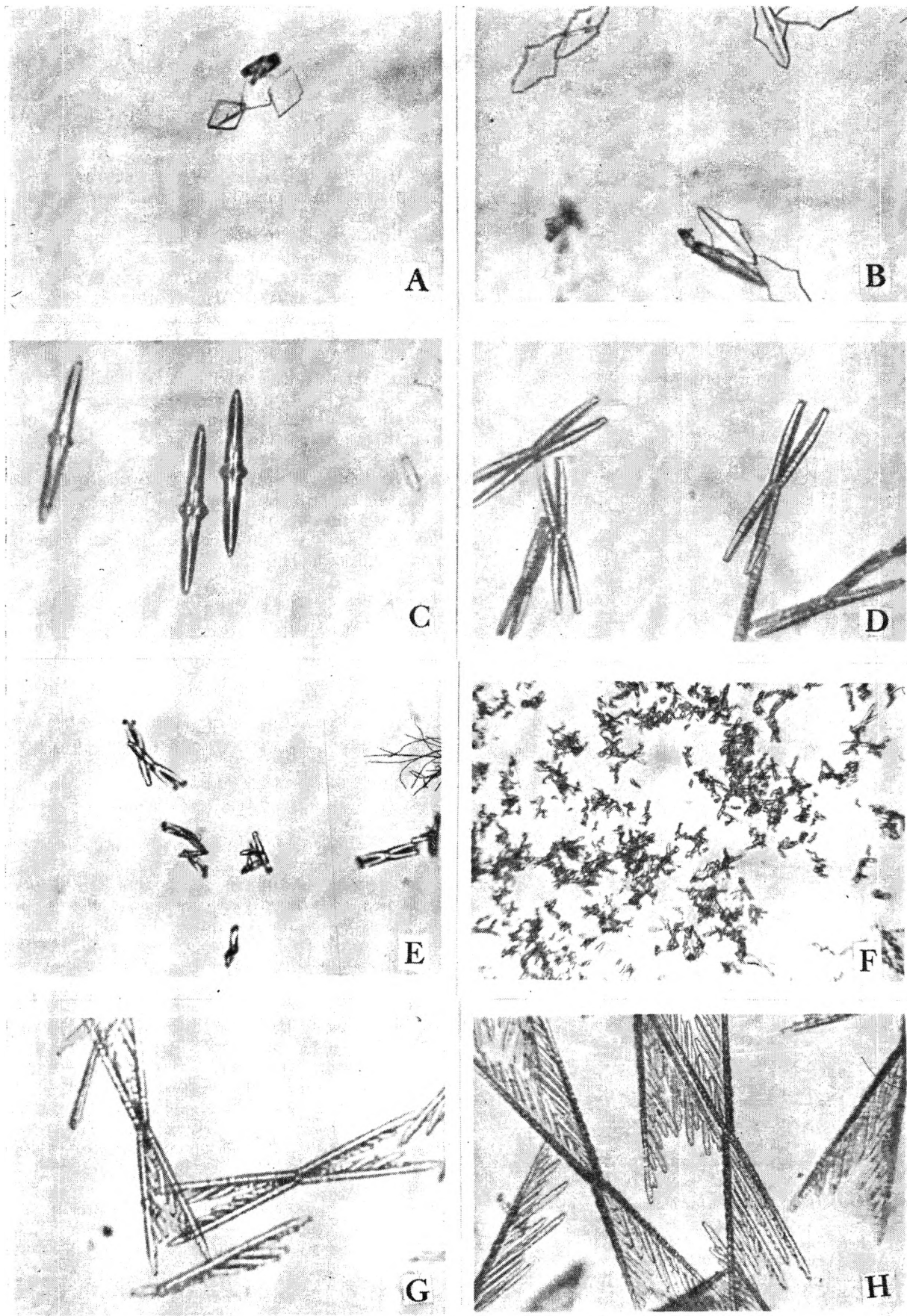


Fig. 3.—Photographs of lead sulfate crystals, 530X; the concentration and kind of reactants are given in text.

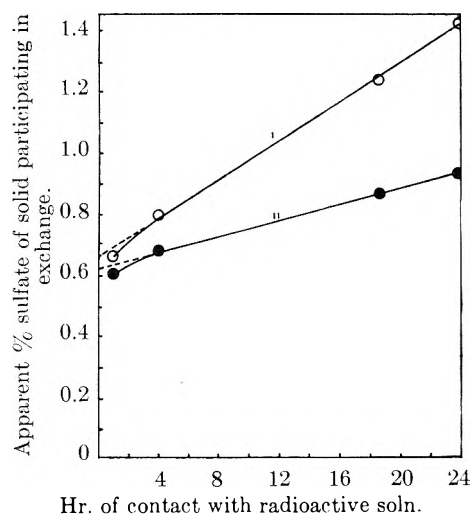


Fig. 4.—Exchange between 205 mg. of lead sulfate and 50 ml. of  $5.0 \times 10^{-5} M$  sulfuric acid: I, solution 80% ethanol; II, solution 90% ethanol.

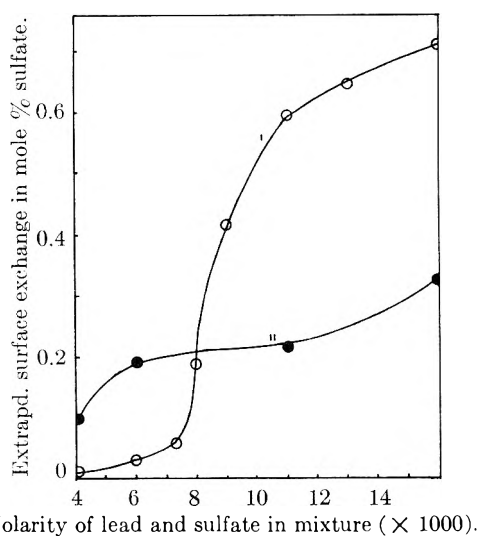


Fig. 5.—Surface exchange of lead sulfate as a function of the concentration in the precipitation mixtures: I,  $\text{Na}_2\text{SO}_4$ ; II,  $\text{K}_2\text{SO}_4$ .

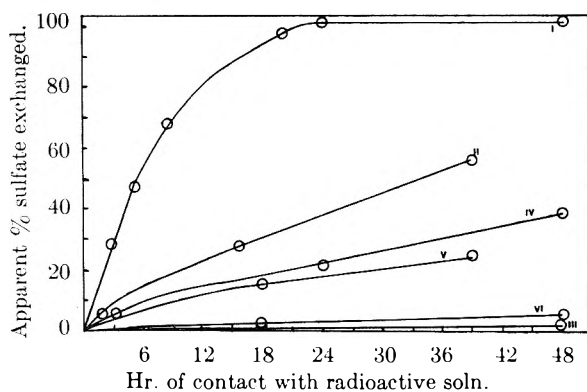


Fig. 6.—Apparent rate of exchange between lead sulfate and aqueous solutions of sodium sulfate. Precipitates from mixtures of solutions of sodium sulfate and lead perchlorate of the following concentrations in the mixture: I, 0.01; II, 0.0075; III, 0.0063  $M$ . Mixtures of potassium sulfate and lead perchlorate solutions were used of the following concentrations in the mixture: IV, 0.01; V, 0.005; VI, 0.003  $M$ .

centration (Fig. 3E:  $7 \times 10^{-3} M$ ; F: 0.01  $M$  lead sulfate).

With potassium sulfate as a precipitant no sharp maximum in particle length was found (curve IV, Fig. 2). Also, the crystal habit was different from those observed at the same lead sulfate concentration with the other sulfates. Figure 3G and H show crystals from solutions  $5 \times 10^{-3} M$  and 0.01  $M$  in lead sulfate, respectively, with potassium sulfate as the precipitant. Crystals from solutions of the same lead sulfate concentrations, but with sodium sulfate as the precipitant, are reproduced in Fig. 3C and F, respectively.

**Specific Surface of Fresh Precipitates.**—The radioactive method of determining the specific surface of lead sulfate in equilibrium with its saturated solution originates with Paneth.<sup>6</sup> Extensive studies by Kolthoff and Rosenblum<sup>8</sup> on the exchange of radioactive lead between lead solutions and solid lead sulfate showed that as a result of recrystallizations the extent of exchange becomes greater than that which corresponds to the original surface and it increases with time of shaking. In order to minimize the effect of recrystallization the exchange experiments were carried out in media which were 60–90% in ethanol.

The apparent exchange was calculated from the following relationship

$$\text{apparent \% exchange} = \frac{M_{\text{sol}}}{M_{\text{prec}}} \times \frac{A_0 - A_t}{A_t} \times 100$$

( $M_{\text{sol}}$  = mmoles of tagged lead or sulfate in solution which contains all the initial radioactivity;  $M_{\text{prec}}$  = mmoles of solid lead sulfate;  $A_0$  = initial activity of an aliquot portion of solution;  $A_t$  = activity of a same aliquot of solution after time  $t$ ). As an example, the variation with time of the extent of exchange between 205 mg. of a 20 minutes old precipitate separated from a mixture which was  $12 \times 10^{-3} M$  in lead sulfate (with sodium sulfate as precipitant) and 50 ml. of  $5.00 \times 10^{-5} M$  radioactive sulfuric acid in 80 and 90% ethanol, respectively, is given in Fig. 4. Because of rupture of crystals upon continuous shaking of the suspensions during exchange experiments the vessels containing crystals and radioactive solution were swirled repeatedly by hand for a few seconds before centrifugation and sampling of the supernatant liquid for activity measurements. The exchange extrapolated to time zero (Fig. 4) yielded a surface corresponding to 0.66 and 0.63 mole % of sulfate in 80 and 90% alcohol, respectively.

It is of interest to mention that the same values were found when radioactive lead instead of sulfate was used in the same alcoholic media containing radioactive lead as lead perchlorate. This result has been found with all precipitates tested and agrees with results obtained by Stow and Spinks<sup>9</sup> with lead sulfate.

Specific surfaces of 20 minutes old precipitates obtained with sodium and potassium sulfate respectively as precipitants from mixtures containing

(8) I. M. Kolthoff and C. Rosenblum, *J. Am. Chem. Soc.*, **55**, 2656 (1933); **56**, 1264, 1658 (1934); **57**, 597, 607, 2573, 2577 (1935); **58**, 116, 171 (1936).

(9) R. M. Stow and J. W. T. Spinks, *Canadian J. of Chem.*, **33**, 938 (1955).

varying amounts of lead sulfate are given in Fig. 5. The differences between sodium and potassium sulfate are given in Fig. 5. The difference between sodium and potassium sulfate is strikingly noticeable. Varying the initial concentration of lead sulfate from 0.005 to 0.01 *M* gave a surface exchange of 0.030 and 0.59 mole % of the solid, respectively, with sodium sulfate and of 0.19 and 0.22% with potassium sulfate as precipitant. This large difference in specific surface of crystals obtained with either sodium or potassium sulfate as precipitant is in qualitative agreement with the results presented in Figs. 2 and 3.

**Degree of Perfection of Precipitates.**—Debye-Scherrer X-ray photographs of crystals formed at all concentrations of reactants gave the normal pattern of orthorhombic lead sulfate. In order to distinguish between different degrees of perfection of crystals obtained at different supersaturations the rate of exchange between radioactive sulfate or lead in solution and solid lead sulfate was determined. After establishment of surface equilibrium the rate of additional exchange is a measure of the rate of recrystallization which indicates the relative degree of perfection of the crystals.

In comparing rates of exchange of various precipitates the weight of precipitate, volume and concentration of the radioactive solutions and method of treatment were kept the same. Under these conditions the surface areas exposed to the solution by the precipitates are different because the specific surface of the various precipitates is different.

Rates of exchange were determined using 0.65 mmole of lead sulfate and 50 ml. of an aqueous solution  $10^{-3}$  *M* in tagged sodium sulfate and  $10^{-3}$  *M* in perchloric acid. After completion of precipitation the crystals were separated by centrifugation, washed twice with  $10^{-3}$  *M* perchloric acid and once with inactive  $10^{-3}$  *M* sodium sulfate solution. The centrifuged precipitates were 20 minutes old before being in contact with the radioactive solution. The mixtures were shaken in 100-ml. bottles in a horizontal shaker with a stroke of 4 cm. The exchange as a function of time is given in Fig. 6 for a variety of precipitates. Exchange with precipitates from solutions 0.005 *M* in lead perchlorate and in sodium sulfate was only 0.5 mole % sulfate after 3 days.

Rates of exchange also were determined between lead sulfate and  $10^{-3}$  *M* tagged lead perchlorate in aqueous  $10^{-3}$  *M* perchloric acid. In these experiments the final washing of the crystals was made with inactive 0.001 *M* lead perchlorate instead of sodium sulfate solution. Rates of exchange were approximately the same as those found in sodium sulfate solutions containing radioactive sulfur.

Precipitates from mixtures 0.01 *M* in lead perchlorate and 0.01 *M* in sodium sulfate gave 100% exchange after 24 hours of contact between crystals and solution. Portions of this precipitate were aged for four hours in various media and the rate of exchange determined. The results, plotted in Fig. 7, show that aging is promoted by increasing concentration of sulfate in the aging medium while an excess of 0.01 *M* lead inhibits the aging.

The influence of adsorbed wool violet on the rate

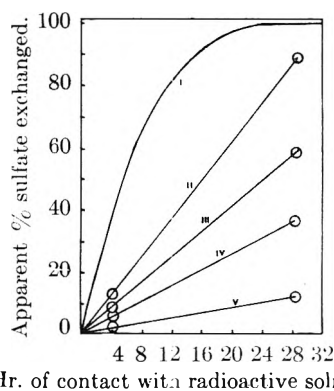


Fig. 7.—Effect of aging on the rate of exchange: I, fresh precipitate (20 minutes old); II, III, IV and V, exchange after 4 hours of aging in the following media, respectively; II, 0.01 *M* lead perchlorate; III, saturated lead sulfate in 0.001 *M* perchloric acid; IV, 0.011 *M*; V, 0.10 *M* sodium sulfate.

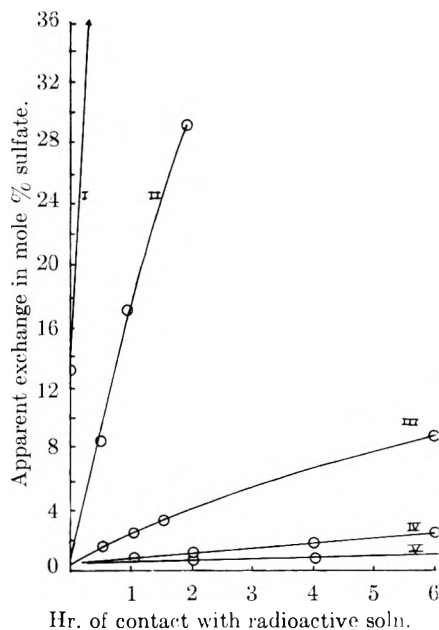


Fig. 8.—Exchange in the presence of the dye wool violet: I, no wool violet; II, 6 mg. W. V./liter (adsorption 17% of saturation value); III, 30 mg. W. V./liter (adsorption 45% of saturation value); IV, 90 mg. W. V./liter (adsorption 78% of saturation value); V, 200 mg. W. V./liter (adsorption 100% surface saturation, the adsorption was 4.55 mg. W. V./g. lead sulfate).

of exchange was determined by addition of varying amounts of the dye to the suspension before adding radioactive sulfate. These experiments were done in aqueous solutions and the measurements of small rates of exchange in sulfate exchange experiments could be done accurately only in solutions with low concentrations of sulfate. The precipitates were prepared by mixing 33.5 ml. of 0.022 *M* lead perchlorate with 33.5 ml. of 0.02 *M* sodium sulfate (*pH* 3.0). Two minutes after mixing and stirring wool violet solution (4 g. of W. V./liter) was added in varying amounts. Five minutes after W. V. addition and stirring the solution was made radioactive by addition of 0.6 ml. of  $H_2S^*O_4$  stock solution and the exchange was determined after various periods of time. From the results in Fig. 8 it is clear that

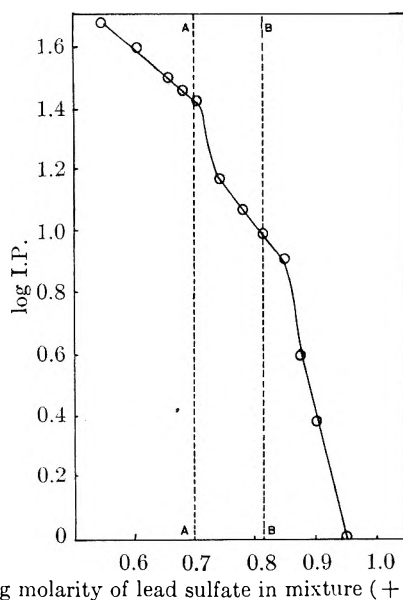


Fig. 9.—Induction periods in precipitation of lead sulfate with sodium sulfate as precipitant.

even very small amounts of W. V. inhibit exchange. However, in agreement with previous results<sup>10</sup> complete coverage of the surface with dye is necessary to prevent exchange as a result of recrystallization.

**Induction Periods (I.P.).**—In determinations of the I.P. at relatively high concentrations the wool violet method was found to give practically the same results as observations of the first appearance of turbidity. The W. V. method was very useful in determination of I. P. in solutions of relatively low supersaturations. In those cases it was difficult to observe the exact time of turbidity in the opaque polyethylene beaker.

In Fig. 9 the log of I.P. in seconds is plotted *vs.* the log of concentration of  $\text{PbSO}_4$  in the original mixtures of lead perchlorate and sodium sulfate. The reproducibility of the determinations was  $\pm 0.5$  second up to I.P.'s of 10 seconds; longer I. P.'s were measured with a precision of  $\pm 5.0\%$ . The supersaturated mixtures were prepared from the same stock solutions of reactants which had a *pH* of 2.8. At concentration A in Fig. 9 the shape of the crystals changes from rectangular to obtuse angle crosses. At concentration B the maximum particle length is attained.

The following empirical relations are derived from Fig. 9: rectangular crosses are formed ( $c_1$  varies between  $3$  and  $5 \times 10^{-3} M$ )

$$\text{I.P.} = k_1 \times c_1^{-n_1}; n_1 = 1.7 \pm 0.07$$

Obtuse angle crosses are formed ( $c_1$  between  $5$  and  $6.8 \times 10^{-3} M$ )

$$\text{I.P.} = k_2 \times c_1^{-n_2}; n_2 = 2.8 \pm 0.15$$

Rapid decrease of particle length with increase of  $c_1$  ( $c_1$  greater than  $6.8 \times 10^{-3} M$ )

$$\text{I.P.} = k_3 \times c_1^{-n_3}; n_3 = \text{approximately } 8.0$$

The molar concentration of lead sulfate in the original mixture is denoted by  $c_1$ .

(10) I. M. Kolthoff and C. Rosenblum, *J. Am. Chem. Soc.*, **57**, 607 (1935).

**Sudden Changes of Supersaturation during Precipitation.**—Supersaturated solutions of lead sulfate were diluted rapidly during and after the induction. A mixture which was  $0.0075 M$  in both lead perchlorate and sodium sulfate had an I. P. of 4.5 seconds. The resulting crystals had a length of about  $10 \mu$ . When the mixture was diluted rapidly 2 to 3 seconds after preparation to a concentration of  $0.005 M$  lead sulfate the length of the crystals was  $55 \mu$  after complete precipitation, the same length as of crystals precipitated from a mixture which was originally  $0.005 M$  in lead sulfate. When the  $0.0075 M$  mixture was diluted to  $0.05 M$  4 seconds after its preparation the crystal length was  $30 \mu$ , and when diluted after 4.5 or more seconds approximately  $10 \mu$  in length. Therefore, dilution after termination of the induction period did not affect the size of the crystals.

The effect of sudden increase or decrease of supersaturation on crystal habit was studied by making solutions more or less supersaturated after the induction period. The crystals present at the end of the induction period formed the center of crystals on which additional growth took place in directions found at original supersaturations identical with the supersaturation after the sudden change. For details on these experiments and photographs the reader is referred to the thesis of the junior author.<sup>1</sup>

### Discussion

The interesting observation can be made that the center of all the crystals has the habit of a rhombohedron. At low supersaturations the final crystals are composed of more or less perfect rhombohedra (Fig. 3A). With increasing supersaturation the rate of crystal growth increases and rectangular crosses are observed (Fig. 3B and C). When the supersaturation is further increased, using sodium sulfate as precipitant, another preferred growth is observed, resulting in the formation of obtuse angle crosses which reach a maximum length at an original concentration of  $6.4 \times 10^{-3} M$  in lead sulfate (Fig. 3D) in the original mixture. This concentration for maximum length is sharply defined and is equal to  $6.2 \times 10^{-3} M$  with lithium sulfate,  $6.6 \times 10^{-3} M$  with ammonium sulfate,  $7.0 \times 10^{-3} M$  with sodium bisulfate, and  $6.9 \times 10^{-3} M$  with sulfuric acid. Above this concentration the rate of formation of nuclei becomes so great that the size of the crystals decreases sharply, but they are obtuse angle crosses, or mixtures of these with needles.

Dilution of a precipitating mixture before the end of the induction period affects the crystal size. The size corresponds closely to that observed when the original mixture was at the same concentration as the diluted mixture. This is no longer true when dilution occurs just before, or at, or after the end of the induction period. These results indicate that the majority of nuclei are formed in the later stages of the I. P. and that under our experimental conditions of high supersaturation the homogeneous nucleation cannot be the only source of formation of nuclei. Apparently, nuclei formed during the I. P. promote the formation of new nuclei.

From Fig. 9 it is evident that the usually valid relation between induction period  $t$  and the concen-

tration  $c_i$  of lead sulfate in the original mixture:  $t = \text{constant} \times c_i^n$  does not hold. In the concentration range between 3 and  $5 \times 10^{-3} M$   $n$  is 1.7, it increases to 2.8 in the region between 5 and  $6.8 \times 10^{-3} M$  (maximum particle length in Fig. 2) and it becomes about 8 at higher concentrations. Nielsen<sup>5</sup> plotted all the known data for the relation between  $\log t$  and  $\log$  concentration in the precipitation of barium sulfate. It is of interest to note that this plot was also composed of three straight lines, although the slopes varied in a different way from those in Fig. 9. This complicated relationship is probably accounted for by the fact that the induction period involves both a rate of nucleation and a rate of growth and that the order of growth reaction varies with the concentration of lead sulfate in the supersaturated solution.

With potassium sulfate as a precipitant the ob-

servations are quite different from those with the other sulfates studied. Potassium sulfate can form a double salt with lead sulfate<sup>11</sup> and at higher concentrations double salt formation may account for the different behavior found with potassium sulfate as a precipitant. While not reported in the experimental part it may be mentioned that the effect of potassium also is observed when part of the sodium sulfate is replaced with potassium sulfate. If lead perchlorate is replaced with lead nitrate, similar particle length curves are obtained as described in the present paper with deviating behavior of potassium sulfate from the other sulfates studied.

Acknowledgment is made to Dr. P. R. O'Connor for help in the performance of radioactive measurements, and to Dr. K. R. Lawless for help in making the photographs.

(11) M. Randall and D. L. Shaw, *ibid.*, **57**, 427 (1935).

## REDUCTION OF DICHROMATE ION BY THALLOUS ION INDUCED BY $\gamma$ -RADIATION

By THOMAS J. SWORSKI<sup>1</sup>

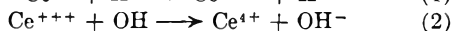
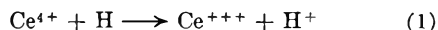
Chemistry Division, Oak Ridge National Laboratory,<sup>2</sup> Oak Ridge, Tennessee

Received December 27, 1958

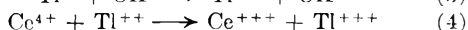
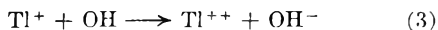
Reduction of dichromate ion in air-saturated 0.4  $M$  sulfuric acid is induced by  $\gamma$ -radiation with  $G(\text{Cr}^{+++}) = \frac{1}{3}[2G_{\text{H}_2\text{O}_2} + G_{\text{H}} - G_{\text{OH}}]$ .  $G(\text{Cr}^{+++})$  is increased to  $\frac{1}{3}[2G_{\text{H}_2\text{O}_2} + G_{\text{H}} + G_{\text{OH}}]$  by addition of thallos ion. Thallos ion is oxidized by OH radical yielding thallium(II) ion which reduces dichromate ion with concomitant production of thallic ion. Neither dichromate ion nor the intermediate chromium(V) and chromium(IV) ions oxidize thallos ion to thallium(II) ion. Chromic ion at concentrations as high as  $10^{-2} M$  has no measurable effect on  $G(\text{Cr}^{+++})$  either in the presence or absence of thallos ion at concentrations as low as  $10^{-4} M$ . The specific reaction rate  $k_{\text{Cr}^{+++}, \text{OH}}$  is so low that (a) chromic ion at concentrations as high as  $10^{-2} M$  does not measurably decrease  $G_{\text{H}_2\text{O}_2}$  and (b)  $k_{\text{TI}^+, \text{OH}}/k_{\text{Cr}^{+++}, \text{OH}}$  cannot be evaluated even with values as high as 100 for  $(\text{Cr}^{+++})/(\text{TI}^+)$ .

### Introduction

$G(\text{Ce}^{+++})$ <sup>3</sup> for the reduction of ceric ion in sulfuric acid solutions has been postulated<sup>4</sup> to be equal to  $2G_{\text{H}_2\text{O}_2} + G_{\text{H}} - G_{\text{OH}}$  according to a mechanism in which H atom reduces ceric ion and OH radical oxidizes cerous ion



This mechanism was evidenced<sup>5</sup> by concomitant oxidation of radioactive cerous ion during reduction of ceric ion.  $G(\text{Ce}^{+++})$  is increased<sup>6,7</sup> to  $2G_{\text{H}_2\text{O}_2} + G_{\text{H}} + G_{\text{OH}}$  by addition of thallos ion according to the sequence of reactions



The oxidation of radioactive chromic ion during

(1) Union Carbide Nuclear Company, P. O. Box 324, Tuxedo, New York.

(2) Operated for the United States Atomic Energy Commission by Union Carbide Nuclear Company.

(3) The 100 e.v. yields of the intermediates H, OH, H<sub>2</sub> and H<sub>2</sub>O<sub>2</sub> are denoted by  $G_{\text{H}}$ ,  $G_{\text{OH}}$ ,  $G_{\text{H}_2}$  and  $G_{\text{H}_2\text{O}_2}$ . The 100 e.v. yield of products of irradiation is denoted by  $G(\text{product})$ .

(4) A. O. Allen, *Radiation Research*, **1**, 85 (1954).

(5) G. E. Challenger and B. J. Masters, *J. Am. Chem. Soc.*, **77**, 1063 (1955).

(6) T. J. Sworski, *ibid.*, **77**, 4689 (1955).

(7) T. J. Sworski, *Radiation Research*, **4**, 483 (1956).

reduction of dichromate ion has been presented<sup>8</sup> as evidence that the mechanisms for reduction of dichromate ion and ceric ion are identical. To further elucidate the mechanism for reduction of dichromate ion, the radiation chemistry of thallos dichromate solutions was investigated.

### Experimental Procedure

Water was purified by a procedure previously established<sup>9</sup> in this Laboratory. The purest chemicals available were used without further purification. Solutions were irradiated with cobalt  $\gamma$ -radiation of homogeneous intensity distribution provided by a cylindrical source.<sup>10</sup> A 2-cm. cylindrical cell could be placed inside of the source positioner of the cobalt source.<sup>10</sup> The rate of energy absorption in solution was determined by use of the ferrous sulfate dosimeter in the same irradiation cell.  $G(\text{Fe}^{+++})$  of 15.6 was determined<sup>11</sup> for the dosimeter by a calorimetric calibration in this Laboratory.

Dichromate ion reduction as a function of energy absorbed was followed in each solution through use of intermittent exposures. The optical density of the dichromate ion solution in the irradiated cylindrical cell was measured after each period of irradiation with a Cary model 11 recording spectrophotometer. Cylindrical cells were obtained from

(8) M. Lefort and M. Lederer, *Compt. rend.*, **242**, 2458 (1956).

(9) C. J. Hochanadel, *This Journal*, **56**, 587 (1952).

(10) J. A. Ghormley and C. J. Hochanadel, *Rev. Sci. Instr.*, **22**, 473 (1951).

(11) C. J. Hochanadel and J. A. Ghormley, *J. Chem. Phys.*, **21**, 880 (1953).



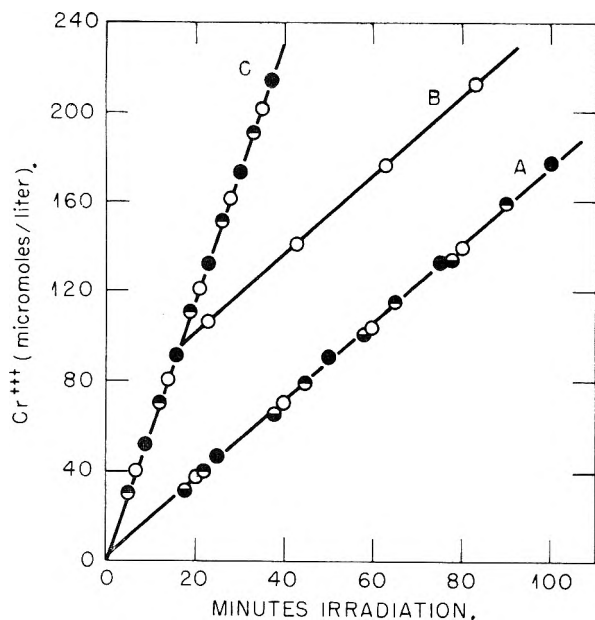


Fig. 1.—Effect of  $\text{Cr}^{+++}$  and  $\text{Tl}^+$  concentrations on the reduction of chromium(VI) ions in air-saturated 0.4  $M$  sulfuric acid. Initial  $\text{Cr}^{+++}$  concentrations were: ●,  $10^{-2} M$ ; ○,  $10^{-3} M$ ; ○,  $10^{-4} M$ ; and ○, none. Initial  $\text{Tl}^+$  concentrations were: A, none; B,  $10^{-4} M$ ; C,  $10^{-3} M$ . Initial  $\text{K}_2\text{Cr}_2\text{O}_7$  concentration in all solutions was  $2 \times 10^{-4} M$ . Fricke dosimeter: 34.9 micromoles/liter of  $\text{Fe}^{++}$  oxidized per minute.

the Pyrocell Manufacturing Company with special fused silica windows for high transparency in the short ultraviolet. No detectable change in optical density of the special fused silica windows was observed either at 305 or 350  $m\mu$ .

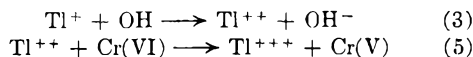
Changes in concentration of dichromate ion were determined by use of a molar extinction coefficient of 2630 at 350  $m\mu$  in 0.4  $M$  sulfuric acid determined relative to a molar extinction<sup>7</sup> for ferric ion of 2210 at 305  $m\mu$  in 0.4  $M$  sulfuric 25°. This evaluation of relative molar extinction coefficients by oxidation of ferrous ion by dichromate ion made an absolute determination of either one unnecessary. Thallous sulfate or chromic sulfate at concentrations up to  $10^{-2} M$  has no measurable effect on the molar extinction coefficient of dichromate ion.

### Results and Discussion

Cobalt  $\gamma$ -radiation induces reduction of dichromate ion in air-saturated 0.4  $M$  sulfuric acid as shown in Fig. 1. The experimental points for a solution initially containing no chromic ion fall on a straight line which does not pass through the origin but has a positive intercept attributed to trace impurities. The addition of chromic ion at concentrations up to  $10^{-2} M$  does not remove the effect of trace impurities. This is surprising since the effect of trace impurities on the reduction of ceric ion is removed<sup>7</sup> by addition of cerous ion at concentrations as low as  $10^{-3} M$ .

The measured value of 0.78 for  $G(\text{Cr}^{+++})$  is equal to  $\frac{1}{3}[2G_{\text{H}_2\text{O}_2} + G_{\text{H}} - G_{\text{OH}}]$  using the previously reported<sup>12</sup> values of  $G_{\text{H}_2\text{O}_2} = 0.78$ ,  $G_{\text{H}} = 3.70$  and  $G_{\text{OH}} = 2.92$ . This value for  $G(\text{Cr}^{+++})$  indicates the reaction mechanism for reduction of dichromate ion is identical to the postulated<sup>4</sup> reaction mechanism for reduction of ceric ion.

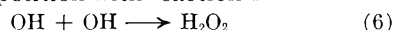
**Effect of Thallous Ion.**— $G(\text{Cr}^{+++})$  in thallous dichromate solutions is increased to  $\frac{1}{3}[2G_{\text{H}_2\text{O}_2} + G_{\text{H}} + G_{\text{OH}}]$  according to the sequence of reactions



$G(\text{Cr}^{+++})$  in thallous dichromate solutions is independent of total energy absorbed or variations in concentration of either dichromate ion or thallous ion as illustrated in Fig. 1. An extremely sharp change in  $G(\text{Cr}^{+++})$  from 2.59 to 0.78 occurs upon depletion of thallous ion in solution. The measured value of 2.59 for  $G(\text{Cr}^{+++})$  is 5% less than the value of 2.75 for  $\frac{1}{3}[2G_{\text{H}_2\text{O}_2} + G_{\text{H}} + G_{\text{OH}}]$  using the previously reported<sup>12</sup> values for  $G_{\text{H}_2\text{O}_2}$ ,  $G_{\text{H}}$  and  $G_{\text{OH}}$ .

The effect of thallous ion is identical in the reduction of dichromate ion and ceric ion. Thallous ion increases  $G(\text{Cr}^{+++})$  by 232% and increases<sup>7</sup>  $G(\text{Ce}^{+++})$  by 231%.  $G_{\text{OH}}$  measured by the increased reduction in the presence of thallous ion is equal to 2.72 for solutions of dichromate ion and 2.77 for solutions of ceric ion. These values for  $G_{\text{OH}}$  are markedly lower than the previously reported<sup>12</sup> value of 2.92. This discrepancy remains unexplained.

$G_{\text{OH}}$  can be determined by the time necessary to deplete thallous ion in solution with the assumption that  $G(\text{Tl}^{+++})$  is equal to  $G_{\text{OH}}$  according to the sequence of reactions 3 and 5.  $G_{\text{OH}}$  increases<sup>7</sup> with increasing thallous ion concentration since reaction 3 is in competition with reaction 6



in regions of high ionization density.  $G_{\text{OH}}$  determined by measurement of  $G(\text{Tl}^{+++})$  will be higher than  $G_{\text{OH}}$  for the pure solvent. Thallous ion in  $10^{-4} M$  concentration is depleted in 16.5 minutes as evidenced by the sharp change in  $G(\text{Cr}^{+++})$  shown in Fig. 1.  $G_{\text{OH}}$  calculated from the data is equal to 2.71 and is evidence that the discrepancy is not attributable to errors in molar extinction coefficients for dichromate ion or ceric ion.

**Effect of Chromic Ion.**—Chromic ion at concentrations as high as  $10^{-2} M$  has no measurable effect on  $G(\text{Cr}^{+++})$  either in the presence or absence of thallous ion. This could be interpreted as evidence that OH radical does not oxidize chromic ion. It is more reasonable to conclude that the specific reaction rate  $k_{\text{Cr}^{+++},\text{OH}}$  is less than  $k_{\text{Ce}^{+++},\text{OH}}$  or  $k_{\text{Tl}^+,\text{OH}}$ . The oxidation of cerous ion by OH radical and the oxidation of chromic ion by ceric ion support this viewpoint. It was not possible to evaluate  $k_{\text{Tl}^+,\text{OH}}/k_{\text{Cr}^{+++},\text{OH}}$  even with  $(\text{Cr}^{+++})/(\text{Tl}^+)$  ratios as large as 100.

$G(\text{Ce}^{+++})$  in ceric solutions is decreased<sup>7</sup> 10% by cerous ion at a concentration of  $10^{-2} M$  due to reaction 2 in competition with reaction 6 in regions of high ionization density. The absence of a measurable effect on  $G(\text{Cr}^{+++})$  by chromic ion in solutions free of thallous ion is evidence that chromic ion at a concentration of  $10^{-2} M$  does not measurably decrease  $G_{\text{H}_2\text{O}_2}$ .

This study of thallous dichromate solutions enables some conclusions to be reached concerning reactions of the intermediate ionic species. Chromium(IV) and chromium(V) ions do not oxidize thallous ions since this would induce a chain reaction. Thallium(II) ion does not oxidize chromic ion since  $G(\text{Cr}^{+++})$  is independent of variations in chromic ion concentrations. The failure to observe these

(12) T. J. Sworski, *J. Am. Chem. Soc.*, **76**, 4687 (1954).

reactions to any measurable extent may be attributed to unfavorable oxidation-reduction potentials. To explain why (a) thallos ion is not oxidized by chromium(IV) ion and (b) thallium(II) ion does not oxidize chromic ion, it can be assumed

that chromium(IV) ions produced during the reduction of dichromate ion are oxyanions while oxidation of chromic ion by a one electron transfer process would yield a positively charged chromium(IV) ion.

## ION-MOLECULE REACTIONS OF 1,3-BUTADIENE, OF ACETYLENE AND OF ACETYLENE-METHANE MIXTURES<sup>1</sup>

By R. BARKER, W. H. HAMILL<sup>2</sup> AND R. R. WILLIAMS, JR.

Department of Chemistry, University of Notre Dame, Notre Dame, Indiana

Received January 9, 1959

The reactions with molecules of positive ions formed in the electron bombardment of 1,3-butadiene, of acetylene and of acetylene-methane mixtures in the ionization chamber of the mass spectrometer have been investigated. Appearance potentials of the more important primary ions of 1,3-butadiene have been measured as well as the appearance potentials of all secondary ions. The heats and cross-sections of ion-molecule reactions have been calculated.

### Introduction

Several studies of the reactions of hydrocarbons involving gaseous positive ions and neutral molecules in the ionization chamber of a mass spectrometer have been reported recently.<sup>3-6</sup> These reactions, in order to be observed, necessarily have large cross-sections and negligible activation energies. Such reactions are certainly of the greatest importance in radiation chemistry. They have been postulated as mechanistic steps in the gas phase radiolysis of methane,<sup>7</sup> methane-argon mixtures<sup>6</sup> and ethane.<sup>8</sup> It must be considered, however, that quite different gas kinetic conditions prevail in the mass spectrometer at *ca.*  $10^{-5}$  mm. and in conventional reaction vessels used for chemical studies. Extrapolation to the liquid state involves still greater uncertainty since it appears that the ejected electron is recaptured by the parent ion within  $10^{-13}$  sec.<sup>9</sup> This recapture may preclude the possibility of an ion-molecule reaction in liquids except under favorable circumstances.<sup>10</sup>

The large cross-sections which characterize ion-molecule reactions arise from the long-range ion-induced dipole interactions.<sup>5</sup> Lind originally proposed that these forces led to the formation of ion-molecule clusters to which he attributed the large ionic yields found for irradiated acetylene.<sup>11</sup> The

present work suggests that the observed high efficiency for acetylene may arise from an exothermic ion-molecule chain reaction.

Unlike the higher alkanes, which exhibit few ion-molecule reactions, the unsaturated hydrocarbons have proven to be rather prolific.<sup>4,5</sup>

### Experimental

The measurements have been made with a Consolidated Electrodynamics Corporation Model 21-103A mass spectrometer. Slight modifications permitted magnetic scanning of ion peaks, adjustable repeller voltage and an ionizing voltage from 9-100 v. which was measured potentiometrically. Distances from the center of the electron beam to the repeller plate and to the exit slit, as supplied by the manufacturer, are 0.124 and 0.135 cm., respectively. The ionization chamber was held at 250°. The ionizing (electron) current was 10.5  $\mu$ amp. throughout. Magnetic scanning was performed mostly at an accelerating voltage of 2260 v.

The concentration of gas within the ionization chamber was found to be  $1.68 \times 10^{10}$  molecules  $\text{cc.}^{-1}$  for each micron of inlet pressure. It was based upon the cross sections reported for the argon-hydrogen reaction and the methanol self reaction.<sup>12,13</sup>

Three types of measurement have been made: (a) the dependence of the ratio of secondary (daughter) ion current to primary (parent) ion current as a function of inlet gas pressure; (b) the dependence of this ratio on ion repeller potential; (c) the appearance potentials of all secondary ions and of the major primary ions of 1,3-butadiene, using the vanishing current method.

The appearance potential of the  $\text{C}_3\text{H}_3^+$  ion from 1,3-butadiene was determined by direct comparison with argon in a suitable mixture. A small contribution from  $\text{C}_3\text{H}_4^+$  to the  $m/e = 40$  peak was corrected from the measured 40/39 ion abundance ratios in 1,3-butadiene alone at the same pressure and over the same range of ionizing voltage. The value 11.99v. for  $\text{C}_3\text{H}_3^+$  so obtained was used as a standard for the other ions from 1,3-butadiene.

**Materials**—Phillips Research Grade 1,3-butadiene was distilled repeatedly from trap to trap, retaining the middle fraction. Argon from Air Reduction Company was used as received. Commercial acetylene was passed through a trap at  $-120^\circ$  to remove acetone and distilled repeatedly from trap to trap. Phillips Research Grade methane and methane-*d*<sub>4</sub> from Tracerlab, Incorporated, were used as received.

### Results and Discussion

**Appearance Potentials.**—In order to characterize the ion-molecule reactions in 1,3-butadiene it

(12) D. P. Stevenson and D. O. Schissler, *J. Chem. Phys.*, **23**, 1353 (1955); D. O. Schissler and D. P. Stevenson, *ibid.*, **24**, 926 (1956).

(13) This value has since been verified using the method described by D. P. Stevenson and D. O. Schissler, *ibid.*, **29**, 282 (1958).

(1) Contribution from the Radiation Project operated by the University of Notre Dame and supported in part under Atomic Energy Commission Contract AT-(11-1)-38. Presented in part at the 132nd Meeting of the American Chemical Society, New York, N. Y., September, 1957.

(2) To whom correspondence and requests for reprints should be sent.

(3) V. L. Tal'roze and A. K. Lybimova, *Doklady Akad. Nauk S.S.S.R.*, **86**, 909 (1952).

(4) (a) F. H. Field, J. L. Franklin and F. W. Lampe, *J. Am. Chem. Soc.*, **79**, 2419 (1957); (b) **79**, 2665 (1957).

(5) D. P. Stevenson, *THIS JOURNAL*, **61**, 1453 (1957).

(6) G. G. Meisels, W. H. Hamill and R. R. Williams, Jr., *ibid.*, **61**, 1456 (1957).

(7) F. W. Lampe, *J. Am. Chem. Soc.*, **79**, 1055 (1957).

(8) L. F. Dorfman, *THIS JOURNAL*, **62**, 29 (1958).

(9) A. H. Samuel and J. L. Magee, *J. Chem. Phys.*, **21**, 1080 (1953).

(10) In the event of electron capture in irradiated liquids, *e.g.*, organic halides, the positive ion would survive long enough to react with neighboring molecules, if reaction were possible.

(11) S. C. Lind, D. C. Bardwell and J. H. Perry, *J. Am. Chem. Soc.*, **48**, 1556 (1926).

TABLE I  
 APPEARANCE POTENTIALS OF PRIMARY IONS FROM 1,3-BUTADIENE

| $m/e$ | Rel. <sup>a</sup><br>intens. | Products                                                                                    | AP or IP, v. | $\Delta H_f$ obsd.,<br>kcal. mole <sup>-1</sup> | $\Delta H_f^b$ lit.,<br>kcal. mole <sup>-1</sup> | Source                               |
|-------|------------------------------|---------------------------------------------------------------------------------------------|--------------|-------------------------------------------------|--------------------------------------------------|--------------------------------------|
| 54    | 79.0                         | C <sub>4</sub> H <sub>5</sub> <sup>+</sup>                                                  | 9.13         | 237                                             | 238 <sup>16</sup>                                | C <sub>4</sub> H <sub>5</sub>        |
| 53    | 58.8                         | C <sub>4</sub> H <sub>5</sub> <sup>+</sup> + H                                              | 12.1         | 252                                             | 264                                              | CH <sub>3</sub> C=CCH <sub>3</sub>   |
| 52    | 9.9                          | C <sub>4</sub> H <sub>3</sub> <sup>+</sup> + H <sub>2</sub>                                 | 13.0         | 326                                             | 329                                              | C <sub>6</sub> H <sub>3</sub>        |
| 51    | 22.0                         | C <sub>4</sub> H <sub>3</sub> <sup>+</sup> + H <sub>2</sub> + H                             | 15.9         | 341                                             | 337                                              | C <sub>6</sub> H <sub>3</sub>        |
| 50    | 26.5                         | C <sub>4</sub> H <sub>2</sub> <sup>+</sup> + 2H <sub>2</sub>                                | 17.8         | 436                                             | 420                                              | CH <sub>3</sub> C=CCH <sub>3</sub>   |
|       |                              | C <sub>4</sub> H <sub>2</sub> <sup>+</sup> + H <sub>2</sub> + 2H                            |              | 332                                             | 351                                              | HC≡CC≡CH                             |
| 39    | 100.0                        | C <sub>3</sub> H <sub>3</sub> <sup>+</sup> + CH <sub>3</sub>                                | 11.99        | 272                                             | 264 <sup>16</sup>                                | C <sub>4</sub> H <sub>3</sub>        |
| 38    | 8.7                          | C <sub>3</sub> H <sub>2</sub> <sup>+</sup> + CH <sub>4</sub>                                | 14.8         | 385                                             | 373                                              | CH <sub>2</sub> =C=C(H) <sub>2</sub> |
| 37    | 8.0                          | C <sub>3</sub> H <sup>+</sup> + CH <sub>3</sub> + H <sub>2</sub>                            |              |                                                 | 282 <sup>4b</sup>                                | C <sub>4</sub> H <sub>6</sub>        |
|       |                              | C <sub>3</sub> H <sup>+</sup> + CH <sub>3</sub> + 2H                                        | 20.7         |                                                 | 328 <sup>4b</sup>                                | C <sub>4</sub> H <sub>6</sub>        |
| 28    | 41.7                         | C <sub>2</sub> H <sub>3</sub> <sup>+</sup> + C <sub>2</sub> H <sub>2</sub>                  | 13.4         | 281                                             | 255                                              | C <sub>2</sub> H <sub>4</sub>        |
| 27    | 65.0                         | C <sub>2</sub> H <sub>3</sub> <sup>+</sup> + C <sub>2</sub> H <sub>3</sub>                  | 16.2         | 317                                             | 307 <sup>16</sup>                                | C <sub>4</sub> H <sub>6</sub>        |
|       |                              | C <sub>2</sub> H <sub>3</sub> <sup>+</sup> + C <sub>2</sub> H <sub>2</sub> + H              |              | 294                                             | 285                                              | C <sub>2</sub> H <sub>4</sub>        |
| 26    | 26.9                         | C <sub>2</sub> H <sub>2</sub> <sup>+</sup> + C <sub>2</sub> H <sub>4</sub>                  | 16.3         | 389                                             |                                                  |                                      |
|       |                              | C <sub>2</sub> H <sub>2</sub> <sup>+</sup> + C <sub>2</sub> H <sub>3</sub> + H              |              | 267                                             |                                                  |                                      |
|       |                              | C <sub>2</sub> H <sub>2</sub> <sup>+</sup> + C <sub>2</sub> H <sub>2</sub> + H <sub>2</sub> |              | 348                                             | 317                                              | C <sub>2</sub> H <sub>2</sub>        |

<sup>a</sup> These values, measured at 70 v., are in good agreement with those reported in the A.P.I. Project 44, National Bureau of Standards Catalog of Mass Spectral Data. <sup>b</sup> Unless otherwise identified the values are taken from ref. 17 for ions derived from molecules in the last column.

 TABLE II  
 ION-MOLECULE REACTIONS

| $m/e$                      | Secondary ion—<br>AP | $m/e$ | Primary ion—<br>AP | Reaction                                                                                                                                                | $-\Delta H_r,^c$ kcal. |
|----------------------------|----------------------|-------|--------------------|---------------------------------------------------------------------------------------------------------------------------------------------------------|------------------------|
| Acetylene <sup>a</sup>     |                      |       |                    |                                                                                                                                                         |                        |
| 37                         | 21.2                 | 13    | 21.7               | CH <sup>+</sup> + C <sub>2</sub> H <sub>2</sub> = C <sub>3</sub> H <sup>+</sup> + H <sub>2</sub>                                                        | 105                    |
| 38                         | 20.3                 | 13    | 21.7               | CH <sup>+</sup> + C <sub>2</sub> H <sub>2</sub> = C <sub>3</sub> H <sub>2</sub> <sup>+</sup> + H                                                        | 2                      |
| 49                         | 20.5                 | 24    | 20.2               | C <sub>2</sub> <sup>+</sup> + C <sub>2</sub> H <sub>2</sub> = C <sub>4</sub> H <sup>+</sup> + H                                                         | 210 <sup>d</sup>       |
| 50                         | 11.7                 | 26    | 11.4               | C <sub>2</sub> H <sub>2</sub> <sup>+</sup> + C <sub>2</sub> H <sub>2</sub> = C <sub>4</sub> H <sub>2</sub> <sup>+</sup> + H <sub>2</sub>                | 20                     |
| 51                         | 11.7                 | 26    | 11.4               | C <sub>2</sub> H <sub>2</sub> <sup>+</sup> + C <sub>2</sub> H <sub>2</sub> = C <sub>4</sub> H <sub>3</sub> <sup>+</sup> + H                             | 16 <sup>e</sup>        |
| Acetylene-methane          |                      |       |                    |                                                                                                                                                         |                        |
| 27                         | 12.1                 | 26    | 11.4               | C <sub>2</sub> H <sub>2</sub> <sup>+</sup> + CH <sub>4</sub> = C <sub>2</sub> H <sub>3</sub> <sup>+</sup> + CH <sub>3</sub>                             | -13(+3) <sup>f</sup>   |
| 39                         | 13.2                 | 16    | 13.1               | CH <sub>4</sub> <sup>+</sup> + C <sub>2</sub> H <sub>2</sub> = C <sub>2</sub> H <sub>3</sub> <sup>+</sup> + H <sub>2</sub> + H                          | -5 <sup>g</sup>        |
| 40                         | 11.7                 | 26    | 11.4               | C <sub>2</sub> H <sub>2</sub> <sup>+</sup> + CH <sub>4</sub> = C <sub>3</sub> H <sub>4</sub> <sup>+</sup> + H <sub>2</sub>                              | 20(15) <sup>h</sup>    |
| 41                         | 11.6                 | 26    | 11.4               | C <sub>2</sub> H <sub>2</sub> <sup>+</sup> + CH <sub>4</sub> = C <sub>3</sub> H <sub>5</sub> <sup>+</sup> + H                                           | 27(17) <sup>h</sup>    |
| 1,3-Butadiene <sup>b</sup> |                      |       |                    |                                                                                                                                                         |                        |
| 65                         | 14.9                 | 38    | 14.7               | C <sub>3</sub> H <sub>3</sub> <sup>+</sup> + C <sub>4</sub> H <sub>6</sub> = C <sub>3</sub> H <sub>5</sub> <sup>+</sup> + C <sub>2</sub> H <sub>3</sub> | 163                    |
| 66                         | 9.1                  | 54    | 9.1                | C <sub>4</sub> H <sub>6</sub> <sup>+</sup> + C <sub>4</sub> H <sub>6</sub> = C <sub>3</sub> H <sub>6</sub> <sup>+</sup> + C <sub>3</sub> H <sub>6</sub> | 27                     |
| 67                         | 9.0                  | 54    | 9.1                | C <sub>4</sub> H <sub>6</sub> <sup>+</sup> + C <sub>4</sub> H <sub>6</sub> = C <sub>3</sub> H <sub>7</sub> <sup>+</sup> + C <sub>3</sub> H <sub>5</sub> | 7                      |
| 76                         | 19.4                 | 50    | 17.9               | C <sub>4</sub> H <sub>2</sub> <sup>+</sup> + C <sub>4</sub> H <sub>6</sub> = C <sub>6</sub> H <sub>1</sub> <sup>+</sup> + C <sub>2</sub> H <sub>4</sub> | 77                     |
| 77                         | 13.3                 | 52    | 13.0               | C <sub>4</sub> H <sub>4</sub> <sup>+</sup> + C <sub>4</sub> H <sub>6</sub> = C <sub>6</sub> H <sub>5</sub> <sup>+</sup> + C <sub>2</sub> H <sub>5</sub> | 26                     |
| 78                         | 9.4                  | 54    | 9.1                | C <sub>4</sub> H <sub>6</sub> <sup>+</sup> + C <sub>4</sub> H <sub>6</sub> = C <sub>6</sub> H <sub>6</sub> <sup>+</sup> + C <sub>2</sub> H <sub>6</sub> | 52                     |
| 79                         | 9.1                  | 54    | 9.1                | C <sub>4</sub> H <sub>6</sub> <sup>+</sup> + C <sub>4</sub> H <sub>6</sub> = C <sub>6</sub> H <sub>7</sub> <sup>+</sup> + C <sub>2</sub> H <sub>5</sub> | ...                    |
| 80                         | 9.2                  | 54    | 9.1                | C <sub>4</sub> H <sub>6</sub> <sup>+</sup> + C <sub>4</sub> H <sub>6</sub> = C <sub>6</sub> H <sub>8</sub> <sup>+</sup> + C <sub>2</sub> H <sub>4</sub> | ...                    |
| 91                         | 12.3                 | 39    | 12.0               | C <sub>3</sub> H <sub>3</sub> <sup>+</sup> + C <sub>4</sub> H <sub>6</sub> = C <sub>7</sub> H <sub>7</sub> <sup>+</sup> + H <sub>2</sub>                | 83                     |
|                            |                      | 53    | 12.1               | C <sub>4</sub> H <sub>5</sub> <sup>+</sup> + C <sub>4</sub> H <sub>6</sub> = C <sub>7</sub> H <sub>7</sub> <sup>+</sup> + CH <sub>4</sub>               | 81                     |
| 92                         | 11.8                 | 39    | 12.0               | C <sub>3</sub> H <sub>3</sub> <sup>+</sup> + C <sub>4</sub> H <sub>6</sub> = C <sub>7</sub> H <sub>8</sub> <sup>+</sup> + H                             | 31                     |
|                            |                      | 53    | 12.1               | C <sub>4</sub> H <sub>5</sub> <sup>+</sup> + C <sub>4</sub> H <sub>6</sub> = C <sub>7</sub> H <sub>8</sub> <sup>+</sup> + CH <sub>3</sub>               | 31                     |
| 93                         | 9.4                  | 54    | 9.1                | C <sub>4</sub> H <sub>6</sub> <sup>+</sup> + C <sub>4</sub> H <sub>6</sub> = C <sub>7</sub> H <sub>9</sub> <sup>+</sup> + CH <sub>3</sub>               | ...                    |

<sup>a</sup> Appearance potentials for secondary ions in this group at  $m/e = 49, 50$  and  $51$  were measured relative to that of C<sub>2</sub>H<sub>2</sub> taken as 11.4 v. Other secondary ions were referred to argon. Appearance potentials of primary ions at  $m/e = 13$  and  $26$  are from the literature<sup>17</sup> while that for ions at  $m/e = 24$  was measured relative to C<sub>2</sub>H<sub>2</sub>. <sup>b</sup> Appearance potentials for secondary ions in this group were referred to that of C<sub>2</sub><sup>13</sup>C<sub>2</sub><sup>12</sup>H<sub>6</sub><sup>+</sup> which was of a convenient intensity. <sup>c</sup> Heats of reaction  $\Delta H_r$  have been calculated from the observed values of  $\Delta H_f$  for the primary ions in Table I. Values of  $\Delta H_f$  for secondary ions are from ref. 17 unless otherwise stated. <sup>d</sup> Based upon  $\Delta H_f(\text{C}_4\text{H}^+) = 312$  kcal. mole<sup>-1</sup>; see ref. 4b. <sup>e</sup> Based upon  $\Delta H_f(\text{C}_4\text{H}_3^+) = 303$  kcal. mole<sup>-1</sup> in ref. 4b. Choosing the value 335 kcal. mole<sup>-1</sup> from ref. 17 gives  $\Delta H_r = 16$  kcal. <sup>f</sup> Depending upon the appearance potential chosen, either 11.4 v. for the primary ion or 12.1 v. for the secondary ion. <sup>g</sup> Based upon  $\Delta H_f(\text{C}_3\text{H}_3^+) = 265$  kcal. mole<sup>-1</sup> from ref. 16. <sup>h</sup> Depending upon the choice of parent ion appearance potential. See ref. 17.

has been necessary to measure the appearance potentials of the more important primary ions. Results appear in Table I. The value for C<sub>3</sub>H<sup>+</sup> is not reliable because of a long exponential tail. It

was not examined more carefully because a similar behavior in a secondary ion could not have been detected.

Values of  $\Delta H_f$  have been obtained from the fol-

lowing data<sup>14,15</sup> all expressed in kcal./mole

$$\begin{aligned} \Delta H_f(\text{H}) &= 52.1, \Delta H_f(\text{CH}_3) = 32.0, \Delta H_f(\text{CH}_4) = -17.89, \\ \Delta H_f(\text{C}_2\text{H}_2) &= 54.19, \Delta H_f(\text{C}_2\text{H}_3) = 83,^{17} \Delta H_f(\text{C}_2\text{H}_4) = 12.50, \\ \Delta H_f(1,3\text{-butadiene}) &= 26.33 \end{aligned}$$

The ion-molecule reactions found for 1,3-butadiene, acetylene and acetylene-methane mixtures are listed in Table II. Heats of reaction  $\Delta H_r$  cannot be determined for reactions yielding secondary ions of masses 79, 80 and 93 because their heats of formation are unknown.

Reaction cross sections  $Q$  have been calculated in terms of ion currents  $I$ , the path length  $l$  of the primary ion and  $n$  the number of molecules per cc. as discussed by Stevenson.<sup>5</sup>

$$I_{\text{sec}} = I_{\text{prim}} nlQ \quad (1)$$

It has been observed that reaction cross sections vary with the applied repeller voltage  $E$  either as  $Q = BE^{-1/2}$  or as  $Q = BE^{-1/2} + C$ . Because of the complexities arising from penetrating fields, space charge and initial kinetic energy we do not consider the difference significant. Either relation is sufficient evidence of the theoretical requirement of an inverse square root dependence of cross section upon repeller field strength.<sup>13</sup> Calculated cross sections are summarized in Table III.

The relative abundances of secondary ions from

TABLE III

CROSS SECTIONS OF ION-MOLECULE REACTIONS AT VARIOUS ION ENERGIES

| Reaction                                                                                        | Cross section $\times 10^{16}$ ,<br>cm. <sup>2</sup> mole <sup>-1</sup> at ion energy |          |          |
|-------------------------------------------------------------------------------------------------|---------------------------------------------------------------------------------------|----------|----------|
|                                                                                                 | 0.1 e.v.                                                                              | 1.0 e.v. | 5.0 e.v. |
| Acetylene                                                                                       |                                                                                       |          |          |
| $\text{CH}^+ + \text{C}_2\text{H}_2 = \text{C}_3\text{H}^+ + \text{H}_2$                        | 385                                                                                   | 104      | 56       |
| $\text{CH}^+ + \text{C}_2\text{H}_2 = \text{C}_3\text{H}_2^+ + \text{H}$                        | 251                                                                                   | 63       | 36       |
| $\text{C}_2^+ + \text{C}_2\text{H}_2 = \text{C}_4\text{H}^+ + \text{H}$                         | 340                                                                                   | 81       | 47       |
| $\text{C}_2\text{H}_2^+ + \text{C}_2\text{H}_2 = \text{C}_4\text{H}_2^+ + \text{H}_2$           | 284                                                                                   | 45       | 24       |
| $\text{C}_2\text{H}_2^+ + \text{C}_2\text{H}_2 = \text{C}_4\text{H}_3^+ + \text{H}$             | 284                                                                                   | 40       | 20       |
| Acetylene-methane                                                                               |                                                                                       |          |          |
| $\text{C}_2\text{H}_2^+ + \text{CH}_4 = \text{C}_2\text{H}_3^+ + \text{CH}_3$                   | 512                                                                                   | 138      | 34       |
| $\text{CH}_4^+ + \text{C}_2\text{H}_2 = \text{C}_3\text{H}_3^+ + \text{H}_2 + \text{H}$         | 917                                                                                   | 242      | 50       |
| $\text{C}_2\text{H}_2^+ + \text{CH}_4 = \text{C}_3\text{H}_4^+ + \text{H}_2$                    | 78                                                                                    | 13       | 3.7      |
| $\text{C}_2\text{H}_2^+ + \text{CH}_4 = \text{C}_3\text{H}_5^+ + \text{H}$                      | 180                                                                                   | 37       | 15       |
| 1,3-Butadiene                                                                                   |                                                                                       |          |          |
| $\text{C}_3\text{H}_2^+ + \text{C}_4\text{H}_6 = \text{C}_3\text{H}_5^+ + \text{C}_2\text{H}_3$ | 222                                                                                   | 103      | 42       |
| $\text{C}_4\text{H}_6^+ + \text{C}_4\text{H}_6 = \text{C}_8\text{H}_6^+ + \text{C}_3\text{H}_6$ | 32                                                                                    | 13       | 7        |
| $\text{C}_4\text{H}_6^+ + \text{C}_4\text{H}_6 = \text{C}_8\text{H}_7^+ + \text{C}_3\text{H}_6$ | 40                                                                                    | 14       | 7        |
| $\text{C}_4\text{H}_2^+ + \text{C}_4\text{H}_6 = \text{C}_8\text{H}_4^+ + \text{C}_2\text{H}_4$ | 17                                                                                    | 7        | 2        |
| $\text{C}_4\text{H}_4^+ + \text{C}_4\text{H}_6 = \text{C}_8\text{H}_5^+ + \text{C}_2\text{H}_3$ | 453                                                                                   | 168      | 61       |
| $\text{C}_4\text{H}_6^+ + \text{C}_4\text{H}_6 = \text{C}_8\text{H}_6^+ + \text{C}_2\text{H}_6$ | 18                                                                                    | 7        | 3        |
| $\text{C}_4\text{H}_6^+ + \text{C}_4\text{H}_6 = \text{C}_8\text{H}_7^+ + \text{C}_2\text{H}_3$ | 97                                                                                    | 32       | 16       |
| $\text{C}_4\text{H}_6^+ + \text{C}_4\text{H}_6 = \text{C}_8\text{H}_8^+ + \text{C}_2\text{H}_4$ | 52                                                                                    | 18       | 8        |
| $\text{C}_3\text{H}_3^+ + \text{C}_4\text{H}_6 = \text{C}_7\text{H}_7^+ + \text{H}_2$           | 31                                                                                    | 10       | 4        |
| $\text{C}_4\text{H}_3^+ + \text{C}_4\text{H}_6 = \text{C}_7\text{H}_7^+ + \text{CH}_4$          | 51                                                                                    | 18       | 6        |
| $\text{C}_3\text{H}_3^+ + \text{C}_4\text{H}_6 = \text{C}_7\text{H}_7^+ + \text{H}$             | 3                                                                                     | 1        | 0.5      |
| $\text{C}_4\text{H}_3^+ + \text{C}_4\text{H}_6 = \text{C}_7\text{H}_8^+ + \text{CH}_3$          | 4                                                                                     | 2        | 1        |
| $\text{C}_4\text{H}_6^+ + \text{C}_4\text{H}_6 = \text{C}_7\text{H}_9^+ + \text{CH}_3$          | 59                                                                                    | 15       | 5        |

(14) F. D. Rossini, *et al.*, Circular 500, National Bureau of Standards, 1952.

(15) F. D. Rossini, *et al.*, "Selected Values of Physical and Thermodynamic Properties of Hydrocarbons and Related Compounds," Carnegie Press, 1953.

(16) J. Collin and F. P. Lossing, *J. Am. Chem. Soc.*, **79**, 5848 (1957).

(17) F. H. Field and J. L. Franklin, "Electron Impact Phenomena," Academic Press, Inc., New York, N. Y., 1957.

the dimer complex of butadiene,  $\text{C}_8\text{H}_{12}^+$ , correspond approximately to those at the same  $m/e$  from 4-ethenylcyclohexene. This compound is the only one of empirical formula  $\text{C}_8\text{H}_{12}$  whose mass spectrum is available.<sup>18</sup> The observed agreement (Table IV) may be dependent upon the fact that 1,3-butadiene readily reacts with itself by a Diels-Alder mechanism to yield 4-ethenylcyclohexene. The pattern for the ions from the butadiene complex is rather dependent upon the available energy (see Table III). The values chosen for Table IV correspond to cross sections for 5 e.v. ions. The only other ions of any prominence in the mass spectrum of 4-ethenylcyclohexene above the  $\text{C}_4$  group occur at  $m/e$  of 91 and 108. The latter is not to be expected in the secondary mass spectrum ("sticky collision"). The former would have a predicted relative abundance of 15 which could easily have been detected if present.

TABLE IV

RELATIVE ABUNDANCES OF IONS FROM THE 1,3-BUTADIENE COMPLEX  $\text{C}_8\text{H}_{12}^+$  AND FROM 4-ETHENYLCYCLOHEXENE

| $m/e$               | 66 | 67 | 78 | 79  | 80 | 93 |
|---------------------|----|----|----|-----|----|----|
| Butadiene           | 44 | 44 | 18 | 100 | 50 | 31 |
| Ethenyl-cyclohexene | 55 | 42 | 24 | 100 | 53 | 31 |

The other ion complexes formed from 1,3-butadiene, together with their daughters, for which there are stable counterparts of known mass spectra, are:  $\text{C}_7\text{H}_8^+(\text{C}_6\text{H}_5^+)$ ;  $\text{C}_8\text{H}_8^+(\text{C}_6\text{H}_4^+)$ ;  $\text{C}_8\text{H}_{10}^+(\text{C}_6\text{H}_5^+)$ . In the spectrum of toluene ( $\text{C}_7\text{H}_8$ ), only ions at  $m/e$  of 65 and 91 are significant. The former corresponds to  $\text{C}_6\text{H}_5^+$  observed, the latter also arises from another reaction of lower appearance potential and so is masked. Styrene ( $\text{C}_8\text{H}_8$ ) has significant peaks at  $m/e$  of 63, 77, 78 (all masked), at 75 (only 4%, not observed) and at 76 (observed). Ethylbenzene and the xylenes ( $\text{C}_8\text{H}_{10}$ ) have significant peaks at  $m/e$  of 78, 79, 91 (all masked). There is a rather minor peak at  $m/e = 77$ . In contrast, the largest cross section for a secondary ion is found at  $m/e = 77$ .

Correlations of this type already have been reported for acetylene self reactions.<sup>4b</sup> For  $\text{C}_2\text{H}_2 + \text{CH}_4$  mixtures there are four reactions involving the complex  $\text{C}_3\text{H}_6^+$ . The mass spectra of propylene and of cyclopropane were examined at several ionizing voltages over the range 13-70 v. No correlation exists between relative abundances in these spectra and in the secondary ion spectrum of acetylene-methane mixtures at  $m/e$  of 27, 39, 40 and 41.

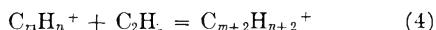
It was thought that a study of these ion-molecule reactions might help to understand the radiation chemistry of acetylene.<sup>11</sup> The ion-pair yield of acetylene consumed is approximately 20. Of this amount 21% goes to form benzene,<sup>19,20</sup> the rest to form cuprene. The invariance of benzene/cuprene with pressure has been explained by Dorfman and Shipko in terms of different trimer states. Specifically, that leading to benzene is assumed to arise from an excited state of acetylene.

(18) A. P. I. Project 44, National Bureau of Standards, Catalog of Mass Spectral Data.

(19) W. Mund and C. Rosenblum, *THIS JOURNAL*, **41**, 469 (1937).

(20) L. M. Dorfman and F. J. Shipko, *J. Am. Chem. Soc.*, **77**, 4723 (1955).

The present work demonstrates the possibility of very efficient ionic polymerizations with unsaturated hydrocarbons. Other work<sup>4,21</sup> extends these observations to include ethylene, benzene and toluene. There is no indication of high specificity and it is plausible that chain reactions of the type



(21) Unpublished observations by R. Barker.

could readily proceed, where  $m/n = 1$ . For the small molecules examined at very low pressure, neutral fragments always formed. For higher pressures and for higher molecular weights, addition without elimination may occur.<sup>22</sup> The possibility of reactions of type (4) is supported by the available thermochemical data<sup>17</sup> for  $m = n = 1, 2, 3, 4, 5, 6$ .

(22) M. Burton and J. L. Magee, *THIS JOURNAL*, **56**, 842 (1952).

## CARBON-HALOGEN BOND ENERGIES AND BOND DISTANCES<sup>1</sup>

BY GEORGE GLOCKLER

*Contribution from the Department of Chemistry, Duke University, Durham, North Carolina*

*Received January 16, 1959*

Bond energy estimates and distances of the cyanogen halides, halomethanes, chloroethanes, carbonyl and acetyl halides show a linear relationship. These regularities and earlier information on carbon-carbon, carbon-oxygen and carbon-hydrogen bond energies and distances are transferred to study chloroacetic acids, chloroaldehydes and chloroalcohols. The method permits estimates to be made of the heats of atomization, formation and combustion of compounds containing carbon-halogen and the above mentioned bonds. Internuclear distances and hence moments of inertia can be estimated by the inverse calculation.

### Introduction

It is believed that the type of calculation presented here will ultimately produce relations of bond energy values and internuclear distances from which estimates of various thermochemical quantities such as heats of atomization, formation and combustion can be obtained for compounds which have not yet been studied thermochemically and others which have not even been synthesized. It would be very timesaving and inexpensive if a proper basis for making such estimates were available for all kinds of molecules. It will obviously be impossible to measure the heats of combustion of all compounds of interest now and in the future. Studies of the type reported here would relieve this situation. For example in another field, empirical equations for calculating isomeric variations in the values of physical properties of hydrocarbons and related compounds are very helpful to the investigator interested in these quantities in cases where they have not yet been determined experimentally.<sup>2</sup>

It is even conceivable that bond lengths obtained by physical methods such as microwave spectroscopy and electron diffraction methods may be measurable with such high accuracy in the future that their use and a well established system of bond energies will be a more satisfactory method of determining heats of formation and combustion than the present day thermochemical experiments. The relation between bond energies and distances will then have to be represented by more complex functions than straight lines. The connection between chemical and physical measurements here discussed can serve both groups of scientists as a check on their own respective experiments. Both

must show that their observations fit the requirements of the other group. For many practical uses it is of great interest to be able to make even rough estimates of thermochemical quantities. They can be made even without knowledge of internuclear distances, if there exist some definite ideas as to the bond picture of the molecule under consideration. As force constants must be transferred from molecule to molecule, so must bond energies be transferred in the present calculations.

**Notation.**— $B(AB, ABC)$  = AB-bond energy (kcal.) in ABC;  $D(Br_2) = 53.4$ ;  $D(Cl_2) = 58$ ;  $D(F_2) = 37.6$ ;  $D(H_2) = 104.2$ ;  $D(I_2) = 51.0$ ;  $D(N_2) = 225.2$ ;  $D(O_2) = 118.2$ ;  $L(C) = 171.7$  kcal.;  $n_A$  = number of A atoms;  $Q_a(ABC)$  = atomic heat of formation (kcal.) of ABC;  $Q_f(ABC)$  = usual heat of formation from the elements A, B and C in their standard states;  $R(AB, ABC)$  = AB-bond length (Å.) in ABC; temperature = 25° (ref. 3, 4). (Note: In Figs. 1-3, full dots indicate that  $R(AB)$  is known experimentally. Open circles show that  $R(AB)$  has been estimated.)

As is the case with carbon-carbon, carbon-hydrogen and carbon-oxygen bonds,<sup>5</sup> it was found here also that large bond energies occur with small internuclear distances and *vice versa*. Most of these distances were obtained by microwave spectroscopy<sup>6</sup> and by electron diffraction by various authors as given in the text. Most  $Q_f$ -values come from the work of Rossini<sup>3</sup> and for fluorocarbons from Margrave.<sup>4</sup>  $R(CH)$  and  $B(CH)$  are related by

(3) Selected Values of Chemical Properties of Hydrocarbons, Cir. 500, Nat. Bur. Standards (U. S. Government Printing Office, Washington 1952).

(4) R. P. Iczkowski, C. A. Neugebauer and J. L. Margrave, Office of Ordnance Research Report No. 1428 (Feb. 1957); C. A. Neugebauer and J. L. Margrave (May 1957) and R. P. Iczkowski and J. L. Margrave (Oct. 1958).

(5) G. Glockler, *THIS JOURNAL*, **61**, 31 (1957); **62**, 1049 (1958).

(6) W. Gordy, W. V. Smith and R. F. Trambarulo, "Microwave Spectroscopy," John Wiley and Sons, Inc., New York, N. Y., 1953.

(1) This research is supported by the Office of Ordnance Research, U. S. Army under Contract No. DA-31-124-ORD-1535. The paper was presented at the Southeastern Regional Meeting, Gainesville, Florida, 11-13 December 1958.

(2) J. B. Greenshields and F. D. Rossini, *THIS JOURNAL*, **62**, 271 (1958).

$$B(\text{CH}) = -36.4 + 148.4/R(\text{CH}) \quad (1)$$

$B(\text{CC})$  and  $R(\text{CC})$  are determined graphically.<sup>5</sup>

**Cyanogen Halides.**—The quantities mentioned in Table I for CNF were estimated by graphical methods from the relations  $R(\text{CX}, \text{CNX})$ ,  $R(\text{CX}, \text{CX}_4)$  and  $R(\text{CN}, \text{CNX})$  with atomic number. The result is  $R(\text{CF}, \text{CNF}) \doteq 1.19$  and  $R(\text{CN}, \text{CNF}) \doteq 1.167 \text{ \AA}$ .<sup>7</sup> From graphs of  $B(\text{CF}$  vs.  $R(\text{CF})$ ,  $B(\text{CF}, \text{CNF}) \doteq 133.0 \text{ kcal.}$  at  $1.19 \text{ \AA}$ . From the relation  $B(\text{CN})$  vs.  $R(\text{CN})$ ,  $B(\text{CN}, \text{CNF}) \doteq 181.6 \text{ kcal.}$  at  $1.167 \text{ \AA}$ ., whence  $Q_a(\text{CNF}) \doteq 314.6 \text{ kcal.}$

Using the  $R(\text{CN})$  values and the relation  $B(\text{CN})$  vs.  $R(\text{CN})$ , the  $B(\text{CN})$  quantities for the other halides were found and finally  $B(\text{CX}) = Q_a(\text{CNX}) - B(\text{CN}, \text{CNX})$  was determined.

The relation of  $B(\text{CX})$  vs.  $R(\text{CX})$  for CNX is shown in Fig. 1a. These quantities and a similar set for the tetrahalomethanes (Fig. 1b) are used to determine the four general relations  $B(\text{CX})$  vs.  $R(\text{CX})$ . It is seen that  $B(\text{CF}) > B(\text{CCl}) > B(\text{CBr}) > B(\text{CI})$  for CNX.

**Tetrahalomethanes.**—These molecules have only been studied by electron diffraction methods since their symmetry precludes light absorption.  $B(\text{CI})$  was determined from an extrapolation of  $B(\text{CX})$  vs.  $R(\text{CX})$  (Fig. 1b).  $Q_a(\text{CI}_4)$  was found from the relation  $Q_a(\text{CX}_4)$  vs.  $R(\text{CX}, (Q_a)(\text{CX}_4))$ . In general internuclear distances obtained from electron diffraction are quoted to be accurate to  $\pm 0.01$  to  $0.02 \text{ \AA}$ . The CF-distance in  $\text{CF}_4$  has been measured lately by two investigators who obtained  $1.317 \text{ \AA}$ .<sup>8</sup> and  $1.323 \pm 0.005$ .<sup>9</sup> The lower value seems to fit much better in a plot of  $R(\text{CF})$  vs.  $n(\text{F})$  of the series  $\text{CF}_4$  to  $\text{CH}_3\text{F}$ . The CCl-distance at  $1.765 \text{ \AA}$ .<sup>10</sup> fits very well into the series  $\text{CCl}_4$  ( $1.765$ ),  $\text{CHCl}_3$  ( $1.767$ ),  $\text{CH}_2\text{Cl}_2$  ( $1.772$ ) and  $\text{CH}_3\text{Cl}$  ( $1.782$ )  $\text{ \AA}$ .<sup>6</sup>

The CBr-distance in  $\text{CBr}_4$  has been determined by three investigators to be  $1.93 \pm 0.02$ ,<sup>11</sup>  $1.92^{12}$  and  $1.942 \pm 0.03 \text{ \AA}$ .<sup>13</sup> However, by a simple extrapolation  $R(\text{CBr}, \text{CBr}_4) = 1.927 \text{ \AA}$ . The electron diffraction results on  $\text{CI}_4$  indicate  $R(\text{CI}, \text{CI}_4) = 2.12 \pm 0.02 \text{ \AA}$ .<sup>11</sup> The value  $2.12 \text{ \AA}$ . was chosen and  $R(\text{CI}, \text{CHI}_3) = 2.128$  and  $R(\text{CI}, \text{CH}_2\text{I}_2) = 2.133 \text{ \AA}$ . were interpolated (Table II).

TABLE II

| TETRAHALOMETHANES |                    |                    |                           |                                     |
|-------------------|--------------------|--------------------|---------------------------|-------------------------------------|
|                   | $Q_f$ ,<br>kcal.   | $Q_a$ ,<br>kcal.   | $B(\text{CX})$ ,<br>kcal. | $R(\text{CX})$ ,<br>$\text{ \AA}$ . |
| $\text{CF}_4$     | 217.2 <sup>a</sup> | 464.1              | 116.0                     | 1.317 <sup>d</sup>                  |
| $\text{CCl}_4$    | 25.5 <sup>b</sup>  | 313.2              | 78.3                      | 1.765 <sup>e</sup>                  |
| $\text{CBr}_4$    | -12.0 <sup>b</sup> | 266.5              | 66.6                      | 1.927 <sup>f</sup>                  |
| $\text{CI}_4$     | -61.0 <sup>c</sup> | 213.1 <sup>c</sup> | 53.4 <sup>c</sup>         | 2.12 <sup>g</sup>                   |

<sup>a</sup> Ref. 4. <sup>b</sup> Ref. 3. <sup>c</sup> Estimated. <sup>d</sup> Ref. 8; see also ref. 9. <sup>e</sup> Ref. 10. <sup>f</sup> Estimated; see ref. 11, 12, 13. <sup>g</sup> Ref. 11.

(7) W. J. O. Thomas, *J. Chem. Phys.*, **20**, 920 (1952).

(8) C. W. W. Hoffman and R. L. Livingston, *J. Chem. Phys.*, **21**, 565 (1953).

(9) O. Brockway, et al., reported by R. L. Livingston, *Ann. Rev. Phys. Chem.*, **5**, 397 (1954).

(10) L. S. Bartell, L. O. Brockway and R. H. Schwendeman, *J. Chem. Phys.*, **23**, 1854 (1955).

(11) Chr. Finbak and O. Hassel, *Z. physik. Chem.*, **B36**, 301 (1937).

(12) L. R. Maxwell, *J. Opt. Soc. Am.*, **30**, 374 (1940).

(13) Chr. Finbak, O. Hassel and O. J. Olaussen, *Tids. Kjem. Bergvaen.*, **3**, 13 (1943).

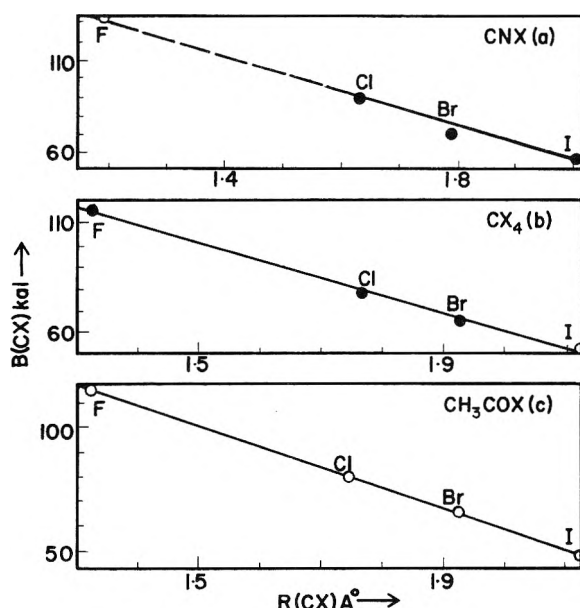


Fig. 1.— $B(\text{CX})$  estimates vs.  $R(\text{RX})$  for: a, cyanogen halides; b, tetrahalomethanes; c, acetyl halides.

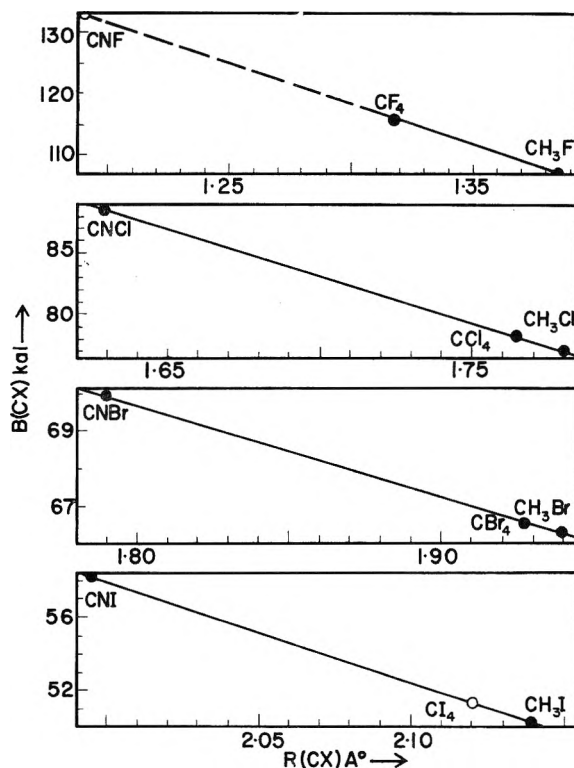


Fig. 2.— $B(\text{CX})$  estimates as functions of  $R(\text{CX})$ , X = F, Cl, Br, I; (CNX,  $\text{CX}_4$  to  $\text{CH}_3\text{X}$ ).

**Methyl Halides.**—The bond energies and distances can be fitted into the straight line determined by the corresponding points from the cyanogen halides and the tetrahalomethanes (Fig. 2). The resulting data are given in Table III. The sections  $\text{CX}_4$  to  $\text{CH}_3\text{X}$  are shown in Fig. 3.

Two estimates have been made of  $Q_f(\text{CH}_3\text{F})$ :  $59 \pm 2$  and  $58.0 \text{ kcal.}$ <sup>4</sup> The  $R(\text{CX})$  values (X = F),<sup>6</sup> (X = Cl, Br, I)<sup>14</sup> were determined by micro-

(14) S. L. Miller, L. C. Aamodt, G. Dousmanis, C. H. Townes and J. Kraitchman, *J. Chem. Phys.*, **20**, 1112 (1952).

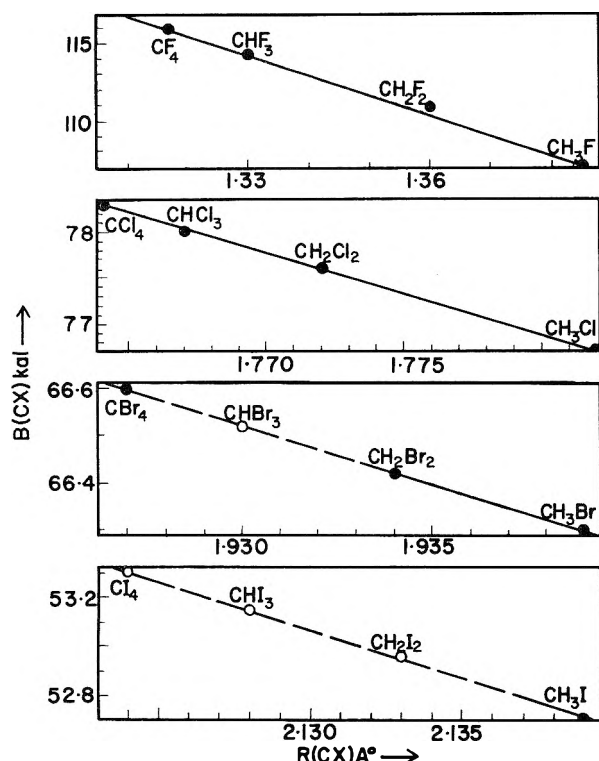


Fig. 3.— $B(CX)$  estimates as functions of  $R(CX)$ ,  $X = F, Cl, Br, I$ ; ( $CX_3$  to  $CH_3X$ ).

TABLE III

## METHYL HALIDES

| $Q_f$ , kcal. | $Q_a$ , kcal.     | $B(CX)$ , kcal. | $R(CX)$ , Å. | $B(CH)$ , kcal.    | $R(CH)$ , Å. |                                          |
|---------------|-------------------|-----------------|--------------|--------------------|--------------|------------------------------------------|
| $CH_3F$       | 57.0 <sup>c</sup> | 403.8           | 107.0        | 1.385 <sup>c</sup> | 98.9         | 1.10 <sup>e</sup><br>1.11 <sup>c,f</sup> |
| $CH_3Cl$      | 19.6 <sup>b</sup> | 376.6           | 76.7         | 1.782 <sup>d</sup> | 99.9         | 1.09 <sup>e</sup><br>1.10 <sup>d,f</sup> |
| $CH_3Br$      | 8.5 <sup>b</sup>  | 363.2           | 66.4         | 1.939 <sup>d</sup> | 98.9         | 1.10 <sup>e</sup><br>1.10 <sup>d,f</sup> |
| $CH_3I$       | -4.9 <sup>b</sup> | 348.7           | 52.6         | 2.139 <sup>d</sup> | 98.7         | 1.10 <sup>e</sup><br>1.10 <sup>d,f</sup> |

<sup>a</sup> Estimate; see ref. 4. <sup>b</sup> Ref. 3. <sup>c</sup> Ref. 6. <sup>d</sup> Ref. 6, 14. <sup>e</sup> Estimate by eq. 1. <sup>f</sup> Ref. 15, 16.

TABLE I

## CYANOGEN HALIDES

| $Q_f$ , kcal. | $Q_a$ , kcal.      | $B(CX)$ , kcal.    | $R(CX)$ , Å.       | $B(CN)$ , kcal.    | $R(CN)$ , Å.       |                    |
|---------------|--------------------|--------------------|--------------------|--------------------|--------------------|--------------------|
| $CNF^a$       | -8.7 <sup>a</sup>  | 314.6 <sup>a</sup> | 133.0 <sup>a</sup> | 1.190 <sup>a</sup> | 181.6 <sup>a</sup> | 1.167 <sup>a</sup> |
| $CNCl$        | -34.5 <sup>b</sup> | 278.8              | 89.8               | 1.629 <sup>c</sup> | 189.0              | 1.163 <sup>c</sup> |
| $CNBr$        | -43.3 <sup>b</sup> | 267.7              | 70.2               | 1.790 <sup>c</sup> | 197.5              | 1.159 <sup>c</sup> |
| $CNI$         | -54.6 <sup>b</sup> | 255.2              | 57.7               | 1.995 <sup>c</sup> | 197.5              | 1.159 <sup>c</sup> |

<sup>a</sup> All values for  $CNF$  are estimates. <sup>b</sup> Ref. 3. <sup>c</sup> Ref. 6.

wave spectroscopy. The  $B(CX)$  quantities were taken from Fig. 2. The energies  $B(CH, CH_3X)$  were obtained from the difference  $Q_a - B(CX)$ . The results are shown in the last column of Table III. They can be compared with the ones determined from microwave spectroscopy work<sup>6,15,16</sup> (Table III, column 7). It is seen that these  $R(CH)$  quantities check to about 0.01 Å, which is the variation of measurement by microwave spectroscopy.

(15) D. P. Stevenson and J. A. Ibers, *Ann. Rev. Phys. Chem.*, **9**, 359 (1958).

(16) C. W. N. Cumper, *Trans. Faraday Soc.*, **54**, 1261 (1958).

copy on account of the influence of zero point vibrations. Internuclear distances determined by electron diffraction measurements are subject to variations of  $\pm 0.01$  to  $0.02$  Å. Of course thermochemical experiments also are affected by errors of 0.1 to 1.0% and even more with many fluorine containing compounds, for example. It is rather interesting that such diverse measurements should yield as good agreement in the determination of molecular distances.

**Methylene Halides** (Table IV).—A preliminary report gave  $R(CF, CH_2F_2)$  as 1.36 and  $R(CH, CH_2F_2)$  as 1.09 Å.<sup>17</sup> An interpolation  $R(CF, CF_4) \rightarrow R(CF, CH_3F)$  resulted in  $R(CF, CH_2F_2) = 1.36$  Å. and  $R(CH, CH_2F_2)$ , calculated) was 1.10 Å. In the molecule  $CH_2Cl_2$  a larger than usual difference in the thermochemical and microwave values of the CH-distance was found. The reason may lie in a discrepancy in the heat of formation of the compound. One value is 21 kcal.<sup>4</sup> while another is 32 kcal., derived from a heat of combustion (106.5 kcal.) due to Berthelot.<sup>15</sup>

TABLE IV

## METHYLENE HALIDES

| $Q_f$ , kcal. | $Q_a$ , kcal.      | $B(CX)$ , kcal. | $R(CX)$ , Å. | $B(CH)$ , kcal.    | $R(CH)$ , Å. |                                        |
|---------------|--------------------|-----------------|--------------|--------------------|--------------|----------------------------------------|
| $CH_2F_2$     | 105.5 <sup>a</sup> | 419.0           | 111.0        | 1.36 <sup>e</sup>  | 98.5         | 1.10 <sup>c</sup><br>1.09 <sup>e</sup> |
| $CH_2Cl_2$    | 21.0 <sup>b</sup>  | 354.9           | 77.6         | 1.772 <sup>d</sup> | 99.9         | 1.09 <sup>e</sup><br>1.07 <sup>d</sup> |
| $CH_2Br_2$    | 1.0 <sup>b</sup>   | 330.3           | 66.4         | 1.934 <sup>c</sup> | 98.7         | 1.10 <sup>c</sup>                      |
| $CH_2I_2$     | -24.0 <sup>c</sup> | 303.0           | 53.0         | 2.133 <sup>c</sup> | 98.5         | 1.10 <sup>c</sup>                      |

<sup>a</sup> Ref. 4. <sup>b</sup> Ref. 3. <sup>c</sup> Estimated by eq. 1. <sup>d</sup> Ref. 6. <sup>e</sup> Ref. 17.

**Haloforms.**—The  $Q_f$ -values (Table V) lead to the  $Q_a$ 's in the usual manner. From Fig. 3 the bond energies are derived from the corresponding distances ( $R(CX)$ ). The CH-distances calculated are compared with the microwave values (column 7, Table V). In bromoform, chloroform and fluoroform, the CH-distances are progressively shorter (1.068, 1.073, 1.098) due presumably to the influence of resonance structures containing double bonds.<sup>6,19</sup> However, this effect also may be ascribed to the difference of s- and p-hybridization affecting the carbon atom radius.<sup>20</sup>

**Chloroethanes.**—The heat of formation of chloroethane is 25.1 kcal.<sup>3</sup> resulting in  $Q_a = 658.5$  kcal. The assumption that  $B(CC, C_2H_6) = 85.9$ ,  $B(CH, C_2H_6) = 98.4$  and  $B(CCl, CH_3Cl) = 76.7$  kcal., leads to a calculated  $Q_a = 654.6$  kcal. (0.6% low).

1,1-Dichloroethane is assumed to have  $B(CC, C_2H_6) = 85.9$ ,  $B(CH, CH_2Cl_2) = 99.9$ ,  $B(CH, C_2H_6) = 98.4$  and  $B(CCl, CH_2Cl_2) = 77.2$  kcal. Since  $Q_f = 29.1$  kcal.,<sup>3</sup>  $Q_a = 639.3$  kcal. while the value from bond energies is 636.2 kcal. (0.6% low).

(17) D. R. Lide, *J. Am. Chem. Soc.*, **74**, 3348 (1952).

(18) P. E. Berthelot and J. Ogier, *Ann. chim. phys.*, [5] **23**, 197 (1881).

(19) S. N. Ghosh, R. Trambarulo and W. Gordy, *J. Chem. Phys.*, **20**, 605 (1952).

(20) C. A. Coulson, Commemorative Volume for Victor Henri "Contribution to Molecular Structure Studies," Desoer, Liège, Belgium, 1948.

TABLE V  
HALOFORMS

|                   | $Q_f$ ,<br>kcal.   | $Q_a$ ,<br>kcal. | $B(CX)$ ,<br>kcal. | $R(CX)$ ,<br>Å.    | $B(CH)$ ,<br>kcal. | $R(CH)$ ,<br>Å.                        |
|-------------------|--------------------|------------------|--------------------|--------------------|--------------------|----------------------------------------|
| CHF <sub>3</sub>  | 162.6 <sup>a</sup> | 442.8            | 114.3              | 1.332 <sup>d</sup> | 99.9               | 1.09 <sup>e</sup><br>1.10 <sup>d</sup> |
| CHCl <sub>3</sub> | 24.0 <sup>b</sup>  | 334.8            | 78.0               | 1.767 <sup>d</sup> | 100.8              | 1.08 <sup>e</sup><br>1.07 <sup>d</sup> |
| CHBr <sub>3</sub> | -3.0 <sup>b</sup>  | 300.8            | 66.5               | 1.930 <sup>d</sup> | 101.3              | 1.08 <sup>e</sup><br>1.07 <sup>d</sup> |
| CHI <sub>3</sub>  | -42.3 <sup>c</sup> | 258.0            | 53.2               | 2.128 <sup>e</sup> | 98.4               | 1.10 <sup>e</sup><br>...               |

<sup>a</sup> Ref. 4. <sup>b</sup> Ref. 3. <sup>c</sup> Estimated by eq. 1. <sup>d</sup> Ref. 6. <sup>e</sup> Estimate.

The isomeric 1,2-dichloroethane has  $Q_f = 32.0$  kcal.,<sup>3</sup> resulting in  $Q_a = 641.8$  kcal. With  $B(CC, C_2H_6) = 85.9$ ,  $B(CH, 0.5 C_2H_6 + 0.5 CH_2Cl_2) = 99.2$  and  $B(CCl, CH_2Cl_2) = 77.6$  kcal.,  $Q_a$  (calcd.) = 637.9 kcal. (0.6% low).

**Hexahaloethanes.**—The heat of formation of hexafluoroethane is 240 kcal.<sup>3</sup> However, a more recent measurement indicates a much higher value,  $303 \pm 2$  kcal.<sup>21</sup> From electron diffraction  $R(CC) = 1.56 \pm 0.03$  Å. and  $R(CF) = 1.32 \pm 0.01$  Å.<sup>22</sup> A study of these quantities leads to the values shown in Table VI. The lower  $Q_f = 240$  kcal. does not fit the electron diffraction results.

TABLE VI

## HEXAHALOETHANES

|                                | $Q_f$ ,<br>kcal.   | $Q_a$ ,<br>kcal. | $B(CX)$ ,<br>kcal. | $R(CX)$ ,<br>Å.    | $B(C-C)$ ,<br>kcal. | $R(C-C)$ ,<br>Å.     |
|--------------------------------|--------------------|------------------|--------------------|--------------------|---------------------|----------------------|
| C <sub>2</sub> F <sub>6</sub>  | 303 <sup>a</sup>   | 759.2            | 112.7              | 1.342 <sup>f</sup> | 82.9                | 1.56 <sup>c</sup>    |
| C <sub>2</sub> Cl <sub>6</sub> | 34 <sup>b</sup>    | 551.4            | 77.6               | 1.772 <sup>f</sup> | 85.9                | 1.543 <sup>d,f</sup> |
| C <sub>2</sub> Br <sub>6</sub> | -16.6 <sup>f</sup> | 487.0            | 66.9               | 1.915 <sup>f</sup> | 85.9                | 1.543 <sup>e,f</sup> |
| C <sub>2</sub> I <sub>6</sub>  | -100 <sup>f</sup>  | 400.0            | 52.3               | 2.15 <sup>f</sup>  | 85.9                | 1.543 <sup>e,f</sup> |

<sup>a</sup> Ref. 21. <sup>b</sup> Ref. 3. <sup>c</sup> Ref. 22. <sup>d</sup> Ref. 23. <sup>e</sup> Ref. 24. <sup>f</sup> Assumed.

The distances for C<sub>2</sub>Cl<sub>6</sub> as given by electron diffraction are  $R(CC) = 1.57 \pm 0.06$  and  $R(CCl) = 1.74 \pm 0.01$ .<sup>23</sup> It was assumed however that  $B(CC, C_2Cl_6) = B(CC, C_2H_6) = 85.9$  kcal. at 1.543 Å. In C<sub>2</sub>Br<sub>6</sub> (crystal),  $R(CBr) = 1.93$  Å. if  $R(CC) = 1.52$  Å.<sup>24</sup> is assumed. However the ethane value for the CC-bond was taken as in C<sub>2</sub>I<sub>6</sub>. The halogens except fluorine are unlikely to change the CC-bond.

**Chlorofluoromethanes.**—The thermochemistry of trichlorofluoromethane has been studied by three investigators:  $Q_f = 70.0 \pm 4$ ,<sup>21</sup> 67<sup>25</sup> and 66.2.<sup>4</sup> The average value is 67.7 kcal. so that  $Q_a = 345.2$  kcal. Its bond energies and distances have been taken as the averages of CF<sub>4</sub> and CCl<sub>2</sub>F<sub>2</sub> since its geometry is not known.

For the dichlorodifluoro compound two values are known for  $Q_f$ ,  $112 \pm 2$ <sup>21</sup> and 113 kcal.<sup>25</sup> Their average leads to  $Q_a = 379.8$  kcal. The electron diffraction results are  $R(CF) = 1.335 \pm 0.02$  and

$R(CCl) = 1.775 \pm 0.02$  Å.<sup>26</sup> Bond energies to satisfy these data are given in Table VII.

TABLE VII

## CHLOROFUOROMETHANES

|                                 | $Q_f$ ,<br>kcal.   | $Q_a$ ,<br>kcal. | $B(CCl)$ ,<br>kcal. | $R(CCl)$ ,<br>Å.   | $B(CF)$ ,<br>kcal. | $R(CF)$ ,<br>Å.      |
|---------------------------------|--------------------|------------------|---------------------|--------------------|--------------------|----------------------|
| CCl <sub>4</sub>                | 25.5 <sup>a</sup>  | 313.2            | 78.3                | 1.765 <sup>d</sup> | ...                | ...                  |
| CCl <sub>3</sub> F              | 67.7 <sup>b</sup>  | 345.2            | 77.7                | 1.770 <sup>e</sup> | 112.1              | 1.348 <sup>e</sup>   |
| CCl <sub>2</sub> F <sub>2</sub> | 112.5 <sup>b</sup> | 379.8            | 77.1                | 1.777 <sup>f</sup> | 112.9              | 1.340 <sup>e,f</sup> |
| CClF <sub>3</sub>               | 163.2 <sup>b</sup> | 420.3            | 76.5 <sup>g</sup>   | 1.785 <sup>g</sup> | 114.6              | 1.328 <sup>g</sup>   |
| CF <sub>4</sub>                 | 217.2 <sup>c</sup> | 464.1            | ...                 | ...                | 116.0              | 1.317 <sup>h</sup>   |

<sup>a</sup> Ref. 3. <sup>b</sup> Estimate; see also ref. 4, 21, 25. <sup>c</sup> Ref. 4. <sup>d</sup> Ref. 10. <sup>e</sup> Estimate. <sup>f</sup> Ref. 26. <sup>g</sup> Assumed; ref. 6, 27, 28. <sup>h</sup> Ref. 8; see also ref. 9.

The heat of formation of trifluorochloromethane has been determined twice,  $Q_f = 171 \pm 1$ <sup>21</sup> and 167 kcal.<sup>25</sup> The average value of  $Q_a$  is then 426 kcal. Microwave spectroscopy in two determinations indicates that  $R(CF) = 1.323$  and  $R(CCl) = 1.765$  Å.<sup>27</sup> or  $R(CF) = 1.328$  and  $R(CCl) = 1.74$  Å.<sup>6</sup> or  $R(CF) = 1.328 \pm 0.002$  and  $R(CCl) = 1.751 \pm 0.004$  Å. by electron diffraction.<sup>28</sup>  $R(CF)$  is definite and leads to  $B(CF) = 114.6$  kcal. Then  $B(CCl) = 426 - (3 \times 114.6) = 82.5$  kcal., a very striking increase indeed since the other  $B(CCl)$  values are 78.3, 77.7 and 77.1 kcal. It seems unlikely that the substitution of another fluorine for a chlorine atom should produce such a marked increase in the  $B(CCl)$  value in CClF<sub>3</sub>. It is possible that the  $Q_f$  values are not accurate. At any rate such a discrepancy should lead to a reinvestigation of the pertinent data. Here it is assumed that  $B(CCl, CClF_3)$  is 76.5 kcal. from the trend noted above. Then  $Q_a(CClF_3) = 420.3$  and  $Q_f = 163.2$  kcal., lower by 3 kcal. than the experimental values mentioned above.

**Carbonyl Halides.**—Two  $Q_f$  values of COF<sub>2</sub> have been determined lately, 143<sup>4</sup> and 150.35 kcal.<sup>29</sup> ( $Q_f = 146.7$  and  $Q_a = 415.6$  kcal.). The geometry of the molecule was studied by electron diffraction.<sup>30</sup> The latter information leads to the following molecular constants:  $Q_a = 417.7$  kcal. with  $B(CF, 1.32 \text{ Å.}) = 115.6$  and  $B(C=O, 1.17 \text{ Å.}) = 186.5$  kcal.

From the microwave spectrum for phosgene it is found that  $R(C=O) = 1.166 \pm 0.002$  and  $R(CCl) = 1.746 \pm 0.004$  Å.<sup>31</sup> Electron diffraction studies give  $1.18 \pm 0.03$  and  $1.74 \pm 0.02$  Å., respectively.<sup>32</sup> The microwave lengths correspond to  $B(C=O) = 190.0$  and  $B(CCl) = 79.8$  kcal., whence  $Q_a = 349.6$  kcal. From thermochemistry  $Q_f = 53.3$ <sup>3</sup> ( $Q_a = 342.6$ ) and 60.6<sup>33</sup> ( $Q_a = 349.6$ ) kcal. Hence the higher value would appear to be the better choice although  $Q_f = 53.3$  kcal. has been found by several investigators.<sup>3</sup>

(26) R. L. Livingston and D. H. Lyon, *J. Chem. Phys.*, **24**, 1283 (1956).

(27) D. K. Coles and R. H. Hughes, *Phys. Rev.*, **76**, 858 (1949).

(28) L. S. Bartell and L. O. Brockway, *J. Chem. Phys.*, **23**, 1860 (1955).

(29) H. v. Wartenberg and G. Riteris, *Z. anorg. Chem.*, **258**, 356 (1949).

(30) T. T. Brown and R. L. Livingston, *J. Am. Chem. Soc.*, **74**, 6084 (1952).

(31) G. W. Robinson, *J. Chem. Phys.*, **21**, 1741 (1953).

(32) V. Schomaker (see P. W. Allen and L. E. Sutton, *Acta Cryst.*, **3**, 46 (1950)).

(33) P. E. Berthelot, *Ann. chim. phys.*, [5] **17**, 129 (1879).

(21) F. W. Kirkbride and F. G. Davidson, *Nature*, **174**, 79 (1954).

(22) D. A. Swick and I. L. Karle, *J. Chem. Phys.*, **23**, 1499 (1955).

(23) D. A. Swick, I. L. Karle and J. Karle, *ibid.*, **22**, 1242 (1954).

(24) G. J. Snaauw and E. J. Wiebenga, *Rec. trav. chim.*, **61**, 253 (1942).

(25) H. v. Wartenberg and J. Schiefer, *Z. anorg. allgem. Chem.*, **273**, 326 (1955).



There is not enough information available for  $\text{COBr}_2$  and  $\text{CCl}_2$  to include these molecules in this study.

**Acetyl Halides.**—Electron diffraction results are available for acetyl chloride<sup>43</sup>:  $R(\text{C}=\text{O}) = 1.22 \pm 0.04$ ,  $R(\text{CC}) = 1.50 \pm 0.04$  and  $R(\text{CCl}) = 1.77 \pm 0.02$  Å. The following distances and bond energies fit all four of these compounds:  $R(\text{C}=\text{O}) = 1.20$  with  $B(\text{C}=\text{O})$  167.0;  $R(\text{CC}) = 1.477$  with  $B(\text{CC}) = 99.1$  and  $R(\text{CH}) = 1.094$  with  $B(\text{CH}) = 99.4$  (Å. and kcal.). The  $\text{C}\text{I}$  and  $\text{CCl}$  bond energies of the carbonyls fit the acetyl compounds. In the case of acetyl bromide and iodide, the  $\text{CBr}$ - and  $\text{CI}$ -bond energies vary only very little in most of their compounds. The heat of formation of acetyl fluoride was obtained from the heat of reaction of the liquid with 0.2*N* sodium hydroxide<sup>35</sup> (Table VIII).

TABLE VIII  
ACETYL HALIDES

|                              | $Q_f$ ,<br>kcal.   | $Q_a$ ,<br>kcal. | $B(\text{CX})$ ,<br>kcal. | $R(\text{CX})$ ,<br>Å. |
|------------------------------|--------------------|------------------|---------------------------|------------------------|
| $\text{CH}_3\text{COF}$      | 101.7 <sup>b</sup> | 680.0            | 115.6                     | 1.32 <sup>d</sup>      |
| $\text{CH}_3\text{COCl}$     | 58.9 <sup>c</sup>  | 646.8            | 79.8                      | 1.746 <sup>e</sup>     |
| $\text{CH}_2\text{ClCOCl}^a$ | 54.9 <sup>c</sup>  | 619.7            | 79.8                      | 1.746 <sup>e</sup>     |
| $\text{CH}_3\text{COBr}$     | 44.6 <sup>c</sup>  | 630.2            | 66.6                      | 1.927 <sup>f</sup>     |
| $\text{CH}_3\text{COI}$      | 30.3 <sup>c</sup>  | 615.2            | 53.3                      | 2.124 <sup>g</sup>     |

<sup>a</sup>  $B(\text{CCl}$  in  $\text{CH}_2\text{Cl}-$ ) = 77.6 kcal. as in  $\text{CH}_2\text{Cl}_2$ . <sup>b</sup> Ref. 35. <sup>c</sup> Ref. 3. <sup>d</sup> As in  $\text{COF}_2$ . <sup>e</sup> As in  $\text{COCl}_2$ . <sup>f</sup> As in  $\text{CBr}_4$ . <sup>g</sup> As in  $\text{Cl}_4$ .

**Chloroacetic Acids.**—All needed bond energies and distances are carried over from acetic acid.<sup>5</sup>  $B(\text{CCl}, \text{CH}_3\text{Cl})$  for mono-,  $B(\text{CCl}, \text{CH}_2\text{Cl}_2)$  for di- and  $B(\text{CCl}, \text{CHCl}_3)$  for trichloroacetic acid were used (Tables III, IV and V). The bond energies and distances of acetic acid are:  $B(\text{CH}, 1.098$  Å.) = 98.9,  $B(\text{CC}, 1.508$  Å.) = 93.0,  $B(\text{OH}, 0.97$  Å.) = 109.0,  $B(\text{C}-\text{O}, 1.34$  Å.) = 106.0 and  $B(\text{C}=\text{O}, 1.21$  Å.) = 170.0 kcal. The heats of formation of these acids in the above order have been measured<sup>3</sup>: 98.0, 106.2 and 108.0 kcal. The corresponding thermochemical  $Q_a$ -values are 745.1, 730.2 and 708.9 kcal. The same quantities calculated from bond energies are: 752.5 (1% high), 732.1 (0.3% high) and 711.1 (0.4% high) kcal.

**Chloraldehydes.**—The bond distances and energies of acetaldehyde<sup>5</sup> are transferred:  $(\text{C}=\text{O}, 1.21, 170.0)$ ,  $(\text{CH}, 1.12, 96.2)$   $(\text{CH}, \text{CH}_3, 1.098, 98.7)$  and  $(\text{CC}, 1.52, 90.5)$  (Å., kcal.) as needed. The  $Q_f$ -values for the monochloro- and the trichloroaldehyde are known<sup>3</sup>: 47.3 and 43.0 kcal, so that  $Q_a = 635.2$  and 584.7 kcal. With  $B(\text{CCl}, \text{CH}_3\text{Cl})$  and  $B(\text{CCl}, \text{CHCl}_3)$  from Tables III and V, respectively, the calculated  $Q_a$  are 0.7% low and 0.4% high.

**2-Chloroethanol.**—The heat of formation of the gaseous substance is 60.4 kcal.<sup>3</sup> whence the experi-

mental  $Q_a = 752.5$  kcal. The bond energy value is 749.5 kcal. (0.3% low). It is derived by transfer of the following bond quantities from other molecules:  $(\text{CC}, \text{C}_2\text{H}_6, 1.543, 85.9)$ ,  $(\text{CH}, \text{C}_2\text{H}_6, 1.102, 98.4)$ ,  $(\text{CH}, \text{CH}_3\text{OH}, 1.098, 98.9)$ ,  $(\text{OH}, 0.967, 109.4)$ ,  $(\text{CO}, \text{CH}_3\text{OH}, 1.420, 82.9)$  and  $(\text{CCl}, \text{CH}_3\text{Cl}, 1.78, 76.7)$  Å. and kcal.

### Discussion

The simple relations here established between bond energies and bond distances of carbon-halogen bonds are considered an improvement over earlier work<sup>36</sup> in the sense that internuclear distances are now becoming known to much higher accuracy through microwave spectroscopy and new methods of carrying out electron diffraction experiments. However, even the present day results by the microwave technique are afflicted with a possible variation of  $\pm 0.01$  Å. in structures of different sets of isotopic species, because of the effect of zero point vibrations. However, progress is being made<sup>37</sup> and a more correct definition of coordinates permits the calculation of satisfactory distances. In the methyl halides no change need be made in the internuclear distances as used.<sup>6</sup>

It is believed that the empirical methods discussed here are of some interest when one considers the great difficulty which exists in the quantum mechanical calculations of bond energy values in order to attain results at all consonant with experimental values.<sup>38</sup> For the simple diatomic hydrides ( $\text{CH}, \text{NH}, \text{OH}, \text{FH}, \text{CH}^+$ ) the calculated dissociation energy is only about 20% of the observed one. Hence it is believed that the present empirical calculations can serve a useful purpose.

Even in this small study it was possible to point out certain discrepancies in thermal quantities cited in the literature. Hexachloroethane has a heat of formation of 303 kcal.<sup>21</sup> since the lower value does not fit with the distances obtained by electron diffraction.<sup>22</sup> The heat of sublimation of iodoform is estimated to be the very likely value of 9 kcal.<sup>3</sup> The  $Q_f$ -value of  $\text{CH}_2\text{Br}_2$  was estimated to be 0.7 kcal. It is given in the literature as 1.0 kcal.<sup>3</sup> The  $\text{CBr}$ -distance in  $\text{CH}_2\text{Br}_2$  is mentioned as being 1.91 Å.<sup>39</sup> A more likely value is 1.934 Å. as estimated here. Most of the cases studied were of course used to establish the bond energy-distance relations. However in fifteen cases the experimental  $Q_a$ -values derived from heats of formation could be compared with the ones obtained from the bond energy *vs.* bond distance system and showed a variation of  $\pm 0.3\%$ . Assuming that the constant terms  $L(\text{C})$ ,  $D(\text{H})_2$ ,  $D(\text{X}_2)$ , are relatively well known, then the total variation would fall onto  $Q_f$ . Since, however, heats of combustion are usually desired, the variation in these quantities would also be relatively small.

(36) H. A. Skinner, *Trans. Faraday Soc.*, **41**, 645 (1945).

(37) C. C. Costain, *J. Chem. Phys.*, **29**, 864 (1958).

(38) M. Krauss, *ibid.*, **28**, 1021 (1958).

(39) J. M. Dowling and A. G. Meister, *ibid.*, **22**, 1042 (1954).

(34) Y. Morino, K. Kuchitsu, M. Iwasaki, K. Arakawa and A. Kuchitsu, *J. Chem. Soc. Japan*, **75**, 647 (1954).

(35) H. O. Pritchard and H. A. Skinner, *J. Chem. Soc.*, 1099 (1950).

# RADIOLYSIS OF WATER BY PARTICLES OF HIGH LINEAR ENERGY TRANSFER. THE PRIMARY CHEMICAL YIELDS IN AQUEOUS ACID SOLUTIONS OF FERROUS SULFATE, AND IN MIXTURES OF THALLOUS AND CERIC IONS

BY MARC LEFORT AND XAVIER TARRAGO

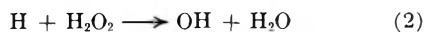
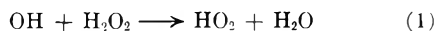
*Département de radiochimie, Laboratoire de Physique Nucléaire de la Faculté des Sciences de Paris, Orsay, France*

*Received January 23, 1959*

In order to measure the primary chemical yields of water radiolysis, mixtures of thallos and ceric ions in aqueous 0.8 *N* H<sub>2</sub>SO<sub>4</sub> solutions were irradiated by polonium  $\alpha$ -particles. Absolute dosimetry measurements were carried out. A *G*-value of  $5.5 \pm 0.1$  was found for ferrous sulfate oxidation. From this value and from results obtained on the ceric system, the following values were determined:  $G_{OH} = 0.50$ ,  $G_{HO_2} = 0.11$ ,  $G_{H_2O_2} = 1.45$ ,  $G_H = 0.60$ ,  $G_{H_2} = 1.57$  and  $G_{H_2O} = 3.62$ . However these yields depend on the concentration of thallos ions which inhibit the intratrack reaction  $H_2O_2 + OH \rightarrow H_2O + HO_2$ . An explanation also is given for the low yield (3.6) obtained for the oxidation of ferrous sulfate in deaerated solutions.

Although a large part of the early work in radiation chemistry was done on mixtures of radon with other gases, studies of radiation<sup>1-4</sup> induced reactions in water were carried out by a number of pioneers among them S. C. Lind<sup>5</sup> who investigated the radiolysis of aqueous potassium iodide solutions by  $\alpha$ -particles. He also wrote the first monograph on radiation chemistry,<sup>6</sup> a book which is of interest even today. In the period between the wars, few papers appeared on the chemical effects of  $\alpha$ -rays,<sup>7,8</sup> while much work was reported on reactions induced by X-rays, probably because the latter are easier and less dangerous to use than the radon techniques. More recently, however, interest has been aroused in the chemical effects of particles of high linear energy transfer (LET) by studies<sup>9-10</sup> on the formation and interaction of radicals in the neighborhood of the tracks produced by the particles. Furthermore, new sources of such particles have become available.

Attempts have been made to determine the molecular and radical yields along tracks of high LET particles. It has been shown recently, mainly with polonium  $\alpha$ -particles that in the radiolysis of water the radical HO<sub>2</sub> is produced inside each spur in nearly the same time as molecular hydrogen and hydrogen peroxide; it is believed that the local following reactions occur



Reaction 1 which was proposed in 1951<sup>11</sup> was later shown to be an *intratrack* reaction because of the high local concentration of OH radicals and H<sub>2</sub>O<sub>2</sub> molecules.<sup>12</sup> It was assumed to explain the produc-

tion of oxygen from pure water irradiated with  $\alpha$ -rays, which shows a linear increase with the absorbed dose. Hart<sup>13</sup> confirmed the primary formation of HO<sub>2</sub> with light particles in his study of  $\gamma$ -ray induced reactions in aqueous ferrous sulfate-cupric sulfate solutions. With similar solutions irradiated by polonium  $\alpha$ -rays, Donaldson and Miller<sup>14</sup> measured the oxygen yield ( $G_{O_2} = 0.23$ ) and suggested that HO<sub>2</sub> is a primary product of water decomposition. Pucheault<sup>15</sup> has assumed that the values of primary yields  $G_{OH}$ ,  $G_H$ ,  $G_{HO_2}$  and  $G_{H_2O}$  could vary in the presence of a solute which might scavenge more or less OH radicals or H atoms and therefore inhibit the local reaction of these species with H<sub>2</sub>O<sub>2</sub> or H<sub>2</sub>. Intratrack reactions are extensively discussed in references 16 and 17.

The purpose of our research was first to make an accurate determination of the oxidation yield of ferrous sulfate in aqueous sulfuric acid solutions irradiated with polonium  $\alpha$ -rays, and second to obtain more information on the magnitude of *intratrack* reactions and on their dependence on different solutes.

We have called "primary products" all those which are formed in dilute solutions from water, without direct interaction of the radiation on solutes. These products may be formed by many mechanisms such as ion neutralization, Stern-Volmer reactions, ion-molecule reactions or radical combinations at a very early stage. For the yield of primary products we have used the notation  $G_H$ ,  $G_{OH}$ , while the measured yields of stable products are written as  $G(H_2O_2)$ ,  $G(H_2)$ , . . .

## A. Oxidation of Ferrous Sulfate in Aerated Aqueous Solutions, 0.8 *N* H<sub>2</sub>SO<sub>4</sub>

### Experimental

Several drops of carefully purified polonium in 0.3 *N* nitric acid (50 microcuries per drop) was evaporated on a steam-bath in a silica crucible which had been irradiated with  $\gamma$ -rays. Following Dr. Hart's advice, we used polonium chloride in several runs instead of a nitric acid solu-

(1) A. T. Cameron and W. Ramsay, *J. Chem. Soc.*, **91**, 931 (1907); **92**, 966 (1908).

(2) J. Duane and O. Scheuer, *Le Radium*, **10**, 33 (1913).

(3) M. Kernbaum, *ibid.*, **6**, 225 (1909).

(4) A. Debiere, *Ann. Phys.*, **2**, 115, 126 (1914).

(5) S. C. Lind, *Le Radium*, **8**, 289 (1911).

(6) S. C. Lind, "The Chemical Effects of  $\alpha$ -Particles and Electrons," Interscience Publishers, New York, N. Y., 1921.

(7) F. C. Lanning and S. C. Lind, *THIS JOURNAL*, **42**, 1229 (1938).

(8) C. Nurnberger, *ibid.*, **38**, 47 (1934); **41**, 431 (1937).

(9) D. E. Lea, *Brit. J. Rad.*, *sup.* 1 (1947).

(10) L. H. Gray, *J. chim. phys.*, **48**, 172 (1951); M. Lefort, *ibid.*, **47**, 624 (1950); L. Monchick, J. L. Magee and A. H. Samuel, *J. Chem. Phys.*, **26**, 935 (1957); H. Fricke, *Ann. N. Y. Acad. Sci.*, **69**, 567 (1955); D. A. Flanders and H. Fricke, *J. Chem. Phys.*, **28**, 1126 (1958).

(11) M. Lefort, *J. chim. phys.*, **48**, 339 (1951).

(12) M. Lefort, "Actions chimiques et biologiques des radiations," *séris* 1, Masson et Cie., Paris, 1955, p. 118.

(13) E. J. Hart, *Radiation Res.*, **2**, 33 (1955).

(14) D. M. Donaldson and N. Miller, *Trans. Faraday Soc.*, **52**, 652 (1956).

(15) J. Pucheault, *Compt. rend. acad. Sci.*, **246**, 409 (1958).

(16) A. O. Allen and H. A. Schwarz, Proceedings of the second international conference on the peaceful uses of atomic energy—Geneva, 1958.

(17) M. Lefort, *Ann. Rev. Phys. Chem.*, **9**, 123 (1958).

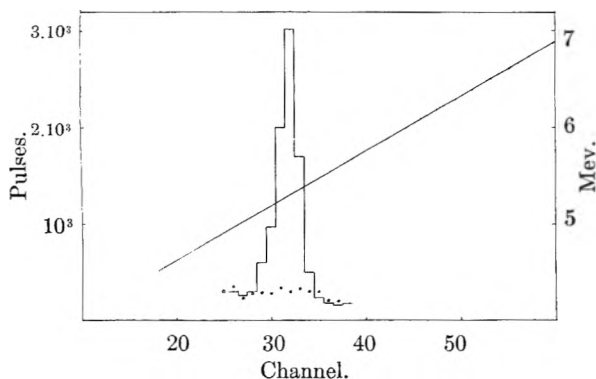


Fig. 1.—The counting of  $\alpha$ -particles for absolute dosimetry:  $\bullet$ , background measurements. The straight line indicates the energy calibration of pulse amplitude.

tion; however, we obtained the same yield in the presence or absence of chloride ion.

The  $10^{-3} M$  ferrous sulfate solution then was added. The solution was stirred and transferred to spectrophotometer cells. Formation of ferric ions was followed by measurement of the optical density at 3040 Å. The cells were thermostated at  $25 \pm 0.02^\circ$  and the extinction coefficient was found to be  $2205 \pm 20 \text{ mole}^{-1} \text{ cm}^{-1}$ . The usefulness of the Fricke dosimeter has been discussed frequently in connection with X- and  $\gamma$ -rays. The polonium activity in the irradiated solution was measured with a pulse ionization chamber collecting free electrons, and a multi-channel system for pulse height recording and measurement. A very small aliquot of the solution was diluted to serve as  $\alpha$ -emitter source. The  $\alpha$ -ray width was measured and compared with that of a pure polonium emitter. When the width was larger because of self absorption, the preparation was not used for dosimetry (Fig. 1). The pulse ionization chamber was filled with a mixture of  $\text{CO}_2$  and argon and worked at 4.500 volts. It had been calibrated with standards and the maximum error of the counting measurements was lower than 1%.

The dilution factor was of the order of 2:10,000. We made several determinations of activity for the same initial solution and checked that the mean square deviation was about 2%.

Schuler and Barr,<sup>18</sup> working with  $10^{-1} M$  ferrous sulfate solutions, report a yield of  $\text{Fe}^{+++}$  of  $4.22 \pm 0.08$  for  $\text{B}(n, \alpha)\text{Li}$  recoils, and  $5.69 \pm 0.12$  for  ${}^6\text{Li}(n, \alpha){}^3\text{He}$ . The first published yields for polonium  $\alpha$ -rays (5.3 Mev.) ranged from 5.9 to 6.2,<sup>19</sup> but recently values of 5.6<sup>20</sup> and 5.2<sup>21</sup> have been reported.

Our results are recorded in Table I from which a value of  $G_{\text{Fe}^{+++}} = 5.5 \pm 0.1$  was obtained. The ferric ion yield was independent of the polonium concentration, *i.e.*, of the dose rate, between 20 and 1000 microcuries per cc.; ( $1.4 \times 10^{16} \text{ e.v. cc}^{-1} \text{ hr}^{-1}$  to  $1 \times 10^{18} \text{ e.v. cc}^{-1} \text{ hr}^{-1}$ ), and remained almost constant throughout the oxidation.  $G_{\text{Fe}^{+++}}$  was also independent of the ferrous sulfate concentration between  $2 \times 10^{-4}$  and  $2 \times 10^{-3} M$ , but with a concentration of  $10^{-2} M$ , we obtained a yield of 5.65 which seems to be definitely higher than that of more dilute solutions. This is in agreement with Schuler and Barr's<sup>18</sup> results on the oxidation rate induced by  $\text{B}(n, \alpha)\text{Li}$  recoils.

(18) R. H. Schuler and N. F. Barr, *J. Am. Chem. Soc.*, **78**, 5756 (1956).

(19) (a) M. Haissinsky and M. C. Anta, *Compt. rend. acad. sci.*, **236**, 1161 (1953); (b) N. Miller, *Trans. Faraday Soc.*, **50**, 690 (1954); (c) R. McDonell and E. J. Hart, *J. Am. Chem. Soc.*, **76**, 2121 (1954).

(20) M. Lefort, *Compt. rend. acad. sci.*, **245**, 1623 (1957).

(21) C. N. Trumbore, *J. Am. Chem. Soc.*, **80**, 1772 (1958).

TABLE I  
OXIDATION OF FERROUS ION IN SOLUTION IRRADIATED WITH  
 $\alpha$ -PARTICLES

| Polonium, $\mu\text{c.}/\text{cc.}$ | Measd. dose rate $\times 10^{17}$ , e.v./cc. | Time of observation, hr. | Oxidation rate $\times 10^{15}$ , ions $\text{cc}^{-1} \text{ hr}^{-1}$ | Mean $G$ -value along the straight line of oxidn. |
|-------------------------------------|----------------------------------------------|--------------------------|-------------------------------------------------------------------------|---------------------------------------------------|
| 20                                  | 0.11                                         | 162                      | 0.60                                                                    | 5.45                                              |
| 50                                  | .30                                          | 80                       | 1.55                                                                    | 5.50                                              |
| 100                                 | .65                                          | 20                       | 3.59                                                                    | 5.52                                              |
| 100                                 | .76                                          | 20                       | 4.25                                                                    | 5.58                                              |
| 200                                 | 1.18                                         | 12                       | 6.50                                                                    | 5.50                                              |
| 250                                 | 1.75                                         | 19                       | 9.50                                                                    | 5.40                                              |
| 250                                 | 1.82                                         | 19                       | 10.20                                                                   | 5.60                                              |
| 1000                                | 6.80                                         | 8                        | 37.40                                                                   | 5.50                                              |

## B. Reduction of Ceric Ion Induced by $\alpha$ -Particles

### Experimental

Several authors<sup>22-24</sup> have studied the reduction of ceric ions in dilute aqueous solutions of  $\text{H}_2\text{SO}_4$  by polonium  $\alpha$ -particles. We determined this yield in 0.8  $N$   $\text{H}_2\text{SO}_4$  by the technique used for ferrous sulfate. Very pure solutions were prepared as described previously.<sup>24</sup> The disappearance of ceric ions was measured directly in spectrophotometer cells at 3200 Å. for the most dilute solutions. We have taken an extinction coefficient of  $5580 \pm 50 \text{ mcl}^{-1} \text{ cm}^{-1}$ . For irradiation in the absence of oxygen, 20 to 30 cc. of solution was degassed under vacuum at the same time as blanks, by trapping and warming up several times.

We found that the ion yield was independent of both the dose rate and the ceric ion concentration. The  $G$ -value was constant up to high doses and dropped off slightly when nearly all the ceric ions had been reduced. As shown in Fig. 2, there was a difference between the reduction yields determined in the presence and in the absence of air.

$$\frac{G_{\text{aer}}}{G_{\text{vac.}}} = 1.05 \pm 0.01 \text{ (Fig. 2)}$$

The ratio  $G(\text{Fe}^{+++})/G(\text{Ce}^{+++})$  also was determined on the same solution by the following procedure: the reduction of ceric ions was followed for some time, and then 1 cc. of  $2 \times 10^{-3}$  molar ferrous sulfate solution was added to 2 cc. of the initial ceric and polonium mixture. After stirring, all the remaining ceric ions were reduced. Ferric ions were measured, and the value obtained was used to verify the direct determination made with the spectrophotometer at 320  $\mu\mu$ . Then the oxidation of the excess ferrous ions in the new solution was followed; the dose rate was  $2/3$  of the initial rate. The ratio  $G(\text{Fe}^{+++})/G(\text{Ce}^{+++})$  could be determined with great precision; we had found that cerous ions have no effect on the oxidation yield of ferric ions.

In presence of air  $G(\text{Fe}^{+++})/G(\text{Ce}^{+++}) = 1.72 \pm 0.02$  (Fig. 3).

Gas analysis was carried out with an apparatus built in the laboratory several years ago,<sup>25</sup> by measuring the total pressure with a McLeod gauge and the ionization current produced in an alphasatron. In this apparatus, the ionization source is a polonium deposit in equilibrium with  $\text{RaD}$  ( $\text{Pb}^{210}$ ). The ionization current produced through the mixture of gases is proportional to energy loss per unit of track length of  $\alpha$ -particles,  $dE/dx$ . This value is proportional to the pressure, and the ionization current is therefore proportional to the pressure.  $dE/dx$  is very dependent on the nature of gases, particularly on the oxygen and hydrogen content of the mixture. After careful calibration we were able to analyze in one minute mixtures of hydrogen and oxygen with a precision of 1%, when the total amount was of the order of 10  $\text{mm}^3$  at atmospheric pressure. Table II gives our results.

TABLE II

| $G(\text{aer. Fe}^{+++})$ | $G(\text{Ce}^{\text{III}} \text{ aer.})$ | $G(\text{Ce}^{\text{III}} \text{ in vacuo})$ | $G(\text{H}_2)$ | $G(\text{O}_2)$ |
|---------------------------|------------------------------------------|----------------------------------------------|-----------------|-----------------|
| $5.5 \pm 0.1$             | $3.20 \pm 0.06$                          | $3.10 \pm 0.06$                              | $1.57 \pm 0.05$ | $1.57 \pm 0.05$ |

(22) M. Lefort and M. Haissinsky, *J. chim. phys.*, **48**, 368 (1951).

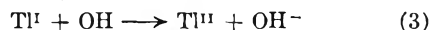
(23) M. C. Anta and M. Haissinsky, *ibid.*, **51**, 33 (1954).

(24) M. Lefort, *ibid.*, **54**, 782 (1957).

(25) M. Lefort, *J. phys. radium*, **17A**, 164 (1956).

### C. Aqueous Acid Solutions of Ceric and Thallous Ions

The previous data are of interest for the following experiments from which primary yields of water decomposition could be calculated. Sworski<sup>26</sup> has shown that the reduction of ceric ions by  $\gamma$ -radiation follows the rate:  $G(\text{Ce}^{\text{III}}) = 2G_{\text{H}_2\text{O}_2} + G_{\text{H}} - G_{\text{OH}}$ ; he also found that the addition of thallous ions at a concentration high enough to scavenge every OH radical increases the reduction yield to  $2G_{\text{H}_2\text{O}_2} + G_{\text{H}} + G_{\text{OH}}$ , according to reactions 3 and 4



If  $\text{HO}_2$  is locally produced through reaction 1, the yield of cerous ions in the absence of thallium is not changed since one ceric ion is reduced by one  $\text{HO}_2$ ; this is strictly equivalent to the reduction of two ions by  $\text{H}_2\text{O}_2$  and the reoxidation of one cerous ion by OH. This is true also for ferric ion formation in the presence of oxygen, since  $3\text{Fe}^{\text{++}}$  ions are oxidized by  $\text{HO}_2$  as well as by  $\text{H}_2\text{O}_2 + \text{OH}$ . Moreover, the addition of thallous ions to ceric sulfate solutions permits the determination of  $G_{\text{HO}_2}$ , as can be seen from the equations

$$G(\text{Ce}^{\text{III}}) = 2G_{\text{H}_2\text{O}_2} + G_{\text{H}} + G_{\text{HO}_2} - G_{\text{OH}} \quad (5)$$

$$G(\text{Fe}^{\text{III}}) = 2G_{\text{H}_2\text{O}_2} + 3G_{\text{H}} - G_{\text{OH}} + 3G_{\text{HO}_2} \quad (6)$$

$$G(\text{Ce}^{\text{III}})(\text{Tl}^{\text{I}} \text{ added}) = 2G_{\text{H}_2\text{O}_2} + G_{\text{H}} + G_{\text{HO}_2} + G_{\text{OH}} \quad (7)$$

$$G(\text{H}_2) = G_{\text{H}_2} = G_{\text{H}_2\text{O}_2} + \frac{1}{2}G_{\text{OH}} - \frac{1}{2}G_{\text{H}} + \frac{3}{2}G_{\text{HO}_2} \quad (8)$$

From Sworski's experiments,<sup>26</sup> equation 7 is obtained with initial concentrations of  $2 \times 10^{-4} M$  for thallous ions and  $10^{-4}$  to  $10^{-3} M$  for ceric ions. Such mixtures were irradiated with dissolved polonium in the absence and presence of air. The disappearance of ceric ions was followed spectrophotometrically until half of the ceric ions had disappeared. A  $10^{-3} M$  ferrous sulfate solution then was added; the ferric ions formed are a measure of the amount of ceric and thallic ions remaining in the solution. Therefore  $G(\text{Tl}^{\text{III}})$  is equal to the difference between  $G_{\text{Fe}^{\text{+++}}}$  and  $G_{\text{Ce}^{\text{+++}}}$  determined above. From the above scheme  $G_{\text{OH}} = G(\text{Tl}^{\text{III}})$ , but the difference is small and the precision is not good.

The results were very reproducible, much more so than for solutions containing only ceric ions (Fig. 4). The yield was constant as long as the ratio of the concentrations of ceric to thallic ions was large. However, the initial concentration of thallous ions has a slight effect on the initial yield of ceric ion reduction. Table III gives the values which were obtained in evacuated solution for several thallous concentrations, together with the yields  $G_{\text{OH}}$ ,  $G_{\text{HO}_2}$ ,  $G_{\text{H}_2\text{O}_2}$ , which can be calculated from the equations

$$(7) - (6) = G(\text{Fe}) - G(\text{Ce Tl}) = 2(G_{\text{H}} + G_{\text{HO}_2})$$

$$(7) - (5) = G(\text{Ce} + \text{Tl}) - G(\text{Ce}) = 2G_{\text{OH}} = 2G(\text{Tl}^{\text{III}})$$

$$(6) - 2(8) = G(\text{Fe}) - 2G(\text{H}_2) = 4G_{\text{H}}$$

$$3(7) - (6) = 3G(\text{Ce} + \text{Tl}) - G(\text{Fe}) = 4G_{\text{H}_2\text{O}_2} + 2G_{\text{OH}}$$

The values given in Table III are in accord with the equation  $G_{(\text{O}_2)} = G_{\text{H}_2\text{O}_2} + G_{\text{HO}_2}$ , a finding which confirms our results. Thus, the radiation induced decomposition of water may be calculated by  $-G_{\text{H}_2\text{O}} = G_{\text{H}} + 2G_{\text{H}_2} - G_{\text{HO}_2} = G_{\text{OH}} + 2G_{\text{HO}_2} + 2G_{\text{H}_2\text{O}_2}$ .

In presence of air the reduction yields were slightly higher, and the ratio  $G_{\text{aer}}/G_{\text{vac}}$  is the same as that found for pure ceric solutions, 1.05.

Although values for the absolute yields are given within 2%, differences between yields, corresponding to differences in thallous ion concentration, have a much better precision.

**Discussion of Table III.**—(1) The increase of  $G(\text{Ce}^{\text{+++}})$  with initial thallous concentration involves an increase of  $G_{\text{OH}}$  and a decrease of  $G_{\text{HO}_2}$ . Intratrack reaction 1 is therefore inhibited by thallous ions. An upper limit of  $0.22 \pm 0.2$  could be extrapolated for  $G_{\text{HO}_2}$ , a value which is in agreement with Donaldson and Miller's results.<sup>14</sup>

(2) It is therefore believable that when solutions containing only ceric ions are irradiated, the initial yield of reduction is equal to  $G_{\text{Ce}^{\text{+++}}} = 2G_{\text{H}_2\text{O}_2} + G_{\text{HO}_2} + G_{\text{H}} - G_{\text{OH}}$  with  $G_{\text{H}_2\text{O}_2} = 1.35$ ;  $G_{\text{HO}_2} =$

(26) T. J. Sworski, *Radiation Research*, **4**, 483 (1956).

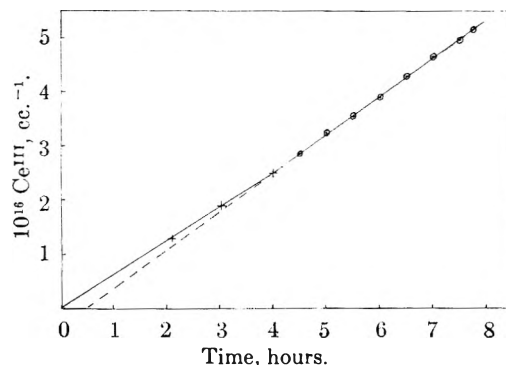


Fig. 2.—The rate of reduction of ceric sulfate:  $\text{Ce}^{\text{IV}}$ ,  $1.4 \times 10^{-4} M$ ; dose rate  $2.2 \times 10^{17}$  e. v. cc.<sup>-1</sup> hr.<sup>-1</sup>; X, reduction in evacuated solution; O, reduction in aerated solution.

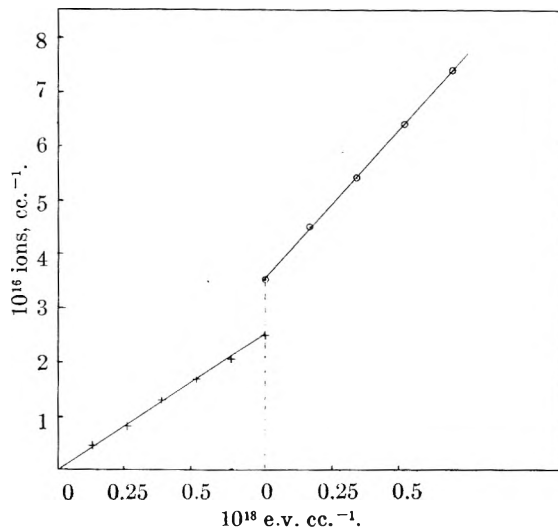


Fig. 3.—The measurement of the reduction of ceric sulfate and the oxidation of ferrous sulfate; —, dose rate:  $0.26 \times 10^{18}$  e. v. cc.<sup>-1</sup> hr.<sup>-1</sup> in ceric ions solution  $10^{-4} M$ ;  $0.175 \times 10^{18}$  e. v. cc.<sup>-1</sup> hr.<sup>-1</sup> in ferrous ions solution; X, the measurement of cerous ions; O, measurement of ferric ions. The dotted line indicates the addition of ferrous solution to the ceric sulfate solution and the first point corresponds to the oxidation of ferrous ions by remaining ceric ions.

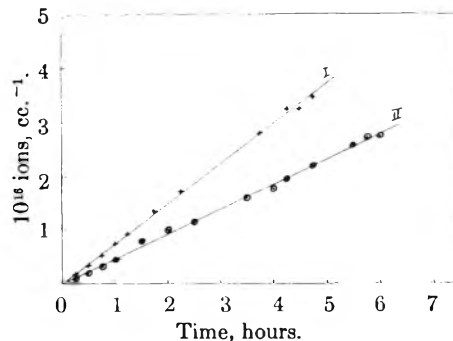


Fig. 4.—The effect of presence of thallous ions in irradiation of deaerated solutions of ceric ions: I,  $\text{Tl } 10^{-3}$ ,  $\text{Ce } 2 \times 10^{-4} M$ , dose rate  $1.81 \times 10^{17}$  e. v. cc.<sup>-1</sup> hr.<sup>-1</sup>; II,  $\text{Ce } 2 \times 10^{-4} M$ , dose rate  $1.44 \times 10^{17}$  e. v. cc.<sup>-1</sup> hr.<sup>-1</sup>.

$0.22$ ,  $G_{\text{OH}} = 0.40$  and  $G_{\text{H}} = 0.60$ . This is in disagreement with Pucheault's calculations<sup>15</sup> in which  $G_{\text{HO}_2}$  was assumed to be negligible for dilute solutions of ceric ion.

(3) At concentrations greater than  $2 \times 10^{-3} M$  thallous ion, the oxygen yield decreases,  $G(\text{Ce}^{\text{+++}})$

TABLE III  
IRRADIATION OF DEAERATED SOLUTION CONTAINING CERIC AND THALLOUS IONS

| Initial<br>Tl <sup>I</sup> concn.,<br><i>M</i> | <i>G</i> (Ce <sup>IV</sup> )<br>±0.1 | <i>G</i> (H <sub>2</sub> ) | <i>G</i> (O <sub>2</sub> ) | <i>G</i> (Tl <sup>III</sup> )<br>±0.2 | <i>G</i> <sub>OH</sub> | <i>G</i> <sub>HO<sub>2</sub></sub> | <i>G</i> <sub>H<sub>2</sub>O<sub>2</sub></sub> | <i>G</i> <sub>H</sub> | - <i>G</i> <sub>H<sub>2</sub>O</sub> |
|------------------------------------------------|--------------------------------------|----------------------------|----------------------------|---------------------------------------|------------------------|------------------------------------|------------------------------------------------|-----------------------|--------------------------------------|
| 3 × 10 <sup>-5</sup>                           | 3.90                                 | 1.57 ± 0.05                | 1.56 ± 0.05                | 0.6                                   | 0.40                   | 0.20                               | 1.36                                           | 0.59                  | 3.52                                 |
| 10 <sup>-4</sup>                               | 4.0                                  | 1.57 ± 0.05                | 1.55                       | .5                                    | .43                    | .16                                | 1.41                                           | .59                   | 3.57                                 |
| 2 × 10 <sup>-4</sup>                           | 4.05                                 | 1.57                       |                            |                                       | .45                    | .15                                | 1.42                                           | .59                   | 3.58                                 |
| 10 <sup>-3</sup>                               | 4.1                                  | 1.57                       | 1.55                       |                                       | .50                    | .11                                | 1.45                                           | .59                   | 3.62                                 |
| 2 × 10 <sup>-3</sup>                           | 4.18                                 | 1.58                       | 1.58 ± 0.05                | .6                                    | .54                    | .08                                | 1.50                                           | .58                   | 3.70                                 |
| 7 × 10 <sup>-3</sup>                           | 4.25                                 | 1.58                       | 1.30 ± 0.1                 | .8                                    | .8                     | .02                                | 1.25                                           | .58                   | 3.70                                 |

is unaffected, and apparently  $G(\text{Tl}^{+++})$  increases. As  $G_{\text{HO}_2}$  cannot be decreased any further, and since  $G_{\text{O}_2} = G_{\text{HO}_2} + G_{\text{H}_2\text{O}_2}$ , it follows that  $G_{\text{H}_2\text{O}_2}$  decreases from about 1.48 to 1.25. The concentration of thallos ions is so high that within each spur, thallos ions compete for OH radicals with the combination of OH radicals and thus inhibit the primary formation of H<sub>2</sub>O<sub>2</sub>. No change is found for  $G(\text{Ce}^{+++})$  since ceric ions which are not reduced by H<sub>2</sub>O<sub>2</sub> are destroyed by Tl<sup>I</sup> according to reaction 4. This effect seems similar to Miller and Donaldson's observation on the decrease of  $G(\text{H}_2)$  when the cupric ion concentration is increased to 10<sup>-2</sup> molar.

(4) It is possible to compare the mean concentration of hydrogen peroxide when it goes into reaction with OH radicals along the  $\alpha$ -track with the H<sub>2</sub>O<sub>2</sub> concentration in the bulk of a solution irradiated by  $\gamma$ -rays. From our results we can assume that a concentration of 2 or 3 × 10<sup>-3</sup> molar thallos ion is necessary to suppress  $G_{\text{HO}_2}$ , while a concentration of 3 × 10<sup>-5</sup> *M* is high enough, from Sworski's experiments, to protect OH radicals against back reactions in the bulk of the solution. This means that the concentration of hydrogen peroxide is about 100 times higher in local cylindrical columns where intratrack reactions occur during expansion of the track, than in the bulk of the solution.

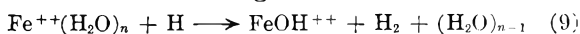
(5) The slightly larger reduction yield in aerated solutions is difficult to understand since HO<sub>2</sub> reduces ceric ions as well as H atoms. Positively oxygen is acting as a strong scavenger for H atoms or free electrons, and therefore the primary yield  $G_{\text{H}}$  is enhanced while  $G_{\text{H}_2}$  decreases.

#### D. Comments on the Yield of Oxidation of Ferrous Sulfate in Deaerated Solutions

If we use the primary yields obtained above for a calculation of ferrous sulfate oxidation in the absence of oxygen,  $G_{(\text{Fe}^{+++})} = 4.36$ .

$$G_{(\text{Fe}^{+++})} = 2G_{\text{H}_2\text{O}_2} + G_{\text{H}} + 3G_{\text{HO}_2} + G_{\text{OH}} = 2.7 + 0.60 + 0.66 + 0.40 = 4.36$$

This is much higher than the value of 3.6 observed by several authors<sup>14,20</sup> together with  $G(\text{H}_2) = 1.8$ . There is no reason to reduce  $G_{\text{HO}_2} = 0.23$  since Donaldson and Miller<sup>14</sup> found a yield of 0.23 when cupric ion is added to ferrous sulfate, under conditions where reaction 1 can occur in the same manner as for pure ferrous ions. On the other hand,  $G_{\text{H}}$  may be calculated from  $G(\text{H}_2) - G_{\text{H}_2}$  since ferric ions are formed through reaction 9



$G_{\text{H}_2}$  has been found to be 1.6 and  $G(\text{H}_2) = 1.8$ . Then with  $G_{\text{H}} = 0.2$ ,  $G_{\text{HO}_2} = 0.23$  and  $G(\text{Fe}^{+++}) = 3.6$

$$2G_{\text{H}_2\text{O}_2} + G_{\text{OH}} = 3.6 - 0.2 - 0.69 = 2.71$$

This value is much lower than in the cupric-ferrous solutions (3.12). But cupric ions, as well as oxygen molecules in aerated solutions of ferrous ions, scavenge atomic hydrogen and therefore inhibit intratrack reaction 2. However, when only ferrous ions are present, reaction 2 occurs and could explain a drop in  $G_{\text{H}_2\text{O}_2}$  from 1.35 to 0.95 because of a yield of 0.4 for reaction 2.  $G_{\text{OH}}$  would increase for the same reason from 0.4 to 0.8 and  $2G_{\text{H}_2\text{O}_2} + G_{\text{OH}}$  would decrease to 2.7.

As it has been suggested several times<sup>15,17,20</sup> it is difficult to assign the same primary yields for all aqueous solutions; for example, aerated and deaerated aqueous solutions of ferrous sulfate support the yields as in Table IV.

TABLE IV

|                                    | <i>G</i> <sub>H</sub> | <i>G</i> <sub>H<sub>2</sub></sub> | <i>G</i> <sub>OH</sub> | <i>G</i> <sub>HO<sub>2</sub></sub> | <i>G</i> <sub>H<sub>2</sub>O<sub>2</sub></sub> | - <i>G</i> <sub>H<sub>2</sub>O</sub> |
|------------------------------------|-----------------------|-----------------------------------|------------------------|------------------------------------|------------------------------------------------|--------------------------------------|
| Fe <sup>+++</sup> + O <sub>2</sub> | 0.59                  | 1.57                              | 0.4                    | 0.22                               | 1.35                                           | 3.55                                 |
| Fe <sup>+++</sup> <i>in vacuo</i>  | 0.2                   | 1.6                               | 0.8                    | 0.23                               | 0.95                                           | 3.2                                  |

The yield of decomposition of water itself varies according to the inhibition of intratrack reactions 1 and 2 by solutes. The lower and upper limits seem to be 3.2 and 3.8 for 5.3 mev.  $\alpha$ -particles.

## IRRADIATION OF POLYETHYLENE. IV. OXIDATION EFFECTS

BY HIROSHI MATSUO<sup>1</sup> AND MALCOLM DOLE*Contribution from the Chemical Laboratory of Northwestern University, Evanston, Illinois**Received February 2, 1959*

The radiolytic oxidation of a linear polyethylene has been studied by measuring changes in total pressure, by observing increases in optical density in the infrared due to carbonyl absorbance and by analyzing gaseous products of oxidation when polyethylene film of different thicknesses was exposed to  $\gamma$ -radiation in the initial presence of a few cm. pressure of oxygen. A steady rate of oxidation was soon established, making valid the use of a solution of the differential equation combining both diffusion and reaction for the steady state. About one fourth of the combined oxygen appeared as carbonyl and one eighth as water. Another eighth of the oxygen formed a mixture of carbon monoxide and dioxide. The rest of the oxygen must have formed mostly peroxides and alcohols. Product yields were linear with amount of oxygen consumed whether during the irradiation or in the dark period subsequent to the irradiation. Hydrogen gas evolution and growth and decay of unsaturation apparently were unaffected by the presence of oxygen, but the dose required to reach the gel point was increased. Chemical mechanisms are discussed.

## Introduction

The oxidation of polyethylene during pile irradiation was first observed<sup>2,3</sup> by chemical analysis and from infrared absorption measurements of irradiated film at 5.8  $\mu$ , the carbonyl absorption band and at 3.0  $\mu$ , the hydroxyl absorption band. As the final percentage of oxygen in films 0.06 mm. thick was about four times as great as that in granules of 2.7 mm. diameter, it was concluded that oxidation depended strongly on the surface area. Charlesby<sup>4</sup> came to the same conclusion by studying weight changes during pile irradiation of polyethylene samples of different sizes and shapes.

In the many oxidation studies<sup>5-14</sup> that have been carried out since then, there have been no measurements of the rate of oxygen uptake during the irradiations, no calculations of  $G(-O_2)$  although Lawton, Powell and Balwit<sup>7</sup> did calculate a related  $G(-O_2)$  and  $G(H_2O + CO_2 + CO)$  for post-irradiation oxidation. There have been no kinetic equations developed, no calculation of  $G$ -values for the individual oxidation products. Such information is essential for a complete understanding of oxidation mechanisms.

## Experimental

**Materials.**—The linear polyethylene, Marlex-50, free of anti-oxidant was kindly supplied by the Phillips Petroleum Co. It was used in the form of films of different thicknesses. Thick films were made by carefully heating and fusing together stacked layers of film between polished aluminum plates.

**Radiation Source and Cells.**—The radiation source and cells were essentially the same as previously described.<sup>15</sup>

(1) On leave from the Electrical Communication Laboratory, Nippon Telegraph and Telephone Public Corporation, Tokyo, Japan.

(2) D. G. Rose, M.S. Thesis, Northwestern University, 1948.

(3) M. Dole, Report of Symposium IX, "Chemistry and Physics of Radiation Dosimetry," Army Chemical Center, Md., 1950, p. 120.

(4) A. Charlesby, *Proc. Roy. Soc. (London)*, **215A**, 187 (1952).

(5) W. C. Sears and W. W. Parkinson, Jr., *J. Polymer Sci.*, **21**, 325 (1956).

(6) E. J. Lawton, J. S. Balwit and R. S. Powell, *ibid.*, **32**, 257 (1958).

(7) E. J. Lawton, R. S. Powell and J. S. Balwit, *ibid.*, **32**, 277 (1958).

(8) K. Schumacher, *Kolloid Z.*, **157**, 16 (1958).

(9) A. Chapiro, *J. chim. phys.*, **52**, 246 (1955).

(10) M. Magat, "International Radiation Research Congress," Burlington, Vt., August, 1958.

(11) N. Bach, ref. 10.

(12) N. A. Bach and V. V. Saraeva, *Zhurn. Fiz. Khim.*, **32**, 209 (1958).

(13) L. E. St. Pierre and H. A. Dewhurst, *J. Chem. Phys.*, **29**, 241 (1958).

(14) P. Alexander and D. Toms, *J. Polymer Sci.*, **22**, 343 (1956).

(15) M. Dole, D. C. Milner and T. F. Williams, *J. Am. Chem. Soc.*, **80**, 1580 (1958).

In order to carry out irradiations at about one eighth the usual dose rate, a holder for the cells was constructed in such a way that the irradiation cell could be supported above the stainless steel blocks containing the Co-60 rather than between them.

**Gas Analysis and Pressure Measurements.**—Before the irradiations, the cells containing the Marlex-50 were evacuated and then filled with pure oxygen at pressures varying from one to six cm. By means of a mercury manometer in a side arm the total pressure could be read at any desired time to  $\pm 0.02$  cm. using a cathetometer. The cell was immersed in a constant temperature bath at 27° during the pressure measurements. The cell contained a second side-arm which could be immersed in liquid nitrogen to freeze out all gaseous products, leaving O<sub>2</sub>, H<sub>2</sub> and CO uncondensed. The pressure was then read and corrected to 27° to give the non-condensable gas pressure at 27°. The sidearm was next immersed in a Dry Ice-acetone bath to freeze out or condense only water, methyl alcohol, acetone, etc. This pressure was read and corrected to 27°. The difference between this pressure and the total was assumed to be water vapor pressure. Sometimes a trace of liquid condensed, at which time the partial pressure of the water became constant. During the time that these pressure measurements were being made, the irradiation cell was removed from the zone of the radiations. The three measurements required about 30 minutes; in this period consumption of oxygen by the post-irradiation effect introduced a negligible error.

Several samples of the gas uncondensable at liquid nitrogen temperature as well as samples of the condensable gas were analyzed in the mass spectrometer either by Dr. D. M. Mason of the Department of Chemical Engineering, Northwestern University or by the Institute of Gas Technology, Chicago.

The volume of the uncondensable gas was measured in a Toepler pump and could be calculated also after a calibration of the volume of the cell. The volume of condensable gases was also measured, when it was possible to do so, in the Toepler pump.

**Measurement of Gel Content and Infrared Technique.**—Estimates of the sol-gel ratio and of vinyl and vinylene group concentrations<sup>15</sup> were carried out as previously described.<sup>16</sup> For estimates of the carbonyl group concentration a value<sup>17</sup> of 188 l. cm.<sup>-1</sup> mole<sup>-1</sup> was taken for the carbonyl molar extinction coefficient<sup>17</sup> at 5.8  $\mu$ . Although growth in the infrared absorption band due to OH had been previously observed during irradiation of polyethylene in air,<sup>2,3</sup> in this work OH could not be detected due to the relatively small doses used and the small pressure of oxygen.

## Results

The general trend of the results in the case of the thinnest film used, 0.0045 cm. thick, is shown in Fig. 1. The top curve represents the total pressure as a function of time. The initial drop in pressure was due to the excess "clean-up" or consumption of oxygen over the hydrogen evolved; the minimum represents the time when most of the oxygen

(16) T. F. Williams and M. Dole, paper submitted for publication.

(17) L. H. Cross, R. B. Richards and H. A. Willis, *Disc. Faraday Soc.*, **9**, 235 (1950).

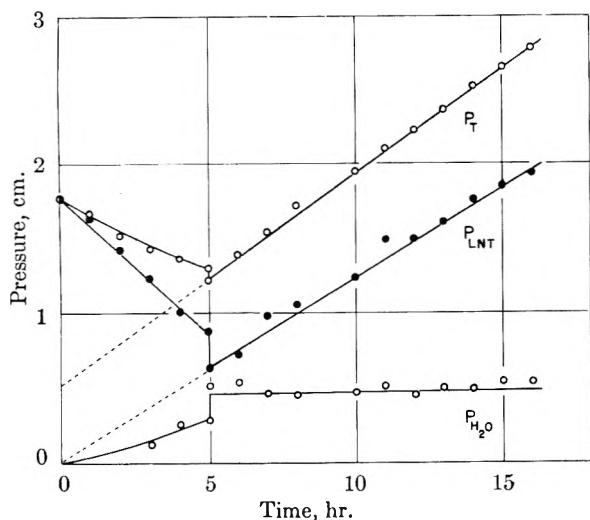


Fig. 1.—Gas pressures in irradiation cell during  $\gamma$ -ray irradiation: upper curve, total pressure; middle curve, pressure corrected to 27° with sidearm in liquid nitrogen trap; lower curve, water partial vapor pressure.

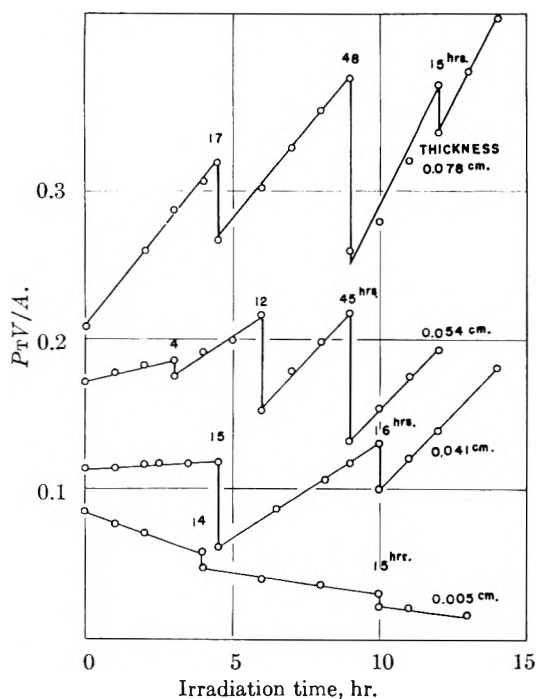


Fig. 2.—Total gas pressure in cell during irradiation multiplied by cell volume and divided by total surface area of polyethylene film. Film thicknesses are given at the right and the numbers over the vertical lines represent the length of the dark period (*i.e.*, no irradiation).

had reacted; and the final linear rising portion of the curve was due to a constant evolution of hydrogen. If this latter curve is extrapolated back to zero time, the intercept on the pressure axis represents the final total pressure of the gaseous oxidation products. In the case of the experimental data of Fig. 1, the extrapolated pressure was about 7.5 mm. while the estimated pressure of water vapor and other gases condensable at Dry Ice temperature was  $5.0 \pm 0.5$  mm. The difference in these pressures, 2.5 mm. can be ascribed to carbon monoxide and carbon dioxide. The total pressure ( $P_{H_2} + P_{CO} + P_{CO_2} + P_{H_2O}$ ) at the end of the

experiment, 27.8 mm., less the pressure ( $P_{H_2} + P_{CO}$ ) at liquid nitrogen temperature (corrected to room temperature) 19.6 mm., less the pressure (chiefly  $P_{H_2O}$ ) of the products condensable at Dry Ice temperature, 5.4 mm., should be the pressure of carbon dioxide, or 2.8 mm. This estimate is somewhat greater than the previous estimate of  $P_{CO} + P_{CO_2}$ , 2.5 mm., which suggests that  $P_{CO}$  could not have been very significant. However, in another experiment where the initial oxygen pressure,  $P_{O_2}^0$ , was much greater, the data of Table I were obtained (estimated for 27°). The pressure of hydrogen was obtained by calculation, assuming  $G(H_2)$  to be 3.8. The pressure of CO could then be obtained by subtracting  $P_{H_2}$  from  $P_{H_2} + P_{CO}$ . In this experiment the pressure of carbon monoxide was seen to be about equal to that of carbon dioxide and 8% of the non-condensable gas pressure at liquid nitrogen temperature. A mass spectrometric analysis of the non-condensable gas yielded 6 and 4% carbon monoxide in two different experiments.

TABLE I

## SUMMARY OF PRESSURE ESTIMATES

Anti-oxidant free Marlex-50 film 0.0388 cm. thick after a total dose of  $6.47 \times 10^{20}$  e.v.g.<sup>-1</sup>

|                                      |          |                                         |      |
|--------------------------------------|----------|-----------------------------------------|------|
| Initial O <sub>2</sub> pressure, mm. | 64.0     |                                         |      |
| Final pressure, mm.                  | 94.7     | Fraction of O <sub>2</sub> converted to |      |
| $P_{H_2}$                            | 66.7     | C=O (carbonyl)                          | 0.25 |
| $P_{CO}$                             | 5.7      | H <sub>2</sub> O                        | .14  |
| $P_{H_2O}$                           | 18.1     | CO <sub>2</sub>                         | .06  |
| $P_{CO_2}$                           | 4.2      | CO                                      | .05  |
| Total                                | 94.7 mm. | Total                                   | 0.50 |
|                                      |          | Peroxides and alcohols<br>by difference | 0.50 |
|                                      |          |                                         | 1.00 |

Figure 2 illustrates the effect of film thickness on the rate of pressure change as well as the post-irradiation oxidation effect. The thicker the film the greater the rate of evolution of hydrogen per cm.<sup>2</sup>, and the thicker the film, the more pronounced is the post-irradiation oxidation effect. In Fig. 2 the vertical lines represent the decrease in oxygen pressure during resting periods when the film was not being irradiated. Note that the post-irradiation effect declines as the pressure of the oxygen drops.

It is interesting to plot the initial slopes of the curves of Fig. 2 as a function of the film thickness. This is done in Fig. 3 where it can be seen that as the films become thicker, the initial slopes change from negative to positive values, and the curves become linear with the thickness  $\delta$ . This is to be expected because per sq. cm. of surface area, the rate of hydrogen evolution should increase linearly with the thickness. At zero thickness there should be no hydrogen evolution, the latter being a volume effect. Actually, the experimentally determined data fail to follow the linear relation because as the film thickness is reduced the negative rate of pressure increase due to oxygen consumption outweighs the positive rate for hydrogen evolution and the ordinates of Fig. 3 become negative. However, at zero thickness there should also be no oxygen consumption.

By extrapolating the straight lines of Fig. 3 to

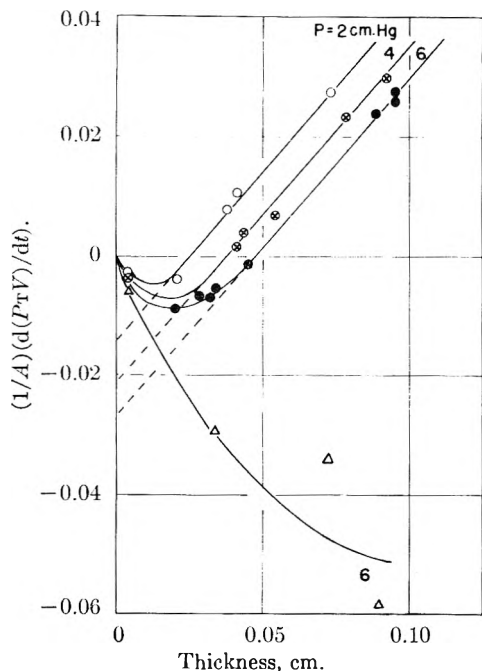


Fig. 3.—Initial rate of change of the function  $PTrV/A$  with time plotted as a function of film thickness for different initial oxygen pressures. The lowest curve represents results obtained in the low intensity experiments, normalized to the same dose rate as the data of the other curves.

zero thickness, the intercept on the ordinate can be obtained. This gives the maximum rate per  $\text{cm.}^2$  of oxygen consumption less the rate of products formed for infinitely thick films. The points at which the extrapolated lines meet the actual curves give the thicknesses at the indicated initial oxygen pressures beyond which no further significant oxygen consumption can be gained. This last point is confirmed by the data of Fig. 4 where the initial rate of oxygen uptake at about 5 cm. pressure is plotted as a function of film thickness. It is seen that the rate approaches a limiting value. The upper curve demonstrates that at an eightfold lower intensity the uptake of oxygen per  $\text{cm.}^2$  per unit of radiation energy absorbed is about twice as great, with the limiting ratio at infinite thickness even greater than this. The middle curve represents the oxygen uptake including both the oxygen consumption during the irradiation and during any subsequent dark period.

If the optical density at  $5.8 \mu$ , the carbonyl absorption band, is plotted as a function of the oxygen uptake, the relationship appears to be linear within the experimental uncertainties both for low and high intensities and demonstrates that the nature of the reaction products did not depend on the amount of oxygen reacted, at least for the extent of reaction involved here. Furthermore, since the ratio of oxygen consumed to product gas formed during the dark periods (periods of no irradiation) seemed to be equal to the ratio for the periods of irradiation ( $\pm 15\%$ ), the conclusion also could be reached that the reactions involving oxygen were the same during both irradiation and no irradiation.

As far as could be told from the data of this re-

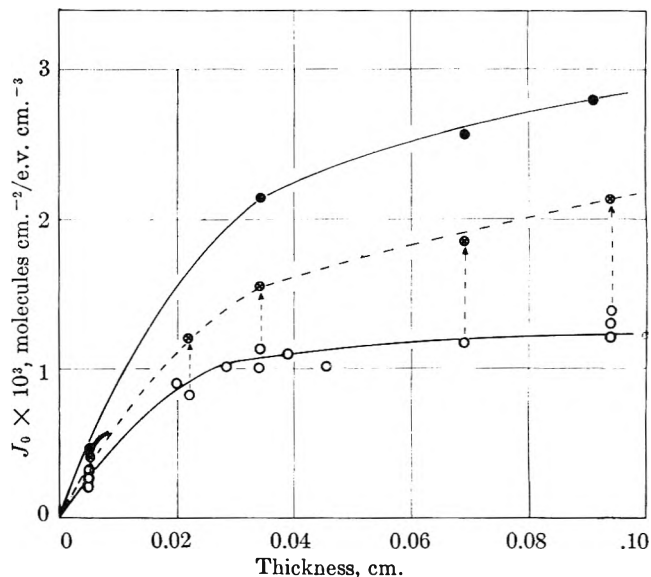


Fig. 4.—Steady-state initial flux of oxygen into film plotted as a function of film thickness: open circles, high intensity experiments; closed circles low intensity experiments corrected to dose rate of high intensity experiments; vertical lines growth of oxygen uptake during resting periods subsequent to the irradiation. Initial oxygen pressure about 5 cm. for all points.

search, hydrogen evolution, vinyl group decay and vinylenes growth and decay were unaffected by the presence of the oxygen. One difficulty in testing the effect of oxygen on changes in unsaturation or hydrogen evolution is that the films must be rather thick to give significant sensitivity; on increasing the thickness of the films the ratio of oxidized regions of the polyethylene to unoxidized decreased. Hence, for a really accurate test of the effect of oxygen on hydrogen evolution, vinyl or vinylenes decay and vinylenes growth, much greater pressures of oxygen should have been used.

In agreement with the observation of many others, the dose required to reach the gel point was about doubled in the case of films 0.03 cm. thick, but hardly affected for films 0.09 cm. thick.

A blank experiment with a mixture of hydrogen and oxygen gas in the irradiation cell showed no change of pressure with time; *i.e.*, there was no perceptible radiolytically induced reaction between oxygen and hydrogen gas. The density of the gas phase was so low relative to that of the polyethylene that no effect would have been expected unless a chain reaction ensued.

As will be seen below,  $G$ -values for oxygen consumption,  $G(-O_2)$ , depend very strongly on many factors, especially on the film thickness, radiation intensity and oxygen pressure. Because of the increase in the rate of oxygen consumption with film thickness as shown in Fig. 4,  $G(-O_2)$  at first increased with film thickness. As the thickness of the film was increased beyond about 0.02 cm. in our experiments,  $G(-O_2)$  decreased, because a greater fraction of the  $\gamma$ -ray energy was absorbed in the interior of the film where no or very little oxygen was available for reaction. The maximum observed  $G(-O_2)$  was 9.9 for a film thickness of 0.021 cm. and an initial oxygen gas pressure of 5.5 cm. Not enough experiments were done using the low inten-



sity radiation to estimate the maximum  $G(-O_2)$  at the optimum film thickness, but under comparable conditions  $G(-O_2)$  for the low intensity experiments was greater by a factor of about 1.2 than  $G(-O_2)$  for the high intensity experiments.

Table II contains estimates of the maximum  $G$ -values of the oxidation products as well as can be calculated from the data.

TABLE II

ESTIMATED MAXIMUM  $G$ -VALUES, MOLECULES/100 E.V.

|                      |      |
|----------------------|------|
| $G(-O_2)$            | 10.0 |
| $G(\text{carbonyl})$ | 5.0  |
| $G(H_2O)$            | 2.5  |
| $G(CO)$              | 1.0  |
| $G(CO_2)$            | 0.6  |

### Kinetic Interpretation of Data

From the foregoing and from previous work of others it is obvious that an interpretation combining simultaneous diffusion theory<sup>18</sup> and reaction must be developed. Let us assume that competitive reactions exist for free radicals between oxygen and other free radicals, then we can write

$$\frac{\partial c}{\partial t} = \frac{k'c}{1 + k''c} \quad (1)$$

where  $c$  is the oxygen concentration in the film and  $t$  is the time. Combining (1) with the diffusion equation for unidirectional diffusion and assuming  $\mathfrak{D}$ , the diffusion coefficient to be independent of concentration and irradiation dosage, eq. 2 results

$$\frac{\partial c}{\partial t} + \frac{k'c}{1 + k''c} = \mathfrak{D} \frac{\partial^2 c}{\partial x^2} \quad (2)$$

The boundary conditions adopted are

$$c = c_0 \text{ at } x = \pm \frac{\delta}{2} \text{ at all } t \quad (3a)$$

$$\frac{\partial c}{\partial x} = 0 \text{ at } x = 0 \text{ at all } t \quad (3b)$$

$$c = c_0 \text{ at all } x \text{ at } t = 0 \quad (3c)$$

In eq. 2 and 3,  $x$  is the distance through the film measured from the mid-point,  $k'$  and  $k''$  are reaction rate constants and  $c_0$  the oxygen concentration in the surface layer. We assume that the rate of attainment of oxygen solubility equilibrium in the surface was rapid compared to reaction and diffusion. If this were not the case, and if the rate of diffusion of oxygen into the film were rate limiting, then the oxygen consumption rate would have been independent of film thickness.

The oxygen pressure decreased during the irradiation, so  $c_0$  must also have decreased with time. For this reason, we shall be chiefly concerned with the initial rate of oxygen uptake. The data indicated that in the high intensity experiments an initial steady-state rate of oxygen uptake was established. The solubility of oxygen at room temperature and 7 cm. pressure (the highest pressure used) was about  $2 \times 10^{-7}$  mole of oxygen per gram of polyethylene.<sup>19</sup> As the maximum observed rate of oxygen consumption was of the order  $10^{-6}$  mole/g. hr. in the high intensity experiments, it is reasonable to

suppose that the oxygen initially dissolved in the film must have reacted fairly rapidly, thereby making possible the establishment of a steady state of oxygen consumption and diffusion, at least within an hour or two. However, a steady state could be expected, theoretically, only if the ambient oxygen pressure remained constant, but if the latter was constant, no rate of oxidation could have been observed by pressure measurements. One of the surprising results of this research was the initially unchanging rate of oxygen consumption despite the continually declining ambient oxygen pressure; a marked change of the oxygen uptake rate occurred usually only after a period of no irradiation. Presumably, a new steady-state concentration gradient of oxygen in the polyethylene was established on renewing the irradiation. Figure 5 illustrates hypothetical curves of the oxygen concentration in the film as a function of distance through the film at different times. It is seen readily that as the oxygen in the film is cleaned up, the concentration gradient in the surface layer of the polyethylene increases. Thus, if the radiation intensity is not too high, an increase with time in the rate of oxygen uptake should have been observable because the flux of oxygen into the film depends on the concentration gradient in the surface layer. Figure 6 illustrates just such an effect in the case of an experiment at the lower  $\gamma$ -ray intensity.

If a steady state does exist, eq. 2 can be simplified to

$$\mathfrak{D} \frac{\partial^2 c}{\partial x^2} = \frac{k'c}{1 + k''c} \quad (4)$$

For high enough concentrations so that  $k''c \gg 1$ , (4) reduces to an equation for diffusion coupled with a zero-order reaction

$$\mathfrak{D} \frac{\partial^2 c}{\partial x^2} = k \quad (5)$$

Integrating twice and evaluating the constants of integration by means of the boundary conditions

$$c - c_m = \frac{k}{2\mathfrak{D}} x^2 \quad (6)$$

where  $c_m$  is the oxygen concentration in the middle of the film at  $x$  equals zero. In the boundary layer at  $x$  equal to  $\delta/2$

$$c_0 - c_m = \frac{k}{2\mathfrak{D}} \left(\frac{\delta}{2}\right)^2 \quad (7)$$

Thus the difference in concentration,  $c_0 - c_m$ , depends on the film thickness. Obviously (7) becomes invalid when the film thickness is so great that a zero-order reaction cannot prevail throughout the film. Differentiating (6) with respect to  $x$ , and multiplying  $\delta c/\delta x$  by  $\mathfrak{D}$  to obtain the flux,  $J$ , one can obtain either

$$J = kx \quad (8a)$$

or

$$J = (c - c_m)^{1/2} (2k\mathfrak{D})^{1/2} \quad (8b)$$

Equation 8a requires that  $J_0$ , the flux in the surface layer, depend only on the film thickness

$$J_0 = k \frac{\delta}{2} \quad (9)$$

This means that the concentration difference ( $c_0 -$

(18) For theories combining both diffusion and reaction see, for example, J. Crank, "The Mathematics of Diffusion," Oxford, 1956, Sec. 8.3.

(19) Unpublished measurements of M. Fallgatter in this Laboratory.

$c_m$ ) is independent of concentration at any fixed value of  $\delta$  but that it increases as the square of  $\delta/2$ .

If  $k''c \ll 1$ , eq. 4 reduces to an equation with diffusion coupled with a first-order reaction

$$D \frac{\partial^2 c}{\partial x^2} = kc \quad (10)$$

A solution<sup>20</sup> satisfying the boundary conditions is

$$c = \frac{c_0}{1 + e^{-(k/D)^{1/2}\delta}} [e^{(k/D)^{1/2}(x-\delta/2)} + e^{-(k/D)^{1/2}(x-\delta/2)}] \quad (11)$$

giving for the flux in the surface layer

$$J_0 = c_0 \times (kD)^{1/2} \frac{1 - e^{-(k/D)^{1/2}\delta}}{1 + e^{-(k/D)^{1/2}\delta}} \quad (12)$$

Equation 12 demonstrates that the flux in the surface layer rapidly becomes independent of the film thickness as the latter is increased; thus for thick films

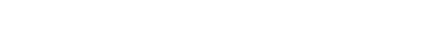
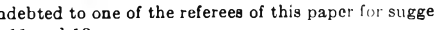
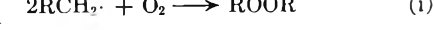
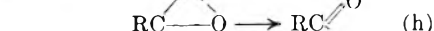
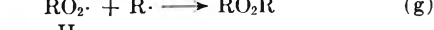
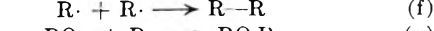
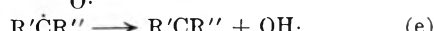
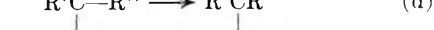
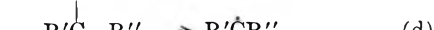
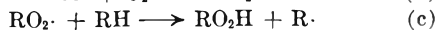
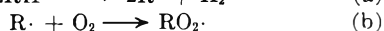
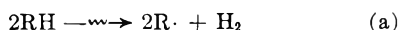
$$J_0 = c_0(kD)^{1/2} \quad (13)$$

As  $\delta$  approaches zero, (12) is reduced in the case of thin films to

$$J_0 = c_0 k \frac{\delta}{2} \quad (14)$$

Both (13) and (14) predict that either for very thick films or for thin films of the same thickness, the oxygen uptake should be proportional to the oxygen pressure to the first power (assuming the validity of Henry's law). This was not observed. On the other hand both (9) and (14) predict that the rate of oxygen consumption should be linear with film thickness for very thin films. The data of Fig. 4 seem to bear out this prediction. Values of  $J_0$  calculated from (12) can be made to approximate the data of Fig. 4, but the theoretical curve rises too steeply at low values of  $\delta$ , and then levels off too abruptly at higher values of  $\delta$ .

We turn now to a consideration of possible reactions which could be used to establish a model of the reaction kinetics. Bach,<sup>11</sup> Bach and Saraeva<sup>12</sup> and Magat<sup>10</sup> have studied the radiolytic oxidation of paraffinic hydrocarbons and polyethylene. They propose the reactions



(20) We are indebted to one of the referees of this paper for suggesting the solutions 11 and 12.

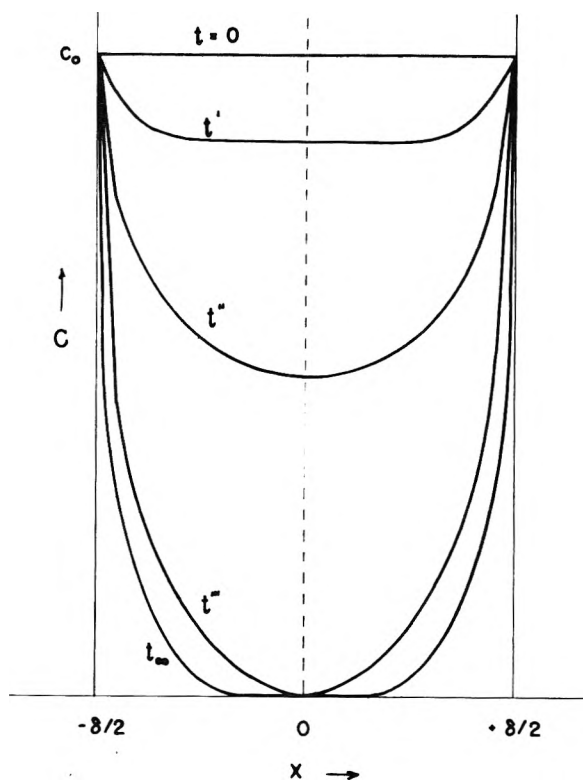


Fig. 5.—Schematic representation of the variation of the concentration of oxygen across the film at different times after the start of the irradiation, assuming no change in external oxygen pressure.

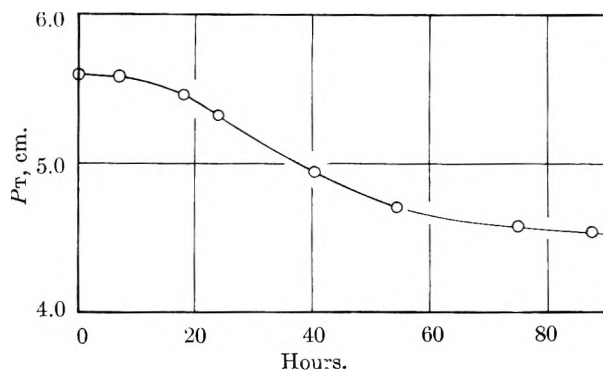
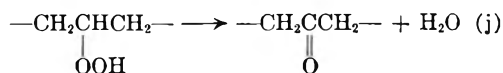


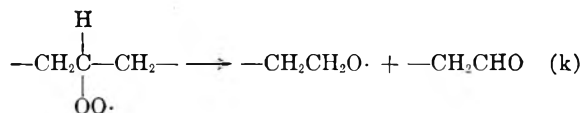
Fig. 6.—Total pressure in irradiation cell during a low intensity radiation experiment; film 0.0723 cm. thick.

Although reactions (b) and (c) constitute a chain, Magat and Bach believe that no chain reaction exists. Bach believes that  $R\cdot$  is formed initially with excess energy which carries over to  $RO_2\cdot$ , but which is lost by the time  $R\cdot$  is formed in reaction (c). The free radical  $R\cdot$  of (c) can react with  $O_2$  to form  $RO_2\cdot$ , but this free radical is not an excited radical and does not have enough energy to overcome the activation energy required for reaction (c).

In the papers of Bach and Magat nothing is said of the formation of gaseous products although the evolution of  $CO$ ,  $CO_2$  and  $H_2O$  is mentioned by Lawton, Powell and Balwit.<sup>7</sup> We have found that on the average carbonyl and water are formed in the molar ratio of 2 to 1, approximately. If carbonyl were formed exclusively from the decomposition of hydroperoxide

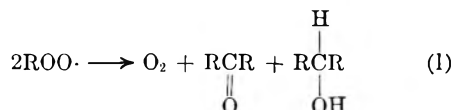


the ratio would be one to one. Water could also be formed by the OH of reaction (e) abstracting a hydrogen atom from a neighboring chain, but the ratio of carbonyl to water would still be one to one. Evidently carbonyl is also formed by reactions such as (h) or by equation (k) suggested by Chapiro<sup>9</sup>

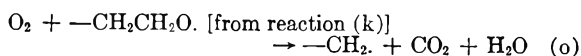
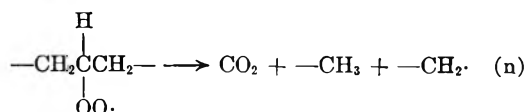
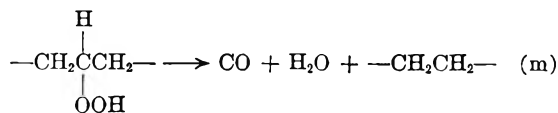


without the concomitant production of water (see also reaction (l)).

Another type of reaction for the termination step has been found by Russell<sup>21</sup> to yield the best explanation for the autoxidation of aralkyl hydrocarbons at 60°. This reaction involves the reaction of two peroxy radicals

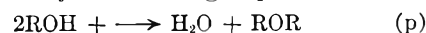


with the liberated oxygen again reacting according to (b). In this case the reaction scheme would involve reactions (a), (b) and (c) with (l) as the termination step. If the kinetic chain length is unity, *i.e.*, one oxygen molecule absorbed per initiating free radical, the total number of oxygen atoms appearing as carbonyl oxygen should be one-fourth the number of the oxygen atoms absorbed. Referring to Table I it is seen that this requirement is fulfilled. Reaction (l) also requires that the number of hydroxyl groups formed should equal the number of carbonyl groups. Neither Russell nor we were able to analyze the product for its hydroxyl content. However, Russell's scheme cannot be completely applicable to the present results, because it does not predict the formation of water. If water is formed exclusively by reaction (j), then the carbonyl content should be greater than one-fourth of the oxygen consumed. This difficulty could be partly resolved if the termination reactions were not exclusively the one suggested by Russell, but included also (f), (g), (i), etc. If water, CO and CO<sub>2</sub> were formed by the reactions



part of the yield of water could be accounted for without the necessity of postulating the simultaneous production of carbonyl, and the presence of CO and CO<sub>2</sub> in the product gas could be explained. Another possibility of water formation without

carbonyl groups being formed is given by the decomposition of adjacent ROH groups



Still another possibility would be provided by the decomposition of two adjacent hydroperoxides

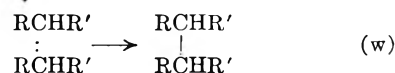
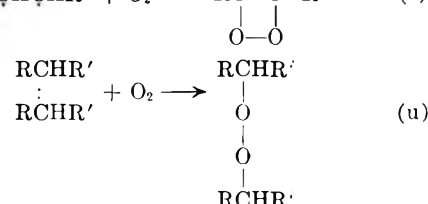
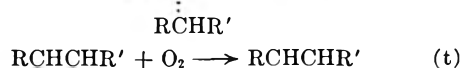
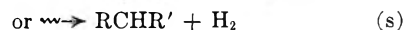


The next problem is to develop kinetic equations corresponding to the different reaction mechanisms. Considering *only* reactions (a), (b), (c) and (l) it is easy to show that the rate of oxygen clean-up must be zero order. For a kinetic chain length of unity, the net rate of oxygen consumption is the rate of (b) less one-third the rate of (l). Assuming homogeneous steady-state kinetics

$$-\frac{\partial c}{\partial t} = \frac{5}{3}\varphi I + k_c \left[ \frac{\varphi I}{k_1} \right]^{1/2} \quad (15)$$

In eq. 15 *t* is the time, *I* the intensity of the radiation,  $\varphi$  the quantum yield,  $k_c$  and  $k_1$  are the reaction rate constants of reactions (c) and (l). The concentration of the polyethylene, [RH], is taken to be a constant at the doses used here. The whole right-hand side of (15) is equal to *k* of eq. 5. The fact that the flux of oxygen into the film, *J*, is not linear with the film thickness,  $\delta$ , as required by eq. 9 demonstrates that oxygen consumption is not zero order throughout the film.

Another reaction scheme which describes only peroxide formation from two closely situated free radicals, but which involves competitive termination reactions is



This sequence yields the rate equation for oxygen consumption

$$-\frac{\partial c}{\partial t} = \varphi I [\text{RH}] \left[ \frac{k_{tc}}{k_{tc} + k_v} + \frac{k_{uc}}{k_{uc} + k_v} \right] \quad (16)$$

In the derivation of (16), the configuration



was considered as a single unit. At high oxygen concentrations (16) reduces to a zero-order rate law and at low concentrations to a first-order rate law.

Turning now to the interpretation of the actual data, the variation in flux, *J*<sub>0</sub>, with the oxygen pressure can be seen in Fig. 3. The intercepts of the curves at zero film thickness, corrected for the rate

(21) G. A. Russell, *Chemistry and Industry*, 1483 (1956); *J. Am. Chem. Soc.*, 79, 3871 (1957).

of product formation, represent the maximum rate of oxygen consumption. The intercepts, given in Table III, seem to be proportional to the square root of oxygen pressure. The rates also are proportional to the function  $k'P/(1 + k''P)$  within the experimental uncertainties. The chief uncertainty in determination of the initial rates is the magnitude of the correction for the gaseous reaction products. There was definite experimental indication of a lag in the build-up of the product pressure, possibly due to a slowness of diffusion of water vapor out of the film.

The conclusion reached is that competitive reac-

tions exist, but this rather obvious deduction, unfortunately, does not permit us to choose any particular reaction scheme as being the most likely one. We believe that our results, in fact, cannot be represented by any one reaction sequence.

Finally, it is interesting to point out that the zero-order rate law constant  $k$  of eq. 9 can be evaluated by estimating the slope of the  $J$ - $\delta$  plot, Fig. 4, at  $\delta$  equal to zero (infinitely thin film). Multiplying by 2 to obtain  $k$  and multiplying the latter by 100 to obtain a theoretical maximum value of  $G(-O_2)$ , the result is  $15 \pm 3$ . If the kinetic chain length for oxygen consumption is unity, then this number represents the maximum number of free radicals produced per 100 e.v. of absorbed  $\gamma$ -ray energy.

**Acknowledgment.**—We gratefully acknowledge the support of the U. S. Atomic Energy Commission and the gift of materials from the Phillips Petroleum Co.

TABLE III  
Max. rate of consumption relative values

| O <sub>2</sub> pressure, cm. | Max. rate of consumption relative values | $\sqrt{P}$<br>Rate |
|------------------------------|------------------------------------------|--------------------|
| 1.7                          | 0.020                                    | 65                 |
| 4.0                          | .030                                     | 66                 |
| 6.2                          | .0386                                    | 65                 |

## THE PHOTOLYSIS OF AMMONIA IN THE PRESENCE OF NITRIC OXIDE<sup>1</sup>

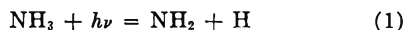
By A. SEREWICZ AND W. ALBERT NOYES, JR.

*Department of Chemistry, University of Rochester, Rochester, New York*

*Received February 2, 1959*

The products of the photolysis of ammonia in the presence of nitric oxide are N<sub>2</sub>, N<sub>2</sub>O, H<sub>2</sub>O and H<sub>2</sub>. The last is a minor product unless the concentration of nitric oxide is very low. A mechanism is proposed.

The photolysis of ammonia has been very extensively studied.<sup>2</sup> In spite of this fact several steps in the mechanism, and in particular the step which leads to production of molecular nitrogen, must still be considered to be uncertain. Nevertheless it may be stated with considerable certainty that the primary process is



with a primary quantum yield of unity. The facts which support these conclusions are as follows. (1) The spectrum of ammonia gas in the region 2000–2400 Å. consists of diffuse bands<sup>2</sup>; (2) hydrazine becomes a major product in a flow system which removes it rapidly from the illuminated zone in which atoms and radicals are present.<sup>3</sup>

Ammonia-nitric oxide mixtures have been previously studied<sup>4</sup> but the importance of nitrous oxide formation seems not to have been emphasized.

It was hoped in undertaking this study that relative rate constants for several reactions of the NH<sub>2</sub> radical might be obtained. This hope has not been fully realized.

(1) This research was supported in part by contract AF18(600) 1528 with the United States Air Force through the Air Force Office of Scientific Research of the Air Research and Development Command. Reproduction in whole or in part is permitted for any purpose by the United States Government. The authors wish to express their appreciation to Dr. P. Ausloos for many helpful discussions and ideas.

(2) Space does not permit a complete bibliography of ammonia photolysis to be given. See W. A. Noyes, Jr., and P. A. Leighton, "The Photochemistry of Gases," Reinhold Publ. Corp., New York, N. Y., 1941, p. 370; C. C. McDonald and H. E. Gunning, *J. Chem. Phys.*, **23**, 532 (1955); H. Gesser, *J. Am. Chem. Soc.*, **77**, 2626 (1955).

(3) C. C. McDonald, A. Kahn and H. E. Gunning, *J. Chem. Phys.*, **22**, 908 (1954).

(4) C. H. Bamford, *Trans. Faraday Soc.*, **35**, 568 (1939). See H. Gesser, ref. 2.

### Experimental

The main features of the vacuum line were similar to those used in other studies in this Laboratory. No stopcocks were used except for a few runs with a portable cell, when a temperature of 0° was required. In these runs two stopcocks were present.

Ammonia from the Ohio Chemical Company was passed through a series of traps at -78° and then outgassed at -159°. Finally the ammonia for each run was outgassed at -196°. Fresh samples of gas were used for each run.

Nitric oxide (Matheson) was passed through several traps at -159°, one at -183° and finally outgassed for several days at -196°. Mass spectrographic analysis showed a purity of 99.6%.

A medium pressure mercury arc (Hanovia S-100) was used without filters except that in some runs the radiation passed through a tube containing mercury vapor to reduce danger of mercury sensitization and in a few runs a path of 5 cm. of water was interposed to reduce short wave lengths. The light was collimated by a quartz lens. Intensities were varied, when necessary, by interposing wire screens whose transmissions were measured by a Beckman ultraviolet photometer.

Most of the runs were made with a cell 5 cm. in diameter and 10 cm. long enclosed in an aluminum block furnace. Temperatures were read by several thermocouples placed on the cell wall. The experiments at 0° were made with a portable cell 5 × 8 cm. irradiated in a brass cylinder with double quartz windows and filled with ice and water.

It was necessary to avoid local depletion of nitric oxide when the pressure of the latter was low. A 6.5 liter bulb was inserted in the line and the gases circulated by a magnetically driven stirrer. Not more than 5% of the nitric oxide and usually not more than 0.2% of the ammonia reacted during a given run.

Nitrogen and hydrogen were removed at -215° and the hydrogen oxidized by cupric oxide at 315°. Hydrogen was determined by difference. Nitric oxide was then removed at -183° (liquid oxygen). Any nitric oxide in the -215° fraction would have been recorded as hydrogen but all analyses were checked with the mass spectrograph. Nitrous oxide was separated at -159° at which temperature ammonia is retained in the trap.

Water was determined by reaction with calcium carbide. The method was checked by formation of water from "water gas." The calcium carbide must be renewed frequently since reaction with water appears to stop once the surface has reacted. Water analyses are less accurate than the others.

### Results

Many preliminary experiments (data not shown) served to show the importance of several variables. In the later runs the effects of the following variables were studied: (1) nitric oxide pressure; (2) temperature; (3) intensity; (4) time of irradiation.

Irradiation of nitric oxide alone produced only nitrogen as the product not condensed at  $-215^{\circ}$  since presumably oxygen reacts with nitric oxide either during the experiment or during the analysis. When mixed with sufficient propane to quench excited mercury atoms (if present) the nitrogen yield was the same as in pure nitric oxide and neither hydrogen nor propene was formed. These results indicate that mercury sensitized reactions did not occur under the conditions of these experiments.

The effects of time of reaction at constant intensity and of rate of reaction as a function of intensity were investigated. There is no conclusive evidence for a change of rate with time and hence the products of the reaction do not interfere

TABLE I

EFFECT OF INTENSITY ON RATE

 $T = 31 \pm 1^{\circ}$ ;  $P_{\text{NH}_3} = 38 \text{ mm.}$ ;  $P_{\text{NO}} = 5 \text{ mm.}$ 

| Intensity (relative) | Time, min. | $\text{N}_2$ moles $\times 10^6$ /hr. | Moles $\times 10^6$ /hr. intensity (relative) |              |                      |       |
|----------------------|------------|---------------------------------------|-----------------------------------------------|--------------|----------------------|-------|
|                      |            |                                       | $\text{N}_2$                                  | $\text{H}_2$ | $\text{H}_2\text{O}$ |       |
| 0.106                | 240        | 0.67                                  | 6.3                                           | 0.24         | 2.0                  | 5.8   |
| 0.297                | 85         | 1.98                                  | 6.6                                           | .55          | 2.8                  | 9.6   |
| 1.00                 | 35         | 6.24                                  | 6.2                                           | 58           | 2.5                  | (8.7) |

TABLE II

EFFECT OF NITRIC OXIDE PRESSURE ON RATES (LOW PRESSURES)

 $T = 31^{\circ}$ ;  $P_{\text{NH}_3} = 38.3 \pm 1 \text{ mm.}$  (Expansion bulb in line)

| $P_{\text{NO}}$ , mm. | $\text{N}_2$ moles $\times 10^6$ /hr. | $\text{H}_2/\text{N}_2$ (A) | $\text{N}_2\text{O}/\text{N}_2$ (B) | $2A + 2B$ |
|-----------------------|---------------------------------------|-----------------------------|-------------------------------------|-----------|
| ..                    | 0.78 <sup>a</sup>                     | 2.8                         | ..                                  | ..        |
| ..                    | 0.86 <sup>a</sup>                     | 2.8                         | ..                                  | ..        |
| 0.11                  | 1.87                                  | 0.38                        | 0.47                                | 1.7       |
| .12                   | 3.54                                  | .34                         | .35                                 | 1.4       |
| .23                   | 3.62                                  | .30                         | .16                                 | 0.92      |
| .29                   | 3.43                                  | .35                         | .19                                 | 1.1       |
| .54                   | 3.51                                  | .26                         | .25                                 | 1.0       |
| 1.07                  | 3.71                                  | .19                         | .31                                 | 1.0       |
| 1.21                  | 3.67                                  | .16                         | ..                                  | ..        |
| 2.39                  | 3.41                                  | .12                         | .48                                 | 1.2       |
| 0.10                  | 1.27 <sup>b</sup>                     | .29                         | ..                                  | ..        |
| 0.22                  | 1.15 <sup>b</sup>                     | .23                         | ..                                  | ..        |
| 0.32                  | 2.19 <sup>b</sup>                     | .21                         | .26                                 | 0.94      |
| 0.14                  | 2.23 <sup>c</sup>                     | .32                         | .15                                 | 0.94      |

Av. (except 1st two) 1.0

<sup>a</sup> Without water filter. <sup>b</sup> Intensity 0.29 of full intensity. <sup>c</sup> Intensity 0.62 of full intensity. NOTE:  $\Phi_{\text{N}_2} = 1$  at sufficiently high NO pressures but this is undoubtedly not true for low NO pressures. Hence  $\text{H}_2\text{O}/\text{N}_2$  is not  $\Phi_{\text{N}_2\text{O}}$  in this table at low NO pressures.

(5) P. J. Flory and H. L. Johnston, *J. Chem. Soc.*, **57**, 2641 (1935).

with the reaction at least at low conversions. Table I shows data on the effect of intensity.

Table II shows the effect of nitric oxide pressure on rates when the nitric oxide pressure is low.

As the nitric oxide pressure increases the  $\text{H}_2/\text{N}_2$  ratio decreases and may approach a constant asymptotically. The  $\text{N}_2\text{O}/\text{N}_2$  ratio is more erratic, possibly due to local depletion of nitric oxide. Table III shows variations over a wide pressure range.

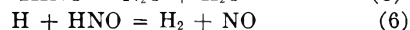
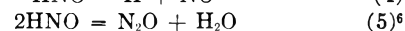
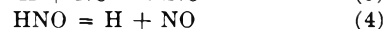
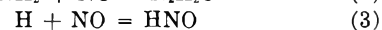
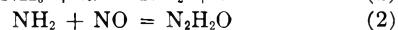
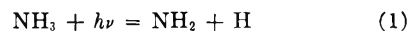
TABLE III

EFFECT OF NITRIC OXIDE PRESSURE ON RATES (HIGH PRESSURES)

| $P_{\text{NO}}$ , mm. | $\text{N}_2$ moles $\times 10^6$ /hr. | $\text{H}_2/\text{N}_2$ (A) | $\text{N}_2\text{O}/\text{N}_2$ (B) | $\text{H}_2\text{O}/\text{N}_2$ (C) | $2A + 2B$ C-A |     |
|-----------------------|---------------------------------------|-----------------------------|-------------------------------------|-------------------------------------|---------------|-----|
|                       |                                       |                             |                                     |                                     | $2A + 2B$     | C-A |
| ..                    | 1.1                                   | 2.8                         | ..                                  | ..                                  | ..            | ..  |
| 3.0                   | 6.6                                   | 0.14                        | 0.32                                | 1.9                                 | 0.92          | 1.6 |
| 6.0                   | 8.2                                   | .09                         | .34                                 | 1.2                                 | .86           | 0.9 |
| 6.3                   | 7.6                                   | .11                         | .34                                 | 1.3                                 | .90           | 1.0 |
| 6.4                   | 7.0                                   | .09                         | .36                                 | 1.6                                 | .90           | 1.2 |
| 10.0                  | 8.7                                   | .04                         | .26                                 | 1.1                                 | .60           | 0.8 |
| 20.0                  | 10.2                                  | < 0.1                       | .14                                 | 1.1                                 | < .30         | 1.0 |
| $T = 0^{\circ}$       |                                       |                             |                                     |                                     |               |     |
| ..                    | 0.15                                  | 3.00                        | ..                                  | ..                                  | ..            | ..  |
| 1.61                  | .087                                  | 0.02                        | 0.50                                | ..                                  | 1.0           | ..  |
| 4.2                   | .073                                  | .05                         | .38                                 | ..                                  | 0.9           | ..  |
| 7.8                   | .089                                  | .03                         | .44                                 | ..                                  | 0.9           | ..  |
| 8.7                   | .088                                  | .04                         | .43                                 | ..                                  | 1.0           | ..  |
| 15.5                  | .087                                  | .02                         | .50                                 | ..                                  | 1.0           | ..  |
| $T = 100^{\circ}$     |                                       |                             |                                     |                                     |               |     |
| 5.5                   | 4.6                                   | 0.05                        | 0.32                                | ..                                  | 0.7           | ..  |
| 4.7                   | 6.3                                   | 0.11                        | 0.36                                | ..                                  | 0.9           | ..  |

### Discussion

Interpretation of the data at low pressures of nitric oxide is complicated by the fact that steps in photolysis of ammonia which lead to nitrogen formation are not known with certainty. At sufficiently high nitric oxide pressures the following steps can be postulated



According to this mechanism

$$1 = \frac{R_{\text{H}_2\text{O}}}{R_{\text{N}_2}} - \frac{R_{\text{N}_2\text{O}}}{R_{\text{N}_2}} \quad (7)$$

$$1 = 2 \left( \frac{R_{\text{H}_2}}{R_{\text{N}_2}} + \frac{R_{\text{N}_2\text{O}}}{R_{\text{N}_2}} \right) \quad (8)$$

In Table II the fifth column shows how well equation 8 is obeyed and in Table III the sixth and seventh columns show how well equation 8 and 7 are obeyed, respectively. As might be expected there is considerable scatter in the results for equation 7 because water analyses are not accurate. The data agree well with equation 8 except for very low and quite high pressures of nitric oxide.

At low pressures of nitric oxide reaction 2 evi-

(6) J. A. Gray and D. W. G. Style, *Trans. Faraday Soc.*, **48**, 1137 (1952); see also J. B. Levy, *J. Am. Chem. Soc.*, **78**, 1780 (1956).

dently does not proceed quantitatively and some of the reactions which occur in pure ammonia must take place. At high nitric oxide pressures the right hand side of equation 8 is below unity thus indicating a lack of material balance, probably due to some unidentified product. The nature of such a product is indicated by the work of Harteck<sup>7</sup> to be possibly a polymer of HNO.

At high nitric oxide pressures the hydrogen atom concentration must be very low and reaction 6 is nearly suppressed. Since there is little or no effect of intensity on the ratios of products one can say that radical-radical reactions do not compete with radical-molecule reactions to an appreciable extent.

The mechanism accounts quantitatively for the products and for the effects of various variables. On the other hand rate expressions may be derived from the mechanism which do not agree well with trends in the data. This may be due partly to wall effects since a change in surface to volume ratio does change the ratio of products. It is also due undoubtedly to the fact that the mechanism embodied in equations 1-6 is not complete since the steps in ammonia photolysis have been omitted.

If  $k_4 = 0$  the following expression is obtained

$$\frac{\left(\frac{R_{N_2}}{R_{H_2}} - 1\right) (R_{N_2O})^{1/2}}{(NO)} = \frac{k_3 k_5^{1/2}}{k_6} \quad (9)$$

(7) P. Harteck, *Ber.*, **66**, 423 (1933).

Table IV shows the application of this equation to a series of runs.

TABLE IV

APPLICATION OF EQUATION 9

 $T = 31^\circ$ ;  $V = 0.196$  l. (Illuminated  $V = 0.188$  l.)

| $P_{NO}$ ,<br>mm. | $R_{N_2}$ ,<br>moles $\times 10^3$ /<br>hr. l. | $R_{N_2}/$<br>$R_{H_2}$ | $R_{N_2O}$ ,<br>moles $\times$<br>$10^3$ /hr. l. | $\frac{k_3 k_5^{1/2}}{k_6} \times 10^{-3}$<br>(concn.,<br>moles/l.,<br>time in hr.) |
|-------------------|------------------------------------------------|-------------------------|--------------------------------------------------|-------------------------------------------------------------------------------------|
| 5.55              | 3.58                                           | 11.3                    | 1.36                                             | 1.3                                                                                 |
| 4.9               | 3.08                                           | 9.7                     | 1.20                                             | 1.2                                                                                 |
| 5.1               | 3.18                                           | 10.8                    | 1.27                                             | 1.3                                                                                 |
| 3.0               | 2.95                                           | 7.6                     | 1.11                                             | 1.4                                                                                 |
| 1.2               | 2.83                                           | 4.4                     | 0.76                                             | 1.5                                                                                 |
| 9.9               | 3.41                                           | 18.6                    | 1.44                                             | 1.3                                                                                 |
| Av.               |                                                |                         |                                                  | $1.3 \pm 0.1$                                                                       |

The assumption that  $k_4 = 0$  is certainly not valid at high temperatures but should be approximately true at  $31^\circ$ . The heat of reaction may not be estimated with any certainty. The figures in the fifth column of Table IV are not very sensitive to trends and hence do not constitute more than supporting evidence for the mechanism.

Thus the mechanism embodied in equations 1-6 is reasonable but is not complete and fully proved.

## THE STRUCTURE OF SILVER CYCLOÏCTATETRAENE NITRATE

By F. SCOTT MATHEWS AND WILLIAM N. LIPSCOMB

*School of Chemistry, University of Minnesota, Minneapolis 14, Minnesota*

Received February 6, 1959

The  $Ag^+$  ion interacts with two non-adjacent " $\pi$ "-bonds of each cyclooctatetraene molecule at  $Ag^+-C$  distances of 2.46, 2.51, 2.78 and 2.84 Å. Slightly longer  $Ag^+-C$  interactions, 3.17 and 3.29 Å., join these units into infinite chains along the  $c$ -axis of the crystal. The short  $Ag^+-O$  distances of 2.36 and 2.43 Å. suggest some covalency. There are four  $AgC_8H_8NO_3$  in a unit cell of symmetry  $P2_1/a$  with parameters,  $a = 16.84$ ,  $b = 8.94$ ,  $c = 5.86$  Å., and  $\beta = 91^\circ 7'$ . Agreement factors for the 1136 observed X-ray diffraction maxima are  $R = \Sigma ||F_0| - |F_c|| / \Sigma |F_0| = 0.112$  and  $r = \Sigma \omega(F_0^2 - F_c^2) / \Sigma \omega F_0^4 = 0.056$ .

### Introduction

Complexes between heavy metal ions and  $\pi$ -bonding systems of unsaturated or conjugated organic compounds have received recent experimental<sup>1-4</sup> and theoretical<sup>5-8</sup> attention. Unfortunately, few crystal structure studies have been carried out, but Zeise's salt,<sup>9</sup> the palladium chloride complexes of ethylene<sup>10</sup> and styrene,<sup>11</sup> and the silver perchlorate-

benzene complex<sup>12,13</sup> have been elucidated in detail. The present study of silver cyclooctatetraene nitrate,<sup>14</sup> previously reported briefly,<sup>15</sup> was undertaken to elucidate the type of interaction between silver ion and a more nearly ethylenic double-bond system than that existing in benzene.

### Experimental

Cyclooctatetraene silver nitrate,  $AgC_8H_8NO_3$ , crystallizes from a mixture of aqueous silver nitrate and cyclooctatetraene (hereafter called COT) dissolved in petroleum ether in the form of needles which decompose easily to  $(COT)_2$  ( $AgNO_3$ )<sub>3</sub> by loss of COT. Thus it was necessary to mount the crystals in an atmosphere of COT. A crystal about 0.15 mm. in diameter was mounted in a thin-walled glass capillary on the X-ray apparatus with the needle axis parallel to the rotation axis. Precession photographs using Mo  $K\alpha$  radiation indicated a monoclinic unit cell with parameters,  $a = 16.84 \pm 0.045$ ,  $b = 8.94 \pm 0.018$ ,  $c = 5.86 \pm$

- J. Chatt and R. G. Wilkins, *Nature*, **165**, 859 (1950).
- J. Chatt, *Chem. Revs.*, **48**, 7 (1951).
- J. Chatt and L. M. Vananzi, *Nature*, **177**, 852 (1956).
- L. J. Andrews, *Chem. Revs.*, **54**, 713 (1954).
- R. S. Mulliken, *J. Chem. Phys.*, **19**, 514 (1951); *J. Am. Chem. Soc.*, **72**, 600 (1950); **74**, 811 (1952).
- J. Chatt, *J. Chem. Soc.*, 3340 (1949).
- J. Chatt and L. A. Dunkanson, *ibid.*, 2939 (1953).
- R. E. Rundle and J. D. Corbett, *J. Am. Chem. Soc.*, **79**, 757 (1957).
- J. A. Wunderlich and D. P. Mellor, *Acta Cryst.*, **7**, 130 (1954); **8**, 57 (1955).
- J. N. Dempsey and N. C. Baenziger, *J. Am. Chem. Soc.*, **77**, 4984 (1955).
- J. R. Holden and N. C. Baenziger, *ibid.*, **77**, 4987 (1955).

- R. E. Rundle and J. Goring, *ibid.*, **72**, 5337 (1950).
- H. G. Smith and R. E. Rundle, *ibid.*, **80**, 5075 (1958).
- A. C. Cope and F. A. Hochstein, *ibid.*, **72**, 2515 (1950).
- F. S. Mathews and W. N. Lipscomb, *ibid.*, **80**, 4745 (1958).

0.008 Å., and  $\beta = 91^\circ 7' \pm 15'$ . Systematic absences observed only for  $h0l$  reflections when  $h$  is odd, and for  $0k0$  reflections when  $k$  is odd, lead unambiguously to the space group  $P2_1/a$ . Assumption of 2, 4 or 6 molecules in the unit cell lead to a calculated density of 1.03, 2.06 or 3.09 g./cc., respectively. A crystal of the compound was observed to sink very slowly in halocarbon oil of density 1.93 g./cc., while a crystal of KBr with density of 2.75 g./cc. about the same size as the  $\text{COTAgNO}_3$  crystal was found to sink relatively rapidly. Thus the density of  $\text{C}_8\text{H}_8\text{AgNO}_3$  is substantially less than 2.75 g./cc. and only a little greater than 1.93 g./cc. Hence we assumed four molecules in the unit cell. For comparison, the density<sup>13</sup> of  $\text{AgC}_6\text{H}_5\text{ClO}_4$  is 2.4 g./cc. Precession photographs at a precession angle  $\bar{\mu} = 30^\circ$  of the  $0kl$ ;  $h0l$ ;  $hhl$ ;  $2k,k,l$ ;  $h1l$  and  $h2l$  reciprocal lattice nets, and at  $\bar{\mu} = 25^\circ$  of the  $h3l$  reciprocal lattice net using Mo  $K\alpha$  radiation, gave 540 independent reflections. Equi-inclination Weissenberg photographs of the same crystal were taken at the  $hk0$ ,  $hk1$ ,  $hk2$ ,  $hk3$  and  $hk4$  levels with the use of Mo  $K\alpha$  radiation. All intensities were estimated by visual comparison with a timed intensity scale prepared from single reflections of this same crystal. After the usual Lorentz and polarization corrections had been applied, the observed structure factors for precession and Weissenberg photographs were placed on a common arbitrary scale by correlation of reflections common to both sets. No attempt was made to correct for absorption of X-rays, since at most only approximately 30% of the radiation was absorbed for this crystal. Weissenberg photographs were also taken with Cu  $K\alpha$  radiation of a second crystal about 0.06 mm. in diameter but, owing to the increased absorption problems, only about 30 additional reflections of the  $hk2$  level were added to the previous list. A final total of 1136 reflections (Table V) were obtained for this study.

**Structure Determination.**—The three-dimensional Patterson map was sharpened by multiplying each  $|F_0|^2$  by  $f^{-2} \exp \beta' \sin^2 \theta / \lambda^2$ , where  $f = \sum f_j / \sum Z_j$  for the  $j$  atoms and  $\beta'$ , the "adjusted" temperature factor, was chosen as  $2 \text{ \AA}^2$ . This map was calculated at intervals of  $a/80$ ,  $b/40$  and  $c/40$  on the Univac Scientific 1103 using the 1136 observed structure factors. A single silver-silver interaction of height 72 (arbitrary units) was found at approximately  $50/80 a$ ,  $17/40 b$ ,  $8/40 c$ , which located a silver atom at  $25/80 a$ ,  $8.5/40 b$ ,  $4/40 c$  in the real centrosymmetric unit cell.

At this point two natural choices presented themselves: (1) calculate structure factors from the position of the silver atom only, in order to determine the relative signs of a majority of the observed structure factors and calculate an electron density map, or (2) employ the "vector convergence method"<sup>16</sup> using a graphical superposition of the three-dimensional Patterson map. The latter method was chosen in order to economize computer time. The origin of the Patterson map was placed on the single silver-silver interaction to give a map in real space with a silver atom at the origin. Although for this centrosymmetric space group only one superposition is necessary, a second superposition using a double silver-silver interaction in a Harker section was performed in the hope of removing spurious peaks. The smallest light atom-heavy atom peaks considered were of height 8, and any peak which did not satisfy the space group symmetry was discarded. A scale model of the unit cell was built utilizing the 68 possible atom sites found. Fifty-two of these formed a plausible ensemble, while the other 16 could be rejected as being chemically improbable. The peak heights of all nitrogen and oxygen atoms ranged from 11 to 19, while those of the carbon atoms ranged from 9 to 14. Of the 16 false atom sites, the peak height of only one exceeded 10. The positions of the four false atom sites in the asymmetric unit are given, along with their average peak heights, in Table I.

The approximate atomic coordinates and individual isotropic temperature factors (initially  $4 \text{ \AA}^2$  for light atoms,  $2 \text{ \AA}^2$  for silver) were refined by seven least-squares<sup>16,17</sup> cycles, which brought  $R = \sum \|kF_0\| - |F_0| / \sum |F_0|$  from 0.371 to 0.158 and  $\tau = \sum w[(kF_0)^2 - F_0^2] / \sum w(kF_0)^2$  from 1.090 to 0.114. At this point, we decided to refine the silver atom temperature factor ( $2.62 \text{ \AA}^2$ ) anisotropically before calculating a difference map. After three such cycles, all

TABLE I

| Patterson superposition |                   |           | UNEXPLAINED PEAKS       |                | Av. ht. (arbitrary units) |     |
|-------------------------|-------------------|-----------|-------------------------|----------------|---------------------------|-----|
| $x, a/80$               | $y, b/40$         | $z, c/40$ |                         |                |                           |     |
| 25.2 <sup>a</sup>       | 11.9              | 11.1      |                         |                |                           | 9.5 |
| 25.2 <sup>a</sup>       | 8.5               | 15.4      |                         |                |                           | 9.5 |
| 25.7                    | 4.5               | 22.2      |                         |                |                           | 8   |
| 25.3 <sup>a</sup>       | 8.4               | 33.4      |                         |                |                           | 8.5 |
| Difference $x, a/80$    | Fourier $y, b/80$ | $z, c/40$ | Int., e.Å <sup>-3</sup> | Closest atom   | Distance, Å.              |     |
| 24                      | 7                 | 7         | 3.0                     | Ag             | 0.6                       |     |
| 26                      | 10                | 0         | 2.5                     | Ag             | 0.6                       |     |
| 27 <sup>a</sup>         | 8.5               | 31        | 2.5                     | C <sub>6</sub> | 1.2                       |     |
| 23 <sup>a</sup>         | 8.5               | 17.5      | 2.0                     | C <sub>5</sub> | 1.0                       |     |
| 25                      | 8.5               | 23.5      | 1.8                     | O <sub>2</sub> | 0.7                       |     |
| 8.5                     | 16                | 33.5      | 1.7                     | C <sub>4</sub> | 0.7                       |     |
| 30                      | 19.5              | 17.5      | 1.6                     | C <sub>3</sub> | 0.5                       |     |
| 30                      | 6.5               | 22.5      | 1.4                     | C <sub>4</sub> | 0.4                       |     |
| 36.5                    | 7.5               | 19        | 1.4                     | C <sub>7</sub> | 0.6                       |     |
| 25 <sup>a</sup>         | 12                | 8.5       | 1.3                     | Ag             | 1.0                       |     |
| 27                      | 23                | 26        | 1.3                     | C <sub>3</sub> | 2.0                       |     |
| 20.5                    | 13                | 21.5      | 1.3                     | C <sub>5</sub> | 1.0                       |     |
| 4                       | 8                 | 29        | -3.8                    |                |                           |     |
| 26                      | 14                | 4         | -3.2                    |                |                           |     |
| 8                       | 14                | 0         | -1.6                    |                |                           |     |
| Electron density map    |                   |           |                         |                |                           |     |
| $x, a/80$               | $y, b/40$         | $z, c/40$ | ht., e.Å <sup>-3</sup>  |                |                           |     |
| 25 <sup>a</sup>         | 12                | 11        | 3.7                     |                |                           |     |
| 25 <sup>a</sup>         | 9                 | 15        | 3.7                     |                |                           |     |
| 25 <sup>a</sup>         | 9                 | 33        | 4.1                     |                |                           |     |
| 25                      | 12                | 36.5      | 3.7                     |                |                           |     |

<sup>a</sup> Peaks common to the three sets of maps.

atoms except hydrogen were used to obtain a difference map, on which the highest positive peak was  $3 \text{ e.}\text{\AA}^{-3}$ . There were 12 positive peaks whose heights were greater than  $1.2 \text{ e.}\text{\AA}^{-3}$ . The position, height and approximate distance from the closest atom are given in Table I for each of these 12 peaks. As can be seen, 7 of these are within  $0.75 \text{ \AA}$ . of an atom. None of the other peaks is a reasonable addition to the present structure, and none suggested a reinterpretation of the structure. In addition, three negative peaks of depth less than  $-1.5 \text{ e.}\text{\AA}^{-3}$  were found, and are also given in Table I.

Finally, three more cycles of least squares were carried out, giving final values for  $R - \tau$  of 0.112-0.056. Final agreement factors are  $R = 0.13$  for  $0kl$ , 0.12 for  $h0l$ , 0.11 for  $hk0$ , 0.11 for  $h$  odd, 0.10 for  $k$  odd, 0.11 for  $l$  odd, 0.11 for  $h + k$  odd, 0.11 for  $k + l$  odd, 0.11 for  $h + l$  odd and 0.11 for  $h + k + l$  odd for, in each class, all observed reflections. After applying the signs calculated during the last cycle to the observed structure factors, a three-dimensional electron density map was calculated. Four unexpected peaks with heights comparable to that of carbon (average  $4.9 \text{ e.}\text{\AA}^{-3}$ ) appeared at positions shown, along with peak height, in Table I. The first three listed have positions close to peaks observed on the difference map (starred) and the false peaks obtained from the Patterson superposition (starred). Series termination could explain the false peaks in the electron density map and possibly also the discrepancies in the difference map. Possibly, also, there are some small systematic errors in the data, such as those caused by absorption or extinction.

In the hopes of minimizing series termination errors, an electron density projection, using  $hk0$  data only, was calculated and is shown in Fig. 1. The largest false peak lies between the silver and the nitrogen atoms, and rough graphical integration of the electron density indicates that it contains approximately 0.16 as many electrons as an oxygen atom.

## Results and Discussion

Final atomic parameters are given in Table II and some important bond distances are given in Table III. The average standard deviations of the

(16) M. G. Rossmann, R. A. Jacobson, F. L. Hirshfeld and W. N. Lipscomb, *Acta Cryst.*, in press.

(17) R. E. Dickerson, P. J. Wheatly, P. A. Howell and W. N. Lipscomb, *J. Chem. Phys.*, **27**, 200 (1957).

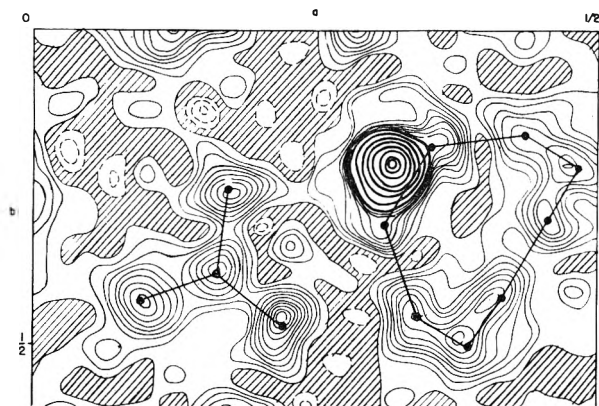


Fig. 1.—Electron density projection along the  $c$ -axis with the light atom framework superimposed. Light contours are at intervals of  $1 e./\text{Å}^2$ , while the heavy contours are at intervals of  $10 e./\text{Å}^2$ . The shaded area is between 1 and  $-1 e./\text{Å}^2$  and the broken contours represent negative electron density.

TABLE II

FINAL ATOMIC PARAMETERS

| Atom           | $x$                                                               | $y$                                                               | $z$                                                              | $B (\text{Å}^2)$ |
|----------------|-------------------------------------------------------------------|-------------------------------------------------------------------|------------------------------------------------------------------|------------------|
| O <sub>1</sub> | 0.173                                                             | 0.250                                                             | 1.047                                                            | 4.21             |
| O <sub>2</sub> | .095                                                              | .433                                                              | 0.949                                                            | 6.00             |
| O <sub>3</sub> | .221                                                              | .470                                                              | .996                                                             | 3.68             |
| N              | .163                                                              | .385                                                              | .996                                                             | 2.29             |
| C <sub>1</sub> | .457                                                              | .298                                                              | .164                                                             | 4.45             |
| C <sub>2</sub> | .410                                                              | .423                                                              | .162                                                             | 2.99             |
| C <sub>3</sub> | .385                                                              | .507                                                              | .361                                                             | 3.92             |
| C <sub>4</sub> | .339                                                              | .456                                                              | .543                                                             | 3.44             |
| C <sub>5</sub> | .311                                                              | .307                                                              | .551                                                             | 3.66             |
| C <sub>6</sub> | .352                                                              | .180                                                              | .570                                                             | 4.64             |
| C <sub>7</sub> | .438                                                              | .163                                                              | .558                                                             | 4.43             |
| C <sub>8</sub> | .484                                                              | .219                                                              | .379                                                             | 4.27             |
| Ag             | .316                                                              | .218                                                              | .097                                                             | $a$              |
| $\alpha$       | $\begin{cases} \beta_1 = 0.0027 \\ \beta_4 = -0.0003 \end{cases}$ | $\begin{cases} \beta_2 = 0.0002 \\ \beta_5 = -0.0103 \end{cases}$ | $\begin{cases} \beta_3 = 0.0261 \\ \beta_6 = 0.0036 \end{cases}$ |                  |

TABLE III

|                                |         |                     |         |
|--------------------------------|---------|---------------------|---------|
| C <sub>1</sub> -C <sub>2</sub> | 1.37 Å. | C <sub>1</sub> -Ag  | 2.51 Å. |
| C <sub>2</sub> -C <sub>3</sub> | 1.46    | C <sub>2</sub> -Ag  | 2.46    |
| C <sub>3</sub> -C <sub>4</sub> | 1.40    | C <sub>5</sub> -Ag  | 2.77    |
| C <sub>4</sub> -C <sub>5</sub> | 1.42    | C <sub>6</sub> -Ag  | 2.84    |
| C <sub>5</sub> -C <sub>6</sub> | 1.33    | O <sub>1</sub> -N   | 1.25    |
| C <sub>6</sub> -C <sub>7</sub> | 1.47    | O <sub>2</sub> -N   | 1.24    |
| C <sub>7</sub> -C <sub>8</sub> | 1.40    | O <sub>3</sub> -N   | 1.24    |
| C <sub>8</sub> -C <sub>1</sub> | 1.51    | O <sub>1</sub> -Ag  | 2.43    |
|                                |         | O <sub>3</sub> '-Ag | 2.36    |
| $\angle C_1C_2C_3$             | 126°    | $\angle C_1AgC_2$   | 32°     |
| $\angle C_2C_3C_4$             | 129     | $\angle C_5AgC_6$   | 27      |
| $\angle C_3C_4C_5$             | 121     | $\angle O_1NO_2$    | 120     |
| $\angle C_4C_5C_6$             | 129     | $\angle O_2NO_3$    | 120     |
| $\angle C_5C_6C_7$             | 127     | $\angle O_3NO_1$    | 118     |
| $\angle C_6C_7C_8$             | 124     |                     |         |
| $\angle C_7C_8C_1$             | 129     |                     |         |
| $\angle C_8C_1C_2$             | 123     |                     |         |

TABLE IV

ANALYSIS OF ANISOTROPIC THERMAL VIBRATION OF SILVER

| Axis | $\phi$ | $\psi$ | $\omega$ | $B (\text{Å}^2)$ | $\sqrt{\mu^2} (\text{Å})$ |
|------|--------|--------|----------|------------------|---------------------------|
| P    | 0.43   | 0.66   | 0.62     | 1.89             | 0.15                      |
| Q    | — .83  | .56    | .01      | 3.06             | .20                       |
| R    | .33    | .52    | — .79    | 4.56             | .24                       |

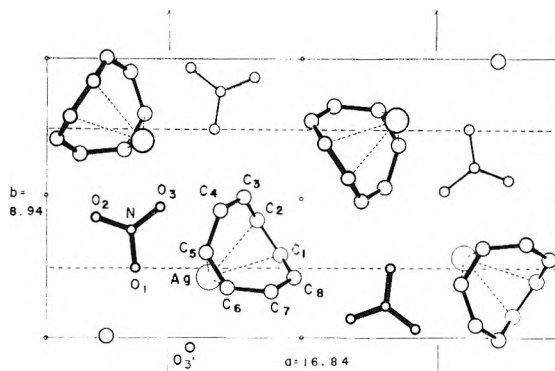


Fig. 2.—Projection along the  $c$ -axis. O<sub>3</sub>' is in the adjacent unit cell. Distances are in Å.

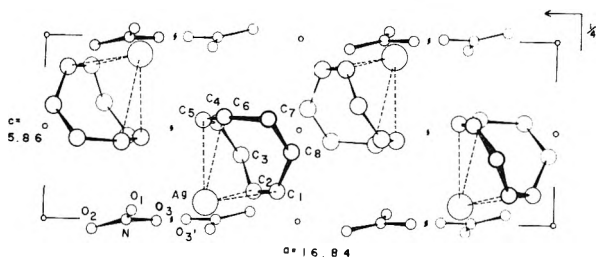


Fig. 3.—Projection along the  $b$ -axis. Distances are in Å.



Fig. 4.—Bonding of silver to COT in infinite chains and to the nitrate groups. The axes P and R of the anisotropic thermal vibration are shown on the upper silver atom, the lengths being proportional to  $B$ . The third axis, Q, is perpendicular to the plane of the figure. Distances are in Å.

bond distances, calculated from residuals of the least-squares treatment,<sup>17</sup> neglecting off-diagonal terms, are Ag-O =  $\pm 0.019$ , Ag-C =  $\pm 0.027$ , O-N =  $\pm 0.025$  and C-C =  $\pm 0.037$  Å. Projections of the unit cell along the  $z$ - and  $y$ -axes are shown in Figs. 2 and 3, respectively. Figure 4 shows perhaps the most significant features of the structure, the bonding in infinite chains of the silver atoms with the cyclooctatetraene double bond systems. The molecule in Fig. 4 is related to the la-



beled molecule of Fig. 3 by a twofold screw axis parallel to  $b$ . The nearest carbon atom neighbors of the silver atom are  $C_1$  and  $C_2$  at an average distance of 2.49 Å., followed by  $C_5$  and  $C_6$  at an average distance of 2.81 Å. Carbon atoms  $C_5$  and  $C_6$  from the unit cell below complete the chain with an average distance of 3.23 Å. The silver atom has two oxygen atom neighbors,  $O_1$  and  $O_3'$  at distances

TABLE V  $F_{\text{obs}} \times 10$ 

00(1-6): 1208, 1309, a, 471, 295, 200; 01(1-7): 982, 1463, 873, 666, 182, a, 221;  
 02(0-6): 1342, 849, 502, 430, 581, 441, 314; 03(1-4): 849, 896, 961, 526; 04(0-5):  
 1203, 760, 501, 83, 359, 285; 05(1-4): 436, 477, 486, 232; 06(0-3): 380, 604, 235,  
 142, 07(3): 247; 08(3): 264; 0.10(0-4): 207, a, a, a, 237; 11(0-4): 212, 518, 644,  
 398, 197; 12(0-5): 147, 397, 148, 279, 499, 213; 13(0-5): 782, 314, 772, 472, a,  
 187; 14(0-4): 1263, 590, a, 446, 470; 15(0-3): 345, 573, 714, 408; 16(0-4): 616,  
 455, a, 386, 527; 17(0-3): 307, 554, 472, 538; 18(0-4): 507, 320, a, 262, 290;  
 19(0-4): 163, 362, 351, 268, 230; 1.10(0-3): 236, a, a, 196; 1.11(0-3): 172, 146,  
 a, 226; 20(0-7): 1084, 308, 505, 551, 640, 174, 248, 159; 21(0-6): 1546, 571, 1150,  
 a, a, 285, 312; 22(0-5): 833, 527, 590, 678, 626, 372; 23(0-6): 953, 1039, 994,  
 586, a, 141, 223; 24(0-4): 784, 278, 149, 502, 392; 25(0-4): 262, 380, 372, 201,  
 164; 26(0-3): 233, a, a, 165; 27(0-3): 199, 166, a, 233; 28(1-2): 176, 276;  
 29(0-1): 224, 208; 2.10(3): 165; 2.11(0-1): 166, 116; 31(0-4): 379, 1089, 179,  
 231, 148; 32(0-4): 308, 259, 617, 533, 242; 33(0-6): 983, 813, 452, a, 396, 176,  
 209; 34(1-4): 196, 816, 505, 409; 35(0-4): 652, 921, 297, a, 361; 36(0-4): 275,  
 242, 624, 619, 366; 37(0-4): 565, 635, 374, 123, 304; 38(0-4): 318, a, 338, 385,  
 294; 39(0-2): 383, 422, 303; 3.10(2-3): 158, 246; 3.11(0-1): 189, 179; 40(0-8):  
 690, 498, 1093, 704, 531, a, 152, 213, 157; 41(0-6): 1171, 914, 170, 341, 700, 528,  
 312; 42(0-6): 360, 1061, 1034, 826, 520, a, 221; 43(0-6): 975, 846, 208, 304, 469,  
 367, 158; 44(1-4): 276, 632, 453, 283; 45(0-4): 446, 281, 205, 109, 176; 46(1-4):  
 262, 234, 159, 262; 48(3): 132; 49(0-2): 211, a, 321; 4.11(0): 181; 51(0-2): 580,  
 231, 216; 52(0-4): 270, 764, 414, 333, 190; 53(0-5): 464, 332, 333, 432, 406, 218;  
 54(0-3): 452, 628, 443, 373; 55(0-5): 827, 450, 259, 323, 513, 322; 56(0-3): 486,  
 828, 591, 528; 57(0-4): 493, 243, 239, 397, 422; 58(0-3): 254, 409, 377, 217;  
 59(0-4): 399, a, a, a, 300; 5.10(1-3): 252, 172, 205; 5.11(0): 182; 60(0-7): 1389,  
 1108, 1195, 444, a, 326, 332, 154; 61(0-5): 1183, 139, 649, 1007, 828, 307; 62(0-5):  
 1422, 1536, 938, 548, 187, 346; 63(0-5): 821, a, 467, 750, 484, 224; 64(0-4): 687,  
 634, 588, 187, 165; 65(0-4): 245, a, 278, 352, 525; 66(0-4): 307, 327, 279, 340,  
 179; 68(4): 224; 69(0): 158; 6.10(0): 183; 6.11(0): 167; 71(0-3): 293, 193, 202,  
 129; 72(0-5): 572, 432, 175, 152, 213, 156; 73(0-5): 245, 209, 662, 553, 345, 166;  
 74(0-4): 504, 521, 368, a, 335; 75(0-4): 275, 197, 372, 561, 299; 76(0-4): 640, 627,  
 370, a, 270; 77(2-4): 381, 425, 260; 78(0-4): 402, 332, 205, a, 268; 79(1-4): 204,  
 a, 309, 286; 7.10(0-2): 191, 242, 171; 80(0-6): 1333, 1113, 473, 383, 454, 368, 269;  
 81(0-4): 366, 667, 1064, 640, 358; 82(0-6): 1222, 678, 322, 369, 381, 302, 187;  
 83(1-4): 486, 636, 532, 262; 84(0-5): 600, 643, 267, 168, 217, 255; 85(0-4): 221,  
 347, 450, 431, 289; 86(0-3): 273, 287, 263, 135; 87(0): 225; 88(3): 140; 8.10(0-3):  
 200, a, a, 170; 91(3): 197; 92(0-4): 232, 218, 254, 224, 237; 93(0-4): 472, 647,  
 708, 317, 161; 94(0-4): 499, 541, 255, 318, 478; 95(0-4): 268, 504, 447, 286, 181;  
 96(0-4): 374, 256, 267, 412, 388; 97(0-3): 166, 455, 407, 234; 98(0-4): 294, 243,  
 251, 225, 267; 99(0-3): 234, 355, 382, 257; 9.10(0-3): 218, a, a, 172; 10.0(0-5):  
 623, 321, 710, 479, 638, 262; 10.1(0-6): 696, 801, 596, 171, 190, 292, 314;  
 10.2(0-5): 313, 142, 392, 535, 419, 254; 10.3(0-5): 380, 625, 451, 252, a, 219;  
 10.4(0-4): 354, 203, 255, 188, 292; 10.5(0-3): 341, 417, 321, 149; 10.6(0-3): 192,  
 a, a, 190; 11.1(1): 206; 11.2(0-3): 124, 147, 236, 219; 11.3(0-5): 462, 632, a, a,  
 297, 156; 11.4(1-4): 252, 458, 398, 206; 11.5(0-4): 415, 459, a, 127, 328;  
 11.6(1-4): 383, 396, 428, 288; 11.7(0-4): 379, 445, 212, a, 241; 11.8(0-4): 150, a,  
 241, 242, 246; 11.9(0-2): 300, 257, 136; 11.10(0-3): 175, a, a, 166; 12.0(0-7):  
 372, 819, 750, 654, 268, a, 201, 109; 12.1(0-6): 736, 529, a, 266, 473, 328, 175;  
 12.2(0-4): 175, 539, 603, 563, 207; 12.3(0-5): 547, 361, 176, 282, 414, 323;  
 12.4(1-4): 273, 319, 279, 221; 12.5(0-4): 293, 187, a, 126, 216; 12.6(0-4): 221,  
 211, 312, 192, 210; 12.9(0): 152; 13.1(3): 270; 13.2(1-3): 260, a, 195; 13.3(0-4):  
 213, 122, 145, 216, 237; 13.4(0-4): 302, 454, 277, 246, 214; 13.5(0-4): 238, 187,  
 a, 264, 238; 13.6(0-3): 242, 366, 353, 255; 13.7(0-4): 263, a, a, 226, 261;  
 13.8(0-3): 211, 224, 239, 167; 13.9(0): 176; 13.10(0): 182; 14.0(0-6): 632, 641,  
 443, a, 193, 289, 222; 14.1(0-5): 396, 158, 308, 452, 311, 207; 14.2(0-2): 535,  
 617, 550; 14.3(0-4): 227, 179, 355, 458, 321; 14.4(0-3): 320, 358, 296, 139;  
 14.5(3-4): 142, 230; 14.6(0-2): 187, 205, 182; 15.1(1-3): 198, 208, 182;

Table V (Continued)

15.2(0-2): 218, 287, 207; 15.3(1-3): 134, 225, 265; 15.4(0-4): 157, 292, a, a, 230; 15.5(3-4): 226, 229; 15.6(0-2): 256, 315, 164; 15.7(2-3): 250, 221; 15.8(0-1): 197, 221; 15.9(3): 171; 16.0(0-5): 347, 189, a, 266, 389, 273; 16.1(1-4): 347, 397, 303, 234; 16.2(0-3): 467, 342, a, 180; 16.3(0-3): 159, 322, 327, 190; 16.4(0-4): 254, 221, a, a, 220; 16.5(0-3): 147, a, a, 182; 17.2(0): 209; 17.3(0-3): 163, 254, 219, 145; 17.4(0-4): 156, a, a, 189, 279; 17.5(0-3): 161, 289, 236, 159; 17.6(0-4): 219, a, a, 187, 271; 17.7(0-1): 163, 254; 18.0(2-5): 260, 388, 320, 156; 18.1(0-2): 298, 314, 282; 18.2(0-3): 195, a, 209, 232; 18.3(0-2): 233, 200, 153; 18.4(3): 202; 18.5(0-1): 159, 211; 19.3(0-1): 163, 154; 19.4(2-3): 175, 183; 19.5(0-4): 233, 235, a, a, 263; 19.6(3): 171; 19.7(0): 193; 20.0(0-3): 197, 260, 324, 262; 20.1(0-1): 247, 176; 20.2(1-2): 222, 225; 20.3(0): 178; 20.4(3): 152; 22.0(0-2): 209, 273, 159; 22.2(0-1): 178, 226; 22.3(1): 252;  $\bar{11}(1-2)$ : 348, 113;  $\bar{12}(1-5)$ : 148, 184, 178, 187, 199;  $\bar{13}(1-4)$ : 580, 392, 523, 398;  $\bar{14}(1-3)$ : 972, 756, 102;  $\bar{15}(1-4)$ : 329, 630, 648, 410;  $\bar{16}(1-4)$ : 694, 318, 176, 291;  $\bar{17}(1-4)$ : 217, 393, 439, 411;  $\bar{18}(1-3)$ : 498, 365, 176;  $\bar{19}(2-4)$ : 316, 277, 281;  $\bar{1.10}(1-3)$ : 304, a, 155;  $\bar{1.11}(3)$ : 176;  $\bar{20}(1-7)$ : 1325, 1556, 577, 379, 499, a, 185;  $\bar{21}(1-6)$ : 205, 725, 1012, 829, 430, 155;  $\bar{22}(1-7)$ : 1029, 1009, 225, a, 317, 284, 199;  $\bar{23}(1-5)$ : 446, 459, 482, 496, 282;  $\bar{24}(1-3)$ : 801, 648, 362;  $\bar{25}(1-4)$ : 144, 362, 379, 373;  $\bar{26}(1-3)$ : 303, 371, 222;  $\bar{28}(3)$ : 159;  $\bar{29}(3)$ : 135;  $\bar{2.10}(1)$ : 181;  $\bar{31}(1-2)$ : 635, 287;  $\bar{32}(1-3)$ : 892, 385, 200;  $\bar{33}(1-5)$ : 404, a, 478, 222, 253;  $\bar{34}(1-3)$ : 795, 748, 529;  $\bar{35}(1-4)$ : 442, a, 549, 414;  $\bar{36}(1-3)$ : 612, 625, 379;  $\bar{37}(1-4)$ : 379, a, 257, 323;  $\bar{38}(1-3)$ : 427, 502, 294;  $\bar{39}(1-4)$ : 272, a, 162, 227;  $\bar{3.10}(2-3)$ : 239, 160;  $\bar{3.11}(1)$ : 146;  $\bar{40}(1-7)$ : 260, 869, 695, 583, a, a, 215;  $\bar{41}(1-6)$ : 607, 659, 402, 462, 476, 330;  $\bar{42}(1-4)$ : 314, 813, 686, 287;  $\bar{43}(1-6)$ : 698, 446, a, 227, 202, 193;  $\bar{44}(1-5)$ : 413, 651, 441, 319, 179;  $\bar{45}(1-4)$ : 260, 350, a, 185;  $\bar{46}(1-4)$ : 211, a, 197, 171;  $\bar{47}(3)$ : 122;  $\bar{51}(1-4)$ : 545, 246, 195, 180;  $\bar{52}(1-4)$ : 250, 604, 568, 201;  $\bar{53}(1-5)$ : 749, 429, a, 188, 260;  $\bar{54}(1-4)$ : 194, 319, 678, 308;  $\bar{55}(1-5)$ : 731, 570, 162, 227, 195;  $\bar{56}(2-4)$ : 372, 413, 266;  $\bar{57}(1-4)$ : 528, 377, a, 249;  $\bar{58}(1-4)$ : 185, 314, 402, 278;  $\bar{59}(1-2)$ : 317, 361;  $\bar{5.10}(2-4)$ : 179, 168, 251;  $\bar{60}(1-6)$ : 214, 226, 506, 435, 290, 166;  $\bar{61}(1-4)$ : 1127, 1048, 495, 182;  $\bar{62}(1-4)$ : 481, 265, 428, 459;  $\bar{63}(1-3)$ : 914, 763, 412;  $\bar{64}(1-4)$ : 161, 277, 430, 384;  $\bar{65}(1-4)$ : 364, 357, 323, 183;  $\bar{66}(2)$ : 248;  $\bar{67}(3-4)$ : 197, 191;  $\bar{68}(1-3)$ : 254, a, 148;  $\bar{71}(1-3)$ : 342, 292, 287;  $\bar{72}(1-5)$ : 448, a, 182, 247, 172;  $\bar{73}(1-3)$ : 330, 336, 262;  $\bar{74}(1-4)$ : 171, a, 289, 237;  $\bar{75}(1-4)$ : 570, 469, 481, 206;  $\bar{76}(1-4)$ : 483, a, 110, 256;  $\bar{77}(1-4)$ : 447, 429, 338, 195;  $\bar{78}(1-4)$ : 242, a, 174, 266;  $\bar{79}(1-3)$ : 219, 243, 223;  $\bar{80}(1-5)$ : 916, 614, 380, 237, 379;  $\bar{81}(1-4)$ : 774, 1068, 703, 465;  $\bar{82}(1-5)$ : 1029, 561, a, 262, 247;  $\bar{83}(1-4)$ : 413, 804, 577, 356;  $\bar{84}(1-5)$ : 661, 323, a, 217, 255;  $\bar{85}(1-4)$ : 152, a, 235, 187;  $\bar{86}(1)$ : 220;  $\bar{87}(3-4)$ : 144, 199;  $\bar{88}(3)$ : 152;  $\bar{91}(1-4)$ : 195, 251, 156, 172;  $\bar{92}(1-2)$ : 391, 296;  $\bar{93}(1-3)$ : 139, a, 277;  $\bar{94}(1-2)$ : 591, 264;  $\bar{95}(1-4)$ : 230, 382, 397, 253;  $\bar{96}(1-2)$ : 452, 347;  $\bar{97}(1-4)$ : 167, 309, 317, 242;  $\bar{98}(1-3)$ : 358, 322, 139;  $\bar{99}(3)$ : 146;  $\bar{10.0}(1-5)$ : 830, 851, 324, a, 191;  $\bar{10.1}(1-5)$ : 210, 119, 567, 368, 273;  $\bar{10.2}(1-3)$ : 512, 602, 310;  $\bar{10.3}(1-5)$ : 237, 109, 287, 337, 202;  $\bar{10.4}(1-3)$ : 331, 470, 282;  $\bar{10.5}(1-3)$ : 207, a, 129;  $\bar{10.6}(1-4)$ : 197, 280, a, 187;  $\bar{10.8}(1)$ : 187;  $\bar{11.1}(1-2)$ : 165, 367;  $\bar{11.2}(1-3)$ : 321, 237, 272;  $\bar{11.3}(1-3)$ : 339, 130, 191;  $\bar{11.4}(1-3)$ : 488, 373, 364;  $\bar{11.5}(1-4)$ : 294, a, 242, 252;  $\bar{11.6}(1-3)$ : 244, 323, 250;  $\bar{11.7}(1-4)$ : 256, a, 129, 234;  $\bar{11.8}(1-3)$ : 211, 314, 202;  $\bar{11.9}(3)$ : 157;  $\bar{11.10}(3)$ : 171;  $\bar{12.0}(1-4)$ : 326, 338, 455, 232;  $\bar{12.1}(1-4)$ : 586, 345, a, 184;  $\bar{12.2}(1-4)$ : 190, 342, 232, 253;  $\bar{12.3}(1-3)$ : 356, 258, 109;  $\bar{12.4}(1-4)$ : 210, 286, 260, 240;  $\bar{12.5}(1-2)$ : 229, 293;  $\bar{12.6}(3)$ : 131;  $\bar{13.1}(4)$ : 179;  $\bar{13.2}(2-4)$ : 163, 189, 197;  $\bar{13.3}(1-4)$ : 396, 230, 201, 149;  $\bar{13.4}(1-4)$ : 167, 261, 287, 211;  $\bar{13.5}(1-3)$ : 381, 282, 142;  $\bar{13.6}(3-4)$ : 191, 230;  $\bar{13.7}(1-3)$ : 290, 236, 149;  $\bar{13.8}(3)$ : 183;  $\bar{13.9}(1)$ : 125;  $\bar{14.0}(1-4)$ : 322, a, 221, 292;  $\bar{14.1}(1-4)$ : 574, 544, 252, 174;  $\bar{14.2}(1-4)$ : 289, 156, 144, 181;  $\bar{14.3}(1-3)$ : 344, 340, 134;  $\bar{14.4}(1-3)$ : 185, a, 135;  $\bar{14.5}(1-3)$ : 226, 294, 149;  $\bar{15.2}(1-4)$ : 195, a, a, 198;  $\bar{15.3}(1-3)$ : 203, 202, 178;  $\bar{15.4}(1)$ : 195;  $\bar{15.5}(1-3)$ : 199, 308, 195;  $\bar{15.6}(1)$ : 198;  $\bar{15.7}(1-3)$ : 216, a, 143;  $\bar{16.0}(1-5)$ : 277, 192, a, 206, 158;  $\bar{16.1}(2-4)$ : 370, 241, 213;  $\bar{16.2}(1-2)$ : 336, 325;  $\bar{16.3}(2-3)$ : 279, 186;  $\bar{16.4}(1-4)$ : 206, a, a, 217;  $\bar{16.5}(3)$ : 167;  $\bar{17.2}(1-2)$ : 217, 279;  $\bar{17.3}(3)$ : 138;  $\bar{17.4}(1)$ : 205;  $\bar{17.5}(3)$ : 157;  $\bar{17.6}(1)$ : 207;  $\bar{17.7}(3)$ : 151;  $\bar{18.0}(1)$ : 226;  $\bar{18.2}(1-3)$ : 238, 304, 168;  $\bar{18.4}(3)$ : 152;  $\bar{19.3}(1)$ : 188;  $\bar{20.0}(2)$ : 194;  $\bar{20.1}(1)$ : 242;  $\bar{22.0}(1)$ : 179.

of 2.43 and 2.36 Å. (overlooked in our earlier report<sup>15</sup>), significantly shorter than the shortest Ag-O distance of 2.68 Å. in the silver benzene perchlorate

complex,<sup>13</sup> and shorter than the sum of ionic radii,<sup>18</sup> 2.46 Å. These distances possibly indicate

(18) L. Helmholz and R. Levine, *J. Am. Chem. Soc.*, **64**, 354 (1942).

some covalent bonding between silver and oxygen,<sup>19,20</sup> in agreement with the cream color of the complex. The usual values<sup>21</sup> for the ionic and covalent sums of radii are 2.66 and 2.19 Å., respectively. The shortest silver-carbon bonds and the silver-oxygen bonds lie roughly in a plane. The COT molecule is tub-shaped with  $D_{2d}$  symmetry, in agreement with previous X-ray<sup>22,23</sup> and electron diffraction studies,<sup>24</sup> with an average C=C distance of 1.37 Å. and C-C distance of 1.46 Å. The variations among the double bond distances and the single bond distances (0.09 Å. at most) are well within three times the C-C standard deviation and are probably not to be considered as significant. The COT bond angles have a standard deviation of approximately  $\pm 5^\circ$ .

The anisotropic thermal parameters were analyzed by methods described elsewhere<sup>25</sup> to determine the directions of the three principal axes P, Q and R of the assumed ellipsoid of vibration. The

(19) J. Donohue and L. Helmholz, *ibid.*, **66**, 295 (1944).

(20) J. Donohue and W. Shand, *ibid.*, **69**, 222 (1947).

(21) L. Pauling, "Nature of the Chemical Bond," Cornell University Press, Ithaca, N. Y., Second Edition, 1948, pp. 164, 179, 346.

(22) H. S. Kaufman, H. Mark and I. Fankuchen, *Nature*, **161**, 165 (1948).

(23) J. Bregman, private communication.

(24) O. Bastiansen, L. Hedberg and K. Hedberg, *J. Chem. Phys.*, **27**, 1311 (1957).

(25) M. G. Rossmann and W. N. Lipscomb, *Tetrahedron*, **4**, 275 (1958).

direction cosines  $\phi$ ,  $\psi$  and  $\omega$ , corresponding to the cell edges  $a$ ,  $b$  and  $c$ , which were assumed to be orthogonal, are given in Table IV for each principal axis, along with the isotropic temperature factor equivalent  $B = 8\pi^2 \bar{\mu}^2$ , and the mean square displacement,  $\sqrt{\bar{\mu}^2}$ . The two sets of atoms  $C_1C_2O_1O_3'$  and  $C_1C_2C_5C_6$  are each approximately coplanar, with the silver atom lying in the plane of the first set and somewhat below the plane of the second. The direction of greatest vibrational motion, R, is roughly  $20^\circ$  from the normal to the plane defined by  $C_1C_2O_1O_3'$  and approximately parallel to the other plane. This motion bends all bonds to the silver atom except the relatively long bonds from Ag to the COT in the adjacent cell. The motion with smallest amplitude has a direction, P, roughly  $20^\circ$  from normal to the plane of  $C_1C_2C_5C_6$  and approximates a stretching of the bonds to the silver atom. Two of these three directions of motion, shown in Fig. 4, are approximately in the plane of this projection, while the third direction is approximately perpendicular to this plane.

**Acknowledgment.**—We wish to thank Professor S. W. Fenton for his suggestion that we undertake this study, the Office of Naval Research and the National Institutes of Health for financial support, and the Minneapolis Honeywell Company for a fellowship to F.S.M.

## THE OXIDATION OF FERROUS IONS IN AQUEOUS SOLUTION BY ATOMIC HYDROGEN

BY GIDEON CZAPSKI AND GABRIEL STEIN

*Department of Physical Chemistry, Hebrew University, Jerusalem, Israel*

*Received February 5, 1959*

Atomic hydrogen—produced in an electrodeless high frequency discharge—oxidizes ferrous ions in aqueous solution. This reaction and the reverse process of reduction of ferric ions were investigated in the presence of  $H_2SO_4$  in the pH range of 0.4–3.0, and the equilibrium ratios established. From the dependence of the rate of oxidation on the concentration of  $Fe^{2+}$  the limiting values of the rate constant of the reaction between  $Fe^{2+}$  and H atoms in the presence of  $H^+$  ions are calculated. The possible mechanisms are discussed.

By virtue of the high energy of formation ( $\sim 104$  kcal./mole) of the H-H bond, hydrogen atoms are capable of acting as dehydrogenating, and thus oxidizing, agents. They dehydrogenate many organic substances, where the C-H bond energy is only of the order of 80–90 kcal./mole. In aqueous solutions containing ferrous ions, and irradiated with ionizing radiations experimental results were obtained<sup>1</sup> which were interpreted as indicating that H atoms are formed in these systems and that these are capable in acid solution of oxidizing ferrous to ferric ions. These results were confirmed.<sup>2,3</sup> Similar results also were obtained when such solutions were irradiated with ultraviolet light.<sup>4</sup> To

account for these results, the formation of  $H_2^{+aq}$  ions from H atoms and  $H^+$  ions was postulated, as the species responsible for the oxidation of  $Fe^{2+}$ .<sup>1,5</sup> It appeared desirable to investigate these processes under conditions where H atoms as such are formed first and then introduced into the system. We produced H atoms in an electrodeless high frequency discharge and observed the oxidation of  $Fe^{2+}$  ions by the H atoms which were introduced into the aqueous solution.<sup>6</sup> At the same time Davis, Gordon and Hart<sup>7</sup> presented similar, more detailed, results. The present paper contains our detailed results.

### Experimental

**The Production of Atomic Hydrogen.**—We have selected the method of electrodeless high frequency discharge. The

(1) T. Rigg, G. Stein and J. Weiss, *Proc. Roy. Soc. (London)*, **A211**, 375 (1952).

(2) N. F. Barr and C. G. King, *J. Am. Chem. Soc.*, **76**, 5565 (1954).

(3) A. O. Allen and W. G. Rothschild, *Radiation Res.*, **7**, 591 (1957); **8**, 101 (1958).

(4) T. Rigg and J. Weiss, *J. Chem. Phys.*, **20**, 1194, (1952); *cf. also*, *J. Chem. Soc.*, 4198 (1952).

(5) J. Weiss, *Nature*, **165**, 728 (1950).

(6) G. Czapski and G. Stein, *ibid.*, **182**, 598 (1958).

(7) T. W. Davis, S. Gordon and E. J. Hart, *J. Am. Chem. Soc.*, **80**, 4487 (1958).

elimination of inner electrodes enables one to avoid the difficulties arising from atomic recombination and hence bad reproducibility, caused by the metal evaporated from the electrodes. We could thus also dispense with the coating of the walls with, *e.g.*, phosphoric acid, and the cleaning of the entire system after every run.<sup>7,8</sup> Our reproducibility was acceptable compared with the results of others.<sup>7,8</sup> The frequency chosen for the discharge was 27–30 Mc. We found as did Jennings and Linnett<sup>9</sup> that operating at lower frequencies good yields of H atoms were obtained. The total possible power input was 2000 watt d.c., with an R.F. power of 1400 watt max. in the R.F. discharge. We usually utilized only 600–700 watts R.F. The discharge tube was made of quartz. It was cleaned with  $\text{CrO}_3\text{-H}_2\text{SO}_4$ , followed by  $\text{HNO}_3$  and then 10% HF and finally several rinses in triple distilled water. Tens of experiments could then be run without dismantling and cleaning, reproducibility being at best  $\pm 10\%$  and usually  $\pm 20\%$ . Our results are given with the appropriate standard deviations.

The hydrogen used was Matheson electrolytic prepurified and was passed through a furnace containing palladized asbestos at  $400^\circ$  and followed by a trap cooled with liquid air. The gas was stored in a large reservoir. This maintained a constant pressure of gas which was supplied to the discharge tube through a reducing valve. The gas was not recirculated but pumped through at a velocity of 50 l./min. at 20–30 mm. The experiments reported here were carried out at this pressure of pure  $\text{H}_2$ . Other experiments included the use of  $\text{H}_2$  or  $\text{H}_2\text{-He}$  mixtures at total pressures of up to 80 mm., up to which the discharge could be efficiently maintained.

The discharge tube was cooled with an air blower and the HF coil was a 7 mm. o.d. copper tube through which cooling water was circulated. The temperature of the tube during discharge exceeded the softening point of Pyrex, but not of the quartz which was used. In view of the high temperature metaphosphoric acid coating was not used, as it reacted and gave  $\text{PH}_3$  and phosphorus under these conditions. Between the reaction vessel and the discharge tube there was a  $90^\circ$  bend in the vacuum line and light shields prevented ultraviolet light from the discharge reaching the reaction vessel. The reaction vessel was fitted with a detachable side arm, in which the solution was placed. The system including the solution was fully evacuated, the solution (25 ml.) tipped into the reaction vessel,  $\text{H}_2$  passed for another 15 minutes and only then was the discharge switched on. Evaporation during this procedure was allowed for. Blank experiments with  $\text{H}_2$  passing, but without discharge were run with  $\text{Fe}^{2+}$  and  $\text{Fe}^{3+}$  solutions. The temperature in the reaction vessel was maintained at about  $5^\circ$  throughout.

Control experiments were run with  $\text{AgNO}_3$  solutions to determine the amount of H atoms available.

**Materials.**—The ferrous ammonium sulfate and sulfuric acid used were "Analar," the ferric sulfate C.P. Triple distilled water was prepared by redistilling glass distilled water from alkaline permanganate, then from phosphoric acid.

**Analysis.**—Using a Hilger Uvispek Spectrophotometer and 1 cm. cells ferric ion was determined as the sulfate at 305  $\mu$  using  $\epsilon$  2180 at  $25^\circ$  in 0.8 N  $\text{H}_2\text{SO}_4$ . The extinction coefficient depends on pH and total sulfate concentration and care was taken of this when reactions were carried out at other pH values.<sup>10</sup> All  $\Delta D_{305}$  values reported in this paper refer to solutions in which  $[\text{H}_2\text{SO}_4]$  was brought to 0.8 N. Ferric ion was determined as the 1,10-phenanthroline complex at 510  $\mu$  using acetate buffer to maintain pH 3.6, and adding NaF, at least 150 times more than the ferric ion concentration, to eliminate the ferric phenanthroline complex.

## Results

**Dependence of  $\Delta[\text{Fe}^{3+}]$  on  $\Delta H$ .**—The dependence of the quantity of ferric ions produced on the quantity of hydrogen passing through the solution was investigated using a discharge in  $\text{H}_2$  at 27 mm.

(8) F. E. Littman, E. M. Carr and A. P. Brady, *Radiation Res.*, **7**, 107 (1957).

(9) K. R. Jennings and J. W. Linnett, *Nature*, **182**, 597 (1958).

(10) Y. Gilat and G. Stein, Proc. 2nd Int. Conf. Peaceful Uses At. Energy, Geneva, 1958.

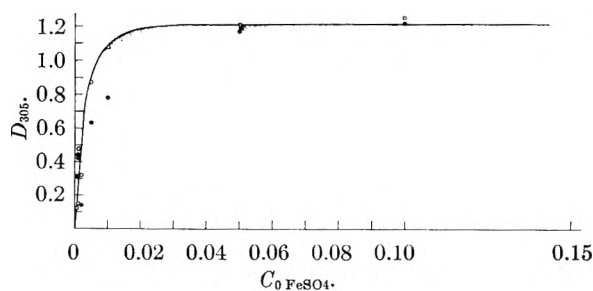


Fig. 1.—Dependence of the oxidation yield on initial  $\text{Fe}^{2+}$  concentration.  $[\text{H}_2\text{SO}_4] = 0.8 N$ .  $\circ$  and  $\bullet$  represent results obtained in two separate series of experiments. The curve is the theoretical one, calculated using the data of Fig. 2.

and 0.01 M  $\text{Fe}^{2+}$  in 0.8 N  $\text{H}_2\text{SO}_4$ . The pumping rate was measured by the time elapsed and also by the pressure decrease in the reservoir. The results shown in Table I represent a separate run for every experimental point.

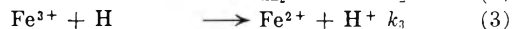
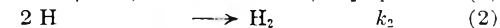
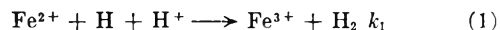
TABLE I  
DEPENDENCE OF  $\Delta[\text{Fe}^{3+}]$  ON  $\Delta H$

| $t$ , sec. | $-\Delta p$ , cm. | $\Delta D_{305}$ |
|------------|-------------------|------------------|
| 130        | 6                 | 0.237            |
| 330        | 15                | .370             |
| 585        | 26.5              | .625             |
| 815        | 38                | .960             |

Thus the yield is a linear function of time and thus of quantity of gas passing the solution at the same pressure. It indicates the degree of constancy of conditions in a series of consecutive runs. It also shows that in investigating the initial yield at this pH the back reaction is not of importance.

**The Oxidation Yield as a Function of Initial  $\text{Fe}^{2+}$  Concentration.**—In 0.8 N  $\text{H}_2\text{SO}_4$  solution the amount of  $\text{Fe}^{2+}$  oxidized was measured as a function of the initial  $\text{Fe}^{2+}$  concentration, keeping  $\text{H}_2$  pressure, flow rate and discharge conditions constant. The yield increases with increasing  $\text{Fe}^{2+}$  concentration, reaching a maximum at higher  $\text{Fe}^{2+}$  concentrations as shown in Fig. 1.

Hydrogen atoms are generated in the discharge and 1 mole l.<sup>-1</sup> sec.<sup>-1</sup> enter the solution. Without deciding what the actual mechanism or the species participating is, H atoms can be considered to disappear by reaction with  $\text{Fe}^{2+}$ , recombination or reaction with  $\text{Fe}^{3+}$



In our system at the relatively low H atom concentrations and under continuous flow, steady state conditions regarding H will prevail, compared with changes in  $\text{Fe}^{2+}$ , so that, assuming homogeneous kinetics

$$d[\text{H}]/dt = 0 = I - k_1[\text{H}][\text{Fe}^{2+}] - k_2[\text{H}]^2 - k_3[\text{H}][\text{Fe}^{3+}] \quad (I)$$

where  $k_1$  is the velocity constant of reaction 1., at a constant  $\text{H}^+$ . Thus

$$[\text{H}] = - \frac{(k_1[\text{Fe}^{2+}] + k_3[\text{Fe}^{3+}])}{2k_2} + \frac{\sqrt{(k_1[\text{Fe}^{2+}] + k_3[\text{Fe}^{3+}])^2 + 4k_2I}}{2k_2} \quad (II)$$

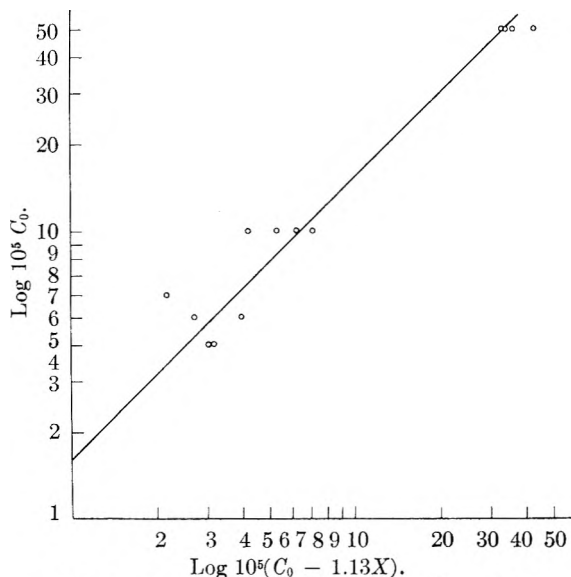


Fig. 2.—Log  $C_0$  as a function of Log  $(C_0 - \beta X)$ .

The rate of formation of  $\text{Fe}^{3+}$  is given by

$$d[\text{Fe}^{3+}]/dt = -d[\text{Fe}^{2+}]/dt = k_1[\text{Fe}^{2+}][\text{H}] - k_3[\text{Fe}^{3+}][\text{H}] \quad (\text{III})$$

Denoting  $k_3/k_1$  by  $\gamma$ , and defining  $\beta = 1 + \gamma$  (where  $\gamma$  and  $\beta$  are pH dependent, as is the ratio of the rate constants) we get, putting  $[\text{Fe}^{2+}]_0 = C_0$  and  $[\text{Fe}^{3+}] = X$

$$dX/dt = k_1[\text{H}](C_0 - X) - k_3X[\text{H}] = k_1[\text{H}](C_0 - \beta X) \quad (\text{IV})$$

so that

$$dX/dt = \frac{k_1^2(C_0 - \beta X)^2}{2k_2} \left( -1 + \sqrt{1 + \frac{4k_2I}{k_1^2(C_0 - \beta X)^2}} \right) \quad (\text{V})$$

At high initial  $[\text{Fe}^{2+}]$ , where  $4k_2I/k_1^2 \ll (C_0 - \beta X)^2$ , expanding into a series we get

$$dX/dt = I \text{ or } \Delta[\text{Fe}^{3+}]/t = I \quad (\text{VI})$$

Thus at high initial  $[\text{Fe}^{2+}]$ , when all H atoms reaching the solution are utilized to oxidize  $\text{Fe}^{2+}$  to  $\text{Fe}^{3+}$ , the yield is independent of  $[\text{Fe}^{3+}]$  and  $I$ , the rate of H atoms entering the solution can be obtained. The calculation gave  $I = 1.1 \times 10^{-6}$  mole l.<sup>-1</sup> sec.<sup>-1</sup>. This value agreed with  $I$  as determined by the reduction of  $\text{AgNO}_3$ . At low initial  $[\text{Fe}^{2+}]$ , where  $(C_0 - \beta X)^2 \ll 4k_2I/k_1^2$  expanding V into a series, we obtain

$$dX/dt = \frac{k_1\sqrt{I}}{\sqrt{k_2}}(C_0 - \beta X) - \frac{k_1^2}{2k_2}(C_0 - \beta X)^2 + \frac{k_1^3}{8k_2^{3/2}\sqrt{I}}(C_0 - \beta X)^3 \quad (\text{VII})$$

At concentrations of  $\text{Fe}^{2+}$  up to  $10^{-4}$  M we shall retain the first term only on the right, so that after integration

$$\ln \frac{C_0}{(C_0 - \beta X)} = \frac{\beta k_1\sqrt{I}}{\sqrt{k_2}} t \quad (\text{VIII})$$

In Fig. 2,  $\log C_0$  versus  $\log (C_0 - \beta X)$  is plotted giving as intercept  $\beta k_1\sqrt{I} t / \sqrt{k_2}$ . Introducing the value of  $I$  obtained at high  $[\text{Fe}^{2+}]$ , we obtain in 0.8 N  $\text{H}_2\text{SO}_4$  the value of  $k_1/\sqrt{k_2} = 0.6$ . Using this

value we calculated the theoretical curve according to equation V. As seen in Fig. 1, the experimental results fit the curve well. This relationship between  $k_1$  and  $k_2$  will be true whatever the actual mechanism. However the pH dependence of  $k_1$  and  $k_2$  and their exact meaning will depend on the species participating in the reaction steps.

**The Dependence of the Oxidation Yield on pH.**—

The dependence of the oxidation yield on the pH was investigated in 0.01 M  $\text{Fe}^{2+}$  solutions, containing varying amounts of added  $\text{H}_2\text{SO}_4$ . Thus ionic strength and sulfate ion concentration also varied at the same time. The yield was determined at constant discharge and flow conditions, for a fixed time of reactions and thus for a constant amount of H atoms passed. The total amount oxidized in all cases was considerably less than the final equilibrium value of  $[\text{Fe}^{3+}]$  at that pH. Table II shows the results.

TABLE II

| DEPENDENCE OF $\Delta[\text{Fe}^{3+}]$ ON THE pH |      |                   |
|--------------------------------------------------|------|-------------------|
| $N_{\text{H}_2\text{SO}_4}$                      | pH   | $\Delta D_{305}$  |
| 0.8                                              | 0.4  | $0.258 \pm 0.073$ |
| .08                                              | 1.3  | $.226 \pm .039$   |
| .04                                              | 1.75 | $.140 \pm .036$   |
| .008                                             | 2.3  | $.100 \pm .039$   |
| .004                                             | 2.65 | $.044 \pm .012$   |
| .0008                                            | 3.3  | $.022 \pm .010$   |

Compared with our preliminary results,<sup>6</sup> where pH dependence was established with certainty only as pH  $\rightarrow$  3, the more detailed results presented in Table II prove a definite pH dependence as the pH is increased to 1.75 and higher.

In this series the pH was varied together with a varying sulfate concentration. In reactions between ions of similar charge, the concentration of ions of opposite charge, which do not themselves react, increases the reaction velocity.<sup>11</sup> Recently it was shown<sup>10</sup> that in the radiation induced oxidation of  $\text{Fe}^{2+}$  (in the presence of  $\text{O}_2$ ), sulfate ions added as  $\text{Na}_2\text{SO}_4$  at a constant pH, influenced the oxidation yield. In the present case we found that for 0.01 M  $\text{Fe}^{2+}$  solutions in 0.004 N  $\text{H}_2\text{SO}_4$  (pH 2.65)  $\Delta D_{305}$  was  $0.044 \pm 0.012$ , whilst in 0.004 N  $\text{H}_2\text{SO}_4$  containing 0.4 M  $\text{Na}_2\text{SO}_4$  (pH 2.75)  $\Delta D_{305}$  was  $0.094 \pm 0.016$ . This significant increase is emphasized by the fact that the slight increase in pH by itself would have decreased the yield.

**The Influence of pH on the Steady State Ratio of  $[\text{Fe}^{3+}]/[\text{Fe}^{2+}]$ .**— $\alpha$ , the final ratio of  $[\text{Fe}^{3+}]/[\text{Fe}^{2+}]$  established under steady-state conditions, at a constant rate of H atoms being passed through the solution was established at several pH values. The steady state is due to the reactions 1 and 3, and as shown in Table III depends sharply on pH. At all pH values the steady state was approached in different experiments from either side. The standard deviations indicated include both types of experiment.

### Discussion

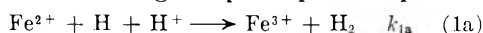
In previous papers<sup>6,7</sup> and in the present work the oxidation of ferrous ions in aqueous solution by

(11) Cf. B. Perlmutter-Hayman and G. Stein, THIS JOURNAL, 63, 734 (1959).

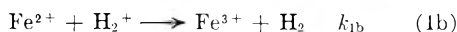
TABLE III  
DEPENDENCE OF THE STEADY STATE VALUE OF  $[\text{Fe}^{3+}]/[\text{Fe}^{2+}]$  ON THE  $p\text{H}$

| $\text{H}_2\text{SO}_4, N$ | $p\text{H}$ | $([\text{Fe}^{3+}]/[\text{Fe}^{2+}])_s = \alpha$ |
|----------------------------|-------------|--------------------------------------------------|
| 0.8                        | 0.4         | $7.4 \pm 0.8$                                    |
| .08                        | 1.3         | $1.05 \pm .05$                                   |
| .008                       | 2.3         | $0.21 \pm .02$                                   |
| .001                       | 3.0         | $0.020 \pm .001$                                 |

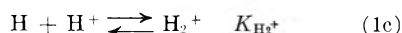
hydrogen atoms was proved. There is however still uncertainty regarding the mechanism of this process. The evidence derived from the radiation chemistry of  $\text{Fe}^{2+}$  in aqueous solution showed that H atoms in the irradiated system oxidize  $\text{Fe}^{2+}$  to  $\text{Fe}^{3+}$  in acid solution.<sup>1,2</sup> This could be due to either of the following two  $p\text{H}$  dependent processes



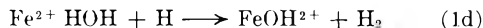
or



where the  $\text{H}_2^+$  ion is present according to the equilibrium



On the basis of the quantitative results, both Rigg, Stein and Weiss<sup>1</sup> and Rothschild and Allen<sup>3</sup> came to the conclusion that reaction 1b involving the species  $\text{H}_2^+$  is likely to be the one occurring in the radiation induced oxidation of  $\text{Fe}^{2+}$ . This conclusion is also supported by the work of Schwarz and Hritz.<sup>12</sup> In the photochemical oxidation of  $\text{Fe}^{2+}$ , Rigg and Weiss<sup>4</sup> found a similar quantitative dependence on  $p\text{H}$  and concluded that here too a mechanism involving  $\text{H}_2^+$  operates. However Lefort and Douzou<sup>13</sup> failed to find any  $p\text{H}$  dependence and suggested that the  $p\text{H}$  independent process



is the one occurring. In view of this contradiction we have recently reinvestigated this reaction<sup>14</sup> and found it to depend on  $p\text{H}$ . Hayon and Weiss<sup>15</sup> have also reinvestigated the photochemical oxidation of  $\text{Fe}^{2+}$  and again found it to be  $p\text{H}$  dependent. The results reported in the present paper, regarding the  $p\text{H}$  dependence of the oxidation of  $\text{Fe}^{2+}$  by H atoms (under conditions where the back reaction of reduction by H atoms of  $\text{Fe}^{3+}$  may be neglected) show a quantitative behavior which is best explained by assuming that  $\text{H}_2^+$  is involved. Theoretically, Coulson<sup>16</sup> considered the evidence in favor of the formation of  $\text{H}_2^+_{\text{aq}}$ . However weighty evidence was obtained through investigation of isotope effects in aqueous solutions irradiated with ionizing radiations, which was interpreted as showing that  $\text{H}_2^+$  ions cannot be involved. Of these the results of Baxendale and Hughes<sup>17</sup> serve to

(12) H. A. Schwarz and J. M. Hritz, *J. Am. Chem. Soc.*, **80**, 5636 (1958).

(13) M. Lefort and P. Douzou, *J. chim. phys.*, **53**, 536 (1956).

(14) J. Jortner and G. Stein, to be published.

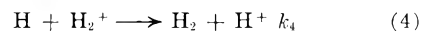
(15) J. Weiss, personal communication.

(16) C. A. Coulson, *J. Chem. Soc.*, 778 (1956).

(17) J. H. Baxendale and G. Z. Hughes, *Z. physik. Chem., N.F.*, **14**, 323 (1958).

eliminate reaction 1a, already considered unlikely by Rothschild and Allen<sup>3</sup>, but are not against reaction 1b. The other results<sup>18,19</sup> can be reconciled with the occurrence of  $\text{H}_2^+$  only if chain reactions carried by H atoms do not occur.

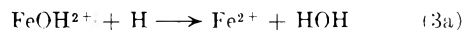
Some results of Friedman and Zeltmann<sup>19</sup> may be interpreted in terms of the intermediate formation of  $\text{H}_2^+$ . Namely investigating the recombination reaction 2, between H atoms, Friedman and Zeltmann found, instead of the expected rate constant of  $10^{10}$  l./mole sec., or higher, a rate constant of only  $1 \times 10^8$  l./mole sec. In acid solutions, in addition to the recombination reaction 2, the likely reaction



will occur. This would be the case in the experiments of Friedman and Zeltmann at  $p\text{H}$  2.  $k_4$  will be smaller than  $k_2$  and the constant obtained by them would be a composite one, showing the relative weights of the two recombination processes.

Taking this into consideration, we shall consider our experimental results which gave the relationship  $k_1 = 0.6 \sqrt{k_2}$ . The recombination velocity constant  $k_2$  would thus have as its highest value  $\sim 10^{10}$  l./mole sec., and would yield an upper limit of  $6 \times 10^4$  l./mole sec. for the velocity constant,  $k_1$ , of the oxidation of  $\text{Fe}^{2+}$  by H atoms, if the recombination process involves only H atoms, as in reaction 2, and  $\text{H}_2^+$  is not involved. If however we take into account the formation of  $\text{H}_2^+$ , " $k_2$ " will have a lower value composed of  $k_4$  and  $k_2$  as indicated by Friedman's results. We obtain then for reaction 1b, a lower velocity constant of the order of  $10^3$  l./mole sec.

The values of  $\alpha = ([\text{Fe}^{3+}]/[\text{Fe}^{2+}])_s$ , obtained by us agree with those obtained by Rothschild and Allen.<sup>3,12</sup> The quantitative  $p\text{H}$  dependence indicates that the reduction process proceeds by a mechanism involving



rather than, e.g.,  $\text{Fe}^{3+}_{\text{aq}}$ . However to establish this point, experiments at constant anion concentration, in different acids, will have to be carried out, to prove that indeed group transfer of this type is involved. The experiments in which at an approximately constant  $p\text{H}$  the anion concentration was increased, resulting in increased oxidation rate, are consistent with the assumption that the oxidation mechanism is indeed 1b, involving two positive ions.

To sum up, the evidence based on the process of oxidation of  $\text{Fe}^{2+}$  by H atoms produced by different methods is decidedly in favor of a  $p\text{H}$  dependent mechanism. However in view of the weighty indirect arguments against it, based on studies of isotope effects, there is no certainty yet that it is actually the species  $\text{H}_2^+_{\text{aq}}$  that is involved.

We thank Mr. J. Jortner for valuable comments.

(18) S. Gordon and E. J. Hart, *J. Am. Chem. Soc.*, **77**, 3981 (1955).

(19) H. L. Friedman and A. H. Zeltmann, *J. Chem. Phys.*, **28**, 878 (1958).

## SOME RADICAL AND MOLECULAR YIELDS IN THE $\gamma$ -IRRADIATION OF SOME ORGANIC LIQUIDS

BY G. E. ADAMS, J. H. BAXENDALE AND R. D. SEDGWICK

*Chemistry Department, The University, Manchester 13, England*

*Received February 9, 1959*

The hydrogen and methane yields from the  $\gamma$ -irradiation of ethanol, isopropyl alcohol, *t*-butyl alcohol, cyclohexanol, cyclohexane, diethyl ether, acetic acid and ethyl acetate have been measured. These yields are decreased by the presence of benzoquinone, which is interpreted in terms of its scavenging effect for H atoms and  $\text{CH}_3$  radicals. Kinetic analysis of the results gives values of primary yields of H,  $\text{CH}_3$ ,  $\text{H}_2$  and  $\text{CH}_4$ . Benzoquinone and ferric chloride have also been used to determine total radical yields.

We have recently shown that the individual radical yields for liquid methanol can be determined using *p*-benzoquinone and ferric salts as free radical and atom scavengers.<sup>1</sup> The present work is an extension of the method to other organic liquids. The yields of all the different radicals produced from more complex molecules are obviously very difficult to obtain, and we have limited ourselves to H and  $\text{CH}_3$ , which, in the absence of scavengers, give  $\text{H}_2$  and  $\text{CH}_4$  by hydrogen abstraction from the compounds irradiated in this work.

With methanol, the total radical yield  $G(\text{R})$  was obtained<sup>1</sup> by measuring the extent of the reduction of hydrated ferric chloride or *p*-benzoquinone by the radicals. Both scavengers gave the same value of  $G(\text{R})$ . However, we find that *p*-benzoquinone cannot be used in this way for all the liquids we have examined. In some cases quinhydrone is precipitated and makes the spectroscopic determination of the quinone impossible. In others, instead of the decrease in optical absorption in the ultraviolet expected as the quinone is reduced, an increase is observed. This clearly indicates that the simple reduction to hydroquinone does not occur, and possibly substitution followed by dimerization of the semiquinone, accounts for the increased density. In such cases we have used hydrated ferric chloride where its solubility allowed. Where benzoquinone has been used we have ensured that no complications are present by establishing that the optical density after prolonged irradiation falls to that of hydroquinone in the same solvent.

### Experimental

**Materials.**—Ethanol and isopropyl alcohol were purified by methods similar to that used for methanol.<sup>1</sup> Acetic acid and *t*-butyl alcohol of analytical grade were further purified by triple fractional crystallization. Cyclohexanol of commercial grade was subjected to multiple fractional distillation. Diethyl ether of anesthetic purity was fractionally distilled after treatment with acidified ferrous sulfate. Spectroscopic grade cyclohexane, and analytical grade ethyl acetate and ferric chloride hexahydrate were used without further purification. *p*-Benzoquinone was purified by low temperature vacuum sublimation.

**Analyses.**—The gases from the radiolysis were collected as described previously<sup>1</sup> and analyzed both qualitatively and quantitatively by the mass spectrometer. Benzoquinone and ferric chloride in organic solvents were determined by ultraviolet absorption.

**Irradiations.**—In all cases 50 ml. of liquid was irradiated in Pyrex vessels, deaerated by pumping and shaking. Where measurement of the rate of consumption of scavenger was required a vessel fitted with a side-arm terminated by a

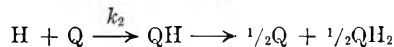
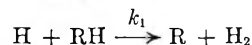
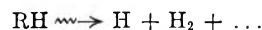
1 cm. quartz cell was used. This allowed successive spectroscopic measurements on the same deaerated sample.

Dose rates between  $3 \times 10^{15}$  and  $7 \times 10^{15}$  e.v./g./min. were obtained from a 10 curie  $\text{Co}^{60}$  source. Total doses were usually about  $2 \times 10^{20}$  e.v. and total gas yields from the 50-cc. samples about  $5 \times 10^{-5}$  mole. Irradiations were done at 18° except for *t*-butyl alcohol which was held at 30° to keep it liquid.

**Dosimetry.**—Dose rates were measured with  $10^{-3}$  M ferrous sulfate in 0.8 N sulfuric acid using  $G(\text{Fe}^{3+}) = 15.6$ . The absorptions of the various liquids were calculated from the mass absorption coefficients of Davisson and Evans.<sup>2</sup>

### Results

For each compound we have measured  $G(\text{H}_2)$  and  $G(\text{CH}_4)$  for the pure liquid. We find that these yields are decreased when benzoquinone (Q) is present and we have assumed that, as for methanol, the following reactions of H atoms occur



From these it follows that

$$G(\text{H}_2) = G_m(\text{H}_2) + k_1(\text{RH})G(\text{H})/[k_1(\text{RH}) + k_2(\text{Q})]$$

where  $G_m(\text{H}_2)$  and  $G(\text{H})$  are molecular and atom yields. When  $(\text{Q}) = 0$

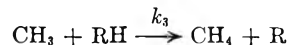
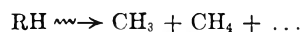
$$G(\text{H}_2) = G(\text{H}_2)_{\text{max}} = G_m(\text{H}_2) + G(\text{H})$$

Hence

$$1/[G(\text{H}_2)_{\text{max}} - G(\text{H}_2)] = 1/G(\text{H}) + k_1(\text{RH})/k_2(\text{Q})G(\text{H}) \quad (1)$$

Thus the plot  $1/[G(\text{H}_2)_{\text{max}} - G(\text{H}_2)]$  vs.  $1/(\text{Q})$  should be linear and give  $G(\text{H})$  and  $k_1/k_2$ .

Analogous equations for  $\text{CH}_3$  and  $\text{CH}_4$  may be written from the reactions



The analogous plot should give  $G(\text{CH}_3)$ ,  $G_m(\text{CH}_4)$  and  $k_3/k_4$ .

Reasonable agreement with this analysis is found for all the liquids although in some cases the yields of  $\text{H}_2$  and  $\text{CH}_4$  are too low to allow of accurate determinations of the above quantities.

Total radical yields have been determined for ethanol, cyclohexanol and acetic acid by measuring the consumption of benzoquinone, and for isopropyl alcohol, *t*-butyl alcohol and ethyl acetate

(1) G. E. Adams and J. H. Baxendale, *J. Am. Chem. Soc.*, **80**, 4215 (1958).

(2) C. M. Davisson and R. A. Evans, *Rev. Mod. Phys.*, **24**, 79 (1952).

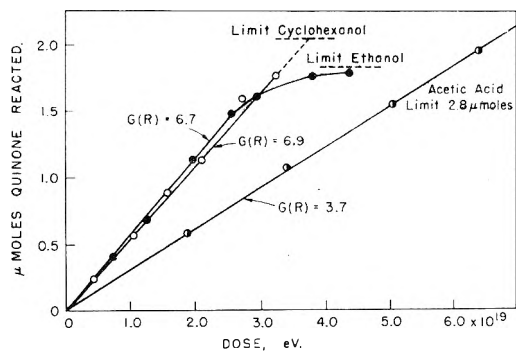


Fig. 1.—Radical yields using benzoquinone. Initial concentrations of benzoquinone are indicated by the limits.

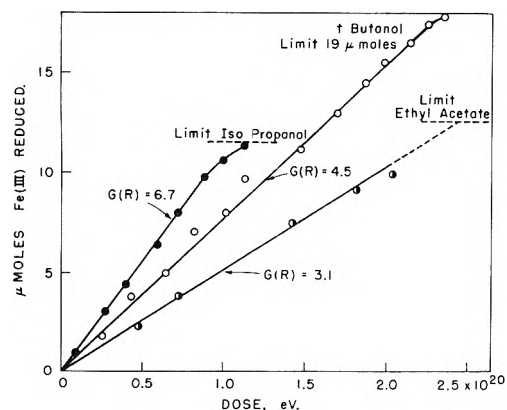


Fig. 2.—Radical yields using ferric chloride. Initial concentrations of  $\text{FeCl}_3 \cdot 6\text{H}_2\text{O}$  are indicated by the limits.

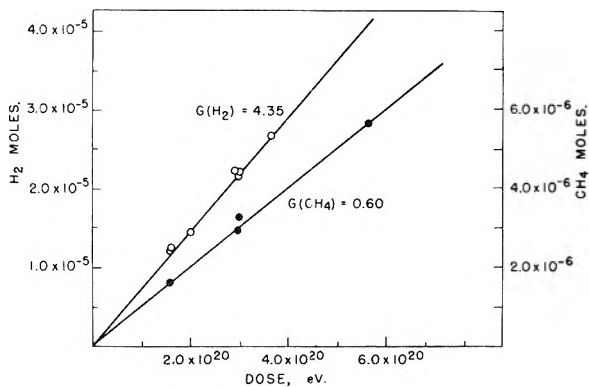


Fig. 3.—Yields of  $\text{H}_2$  and  $\text{CH}_4$  from ethanol.

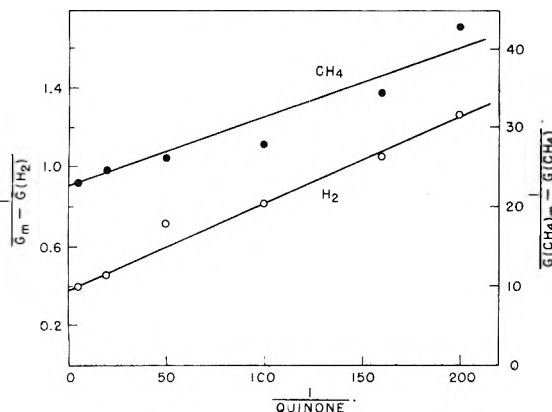


Fig. 4.—Plot of equation 1 for  $\text{H}_2$  and  $\text{CH}_4$  yields from ethanol containing benzoquinone.

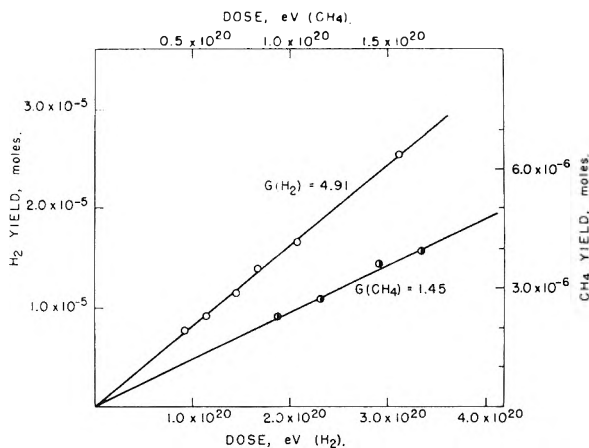


Fig. 5.—Yields of  $\text{H}_2$  and  $\text{CH}_4$  from isopropyl alcohol.

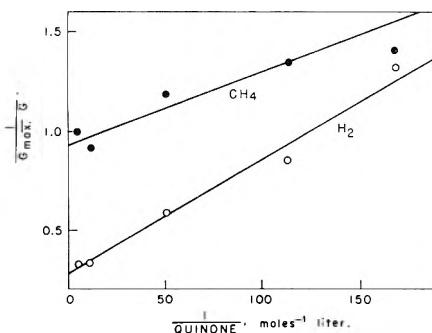


Fig. 6.—Plot of equation 1 for  $\text{H}_2$  and  $\text{CH}_4$  yields from isopropyl alcohol containing benzoquinone.

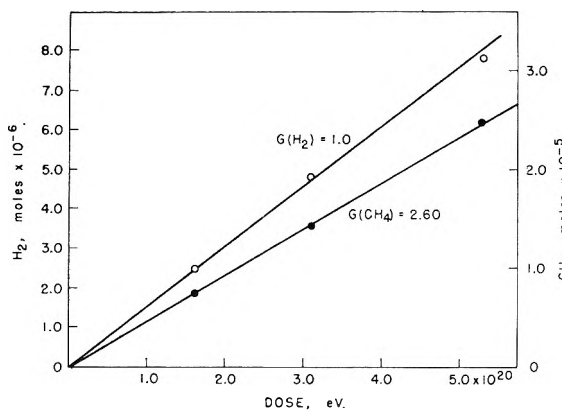


Fig. 7.—Yields of  $\text{H}_2$  and  $\text{CH}_4$  from *t*-butyl alcohol.

from the consumption of ferric chloride. It is assumed in each case that a radical reacts to reduce one equivalent of the scavenger and that all radicals are scavenged. The latter was established by showing that the consumption of scavenger is linear with dose for at least a fivefold change in scavenger concentration. The consumption curves are given in Figs. 1 and 2, and the values of  $G(R)$  are collected in Table I.

**Ethanol.**—Small amounts of ethane, ethylene and carbon monoxide were observed in addition to the main gaseous products hydrogen and methane. The productions of the latter with dose are given in Fig. 3. They give  $G(\text{CH}_4) = 0.60$  and  $G(\text{H}_2) = 4.35$ . Burr<sup>3</sup> has reported  $G(\text{H}_2) = 3.66$  for ethanol

(3) J. G. Burr, *This Journal*, **61**, 1477 (1957).



TABLE I

| Solvent               | $G(H)$ | $G_m(H_2)$ | $G(CH_4)$ | $G_m(CH_4)$ | $k_2/k_1$ | $k_4/k_3$ | $G(R)$ |
|-----------------------|--------|------------|-----------|-------------|-----------|-----------|--------|
| Methanol <sup>a</sup> | 2.40   | 1.70       | 1.00      | 0.20        | 6,000     | 76,000    | 6.1    |
| Ethanol               | 2.70   | 1.65       | 0.44      | .16         | 1,450     | 4,500     | 6.9    |
| Isopropyl alc.        | 3.64   | 1.27       | 1.06      | .39         | 620       | 3,500     | 6.7    |
| <i>t</i> -Butyl alc.  | 0.43   | 0.57       | 1.70      | .90         | 3,700     | 100,000   | 4.5    |
| Cyclohexanol          | .68    | 2.17       | ...       | ...         | 840       | ...       | 6.7    |
| Cyclohexane           | 3.17   | 2.10       | ...       | ...         | 680       | ...       | ...    |
| Ethyl ether           | 1.32   | 2.01       | 0.22      | .09         | 680       | 1,360     | ...    |
| Acetic acid           | 0.21   | 0.30       | 2.82      | .60         | 16,000    | 39,000    | 3.7    |
| Ethyl acetate         | .35    | .55        | ...       | ...         | 3,700     | ...       | 3.1    |

<sup>a</sup> From reference 1.

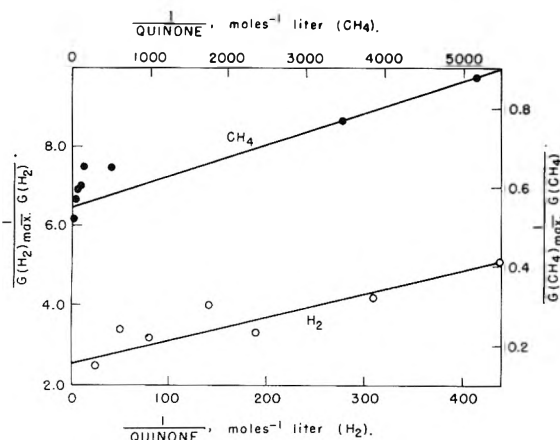


Fig. 8.—Plot equation 1 for  $H_2$  and  $CH_4$  yields from *t*-butyl alcohol containing benzoquinone.

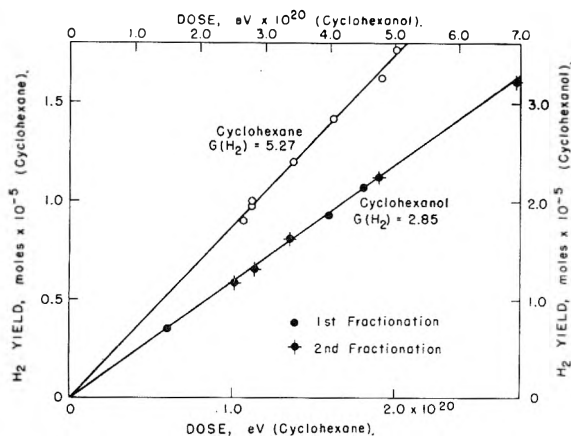


Fig. 9.—Yields of  $H_2$  from cyclohexanol and from cyclohexane.

using higher doses than ours. The competition plots for  $G(H_2)$  and  $G(CH_4)$  in the presence of benzoquinone are given in Fig. 4, and the primary yields calculated using equations 1 above are given in Table I.

**Isopropyl Alcohol.**—Yields of hydrogen and methane with dose for pure isopropyl alcohol are given in Fig. 5. These give  $G(H_2) = 4.91$  and  $G(CH_4) = 1.45$ . The plots according to equation 1 are given in Fig. 6 and the primary yields calculated from these collected in Table I.

***t*-Butyl Alcohol.**—Figure 7 shows the production of hydrogen and methane with dose from which  $G(H_2) = 1.00$  and  $G(CH_4) = 2.60$  are obtained. The plots of equation 1 are given in Fig. 8. The variations of  $G(H_2)$  and  $G(CH_4)$  with added benzo-

quinone are rather small and the resulting primary yields (Table I) are consequently not very accurate.

**Cyclohexanol.**—Hydrogen was the only gas present in an appreciable quantity.  $G(H_2) = 2.85$  is given by the results in Fig. 9. Equation 1 is plotted in Fig. 10 and the primary yields given in Table I.

**Cyclohexane.**—Again only hydrogen was measured and  $G(H_2) = 5.27$  obtained from Fig. 9. This compares with 5.4 obtained by Schuler,<sup>4</sup> 5.9 by Burton, *et al.*,<sup>5</sup> and 4.85 by Swallow. Burton also found that  $G(H_2)$  is decreased to 3.8 by  $10^{-2}M$  iodine. We observed  $G(H_2) = 3.93$  in the presence of  $10^{-2}M$  benzoquinone, and 2.85 with  $4.35 \times 10^{-2}M$ . The plot of the effect of benzoquinone according to equation 1 is given in Fig. 10. This gives  $G(H) = 3.17$  and  $G(H_2) = 2.1$ . The latter is about the same as  $G(\text{cyclohexene}) = 2.3$  obtained by Dewhurst<sup>6</sup> and suggests that adjacent atoms are abstracted to form molecular hydrogen.

**Diethyl Ether.**—Productions of hydrogen and methane with dose are given in Fig. 11. These give  $G(H_2) = 3.43$  and  $G(CH_4) = 0.31$ . Both are reduced by the presence of benzoquinone and the plots of equation 1 are given in Fig. 12. Primary yields are collected in Table I.

**Acetic Acid.**—Carbon dioxide is the main gaseous product with  $G(CO_2) = 4.25$ .  $G(H_2) = 0.51$  and  $G(CH_4) = 3.42$  are given by the lines in Fig. 13.  $G(CO) = 0.29$  and  $G(C_2H_6) = 0.45$  were also obtained. Burr<sup>3</sup> has reported  $G(H_2) = 0.45$  and  $G(CH_4) = 3.13$ .  $G(CO_2)$ ,  $G(CO)$  and  $G(C_2H_6)$  were unchanged in the presence of benzoquinone which indicates that they are either produced primarily as molecules or that the radicals from which they are formed react with benzoquinone to produce them more quickly than they react with benzoquinone. In the sense used here we would call these "molecular" products.  $G(H_2)$  and  $G(CH_4)$  however are both decreased in these conditions and the plots of equation 1 are given in Fig. 14.

**Ethyl Acetate.**—The main gaseous products are hydrogen, methane and carbon monoxide although smaller amounts of ethane, ethylene and carbon dioxide were observed.  $G(H_2) = 0.90$ ,  $G(CH_4) = 1.58$  and  $G(CO) = 1.13$  are obtained from Fig. 15. These yields are reduced by benzoquinone but plotting the yields according to equation 1 gives a straight line for hydrogen only (Fig. 16). The re-

(4) R. H. Schuler, *THIS JOURNAL*, **62**, 1472 (1958).

(5) M. Burton, J. Chang, S. Lipsky and M. P. Reddy, *J. Chem. Phys.*, **26**, 1337 (1957).

(6) H. A. Dewhurst, *ibid.*, **24**, 1254 (1956).

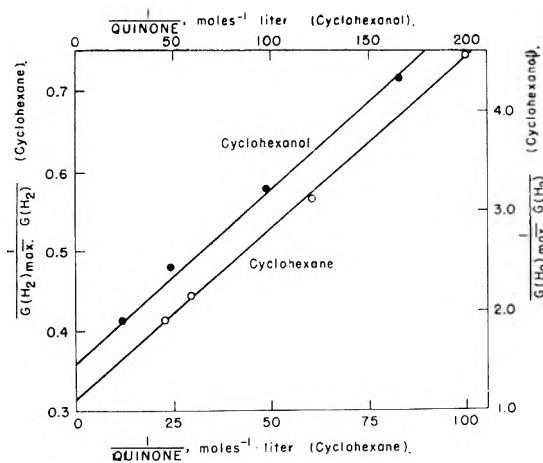


Fig. 10.—Plots of equation 1 for  $H_2$  yields from cyclohexanol and from cyclohexane containing benzoquinone.

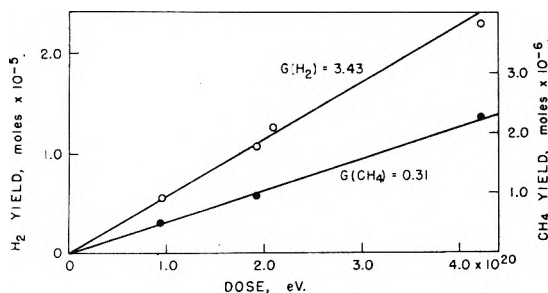


Fig. 11.—Yields of  $H_2$  and  $CH_4$  from diethyl ether.

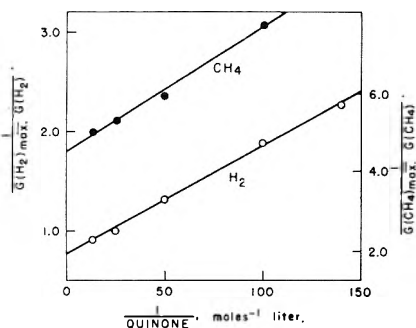


Fig. 12.—Plot of equation 1 for  $H_2$  and  $CH_4$  yields from ether in the presence of benzoquinone.

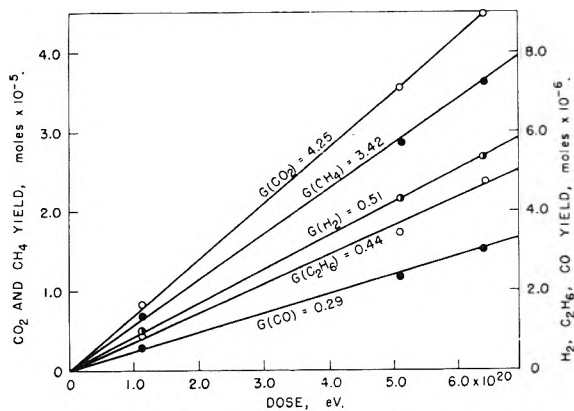


Fig. 13.—Yields from acetic acid.

duction in  $G(CO)$  suggests that carbon monoxide originates in part from  $CH_3CO$  decomposition. If this were the case and the decomposition com-

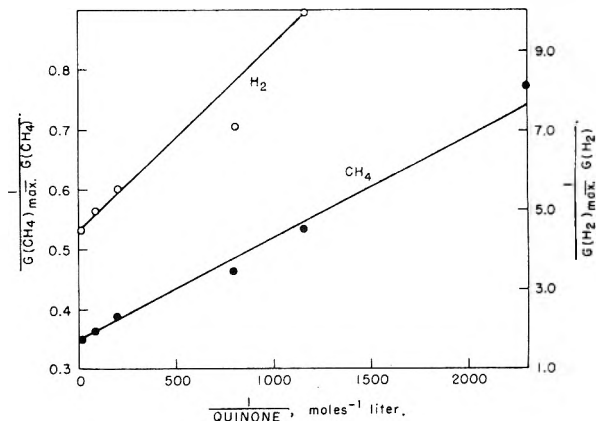


Fig. 14.—Plot of equation 1 for  $H_2$  and  $CH_4$  yields from acetic acid containing benzoquinone.

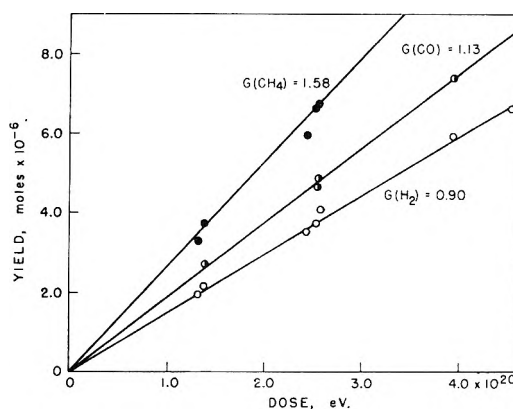


Fig. 15.—Yields from ethyl acetate.

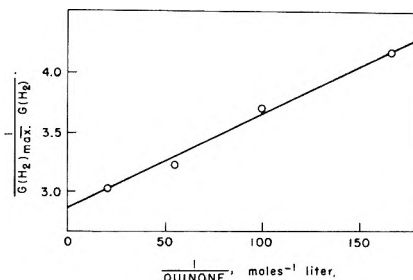


Fig. 16.—Plot of equation 1 for  $H_2$  yields from ethyl acetate in the presence of benzoquinone.

peted with the reaction with benzoquinone, then an equation of the form of 1 would not necessarily apply to  $G(CH_4)$  and  $G(CO)$ . However, from the values of  $G(CH_4)$  at the highest quinone concentrations we can say  $G_m(CH_4) < 0.4$ .

### Discussion

The total radical and the individual radical and molecular yields obtained are given in Table I. The rate constant ratios  $k_2/k_1$  ( $H + Q$  compared with  $H + RH$ ) and  $k_4/k_3$  ( $CH_3 + Q$  compared with  $CH_3 + RH$ ) are also collected in Table I.

**Rate Constants.**—If it may be assumed that the rates of the  $H + Q$  and  $CH_3 + Q$  reactions will be only little dependent on the solvent (which seems reasonable except perhaps for cyclohexane which is much less polar and acetic acid on account of its acidity) then the ratios are a measure of the relative rates of abstraction of hydrogen from the

different molecules. In the alcohol series the rates are in the order expected for abstraction of the carbon hydrogen from methanol and *t*-butyl alcohol, the secondary hydrogen from ethanol and the tertiary hydrogen from isopropyl alcohol. The rates suggest that in ether the secondary hydrogen is removed whilst in ethyl acetate the primary hydrogen of the ethyl group is involved. Probable solvent effects on the quinone reactions prevent any conclusions being drawn from the reaction rates in cyclohexane and acetic acid.

**Primary Yields.**—The results in Table I indicate a tendency for total radical yields to be higher when  $G(\text{H})$  is high. Thus the compounds fall into two groups, the primary and secondary alcohols for which  $G(\text{H}) > 2$  and  $G(\text{R}) > 6$ , and the others for which  $G(\text{H}) < 0.5$  and  $G(\text{R})$  is 4.5 to 3.1. This tendency may result from the greater ease with which hydrogen atoms escape solvent cage reactions. It seems odd that  $G(\text{H})$  for cyclohexanol is so small. One would expect a value similar to the  $G(\text{H})$  for either cyclohexane or isopropyl alcohol as is the case for  $G_{\text{m}}(\text{H}_2)$  and  $G(\text{R})$ . It is possible that traces of unsaturated materials are responsible for the anomaly, but further fractional distillation left  $G(\text{H}_2)$  unchanged (Fig. 9).

For the other alcohols  $G(\text{H})$  increases in the order MeOH, EtOH, iso-PrOH. This variation is in the opposite sense to that expected from the mass

spectra of the vapors. Here the relative abundance of the ion corresponding to the production of H atoms (*i.e.*, parent ion less one) decreases appreciably along the series. This suggests that ionization processes are not a predominant primary source of H atoms and that possibly dissociative electron capture of the type



or charge neutralization are more important. However, it is not immediately obvious how these mechanisms account for the much lower  $G(\text{H})$  for butanol. One possibility is that the slightly higher O–H bond energy compared with the other alcohols<sup>7</sup> makes the electron capture process less efficient.

The values of  $G(\text{CH}_3)$  for the alcohols (except methanol which may involve a special mechanism for  $\text{CH}_3$  production<sup>1</sup>) fall in line with the abundance of the corresponding ion (*i.e.*, parent ion less 15) in the mass spectra. This would be consistent with  $\text{CH}_3$  as a primary product of the ionization processes.

We gratefully acknowledge the financial support of the U.K. Atomic Energy Authority (Research Group Harwell) and the Department of Scientific and Industrial Research.

(7) P. Gray, *Trans. Faraday Soc.*, **52**, 344 (1956).

## ABSOLUTE RATE CONSTANTS FOR H ATOM REACTIONS IN AQUEOUS SOLUTIONS<sup>1</sup>

BY PETER RIESZ<sup>2</sup> AND EDWIN J. HART

*Argonne National Laboratory, Lemont, Illinois*

*Received February 9, 1959*

In order to determine the absolute rate constant of the reaction  $\text{H} + \text{Fe}^{\text{III}} = \text{Fe}^{\text{II}} + \text{H}^+$ , we have measured the relative rate constant ratio  $k_{(\text{H} + \text{Fe}^{\text{III}})}/k_{(\text{H} + \text{D}_2)}$  and then calculated  $k_{(\text{H} + \text{Fe}^{\text{III}})}$  by assuming that  $k_{(\text{H} + \text{D}_2)}$ , known from gas phase studies, remains unchanged in solution. The initial HD yields from the  $\gamma$ -irradiation of water containing dissolved deuterium gas, ferric sulfate and ferrous sulfate have been measured at various  $\text{Fe}^{\text{III}}/\text{D}_2$  ratios. From these studies we have calculated the rate constant ratio  $k_{(\text{H} + \text{Fe}^{\text{III}})}/k_{(\text{H} + \text{D}_2)} = 120 \pm 30$  in 0.01 *N*  $\text{H}_2\text{SO}_4$ . Since the rate constant of the gas reaction,  $\text{H} + \text{D}_2 = \text{HD} + \text{D}$ , equals  $0.4 \times 10^6$  l. mole<sup>-1</sup> sec.<sup>-1</sup>, it follows that the rate constant of the reaction  $\text{H} + \text{Fe}^{\text{III}} = \text{Fe}^{\text{II}} + \text{H}^+$  in 0.01 *N*  $\text{H}_2\text{SO}_4$  is  $(0.48 \pm 0.1) \times 10^7$  l. mole<sup>-1</sup> sec.<sup>-1</sup> at 25°. Using this result, we have calculated a number of absolute rate constants for H atom reactions.

### Introduction

For a better understanding of aqueous radiation chemistry, a knowledge of the absolute rate constants of H atom reactions with a variety of inorganic and organic substances is desirable. Such rate constants are of theoretical interest in the development of the radical diffusion model<sup>3,4</sup> and in testing its ability to predict the effect of solutes on the molecular  $\text{H}_2$  yield.

In order to calculate absolute rate constants from the large number of published relative rate constants for H atom reactions,<sup>5-8</sup> one requires the

absolute value of the rate constant for a single suitable reaction. Since the rate constant for the reaction  $\text{H} + \text{D}_2 = \text{HD} + \text{D}$  is known from gas phase studies,<sup>9</sup> our procedure was to measure the relative rate constant ratio,  $k_{(\text{H} + \text{Fe}^{\text{III}})}/k_{(\text{H} + \text{D}_2)}$ , and then to calculate  $k_{(\text{H} + \text{Fe}^{\text{III}})}$  by assuming that  $k_{(\text{H} + \text{D}_2)}$  is the same in solution as in the gas phase. When this work was started, it was hoped that the competition of ferric ions and deuterium molecules for hydrogen atoms could be studied by measuring the initial HD yield from  $\gamma$ -irradiated

(1) Based on work performed under the auspices of the U. S. Atomic Energy Commission.

(2) Radiation Branch, National Cancer Institute, N. I. H., Bethesda 14, Md.

(3) D. A. Flanders and H. Fricke, *J. Chem. Phys.*, **28**, 1126 (1958).

(4) H. A. Schwarz, *J. Am. Chem. Soc.*, **77**, 4960 (1955).

(5) J. H. Baxendale and D. H. Smithies, *Z. physik. Chem.*, **6**, 242 (1956).

(6) J. H. Baxendale and G. Hughes, *ibid.*, **14**, 306 (1958).

(7) J. H. Baxendale and G. Hughes, *ibid.*, **14**, 323 (1958).

(8) W. G. Rothchild and A. O. Allen, *Rad. Res.*, **8**, 101 (1958).

(9) G. Boato, G. Careri, A. Cimino, E. Molinari and G. G. Volpi, *J. Chem. Phys.*, **24**, 783 (1956).

solutions containing dissolved deuterium gas at various  $\text{Fe}^{\text{III}}/\text{D}_2$  ratios.

### Experimental

Triply distilled water<sup>10</sup> was used in all experiments. Stock solutions with known  $\text{Fe}^{\text{II}}/\text{Fe}^{\text{III}}$  ratios were prepared by addition of standardized hydrogen peroxide to ferrous sulfate solutions in 0.10 *N*  $\text{H}_2\text{SO}_4$ . The total iron content of the ferrous sulfate solutions was determined by oxidation to ferric sulfate with excess  $\text{H}_2\text{O}_2$ . Ferric ion concentrations were determined by absorption spectroscopy at 3020 Å.

Solutions used in irradiation experiments were made up from the stock solutions just prior to irradiation and were 0.010 *N* in  $\text{H}_2\text{SO}_4$ . The pH's of these solutions were measured on a Beckman pH meter and found to be  $2.12 \pm 0.02$ .

Deuterium gas supplied by the Stuart Oxygen Co. and assaying >99.5% in deuterium atom content was used without further purification except to pass it through a liquid nitrogen trap. The procedures to degas the solutions, dissolve the deuterium gas and fill the 100-ml. syringes have been described previously.<sup>10</sup>

All solutions prepared by the above procedure contained no gas phase and were irradiated with  $\text{Co}^{60}$   $\gamma$ -rays in a specially designed chamber.<sup>11</sup> The dosage rates for each syringe used in these experiments were measured for the volumes employed by use of the ferrous sulfate dosimeter, and a value of 15.6  $\text{Fe}^{\text{III}}/100$  e.v. was used to convert chemical yield to e.v./l.

For each experiment two or three syringes were used. After irradiation 10 ml. of solution was added to 10 ml. of 1.6 *N*  $\text{H}_2\text{SO}_4$  and the optical density at 3020 Å. determined in cells of 5- or 1-cm. path length. Approximately 15–20 ml. of solution was introduced into a Van Slyke apparatus, the gas extracted and its volume and pressure measured. Two such gas samples at each dosage were combined for mass spectrometric determination of  $\text{H}_2$ , HD and  $\text{D}_2$ .  $\text{N}_2$  and  $\text{O}_2$  were determined as a check on the absence of dissolved air. The initial concentration of deuterium was measured in each syringe by extracting the gas from an aliquot of the solution removed prior to irradiation. Mass spectrometric analyses were carried out on a Type 21-620 Consolidated Electrodynamics machine. Precision is estimated as  $\pm 3\%$  for points other than blank determinations of HD present initially in  $\text{D}_2$  where it is  $\pm 6\%$ . The percentage compositions of  $\text{H}_2$ , HD and  $\text{D}_2$  obtained by the mass-spectrometer, together with the micromoles of total gas measured by the Van Slyke, were used to calculate the micromoles of HD and  $\text{H}_2$  produced and of  $\text{D}_2$  consumed.

### Results and Discussion

In some preliminary experiments solutions of either ferric sulfate or ferrous sulfate (205  $\mu\text{m.}/\text{l.}$ ) in 0.01 *N*  $\text{H}_2\text{SO}_4$  containing about 670  $\mu\text{m.}/\text{l.}$  of dissolved deuterium gas were irradiated. A steady-state  $\text{Fe}^{\text{III}}/\text{Fe}^{\text{II}}$  ratio is rapidly approached in both cases. The results for ferrous sulfate are shown in Fig. 1. It is evident from these experiments that precise initial HD yields ( $\pm 3\%$  for a given dose) cannot be determined for solutions containing only ferric ions without a substantial concentration of ferrous ions or *vice versa*. Hence subsequent experiments were carried out at steady-state  $\text{Fe}^{\text{III}}/\text{Fe}^{\text{II}}$  ratios.

The initial  $G(\text{HD})$  and  $G(\text{H}_2)$  values of experiments carried out at approximately steady-state  $\text{Fe}^{\text{III}}/\text{Fe}^{\text{II}}$  ratios in 0.01 *N*  $\text{H}_2\text{SO}_4$  containing about 600  $\mu\text{m.}/\text{l.}$  of dissolved  $\text{D}_2$  for various  $\text{Fe}^{\text{III}}/\text{D}_2$  ratios are shown in Table I. In every experiment reported here the formation of HD and  $\text{D}_2$  is a linear function of dose for low conversion. Some typical results (experiment 3 of Table I) are shown in Fig. 2. For experiments in which

(10) E. J. Hart, S. Gordon and D. A. Hutchinson, *J. Am. Chem. Soc.*, **75**, 6165 (1953).

(11) R. A. Blomgren, E. J. Hart and L. S. Markheim, *Rev. Sci. Instr.*, **24**, 298 (1953).

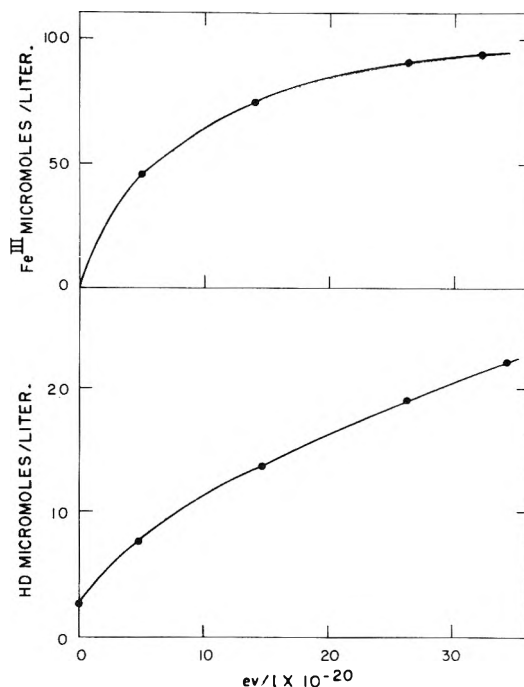


Fig. 1.— $\text{Fe}^{\text{III}}$  and HD yields from  $\gamma$ -irradiated  $\text{FeSO}_4$  solutions containing dissolved  $\text{D}_2$ .

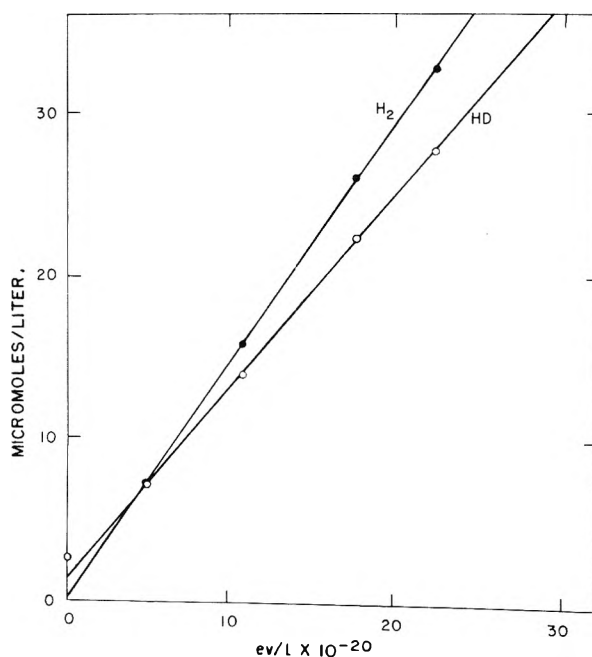


Fig. 2.—Initial HD and  $\text{H}_2$  yields from  $\gamma$ -irradiated solutions containing dissolved  $\text{D}_2$  at the steady state  $\text{Fe}^{\text{III}}/\text{Fe}^{\text{II}}$  ratio.

the initial  $\text{Fe}^{\text{III}}/\text{Fe}^{\text{II}}$  ratio is not exactly equal to the steady-state ratio, the HD yield does not extrapolate to the HD content of the  $\text{D}_2$  gas at zero dose. Curvature becomes noticeable on such plots when the concentration of the products, hydrogen and hydrogen deuteride, is about 10% of the total dissolved gas.

In all experiments the total amount of gas was found to be constant; that is, the amount of deuterium consumed was always equal to the hydrogen and hydrogen deuteride produced. This observation can be understood by a consideration of the

TABLE I  
 $G(\text{HD})$  AND  $G(\text{H}_2)$  FOR AQUEOUS SOLUTIONS CONTAINING  $\text{D}_2$ ,  $\text{Fe}^{\text{III}}$  AND  $\text{Fe}^{\text{II}}$  IN 0.01 N  $\text{H}_2\text{SO}_4$

| Expt. | $\text{D}_2$ av.,<br>$\mu\text{M/l.}$ | $\text{Fe}^{\text{III}}$ av.,<br>$\mu\text{M/l.}$ | $\text{Fe}^{\text{II}}$ av.,<br>$\mu\text{M/l.}$ | $G(\text{HD})$ | $G(\text{H}_2)$ | $\beta$ | $\frac{g(\text{H}_2)\gamma}{G(\text{HD})-\beta}$ | $\frac{(\text{Fe}^{\text{III}})}{\text{D}_2} + \frac{6.7(\text{H}_2\text{O}_2)_{\text{ss}}}{\text{D}_2}$ | $x$   |
|-------|---------------------------------------|---------------------------------------------------|--------------------------------------------------|----------------|-----------------|---------|--------------------------------------------------|----------------------------------------------------------------------------------------------------------|-------|
| 1     | 610                                   | 11.6                                              | 22.4                                             | 1.38           | 0.90            | 0.46    | 4.04                                             | 0.0241                                                                                                   | 0.039 |
| 2     | 460                                   | 31.5                                              | 36.2                                             | 0.54           | .76             | .18     | 10.1                                             | .079                                                                                                     | .091  |
| 3     | 675                                   | 26.7                                              | 41.0                                             | 0.72           | .89             | .31     | 8.18                                             | .048                                                                                                     | .055  |
| 4     | 630                                   | 11.5                                              | 22.1                                             | 1.33           | .85             | .46     | 4.27                                             | .0232                                                                                                    | .038  |
| 5     | 610                                   | 101                                               | 101                                              | 0.218          | .72             | .086    | 28.0                                             | .189                                                                                                     | .192  |
| 6     | 620                                   | 64.5                                              | 70.2                                             | 0.380          | .80             | .13     | 14.6                                             | .120                                                                                                     | .125  |
| 7     | 600                                   | 11.1                                              | 22.5                                             | 1.47           | .95             | .51     | 3.76                                             | .0237                                                                                                    | .028  |

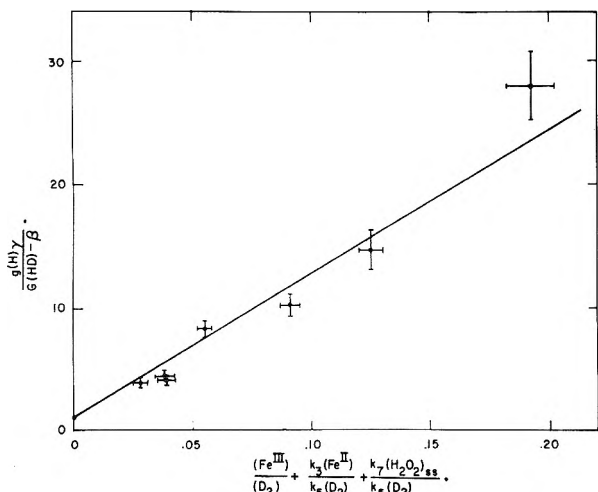
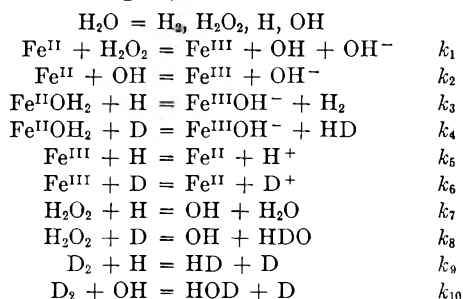


Fig. 3.—Initial HD yields plotted for determination of  $k_{(\text{H} + \text{Fe}^{\text{III}})}/k_{(\text{H} + \text{D}_2)}$ . The line is drawn with an intercept of one.

oxidation-reduction balance, since there is no production of oxygen or hydrogen peroxide and no change in the  $\text{Fe}^{\text{III}}/\text{Fe}^{\text{II}}$  ratio.

The following reactions take place when aqueous solutions containing  $\text{D}_2$ ,  $\text{Fe}^{\text{III}}$  and  $\text{Fe}^{\text{II}}$  are irradiated



The secondary reactions  $\text{H} + \text{HD} = \text{H}_2 + \text{D}$  and  $\text{D} + \text{H}_2 = \text{HD} + \text{H}$  can be neglected at low conversion. Reactions involving two atoms or radicals have been excluded, since the product of their stationary state concentrations is negligible.

Let  $a$ ,  $b$  and  $c$  be the rates of production (moles  $\text{l}^{-1} \text{sec}^{-1}$ ) of  $\text{H}$ ,  $\text{OH}$  and  $\text{H}_2\text{O}_2$ , respectively. Then by applying the stationary state method to the intermediates  $\text{H}$ ,  $\text{D}$ ,  $\text{OH}$  and  $\text{H}_2\text{O}_2$  the following results are obtained

$$(\text{H}_2\text{O}_2)_{\text{ss}} = \frac{c}{k_1(\text{Fe}^{\text{II}}) + k_7(\text{H}) + k_8(\text{D})} \quad (1)$$

$$(\text{H})_{\text{ss}} = \frac{a}{k_3(\text{Fe}^{\text{II}}) + k_5(\text{Fe}^{\text{III}}) + k_7(\text{H}_2\text{O}_2)_{\text{ss}} + k_9(\text{D}_2)} \quad (2)$$

$$(\text{OH})_{\text{ss}} = \frac{b + c}{k_2(\text{Fe}^{\text{II}}) + k_{10}(\text{D}_2)} \quad (3)$$

$$(\text{D})_{\text{ss}} = \frac{k_9(\text{D}_2)(\text{H}) + k_{10}(\text{D}_2)(\text{OH})}{k_4(\text{Fe}^{\text{II}}) + k_6(\text{Fe}^{\text{III}}) + k_8(\text{H}_2\text{O}_2)_{\text{ss}}} \quad (4)$$

$$G(\text{HD}) = \frac{g(\text{H})\gamma}{1 + \frac{k_6}{k_9} \left[ \frac{(\text{Fe}^{\text{III}})}{(\text{D}_2)} + \frac{k_3(\text{Fe}^{\text{II}})}{k_5(\text{D}_2)} + \frac{k_7(\text{H}_2\text{O}_2)_{\text{ss}}}{k_5(\text{D}_2)} \right]} + \beta \quad (5)$$

where

$$\beta = \frac{g(\text{OH}) + g(\text{H}_2\text{O}_2)}{\left[ 1 + \frac{k_2}{k_{10}} \frac{(\text{Fe}^{\text{II}})}{(\text{D}_2)} \right] \left[ 1 + \frac{k_6}{k_4} \frac{(\text{Fe}^{\text{III}})}{(\text{Fe}^{\text{II}})} + \frac{k_8}{k_4} \frac{(\text{H}_2\text{O}_2)_{\text{ss}}}{(\text{Fe}^{\text{II}})} \right]}$$

and

$$\gamma = 1 + \frac{1}{\left[ 1 + \frac{k_6}{k_4} \frac{(\text{Fe}^{\text{III}})}{(\text{Fe}^{\text{II}})} + \frac{k_8}{k_4} \frac{(\text{H}_2\text{O}_2)_{\text{ss}}}{(\text{Fe}^{\text{II}})} \right]}$$

$g(\text{H})$ ,  $g(\text{OH})$  and  $g(\text{H}_2\text{O}_2)$  are the primary radical and molecular yields and  $G(\text{HD})$  is the observed HD yield (molecules/100 e.v.). From equation 5 it follows that a plot of  $g(\text{H})\gamma/[G(\text{HD}) - \beta]$

$$\text{against } x = \frac{(\text{Fe}^{\text{III}})}{(\text{D}_2)} + \frac{k_3(\text{Fe}^{\text{II}})}{k_5(\text{D}_2)} + \frac{k_7(\text{H}_2\text{O}_2)_{\text{ss}}}{k_5(\text{D}_2)}$$

should be a straight line with a slope equal to  $k_5/k_9$  and an intercept equal to one.

Fortunately, several of the important rate constant ratios which appear in equation 5 have been determined in the course of previous investigations. The ratio  $k_5/k_3$  has been measured by Allen and Rothchild<sup>8</sup> in 0.01 N  $\text{H}_2\text{SO}_4$  and is equal to  $7.2 \pm 0.7$ .

From the work of Baxendale and Hughes,<sup>7</sup> we can infer that  $k_6/k_4 = k_5/k_3$ . These authors find no isotope effect in the reaction of  $\text{H}$  or  $\text{D}$  atoms with  $\text{Fe}^{\text{III}}$ . Since reactions 4 and 3 both involve the rupture of an O-H bond in the transition state, there should be little change in rate when the reactant is changed from  $\text{H}$  to  $\text{D}$ .

The ratio  $k_{(\text{OH} + \text{Fe}^{\text{II}})}/k_{(\text{OH} + \text{H}_2)}$  has been determined by Dainton and Hardwick,<sup>12</sup> Hardwick,<sup>13</sup> and by Rothchild and Allen,<sup>8</sup> and was found to be 6.7, 8.6 (for 0.1 N  $\text{HClO}_4$ ) and 5.7 (for 0.01 N  $\text{H}_2\text{SO}_4$ ), respectively. A value of 3.5 has been reported<sup>14,15</sup> for the ratio  $k_{(\text{OH} + \text{H}_2)}/k_{(\text{OH} + \text{D}_2)}$ .

(12) F. S. Dainton and T. J. Hardwick, *Trans. Faraday Soc.*, **53**, 333 (1957).

(13) T. J. Hardwick, *Can. J. Chem.*, **35**, 437 (1957).

(14) Atomic Energy of Canada, Ltd., Chalk River, Ontario, PR-CM-6-C.

(15) H. L. Friedman and A. H. Zeltmann, *J. Chem. Phys.*, **28**, 878 (1958).

Combining the isotope effect of 3.5 with the intermediate value of 6.7 we find

$$\frac{k_2}{k_{10}} = \frac{k_{(\text{OH} + \text{Fe}^{\text{II}})}}{k_{(\text{OH} + \text{D}_2)}} = 23$$

However, it is interesting to note that even if we choose  $k_2/k_{10} = 30$ , this produces only a 15% decrease in the final result for  $k_5/k_9$ .

The ratio  $k_7/k_5$  was calculated from experiments 4 and 7, in which the  $\gamma$ -ray intensity was varied by a factor of 6.8 keeping the ferrous, ferric and D<sub>2</sub> concentrations approximately constant. The stationary state H<sub>2</sub>O<sub>2</sub> concentrations at the higher intensity (expt. 4,  $I = 2 \times 10^{19}$  e.v.l.<sup>-1</sup> min.<sup>-1</sup>) was measured by following the post-irradiation increase in the ferric ion concentration and was found to be  $1.4 \pm 0.1 \mu\text{m./l.}$  by extrapolation.

If we assume no reaction between H<sub>2</sub>O<sub>2</sub> and H or D atoms, we find from equation 1,  $(\text{H}_2\text{O}_2)_{\text{ss}} = c/k_1(\text{Fe}^{\text{III}}) = 2.5 \mu\text{m./l.}$  ( $k_1 = 71$  l. moles<sup>-1</sup> sec.<sup>-1</sup>).<sup>12</sup> This indicates that about one-half of the hydrogen peroxide formed in experiment 4 is removed by reaction with H and D atoms. Since the steady-state concentrations of H and D atoms are approximately proportional to the  $\gamma$ -ray intensity, we find  $(\text{H}_2\text{O}_2)_{\text{expt. 4}}/(\text{H}_2\text{O}_2)_{\text{expt. 7}} = 3.9$ . From the observed  $G(\text{HD})$  values of experiments 4 and 7 we find by substitution into equation 5 that  $k_7/k_5 = 6.7$  and  $k_8/k_9 = 65$ . The contribution of the term,  $(k_7/k_5)[(\text{H}_2\text{O}_2)_{\text{ss}}/(\text{D}_2)]$ , to the value of  $x$  is appreciable only at low total ferrous plus ferric concentrations and is shown in Table I.

The ratio  $k_8/k_4$  will not differ by more than a factor of 2 or 3 from  $k_7/k_5$ , which is equal to  $(k_7/k_5) \cdot (k_5/k_3)$ . Hence we find that the term  $(k_8/k_4)[(\text{H}_2\text{O}_2)_{\text{ss}}/(\text{Fe}^{\text{II}})]$  is negligible compared to  $(k_6/k_4)[(\text{Fe}^{\text{III}})/(\text{Fe}^{\text{II}})]$ .

From the experimental data of Table I and the rate constant ratios in the literature, the quantities  $g(\text{H})\gamma/(G(\text{HD}) - \beta)$  and  $x$  were calculated and are given in Table I. The primary radical and molecular yields at pH 2.1 are  $g(\text{H}) = 3.3$ ,<sup>8</sup>  $g(\text{OH}) = 2.6$  (by material balance),  $g(\text{H}_2) = 0.45$  and  $g(\text{H}_2\text{O}_2) = 0.80$ . A plot of  $g(\text{H})\gamma/(G(\text{HD}) - \beta)$  vs.  $x$  was found to be linear (Fig. 3). The straight line, drawn by inspection and with an intercept of one, has a slope equal to  $k_{(\text{H} + \text{Fe}^{\text{III}})}/k_{(\text{H} + \text{D}_2)} = 120 \pm 30$ .

The rate constant for the reaction,  $\text{H} + \text{D}_2 = \text{HD} + \text{D}$ , in the gas phase<sup>9,15,16</sup> at 25° is  $0.4 \times 10^5$  l. moles<sup>-1</sup> sec.<sup>-1</sup>. Assuming that the rate constant,  $k_{(\text{H} + \text{D}_2)}$ , remains unchanged in solution, we find

$k_{(\text{H} + \text{Fe}^{\text{III}})} = (48 \pm 12) \times 10^5$  l. moles<sup>-1</sup> sec.<sup>-1</sup> at 25° for 0.01 N H<sub>2</sub>SO<sub>4</sub>. Although it is possible that the ratio  $k_{\text{soln}}/k_{\text{gas}}$  for the reaction  $\text{H} + \text{D}_2 = \text{HD} + \text{D}$  at ordinary temperatures might be as large as two to three,<sup>17</sup> the assumption which we have made seems reasonable, since it has been found<sup>18</sup> that the conversion of para to orthohydrogen takes place 1.2 times as fast in aqueous solution as in the gas phase when catalyzed by oxygen. The corresponding figure for nitric oxide, a polar molecule which is probably more strongly solvated, is 2.2. This provides evidence that the collision numbers in the two phases are in the same ratio.

TABLE II  
APPROXIMATE RATE CONSTANTS FOR R + H AT 25°

| R                                 | $k \times 10^{-5}$<br>l. moles <sup>-1</sup><br>sec. <sup>-1</sup> | pH                                    |
|-----------------------------------|--------------------------------------------------------------------|---------------------------------------|
| D <sub>2</sub>                    | 4                                                                  | Gas                                   |
| Fe <sup>III</sup>                 | 48                                                                 | 2.1 (H <sub>2</sub> SO <sub>4</sub> ) |
| Fe <sup>II</sup>                  | 3.7                                                                | 2.1 (H <sub>2</sub> SO <sub>4</sub> ) |
| O <sub>2</sub>                    | 1000                                                               | ...                                   |
| HCOOH                             | 1                                                                  | 3 and 1                               |
| CH <sub>3</sub> COOH              | 1.9 <sup>c</sup>                                                   | 1 (H <sub>2</sub> SO <sub>4</sub> )   |
| CH <sub>3</sub> COCH <sub>3</sub> | 3.5 <sup>c</sup>                                                   | 1 (H <sub>2</sub> SO <sub>4</sub> )   |
| CH <sub>3</sub> OH                | 23 <sup>c</sup>                                                    | 1 (H <sub>2</sub> SO <sub>4</sub> )   |
| HCHO                              | 9 <sup>c</sup>                                                     | 1 (H <sub>2</sub> SO <sub>4</sub> )   |
| DCO <sub>2</sub> H <sup>a</sup>   | 13 <sup>c</sup>                                                    | 1 (H <sub>2</sub> SO <sub>4</sub> )   |
| EtOH                              | 27 <sup>c</sup>                                                    | 1 (H <sub>2</sub> SO <sub>4</sub> )   |
| Cu <sup>2+</sup> <sup>b</sup>     | 106 <sup>c</sup>                                                   | 1 (H <sub>2</sub> SO <sub>4</sub> )   |
| Benzoquinone                      | 5700 <sup>c</sup>                                                  | 1 (H <sub>2</sub> SO <sub>4</sub> )   |

<sup>a</sup> For D abstraction. <sup>b</sup> For  $\text{Cu}^{2+} + \text{H} = \text{Cu}^+ + \text{H}^+$ .  
<sup>c</sup> From the data of Baxendale and Smithies, reference 5.

A list of approximate rate constants for the reactions of some inorganic and organic compounds with H atoms is given in Table II. Rothchild and Allen<sup>8</sup> have found that the ratio  $k_{(\text{H} + \text{O}_2)}/k_{(\text{H} + \text{Fe}^{\text{III}})}$  in 0.01 N H<sub>2</sub>SO<sub>4</sub> is equal to  $208 \pm 40$ . Therefore, it follows that the rate constant  $k_{(\text{H} + \text{O}_2)} = (10 \pm 3) \times 10^8$  l. moles<sup>-1</sup> sec.<sup>-1</sup>. From Hart's<sup>19</sup> value for the ratio  $k_{(\text{H} + \text{O}_2)}/k_{(\text{H} + \text{HCOOH})} = 540 \pm 80$ , we find  $k_{\text{H} + \text{HCOOH}} = (19 \pm 6) \times 10^5$  l. moles<sup>-1</sup> sec.<sup>-1</sup> at pH 3 and 25°.

This value of  $k_{(\text{H} + \text{HCOOH})}$  was used to calculate several of the rate constants of Table II from the data of Baxendale and Smithies,<sup>5</sup> who have measured the rates of a number of H atom reactions relative to the rate of the reaction  $\text{H} + \text{HCOOH} = \text{H}_2 + \text{COOH}$  at pH 1.

(17) R. P. Bell, *Ann. Rep. Chem. Soc.*, **36**, 82 (1939).

(18) L. Farkas and U. Garbatski, *Trans. Faraday Soc.*, **35**, 263 (1939).

(19) E. J. Hart, *J. Am. Chem. Soc.*, **76**, 4312 (1954).

(16) J. Hirschfelder, H. Eyring and B. Topley, *J. Chem. Phys.*, **4**, 170 (1936).

## THE ACTION OF $^{60}\text{Co}$ $\gamma$ -RADIATION ON AQUEOUS SOLUTIONS OF ACETYLENE

By P. G. CLAY, G. R. A. JOHNSON AND J. WEISS

*Department of Chemistry, King's College, University of Durham, Newcastle on Tyne, England*

*Received February 9, 1959*

$^{60}\text{Co}$   $\gamma$ -irradiation of water saturated with acetylene (1 atm.) in the absence of oxygen, yielded  $\text{C}_1$ ,  $\text{C}_2$  and  $\text{C}_4$ -aldehydes and a white solid polymer. The irradiated solution showed a very strong, broad absorption band with a maximum at about 200  $\text{m}\mu$ . Aqueous solutions of acetylene-oxygen mixtures, on irradiation, yielded glyoxal and hydrogen peroxide, with small amounts of an organic hydroperoxide ( $G \sim 0.3$ ). The formation of the radiation products has been studied at different ratios of oxygen/acetylene, as a function of pH and in the presence of added ferrous sulfate. Under certain conditions, glyoxal is apparently formed by a chain reaction.

### Introduction

Much work has been done on the radiation chemistry of acetylene, in the gas phase, notably by Lind and his co-workers.<sup>1</sup> In the absence of oxygen, using various radiations, a yellow solid polymer was formed and some aromatic compounds also were produced. In the case of acetylene irradiated with  $\alpha$ -particles, benzene accounted for about 15% of the products.<sup>2</sup> In the presence of oxygen, gas phase irradiation of acetylene resulted in the formation of carbon dioxide, carbon monoxide and a liquid polymer.<sup>3</sup>

We have studied the action of  $^{60}\text{Co}$   $\gamma$ -rays on acetylene in aqueous solutions as part of a program investigating the radiation chemistry of aqueous solutions of simple unsaturated compounds.

### Experimental

**Preparation of Solutions.**—Ordinary distilled water was redistilled from alkaline potassium permanganate and then from dilute sulfuric acid. The pH of this water was about 5.5, solutions of lower pH were obtained by adding sulfuric acid and higher values by the addition of sodium hydroxide.

Acetylene was used from a cylinder (British Oxygen Co. Ltd.), after washing with 10% sodium bisulfite solution followed by 20% sodium hydroxide solution. After this treatment no acetone could be detected in the solutions prepared for radiation. Oxygen (British Oxygen Co. Ltd., medical grade) was used directly from the cylinder.

The solutions were prepared and irradiated in cylindrical Pyrex vessels equipped with a side arm and tap. The vessels were deaerated by repeated pumping with a two stage oil pump and shaking. The appropriate gas mixtures were prepared in a gas buret of conventional design and were admitted to the vessel by the side arm. The vessel and its contents was shaken in contact with the gas to bring about saturation of the solution. For the experiments in the absence of oxygen the acetylene was condensed out in a trap cooled by liquid nitrogen and freed from any non-condensable gases by repeated melting and pumping. The vessel and side arm, previously evacuated, were opened to the container holding the solid acetylene and the latter allowed to warm up. The vessel was agitated during the time when the acetylene pressure was building up in the apparatus and for some time after atmospheric pressure was reached.

**Irradiation Arrangements.**—The samples were irradiated with  $^{60}\text{Co}$   $\gamma$ -rays from a 500 Curie source of the type described by Hochanadel and Ghormley.<sup>4</sup> The dose rate, measured by the ferrous sulfate dosimeter ( $10^{-3} M$  ferrous sulfate in 0.1  $N$  sulfuric acid) was  $0.86 \times 10^{-7}$  (e.v./ $N$ )  $\text{ml.}^{-1}$  based on  $G_{\text{Fe}^{3+}} = 15.5$ .

**Identification and Determination of Products.**—(i) Hydrogen peroxide was identified and determined by the titanium sulfate reagent.<sup>5</sup> Since the products of irradiation, in the absence of oxygen, absorbed strongly at 405  $\text{m}\mu$ , hydrogen peroxide formed under these conditions was measured by the ferrous thiocyanate method. (ii) Organic hydroperoxides, under normal conditions, do not react with the titanium sulfate reagent but oxidize iodide<sup>6</sup> and react with ferrous thiocyanate.<sup>7</sup> Determination of the total peroxide in the irradiated solutions showed the presence of an organic hydroperoxide. As its yield was rather low ( $G \sim 0.3$ ) the identity of this hydroperoxide has not yet been established. (iii) Formaldehyde and acetaldehyde were identified by paper chromatography of their 2,4-dinitrophenylhydrazones according to the method of Gasparic and Vecera.<sup>8</sup> Crotonaldehyde was identified on the chromatogram by its 2,4-dinitrophenylhydrazone. Further evidence was provided by elution of the 2,4-dinitrophenylhydrazone spot with alcohol and the spectra of the eluted spot in the neutral and alkaline alcoholic solution were compared with those of an authentic sample of crotonaldehyde 2,4-dinitrophenylhydrazone and shown to be identical. The aldehydes were determined by the method of Johnson and Scholes.<sup>9</sup> (iv) Glyoxal and glycolaldehyde were identified by the purple-blue color of their 2,4-dinitrophenylhydrazones in strongly alkaline solution. The irradiated solution was treated with the dinitrophenylhydrazine reagent and the resulting red ppt. filtered off, dried and dissolved in benzene, addition of ethanolic sodium hydroxide produced the characteristic purple-blue color indicating the presence of either glyoxal or glycolaldehyde. The method of Dechary, *et al.*,<sup>10</sup> was used to distinguish between these two compounds and to estimate them. The method depends on the formation of a blue colored derivative when solutions of glyoxal or glycolaldehyde are treated with the 2,3-diaminophenazine reagent. Glyoxal reacts with the reagent in acetic acid solution; glycolaldehyde reacts only under conditions where conversion into glyoxal can occur, *i.e.*, in 10  $N$  sulfuric acid. (v) Oxygen was determined by the Winkler method<sup>11</sup> in the following way: solutions of acetylene and oxygen were made up exactly as for irradiation, the side arm was removed and 15 ml. of petroleum ether placed on the top of the solution. One ml. of saturated  $\text{MnCl}_2$  solution was added below the surface of the pet. ether and the flask gently shaken until the solutions were mixed. One ml. of solution of 33%  $\text{NaOH}$  and 10%  $\text{KI}$  was added and shaken in a similar fashion and the ppt. formed was allowed to settle for 2 minutes when 5 ml. of concd.  $\text{HCl}$  was added. The liberated iodine was titrated against thiosulfate.

### Results

**Irradiations in the Absence of Oxygen.**—Irradiation of water saturated with acetylene (1 atm.)

(1) Cf. S. C. Lind, "The Chemical Effects of Alpha Particles and Electrons," 2nd edition, The Chemical Catalog Co., New York, N. Y., 1928.

(2) C. Rosenblum, *THIS JOURNAL*, **52**, 474 (1948).

(3) S. C. Lind, D. C. Bardwell and J. H. Perry, *J. Am. Chem. Soc.*, **48**, 1556 (1926).

(4) C. J. Hochanadel and J. A. Ghormley, *Rev. Sci. Instr.*, **22**, 273 (1951).

(5) G. M. Eisenberg, *Ind. Eng. Chem., Anal. Ed.*, **15**, 327 (1943).

(6) C. J. Hochanadel, *THIS JOURNAL*, **56**, 597 (1952).

(7) A. C. Egerton, A. J. Everett, G. J. Minkoff, S. Rudrakanchana and K. C. Salooja, *Anal. Chim. Acta*, **10**, 422 (1954).

(8) J. Gasparic and M. Vecera, *Coll. Czech. Chem. Commun.*, **22**, 1426 (1957).

(9) G. R. A. Johnson and G. Scholes, *Analyst*, **77**, 937 (1954).

(10) J. M. Dechary, E. Kun and H. C. Pitot, *Anal. Chem.*, **26**, 449 (1954).

(11) Cf. W. W. Scott, "Standard Methods of Chemical Analysis," London, 1926, p. 1436.

at pH 1.2 yielded a yellow-white solid polymer and several different aldehydes. The irradiated solution exhibited a broad absorption band with a maximum at 200 m $\mu$ . Chromatography of the 2,4-dinitrophenylhydrazones of the aldehydes produced in the irradiation, showed the presence of some formaldehyde and larger quantities of acetaldehyde and crotonaldehyde. Examination of the absorption spectrum of aqueous crotonaldehyde ( $10^{-4}$  M) showed a sharp absorption maximum at 210 m $\mu$ , indicating that crotonaldehyde was not entirely responsible for the absorption of the irradiated solution. An additional dinitrophenylhydrazone derivative of a higher  $R_f$  was present on the chromatogram but this has not yet been identified. Glycolaldehyde also was formed as an irradiation product, but the observed yields were rather irreproducible. Quantitative studies showed the yields of the measured products, other than that of glycolaldehyde, to be linear with dose up to the highest doses used, *viz.*,  $4.9 \times 10^{-6}$  (e.v./N) ml.<sup>-1</sup>. The yields were ( $G$  = molecules/100 e.v.):  $G(\text{acetaldehyde}) = 0.2$ ;  $G(\text{crotonaldehyde}) = 0.2$ ;  $G(\text{hydrogen peroxide}) = 0.5$ . The  $G(\text{glycolaldehyde})$  was of the same order as those of the other two aldehydes although somewhat irreproducible.

**Irradiations in the Presence of Oxygen.**—Glyoxal and hydrogen peroxide were the main products formed in the irradiation of aqueous solutions saturated with acetylene-oxygen mixtures (1 atm.). Small amounts of an unidentified hydroperoxide were also formed. No aldehydes other than glyoxal could be detected.

Preliminary quantitative experiments using a gas mixture of acetylene/oxygen (1:1, total press. 1 atm.) showed that the formation of glyoxal was markedly dependent on the pH of the solution; for the range of pH 1.2 to 9, the yields of the products were also determined as a function of the radiation dose. Figures 1 and 2 show typical dose-yield plots, for pH 1.2 and 5.5, respectively. At all the pH values studied the yield-dose curves were initially linear, but eventually showed a marked diminution in the yield per unit dose, presumably attributable to the consumption of molecular oxygen in the radiation-induced reactions. In the case of solutions irradiated at pH 1.2, it was noted that the change of slope of the dose-yield curve occurred at a lower total dose for the glyoxal than for the hydrogen peroxide. At pH 5.5, however, the changes in slope of the glyoxal and hydrogen peroxide dose-yield plots occurred at about the same total dose.

A plot of the initial  $G$ -values of the products against pH is shown in Fig. 3:  $G(\text{glyoxal})$  decreased smoothly from  $G = 14$  at pH 1.2 to  $G = 7$  at pH 9. Between pH 1.2 and pH 9, the  $G(\text{H}_2\text{O}_2)$  was found to be independent of pH. Above pH 9, the results were somewhat irreproducible, with mean values of  $G(\text{glyoxal}) \sim 1$ ,  $G(\text{formaldehyde}) \sim 1.5$ .

The shape of the dose-yield plot in acid solution suggested that  $G(\text{glyoxal})$  was dependent upon the ratio of acetylene/oxygen in the solution. To investigate this point further, solutions of gas mixtures containing different proportions of oxygen

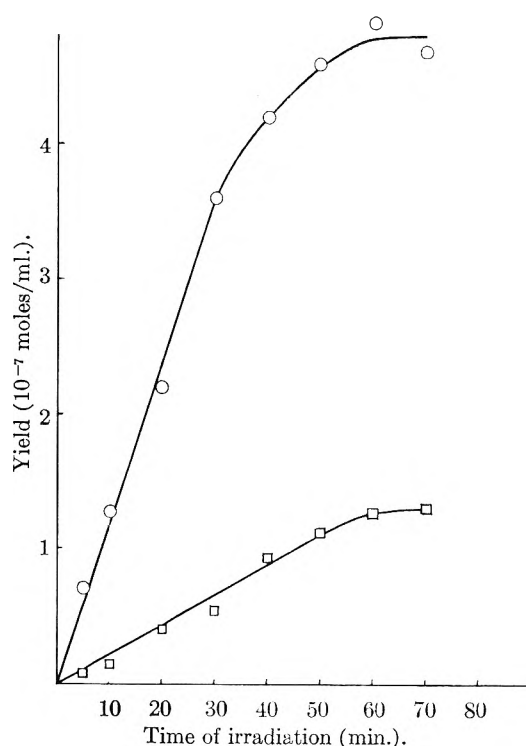


Fig. 1.—Irradiation of aqueous solutions of acetylene-oxygen mixtures (1:1) with  $^{60}\text{Co}$   $\gamma$ -rays at pH 1.2; dose rate =  $0.86 \times 10^{-7}$  (e.v./N) ml.<sup>-1</sup> min.<sup>-1</sup>. Yield dose dependence for the formation of glyoxal and hydrogen peroxide: O, glyoxal; □, hydrogen peroxide.

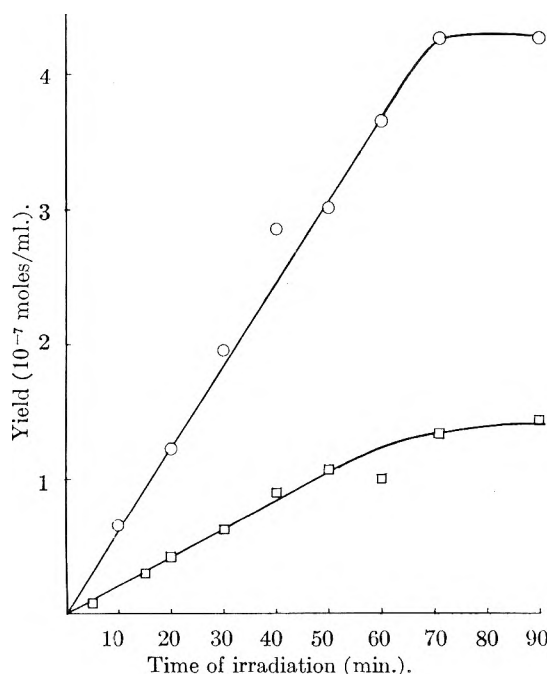


Fig. 2.—Irradiation of aqueous solutions of acetylene-oxygen mixtures (1:1) with  $^{60}\text{Co}$   $\gamma$ -rays at pH 5.5; dose rate =  $0.86 \times 10^{-7}$  (e.v./N) ml.<sup>-1</sup> min.<sup>-1</sup>. Yield dose dependence for the formation of glyoxal and hydrogen peroxide at pH 5.5: O, glyoxal; □, hydrogen peroxide.

and acetylene were irradiated at pH 1.2. The total pressure in the vessels was kept constant at 1 atm., by the addition of the appropriate amounts of nitrogen. Figure 4 shows the dependence of the initial  $G$ -values (each obtained from an appropriate



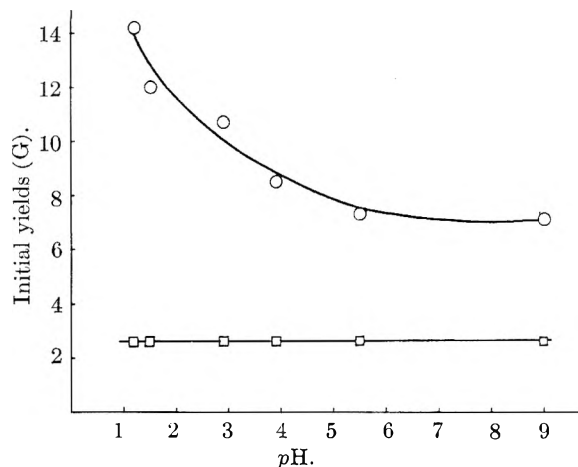


Fig. 3.—Irradiation of aqueous solutions of acetylene-oxygen mixtures (1:1) with  $^{60}\text{Co}$   $\gamma$ -rays; dose rate =  $0.86 \times 10^{-7}$  (e.v./N) ml. $^{-1}$  min. $^{-1}$ . pH dependence of the initial yields: O, glyoxal;  $\square$ , hydrogen peroxide.

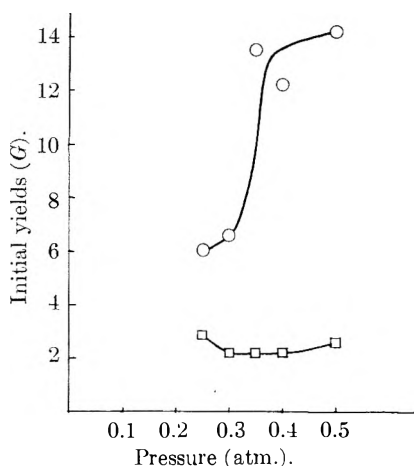


Fig. 4.—Irradiation of aqueous solutions of acetylene-oxygen mixtures (1:1) with  $^{60}\text{Co}$   $\gamma$ -rays at pH 1.2; dose rate =  $0.86 \times 10^{-7}$  (e.v./N) ml. $^{-1}$  min. $^{-1}$ . Dependence of the initial yields on the total pressure of acetylene and oxygen: O, glyoxal;  $\square$ , hydrogen peroxide.

dose-yield plot) on the *total* pressure of acetylene/oxygen mixtures, when the partial pressures of both gases were the same. It is seen that  $G$ (glyoxal) is dependent upon the solute concentration. On the other hand,  $G(\text{H}_2\text{O}_2)$  was found to change very little in the range of solute concentrations studied.

In a further series of experiments, the partial pressure of the acetylene was kept constant at 0.25 atm. the pressure of oxygen being varied from 0.25 to 0.75 atm. In each case the total pressure of the gas mixture was adjusted to 1 atm. by the addition of nitrogen. The variation of the initial  $G$ -values is shown in Fig. 5. Hydrogen peroxide formation appeared to be independent of the oxygen/acetylene ratio. On the other hand, the glyoxal formation showed a marked dependence on the partial pressure of the oxygen.

Figure 6 shows the variation of the initial  $G$ (glyoxal) and  $G(\text{H}_2\text{O}_2)$  when, at a partial pressure of oxygen of 0.25 atm., the pressure of acetylene was changed from 0.25 to 0.75 atm. As before, the total pressure was always adjusted to 1 atm. with

nitrogen.  $G(\text{H}_2\text{O}_2)$  was found to be independent of the partial pressure of acetylene between 0.25 and about 0.6 atm., beyond which it dropped off somewhat.  $G$ (glyoxal) depended markedly on the partial pressure of the acetylene in the gas mixture. At low pressures,  $G$ (glyoxal) = 6, but when the partial pressure of acetylene exceeded 0.5 atm., the yield of glyoxal increased rapidly. At higher acetylene pressures  $G$ (glyoxal) decreased corresponding to the decrease of hydrogen peroxide.

Some experiments were carried out in the presence of added ferrous sulfate; the results are shown in Table I, which gives the initial  $G$ -values for the products and for the oxidation of ferrous to ferric, at two different acetylene-oxygen concentrations. These concentrations were chosen to correspond to conditions where, in the absence of ferrous salt, in the one case, the yield of glyoxal was high ( $G = 14.2$ ) and in the other case it was low ( $G = 6$ ).

TABLE I

EFFECT OF ADDED FERROUS SULFATE ON THE INITIAL YIELDS IN THE IRRADIATION OF AQUEOUS SOLUTIONS OF ACETYLENE-OXYGEN MIXTURES WITH  $^{60}\text{Co}$   $\gamma$ -RAYS

(dose rate =  $0.75 \times 10^{-7}$  (e.v./N) ml. $^{-1}$  min. $^{-1}$ ) at pH 1.2

[ $\text{Fe}^{2+}$ ], moles/l.  $G$ (glyoxal)  $G$ (formaldehyde)  $G$ (glycolaldehyde)  $G(\text{Fe}^{3+})$   
Saturating gas mixture: oxygen:acetylene = 1:1 (total pressure 1 atm.)

|           |      |     |     |    |
|-----------|------|-----|-----|----|
| 0         | 14.2 | 0   | 0   | .. |
| $10^{-3}$ | 50   | 2.0 | 2.0 | 50 |
| $10^{-2}$ | 12.5 | 1.7 | 3.0 | 22 |

Saturating gas mixture: oxygen:acetylene:nitrogen = 2.5:3.5:5.4 (total pressure 1 atm.)

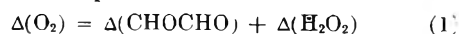
|           |    |     |   |    |
|-----------|----|-----|---|----|
| 0         | 6  | 0   | 0 | .. |
| $10^{-3}$ | 11 | 3.3 | 0 | 30 |
| $10^{-2}$ | 8  | 3.3 | 0 | 30 |

Irradiation of solutions of acetylene/oxygen (1:1) in the presence of ferric sulfate ( $4 \times 10^{-4}$  M) gave  $G$ (glyoxal) = 13.0, a value close to that ( $G = 14$ ) found in the absence of ferric ion. This indicates that the ferric ions formed in the irradiation in the presence of ferrous sulfate, do not play an important part in this reaction.

### Discussion

With a solute of relatively simple structure such as acetylene, it might be expected that its chemical behavior would be comparatively straightforward and amenable to interpretation on the basis of present concepts in the radiation chemistry of aqueous solutions. In actual fact, however, this study has revealed a rather complex picture and it is not possible as yet to give a complete mechanism capable of explaining all the experimental results.

An interesting feature of the acetylene-oxygen system is the finding that only one major oxidation product is formed. A qualitative investigation failed to reveal the presence of other possible oxidation products. This finding is further confirmed by the observation that after taking into account any oxygen derived from the water, the oxygen consumed is that expected from the stoichiometric relationship



For instance, in a particular experiment, the

measured concentration of oxygen in solutions saturated with acetylene/oxygen (1:1, 1 atm.) at pH 1.2 was  $5.2 \times 10^{-7}$  mole/ml., whereas the uptake of molecular oxygen calculated from the yields of glyoxal and hydrogen peroxide at the break point was found to be  $4.96 \times 10^{-7}$  mole/ml.

No previous studies of the radiation-induced oxidation of acetylenic compounds in aqueous solution have been made but, in the cases of other unsaturated solutes, (e.g., ethylene,<sup>12</sup> benzene<sup>13</sup>) a number of different oxidation products were found.

The acetylene-oxygen system is somewhat unusual also, in that the yield of the oxidation product is relatively high showing  $G$ -values of 6 to 15. The yield is very much influenced by both the acetylene and the oxygen concentrations in the concentration range which was studied; acetylene was varied from  $0.8 \times 10^{-2}$  to  $2.4 \times 10^{-2}$   $M$ ; oxygen from  $2.6 \times 10^{-4}$  to  $7.8 \times 10^{-4}$   $M$ , a very sharp increase resulting as the concentrations are increased (Fig. 4).

The  $G$ -values for the formation of free radical and molecular products from the radiolysis of water according to<sup>14,15</sup>

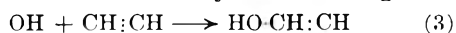


may be taken as

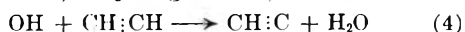
$G_{\text{H}}^{\bullet} = 3.65$ ,  $G_{\text{OH}}^{\bullet} = 2.85$ ,  $G_{\text{H}_2\text{O}_2} = 0.80$ ,  $G_{\text{H}_2} = 0.40$ , where  $G^{\bullet}$  refers to the yield in molecules per 100 e.v. of radiation energy absorbed by the water.<sup>16</sup>

The relatively high  $G$ -values found for the formation of glyoxal show, therefore, that more than one molecule of glyoxal is formed for each radical produced by the radiation. The occurrence of a short chain-reaction leading to glyoxal formation is suggested also by the marked dependence of yield on the solute concentrations.

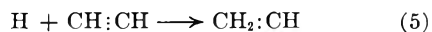
The most likely initiation reaction involves addition of an OH radical to acetylene according to



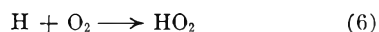
the alternative, dehydrogenation, reaction



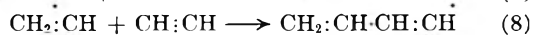
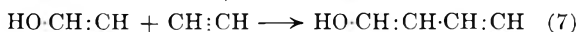
is less probable on energetic grounds and would not explain the observed formation of glyoxal. Addition of hydrogen atoms to acetylene according to



may also occur, but, in the presence of oxygen, will be in competition with the reaction



Subsequent reactions of the free-radicals formed in reactions 3 and 5 with acetylene and with oxygen must be considered, *viz.*



(12) P. G. Clay, G. R. A. Johnson and J. Weiss, *J. Chem. Soc.*, 2175 (1958).

(13) M. Daniels, G. Scholes and J. Weiss, *ibid.*, 832 (1956).

(14) J. Weiss, *Nature*, **163**, 748 (1944).

(15) A. O. Allen, C. J. Hochanadel, J. A. Ghormley and T. W. Davis, *THIS JOURNAL*, **56**, 575 (1952).

(16) Cf. G. R. A. Johnson and J. Weiss, *Proc. Roy. Soc. (London)*, **A240**, 189 (1957).

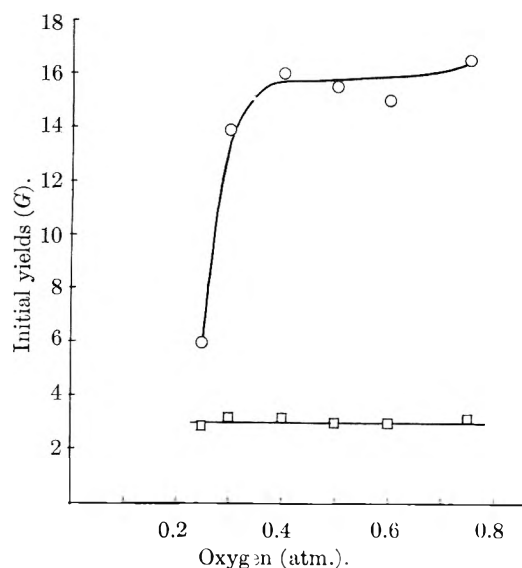


Fig. 5.—Irradiation of aqueous solutions of acetylene-oxygen mixtures with  $^{60}\text{Co}$   $\gamma$ -rays at pH 1.2; dose rate =  $0.86 \times 10^{-7}$  (e.v./N) ml.<sup>-1</sup> min.<sup>-1</sup> Dependence of the initial yields on the partial pressure of oxygen; acetylene pressure = 0.25 atm.: O, glyoxal; □, hydrogen peroxide.

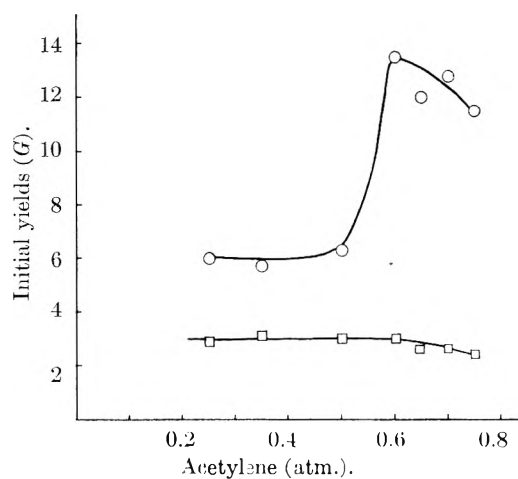
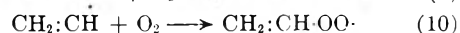


Fig. 6.—Irradiation of aqueous solutions of acetylene-oxygen mixtures with  $^{60}\text{Co}$   $\gamma$ -rays at pH 1.2; dose rate =  $0.86 \times 10^{-7}$  (e.v./N) ml.<sup>-1</sup> min.<sup>-1</sup> Dependence of the initial yields on the partial pressure of acetylene; oxygen pressure = 0.25 atm.: O, glyoxal; □, hydrogen peroxide.

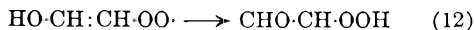


In the case of irradiations carried out in the absence of dissolved oxygen, the polymeric product and the product which absorbs in the region of 200  $m\mu$  (probably a conjugated polyenic compound) may be the end result of reactions 7 and 8. The apparent absence of such products in the presence of oxygen suggests that reactions of the radicals with oxygen, *viz.*, reactions 9 and 10 are more rapid than the reactions with acetylene.

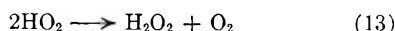
It is not easy to find a chain propagation reaction which would account adequately for all the results obtained, particularly since nothing is known about the reactions of radicals such as the peroxy radical formed in reaction 9. A simple propagation step which would lead to glyoxal is



This type of OH elimination reaction has been shown to occur in the mercury photo-sensitized chain-oxidation of certain hydrocarbons in the gas phase.<sup>17</sup> In these reactions the pre-exponential factor is usually low, because of the molecular rearrangement which must occur prior to OH elimination and it is difficult to predict whether the type of rearrangement, *viz.*



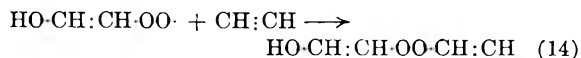
would occur with any facility in the case of the peroxy radical formed in solution. Reaction 11 together with the termination reactions involving interaction of the OH radicals with themselves and with HO<sub>2</sub> radicals could account for the dependence of *G*(glyoxal) on acetylene concentration and, together with the reaction



would be consistent with the observed *G*(H<sub>2</sub>O<sub>2</sub>). The results obtained in the presence of added ferrous salt, however, suggest that acetylene is at least as reactive as Fe<sup>2+</sup> toward OH radicals, which means that radical-radical termination reactions involving OH radicals are unlikely in the presence of acetylene, so that the chains would probably be much longer than those observed if reaction 11 were the propagation step. Chain termination could, of course, also occur by the interaction of two RO<sub>2</sub> radicals.

The dependence on oxygen concentration implies that reactions such as (9) and (10) are in competition with the propagation reactions. As pointed out above, however, a search for possible specific end-products of these reactions has so far been unsuccessful.

An alternative mode of glyoxal formation might involve addition of the peroxy radical formed in reactions 9 or 10, to acetylene, leading to a polyperoxide radical, in some respects similar to the polymeric organic peroxide observed by Staudinger<sup>18</sup> (*cf.* also Mayo<sup>19</sup> and Hargrave and Morris<sup>20</sup>)



(17) R. H. Burgess and J. C. Robb, *Trans. Faraday Soc.*, **54**, 1015 (1958).

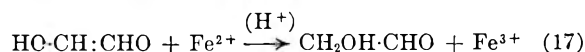
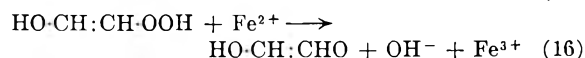
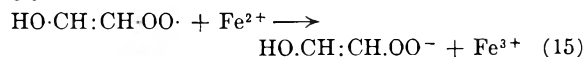
(18) H. Staudinger, *Ber.*, **58**, 1075 (1925).

(19) F. R. Mayo, *J. Am. Chem. Soc.*, **80**, 2465 (1958).

(20) F. R. Hargrave and A. L. Morris, *Trans. Faraday Soc.*, **54**, 1015 (1958).

Glyoxal formation could then result from a breaking up of the polymeric peroxide, with chain breaking between two RO<sub>2</sub>-type radicals. However, such a scheme must be merely speculative at present, since little is known about the reactions of such intermediates.

The experiments in the presence of ferrous salt were carried out in an endeavor to obtain more information about the oxidation reaction. Reaction of the ferrous ion with the peroxy-radical formed in reaction 9 might be expected to lead to glycolaldehyde

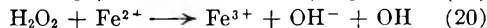
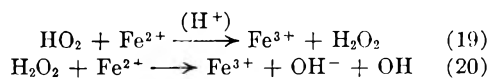


In fact, glycolaldehyde was formed under these conditions (Table I). Moreover, the yields of glyoxal were markedly influenced by the presence of Fe<sup>2+</sup>, at sufficiently high oxygen-acetylene concentrations values as high as *G*(glyoxal) = 50 were observed when the ferrous concentration was 10<sup>-3</sup> *M*. At higher Fe<sup>2+</sup> concentrations lower yields were found, possibly due to the competition of



with reaction 3.

The results with added Fe<sup>2+</sup> do not help greatly to elucidate the mechanism of glyoxal formation but do suggest that reaction 11 is not the propagation step; this reaction, together with the reactions



leading to further OH production could account for relatively high yields of glyoxal being produced in the presence of Fe<sup>2+</sup>, but would not explain the very high yield of the simultaneously produced ferric, which amounts to *G*(Fe<sup>3+</sup>) = 50, since, on the basis of reactions 11, 19 and 20, the ferric yield could not exceed (*G*<sub>OH</sub> + 3*G*<sub>HO<sub>2</sub></sub> + 2*G*<sub>H<sub>2</sub>O<sub>2</sub></sub>) = 15.5.

We wish to thank the United Kingdom Atomic Energy Authority Research Group, Harwell, for support and for permission to publish this paper, and the Rockefeller Foundation for financial support.

# $\alpha$ -RAY OXIDATION OF FERROUS SULFATE IN 0.4 M SULFURIC ACID SOLUTIONS. THE EFFECT OF 0 TO 0.4 M OXYGEN<sup>1</sup>

BY CONRAD N. TRUMBORE<sup>2</sup> AND EDWIN J. HART

Contribution from the Chemistry Division, Argonne National Laboratory, Lemont, Illinois, and the Department of Chemistry, University of Rochester, Rochester, N. Y.

Received February 9, 1959

$G(\text{Fe}^{+++})$  has been measured as a function of dissolved oxygen concentration in ferrous sulfate solutions in 0.4 M sulfuric acid irradiated by the 5.3 Mev.  $\alpha$ -particles of dissolved polonium-210. Studies on product yields with identical solutions containing no dissolved ferrous sulfate have been obtained and are used to explain the ferric ion yields. Both  $G(\text{H}_2\text{O}_2)$  and  $G(\text{Fe}^{+++})$  increase with increasing oxygen concentration, reaching yields of 1.9 and 9.8, respectively, at an oxygen concentration of 0.4 M. These results have been treated by diffusion theory. On the assumption that the radical-radical rate constant is  $1.0 \times 10^{-11}$  cc. molecule<sup>-1</sup> sec.<sup>-1</sup>, a rate constant is derived for  $k_{(\text{H} + \text{O}_2)}$  of  $2.5 \times 10^{-12}$  cc. molecule<sup>-1</sup> sec.<sup>-1</sup>. Information is deduced regarding the relative rate constants for the reactions:  $\text{H} + \text{O}_2 = \text{HO}_2$ ,  $k_1$ ;  $\text{H} + \text{H} = \text{H}_2$ ,  $k_2$  and  $\text{HO}_2 + \text{HO}_2 = \text{H}_2\text{O}_2 + \text{O}_2$ ,  $k_3$ ;  $k_2 k_1 \sim k_2 \gg k_3$ .

Theoretical studies on the radiation chemistry of water indicate that the molecular products, hydrogen and hydrogen peroxide, are formed by the recombination of hydrogen atoms and hydroxyl radicals in the track. Flanders and Fricke<sup>3</sup> have treated the general cases of spherical and cylindrical diffusion and radical recombination for a one radical model. Our present work on  $G(\text{Fe}^{+++})$  and  $G(\text{H}_2\text{O}_2)$  for polonium  $\alpha$ -particles was designed to provide a test of cylindrical diffusion theory.

Molecular oxygen is an efficient hydrogen atom scavenger in aqueous solutions and it is particularly effective in promoting oxidation in the Fricke dosimeter (ferrous sulfate in 0.4 M sulfuric acid). For this reason, the increase in  $G(\text{Fe}^{+++})$  provides a measure of the effectiveness of oxygen in scavenging hydrogen atoms.

$G(\text{Fe}^{+++})$  increases with increasing dissolved oxygen concentrations from zero up to the highest oxygen concentrations obtainable in this investigation, about 0.4 M (680 atm.  $\text{O}_2$ ). In addition, a study of the hydrogen, hydrogen peroxide and oxygen yields was made on several 0.4 M  $\text{H}_2\text{SO}_4$  solutions with and without ferrous sulfate added. Hydrogen peroxide measurements also were made on ferrous-free solutions at high oxygen concentrations.

The correlation of experimental results with cylindrical diffusion theory of a one radical model is remarkably good considering the crude nature of the model.

## Experimental

**Materials.**—Baker and Adamson special reagent grade ferrous sulfate, Mallinckrodt analytical reagent grade sodium chloride and du Pont reagent grade concentrated sulfuric acid were used without further purification for ferrous sulfate solutions. Triply distilled water whose purification has been described elsewhere was used for all solutions.<sup>4</sup> Oxygen gas designated "99.5% pure and dry, U.S.P." was obtained from Liquid Carbonic Corporation and was used without further treatment. About 60 millicuries of polonium-210 was obtained from Mound Laboratory as a solid chloride deposit in a 5-ml. volumetric flask. The stock solution of polonium was prepared and stored in this flask. Deuterium gas was obtained from Stuart Oxygen Company and was greater than 99.5% isotopic purity.

(1) Based on work performed under the auspices of the U. S. Atomic Energy Commission. Support for part of this research was obtained from Atomic Energy Commission contract AT(30-1)-2263, granted to the University of Rochester.

(2) Department of Chemistry, University of Rochester.

(3) D. A. Flanders and H. Fricke, *J. Chem. Phys.*, **28**, 1126 (1958).

(4) H. Fricke, E. J. Hart and H. P. Smith, *ibid.*, **6**, 229 (1938).

**Preparation of Solutions.**—One ml. of concentrated sulfuric acid was added to the dry polonium chloride deposit and refluxed for 10–15 hours at 130–150° to provide a stock solution. Less drastic treatment than this extended digestion resulted in a colloidal suspension. Solution of the polonium was checked by assaying for polonium  $\alpha$ -activity, then centrifuging an aliquot of this solution in a Vaseline coated tube and reassaying.

For irradiation runs, an aliquot of the stock solution was diluted with water and ferrous sulfate in such a manner that the resulting solution contained 0.003 M ferrous sulfate, 0.001 M sodium chloride and 0.4 M sulfuric acid. The diluted solution was then bubbled with filtered air for about 30 minutes to remove all gaseous decomposition products of the self-irradiation of the concentrated polonium-sulfuric acid solutions.

**$G(\text{Fe}^{+++})$  Determinations.**— $G(\text{Fe}^{+++})$  was obtained by the following procedure for aerated solutions: a 3-ml. portion of the above reaction solution was transferred to a stoppered 1 cm. silica absorption cell and the optical density of the contents was read as a function of time in a Beckman DU spectrophotometer. At 3020 Å. and at 25°, the molar extinction coefficient,  $\epsilon(\text{Fe}^{+++})$ , is 2220. In all cases the increase in optical density was linear with dose up to 50% ferrous ion oxidation. These dosage curves were made during each run in order to check the reproducibility of experimental conditions from run to run and to provide a standard deviation for  $G(\text{Fe}^{+++})$  for air saturated solutions.

For oxygen concentrations less than  $2.2 \times 10^{-4}$  M (air saturated solutions), a calibrated hemispherical Pyrex cell was equipped with a 1 cm. silica absorption cell, a stopcock and ground glass joint, a detachable calibrated bulb and a magnetic stirring device. Polonium solution was introduced into the cell which was then sealed and evacuated. A known pressure of oxygen was added to the system by expanding oxygen of known pressure from the small bulb into the reaction cell. It was possible to invert the cell so that the optical density of the solution could be followed spectrophotometrically as a function of time. The ratio of gas to liquid volume in the cell was high to avoid serious depletion of oxygen and the solutions were stirred frequently to assure equilibrium with the oxygen in the gas phase.

For oxygen concentrations greater than atmospheric pressure saturated solutions ( $1.1 \times 10^{-3}$  M  $\text{O}_2$ ), a stainless steel high pressure bomb was used. The bomb, obtained from the American Instrument Company had an i.d. of 1 $\frac{5}{16}$ "', an o.d. of 2 $\frac{9}{16}$ "' and a depth of 8 $\frac{1}{4}$ "'. An aluminum holder supported 6 cells in the bomb. The cells were hemispherical with a flat bottom (diameter 1") and had narrow necks with calibration marks for 3-ml. cell volume. After 0.50 ml. of reaction solution was pipetted into the cell, a loose fitting cap was placed on the neck of the cell and the cells were lowered into the bomb which was then sealed and connected to a high pressure oxygen tank. The bomb was fitted with a capillary leak of 0.004" diameter and a stainless steel filter so as to prevent any sudden change in pressure, possible frothing of the solution and spreading of  $\alpha$ -activity. The bomb was charged with high oxygen pressure initially and then vented to exhaust most of the air present originally in the bomb cavity. It then was filled with oxygen to the desired pressure and sealed. Because of a surface to volume ratio of 10 to 1, a 5 minute gentle agita-

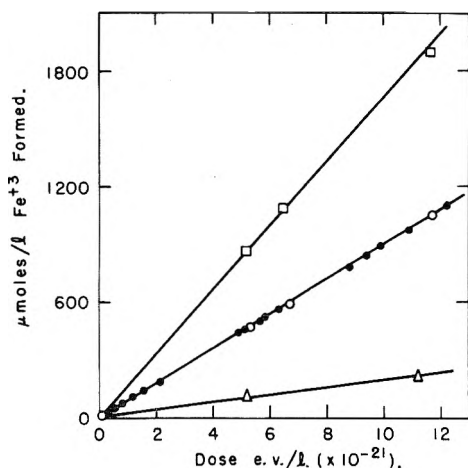


Fig. 1.—Dose dependence of ferric ion yields in a typical run: ○, 3 mM ( $\text{Fe}^{++}$ ), 1 mM NaCl, 0.4 M  $\text{H}_2\text{SO}_4$ ,  $2.2 \times 10^{-4}$  M  $\text{O}_2$  (air-satd.), 0.32 mc./ml.  $\text{Po}^{210}$ ; △, same as ○, contains no  $\text{Po}^{210}$  and ( $\text{O}_2$ ) =  $9.7 \times 10^{-2}$  M; □, same as ○, ( $\text{O}_2$ ) =  $9.7 \times 10^{-2}$  M; ●, Beckman control, same as ○, only in 1 cm. silica Beckman cell during high pressure oxidation.

tion of the bomb and contents at high oxygen pressure assured saturation of the solution with oxygen. After a predetermined time interval, the cells were removed from the bomb and the solutions were diluted to 3.0 ml. with 0.4 M  $\text{H}_2\text{SO}_4$ , mixed thoroughly and transferred to 1 cm. spectrophotometer cells for measurement. The ferric ion concentration of these solutions and blanks (identical reaction solutions which had not been exposed to high oxygen pressures) were obtained.

Since ferrous ion is oxidized by oxygen in the absence of  $\alpha$ -particle radiation, it was necessary to correct all results for the "dark" oxidation. Controls, identical in composition with the active solutions but containing no polonium were exposed to oxygen at the same time as the irradiated solutions. In general this thermal oxidation accounted for less than 10% of the total ferrous oxidation. In calculations of  $G(\text{Fe}^{+++})$  the dark oxidation was subtracted directly from the total oxidation and corrections were made for radiation induced oxidation before and after exposure to the high oxygen pressures. Since the dark oxidation increased as the square of the initial ferrous ion concentration, thermal oxidation corrections were high in runs where the ferrous concentration was above 3 mM. In one experiment at 25 mM ferrous ion the non-radiation induced oxidation accounted for about 60% of the total oxidation. Experiments on the extent of the dark oxidation carried out with different volumes of blank solutions confirmed our conclusion that the dissolved oxygen was in equilibrium with the gas phase for the 0.50 cc. solutions in the cells as described above.

After subtraction of the thermal reaction, the net radiation induced oxidation of ferrous ion was obtained. Several experiments showed that this net oxidation was linear with dose (see Fig. 1). Subsequent experimental ferric ion yields were calculated on the basis of two experimental points, one at the beginning of the oxygen exposure and one at the completion, the difference being the net oxidation of ferrous ion. By knowing the energy input over this period of time (obtained by a radiochemical assay technique to be described) it is possible to calculate  $G(\text{Fe}^{+++})$ , the number of ferric ions formed per 100 e.v. absorbed from the 5.3 Mev.  $\alpha$ -particles.

Several experiments were performed at oxygen pressures of 340 and 680 atm. A special compression apparatus built by the American Instrument Company and modified for high oxygen pressure use was employed for these runs. The compression fluid and lubricant for the pump was water and the entire pumping system was free from organic matter.

**Oxygen Concentration.**—The solubility of oxygen in 0.4 M  $\text{H}_2\text{SO}_4$  solutions was measured in the Van Slyke gas analysis apparatus for oxygen solutions saturated at atmospheric pressure and oxygen is 90% as soluble in 0.4 M sulfuric acid as in water at 25°. Following the suggestion of Smith and

Katz,<sup>5</sup> we assume that the ratio of solubility of oxygen in a salt solution to that in pure water is independent of pressure. The data of Zoss, Suci and Sibbitt<sup>6</sup> on the solubilities of oxygen in water at various pressures (up to 140 atm.) were used to estimate the solubility of the oxygen in reaction solutions. Huffman and Davidson<sup>7</sup> studied the kinetics of the thermal oxidation of ferrous sulfate in sulfuric acid solutions and measured a ternolecular rate constant for room temperature oxidation. We confirm this rate constant at very high oxygen concentrations (up to 0.1 M). At these concentrations the dark oxidation is first order in oxygen concentration and second order in ferrous ion concentration. Using these data the oxygen concentrations at 340 and 680 atm. were estimated by extrapolation of rates of ferrous oxidation vs. oxygen concentration to those found in dark oxidation at these very high pressures. The effects of pressure alone on constitution of water may, however, become serious at these pressures so the data on solubility at these pressures must be somewhat uncertain.

**Assaying of  $\text{Po}^{210}$  Activity.**—Aliquots of the irradiated solutions were taken and diluted by at least a factor of  $10^6$  with 3 M HCl. An aliquot of the diluted solution, usually 0.025 ml., was deposited on a 0.003" Pt plate by micropipet techniques. The solution on the plate was slowly evaporated with an infrared lamp and a hotplate below 200°. With 0.4 M sulfuric acid solutions, the original dilution must be at least by a factor of  $10^5$  or trouble is encountered in evaporating the sulfuric acid completely at 200°. After the plates were cooled they were counted for  $\alpha$ -activity in a calibrated pulse ionization chamber. The energy absorbed by the solution from  $\alpha$ -particle decay was then calculated from the number of counts/sec., the geometry, the dilution factor and the  $\alpha$ -particle energy. There was no indication that adsorption of the polonium on glass surfaces of the reaction cell occurred. In all cases the solutions maintained their original polonium assay for at least a week and activity was not lost by adsorption when solutions were transferred from one vessel to another. All plates which were counted decayed with the 138 day half-life of  $\text{Po}^{210}$ .

Glassware which was used repeatedly with polonium activity was cleaned by soaking in 3 M HCl overnight and by rinsing at least 5 times with triply distilled water. While some activity remained on the glass surface it was negligible compared to the activities used during irradiation. (Solutions were normally about 0.4 mc./cc.)

**Measurements on Ferrous Free Solutions.**—The yields of hydrogen and oxygen from 0.4 M  $\text{H}_2\text{SO}_4$  solutions irradiated at atmospheric pressure were obtained by our syringe and Van Slyke techniques.<sup>8</sup> Total gas concentrations were determined by the Van Slyke method and per cent. composition of the gas was determined by mass spectrometric analysis. Hydrogen peroxide yields for this solution containing no ferrous sulfate were determined by oxidation of ferrous sulfate by an aliquot of the syringe solution. Solutions of polonium-free hydrogen peroxide in 0.4 M  $\text{H}_2\text{SO}_4$  were unchanged in peroxide concentration for at least one week.

## Results

The increase in ferric ion concentration with dose is linear up to at least 50% oxidation in 3.0 mM ferrous solutions. (Corrections for the dark reactions have been made for all yields reported.) From the slopes of these curves ferric ion yields,  $G(\text{Fe}^{+++})$ , the number of ferric ions formed per 100 e.v. energy absorbed, were calculated.

The ferric ion yield for air saturated ferrous sulfate solutions (3 mM  $\text{FeSO}_4$ , 1 mM NaCl, 0.4 M  $\text{H}_2\text{SO}_4$ ) is  $5.10 \pm 0.10$ . As previously reported,<sup>9</sup> this value is lower than that found by earlier investigators<sup>10</sup> and is believed to be more reliable. This

(5) A. Smith and J. Katz, ORNL Report #1069, September 24, 1951.

(6) A. Zoss, S. N. Suci and W. I. Sibbitt, *Trans. Am. Soc. Mech. Eng.*, **76**, 69 (1954).

(7) R. E. Huffman and N. Davidson, *J. Am. Chem. Soc.*, **78**, 4836 (1956).

(8) S. Gordon and E. J. Hart, *ibid.*, **77**, 3981 (1955).

(9) C. N. Trumbore, *ibid.*, **80**, 1772 (1958).

(10) (a) N. Miller and J. Wilkinson, *Trans. Faraday Soc.*, **50**, 690 (1954); (b) W. R. McDonell and E. J. Hart, *J. Am. Chem. Soc.*, **76**,

value derives from twenty-one independent and absolute determinations made on solutions used as controls in various runs. All yields reported in this work were normalized to this average value. Aliquots from each run were counted independently and checked against the ferric ion yield of 5.10 for air saturated solutions. The concentration of polonium in air saturated ferrous sulfate solutions was varied from 0.9 to 0.01 mc./ml. and within experimental error there was no change in  $G(\text{Fe}^{+++})$ .

Table I gives the dependence of  $G(\text{Fe}^{++})$  on initial ferrous ion concentration,  $(\text{Fe}^{++})_0$ , for runs in which  $(\text{Fe}^{++})_0$  was different from 3 mM. Results with air saturated solutions show that  $G(\text{Fe}^{+++})$  increases slightly with increasing ferrous sulfate concentrations. At higher oxygen concentrations there is no definite effect of ferrous sulfate concentration. Here the data are less reliable than the 3 mM  $(\text{Fe}^{++})_0$  data because of the higher corrections necessary for the dark oxidation.

TABLE I

| EFFECT OF FERROUS ION CONCENTRATION ON $G(\text{Fe}^{++})^a$ |                                  |                     |                                               |
|--------------------------------------------------------------|----------------------------------|---------------------|-----------------------------------------------|
| $(\text{Fe}^{++})_0$ , mM                                    | $G(\text{Fe}^{++})_{\text{O}_2}$ | $(\text{O}_2)$ , mM | $G(\text{Fe}^{++})_{\text{air satd.}}$ (3 mM) |
| 0.22                                                         | 5.00                             | 0.22 (air satd.)    | 5.10                                          |
| 0.66                                                         | 5.00                             | .22 (air satd.)     | 5.10                                          |
| 0.5                                                          | 5.02                             | .22 (air satd.)     | 5.10                                          |
| 1.6                                                          | 5.21                             | .22 (air satd.)     | 5.10                                          |
| 4.1                                                          | 5.19                             | .22 (air satd.)     | 5.10                                          |
| 5                                                            | 5.24                             | .22 (air satd.)     | 5.10                                          |
| 10                                                           | 5.33                             | .22 (air satd.)     | 5.10                                          |
| 25                                                           | 5.38                             | .22 (air satd.)     | 5.10                                          |
| 5                                                            | 7.60                             | 17.0                | 7.73 <sup>b</sup>                             |
| 5                                                            | 7.64                             | 61.0                | ..                                            |
| 5                                                            | 3.70                             | 0.0                 | 3.57                                          |
| 5                                                            | 6.17                             | 1.1                 | 5.49                                          |
| 10                                                           | 7.31                             | 41                  | 7.60                                          |
| 10                                                           | 7.47                             | 25                  | 7.53                                          |
| 25                                                           | 9.51 <sup>c</sup>                | 62                  | 8.43                                          |

<sup>a</sup> Solutions were 0.4 M  $\text{H}_2\text{SO}_4$ , 1 mM NaCl containing 0.2-0.8 mc./ml.  $\text{Po}^{210}$ . <sup>b</sup> Extrapolated value from Fig. 2. <sup>c</sup> Dark reaction 75% of total oxidation.

Over the oxygen concentration range from 0 to 0.4M, Fig. 2 shows the effect of oxygen concentration on  $G(\text{Fe}^{+++})$  for solutions which were 0.4 M in  $\text{H}_2\text{SO}_4$ , 3 mM in  $\text{FeSO}_4$ , 1 mM in NaCl. The plot is arbitrarily made on a log-oxygen concentration basis so as to encompass the wide range of oxygen concentrations used in this work. The air-free ferric ion yield was 3.57.

Figure 3 shows that  $G(\text{Fe}^{+++})$  remains unchanged until the ferrous ion is nearly exhausted. These solutions contained 0.22 and 0.66 mM  $\text{FeSO}_4$  (1 mM NaCl) in air saturated 0.4 M  $\text{H}_2\text{SO}_4$ .

Several runs were carried out with 3 mM ferrous sulfate in 0.4 M sulfuric acid (1 mM chloride ion) in which the hydrogen and oxygen yields were determined for two initial oxygen concentrations. One syringe had no oxygen, the other initially had 0.140 mM oxygen. The results of these experiments are reported in Table II where the yields are the averages of two measurements per run. The estimated drop in  $G(\text{Fe}^{+++})$  yield during the run due to the observed oxygen depletion was from 4.9

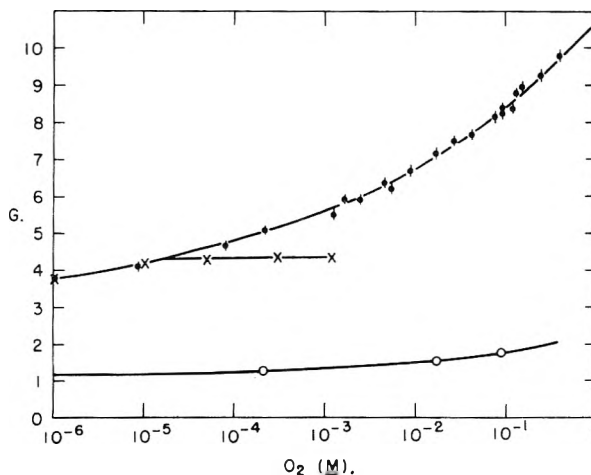


Fig. 2.—Dependence of  $G(\text{Fe}^{+++})$  and  $G(\text{H}_2\text{O}_2)$  on oxygen concentration [ $G$  vs.  $(\text{O}_2)$  M]: ●,  $G(\text{Fe}^{+++})$  for 3 mM  $(\text{Fe}^{++})$ , 1 mM NaCl, 0.4 M  $\text{H}_2\text{SO}_4$  solutions containing dissolved  $\text{Po}^{210}$ ; ×,  $G(\text{Fe}^{+++})$  predicted from equation 13; ○,  $G(\text{H}_2\text{O}_2)$  for 0.4 M  $\text{H}_2\text{SO}_4$  solutions containing dissolved  $\text{Po}^{210}$ .

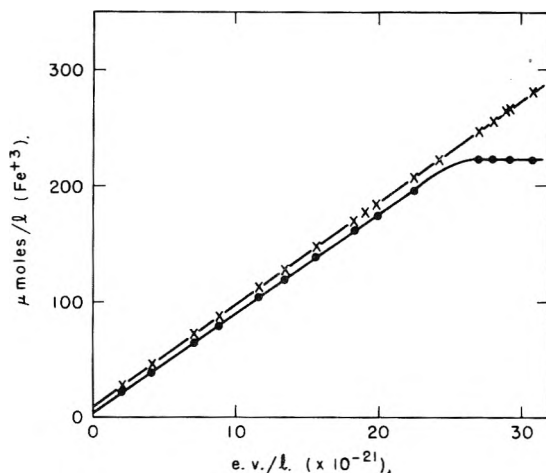


Fig. 3.—Effect of ferrous ion depletion [ $\mu\text{moles Fe}^{+++}/\text{l.}$  vs. e.v./l. ( $\times 10^{-21}$ ): ●, 0.22 mM  $(\text{Fe}^{++})$ , 1 mM NaCl, 0.4 M  $\text{H}_2\text{SO}_4$  containing 0.4 mc./ml.  $\text{Po}^{210}$ ; ×, 0.66 mM  $(\text{Fe}^{++})$ , 1 mM NaCl, 0.4 M  $\text{H}_2\text{SO}_4$  containing 0.4 mc./ml.  $\text{Po}^{210}$ .

to 4.4 and the calculated  $G(\text{Fe}^{+++})$  average for this oxygen concentration range was 4.7, in good agreement with the data of Fig. 2 at this oxygen concentration.

TABLE II

YIELDS IN 0.4 M SULFURIC ACID SOLUTIONS IRRADIATED WITH  $\text{Po}^{210}$   $\alpha$ -PARTICLES

| $(\text{Fe}^{++})_0$ , mM | (NaCl), mM | $(\text{O}_2)$ , mM | $G_{\text{air}}$ ( $\text{Fe}^{+++}$ ) | $G(\text{H}_2)$ | $G_{\text{air}}$ ( $\text{H}_2\text{O}_2$ ) | $G(\text{O}_2)$ |
|---------------------------|------------|---------------------|----------------------------------------|-----------------|---------------------------------------------|-----------------|
| 3.0                       | 1.0        | 0.0                 | 3.54                                   | 1.69            | ..                                          | ..              |
| 3.0                       | 1.0        | 0.14                | ..                                     | 1.28            | ..                                          | ..              |
| ..                        | ..         | ..                  | ..                                     | 1.40            | 1.10                                        | 0.07            |
| ..                        | ..         | 0.22 (air)          | ..                                     | ..              | 1.25                                        | ..              |
| ..                        | ..         | 17.5                | ..                                     | ..              | 1.45                                        | ..              |
| ..                        | ..         | 98.5                | ..                                     | ..              | 1.70                                        | ..              |

In order to obtain data regarding the hydrogen atom yields for  $\alpha$ -particles, some runs were made with dissolved deuterium. Figure 4 shows the yields of hydrogen ( $\text{H}_2$ ), HD,  $\text{H}_2\text{O}_2$  and  $\text{O}_2$  as a function of dose in an aqueous solution 0.4 M in sulfuric

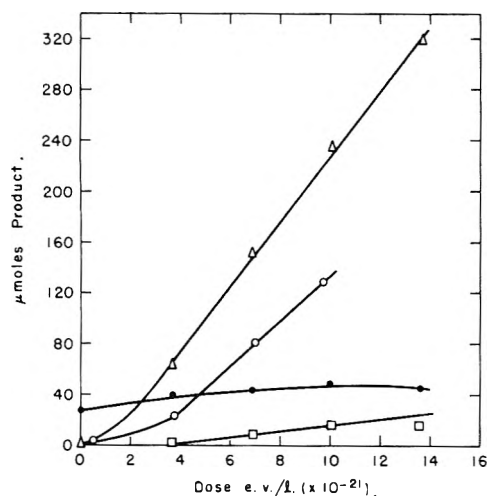
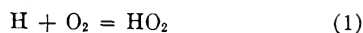


Fig. 4.—Product yields in deuterium saturated solution. [ $\mu$ moles product vs. e.v./l. ( $\times 10^{-21}$ )]. The solution was initially  $680 \mu M$  in  $D_2$ ,  $0.4 M$  in  $H_2SO_4$  and contained  $0.2$  mc./ml. dissolved  $Po^{210}$ :  $\square$ , oxygen;  $\bullet$ , HD;  $\circ$ ,  $H_2O_2$ ;  $\Delta$ , total hydrogen ( $H_2$ , HD,  $D_2$ ).

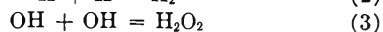
acid containing  $0.670 M$  dissolved deuterium gas. A  $G(HD)$  of  $0.19$  was found. Table II gives  $G(H_2)$ ,  $G(O_2)$  and  $G(H_2O_2)$  in  $0.4 M$  sulfuric acid solution for zero initial oxygen concentration. Peroxide yields also are reported for air saturated solutions and for two high oxygen concentrations. In all cases the dosage curves were linear up to  $10^{19}$  e.v./ml. total absorbed dose.

### Discussion

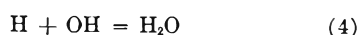
According to present ideas about the mechanism of the radiolytic decomposition of water, dissolved oxygen reacts with a hydrogen atom to form the hydroperoxy radical, as shown in reaction 1



Since hydrogen and hydrogen peroxide originate from pairwise radical recombination reactions 2 and 3



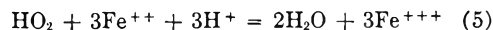
in regions of high radical concentration, reaction 4 also occurs, although it cannot be confirmed experimentally.



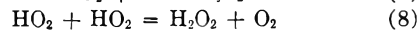
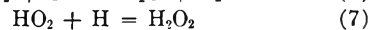
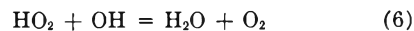
Reaction 1 will compete with (2) and (4) if the oxygen concentration in the  $\alpha$ -ray track is sufficiently high. From theoretical considerations (see later discussion where an initial track radius of  $20 \text{ \AA}$ . is derived) the calculated concentration of radicals in the track is  $1$  to  $2 M$ . Therefore the rate constant of (1) must be within an order of magnitude of the rate constants for the recombination reactions 2, 3 and 4 in order that hydrogen atoms react to an appreciable extent with oxygen in  $0.4 M$   $O_2$  solutions. The fact that  $G(Fe^{+++})$  in Fig. 3 increases with increasing oxygen concentration demonstrates that hydrogen atoms still remain in the  $\alpha$ -ray track in  $0.4 M$  oxygen.

The scavenging action of oxygen is complicated by the fact that the hydroperoxy radical formed undergoes further chemical reactions. When this radical diffuses into the bulk of the ferrous sulfate

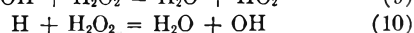
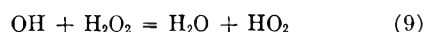
solution it reacts according to (5), thus causing a net oxidation of three ferrous ions per hydroperoxy radical.



In track regions where free radical concentrations are high, other possible reactions with the hydroperoxy radical are



Each of these reactions lowers the efficiency of oxygen as a scavenger since (6) gives only water and oxygen and (7) and (8) give one hydrogen peroxide, which is capable of oxidizing only two ferrous ions. To complicate matters even further, the following secondary reactions may occur<sup>11,12</sup>

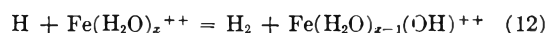


If these reactions occur, they probably take place only in regions of high radical concentrations at our ferrous sulfate concentrations. Reaction 10 competes with (1) for hydrogen atoms. An increase in the concentration of OH radicals in the track may tend to increase the rate of reaction 9. Another secondary reaction which may be affected indirectly by oxygen is<sup>13</sup>



We propose to correlate the increase in  $G(Fe^{+++})$  with an increase in the number of hydrogen atoms scavenged by reaction 1.

**Low Oxygen Concentrations.**—Increases in  $G(Fe^{+++})$  at very low oxygen concentration (less than  $10^{-5} M$ ) are due almost entirely to an increase in the rate of reaction 1 followed by 5, and a corresponding decrease in the rate of reaction 12



in the bulk of the solution. Thus increases in oxygen concentration in these regions of low oxygen concentration contribute no additional scavenging action to that afforded by the  $3.0 M$  ferrous ions present. This conclusion is based on calculations using equation 13, which is derived from steady-state kinetics.  $g(H)_{vac}$ , the yield of hydrogen radicals scavenged via (12) by  $3 M$  ferrous ions

$$G(Fe^{+++})_{O_2} - G(Fe^{+++})_{vac} = \frac{2g(H)_{vac}}{1 + \frac{k_{12}f(Fe^{++})}{k_1(O_2)}} \quad (13)$$

in the absence of oxygen, is assumed constant.  $G(Fe^{+++})_{O_2}$  is the ferric ion yield in the presence of oxygen and  $G(Fe^{+++})_{vac}$  is the ferric yield in the absence of oxygen. The hydrogen atom rate constant ratio,  $k_1/k_{12}$ , for reactions 1 and 12, is  $1200^{14}$  and  $g(H)_{vac}$  equals  $0.42$ . The latter value is computed from (14)

(11) J. Pucheault and C. Ferradini, *Radiation Research*, **9**, 168 (1958).

(12) A. O. Allen, "Proceedings of the Second International Conference on Peaceful Uses of Atomic Energy," 1958.

(13) N. Barr and A. O. Allen, presented at American Chemical Society Meeting, San Francisco, April, 1958.

(14) A. O. Allen and W. G. Rothschild, *Radiation Research*, **7**, 591 (1957).

$$G(\text{H}_2)_{\text{vac}} - G(\text{H}_2)_{\text{O}_2} = \frac{g(\text{H})_{\text{vac}}}{1 + \frac{k_{12}(\text{Fe}^{++})}{k_1(\text{O}_2)}} \quad (14)$$

which was derived in a manner similar to that described for equation 12. The data in the first two rows of Table II are used to calculate  $g(\text{H})_{\text{vac}}$  by equation 14. The agreement between the predicted values of  $G(\text{Fe}^{+++})_{\text{O}_2}$  from (12) and the experimental values given in Fig. 2 is excellent up to an oxygen concentration of  $10^{-5} M$ , where the experimental value increases faster than the predicted value (compare circles with x's of Fig. 2). It is clear that above  $10^{-5} M \text{O}_2$  the first direct scavenging action of H atoms by oxygen in reaction 2 occurs. Here reaction 1 begins to compete with (2), (4) or (10) for hydrogen atoms.

The yields obtained from the above calculation are consistent with but slightly lower than those reported by other investigators who have studied oxygen-free aqueous polonium solutions.<sup>10</sup> A yield of  $\text{HO}_2$  radicals from the track in the absence of oxygen, presumably arising from the occurrence of (9) in the dense free radical track, is calculated as the difference between  $g(\text{HO}_2)_{\text{vac}}$  and  $g(\text{H})_{\text{vac}}$ , or 0.13. This value agrees very well with a similar yield predicted from the experimental value of  $g(\text{O}_2)$ , equal to 0.07 as found in Table II.

**High Oxygen Concentrations.**—Above  $10^{-4} M$  oxygen, the difference between  $G(\text{Fe}^{+++})_{\text{O}_2}$  and 4.4, the ferric ion yield when all the free hydrogen atoms of the  $g(\text{H})_{\text{vac}}$  yield are scavenged by oxygen, represents the increase in ferric ion yield due to additional oxidizing species,  $\text{HO}_2$ , OH or  $\text{H}_2\text{O}_2$ , escaping from the track. We wish now to speculate on the nature of the species emerging from the densely populated  $\alpha$ -particle track.

The yield,  $G(\text{Fe}^{+++})$ , increases six times as rapidly as  $G(\text{H}_2\text{O}_2)$  over the oxygen concentration range above  $10^{-3} M \text{O}_2$ . After correcting for the competition between oxygen and ferrous ions for hydrogen atoms (reactions 1 and 14), the ratio,  $\Delta G(\text{Fe}^{+++})/\Delta G(\text{H}_2\text{O}_2)$  (where  $\Delta$  is a change caused by a change in oxygen concentration), is six over the entire oxygen concentration range. From this result we conclude that hydroperoxy radicals escape recombination as the track expands in ferrous sulfate solutions. Each two radicals oxidize six ferrous ions by reaction 5. In the absence of ferrous sulfate, two hydroperoxy radicals recombine according to reaction 11 and form but one hydrogen peroxide molecule.

The above conclusion that hydroperoxy radicals escape recombination reaction 8 and react with  $0.003 M$  ferrous ions implies that the rate constant of (8) is much smaller than that of reaction 2. Cylindrical diffusion theory supports this conclusion. Suppose that the rate constant for (8),  $k_8 = k_2 = 10^{-11} \text{ cc. molecule}^{-1} \text{ sec.}^{-1}$  and make the extreme assumption that all scavenged hydrogen atoms producing  $\text{H}_2$  via (2) are converted to  $\text{HO}_2$  radicals in  $0.4 M \text{O}_2$ , then the maximum expected number of  $\text{HO}_2$  radicals diffusing out of the  $\alpha$ -particle track can be calculated by using Fig. 1b of the Flanders-Fricke (F,F) paper.<sup>3</sup> At an  $E_\alpha$  of 2.10 for  $0.003 M$  ferrous sulfate, only 20% of the  $\text{HO}_2$  radicals will escape recombination. Since  $g(\text{H}_2)$

equals 1.27, the expected  $\Delta G(\text{Fe}^{+++})$  above  $10^{-4} M \text{O}_2$  is only 1.52. Instead the experimental  $\Delta G(\text{Fe}^{+++})$  in the concentration range from  $10^{-4}$  to  $0.4 M \text{O}_2$  is 5.0 (see Fig. 3).

Rate constant studies on the radiation induced decomposition of hydrogen peroxide also show that the rate constant of reaction 8 is low. Below  $1.0 M \text{H}_2\text{O}_2$ , the recombination reaction is termolecular<sup>15</sup> and above  $1.0 M$  it is bimolecular with a rate constant of  $0.5 \times 10^{-14} \text{ cc. molecule}^{-1} \text{ sec.}^{-1}$ .<sup>16</sup>

Diffusion theory has not developed to a point where one can work out the kinetics for the complex reactions occurring in an expanding  $\alpha$ -ray track. However, we wish to retain the assumption that reaction 8 is slow and now discuss briefly two limiting cases: each hydroxyl radical liberated in (4) reacts with: (a) an  $\text{HO}_2$  radical and (b) with a hydrogen peroxide molecule.

**Case (a). Hydroxyl Radicals Released in (4) React with Hydroperoxy Radicals.**—If the rate constant for reaction 4 is twice that for (2), then equal numbers of hydrogen atoms are scavenged from each of these reactions. (Because reaction 4 involves unlike radicals, the statistical factor of two is involved.) We assume now that all  $\text{HO}_2$ 's escape recombination reaction 8 but that all the OH's from reaction 4 react according to (6). Then we have for the ferric ion yield

$$G(\text{Fe}^{+++}) = 2g(\text{H}_2\text{O}_2) + g(\text{OH}) + 3g(\text{HO}_2) \quad (15)$$

in which  $g(\text{X})$  represent the yield of oxidizing species (X), which has escaped from the track and reacts with ferrous ions in the bulk of the solution.

A similar equation, eq. (16), holds for  $G(\text{H}_2\text{O}_2)$  in ferrous-free sulfuric acid solutions.<sup>17,18</sup>

$$G(\text{H}_2\text{O}_2) = g(\text{H}_2\text{O}_2) - \frac{1}{2}g(\text{OH}) + \frac{1}{2}g(\text{HO}_2) \quad (16)$$

The two equations, (15) and (16), represent a pair of simultaneous equations if it is assumed that the track yield,  $g(\text{X})$ , is identical in the two chemical systems at the same oxygen concentration. This is a reasonable approximation since the ferrous ion is a relatively weak scavenger compared with oxygen. At low oxygen concentrations the approximation will be more in error than at millimolar or higher oxygen concentrations. By assuming that  $g(\text{H}_2\text{O}_2)$  is independent of oxygen concentration, the values for  $g(\text{OH})$  and  $g(\text{HO}_2)$  appearing in columns 3 and 4 of Table III are calculated. Note that  $g(\text{OH})$  remains nearly constant whereas  $g(\text{HO}_2)$  rises with increasing oxygen concentration. Under the conditions assumed above, each observed hydroperoxy radical corresponds to one hydrogen atom not reacting in (2). This reduces the molecular hydrogen yield by one half molecule. Therefore

$$\Delta g(\text{HO}_2) = \frac{\Delta g(\text{H}_2)}{2} \quad (17)$$

$g(\text{H}_2)$ 's calculated from  $\Delta g(\text{HO}_2)$  appear in column

(15) E. J. Hart and M. S. Matheson, *Disc. Faraday Soc.*, **12**, 169 (1952).

(16) F. S. Dainton and J. Rowbottom, *Trans. Faraday Soc.*, **49**, 1160 (1953).

(17) C. J. Hochanadel, *Proc. of the Intl. Conf. on the Peaceful Uses of Atomic Energy*, **7**, 521 (1956).

(18) This equation assumes a mechanism of hydrogen peroxide formation similar to that postulated in the case of  $\gamma$ -rays.



TABLE III  
FRACTION OF HYDROGEN ATOMS RECOMBINING IN THE Po<sup>210</sup>  $\alpha$ -RAY TRACK

| O <sub>2</sub> , <i>M</i>     | O <sub>2</sub> (eff.) <sup>a</sup> | <i>g</i> (OH) | <i>g</i> (HO <sub>2</sub> ) <sup>c</sup> | $\Delta g(\text{HO}_2)$ |        | Case (a) eq. 17            |                           |                                         | Case (b) eq. 18            |                           |                                         |
|-------------------------------|------------------------------------|---------------|------------------------------------------|-------------------------|--------|----------------------------|---------------------------|-----------------------------------------|----------------------------|---------------------------|-----------------------------------------|
|                               |                                    |               |                                          | Case a                  | Case b | <i>g</i> (H <sub>2</sub> ) | <i>I</i> <sub>reac.</sub> | <i>I</i> <sub>theor.</sub> <sup>d</sup> | <i>g</i> (H <sub>2</sub> ) | <i>I</i> <sub>reac.</sub> | <i>I</i> <sub>theor.</sub> <sup>d</sup> |
| 0                             | $2.5 \times 10^{-6}$               | 0.55          | 0.55                                     | ..                      | ..     | 1.27                       | 0.91                      | ..                                      | 1.27                       | 0.91                      | ..                                      |
| 10 <sup>-6</sup>              | $3.5 \times 10^{-6}$               | .55           | .55                                      | ..                      | ..     | 1.27                       | .91                       | 0.90                                    | 1.27                       | .91                       | 0.90                                    |
| 10 <sup>-5</sup>              | $1.25 \times 10^{-6}$              | .40           | .60                                      | 0.05                    | 0.04   | 1.24                       | .89                       | .88                                     | 1.26                       | .90                       | .89                                     |
| 10 <sup>-4</sup>              | $1.03 \times 10^{-4}$              | .44           | .72                                      | .17                     | .15    | 1.18                       | .84                       | .85                                     | 1.23                       | .88                       | .87                                     |
| 10 <sup>-3</sup>              | 10 <sup>-3</sup>                   | .55           | .95                                      | .40                     | .34    | 1.07                       | .76                       | .79                                     | 1.18                       | .84                       | .85                                     |
| 10 <sup>-2</sup>              | 10 <sup>-2</sup>                   | .63           | 1.30                                     | .75                     | .64    | 0.89                       | .64                       | .66                                     | 1.11                       | .79                       | .80                                     |
| 10 <sup>-1</sup> <sup>b</sup> | 10 <sup>-1</sup>                   | .56           | 1.70                                     | 1.35                    | 1.16   | 0.59                       | .42                       | .42                                     | 0.98                       | .69                       | .69                                     |
| $4 \times 10^{-1}$            | $4 \times 10^{-1}$                 | .60           | 2.3                                      | 1.75                    | 1.50   | 0.39                       | .28                       | .20                                     | 0.89                       | .64                       | .56                                     |

$$B = 3.3 (\text{O}_2) \quad 0.25 (\text{O}_2)$$

<sup>a</sup> Effective oxygen concentration based on the scavenging power of ferrous ion being 1/1200 that of molecular oxygen. <sup>b</sup> Values of *I*<sub>reac.</sub> and *I*<sub>theor.</sub> are matched at this oxygen concentration. <sup>c</sup> Assuming *g*(H<sub>2</sub>O<sub>2</sub>) = 1.1. <sup>d</sup> *E* = 2.1 ( $\alpha = 10^{-11}$  molecules cc.<sup>-1</sup> sec.<sup>-1</sup>).

7 of Table III. Before applying these results to diffusion theory, let us consider the consequences of the case (b).

**Case (b). Hydroxyl Radicals Released in Reaction 4 React with Hydrogen Peroxide.**—While this second limiting case will never be fully realized in practice, oxygen liberation in ferrous sulfate-cupric sulfate solutions demonstrates that reaction 9 occurs not only in  $\alpha$ -tracks but also in  $\gamma$ -ray spurs. Besides the relatively slow growth of hydrogen peroxide in the ferrous-free Po<sup>210</sup> irradiations supports this hypothesis. If all the hydroxyl radicals react with hydrogen peroxide *via* (9), then hydroperoxy radicals scavenged from reactions 2 and 4 may react with ferrous ions. The OH released in (4) reacts with H<sub>2</sub>O<sub>2</sub> to give an HO<sub>2</sub> radical, consequently one ferric ion is produced by this OH radical and the increase in Fe<sup>+++</sup> is  $\Delta g(\text{HO}_2)/2$ . The ferric ion yield is

$$\Delta G(\text{Fe}^{+++}) = 3\Delta g(\text{HO}_2) + \frac{\Delta g(\text{HO}_2)}{2}$$

If we assume that *g*(OH) and *g*(H<sub>2</sub>O<sub>2</sub>) remain independent of oxygen concentration then  $\Delta g(\text{HO}_2)$  for case (b) is derived from column 5 of Table II by multiplying  $\Delta g(\text{HO}_2)$  by 3/3.5. This gives the  $\Delta g(\text{HO}_2)$ 's of column 6. Since we postulate that all hydroperoxy radicals escape and that we are scavenging H atoms from reactions 2 and 4,  $\Delta g(\text{H}_2)$  is given by

$$\Delta g(\text{H}_2) = \frac{\Delta g(\text{HO}_2)}{4} \quad (18)$$

The calculated hydrogen yields appear in column 10 of Table III. We next compare these *G*(H<sub>2</sub>)'s with diffusion theory and estimate the value of the H + O<sub>2</sub> rate constant compared to the H + H rate constant.

**Comparison with Diffusion Theory.**—Since general diffusion theory has not been worked out for the two radical model, we compare our estimated *g*(H<sub>2</sub>)'s of Table III with the simple one radical model treated by Flanders and Fricke.<sup>3</sup> At the outset, we recognize that the actual track conditions and reactions are more complex than assumed in this theory. Nevertheless, conclusions can be drawn that demonstrate the merits of the (F,F) treatment. First we estimate the initial radius of the radiation spurs.

To employ diffusion theory we must compute the

(F,F) parameters, *b*, *E* and *B*, applicable to cylindrical diffusion from a 5.3 Mev  $\alpha$ -track.

These parameters are defined by the equations

$$E_{\text{sphere}} = \frac{\alpha N_0}{\pi^{3/2} b D} \quad (19a)$$

$$E_{\text{cyl.}} = \frac{\alpha N_{\text{H}}}{2\pi D_{\text{H}}} \quad (19b)$$

$$B = \frac{b^2 \beta C}{4D_{\text{H}}} \quad (19c)$$

where  $\alpha = 1.0 \times 10^{-11}$  cc. molecule<sup>-1</sup> sec.<sup>-1</sup>, rate constant for reaction 2<sup>19</sup>;  $\beta$  = rate constant for the H + O<sub>2</sub> reaction 1; *N*<sub>0</sub> = 11.6, total H and OH radicals initially formed per spur for the spherical case<sup>20</sup>; if 100 e.v. is the average energy dissipated/spur, then *N*<sub>0</sub> = *g* (total radicals) = *g*(H) + *g*(OH) + 2*g*(H<sub>2</sub>) + 2*g*(H<sub>2</sub>O<sub>2</sub>) + 2.5<sup>21</sup>; *D* =  $4.5 \times 10^{-5}$  cm.<sup>2</sup> sec.<sup>-1</sup>, diffusion constant for mixed H and OH radicals; *D*<sub>H</sub> =  $6.0 \times 10^{-5}$  cm.<sup>2</sup> sec.<sup>-1</sup>, diffusion constant for H atoms; *b* = 20 Å., radius of the initial diffusion sphere in the  $\gamma$ -ray case or the radius of the initial cylinder in the  $\alpha$ -ray case (see discussion below); *N*<sub>H</sub> =  $0.79 \times 10^8$ , no. of hydrogen atoms/cm. track for 5.3 Mev.  $\alpha$ -particles; *C* = oxygen concentration in molecules/cc.

From Fig. 2 of the (F,F) paper<sup>3</sup> we determine *E*<sub>sphere</sub> from the fraction of radicals escaping recombination for  $\gamma$ -rays in order to compute *b*, the initial radius of the spur, from *E*<sub>sphere</sub>. *b* is used below to calculate  $\beta$  from equation 19c. For *I*<sub>s</sub>, fraction of escaping radicals in 0.4 *M* sulfuric acid irradiated by  $\gamma$ -rays,<sup>20</sup> we take 6.6/11.6 = 0.57. Then at an *I*<sub>s</sub> of 0.57 we find that *E*<sub>sphere</sub> equals 2.3, and from equation 19a that *b* equals 20 Å. *E*<sub>cyl.</sub> is next calculated from equation 19b. We find that *E*<sub>cyl.</sub> = 2.1 for the specific case of hydrogen atom diffusion from a 5.3 Mev.  $\alpha$ -track. A theoretical scavenger curve applicable to 5.3 Mev.  $\alpha$ -rays is obtained by the following procedure: first construct an *I*<sub>r</sub> (*I*<sub>r</sub> = 1 - *I*<sub>s</sub>) versus *B*<sub>cyl.</sub> curve from *I*<sub>s</sub> and *E* for each *B* from Table I (F,F); then construct an *I*<sub>r</sub> versus *B* curve at *E*<sub>cyl.</sub> = 2.1. Finally by matching our *I*<sub>r</sub> calculated results of Table III columns 8 or 11 at any one oxygen concentration, one obtains the theoretical fraction of hydrogen atoms escaping recombination,

(19) H. Fricke, *Ann. N. Y. Acad. Sci.*, **69**, 456 (1955).

(20) N. F. Barr and R. H. Schuler, *Radiation Research*, **7**, 302 (1957).

(21) 1.25 water molecules are assumed to be reformed *via* reaction 4.

$I_{r\text{theor}}$  (see columns 9 and 12 of Table III). We used 0.1 *M* oxygen as our reference point in these calculations because there is greater uncertainty in the yields and oxygen concentration at the 0.4 *M* point. Except at 0.4 *M* O<sub>2</sub>, the agreement between calculated  $I_r$ 's and theoretical  $I_r$ 's is satisfactory.

From the  $I_r$  versus *B* curve constructed for  $E_{\text{cyl}} = 2.1$ , we compute a value for  $\beta$ , the H + O<sub>2</sub> rate constant relative to an H + H rate constant of  $10^{-11}$  cc. molecule<sup>-1</sup> sec.<sup>-1</sup>. In 0.1 *M* oxygen for case a, *B* equals 0.33 at an  $I_r$  of 0.42, and for case b, *B* equals 0.025 at an  $I_r$  of 0.69. Solving (19c) for  $\beta$ , one obtains  $3.3 \times 10^{-11}$  and  $2.5 \times 10^{-12}$  cc. molecule<sup>-1</sup> sec.<sup>-1</sup> for cases a and b, respectively.

The rate constant  $k_{(\text{H} + \text{O}_2)}$  for reaction 1 has been determined as  $1.5 \times 10^{-12}$  cc. molecule<sup>-1</sup> sec.<sup>-1</sup> from relative rate constants of the reaction: H + D<sub>2</sub>; H + Fe<sup>++</sup>.<sup>22</sup> The rate constants calculated for the two possible cases treated in this paper are both within order-of-magnitude agreement with this value, although case b seems to

(22) P. Riesz and E. J. Hart, unpublished results.

provide the best agreement. Since this agreement between experiment and theory is better than expected for the one radical model, we believe that the  $g(\text{HO}_2)$  yields in Table II are realistic. Thus hydrogen atoms may be scavenged by oxygen from a volume originally about 1.0 *M* in hydrogen atoms. The results show further that a more efficient scavenger than oxygen is desirable to test diffusion theory. More critical still is the need for the complete diffusion theory for the actual multi-radical kinetics prevailing during radical diffusion out of the  $\alpha$ -track.

**Acknowledgments.**—The authors are indebted to the following individuals for assistance in carrying out this research project: Drs. H. Fricke, N. Miller and D. J. Wilson for stimulating discussions; Misses Patricia Walsh and Vicki Meyers for technical assistance; Mr. Chester Plucinski for mass spectral analyses; and Dr. Malcolm Daniels, Burton Snyder and Harry Youngquist who redesigned and tested the high pressure oxygen equipment.

## THE RADIOLYSIS OF ORGANIC SOLUTIONS. II. THE BENZOPHENONE-PROPANOL-2 SYSTEM<sup>1</sup>

By J. G. BURR AND J. D. STRONG

Contribution from the Research Department of Atomic International, A Division of North American Aviation Company, Canoga Park, Cal.

Received February 9, 1959

Mixtures of benzophenone with propanol-2 have been irradiated with cobalt-60  $\gamma$ -rays. It has been found that the yield of hydrogen from propanol-2 is very sensitive to benzophenone addition; 1% benzophenone lowers  $G(\text{H}_2)$  from 3.0 to 2.0. Addition of benzophenone also lowers the yield of methane from propanol-2. It is concluded that benzophenone probably functions principally as a hydrogen atom scavenger. It was also observed that radiolysis of these mixtures produced benzpinacol with a *G* of 6.60 (as semi-pinacol units) concurrent with a disappearance of benzophenone with a *G* of 7.2 and the formation of acetone with a *G* of 9.1. It is concluded that hydrogen transfer between the components of a system composed of a ketone molecule solvated with carbinol molecules is an important factor in the formation of the pinacol.

### I. Introduction

In a previous paper<sup>2</sup> we discussed the possibility that ketones could serve as scavengers for radiolytically produced hydrogen atoms and presented evidence to show that acetone did indeed scavenge the hydrogen atoms produced in the radiolysis of propanol-2. The present paper reports an extension of this investigation to the ketone, benzophenone. We have evaluated the ability of benzophenone to scavenge the radiolytic hydrogen atoms from propanol-2.

An interesting side issue accompanied study of the benzophenone-propanol-2 system—the radiation-induced formation of acetone and benzpinacol. It is well known in photochemistry that illumination with sunlight or ultraviolet light of solutions of benzophenone in propanol-2 (and other carbinols) converts the benzophenone quantitatively into benzpinacol (1,1,2,2-tetrahydroethanediol-1,2) and an equivalent amount of propanol-2 into acetone.<sup>3</sup>

Pinacols can similarly be produced by ultraviolet irradiation of numerous other ketone-carbinol solutions.<sup>3</sup> More recent work<sup>4</sup> has suggested that a complex radical formed by addition of a semi-pinacol radical to another ketone molecule is intermediate in pinacol formation. It also has been shown<sup>4</sup> by carbon-14 labeling that the benzpinacol formed by reaction between benzophenone and benzhydrol arises entirely from the ketone. The quantum yield of benzpinacol has been observed to be 0.5.<sup>4</sup>

The absorption of energy in the photochemical reaction is entirely by the benzophenone, since this substance possesses absorption maxima<sup>5</sup> at 258 *m* $\mu$  (aromatic ring) and 338 *m* $\mu$  (carbonyl group), whereas propanol-2 like other saturated aliphatic carbinols is transparent in the near ultraviolet region. Thus formation of the pinacol must be initiated by excitation of the ketone and proceed by interaction of the excited ketone molecule with carbinol molecules. In the radiation-induced process, on the other hand, the absorption of ionizing ra-

(1) Work performed under AEC Contract AT-(11-1)-Gen-8.

(2) J. D. Strong and J. G. Burr, *J. Am. Chem. Soc.*, **81**, 775 (1959).

(3) W. A. Noyes, "Technique of Organic Chemistry," Vol. II, 2nd Ed., Interscience Publishers, Inc., New York, N. Y., 1956, pp. 315-317.

(4) G. O. Schenck, University of Göttingen, personal communication.

(5) R. N. Jones, *J. Am. Chem. Soc.*, **67**, 2141 (1945).

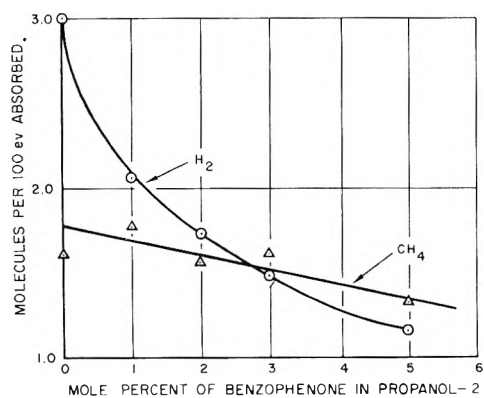


Fig. 1.—The 100 e.v. yields of hydrogen and methane in the radiolysis of solutions of benzophenone in propanol-2; the dose was about  $1.1 \times 10^{21}$  e.v./g., at a rate of  $1.50 \times 10^{18}$  e.v./ml. water-min.

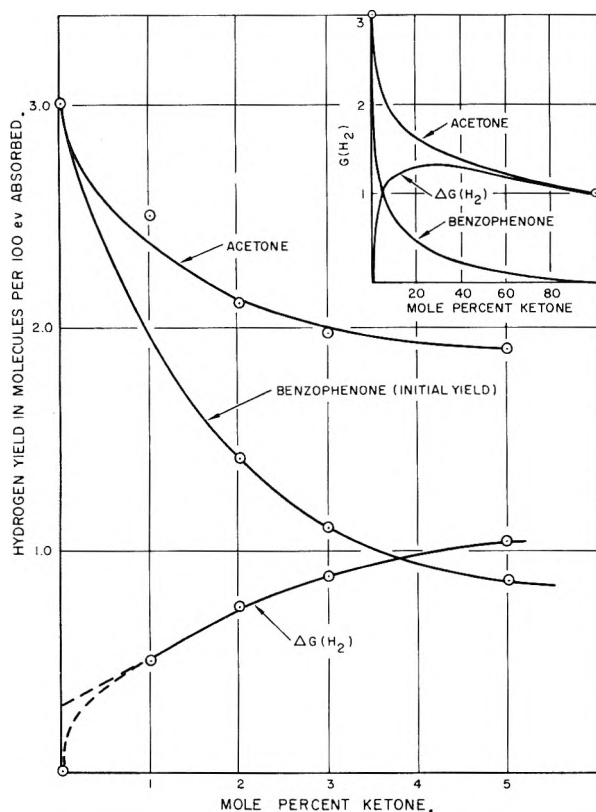


Fig. 2.—The initial 100 e.v. yield of hydrogen in the radiolysis of solutions of benzophenone in propanol-2 with corresponding data for solutions of acetone in propanol-2. The curve marked  $\Delta G(H_2)$  was obtained by subtracting the data for benzophenone solutions from the data for acetone solutions of equal concentration.

diation by the two components is in proportion to the electron fraction of each in the mixture. For the concentration of ketones employed here (1–5 mole %), the absorption of energy is predominantly by the carbinol. Thus one must distinguish between pinacolization initiated by excitation (or ionization) of the carbinol and that initiated by excitation of the ketone. This distinction will be important in the later discussion.

### Experimental

**Materials.**—Propanol-2, Mallinckrodt analytical reagent grade, was carefully fractionated in a fifty plate column and

the heart fraction dried over Drierite. Very high chemical purity was confirmed by examination in the gas chromatograph. Benzophenone was purchased from Eastman Kodak Company, white label grade, which was assumed to be essentially free from isomers, homologs and impurities. This was then vacuum distilled twice, each time retaining the heart fraction. A purity check on the gas chromatograph was unsuccessful as the benzophenone decomposed inside the column of the instrument. No impurities could be seen by infrared spectrophotometer analysis. Mixtures of benzophenone in isopropyl alcohol were made up in molar concentrations of 1, 2, 3 and 5% benzophenone. These solutions were noticeably unstable to the fluorescent light of the laboratory so they were either stored in the dark or freshly prepared for the radiolyses.

**Irradiations.**—Ampules for the benzophenone–propanol solutions were prepared from sections of 12 mm. Pyrex tubing, constricted to capillary diameter at one end and sealed at the other end. The internal volumes were about 2.5 ml., and the over-all lengths about 60–70 mm. One-ml. samples of the solutions were pipetted into the ampules through the constriction, the liquids degassed on a high vacuum line by the conventional freeze-melt technique, and the ampules then sealed off under vacuum.

The benzophenone–propanol-2 solutions were irradiated to a total dose of about  $1.1 \times 10^{21}$  e.v. The intensity of the source was  $1.50 \times 10^{18}$  e.v./ml. water-min., and the ambient temperature was about  $40^\circ$ .

**Benzpinacol Formation.**—Essentially 100% conversion of benzophenone to benzpinacol could be accomplished by irradiating the degassed benzophenone–propanol-2 solutions. The pinacol crystallized spontaneously from the solutions. Irradiation of solutions open to the air produced a much lower yield of pinacol (10–15%). The pinacol crystals obtained from either solution were colored, but since the color annealed out upon heating, it was evidently normal F-center coloring. The pinacol was identified by melting point, mixture melting point with authentic benzpinacol, and iodine-catalyzed conversion to benzpinacolone.<sup>5</sup>

**Analyses.**— $G$ -values for gaseous products were measured by opening the ampules in a high vacuum system containing a liquid nitrogen-cooled trap. The non-condensable gases were toeplered into a calibrated gas buret<sup>2</sup> where the volumes and temperatures were measured. Composition of the gaseous products was determined by mass spectrometry on a modified Consolidated 21-620 mass spectrometer.

After removal of the non-condensable gases from the irradiated benzophenone–propanol-2 solutions, the volatile components of the solution were distilled into the liquid nitrogen-cooled trap of the vacuum line and then removed. This fraction was analyzed for volatile ketone (acetone) by measuring the transmission in the infrared at  $5.84 \mu$ . Solutions of acetone in propanol-2 were used as standards and a portion of the unirradiated radiolysis solution used as the reference standard for zero ketone content. The non-volatile fraction of the radiolysis product was removed from the vacuum line, dissolved in chloroform and made up to the volume of the original radiolysis sample. Benzophenone content was measured by the transmission in the infrared at  $6.02 \mu$ , and non-volatile carbinol by the transmission at  $2.80 \mu$ . Reference standards were solutions of benzophenone in chloroform and solutions of benzpinacol in carbon disulfide (the molar transmission of the OH stretching band for benzpinacol was shown to be the same in carbon disulfide and in chloroform). Although this non-volatile carbinol probably includes some glycol from the propanol, no attempt was made to distinguish this carbinol from the benzpinacol, and the analyses are reported as per cent benzpinacol (since the atmospheric boiling point of pinacol is  $176^\circ$ , and the working pressure of the vacuum line was about  $10^{-5}$  mm., it was considered probable that most of the glycol distilled away from the benzpinacol).

### Discussion and Conclusions

**Hydrogen Atom Scavenging and Energy Transfer.**—Evidence was presented in the previous

(6) It was observed that the melting point of the pinacol depends markedly upon the rate of heating, and the literature value could be approached only if the rate of heating were quite slow as with a capillary tube and heating bath. Faster heating as on a hot bench produced a melting point raised by  $20$ – $30^\circ$ .

paper<sup>2</sup> of this series to show that the effect of dissolved acetone upon the yield of radiolytic hydrogen from propanol-2 could be explained by trapping of hydrogen atoms (from the propanol-2) by the carbonyl group of the ketone. This evidence consisted principally in the fact that the hydrogen and methane originated from the acetone in yields which were directly proportional to the absorption of energy in the acetone. The yields of hydrogen and methane from radiolysis of solutions of benzophenone in propanol-2 are shown in Fig. 1. It was subsequently found that, for reasons discussed below, benzophenone disappeared from these solutions at a very high rate (in contrast to the acetone solutions,<sup>2</sup> where acetone concentration remained essentially constant). During the irradiations whose results are cited in Fig. 1, approximately one-half of the benzophenone was consumed and an amount of acetone was formed nearly equivalent to the amount of benzophenone consumed. Therefore, we studied the yields of hydrogen and methane from a 2% solution of benzophenone in propanol-2 as a function of dose. The yields so obtained were linear with dose and could be extrapolated to zero dose to obtain initial yields. The data of Fig. 1 thus corrected to present the initial yields of hydrogen are shown in Fig. 2, together with the corresponding data for solutions of acetone in propanol-2. Figure 2 also contains curves for the difference in hydrogen yield ( $\Delta G(\text{H}_2)$ ) for these two types of solution at equal molar concentrations of the two ketones.

It is instructive to compare the results obtained in this investigation with the corresponding data for solutions of acetone in propanol-2. This comparison is shown in Fig. 2. At low concentrations of ketone (0.5%), the slope  $\Delta G(\text{H}_2)/\Delta(\text{ketone})$  for benzophenone solutions is about twice that for the acetone solutions; thus benzophenone is about twice as effective as acetone in reducing the hydrogen yield from propanol-2.

Acetone had no observable effect upon the methane yield from propanol-2 (this was measured with the use of acetone-*d*<sub>6</sub>), whereas 2% of benzophenone reduces the methane yield from 1.8 to 1.4. In the case of solute acetone, it was possible to show that the carbonyl group of the acetone does not appear able to trap methyl radicals.

This difference in effectiveness of two solutes so similar in structure (namely, each consisting of two hydrocarbon residues attached to a carbonyl group) is quite in contrast to the similar effectiveness of other solutes in reducing hydrogen yields. For example, Schuler<sup>7</sup> found that iodine, methyl iodide, ethyl iodide, methyl bromide, sulfur dioxide, methyl iodide plus iodine, and methyl iodide plus triphenylmethane were equally effective in reducing the hydrogen yield from cyclohexane. Similarly Ausloos and Paulson<sup>8</sup> found that both iodine and DPPH were about equally effective in reducing the hydrogen yield and methane yield from irradiated liquid acetone.

It appears then that the differences in structure between acetone and benzophenone are quite im-

portant. This fact can be best rationalized on the basis that the effect of both ketones upon the hydrogen yield from propanol-2 is caused by the scavenging of hydrogen atoms. It is well known that aryl rings can trap hydrogen atoms by an addition reaction, both in the gas phase<sup>9</sup> and in the liquid phase.<sup>10</sup> It is also known that methyl radicals add readily to aromatic rings.<sup>11</sup> Benzophenone, for the purposes of this discussion, can be regarded as a collection of six carbon-carbon double bonds and one carbon-oxygen double bond; each double bond is capable of scavenging at least the hydrogen atoms. Thus a solution of benzophenone, equal in molar concentration to a particular acetone solution, contains a concentration of scavenger groups seven times that of the acetone solution. This is consistent with our observation that benzophenone is more effective in reducing hydrogen yield than acetone.

We produced evidence in the earlier paper that the acetone carbonyl group does not scavenge the thermal methyl radicals produced in the radiolysis of acetone; presumably the carbonyl group of benzophenone would be even less effective as a methyl radical scavenger owing to the greater steric demand of that carbonyl group. However, the ability of dissolved benzophenone to reduce the methane yield from propanol-2 can be logically attributed to scavenging of the methyl radicals by the aromatic rings of the benzophenone.

We have no direct evidence to exclude energy transfer as an important factor in the radiolysis of the benzophenone-propanol-2 solutions. However, it is difficult to reconcile the assumption of extensive energy transfer here with the indicated absence of such processes in the acetone-propanol-2 radiolysis,<sup>2</sup> because energy transfer from propanol-2 to acetone seems at least as energetically favorable as that from propanol-2 to benzophenone. The excitation energies and ionization potentials of the two ketones are quite similar (since in both cases the electrons of the carbonyl oxygen unshared pair are the ones principally involved in these transitions).

**Benzpinacol Formation.**—The yields of acetone and benzpinacol and the yield for benzophenone consumption were measured as a function of dose. All three yields were found to be linear with dose; the data for acetone and benzpinacol formation could be extrapolated to indicate zero yield at zero dose. We suggest, therefore, that these data represent observation of primary chemical reactions in the radiolyses.

The yield for acetone formation was found to be 9.1 molecules per 100 e.v. absorbed; the yield of benzpinacol (as semi-pinacol units) to be 6.6 units per 100 e.v. absorbed; and the yield for consumption of benzophenone to be 7.2 molecules per 100 e.v. absorbed. It may be noted that the yield of semi-pinacol units and the yield for consumption of benzophenone are nearly equal, *i.e.*, one-half

(9) H. W. Melville and J. C. Robb, *Proc. Roy. Soc. (London)*, **202**, 181 (1950); P. E. M. Allen, H. W. Melville and J. C. Robb, *ibid.*, **218**, 311 (1953).

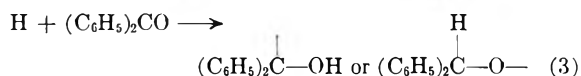
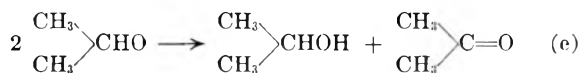
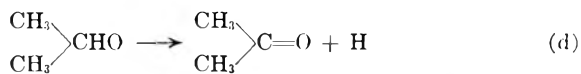
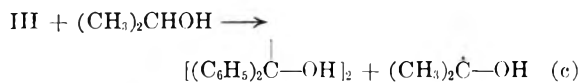
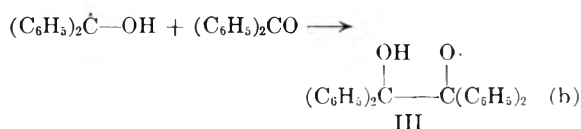
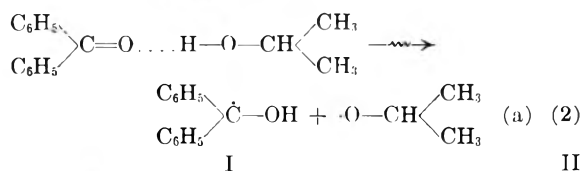
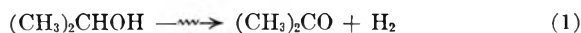
(10) W. N. Patrick and M. Burton, *This Journal*, **58**, 424 (1954).

(11) J. Smid and M. Szwarc, *J. Am. Chem. Soc.*, **78**, 3322 (1956) and earlier papers.

(7) R. H. Schuler, *This Journal*, **61**, 1472 (1957).

(8) P. Ausloos and J. F. Paulson, *J. Am. Chem. Soc.*, **80**, 5117 (1958).

molecule of benzpinacol appears for every molecule of benzophenone which disappears. On the other hand the yield of acetone is distinctly higher. The higher yield of acetone than semi-pinacol units may be accounted for by postulating that acetone is formed *via* two processes: (1) the direct radiolysis of propanol-2, and (2) a radiation-induced reaction between the ketone and the carbinol.



The radiolysis of propanol-2 is known<sup>12</sup> to produce acetone with a *G*-value of about 3; the difference between our *G* for acetone, 9.1, and the *G* for semipinacol formation, 6.6, is 2.5. The fact that the *G*-value for benzophenone consumption is higher than the *G*-value for pinacol production can be attributed to consumption of benzophenone through hydrogen atom trapping (eq. 3). However, the accuracy of these values is insufficient to warrant much discussion of processes which are measured by the differences among the observed values. We can

(12) W. McDonnell and A. S. Newton, *J. Am. Chem. Soc.*, **76**, 4651 (1954).

simply say that these differences are in the right directions and of reasonable magnitudes.

It is also to be noted that the *G*-values reported above are based upon the energy absorption *by the entire solution*. If the consumption of benzophenone is calculated upon the basis of energy absorption only by benzophenone, the *G*-value is about 350. This very high value suggests (a) a high rate of energy transfer from propanol-2 to benzophenone; or (b) a chain reaction for benzophenone consumption; or (c) a reaction which can be initiated by absorption of very small amounts of energy, *i.e.*, of the order of 0.3 e.v., or about 6-7 kcal./mole. In the foregoing discussion it was concluded that energy transfer from propanol-2 to the dissolved benzophenone was not likely in these radiolyses. We have been unable to think of any logical or defensible chain reaction involving benzophenone and propanol-2, so we think explanation (b) is unlikely.

However, it is highly probable that a substantial amount of hydrogen bonding exists between the ketone and the carbinol hydroxyl hydrogen, as shown in equation 2a. It seems quite probable that absorption of a relatively small amount of radiant energy could effect a reversible shift of the hydrogen atom from the carbinol oxygen to the ketone oxygen. The two radicals I and II thus produced could be the source of the two reaction products, benzpinacol and acetone.

We have no evidence bearing upon the mechanism of pinacol and acetone formation subsequent to the presumed formation of the two semi-pinacol intermediates. We can say that formation of acetone from II by reaction 2d is endothermic and thus unlikely; that formation of acetone directly from II by the disproportionation, 2e, can be ruled out since this would produce only one acetone molecule for every two benzophenone molecules consumed. We can also say that the sequence of reactions 2a, b, c, is in agreement with the stoichiometry observed, and seems the most probable sequence which can be proposed in the absence of any specific knowledge of the reaction intermediates. We do not know what process converts the  $(\text{CH}_3)_2\text{COH}$  radicals into acetone.

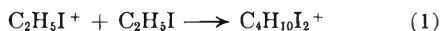
# PERSISTENT ION-MOLECULE COLLISION COMPLEXES OF ALKYL HALIDES<sup>1</sup>

BY ROSWELL F. POTTIE AND WILLIAM H. HAMILL<sup>2</sup>

Received February 11, 1959

The first examples of persistent collision complexes between an ion and a molecule have been observed by mass spectrometry. The processes are of the type  $RX^+ + RX \rightarrow R_2X_2^+$  for ethyl iodide, propyl iodide and ethyl bromide. Methyl iodide and methyl bromide gave negative results but  $C_3H_8I_2^+$  was observed with a mixture of methyl and ethyl iodides. Reaction cross-section falls to zero above a critical ion velocity.

In the course of a study of ion-molecule reactions of ethyl iodide in the ionization chamber of a mass spectrometer we found evidence for an ionic species at, or close to,  $m/e = 312$ . This mass corresponds to  $C_4H_{10}I_2^+$  which suggests its formation in the bimolecular process



This reaction, if verified, would be of particular interest as the first example (to our knowledge) of a persistent collision complex, or "sticky collision."<sup>3</sup>

Although previously unobserved in mass spectrometry, such collision complexes are not unanticipated. In conventional gaseous systems the dimeric ion should occur more frequently because it is susceptible to collisional stabilization by removal of excess energy. Similarly, it can be expected to grow by accretion of additional molecules and this concept is the basis of Lind's "cluster theory."<sup>4</sup>

According to a recent simple treatment<sup>5</sup> of ion-molecule "sticky collisions" the lifetime  $\tau$  of the complex is given by

$$\tau = \nu^{-1}(1 - E_b/E)^{1-\alpha} \quad (2)$$

where  $E$  is the total internal energy,  $E_b$  the energy required to dissociate the complex and  $\alpha$  the number of effective degrees of vibrational freedom. To be detected in a mass spectrometer the complex must have a lifetime approximating  $10^{-6}$  sec.

## Results

The general experimental procedure for this work follows Stevenson and Schissler.<sup>6</sup> Details have been described elsewhere.<sup>7</sup>

In order to confirm the reaction 1, as indicated by preliminary experiments, it was next established that peak height tentatively assigned to  $C_4H_{10}I_2^+$  varied as the square of the inlet pressure of ethyl iodide. Further, its ion intensity varied inversely with the repeller field strength at values in excess of 10 v. cm.<sup>-1</sup> both for 70 v. and for 10.5 v.

(1) Contribution from the Radiation Project operated by the University of Notre Dame and supported in part under Atomic Energy Commission Contract AT-(11-1)-38.

(2) To whom correspondence and requests for reprints should be sent.

(3) Dr. N. A. I. M. Boelrijk, working in these laboratories, has examined many systems for evidence of this phenomenon, without success. J. L. Franklin, F. H. Field and F. W. Lampe, in a preprint of a paper presented at the Joint Conference on Mass Spectrometry, London, September, 1958, have remarked upon the absence of peaks attributable to such species in mass spectra containing evidence of other ion-molecular reactions.

(4) S. C. Lind, "The Chemical Effects of Alpha Particles and Electrons," 2nd ed., Chemical Catalog Co., New York, N. Y., 1929.

(5) M. Burton and J. L. Magee, *THIS JOURNAL*, **56**, 842 (1952).

(6) D. P. Stevenson and D. O. Schissler, *J. Chem. Phys.*, **29**, 282 (1958).

(7) R. F. Pottie, R. Barker and W. H. Hamill, *Rad. Res.*, in press.

electrons. The lower value corresponds to the position of the maximum in Fig. 1. A number of ion-molecule reactions are known to exhibit such an inverse dependence of ion abundance upon repeller field strength,<sup>8</sup> although an inverse square root dependence is considered normal.

The resolving power at  $m/e = 312$  is unfavorable and special care was necessary to identify the ion. This was accomplished, in part, by using the metastable suppressor electrode to improve the resolution. The mass spectrum in this region was calibrated at mass-to-charge ratios of 296, 310 and 338 using propylene diiodide, tetramethylene diiodide and hexamethylene diiodide, respectively. In this manner it was definitely established that an ion-molecule reaction product of  $m/e = 312$  had been formed from ethyl iodide. Furthermore, it follows that reaction (1) is occurring.

As a final, confirmatory test we compared the ionization efficiency curve for the parent molecule-ion  $C_2H_5I^+$  with that of the daughter. The vanishing current method gave an appearance potential at  $m/e = 312$  which agreed, within experimental error, with that at  $m/e 156$ . Rather unexpectedly, the curves show a striking difference. The ionization efficiency curve for the primary ion (see Fig. 1) is normal. In contrast, the curve for  $C_4H_{10}I_2^+$  rises sharply from the onset of ionization to a well-defined maximum about 1.5 v. higher. Then, following a small subsequent decrease, the curve behaves normally over an interval of several volts and reaches a plateau only 6 v. above its appearance potential, decreasing slightly at 70 v. The similarity and difference of the two curves in Fig. 1 have been emphasized by choosing an appropriate scale factor to equalize ion abundances at higher ionizing voltages.

A similar reaction has been found yielding  $C_4H_{10}Br_2^+$  from ethyl bromide,  $C_6H_{14}I_2^+$  from propyl iodide and  $C_3H_8I_2^+$  from a mixture of methyl and ethyl iodides. No reaction was found for methyl iodide, methyl bromide or propyl chloride. The latter is an unfavorable case for test because of a low abundance of  $C_3H_7Cl^+$ . The calculated cross sections  $\sigma$  for reactions in one-component systems at 70 v. ionizing voltage and 4 v. cm.<sup>-1</sup> repeller field strength appear in Table I.

The ion abundance curves for  $C_2H_5Br^+$  and  $C_4H_{10}Br_2^+$  strongly resemble the corresponding curves in Fig. 1. For  $C_6H_{14}I_2^+$  there is slight evidence of structure in the ion abundance curve and the abundance ratio of primary to secondary ion is substantially constant over a 10 v. range above

(8) G. Gioumousis and D. P. Stevenson, *J. Chem. Phys.*, **29**, 294 (1958).

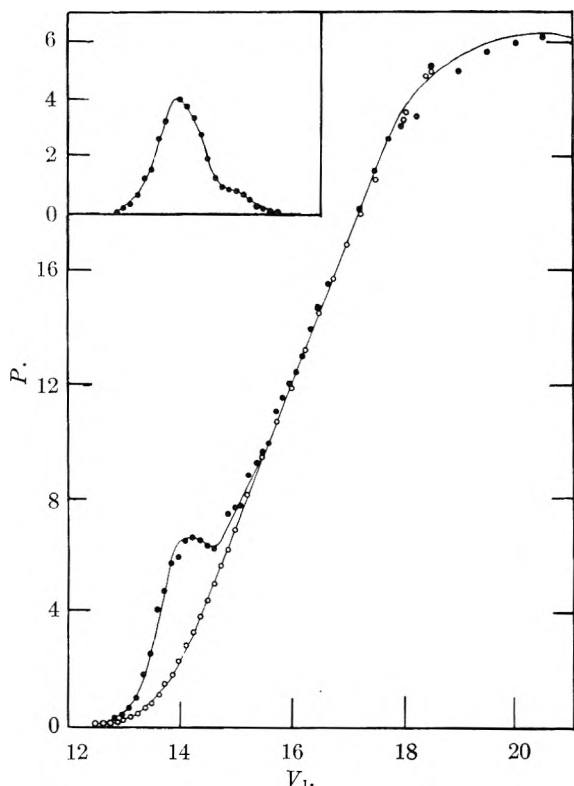


Fig. 1.—Peak height  $P$  vs. ionizing voltage  $V_1$  for  $C_4H_{10}I_2^+$  (●) from  $C_2H_5I^+$  (○) at 4 v.  $cm^{-1}$  ion repeller field strength.

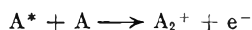
TABLE I

| CROSS-SECTIONS FOR PERSISTENT COLLISION COMPLEXES   | $\sigma \times 10^{16}$<br>$cm.^2$ at 4 v.<br>$cm.^{-1}$ |
|-----------------------------------------------------|----------------------------------------------------------|
| $C_2H_5I^+ + C_2H_5I \rightarrow C_4H_{10}I_2^+$    | 1.5                                                      |
| $C_2H_5Br^+ + C_2H_5Br \rightarrow C_4H_{10}Br_2^+$ | 3.2                                                      |
| $C_3H_7I^+ + C_3H_7I \rightarrow C_6H_{14}I_2^+$    | 12                                                       |

their common appearance potential. The ion abundance curve for  $C_3H_8I_2^+$  resembles Fig. 1 in having a maximum 1.5 v. above the appearance potential. In addition, there is a second maximum about 3.5 v. above the appearance potential, followed by the plateau some 5 v. higher which persists to 70 v.

For the three reactions in Table I the difference between the ionization potential of the primary ion and the appearance potential of the secondary ion does not exceed 0.2 v. For  $C_3H_8I_2^+$  the primary ion cannot be distinguished because the ionization potentials of methyl iodide and of ethyl iodide differ by less than 0.2 v.

Although no difference could be distinguished between appearance potentials of primary and secondary ions, the maxima in the ion abundance curves suggested contributions to the observed reactions from resonance excitations of parent molecules. Reactions of the type



are well known for atoms and have been observed by mass spectrometry.<sup>9</sup> For comparison with the alkyl halides we measured the  $Ar_2^+$  intensity from argon as a function of repeller field strength.

(9) J. A. Hornbeck and J. P. Molnar, *Phys. Rev.*, **84**, 621 (1951).

At 20 v. ionizing voltage, corresponding to the maximum in the ionization efficiency curve, the observed ion intensity dependence for  $m/e = 80$  was characteristic of primary ions, as expected. In contrast, for ethyl iodide at 70 v. ionizing voltage, where the contribution from the low energy component should be negligible, the peak height for the ion at  $m/e = 312$  decreased in a manner characteristic of secondary ions with increasing repeller field strength. When the ionizing voltage was then decreased to a value corresponding to the maximum in Fig. 1, the peak height again decreased in a similar manner with increasing repeller field strength. We conclude that the energy-rich precursor for the ion at  $m/e = 312$  is an ion, and not an excited neutral molecule, over the entire range of ionizing voltage.

Ions at double the parent mass were not found for methyl bromide or methyl iodide at 70 v. ionizing voltage but there is still the possibility of a resonance process at some lower electron energy. The appropriate mass regions were therefore scanned repeatedly, over small voltage intervals, from 2 v. below to 10 v. above the appearance potentials of the parent molecule ions. No collision complex ion was detected in either instance.

#### Discussion

Stevenson and Schissler<sup>6</sup> have pointed out that parent ion-daughter ion relationship is better established by constancy of their abundance ratios at low ionizing voltages than by simple agreement of their appearance potentials. The ions  $C_4H_{10}I_2^+$  and  $C_4H_{10}Br_2^+$  are exceptional in this respect over the lower range of voltage while agreeing excellently over the medium and higher range. The curves in Fig. 1 strongly suggest two processes and, if so, the facts require that  $C_2H_5I^+$  is involved in each. To account for the results it is postulated that there are two isomeric ionic species of the empirical formula  $C_2H_5I^+$  and of unequal reaction cross-sections. If one species behaves normally in giving a constant parent ion-daughter ion ratio, the contribution of the abnormal variety can be isolated by subtracting the parent curve from the daughter curve. This difference curve is plotted in the panel of Fig. 1 and suggests a resonance process.

Before attempting to explain this effect it is first necessary to consider the possibility that it is merely an artifact. Appearance potentials were measured at repeller field strengths of 4 v.  $cm^{-1}$  in order to maximize secondary ion current, but at the risk of instability. The ionization efficiency curves for primary ions were all normal, as for the one illustrated, while those for collision complex ions exhibit the features mentioned. Also, ionization efficiency curves for many secondary ions which are not collision complexes have been determined with the same instrument and at the same repeller field strength but with no evidence of the anomalies reported here, not excluding such ions resulting from alkyl halides.

There is no necessary inconsistency between the structure reported for the secondary ion abundance curves and the apparent lack of structure in the corresponding primary ion curves. The

electron energy resolution of the instrument is so low that negative evidence is simply inconclusive. One is inclined to attempt to correlate the maxima in the secondary ion abundance curves with the double series of electronic states observed for the alkyl halides.<sup>10</sup> These series lead to ionization potentials separated by 0.64 and 0.59 v. for methyl and ethyl iodides and by 0.33 and 0.33 v. for methyl and ethyl bromides. A serious deficiency of this proposal is that it cannot account for the break in the curve for  $C_3H_5I_2^+$  at an electron energy ca. 3.5 v. above the ionization potential. It would also be necessary to assume that formation of one of these states was sharply resonant, although the probability of ion formation by electron impact is normally linear in the excess energy.

Whatever may be the detailed explanation of these effects, it is rather likely that the sensitivity of the collision complex to small energy differences will amplify the effect, particularly so if only a small fraction of complexes survive long enough to be collected. Referring to equation 2 let

$$E = E_b + E_t + E_v + 3kT$$

$E_t$  is the kinetic energy of the primary ion arising from the repeller field. Its maximum value was 0.5 e.v. and since  $\sigma$  varies as  $E_t^{-1/2}$  we take  $E_t = 0.1$  e.v. as representative.  $E_v$  is the vibrational energy of the primary ion resulting from vertical ionization. The ionization potential of ethyl iodide by electron impact<sup>11</sup> is 9.47 e.v. and the spectroscopic value<sup>10</sup> is 9.34 e.v., giving  $E_v = 0.12$  e.v. At the temperature of the ionization chamber (250°),  $3kT$  is 0.14 e.v. The value of  $E_b$  is very uncertain but 1 e.v. is a plausible value. Letting

(10) W. C. Price, *J. Chem. Phys.*, **4**, 539, 547 (1936).

(11) J. D. Morrison and A. J. C. Nicholson, *ibid.*, **20**, 1021 (1952).

$\tau = 10^{-6}$  sec. and  $\nu = 10^{13}$  sec.<sup>-1</sup> leads to a required minimum 13 degrees of vibrational freedom. Considering the high internal energy, heavy atoms and relatively weak C-C bonds, this is an acceptable value. For these values of the parameters, decreasing the internal energy of the collision complex by only 0.03 e.v. would more than double the value of  $\tau$ . If the very small cross-section for  $C_3H_5I_2^+$  can be interpreted as inefficient collection due to extensive decomposition of the collision complex, then doubling the value of  $\tau$  will have a large effect upon  $\sigma$ .

Considering the sensitivity of the value of  $\tau$  to the internal energy of the complex we may consider that  $\tau$  changes discontinuously to zero at some critical value,  $E_c$ , of the translational energy of the primary ion. There is a corresponding critical limit,  $l_c$ , of the length of the ion track (measured from the electron beam toward the exit slit), along which a viable complex can form. This distance is shorter, the greater the repeller field strength,  $F$ . The yield of complexes is proportional to

$$\int_0^{l_c} \sigma(E) dl = \int_0^{E_c} \sigma(E) F^{-1} dE$$

The cross-section for collision,  $\sigma(E)$ , is presumed to depend upon  $E^{-1/2}$  but it is clear that regardless of the functional dependence, the yield of secondary ions varies inversely with field strength, provided that  $E_c$  is less than the maximum energy attainable by the primary ion.<sup>12</sup>

**Acknowledgment.**—It is a pleasure to acknowledge helpful conversations with Professor John L. Magee.

(12) N. A. I. M. Boelrijk and W. H. Hamill, to be published in further detail.

## RADIOLYSIS OF LIQUID *n*-PENTANE<sup>1</sup>

BY ADOLF E. DE VRIES<sup>2</sup> AND AUGUSTINE O. ALLEN

*Contribution from Department of Chemistry, Brookhaven National Laboratory, Upton, N. Y.*

*Received February 11, 1959*

Product distribution in *n*-pentane radiolysis is the same for beams of 14 Mev. He<sup>++</sup> ions as for 2 Mev. electrons, in marked contrast to the behavior of aqueous solutions. The various branched- and straight-chain products heavier than pentane contain little or no unsaturation and their relative yields are consistent with their being formed by random combination of free radicals produced by breakup of pentane without rearrangement. Hydrocarbon products lighter than pentane must be formed by some other mechanism.

### Introduction

A good deal of work has recently been reported on radiolysis products of liquid paraffinic hydrocarbons, using radiations of low ionization density, such as fast electrons.<sup>3-5</sup> The present work was undertaken to determine the effects of changing radiation quality on the product distribution in the radiolysis of *n*-pentane.

(1) Research performed under the auspices of the U. S. Atomic Energy Commission.

(2) Lab. v. Massaspektrografic, Amsterdam, Netherlands.

(3) H. A. Dewhurst, *THIS JOURNAL*, **61**, 1466 (1957).

(4) H. A. Dewhurst, *ibid.*, **62**, 15 (1958).

(5) J. J. Keenan, R. M. Lincoln, R. L. Rogers and H. Burwasser, *J. Am. Chem. Soc.*, **79**, 5125 (1957).

### Experimental

Matheson's best pentane was washed with H<sub>2</sub>SO<sub>4</sub> and KOH, fractionated through a 20-plate column and passed through 1.5 m. of silica gel. One-gram samples of thoroughly deaerated pentane were sealed under vacuum into small radiation cells fitted with thin glass windows.

Electron-beam irradiations were performed at 2 Mev. and 0.5  $\mu$ amp. with a Van de Graaff generator to total doses of  $1.5 \times 10^{21}$  or  $6 \times 10^{21}$  e.v. Cyclotron irradiations were performed with He<sup>++</sup> ions ( $\alpha$ -rays) having their energy reduced by absorbers to 14 Mev. (their original energy is 40 Mev.); the current was about 0.06  $\mu$ amp. and the total dose was about  $3 \times 10^{21}$  e.v., but was determined only approximately because of difficulties in reading the current, due to the low electrical conductivity of pentane.

After irradiation the sample tubes were opened on a vacuum line; H<sub>2</sub> and CH<sub>4</sub> were pumped from the sample at



liquid nitrogen temperature and determined by combustion. The remaining sample was analyzed by gas chromatography, using a Burrell Kromo-Tog. Either the light fraction ( $C_2$ - $C_5$ ) or the heavy fraction ( $C_6$ - $C_{10}$ ) could be determined on a given sample. For determining the light fraction, the whole sample was expanded as a vapor into a large bulb (to avoid fractionation in sampling) and a convenient sample of the vapor introduced into the 1.8-m. column containing tricresyl phosphate supported on firebrick. For the heavy fraction, the liquid sample was fed into a Dow-Corning silicone-oil 710 column at 80–110°. For each component appearing as a peak on the recorder trace, the area under the peak was measured and converted into actual amount of material by calibration factors obtained by running through known quantities of known materials. It was found that peak areas were proportional neither to the number of moles nor to the number of grams of material, but calibration factors varied smoothly with molecular weight. The normal paraffins from  $C_6H_{14}$  to  $C_{10}H_{22}$  gave well resolved peaks, but their branched isomers were not always well resolved from one another, and no attempt was made to determine which branched isomers were present. To establish the identity of some of the peaks, mass spectrometric patterns were obtained of samples trapped out after leaving the column. Since the silicone oil did not separate saturated and unsaturated compounds, the fractions were trapped out separately and unsaturation determined in each by bromine titration. The sample was added to a mixture of  $HgCl_2$ ,  $HBr$ ,  $HCl$  dissolved in methanol, and a solution of  $Br_2$  in  $CCl_4$  was added until a small electrical conductivity was observed which did not disappear within one minute.<sup>6</sup>

### Results

Table I shows the 100 e.v. yields ( $G$ ) for the various products produced by electrons. Other products were found in traces ( $G < 0.05$ ): acetylene, isopentane and butane isomers. The bromine titration showed that fractions  $C_6$ - $C_9$  contained no unsaturation, and  $C_{10}$  only a small amount:  $G(C_{10}H_{20}) \leq 0.1$ . The low degree of unsaturation of the  $C_{10}$  fraction was confirmed by infrared spectroscopy. This low unsaturation in

TABLE I

PRODUCTS OF ELECTRON BEAM IRRADIATION OF NORMAL PENTANE

| Product                | $G$<br>(obsd.) | Formula for<br>calcd. yield | $G$<br>(calcd.) |
|------------------------|----------------|-----------------------------|-----------------|
| $H_2$                  | 4.20           | ...                         | ...             |
| $CH_4$                 | 0.22           | ...                         | ...             |
| $C_2H_4$               | .36            | ...                         | ...             |
| $C_2H_6$               | .27            | ...                         | ...             |
| $C_3H_6$               | .29            | ...                         | ...             |
| $C_3H_8$               | .33            | ...                         | ...             |
| Butene-1               | .06            | ...                         | ...             |
| $n$ - $C_4H_{10}$      | .09            | ...                         | ...             |
| Pentenes               | .71            | ...                         | ...             |
| $iso$ - $C_6H_{14}$    | .03            | $AE/R$                      | 0.05            |
| $n$ - $C_6H_{14}$      | .14            | $AF/R + BD/R + 2C^2/R$      | .11             |
| $iso$ - $C_7H_{16}$    | .41            | $BE/R$                      | .57             |
| $n$ - $C_7H_{16}$      | .45            | $CD/R + BF/R$               | .28             |
| $iso$ - $C_8H_{18}$    | .59            | $CE/R$                      | .52             |
| $n$ - $C_8H_{18}$      | .20            | $D^2/2R + CF/R$             | .23             |
| $iso$ - $C_9H_{20}$    | .21            | $DE/R$                      | .15             |
| $n$ - $C_9H_{20}$      | ~0             | $DF/R$                      | .07             |
| $iso$ - $C_{10}H_{22}$ | 2.40           | $E^2/2R + EF/R$             | 2.42            |
| $n$ - $C_{10}H_{22}$   | 0.28           | $F^2/2R$                    | 0.25            |

the large "dimer" fraction agrees with Dewhurst's findings on hexane,<sup>4</sup> but is in sharp contrast to the result reported by Keenan, Lincoln, Rogers and Burwasser<sup>5</sup> on liquid butane. Their highly un-

saturated products may have resulted from secondary reactions brought about in the electron beam as a result of the very high current density they used. Dewhurst's  $G(H_2)$  for pentane agrees exactly with ours, but his  $G(CH_4)$  is higher. We believe our absolute  $G$ -values for the various condensable fractions have a probable error of about 15%, or  $\pm 0.05$  (whichever is larger).

Our material balance appears to be very good; thus for total H and C atoms appearing in the products per 100 e.v. we find, respectively, 118.79 and 49.57, ratio 2.396, while in pentane the ratio is 2.40. Another test for material balance is the equation  $G(H_2) = G(\text{unsaturation}) + G(C_{10}) + 0.8 G(C_9) + 0.6 G(C_8) + 0.4 G(C_7) + 0.2 G(C_6) - 0.2 G(C_4) - 0.4 G(C_3) - 0.6 G(C_2) - 0.8 G(C_1)$ . If we neglect the small amount of unsaturation in  $C_{10}$ , we find for the two sides of this equation 4.20 and 4.29.

The cyclotron results are less complete. Not only was the dosimetry uncertain, but a reliable relationship was not obtained between the absolute yields of the  $H_2$ - $CH_4$  fraction and the heavier fractions. We do have reliable ratios between  $CH_4$  and  $H_2$  and between the various heavier products. Several such product ratios are shown in Table II, with the electron-beam values for comparison. No significant difference is found in the product distribution given by the two radiations.

TABLE II

COMPARISON OF PRODUCT DISTRIBUTIONS FOR 14 MEV.  $He^{++}$  AND 2 MEV. ELECTRON BEAMS

| Product ratio                         | Electron<br>value | Cyclotron<br>value |
|---------------------------------------|-------------------|--------------------|
| $CH_4/H_2$                            | 0.052             | 0.054              |
| $C_3(\text{total})/C_2(\text{total})$ | .99               | 1.02               |
| $C_3H_6/C_3H_8$                       | .88               | 1.0                |
| $C_4H_{10}/C_2(\text{total})$         | .14               | 0.15               |
| $C_4H_8/C_4H_{10}$                    | .67               | 0.83               |
| $C_5H_{10}/C_2(\text{total})$         | 1.13              | 1.10               |
| $C_8(\text{total})/C_7(\text{total})$ | 0.92              | 0.92               |
| $iso$ - $C_8/n$ - $C_8$               | 2.95              | 2.43               |
| $iso$ - $C_9/C_8(\text{total})$       | 0.27              | 0.27               |
| $iso$ - $C_{10}/iso$ - $C_9$          | 4.06              | 4.5                |

### Discussion

Free radicals undoubtedly play a major role in the formation of products heavier than pentane, as shown by observations of Dewhurst<sup>5</sup> and of Davison<sup>7</sup> that these products are suppressed in dilute solutions of radical scavengers such as iodine and oxygen. These radicals combine randomly in pairs to form the observed products; whether they are formed close together in the  $\alpha$ -particle track or far apart in the tracks of fast electrons makes no difference as long as no reaction first order in radicals competes with the recombination. Thus the similarity of products formed by radiations of different quality shows that smaller radicals do not often abstract hydrogen from the pentane under the experimental conditions:  $R \cdot + C_5H_{12} = RH + C_5H_{11}$ . If this reaction occurred frequently in competition with radical recombination, we should expect to find relatively less  $C_{10}H_{22}$  with  $\alpha$ -particles

(7) W. H. T. Davison (a) in "Reactions of Free Radicals in the Gas Phase," The Chemical Society, London, 1957, p. 151; (b) *Chem. and Ind.*, 662 (1957).

(6) K. G. Stone, "Determination of Organic Compounds," McGraw-Hill Book Co., New York, N. Y., 1956, p. 19.

than with electrons. The great effect of radiation quality in water, in contrast, is due to the active competition in the particle tracks between first- and second-order radical reactions.

If the smaller radicals are formed by breakup of pentane molecules they should all be "primary" radicals with the free valence at the end of the chain. The  $C_5H_{11}$  could be primary, or either of two secondary forms, depending on where the hydrogen atom was lost from pentane. A random recombination of such radicals imposes considerable restriction on the relative yields of the various products. Thus if the 100-e.v. yields of methyl, ethyl, propyl, butyl, *sec*-amyl and *n*-amyl are denoted, respectively, by  $A$ ,  $B$ ,  $C$ ,  $D$ ,  $E$  and  $F$ , and the sum of these six (the total radical yield) by  $R$ , we will have for observed yields of heavy products the expressions shown in the third column of Table I. We

have ten observations to fit with six parameters. A fairly good fit, shown in Table I (not necessarily the best fit) has been obtained by assuming  $A = 0.1$ ,  $B = 1.1$ ,  $C = 1.0$ ,  $D = 0.3$ ,  $E = 5.0$ ,  $F = 2.2$ , so that  $R = 9.7$ . Except for the ratio of normal heptane to isoheptane, agreement with observation is within the expected experimental error. The radical yields found are entirely reasonable; and it is gratifying that the yields of ethyl and propyl are practically equal, and of methyl and butyl not far different, as expected for the breakup of normal pentane.

**Acknowledgment.**—We are indebted to A. P. Irsa for mass spectrometric measurements and to H. A. Schwarz for valuable advice and for his assistance in the cyclotron irradiations. We owe to C. D. Wagner the suggestion for calculation of product yields by random radical combination.

## ON THE ADSORPTION OF SOME FISSION PRODUCTS ON VARIOUS SURFACES

By J. BELLONI, M. HAISSINSKY AND HALIM N. SALAMA

*Laboratoire Curie, 11, rue Pierre Curie, Paris, France*

*Received February 12, 1959*

The adsorption of promethium and tagged cerium and ruthenium from aqueous acid solutions has been studied on various surfaces. Certain apparently anomalous effects in the kinetics of the adsorption processes have been observed and interpreted. The quantities adsorbed at equilibrium increased with  $pH$  and, in most cases, passed through a maximum. The lanthanides obey the Langmuir isotherm, whereas the adsorption of ruthenium follows Henry's law. No temperature effect was observed on the adsorption of the lanthanides; the adsorption of ruthenium increases with temperature and is partly irreversible, whereas the adsorption of cerium and promethium is reversible. Possible mechanisms for these processes are discussed in the light of these results and those of other workers.

The advantages of radiochemical methods in the study of the adsorption phenomena in aqueous solutions are well known and need not be outlined here. There is already, therefore, a great number of publications on the subject, especially on adsorption on the radioactive indicator scale. Few authors, however, have carried out systematic studies of the principal factors on which the features of adsorption depend, *viz.*: nature of the adsorbate molecules or ions, nature and state of the adsorbent surface, effect of concentration, of  $pH$ , of ions of opposite charge, of the temperature, etc.

At the Laboratoire Curie, we have undertaken such a study on different radioelements,<sup>1</sup> most particularly on several fission products, on protactinium<sup>2</sup> and on plutonium.<sup>3,4</sup> This paper, however, will be limited to the experiments on promethium and on trivalent radio-cerium and radio-ruthenium. The choice of these elements has been dictated by the following considerations: promethium and cerium are typical representatives of the lanthanides, which are among the most important of the fission products. These elements are strongly electropositive and their ions have a noble gas electronic structure, in contrast with ruthenium

which is a transition element belonging to the group of noble metals. Ruthenium, moreover, because of its multiple valency states, offers the possibility of studying the influence of valence on the adsorption of the same metal. The radioactive properties of some of their isotopes ( $^{147}Pm$ ,  $^{144}Ce$  and  $^{106}Ru$ ) allow the measurement of extremely small quantities, such as are generally adsorbed on small surface areas.

### Experimental

The promethium of mass 147 ( $T_{1/2} = 2.6$  years) was supplied by the Isotope Service of Oak Ridge, in the form of the chloride. In the solutions generally used in our experiments, the activity corresponded to a concentration of  $2.5 \times 10^{-6}$   $\mu\text{moles/cm}^3$  ( $0.44 \mu\text{C./cm}^3$ ). We have verified that the sample was pure from the radioactive point of view. It is therefore very probable that the inactive impurities, especially other lanthanides, were also eliminated during the purifications, but one cannot exclude the possibility that a certain amount of these have accumulated by the end of the operations, for instance, by radioactive decay. It is difficult to calculate exactly this amount, but we shall assume, somewhat arbitrarily, that the concentration of promethium and other lanthanides in the product is of the order of  $5 \times 10^{-9} M$ . A knowledge of these concentrations is of no importance, however, in all the experiments where only the relative changes of concentration need to be known (effect of  $pH$ , of the anion, of the temperature, reversibility, etc.).

The radio-cerium,  $^{144}Ce$  ( $T_{1/2} = 285$  days), was obtained also as the chloride, from AERE at Harwell. It is in radioactive equilibrium with its decay product  $^{144}Pr$  (17.3 min.) which emits very penetrating  $\beta$ -rays ( $\sim 3$  Mev.). The concentration of  $^{144}Pr$ , chemically very similar to cerium, is al-

(1) These studies are related to problems interesting the Commissariat à l'Energie Atomique de France, which we thank for financial assistance.

(2) C. Rougée, Diplôme d'Etudes Supérieures, Paris, 1958.

(3) M. Haissinsky and Y. Laflamme, *J. chim. phys.*, **56**, 510 (1958).

(4) M. Haissinsky and Y. Paiss, *ibid.* (in press).

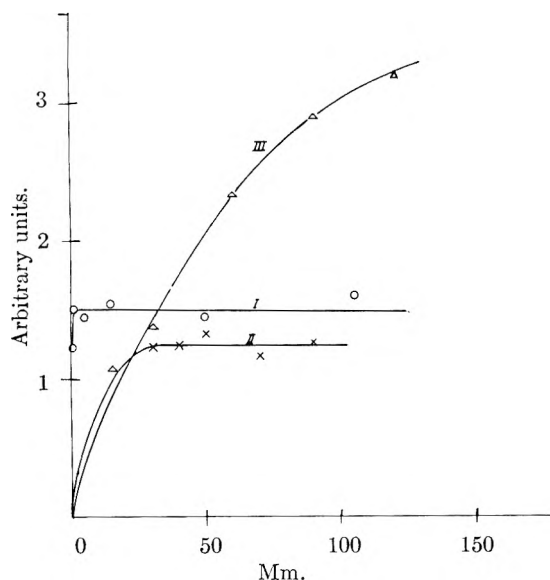


Fig. 1.—Kinetics of adsorption of ruthenium and of promethium: I, Pm, successive foils of platinum; II, Ru, successive foils of platinum; III, Ru, the same foil of platinum.

ways negligible. The measured activity of the solution used corresponded to a concentration of  $8 \times 10^{-4}$   $\mu$ moles Ce/cm.<sup>3</sup>. The product was stated to contain 2.8 mg. of inactive impurities. We shall see later on from the adsorption behavior of these impurities, which is very close to that of cerium, that they are all very probably lanthanides, if not cerium itself.

The radio-ruthenium, obtained also from Harwell, was initially a mixture of <sup>103</sup>Ru (39.8 days) and <sup>106</sup>Ru (1.00 year). Given the age of our sources, we could neglect the presence of <sup>103</sup>Ru, which had already disappeared by decay. The isotope <sup>106</sup>Ru is in radioactive equilibrium with its descendant <sup>106</sup>Rh (30 sec.) and can be estimated easily by the penetrating  $\beta$ -rays of the latter. As in the case of promethium, it is also difficult to determine the exact concentration of ruthenium, in which the stable isotopes of masses 99, 101 and 102, constitute fission chain ends. Moreover, the stable isotope of rhodium, <sup>103</sup>Rh, being formed by the decay of <sup>103</sup>Ru is probably, in its absorption behavior, very similar to ruthenium. In the experiments without carrier, therefore, the real concentration of ruthenium is known to within a factor of about 5. We estimate it to be about  $10^{-9}$   $M$ . The activity of our solution was usually 0.076  $\mu$ curie/cm.<sup>3</sup>.

The ruthenium was delivered in the form of the nitrate of the nitroso salt,  $\text{RuNO}(\text{NO}_3)_3$ . This is probably the form of ruthenium in the solutions of fission products when they have been treated by concentrated nitric acid. We have studied the adsorption of ruthenium only in its nitroso form. The chloride and sulfate of nitrosyl ruthenium were obtained by treating the nitrate with the corresponding acid after treatment by aqua regia.

**Adsorbents.**—As adsorbent surfaces, we have used platinum, gold, silver, stainless steel (Inox Ugine NS-225), "Thüringe" glass and polyvinyl chloride. Some experiments of adsorption of ruthenium also were carried out on nickel. All the adsorbents had the form of thin foils with a surface area of  $2 \times 10 \times 10$  mm.<sup>2</sup>, with the exception of the slides of glass which were of  $2 \times 9 \times 18$  mm.<sup>2</sup>.

The platinum and gold were cleaned before use by treatment with boiling, concentrated nitric acid and thoroughly washed with twice distilled water. The silver was treated with 5  $N$  HCl, and the glass with a sulfochromic mixture. The pH of the solutions was adjusted by the addition of the appropriate amount of the corresponding acid to the active solutions. All the experiments were carried out in 10 cm.<sup>3</sup> of solution, in which the foil of the adsorbent rotated at a speed of 60 turns/min. All experiments were carried out at room temperature ( $20 \pm 2^\circ$ ) except when the effect of temperature was to be studied, when the solutions were placed in a "Hoopler" thermostat regulated to  $\pm 0.05^\circ$ . At the end of each experiment, the foil was either washed rapidly

with twice distilled water and dried, or carefully shaken and the last adherent droplet on the edge removed by fine filter paper. We have verified that no activity was lost during the washing.

Activity measurements were carried out with Geiger-Müller counters. Absorption measurements were used in order to correct activity measurements on one face of the foil for the radiation penetrating from the other.

### Experimental Results

**Kinetics. Reproducibility.**—It is well known that it is difficult to obtain good reproducibility of surface phenomena, probably because of the difficulties of obtaining reproducible surfaces. Nevertheless, when we have taken into account three apparent anomalies, which we are going to point out, the reproducibility of our results becomes satisfactory enough. In carrying out, for each point, a large number of experiments, we can estimate that the precision of the mean values was generally  $\pm 10\%$ . It is less accurate for the solutions of high pH, where the equilibria between the different ionic and molecular forms in the solutions themselves are established slowly. In any case, these results, as we shall see, show clearly the effects of pH, concentration and temperature on the adsorption.

The first observed anomaly for promethium, cerium and ruthenium, and which has also been observed for protactinium<sup>2</sup> and plutonium,<sup>4</sup> may be described as follows. If we determine adsorption as a function of time by using a fresh foil of metal or polyvinyl chloride at each immersion, the quantities adsorbed increase with time of immersion up to a limiting value, indicating saturation. This equilibrium is generally attained within about 2 or 3 minutes, if not less, with the solutions of promethium or cerium, and after about 30 minutes with ruthenium. The time necessary for the attainment of saturation fluctuates considerably and varies with the conditions of the medium. If, on the contrary, we repeatedly dip the same foil in the active solution for increasing periods of time (after washing and drying), the adsorbed activity continues to increase without reaching a limiting value; or, at least, the adsorbed amount at the apparent equilibrium is much greater than in the first case.

In Fig. 1, curve III illustrates the latter phenomenon for  $10^{-9}$   $M$  ruthenium in nitric acid solution of pH 3. Curve II illustrates the limiting adsorption obtained with successive foils of platinum in the same solution, as for curve I. Curve I shows the same effect for  $5 \times 10^{-9}$   $M$  promethium in 0.5  $N$  HNO<sub>3</sub> solution. We shall discuss later a probable explanation for this anomalous behavior. All the following results correspond to experiments performed with the technique of successive foils and to saturation values.

Another anomaly has been observed in the adsorption of promethium or cerium on glass in nitric acid solutions. In this case, even if we use successive slides, the adsorbed quantities pass through a maximum, then diminish (after about 30 minutes) to a constant value. This same constant value is obtained without passing through a maximum if we first immerse the glass slide for 10 to 15 hours in a solution of the same pH con-

taining no lanthanide. The time of the pretreatment is shorter for higher acidities. It seems, therefore, that the "acidity" of the surface of glass is modified during contact with the solution, arriving at an equilibrium state after a certain time. As long as this equilibrium is not reached, neither can the adsorption of promethium or cerium be at equilibrium.

Finally, the quantities of ruthenium adsorbed in its nitrosyl form are relatively high from freshly prepared solutions, but diminish continuously with the age of the solution to a reproducible lower limit. The time required to reach this lower limit was found to be shortened when the solution was in contact with any of the metallic adsorbents used. It is also shorter for solutions of higher acidity and higher concentration of ruthenium. The general characteristics of this phenomenon are independent of the nature of the anion:  $\text{NO}_3^-$ ,  $\text{Cl}^-$  or  $\text{SO}_4^{2-}$ , but appear more clearly with the first. The aging anomaly is probably related to the slow evolution toward a state of equilibrium between the simple and polynuclear forms of  $\text{Ru}(\text{NO})_{\text{III}}$ , which are known<sup>5</sup> to coexist in aqueous solutions. All the results which are given for this radioelement were consequently obtained with aged solutions when the results have become reproducible.

**Effect of pH and the Anion.**—The variation of adsorption of promethium and ruthenium on different surfaces at equilibrium, as a function of the pH of nitric acid solutions, is shown in Figs. 2 and 3. We notice, first, that the amounts adsorbed are always extremely small and are but very small fractions of the quantities remaining in solution. In nitric acid solutions of 1 *N*, or higher normalities, the adsorption of promethium is hardly measurable. At pH 3, only 0.008% of promethium and 0.026% of ruthenium are adsorbed per  $\text{cm}^2$  of platinum (from a volume of 10  $\text{cm}^3$ ). Taking into consideration the previously mentioned approximations for the evaluation of absolute concentrations, these values correspond to  $5 \times 10^{-15}$  mole/ $\text{cm}^2$  of promethium and  $2.6 \times 10^{-15}$  mole/ $\text{cm}^2$  of ruthenium. If we suppose that the adsorbate is fixed on the surface in an ionic form and take the ionic radius of  $\text{Pm}^{3+}$  to be 0.98 Å., and that of ruthenium to be about 1.0 Å., we estimate the coverage to be  $1 \times 10^{-6}$  for promethium and  $6 \times 10^{-7}$  of a geometric monoatomic layer, for ruthenium. The radius of the ruthenium ion which we have taken is almost certainly too small since the distance Ru-N is probably of the order of 1 Å. An exact estimate, in any case, cannot be made, since we are ignorant of the form of the adsorbed ruthenium (which may even be atomic; see Discussion). We shall see that more exact information is unnecessary for the understanding of the results.

On the other hand, Figs. 2 and 3 show that the adsorption increases with the pH, attains a maximum (at pH 5.6 for Pm and 4.5 for Ru), then decreases. At the maxima, the adsorbed quantities and the atomic coverages on platinum are increased 7.7 times for ruthenium and 8 times for prome-

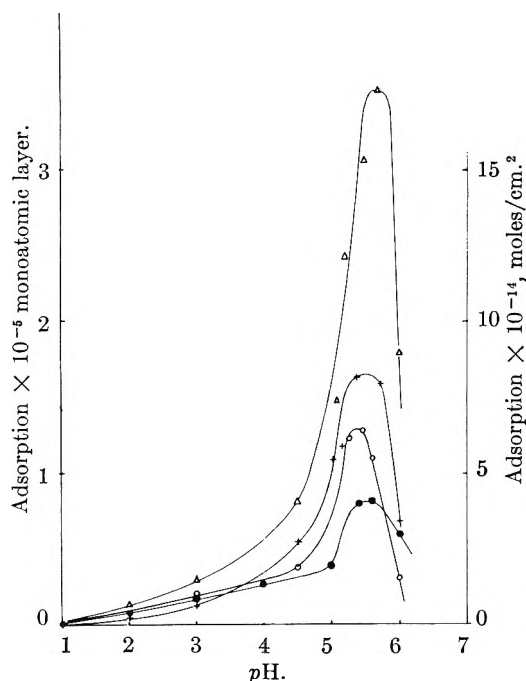


Fig. 2.—Adsorption of Pm as function of pH: ●, platinum; ○, silver; +, stainless steel; △, polyvinyl chloride.

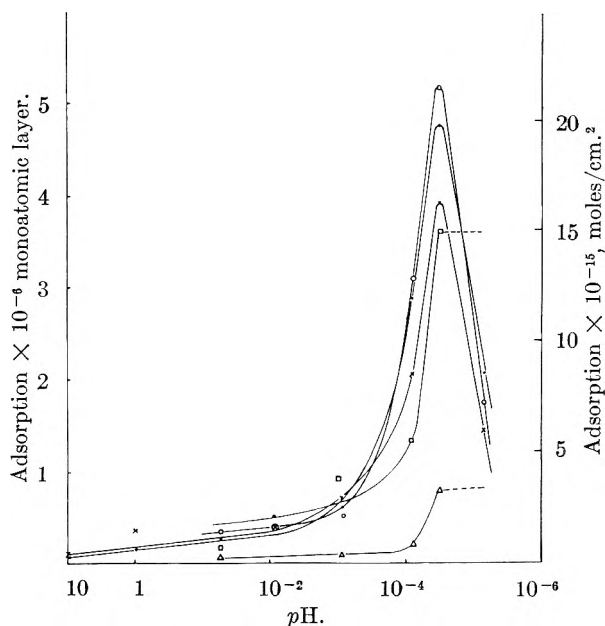


Fig. 3.—Adsorption of Ru as function of pH: △, glass; □, polyvinyl chloride; ×, gold; ●, platinum; ○, silver.

thium. The variation with pH is qualitatively the same for the adsorption of promethium on silver, stainless steel and polyvinyl chloride, and for the adsorption of ruthenium on silver, gold and polyvinyl chloride. We shall see that under certain other conditions, the adsorption of ruthenium is quite high, but nevertheless remains very slight compared with the quantities remaining in solution (on an adsorbent surface of 1 or 2  $\text{cm}^2$  and 10  $\text{cm}^3$  of solution).

We have found the same pH effects for the adsorption of cerium from nitric acid solutions. The maximum in this case is at pH 4.5. For cerium

(5) J. M. Fletcher, I. L. Jenkins, F. M. Lever, F. S. Martin, A. R. Powell and R. Todd, *J. Inorg. Nucl. Chem.*, **1**, 378 (1955).

too, the positions of the maxima are independent of the nature of the adsorbent surface (Pt, Au, Ag, stainless steel, polyvinyl chloride and glass).

The adsorption of promethium on platinum in hydrochloric acid solutions increases with decreasing acidity (studied to pH 2), as in nitric acid solutions, but the amounts adsorbed are about half as great.

The adsorption of ruthenium from 10 *N* HCl is practically zero. Between pH 0 and 5.20, its adsorption on gold also passes through a maximum at pH 4.5. On platinum and polyvinyl chloride, a rapid increase of adsorption is observed up to pH 5, where it attains  $155 \times 10^{-15}$  mole/cm.<sup>2</sup> on platinum and  $103 \times 10^{-15}$  mole/cm.<sup>2</sup> on polyvinyl chloride.

The adsorption of ruthenium on platinum or gold from sulfuric acid solutions is considerably higher than from nitric acid, but after an initial increase of adsorption as the pH rises to zero, no regular variation with the pH is observed.

The following table indicates the amounts adsorbed from H<sub>2</sub>SO<sub>4</sub> solutions, in units of 10<sup>-15</sup> mole/cm.<sup>2</sup>, at different pH values.

| pH       | (10 <i>N</i> ) | 1.3   | 2     | 3    | 4     | 5.2   |
|----------|----------------|-------|-------|------|-------|-------|
| Platinum | 9.45           | 90.4  | 43.05 | 90.4 | 64.55 | 86    |
| Gold     | 6.5            | 68.85 | 77.5  | 94.7 | 60.25 | 64.55 |

Adsorption-pH data showing maxima have been observed already by Starik and co-workers for the adsorption of promethium<sup>6</sup> and Ru<sup>III</sup> (containing no NO group)<sup>7</sup> on glass. They give the maxima for adsorption of promethium on this surface at pH 6.2. The same authors have also found maxima for the adsorption of La and of Ru<sup>IV</sup> on glass.

Maxima have been observed by other authors for thorium,<sup>8</sup> yttrium, cerium and cobalt,<sup>9</sup> while the increase of adsorption with pH, has been observed for Pa<sup>2</sup> and Pu<sup>3</sup> and in certain other cases.

**Nature of the Adsorbent Surface.**—The quantitative differences between the observed adsorptions on the metallic surfaces are generally so small that, when varying the experimental conditions, inversions in the order of adsorption can take place. Thus, *e.g.*, at the maximum of adsorption of promethium from nitric acid solutions, the different surfaces which we have examined can be arranged in the order of increasing adsorption Pt < Ag < stainless steel < polyvinyl chloride, while for cerium, the order is stainless steel < Au, Pt, Ag < glass < polyvinyl chloride. For the adsorption of ruthenium from nitric acid solutions at pH 3, the order is glass < Ag < Pt < Au < polyvinyl chloride < Ni, while at the maximum adsorption (pH 4.5), the order becomes glass < polyvinyl chloride < Au < Pt < Ag.

Some measurements have been carried out on nickel. In spite of the visible dissolution of the metal, the adsorbed amounts are much greater than those on the noble metals, nearly 100 times at pH 2.

In hydrochloric acid solutions, depending on the

pH, polyvinyl chloride adsorbs more than platinum or gold (pH < 3) or less (pH ~ 4).

The inversion in the relative adsorption capacities of noble metals and glass has already been observed in other cases: thorium is more extensively adsorbed on glass than on platinum,<sup>8</sup> while the inverse has been observed for the adsorption of plutonium from sulfuric acid solutions.<sup>3</sup> In the adsorption of protactinium, glass stands between platinum (which adsorbs more) and gold.<sup>2</sup>

**Effect of Concentration and Temperature.**—In labelling a nitric acid solution (pH 3) of inactive Ru(NO)(NO<sub>3</sub>)<sub>3</sub> with <sup>106</sup>Ru, we were able to examine the variation with concentration of adsorption on platinum, between 10<sup>-9</sup> and 10<sup>-3</sup> *M* at 20 and 60°. At both temperatures, the amount adsorbed *a*<sub>ad</sub> follows Henry's law, *i.e.*, it is proportional to the quantity remaining in solution, *a*<sub>s</sub>

$$a_{ad} = k a_s \quad (1)$$

The value of the constant *k* at 20° is  $5.6 \times 10^{-6}$  cm.<sup>-1</sup>, and increases to 10<sup>-5</sup> cm.<sup>-1</sup> at 60°.

The same law holds for the adsorption of ruthenium on platinum from 1 *N* hydrochloric acid at 20°, and from hydrochloric acid of pH 2.5 at 20, 40 and 60°, where the values of *k* are  $1.41 \times 10^{-6}$ ,  $3.55 \times 10^{-6}$  and  $7.08 \times 10^{-6}$  cm.<sup>-1</sup>, respectively.

The application of the Clapeyron-Clausius equation gives the values of the heats of adsorption which are, *Q* = 1.5 kcal./mole in nitric acid solutions and 3.15 kcal./mole in hydrochloric acid solutions.

At 20°, a monoatomic layer of ruthenium is adsorbed on platinum from a solution of about 10<sup>-3</sup> *M* in nitric acid at pH 3, and about  $5 \times 10^{-6}$  *M* in hydrochloric acid at pH 2.5, assuming that the apparent surface area is the true one. Balaschova estimates the roughness factor of smooth platinum to be 1.5.<sup>10</sup> The error introduced by neglecting this factor is probably overcompensated for by our choice of ionic radius.

On the other hand, we have not found any measurable effect of temperature between 20 and 60° on the adsorption of promethium (about 10<sup>-7</sup> *M*, in nitric acid, of pH 2), on platinum or polyvinyl chloride, nor on the adsorption of cerium (about 10<sup>-5</sup> *M*, in nitric acid of pH 3), on platinum. The isotherms of adsorption of promethium and of cerium on platinum at 20° are also different from those of ruthenium. These isotherms were determined, as above, in nitric acid solutions, at pH 2 in the case of promethium, and at pH 3 in that of cerium.

In order to study the effect of concentration on adsorption of promethium, and given that the maximum concentration of our solutions of promethium was about 10<sup>-8</sup> *M*, we have measured the adsorption of samarium, labelled with promethium, from solutions of 10<sup>-7</sup> to 10<sup>-3</sup> *M*. It is reasonable to assume that the adsorbabilities of promethium and samarium, near neighbors in the lanthanide family and whose radii differ only by 0.01 Å., are identical within the limits of experimental error. The concentrated solutions of cerium were prepared from the inactive nitrate, labelled with

(6) I. E. Starik and M. C. Lambet, *J. Inorg. Chem. (Russian)*, **3**, 136 (1958).

(7) I. E. Starik and A. B. Kossitsyn, *ibid.*, **2**, 444 (1957).

(8) J. Rydberg and B. Rydberg, *Svensk Kem. Tid.*, **64**, 199 (1952).

(9) J. Siejka and I. G. Campbell, 2nd U. N. Internat. Conf. on Peaceful Uses of Atom. Energy, P/1589 (1958).

(10) N. A. Balaschova, *Z. physik. Chem.*, **207**, 340 (1957).

$^{144}\text{Ce}$ . It is to be noted that the concentrations of these last solutions (which we shall call "macroscopic") were accurately known, while, as we have already mentioned, the absolute concentrations of the active (microscopic) solutions from Harwell, were uncertain. Therefore, we plotted, separately, the amounts adsorbed, at equilibrium, as a function of the absolute concentration of the macroscopic solutions (curve A), and as a function of the relative, microscopic, concentrations (curve B). We have then adjusted one of the points of curve B in such a way that it falls on curve A and calculated the corresponding concentration. This permitted the calculation of the absolute concentrations of all the other points of curve B so that the two curves overlap. This result has shown that the ponderable impurities which accompanied the radio-cerium source consisted either of cerium itself or another lanthanide having similar properties. The concentrations employed were from  $3.5 \times 10^{-8}$  to  $3.5 \times 10^{-4}$   $M$ . This curve was traced in logarithmic coordinates to cover the whole range of concentrations studied. For the smallest concentrations, the curve is approximately linear, but levels off for concentrations higher than  $10^{-5}$   $M$ . The same form is shown by the corresponding curve for Pm-Sm. The Freundlich isotherm, which corresponds to a linear variation of  $\log a_{ad}$  as a function of  $\log a_s$  for all concentrations must therefore be excluded.

The range of concentration examined was too extensive to permit the usual graphical tests for the applicability of the Langmuir isotherm

$$a_d = \frac{a_m b a_s}{1 + b a_s} \quad (2)$$

by plotting, for example  $a_s/a_d$  against  $a_s$  which should give a straight line. We were nevertheless able to show by calculation that the experimental results agree satisfactorily with this isotherm if the following values of the constants are adopted

Pm-Sm

$$a_m = 5 \times 10^{-3} \text{ monoatomic layer; } b = 4 \times 10^4 M^{-1} \\ (\tau_{\text{Pm}^{3+}} = 0.98 \text{ \AA.})$$

Ce

$$a_m = 4.8 \times 10^{-3} \text{ monoatomic layer; } b = 2.8 \times 10^5 M^{-1} \\ (\tau_{\text{Ce}^{3+}} = 1.02 \text{ \AA.})$$

The maximum coverage, therefore, corresponds only to a very small fraction of the surface.

Before discussing the significance of this result, we have also to consider the possible adsorption of the ions  $\text{H}^+$  and the anions. We have seen that the adsorption of  $\text{Pm}^{3+}$  and of  $\text{Ce}^{3+}$  or partly hydrolyzed forms diminishes with increasing  $\text{H}^+$  concentration. Furthermore, the parts of the  $p\text{H}$  curves between zero and the maximum of adsorption (Fig. 2 for promethium) could be considered to be hyperbolic. We can therefore interpret this variation as a consequence of the competition between the two ionic species ( $\text{Pm}^{3+}$  or  $\text{Ce}^{3+}$  and  $\text{H}^+$ ) and assume that the adsorption of  $\text{H}^+$  also follows Langmuir's law and apply the isotherm of binary mixtures<sup>11</sup> where the index<sup>1</sup> corresponds to a

$$a_d' = \frac{a_m b' a_s'}{1 + b' a_s' + b'' a_s''} \quad (3)$$

trivalent ion,  $\text{Pm}^{3+}$  or  $\text{Ce}^{3+}$  and  $''$  to  $\text{H}^+$  ions.

Equation 3 shows that at constant  $a_s'$ , the variation of adsorption ( $a_d'$ ) with  $a_s''$  ( $\text{H}^+$ ) is hyperbolic. In the usual interpretation of Langmuir's isotherm,  $a_m$  is independent of the nature of the adsorbate and corresponds to a monoatomic layer, although these assumptions are not always experimentally valid.<sup>12</sup> We have however attempted to choose values for the constants  $a_m$ ,  $b'(\text{Pm}^{3+} + \text{Sm}^{3+})$ ,  $b'(\text{Ce}^{3+})$  and  $b''(\text{H}^+)$  which would enable us to calculate the isotherms and the variations of adsorption with  $p\text{H}$  at a constant adsorbate concentration.

The results of these calculations are compared below with the experimental results (Table I and II) taking

for Pm + Sm at  $p\text{H}$  2

$$a_m = 5 \times 10^{-3} \text{ monoatomic layer} \\ b' = 2 \times 10^5 M^{-1} \\ b''(\text{H}^+) = 2.5 \times 10^2 M^{-1}$$

for Ce at  $p\text{H}$  3

$$a_m = 4.8 \times 10^{-3} \text{ monoatomic layer} \\ b' = 4.4 \times 10^5 M^{-1} \\ b''(\text{H}^+) = 4 \times 10^2 M^{-1}$$

Given the limits of experimental errors, which are relatively high for the phenomena studied, the agreement is satisfactory. Satisfactory agreement has also been obtained with an adsorption isotherm of Pm + Sm in 0.5  $N$   $\text{HNO}_3$ , taking

$$a_m = 5 \times 10^{-3} \text{ monoatomic layer} \\ b' = 2.5 \times 10^5 M^{-1} \\ b'' = 2.5 \times 10^2 M^{-1}$$

In comparing the values of  $b'$ , which express the probability of fixation of the adsorbate on the surface, it is found that  $\text{Ce}^{3+}$  is slightly more adsorbable than  $\text{Pm}^{3+}$ . The  $\text{H}^+$  ions are about a thousand times less adsorbable than the trivalent lanthanide ions, and the ratio  $b'/b''$  seems to be approximately constant for the three isotherms.

The fact that the maximum adsorption of these cations is much less than a monoatomic layer is probably related to the mechanism of the adsorption process. We notice first that the adsorption maxima ( $a_m$ ) are of the order of magnitude necessary to charge the molecular condenser of Helmholtz. The maximum charge carried by the adsorbed ions  $q = a_m z F$  (where  $z$  is the valency, and  $F$ , the faraday), is found for Pm + Sm to be  $2.5 \times 10^{-11} \times 3 \times 965000 \approx 7.2 \times 10^{-6}$  coulombs/cm.<sup>2</sup>; for Ce to be about  $5.5 \times 10^{-6}$  coulombs/cm.<sup>2</sup>. Furthermore, the capacity of the double layer at the surface of platinum is of the order of 20 microfarads/cm.<sup>2</sup><sup>13</sup> and we may assume that the potential difference of the Helmholtz molecular condenser is between 0.1 and 0.2 volt. This gives for  $q$  a value of 2 to  $4 \times 10^{-6}$  coulomb/cm.<sup>2</sup>, a little less than those found experimentally using the geometric area, which, as we have seen, is 30% smaller than the real one. It must also be taken into account that at the  $p\text{H}$  of our isotherms, a part of the

(12) S. Brunauer, "The Adsorption of Gases and Vapors," Vol. 1, Princeton University Press, Princeton, N. J., 1945.

(13) Th. G. Overbeek, "Electrochemistry of the Double Layer," in M. R. Kruyt, "Colloid Science," Vol. 1, Amsterdam, 1952, p. 115.

(11) E. C. Markham and A. F. Benton, *J. Am. Chem. Soc.*, **53**, 497 (1931).

TABLE I

| ADSORPTION OF PROMETHIUM + SAMARIUM (IN MONOATOMIC LAYERS) AS A FUNCTION OF CONCENTRATION ( $\text{HNO}_3$ at pH 2) |                        |                       |                      |                      |                      |                       |                      |                      |                      |
|---------------------------------------------------------------------------------------------------------------------|------------------------|-----------------------|----------------------|----------------------|----------------------|-----------------------|----------------------|----------------------|----------------------|
| $a_s$ (M)                                                                                                           | $1.35 \times 10^{-10}$ | $3.7 \times 10^{-10}$ | $1.2 \times 10^{-9}$ | $5 \times 10^{-9}$   | $7.5 \times 10^{-9}$ | $1.25 \times 10^{-7}$ | $10^{-5}$            | $10^{-3}$            | $10^{-1}$            |
| $a_d$ measd.                                                                                                        | $1.6 \times 10^{-7}$   | $3.2 \times 10^{-7}$  | $7 \times 10^{-7}$   | $7 \times 10^{-7}$   | $10^{-6}$            | $2 \times 10^{-6}$    | $2 \times 10^{-5}$   | $1.5 \times 10^{-3}$ | $5 \times 10^{-2}$   |
| $a_d$ calcd.                                                                                                        | $2.5 \times 10^{-8}$   | $7.4 \times 10^{-8}$  | $2.4 \times 10^{-7}$ | $2.4 \times 10^{-7}$ | $10^{-6}$            | $2.5 \times 10^{-5}$  | $2 \times 10^{-5}$   | $2 \times 10^{-3}$   | $4.9 \times 10^{-3}$ |
| AS A FUNCTION OF ACIDITY ( $a_s = 5 \times 10^{-9} M$ )                                                             |                        |                       |                      |                      |                      |                       |                      |                      |                      |
| $\text{HNO}_3$ (V)                                                                                                  | 10                     | 1                     | $10^{-1}$            | $10^{-2}$            | $10^{-3}$            | $10^{-4}$             | $10^{-4}$            | $10^{-5}$            | $10^{-5}$            |
| $a_d$ measd.                                                                                                        | 0                      | 0                     | $2 \times 10^{-7}$   | $10^{-6}$            | $2 \times 10^{-6}$   | $2 \times 10^{-6}$    | $3 \times 10^{-6}$   | $4 \times 10^{-6}$   | $4 \times 10^{-6}$   |
| $a_d$ calcd.                                                                                                        | $2 \times 10^{-5}$     | $2 \times 10^{-5}$    | $2 \times 10^{-7}$   | $2.4 \times 10^{-6}$ | $4 \times 10^{-6}$   | $4 \times 10^{-6}$    | $4.6 \times 10^{-6}$ | $4.8 \times 10^{-6}$ | $4.8 \times 10^{-6}$ |

TABLE II

| ADSORPTION OF CERIUM (IN MONOATOMIC LAYERS) AS A FUNCTION OF CONCENTRATION ( $\text{HNO}_3$ at pH 3) |                      |                      |                      |                      |                      |                      |                      |                      |                      |                      |                      |
|------------------------------------------------------------------------------------------------------|----------------------|----------------------|----------------------|----------------------|----------------------|----------------------|----------------------|----------------------|----------------------|----------------------|----------------------|
| $a_s$ (M)                                                                                            | $3.5 \times 10^{-8}$ | $7.4 \times 10^{-8}$ | $2.4 \times 10^{-7}$ | $4 \times 10^{-7}$   | $6.8 \times 10^{-7}$ | $8 \times 10^{-7}$   | $10^{-6}$            | $2.4 \times 10^{-6}$ | $3.2 \times 10^{-6}$ | $4 \times 10^{-6}$   | $8 \times 10^{-6}$   |
| $a_d$ measd.                                                                                         | $8.6 \times 10^{-5}$ | $1.3 \times 10^{-4}$ | $2.8 \times 10^{-4}$ | $4.3 \times 10^{-4}$ | $5.7 \times 10^{-4}$ | $7.6 \times 10^{-4}$ | $1.9 \times 10^{-3}$ | $2.2 \times 10^{-3}$ | $3.8 \times 10^{-3}$ | $2.1 \times 10^{-3}$ | $2.9 \times 10^{-3}$ |
| $a_d$ calcd.                                                                                         | $4.8 \times 10^{-5}$ | $1 \times 10^{-4}$   | $3.3 \times 10^{-4}$ | $4.8 \times 10^{-4}$ | $7.6 \times 10^{-4}$ | $9 \times 10^{-4}$   | $1.7 \times 10^{-3}$ | $2 \times 10^{-3}$   | $4.3 \times 10^{-3}$ | $4.4 \times 10^{-3}$ | $4.6 \times 10^{-3}$ |
| AS A FUNCTION OF ACIDITY ( $a_s = 8 \times 10^{-7} M$ )                                              |                      |                      |                      |                      |                      |                      |                      |                      |                      |                      |                      |
| $\text{HNO}_3$ (V)                                                                                   | 10                   | 2                    | 1                    | $10^{-1}$            | $10^{-2}$            | $10^{-3}$            | $10^{-3}$            | $10^{-4}$            | $10^{-4}$            | $10^{-4}$            | $10^{-4}$            |
| $a_d$ measd.                                                                                         | 0                    | 0                    | 0                    | $4.5 \times 10^{-5}$ | $2.7 \times 10^{-5}$ | $3.6 \times 10^{-4}$ | $3.6 \times 10^{-4}$ | $7.6 \times 10^{-4}$ | $1.9 \times 10^{-3}$ | $1.7 \times 10^{-3}$ | $1.7 \times 10^{-3}$ |
| $a_d$ calcd.                                                                                         | $4.5 \times 10^{-7}$ | $2.2 \times 10^{-6}$ | $2.2 \times 10^{-6}$ | $4.5 \times 10^{-6}$ | $4.4 \times 10^{-5}$ | $3.6 \times 10^{-4}$ | $3.6 \times 10^{-4}$ | $1.3 \times 10^{-3}$ | $1.3 \times 10^{-3}$ | $1.3 \times 10^{-3}$ | $1.3 \times 10^{-3}$ |

lanthanide ions are hydrolyzed and carry a charge smaller than 3 ( $\text{PmOH}^{2+}$ ,  $\text{PmO}^+$ , etc).

On the other hand, it has been shown by Frumkin and co-workers, using electrochemical methods,<sup>14</sup> that at potentials more negative than that corresponding to the zero point of charge, the surface of a metal adsorbs the cations, while at more positive potentials, it is the anions which are primarily adsorbed and which, in turn, attract the cations electrostatically (outer Helmholtz plane of Grahame<sup>15</sup>). These results have been confirmed recently by Balaschova<sup>10,16</sup> for the case of platinum, with the help of radioactive indicators. The spontaneous potential of platinum in our solutions, was found, depending on the pH, to be from +0.74 to +0.85 v., with respect to the normal hydrogen electrode. We suggest, therefore, that the adsorption of  $\text{Ce}^{3+}$  and of  $\text{Pm}^{3+}$  which we observe is of this secondary origin. It would not be surprising should the amounts adsorbed be a little higher than that necessary to charge the Helmholtz condenser, since the adsorption of anions is due, not only to coulombic forces, but also to chemical, or van der Waals, forces (*specific adsorption*). Experiments on the adsorption of anions and tritium will perhaps enable us to verify the proposed mechanism.

With regard to the anomalous effect which consisted in the continuous increase of adsorption after each immersion of the adsorbent, it may now be supposed that each time the metallic foil is withdrawn from the solution and dried, the double layer is destroyed and surface reactions occur which immobilize the adsorbed cations in such a way that they cannot participate in the adsorption equilibrium when the foil is replaced in the solution (*e.g.*, oxide or hydroxide formation). The ionic double layer must be rebuilt, increasing the adsorption, on a new immersion.

**Desorption. Reversibility.**—When foils of platinum or polyvinyl chloride, which have adsorbed promethium or cerium from a slightly acid solution, are placed in strong acid solutions of the same radioelement, they are completely deactivated in one or two hours. Similarly, when a foil in equilibrium with a solution of promethium of a given concentration and pH is placed in a solution of the same pH but of a smaller concentration of promethium, it retains, at the end of the operation, an adsorbed quantity which is only slightly higher than that which would correspond to equilibrium with the less concentrated solution.

The adsorption of ruthenium, on the contrary, is partially irreversible. For example, having obtained at pH 2.4 an activity of Rd-Ru of 319 counts/min. on a foil of platinum, we have immersed it in a solution of the same concentration of Rd-Ru but of pH 0. After 3.5 hours, the residual activity was 135 counts/min; and after 8.5 hours, 131 counts/min. On the other hand, the activity obtained by immersing a foil in a solution of pH 0 was increased from 63 to 227

(14) A. N. Frumkin, V. S. Bagotsky, Z. A. Iofa and B. N. Kabanov, "Kinetics of Electrode Processes," Moscow, 1952.

(15) D. C. Grahame, *Chem. Revs.*, **41**, 441 (1947).

(16) N. A. Balaschova, B. A. Ivanov and V. E. Kazarinov, *C. R. Acad. Sci. U.S.S.R.*, **115**, 336 (1957).

counts/min., by 20 minutes immersion in a solution of pH 2.4. Similar phenomena occur when we replace a solution by another of the same pH, but of a higher or lower concentration of ruthenium: *i.e.*, very slow and incomplete desorption (from 1863 to 1493 counts/min. in 18 hours), but rapid adsorption (from 329 to 1745 counts/min. in 30 minutes).

### Discussion

Our observations as a whole, illustrate the contrasting adsorption behavior of promethium (or, more generally, of the lanthanides) with that of ruthenium, particularly on platinum, which was examined more thoroughly than the other adsorbents. To summarize, we have observed: (1) reversible adsorption of promethium and cerium, partially irreversible adsorption of ruthenium; (2) no effect of temperature for promethium and cerium; an increase of adsorption for ruthenium; (3) Langmuir's isotherm is satisfied for promethium and cerium; Henry's law for ruthenium; (4) maximum surface coverage of about  $5 \times 10^{-3}$  of a monoatomic layer for promethium and cerium; one or more monoatomic layers from sufficiently concentrated solutions for ruthenium.

These contrasts in behavior probably correspond to different adsorption mechanisms. We have assumed for the lanthanides that their adsorption on platinum is due to the electrostatic attraction of a primary layer of adsorbed anions and have explained the effect of pH by the competitive adsorption of H<sup>+</sup> ions. The diminution of adsorption after the maximum may then be attributed to the formation of colloidal micelles, slightly adsorbable or poorly adherent to the surface. In the case of cerium, which is less basic than promethium, the formation of insoluble basic salts or the hydroxide must take place at a lower pH, in agreement with our observations.

At pH 3, at which the isotherms were determined, ruthenium is mostly hydrolyzed and is positively charged. We can therefore assume, for it, the same adsorption mechanism as for the lanthanides. At higher acidities, the Ru is probably partly in the form of anionic complexes, but these may be assumed to be sufficiently unstable, in the neighborhood of the double layer, to dissociate as a result of the electrostatic repulsion between the anionic component of the complex and the NO<sub>3</sub><sup>-</sup> ions adsorbed on the surface. The ruthenium being a noble metal, its adsorption may then be followed by electrochemical displacement of platinum and concomitant deposition, the extent of which would depend on the potential of platinum in the given medium. This would explain the partial irreversibility of adsorption and, perhaps, the low heats of adsorption (0.065 v., in nitric acid and 0.137 v. in hydrochloric acid), since ruthenium and platinum have very similar properties. The absence of saturation in the isotherm would then

be due to discharge of some of the ions on the surface (leaking condenser) and their replacement by adsorption of more ions of the same kind.

The pH effect could then be explained not only by competition with H<sup>+</sup> ions but also by the diminution of the potential of platinum with increasing pH, which favors the discharge of cations. We have found in fact that this potential with respect to the saturated calomel electrode takes the values, +0.66 in 0.5 N HNO<sub>3</sub>, +0.55 in 10<sup>-2</sup> N HNO<sub>3</sub> and +0.43 in 10<sup>-3</sup> N HNO<sub>3</sub>.

Independently of the above mechanisms, our experimental results exclude, for adsorption on platinum, the hypotheses of Starik and Kossytsin,<sup>7</sup> according to which the initial increase of adsorption of Ru<sup>III</sup> (without NO group) on glass is due to an increased formation of positively charged colloidal micelles and the diminution, after the maximum, to inversion of the sign of the micellar charge, glass being charged negatively. Since the surface of platinum, as we have seen, is positively charged, the mechanism of Starik and Kossytsin would lead to a pH effect which would be the opposite of that actually observed.

The mechanism of adsorption may of course vary with the nature of the adsorbent as well as with the nature of the adsorbate. For instance, the effect of acidity on the adsorption of thorium on glass is attributed by Rydberg and Rydberg<sup>8</sup> to the increasing ionic dissociation of silicic acid in the glass with increasing pH. These various interpretations are not necessarily contradictory. On the other hand, the attempts to these authors and of Starik and co-workers<sup>6,7</sup> to determine, even approximately, the solubility products of Th(OH)<sub>4</sub> or of Pm(OH)<sub>3</sub> from the adsorption behavior (the maximum on the adsorption-pH curves) of the radioelements on the indicator scale, do not seem justified.

It might be remembered, in fact that the whole problem of radiocolloids, which has given rise to so many controversies, began as a result of the incompatibility of their behavior with the solubility product values obtained from measurements on the macroscopic scale.

It has been shown<sup>17</sup> that the radiocolloids are systems which are not in the thermodynamic equilibrium, but in a polydispersed state which evolves very slowly toward equilibrium, increasing the proportion in the colloidal form. Consequently, it must be expected that the adsorption, at and after the pH corresponding to the maximum (the pH range corresponding to colloid formation) will diminish with the age of the solutions, in agreement with our observations.

The authors wish to thank Dr. A. M. Peers for help with the preparation of the English text.

(17) M. Hajssinsky, *Acta Phys. Chem. U.R.S.S.*, **3**, 517 (1935); "Les Radiocolloides," ed. Hermann, Paris, 1935. See also G. Schweitzer and W. Jackson, *J. Chem. Educ.*, **29**, 513 (1952).



THE REDUCTION OF CERIC IONS BY  $\text{Po}^{210}$  ALPHA PARTICLESBY J. WEISS<sup>1a</sup> AND N. MILLER<sup>1b</sup>*Department of Natural Philosophy, University of Edinburgh, Edinburgh, England**Received February 12, 1959*

Solutions of ceric sulfate, cerous sulfate and thalious sulfate in 0.8 *N* sulfuric acid have been irradiated using a one-curie  $\text{Po}^{210}$   $\alpha$ -source external to the solutions. The yield of ceric ion reduction was determined and a qualitative explanation of the results given. The  $G(\text{Ce}^{3+})$  without added solute was found to be  $2.88 \pm 0.02$  for 3.4 Mev.  $\alpha$ -particles.

## Introduction

The mechanism for the reduction of ceric ions by  $\gamma$ -radiation has been postulated by Allen<sup>2a</sup> and confirmed by Sworski.<sup>2b</sup> Sworski also studied the effect of added thalious ion on the reduction of ceric ion by radiation. The present work was undertaken to determine how the reduction of ceric ion, with and without added thalious ion, would be affected when  $\alpha$ -particles are used as the source of radiation.

## Experimental Procedure

Water distilled from acid permanganate solution and then from alkaline permanganate solution and finally through silica tubing at  $900^\circ$  was used to make up all solutions. Reagent grade ceric sulfate and cerous sulfate, C.P. thalious sulfate and reagent grade sodium chloride and ferrous ammonium sulfate were used without further purification.

The irradiations were carried out in a facility developed by Hart and Terandy<sup>3</sup> at the Argonne National Laboratory.  $\alpha$ -Particles from a source of  $\text{Po}^{210}$  on a tantalum backing passed through a space 1 cm. across, filled with helium at atmospheric pressure, and emerged into the air through a window 6 mm. in diameter, covered with mica of 1.09 mg./cm.<sup>2</sup> mass thickness, which served to contain the polonium contamination within the source holder. The irradiation cells, which could be placed so closely adjacent to the source holder that only a 1 mm. air gap was traversed by the  $\alpha$ -particles in going from one to another, also had a mica window 1.09 mg./cm.<sup>2</sup> in mass thickness, somewhat larger in diameter than that of the source holder, so that the reproducible positioning of the cells was not highly critical.

The mean energy of the  $\alpha$ -particles on reaching the solution was calculated by using the values for the stopping power of mica given by Riezler<sup>4</sup> and the range-energy relationships of Jesse and Sadauskis.<sup>5</sup> The geometry of the arrangement was such that the  $\alpha$ -particles entered the solution at angles up to  $31^\circ$  from the normal. Eighty-five per cent. of the total mass thickness of material traversed by the  $\alpha$ -particles before reaching the solution was represented by that of the two mica windows, the helium and air-filled gaps accounted for the remainder. A normally incident  $\alpha$ -particle, entered the solution with an energy of 3.5 Mev., and one at  $30^\circ$  from the normal at 3.2 Mev. The mean energy could, therefore, be taken at  $3.4 \pm 0.1$  Mev.

The cells were made of Pyrex glass and had an irradiation zone in the form of a flat cylinder 3 cm. in diameter and 1 cm. deep, with a mica window in the center of one face. The cell had two side arms of 1 mm. bore capillary tubing about 10 cm. long, one of which terminated in a 5/20 cone joint. After the cells had been filled, the end of the side arm could be sealed with a 5/20 cap, while the other capillary side arm was left open to the atmosphere. During irradiation, the contents were agitated by a magnetically operated stirrer.

No absolute measurements of the energy reaching the solutions were attempted. The yields were determined by measuring the ferric yield in the standard dosimeter solution irradiated in the same apparatus for which a  $G$ -value of 4.7

ferric ions per 100 e.v. was used based on previously published data<sup>6</sup> and comparing this to the ceric conversion.

The changes in the ceric ion concentration were determined spectrophotometrically at 320  $m\mu$  using 5580 for the molar extinction coefficient. A molar extinction coefficient of 2199 at  $24.9^\circ$  was used for ferric ion at 304  $m\mu$ .

## Experimental Results

The standard Fricke ferrous sulfate dosimetric solution was used to calibrate the  $\text{Po}^{210}$  source and determine the  $G$ -value for  $\text{Ce}^{3+}$  production. Using a value of 4.7 for  $G(\text{Fe}^{3+})$ , a value of  $2.88 \pm 0.02$  was obtained for  $G(\text{Ce}^{3+})$ . The reduction of ceric ion was independent of initial ceric ion concentration from  $10^{-3} M$  to  $10^{-5} M$  (Fig. 1).

When thalious ion is added to the system, the effect on the yield of cerous ion is significantly different for  $\alpha$ -particle and  $\gamma$ -ray irradiations. In the case of  $\gamma$ -rays, Sworski<sup>2</sup> found that the yield of cerous ion went from 2.39 without thalious ion

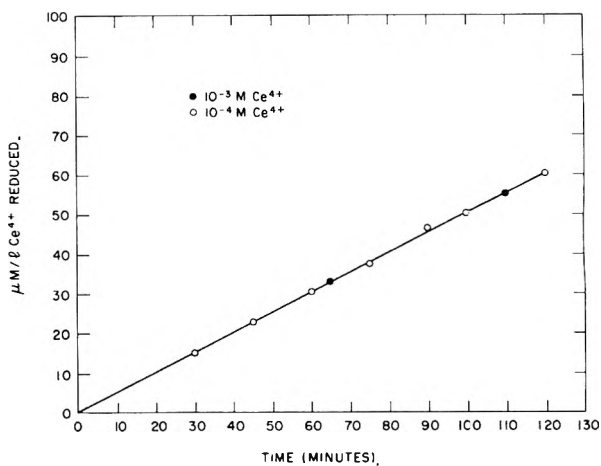


Fig. 1.—Reduction of ceric ion as a function of time. Initial ceric concentration was varied from  $10^{-3}$  to  $10^{-5} M$ .

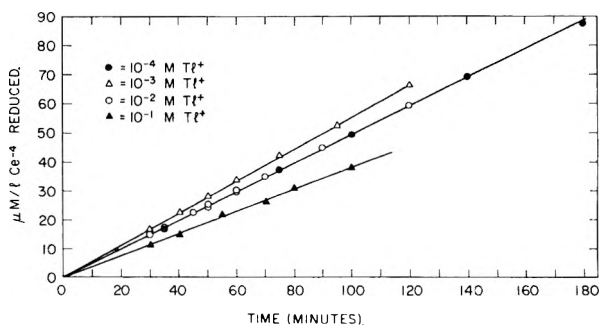


Fig. 2.—Effect of varying thalious ion concentration on the reduction of ceric ion. The rate of reduction with no thalious ion coincided with the rate with  $10^{-4}$  and  $10^{-2} M \text{ Tl}^{3+}$ .

(1) (a) Brookhaven National Laboratory, Upton, N. Y.; (b) Deceased, May 4, 1958.

(2) (a) A. O. Allen, *Rad. Res.*, **1**, 85 (1954); (b) T. J. Sworski, *ibid.*, **4**, 483 (1956).

(3) E. J. Hart and V. Terandy, *Rev. Sci. Instr.*, **29**, 962 (1958).

(4) W. Riezler, *Ann. Phys.*, **36**, 350 (1939).

(5) W. P. Jesse and J. Sadauskis, *Phys. Rev.*, **78**, 1 (1950).

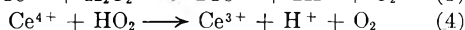
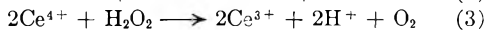
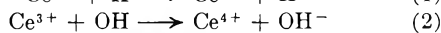
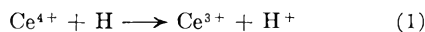
(6) N. Miller, *Rad. Res.*, **7**, 653 (1958).

to 7.92 when thalious ion was added. The effect of added thalious ion in the present work is shown in Fig. 2 and Fig. 3.

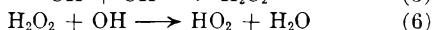
The reduction of ceric ion was also determined as a function of the concentration of initially added cerous ion. The results obtained are shown in Fig. 4 and Fig. 5.

### Discussion

The reduction of ceric ion by radiation proceeds according to the same mechanism whether the irradiation source be alpha particles or  $\gamma$ -rays.



Reaction 4 is important only in the case of high ion density where reactions 5 and 6 play an important part.



The effects observed on the addition of thalious and cerous ion can be explained qualitatively on the basis of reactions 5 and 6. If one assumes that reaction 6 takes place outside the main body of the  $\alpha$ -particle track, then relatively small concentrations of thalious or cerous ion can compete

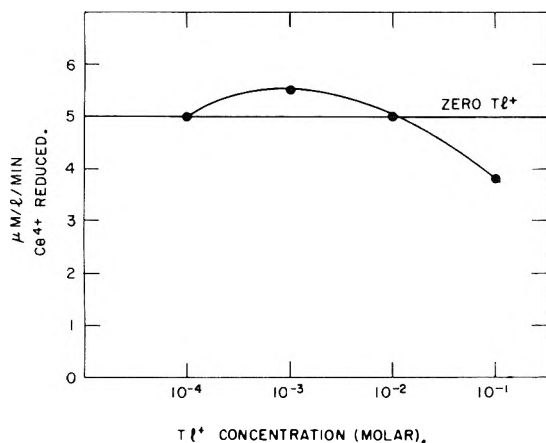


Fig. 3.—The rate of ceric ion reduction as a function of initial thalious ion concentration.

with  $\text{H}_2\text{O}_2$  for the OH radicals. If cerous ion scavenges an OH radical which would have reacted according to reaction 6 there will be no net effect on the  $G(\text{Ce}^{3+})$ . If thalious ion does the scavenging there will be a net increase in reducing equivalents and the  $G(\text{Ce}^{3+})$  will increase. As the concentration of scavenger is increased, reaction

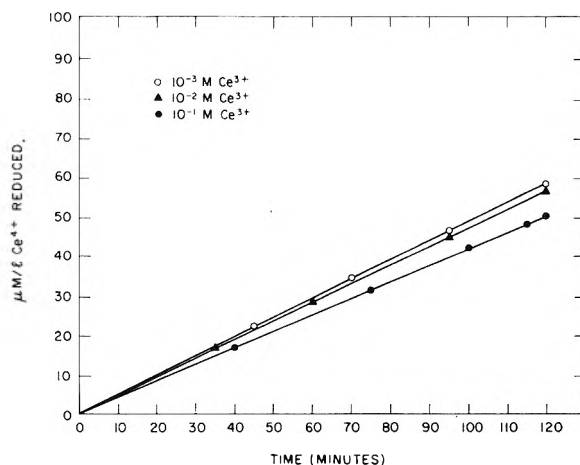


Fig. 4.—Effect of varying the initial cerous ion concentration on the reduction of ceric ion. The rate of reduction with no added cerous ion coincided with the curve for  $10^{-3}$  M initial cerous ion.

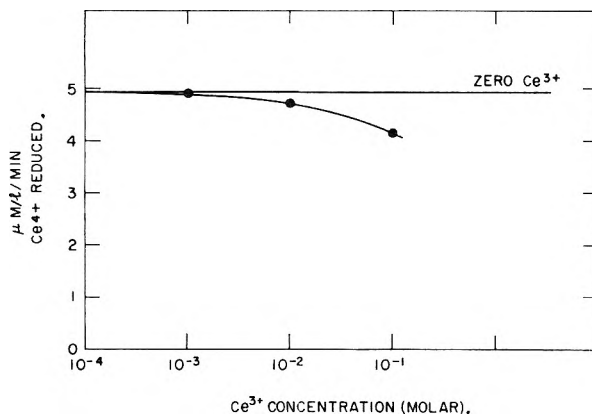


Fig. 5.—The rate of ceric ion reduction as a function of initial cerous ion concentration.

5 becomes significantly affected and the  $G(\text{H}_2\text{O}_2)$  as well as the  $G(\text{Ce}^{3+})$  decreases.

It is felt that a clearer picture of the mechanism of this reaction would be obtained if the thalious ion concentration could be determined and if the oxygen yields were also determined.

**Acknowledgments.**—We would like to record our gratitude to Dr. J. Stevenson, Radiochemical Center, Amersham, for supplying the Po source as well as a supply of very thin mica. One of us (J.W.) wishes to make acknowledgment to the University of Edinburgh for the grant of a Dewar Research Fellowship, during the tenure of which this work was carried out, and also wishes to thank A. O. Allen and H. Schwarz for many helpful suggestions and discussions.

## KINETICS OF THE RUTHENIUM-CATALYZED ARSENIC(III)-CERIUM(IV) REACTION<sup>1</sup>

By C. SURASITI AND E. B. SANDELL

*School of Chemistry, University of Minnesota, Minneapolis, Minn.*

*Received February 13, 1959*

The rate of the ruthenium-catalyzed reaction of cerium(IV) with arsenic(III) in sulfuric acid solution is independent of arsenic(III), arsenic(V), cerium(III) and hydrogen-ion concentrations. The rate expression (25°) is  $-d[\text{Ce(IV)}]/dt = \{4.0 \times 10^{10}[\text{Ru}][\text{Ce(IV)}]^{2.6}/\{1 + 2.1 \times 10^3[\text{Ce(IV)}]^{1.6}\}$ , in which concentrations are given in moles per liter and time in minutes.

The very slow reaction between arsenic(III) and cerium(IV) in sulfuric acid solution is strongly catalyzed by iodine, osmium and ruthenium. The catalysis by iodine and osmium has already received attention especially because of its importance in the determination of traces of these elements. The study summarized here dealt with the kinetics but not the mechanism of the ruthenium-catalyzed reaction.

### Experimental

**Reagents. Arsenious Oxide, 0.2000 N Solution.**—Reagent grade  $\text{As}_2\text{O}_3$  (9.892 g.) was dissolved in 30 ml. of 1 *M* sodium hydroxide and the solution was diluted to 1 liter after acidification with sulfuric acid.

**Ceric Ammonium Sulfate Solution, 0.2000 N.**—A solution obtained by dissolving 126 g. of the dihydrate in 2 *M* sulfuric acid and diluting to 1 liter was allowed to stand for two weeks, filtered and standardized against arsenious oxide. This solution was diluted with 2 *M* sulfuric acid to make the ceric concentration 0.2000 *N*, and the normality was verified by restandardization.

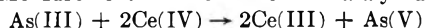
**Ruthenium(IV) Sulfate.**—A solution of potassium ruthenate, obtained by fusing metallic ruthenium with a mixture of potassium hydroxide and sodium peroxide in a gold crucible, was added slowly with vigorous stirring to 1 *M* sulfuric acid. The resulting solution was treated with 30% hydrogen peroxide and evaporated to half its volume. The evaporation was repeated several times after addition of water and hydrogen peroxide. This treatment served to remove any osmium present. Ruthenium tetroxide was distilled from the resulting solution after addition of ceric ammonium sulfate and absorbed in ice-cooled sulfuric acid solution containing hydrogen peroxide. This solution was heated overnight to destroy hydrogen peroxide and filtered through sintered glass. The ruthenium concentration of the solution was obtained by hydrolytic precipitation of hydrous ruthenium(IV) oxide (sodium bicarbonate as neutralizing agent), followed by ignition of the precipitate to ruthenium metal in hydrogen and nitrogen. The metal was leached with hot water to remove any soluble salts present.

The stock ruthenium sulfate solution was suitably diluted to obtain working solutions. Solutions as dilute as 0.01  $\gamma$  Ru per ml. (in 2 *M* sulfuric acid) showed no change in concentration in a year's time.

**Ruthenium Tetroxide.**—The tetroxide, obtained as described above, was swept through anhydrous magnesium perchlorate in a stream of nitrogen and trapped in a U-tube immersed in Dry Ice-acetone. The collected tetroxide was distilled into another cooled trap. Solutions of ruthenium tetroxide were prepared by dissolving weighed amounts in 1 *M* sulfuric acid.

**Water.**—Deionized water was doubly distilled, first from alkaline permanganate in a tin still, then from alkaline permanganate in a Pyrex still with a 40 cm. Vigreux column to trap spray.

**Rate Measurements.**—The rate of the catalyzed reaction



was obtained by determining spectrophotometrically the concentration of cerium(IV) in the reaction mixture as a function of time. The ceric ammonium sulfate solution,

to which ruthenium had been added as the sulfate(IV) or tetroxide, was added by means of a hypodermic syringe to the magnetically stirred arsenious oxide solution. A Beckman DU spectrophotometer was used in conjunction with a percentage transmittance-time recorder (Varian graphic recorder model G-10) for the photometric measurements. All solutions were thermostated at  $25.0 \pm 0.1^\circ$  before mixing and during the transmittance measurements.

The percentage transmittance-time curve was transformed into a concentration-time curve with the aid of standard curves prepared from cerium(IV) solutions containing appropriate amounts of arsenic(III) and arsenic(V), which affect the absorbance of cerium(IV). The concentration-time curve was extrapolated to zero time and the initial rate was obtained by finding the slope of the curve at zero time.

When the initial reaction rate was not needed, the "reaction time" was measured, this being the time required for a given fraction of cerium(IV) to react. Usually the time required for one-half of the original amount of cerium(IV) to be reduced was taken as the reaction time.

### Results

#### Effect of Initial Oxidation State of Ruthenium.

The results obtained will be summarized without presenting the data. Provided that ruthenium is added to the ceric solution before this is mixed with the arsenite solution, the rate of the catalyzed reaction is the same whether ruthenium(IV) sulfate or ruthenium tetroxide is used. Ruthenium(IV) is completely oxidized to ruthenium(VIII) by ceric sulfate within 10 seconds. However, if ruthenium(IV) sulfate is added first to the arsenite solution, the reaction rate is markedly lower.

If ruthenium tetroxide solution is added with good stirring to excess arsenite solution acidified with sulfuric acid, the reaction rate is almost the same as when the tetroxide is added to the ceric solution and, moreover, does not depend on the time elapsing before the arsenite-ruthenium solution is mixed with the ceric solution. But if the mixing is poor so that there is an appreciable local excess of the tetroxide, the reaction rate decreases and is irreproducible.

It was observed that treatment of a ruthenium tetroxide solution with arsenious oxide in the amount needed to reduce ruthenium(VIII) to ruthenium(IV) gave a reddish brown solution (the color of  $\text{Ru(SO}_4)_2$ ), which did not change on subsequent addition of more arsenious oxide. On the other hand, if a large excess of arsenious oxide was added to well-stirred ruthenium tetroxide solution, a straw-yellow color characteristic of ruthenium(III) was produced. The conclusion may be drawn that, once formed, ruthenium(IV) is stable, and can be obtained in a form which is not very active catalytically. Further, ruthenium(III) in arsenious oxide solution shows a catalytic

(1) From the Ph.D. thesis of C. Surasiti, University of Minnesota, 1957.

activity much the same as that of ruthenium-(VIII) originally present in ceric solution.

**Effect of Arsenic(III) Concentration.**—The initial rate of the catalyzed reaction as a function of the arsenious oxide concentration was determined at a constant cerium concentration of 0.0250 *N* and a constant ruthenium concentration of  $2.46 \times 10^{-7}$  *M* in a 2.0 *M* sulfuric acid solution at 25.0°. The rate was found to be independent of the arsenic-(III) concentration. An average value of 0.0286 mole l.<sup>-1</sup>min.<sup>-1</sup> was found for  $(-d[\text{As(III)}]/dt)_0$  over the range 0.01 – 0.08 *M* As(III), the lowest and highest values of eight measurements being 0.0274 and 0.0296. The ionic strength was maintained constant in this series with sodium sulfate.

**Effect of Arsenic(V) and Cerium(III) Concentrations and Other Factors.**—The effect of these on the rate was tested in a mixture which was 0.030 *N* in As(III), 0.020 *N* in Ce(IV) and 2.0 *M* in sulfuric acid, and which contained 0.02  $\gamma$  Ru/ml. ( $1.96 \times 10^{-7}$  *M*). Sodium perchlorate was added to keep the ionic strength constant. The rate remained constant over the range of concentrations examined: As(V), 0–0.025 *M*; Ce(III), 0–0.04 *M*.

Variation in ionic strength has but a small effect on the rate of the catalyzed reaction (Table I), the rate increasing slightly as the ionic strength is raised.

TABLE I

RECIPROCAL OF HALF-REACTION TIME<sup>a</sup> AS FUNCTION OF IONIC STRENGTH  
(0.0075 *N* As(III), 0.005 *N* Ce(IV), 0.020  $\gamma$  Ru/ml., 0.5 *M* H<sub>2</sub>SO<sub>4</sub>)

|                                                 |      |      |      |      |      |      |
|-------------------------------------------------|------|------|------|------|------|------|
| Ionic strength                                  | 0.5  | 1.1  | 1.7  | 2.3  | 2.9  | 3.5  |
| 1/ <i>t</i> <sub>1/2</sub> , min. <sup>-1</sup> | 8.56 | 7.80 | 7.11 | 7.40 | 6.67 | 7.11 |

<sup>a</sup> The half-reaction time, *t*<sub>1/2</sub>, is defined as the time required for one-half of the Ce(IV) to be reduced.

Variation in the concentration of sulfuric acid from 0.5 to 2.0 *M* in a mixture of 0.0050 *N* cerium-(IV) and 0.0075 *N* arsenic(III) containing 0.04  $\gamma$  Ru/ml., in which the ionic strength was maintained constant with sodium bisulfate, produced no change in reaction rate.

Chloride reduces the reaction rate markedly. Thus, in a mixture which was 0.020 *N* in Ce(IV), 0.025 *N* in As(III) and 2.0 *M* in sulfuric acid, and which contained 0.0060  $\gamma$  Ru/ml., the half-reaction times (minutes) varied as follows with the indicated sodium chloride concentrations: 0.0000 *M*, 1.05; 0.0005 *M*, 1.73; 0.0010 *M*, 3.49; 0.0020 *M*, 10.5; 0.0050 *M*, 22.5. In these experiments the sodium chloride was added to the ceric solution before mixing with arsenite.

**Initial Rate of Catalyzed Reaction as a Function of the Ce(IV) and Ruthenium Concentrations.**—In this series of experiments, the ionic strength was maintained constant by the addition of ammonium sulfate. The results are given in Table II.

The rate is first order with respect to ruthenium over the whole range investigated (to concentrations as low as  $5 \times 10^{-8}$  *M* or 5  $\gamma$  Ru/liter).

The rate is not a simple function of the cerium-(IV) concentration. Analysis of the data in the last column of Table II leads to the following expression for the rate of the catalyzed reaction

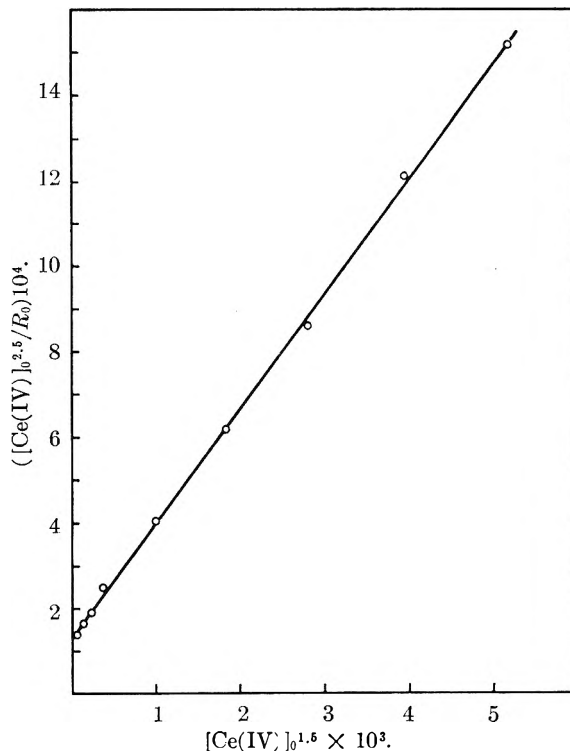


Fig. 1.—Plot of  $[\text{Ce(IV)}_0]_0^{2.5}/R_0$  vs.  $[\text{Ce(IV)}_0]_0^{1.5}$ . *R*<sub>0</sub> is the initial rate of the catalyzed reaction (mole l.<sup>-1</sup> min.<sup>-1</sup>).

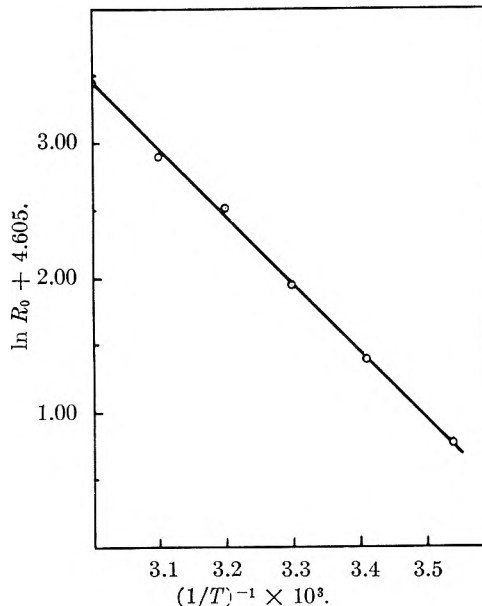


Fig. 2.—Plot of  $\ln R_0$  (initial rate of catalyzed reaction) vs. reciprocal of absolute temperature (0.020 *N* Ce(IV), 0.03 *N* As(III), 2 *M* sulfuric acid, 0.020  $\gamma$  Ru/ml.).

$$-\frac{d[\text{Ce(IV)}]}{dt} = \frac{k_1[\text{Ru}][\text{Ce(IV)}]^{2.5}}{1 + k_2[\text{Ce(IV)}]^{1.5}}$$

When  $k_2[\text{Ce(IV)}]^{1.5} \gg 1$ , this equation reduces to

$$-\frac{d[\text{Ce(IV)}]}{dt} = \frac{k_1}{k_2} [\text{Ru}][\text{Ce(IV)}]$$

and when  $k_2[\text{Ce(IV)}]^{1.5} \ll 1$ , it becomes

$$-\frac{d[\text{Ce(IV)}]}{dt} = k_1[\text{Ru}][\text{Ce(IV)}]^{2.5}$$

Above an initial cerium(IV) concentration of

TABLE II

INITIAL RATE OF RUTHENIUM-CATALYZED Ce(IV)-As(III) REACTION AS A FUNCTION OF RUTHENIUM AND INITIAL Ce(IV) CONCENTRATIONS

$$([\text{As(III)}]_0 = 0.040 M, \text{H}_2\text{SO}_4 = 2 M, 25^\circ)$$

| [Ce(IV)] <sub>0</sub> ,<br>mole l. <sup>-1</sup> × 10 <sup>3</sup> | $\left(\frac{-d[\text{Ce(IV)}]}{dt}\right)_0$ , mole l. <sup>-1</sup> min. <sup>-1</sup> |                                               |                                               |                                               |
|--------------------------------------------------------------------|------------------------------------------------------------------------------------------|-----------------------------------------------|-----------------------------------------------|-----------------------------------------------|
|                                                                    | [Ru], mole l. <sup>-1</sup> × 10 <sup>2</sup>                                            | [Ru], mole l. <sup>-1</sup> × 10 <sup>2</sup> | [Ru], mole l. <sup>-1</sup> × 10 <sup>2</sup> | [Ru], mole l. <sup>-1</sup> × 10 <sup>2</sup> |
|                                                                    | 1.49                                                                                     | 0.99                                          | 1.48                                          | 1.98                                          |
| 1.25                                                               |                                                                                          |                                               |                                               | 0.0004                                        |
| 2.50                                                               |                                                                                          |                                               |                                               | .0019                                         |
| 3.75                                                               |                                                                                          |                                               |                                               | .0045                                         |
| 5.00                                                               | 0.0019                                                                                   | 0.0037                                        | 0.0051                                        | .0071                                         |
| 10.00                                                              | 0.060                                                                                    | .0120                                         | .0184                                         | .0248                                         |
| 15.00                                                              | 0.136                                                                                    | .0256                                         | .0352                                         | .0448                                         |
| 20.00                                                              | 0.168                                                                                    | .0336                                         | .0488                                         | .0656                                         |
| 25.00                                                              | 0.248                                                                                    | .0420                                         | .0641                                         | .0816                                         |
| 30.00                                                              | 0.280                                                                                    | .0504                                         | .0720                                         | .1024                                         |
| 35.00                                                              | 0.340                                                                                    | .0600                                         | .0872                                         | .1216                                         |

about 0.005 *M*, the initial rate increases linearly with the ceric concentration.

The constants  $k_1$  and  $k_2$  are found (Fig. 1) to have the values  $4.0 \times 10^{10}$  and  $2.1 \times 10^3$ . The rate expression then becomes

$$-\frac{d[\text{Ce(IV)}]}{dt} = \frac{4.0 \times 10^{10} [\text{Ru}] [\text{Ce(IV)}]^{2.5}}{1 + 2.1 \times 10^3 [\text{Ce(IV)}]^{1.5}} \quad (25^\circ) \quad (1)$$

where all concentrations are in moles per liter and  $t$  is in minutes. Since the rate is not altered by cerium(III) and arsenic(V), this expression holds not only initially but also for the whole course of the reaction. The rate of the uncatalyzed re-

action has been neglected in equation 1 as being insignificant compared to that of the catalyzed reaction. This simplification is justified for half-reaction times of less than 20 minutes.

It may be noted that the rate of the osmium-catalyzed As(III)-Ce(IV) reaction is determined by the arsenious oxide concentration, not the ceric concentration.<sup>2</sup>

The effect of temperature on the initial reaction rate at a cerium(IV) concentration of 0.02 *N* is shown in Fig. 2. At this ceric concentration, the initial rate may be expressed by

$$\left(\frac{-d[\text{Ce(IV)}]}{dt}\right)_0 = k[\text{Ru}][\text{Ce(IV)}]_0 \quad (k = k_1/k_2)$$

and

$$\ln \left(\frac{-d[\text{Ce(IV)}]}{dt}\right)_0 = \ln k + \ln [\text{Ru}][\text{Ce(IV)}]_0$$

From the Arrhenius law

$$\ln k = -\frac{E}{RT} + \text{const.}$$

$$\therefore \ln \left(\frac{-d[\text{Ce(IV)}]}{dt}\right)_0 = -\frac{E}{RT} + \text{const.}$$

From the slope of the line in Fig. 2 ( $= -E/R$ ),  $E$  is found to have the value 9.77 kcal. This may be compared with the value 14.35 kcal. for the uncatalyzed reaction.<sup>3</sup>

(2) R. D. Sauerbrunn and E. B. Sandell, *Mikrochim. Acta*, 22 (1953).

(3) V. F. Stefanovskii and M. S. Gaukham, *J. Gen. Chem. U.S.S.R.*, 11, 970 (1941).

## KINETICS OF THE RADIATION-INDUCED REACTION OF IRON(III) WITH TIN(II)

BY J. W. BOYLE, S. WEINER<sup>2</sup> AND C. J. HOCHANADEL

*Contribution from the Oak Ridge National Laboratory,<sup>1</sup> Chemistry Division, Oak Ridge, Tenn.*

*Received February 14, 1959*

Cobalt  $\gamma$ -rays induce reaction of Fe(III) with Sn(II). For dilute solutions in deaerated 0.4 *M* H<sub>2</sub>SO<sub>4</sub>, the initial product yields per 100 e.v. of energy absorbed are  $G(\text{Fe(II)}) = 6.62$ ,  $G(\text{Sn(IV)}) = 3.75$ , and  $G(\text{H}_2) = 0.45$ . Assuming the primary chemical species in the decomposition of water to be H, OH, H<sub>2</sub> and H<sub>2</sub>O<sub>2</sub> produced with yields  $G_{\text{H}}$ ,  $G_{\text{OH}}$ ,  $G_{\text{H}_2}$  and  $G_{\text{H}_2\text{O}_2}$ , the initial product yields are related to these quantities as follows:  $G(\text{Fe(II)}) = G_{\text{H}} + G_{\text{OH}}$ ,  $G(\text{Sn(IV)}) = G_{\text{H}_2\text{O}_2} + G_{\text{OH}}$ , and  $G(\text{H}_2) = G_{\text{H}_2}$ . The initial yields indicate a mechanism in which Sn(II) is reduced by H to Sn(I) and oxidized by OH to Sn(III), Fe(III) is reduced by Sn(I) and Sn(III), and Fe(II) is oxidized by H<sub>2</sub>O<sub>2</sub>. The presence of Sn(II) in deaerated Fe(II) solutions lowers the yield for oxidation of Fe(II) and, at concentration ratios  $(\text{Sn(II)})/(\text{Fe(II)}) > 0.02$ , oxidation of Fe(II) is completely suppressed. Irradiation of deaerated Sn(II) solution produces Sn(IV) and H<sub>2</sub> with a yield 0.49 which is equivalent to  $G_{\text{H}_2}$ . On the basis of proposed mechanisms and the dependence of yields on relative concentrations, the following ratios of rate constants were evaluated:  $k_{(\text{Fe(II)}+\text{H})} : k_{(\text{Sn(II)}+\text{OH})} = 1:7.0$ ;  $k_{(\text{Fe(II)}+\text{OH})} : k_{(\text{Sn(II)}+\text{H})} : k_{(\text{Sn(IV)}+\text{H})} : k_{(\text{Fe(II)}+\text{H})} = 1 : \sim 5000:0.16:0.081$ ;  $k_{(\text{Fe(II)}+\text{H}_2\text{O}_2)} : k_{(\text{Sn(II)}+\text{H}_2\text{O}_2)} = 100:1$ . The rapid rate of reduction of Sn(II) by H atoms is especially noteworthy.

### Introduction

Water is decomposed by high energy radiations into several reactive intermediates, the character and yields of which are usually inferred from the nature and extent of reactions produced with various solutes. On this basis, the important long-lived chemical intermediates are considered to be

(1) Work performed for the U. S. Atomic Energy Commission at the Oak Ridge National Laboratory, Oak Ridge, Tennessee, operated by Union Carbide Nuclear Company.

(2) Guest scientist, summer 1958, from the University of Wisconsin, Wausau Extension Center, Wausau, Wisconsin.

H, OH, H<sub>2</sub> and H<sub>2</sub>O<sub>2</sub>, produced with yields,<sup>3</sup> 3.68, 2.94, 0.45 and 0.81 in the irradiation of 0.4 *M* H<sub>2</sub>SO<sub>4</sub> solution with cobalt  $\gamma$ -rays. Studies of the effects of concentration, pH, temperature, phase, isotopic substitution, etc., on product yields may also provide information on the initial spatial distribution of these intermediates and, possibly, information on the shorter-lived ionic and excited-state precursors.

(3) For one of the recent determinations, see H. A. Mahlman and J. W. Boyle, *J. Am. Chem. Soc.*, 80, 773 (1958).

This paper describes kinetic studies of  $\gamma$ -ray-induced reactions in deaerated 0.4 *M* sulfuric acid solutions of Sn(II); Sn(II) and Fe(II); and Sn(II) and Fe(III). Results are interpreted on the basis of reactions with H, OH, H<sub>2</sub> and H<sub>2</sub>O<sub>2</sub>. Ratios of rate constants for reactions of the various solutes with the intermediates are evaluated. The unstable valence states Sn(I) and Sn(III) play an important part in the mechanisms.

### Experimental

**Preparation of Solutions.**—Solutions irradiated were oxygen-free and contained initially either Sn(II), Sn(II) + Fe(II), or Sn(II) + Fe(III), all in 0.4 *M* H<sub>2</sub>SO<sub>4</sub>. Because of rapid air oxidation of Sn(II) it was necessary to maintain oxygen-free conditions during preparation, irradiation and analyses of solutions. The apparatus for carrying out the various operations is shown in Fig. 1.

Sn(II) solution was prepared by anodic oxidation of mossy tin using a platinum wire as cathode. Approximately 500 ml. of 0.4 *M* H<sub>2</sub>SO<sub>4</sub> was placed in the generator shown in the upper left of Fig. 1a. Purified helium was bubbled through the solution until the solution and auxiliary apparatus were thoroughly purged of air. The tin anode was then lowered into the acid, and using a 6 v. storage battery, a current of 10 to 30 ma. was passed through solution until approximately the desired concentration of Sn(II) was obtained. During this process helium escaped around the anode lead-in tube thus preventing air from entering the system. The tin anode then was removed from solution and the anode lead-in tube resealed by the inverted standard taper joint A.

By manipulation of stopcocks, the tin solution could be forced by helium pressure either directly into the irradiation cell attached at B, or into the deaerator-mixer vessel containing either deaerated Fe(II) or Fe(III) solution. The mixer vessel was calibrated so that desired mixtures could be approximated. The irradiation vessel was first purged with helium and then filled to overflowing and stoppered (leaving no gas space) while solution was flushing out the neck of the cell. Joints and stopcocks were lubricated with solution only. A test of the technique by checking the known yield<sup>4</sup> for Fe(II) oxidation in oxygen-free solution indicated that oxygen was effectively eliminated.

At the acidity and concentrations employed ( $<10^{-3}$  *M*) deaerated solutions were stable for several days. Also, thermal reaction of Sn(II) with Fe(III) was negligible.

**Materials.**—Water from a Barnstead still was redistilled from acid permanganate then alkaline permanganate solution. A final distillation was made in an all silica system and the water was stored in silica vessels.

The mossy tin and FeSO<sub>4</sub> were Mallinckrodt analytical reagent grade. The H<sub>2</sub>SO<sub>4</sub> and Fe<sub>2</sub>(SO<sub>4</sub>)<sub>3</sub> were Baker and Adamson reagent grade.

Pure helium was passed over hot copper and then through a scrubber containing 0.4 *M* H<sub>2</sub>SO<sub>4</sub> solution.

**Irradiation.**—Solutions were irradiated in a completely filled and stoppered cylindrical silica optical cell with a 1 cm. light path and a total volume  $\sim 3.5$  ml. The cells (obtained from Pyrocell Mfg. Co.) were made with special silica optical windows which are not colored in the spectral region 2000 to 6000 Å. by  $\gamma$ -irradiation. Solutions were irradiated in the central position of an 800 curie cobalt source<sup>5</sup> at a dose rate  $\sim 6 \times 10^{17}$  e.v. g.<sup>-1</sup> min.<sup>-1</sup>. Dose rate was determined using the ferrous sulfate dosimeter taking  $G(\text{Fe(III)})$  as 15.6.<sup>6</sup>

**Analyses.**—Ferric ion was measured by its absorption at 3050 Å. on a Model 11 Cary recording spectrophotometer using a molar extinction coefficient of 2206 at 25°. The presence of Fe(II), Sn(II) or Sn(IV) did not affect the measurement. Ferrous concentration was obtained by subtracting the ferric concentration from the total iron concentration. Since Fe(III) was measured by direct optical absorption, a

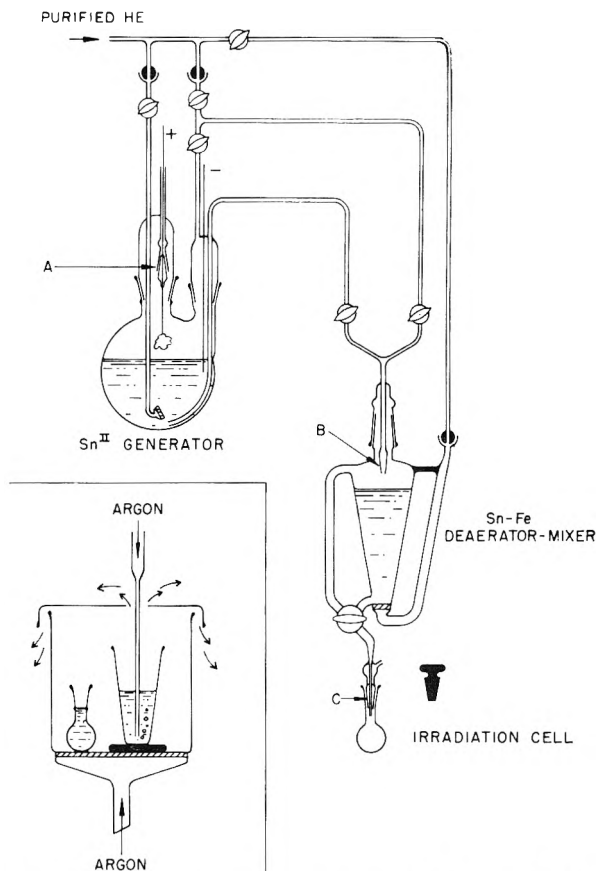


Fig. 1b.—Inert atmosphere vessel for transferring solutions.

Fig. 1a.—Apparatus for preparation of solutions.

complete dose *vs.* concentration curve could be obtained using a single sample by intermittent irradiation-measurement procedure.

Sn(II) was determined by oxidizing an aliquot with excess Ce(IV) in absence of air, and measuring the unreacted Ce(IV) spectrophotometrically at 3200 Å. using a molar extinction coefficient of 5608 for solution in 0.4 *M* H<sub>2</sub>SO<sub>4</sub> at 25°. The reaction between Sn(II) and Ce(IV) is not instantaneous, and it was necessary to allow  $\sim 10$  min. to ensure essentially complete reaction. The solution taken from the Sn(II) generator was assumed to contain no Sn(IV). The amount of Sn(IV) produced by radiolysis was assumed to be equal to Sn(II) depletion. For solutions containing both Sn(II) and Fe(II), the concentration of each was calculated from the total reducing power of the solution as measured by Ce(IV), the measured Fe(III) concentration, and the known total iron concentration. It was necessary to use a new sample for each Sn(II) determination.

For transferring and mixing these solutions under air-free conditions, the apparatus shown in Fig. 1b was employed. This relatively simple inert atmosphere vessel consisted of a sintered glass filter funnel covered with a petri dish having a 1 cm. opening near the center. Flowing argon or CO<sub>2</sub> maintained air-free conditions, and the opening at the top allowed insertion of tubes for deaerating and pipetting solutions.

Hydrogen was assumed to be the other product of irradiation, and the amount was calculated on the basis of stoichiometry. Hydrogen measurements are planned, however, in view of the interest Sn(II) offers as scavenger for precursors of "molecular" hydrogen.

### Results and Discussion

For the sake of simplicity and for lack of information on the exact nature of the species present in solution, the various valence states of the ions are indicated by Roman numerals. For

(4) A. O. Allen and W. G. Rothschild, *Radiation Research*, **7**, 591 (1957).

(5) J. A. Ghormley and C. J. Hochanadel, *Rev. Sci. Instr.*, **22**, 473 (1951).

(6) C. J. Hochanadel and J. A. Ghormley, *J. Chem. Phys.*, **21**, 880 (1953).

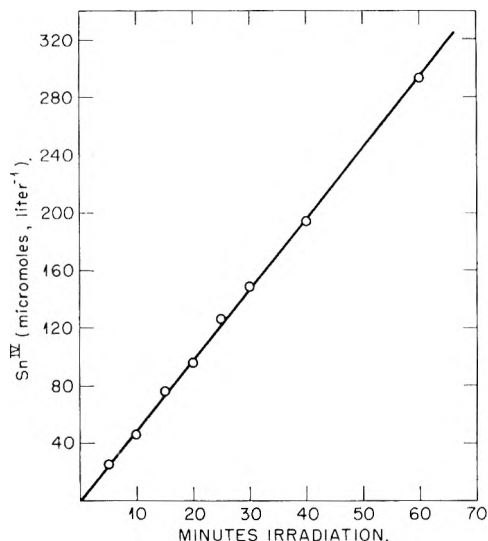


Fig. 2.—Formation of Sn(IV) in deaerated solution of Sn(II) in 0.4 M H<sub>2</sub>SO<sub>4</sub>. Initial (Sn(II)) = 534 μ moles per liter; γ-ray dose rate = 6.1 × 10<sup>20</sup> e.v. l.<sup>-1</sup> min.<sup>-1</sup>.

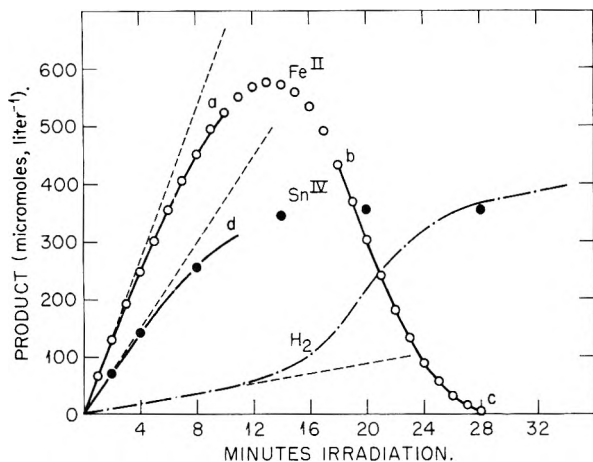
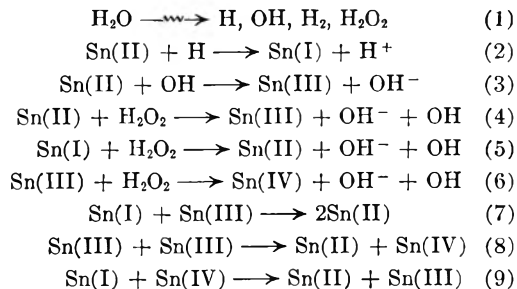


Fig. 3.—Formation of Sn(IV), Fe(II) and H<sub>2</sub> in deaerated 0.4 M H<sub>2</sub>SO<sub>4</sub> solution containing Sn(II) and Fe(III). Initial concentrations (Sn(II)) = 356, (Fe(III)) = 950 μ moles per liter. γ-ray dose rate = 6.1 × 10<sup>20</sup> e.v. l.<sup>-1</sup> min.<sup>-1</sup>. Dotted lines are theoretical initial rates assuming no effect of solutes on yields of intermediates. G(Fe(II)) = 6.62, G(Sn(IV)) = 3.75, G(H<sub>2</sub>) = 0.45. Solid curve oa is given by equation 24, od by equation 23, and bc by equation 20. The dashed curve for H<sub>2</sub> is calculated from material balance.

example, tetravalent tin is represented by Sn(IV) even though it may be present as Sn(SO<sub>4</sub>)<sub>3</sub><sup>-</sup> aq., or in some other form. It is recognized, however, that the structure of the species may determine its reactivity with the various intermediates.

**Radiation Induced Oxidation of Sn(II) in Oxygen-Free 0.4 M H<sub>2</sub>SO<sub>4</sub> Solution.**—Irradiation produced a net decrease in reducing power of the tin solutions as determined by analysis with Ce(IV). Also, addition of Fe(II) solution immediately following irradiation gave no Fe(III), indicating the absence of peroxide. It was therefore concluded that the net reaction is oxidation of Sn(II) to Sn(IV) with formation of an equivalent amount of hydrogen. The rate of oxidation was essentially linear with dose over the range studied as shown in Fig. 2. The yield  $G(\text{Sn(IV)}) = G-$

$(\text{H}_2) = 0.49$  is equivalent to  $G_{\text{H}_2} = G_{\text{H}_2\text{O}_2} - (G_{\text{H}} - G_{\text{OH}})/2$  and indicates net oxidation by H<sub>2</sub>O<sub>2</sub> and OH and reduction by H, possibly according to the sequence



According to this mechanism Sn(II) reacts with both H and OH to form the unstable valence states Sn(I) and Sn(III), respectively. The unstable valence states then react according to 5-9. Reduction of Sn(IV) by H would give the same stoichiometry. However, evidence to be presented later from irradiation of solutions containing both tin and iron indicates that reduction of Sn(II) by H is about 30,000 times faster than reduction of Sn(IV) by H. The results also indicate no oxidation of Sn(II) by H as in the case of Fe(II). Results to be presented in the next section also indicate that oxidation of Sn(II) by H<sub>2</sub>O<sub>2</sub> is a slow reaction, and therefore reactions 5 and 6 are postulated for removing at least part of the peroxide.

The yield 0.49 is somewhat higher than values reported for the "molecular" hydrogen yield at solute concentrations approaching zero,  $G_{\text{H}_2} = 0.45$ . In view of the high reactivity of Sn(II) with H atoms, the "molecular" yield should be reduced somewhat by scavenging in the particle tracks. Accurate hydrogen yields are needed in order to clarify this point.

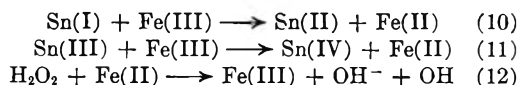
**Thermal Reaction of Sn(II) with H<sub>2</sub>O<sub>2</sub>.**—To establish mechanisms for reactions in these systems it was necessary to determine the fate of the H<sub>2</sub>O<sub>2</sub>. Both Sn(II) and Fe(II) react with peroxide. The rate constant for reaction of Fe(II) with H<sub>2</sub>O<sub>2</sub> ( $k_{12}$ ) is known<sup>7</sup> to be 71 l. mole<sup>-1</sup> sec.<sup>-1</sup> at 25°. The rate constant for reaction of Sn(II) with H<sub>2</sub>O<sub>2</sub> ( $k_4$ ) was measured by mixing air free solutions in the apparatus shown in Fig. 1b. The initial concentration of Sn(II) was 320 μM and H<sub>2</sub>O<sub>2</sub> was 85 μM. After various reaction times, aliquots were mixed with air-free Fe(II) solution and the Fe(III) concentration measured as described previously. This gave a measure of H<sub>2</sub>O<sub>2</sub> remaining in solution. Since Sn(II) and Fe(II) compete for OH radicals produced by reaction of Fe(II) with H<sub>2</sub>O<sub>2</sub> (see reactions 12, 3 and 13), it was necessary to ensure a concentration ratio (Fe(II))/(Sn(II)) > 100 in the analysis. The results followed a second-order plot from which the rate constant  $k_{(\text{Sn(II)} + \text{H}_2\text{O}_2)}$  was estimated to be 0.7 l. mole<sup>-1</sup> sec.<sup>-1</sup>, and the ratio of rate constants  $k_{(\text{Fe(II)} + \text{H}_2\text{O}_2)}/k_{(\text{Sn(II)} + \text{H}_2\text{O}_2)}$  was taken to be 100.

**Radiation-induced Reaction of Sn(II) with Fe(III) in Oxygen-free 0.4 M H<sub>2</sub>SO<sub>4</sub> Solution.**—With a stoichiometric excess of Fe(III) initially

(7) See e.g., G. S. Dainton and T. J. Hardwick, *Trans. Faraday Soc.*, **53**, 333 (1957).

present in Sn(II) solution, the sequence shown in Fig. 3 occurs upon irradiation. Sn(II) is oxidized at a rate which diminishes with increased dose until it is completely oxidized. The initial yield,  $G(\text{Sn(IV)}) = 3.75$ . Fe(III) is first reduced to Fe(II) at a rate which decreases with increased dose; the concentration of Fe(II) reaches a maximum just before the Sn(II) is completely oxidized, after which the Fe(II) is reoxidized to Fe(III). The initial yield  $G(\text{Fe(III)}) = 6.62$ . Presumably,  $\text{H}_2$  is the other reduced species and, from stoichiometry, follows the dashed curve in Fig. 3. The calculated initial yield  $G(\text{H}_2) = 0.45$ .

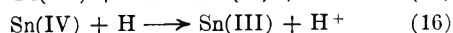
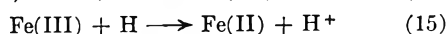
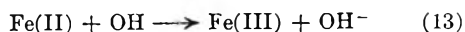
The measured initial yields are interpreted on the basis of reaction of Sn(II) with H and OH (reactions 2 and 3), followed by scavenging of the unstable valence states Sn(I) and Sn(III) by Fe-



(III).  $\text{H}_2\text{O}_2$  reacts with Fe(II). Accordingly, the initial yields are related to yields of intermediates by:  $G(\text{Sn(IV)}) = G_{\text{H}_2\text{O}_2} + G_{\text{OH}} = 3.75$ ;  $G(\text{Fe(II)}) = G_{\text{H}} + G_{\text{OH}} = 6.62$ , and  $G(\text{H}_2) = G_{\text{H}_2} = 0.45$ . The values are in good agreement with yields of intermediates determined using other systems.

At the very start of irradiation, with no Fe(II) present, if Sn(II) reacted with  $\text{H}_2\text{O}_2$  according to reaction 4 the "actual" initial yields would be  $G(\text{Fe(II)}) = G_{\text{H}} + G_{\text{OH}} + 2G_{\text{H}_2\text{O}_2} = 8.24$ ,  $G(\text{Sn(IV)}) = G_{\text{OH}} + 2G_{\text{H}_2\text{O}_2} = 4.56$ , and  $G(\text{H}_2) = G_{\text{H}_2} = 0.45$ . However, because Fe(II) reacts with  $\text{H}_2\text{O}_2$  100 times faster than does Sn(II), a small concentration of Fe(II) either produced by radiation or adventitiously present at the start would suffice to eliminate reaction 4. The high yield would be observed only during the first fraction of a minute irradiation and this could only be detected by a small positive intercept at zero time. From three experiments of the type shown in Fig. 3, it was not possible to determine whether or not "actual" initial yields were high. In the concentration region of interest, reaction 4 is assumed to be negligible and the above mechanism is assumed to hold. An alternative would be oxidation of Sn(II) to Sn(IV) by  $\text{H}_2\text{O}_2$  in a one step process with no OH radical intermediate. This would also give the observed yields. From our results we could not determine whether this reaction is a one step or two step process.

The dependence of yields on relative concentrations of solutes indicates several competing reactions. These are considered to be: competition of Sn(II) and Fe(II) for OH radicals, (reactions 3 and 13); Sn(II), Fe(II) Fe(III) and Sn(IV) for H atoms (reactions 2, 14, 15 and 16); and Fe(II) and Sn(II) for  $\text{H}_2\text{O}_2$  (reactions 12 and 4).



The general rate equations based upon reactions 1-4 and 10-16 are

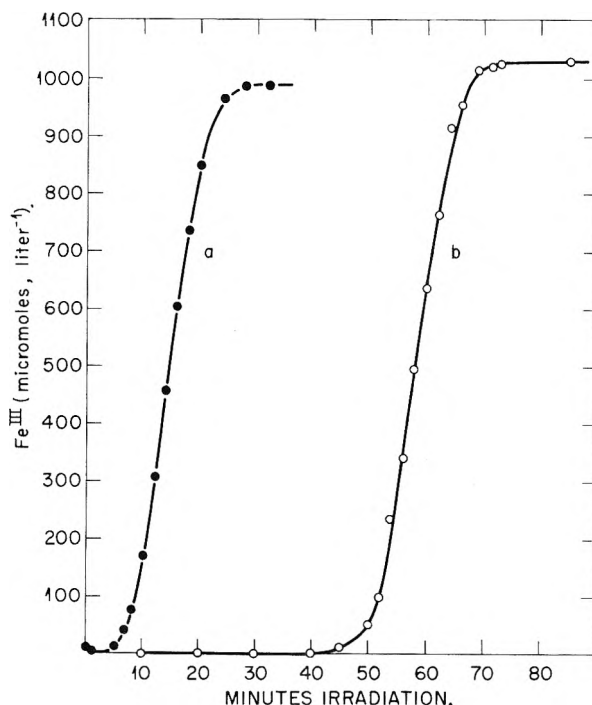


Fig. 4.—Formation of Fe(III) in deaerated 0.4 M  $\text{H}_2\text{SO}_4$  solution containing Fe(II) and Sn(II). Initial concentrations of (Sn(II)): (a)  $\sim 50$ ; (b)  $\sim 250$   $\mu$  moles per liter.  $\gamma$ -ray dose rate =  $6.1 \times 10^{20}$  e.v.  $\text{l}^{-1} \text{min}^{-1}$ .

$$\begin{aligned} G(\text{Sn(IV)}) &= G_{\text{H}_2\text{O}_2} \left[ \frac{(k_4/k_{12})(\text{Sn(II)})}{(k_4/k_{12})(\text{Sn(II)}) + (\text{Fe(II)})} \right] \\ &+ [G_{\text{OH}} + G_{\text{H}_2\text{O}_2}] \left[ \frac{(k_3/k_{13})(\text{Sn(II)})}{(k_3/k_{13})(\text{Sn(II)}) + (\text{Fe(II)})} \right] \quad (17) \end{aligned}$$

$$\begin{aligned} G(\text{Fe(II)}) &= \\ G_{\text{H}} &\left[ \frac{(k_2/k_{14})(\text{Sn(II)}) + (k_{16}/k_{14})(\text{Sn(IV)}) + (k_{16}/k_{14})(\text{Fe(III)}) - (\text{Fe(II)})}{(k_2/k_{14})(\text{Sn(II)}) + (k_{16}/k_{14})(\text{Sn(IV)}) + (k_{16}/k_{14})(\text{Fe(III)}) + (\text{Fe(II)})} \right] \\ &+ [G_{\text{OH}} + G_{\text{H}_2\text{O}_2}] \left[ \frac{(k_3/k_{13})(\text{Sn(II)}) - (\text{Fe(II)})}{(k_3/k_{13})(\text{Sn(II)}) + (\text{Fe(II)})} \right] \\ &+ G_{\text{H}_2\text{O}_2} \left[ \frac{k_4/k_{12}(\text{Sn(II)}) - (\text{Fe(II)})}{(k_4/k_{12})(\text{Sn(II)}) + (\text{Fe(II)})} \right] \quad (18) \end{aligned}$$

The kinetics are considerably simplified for the regions of the curves labelled bc and oa in Fig. 3. The portion of the curve bc describes the oxidation of Fe(II) after Sn(II) has been completely oxidized. The solution contains only Fe(II), Fe(III) and Sn(IV). Fe(II) reacts with all OH and  $\text{H}_2\text{O}_2$ , and competes with Fe(III) and Sn(IV) for H atoms. The rate equation is given by

$$\begin{aligned} G(\text{Fe(III)}) &= G_{\text{OH}} + 2G_{\text{H}_2\text{O}_2} - \\ G_{\text{H}} &\left[ \frac{(k_{15}/k_{14})(\text{Fe(III)}) + (k_{16}/k_{14})(\text{Sn(IV)}) - (\text{Fe(II)})}{(k_{15}/k_{14})(\text{Fe(III)}) + (k_{16}/k_{14})(\text{Sn(IV)}) + (\text{Fe(II)})} \right] \quad (19) \end{aligned}$$

The integrated form (eq. 20) is shown as the solid curve bc

$$\begin{aligned} \text{dose} &= 67.8(\text{Fe(III)}) - [12.4(\text{Fe}^0) + 24.8(\text{Sn(IV)})] \\ \log [1 - (\text{Fe(III)}) / (1.01(\text{Fe}^0) + 0.0175(\text{Sn(IV)})] & \quad (20) \end{aligned}$$

(dose is given as  $10^{17}$  e.v.  $\text{l}^{-1}$ ; concentrations as micromoles per liter;  $(\text{Fe}^0)$  as total iron concentration). The ratio of rate constants  $k_{15}/k_{14} = 0.081$



was taken from the literature<sup>4</sup> and the ratio  $k_{16}/k_{14}$  was evaluated to be 0.16.

In the region oa the main competition is that of Fe(II) and Sn(II) for OH radicals. Fe(II) reacts with essentially all  $H_2O_2$ . Sn(II) reacts with nearly all H atoms as is indicated by the fact that the chief competitor, Fe(II), which produces  $H_2$  on reaction with H, does not react appreciably with H until the Sn(II) is nearly depleted (region ab). The rate equations for region od and oa then become

$$G(\text{Sn(IV)}) = [G_{H_2O_2} + G_{OH}] \left[ \frac{(k_3/k_{13})(\text{Sn(II)})}{(k_3/k_{13})(\text{Sn(II)}) + (\text{Fe(II)})} \right] \quad (21)$$

$$G(\text{Fe(II)}) = G_H - G_{H_2O_2} + [G_{OH} + G_{H_2O_2}] \left[ \frac{(k_3/k_{13})(\text{Sn(II)}) - (\text{Fe(II)})}{(k_3/k_{13})(\text{Sn(II)}) + (\text{Fe(II)})} \right] \quad (22)$$

The integrated forms (equations 23 and 24) are shown as the solid curves od and oa. The ratio of rate constants  $k_3/k_{13}$  was evaluated to be 7.0.

$$\text{dose} = 120(\text{Sn(IV)}) - 93.2(\text{Sn}^0) \log [1 - (\text{Sn(IV)})/(\text{Sn}^0)] \quad (23)$$

$$\text{dose} = 65.8(\text{Fe(II)}) - 99(\text{Sn}^0) \log [1 - 0.585(\text{Fe(II)})/(\text{Sn}^0)] \quad (24)$$

For the system represented by the portion ab of the curve, a small concentration of Sn(II) is competing with Fe(II), Fe(III) and Sn(IV) for H atoms, and with Fe(II) for OH radicals. The only remaining adjustable factor is the reactivity of Sn(II) (relative to the other three solutes) for H atoms. The ratios of rate constants were ad-

justed until yields calculated using the general rate equations gave the best agreement with yields estimated from slopes taken from portion ab of the curve. On this basis the relative rate constants were  $k_{14} : k_2 : k_{16} : k_{15} = 1 : \sim 5000 : 0.16 : 0.08$ . Because of the inaccuracy in estimating Sn(II) concentrations accurately at concentrations  $< 10 \mu M$ , and, in estimating slopes, ratios of rate constants involving  $k_2$  are inaccurate. For example, an error of 50% in estimating the  $10 \mu M$  Sn(II) concentration will make  $k_2/k_{14}$  in error by an order of magnitude. The ratios of rate constants not involving  $k_2$  are believed to be accurate to  $\pm 10\%$ .

**Radiolysis of Oxygen-free Solutions Containing Sn(II) and Fe(II) in 0.4 M  $H_2SO_4$ .**—In degassed ferrous sulfate solution Fe(II) is oxidized with a yield  $G(\text{Fe(III)}) = 8.2 = G_H + G_{OH} + 2G_{H_2O_2}$ . Addition of Sn(II) lowers this yield until, at a concentration ratio  $(\text{Sn(II)})/(\text{Fe(II)}) > 0.02$ , oxidation of Fe(II) is completely suppressed. Sn(IV) and  $H_2$  then are produced with a yield  $0.45 = G_H$ . Typical experiments are shown in Fig. 4. The small amount of Fe(III) which may be present initially is first reduced to Fe(II). After the Sn(II) is nearly depleted, Fe(II) is oxidized at a rate which depends on relative concentrations of Sn(II), Fe(II), Fe(III) and Sn(IV). Inability to analyze accurately a small amount of Sn(II) in presence of a large amount of Fe(II) precluded the possibility of accurate kinetic analysis of the data from this particular system. However, the results confirm the fact that Sn(II) is reduced rapidly by H and oxidized by OH.

## ON THE USE OF AQUEOUS SODIUM FORMATE AS A CHEMICAL DOSIMETER

BY T. J. HARDWICK AND W. S. GUENTNER

*Gulf Research & Development Company, Pittsburgh, Pennsylvania*

*Received February 14, 1959*

On radiolysis, sodium formate in aqueous solution gives products which may be quantitatively titrated with acid permanganate. This system is proposed as a chemical dosimeter in the range 1–80 Mrad. and is particularly convenient for use in metal systems. The chemical change is proportional to the energy absorbed, and the yield of reductant ( $G = 3.40$  mol. equiv./100 e. v.) is independent of dose rate, formate ion concentration over a wide range and temperature.

### Introduction

Until quite recently the irradiation of liquids was largely carried out using glass vessels. With increasing use of fast electrons as a source of ionizing radiation, it has been found that glass is unsuitable in many applications. When electron beams are used, materials for irradiation cells are required (a) to be mechanically strong, (b) to be available in uniform and reproducible thickness, and (c) to conduct heat and electricity. Metals are obviously the most suitable materials of construction, and among those used, brass and aluminum have many advantageous characteristics.

Conventional dosimeters cannot be used in many metallic systems. Both the ferrous ion and ceric ion dosimeters have 0.8 N sulfuric acid as the sol-

vent medium. Air-free formic acid solutions are too acidic for use. The application of the continuous production of electrolytic gas from potassium iodide solutions<sup>1</sup> is limited mostly to rate measurements, and furthermore has the disadvantage of contaminating any metal system with traces of iodine. Oxalic acid solutions,<sup>2</sup> like those of formic acid, attack many metals.

A need exists, therefore, for a dosimeter which is suitable in commonly used metal systems.

Organic compounds immediately suggest themselves by virtue of their inertness to metals. However, we have been unable to find any common

(1) E. J. Hart and S. Gordon, *Nucleonics*, **12**, No. 4, 40 (1954).

(2) J. Sutton, I. Draganic and H. Hering, *Int'l. Conf. Peaceful Uses of Atomic Energy*, **14**, 160 (1956).

organic liquid in which an easily measured chemical change occurs which is proportional to the energy absorbed over a wide range. In most systems the products are equally, if not more, reactive to intermediate ions and radicals than is the parent compound. Finally, there is the difficulty in obtaining the necessary purity for radiation work. Small quantities of impurities may be present, but they must be identified and shown not to affect the course of reaction.

The choice appears to be limited therefore to an aqueous system, using a neutral solute. We have found that the radiation-induced conversion of sodium formate to products quantitatively oxidized by acid permanganate is suitable for chemical dosimetry. The remainder of this paper will be devoted to testing the effect of the usual variables on the sodium formate dosimeter, and to measuring the absolute yield.

### Experimental

**Materials and Reagents.**—All chemicals used were Merck Reagent Grade. The water used was either ordinary distilled water or water redistilled from alkaline permanganate. No difference in results was observed on interchanging the two sources of water.

**Source of Radiation.**—The source of radiation was an electron beam from a Van de Graaff accelerator of 3 Mev., 1 ma. capacity (High Voltage Engineering Corporation, Model KS). In our experiments the current was 20–40  $\mu$ amp. and was used as a spot beam.

**Absolute Measurement of Energy Absorption.**—The experimental apparatus used in measuring the energy output of the electron beam is shown in Fig. 1. A wide-mouth (6") dewar was filled with 1500 ml. of hydrogen-saturated water and centered with the lip one inch below the scanning tube of the accelerator. A collecting wire, dipped in the water, conducted the spent electrons to the accelerator controls. A film of polyethylene (7 mg./cm.<sup>2</sup>) was placed flatly over the dewar to prevent gross admission of air. The water was stirred by a small bar magnet actuated by a horseshoe magnet which rotated beneath the dewar.

The temperature of the water was measured by a Beckmann thermometer just before and after irradiation. On the average, a temperature increase of 3° was observed. The energy input into the water was taken as the heat capacity of the water and dewar multiplied by the measured temperature difference. The usual time-temperature extrapolations were made prior to and after irradiations, but in no case did the correction amount to more than 0.2%. The heat capacity of the dewar was measured by conventional mixing techniques and amounted to 160  $\pm$  4 g. of water equivalent.

In order to compare the calorimetric measurements with the radiation-induced reaction in the sodium formate system, it was necessary to standardize the operation of the accelerator. The collected beam current was passed through a current integrator (Eldorado Electronics Company, Model CI-100) and the total charge accurately measured. Although the absolute accuracy of the voltage registered on the accelerator controls was probably no better than  $\pm$ 5%, preliminary tests showed that a reproducibility of  $\pm$ 1% was obtained at 2.5 Mev. This error was probably due to difficulty in setting the machine at exactly the same voltage on successive runs.

In a series of experiments, the total energy absorbed in the water was measured for irradiations at various voltages and total electron charges. This, in effect, monitored the output of the Van de Graaff accelerator for various voltage and current settings. In the data reported for sodium formate irradiations, the energy absorption was, in all cases, based on the calorimetric results.

**Irradiation of Sodium Formate Solutions.**—The volume of liquid used for energy calibration was inconveniently large for kinetic experiments. Accordingly, the dewar was replaced by an aluminum dish, 3.5 inches in diameter and 2 inches deep. During irradiations this dish was placed in a constant temperature bath and the contents stirred magnetically as before.

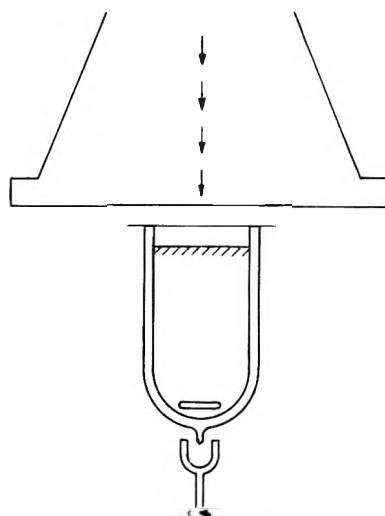


Fig. 1.—Experimental arrangement for calorimetric measurement of the electron beam.

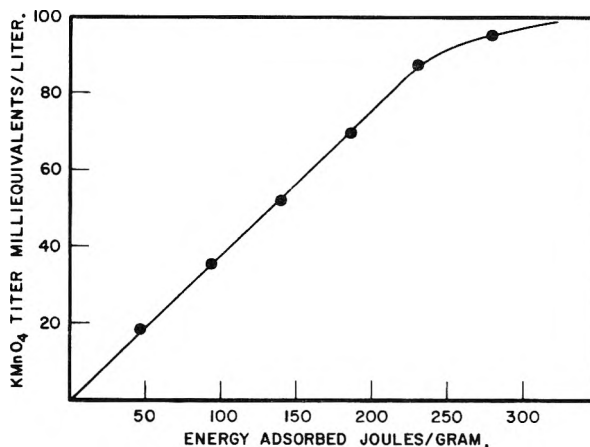


Fig. 2.—Equivalents of  $\text{KMnO}_4$  titer as a function of energy absorbed for a 200-g. sample of 0.10  $M$  sodium formate.

A 200-ml. volume of nitrogen-purged sodium formate solution was put in the dish, filling it to a depth of about 2 inches. Polyethylene film of the same thickness as before was placed over the dish and the unit centered beneath the electron beam at the same distance from the window as the dewar. Minor variations in positioning were shown to have no effect on the results. For a given voltage setting and total charge, it was assumed that the sodium formate solution absorbed the same amount of energy as the water in the dewar in calorimetric experiments. A few experiments using sodium formate solutions in the dewar confirmed this.

**Analysis.**—As will be shown in a subsequent paper, the products of irradiation are hydrogen gas and sodium oxalate, plus small amounts of formaldehyde and glyoxalic acid. Analysis was carried out by making the solution 2  $N$  in sulfuric acid and titrating with 0.1  $N$  potassium permanganate at a temperature above 80°. Under these conditions, a reproducible end-point is found. The total equivalent titer of permanganate is, for convenience, called the amount of reductant produced. The radiolysis products are stable, for aliquots of the irradiated solution gave identical values in determinations made immediately after irradiation and one week later.

### Results

**Effect of Energy Absorbed.**—The production of reductant as a function of energy absorbed is shown in Fig. 2. The response is linear to at least 80% of complete reaction. Although some of the

products are known to react with H and OH radicals, they are well protected by formate ion under our conditions.

**Effect of Sodium Formate Concentration.**—Air-free solutions of sodium formate of various concentrations were irradiated to varying doses. All showed a response proportional to energy absorbed to at least 80% formate ion destruction. In Table I are found the yield of reducing equivalents for various initial formate ion concentrations. No effect of formate concentration on the reductant yield was found in the range 0.05–0.30 *M*. Above 0.5 *M* sodium formate, a slight increase in reductant yield was apparent. This may be due to direct action effects.

TABLE I  
EFFECT OF SODIUM FORMATE CONCENTRATION  
ON REDUCTANT YIELD

| Initial concn. of sodium formate, moles/l. | Reductant yield Mol. equiv. per 100 e.v. |
|--------------------------------------------|------------------------------------------|
| 0.30                                       | 3.41                                     |
| .10                                        | 3.40                                     |
| .05                                        | 3.43                                     |

From these data it can be estimated that the useful range of this system is 1–80 Mrad.

**Effect of Temperature.**—Irradiations were made at various temperatures using 0.1 *N* sodium formate solution in a circulation loop system.<sup>3</sup> In the temperature range 0–40° no difference in reductant yield due to temperature was observed.

**Effect of Oxygen.**—When oxygen was bubbled continuously through the system during irradiation, erratic results were found. This was attributed to the hydrogen peroxide formed which may catalytically decompose and/or scavenge radicals. In most practical systems for which the dosimeter is to be used, the effect due to oxygen present in

(3) T. J. Hardwick, to be published.

solution from dissolved air is barely measurable. A simple purge with nitrogen or hydrogen removes all interferences.

**Effect of Dose Rate.**—The specific rate of energy absorption is difficult to estimate when a spot beam of electrons strikes a rapidly-stirred solution. However, with constant geometry and the same rate of stirring, an increase in the beam current by a factor of two did not change the yield of reductant.

**pH Change.**—The pH of sodium formate solutions in ordinary distilled water is about 7.5. On irradiation, the pH rises rapidly to 10–11 and remains steady. At this pH, aluminum is attacked slightly at temperatures above 35°. Traces of aluminum thus produced in the dosimeter solution do not affect the course of irradiation or the analysis. Disodium hydrogen phosphate in 0.1 molar concentration prevents any such attack on aluminum and does not change the reductant yield. Sodium bicarbonate is unsuitable as a buffer since, on making the initial sodium formate solution 0.1 *M* in sodium bicarbonate, an unexplained increase (20%) in the reductant yield was found.

### Conclusion

The conversion of sodium formate in aqueous solution is suitable as a chemical dosimeter for light particle ionizing radiation. The useful range is approximately 1–80 megarad. The advantages of this system are: (1) linear response with energy absorption to at least 80% destruction; (2) in the range normally used, the effect of oxygen initially dissolved in the solution is almost negligible; (3) the response measured (*i.e.*, reductant production) increases from zero; (4) initial materials (sodium formate and distilled water) are readily available; (5) analysis follows a standard analytical procedure; (6) The system is non-corrosive to normal structural metals at room temperature; (7) the system is temperature independent.

EFFECTS OF SOLUTE CONCENTRATION IN RADIOLYSIS OF WATER<sup>1</sup>

BY MILTON BURTON AND K. C. KURIEN

*Department of Chemistry, University of Notre Dame, Notre Dame, Indiana**Received February 14, 1959*

Effects of halide scavenger on  $G(\text{H}_2\text{O}_2)$  in aerated 0.8  $N$   $\text{H}_2\text{SO}_4$  solutions irradiated in separate experiments with average-24 Mev. X-rays,  $\text{Co}^{60}$   $\gamma$ -rays, 50 kev. X-rays and 3.4 Mev. alphas are in substantial agreement with the expanding-spur treatment of the theory of the radiolysis of water, both in the Ganguly-Magee form and in the earlier Magee form. On the other hand,  $G^0$ , the 100 e.v. yield of initial decomposition, seems to vary with velocity of the impinging particle in a manner not predicted by any current theory. Furthermore, there appears to be an inconsistency in the application of the present, necessarily simplified, theory to the results. The  $G^0$  values found are significantly larger than those corresponding to the Ganguly-Magee model. At the same time, they suggest participation of both ionized and excited molecules in the radiolysis but to a degree considerably less than might be expected on the basis of the vapor phase result of Firestone. The latter is shown to correspond to the assumption that all primarily ionized and excited molecules contribute to the chemistry of the vapor. Apparently, part of the excitation energy is dissipated in the liquid state prior to decomposition to scavengeable free radicals. The results of experiments with "24 Mev." X-rays are qualitatively similar to, but quantitatively different from, those with  $\text{Co}^{60}$   $\gamma$ -rays. The expanding-spur theory would not in any presently existent treatment predict such a result. The specific rates of the scavenger reaction  $\text{X}^- + \text{OH} \rightarrow \text{X} + \text{OH}^-$  have been calculated on the basis of the Ganguly-Magee model to be  $1.6 \times 10^{10}$  l. mole<sup>-1</sup> sec.<sup>-1</sup> for  $\text{Br}^-$  and  $4 \times 10^9$  l. mole<sup>-1</sup> sec.<sup>-1</sup> for  $\text{Cl}^-$ .

## 1. Introduction

A study of fission-fragment-induced decomposition of aqueous thorium nitrate solutions by Boyle and Mahlman<sup>2</sup> shows, on detailed analysis, that  $G(\text{N}_2)$  increases linearly with the first power of the nitrate concentration and that  $G(\text{H}_2)$  decreases linearly with the square-root of the same concentration. Such results suggest that the nitrogen is the product of the direct interaction of the radiation with the nitrate and that the hydrogen results from a simple diffusion-controlled reaction involving free radicals, presumably hydrogen atoms. An indication that the true situation is somewhat more complicated was given earlier by Sworski<sup>3</sup> who pointed out that in air-saturated acid solution of KBr,  $G(\text{H}_2\text{O}_2)$  decreases linearly with the cube-root of concentration when the solution is irradiated with  $\text{Co}^{60}$   $\gamma$ -rays. Shortly thereafter, Magee<sup>4</sup> presented a quantitative theory of diffusion-controlled reactions related essentially to the number of spurs per ionization track.

The conclusions of Magee pertinent to the results may be summarized as follows. The cube-root relationship is fortuitous and only approximate. No single exponential relationship holds over the entire range of solute concentration. However, if the approximate value of the exponent is considered, it will be found to vary with the energy of the impinging radiation from a low value for slow particles like alphas to values approaching 0.5 when the number of spurs per ionization track approaches infinity (as in fission-recoil tracks). The values of the "exponents" are characteristic of the radiation and not of the solute nor indeed of the solvent system under investigation.

Following the initial results of Sworski, a significant number of aqueous systems irradiated with  $\text{Co}^{60}$   $\gamma$ -radiation was found to obey the cube-root relationship. They are summarized in Table I.<sup>3,5-12</sup>

(1) Contribution from the Radiation Project operated by the University of Notre Dame and supported in part under U. S. Atomic Energy Commission Contract AT(11-1)-38. Abstract from a portion of a thesis submitted by K. C. Kurien in partial fulfillment of the requirements for the degree of Doctor of Philosophy.

(2) J. W. Boyle and H. A. Mahlman, *Nuc. Sci. Eng.*, **2**, 492 (1957).

(3) T. J. Sworski, *J. Am. Chem. Soc.*, **76**, 4687 (1954).

(4) J. L. Magee, *J. chim. phys.*, **52**, 528 (1955).

(5) T. J. Sworski, *Radiation Research*, **2**, 26 (1955).

In addition, Sowden<sup>13</sup> found a similar relationship for  $\text{H}_2$  production with  $\text{NO}_3^-$  ion scavenger in an unbuffered  $\text{Ca}(\text{NO}_3)_2$  solution irradiated in a pile with mixed fast neutrons and gammas.

A more elaborate version of the theory by Ganguly and Magee<sup>14</sup> considered the distribution of spurs along the ionization track and made more detailed predictions regarding effect of solute concentration on the so-called "radical yield" in water. These predictions are qualitatively supported in a limited range by the results of Schuler and Allen<sup>15</sup> and also by those of Donaldson and Miller.<sup>16</sup> Schwarz<sup>17</sup> has studied the effect of  $\text{Co}^{60}$   $\gamma$ -rays, 18 Mev. deuterons and 33 Mev. helium ions on  $\text{H}_2$  yield as affected by  $\text{NO}_2^-$  concentration and on  $\text{H}_2\text{O}_2$  yield as affected by  $\text{Br}^-$  concentration.

This paper is a report of a study of  $\text{H}_2\text{O}_2$  yield in radiolysis of bromide and chloride solutions as a function of halide concentration over a broader range of incident-particle velocities than has heretofore been described.

## 2. Experimental

2.1. Chemicals, Solutions, Analyses.—All chemicals used in this work were Baker's A. R. grade. Water used was twice distilled from alkaline permanganate and finally from acid dichromate solution. Special care was exercised to avoid contamination by organic vapors. The general method employed in this work followed Sworski.<sup>3,5</sup> Air-saturated solutions of 0.8  $N$   $\text{H}_2\text{SO}_4$  containing various concentrations of KBr and KCl were employed. Hydrogen peroxide yield was determined by ceric reduction. Spec-

(6) A. O. Allen and R. A. Holroyd, *J. Am. Chem. Soc.*, **77**, 5852 (1955).

(7) H. A. Schwarz, *ibid.*, **77**, 4960 (1955).

(8) H. A. Schwarz and A. O. Allen, *ibid.*, **77**, 1324 (1955).

(9) C. J. Hochanadel and J. A. Ghormley, *Radiation Research*, **3**, 227 (1955).

(10) H. A. Mahlman and J. W. Boyle, *J. Chem. Phys.*, **27**, 1434 (1957).

(11) H. A. Schwarz and J. M. Hritz, *J. Am. Chem. Soc.*, **80**, 5636 (1958).

(12) K. C. Kurien, P. V. Phung and M. Burton, *Radiation Research*, in press.

(13) R. G. Sowden, *J. Am. Chem. Soc.*, **79**, 1263 (1957).

(14) A. K. Ganguly and J. L. Magee, *J. Chem. Phys.*, **25**, 129 (1956).

(15) R. H. Schuler and A. O. Allen, *J. Am. Chem. Soc.*, **79**, 1565 (1957).

(16) D. M. Donaldson and N. Miller, *Radiation Research*, **9**, 487 (1958).

(17) H. A. Schwarz, J. M. Caffrey and G. Scholes, *J. Am. Chem. Soc.*, **81**, in press (1959).

TABLE I

| SUMMARY OF EXPERIMENTS ON CUBE-ROOT RELATIONSHIP IN $\text{Co}^{60}$ $\gamma$ -IRRADIATED AQUEOUS SYSTEMS |                        |                                                                                       |                                        |
|-----------------------------------------------------------------------------------------------------------|------------------------|---------------------------------------------------------------------------------------|----------------------------------------|
| Scavenger                                                                                                 | Product measd.         | Systems studied                                                                       | Investigators                          |
| $\text{Br}^-$                                                                                             | $\text{H}_2\text{O}_2$ | Air-satd. KBr soln. $\text{H}_2\text{SO}_4 = 0.8 N$ or $\text{pH } 2$                 | Sworski <sup>3</sup>                   |
| $\text{Cl}^-$                                                                                             | $\text{H}_2\text{O}_2$ | Air-satd. KCl soln. $\text{H}_2\text{SO}_4 = 0.8 N$ or $\text{pH } 2$                 | Sworski <sup>3</sup>                   |
| $\text{Br}^-$                                                                                             | $\text{H}_2\text{O}_2$ | Air-satd. $\text{Br}^-$ soln. without $\text{H}_2\text{SO}_4$ , $\text{pH} \approx 5$ | Allen and Holroyd <sup>6</sup>         |
| $\text{NO}_2^-$                                                                                           | $\text{H}_2$           | Unbuffered, degassed $\text{KNO}_3$ soln.                                             | Schwarz <sup>7</sup>                   |
| $\text{Cu}^{++}$                                                                                          | $\text{H}_2$           | Unbuffered, degassed $\text{CuSO}_4$ soln.                                            | Schwarz <sup>7</sup>                   |
| $\text{NO}_2^-$                                                                                           | $\text{H}_2\text{O}_2$ | Unbuffered, air or $\text{O}_2$ -satd. $\text{KNO}_3$ soln.                           | Schwarz and Allen <sup>8</sup>         |
| $\text{H}_2\text{O}_2$                                                                                    | $\text{H}_2$           | $\text{H}_2\text{O}_2$ soln.                                                          | Hochanadel and Ghormley <sup>9</sup>   |
| $\text{NO}_3^-$                                                                                           | $\text{H}_2$           | $\text{NaNO}_3$ soln.                                                                 | Mahlman and Boyle <sup>10</sup>        |
| $\text{Fe}^{+++}$                                                                                         | $\text{H}_2$           | Deaerated $0.4 N$ HCl containing $\text{FeCl}_2$ , $\text{Fe}^{+++}$                  | Schwarz and Hritz <sup>11</sup>        |
| $\text{C}_6\text{H}_5\text{OH}$                                                                           | $\text{Fe}^{+++}$      | Oxygenated "Fricke soln." containing phenol                                           | Kurien, Phung and Burton <sup>12</sup> |

trometric measurements were made as quickly as possible in order to avoid any effect of the slow oxidation of  $\text{Br}^-$  ion with ceric ion. The extinction coefficient of ceric ion at  $320 \mu$  at  $25^\circ$  was taken as  $5580 \text{ l. mole}^{-1} \text{ cm.}^{-1}$ .

2.2.  $\gamma$ -Ray Studies.—Twenty-five-cc. sample solutions were irradiated in a 1200 curie underground source, according to methods customary in our laboratory. Energy absorption was determined with a Fricke dosimeter,  $G(\text{Fe}^{+++}) = 15.6$ .

2.3. 50 kv. X-Ray Studies.—A 50 kv. X-ray beam with a maximum intensity at 27 kV,<sup>18</sup> was obtained from an Industrial X-ray Unit (Standard X-ray Co.). For each run two similar cells (1 cm. diameter, 2.5 cm. long) were precisely and reproducibly positioned, in front of the X-ray window. For check of reproducibility, both cells were filled with Fricke dosimeter solution and the ratio of ferric yields after irradiations was determined. In several such trials, the ratio remained constant. With this ratio and the ferric yield in one of the cells known, the energy absorbed in the other cell, when used as the unknown, could be evaluated. Thus, one of the cells served as a dosimeter for the second, sample-containing cell. The value of  $G(\text{Fe}^{+++})$  in the Fricke dosimeter for X-rays in this range was taken as 13.1.<sup>19</sup> The dose rate in this work was one-tenth of that in the case of  $\gamma$ -rays. Employment of smaller dose ensured absence of any effect attributable to depletion of  $\text{O}_2$  in the system.

2.4.  $\alpha$ -Ray Studies.—The samples were irradiated at the Argonne National Laboratory using a  $\text{Po}^{210}$   $\alpha$ -source according to a technique described by Hart and Terandy.<sup>20</sup> The collimated  $\alpha$ -rays from the source entered the cell through a mica window which reduced their energy to 3.4 Mev. The sample solution was stirred vigorously at constant speed by means of a magnetic stirrer. The value of  $G(\text{Fe}^{+++})$  for the Fricke dosimeter in this range was taken as 4.7.<sup>20</sup>

2.5. Betatron X-Rays.—In this series of experiments, two cells were arranged in fixed, reproducible position one behind the other, in the maximum intensity region of the 24 Mev. X-rays from the University of Illinois betatron.<sup>21</sup> The dose rate was  $\approx 2 \times 10^{19} \text{ e.v. l.}^{-1} \text{ min.}^{-1}$ . In order to check reproducibility, a Fricke dosimeter solution was placed in both cells and the ratio of ferric yields after irradiation was determined. In a series of experiments, the ratio of front-cell to back-cell yields remained constant at  $1.11 \pm 0.01$ . In subsequent experiments the solution under investigation was placed in the front cell and Fricke solution was placed in the back cell. From the known ratio of ferric yields in both cells and the measured ferric yield in the back cell in each experiment, the energy absorbed by solution in the front cell could be computed provided  $G(\text{Fe}^{+++})$  for radiation of this quality were known. In the ensuing presentation, the as-

sumption is made that, just as for  $\text{Co}^{60}$   $\gamma$ -radiation,  $G(\text{Fe}^{+++}) = 15.6$ .<sup>22</sup>

2.6. Test of Effect of Dose on  $\text{H}_2\text{O}_2$  Yield. (a)  $\alpha$ -Rays.—Air saturated  $0.8 N$   $\text{H}_2\text{SO}_4$  solutions containing, respectively, KBr and KCl were irradiated for various times at a dose rate  $\approx 1 \times 10^{19} \text{ e.v. l.}^{-1} \text{ min.}^{-1}$  in the whole volume of solution<sup>23</sup> and the yield of  $\text{H}_2\text{O}_2$  was determined. Over a period of 50 minutes,  $\text{H}_2\text{O}_2$  yield was linear with dose.

(b) 50 kv. X-Rays.—Fricke dosimeter solution was placed in both cells and irradiated at a dose rate  $\approx 1.3 \times 10^{20} \text{ e.v. l.}^{-1} \text{ min.}^{-1}$  (in the region immediately behind the window); because of small fluctuations in current, dose was not exactly proportional to duration of irradiation. O.D.<sub>300</sub> of  $\text{Fe}^{+++}$  produced was determined; Fig. 1 shows a linear relationship between yield of  $\text{Fe}^{+++}$  in one cell and time of irradiation over a period of 15 minutes; as related in Section 2.3, the yield in the other cell bore a constant ratio to the values given. In the determination of  $\text{H}_2\text{O}_2$  yield in KBr and KCl solutions, the samples were irradiated for only 5 minutes each. In these systems, oxygen consumption is about one-half that in the case of Fricke solution. As is evident from Fig. 1, even in Fricke solution, 5 minute irradiation is far below the range where there could be an effect due to  $\text{O}_2$  depletion.

### 3. Results

The effect of halide in all cases was to decrease  $G(\text{H}_2\text{O}_2)$ . Table II summarizes the results. The effect of  $\text{Cl}^-$  ion in diminution of  $\text{H}_2\text{O}_2$  yield is consistently less than that of  $\text{Br}^-$  ion.

### 4. Discussion

4.1. Plot of the Data.—In the light of present knowledge of the radiation chemistry of aqueous systems, the theoretically most satisfactory plot of the data would accord with the treatment of Ganguly and Magee.<sup>14</sup> This is a plot of fraction of free radicals unscavenged  $(1 - S)$  as a function of a quantity  $q$ . The latter is itself the product  $k_s c_s t_0$ , where  $k_s$  is the rate constant for the radical-scavenging reaction



$c_s$  is concentration of scavenger solute, and  $t_0$  is a defined initial time characteristic of the spur. In the single-radical theory water is treated as a symmetrical two-radical compound  $\text{R}_2$  and  $\text{H}_2$ ,  $\text{H}_2\text{O}_2$  and  $\text{H}_2\text{O}$  are the equivalent products of a recombination reaction



Figure 2 includes, among other curves, the theoretical Ganguly-Magee plot for 0.5 Mev. electron irradiation which corresponds rather closely to what would be expected for  $\text{Co}^{60}$   $\gamma$ -irradiation.

(22) J. Zsula, A. Liuzzi and J. S. Laughlin, *Radiation Research*, **6**, 661 (1957).

(23) The actual energy absorbed was ca.  $5 \times 10^{16} \text{ e.v. min.}^{-1}$  in a volume (directly behind the window) of ca.  $5 \times 10^{-1} \text{ cc.}$  of solution.

(18) Cf. M. A. Liechti, "Roentgen Physik," Verlag von Julius Springer, Wien, 1939, p. 86.

(19) This is an estimated value derived from  $G(\text{Fe}^{+++}) = 12.9 \pm 0.2$  for tritium  $\beta$ -irradiation, given by W. R. McDonell and E. J. Hart, *J. Am. Chem. Soc.*, **76**, 2121 (1954);  $G(\text{Fe}^{+++}) = 13.1 \pm 0.5$  for 60 kVp. X-rays of effective mean energy = 21 kev. given by J. L. Haybittle, R. D. Saunders and A. J. Swallow, *J. Chem. Phys.*, **25**, 1213 (1956).

(20) E. J. Hart and J. Terandy, *Rev. Sci. Instr.*, **29**, 962 (1958).

(21) The X-ray distribution (i.e., the photon intensity) of this instrument is said to be fairly homogeneous over the entire energy range up to 24 Mev.

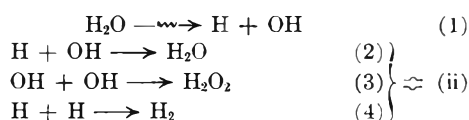
TABLE II

$G(\text{H}_2\text{O}_2)$  AND  $G_w(\text{H}_2\text{O}_2)$  IN AIR-SATURATED 0.8 N  $\text{H}_2\text{SO}_4$  AS A FUNCTION OF HALIDE CONCENTRATION FOR VARIOUS CONDITIONS OF IRRADIATION

| Radiation<br>cs, $M$ | $\text{Co}^{60}\text{-}\gamma^a$ |                               | $<50$ kev. X-ray <sup>b,21</sup> |                               | 3.4 Mev. $\alpha^c$         | $\text{Co}^{60}$ X-ray <sup>d</sup> |                               |
|----------------------|----------------------------------|-------------------------------|----------------------------------|-------------------------------|-----------------------------|-------------------------------------|-------------------------------|
|                      | $G(\text{H}_2\text{O}_2)$        | $G_w(\text{H}_2\text{O}_2)^e$ | $G(\text{H}_2\text{O}_2)$        | $G_w(\text{H}_2\text{O}_2)^e$ | $G(\text{H}_2\text{O}_2)^f$ | $G(\text{H}_2\text{O}_2)^f$         | $G_w(\text{H}_2\text{O}_2)^e$ |
| 0                    | 1.21                             | 0.805                         | 1.33                             | 0.99                          | 1.65 <sup>g</sup>           | 1.18                                | 0.79                          |
| KBr                  |                                  |                               |                                  |                               |                             |                                     |                               |
| $10^{-5}$            |                                  |                               |                                  |                               | 1.57                        | 1.13                                | .765                          |
| $2 \times 10^{-5}$   |                                  |                               | 1.23                             | .94                           |                             |                                     |                               |
| $5 \times 10^{-6}$   | 1.15                             | .775                          |                                  |                               | 1.52                        | 1.05                                | .725                          |
| $10^{-4}$            |                                  |                               | 1.18                             | .915                          |                             |                                     |                               |
| $5 \times 10^{-4}$   | 1.075                            | .74                           |                                  |                               | 1.53                        | 1.00                                | .70                           |
| $10^{-3}$            |                                  |                               | 1.07                             | .86                           |                             |                                     |                               |
| $5 \times 10^{-3}$   | 0.93                             | .67                           | 0.99                             | .82                           | 1.45                        | 0.79                                | .595                          |
| KCl                  |                                  |                               |                                  |                               |                             |                                     |                               |
| $10^{-4}$            |                                  |                               |                                  |                               |                             | 1.14                                | .77                           |
| $10^{-3}$            | 1.10                             | .75                           | 1.145                            | .90                           | 1.53                        | 1.03                                | .715                          |
| $10^{-2}$            | 0.98                             | .69                           | 0.97                             | .81                           | 1.49                        | 0.95                                | .675                          |
| $3 \times 10^{-2}$   | 0.88                             | .64                           | 0.855                            | .75                           | 1.37                        |                                     |                               |
| $10^{-1}$            | 0.72                             | .56                           | 0.73                             | .69                           |                             | 0.62                                | .51                           |

<sup>a</sup>  $G_F$  taken as 0.40. <sup>b</sup>  $G_F$  taken as 0.65 from the value for 10 kev. X-rays. <sup>c</sup> Measured value of  $G(\text{H}_2\text{O}_2)$  is taken as  $G_w(\text{H}_2\text{O}_2)$  because contribution due to radicals escaping from the spur is negligible. <sup>d</sup>  $G_F$  taken as 0.40 by analogy with  $\text{Co}^{60}$   $\gamma$ -ray value, which pertains to essentially isolated spurs. <sup>e</sup> Calculated as described in Section 4.2. See also footnote 25. <sup>f</sup> The reliability of the relative values is good; the reliability of the absolute values is not established. <sup>g</sup> Cf.  $G_w(\text{H}_2\text{O}_2)$  in Table III.

When  $\text{H}_2\text{O}_2$  is the product by which a scavenging effect is studied, it would appear that  $G_w(\text{H}_2\text{O}_2) + G_w(\text{H}_2)^{25} + G_r$ , where  $G_r$  is the yield of a reverse reaction in the spur (see Section 4.2), is the summed yield which is to be related to  $(1 - S)$ . In terms of the Ganguly-Magee model, the significant reactions of the radicals are



Halide scavenger (see Section 4.2) affects only concentration of OH; thus it has no direct effect on reaction 4 and but little on reaction 2 as compared with reaction 3. It follows that as a matter of theory and convenience  $G_w(\text{H}_2\text{O}_2)$  is the quantity which can be most directly related, in a first approximation, to  $(1 - S)$ .

We define a factor  $f$  so that

$$f \cdot G_w(\text{H}_2\text{O}_2) \approx (1 - S) \quad (1)$$

In the range of low  $g$ , or low  $c_s$ ,  $(1 - S)$  for 0.5 Mev. electrons  $\approx 0.49$  and changes very slowly. Examination of the data for both  $\text{Br}^-$  and  $\text{Cl}^-$  as scavenger shows  $f = 0.63$ .

In order to complete the plot, one notes that

$$\log c_s + \log \Delta = \log g \quad (2)$$

where

$$\Delta = k_2 t_0 \quad (3)$$

and  $\Delta$  is therefore a quantity characteristic of a particular scavenger and independent of the quality of the radiation. The quantities

$$\begin{aligned} \Delta(\text{Br}^-) &= 2 \\ \Delta(\text{Cl}^-) &= 1/2 \end{aligned}$$

are thus obtained by simple fitting of the quantity  $f \cdot G_w(\text{H}_2\text{O}_2)$  for  $\text{Co}^{60}$   $\gamma$ -rays to the Ganguly-

(24) M. Lefort, *Ann. Rev. Phys. Chem.*, **9**, 123 (1958).

(25) The 100 e.v. yields of  $\text{H}_2\text{O}_2$  and  $\text{H}_2$ , respectively, from water itself at the earliest detectable stage; we follow the convention of H. A. Dewhurst and M. Burton, *J. Am. Chem. Soc.*, **77**, 5781 (1955).

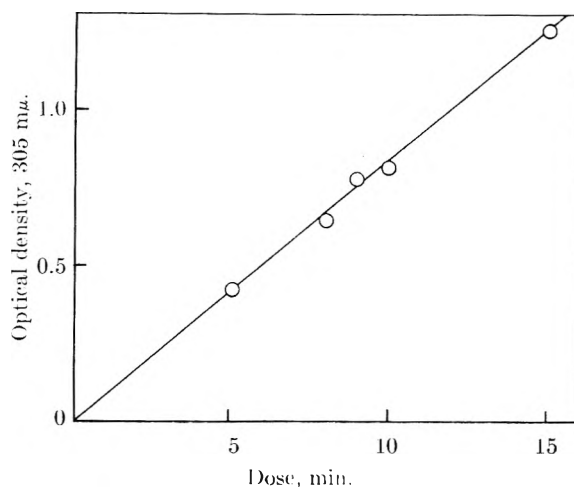


Fig. 1.—Dependence of  $\text{Fe}^{+++}$  yield on irradiation time in Fricke dosimeter exposed to  $<50$  kev. X-rays; dose rate  $\sim 1.3 \times 10^{20}$  e.v.  $\text{l}^{-1} \text{min}^{-1}$ .

Magee plot. According to Ganguly and Magee  $t_0 = 1.25 \times 10^{-10}$  sec. Substitution of the appropriate values of  $\Delta$  and  $t_0$  in equation 3, yields the specific rates of the scavenger reaction  $\text{X}^- + \text{OH} \rightarrow \text{X} + \text{OH}^-$  as  $1.6 \times 10^{10}$  liter mole $^{-1}$  sec. $^{-1}$  for  $\text{Br}^-$  and  $4 \times 10^9$  liter mole $^{-1}$  sec. $^{-1}$  for  $\text{Cl}^-$ .

Figure 2 shows that the data for the effect of  $\text{Br}^-$  and  $\text{Cl}^-$  on  $G(\text{H}_2\text{O}_2)$  in solutions irradiated by  $\text{Co}^{60}$   $\gamma$ -rays may be fitted rather smoothly to the Ganguly-Magee curve for 0.5 Mev. electrons. It also shows that when the same values of  $f$  and  $\Delta$  are applied to the data obtained with other types of irradiation, the resultant curves also approximate rather closely to what one might expect on the basis of the original Ganguly-Magee calculations.

One feature of Fig. 2 is particularly notable. The curve for 24 Mev. X-rays lies below the  $\text{Co}^{60}$   $\gamma$ -curve. This range of irradiation has not yet been theoretically examined for possible effect on  $(1 - S)$ . However, Professor A. Kuppermann,

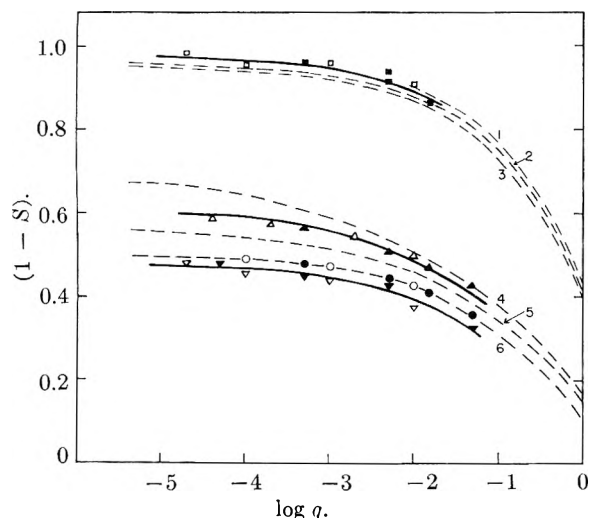


Fig. 2.—Plot of data according to model of Ganguly and Magee. Theoretical Ganguly-Magee plots: (1) 2.0 Mev.  $\alpha$ ; (2) 7.68 Mev.  $\alpha$ ; (3) 10.0 Mev.  $\alpha$ ; (4) 0.01 Mev.  $\beta$ ; (5) 0.05 Mev.  $\beta$ ; (6) 0.5 Mev.  $\beta$ . Experimental results:  $\square$ , KBr for 3.4 Mev.  $\alpha$ -irradiation;  $\blacksquare$ , KCl for 3.4 Mev.  $\alpha$ -irradiation;  $\triangle$ , KBr for <50 Kev. X-rays irradiation;  $\blacktriangle$ , KCl for <50 kev. X-rays irradiation;  $\circ$ , KBr for  $\text{Co}^{60}$   $\gamma$ -irradiation;  $\bullet$ , KCl for  $\text{Co}^{60}$   $\gamma$ -irradiation;  $\nabla$ , KBr for 24 Mev. X-rays irradiation;  $\blacktriangledown$ , KCl for 24 Mev. X-rays irradiation.

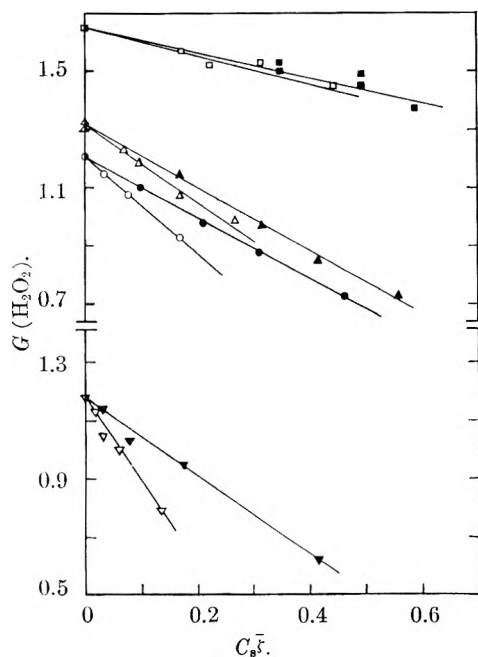


Fig. 3.—Sworski-type plot of  $G(\text{H}_2\text{O}_2)$  values in air-saturated 0.8N  $\text{H}_2\text{SO}_4$  solutions of KCl and KBr for different radiations. The concentration of solute is  $C_s$ .

$\blacksquare$ , KCl for 3.4 Mev.  $\alpha$ -irradiation }  $\bar{s} = 0.15$   
 $\square$ , KBr for 3.4 Mev.  $\alpha$ -irradiation }  
 $\blacktriangle$ , KCl for <50 kev. X-rays irradiation }  $\bar{s} = 0.26$   
 $\triangle$ , KBr for <50 kev. X-rays irradiation }  
 $\bullet$ , KCl for  $\text{Co}^{60}$   $\gamma$ -irradiation }  $\bar{s} = 0.33$   
 $\circ$ , KBr for  $\text{Co}^{60}$   $\gamma$ -irradiation }  
 $\blacktriangledown$ , KCl for 24 Mev. X-rays irradiation }  $\bar{s} = 0.38$   
 $\nabla$ , KBr for 24 Mev. X-rays irradiation }

who has been doing machine calculations on the basis of the Ganguly-Magee model, tells us that the inter-spur distance is already so great in the case of  $\text{Co}^{60}$   $\gamma$ -irradiation that no further effect is to be expected as the result of any possible increase in such distance with irradiation of higher average

energy. Resort to some other explanation of these results seems necessary.

**4.2. Elementary Reactions and Yields.**—According to the simple free-radical model of the radiation chemistry of aqueous solutions, we note that the first steps are reactions 1 and 2. The 100 e.v. yield of water molecules initially decomposed, represented by reaction 1, is  $G^0$ . The yield of radicals available for scavenging is decreased, according to the Ganguly-Magee model by reverse reaction 2 as well as by reactions 3 and 4, all of which take place in the spur and the sum of which is formally equivalent to the "recombination reaction"  $\bar{r}$ . On that model the total number of radicals available for subsequent reaction is

$$G_R = 2[G^0 - G_w(\text{H}_2\text{O}_2) - G_w(\text{H}_2) - G_r] \quad (4)$$

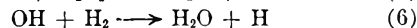
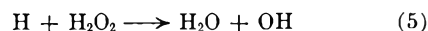
$$= G_w(\text{H}) + G_w(\text{OH}) \quad (5)$$

The quantity  $(1 - S)$  of Ganguly and Magee is *not* simply related to the actualities of water. A convenient "experimental" relationship is

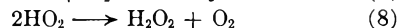
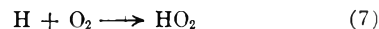
$$(1 - S)_e \approx \xi/2G^0 \quad (6)$$

where  $\xi$  is a quantity the nature of which remains to be established.

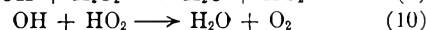
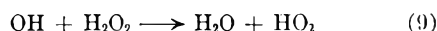
The yields of reactions 3 and 4, which are presumed to take place within the spur are given, respectively, for  $\text{Co}^{60}$   $\gamma$ -irradiation, as  $G_w(\text{H}_2\text{O}_2) \approx 0.78$  and  $G_w(\text{H}_2) \approx 0.39$ .<sup>26</sup> In the absence of scavenger, products so formed (as well as any products produced outside the spur) are destroyed by the reactions<sup>27</sup>



When  $\text{O}_2$  is present, the free H atoms are intercepted



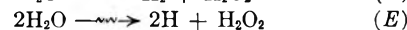
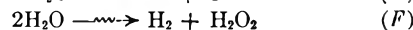
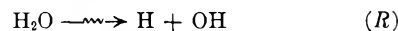
but the yield of  $\text{H}_2\text{O}_2$  so produced is decreased by the reactions<sup>28</sup>



so that the total 100 e.v. yield of  $\text{H}_2\text{C}_2$  in presence of oxygen becomes

$$G(\text{H}_2\text{O}_2) = G_w(\text{H}_2\text{O}_2) + \frac{1}{2}[G_w(\text{H}) - G_w(\text{OH})] \quad (7)$$

At this stage of the considerations, it is convenient to introduce the stoichiometric relationships of Allen as they were employed by Sworski.<sup>3</sup>

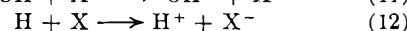
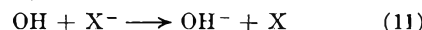


In the terminology employed in this paper

$$G_w(\text{H}_2\text{O}_2) = G_F + G_E \quad (8)$$

$$G(\text{H}_2\text{O}_2) = G_F + 2G_E \quad (9)$$

When, in addition to oxygen, the solution contains halide ion, the reactions



can replace reactions 5, 6, 7, 9 and 10 to some ex-

(26) H. A. Mahlman and J. W. Boyle, *Radiation Research*, **7**, 436 (1957).

(27) A. O. Allen, *Disc. Faraday Soc.*, **12**, 79 (1952).

(28) A. O. Allen, *Radiation Research*, **1**, 85 (1954).

tent. Sworski effectively short-circuited the involved considerations of mechanism and considered simply that the reaction sequence 11, 12 effectively decreases only  $G_E$ . With  $G_F$  thus taken constant, it follows that  $G_E$  in any case can be calculated from relation 9 and  $G_w(\text{H}_2\text{O}_2)$  is then given by equation 8. This is the procedure used in calculation of the  $G_w(\text{H}_2\text{O}_2)$  values shown in Table II.

**4.3. Initial Decomposition.**—In order to make expression 6 directly applicable in the Ganguly-Magee theory we must take into account the fact that, in the actual case, unlike the theory, only one portion of the radicals (*i.e.*, the OH radicals) can be directly affected by halide. Thus, for purposes of comparison with the Ganguly-Magee treatment,  $\xi$  is not simply  $2G_w(\text{H}_2\text{O}_2)$ , but is instead equal to a term which includes all unscavenged radicals, (*cf.* Section 4.1); *i.e.*

$$\xi = 2[G_w(\text{H}_2\text{O}_2) + G_w(\text{H}_2) + G_r] \quad (10)$$

The quantity  $G_r$  can be very roughly estimated on the basis of simple combinations provided we neglect consideration of relative specific rates of reactions 2, 3 and 4. The two cases, which must be considered, are the continuous column of ionization and the column of separate spurs. In the former case  $G_r = G_w(\text{H}_2\text{O}_2) + G_w(\text{H}_2)$ . In the latter case, we may for simplicity (and with some further introduction of error) consider only the "average spur," which is assumed to contain originally 3H and 3OH radicals.<sup>14</sup> Consideration of the possible combinations indicates that for this case  $G_r = 1.5 [G_w(\text{H}_2\text{O}_2) + G_w(\text{H}_2)]$ . The values of  $G_r$  so obtained are applied to actual cases to obtain values of  $\xi$  and  $G^0$  shown in Table III.

TABLE III

SOME CHARACTERISTIC PARAMETERS FOR VARIOUS RADIATIONS

| Radiation                        | $G_w(\text{H}_2)$ | $G_w(\text{H}_2\text{O}_2)$ | $G_w(\text{H})$ | $G_w(\text{OH})$ | $\xi^a$ | $G^0$ | $(1 - S)_e$ |
|----------------------------------|-------------------|-----------------------------|-----------------|------------------|---------|-------|-------------|
| $\alpha^{b,24}$                  | 1.70              | 1.65                        | 0.55            | 0.65             | 13.4    | 7.3   | 0.92        |
| <50 kv. X <sup>c,24</sup>        | 0.65              | 1.0                         | 2.90            | 2.20             | 8.2     | 6.7   | 0.62        |
| Co <sup>60</sup> - $\gamma^{26}$ | 0.39              | 0.78                        | 3.7             | 2.92             | 5.8     | 6.3   | 0.47        |

<sup>a</sup> For Co<sup>60</sup>  $\gamma$ -radiation this is the value of  $\xi$  at  $q = 10^{-4}$ . The other values are simply for "low concentration" of scavenger. <sup>b</sup> These are the values for 5.3 Mev.  $\alpha$ 's. The residual energy of the  $\alpha$ 's used in the present work was 3.4 Mev. <sup>c</sup> The values of the  $G$ 's used in the table are the nearest known values; *i.e.*, those for 10 kv. X-rays.

The values of  $(1 - S)_e$  shown in Table III are in reasonably good agreement with the Ganguly-Magee values of  $(1 - S)$  shown in Fig. 2. Since the latter values in turn are fitted very well by experimental data adduced in this paper, it is reasonable to conclude that the results shown in Table III support the method of approximate calculations of  $G_r$  and thus of  $G^0$ .

Three points regarding the values of  $G^0$  are worthy of comment. First, the value of  $G^0$  is greater for the slow  $\alpha$ -particles. There is nothing in the Ganguly-Magee picture which would predict such an effect.<sup>29</sup> Second, the values of  $G^0$  are less

(29) P. J. Dyne and J. M. Kennedy, *Can. J. Chem.*, **36**, 1518 (1958), assume  $6 \pm 1$  "radical pairs" per "average spur." The approximation used here, that  $G_r = 1.5[G_w(\text{H}_2\text{O}_2) + G_w(\text{H}_2)]$  for Co<sup>60</sup>  $\gamma$ -rays and 24 Mev. X-rays, tends to bring the calculated  $G^0$  values closer together. If the Dyne-Kennedy picture of the average spur is employed,

than the value  $11.7 \pm 0.6$  obtained by Firestone<sup>30</sup> in a study of water vapor containing T<sub>2</sub>O and D<sub>2</sub>. Third, the "average spur," presumed to contain 6 radicals,<sup>14</sup> is presumed also to contain 3 ions.<sup>31</sup> Noting the value  $W(\text{H}_2\text{O})$ , the energy per ion pair for water vapor,  $\sim 30$  e.v.<sup>32</sup> it follows (if one may use the same value for liquid water<sup>33</sup>) that the energy per average spur is 90 e.v. Unless  $W(\text{H}_2\text{O})_{\text{liquid}}$  is really only about  $1/2 W(\text{H}_2\text{O})_{\text{gas}}$  and if ionized molecules are the sole source of radicals, one might expect for both Co<sup>60</sup>  $\gamma$  and low-energy X-rays, on the basis of the Ganguly-Magee model, a maximum value

$$G^0 = \frac{100}{90} \times 3 = 3.3$$

The alternative view is that excited water molecules contribute significantly to the radiolysis of liquid water; under any circumstances, they appear to participate significantly in the radiolysis of water vapor. The assumption that all ionized and excited molecules contribute to the radiolysis of water vapor leads to the maximum value

$$G^0_{\text{max}} = \frac{100}{W(\text{H}_2\text{O})} + \frac{100}{E} \left[ 1 - \frac{I}{W(\text{H}_2\text{O})} \right] \quad (11)$$

where  $I$  is the lowest ionization potential, 12.56 e.v.<sup>34</sup> and  $E$  the lowest excitation potential, 6.5 e.v.<sup>35</sup> of water vapor. Thus,  $G^0_{\text{max}} = 12.2$ , which may be compared with the Firestone value  $G^0 = 11.7 \pm 0.6$

**4.4. Values of the "Exponent."**—In the Magee treatment,  $-\log(S - S_0)$  is plotted against  $-\log q$ . A series of curves is obtained which depart only slightly from straight lines; the average slopes are characteristic of the number of spurs per ionization track and of the nature of the impinging particle. In an equivalent treatment, the log of the decrease in  $G(\text{H}_2\text{O}_2)$ , *i.e.*,  $\log[-\Delta G(\text{H}_2\text{O}_2)]$ , may be plotted as a function of  $\log c_a$ . Any error in the absolute value of  $G(\text{H}_2\text{O}_2)$  is without effect on the slope. Thus, this sort of plot permits comparison of experiment with theory without introduction of any additional calculations or assumptions regarding dose measurement or determination of  $G(\text{H}_2\text{O}_2)$ . Such plots exaggerate the significance of small experimental errors, particularly at low  $c_a$ . On the other hand, the method does enable establishment of the average exponent in the approximate relation

$$G(\text{H}_2\text{O}_2) \approx G_0(\text{H}_2\text{O}_2) - kc_a\bar{\zeta} \quad (12)$$

where  $G_0(\text{H}_2\text{O}_2)$  refers to the yield in absence of halide. Table IV summarizes the values of  $\bar{\zeta}$ .

The fit of the data on the Sworski<sup>3</sup> type of plot,  $G(\text{H}_2\text{O}_2)$  vs.  $c_a\bar{\zeta}$ , is shown in Fig. 3. The values of  $\bar{\zeta}$  are in obviously good agreement with the predictions of the Magee treatment, except (*cf.* Section

the factor 1.5 is reduced to about 1.2 and the calculated  $G^0$  values would be thus thrust even farther apart.

(30) R. F. Firestone, *J. Am. Chem. Soc.*, **79**, 5593 (1957).

(31) E. Kara-Michailoua and D. E. Lea, *Proc. Cambridge Phil. Soc.*, **36**, 101 (1940).

(32) A. K. Appleyard, *Nature*, **164**, 838 (1949).

(33) *Cf.* U. Fano, *Phys. Rev.*, **70**, 44 (1946).

(34) W. C. Price and T. M. Sugden *Trans. Faraday Soc.*, **44**, 108 (1948).

(35) H. Sponer, "Molekulspektren und ihre Anwendung auf Chemische Probleme, Vol. I, Tabellen," Verlag von Julius Springer, Berlin, 1935, p. 102.



4.1) that nothing in the present state of the model would lead to the expectation that the  $\bar{\zeta}$  value for "24 Mev." X-rays should exceed that for Co<sup>60</sup>  $\gamma$ -rays.

TABLE IV  
VALUES OF THE "EXPONENT,"  $\bar{\zeta}$ , FOR DIFFERENT RADIATIONS

| Radiation                   | Scavenger       |                 |
|-----------------------------|-----------------|-----------------|
|                             | Cl <sup>-</sup> | Br <sup>-</sup> |
| "24 Mev." X-rays            | 0.38            | 0.38            |
| Co <sup>60</sup> - $\gamma$ | .34             | .32             |
| 50 kev. max. X-rays         | .26             | .26             |
| 3.4 Mev. $\alpha$           | .15             | .15             |

### Conclusion

In many respects the data for effect of scavenger in the radiolysis of water show results in agreement with the Ganguly-Magee and Magee treatment of the expanding-spur theory. However, more detailed quantitative examination of the results show curious discrepancies which will

ultimately require some refinement of the mode and which may reveal some presently unexpected features of the mechanism of the radiolysis of liquid water.

It appears clear that both ions and excited molecules contribute to free-radical formation in the cases studied but that some reverse reaction of free radicals occurs so rapidly that it is inaccessible to the effect of scavenger.

**Acknowledgment.**—The authors are indebted to Dr. E. J. Hart and the Argonne National Laboratory for use of their Po  $\alpha$ -source, to the University of Illinois for access to the 24 Mev. betatron, to Professor A. Kuppermann, who made arrangements for such use and who assisted in the experiments and gave generously of his time for theoretical discussion, and to Professor J. L. Magee for his repeated advice on theoretical aspects of this work, and for access to his original computations, which permitted a more exact plot than do the original published curves.

## RADIATION CHEMICAL PROCESSES IN RIGID SOLUTIONS

BY H. T. J. CHILTON AND G. PORTER

*Chemistry Department, University of Sheffield, Sheffield, England*

*Received February 14, 1969*

Gamma radiolysis of rigid solutions of aromatic molecules in paraffin solution at 77°K. results in the formation of aromatic radicals which have been trapped and identified by means of their electronic absorption spectra. Studies of the radicals which result from the radiolysis of toluene and a number of its derivatives show that although the primary fission processes are very similar to those which follow irradiation at 2537 Å. there are also significant differences. *G*-values of formation of triphenylmethyl from solutions of triphenylmethane have been determined and it is shown that dissociation of the solute is brought about principally by energy transferred from the solvent and that the efficiency of this transfer is 800 l. solvent/mole solute.

The absorption of ionizing radiations is an un-specific process and most of the energy taken up by a dilute solution is absorbed by the solvent. The matrix isolation technique therefore appears less promising for the study of primary radiation chemical processes than for photochemical processes since, in the former case, the trapped primary products which are observed might be expected to arise principally from the matrix rather than from the solute. For this reason, although studies of the free radicals which result from the photochemical dissociation of a solute in a dilute rigid solution are of great value in the elucidation of primary photochemical processes<sup>1-3</sup> most radiation chemical studies using the trapped radical technique have been concerned with pure substances.<sup>4,5</sup>

A system which has proved particularly appropriate for the study of primary photochemical processes is one in which an aromatic molecule, especially toluene or one of its derivatives, is dissociated by ultraviolet irradiation in dilute solutions at low temperatures. Most of the benzyl type radicals which result from such dissociations have

been identified spectroscopically and the main features of the primary photochemical dissociation at the  $\beta$ -bond have been elucidated.<sup>3</sup> In the present work we have extended this type of study to the primary processes of radiation chemical dissociation. Contrary to the considerations of the last paragraph we have found that the species which are trapped and observed under these conditions are few in number and remarkably specific. It appears that energy absorbed by the solvent results in dissociation of the solute, even when the latter is in concentrations as low as  $10^{-3}$  *M* and when the solvent is quite rigid. Further, of the many primary products of solute dissociation which are energetically possible, only one is observed in most cases.

### Experimental

The basic experimental technique was that of Norman and Porter<sup>2</sup> except that the ultraviolet source was replaced by one for  $\gamma$ -irradiation.

A quartz cell of 12.5 mm. path length was used to contain the solutions which were always outgassed before freezing in liquid nitrogen. The cell could be clamped rigidly in a fixed position in a large Dewar flask of liquid nitrogen which was placed in front of a Co-60  $\gamma$ -ray source of approximately 70 Curie. Dose rates of up to  $2.6 \times 10^4$  rad./hr. could be obtained and were measured by means of the standard ferrous sulfate dosimeter.<sup>6</sup> After irradiation, the cell containing

(1) G. N. Lewis and D. Lipkin, *J. Am. Chem. Soc.*, **64**, 2801 (1942).

(2) I. Norman and G. Porter, *Proc. Roy. Soc. (London)*, **A230**, 399 (1955).

(3) G. Porter and E. E. Strachan, *Trans. Faraday Soc.*, **54**, 1595 (1958).

(4) C. F. Luck and W. Gordy, *J. Am. Chem. Soc.*, **78**, 3240 (1956).

(5) M. S. Matheson and B. Smaller, *J. Chem. Phys.*, **23**, 521 (1955).

(6) G. Weiss, "Peaceful Uses of Atomic Energy," **14**, 179, United Nations (1956).

the frozen solution was transferred to a Dewar vessel containing liquid nitrogen, the design of which is shown in Fig. 1. It is made up of several easily replaceable parts and has a number of advantages over the original all quartz spectroscopy Dewar of Norman and Porter.

Spectra were recorded using a Hilger E484 spectrograph and SeloChrome plates in conjunction with either a tungsten lamp or a hydrogen discharge lamp. For the quantitative work on triphenylmethane a Unicam SP500 spectrophotometer, which had been modified to take a pair of spectroscopic Dewars in place of the normal quartz cells, was used. Super purity quartz, which does not discolor when irradiated, eventually was used for the cells. In earlier runs, where the super purity quartz could not be used, correction for the quartz absorption was applied and any discoloration was removed by heating the cell at the completion of each experiment.

The solvents used to form glasses were E.P.A. (ether, isopentane and ethanol in the proportions 5:5:2 by volume) and M.P. (methylcyclohexane and isopentane in the proportions 2:3 by volume). They were carefully purified and dried.<sup>2</sup> Pure samples of a number of solutes used in similar photochemical work<sup>3</sup> were supplied by Dr. E. Strachan, namely benzhydrol, benzyl chloride, benzylamine, benzotrichloride, diphenylmethane, triphenylmethane, *t*-butylbenzene and isopropylbenzene. Ethylbenzene was purified by the method of Vogel<sup>7</sup> and other solutes by fractional distillation or recrystallization.

### Results

**Preliminary Observations.**—Irradiation of the pure solvents E.P.A. and M.P. at  $-196^\circ$ , with doses similar to those used in the later work on solutions ( $4 \times 10^5$  rad.), produced no permanent change which could be detected by ultraviolet spectroscopic or chromatographic analysis of the liquid after warming to room temperature. The rigid E.P.A. glass, after irradiation, showed an intense absorption throughout the visible and ultraviolet region which remained as long as the glass was held at  $-196^\circ$ . The glass was violet in color after short irradiations and became quite opaque in a 1 cm. path after a dose of  $10^5$  rad. The color disappeared completely as the temperature of the glass was raised to softening point. The absorption spectrum extended from 7000 Å. to shorter wave lengths and may arise from "trapped electrons" or from radicals such as  $\text{CH}_3\text{CHOH}$ .<sup>8</sup> The E.P.A. glass is clearly unsuitable for the ultraviolet spectroscopic study of  $\gamma$ -irradiated solutions.

The pure hydrocarbon M.P. glass showed no such effect on irradiation at  $-196^\circ$  and remained quite transparent throughout the visible and quartz ultraviolet region of the spectrum after a dose of  $4 \times 10^5$  rad. It was therefore used for all subsequent investigations.

Irradiation of solutions of various aromatic molecules in M.P. glass at  $-196^\circ$ , followed by spectroscopic investigation at the same temperature, showed characteristic sharp banded absorption spectra which disappeared when the glass was brought to room temperature and which closely resembled the spectra of benzyl and its derivatives, found after photolysis of the same compounds. The spectra were, in most cases, more intense than the strongest absorptions so far obtained in photochemical studies of rigid solutions, using the same path length and were comparatively free from other diffuse absorption spectra such as those of hexa-

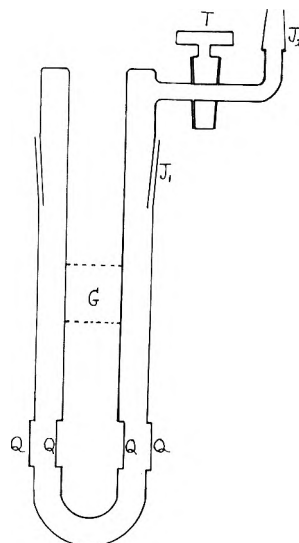


Fig. 1.—G = quartz/Pyrex graded seal; J<sub>1</sub>, J<sub>2</sub> = standard joints; Q = quartz windows; T = vacuum tap. Optical dewar vessel used for ultraviolet absorption spectroscopy.

triene derivatives. The spectra of these solutions showed no measurable permanent change after warming, except for some small continuous absorption at shorter wave lengths in a few cases which was, however, generally much smaller than in the corresponding photochemical experiment, in spite of the greater concentration of radicals originally present in the irradiated glass.

On warming the glassy solutions after irradiation, the rise in temperature was accompanied by an emission of light, readily visible in subdued daylight. The glow was quite separate and readily distinguishable from that of quartz, being more intense, of different color and observed over a different temperature range. Furthermore, the warm-up glow of the solutions varied in color from one solute to another. For example the luminescences of solutions of toluene, benzyl chloride and ethylbenzene solutions were green, whilst those of *t*-butylbenzene and diphenylmethane were pale yellow. The warm-up glows must therefore involve the solute molecule or its products but their origin is not yet known. There is no correlation with the observed radical spectra since not only solutions of benzene and chlorobenzene but also the pure M.P. solvent showed a luminescence after irradiation. On the other hand no phosphorescence of comparable intensity was observed on warming irradiated E.P.A. glass. Attempts to record the spectrum of the warm-up glow were not successful.

**Identification of the Absorption Spectra and Dissociation Processes.**—As already mentioned, the solutions investigated showed absorption spectra which closely resembled those obtained after ultraviolet irradiation under the same conditions. There were, however, significant differences. For example rigid carbon disulfide solutions, which yield the CS radical after short exposure to ultraviolet light, showed no such spectrum after  $\gamma$ -irradiation, although some changes took place as evidenced by a weak continuous absorption, a green color of the solution which disappeared on warming, and a smell of garlic in the products. Again, rigid solutions of

(7) A. I. Vogel, *J. Chem. Soc.*, 607 (1948).

(8) M. C. R. Symons and M. Townsend, *J. Chem. Phys.*, **25**, 1299 (1956).

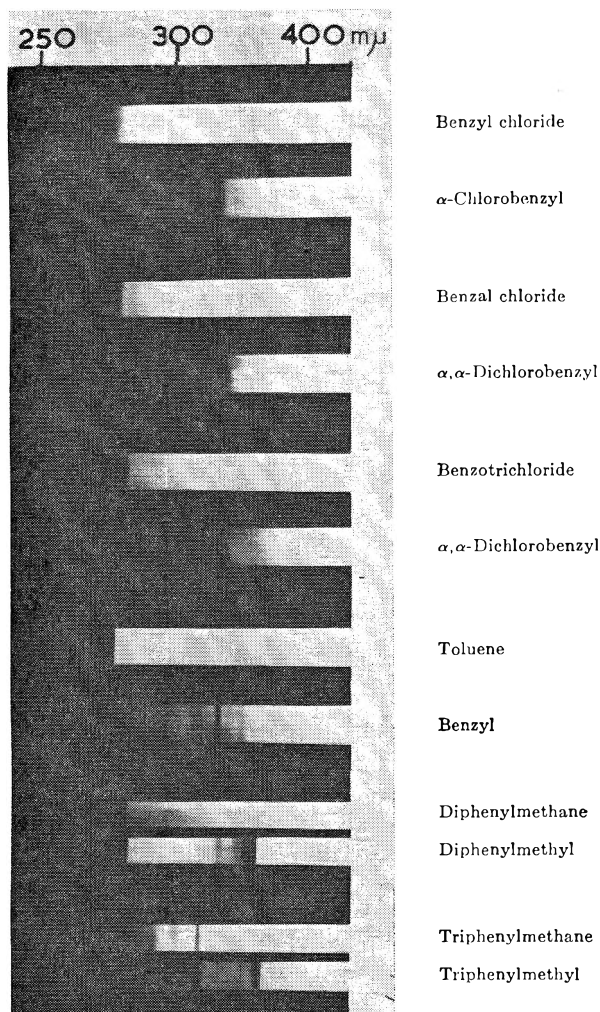


Fig. 2.—Radical spectra resulting from the radiolysis of aromatic molecules at 77°K. In each case the first spectrum is recorded before and the second after irradiation of the rigid solution.

benzene which, when subjected to ultraviolet irradiation, yield intense absorption bands attributed to hexatriene, showed no such spectrum after  $\gamma$ -irradiation.

On the other hand toluene and its derivatives gave strong banded absorption spectra when irradiated with  $\gamma$ -rays in M.P. solution at  $-196^\circ$ . Their assignments and relationships to spectra observed under similar conditions after photolysis provide information concerning the primary processes taking place. Three classes of compound have been investigated in which the hydrogens of the methyl group of toluene are successively substituted by phenyl, chlorine and methyl, respectively. Typical spectrographic records of the glasses before and after irradiation are shown in Fig. 2.

**Phenylmethanes.**—These compounds, and the related molecule benzhydrol, gave absorption spectra whose main bands were identical, within the limits of measurement, with those obtained from the photochemical dissociation of the same compounds in M.P. glass. The identity was confirmed by direct comparison of the plates and, in the case of triphenylmethane, by spectrophotometric measurements.

Wave lengths of band maxima, with approximate relative intensities on a scale of ten, are given in Table I. The measurements were made independently on each plate and the error in wave length is estimated at about  $\pm 5 \text{ \AA}$ . for the sharp bands and  $\pm 10 \text{ \AA}$ . for the broader bands.

The assignments of the main absorption bands to benzyl, diphenylmethyl and triphenylmethyl can be made with confidence in view of the evidence already put forward in support of those assignments by Porter and Strachan.<sup>3</sup> The assignment of the radical from benzhydrol to diphenylmethyl cannot however be considered definite until the spectrum of the semipinacone is known. Some of the weaker unidentified bands may also belong to the same radicals since the absorption was stronger in the  $\gamma$ -ray work and the weakest bands would have been below the limit of detection in the photochemical experiments. In at least one case, that of toluene, there are bands at longer wave lengths which are absent after photochemical dissociation and which cannot be attributed to the benzyl radical.

**Chlorine Substituted Derivatives.**—The radical spectra from the three compounds of this class, as well as from toluene itself, were very similar, consisting principally of one strong band and a weaker doublet at shorter wave lengths. The spectra derived from benzal chloride and benzotrìchloride were identical within the accuracy to which plates could be compared. The spectrum derived from benzyl chloride was definitely different from these and from that of benzyl. These facts, and comparison with the wave lengths of the radical spectra previously measured, lead to the assignments of radicals formed which are given in Table II.

There were very few additional bands from the chlorinated molecules but a weak band at 3179  $\text{\AA}$ . obtained from benzyl chloride may indicate that a small amount of benzyl also is formed.

Comparison with the photochemical dissociation processes of these molecules reveals that, unlike the previous class of phenylmethanes, the chlorine compounds show differences in their behavior to  $\gamma$  and to ultraviolet irradiation. The clearest example of this difference is found in benzyl chloride which with 2537  $\text{\AA}$ . irradiation, yields benzyl whilst, with  $\gamma$ -rays, little or no benzyl is found and  $\text{C}_6\text{H}_5\text{CHCl}$  is the main product observed. Only in toluene and benzotrìchloride are the products the same with both kinds of irradiation. The  $\beta$ -bond fission processes of these molecules therefore depend on the type of irradiation. With  $\gamma$ -irradiation the H atom separates in preference to the chlorine atom whilst the converse is true with ultraviolet irradiation.

**Ethyl-, Isopropyl- and *t*-Butylbenzenes.**—The band maxima of radicals derived from these hydrocarbons, with their probable assignments, are given in Table III. These spectra were weaker and more diffuse and there were also some relatively intense additional bands so that the assignments are less definite than in the two previous classes of compound. Again, however, the spectra from isopropyl- and *t*-butylbenzene were quite different

TABLE I

| Molecule         | Band max. assigned to radical $\lambda$ (Å.) |          |          | Radical        | Unassigned band max. $\lambda$ (Å.) |          |
|------------------|----------------------------------------------|----------|----------|----------------|-------------------------------------|----------|
| $C_6H_5CH_3$     | 3179 (10)                                    | 3071 (3) | 3044 (3) | $C_6H_5CH_2$   | 3339 (4)                            | 3242 (2) |
| $(C_6H_5)_2CH_2$ | 3365 (10)                                    | 3314 (2) |          | $(C_6H_5)_2CH$ | 3270 (2)                            | 3237 (2) |
| $(C_6H_5)_2CHOH$ | 3377 (10)                                    | 3333 (2) |          | $(C_6H_5)_2CH$ | 3121 (6)                            | 3015 (2) |
| $(C_6H_5)_3CH$   | 3425 (10)                                    | 3293 (2) |          | $(C_6H_5)_3C$  | 3252 (1)                            | 3141 (6) |
|                  |                                              |          |          |                | 3067 (1)                            |          |
|                  |                                              |          |          |                | 2790-2800 (6)                       |          |

TABLE II

| Molecule       | Band max. assigned to radical $\lambda$ (Å.) |          |          | Radical       | Unassigned band max. $\lambda$ (Å.) |          |
|----------------|----------------------------------------------|----------|----------|---------------|-------------------------------------|----------|
| $C_6H_5CH_3$   | 3179 (10)                                    | 3071 (3) | 3044 (3) | $C_6H_5CH_2$  | 3339 (4)                            | 3242 (2) |
| $C_6H_5CH_2Cl$ | 3225 (10)                                    | 3112 (3) | 3075 (3) | $C_6H_5CHCl$  | 3179 (2)                            | 2994 (1) |
| $C_6H_5CHCl_2$ | 3243 (10)                                    | 3131 (3) | 3105 (3) | $C_6H_5CCl_2$ | 2959 (1)                            |          |
| $C_6H_5CCl_3$  | 3243 (10)                                    | 3137 (3) | 3101 (3) | $C_6H_5CCl_2$ | 3334 (1)                            |          |
|                |                                              |          |          |               | ...                                 |          |

TABLE III

| Molecule           | Band max. assigned to radical $\lambda$ (Å.) |          |          | Radical           | Unassigned band max. $\lambda$ (Å.) |           |
|--------------------|----------------------------------------------|----------|----------|-------------------|-------------------------------------|-----------|
| $C_6H_5CH_2CH_3$   | 3236 (10)                                    | 3163 (2) | 3098 (2) | $C_6H_5CHCH_3$    | 3355 (2)                            | 3328 (6)  |
|                    |                                              |          | 3078 (4) |                   |                                     |           |
| $C_6H_5CH(CH_3)_2$ | 3245 (10)                                    |          |          | $C_6H_5C(CH_3)_2$ | 3439 (4)                            | 3325 (10) |
| $C_6H_5C(CH_3)_3$  |                                              | ...      |          | ...               | 3313 (10)                           | 3228 (7)  |

from benzyl derived from toluene whilst the radical spectrum derived from ethylbenzene was unique and showed no bands of benzyl. The corresponding spectra obtained after ultraviolet irradiation of these substances are also relatively weak and have been measured in E.P.A. solution only, but it seems probable that the principal processes of  $\beta$ -bond fission are the same with both types of irradiation and that the hydrogen atom separates in preference to the methyl group.

All the  $\beta$ -bond fission processes discussed and given in Tables I, II and III are summarized by the following statement. The  $\gamma$ -irradiation of solutions of toluene and its derivatives in rigid M.P. solution leads to fission of a  $\beta$ -bond, and, when more than one type of  $\beta$ -bond is present in such a molecule, the probability of separation of a hydrogen atom is greater than that of  $CH_3$ ,  $C_2H_5$  or a chlorine atom.

This is the same as was found for ultraviolet irradiation under similar conditions with the important exception that the order of probabilities of fission of C-H and C-Cl bonds is reversed.

#### G-Values and their Concentration Dependence.

—The  $G$ -values of radical formation have been studied for the formation of triphenylmethyl from triphenylmethane. This particular case was chosen first because its photochemical quantum yield has been determined under similar conditions and second because triphenylmethyl is the only one of the radicals which we have studied whose absolute extinction coefficient is known, having been measured at 77°K. by Chu and Weissman.<sup>9</sup>

Solutions of triphenylmethyl in M.P. were irradiated for 16 hours under identical conditions at  $-196^\circ$  and the concentration of the triphenylmethyl radical formed was measured in the modified Unicam spectrophotometer, the comparison cell containing an identical solution which had not been irradiated. The dose rate in these runs, deter-

mined by standard ferrous sulfate dosimetry, was  $2.6 \times 10^4$  rad./hr. and the total dose was  $4.2 \times 10^5$  rad. After small corrections for the different absorption coefficients of the solutions this leads to a  $G$ -value of triphenylmethyl formation from a  $5.33 \times 10^{-3}$  molar solution of triphenylmethane of 0.17 radicals/100 e.v.

The  $G$ -value of 0.17 is calculated per 100 e.v. of energy absorbed by the solution. Most of this energy is absorbed in the first place by the solvent, the proportion absorbed by the solute, calculated on the basis of absorption of energy by Compton scattering, is equal to the ratio of electron densities in solute and solvent and is  $1.7 \times 10^{-3}$  for a  $5.33 \times 10^{-3}$  M solution. The energy used in the dissociation of the solute must therefore be derived mainly from energy originally absorbed by the solvent.

Further evidence that energy transferred from the solvent is mainly responsible for dissociation of the solute was obtained from studies of the radical yield as a function of solute concentration. Owing to the fact that the  $\gamma$ -ray source is no longer available to us we have not yet been able to obtain as complete data on this important factor as we would wish. The data so far available are, however, sufficient to show that the radical yields are not proportional to solute concentration, as would be the case if only energy absorbed by the solute were utilized for dissociation, but tend to a limiting value at higher concentrations, indicating that the process of energy transfer from the solvent is approaching unit efficiency. The radical yields, as a function of solute concentration, are shown in Fig. 3.

#### Discussion

There is much previous evidence to show that radiation chemical change in a solute may be brought about as a result of energy originally absorbed by the solvent. The particular significance of studies of such effects in rigid solutions,

(9) T. L. Chu and S. I. Weissman, *J. Chem. Phys.*, **22**, 21 (1954).

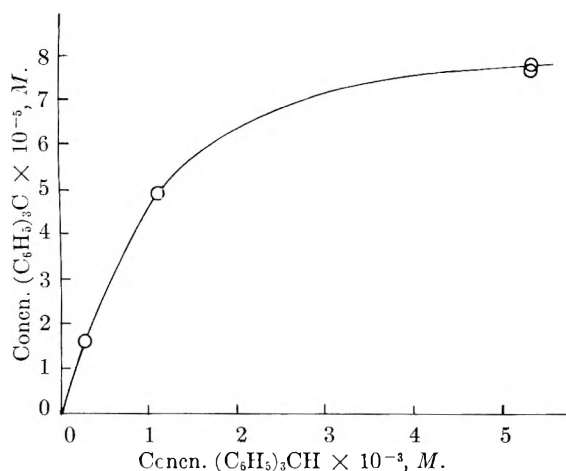
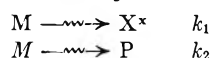


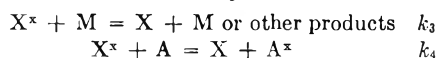
Fig. 3.—Variation of triphenylmethyl radical concentration with triphenylmethane concentration at constant dose.

apart from the directness of the observation of the intermediate products, lies in the fact that processes involving molecular diffusion are eliminated.

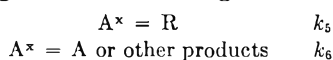
The energy absorbed by the matrix or solvent M appears as potential energy of separation of ions  $M^+$  and electrons and of free radicals, as electronic excitation of matrix molecules and as residual kinetic energy of these products, particularly as sub-excitation electrons.<sup>10</sup> At least one of these forms of energy must be transferred, in the present experiments, to the solute molecules which are in relatively low concentration in the rigid solvent. We shall describe the energetic product or products whose energy is transferred to the solute by the symbol  $X^x$  and all other products derived from irradiation of the solvent by P



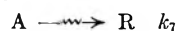
Now  $X^x$  may lose its energy by the matrix or may transfer it in some way to the solute A



and  $A^x$  may dissociate to give the observed radical R or undergo some other change not forming R



Finally, in more concentrated solutions, radicals may be formed by direct irradiation of the solute



Steady-state treatment of this scheme leads to the following expression for the concentration [R] of radicals formed in unit time

$$[R] = \frac{k_1 k_4 k_5 [A] [M]}{(k_5 + k_6)(k_3 [M] + k_4 [A])} + k_7 [A]$$

when  $k_1$  and  $k_7$  are the rates of reactions 1 and 7 for unit concentrations of M and A, respectively.

In dilute solution  $k_7 [A] \ll k_1 [M]$  and the second

(10) R. L. Platzman, *Radiation Research*, **2**, 1 (1955).

term in this expression is negligibly small. Then

$$\frac{1}{[R]} = \frac{k_3}{k_1 k_4 [A]} + \frac{k_3 k_6}{k_1 k_4 k_5 [A]} + \frac{1}{k_1 [M]} + \frac{k_6}{k_1 k_5 [M]}$$

A plot of  $1/[R]$  versus  $1/[A]$  should therefore be linear for dilute solutions and

$$\frac{\text{Intercept}}{\text{Slope}} = \frac{k_4}{k_5 [M]} \text{ l. mole}^{-1} = P_0$$

$P_0$  is the energy transfer probability for unit solute concentration.

The data of Fig. 3. are in accord with this relation and lead to the value

$P_0 = 830 \text{ l. mole}^{-1} = 7000 \text{ molecules solvent/molecule solute}$  i.e., the probability of transfer of the energy to a molecule of triphenylmethane is approximately 7000 times greater than that of its degradation by a solvent molecule.

In addition to the efficiency of the energy transfer process from  $X^x$  to A there are indications that the intermediate  $X^x$  must be formed efficiently in process 1 and is a major product of the primary processes. The quantum yields of photochemical dissociation of aromatic hydrocarbons are usually small and the quantum yield of the particular process under consideration, viz., the dissociation of triphenylmethane to triphenylmethyl radicals in a rigid glass at  $-196^\circ$ , has been measured and found to be 0.01 at  $2537 \text{ \AA}$ .<sup>3</sup> If  $A^x$  in our present scheme were identical with the excited triphenylmethane formed by  $2537 \text{ \AA}$ . irradiation, i.e., the lowest excited singlet state, it would follow that the G-value of formation of  $A^x$  at high concentrations of A was  $\sim 20$  and that since the excitation potential of the first singlet state in triphenylmethane is 4.6 e.v.,<sup>11</sup> more than half the total energy absorbed by the solution is used in excitation of the solute. In fact  $A^x$  probably contains considerably more energy than the molecule excited by  $2537 \text{ \AA}$ . light and may therefore have a somewhat greater dissociation probability.

Although molecular diffusion processes are eliminated in the present experiments several alternative explanations of the energy transfer mechanism are possible. Discussion of these will be postponed until further data on the concentration dependence of radical yield become available. The results of this present investigation show that studies of trapped radicals formed by radiolysis of dilute rigid solutions provide a promising approach to the study of primary radiation chemical processes and energy transfer.

We are grateful to the director and staff of the David Morrison Research Department, of the Sheffield National Centre for Radiotherapy, for the opportunity of using their  $\text{Co}^{60}$  source. We are also grateful to the General Electric Research Laboratory of Schenectady, N.Y. for financial support which made this work possible.

(11) R. A. Friedel and M. Orchin, "Ultraviolet Spectra of Aromatic Compounds," John Wiley and Sons, Inc., New York, N. Y., 1951.

# THE RADIATION-INDUCED POLYMERIZATION OF ISOBUTENE: A LIQUID PHASE IONIC REACTION

By E. COLLINSON, F. S. DAINTON AND H. A. GILLIS

Department of Physical Chemistry, The University, Leeds 2, England

Received February 14, 1959

New evidence is presented in support of the suggestion that the  $\gamma$ -ray induced polymerization of liquid isobutene at  $-78^\circ$  proceeds solely by a cationic mechanism. Attempts to polymerize isobutene at  $-78^\circ$  with free radicals from the photolysis of diacetyl, benzoin and benzil were unsuccessful but the benzil solution irradiated with ultraviolet light at  $77^\circ\text{K}$ . was shown by electron spin resonance measurements to give rise to radicals from the isobutene. Isobutene irradiated in the pure state at a  $\gamma$ -ray dose rate of  $7 \times 10^{17}$  e.v. ml.<sup>-1</sup> min.<sup>-1</sup> polymerized with  $G(-\text{C}_4\text{H}_8) = 3.0 \pm 1.7 \times 10^2$ . Solutions of  $\text{FeCl}_3$ , DPPH, benzoquinone and iodine in isobutene were also irradiated with  $\gamma$ -rays. Of these solutes, only benzoquinone reduced the polymerization rate to zero, and DPPH had no significant effect. The effects of  $\text{FeCl}_3$  and  $\text{I}_2$  on the polymerization were complicated by other factors. The measured yields of conversion of the solutes after irradiation were  $G(-\text{DPPH}) = 3.7 \pm 0.2$ ,  $G(\text{Fe(II)}) = 3.0 \pm 0.5$  and  $G(-\text{Q}) = 1.5 \pm 0.2$ . The electron spin resonance spectrum of isobutene irradiated with  $\gamma$ -rays at  $77^\circ\text{K}$ . showed the presence of H atoms which disappeared rapidly, and a more stable radical, the spectrum of which consisted of 6 peaks having an over-all spacing of 158 gauss at the operating frequency of 9400 Mc. sec.<sup>-1</sup>. The same six peak pattern was obtained from cyclopropane irradiated with  $\gamma$ -rays at  $77^\circ\text{K}$ . and from a solution of benzil in isobutene irradiated with ultraviolet light at  $77^\circ\text{K}$ . It is concluded that the radical responsible for this spectrum is either the cyclopropyl radical or the methyl substituted allyl radical, the latter being the less likely. The most likely initiating ion is considered to be  $(\text{CH}_3)_3\text{C}^+$ , and a mechanism consistent with the available data is proposed.

## Introduction

In 1947, after some 37 years of active work in Radiation Chemistry S. C. Lind<sup>1</sup> summarized the mechanistic dilemma in the words "Generally two ideas have dominated the theory of radiation chemistry: One is that the ions themselves are the direct agents in the reactions. There is a great deal of exact quantitative evidence in favor of this theory but little theoretical support. A second idea that has had great support in recent years is that the chemical effects of radiation are brought about by the action of free radicals or atoms. There is strong theoretical but little experimental evidence of quantitative character supporting this view." Whilst it is still true that there is convincing experimental evidence supporting the first idea, at least in relation to certain gas phase reactions, the application of modern physical and chemical methods of radical identification and estimation during the past 11 years has demonstrated that radicals and atoms are essential intermediates in the vast majority of radiation-chemical reactions in the liquid phase. Although recent studies, especially those concerned with mass spectrometry, serve as a reminder that the essential radicals originate in part from earlier reactions of ions with molecules or from breakdown of unstable molecular ions or from charge neutralization processes, it is difficult to specify a single radiation-chemical reaction occurring in an organic liquid for which ions are the sole cause of the major chemical change observed. In the main this difficulty stems from the scarcity of reactions for which a radical mechanism could not give rise to some, if not all, of the observed products. Our purpose in this paper is to consider whether the radiation-induced polymerization of liquid isobutene is a reaction which can only proceed by an ionic mechanism, as proposed by Davison, Pinner and Worrall.<sup>2</sup>

Isobutene may be polymerized in the vapor or liquid phase either by radiation or by Friedel-

Crafts type catalysts.<sup>3</sup> As might be expected for a monomer of such low heat of polymerization the vapor phase polymerization at temperatures slightly above room temperature is accompanied by depropagation reactions which are largely responsible for the marked negative temperature coefficient.<sup>4</sup> The polymerization of pure liquid isobutene at room temperatures and below is free from this complication, is very readily induced by traces of Friedel-Crafts catalysts and is one of the classic examples of polymerization by the cationic mechanism. Polymerization of liquid isobutene by a free-radical mechanism has not been observed and radical-initiated copolymerization experiments with, for example, vinyl chloride<sup>5</sup> and sulfur dioxide,<sup>6</sup> indicate that the isobutyl radical has no tendency to add to an isobutene molecule.

The work of Davison, Pinner and Worrall<sup>2</sup> on the polymerization of liquid isobutene, initiated by irradiation with  $^{60}\text{Co}$   $\gamma$ -rays or 2 Mev. electrons, indicated that the polymer formed is indistinguishable from that produced by chemical initiation. On the other hand the  $G$ -value for chain initiation (calculated from the rate and the viscosity average molecular weight on the assumption that chain transfer is absent) is very low (about 0.1) unless a solid such as zinc oxide is present, when it may become as large as 2.8. In the absence of added solids the rate of polymerization is proportional to the dose rate, as would be expected for an ionic reaction. In contrast, oxygen and benzoquinone, two classical inhibitors of free-radical polymerizations, also inhibited this reaction.

## Experimental

**Materials.**—Isobutene from a cylinder supplied by The

(3) (a) Vapor: Radiation—W. Mund and P. Huyskens, *Bull. classe sci. Acad. roy. Belg.*, **36**, 610 (1950); W. Mund, C. Guidee and J. Vanderauwera, *ibid.*, **41**, 805 (1955); (b) Vapor:  $\text{BF}_3$ —A. G. Evans, G. W. Meadows and M. Polanyi, *Nature*, **160**, 869 (1947); (c) Liquid: radiation—Ref. 2 above; S. H. Pinner and R. Worrall, *J. Polymer Sci.*, **34**, 229 (1959); (d) Liquid: Friedel-Crafts catalysts—see D. C. Pepper, *Quart. Revs.*, **8**, 88 (1954).

(4) F. S. Dainton and K. J. Ivin, *ibid.*, **12**, 61 (1958).

(5) A. G. Evans and M. Polanyi, *J. Chem. Soc.*, 252 (1947).

(6) L. L. Ryden and C. S. Marvel, *J. Am. Chem. Soc.*, **57**, 2311 (1935).

(1) S. C. Lind, *THIS JOURNAL*, **52**, 437 (1948).

(2) W. H. T. Davison, S. H. Pinner and R. Worrall, *Chemistry and Industry*, 1274 (1957).

Distillers' Company Limited was fractionated at reduced pressure through a 3-foot vacuum jacketed column packed with Fenske helices and provided with a vapor take-off. The condensate was dried by agitation over specially prepared barium oxide and stored under vacuum.

Commercial samples of diacetyl, resublimed iodine and British Oxygen Company cyclopropane were used as received. Commercial samples of benzil and benzoin were recrystallized from ligroin and ethyl alcohol, respectively. Diphenylpicrylhydrazyl (DPPH) was kindly provided by Dr. K. E. Russell and had been recrystallized from solution in a mixture of pure benzene and chloroform. The benzoquinone was a commercial sample which had been recrystallized from ligroin and dried under vacuum. Ferric chloride was prepared by the action of dry chlorine on very pure iron wire and subsequently purified by sublimation into small glass bulbs provided with break-seals.

**Apparatus.**—The source consisted of 1800 curies  $^{60}\text{Co}$ . Two types of irradiation cell were used. The cells for following the course of the polymerization dilatometrically consisted of test-tubes, 11 mm. i.d. and containing 6 ml., sealed to precision bore capillary tubing of 1.0 mm. i.d. For experiments in which the disappearance of radical scavengers was followed spectrophotometrically, the irradiation cells were provided with a side-arm connected through a graded Pyrex to quartz seal to a plane ended cylindrical quartz cell which could be precisely fitted into the appropriate holder of a Unicam SP 500 Spectrophotometer. Most of the kinetic experiments were effected on isobutene at  $-78^\circ$ . Temperature control to  $\pm 2^\circ$  was achieved by immersing the bulk of the irradiation cell in a Dry Ice-acetone mixture contained in a transparent Dewar vessel.

**Procedure.**—Before all experiments the irradiation cells were cleaned as follows. After immersion for at least 30 min. in a boiling mixture of nitric and sulfuric acids the cells were washed successively with distilled water, ammonium hydroxide solution and distilled water, then steamed out for not less than 30 min. and dried. The cell and degassing manifold were always evacuated for 8 hours and then flamed out before admission of any reagents. Weighed quantities of solute were distilled or sublimed into the irradiation cell first and followed by distillation of the required quantity of isobutene, which had been exhaustively deaerated by the usual freezing-melting cycles under vacuum. The reaction cell then was sealed off, time was allowed for dissolution of any solute, and measurement of the optical density of the solution at the selected wave length was measured. The cell was then immersed in the cryostat for sufficient time to ensure thermal equilibration and the irradiation was begun. Dosimetric measurements were made with the Fricke dosimeter in cells of identical shape and position to those of the irradiation cells. The dose rates for all these experiments were in the range  $2$  to  $10 \times 10^{17}$  e.v. ml. $^{-1}$  min. $^{-1}$ .

**Analysis.**—Spectrophotometric analysis by established methods was used as described below.

## Results

**1. Failure to Achieve Free-radical Polymerization at  $-78^\circ$ .**—It was clearly necessary to eliminate any possibility that isobutene could undergo free-radical polymerization at  $-78^\circ$ . Since there is in this system no suitable method of generating radicals homogeneously by thermal means, it was decided to use photosensitizers. Azo bisisobutyronitrile seemed on general grounds to be an appropriate substance but preliminary experiments showed it to be insufficiently soluble. Biacetyl does not suffer from this disadvantage, is known to be a photosensitizer for free radical polymerization and has the added merit of an absorption band in the blue ( $\lambda_{\text{max}} = 4200 \text{ \AA.}$ ) region of the spectrum. A solution of 0.02 ml. of biacetyl in 3 ml. of isobutene had an optical density of 0.273 at 4200  $\text{\AA.}$  No detectable polymer was produced when this solution was irradiated for a prolonged period with unfiltered light from a high pressure mercury arc, the quartz reaction vessel being immersed in a Dry Ice-acetone bath. After two hours irradiation

the optical density at 4200  $\text{\AA.}$  had dropped to 0.05, suggesting that at least 80% of the biacetyl had been destroyed. The single absorption band with a maximum at wave length 2650  $\text{\AA.}$  was partially replaced by two absorption bands, one of which, having  $\lambda_{\text{max}} = 2900 \text{ \AA.}$ , was strongly reminiscent of the spectrum of acetaldehyde in hydrocarbon solution.

Similar experiments were performed with benzil and benzoin as photosensitizers. No polymer was produced when a solution of 0.0175 g. of benzil in 4 ml. of isobutene was irradiated at  $-78^\circ$  for one hour with the full light of the mercury lamp, despite the fact that very marked spectral changes indicated substantial photolysis of the benzil. Likewise the photolysis of a saturated solution of benzoin in isobutene gave no polymer in 4 hours irradiation, and the resulting spectrum was consistent with the production of benzaldehyde.

**2. Kinetics of Polymerization of "Pure" Isobutene.**—The rates of polymerization were rather irreproducible. Of fourteen runs performed with isobutene which had been subjected only to trap-to-trap distillation and then dried by a variety of methods, including distillation from a storage reservoir at  $-78^\circ$ , filtration through a fine sintered glass disc at  $-78^\circ$ , distillation through barium oxide columns, and distillation through a column of sodium-coated glass helices, the fastest rate was 30 times greater than the slowest and the standard deviation was 160% of the mean rate. For eight runs using isobutene which had been fractionally distilled and subjected to the same drying procedure (known to be very effective in the case of styrene) it was found that  $G(-\text{C}_4\text{H}_8) = (3.0 \pm 1.7) \times 10^2$  (standard deviation) which is somewhat lower than the values quoted by others.<sup>2</sup> Some of this lack of reproducibility may be due to impurities generated in the sealing off process, since heating of the tip of the dilatometer comparable to that necessary for sealing off caused a 35% reduction in rate.

In other respects the experiments were very satisfactory. No induction periods were observed, the shrinkage-dose curves were linear up to 4% polymerization (see Fig. 1) and the separation of small transparent globules of swollen polymer did not appear to influence the reaction.

**3. Irradiation of Solutions of DPPH in Isobutene.**—The molar decadic extinction coefficients of DPPH in isobutene at  $20^\circ$  were found to be 9,200 at 5100  $\text{\AA.}$  and 720 at 7,500  $\text{\AA.}$  As illustrated in Fig. 2 the optical density decreases linearly with dose up to about  $14 \times 10^{17}$  e.v./ml. for the solution of highest concentration and then diminishes more slowly. This change in slope in the later stages of the reaction is due partly to light scattering by suspended polymer particles and partly to the fact that the products of the DPPH reaction also absorb light of these wave lengths. The initial slopes of the optical density-dose curves indicate that  $G(\text{DPPH})$  is  $3.7 \pm 0.2$  for solute concentrations in the range 150 to 750  $\mu\text{M}$ .

DPPH had no significant effect on the rate of polymerization. Thus in two pairs of runs  $G(-\text{C}_4\text{H}_8)$  for a saturated solution of DPPH in iso-

butene was 20% larger and 41% smaller than  $G(-C_4H_8)$  for the samples of isobutene subjected to the same purification but containing no solute.

**4. Irradiation of Solutions of Ferric Chloride in Isobutene.**—Like other electron donating organic substances<sup>7</sup> isobutene will dissolve a limited amount of ferric chloride and the resultant slightly yellow solution shows an absorption spectrum characteristic of tetravalent Fe(III) with a maximum at 3450 Å. On standing, either at room temperature or  $-78^\circ$ , polymerization occurs and is accompanied by a decrease in the characteristic absorption spectrum. These changes are comparatively slow if the isobutene and ferric chloride are very carefully dried and therefore we presume they are both associated with the cationic polymerization of isobutene catalyzed by  $FeCl_3$  and cocatalyzed by some unidentified substance which is probably water. Using drastically dried materials the optical density of a solution of  $FeCl_3$  in isobutene irradiated at  $-80^\circ$  diminishes linearly with dose at 3700, 3900 and 4000 Å., up to a dose of about  $2 \times 10^{18}$  e.v. ml.<sup>-1</sup> as shown in Fig. 3. Above this dose the separation of polymer particles causes deviations from linearity. If after irradiation the isobutene is evaporated and ethanol added, Fe(II) may be detected in the resultant solution by addition of *o*-phenanthroline. The mean value of  $G(Fe(II))$  for the complete irradiation is then found to be  $3.0 \pm 0.5$ . It is difficult to obtain reliable values of the extinction coefficients of  $FeCl_3$  in isobutene, but taking  $\epsilon^{3450} = 6000$  and  $\epsilon^{4000} = 1800$  l. mole<sup>-1</sup> cm.<sup>-1</sup>, which values are similar to the values in similar solvents such as hexadecene-1,<sup>7</sup>  $G(-Fe(III))$  may be calculated to be 3.0.

**5. Irradiation of a Solution of Benzoquinone in Isobutene.**—The extinction coefficient of benzoquinone in isobutene is 207 l. mole<sup>-1</sup> cm.<sup>-1</sup> at  $\lambda = 3200$  Å. Irradiation of a 3 mM solution resulted in a linear decrease of optical density with time until almost 50% of the benzoquinone had been destroyed, when the optical density decreased ever more slowly as the reaction proceeded (see Fig. 3). The constant value of  $G(-Q)$ , where Q denotes benzoquinone, in the early stages was  $1.3 \pm 0.2$ . When benzoquinone was present no polymer was produced.

**6. Irradiation of Solutions of Iodine in Isobutene.**—Solutions of iodine in isobutene are decolorized on irradiation but on prolonged standing color is nearly completely regenerated. The optical density at  $\lambda_{max} = 4800$  Å. decreases linearly with dose up to about  $4 \times 10^{18}$  e.v. ml.<sup>-1</sup> (see Fig. 3) after which the separation of the polymer particles interferes with the light absorption. The apparent extinction coefficient at 4800 Å., based on the known total iodine concentration, is 61. This value is only about 5% of the value of the extinction coefficient of iodine in a number of saturated hydrocarbons at this wave length and would lead to an absurdly high value for  $G(-I_2)$  of the order of  $10^2$ . A reasonable, but as yet unverified, explanation of these phenomena is that a large fraction (>90%) of the iodine in isobutene exists

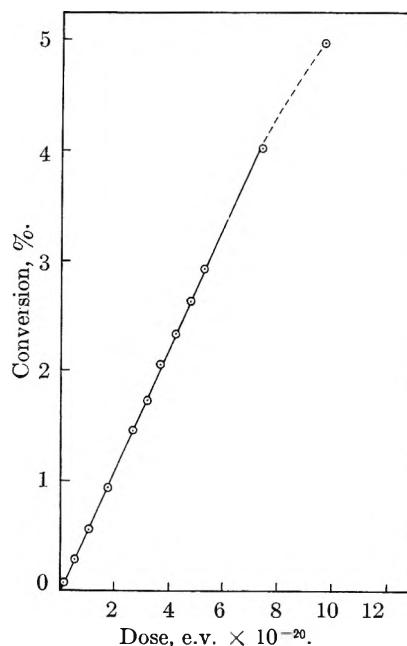


Fig. 1.—Shrinkage-dose curve for "pure" isobutene at  $-78^\circ$ . Dose rate =  $7 \times 10^{17}$  e.v. ml.<sup>-1</sup> min.<sup>-1</sup>; dilatometer bulb volume = 6.0 ml.; capillary internal diameter = 1 mm.,  $G(-C_4H_8) = 205$ .

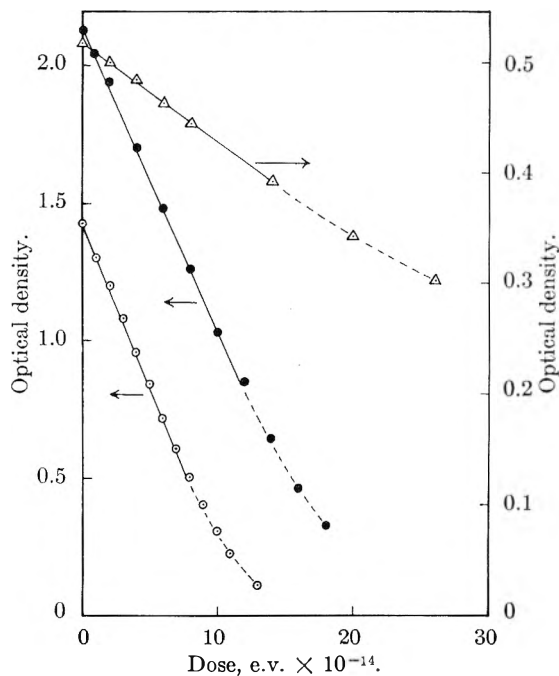


Fig. 2.—Decrease in optical density of solutions of DPPH in isobutene irradiated with  $^{60}Co$   $\gamma$ -rays at  $-78^\circ$ :  $\circ$ , [DPPH] = 155  $\mu M$   $\lambda = 5100$  Å., dose rate  $2.0 \times 10^{17}$  e.v. ml.<sup>-1</sup> min.<sup>-1</sup>,  $G(-DPPH) = 3.9$ ;  $\bullet$ , [DPPH] = 232  $\mu M$   $\lambda = 5100$  Å., dose rate  $2.0 \times 10^{17}$  e.v. ml.<sup>-1</sup> min.<sup>-1</sup>,  $G(-DPPH) = 3.6$ ;  $\Delta$ , [DPPH] = 719  $\mu M$   $\lambda = 7500$  Å., dose rate  $2.0 \times 10^{17}$  e.v. ml.<sup>-1</sup> min.<sup>-1</sup>,  $G(-DPPH) = 3.7$ .

in the form of a complex, which may be a charge transfer complex, and which makes a negligible contribution to light absorption at 4800 Å. This is certainly the case for other alkenes. Thus Freed and Saucier<sup>8</sup> found complexing between iodine and

(7) E. A. Cherniak, E. Collinson, F. S. Dainton, G. M. A. C. Meaburn and D. C. Walker, Proc. 2nd U. N. International Conference on Peaceful Uses of Atomic Energy, Geneva, 1958.

(8) S. Freed and K. M. Saucier, *J. Am. Chem. Soc.*, **74**, 1273 (1952); L. J. Andrews and R. M. Keefer, *ibid.*, **74**, 458 (1952); J. A. A. Ketelaar and C. van de Stolpe, *Rec. trav. chim.*, **71**, 805 (1955).



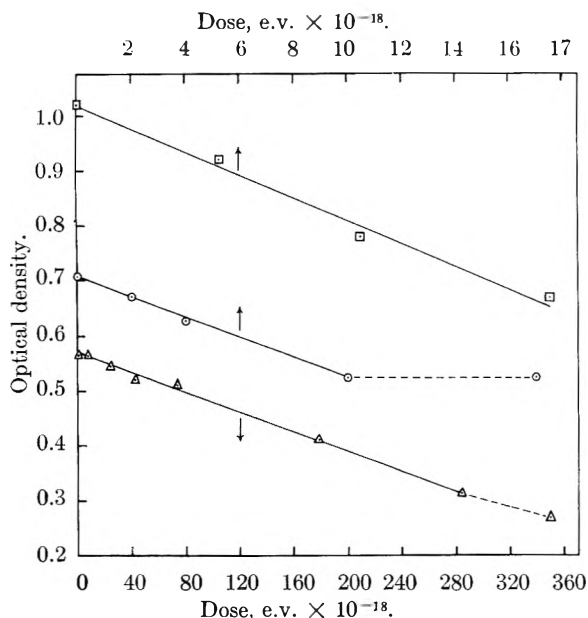


Fig. 3.—Decrease in optical densities of solutions of ferric chloride, benzoquinone or iodine in isobutene irradiated with  $^{60}\text{Co}$   $\gamma$ -rays at  $-78^\circ$ :  $\circ$ ,  $\text{FeCl}_3 = 3.9 \times 10^{-4} M$ ;  $\lambda = 4000 \text{ \AA}$ .; dose rate =  $2 \times 10^{17} \text{ e.v. ml.}^{-1} \text{ min.}^{-1}$ . If  $\epsilon^{4000} = 1800 \text{ l. mole}^{-1} \text{ cm.}^{-1}$   $G(-\text{Fe(III)}) = 3.0$ .  $\Delta$ , benzoquinone =  $3 \times 10^{-3} M$ ;  $\lambda = 3200 \text{ \AA}$ .; dose rate =  $7 \times 10^{17} \text{ e.v. ml.}^{-1} \text{ min.}^{-1}$ ;  $\square$ , "total" iodine =  $1.5 \times 10^{-2} M$ ;  $\lambda = 4800 \text{ \AA}$ .; dose rate =  $7 \times 10^{17} \text{ e.v. ml.}^{-1} \text{ min.}^{-1}$ .

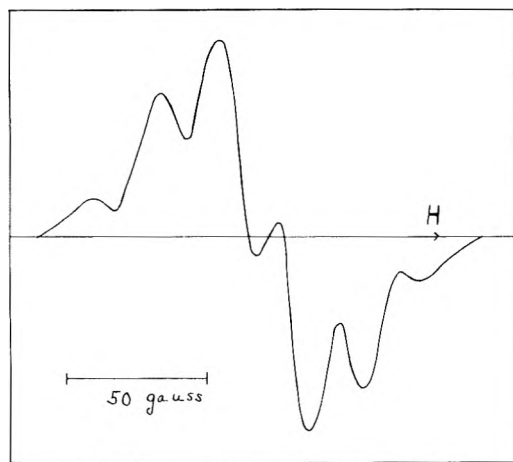


Fig. 4.—Paramagnetic resonance spectrum at  $-196^\circ$  of solid isobutene irradiated with a dose  $2.4 \times 10^{20} \text{ e.v./ml.}$  Separation of individual components of spectrum =  $20 \pm 1$  gauss. Ordinate is the first derivative of signal with respect to  $H$ .

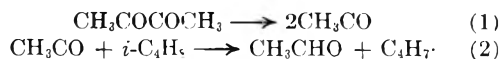
propylene, *cis*-butene-2, *trans*-butene-2 and cyclopropane; Andrews and Keefer<sup>8</sup> found  $K$  for cyclohexene-iodine complexes in *n*-hexane solution to be  $3.4 \text{ l. mole}^{-1}$  and Ketelaar and van de Stolpe<sup>8</sup> found  $K$  for 1-*t*-butyl-2,2'-dimethylethylene and iodine in *n*-hexane to be 3.7, both at room temperature. If the value for isobutene-iodine complex is 3.7 at room temperature and  $\Delta H = -200 \text{ cal. mole}^{-1}$  the value at  $-78^\circ$  will still be less than 10 so that a significant fraction of the iodine will be uncomplexed. The species destroyed during the irradiation is the uncomplexed iodine and after the irradiation the complex dissociates at a measurable speed replacing almost all the iodine which has

reacted and thereby increasing the optical density of the solution at  $4800 \text{ \AA}$ . to a limiting value only slightly less than that of the original solution.<sup>9</sup> Assuming that the "free" iodine in isobutene has the same extinction coefficient at  $5200 \text{ \AA}$ . as the iodine in alkane solutions,  $\epsilon^{4800}$  may be calculated to be  $1300 \text{ l. mole}^{-1} \text{ cm.}^{-1}$  and hence  $G(-\text{I}_2) = 4.8$ . However, in view of the displacement to shorter wave lengths when propylene is present, there may be "contact enhancement" of the transition in iodine responsible for the band at  $4800 \text{ \AA}$ . and the value 4.8 is probably an upper limit for  $G(-\text{I}_2)$ .

**7. Electron Spin Resonance of Irradiated Solid Isobutene.**—Isobutene contained in a special high purity quartz capillary tube was irradiated at  $-196^\circ$  and then transferred to the cooled cavity of an electron paramagnetic resonance spectrometer operating at  $9400 \text{ Mc./sec.}$ , which will be described elsewhere. Two spectra were obtained. The first was the normal hydrogen atom doublet of 473 gauss which disappeared after a few hours standing at  $-196^\circ$  or could be "wiped off" the walls on which they were presumed to be adsorbed merely by running the palm of the hand over the outside of the tube. The second spectrum is shown in Fig. 4. It had 6 peaks and was much more permanent, persisting for several days at  $-196^\circ$  and only disappearing when the sample was warmed to the melting point ( $-140^\circ$ ).

## Discussion

**1. Absence of Free-radical Polymerization.**—The fact that ultraviolet irradiation of solutions of biacetyl in isobutene results in destruction of biacetyl and appearance of a band in the ultraviolet very similar to that given by acetaldehyde suggests that the principal processes which occur are



Reaction 2 will be exothermic even if the acetyl radicals emerging from reaction 1 are not "hot" because of the resonance stabilization of the  $\text{C}_4\text{H}_7\cdot$  radical which has the structural formula  $\text{CH}_2\text{---}\overset{\text{CH}_3}{\text{C}}\text{---CH}_2$ . Reactions corresponding to (1)

and (2) probably occur also with benzoin or benzil as photosensitizers, since the ultraviolet absorption spectra indicate some production of benzaldehyde. On the other hand the electron spin resonance spectrum of a solid solution of benzil in isobutene which had been irradiated at  $77^\circ\text{K.}$  with ultraviolet light showed two overlapping spectra. Benzil alone, treated in the same way, gave a single line spectrum which was quite distinct. One of the overlapping spectra, a 5-line pattern, was consistent with the production of an allyl type radical; the other, which was predominant, was the same 6-line spectrum as that obtained from the  $\gamma$ -ray irradiation of pure isobutene. If the radical responsible for the 6-line spectrum is the same in each case and if this is the cyclopropyl radical

(9) Curious color loss and restoration phenomena in iodine solutions are common, see e.g., Freed and Saucier.<sup>9</sup>

$\begin{array}{c} \text{CH} \\ \diagup \quad \diagdown \\ \text{CH}_2 - \text{CH}_2 \end{array}$  (see below), it is difficult to see how this is formed unless a  $\text{CH}_3$  group is removed from the isobutene to give acetophenone.

The absence of polymerization is not surprising since formation of poly-isobutene by a free radical mechanism has never been achieved even at higher temperatures than  $-78^\circ$ . The situation is analogous to that observed by Worsfold and Bywater<sup>10</sup> who were unable to achieve the polymerization of  $\alpha$ -methylstyrene photosensitized by benzoin between  $-20$  and  $+60^\circ$ . In both these monomers addition of a monomer to a radical containing 2 or more monomer units requires an unusually high energy of activation because of the steric strain involved. It is for this reason that free radical copolymerization of isobutene or  $\alpha$ -methylstyrene with other monomers never results in incorporation of more than 50 mole % of isobutene or  $\alpha$ -methylstyrene in the copolymer. Any free radical polymer chains in liquid isobutene initiated by  $\text{CH}_3\text{CO}\cdot$ ,  $\text{C}_6\text{H}_5\text{CO}\cdot$ ,  $\text{C}_6\text{H}_5\text{CHOH}\cdot$ ,  $\text{C}_3\text{H}_5\cdot$  or  $\text{C}_4\text{H}_7\cdot$  will therefore be very slowly propagated but rapidly terminated.

**2. The Cationic Polymerization Mechanism and the Action of Additives.**—Of the possible ionic mechanisms for the radiation-induced polymerization, the cationic one is by far the most likely, since isobutene cannot be polymerized anionically and is known to polymerize with great rapidity in the presence of suitable proton donors. Furthermore it has been shown<sup>11</sup> that the first ion found in the acid-catalyzed polymerization of isobutene is the *t*-butyl ion  $(\text{CH}_3)_3\overset{\oplus}{\text{C}}$ , which, as discussed in section 3 below, is likely to be a major constituent of the primary products during the  $\gamma$ -irradiation of liquid isobutene. The structural identity of the products of the radiation-induced polymerization and the cationically-induced polymerization also supports this view.

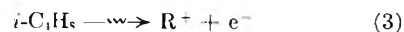
A test of mechanism of a polymerization is that, in general, inhibitors of free radical and anionic polymerizations do not markedly influence cationic polymerization rates and *vice versa*. The fact that DPPH, known to be an extremely effective inhibitor of free radical polymerization<sup>12</sup> has no influence on the rate of the radiation-induced polymerization of isobutene, although it is evidently reacting, again implies that the mechanism is cationic. A similar interpretation can be given to the effect of iodine which is also a well known radical scavenger and inhibitor of polymerizations catalyzed by free radicals, though this will be discussed further below. Ferric chloride is also a radical scavenger and a poly-radical chain terminator, but the concurrent cationic polymerization to which it gives rise prevents our drawing any conclusions about the mechanism of the polymerization from the results given in section 4 of the Results.

(10) D. J. Worsfold and S. Bywater, private communication from Dr. S. Bywater to F.S.D.

(11) F. S. Dainton and G. B. M. Sutherland, *J. Polymer Sci.*, **4**, 37 (1949).

(12) P. J. Flory, "Principles of Polymer Chemistry," Cornell University Press, New York, N. Y., 1953, p. 162.

Superficially the effects of oxygen<sup>2</sup> and benzoquinone (ref. 2 and above) which are also known inhibitors of free-radical polymerization, are anomalous. Closer consideration leads to an understanding of these inhibitory actions on the radiation-induced polymerization. Schematically one may write the primary radiation-chemical act as



where  $\text{R}^+$  denotes one of the many positive ions which are formed either directly, by ion breakdown, or by ion-molecule type reactions. Most of the secondary electrons will be recaptured within  $10^{-12}$  sec. in processes which lead to the liberation of heat or the formation of radicals. This period of time is far shorter than the interval between propagation steps so that cationic polymerization cannot occur unless electron recapture processes are partially suppressed. Pinner and Worrall<sup>2c</sup> suggest that solid powders such as zinc oxide and silica, the presence of which they found greatly to increase the *G*-value for chain initiation, are effective because they have suitable sites on which electrons can be retained. The excess unneutralized carbonium ions in the solution can then propagate polymerization chains which will only be terminated

when the growing carbonium ion  $\overset{\oplus}{\text{C}}(\text{CH}_3)_2$  reaches the solid surface and is electrically neutralized by the bound electron, probably by proton expulsion. Although the propagation step in the cationic polymerization of isobutene is believed to be very fast,  $k_p$  is unlikely to exceed  $10^6 e^{-1} \text{ kcal./} 200^\circ \text{ l. mole sec.}^{-1}$  at  $-78^\circ$ , and hence the interval between successive propagation steps in liquid isobutene is not likely to be less than  $10^{-6}$  sec. If the number average degree of polymerization is  $10^4$ , and there is no monomer transfer, the lifetime of the chain between initiation in the liquid and termination on the solid will be about  $10^{-2}$  sec., in which time the chain will have undergone a translational displacement of  $10^{-1} (2D)^{1/2}$  cm. Taking a mean diffusion constant (*D*) of  $0.5 \times 10^{-6} \text{ cm.}^2/\text{sec.}$  as appropriate (observed value of *D* for serum albumin of mol. wt. 60,000 in water<sup>13</sup>), this distance becomes  $10^{-4}$  cm. On the average only a small fraction of the secondary electrons are likely to escape the coulomb field of their parent ions and travel a distance of this magnitude to a suitable site, but this fraction will increase as more finely divided solid is added.

If this mechanism is correct the logical deduction would be that in the absence of solid no polymerization would take place, and that some solid is always present which is capable of performing this function, even when no solid is deliberately added. We consider that this solid comprises the walls of the reaction vessel and the inevitable dust particles, some of which are sub-microscopic flakes of the friable, rough Pyrex walls. These particles will be present in very variable amounts and this variation would account for the irre-

(13) T. Svedberg and K. Pedersen, "The Ultracentrifuge," Oxford University Press, 1940, p. 406. A similar value of *D* may be calculated for polyisobutene of mol. wt. = 60,000 as follows.  $D = kT/\alpha\eta_0 P(\eta_0^2/M)^{1/2} M^{1/2}$  taking  $\eta_0 = 5 \times 10^{-3}$  and  $\eta_0^2/M = 85 \times 10^{-2}$ ,  $D \geq 5 \times 10^{-7}$  c.g.s.

TABLE I  
 MASS SPECTRUM OF ISOBUTENE

| No. | Ion        | Ap-<br>pearance<br>potential<br>(v.) | Associated<br>products        | Relative abundance     |                        |                        | Ref.<br>18<br>(70 v.) | Reaction                                         |
|-----|------------|--------------------------------------|-------------------------------|------------------------|------------------------|------------------------|-----------------------|--------------------------------------------------|
|     |            |                                      |                               | Ref.<br>17a<br>(50 v.) | Ref.<br>17b<br>(50 v.) | Ref.<br>17c<br>(50 v.) |                       |                                                  |
| 4   | $C_4H_8^+$ | 9.35                                 | Nil                           | 44.5                   | 45                     | 51.5                   | 47                    | $C_4H_8 \rightarrow e^+ + (CH_3)_2C=CH_2^+$      |
| 5   | $C_4H_7^+$ | 11.32                                | H                             | 16                     | 16                     | 24                     |                       | $CH_2=C(CH_3)-CH_2^+ + H$                        |
| 6   | $C_3H_5^+$ | 11.44                                | $CH_3$                        | 100                    | 100                    | 100                    | 100                   | $CH_2=C-CH_3^+ + CH_3$                           |
| 7   | $C_3H_4^+$ | 11.62                                | $CH_4$                        | 10                     | 11                     | 9                      |                       | $CH_2-C=CH_2^+ + CH_4$                           |
| 8   | $C_3H_3^+$ | 14.2                                 | $CH_3 + H_2$ or<br>$CH_4 + H$ | 45                     | 47                     | 40                     | 40                    | $CH_2=C=CH^+ + CH_3 + H_2$<br>or $CH_4 + H$      |
| 9   | $C_2H_5^+$ | 15                                   | $C_2H_3$ or<br>$C_2H_2 + H$   | 11                     | 10                     | 10                     |                       | $CH_3CH_2^+ + CH\equiv CH + H$<br>or $CH_2=CH^+$ |
| 10  | $C_2H_4^+$ | 12.15                                | $C_2H_4$                      | 22                     | 21                     | 19                     | 27                    | $CH_2^+=CH_2 + CH_2=CH_2$                        |
| 11  | $C_2H_3^+$ | 15.2                                 | $C_2H_4 + H$                  | 22                     | 21.5                   | 16                     | 25                    | $CH_2=CH^+ + CH_2=CH_2 + H$                      |

\* Some of these ions may in fact be derivatives of isomeric methyl cyclopropane, e.g.,  $C_3H_5^+$ , given the structure  $CH_2-\overset{+}{C}-CH_2$  may be  $\begin{array}{c} CH_2-CH \\ | \\ CH_2 \end{array}$ .

producibility of rates referred to in section 2 of Results.

On this mechanism the inhibiting action of oxygen and benzoquinone may be ascribed to the fact that they are competitive electron traps. The electron affinity of  $O_2$  is 0.9 e.v.<sup>14</sup>; that of benzoquinone is unknown but from the known stability of semi-benzoquinone and the quinone-semiquinone reduction potentials in water it seems probable that electrons of energy less than 0.5 e.v. will be readily captured by this substance. At the concentrations of each ( $\sim 10^{-3} M$ ) at which inhibition is complete, the mean separation of the inhibitor molecules will be about 100 Å., so that the majority of electrons which would otherwise have become immobilized on a solid particle will be intercepted and transformed to  $O_2^-$  or  $Q^-$ . These latter entities are freely mobile and hence in the presence of these inhibitors, some  $10^{-12}$  sec. after the passage of the primary particle each  $R^+$  ion will have a freely moving  $O_2^-$  or  $Q^-$  ion within about  $10^3$  Å. Collision of such oppositely charged ions will occur within about  $10^{-5}$  to  $10^{-6}$  sec., and whatever the nature of the products ( $RO_2$  or molecule +  $QH$ ) the carbonium ion will be destroyed before it has added more than a very few isobutene molecules.

The question arises as to why iodine, DPPH and ferric chloride cannot function in this fashion. We conclude that either the electron affinity is too low for the electron to be intercepted or that it is sufficiently high for the ion pair  $R^+$  Additive $^-$  to continue chain propagation. If the latter explanation is correct we would expect certain soluble additives to be catalysts. In this connection it is perhaps significant that iodine which is known to catalyze the cationic polymerization of vinyl ethers because of the stability of  $R^+ I_3^-$  ion pairs<sup>15</sup> does seem from Worrall's results<sup>16</sup> to increase the initiation  $G$ -value.

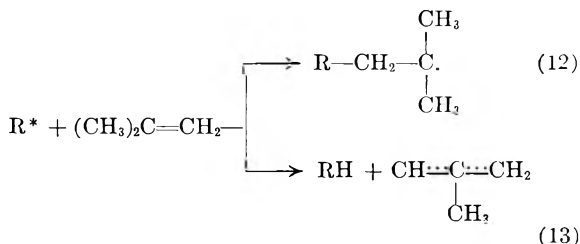
(14) H. O. Pritchard, *Chem. Revs.*, **52**, 529 (1953).

(15) D. D. Eley and A. W. Richards, *Trans. Faraday Soc.*, **45**, 425 (1949).

(16) R. Worrall, private communication to F.S.D.

(17) American Petroleum Institute, Mass Spectral Data, Project 44 (1948). Contributions from (a) the National Bureau of Standards;

3. The Ions and Radicals Produced in the Primary Act.—The most abundant ion in the mass spectrum of isobutene is  $C_3H_5^+$ . The relative abundances of all other ions responsible for ion currents  $\geq 10\%$  of that for this peak are listed in the Table I. These data indicate that over half the ionizations result in dissociation of the isobutene to form at least one radical ( $CH_3$  or  $H$ ) (reaction 5, 6, 8, 9 and 11); that molecular products ( $H_2$ ,  $CH_4$ ,  $C_2H_2$ ,  $C_2H_4$ ) result from only about 30% of the ionizations and that the most favored process is detachment of a methyl radical. The fate of the positive ions in liquid isobutene is in doubt. If the secondary electron returns to the parent ion after a dissociative vibration the following species will be formed in a hot condition:  $C_4H_8$ ,  $C_4H_7$ ,  $C_3H_5$ ,  $CH_2=C=CH_2$ ,  $CH_2=C=CH$ ,  $C_2H_5$ ,  $C_2H_4$  and  $C_2H_3$ . Of these the hot radicals  $C_3H_3$ ,  $C_2H_5$  and  $C_2H_3$ , which we will designate  $R^*$ , will almost certainly either add to an isobutene molecule (reaction 12) or detach a hydrogen atom from it (reaction 13) and each of the resultant



radicals will be relatively long lived, the first because of steric repulsions and the second because of resonance stabilization. For this latter reason the radicals  $C_4H_7$  and  $C_3H_5$  may be sufficiently stable not to react as in (12) or (13). However there is also the possibility that one of the parent positive ions will surrender a proton to isobutene, which has a relatively high proton affinity since the resultant *t*-butyl carbonium ion  $(CH_3)_3C^+$  is one (b) the Socony-Vacuum Laboratories; (c) the Phillips Petroleum Company.  
(18) D. P. Stevenson and J. A. Hipple, *J. Am. Chem. Soc.*, **64**, 2769 (1942).

of the most stable of the simple alkyl carbonium ions. The parent ion  $C_4H_8^+$  should be particularly prone to this because of the stability of the  $CH_2^{\sim}C(CH_3)=CH_2$  radical which is thereby formed. The most common free-radical species produced in the primary act are therefore likely to be the methyl



substituted allyl radical  $CH_2^{\sim}C(CH_3)=CH_2$  and the radical  $C_3H_5^{\cdot}$ . The 6-line pattern of the electron spin resonance spectrum of  $\gamma$ -irradiated solid isobutene is not the same as the 5-line spectrum of the allyl radical observed by Matheson and Smaller<sup>19</sup> and consequently if the radical  $C_3H_5^{\cdot}$  is produced it presumably exists in some other form. One possibility is the cyclopropyl radical  $CH_2-CH_2$



which, by analogy with radicals of the type  $\sim CH_2-\dot{C}H-CH_2\sim$  may be expected to show a 6-line spectrum of the spread observed.<sup>19</sup> In support of this, the 6-line spectrum given by cyclopropane irradiated with  $\gamma$ -rays at 77°K. coincided almost completely with that of  $\gamma$ -ray irradiated isobutene. Cyclopropane irradiated with  $\gamma$ -rays to a dose of about  $1.5 \times 10^{20}$  e.v. ml.<sup>-1</sup> also gave indications of a 5-line pattern superimposed on the much more marked 6-line spectrum. At higher doses the 5-line pattern became less significant. This result was very similar to that for the photolysis of solid solutions of benzil in isobutene, and the spacing of the 5-line spectrum in each case was consistent with its origin being the allyl radical. The 2-methyl substituted allyl radical might be expected to give a similar electron spin resonance spectrum to that of the allyl radical. If this is so our observations indicate that the extent of its formation in  $\gamma$ -ray irradiated isobutene is, surprisingly, negligibly small. An abundant positive ion will be  $(CH_3)_3C^+$  and since it is known that this ion does initiate cationic polymerization in liquid isobutene,<sup>11</sup> ions of this type, which escape neutralization because their conjugate electrons are captured, are presumably responsible for the observed radiation-induced polymerization.

**4. Reactions of the Primary Products with Solutes.**—Oxygen and all the solutes we have used are known to react readily with free radicals. In view of the uncertainty of the chemistry of the reaction with benzoquinone (see ref. 12) and uncertainty as to the true extinction coefficient of iodine at 4,800 Å. in isobutene solution, the radical yield will be closest to  $G(-DPPH)$  and  $g(-Fe(III))$  and less than  $G(-I_2)$ . We shall accept the value of 3.4, which is not greatly different from the value for hexadecene-1 ( $g(-Fe(III))3.1$ ). When oxygen and benzoquinone capture electrons the resultant anions will probably react with the predominant polymerization initiating cation  $(CH_3)_3C^+$  to form  $(CH_3)_2C=CH_2 + HO_2$  or  $(CH_3)_3CO_2^{\cdot}$ .

(19) B. Smaller and M. S. Matheson, *J. Chem. Phys.*, **28**, 1169 (1958).

and  $(CH_3)_2C=CH_2 + QH$ . If the stable semibenzoquinone radical QH persists it may well react with the isobutyl radical or the cyclopropyl radical regenerating quinone, which could account for the fact that  $2G(-Q) < 3.4$ .

### Conclusions

The main conclusions to be drawn from this and other studies of the radiation chemistry of isobutene are: (1) the polymerization is caused by positive ions, mainly  $(CH_3)_3C^+$ , which escape neutralization by conjugate electrons because these electrons have been spatially immobilized about  $10^4$  Å. from the ion by capture on suitable sites on submicroscopic particles or on added inorganic solids; (2) polymerization may be suppressed by quinone or oxygen which capture a significant fraction of secondary electrons not more than  $10^3$  Å. from the parent ion, but the resultant anions  $O_2^{\cdot-}$  and  $Q^{\cdot-}$ , being mobile, return to and destroy the  $(CH_3)_3C^+$  ion before the latter has had sufficient time to add more than a very few monomer molecules, (3) radicals are also formed, the most im-



portant being  $CH_2-CH_2$  and  $CH_2^{\sim}C(CH_3)=CH_2$  and  $G-$



(radicals) =  $\sim 3.4$ . The radicals react with radical scavengers  $O_2$ ,  $I_2$ ,  $Q$ ,  $FeCl_3$  and DPPH in the usual way; (4) iodine may also capture electrons forming  $I_2^{\cdot-}$  ions, which may combine with a radical to form the ion  $I_3^{\cdot-}$ . This is known to be sufficiently stable not to terminate poly-isobutene carbonium ions and iodine is therefore a mild catalyst of the polymerization.

These conclusions are perhaps especially appropriate to the occasion of Dr. Lind's 80th birthday. He has so often reminded us of the important role which ions play in gaseous reactions, whilst the prevailing fashion has been to interpret most of these, and all radiolyses of organic liquids, in terms of uncharged free radicals and atoms. The radiation-induced polymerization of liquid isobutene provides a clear example of a liquid phase ionic reaction. It also serves as a reminder that so-called "radical scavengers" such as  $O_2$  and benzoquinone, may be acting in part as "electron scavengers" and that the over-all stoichiometry of the scavenger disappearance can provide no information as to the relative importance of the two functions.

**Acknowledgments.**—We are grateful to the Rockefeller Foundation which made possible the purchase of the source; to the General Electric Research Laboratory, Schenectady, U. S. A., for a grant and to the Department of Scientific and Industrial Research for the gift of the electron spin resonance spectrometer, on which Dr. P. B. Ayscough and Mr. A. P. McCann kindly measured the spectra.

# MASS SPECTROMETRIC STUDIES OF IONIC INTERMEDIATES IN THE $\alpha$ -PARTICLE RADIOLYSIS OF THE $C_2$ HYDROCARBONS. I. ACETYLENE<sup>1</sup>

BY P. S. RUDOLPH AND C. E. MELTON

*Chemistry Division, Oak Ridge National Laboratory, Oak Ridge, Tennessee*

*Received February 16, 1959*

Ionic intermediates from the  $\alpha$ -particle radiolysis of acetylene were systematically studied as a function of pressure by magnetic mass separation of the ions. "Polymeric" ions,  $C_4H_n^+$  and  $C_6H_n^+$  have been identified and their per cent. abundance determined. The most probable mechanisms for formation of the observed "polymeric" ions are evaluated.

"Polymeric" ions induced in the  $\alpha$ -particle radiolysis of  $C_2H_2$  were observed during preliminary investigations,<sup>2</sup> using a modified research mass spectrometer<sup>2,3</sup> to identify the primary ions formed by  $\alpha$ -particles. The term "polymeric" as used in this report refers to a chemical species containing more carbon atoms than the parent compound. The strikingly simple mass spectrum of  $C_2H_2$  observed in this preliminary work indicated that a systematic study of the polymeric ions observed would be useful in elucidating the mechanism for the formation of these polymeric species.

The importance of ions in radiation chemistry was postulated as early as 1911 by Lind.<sup>4</sup> These postulates were later overshadowed by the concepts of excitation and free radicals<sup>5</sup> for which there was considerable experimental evidence from photolysis studies. Because of this evidence, the role of ions in radiation chemistry was relegated to minor importance in the elucidation of chemical mechanisms.

Despite the observation of products formed by ion-molecule reactions in the earliest days of mass spectrometry,<sup>6</sup> practically no systematic investigations of these reactions had been made until recently. Experimental difficulties encountered, principally because of the high pressure required to study these reactions, are largely responsible for the neglect of such studies. In recent years many investigators have made systematic studies of both positive<sup>7-11</sup> and negative<sup>12</sup> ion-molecule reactions. The usual method<sup>7</sup> for investigating ion-molecule reactions with a mass spectrometer consists of studying the pressure dependence of the relative abundance of ions formed by electrons from a hot tungsten filament.

The purpose of this investigation was to study ionic intermediates formed in  $C_2H_2$  using  $\alpha$ -particles as the ionizing medium. The use of  $\alpha$ -particles eliminated the principal disadvantage,

the high temperature from the hot filament, necessarily encountered in all previous mass spectrometric studies of ion-molecule reactions. It was anticipated that the use of pressures, in the reaction chamber, higher than heretofore used would induce consecutive bimolecular reactions. Although the authors are cognizant of the importance of free radical and excited state reactions, their discussion is limited to ionic reactions for which their apparatus was designed.

## Experimental

"Purified"  $C_2H_2$  (99.5%) obtained from the Matheson Co. was further purified by the method of Fernelius,<sup>13</sup> giving  $C_2H_2$  of 99.9% purity.<sup>14</sup>

The modified research mass spectrometer used for this study has been described in detail elsewhere.<sup>2,3,15</sup>

The spectrum of  $C_2H_2$  was studied as a function of the pressure in the reaction chamber over a tenfold range from a minimum of approximately 0.01 mm.

Equal aliquots of the reactant gas were condensed into a ballast reservoir which held each pressure constant in the reaction chamber. This technique gave accurate pressure increments although the absolute pressures were approximate. Reactant ions were produced exclusively by  $\alpha$ -particle emission from a  $Po^{203}$  source.<sup>2</sup> The temperature of the reaction chamber was maintained at 23° in all of these studies.

Known mass spectra from  $C_2H_6$ , Ar,  $CO_2$  and Kr produced by 75 e.v. electrons from a thoria-iridium filament<sup>16</sup> were used to calibrate the alpha induced mass spectra of  $C_2H_2$  at the end of each determination.

## Results

The per cent. of ionic species observed in  $C_2H_2$  as a function of pressure are given in Table I. These data are presented as ratios of the absolute intensity for each ion to the total ion intensity. Percentages of individual ions were not tabulated in those cases where their absolute intensities were too low to be determined accurately. In most cases, the per cent. shown were reproducible to within 5% over extended periods of time.

Since primary ionization is a first-order reaction with respect to pressure, the per cent. of ions resulting from primary ionization are independent of pressure. The apparent disagreement of the data in Table I, for primary ions, with the first-order law indicates that these ions are enhanced or depleted by other reactions. Ions resulting from ion-molecule collision reactions are second order or higher, with respect to pressure, depending upon the number of consecutive reactions involved. Hence, the per cent. of product ions formed by ion-

(1) This paper is based on work performed for the U. S. Atomic Energy Commission by Union Carbide Nuclear Company, a division of Union Carbide Corporation, at the Oak Ridge National Laboratory.

(2) C. E. Melton and P. S. Rudolph, *J. Chem. Phys.*, **30**, 847 (1959).

(3) C. E. Melton, Gus A. Ropp and P. S. Rudolph, *ibid.*, **29**, 968 (1958).

(4) S. C. Lind, *Am. J. Chem.*, **47**, 397 (1911).

(5) H. Eyring, J. O. Hirschfelder and H. S. Taylor, *J. Chem. Phys.*, **4**, 479, 570 (1936).

(6) F. W. Aston, *Proc. Cambridge Phil. Soc.*, **19**, 317 (1920).

(7) V. L. Tal'roze and A. K. Lyubimova, *Doklady Akad. Nauk, S.S.S.R.*, **86**, 909 (1952).

(8) F. J. Norton, Natl. Bur. Standards Circ. No. 522, 201 (1953).

(9) D. A. Hutchison, *J. Chem. Phys.*, **22**, 1789 (1954).

(10) D. P. Stevenson and D. O. Schissler, *ibid.*, **23**, 1353 (1955).

(11) C. E. Melton, *ibid.*, **28**, 359 (1958).

(12) C. E. Melton and Gus A. Ropp, *J. Am. Chem. Soc.*, **80**, 5573 (1958).

(13) W. C. Fernelius, "Inorganic Syntheses," McGraw-Hill Book Co., Inc., New York, N. Y., 1946, First edition, Vol. 2, p. 76.

(14) C. E. Melton, M. M. Bretscher and Russell Baldock, *J. Chem. Phys.*, **26**, 1302 (1957).

(15) G. F. Wells and C. E. Melton, *Rev. Sci. Instr.*, **28**, 1065 (1957).

(16) C. E. Melton, *ibid.*, **29**, 250 (1958).

TABLE I  
PER CENT. OF IONIC INTERMEDIATES IN THE RADIOLYSIS OF  $C_2H_2$  AS A FUNCTION OF PRESSURE  
(FROM 0.01 TO 0.1 MM.)

| Mass | + Ion      | Equal increments of pressure |       |       |       |       |       |       |       |       |          |
|------|------------|------------------------------|-------|-------|-------|-------|-------|-------|-------|-------|----------|
|      |            | $P_1$                        | $P_2$ | $P_3$ | $P_4$ | $P_5$ | $P_6$ | $P_7$ | $P_8$ | $P_9$ | $P_{10}$ |
| 26   | $C_2H_2^+$ | 77.9                         | 60.6  | 49.1  | 41.6  | 34.1  | 28.2  | 22.9  | 18.2  | 15.0  | 13.1     |
| 27   | $C_2H_3^+$ |                              |       | 0.8   | 1.2   | 1.5   | 2.1   | 2.3   | 2.5   | 2.7   | 3.1      |
| 50   | $C_4H_2^+$ | 8.2                          | 15.7  | 21.1  | 22.5  | 23.8  | 23.1  | 22.7  | 25.2  | 22.4  | 21.7     |
| 51   | $C_4H_3^+$ | 13.9                         | 23.6  | 29.0  | 34.8  | 40.5  | 40.2  | 39.6  | 38.8  | 40.5  | 40.9     |
| 52   | $C_4H_4^+$ |                              |       |       |       |       | 1.8   | 2.5   | 2.5   | 2.4   | 3.0      |
| 74   | $C_6H_2^+$ |                              |       |       |       |       |       | 0.7   | 1.2   | 1.4   | 1.8      |
| 75   | $C_6H_3^+$ |                              |       |       |       |       |       | 0.8   | 1.2   | 1.7   | 1.8      |
| 76   | $C_6H_4^+$ |                              |       |       |       |       | 2.6   | 4.6   | 5.6   | 7.3   | 7.5      |
| 77   | $C_6H_5^+$ |                              |       |       |       |       | 2.1   | 3.9   | 4.9   | 6.5   | 7.0      |

TABLE II  
IONIC INTERMEDIATES IN THE RADIOLYSIS OF  $C_2H_2$  AT A PRESSURE OF APPROXIMATELY 0.1 MM.

| Mass | Positive ion | Abundance, % | Probable reaction                                                                                          | $\Delta H_i$ , e.v. | Remarks                                                                                                                                                                                                                                                                                    |
|------|--------------|--------------|------------------------------------------------------------------------------------------------------------|---------------------|--------------------------------------------------------------------------------------------------------------------------------------------------------------------------------------------------------------------------------------------------------------------------------------------|
| 26   | $C_2H_2^+$   | 13.0         | $C_2H_2 \rightsquigarrow C_2H_2^+ + e^-$                                                                   | 11.4                | Primary ionization                                                                                                                                                                                                                                                                         |
| 27   | $C_2H_3^+$   | 3.1          | $C_4H_3^+ + C_2H_2 \rightarrow C_2H_3^+ + C_4H_2$<br>$C_2H_2^+ + C_2H_2 \rightarrow C_2H_3^+ + C_2H$       | 1.0<br>-0.2         | No exptl. evidence to distinguish between these reactions                                                                                                                                                                                                                                  |
| 50   | $C_4H_2^+$   | 21.7         | $C_2H_2^+ + C_2H_2 \rightarrow C_4H_2^+ + H_2$                                                             | 0.3                 | The % of $C_2H_2^+$ decreases rapidly with increasing pressure paralleling the rapid increase in %'s of $C_4H_2^+$ and $C_4H_3^+$ to 0.05 mm., Fig. 1 and Table I. These observations plus the fact that $C_2H_2^+$ is the predominant primary ion <sup>2</sup> substantiate this reaction |
| 51   | $C_4H_3^+$   | 40.9         | $C_2H_2^+ + C_2H_2 \rightarrow C_4H_3^+ + H$                                                               | 0.3                 | Same as for $C_4H_2^+$ (50)                                                                                                                                                                                                                                                                |
| 52   | $C_4H_4^+$   | 3.0          | $C_2H_2^+ + C_2H_2 \rightarrow C_4H_4^+$                                                                   | -2.3                | There is insufficient exptl. evidence to substantiate this reaction                                                                                                                                                                                                                        |
| 74   | $C_6H_2^+$   | 1.8          | $C_4H_2^+ + C_2H_2 \rightarrow C_6H_2^+ + H_2$<br>or<br>$C_4H_3^+ + C_2H_2 \rightarrow C_6H_2^+ + H_2 + H$ | -3.3<br>-3.3        | % of this ion too low to determine its origin conclusively                                                                                                                                                                                                                                 |
| 75   | $C_6H_3^+$   | 1.8          | $C_4H_3^+ + C_2H_2 \rightarrow C_6H_3^+ + H_2$<br>or<br>$C_4H_2^+ + C_2H_2 \rightarrow C_6H_3^+ + H$       | -0.9<br>-0.9        | % of this ion too low to determine its origin conclusively                                                                                                                                                                                                                                 |
| 76   | $C_6H_4^+$   | 7.5          | $C_4H_2^+ + C_2H_2 \rightarrow C_6H_4^+$                                                                   | 0.2                 | This reaction is substantiated by the simultaneous appearance at 0.05 mm. of a continuous plateau in the % of $C_4H_2^+$ and the initial detection of $C_6H_4^+$ , the % of which ion continues to increase with increasing pressure, Fig. 1 and Table I                                   |
| 77   | $C_6H_5^+$   | 7.0          | $C_4H_3^+ + C_2H_2 \rightarrow C_6H_5^+$                                                                   | -4.0                | Evidence for this reaction is analogous to that for the formation of $C_6H_4^+$ (76)                                                                                                                                                                                                       |

molecule collision reactions increase with increasing pressure while the per cent. of reactant ions consumed in ion-molecule collision reactions show a corresponding decrease with increasing pressure. The data in this table conclusively show that all of the ionic species are either involved in or formed by ion-molecule collision reactions. This is further corroborated by the curves in Fig. 1. Although the per cent. of the individual species change drastically with pressure as shown by these curves, the total ion intensity is a linear function of pressure, Fig. 2. This indicates that the reactant ions consumed in ion-molecule collision reactions are collected as product ions.

A summary of the reaction mechanisms for the ionic species observed in  $C_2H_2$  is given in Table II. The primary ionization reactions as shown are merely a convention and do not preclude the existence of such products as  $H^-$ ,  $HeH^+$ ,  $He^+$ , etc. The structure and energetics of the ionic and neutral products are not known. Only the per cent. and  $M/e$  of the ionic species are known accurately.

Values for  $\Delta H$  shown were calculated from data published by Field and Franklin<sup>17</sup> and Pauling.<sup>18</sup>

(17) F. H. Field and J. L. Franklin, "Electron Impact Phenomena," Academic Press, Inc., New York, N. Y., 1957, p. 243 ff.

(18) L. Pauling, "Nature of the Chemical Bond," 2nd Ed., Cornell University Press, Ithaca, N. Y., 1944, pp. 53, 131.

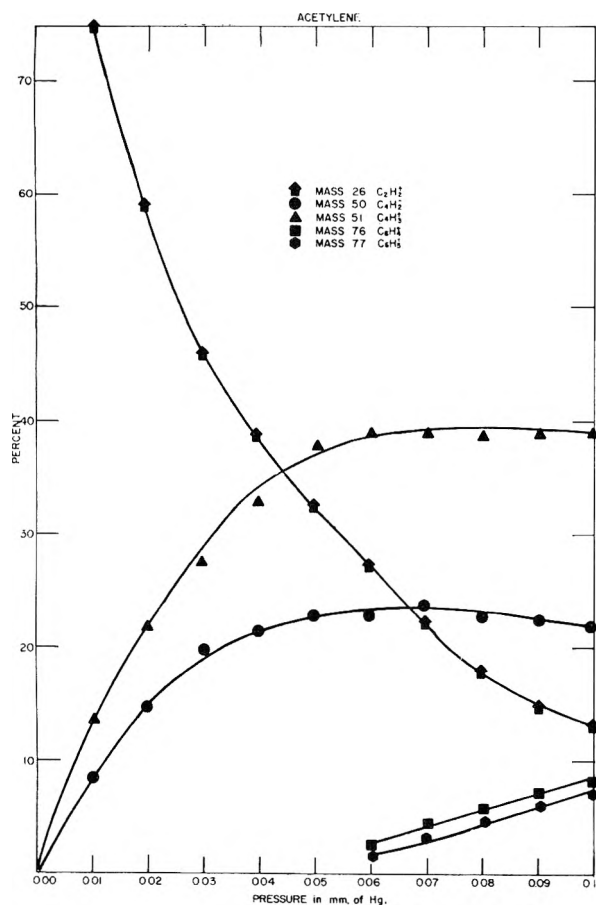


Fig. 1.—The per cent. abundance of various ionic species from acetylene as a function of pressure.

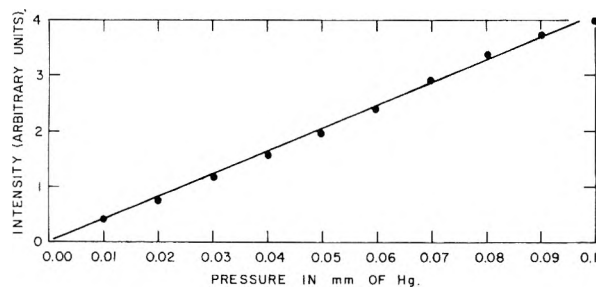


Fig. 2.—The intensity of total ions from acetylene as a function of pressure.

These values represent ground state transitions, hence they may not be applicable to the postulated reactions. In addition to this possible discrepancy, neither the structure of the observed ions nor the

structure of the ions for which the appearance potentials<sup>17</sup> were given is known. In view of these uncertainties, it is not surprising that apparently endothermic reactions are observed. In most cases, the per cent. of ions resulting from such reactions are small, *e.g.*, C<sub>2</sub>H<sub>3</sub><sup>+</sup>(27) in Table II, suggesting that excited ions are involved. Postulated reactions are substantiated by experimental observations as summarized in the "Remarks" columns of this table.

A comparison of these results with those obtained from electron impact studies<sup>19</sup> shows striking differences. For example, Field, *et al.*,<sup>19</sup> show "important" polymeric ions of mass 37, 38 and 49 produced by ion-molecule collision reactions of fragment ions CH<sup>+</sup> and C<sub>2</sub><sup>+</sup> with acetylene. These masses could not be observed in the present study due to the absence of these fragment ions. In the electron impact studies, a value of 1.2 was found for the abundance ratio C<sub>4</sub>H<sub>3</sub><sup>+</sup>/C<sub>4</sub>H<sub>2</sub><sup>+</sup> compared to 1.9 found in the  $\alpha$ -particle study. Polymeric ions of masses 74 through 77 were found in the present study and were not reported in the electron impact study. These dissimilarities were anticipated due to the following marked differences. In this study a different ionizing medium was used, vastly lower temperatures and higher pressures were employed, and strikingly simpler primary ion patterns were observed.

#### Conclusions

This study demonstrates the applicability of a research mass spectrometer to elucidate ionic reactions induced by  $\alpha$ -particles. A study of ions produced in C<sub>2</sub>H<sub>2</sub> as a function of pressure conclusively shows that all ionic species are involved in ion-molecule collision reactions. This investigation evinces the importance of ionic reactions in the radiolyses of C<sub>2</sub>H<sub>2</sub>. The observed C<sub>6</sub>H<sub>n</sub><sup>+</sup> ions may be the precursors of benzene and "cuprene," known products in the radiolyses of acetylene.

**Acknowledgment.**—The authors would like to acknowledge valuable suggestions stemming from stimulating discussions with Professor P. H. Emmett of Johns Hopkins University; Professors M. Burton and J. L. Magee of Notre Dame University; and R. Baldock and E. H. Taylor of this Laboratory.

The authors are happy to have this opportunity to express their gratitude to Dr. S. C. Lind whose encouragement and interest in this work were a source of inspiration.

(19) F. H. Field, J. L. Franklin and F. W. Lampe, *J. Am. Chem. Soc.*, **79**, 2665 (1957).

## RECOIL REACTIONS WITH HIGH INTENSITY SLOW NEUTRON SOURCES.

III. THE RADIATION DECOMPOSITION OF CRYSTALLINE  $\text{KBrO}_3$ 

BY G. E. BOYD AND J. W. COBBLE

*Contribution from Oak Ridge National Laboratory  
Oak Ridge, Tennessee**Received February 16, 1959*

The relative contributions of energetic neutrons,  $\gamma$ - and  $\beta$ -rays to the radiation decomposition of crystalline  $\text{KBrO}_3$  in the Oak Ridge graphite pile were determined as approximately 20, 40 and 40%, respectively. Decomposition yields (*i.e.*, " $G$ "-values) for  $\beta$ -rays and pile  $\gamma$ -rays were  $1.0 \pm 0.1$  molecule per 100 e.v. energy absorbed, while for energetic neutrons yields varying from 23 to 30, dependent on neutron energy, were found. The much greater efficiency for decomposition by fast neutrons was attributed to the mechanism whereby these particles transfer energy to bromate radicals.

Previous studies<sup>1,a,b</sup> with high intensity slow neutron sources have shown that the enrichment,  $E$ , in the specific activity of 35.8 h.  $\text{Br}^{82}$  obtainable using a Szilard-Chalmers recoil separation with crystalline  $\text{KBrO}_3$  was governed to a fair approximation by the relation

$$E = \phi / k_T p t \quad (1)$$

where  $\phi$  is the fraction of the total  $\text{Br}^{82}$  chemically separable from bromate,  $k_T$ , the specific radiation decomposition rate constant for  $\text{KBrO}_3$ ,  $p$ , the intensity of the decomposing radiations, and  $t$ , the time. The enhancement in specific activity over that attainable on irradiating pure bromine according to eq. 1 should diminish with decreasing  $\phi$  and with increasing radiation dose,  $pt$ . The quantity  $\phi$  did not depart appreciably from unity and, hence, was much less important in establishing the magnitude of  $E$  than was the product,  $k_T p t$ , which measured the radiation decomposition and varied by several powers of ten.

The radiations in the Oak Ridge National Laboratory graphite, natural uranium chain reactor responsible for the decomposition of  $\text{KBrO}_3$  were energetic neutrons and  $\beta$ - and  $\gamma$ -rays; the effects of fission-product recoils could be ignored. The electromagnetic component was made up from prompt  $\gamma$ -rays emitted in  $\text{U}^{235}$  fission or produced by neutron capture in uranium and in structural materials, and from delayed  $\gamma$ -rays emitted by the fission products. The  $\beta$ -rays originated largely from the short-lived bromine activities formed by the capture of thermal neutrons in the compound itself.

This paper will be concerned with estimating the relative contributions from each of the above mentioned types of radiations in the Oak Ridge graphite reactor to the observed gross decomposition of  $\text{KBrO}_3$ . Additionally, " $G$ "-values (*i.e.*, molecules of  $\text{KBrO}_3$  decomposed per 100 e.v. absorbed) will be derived for each radiation type in an attempt to gain an insight as to the mechanisms of their action.

The method for disentangling the total radiation effects was to measure independently the decomposing actions of  $\beta$ -rays (1.15 Mev. Van der Graaff electrons), of  $\gamma$ -rays ( $\text{Co}^{60}$ ) and of energetic neutrons in which the attendant  $\gamma$ -rays were of relatively negligible intensity. Additivity of the consequences of these separate kinds of radiation

in the pile was assumed, such that

$$k_T = k_\beta + k_\gamma + k_n \quad (2)$$

where  $k_\beta$ ,  $k_\gamma$  and  $k_n$  are the specific decomposition rate constants for the  $\beta$ - and  $\gamma$ -rays and for neutrons, respectively.

## Experimental

The purification of the C.P. grade, crystalline  $\text{KBrO}_3$  preparations employed and the method for the analysis of total bromine (bromine + bromide + hypobromite) produced in the compound by radiation decomposition have been described.<sup>1a</sup> Briefly, the latter procedure consisted in dissolving *ca.* 0.5 g. of irradiated salt in water containing 150  $\mu$ l of a 2% sodium arsenite solution to reduce all valence states of bromine, except bromate, to bromide which was assayed by a micro-potentiometric titration with 0.01 *N*  $\text{AgNO}_3$ . Determinations with unirradiated  $\text{KBrO}_3$  were performed at the same time as the analyses on irradiated samples; these blanks indicated an initial  $25 \pm 3$  p.p.m. by weight of bromide which was subtracted from the value for the irradiated salt. The reliability of the analysis for bromide was demonstrated in a special study by the material balances found on adding a wide range of known amounts of  $\text{KBr}$  to irradiated  $\text{KBrO}_3$ .

Thermal decomposition measurements were made because environmental temperatures up to 125° were expected in some irradiations. Potassium bromate is known to decompose to oxygen gas and potassium bromide at approximately 370°. An appreciable thermodynamic instability even at 25° was indicated also by the estimated standard free energy change of  $-32.4$  kcal. mole<sup>-1</sup> for this reaction. Prolonged (*ca.* 100 hr.) heating at 81°, however, gave no increase in bromide content above a 23 p.p.m. blank. Decomposition rates of 1.6 and 42.6 p.p.m. bromide per hour were found at 153 and 190°, respectively, so that for practical purposes a threshold between these temperatures existed.

The radiation decompositions of  $\text{KBrO}_3$  whose explanation was the object of this research were effected in two experimental facilities in the ORNL graphite moderated-natural uranium reactor:<sup>2</sup> (a) Hole 22 South in which a general usage pneumatic transfer tube had been placed for the irradiation of small samples at *ca.* 80°, and (b) Hole 12 in which a vertical water-cooled tube had been installed for irradiations at 30–40°. Approximately one-gram aliquots of pure crystalline salt were bombarded in Hole 22 in air in 10 mm. i.d. quartz tubes held in a plastic capsule or "rabbit" (3.8 mm. wall thickness) which could be blown rapidly into and out of the pile by compressed  $\text{CO}_2$ . An approximate calculation of the attenuation by self-absorption and by the "rabbit" and quartz tube walls of the  $\beta$ -rays from 2.4 m.  $\text{Al}^{28}$  induced in the one-eighth-inch aluminum transfer tube showed that virtually no decomposition (*i.e.*,  $<0.3$  p.p.m. hr.<sup>-1</sup>) of  $\text{KBrO}_3$  could be attributed to these radiations. In some cases the samples were wrapped with boron impregnated plastic, or with Cd or Pb sheet to minimize certain pile radiations. The graphite pile when operated at a nominal maximum power of 3500 Kw. had a central flux of thermal neutrons,  $(n\nu)_{th}$ , of  $1.05 \pm 0.05 \times 10^{12}$  cm.<sup>-2</sup> sec.<sup>-1</sup>.

(1) (a) G. E. Boyd, J. W. Cobble and S. Wexler, *J. Am. Chem. Soc.*, **74**, 237 (1952); (b) J. W. Cobble and G. E. Boyd, *ibid.*, **74**, 1282 (1952).

(2) M. E. Ramsey and C. D. Cagle, "Proceedings of the International Conference on the Peaceful Uses of Atomic Energy," Vol. 2, United Nations, 1956, p. 281.



These neutrons possess an average energy of 0.034 e.v. and an approximately Maxwellian velocity distribution which was assumed to extend out to 1 e.v. For neutron energies,  $E$ , between 1 and  $10^6$  e.v., a second group of resonance or "epithermal" neutrons may be distinguished whose flux per unit energy is proportional to  $1/E$ . Finally, a group of "fast" neutrons defined as those with energies above 1 Mev. must be considered. The majority of the neutrons are slow; practically all are slow plus epithermal.

The measured  $(\bar{n}\bar{v})_{th}$  at the terminus of Hole 22 for a "steady state" power of 3500 Kw. was  $6.0 \pm 0.2 \times 10^{11}$  cm.<sup>-2</sup> sec.<sup>-1</sup>. This flux has been shown<sup>3</sup> to vary linearly with the power from 1800 to 3750 Kw. A Co wire flux monitor was included in every bombardment of KBrO<sub>3</sub> that the decompositions might be corrected for changes in pile power, loading, etc., to a nominal value for 3500 Kw. A value of  $3.3 \times 10^{11}$  cm.<sup>-2</sup> sec.<sup>-1</sup> was estimated<sup>4</sup> for the epithermal flux,  $(\bar{n}\bar{v})_E$ . The S<sup>32</sup> (n,p) 14.3 d. P<sup>32</sup> reaction in sulfur monitors was used to derive a value of  $2.1 \times 10^{10}$  for the fast flux,  $(\bar{n}\bar{v})_f$ . The average neutron energy,  $\bar{E}_n$ , above one Mev. was calculated as 2.2 Mev. by graphical integration of the spectrum reported by Bopp and Sisman.<sup>4</sup> A  $\gamma$ -ray dose rate of  $5.33 \times 10^{17}$  e.v. g.<sup>-1</sup> min.<sup>-1</sup> in water was computed for Hole 22 using calorimetric measurements<sup>5</sup> of the  $\gamma$ -heating in Hole 12, the thermal flux ratio (0.80) between these holes, and a factor of 0.97 to correct for differences in  $\gamma$ -ray absorption. The pile  $\gamma$ -ray energy spectrum is not known; however, there is reason to suppose that the distribution shows a pronounced peak at about 0.1 Mev. which is near the photoelectric absorption threshold for carbon. An average energy  $\bar{E}_\gamma$  of  $0.85 \pm 0.10$  Mev. can be deduced by comparing the heat evolutions<sup>6</sup> in carbon and in bismuth metal, respectively. A  $\gamma$ -ray flux of  $4 \times 10^{11}$  photons cm.<sup>-2</sup> sec.<sup>-1</sup> may be estimated from  $\bar{E}_\gamma$  and the heat evolution in water.

Bombardments of KBrO<sub>3</sub> also were performed in the Los Alamos Fast Plutonium Reactor<sup>5</sup> where the neutrons were predominantly "fast." Approximately 0.5-g. amounts of salt were irradiated in air in quartz tubes contained in cold-rolled, mild steel capsules placed at the center position (67.5 inches from the west face) of tangential hole 2W in the uranium metal reflector where the temperature was ca. 100°. Measurements<sup>6</sup> of fission rates in U<sup>235</sup>, Np<sup>237</sup> and U<sup>238</sup> in this location gave thermal and energetic neutron fluxes above 0.6 and 1.4 Mev. as  $6.4 \times 10^9$ ,  $6.5 \times 10^{11}$  and  $1.8 \times 10^{11}$  cm.<sup>-2</sup> sec.<sup>-1</sup>, respectively, for a nominal maximum power of 25 Kw. Self-decomposition of KBrO<sub>3</sub> by induced bromine and potassium activities can be ignored because of the relatively small  $(\bar{n}\bar{v})_{th}$  and because of the small activation cross-section (42.5 mb.) for Br<sup>79</sup> for neutrons in the fission energy range. All bombardments were monitored using sulfur pellets. A value,  $(\bar{n}\bar{v})_f = 3.9 \times 10^{11}$  cm.<sup>-2</sup> sec.<sup>-1</sup>, at 15 Kw. was obtained which agreed poorly with the value  $2.5 \times 10^{11}$  cm.<sup>-2</sup> sec.<sup>-1</sup> interpolated from the aforementioned fission rate measurements. The latter fast flux value will be employed in the calculations presented later in this paper. An average neutron energy,  $\bar{E}_n = 0.6$  Mev., was calculated by a graphical integration of measurements<sup>7</sup> of the neutron number-energy spectrum. The  $\gamma$ -ray energy distribution in the center of the reactor has been measured and  $\bar{E}_\gamma$  has been given as approximately one Mev.<sup>8</sup> Because of the efficient absorption of  $\gamma$ -rays by uranium metal, however, samples irradiated in Hole 2W were considered to be decomposed exclusively by energetic neutrons.

Irradiations of KBrO<sub>3</sub> with U<sup>235</sup> fission neutrons were carried out by placing ca. 0.5 g. of salt wrapped in aluminum foil inside a 50-g. U<sup>235</sup> metal (95% purity) "pill-box" which in turn was placed in the thermal column of the Los Alamos

Fast Reactor at a point where the thermal flux<sup>6</sup> was  $2.8 \times 10^{10}$  cm.<sup>-2</sup> sec.<sup>-1</sup>. Thermal neutrons were absorbed completely by this convertor, and the salt was exposed to a fission neutron flux of  $2.76 \times 10^{10}$  cm.<sup>-2</sup> sec.<sup>-1</sup> measured using sulfur monitors. Measurements of the fission neutron energy spectrum have been reported<sup>9</sup>; the average neutron energy,  $\bar{E}_n = 2.0$  Mev. The ratio of fast neutron to  $\gamma$ -ray flux in the convertor was sufficiently large because of the strong absorption of the latter that the decomposition was ascribed entirely to the former radiations.

Bombardments of KBrO<sub>3</sub> were conducted with neutrons of 6.1 Mev. average energy produced by 15 Mev. deuterons incident on thick beryllium metal internal, water-cooled targets in the 60-inch cyclotron at the Department of Terrestrial Magnetism, Carnegie Institution of Washington, Washington, D. C. Samples of the salt were irradiated in quartz tubes located about 2.5 cm. behind the target. Sulfur monitors were employed in separate determinations of the variation of the fast neutron flux with the power output by the deuteron beam as measured by a 14-junction thermocouple in the cooling water line. Because of short period fluctuations in the intensity of the deuteron beam (usually ca. 30  $\mu$ a.) a continuous recording of the power was made from which an average  $(\bar{n}\bar{v})_f$  could be calculated by numerical integration. Fluxes between  $5$  and  $10 \times 10^9$  cm.<sup>-2</sup> sec.<sup>-1</sup> were obtained. The energy distribution of Be(d,n) neutrons has been measured<sup>10</sup> and was employed to estimate  $\bar{E}_n$  given above and to compute  $(\bar{n}\bar{v})_f$  from the sulfur monitor activations. The  $\gamma$ -ray contamination of the fast neutron flux was estimated to be negligibly small.

Gamma-ray decompositions of KBrO<sub>3</sub> were accomplished using a 300 curie source of Co<sup>60</sup> radiations of 1.25 Mev. average energy. The irradiations employed a shielded, constant geometry arrangement<sup>11</sup> wherein neutron irradiated cobalt pellets were placed symmetrically around the surface of a brass cylinder 10 cm. long and about 4 cm. in diameter. One-gram samples contained in quartz tubes were exposed in air at room temperature inside the cylinder. The intensity of the source was measured calorimetrically and, at the time of these experiments, the dose rate was  $2.82 \times 10^{17}$  e.v. g.<sup>-1</sup> min.<sup>-1</sup> in water.

Thermal neutron flux measurements were performed using unshielded, weighed Co wires of the highest purity. The induced  $\gamma$ -ray activity was assayed quantitatively using a 4 $\pi$  geometry, high pressure, argon-filled ionization chamber previously calibrated by coincidence count rate measurements to give absolute disintegration rates. An activation cross-section of 36 b. and a half-life of 5.3 y. for Co<sup>60</sup> were assumed in the computation of  $(\bar{n}\bar{v})_{th}$ .

The estimation of fast neutron fluxes requires  $\beta$ -disintegration rate measurements on 14.3 d. P<sup>32</sup> formed by an (n,p) reaction with sulfur. These assays were performed with end-window G.M. or proportional counters under known geometry, scattering and self-absorption after a time sufficient to allow for the complete decay of 2.6 h. Si<sup>31</sup> activity also formed by an (n, $\alpha$ ) reaction on S<sup>34</sup>. Because of the energy dependence of the cross-section,  $\sigma(E)$ , for the formation of P<sup>32</sup> above the threshold of 0.95 Mev., and because of the neutron energy distribution,  $n(E)$ , the flux  $(\bar{n}\bar{v})_{2.9}$ , was estimated as that above an effective threshold energy  $E_{eff} = 2.9$  Mev. for the reaction. The effective reaction cross-section,  $\sigma_{eff}$ , employed depended on the adopted  $E_{eff}$  according to

$$\sigma_{eff} = \frac{\int_0^\infty n(E)\sigma(E) dE}{\int_{E_{eff}}^\infty n(E) dE} \quad (3)$$

A value,  $\sigma_{eff} = 0.30$  b. was calculated using a fission spectrum<sup>9</sup> for  $n(E)$ . The fast flux,  $(\bar{n}\bar{v})_f$ , was then derived from

$$(\bar{n}\bar{v})_f = (\bar{n}\bar{v})_{2.9} \frac{\int_0^\infty n(E) dE}{\int_{E_{eff}}^\infty n(E) dE} \quad (4)$$

(9) B. E. Watt, *ibid.*, **87**, 1037 (1952).

(10) B. L. Cohen and C. E. Falk, *ibid.*, **84**, 173 (1951).

(11) J. A. Ghormley and C. J. Hohanadel, *Rev. Sci. Instr.*, **22**, 473 (1951).

(3) J. W. Jones, H. M. Clark and R. T. Overman, Oak Ridge National Laboratory Report, MonC-398, February 27, 1948; declassified May 31, 1952.

(4) C. D. Bopp and O. Sisman, Oak Ridge National Laboratory Report, ORNL-525, July 28, 1950, declassified Feb. 29, 1956.

(5) D. M. Richardson, A. O. Allen and J. W. Boyle, "Proceedings of the International Conference on the Peaceful Uses of Atomic Energy," Vol. 14, 1956, United Nations, p. 209.

(6) E. T. Journey, J. H. Hall, D. B. Hall, *et al.*, Los Alamos Scientific Laboratory Report, LA-1679, May, 1954, declassified May 2, 1958. (See also: TID-10048).

(7) N. Nereson, Los Alamos Scientific Laboratory Report, LA-1192, December 15, 1950, declassified March 31, 1957.

(8) J. W. Motz, *Phys. Rev.*, **86**, 753 (1952).

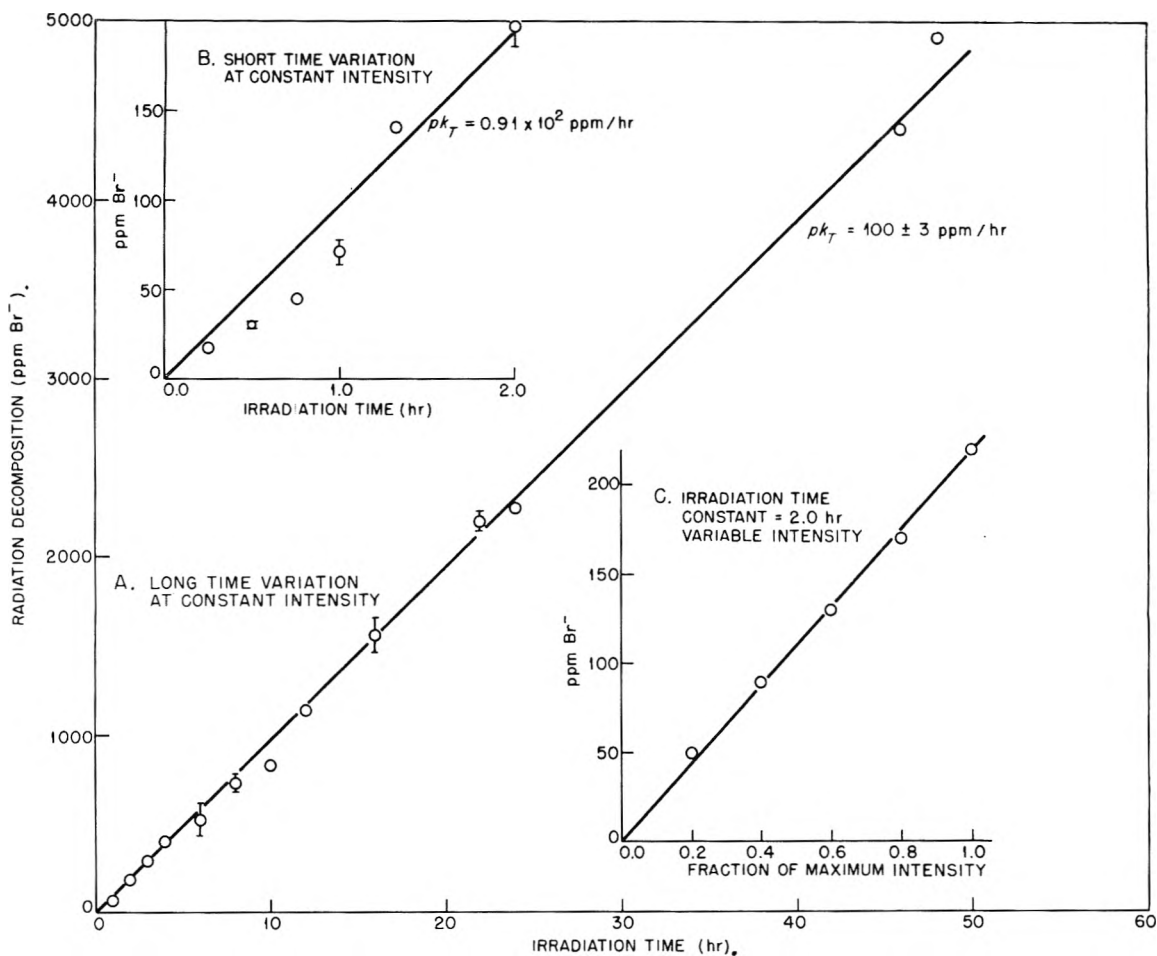


Fig. 1.—Variation of the radiation decomposition of  $\text{KBrO}_3$  in the Oak Ridge Graphite Reactor with time and reactor power (Hole 22).

### Experimental Results

The observed decompositions of pure, crystalline  $\text{KBrO}_3$  on exposure to the radiations near the center of the Oak Ridge graphite reactor are plotted in Fig. 1 as functions of exposure time at constant reactor power and of pile power,  $p$  (radiation intensity) at constant time. The decomposition was linear with the dose rate,  $p$ , and with the radiation dose,  $pt$ , within experimental errors after the first 90 minutes. The departure from an apparent long time average rate of  $100 \pm 3$  p.p.m.  $\text{hr}^{-1}$  for irradiations up to two hours' duration is believed to be real, and to be caused by the self-decomposition of  $\text{KBrO}_3$  under the action of the  $\beta$ -rays from 17.6 m.  $\text{Br}^{80}$  induced in the sample by thermal neutron capture.

The rates of decomposition found when  $\text{KBrO}_3$  was shielded by boron impregnated plastic, cadmium or lead foils are presented in Fig. 2. When the salt was wrapped in a 4 mm. thickness of plastic containing 52% by weight of natural boron (density = 1.67) the rate was lowered to 80 p.p.m.  $\text{hr}^{-1}$ . This amount of boron was sufficient to remove all thermal and an estimated 16% of all epithermal neutrons incident on the sample.

In another set of experiments samples were wrapped in a 40 mil thickness of cadmium sheet to remove all pile radiations except  $\gamma$ -rays and energetic

neutrons. Instead of the expected reduction in the decomposition rate, however, a nearly threefold increase over the unshielded rate was found (*i.e.*, 265 p.p.m.  $\text{hr}^{-1}$ ). This enhancement probably reflects the increase in  $\gamma$ -ray intensity on the sample caused by the neutron capture  $\gamma$ -rays of  $\text{Cd}^{114}$ . A large fraction of the neutron binding energy, 9.046 Mev., released on capture is known to be emitted in cascades of relatively low energy quanta; for example,<sup>12</sup> 85% of the thermal neutrons captured give a 0.559 and 23% to a 0.654 Mev.  $\gamma$ -ray in coincidence with the former transition. The observed increased decomposition rate of  $\text{KBrO}_3$  (*ca.* 160 p.p.m.  $\text{hr}^{-1}$ ) can be explained qualitatively using the observation<sup>13</sup> that 4.1  $\gamma$ -rays in cascade are produced by  $\text{Cd}^{113}(n,\gamma)\text{Cd}^{114}$ .

In the absorption of thermal neutrons by the boron plastic one 0.466 Mev.  $\gamma$ -ray is emitted<sup>14</sup> per neutron absorbed by  $\text{B}^{10}$ . The increase in  $\gamma$ -ray decomposition from these radiations, unfortunately, cannot be calculated from the thermal neutron flux in the absence of boron because of an unknown flux depression. Qualitatively, the lowering of the decomposition rate was the net result of a lowering of the self-decomposition by bromine activities from thermal neutron capture and an in-

(12) H. T. Motz, *Phys. Rev.*, **104**, 1353 (1956).

(13) C. O. Muehlhause, *ibid.*, **79**, 277 (1950).

(14) B. Rose, *Canadian J. Res.*, **26A**, 366 (1948).

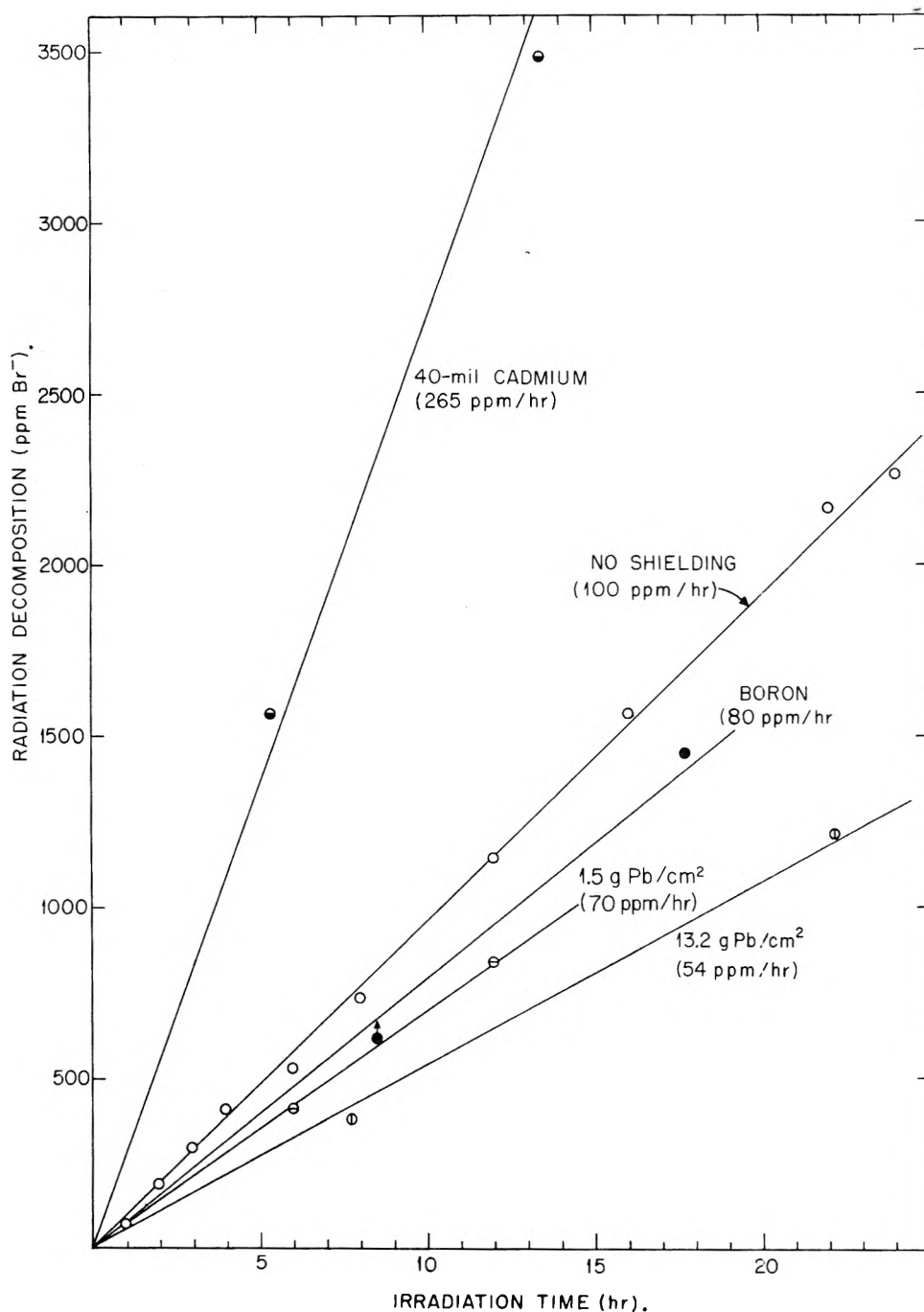


Fig. 2.—The radiation decomposition of  $\text{KBrO}_3$  when shielded by various materials (Oak Ridge Graphite Reactor): values for  $13.2 \text{ g. Pb cm.}^{-2}$  for Hole 12. Corrected rate for Hole 22 was  $57 \text{ p.p.m. hr.}^{-1}$ .

crease from an increased  $\gamma$ -ray flux on the sample.

Varying thicknesses of lead were employed to reduce decomposition by pile  $\gamma$ -rays without altering the thermal neutron flux. Unfortunately, however, the decrease in photon flux across the samples could not be computed, because the  $\gamma$ -ray energy spectrum was unknown. The relatively large decrease in decomposition rate on screening with  $1.5 \text{ g. Pb cm.}^{-2}$  cannot be explained by the absorption of average  $0.85 \text{ Mev.}$  pile  $\gamma$ -rays. The mass absorption coefficient for lead for  $0.1 \text{ Mev.}$  photons, however, is sufficiently large that radiations of this energy would be absorbed quantitatively.

The decompositions found in the  $300 \text{ curie Co}^{60}$  source at  $25^\circ$  are summarized in Table I. A plot of these data revealed that the decomposition was linear with dose, and that the rate constant was  $20 \text{ p.p.m. hr.}^{-1}$ . The point measured at  $80^\circ$  lay on the same straight line as the other measurements indicating the absence of a temperature coefficient for  $\gamma$ -ray decomposition between  $25$  and  $80^\circ$ .

Measurements of energetic neutron decompositions in the Los Alamos Fast Reactor are presented in Fig. 3 from which it may be seen that the decomposition of  $\text{KBrO}_3$  was linear with dose and with dose rate. The first-order rate constant was  $161 \text{ p.p.m. hr.}^{-1}$  for a flux above one  $\text{Mev.}$  of  $4.2 \times$

$10^{11}$  cm.<sup>-2</sup> sec.<sup>-1</sup>. The rate corresponding to the fast flux in the ORNL graphite reactor was computed from the flux ratio to be 8.1 p.p.m. hr.<sup>-1</sup>. Irradiation of the salt in a U<sup>235</sup> fast neutron converter placed in the thermal column of the fast reactor gave a rate of 24 p.p.m. hr.<sup>-1</sup> for  $(\bar{n}\bar{v})_f = 2.8 \times 10^{10}$  cm.<sup>-2</sup> sec.<sup>-1</sup>. Adjusted to a fast flux of  $2.1 \times 10^{10}$  cm.<sup>-2</sup> sec.<sup>-1</sup> for the graphite pile the rate was 18 p.p.m. hr.<sup>-1</sup>.

TABLE I  
DECOMPOSITION OF KBrO<sub>3</sub> AT ROOM TEMPERATURE BY Co<sup>60</sup>  
γ-RADIATIONS

| Irradiation time (hr.) | Decomposition (p.p.m. Br) |
|------------------------|---------------------------|
| 15.8                   | 322                       |
| 24.1                   | 520                       |
| 25.7                   | 533 (80°)                 |
| 43.2                   | 852                       |
| 64.3                   | 1332                      |
| 111.7                  | 2253                      |

Av. rate: 20 p.p.m. hr.<sup>-1</sup>

Decompositions produced by 6.1 Mev. average energy neutrons are summarized in Table II. A mean rate of  $37 \pm 5$  p.p.m. hr.<sup>-1</sup> for a fast flux of  $2.1 \times 10^{10}$  cm.<sup>-2</sup> sec.<sup>-1</sup> was calculated from these values. The energy dependence of the flux-adjusted rates is shown in Fig. 4.

TABLE II  
DECOMPOSITION OF KBrO<sub>3</sub> BY 6.1 MEV. AVERAGE ENERGY  
NEUTRONS

| Bombardment time (hr.) | Fast neutron flux (cm. <sup>-2</sup> sec. <sup>-1</sup> ) | Decomposition (p.p.m. Br) |
|------------------------|-----------------------------------------------------------|---------------------------|
| 4.20                   | $6.1 \times 10^9$                                         | 65                        |
| 7.92                   | $1.0_2 \times 10^{10}$                                    | 125                       |

### Discussion

Estimates of the relative contributions of the β- and γ-ray and neutron components of the ORNL graphite pile radiations to the total decomposition rate for solid KBrO<sub>3</sub> may be carried out using the data presented above. For example, a value for the pile γ-ray decomposition rate constant  $k_\gamma = 38$  p.p.m. hr.<sup>-1</sup> can be computed from the decomposition rate of 20 p.p.m. hr.<sup>-1</sup> found with the Co<sup>60</sup> source and the ratio of the dose rate of this source to that of Hole 22 (*i.e.*, 0.53). This computation employed the demonstrably correct assumption that the ratio of the energy absorption coefficients at 0.85 and 1.25 Mev. for KBrO<sub>3</sub> is equal to the same ratio for water. On comparing  $k_\gamma$  with  $k_T = 100 \pm 3$  p.p.m. hr.<sup>-1</sup> it was concluded that pile γ-rays caused about 40% of the total decomposition. The fast neutron decomposition rate may be estimated as 19 p.p.m. hr.<sup>-1</sup> using the curve in Fig. 4 and an average energy of 2.2 Mev. for the fast neutrons in the Oak Ridge graphite reactor. The difference between  $k_T$  and the sum of the foregoing fast neutron and γ-ray decomposition rates indicated that approximately 40% of the total rate remained to be assigned to β-ray and/or to epithermal neutron decomposition.

The thermal neutrons in the pile do not possess sufficient kinetic energies to decompose KBrO<sub>3</sub> by elastic collisions. Capture of these neutrons by

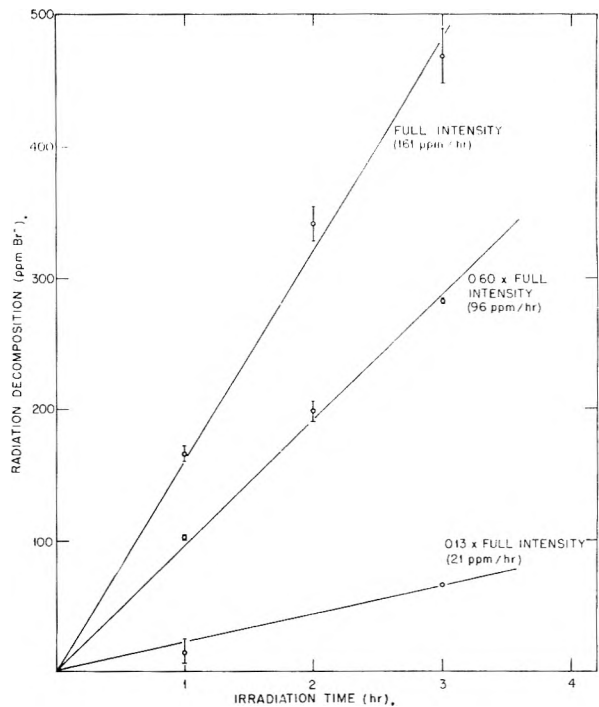


Fig. 3.—Variation of the radiation decomposition of KBrO<sub>3</sub> in the Los Alamos Fast Plutonium Reactor with time and reactor power.

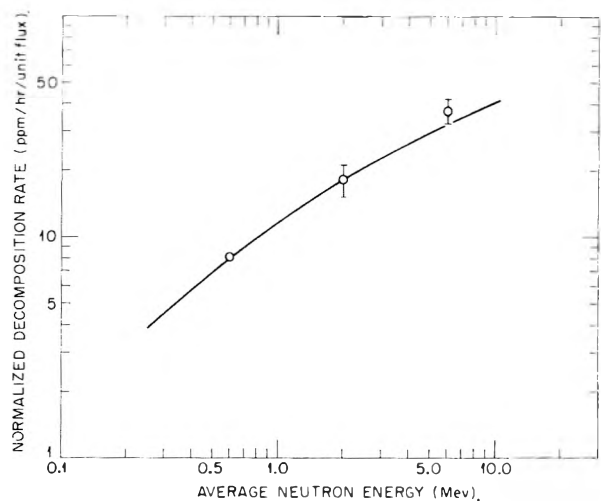


Fig. 4.—Energy dependence of the fast neutron decomposition of KBrO<sub>3</sub> (flux unit was  $2.1 \times 10^{10}$  cm.<sup>-2</sup> sec.<sup>-1</sup>).

Br<sup>79</sup> and Br<sup>81</sup> and by K<sup>39</sup> and K<sup>41</sup>, on the other hand, will produce radioactive recoil atoms whose effects must be considered. Assuming the recoil energies,  $E_r$ , are given by:  $E_r = 537E_\gamma^2/M$ , where  $M$  is the mass of the nucleus emitting a γ-ray of energy  $E_\gamma$  (Mev.)<sup>15</sup> values of  $E_r$  between 30 and 100 e.v. were obtained on taking  $E_\gamma$  as the quotient of the neutron binding energy and the average number of γ-rays emitted per capture. The range of recoils of these energies in crystalline KBrO<sub>3</sub> was estimated as less than *ca.* 5 Å.<sup>16</sup> If every bromate

(15) Capture by oxygen nuclei is neglected because the cross-sections for these are extremely small.

(16) K. O. Nielsen, "Electromagnetically Enriched Isotopes and Mass Spectrometry," Academic Press, Inc., New York, N. Y., 1956, Ch. 9, pp. 68-81.

ion within a sphere of 5 Å. radius were decomposed the yield would be only six bromide ions per neutron captured. A negligible decomposition rate (ca. 0.05 p.p.m. hr.<sup>-1</sup>) will occur therefore when  $(\bar{n}\bar{v})_{\text{th}} = 6.7 \times 10^{11}$  cm.<sup>-2</sup> sec.<sup>-1</sup>. After coming to rest in the KBrO<sub>3</sub> crystal lattice these recoils will undergo radioactive disintegration with the release of additional energy. Decay β-rays, because they are absorbed efficiently, can produce an appreciable decomposition. The extent of their action was calculated assuming one bromate decomposed per 100 e.v. β-energy absorbed (i.e., a "G"-value of unity), and it was found that the β-radiations from 17.6 m. Br<sup>80</sup> were of predominant importance. This activity was produced with a relatively large thermal neutron capture cross-section (8.5 b.) and, because of its short half-life, reached saturation within one hour. It was also formed by the decay of 4.4 h. Br<sup>80m</sup> produced with a cross-section of 2.9 b. Absorption of 91% of all of the β-rays emitted by 17.6 m. Br<sup>80</sup> was estimated from their average energy and range in KBrO<sub>3</sub>. The time dependence of the internal β-ray induced decomposition was derived as

$$k_{\beta}(\text{p.p.m. hr.}^{-1}) = 38.3 - 27.9e^{-\lambda_2 t} - 10.4e^{-\lambda_3 t} \quad (5)$$

where  $\lambda_2$  and  $\lambda_3$  are the decay constants for the 4.4 h. Br<sup>80m</sup> and 17.6 m. Br<sup>80</sup> activities, and  $t$  is the time of bombardment, respectively. Interestingly, eq. 5 predicts a "steady-state" rate of about 38 p.p.m. hr.<sup>-1</sup> and that this limit will be reached after 30–40 hours' bombardment. This result taken together with the values found for  $k_{\gamma}$  and for the fast neutrons has appeared to imply that relatively little decomposition was to be assigned to the epithermal neutron flux. After considering the neutron decomposition yields some support for this conclusion will be adduced.

Estimations of the number of bromate ions decomposed per 100 e.v. absorbed were conducted to understand better the mechanisms of decomposition by pile γ-rays and fast neutrons. A value of  $G = 1.0 \pm 0.1$  was computed for γ-rays from  $k_{\gamma} = 38$  p.p.m. hr.<sup>-1</sup> and a dose rate of  $5.33 \times 10^{17}$  e.v. g.<sup>-1</sup> min.<sup>-1</sup> in water assuming that the energy absorbed per gram of KBrO<sub>3</sub> may be derived from that for water by multiplying by the ratio of the number of electrons per gram in each compound. A γ-ray yield value of this order of magnitude was not unreasonable; recent measurements of the radiolysis of crystalline nitrates with Co<sup>60</sup> γ-rays have given  $G = 1.57 \pm 0.05$  for KNO<sub>3</sub>, for example.<sup>17</sup> The mechanisms for decomposition of bromate and nitrate very well may be similar and both involve the dissociation of excited ions to give oxygen atoms which may undergo secondary reactions.

The mechanism for the decomposition of KBrO<sub>3</sub> by β-rays would be expected to resemble that by γ-rays and their "G"-values should be nearly the same. This expectation appeared to be confirmed in a four-hour irradiation of ca. 0.5 g. of KBrO<sub>3</sub> with a  $2.6 \times 10^{-3}$  μa. beam of 1.15 Mev. electrons from a Van der Graaff accelerator where a decomposition rate of 129 p.p.m. hr.<sup>-1</sup> was observed.

(17) C. J. Hochanadel and T. W. Davis, *J. Chem. Phys.*, **27**, 333 (1957).

A "G"-value of about unity can be computed from this result if the entire energy in the electron beam was deposited in the polycrystalline solid.

A knowledge of the energy deposition by energetic neutrons is necessary to infer yield values from observed decomposition rates in fast neutron fluxes. It was assumed because of the large mean free path (10–100 cm.) for such neutrons that the "knock-on" energy was transmitted in a single, elastic collision between a given oxygen or bromine nucleus and a fast neutron which was scattered isotropically. Further, because of the large initial energies of the recoiling oxygen or bromine nuclei their binding in a bromate radical was ignored. The number per second,  $Z$ , of collisions per bromate will be given by  $Z = (\bar{n}\bar{v})_f \bar{\sigma}_s N$ , where  $(\bar{n}\bar{v})_f$  is the fast flux,  $\bar{\sigma}_s$  the neutron scattering cross-section and  $N$  the number of bromate groups per unit volume. The value of  $\bar{\sigma}_s$  for the bromate group was taken as the sum of three times the  $\sigma_s$  for oxygen plus the  $\sigma_s$  for bromine. In an elastic collision a given neutron will lose, on the average, the same fractional amount of kinetic energy irrespective of its incident energy. The average change in the logarithm of the neutron energy,  $\xi$ , can be given to a satisfactory approximation by the relation<sup>18</sup>:  $\xi = 2/(A + 2/3)$ , where  $A$  is the atomic mass number; for the bromate group;  $\xi_{\text{BrO}_3^-} = (3\xi_{\text{O}} + \xi_{\text{Br}})/4 = 0.0962$ . The amount of energy absorbed per unit volume per second,  $W$ , will be given by  $W = Z\Delta E$ , where  $\Delta E = E_i - E_s$  is the difference between the energies of the incident and scattered neutrons, respectively, and the value of  $E_s$  is defined by:  $\ln E_s = \ln E_i - \xi$ . If  $M$  is the number of bromate ions decomposed per unit volume per second, the yield is given by  $G = 100 (M/W)$ .

Decomposition yield calculations for each neutron energy in Fig. 4 are summarized in Table III.

TABLE III  
FAST NEUTRON DECOMPOSITION YIELDS  
(Unit flux =  $2.1 \times 10^{10}$  cm.<sup>-2</sup> sec.<sup>-1</sup>)

|                                                                          |      |        |        |
|--------------------------------------------------------------------------|------|--------|--------|
| $E_n$ (Mev.)                                                             | 0.6  | 2.0    | 6.1    |
| $\Delta E \times 10^{-4}$ (e.v.)                                         | 5.5  | 18.3   | 56     |
| $\bar{\sigma}_s \times 10^{24}$ (cm. <sup>2</sup> molec. <sup>-1</sup> ) | 15.3 | 8.7    | 7.9    |
| $Z \times 10^{-9}$ (cm. <sup>-3</sup> sec. <sup>-1</sup> )               | 3.9  | 2.2    | 2.0    |
| $W \times 10^{-14}$ (e.v. cm. <sup>-3</sup> sec. <sup>-1</sup> )         | 2.1  | 4.0    | 11.2   |
| $k_T$ (p.p.m. hr. <sup>-1</sup> )                                        | 8.1  | 18 ± 3 | 37 ± 5 |
| $M \times 10^{-13}$ (cm. <sup>-3</sup> sec. <sup>-1</sup> )              | 5.5  | 12.3   | 25     |
| $G$ (molec./100 e.v.)                                                    | 26   | 30     | 23     |

The magnitude of the values and their apparent energy dependence merit comment. The decomposition efficiency of fast neutrons undoubtedly is many times larger than that for β- or γ-rays despite fairly large experimental uncertainties. This difference is believed to be the consequence of a difference in the mechanism for the absorption of energy by KBrO<sub>3</sub> from these types of pile radiation: With neutrons energy is dissipated largely by collisional processes wherein primary "knock-on" atoms in turn produce secondary and higher order recoils which give additional decomposition; with elec-

(18) S. Glasstone and M. C. Edlund, "The Elements of Nuclear Reactor Theory," D. Van Nostrand Co., Inc., New York, N. Y., 1952, p. 144.

trons and  $\gamma$ -rays energy is imparted by ionization and excitation and the process is relatively inefficient insofar as molecular disruption is concerned.

An additional description of the decomposition produced by fast neutrons may be of interest. Considering an incident 1 Mev. neutron, the average kinetic energy,  $\bar{T}$ , given to an atom of mass  $A$  in an elastic collision will be:  $\bar{T}(\text{Mev.}) = A/(A + 1)^2$ , or 24 Kev. for a bromine and 110 Kev. for an oxygen atom, respectively. The velocity of the bromine atom is sufficiently low that it will transfer its energy solely by elastic collisions, while that for an oxygen atom is such that energy will be lost by ionization and excitation as well as by collisions. The mean number of displaced atoms in  $\text{KBrO}_3$ , including the primary knock-on itself, produced by a primary knock-on energy  $\bar{T}$ , is given approximately by<sup>19</sup>  $\bar{T}/2E_d$ , where  $E_d$  is the displacement energy. If the rupture of a Br-O bond is considered sufficient to decompose a bromate group, then  $E_d$  will be equal to the bond energy,<sup>20</sup>  $2.2 \pm 0.5$  e.v., for the displacement of oxygen and roughly to  $6.6 \pm 1.5$  e.v. for the displacement of bromine atoms, neglecting the resonance stabilization energy. With an average 110 Kev. oxygen primary, approximately 25,000 and with a bromine primary approximately 1700 decompositions will be produced. The energy deposition per 1 Mev. neutron will be  $9.17 \times 10^4$  e.v.; hence  $G = 19$  molecules will be decomposed per 100 e.v. absorbed on the average. The general agreement of this yield with those derived from experiment (Table III) suggests that fairly good account of the decomposition mechanism can be obtained even from a primitive model. A refinement of this picture of

the fast neutron decomposition of  $\text{KBrO}_3$  will not be undertaken: it must suffice to point out that the apparent decrease in  $G$  with energy (Table III) might be explained by the breakdown of the assumption of isotropic scattering of 6.1 Mev. neutrons. In addition, the oxygen recoils will transmit less energy than estimated on the basis of elastic collisions because of ionization effects.

The foregoing model of the mechanism for neutron decomposition requires that the  $G$ -value be independent of the neutron energy. Using  $G = 19$  and assuming the epithermal flux per unit energy varies accurately as  $1/E$  from 0.1 Mev. to 1 e.v., it may be calculated that a decomposition rate of only about 1.5 p.p.m. hr.<sup>-1</sup> will occur because of elastic collisions. Most of this decomposition will occur in the interval between 0.01 and 0.1 Mev. by reason of the linear energy dependence of  $\Delta E$  on  $E_i$ . Only a rough estimate of 8 p.p.m. hr.<sup>-1</sup> for the decomposition for the interval between 0.1 and 1 Mev. can be made; the  $1/E$  law is quite inaccurate because the fission neutron spectrum extends to nearly 0.5 Mev. The epithermal neutron contribution to the decomposition will therefore be less than 10 p.p.m. hr.<sup>-1</sup>.

**Acknowledgments.**—It is a pleasure to acknowledge the interest and helpful criticism of our colleagues, including Drs. E. H. Taylor, C. J. Hochanadel and G. H. Jenks, at the Oak Ridge National Laboratory with whom the authors have discussed various aspects of this research. Thanks also are expressed to the staff of the Los Alamos Fast Plutonium Reactor and to Dr. C. W. Zabel for their assistance in the fast pile neutron bombardments, and to Drs. M. A. Tuve and Dean Cowie of the Department of Terrestrial Magnetism of the Carnegie Institution of Washington for their hospitality during our experiments with the 60-inch cyclotron.

(19) G. J. Dienes and G. H. Vineyard, "Radiation Effects in Solids," Interscience Publishers, Inc., New York, N. Y., 1957, p. 26.

(20) T. L. Cottrell, "The Strength of Chemical Bonds," Butterworth's Scientific Publications, London, 1954, p. 221.

## RADICAL PRODUCTION IN HYDROCARBONS BY HEAVY PARTICLE RADIATIONS<sup>1</sup>

BY ROBERT H. SCHULER

*Contribution from Radiation Research Laboratories, Mellon Institute, Pittsburgh, Pennsylvania*

*and*  
*Department of Chemistry, Brookhaven National Laboratory, Upton, N. Y.*

*Received February 16, 1959*

Previous experiments on the use of iodine to scavenge radicals produced in hydrocarbons by  $\gamma$ -rays have been extended to the heavy particle radiations available at the Brookhaven 60-inch cyclotron. It has been shown that at beam currents of the order of  $10^{-9}$  ampere depletion effects can be avoided in millimolar iodine solutions and that significant radical yields can be determined. Hexane, cyclohexane and 2,2,4-trimethylpentane were studied. In experiments with 18-Mev. deuterons (LET = 0.5 e.v./ $\text{\AA}$ .) and with 33-Mev. helium ions (LET = 2 e.v./ $\text{\AA}$ .) the observed yields are approximately 10 and 30% less than those found in similar fast electron experiments. This decrease in radical yield is somewhat less than observed in similar comparisons of the effect of light and heavy particles on aqueous systems.

Extensive studies of the radiolysis of aqueous solutions by various densely ionizing radiations have shown that bimolecular radical reactions occur to an important extent within the track of the ionizing particle. These reactions significantly reduce the yield of radicals which escape from the track and alter the over-all radiation chemical

process. To date very little comparative work on the effects of light and heavy particles on liquid organic systems has appeared in the literature. By analogy with the results from aqueous solutions, however, one might expect to be able to observe a decrease in the yield of radicals and a corresponding increase in certain "molecular" products in going from fast electrons to more densely ionizing radia-

(1) Supported, in part, by the U. S. Atomic Energy Commission.

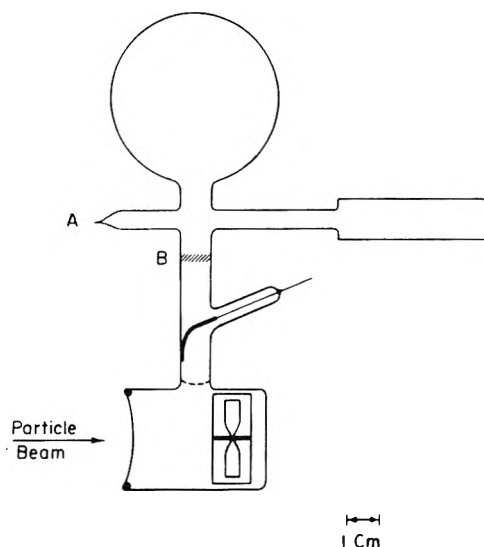


Fig. 1.—Irradiation cell. Sample degassed in large bulb (50 cc.) and sealed at A. Cell coated up to B with conducting film of stannic oxide.

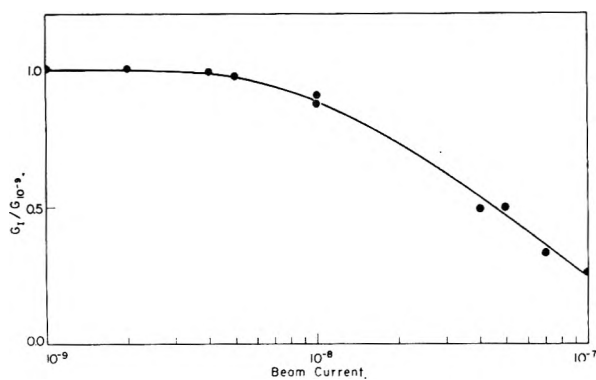


Fig. 2.—Dependence of yield on beam current for solutions  $0.2 \times 10^{-3} M$  in iodine (for 34 Mev. helium ions).

tions. Preliminary comparative investigations of the effects of different types of radiations on the radiolysis of hexane and cyclohexane have not shown any effect of linear energy transfer (LET) on the over-all radiation chemistry.<sup>2</sup> The present work represents the initial investigation of the dependence of the yield of observable radicals upon LET when an active radical scavenger is present. Iodine scavenging was employed in experiments similar to those previously described<sup>3</sup> to measure the radical yields produced by the radiations available at the Brookhaven 60-inch cyclotron. Studies were carried out on hexane, cyclohexane and 2,2,4-trimethylpentane. These typical non-aromatic hydrocarbons have been the subject of numerous other recent radiation-chemical investigations.

### Experimental

Phillips Research Grade hydrocarbons were used. Samples (usually 25 cc.) containing the desired amount of dissolved iodine were sealed, after thorough degassing, into Saldick-type<sup>4</sup> irradiation cells fitted with a magnetic stirrer and a Pyrex 1-cm. cuvette on a side-arm (Fig. 1). Iodine concen-

trations were determined at intervals during a run by spectrophotometry at 520  $\mu$ . The molar extinction coefficient of iodine is 910 in hexane, 930 in cyclohexane and 940 in 2,2,4-trimethylpentane.

The inside surface of the cell was coated with a thin electrically-conducting but chemically inert film of stannic oxide which was fused into the glass at high temperature. This allowed the beam current to be collected by an electrode sealed through the cell wall and conducted to ground through the measuring instrument (a Higginbotham-Rankowitz integrator), while maintaining the required high insulation resistance ( $>10^{10}$  ohms) between the current collecting system and ground. The beam energies were determined as previously described,<sup>5</sup> and appropriate current corrections made.<sup>6</sup> In the  $\gamma$ -ray studies, doses were determined by the Fricke dosimeter, assuming  $G(\text{Fe}) = 15.5$  and energy absorption proportional to the electron density of irradiated samples.

### Results and Discussion

Because of the short range of the particles used in the experiments at the cyclotron (340 mg./cm.<sup>2</sup> in aluminum for 20 Mev. deuterons and 170 mg./cm.<sup>2</sup> for 40 Mev. helium ions) only a thin layer next to the cell window is irradiated at any one instant. In the present studies the beam was restricted to a cross sectional area of 0.31 cm.<sup>2</sup> so that the irradiated volume was approximately 0.1 cc., *i.e.*, less than 1% of the total sample. At high currents bulk depletion of the scavenger within this volume can become a significant problem. For example, at iodine concentrations of  $10^{-4} M$  a total charge input corresponding to  $10^{-9}$  coulomb of 20 Mev. particles will produce sufficient radicals to react with all of the scavenger present. At currents above  $10^{-8}$  ampere depletion of the solute within the irradiation zone will occur within one tenth of a second. Significant experiments can therefore be carried out only at low beam currents and only with sufficient stirring to replace adequately the solution within the irradiation zone.

Some indication of the efficiency of stirring is given in Fig. 2 where the dependence of the relative yield of iodine consumption is given as a function of beam current for solutions approximately  $0.2 \times 10^{-3} M$  in iodine. From the onset of depletion at a current of  $5 \times 10^{-6}$  ampere we estimate that the irradiated volume is completely replaced at least 20 times per second under the stirring conditions employed here (600 r.p.m.). For solutions of higher concentration (*i.e.*,  $10^{-2} M$ ) and lower currents ( $10^{-9}$  ampere) depletion effects should be negligible. Thus the radical yields determined in this way should be significant and characteristic of the particular radiations under investigation.

Typical results of the reaction induced by 30-Mev. helium ions between iodine and hexane are illustrated in Fig. 3. Approximate zero-order dependence is indicated. This behavior is very similar to that found with X-rays<sup>7</sup> although a slight curvature is observed in the points obtained at the highest concentration. This is due in part to the dependence of yield on concentration and in part to the interference of some product, probably hydrogen iodide, formed by complications which appear at

(5) R. H. Schuler and A. O. Allen, *J. Am. Chem. Soc.*, **79**, 1565 (1957).

(6) R. H. Schuler and A. O. Allen, *Rev. Sci. Instr.*, **26**, 1128 (1955).

(7) P. F. Forsyth, E. N. Weber and R. H. Schuler, *J. Chem. Phys.*, **2**, 60 (1954).

(2) H. A. Dewhurst and R. H. Schuler, *J. Am. Chem. Soc.*, **81**, in press (1959).

(3) R. W. Fessenden and R. H. Schuler, *ibid.*, **79**, 273 (1957).

(4) J. Saldick and A. O. Allen, *J. Chem. Phys.*, **22**, 438 (1954).

higher iodine concentrations.<sup>8</sup> That this curvature is not entirely due to a concentration dependence is exemplified by the fact that the curves in Fig. 3 for solutions 0.2 and 0.4 mM in iodine are of more nearly the same slope as that described initially than that observed after 60 and 80% reaction for the more concentrated sample. The presence of hydrogen iodide in the sample would result in production of iodine<sup>9</sup> rather than its elimination and would therefore have an exaggerated effect on the curves of Fig. 3. Similar data to those given in Fig. 3 were obtained for all solutions. The yields calculated from the initial slopes of these curves are given in Fig. 4 for hexane and are summarized in Table I for the various experiments carried out in this study.

TABLE I  
RADIATION-INDUCED REACTION OF  
IODINE AND HYDROCARBONS

| Radiation              | Beam current, amp. $\times 10^9$ | Iodine concn., mM | $G(-1/2 I_2)^a$   |
|------------------------|----------------------------------|-------------------|-------------------|
| Hexane                 |                                  |                   |                   |
| Co60 $\gamma$ -rays    | ...                              | 0.81              | 5.60              |
| 2 Mev. $e^-$           | 30                               | 1.02              | 5.55              |
| 19.0 Mev. $D^+$        | 1                                | 1.00              | 5.20              |
| 18.9 Mev. $D^+$        | 1                                | 0.41              | 4.95              |
| 18.5 Mev. $D^+$        | 1                                | 0.19              | 4.87              |
| 34.2 Mev. $He^{++}$    | 1                                | 1.00              | 4.13              |
| 31.0 Mev. $He^{++}$    | 1                                | 0.80              | 3.80              |
| 34.0 Mev. $He^{++}$    | $10^b$                           | .78               | 3.95              |
| 34.0 Mev. $He^{++}$    | 1                                | .39               | 3.85              |
| 34.0 Mev. $He^{++}$    | 10                               | .38               | 4.01              |
| 30.5 Mev. $He^{++}$    | 1                                | .19               | 3.55              |
| (34.0 Mev. $He^{++}$ ) | 100                              | .4                | 2.2) <sup>c</sup> |
| (34.0 Mev. $He^{++}$ ) | $100^d$                          | .4                | 1.4) <sup>c</sup> |
| (34.0 Mev. $He^{++}$ ) | 10                               | .1                | 2.0) <sup>c</sup> |
| 17.6 Mev. $He^{++}$    | 2                                | .26               | 2.85              |
| 11.8 Mev. $He^{++}$    | 2                                | .48               | 2.88              |
| Cyclohexane            |                                  |                   |                   |
| Co-60 $\gamma$ -rays   | ...                              | 0.85              | 5.50              |
| Co-60 $\gamma$ -rays   | ...                              | .80               | 5.70              |
| 2 Mev. $e^-$           | 10                               | .99               | 5.62              |
| 2 Mev. $e^-$           | 10                               | .82               | 5.59              |
| 18.5 Mev. $D^+$        | 1                                | .95               | 5.25              |
| 18.0 Mev. $D^+$        | 1                                | .40               | 5.00              |
| 33.5 Mev. $He^{++}$    | $10^b$                           | 1.02              | 3.33              |
| 34.2 Mev. $He^{++}$    | 1                                | 0.92              | 3.94              |
| 31.0 Mev. $He^{++}$    | 1                                | .82               | 3.41              |
| 34.2 Mev. $He^{++}$    | 1                                | .38               | 3.64              |
| 34.0 Mev. $He^{++}$    | 1                                | .19               | 3.20              |
| 12.2 Mev. $He^{++}$    | 2                                | .37               | 2.72              |
| Isooctane              |                                  |                   |                   |
| Co-60 $\gamma$ -rays   | ...                              | 0.70              | 5.65              |
| 2 Mev. $e^-$           | 10                               | .85               | 5.33              |
| 18.5 Mev. $D^+$        | 1                                | .78               | 5.12              |
| 34.0 Mev. $He^{++}$    | 1                                | .85               | 4.15              |

<sup>a</sup> Absolute radiation yields as atoms of iodine reacting per 100 e.v. of absorbed energy. <sup>b</sup> Current collected from cell coated externally with film of "dag." <sup>c</sup> These results show significant depletion effects at the high currents employed; cf. also Fig. 2. <sup>d</sup> Sample not stirred during the irradiation.

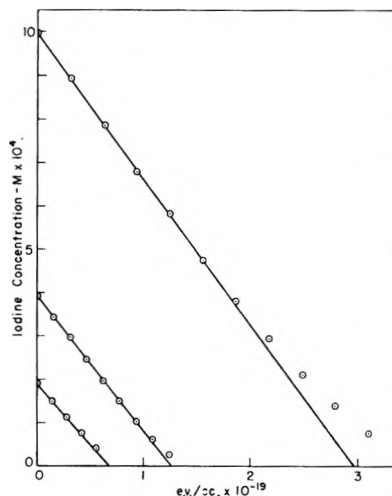


Fig. 3.—Reaction of iodine with hexane induced by 34 Mev. helium ions.

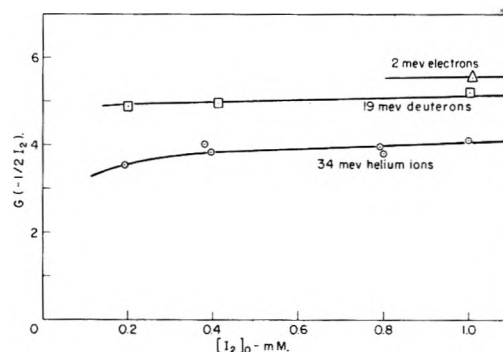


Fig. 4.—Yields of reaction between iodine and hexane as a function of initial iodine concentration.

For each of the hydrocarbons studied the yields for iodine consumption in millimolar solution for 18-Mev. deuterons (LET = 0.5 e.v./ $\text{\AA}$ .) and for 34-Mev. helium ions (LET = 2.0 e.v./ $\text{\AA}$ .) are, respectively, 10 and 30% lower than those found for fast electrons. Since the densities of total energy dissipation are quite similar in the deuteron and helium ion experiments the 20% difference noted here must almost certainly be due to a track effect rather than bulk depletion of the scavenger. For the densely ionizing helium ions a slight decrease with decreasing iodine concentration is indicated in Fig. 4 although it is of course difficult to be sure that depletion effects are not involved at the low concentrations. The effect of LET is very nearly the same in each of the cases studied, being slightly greater for cyclohexane than for the two aliphatic hydrocarbons.

For helium ions of energies lower than the maximum available at the cyclotron a further decrease in yield is observed. The differential yield ( $G_i = d(G_0 E_0)/dE_0 \sim \Delta(G_0 E_0)/\Delta E_0$ ) can be calculated for 25 Mev. helium ions (LET = 3 e.v./ $\text{\AA}$ .) from the data of Table I. Values of 4.6 and 4.2 are obtained, respectively, for hexane and cyclohexane. If these yields are taken as representative of the integral values for 5 Mev. deuterons then differential yields of 5.1 and 5.3 are estimated for 10 Mev. deuterons (LET = 1 e.v./ $\text{\AA}$ .). The fact that these differential yields are slightly lower than

(8) Cf. C. E. McCauley and R. H. Schuler, *J. Am. Chem. Soc.*, **79**, 4008 (1957).

(9) R. H. Schuler, *THIS JOURNAL*, **61**, 1472 (1957).



those observed for fast electrons shows that the decreases found in the heavy particle studies are not due entirely to effects which occur at the extreme range of the track but rather to reactions which gradually increase in importance as the LET increases.

The fact that the differences in yields between fast electrons and heavy particle radiations are as small as those indicated here demonstrates that most of the radicals readily escape from the ionization track. For radiations having a LET of 2 e.v./Å. one radical is produced on the average along every 10 Å. of path length. For a solution  $10^{-3} M$  in iodine the track must expand to a radius of several hundred angstroms before it itself contains sufficient iodine to quench all of the radicals formed. Reactions between radicals within the track, which compete with the scavenging process, might well be expected, because of the high initial concentration at which the radicals are formed and because of depletion of scavenger within the track. Such reactions are of lesser importance here than in

aqueous solutions.<sup>10</sup> That such reactions do not contribute in a more important way is on first reflection somewhat surprising. Diffusion of the radicals out of the track apparently competes successfully with the bi-molecular process. These results are in accord with the previously observed fact that the over-all radiation chemistry of these simple hydrocarbons is relatively unaffected by the LET of the radiation.<sup>2</sup> Only through very detailed quantitative comparisons of the effects of light and heavy particles such as the present is it possible to discover significant effects of LET on the radiation chemistry of the system.

**Acknowledgment.**—We wish to thank Dr. A. O. Allen for extensive discussions on the subject of this paper, Mr. Irving Meyer for his aid in the development of the very fine irradiation cells which have made these measurements possible and the members of the staff of the Brookhaven 60-inch cyclotron for their assistance with these measurements.

(10) N. F. Barr and R. H. Schuler, *THIS JOURNAL*, **63**, 808 (1959).

## HYDROGEN ATOMS IN THE RADIOLYSIS OF WATER<sup>1</sup>

BY NATHANIEL F. BARR AND AUGUSTINE O. ALLEN

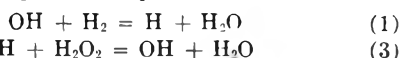
*Contribution from Department of Chemistry, Brookhaven National Laboratory, Upton, N. Y.*

*Received February 16, 1959*

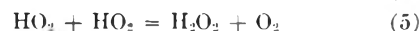
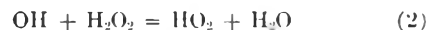
In the radiolysis of aqueous solutions containing  $H_2$ ,  $H_2O_2$  and  $O_2$ , the "H atom" formed by free-radical oxidation of  $H_2$  is shown to react with  $O_2$  much faster than with  $H_2O_2$ ; but in solutions containing  $O_2$  and  $H_2O_2$  only, the "H atom" formed from water by radiolysis attacks  $O_2$  and  $H_2O_2$  at comparable rates. It is concluded that the two kinds of "H atom" are in fact different, and may be basic and acid forms of H, *i.e.*, the solvated electron, or the ion  $E_2^+$ .

The mechanism of water decomposition by radiation, including the back-reaction, appears to be fairly well understood.<sup>2</sup> Water is dissociated into free radicals, denoted H and OH. Some of these combine to form molecular  $H_2$  and  $H_2O_2$ ; others escape this initial recombination and react with dissolved materials present. In the absence of other materials the radicals act on the molecular decomposition products. Peroxide is thereby converted in part into molecular oxygen, and hydrogen is combined with this oxygen and with the peroxide to re-form water. To elucidate the process, a number of studies have been made in which solutions of these decomposition products in water have been irradiated with  $\gamma$ -rays.

As long as only two of the three decomposition products are present, the observed reaction kinetics are satisfactorily explained by plausible reactions of the free radicals H and OH. Thus when solutions containing hydrogen gas and hydrogen peroxide are irradiated with  $\gamma$ -rays the two solutes react together to form water, with a high yield which indicates that a chain reaction occurs.<sup>3</sup> This chain must presumably be written as



When only oxygen and peroxide are present the OH reacts with the peroxide and H with both oxygen and peroxide.



If only oxygen is present peroxide formed as a result of reactions 4 and 5 is partially destroyed by reaction 2, but since the free H is formed in larger quantity than free OH a net formation of peroxide is observed with a yield equal to  $G_{H_2O_2} + G_H - G_{OH}$ .<sup>4</sup> As soon as appreciable peroxide accumulates, however, the rate diminishes and a steady state is reached in which the peroxide is present at a concentration about one-third that of the oxygen.<sup>5</sup> Not only the steady state levels at different oxygen concentrations, but the entire course of the curve shown in Hochanadel's latest publication<sup>5</sup> on this subject agree with the above mechanism if the specific rate constants for reaction of H with  $O_2$  and  $H_2O_2$  are of the same order of magnitude. This result has also been checked by measurements made

(4) The net yields of the radical and molecular products from water radiolysis, in molecules produced per 100 e.v. absorbed, are denoted here by  $G$  with an appropriate subscript. Actual observed yields of various products are denoted by  $d(\text{Product})/d(\text{Dose})$ , taken again in units of molecules per 100 e.v.

(5) C. J. Hochanadel, *Proc. Intl. Conf. Peaceful Uses of Atomic Energy*, **7**, 521 (1955) (United Nations).

(1) Research performed under the auspices of the U. S. Atomic Energy Commission.

(2) A. O. Allen, *Proc. Intl. Conf. Peaceful Uses of Atomic Energy*, **7**, 513 (1955) (United Nations).

(3) C. J. Hochanadel, *J. Phys. Chem.*, **56**, 587 (1952).

in this Laboratory by Schwarz,<sup>6</sup> who obtains for the rate constant ratio  $k_4/k_3$  the value 1.85.

In solutions containing only hydrogen and oxygen, the two molecules combine to form hydrogen peroxide. The rate is shown by Hochanadel to be practically independent of the concentrations of hydrogen and oxygen, and one must conclude that all free OH is reacting with  $H_2$  to form H; all H then reacts with  $O_2$  to form  $HO_2$  which in turn eventually reacts with itself to form peroxide. The number of molecules of peroxide formed here, 3.2 per 100 e.v., is therefore taken as a measure of half the total yield of free radicals plus the direct yield of molecular peroxide;  $G_{OH}/2 + G_H/2 + G_{H_2O_2} = 3.2$ . From these and similar experiments, the radical and molecular yields are obtained:  $G_{H_2} = 0.45$ ,  $G_{H_2O_2} = 0.70$ ,  $G_H = 2.75$ ,  $G_{OH} = 2.25$ .

When all three substances, hydrogen, hydrogen peroxide and oxygen, are present together the system no longer behaves as expected on the basis of the above reactions. An example of such discrepancy is found in Hochanadel's work<sup>2</sup> on solutions initially containing much hydrogen and relatively little oxygen, when the reaction continues into regions where the peroxide concentration becomes comparable to that of the oxygen. In this system, since hydrogen is in large excess over peroxide, practically all OH reacts with  $H_2$  rather than  $H_2O_2$ , and the rate of consumption of oxygen is expected to be constant and equal to  $G_{OH}/2 + G_H/2$ . Reaction 3 will reduce the peroxide yield but should not affect the yield of oxygen consumption, since the OH formed in (3) will react with  $H_2$  by (1) to regenerate H which can then react with  $O_2$ . In a solution containing hydrogen and a relatively small quantity of oxygen the dose at which the oxygen is all consumed can then be calculated. At approximately half this dose the oxygen and peroxide will be present in equal concentrations, and according to the experiments mentioned above on solutions containing only oxygen and peroxide the  $O_2$  and  $H_2O_2$  should be competing for H and the rate of peroxide formation should be greatly reduced. Reaction 3 destroys one mole of peroxide, while (4) followed by (5) produces one-half mole. Then when the rate of (3) exceeds one-half the rate of (4), the effect of the radical reactions is to give a net destruction of peroxide. If  $k_4/k_3 = 1.85$ , this condition will occur when the  $H_2O_2$  concentration becomes greater than 1.85/2 or 0.925 of the  $O_2$  concentration. As further oxygen is consumed the rate of peroxide destruction by radicals will exceed its rate of formation from the water, the peroxide concentration should then begin to drop, and by the time the oxygen is all consumed no peroxide should be left. The equation for peroxide concentration on the above mechanism, consisting of reactions 1, 3, 4 and 5 and including the contribution of the molecular yield by assuming reaction 2 to be negligible, is

$$\frac{d(H_2O_2)}{d(\text{Dose})} = G_{H_2O_2} + (G_{OH} + G_H) \left( \frac{1}{2} - \frac{k_3(H_2O_2)}{k_4(O_2)} \right) \quad (A)$$

where  $(O_2)$  will be given by  $(O_2)_0 - 1/2(G_{OH} + G_H)(\text{Dose})$ . Hochanadel's data on a solution

initially containing  $45 \mu M O_2$  and  $440 \mu M H_2$  do not follow this expected curve at all. Data shown in Fig. 6 of his paper<sup>3</sup> indicate that the peroxide keeps on climbing at almost the initial rate until the expected dose for complete consumption of oxygen is exceeded. Then the concentration of peroxide drops very suddenly, presumably by the chain reaction between hydrogen and hydrogen peroxide, which is well known from the study of solutions containing only these two components. It seemed that the competition between  $O_2$  and  $H_2O_2$  for H atoms was not proceeding at all in the presence of hydrogen as expected from experiments on solutions not containing hydrogen. Other data on these systems also seem to indicate difficulties. We therefore undertook a more detailed study of the course of peroxide formation in aqueous solutions of hydrogen and oxygen exposed to  $\gamma$ -rays.

### Experimental

Water was purified by multiple distillation and radiolysis as previously described.<sup>7</sup> Water was saturated with hydrogen by bubbling and the two solutions mixed by drawing a portion of each into a glass hypodermic syringe. A glass ring was placed in the syringe to ensure thorough mixing when the syringe was shaken. Irradiations were made at  $23^\circ$  in the syringe using the  $\gamma$ -ray source described by Schwarz and Allen.<sup>8</sup> At intervals the syringe was removed from the source, a sample of liquid ejected for analysis, and the remainder replaced for further irradiation. Special experiments showed that the amount of oxygen leaking into the syringe from the air during these manipulations was negligible compared to the amounts of oxygen present in the experiments.

### Results

A number of experiments showed that for solutions of different oxygen concentrations with hydrogen at about  $360 \mu M$  the initial yield of peroxide appeared to be independent of the oxygen concentration and equal to 3.2, in exact agreement with Hochanadel's value. At a concentration of  $H_2$  of  $160 \mu M$  the initial yield appeared to be about 9% smaller. This effect, if real, is reminiscent of the drop in peroxide yield found by Jayson, Scholes and Weiss,<sup>9</sup> in aqueous solutions of oxygen and alcohol, when the alcohol concentration is reduced to very low levels. We believe these effects may be ascribed to a direct reaction between OH and  $HO_2$  which sets in when the amount of all other materials capable of reaction with OH is small. Figure 1 shows the results obtained from a number of solutions initially containing approximately  $700 \mu M H_2$  and much smaller concentrations of  $O_2$ . In every case the form of the curve resembles that reported by Hochanadel; *i.e.*, the peroxide concentration continues to rise until the total dose reaches a value at which oxygen is expected to be completely consumed; then at a slightly greater dose a precipitous fall occurs. The results are highly reminiscent of those reported by Hart<sup>10</sup> for solutions containing formic acid and hydrogen peroxide in the presence of oxygen.

(7) A. O. Allen and R. A. Holroyd, *J. Am. Chem. Soc.*, **77**, 5852 (1955).

(8) H. A. Schwarz and A. O. Allen, *Nucleonics*, **12**, No. 2, 58 (1954).

(9) G. G. Jayson, G. Scholes and J. Weiss, *J. Chem. Soc.*, 1358 (1957).

(10) E. J. Hart, *J. Am. Chem. Soc.*, **73**, 68 (1951).

(6) A. O. Allen and H. A. Schwarz, *Second Intl. Conf. Peaceful Uses of Atomic Energy*, (1958), in press (1958).

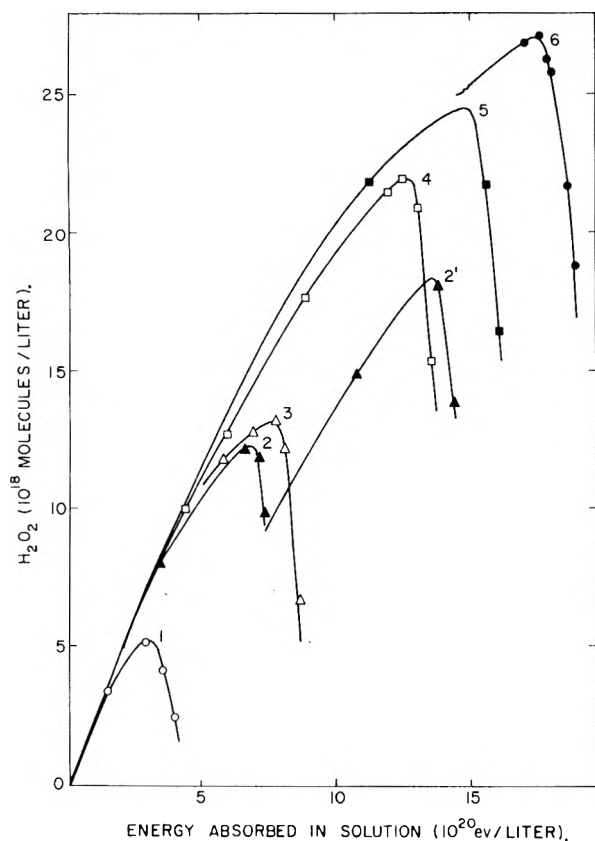


Fig. 1.—Peroxide formation in  $H_2$ -saturated solutions containing various amounts of oxygen (see Table I).

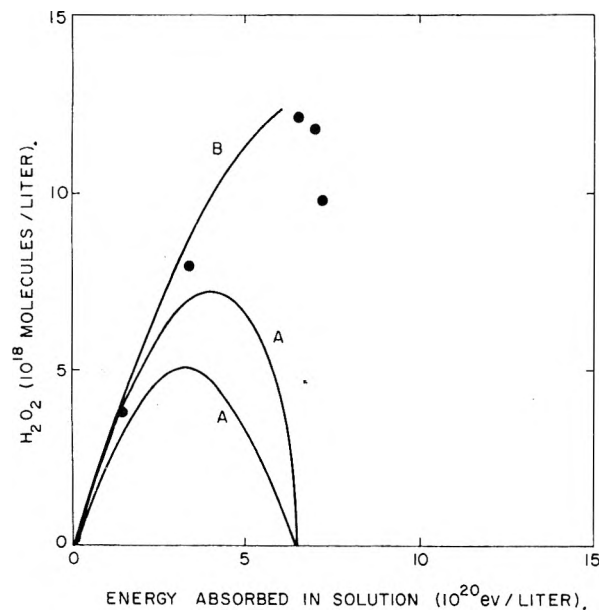


Fig. 2.—Points from expt. 2 replotted to show comparison with curves obtained by integration of Equations A and B.

There also the peroxide was not consumed while any oxygen was present, but instead the formic acid and oxygen reacted together to form peroxide and  $CO_2$ . When all oxygen was consumed a chain reaction between peroxide and formic acid to yield  $CO_2$  and water suddenly set in.

In experiment 2 of Fig. 1 more oxygenated water was added to the syringe after the peroxide concen-

tration started to decrease. The result was a second rise and subsequent fall in peroxide, similar to that produced initially. In Table I the values

TABLE I  
CHARACTERISTICS OF THE PEROXIDE CONCENTRATION-DOSE CURVES

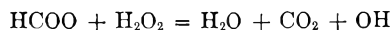
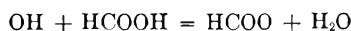
| Expt. | $(O_2)_0$ ,<br>molec./l.<br>$\times 10^{-18}$ | $D_{max}$ ,<br>e.v./l.<br>$\times 10^{-20}$ | $(O_2)_0/D_{max}$ ,<br>molec./<br>100 e.v. | $(H_2O_2)_{max}$ ,<br>molec./l.<br>$\times 10^{-18}$ | $(H_2O_2)_{max}/$<br>$(O_2)_0$ |
|-------|-----------------------------------------------|---------------------------------------------|--------------------------------------------|------------------------------------------------------|--------------------------------|
| 1     | 6.79                                          | 3.1                                         | 2.19                                       | 5.15                                                 | 0.76                           |
| 2     | 15.07                                         | 6.9                                         | 2.18                                       | 12.1                                                 | .80                            |
| 2'    | 13.66                                         | 6.3                                         | 2.17                                       | 17.9                                                 | <sup>a</sup>                   |
| 3     | 15.56                                         | 7.4                                         | 2.11                                       | 13.0                                                 | .84                            |
| 4     | 26.19                                         | 12.6                                        | 2.08                                       | 21.8                                                 | .83                            |
| 5     | 32.42                                         | 14.8                                        | 2.09                                       | 24.2                                                 | .75                            |
| 6     | 36.97                                         | 17.3                                        | 2.14                                       | 27.2                                                 | .75                            |

<sup>a</sup> Calculated  $(H_2O_2)_{max} = 16.6$ . For this run equation (B) was integrated with a different boundary condition, since  $(H_2O_2)$  was not zero at the start.

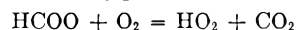
of the dose required to produce maximum peroxide concentration are shown together with the ratio to this dose of the initial oxygen concentration. If the rate of oxygen uptake is constant at  $G_{OH}/2 + G_{OH}/2$ , the dose to consume all oxygen should be 2.5 times the initial oxygen concentration. The required dose to maximum peroxide actually exceeds this value by about 15%, instead of being considerably smaller as might be expected from the competition for H between  $H_2O_2$  and  $O_2$ . Figure 2 replots the points from experiment 2 of Fig. 1. The two lower curves are calculated from equation A, assuming the rate constant ratio  $k_4/k_3$  to have the value 1.0 or 2.0, respectively.

#### Discussion

The present data show that solutions containing hydrogen, oxygen and hydrogen peroxide behave quite similarly to those containing formic acid, oxygen and hydrogen peroxide. The indication seems clear that as long as any oxygen is present, hydrogen peroxide will not react with hydrogen to form water under  $\gamma$ -radiation. As soon as oxygen is all used up a rapid chain reaction sets in between the hydrogen and the peroxide. This reaction is stopped by very small quantities of oxygen. In the case of formic acid this behavior was explained<sup>10</sup> by supposing that the chain reaction between peroxide and formic acid was carried by the reactions



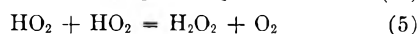
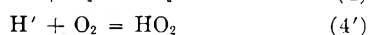
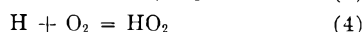
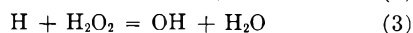
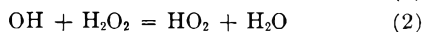
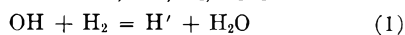
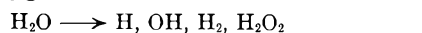
This chain is stopped by small quantities of oxygen because the chain carrier HCOO reacts very much more rapidly with oxygen than with peroxide



to form the relatively unreactive  $HO_2$  radical which cannot carry on the chain. In the case of hydrogen the corresponding chain reaction, as we have already seen, consists of reactions 1 and 3. Here also the data suggest that the chain carrier H must react much more rapidly with  $O_2$  than with  $H_2O_2$  in order to explain the inhibition of this reaction by small quantities of  $O_2$ . Yet we have seen that in the irradiation of water containing only  $H_2O_2$  and  $O_2$  these two substances compete on approximately equal terms for reaction with the

reducing free radical H formed from the water by radiation.

In order to explain this discrepancy we have reluctantly been forced to conclude that the "H atom" produced by the oxidation of H<sub>2</sub> in reaction 1 behaves differently from the "H atom" formed from water by radiolysis. In writing reaction schemes we consequently generally denote the product of reaction 1 by H', and in systems where oxygen is present we can obtain the observed kinetics by assuming that H' reacts exclusively with oxygen in preference to peroxide. The reaction scheme for the formation of peroxide in the presence of hydrogen and oxygen then becomes



By equating rates of formation and consumption of each of the intermediates H, H', OH and HO<sub>2</sub> in the usual manner, we find for the rate of H<sub>2</sub>O<sub>2</sub> formation

$$\frac{d(\text{H}_2\text{O}_2)}{d(\text{Dose})} = G_{\text{H}_2\text{O}_2} + \frac{G_{\text{H}}}{2} + \frac{G_{\text{OH}}}{2} - \frac{G_{\text{OH}}}{1 + \frac{k_1(\text{H}_2)}{k_2(\text{H}_2\text{O}_2)}} - \frac{G_{\text{H}}}{1 + \frac{k_4(\text{H}_2)}{k_3(\text{H}_2\text{O}_2)}} \left[ 1 + \frac{1}{1 + \frac{k_1(\text{H}_2)}{k_2(\text{H}_2\text{O}_2)}} \right]$$

If (H<sub>2</sub>O<sub>2</sub>) is small compared to (H<sub>2</sub>), so that (2) can be neglected, the equation reduces to

$$\frac{d(\text{H}_2\text{O}_2)}{d(\text{Dose})} = G_{\text{H}_2\text{O}_2} + \frac{1}{2} (G_{\text{OH}} + G_{\text{H}}) - \frac{G_{\text{H}}}{1 + \frac{k_4(\text{O}_2)}{k_3(\text{H}_2\text{O}_2)}} \quad (\text{B})$$

where again (O<sub>2</sub>) may be assumed equal to (O<sub>2</sub>)<sub>0</sub> - 1/2(G<sub>OH</sub> + G<sub>H</sub>)(Dose).

The course of the curves in Fig. 1 should be calculable by integration of equation B, with the assumption that maximum peroxide occurs when all the oxygen is gone. Integration is accomplished by taking as variables (O<sub>2</sub>) and  $y = (\text{H}_2\text{O}_2)/(\text{O}_2)$ . Putting in the numbers for the various G's and 1.85 for k<sub>4</sub>/k<sub>3</sub>, we find, for the boundary condition  $y = 0$  when (O<sub>2</sub>) = (O<sub>2</sub>)<sub>0</sub>

$$-\ln \frac{(\text{O}_2)}{(\text{O}_2)_0} = \frac{1}{2} \ln \left( \frac{y^2 + 2.03y + 2.368}{2.368} \right) + 0.7219 \left( \tan^{-1} \frac{2y + 2.03}{2.313} - \tan^{-1} \frac{2.03}{2.313} \right)$$

To evaluate the expected maximum peroxide corresponding to (O<sub>2</sub>) = 0 and  $y = \infty$ , we may conveniently multiply the equation by 2, combine the logarithmic terms, replace  $y$  under the logarithm by (H<sub>2</sub>O<sub>2</sub>)/(O<sub>2</sub>), and find

$$-\ln \frac{(\text{O}_2)^2}{2.368(\text{O}_2)_0^2} \left[ \frac{(\text{H}_2\text{O}_2)^2}{(\text{O}_2)^2} + \frac{2.03(\text{H}_2\text{O}_2)}{(\text{O}_2)} + 2.368 \right] = 1.4438 \left( \tan^{-1} \frac{2y + 2.03}{2.313} - \tan^{-1} \frac{2.03}{2.313} \right)$$

When (O<sub>2</sub>) = 0, only the first term under the logarithm remains; when  $y = \infty$ , the first  $\tan^{-1}$  becomes  $\pi/2$ . Then

$$-\ln \frac{(\text{H}_2\text{O}_2)_{\text{max}}^2}{2.368(\text{O}_2)_0^2} = 1.4438 \left[ \frac{\pi}{2} - \tan^{-1} 0.8776 \right]$$

Thus the maximum (H<sub>2</sub>O<sub>2</sub>) is proportional to the initial O<sub>2</sub> concentration, and evaluation of the constant from the above equation gives (H<sub>2</sub>O<sub>2</sub>)<sub>max</sub>/(O<sub>2</sub>)<sub>0</sub> = 0.833. Table I includes experimental values of this ratio obtained from the curves drawn in Fig. 1. Agreement is remarkably good. Figure 2 shows the curve calculated by integration of (B) for (O<sub>2</sub>)<sub>0</sub> = 15.07 × 10<sup>-3</sup> molec./l. along with the corresponding experimental points (from expt. 2).

The main discrepancy of all the runs from the theory lies in the size of the dose required to consume all oxygen, which is stated above is 15% greater than expected. Some but not all the discrepancy may be ascribed to a slight contribution of reaction 2, which has been neglected in the above treatment.

Obviously at least one of the two entities, H and H', must be something other than a simple hydrogen atom. In water, radicals are quite likely to exist in acidic or basic forms corresponding to loss or gain of a proton. Possibilities here are the solvated electron, which may be regarded as the basic form of H, and the much-discussed acidic form H<sub>2</sub><sup>+</sup>. In neutral water the radical lifetime may be too short to allow equilibrium to be established between acidic and basic forms, so that these species react independently. The entity formed in water radiolysis could be a solvated electron, which might eventually react with water to form H, but only after a time long compared to its ordinary lifetime in solutions containing appreciable oxygen or peroxide concentrations. If this were the case it must be supposed that solvated electrons formed close together can react readily with one another to form molecular hydrogen.

Another possibility is that the radical formed in water radiolysis is really a hydrogen atom, while the reaction of OH with H<sub>2</sub> in aqueous environment leads not to disruption of the H-H bond but merely to an electron transfer, giving H<sub>2</sub><sup>+</sup> as the product. A suggestion has been offered<sup>11</sup> that H<sub>2</sub><sup>+</sup> may be a fairly weak acid. It would then be expected to live long enough on the average in neutral solutions to be able to react as such with active solutes like oxygen.

**Acknowledgment.**—Throughout this work we have greatly profited by discussions with Dr. Harold A. Schwarz.

(11) W. G. Rothschild and A. O. Allen, *Radiation Research*, **8**, 101 (1958).

# APPLICATION OF OPTICAL ROTATION MEASUREMENTS IN STUDYING THE STRUCTURAL DEGRADATION OF $\gamma$ -IRRADIATED OVALBUMIN<sup>1</sup>

BY HUGO FRICKE, WENDELL LANDMANN, CHARLES LEONE AND JAMES VINCENT

*Contribution from the Chemistry Division and Biological and Medical Research Division, Argonne National Laboratory, Lemont, Illinois*

*Received February 16, 1959*

Earlier work led to the conclusion that ovalbumin treated with high energy radiations contains a broad range of protein molecules in various stages of structural breakdown. This view has now been supported by optical rotation studies on solutions of ovalbumin after treating in the lyophilized state, under vacuum, with  $\gamma$ -rays. The specific levorotation  $-\alpha_{5461}^{25}$  of the isoelectrically coagulable fraction and of three thermolabile fractions of increasing stability obtained from ovalbumin treated with 58.5 electronic volts per protein molecule, were found to be 60.2, 47.7, 42.1 and 39.5°, respectively, as compared to 85.0° for ovalbumin denatured by heating at pH 7.2 and 36.9° for the native protein. These values for the specific levorotations of the various fractions are discussed with reference to the serological activities of these same fractions, as measured by their reaction with antinative rabbit serum.

Thermal stability and serological studies<sup>2-5</sup> led to the conclusion that ovalbumin treated with high energy radiations contains a spectrum of protein molecules in which the secondary, H-bonded structure is in various stages of unfolding. The most strongly degraded molecules exhibit a characteristic coagulation reaction at the isoelectric point of the native protein. Other molecules in more moderately injured configurations, were discovered because upon heating they are changed more easily than native molecules to the coagulable state. In solutions of  $\gamma$ -irradiated ovalbumin, the whole or nearly the whole loss of serological activity, as measured by the reaction of the antigen with antinative rabbit serum, was found to be associated with the coagulable and thermolabile constituents. The coagulable fraction suffered a large but not a complete loss of activity, suggesting that it is in a less strongly degraded state than protein degraded by heating. The activities of the thermolabile constituents lay intermediately between those of the coagulable and native protein and increased with increasing stability of the fractions.

Measurement of the optical rotation of proteins in solution is a sensitive method for studying the disruption of their secondary structure. This paper describes the use of the method in elucidating the structural state of the protein molecules in solutions obtained from lyophilized ovalbumin that was exposed, under vacuum, to  $\gamma$ -rays. As in earlier works, a number of fractions of decreasing structural breakdown were precipitated progressively by application of pH and heat. By measuring the optical rotation of the series of supernatants obtained in this process, we calculate the specific rotations of the precipitated fractions in the state in which they were present in the original solution.

## Materials and Methods

The general procedures used were the same as those employed in our earlier works. In the following, they will be described in a somewhat more detailed manner than was done before.

(1) Based on work performed under the auspices of the U. S. Atomic Energy Commission.

(2) H. Fricke, *Nature*, **169**, 965 (1952).

(3) H. Fricke, *This Journal*, **56**, 789 (1952).

(4) H. Fricke, C. A. Leone and W. Landmann, *Nature*, **180**, 1423 (1957).

(5) C. A. Leone, W. Landmann and H. Fricke, "Proceedings of the Second International Conference on the Peaceful Uses of Atomic Energy," Geneva, 1958.

The ovalbumin was recrystallized three times with Na<sub>2</sub>SO<sub>4</sub>.<sup>6</sup> Nearly all the salt was dialyzed off following the last crystallization and 90 to 92% of the water, as determined by heating the protein to constant weight at 110°, was removed by lyophilization.

The lyophilized protein was placed under vacuum in glass ampules and irradiated at 0° in a homogeneous,  $\gamma$ -ray field at  $1.5 \times 10^6$  rad./hr. Radiation dosage was determined with the ferrous sulfate dosimeter ( $G[\text{Fe}^{+++}] = 15.5$ ) and expressed in terms of electron volts absorbed per protein molecule (e.v./mol.). In this calculation, we used 45000 as the molecular weight of ovalbumin and 7% H, 50% C, 15.5% N, 26% O, 0.1% P, 1.6% S as its elementary composition. Photoelectric and recoilelectric absorption values were obtained from Lea.<sup>7</sup>

Irradiated ovalbumin is stable if it is kept in the lyophilized form and under vacuum at 0°. When placed in solution its relative instability toward temperature and pH (Fig. 1) must be kept in mind during solvation and in storing and testing it. To avoid or reduce secondary degradation, all initial processing was carried out near 0°, and as close to neutral pH as possible.

Owing in part to crosslinkage, and in part to structural unfolding, irradiated protein is more difficult to dissolve than native. It dissolves at an impractically slow rate at neutral pH. Dissolution is hastened at both acid and basic pH values and since the coagulable constituents are insoluble in the acid region pH 3.5 to 6, dissolving the protein was carried out at basic pH. In the dosage range used, up to 120 e.v./mol., the irradiated protein went rapidly into solution at pH 9. The irradiated powder was added a few milligrams at a time to water adjusted to pH 9 with NaOH. The solutions were prevented from dropping below pH 7 by the periodic addition of small volumes of 0.1 N NaOH. The dissolution process required about 90 min. Tests showed that dissolved protein treated with 58.5 e.v./mol. could be kept for two hours at pH 9 without noticeable increase in structural degradation.

After being dissolved, the irradiated protein was brought to pH 7.2 and traces of insoluble material removed by centrifugation. At this pH and 0°, the solutions of irradiated protein were stable for several hours, during which period the optical rotation was measured.

Ovalbumin is fragmented under the influence of ionizing radiations, but this effect was small enough in our work, to not cause a significant rise in non-protein nitrogen as determined by the micro-Kjeldahl procedure. Therefore, total nitrogen determinations on the whole irradiated systems or on fractions derived from them were converted to protein by using the conversion factor, 6.45, of the native ovalbumin.

**Fractionation.**—(a) The coagulable fraction of a solution of irradiated protein was obtained by lowering the pH with 0.1 N HCl to 4.85, which is the isoelectric point of native ovalbumin. The coagulation process went to completion within 10 to 20 minutes. The supernatant, after centrifugation, remained clear for a few hours, showing that the coagulable and thermolabile fractions could be cleanly separated from each other. Further tests revealed

(6) R. A. Kekwick and R. K. Cannan, *Biochem. J.*, **30**, 227 (1936).

(7) D. E. Lea, "Actions of Radiations on Living Cells," Cambridge University Press, 1947, p. 347.

TABLE I  
OPTICAL ROTATION MEASUREMENTS ON FRACTIONATED SOLUTIONS OF  $\gamma$ -IRRADIATED OVALBUMIN

| Dosage,<br>e.v./mol. | Relative concn. |                |                | Obsd. $[\alpha]_{5461}^D$ |                |                |                |                       | Caled. $[\alpha]_{5461}^D$ |                |                |
|----------------------|-----------------|----------------|----------------|---------------------------|----------------|----------------|----------------|-----------------------|----------------------------|----------------|----------------|
|                      | D               | L <sub>1</sub> | L <sub>2</sub> | I                         | S <sub>1</sub> | S <sub>2</sub> | S <sub>3</sub> | D<br>redis-<br>solved | D                          | L <sub>1</sub> | L <sub>2</sub> |
| 0                    |                 |                |                | 36.9                      |                |                |                |                       |                            |                |                |
| 15.0                 | 0.062           | 0.21           |                | 40.3                      | 39.0           | 37.0           |                | 60.9                  | 61.2                       | 46.2           |                |
| 30.3                 | .123            | .24            |                | 42.1                      | 40.0           | 36.7           |                | 59.0                  | 57.0                       | 49.2           |                |
| 58.5                 | .25             | .28            | 0.21           | 47.1                      | 43.4           | 40.8           | 39.5           | 61.4                  | 58.3                       | 47.7           | 42.1           |
| 90                   | .355            |                |                | 51.7                      | 47.2           |                |                | 62.9                  | 61.3                       |                |                |
| 120                  | .51             |                |                | 57.1                      | 50.9           |                |                | 63.1                  | 63.1                       |                |                |

that no additional coagulate was formed when pH of the supernatant was varied with HCl and NaOH over a broad range, pH 3 to 6, proving that pH 4.85 was close enough to the isoelectric point of all coagulable constituents to secure their complete precipitation.

(b) After the coagulable fraction had been removed, two fractions of thermolabile constituents were precipitated successively by exposing the supernatant to 49.25° for 6 hr. and 62.05° for 4 hr. at pH 7.2. After the first heat treatment the supernatant was adjusted to pH 4.85 with HCl. The precipitate that formed was removed and pH of the new supernatant solution readjusted to pH 7.2, with NaOH and then the process was repeated at the higher temperature. The native protein is practically stable at 49.25°, pH 7.2, so the fraction of irradiated protein removed at this temperature contained no appreciable admixture of native protein.

**Terminology.**—Solutions of native and irradiated protein are called N and I, respectively. The coagulable fraction of I is called D and the labile fractions separated successively by the use of any particular process are called L<sub>1</sub>, L<sub>2</sub>, L<sub>3</sub>, etc. The series of supernatants obtained in the progressive removal of these fractions, are called S<sub>1</sub>, S<sub>2</sub>, S<sub>3</sub>, S<sub>4</sub>, etc. The concentrations of D, L<sub>1</sub>, L<sub>2</sub>, L<sub>3</sub>, etc., calculated as fractions of the protein concentrations of I, are called [D], [L<sub>1</sub>], [L<sub>2</sub>], [L<sub>3</sub>], etc.

**Optical Rotation.**—Measurements were made with a Rudolph precision polarimeter, graduated to 0.01 degree, using the mercury line 5461 Å. and 1 and 2 dm. tubes. The measurements were made in a cold room near 0°.

### Experimental Results

The data on the optical rotation of solutions of irradiated ovalbumin are presented in Table I. For the native protein the specific levorotation,  $[\alpha]_{5461}^D$ , obtained was 36.9°, which agrees satisfactorily with the results of earlier workers.<sup>8,9</sup> The  $\gamma$ -irradiated protein has an increased specific levorotation, which varies linearly with radiation dosage. A linear relationship is found also for the variation of [D] with radiation dosage.

The table shows that the increased levorotation of I is, in part but only in part, associated with the coagulable constituents, the levorotation of S<sub>1</sub> being lower than that of I, but higher than that of N. Some of the isoelectrically soluble constituents of I must possess a relatively high levorotation.

Since tests showed that the specific rotation of I did not depend on the protein concentration used in its measurement, we may assume that the rotation of I is the sum of the rotations of its various fractions. Furthermore, the operations used in removing D would not be expected to affect the rotation of the soluble constituents of I. As a result of the manipulation of pH of I to 4.85 and the subsequent readjustment of S<sub>1</sub> to pH 7.2, the latter solution contains somewhat more NaCl than I, but tests revealed that such small

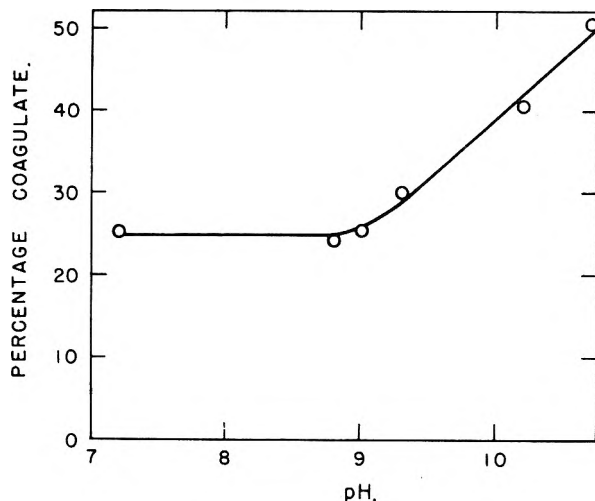


Fig. 1.—Structural degradation of  $\gamma$ -irradiated ovalbumin exposed for 3.5 hours to NaOH at different pH values; radiation dosage 58.5 e.v./mol. The native protein is stable in this pH range. The coagulate was collected at pH 4.85; temp. 0°.

concentrations of salt did not affect the optical rotation. Hence, we may calculate the specific levorotation for D, in the structural state in which it exists in I, from eq. 1.

$$[D][\alpha_D] + (1 - [D])[\alpha_{S_1}] = [\alpha_I] \quad (1)$$

where  $[\alpha_I]$ ,  $[\alpha_{S_1}]$  and  $[\alpha_D]$  are the specific levorotations of I, S<sub>1</sub> and D, respectively. The values of  $[\alpha_D]$  thus calculated are shown in Table I. They lie in the range of 57.0 to 63.1° and have a mean value of 60.2°. They show no apparent dependence on radiation dosage.

In order to measure the optical rotation of D directly, the coagulate obtained on shifting pH of I to 4.85 was centrifuged off, carefully washed with pH 4.85 HCl and then redissolved in pH 9.0 NaOH. The values of  $[\alpha_D]$  obtained from the solutions of these dissolved coagulates are given in Table I. They agree well with the calculated values, indicating first that the assumptions used in deriving eq. 1 are valid and, second, that D can be precipitated and redissolved without altering its molecular structure.

In order to establish the role played by the thermolabile constituents in the increased levorotation of S<sub>1</sub> over native ovalbumin, the thermal fractionation procedure was applied to the samples that had absorbed 15.0, 30.3 and 58.5 e.v./mol. The second heat-treatment was applied only to protein treated with 58.5 e.v./mol. The optical rotations that were determined for the several

(8) H. F. Holden and M. Freeman, *Australian J. Exp. Biol. Med.*, **7**, 13 (1930).

(9) H. A. Barker, *J. Biol. Chem.*, **103**, 1 (1933).

supernatants are given in Table I. The results show that the increased levorotation of the several  $S_1$ 's over native ovalbumin is associated wholly or mainly with the thermolabile constituents, their removal causing the optical rotation to approach that of the native protein. In the samples that adsorbed the two lower dosages of radiation, the specific levorotations of the  $S_2$  solutions were not significantly different from that of native ovalbumin showing that the increased levorotation of the  $S_1$  solutions was essentially derived from the  $L_1$ 's. In the sample that absorbed 58.5 e.v./mol. the removal of even the  $L_2$  fraction did not completely restore the levorotation of the  $S_3$  to that of native ovalbumin. At this relatively high dose of radiation there may be no appreciable amount of structurally uninjured protein left in I.

In order to draw quantitative conclusions from these experiments we must assume that the heatings did not affect the isoelectrically soluble constituents remaining in the supernatants of the heated systems. Strict proof cannot be given, but supporting evidence is provided by the fact that for the smaller dosages, removal of the thermolabile constituents brought the optical rotation of  $S_1$  back to that of N. Further support is given by the fact that the thermal conversion of native ovalbumin to the coagulable form is a first-order reaction.<sup>3,10-15</sup> This indicates that at least for the native protein the degradation of the molecular structure by heat is an all-or-none reaction, which is not accompanied by structural changes in the soluble molecules.

Direct evidence that heating native ovalbumin leaves the isoelectrically soluble protein molecules unaltered was obtained earlier from serological studies.<sup>5</sup> We have now further verified this conclusion by means of optical rotation measurements. Solutions of native ovalbumin at pH 7.2 were heated at several selected temperatures between 62.0 and 71.0° so as to convert various proportions of the protein into the coagulable form. The altered protein was coagulated by adjusting the systems to pH 4.85. The specific optical rotations of the cleared supernatants were measured. No significant changes from the value for the original native protein were obtained.

Although the question whether the thermal degradation of irradiated ovalbumin is an all-or-none reaction remains undecided, we shall tentatively assume that this is the case. We may then calculate the specific levorotation  $[\alpha_{L_1}]$  of the thermolabile fraction  $L_1$  from an analog of eq. 1

$$[L_1][\alpha_{L_1}] + (1 - [D] - [L_1])[\alpha_{S_1}] = (1 - [D])[\alpha_{S_1}] \quad (2)$$

A similar equation was used for calculating the specific levorotation  $[\alpha_{L_2}]$  of  $L_2$ . The values of  $[\alpha_{L_1}]$  in Table I show no dependence upon radiation dosage. The mean value is  $-47.7^\circ$ . The value for the one calculated  $[\alpha_{L_2}]$  is  $-42.1^\circ$ .

(10) H. Chick and C. J. Martin, *J. Physiol. (London)*, **40**, 404 (1910).

(11) H. Chick and C. J. Martin, *ibid.*, **43**, 1 (1911).

(12) H. Chick and C. J. Martin, *ibid.*, **45**, 61 (1912).

(13) H. Chick and C. J. Martin, *Kolloidchem. Beih.*, **5**, 49 (1914).

(14) P. S. Lewis, *J. Biochem. J.*, **20**, 965 (1926).

(15) H. K. Cubin, *ibid.*, **29**, 25 (1929).

## Discussion

We showed earlier<sup>4,5</sup> that the loss of serological activity of solutions of  $\gamma$ -irradiated ovalbumin, as measured by the reaction of the antigen with anti-native rabbit serum, was associated wholly or nearly wholly with the coagulable and thermolabile fractions. The coagulable fraction suffered a marked but not a complete loss of activity, the residual activity being about 16% of that of the native protein. The losses suffered by the thermolabile fractions were smaller and decreased with increasing stability of the fractions. It was suggested that not only the coagulable fraction but also the thermolabile fractions are in states of partial structural unfolding, the extent of which in any particular fraction increased with decreasing stability of that fraction. The fact that the coagulable fraction retained an appreciable amount of activity, indicated that it had not undergone complete unfolding.

Disruption of the H-bonded secondary structure of proteins with the resultant unfolding of the polypeptide chain has been found invariably to lead to a large increase in levorotation of solutions containing them.<sup>8,9,16,17,17a</sup> The effect has been discussed theoretically by Fitts and Kirkwood.<sup>18,19</sup> The increase in levorotation depends on the denaturing agent used. Holden and Freeman<sup>8</sup> measured the levorotation of ovalbumin subjected to a variety of treatments resulting in coagulation at the isoelectric point and found values in the range of 58 to 100° (at 5461 Å.). These different values might at least in part reflect differences in the extent of unfolding obtained in the different cases.

The increased levorotation values found for the various fractions studied in irradiated ovalbumin supports the conclusions as to structural unfolding drawn from the serological evidence. The levorotation of the coagulable fraction lies in the lower range of values found in Holden and Freeman's study, suggesting that the molecules of this fraction are not in a completely unfolded state. The

TABLE II

COMPARISON OF OPTICAL ROTATION AND SEROLOGICAL ACTIVITY OF DIFFERENT FRACTIONS OF A SOLUTION OF  $\gamma$ -IRRADIATED OVALBUMIN. RADIATION DOSAGE 58.5 e.v./MOL.

| Fraction | Relative concn. <sup>a</sup> | - $[\alpha]_{5461}$ | Serological activity | Relative degree of unfolding in terms of |                      |
|----------|------------------------------|---------------------|----------------------|------------------------------------------|----------------------|
|          |                              |                     |                      | Optical rotation                         | Serological activity |
| D        | 0.25                         | 58.3                | 0.17                 | 1                                        | 1                    |
| $L_1$    | .28                          | 47.7                | .51                  | 0.50                                     | 0.59                 |
| $L_2$    | .21                          | 42.1                | .77                  | 0.24                                     | 0.28                 |
| $S_3$    | .25                          | 39.5                | .89                  | 0.12                                     | 0.13                 |
| N        |                              | 36.9                | 1                    | 0                                        | 0                    |

<sup>a</sup> With reference to concentration of protein in I.

(16) P. Doty and E. P. Geidushek in: H. Neurath and K. Bailey, "The Proteins," Academic Press, New York, N. Y., 1953, Vol. **1A**, p. 393.

(17) C. Cohen, *Nature*, **175**, 129 (1955).

(17a) J. A. Schellman, *Compt. Rend. Trav. Lab. Carlsberg, Sér. chim.* **30**, 363 (1956-58).

(18) D. D. Fitts and J. G. Kirkwood, *J. Am. Chem. Soc.*, **78**, 2650 (1956).

(19) D. D. Fitts and J. G. Kirkwood, *Proc. Natl. Ac. Sci. (U.S.)*, **42**, 33 (1956).

levorotations of the different thermolabile fractions lie intermediately between the values for the coagulable fraction and the native protein and decrease with increasing stability of the fraction.

In order to show the correlation with the serological activities, we present in Table II, for the radiation dosage 58.5 e.v./mol., the specific levorotations of the different fractions, taken from Table I, and the relative serological activities measured on the same preparations.<sup>5</sup> To compare these two sets of data, we calculate the quantity

$$([\alpha_F] - [\alpha_N])/([\alpha_D] - [\alpha_N])$$

and the quantity obtained when the  $[\alpha]$ 's are replaced by the corresponding values for the serological activities. (F denotes any particular fraction.) These two quantities may be described as representing the relative degrees of unfolding of the fraction F, in terms of levorotation and serological activity, respectively. The correlation between the two sets of values is seen to be quite good. Although the meaning of this comparison is not wholly clear, it is felt that it gives further support to the view that the relation of the serological activity to the extent of unfolding in the various fractions is a causal one.

## THE EFFECT OF $\alpha$ -RADIATION ON AQUEOUS GLYCINE

BY CHARLES R. MAXWELL AND DOROTHY C. PETERSON

Department of Health, Education and Welfare, Public Health Service, National Institutes of Health, National Cancer Institute, Radiation Branch, Bethesda, Md.

Received February 16, 1959

Oxygen-saturated and oxygen-free 1 M solutions of glycine have been irradiated with  $\alpha$ -particles from an exterior Po<sup>210</sup> source. Yields of HCHO, NH<sub>3</sub>, HCOCOOH and H<sub>2</sub>O<sub>2</sub> are reported as a function of dose. The relative yields of these compounds are quite different from those previously reported for X-rays. The specific yields of these products are greater, particularly in the oxygen-saturated solutions, than would be predicted by an indirect free radical mechanism in the bulk of the solution.

### Introduction

No concerted effort has been made to determine the effect of the rate of linear energy transfer (LET) upon the radiolysis of aqueous glycine. The effect of X-rays has been studied by Dale, Davies and Gilbert,<sup>1</sup> Stein and Weiss,<sup>2</sup> Barron, Ambrose and Johnson,<sup>3</sup> and Maxwell, Peterson and Sharpless.<sup>4</sup> The effect of electrons upon the system has been reported by Maxwell, Peterson and White<sup>5</sup> who showed that the yields of the products were the same for 50 Kv. X-rays at a dose rate of  $1 \times 10^{20}$  e.v./l. min. as for 150 Kv. electrons at a dose rate of  $\approx 1.6 \times 10^{23}$  e.v./l. min. However, the LET for these two irradiations are essentially the same. Dale, Davies and Gilbert<sup>6</sup> have reported the yield of NH<sub>3</sub> from alkaline air-saturated solutions of glycine irradiated with the recoil particles from the B<sup>10</sup> ( $n\alpha$ ) Li<sup>7</sup> reaction. However only very large doses of the order of  $1.5 \times 10^{25}$  e.v./l. were used and only the yield of NH<sub>3</sub> was determined. Weeks<sup>7</sup> has studied the effect of 30 Mev. He ions upon aqueous glycine but his experiments were designed primarily for the detection and estimation of compounds produced in low yield. The reported yields at the very large doses necessarily used probably do not represent the initial yields of these products before the onset of secondary reactions.

The experiments described here on the radiolysis of aqueous glycine with  $\alpha$ -particles from Po<sup>210</sup> have been restricted to the measurements of the major products at small doses. Where possible the yields have been determined as a function of dose and the initial yields evaluated as the slopes of the plots of these data.

### Experimental

$\alpha$ -Particles were introduced into the glycine solution through a mica window submerged in the solution. The polonium source was a thin spot of metal approximately 1 cm. in diameter on the end of a  $9/16$ " tantalum rod housed in a tight fitting glass tube closed at one end with a mica window. This window was between 1.0 and 1.2 mg./cm.<sup>2</sup> thick and was sealed to the glass with black wax. The tantalum rod could be moved so that the polonium was in contact with the window during an irradiation. The source and housing were completely inside the sample handling and degassing system so that there was never more than a few millimeters pressure differential across the window.

The all-glass apparatus consisted of a degassing chamber and an irradiation chamber. These chambers were connected to each other and to a vacuum line in a manner which allowed individual evacuation and the transfer, by gravity, of solution from the degassing chamber to the irradiation chamber.

For gas-free vacuum runs the solution to be irradiated was degassed by boiling under the low pressure obtained with a mechanical pump. The solution was placed in the degassing chamber where it was stirred violently by a Teflon bar for 20 minutes during which time it was opened frequently for short periods to the vacuum line for the removal of evolved gases. The irradiation chamber was evacuated with the same vacuum line and then swept free of any last traces of gases with water vapor from the degassed solution. Sample was drained from the degassing chamber into the irradiation chamber until the mica window was submerged approximately 3 mm. The sample was stirred gently during the irradiation by another Teflon bar rotating at 120 r.p.m. After the irradiation the sample size was determined by weight. Sample size varied from 15 to 25 ml. depending upon the radiation chamber used.

For oxygen saturated runs, the entire system was evacuated and the solution partially degassed. Oxygen was admitted to atmospheric pressure. The solution was then

(1) W. M. Dale, J. V. Davies and C. W. Gilbert, *Biochem. J.*, **45**, 93 (1949).

(2) G. Stein and J. Weiss, *J. Chem. Soc.*, 3256 (1949).

(3) E. S. G. Barron, J. Ambrose and P. Johnson, *Radiation Research*, **2**, 145 (1955).

(4) C. R. Maxwell, D. C. Peterson and N. E. Sharpless, *ibid.*, **1**, 530 (1954).

(5) C. R. Maxwell, D. C. Peterson and W. C. White, *ibid.*, **2**, 431 (1955).

(6) W. M. Dale, J. V. Davies and C. W. Gilbert, *Biochem. J.*, **45**, 543 (1949).

(7) B. M. Weeks, University of California Radiation Laboratory Report UCRL-3071 (July 1955).



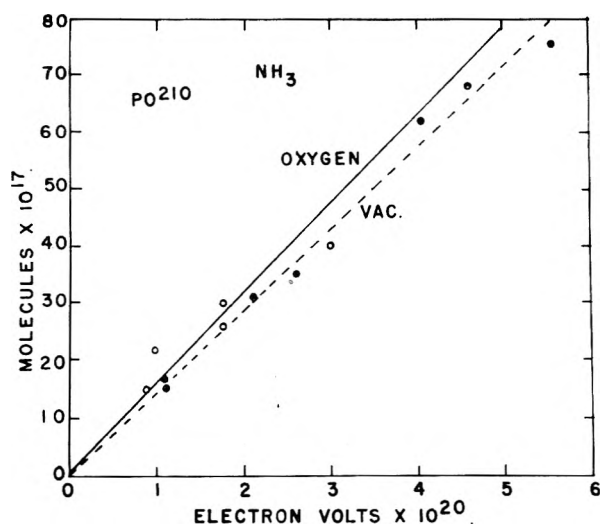


Fig. 1.—Yield of  $\text{NH}_3$  from 1  $M$  glycine when irradiated in oxygen and *in vacuo* with  $\alpha$ -particles.

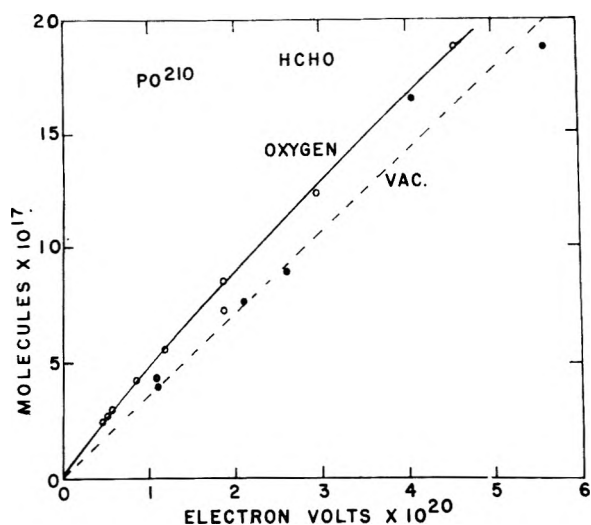


Fig. 2.—Yield of  $\text{HCHO}$  from 1  $M$  glycine when irradiated in oxygen and *in vacuo* with  $\alpha$ -particles.

stirred for 5 minutes in the degassing chamber to ensure liquid-gas equilibration and the irradiation carried out as above.

**Analytical.**—Triple distilled water and recrystallized glycine<sup>4</sup> were used in all solutions. Formaldehyde, glyoxalic acid, hydrogen peroxide and methylamine were determined by methods previously described.<sup>4</sup> Ammonia was determined by diffusion in a Conway disk followed by Nesslerization. Acetic acid was steam distilled<sup>4</sup> from  $\text{MgSO}_4$  and  $\text{H}_3\text{PO}_4$ , neutralized with  $\text{NaOH}$ , concentrated on a steam-bath and assayed enzymatically with acetokinase. The preparation and properties of the enzyme and the test are described by Rose, Grunberg-Manago, Korey and Ochoa.<sup>8</sup> This enzyme in the presence of adenosine triphosphate and hydroxylamine converts the acetate to acethydroxamic acid which may be determined according to Lipmann and Tuttle with  $\text{FeCl}_3$ .<sup>9</sup> We found it necessary with our enzyme preparation to incubate the enzyme and acetic acid longer than the hour suggested by Rose, *et al.*, and usually incubated overnight at room temperature. The steam distillation was necessary to concentrate the acetic acid to an assayable concentration and to separate it from  $\text{HCOCOOH}$  which interferes with the hydroxamic acid test.

Catalase was added to all irradiated solutions immediately after the removal of an aliquot for the  $\text{H}_2\text{O}_2$  determina-

tion in order to prevent any subsequent reactions due to  $\text{H}_2\text{O}_2$ .

**Dosimetry.**—The energy delivered to the irradiated solution was evaluated both by a calculation based upon the activity of the source and the energy loss in the mica window and by a measurement of the ferrous oxidation in a ferrous sulfate dosimeter.

Although  $\text{Po}^{210}$  emits a 5.3 Mev.  $\alpha$ -particle, the  $\alpha$ -particles entering the solution have a spectrum of energies from zero to approximately 4.5 Mev. as a result of energy loss in the mica window. The exit energy of  $\alpha$ -particles traversing the mica window at various incident angles and the number of particles traversing the window within  $2.5^\circ$  of these angles were calculated with the assumptions that the polonium was a point source in contact with a flat sheet of mica, that there was no scattering and no self-absorption and that the data of Holloway and Livingston<sup>10</sup> for the range of alpha particles in air are valid for mica when corrected for density differences.

These calculations showed that with a 1.1 mg./cm.<sup>2</sup> window 76% of the  $\alpha$ -particles emitted in the forward direction entered the solution and that they had a maximum energy of 4.45 Mev., an average energy of 3.47 Mev. and a median energy of 3.95 Mev. The dose rate during an irradiation was then calculated by a numerical integration over this spectrum using the assay of the source supplied by the manufacturer and the known half-life of  $\text{Po}^{210}$ .

Four 40 minute irradiations of an oxygen saturated 0.4 mM  $\text{Fe}^{++}$ -0.4  $M$   $\text{H}_2\text{SO}_4$  dosimeter showed a ferrous oxidation rate of  $6.31 \pm 0.18 \times 10^{14}$  ions/min. The effective  $G(\text{Fe})$  for  $\alpha$ -particles with the above spectrum was calculated to be 4.5, with the formula  $G_0(\text{Fe}) = 3.6 + 10/(1 + 38/\text{Mev.})$  proposed by Schuler and Allen<sup>11</sup> for monoenergetic  $\alpha$ -particles. Thus the dose rate for our 600 mc. source at the beginning of the series of irradiations was  $1.40 \times 10^{18}$  e.v./min. according to the ferrous yield and  $1.76 \times 10^{18}$  e.v./min. according to the calculated spectrum and the manufacturer's assay. We have used the intermediate value of  $1.5 \times 10^{18}$  e.v./min. in evaluating our data.

Unfortunately the mica windows deteriorated under the  $\alpha$ -irradiation and the flexing necessarily associated with the degassing technique, and on three occasions broke during an irradiation with considerable loss of polonium from the source. After these breaks the remaining activity of the source relative to the activity of the original source was determined by comparing the  $\text{HCHO}$  and  $\text{NH}_3$  yields from at least two irradiations *in vacuo* with similar yields observed with the original source. After the first break the remaining activity was 525 mc. The second break reduced this to 160 mc. and after the third break the source was too weak to justify further experimentation.

We did not use the  $\text{Fe}^{++}$ - $\text{H}_2\text{SO}_4$  dosimeter for these calibrations for fear that a break of a window during a calibration would result in the complete loss of the source.

## Results and Discussion

The yields of  $\text{H}_2\text{O}_2$ ,  $\text{HCHO}$ ,  $\text{HCOCOOH}$  and  $\text{NH}_3$  as a function of dose in both evacuated and oxygen-saturated solutions are shown in Figs. 1 to 4. The *in vacuo* yields of  $\text{HCHO}$  and  $\text{NH}_3$  were measured using the original 600 mc. source. The *in vacuo* yields of  $\text{H}_2\text{O}_2$  and  $\text{HCOCOOH}$  were measured using both the 600 and 525 mc. source. All oxygen-saturated solutions were irradiated with the 160 mc. source.

In addition one *in vacuo* irradiation with the 525 mc. source for a dose of  $53.1 \times 10^{19}$  e.v. gave a yield of  $12.5 \times 10^{17}$  molecules of  $\text{CH}_3\text{NH}_2$ . Two *in vacuo* irradiations with the 160 mc. source for doses of 40 and  $41 \times 10^{19}$  e.v. gave yields of 6.7 and  $6.0 \times 10^{17}$  molecules of  $\text{CH}_3\text{COOH}$ . These are not necessarily the correct initial yields but the dose-yield data previously observed with X-rays<sup>4</sup> indicate that these products are not readily subject to sec-

(8) I. A. Rose, M. Grunberg-Manago, S. R. Korey and S. Ochoa, *J. Biol. Chem.*, **211**, 737 (1954).

(9) F. Lipmann and L. C. Tuttle, *ibid.*, **159**, 21 (1945).

(10) M. G. Holloway and M. S. Livingston, *Phys. Rev.*, **64**, 13 (1938).

(11) R. H. Schuler and A. O. Allen, *J. Am. Chem. Soc.*, **79**, 1565 (1957).

TABLE I  
YIELD OF PRODUCTS FROM THE RADIOLYSIS OF UNBUFFERED 1 M GLYCINE FOR VARIOUS TYPES OF RADIATION

| Product                                          | Molecules/100 e.v. |                   |                    |             |                    |  |
|--------------------------------------------------|--------------------|-------------------|--------------------|-------------|--------------------|--|
|                                                  | Evacuated          |                   | Oxygen-satd        |             |                    |  |
|                                                  | $\alpha$           | Hc <sup>++a</sup> | X-Ray <sup>b</sup> | $\alpha$    | X-Ray <sup>c</sup> |  |
| NH <sub>3</sub>                                  | 1.67               | 1.12              | 3.97               | 1.80        | 4.3                |  |
| CH <sub>3</sub> NH <sub>2</sub>                  | 0.24               | 0.11              | 0.19               |             | 0.16               |  |
| HCOCOOH                                          | 1.1 > 0.61         | 0.2               | 2.10               | 1.23 > 0.84 | 3.4                |  |
| HCHO                                             | 0.42               | 0.3               | 0.53               | 0.57        | 1.1                |  |
| CH <sub>3</sub> COOH                             | 0.16               | ..                | 1.20               |             |                    |  |
| HOOCCH <sub>2</sub> CH(NH <sub>2</sub> )COOH     | ..                 | .09               | 0.25 <sup>d</sup>  |             |                    |  |
| HOOCCH(NH <sub>2</sub> )CH(NH <sub>2</sub> )COOH | ..                 | ≈ .05             | 0.08 <sup>d</sup>  |             |                    |  |
| H <sub>2</sub> O <sub>2</sub>                    | >0.6               |                   | <0.01              | ≈0.8        | 3.6                |  |

<sup>a</sup> Reference 7 and 12. <sup>b</sup> Reference 4. <sup>c</sup> Reference 5. <sup>d</sup> For Co<sup>60</sup>  $\gamma$ -rays reference 12.

ondary reactions at these doses and it is believed that these may be taken as approximately correct. The loss of our source prevented us from obtaining as many data as we desired.

These data and the initial yields for NH<sub>3</sub>, HCHO, HCOCOOH and H<sub>2</sub>O<sub>2</sub> evaluated as the initial slopes of the curves in Figs. 1 → 4 are listed in the second and fifth columns in Table I. The upper limits set for the yields of HCOCOOH were taken as the difference between the NH<sub>3</sub> yields and the sum of the HCHO and CH<sub>3</sub>COOH yields.

Also listed in Table I are the yields reported by Weeks<sup>7</sup> and Weeks and Garrison<sup>12</sup> for irradiation made with 30 Mev. He ions. These yields were observed with doses of the order of  $3 \times 10^{23}$  e.v./l. and may not reflect the initial yields. The low values reported for the yields of HCOCOOH and H<sub>2</sub>O<sub>2</sub> are almost certainly the result of secondary reactions at this dose. For evidence notice the maxima approached in Figs. 3 and 4 where the maximum dose is of the order of  $3 \times 10^{22}$  e.v./l.

The data for X-ray yields are included for ready comparison. Such a comparison shows that the same products are formed in all cases but that their relative yields are quite different. Such differences are of course not surprising in view of the well established differences in the relative yields of the active intermediate species—H, OH and H<sub>2</sub>O<sub>2</sub>—from which most of these products presumably arise. It would seem appropriate at this time to examine these data in terms of the mechanisms recently proposed by Weeks and Garrison<sup>12</sup> in a paper on the radiolysis of aqueous glycine. However, the results of current experiments in this Laboratory with X-rays indicate that a detailed analysis may be premature and only a few general observations will be made.

The low yields of nearly all the products observed with  $\alpha$ -particles are consistent with a free radical mechanism since the number of free radicals produced by  $\alpha$ -particles is much less than those produced with X-rays. The essentially constant yield of CH<sub>3</sub>NH<sub>3</sub> is consistent with the proposed direct formation of this product. The very low yield of CH<sub>3</sub>COOH is consistent with the proposal that this product is formed by some fraction of the H atoms which escape into the bulk of the solution. The large yields of HCOCOOH and HCHO in the evacuated system are consistent with the proposal that the free radical production of these products is

(12) B. M. Weeks and W. M. Garrison, *Radiation Research*, 9, 291 (1958).

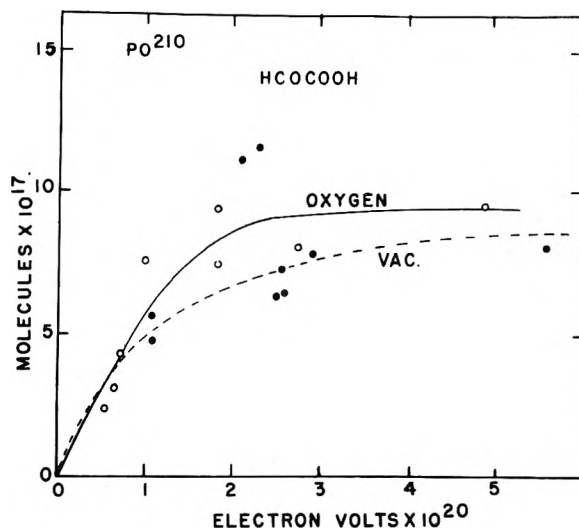


Fig. 3.—Yield of HCOCOOH from 1 M glycine when irradiated in oxygen and *in vacuo* with  $\alpha$ -particles.

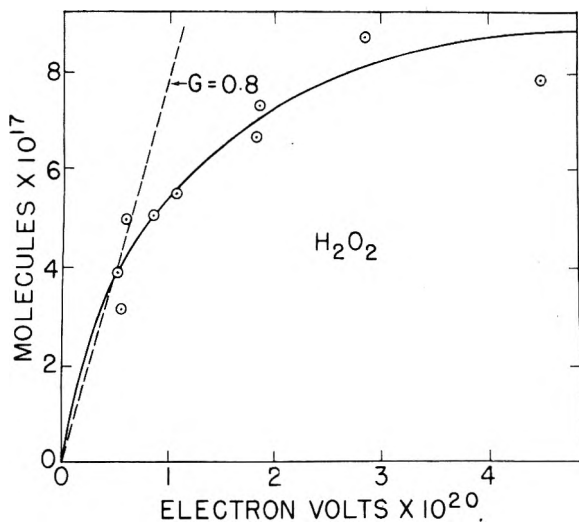


Fig. 4.—Yield of H<sub>2</sub>O<sub>2</sub> from 1 M glycine when irradiated in oxygen and *in vacuo* with  $\alpha$ -particles.

supplemented by a radical induced chain oxidation of glycine by H<sub>2</sub>O<sub>2</sub>. However, the large HCHO/HCOCOOH ratio is inconsistent with our observation (unpublished data) that little HCHO is formed by this latter reaction.

The large yields of all products in the oxygen-saturated solution is inconsistent with the proposal

that, in the presence of oxygen, glycine reacts only with the OH radicals. It is generally agreed<sup>13</sup> that  $G(\text{OH})$  for  $\alpha$ -particles is of the order of 0.1–0.3, which is much too low to account for the observed yields. This proposed reaction may well account for most of the effect produced by X-rays but it appears that other reactions are of considerable importance with  $\alpha$ -particle irradiation. These are probably re-

(13) A. O. Allen, *Radiation Research*, **1**, 85 (1954).

actions within the track itself. In fact we are rapidly coming to the conclusion in this Laboratory that the formation of HCHO even with X-rays may be almost entirely in the "spurs" or regions of high local concentration of radicals and excited molecules. A study of the initial yield of all the products as a function of glycine concentration and particularly studies in the presence of oxygen with He ions or  $\alpha$ -particles, should be most rewarding.

## THE MOLECULAR COMPOSITION OF SODIUM IODIDE VAPOR FROM MOLECULAR WEIGHT MEASUREMENTS

BY SHELDON DATZ AND WILLIAM T. SMITH, JR.

Contribution from the Chemistry Division, Oak Ridge National Laboratory,<sup>1</sup> Oak Ridge, Tenn., and the Department of Chemistry University of Tennessee, Knoxville, Tenn.

Received February 16, 1959

A technique has been developed for the determination of the molecular weight of vapors at high temperatures, by measurement of the pressure at constant vapor density, the pressure measuring device being a molten gold manometer. For the dissociation of  $\text{Na}_2\text{I}_2$  into  $\text{NaI}$  measurements from 1175 to 1350°K. indicate a  $\Delta E^\circ$  of 40.2 kcal. mole<sup>-1</sup> and a  $\Delta S^\circ$  of 27.0 e.u. at 1260°K.

### Introduction

Considerable effort has been put forth in recent years in the determination of molecular association in alkali halide vapors. Of the experimental methods employed, the most satisfactory has been that of effusive velocity distribution analysis devised by Miller and Kusch.<sup>2,3</sup> Mass spectroscopic investigations<sup>4–7</sup> have yielded much valuable information, but uncertainties in ionization cross sections and modes of dissociation on electron impact preclude quantitative measurements of the degree of association. Infrared absorption studies of alkali halide vapors have indicated the presence of dimer,<sup>8</sup> but quantitative measurements of amounts present are at best very difficult. Since even the most precise of the above methods is highly complex in both execution and interpretation, the present research was undertaken to provide a more simple and direct method of measurement, and to extend the measurements over a wide range of temperature and pressure.

In this work, the association equilibrium of sodium iodide vapor was studied by the measurement of molecular weight as a function of temperature. The molecular weight was determined by measurement of the absolute pressure exerted by a known weight of completely vaporized salt contained in an isothermal bulb of known volume. The choice of fused silica for use in fabrication of the

bulb was dictated by the requirements of high temperature dimensional stability, non-reactivity with halide vapors and the ability to be degassed and sealed off at high temperatures. The pressure measuring device must have its sensing element at a temperature higher than the condensation point of the gas, and must be accurate to  $\pm 0.1$  mm. Initially a vitreous silica Bourdon sickle gauge was used, but it was found that at 1000° the rapid diffusion of argon (used to balance the gauge pressure) through the thin membrane of the gauge caused large errors in pressure measurement. The gauge used in the measurements reported here was a balanced manometer in which the manometric fluid was molten gold. The two arms of the manometer could be observed through a window in the furnace and the external pressure of argon required to balance the bulb pressure was read from an external mercury manometer. The choice of molten gold for the manometric fluid was made on the basis of the temperature range over which it is a liquid, its lack of chemical reactivity and its low vapor pressure over the required temperature range.

### Experimental

**Apparatus.**—The bulb was fabricated from 80 mm. i.d. 82 mm. o.d. clear silica tubing with end plates cut from 3.2 mm. thick silica plates made slightly convex to resist high temperature distortion. The bulb is 16 cm. in length and has a volume of ca. 800 ml. The pressure transmitting tube, which connects the top of the bulb to the top of the manometer which is mounted vertically above it, is 8 mm. i.d. and 30 cm. in length. The manometer tube is 10 mm. i.d. and contains 130 g. of gold (7.6 cc. when molten) giving a height of 3 cm. in each arm. Additional mechanical support of the bulb is provided by two 4 mm. silica rods which bridge the manometer. Additional 6 mm. tubes are sealed to the top of the bulb for sample loading and pumping. The pressure balancing arm is connected to a Pyrex pressure manifold through a graded seal located away from the high temperature region.

Pressure in the manifold is adjusted by manipulation of two vacuum stopcocks, one connected to a vacuum system and the other to a bulb containing argon at a pressure slightly above the maximum anticipated pressure. Flow

(1) Operated for the United States Atomic Energy Commission by the Union Carbide Corporation.

(2) R. C. Miller and P. Kusch, *J. Chem. Phys.*, **25**, 860 (1956); **27**, 981 (1957), hereinafter referred to as MK.

(3) M. Eisenstadt, G. M. Rothberg and P. Kusch, *J. Chem. Phys.*, **29**, 797 (1958).

(4) L. Friedman, *ibid.*, **23**, 477 (1955).

(5) T. A. Milne, H. M. Klien and D. D. Cubicciotti, *ibid.*, **28**, 718 (1958).

(6) R. C. Schoonmaker and R. F. Porter, *ibid.*, **30**, 283 (1959); **29**, 1070 (1958).

(7) J. Berkowitz and W. A. Chupka, *ibid.*, **29**, 653 (1958).

(8) W. Klemperer, Chemistry Dept., Harvard Univ., private communication.

rates through the stopcocks are kept at a convenient level for manipulation by plugging the bore entirely with paraffin and then piercing a hole with a 0.004 in. tungsten wire.

**Furnaces.**—The heating system consists of three electric tube furnaces. The bulb furnace is a "Kanthal" wound "Marshall" tube furnace 16 in. long with a 3.5 in. i.d. Its temperature is controlled by a "Speedomax" controller with a 10 mv. span, using a chromel-alumel thermocouple as a sensing element. Gradients over the length of the bulb may be adjusted by shunting sections of the furnace winding. With this system, the temperature can be maintained constant to  $\pm 0.5^\circ$  for several hours and the gradients over the length of the bulb range from  $1^\circ$  at the lowest operating temperature to  $5^\circ$  at the highest. To facilitate loading, pumping and sealing, the furnace may be lowered 4.5 in. by a counterweight system.

The manometer is heated by a "Kanthal" wound "Marshall" furnace 16 in. long and having a 2.5 in. bore. The furnace is fitted with two 1 in. diameter windows set at  $180^\circ$  to each other and centered 8 in. from the end of the furnace. The temperature control of this furnace is accomplished with a "Micromax" controller using a chromel-alumel thermocouple. This furnace is mounted in a fixed position directly above the bulb furnace such that there is a  $1/2$  in. gap between furnaces.

In order to prevent condensation in the pressure transmitting tube, a third furnace was made of a MgO swaged "Kanthal" heater contained in a  $1/8$  in. Inconel sheath wrapped in the form of a helix and welded to a 2.5 in. i.d. Inconel tube 6 in. long. The tube is mounted firmly to the bottom of the manometer furnace such that three inches extend up into the upper furnace tube and 2.5 in. into the lower furnace.

The furnace ends are sealed with fire brick and fire brick dust and the gap is lagged with "Fiberfrax" packing.

**Gold Manometer.**—The purest gold commercially available contains considerable amounts of dissolved gas and small amounts of other impurities which tend to collect at the liquid surface. For this reason, it is further purified as follows. Gold wire is first de-greased and washed in hot  $\text{HNO}_3$ . It is then melted in a silica tube under vacuum and pumped for several hours. After cooling, the cast ingot is removed and cleaned again in boiling  $\text{HNO}_3$ .

Once the gold has been melted in the manometer, the manometer temperature should not be dropped below  $600^\circ$  since, if the temperature drops to ca.  $500^\circ$ , the silica will crack. This effect may be due to a slight wetting of the silica by the gold, although the markedly convex appearance of the gold meniscus suggests that the silica is not wet. The temperature at which fracture occurs might be associated with the sharp decrease in coefficient of expansion of quartz occurring at  $550^\circ$ , although no such transition is observed in vitreous silica.<sup>9</sup>

**Sample Purity.**—The samples were prepared from reagent grade NaI (99.95% pure) which was heated under vacuum to  $500^\circ$  and then melted and recrystallized under argon pressure.<sup>10</sup> Optically clear crystals were selected and a single piece cleaved from the center of a crystal constituted a sample. All handling was done in a nitrogen filled  $\text{P}_2\text{O}_5$  dry box.

**Procedure.**—Initially, the system is evacuated ( $p = 10^{-6}$  mm.) and degassed at  $1000^\circ$  for 24 hours with an external atmosphere of argon supplied through a silica feed tube. After cooling, the bulb furnace is lowered, argon is admitted to the bulb and the sample is introduced through the loading tube, which is then resealed. The bulb containing the sample then is evacuated and heated to  $200^\circ$  for several hours. The pumping tube is then sealed at a point 1 in. away from the bulb. The bulb furnace is raised into position and the gap between furnaces filled with "Fiberfrax." The bulb then is heated in an argon atmosphere. Pressure readings are made by measuring with a cathetometer the argon pressure necessary to balance the gold manometer. Temperature measurements are made with calibrated Pt-90% Pt 10% Rh thermocouples placed along the length of the bulb.

Since it has been observed that some gas appears to diffuse into the bulb, especially at high temperatures, the tempera-

ture of the bulb is dropped below the point where the salt vapor pressure is measurable and a determination of the residual gas pressure is made with the manometer.

To change samples the vacuum is broken and the pumping tube is reconnected to the pumping system. The old sample is then distilled out of the bulb to a cold portion of the pumping tube and the new sample introduced.

**Errors.**—Errors in the measurement of sample weight and volume (after correction for thermal expansion) amount to less than 0.5%, which is negligible. Absolute temperature measurements are accurate to  $\pm 1^\circ$  (0.1%). Since a temperature difference of  $4^\circ$  will vary the equilibrium constant by 3%, a weighted average temperature of the bulb is used in the calculation of the equilibrium constants. The larger gradients existing along the pressure transmitting tube and the manometer itself do not significantly contribute to the error, since the volume involved is only 1.5% of the total. Pressure measurements were found to be reproducible to within  $\pm 0.05$  mm., which introduces a maximum error of 1% in the measured pressure range (10 to 30 mm.). A precise knowledge of the density of the molten gold (ca. 17.0) is not necessary since a null method is used.

The largest error introduced is in the correction of the pressure for permanent gas diffusion into the bulb. This pressure was measured at  $200^\circ$ , corrected to the temperature of the observation and subtracted from the total pressure observed. The leak rate varies greatly with temperature from 0.4 mm. per hour at  $1350^\circ\text{K}$ . to essentially zero at  $1200^\circ\text{K}$ . The largest pressure correction required in measurements recorded here was 5 mm. in a total pressure of 30 mm. Confidence in the validity of this correction was gained from an experiment in which a separate sample was heated rapidly to  $1250^\circ\text{K}$ . and then rapidly cooled to avoid any measurable leak up. The point thus obtained was in good agreement with the curve obtained from measurements made on vapor pressure (*i.e.*, at temperatures below complete vaporization) in which both the slope of the  $\ln P$  vs.  $1/T$  line and the magnitude of the pressures agree well with previously reported values when the pressure correction was made. In addition, the data are self-consistent and reproducible over the complete range of total pressure and pressure correction values.

If the source of permanent gas is either the argon diffusing through the silica or the release of carbon monoxide dissolved in silica,<sup>11</sup> the above correction is valid. There is, however, a bare possibility that the NaI reacts with the silica to yield iodine which would be measured as a permanent gas. To determine this, a 41-mg. sample was kept at  $1350^\circ\text{K}$ . for eight hours, after which a total gas pressure of 2 mm. was observed at  $400^\circ\text{K}$ . Visual comparison of the color of the gas in the bulb with an equivalent bulb containing  $\text{I}_2$  gas at known pressures indicated that if any  $\text{I}_2$  gas was present, an upper limit could be placed at a value of 0.1 mm. An error of this sort would affect the value of  $K_C$  in two ways. First, the effective sample weight is diminished and second, the residual gas correction extrapolated from a low temperature measurement should be increased to take into account the dissociation of  $\text{I}_2$  at high temperature. These effects tend to cancel each other and the combined effect is to alter  $K_C$  by only 2%.

## Results and Discussion

The mole fraction of dimer  $N_d$  is given by

$$N_d = (M_{\text{exp}}/M_{\text{NaI}}) - 1$$

where  $M_{\text{exp}}$  is the molecular weight obtained from the ideal gas law with the measured values of pressure and temperature and  $M_{\text{NaI}}$  is the formula weight of NaI. The equilibrium constant  $K_C$  for the reaction  $\text{Na}_2\text{I}_2 \rightarrow 2\text{NaI}$  is then obtained from

$$K_C = \frac{C_m^2}{C_d} = \frac{P}{R_{l.a.} T} \frac{N_m^2}{N_d}$$

where  $P$  is in atmospheres,  $R_{l.a.}$  in l. atm. mole<sup>-1</sup> deg.<sup>-1</sup> and the subscripts m and d refer to monomer and dimer, respectively.

In Table I are listed the experimental values ob-

(11) E. Machol and E. F. Westrum, USAEC Report AECU-3753. (1958).

(9) R. B. Sosman, "The Properties of Silica," Chemical Catalog Co., New York, N. Y., 1927.

(10) J. W. Johnson, M. A. Bredig and Wm. T. Smith, Jr., *J. Am. Chem. Soc.*, **77**, 307 (1955).

TABLE I  
MEASURED EQUILIBRIUM CONSTANTS FOR  $\text{Na}_2\text{I}_2$  DISSOCIATION

|                | $C^a$ | $T$ ,<br>°K. | $P$ , mm. | $-\log K_C$<br>(expt.) | $K_C$ (calcd.) -<br>$K_C$ (expt.) |
|----------------|-------|--------------|-----------|------------------------|-----------------------------------|
| NaI            | 6     | 1212         | 17.59     | 3.902                  | -0.062                            |
| Sample         | 7     | 1256         | 19.82     | 3.561                  | .025                              |
| Wt. = 42.0     | 4     | 1262         | 20.00     | 3.542                  | .011                              |
| mg.            | 2     | 1295         | 21.23     | 3.407                  | -.032                             |
| Vol. = 796 cc. | 5     | 1297         | 21.37     | 3.386                  | -.022                             |
| (at 300°K.)    | 3     | 1301         | 21.76     | 3.327                  | .016                              |
|                | 8     | 1344         | 23.95     | 3.066                  | .062                              |
|                | 1     | 1353         | 24.06     | 3.074                  | .010                              |
| NaI            | 9     | 1179         | 8.27      | 4.009                  | .034                              |
| Sample         | 10    | 1207         | 8.78      | 3.866                  | .004                              |
| Wt. = 20.0     | 11    | 1233         | 9.34      | 3.704                  | .012                              |
| mg.            | 12    | 1260         | 9.85      | 3.578                  | -.003                             |
|                | 13    | 1286         | 10.41     | 3.431                  | .013                              |
| Vol. = 830 cc. | 14    | 1314         | 10.92     | 3.315                  | -.022                             |
| (at 300°K.)    | 15    | 1337         | 11.33     | 3.224                  | -.047                             |

<sup>a</sup> Chronological order of experiments.

the values in these three papers were given at 817°K., they have been adjusted to 1260°K. by a statistical calculation using the vibrational frequencies assumed by BDP for the change in entropy and the expression given by MC for the change in  $\Delta H^0$  with temperature.

The agreement between our value of  $\Delta E^0$  and that of MK appears excellent. The value given by BDP is also in good agreement, but it is not an independent check since this number was obtained from their calculation of the entropy and the assumption of the validity of the  $\Delta F^0$  obtained by MK. The value calculated by MC falls outside the experimental error stated here and by MK. The entropy value obtained here is in reasonable agreement with MK but differs significantly from that of BDP and MC. Since the standard error stated here is that given by the least squares fit, systematic errors in measurement may account for the difference. Whether a discrepancy with theory really exists must await measurement of the vibra-

TABLE II  
COMPARISON OF EXPERIMENTAL AND CALCULATED VALUES FOR SODIUM IODIDE ASSOCIATION<sup>a</sup>

|                                  | $\Delta E^0$ (kcal./mole) |            | $\Delta S_P^0$ (e.u.) |            |
|----------------------------------|---------------------------|------------|-----------------------|------------|
|                                  | 817°K.                    | 1260°K.    | 817°K.                | 1260°K.    |
| Datz and Smith (expt.)           | [41.1]                    | 40.2 ± 1.2 | [27.8]                | 27.0 ± 1.0 |
| Miller and Kusch (exptl.)        | 38.6 ± 3.4                | [37.5]     | 28.5 ± 4.2            | [27.7]     |
| Bauer, Diner and Porter (calcd.) | 39.9 <sup>b</sup>         | [39.0]     | 30.1                  | [29.3]     |
| Milne and Cubicciotti (calcd.)   | 45.0                      | [44.1]     | 31.7 <sup>c</sup>     | [31.0]     |

<sup>a</sup> Bracketed values are extrapolated. <sup>b</sup> Computed by BDP with their calculated  $\Delta S^0$  and the MK value of  $K_C$ . <sup>c</sup> Given at 852°K.

tained from two samples, together with the deviations of the experimental points from the least squared straight line obtained from a plot of  $\log K_C$  vs.  $1/T$ . The slope of this line yields a value of  $\Delta E^0 = 40.2$  kcal. mole<sup>-1</sup> with a standard error of ±1.3 and  $\log K_C = -3.56$  at 1260°K. From the zero intercept,  $\Delta S_V^0$  is found to be  $15.8 \pm 1.0$  e.u. for a standard state of one mole per liter. The entropy change for a standard state of one atmosphere,  $\Delta S_P^0$ , is then  $27.0 \pm 1.0$  e.u., since

$$\Delta S_P^0 = \Delta S_V^0 + R(1 + \ln R_{1.0} T)$$

In Table II, these values are listed and compared with those of Miller and Kusch<sup>2</sup> and with some recent theoretical calculations by Bauer, Diner and Porter,<sup>12</sup> and by Milne and Cubicciotti.<sup>13</sup> Since

(12) S. H. Bauer, R. M. Diner and R. F. Porter, *J. Chem. Phys.*, **29**, 991 (1958), hereinafter referred to as BDP.

(13) T. A. Milne and D. Cubicciotti, *J. Chem. Phys.*, **29**, 846 (1958), hereinafter referred to as MC.

tional frequencies and dimensions of the dimer, since these are at present only estimated.

For potassium iodide and rubidium chloride, much larger discrepancies exist between the measured and calculated  $\Delta S^0$  values. We are presently trying to resolve the issue by measurements on these systems.

Vapor density measurement on fluorides or lithium salts may not be feasible in our equipment, due to the possibility of reaction with silica. However, the method should prove generally useful for temperatures up to ca. 1500°K. Above this temperature, devitrification of silica becomes rapid. The objectionable diffusion of ambient gas at temperatures above 1300°K. may be overcome by vacuum jacketing the apparatus.

**Acknowledgments.**—We wish to thank E. H. Taylor and R. E. Minturn for many helpful discussions, and M. J. Nesbit for his patience and skill in the construction of the silica apparatus.

## INFRARED STUDIES OF PROPELLANT FLAMES

BY HENRY A. BENT AND BRYCE CRAWFORD, JR.

*School of Chemistry, University of Minnesota, Minneapolis 14, Minnesota**Received February 17, 1959*

Application of a fast-scanning infrared spectrometer to the study of the pressure-supported flame of a solid double-base propellant is described. In the region from 700 to 4000  $\text{cm}^{-1}$  the flame spectrum in emission contains twelve characteristic bands. With but one exception, these bands correspond to the prominent bands in the absorption spectrum of the quenched products and have been assigned to  $\text{CO}_2$ ,  $\text{CO}$ ,  $\text{N}_2\text{O}$ ,  $\text{H}_2\text{O}$ ,  $\text{NO}$ ,  $\text{NO}_2$ ,  $\text{C}_2\text{H}_2$  and  $\text{HCN}$ . A Rice-Herzfeld-type free-radical mechanism appears capable of accounting for the principal features of the thermal decomposition of both nitroglycerine and nitrocellulose. The direct detection of  $\text{NO}_2$  is described, and the peculiar role of nitric oxide in nitrate ester flames is pointed out. Some suggestions are forwarded concerning a perplexing, broad and intense absorption at 2600–2700  $\text{cm}^{-1}$ .

## Introduction

The combustion of double-base propellants has been under investigation at Minnesota since 1942. Early experimental studies were concerned, in part, with the determination of the rate of those chemical processes by which a solid propellant, once ignited, is converted spontaneously into (largely) gaseous products, without the addition of any oxidizing agent. This over-all kinetic constant, the burning rate, is one of the most important properties of a propellant, and a simple, convenient method was devised for direct measurement of linear burning rates.<sup>1</sup> The mechanism of burning of double-base propellants and the dependence of the burning rate on pressure and composition have been considered by Crawford, Huggett and McBrady.<sup>2</sup> A physical theory based on a three stage flame-foam-fizz model was developed by Parr and Crawford.<sup>3</sup> These theories have been reviewed by Geckler.<sup>4</sup> As a logical extension of this work, recent experimental work in this Laboratory has centered attention on infrared studies of the propellant flame. One of the obvious advantages of this technique is that one may look at the flame without sensibly disturbing it, and in principle one should be able not only to identify reactants, intermediates and products, but also to measure their concentration and (effective) temperature throughout the flame.

For flames that can be maintained accurately stationary for long periods of time, the infrared spectrum could be obtained with a conventional spectrometer in about 20 minutes.<sup>5</sup> However, in the investigation of the burning of solid propellants, it would be difficult to maintain a flame stationary for 20 minutes because (i) the flame is not steady enough, (ii) burning rates vary considerably from powder to powder and even along the length of a given powder strand, and (iii) it is not practicable to extrude or handle the lengths of powder strands that would be necessary. One might hope to slow down the rate of motion of the flame with respect to the spectrometer by, say, a factor of 10 by movement of the propellant strand, but this would still

fall far short of the requirements of a conventional spectrometer. Rather than attempting to slow down the flame it was decided to speed up the spectrometer. To this end a fast-scanning infrared-recording spectrometer was built in 1951. Earlier reports have described the basic instrument<sup>6</sup> and its modifications for studies of gas-phase reactions<sup>7–10</sup> and for preliminary studies on propellant flames.<sup>11,12</sup> The present report is concerned with recent work with this fast-scanning spectrometer on the infrared spectra of propellant flames in the region 700–4000  $\text{cm}^{-1}$ .

## Experimental

Since propellants seldom burn with a self-sustaining flame at pressures below 50 p.s.i., it was necessary to construct a special high-pressure cell (Fig. 1). This cell was designed to withstand static pressures up to 500 p.s.i.; the usual operating pressure, in runs with nitrogen as the pressurizing and sweep gas was 100 p.s.i. (gauge pressure). The main frame of the cell was constructed from three-quarter inch steel stock, grooved to take a lead "O"-ring gasket. The  $\frac{3}{8}$ " thick front and rear plates were bolted to the frame with thirty-two tempered steel Allen-head bolts. Three or four days were usually required to draw down the cover plates to a tight fit after the cell had been dismantled for cleaning or modifications.

The cell has two sets of windows: one set of crystal windows, usually KBr, for the infrared beam of the spectrometer or emission spectra of the flame itself; and one set of Plexiglass windows for visual or photographic observation.

An important feature of this cell was provision for continuous removal of the combustion products to prevent their recirculating back into the flame. At elevated pressures this requires a relatively large flow of nitrogen or other sweep gas during a run. A large inlet at the end below the strand was connected to two commercial nitrogen cylinders; at the other end of the cell, an exit orifice of adjustable diameter led directly to an exhaust system with provision for sampling the combustion products. Baffle screens at B (Fig. 1) served to smooth out the flow. In this way a linear flow of gas matched to the natural velocity of the flame products (approximately 1 meter/second) could be maintained for the duration of a run (approximately 20–30 seconds). There is also provision for mechanically advancing the strand to slow the motion of the flame with respect to the spectrometer.

In early use,<sup>12</sup> this cell lay bolted horizontally on the main

(1) B. L. Crawford, Jr., C. Huggett, F. Daniels and R. E. Wilfong, *Anal. Chem.*, **19**, 630 (1947).

(2) B. L. Crawford, Jr., C. Huggett and J. J. McBrady, *THIS JOURNAL*, **54**, 854 (1950).

(3) R. G. Parr and B. L. Crawford, Jr., *ibid.*, **54**, 929 (1950).

(4) R. D. Geckler, "Selected Combustion Problems," AGARD, Butterworths, London, 1954, p. 289.

(5) (a) D. P. Needham and J. Pwling, *Proc. Roy. Soc. (London)*, **323A**, 337 (1955); (b) D. A. Dows, E. Whittle and G. C. Pimentel, *J. Chem. Phys.*, **23**, 499 (1955); (c) R. E. Donovan and W. A. Agnew, *ibid.*, **23**, 1592 (1955).

(6) P. J. Wheatley, E. R. Vincent, D. L. Rotenberg and G. R. Cowan, *J. Op. Soc. Am.*, **41**, 665 (1951).

(7) G. R. Cowan, E. Vincent and B. Crawford, Jr., *ibid.*, **43**, 710 (1953).

(8) R. E. Nightingale, G. R. Cowan and B. L. Crawford, Jr., *J. Chem. Phys.*, **21**, 1398 (1953).

(9) G. R. Cowan, D. L. Rotenberg, A. Downie, B. L. Crawford, Jr., and R. A. Orr, Jr., *ibid.*, **21**, 1397 (1953).

(10) I. C. Hisatsune, A. P. McHale, R. E. Nightingale, D. L. Rotenberg and Bryce Crawford, Jr., *ibid.*, **23**, 2467 (1955).

(11) H. F. White, G. R. Cowan, D. Rotenberg and B. Crawford, Jr., *ibid.*, **21**, 1399 (1953).

(12) A. D. Dickson, B. L. Crawford and D. L. Rotenberg, *Ind. Eng. Chem.*, **48**, 759 (1956).

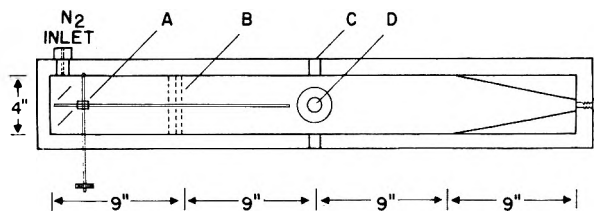


Fig. 1.—High pressure cell; A, strand holder and feed; B, baffle screens; C, crystal windows; D, glass windows.

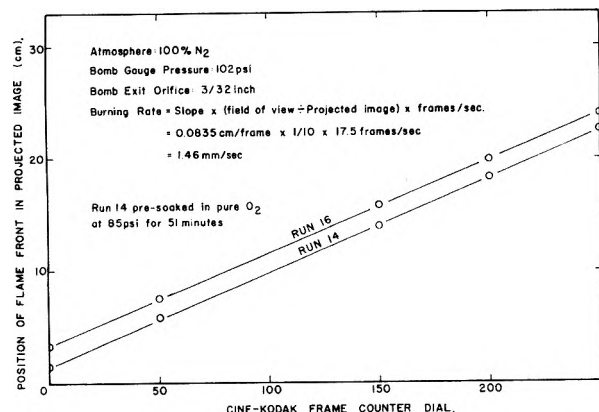


Fig. 2.—Determination of propellant linear burning rate.

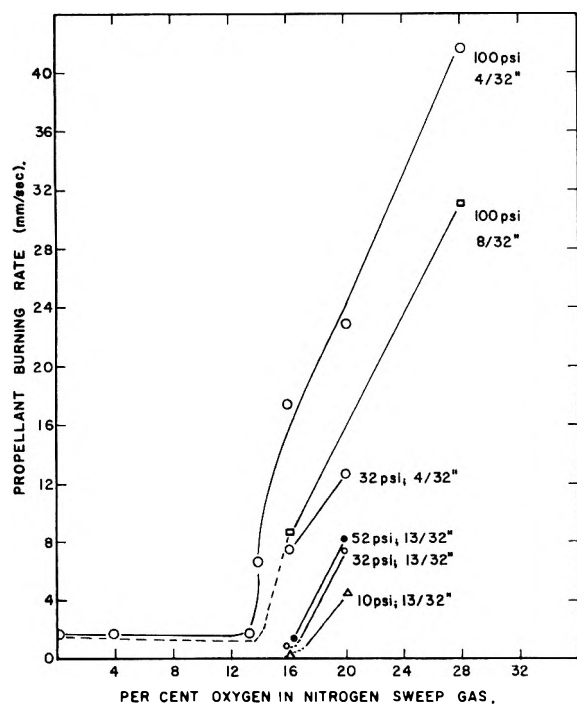


Fig. 3.—Propellant burning rate vs. per cent. oxygen in nitrogen sweep gas.

frame of the spectrometer; naturally, in this position the flame had a tendency to lift. For this reason, a second optical system was constructed and mounted at right angles to the first. This system permitted vertical mounting of the propellant strand, with the image of the flame twisted through 90° and focussed across the slit of the monochromator. The spectra displayed in the figures have been obtained with this arrangement.

In a typical run, a piece of propellant measuring 4" × 1" × 3/8" was cut from standard stock on a band saw, and drilled at one end to accommodate an igniter tip and at the other to fit onto the strand holder (Fig. 1). This propellant, mounted on the strand holder, was advanced until the igniter tip pressed against a wire that could be heated electrically. The

strand in final position extended approximately one inch above the space normally traversed by the beam, thereby blocking the beam. This provided time for the crater-like ignition area to develop into a flat flame front before the spectrometer saw the flame. Finally, the front plexiglass observation windows were bolted into place and the pressurizing sweep gas started through the cell. When the cell pressure was steady, the igniter was energized and shortly thereafter the scope camera was started. For emission runs, a blank would usually be run before and immediately after each burn. When desired, the entire optical path outside the flame could be swept free of atmospheric carbon dioxide and water with dry nitrogen; however, these atmospheric bands were sometimes retained as convenient calibration points. The amplification of the signal from the Golay and the scanning speed of the Littrow were checked each time with a standard 60-cycle signal.

The appearance of a pattern on the scope was influenced by several factors: the cell pressure, the slit opening, the scope amplification, the camera speed, the scanning speed, the prism used, the drum setting and the scanning amplitude. The higher the cell pressure, the brighter the flame in emission; thus the spectral resolution and signal-to-noise ratio could be increased by raising the pressure; however, this compressed the characteristic zones in the flame and diminished the geometrical resolution. The greater the scanning speed, the less the difficulties on any individual scan with random fluctuations in the flame, and the better the geometrical but the poorer the spectral resolution. As a compromise, most emission spectra were run at 100 p.s.i. (gauge pressure) at a scanning speed of 15 scans/second.

In view of the instrumental factors peculiar to the fast scanner we calibrated each scanned spectral region directly against known standards, such as polystyrene, atmospheric water and carbon dioxide, or specific calibrating gases (chiefly NO, NO<sub>2</sub>, C<sub>2</sub>H<sub>2</sub> and HCN). The spectra of the individual oxides of nitrogen have been published previously.<sup>13</sup>

The general procedure followed in surveying the spectrum of the propellant flame was to scan the spectral region covered by each prism in two series of overlapping scans: first an initial survey with the Littrow mirror oscillating with a large amplitude (wide scan), then a more detailed series of overlapping scans of smaller scanning amplitude (narrow scan), with special emphasis in the second series on the promising regions of the spectrum. For example, the calcium fluoride region (1400–5000 cm.<sup>-1</sup>) was scanned twice, in a series of 6 overlapping wide scans and a series of 26 overlapping narrow scans, with special emphasis on the region around 2600–2700 cm.<sup>-1</sup> just above the CO<sub>2</sub> band at 2350 (Figs. 11, 12). The region from about 1850 to 5000 cm.<sup>-1</sup> also was scanned in a series of 11 medium scans using a LiF prism.

Likewise, the sodium chloride region (670–1400 cm.<sup>-1</sup>) was scanned twice, first in a series of 6 overlapping wide scans and later with a series of 14 overlapping narrow scans. Several special high-resolution scans were made in regions of special interest, as when looking specifically at NO, NO<sub>2</sub>, HCN or the separation of the P and R branches of CO<sub>2</sub>.

The procedure in the exhaust collection runs was to burn the propellant, under pressure with the sweep gas exhausting through liquid-nitrogen surrounded traps. The contents of the traps were then fractionated, successively, with a microcolumn loaned us by Dr. John Overend, into storage bulbs, and from thence into an 8-cm. infrared gas cell equipped with silver chloride windows. Representative spectra of the gases collected in this way are shown in Figs. 15 and 16. These were obtained with a Perkin-Elmer Model 21 double-beam spectrometer.

The method by which the linear burning rate of the propellant was determined photographically is summarized in Fig. 2. It was observed that the burning rate slowly increases with increasing oxygen content of the ambient atmosphere, and with decreasing exit-orifice diameter, until some critical velocity, between 1.78 and 3.10 mm./sec., is reached, when, suddenly, the propellant begins to burn down the side at a much increased rate (Fig. 3). These side burns have been fairly reproducible; can be sustained to low pressures; are quite sensitive to oxygen content, pressure and sweep-gas flow rate; and are quite brilliant. In separate experiments, it has been found that to a first approximation the linear flow

(13) R. E. Nightingale, A. R. Downie, D. L. Rotenberg, Bryce Crawford, Jr., and R. A. Ogg, Jr., *THIS JOURNAL*, **68**, 1047 (1954).

rate of gas through the high pressure cell is nearly independent of the cell pressure, depending principally on the exit-orifice diameter.

### Results and Discussion

With a  $\text{CaF}_2$  prism, the infrared absorption spectrum from  $1400$  to  $4000\text{ cm.}^{-1}$  of propellant flames supported by an atmosphere of nitrogen at  $100\text{ p.s.i.}$  (gauge pressure) was obtained, in 12 overlapping scans, at a scanning speed of 15 scans/second. While some moderately strong absorption bands were observed<sup>11</sup> particularly in the region of the  $\text{CO}_2$   $2350\text{ cm.}^{-1}$  band, the spectra on the whole were disappointingly like the black-body radiation of the globar. On increasing the bomb pressure to  $350\text{ p.s.i.}$ , emission of infrared radiation from the flame itself began to predominate over the black-body emission of the globar, as evidenced by the fact that the oscilloscope trace was deflected off scale when the luminous part of the flame reached the level of the beam. However, it was evident from the few scans obtained on these flames that, on the whole, more structure was to be observed from the flame in emission than in absorption; hence we turned our attention to the emission spectrum. All flame spectra reported here are of the flame in emission. Burning at  $100\text{ p.s.i.}$ , the peak energy collected at the detector from the flame of a strand  $1'' \times \frac{3}{8}''$  in cross-section was roughly one-quarter that from the globar, operating at 4.6 amperes. These figures represent our first extensive report on the spectra of solid-propellant flames as viewed by the Minnesota fast-scanning infrared spectrometer.

The solid curves in the figures are traces of the photographic oscilloscope record. Oscilloscope deflection is plotted vertically, wave numbers scanned horizontally, increasing from left to right; the approximate scan center is indicated in the upper left-hand corner, together with the prism, cell pressure and spectrometer slits in microns. The solid curve labeled I represents the spectra obtained early in a run, from a zone close to the surface of the burning propellant; II and III indicate zones progressively further out in the flame. For comparison, the dashed curve labeled GB is the globar; for calibration purposes, the dotted curve labeled PS is the absorption spectrum of polystyrene, as recorded immediately after a run. These traces are quite characteristic and, for all their peculiar structure, quite reproducible.

The first question raised by these traces is whether they portray peaks of emission or valleys of absorption—or both. In a chemically and physically similar system, the flame decomposition of ethyl nitrate, Needham and Powling<sup>5a</sup> find, in the main, emission peaks (for  $\text{H}_2\text{O}$ ,  $\text{CH}_4$  and  $\text{CO}_2$ ). Close examination of the region about the  $\text{CO}_2$  doublet at  $2350\text{ cm.}^{-1}$ , has enabled us to resolve the  $\text{CO}_2$  doublet *in absorption*—precisely where one should ordinarily find it, except for a slightly increased separation of the P and R branches. Indeed, this  $\text{CO}_2$  band in "emission" appears in nearly every way like the  $\text{CO}_2$  band in absorption reported previously.<sup>12</sup>

There are other clues; the flames are sooty and luminous; and the "spectrophotometric gradient" of the early traces (I) resembles rather closely that

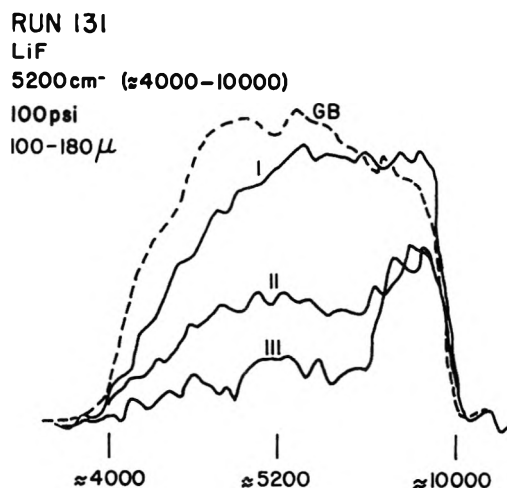


Fig. 4.—Flame spectrum: black-body radiation peak.

of the black-body globar blank. Increasing the cell pressure increases both the visible luminosity of the flame and the intensity of the black-body radiation and, also, the separation of the P and R branches of  $\text{CO}_2$ . Furthermore, in both absorption and emission the optical density of the  $\text{CO}_2$  band was roughly independent of the cross-sectional dimensions of the strand.

These facts suggest that what we are observing is a small sun of luminous soot particles radiating a black-body continuum, surrounded by a mantle, of increasing thickness as one progresses outward in the flame, of cooler infrared-absorbing gases.

The outer envelope of flame gases is presumably quenched by the nitrogen sweep gas, which enters the bomb some 20 or 30 degrees below room temperature at a Reynolds number in excess of 3200. The importance of diffusion into a flame from the surrounding gases recently has been emphasized by Gaydon and Wolfhard.<sup>14</sup> Under even mild conditions, mixing can occur; in our cell conditions are quite turbulent and extended mixing must certainly occur.

We have estimated the temperature of the soot particles responsible for the infrared continuum in this way. Where the envelope of quenched gases is optically thin, as at the base of the flame, the spectrometer sees directly into the hot interior of the flame. The soot particles there are probably nearly in temperature equilibrium with their surroundings,<sup>14</sup> although the radiation from them may be not quite Planckian. Absolute intensity measurements on the spectrophotometric gradient of the flame black-body emission are, of course, meaningless.<sup>15</sup> From the black-body radiation peak, however (Fig. 6, trace I), one estimates for the case of a spectrometer sampling equal wave length intervals<sup>16</sup> that  $T = (\text{max})/3.45 \approx 1200\text{--}1300^\circ$  (for the inner cone of a flame burning in an atmosphere of  $\text{N}_2$  at  $100\text{ p.s.i.}$  and streaming by at approximately 1 meter/sec.). This temperature is reasonable for our

(14) A. G. Gaydon and H. G. Wolfhard, "Flames," Chapman and Hall, Ltd., London, 1953.

(15) G. H. Dieke, "Temperature," Vol. 2, Reinhold Publ. Corp., New York, N. Y., 1955, Chapter 3.

(16) Max Planck, "The Theory of Heat Radiation," F. Blakiston's Son and Co., Philadelphia, 1914.



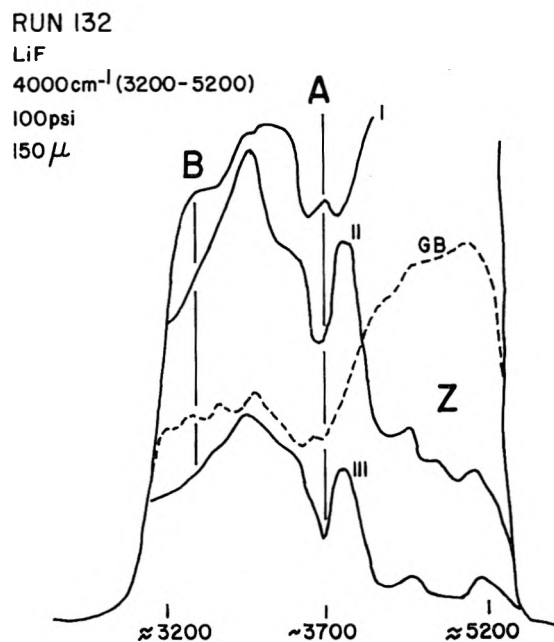
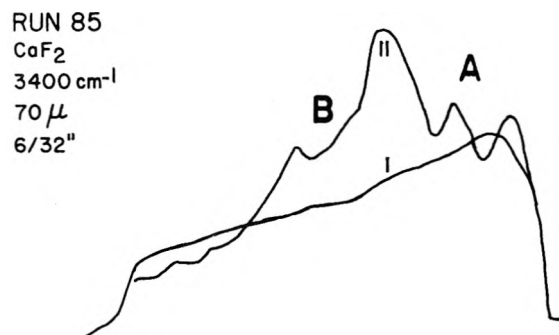
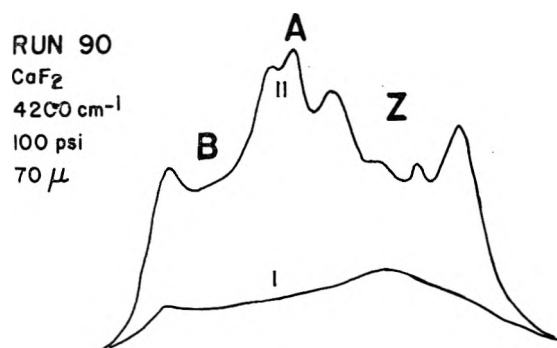


Fig. 5.—Flame spectrum: O-H stretching region; CO<sub>2</sub> combination bands.

Fig. 6.—Flame spectrum: hydrogen stretching region (LiF prism).

flames, though possibly a bit on the high side.<sup>5a</sup> We shall return to this point later, in our discussion of the mechanism of the flame reactions and the possible role of surface catalysis.

The temperature of the outer mantle of the flame has been estimated from the separation of the peaks of the P and R branches of the 2350 CO<sub>2</sub> band.<sup>17</sup> The spectrometer naturally reports an average of what it sees along its line of sight into the flame.

(17) G. Herzberg, "Molecular Spectra. I." D. Van Nostrand Co., New York, N. Y., 1950, Chapter 3.

For this average, we find values ranging from 200–800°, depending on the pressure and turbulence of the nitrogen sweep gas.

These temperature estimates serve to confirm the picture of a hot core of solid particles, radiating a continuum, surrounded by an envelope of cooler gas. With this picture in mind, the traces have been examined from the point of view of absorption. The main "bands," whose structures have been verified repeatedly under varying conditions, are listed in the first column of Table I by their designation in the figures, together with their approximate frequency and intensity. Our confidence in this interpretation of the over-all emission spectra of the flame as being that of essentially discrete absorption bands superimposed on a continuous black-body background will depend in part on the extent to which logical assignments can be offered for these bands.

TABLE I

| Obsd. bands (cm. <sup>-1</sup> ) | Figures | Assignments                                                                                |
|----------------------------------|---------|--------------------------------------------------------------------------------------------|
| Z(s) 5-6000                      | 5       | Overtones; combinations                                                                    |
| A(ms) 3700                       | 5, 6    | O-H (H <sub>2</sub> O, OH, HONO)<br>CO <sub>2</sub> ( $\nu_1 + \nu_2$ ; $2\nu_2 + \nu_1$ ) |
| B(m) 3300                        | 5, 6    | HCN; C <sub>2</sub> H <sub>2</sub> ; N-H                                                   |
| C(m) 3085                        | 7       | C-H                                                                                        |
| D(vs) 2600-2700                  | 8, 9    | ?                                                                                          |
| E(s) 2350                        | 8, 9    | CO <sub>2</sub>                                                                            |
| F(w) 2100                        | 9       | CN (?)                                                                                     |
| G(m) 2000                        | 10      |                                                                                            |
| H(m) 1860                        | 10      | NO                                                                                         |
| I(vs) 1620                       | 11      | NO <sub>2</sub>                                                                            |
| J(ms) 1500                       | 11, 12  | C-NO <sub>2</sub>                                                                          |
| K(w) 1600 region                 | 11      | H <sub>2</sub> O                                                                           |
| L(s) 700-1000                    | 13, 14  | HCN, C <sub>2</sub> H <sub>2</sub> ; HONO; C <sub>2</sub> H <sub>4</sub>                   |

In trying to assign these bands, several problems are encountered immediately. First, there are factors involving the flame itself: whether it contains normal molecules, excited molecules, free radicals or some complex mixture of all these. Secondly, there are purely instrumental factors: the appearance of an absorption band as recorded by the fast scanner depends on many factors, and any similarity between the appearance of a band on the fast scanner with that obtained with an unmodified 12C spectrometer on slow scan is purely coincidental!

The simplest and most direct approach to these two problems is to assume that the absorbing entities in the turbulent flame envelope are normal molecules in thermodynamic equilibrium with their environment and to compare where possible the spectrum of the flame directly with that of suspected absorbing entity in an ordinary gas cell, either just before or immediately following a run. Such comparisons were made for water vapor (Fig. 11), carbon dioxide (Fig. 9), nitric oxide, nitrogen dioxide and hydrogen cyanide.

If the principal absorbing entities are stable molecules, it should be possible to collect them from the exhaust gases and to observe their spectra as quenched products at room temperature. Figure 15 shows the spectrum on a model 21 double-beam spectrometer of the volatile products from two modes of decomposition: thermal decomposition *in*

*vacuo* (the dashed line), and flame decomposition at 114 p.s.i. (the solid line). The similarities are striking: in both instances one finds  $\text{CO}_2$ , CO and  $\text{N}_2\text{O}$ , NO,  $\text{NO}_2$ , HONO, probably  $\text{HNO}_3$ ,  $\text{C}_2\text{H}_2$ , HCN and  $\text{C}_2\text{H}_4$ . As we shall see later, most of these products are kinetically quite plausible.

The same species, less those involving  $\text{H}_2\text{O}$ , are displayed in a fractionated sample in Fig. 16. Across the bottom of this figure we have indicated the bands seen in absorption in the flame spectra. (The vertical pips indicate the bands reported by Wolfrom, *et al.*,<sup>18</sup> for the gaseous products from the slow controlled thermal decomposition of nitrocellulose.) Again, the correspondence is striking.

With one exception, all of the major flame bands correspond to prominent bands in the quenched products. Perhaps this is not surprising: in the one case the quenching is with gaseous nitrogen at approximately  $0^\circ$ , in the other with liquid nitrogen. The two bands of  $\text{CO}_2$  at approximately 3600 and 3700 are clearly seen in both instances (Figs. 15, 16; and 5, 6). Removal of the water clearly reveals band B in the quenched exhaust gases, and the relatively weak band C. Next is the relatively strong  $\text{CO}_2$  band at 2350, with the CO- $\text{N}_2\text{O}$  structure on its lower wing. From here on down to 1400 the principal absorptions are due to NO and  $\text{NO}_2$ .  $\text{N}_2\text{O}_4$ , which is detected in the exhaust gases, would, of course, not be present at any appreciable concentration at  $200^\circ$  above, and in the flame the region extending from approximately 1350 down to 1050 showed no strong absorption bands. The flame spectrum from approximately 1000 to 700 is one broad fairly intense band with a certain amount of fine structure. This region is nicely covered by  $\text{C}_2\text{H}_4$ , HONO,  $\text{C}_2\text{H}_2$  and HCN in that manner. The only intense flame band unaccounted for in this way is band D at 2600-2700  $\text{cm}^{-1}$ .

From the optical densities of the non-overlapping bands in Figs. 15 and 16, one finds that carbon dioxide and nitric oxide are the principal constituents of the volatile exhaust gases. Exclusive of any nitrogen, hydrogen, oxygen or water that may be formed, these two gases together account for over 80% of the volatile, infrared active products. Table II gives the relative partial pressures of the identifiable products based on 100 for  $P_{\text{NO}}$ .

TABLE II

| Substance              | Relative partial pressure | Substance              | Relative partial pressure |
|------------------------|---------------------------|------------------------|---------------------------|
| $\text{CO}_2$          | 170                       | $\text{NO}_2$          | 8                         |
| NO                     | 100                       | $\text{C}_2\text{H}_4$ | 6                         |
| HCN                    | 35                        | $\text{N}_2\text{O}$   | 0.2                       |
| $\text{C}_2\text{H}_2$ | 12                        |                        |                           |

The carbon-to-nitrogen ratio for the gaseous mixture represented by Table II comes out to 1.68, compared to a calculated value of approximately 1.70 for the propellant itself. Since neither carbon nor nitrogen are included in the experimental count, this agreement is either fortuitous, or indicates that the relative amount of soot and reduced nitrogen formed is small.

(18) M. L. Wolfrom, J. H. Frazer, L. P. Kuhn, E. E. Dickey, S. M. Olin, R. S. Bower, G. G. Maher, J. D. Murdock, A. Chaney and E. Carpenter, *J. Am. Chem. Soc.*, **78**, 4695 (1956).

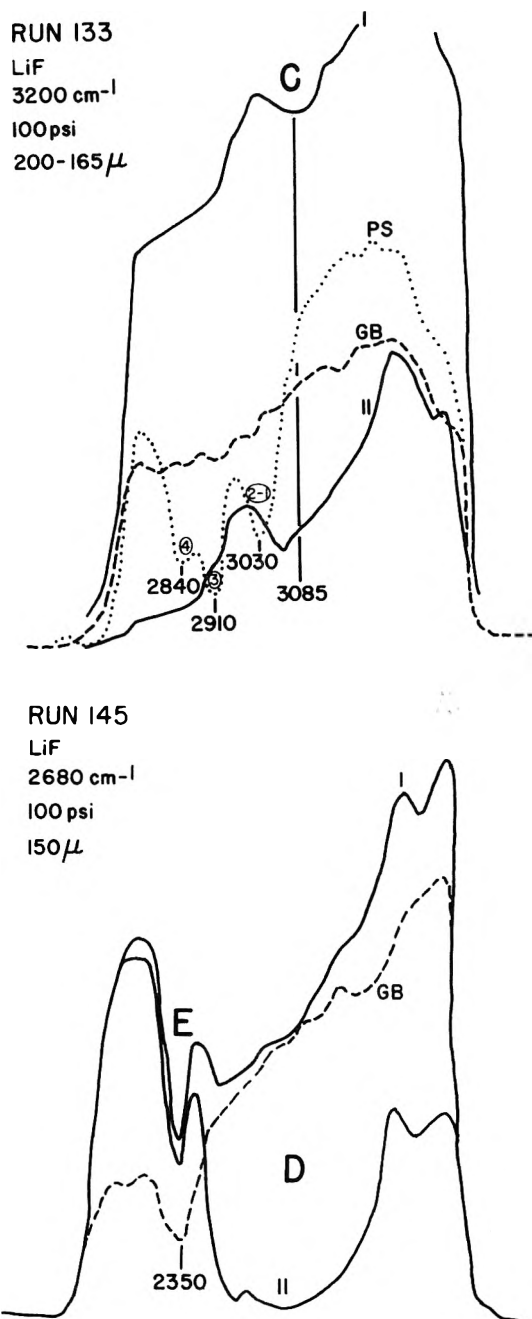


Fig. 7.—Flame spectrum: C-H stretching region.  
Fig. 8.—Flame spectrum: band D and  $\text{CO}_2$  (band E).

From Table II it may be seen that nitric oxide constitutes approximately one-third of the total pressure (exclusive of any  $\text{N}_2$ ,  $\text{O}_2$ ,  $\text{H}_2$  and  $\text{H}_2\text{O}$ ). Much the same conclusion is reached from an inspection of the traces.

It is interesting to compare these results with those of Needham and Powling on the flame decomposition of ethyl nitrate at atmospheric pressure.<sup>5a</sup> They find the products listed in Table II, together with methane (which we would not have detected at the low level they report), hydrogen and nitrogen, nitromethane and the partially oxidized products methyl nitrite, acetaldehyde, formaldehyde and methyl alcohol. Most strikingly, whereas we find much  $\text{CO}_2$ , and little CO, they

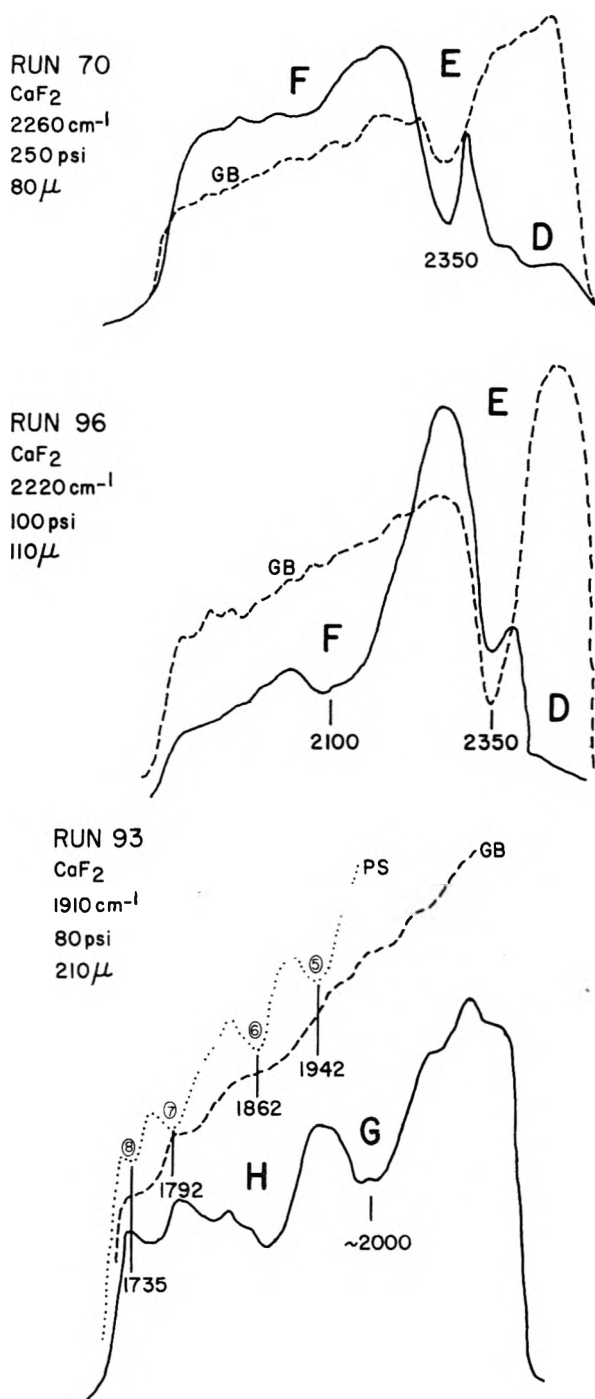
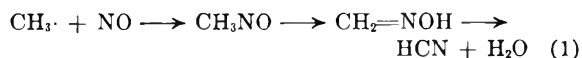


Fig. 9.—Flame spectrum: 2200  $\text{cm}^{-1}$  region.  
 Fig. 10.—Flame spectrum: 1900  $\text{cm}^{-1}$  region.

find mainly  $\text{CO}$ , with little  $\text{CO}_2$ , no  $\text{NO}_2$  and no soot. Also, we find relatively more  $\text{HCN}$ —indeed, several hundred millimeters of it in the flame under combustion conditions.

The  $\text{HCN}$  formed in the flame is probably a synthetic product, since there are relatively few  $\text{C-N}$  bonds in the double-base propellant, and none at all in either of the major components, nitroglycerine and nitrocellulose. Other synthetic products are  $\text{N}_2\text{O}$ ,  $\text{CO}_2$  and  $\text{H}_2\text{O}$ .  $\text{CO}$ ,  $\text{NO}$ ,  $\text{NO}_2$  and  $\text{C}_2\text{H}_2$ , on the other hand, presumably are decomposition products.

The formation of  $\text{HCN}$  is interesting, because it is usually assumed<sup>19-23</sup> that this molecule is formed by the reaction of a methyl radical with nitric oxide



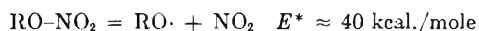
Under cracking conditions at  $1000^\circ$ ,  $\text{HCN}$  has, in fact, been manufactured from  $\text{NO}$  and methane.<sup>24</sup> It is known that  $\text{CH}_2\text{NOH}$  decomposes at moderate temperatures<sup>25</sup> and that  $\text{HCN}$  is produced in the reaction of methyl radicals with  $\text{NO}$ .<sup>23,26</sup>  $\text{HCN}$  has been reported before in flames,<sup>5a,27</sup> and by Wolfrom, *et al.*,<sup>18</sup> in the slow controlled thermal decomposition of nitrocellulose. Our system, as previously noted, is flooded with nitric oxide; however, neither of the major components contain methyl groups, which may come from the additives, a possibility also considered by others.<sup>18</sup> Another possibility is suggested by the reaction



which has an activation energy of approximately 7 kcal.<sup>28</sup> This is not to suggest that  $\text{CN}$ , for which we have some slight evidence (band F, Fig. 19), abstracts hydrogen atoms in the flame from  $\text{H}_2$ , for which we have no direct evidence, but rather, since  $D(\text{H-H})$  and  $D(\text{C-H})$  are comparable, that  $\text{CN}$  if present (as ultraviolet emission studies would suggest<sup>14</sup>) could abstract hydrogen atoms from hydrocarbons with an activation energy of 7 kcal. or less and form free radicals still more easily.

To facilitate comparisons of this sort, we have in Table III listed some representative activation energies for a number of elementary kinetic processes that might be thought to occur in a nitrate-ester flame.

The elementary processes in Table III may be divided into two classes, with activation energies, respectively, greater or less than that for rupture of the weakest bond in a nitrate ester. This activation energy is approximately 40 kcal./mole,<sup>19,29</sup> and corresponds to the bond dissociation energy of the  $\text{RO-NO}_2$  bond. The first step in the thermal decomposition of a nitrate ester is, then, generally postulated as being the homolytic scission of this bond to give two free radicals, an alkoxy radical and nitrogen dioxide



Fairly conclusive proof that  $\text{NO}_2$  is in fact formed in some such step as this recently has been obtained in a study of the thermal decomposition of

(19) E. W. R. Steacie, "Atomic and Free Radical Reactions," Reinhold Publ. Corp., New York, N. Y., 1954.

(20) A. F. Trotman-Dickenson, "Gas Kinetics," Academic Press, Inc., New York, N. Y., 1955.

(21) H. A. Taylor and H. Bender, *J. Chem. Phys.*, **9**, 761 (1941).

(22) C. S. Coe and T. F. Doumani, *J. Am. Chem. Soc.*, **70**, 1516 (1948).

(23) W. A. Bryce and K. U. Ingold, *J. Chem. Phys.*, **23**, 1968 (1955).

(24) M. Patry and G. Engel, *Comp. rend.*, **231**, 1302 (1950).

(25) G. K. Adams, W. G. Parker and H. G. Wolfhard, *Disc. Faraday Soc.*, **14**, 97 (1953).

(26) P. Hartek, *Ber.*, **66**, 423 (1933).

(27) E. A. Arden and J. Powling "Sixth Symposium (International) on Combustion," Reinhold Publ. Corp., New York, N. Y., 1957, p. 177.

(28) Ref. 19, p. 644.

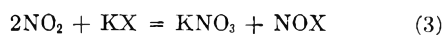
(29) P. Gray, *Trans. Faraday Soc.*, **51**, 1367 (1955).

TABLE III

## ACTIVATION ENERGIES OF SOME ELEMENTARY REACTIONS

| Reaction                                                                                          | $E^*$<br>(kcal./mole) | Ref.                   |
|---------------------------------------------------------------------------------------------------|-----------------------|------------------------|
| $\text{CH}_3 + \text{NO}$                                                                         | 0                     | 19, p. 646             |
| $\text{C}=\text{C} + \text{NO}_2 \rightarrow \text{C}(\text{NO}_2)\text{-C}$                      | 0                     | 32                     |
| $\text{C}_2\text{H}_5 + \text{C}_2\text{H}_5$                                                     | 1                     |                        |
| $\text{C}=\text{C} + \text{H}$                                                                    | 4-5                   | 20, p. 284             |
| $\text{C}=\text{C} + \text{CH}_3$                                                                 | 6-7                   | 20, p. 296             |
| $\text{H} + \text{H}_2\text{CO}$                                                                  | 3.6                   | 19, p. 616             |
| $\text{CH}_3 + \text{H}_2\text{CO}$                                                               | 5.6                   | 19, p. 616             |
| $\text{CN} + \text{H}_2 \rightarrow \text{HCN} + \text{H}$                                        | 7                     | 19, p. 644             |
| $\text{RO}\cdot$ dismutating by C-C<br>rupture                                                    | 3-13                  | 39a                    |
| $\text{RO}\cdot$ dismutating by C-H<br>rupture                                                    | 12-25                 | 39a                    |
| $\text{C}_2\text{H}_2 + \text{NO}_2 \rightarrow$ glyoxal<br>(over-all)                            | 15                    | 51                     |
| $\text{CHO} \rightarrow \text{CO} + \text{H}$                                                     | 13-14                 | 19, p. 609; 20, p. 306 |
| $\text{H}_2\text{CO} + \text{NO}_2 \rightarrow \text{HONO}$<br>+ $\text{CHO}$                     | 15-19                 | 32                     |
| $\text{CHO}\cdot\text{CHO} + \text{NO}_2 \rightarrow$<br>$\text{HONO} + \text{CHO}\cdot\text{CO}$ | 20                    | 20, p. 212             |
| $\text{R} + \text{ONO} \rightarrow \text{RO} + \text{NO}$                                         | 20 (H)                | 39a                    |
| $\text{CH}_4 + \text{NO}_2 \rightarrow \text{HONO}$<br>+ $\text{CH}_3$                            | 21                    | 32                     |
| $\text{R}\cdot$ dismutating by C-C<br>rupture                                                     | 24                    | 20                     |
| $\text{R}\cdot$ dismutating by C-H<br>rupture                                                     | 40                    | 20                     |
| $\text{HCHO}$ oxidation ( $350^\circ$ )                                                           | 21                    | 43                     |
| $\text{NO}_2 + \text{CO} \rightarrow \text{CO}_2 + \text{NO}$                                     | 28                    | 20                     |
| $2\text{NO}_2 \rightarrow 2\text{NO} + \text{O}_2$                                                | 25                    | 20                     |
| $D(\text{RO}-\text{NO})$                                                                          | 38                    | 39a                    |
| $D(\text{RO}-\text{NO}_2)$                                                                        | 40                    | 19, p. 241             |
| $\text{NO} + \text{CO} \rightarrow \text{CO}_2 + \frac{1}{2}\text{N}_2$                           | 50                    | 55                     |
| $D(\text{R}-\text{ONO})$                                                                          | 57                    | 39a                    |
| $D(\text{R}-\text{NO}_2)$                                                                         | 58                    | 39a                    |
| $2\text{NO} \rightarrow \text{N}_2\text{O} + \text{O}$                                            | 63                    | 48                     |
| $D(\text{NN}-\text{O})$                                                                           | 55                    | 48                     |
| $\text{HCHO} \rightarrow \text{CO} + \text{H}_2$<br>( $510-607^\circ$ )                           | 45                    | 44                     |
| $\text{NO} + \text{H}_2$                                                                          | 49                    | 47                     |
| $\text{C}_2\text{H}_5 \rightarrow \text{C}_2\text{H}_4 + \text{H}_2$                              | 70                    | 20                     |
| $D(\text{C}-\text{C})$                                                                            | 80-85                 | 20                     |
| $D(\text{C}-\text{H})$ , prim., sec, ter.                                                         | 100, 94, 90           | 20                     |
| $\text{C}_2\text{N}_2 \rightarrow 2\text{CN}$                                                     | 114                   | 19, p. 645             |

several nitrate esters in potassium halide matrices. Free  $\text{NO}_2$  is known to react quickly at room temperature with alkali halides according to the equation<sup>30</sup>



The nitrate ion that is produced should be readily detectable in the infrared. Using this diagnostic test for  $\text{NO}_2$  we have, in fact, found strong proof of the formation of  $\text{NO}_2$  in the controlled thermal decomposition of ethyl nitrate, nitrocellulose and the double-base propellant itself.<sup>31</sup>

The nitrogen dioxide may react in a host of ways. Gray and Yoffe<sup>32</sup> have recently published a system-

(30) D. M. Yost and H. Russell, "Systematic Inorganic Chemistry," Prentice-Hall, Inc., New York, N. Y., 1946.

(31) H. A. Bent and B. L. Crawford, Jr., *J. Am. Chem. Soc.*, **79**, 1793 (1957).

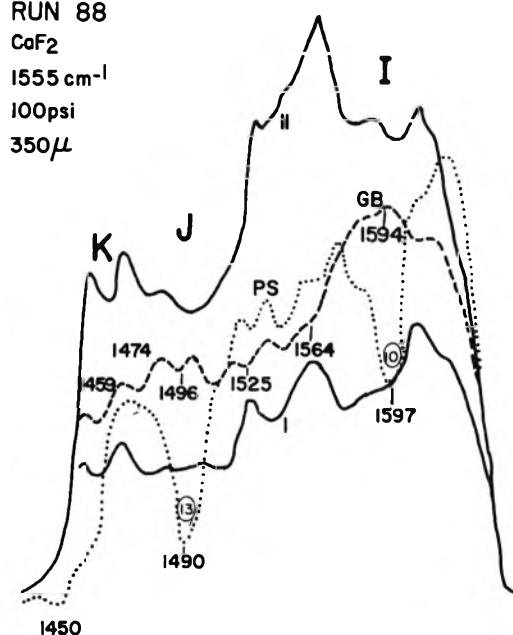
(32) P. Gray and A. D. Yoffe, *Quart. Revs.*, **IX**, 362 (1955); also, *Chem. Revs.*, **55**, 1070 (1955).

## RUN 88

CaF<sub>2</sub>1555 cm<sup>-1</sup>

100psi

350μ



## RUN 129

NaCl

1334 cm<sup>-1</sup>

100psi

150-270μ

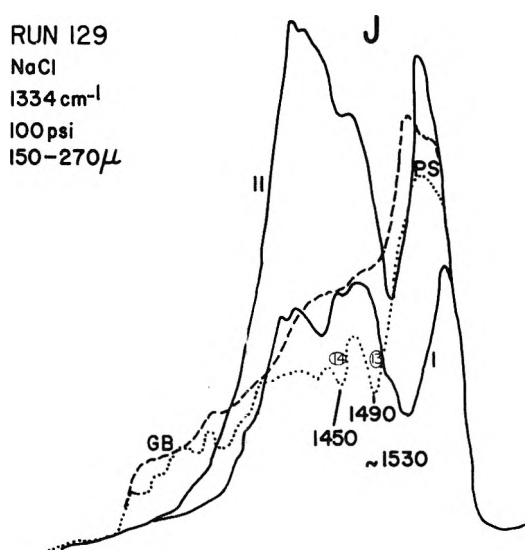


Fig. 11.—Flame spectrum: C-NO<sub>2</sub> region (CaF<sub>2</sub> prism).  
Fig. 12.—Flame spectrum: C-NO<sub>2</sub> region (NaCl prism).

atic review of many of its reactions. Essentially, in one way or another,  $\text{NO}_2$  loses oxygen to become  $\text{NO}$ , a radical that is unusually stable under flame conditions.<sup>14,40</sup> This is indeed one of the great problems of nitrate ester combustion: the reduction of nitrogen beyond  $\text{NO}$ .<sup>33</sup> However, we defer further consideration of these radicals until we have considered the probable fate of the alkoxy radical, and the products derived from it, some of which are known to react quite readily with  $\text{NO}_2$ .

Enough is known of bond dissociation energies and activation energies of simple gas phase reactions (*cf.* Table III), to be a fairly detailed guide as to the probable mode of decomposition of a complex ester like nitroglycerine or nitrocellulose. We shall start, somewhat arbitrarily, with nitroglycerine.

(33) P. Gray and M. W. T. Pratt, "Sixth Symposium (International) on Combustion," Reinhold Publ. Corp., New York, N. Y., 1957, p. 183.

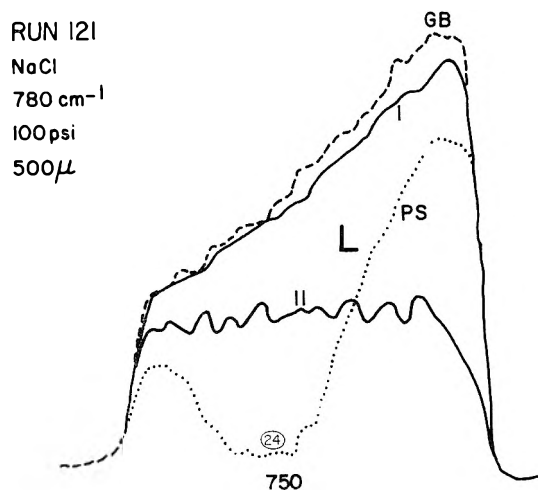
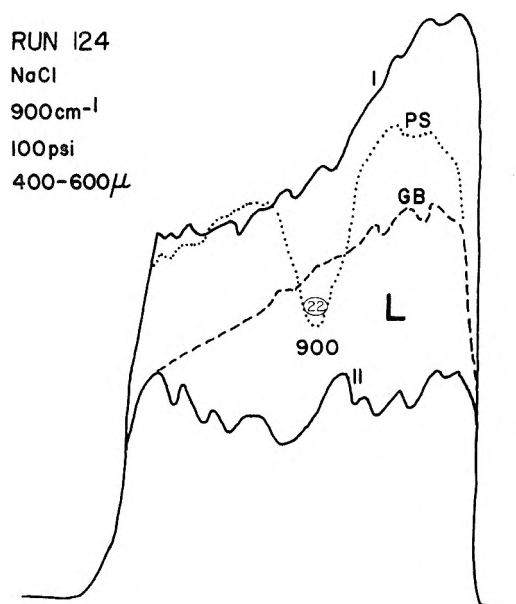
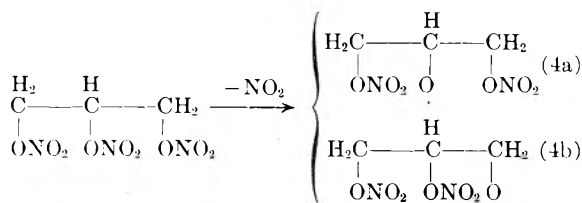


Fig. 13.—Flame spectrum: 900 cm.<sup>-1</sup> region.  
Fig. 14.—Flame spectrum: 780 cm.<sup>-1</sup> region.

According to the discussion above (reaction 3), the first step in the decomposition of this ester is probably scission of an O-N bond. There are two possibilities

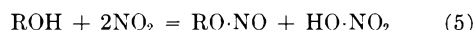


In what follows, both of these alkoxy radicals will yield essentially the same products; we shall consider only one of them, (b).

An alkoxy radical is isoelectronic with an ordinary alkyl radical, the terminal CH<sub>2</sub> group of the latter having been replaced by a terminal oxygen atom with an unpaired electron. As such, it may be expected to undergo very much the same sequence of reaction as postulated by Rice and Herzfeld for the alkyl radicals in the thermal decompo-

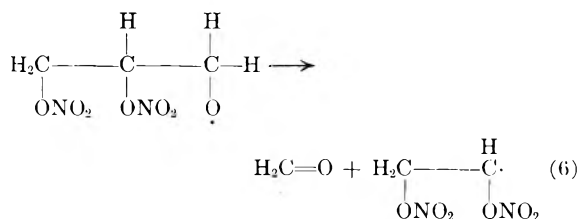
sition of the paraffins.<sup>34,19</sup> According to the Rice-Herzfeld mechanism, and studies of alkoxy radicals,<sup>31,35-38</sup> one may expect two reactions to dominate the further decomposition of our nitrate ester radical (b): (i) hydrogen abstraction and (ii) radical dismutation.

The activation energies for these two alternatives are not known with certainty (Table III), but presumably both alternatives are important at any temperature where the initial RO-NO<sub>2</sub> bond scission is occurring at a significant rate. We may, however, ignore hydrogen abstraction for the following reasons. This abstraction process forms alcohols, which are known to react rapidly with NO<sub>2</sub> to give nitrites and nitric acid<sup>9,32</sup>

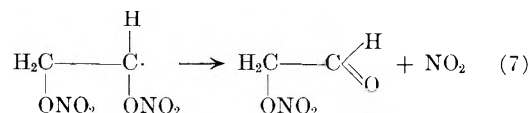


This reaction is, in fact, merely the alkyl analog of the reaction of water with NO<sub>2</sub> to yield nitrous acid and nitric acid, which occurs rapidly at room temperature.<sup>30</sup> Inasmuch as a normal RO-NO bond is kinetically equivalent to an RO-NO<sub>2</sub> bond (Table III; see also ref. 29), the mixed nitrite-nitrate ester formed in this way is essentially equivalent, kinetically, to the original nitrate ester. Given a source of readily abstractable hydrogen, such as an aldehyde (see later), this sequence merely changes nitrate groups in our original kinetic entity to nitrite groups. Eventually the intermediate radical will presumably find an opportunity to dismutate, particularly since this latter alternative is presumably less discriminating in the type of collision required (because of the higher steric factor).

An alkoxy radical may decompose in either of two ways: (i) by splitting homolytically an alpha C-H bond, or (ii) by splitting an alpha C-C bond. Since C-C bonds are the weaker, the latter alternative is the most likely, just as with alkyl radicals (Table III, ref. 39a, b), where, instead of forming a C=C double bond, there is formed a carbon-oxygen double bond



The radical thus formed will be much less stable than the parent molecule, for it can dismutate by breaking a relatively weak O-N bond



(34) F. O. Rice and K. F. Herzfeld, *J. Am. Chem. Soc.*, **56**, 284 (1934).

(35) J. H. Daley, F. F. Rust and W. E. Vaughan, *ibid.*, **70**, 88 (1948).

(36) J. B. Levy, *ibid.*, **75**, 1801 (1953).

(37) E. W. R. Steacie, ref. 19, p. 232.

(38) A. V. Tobolsky and R. E. Mesrobian, "Organic Peroxides," Interscience Publishers, New York, N. Y., 1954.

(39) (a) P. Gray, "Fifth Symposium on Combustion," Reinhold Publ. Corp., New York, N. Y., 1955, p. 535. (b) D. G. Alder, M. W. T. Pratt and P. Gray, *Chemistry and Industry*, 1517 (1955).

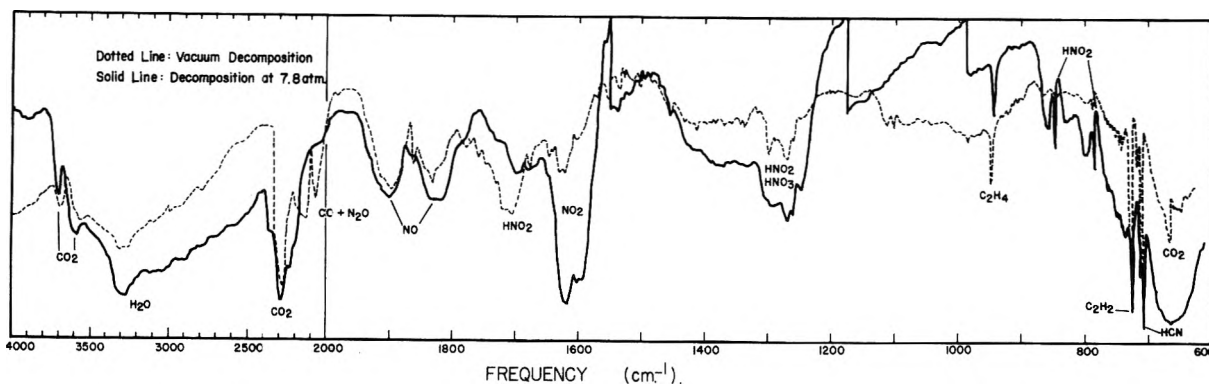


Fig. 15.—Spectra of quenched combustion products: solid line, decomposition at 114 p.s.i.; dashed line, vacuum decomposition.

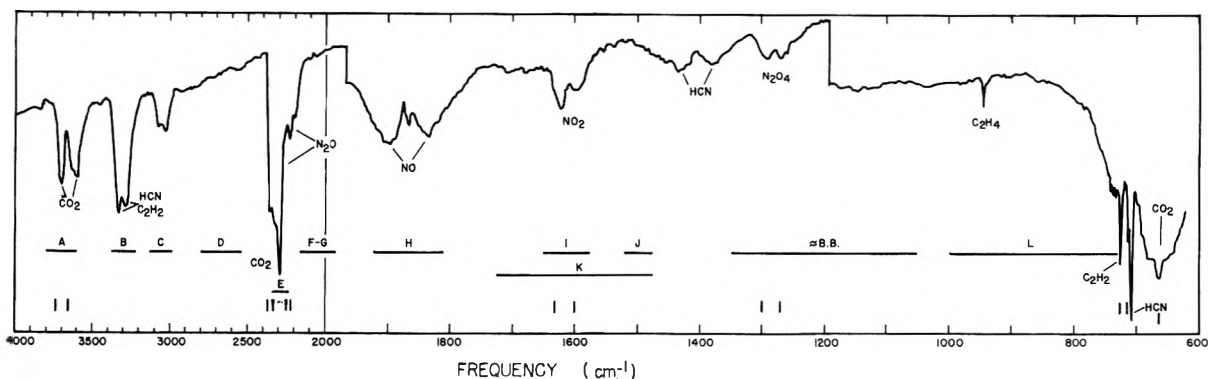
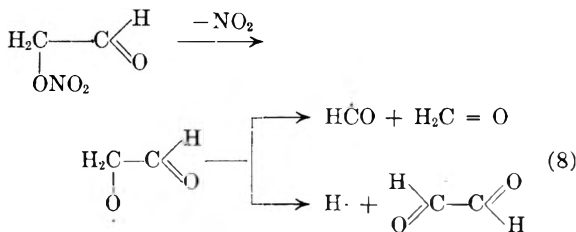


Fig. 16.—Flame spectra (bands A, B, ..., L) compared with spectra of quenched combustion products (continuous solid line) and the results of Wolfrom, *et al.*,<sup>18</sup> (vertical pips) on the spectra of the gaseous products from the slow thermal decomposition of nitro cellulose.

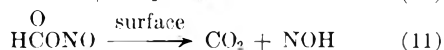
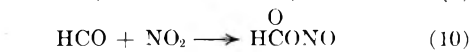
followed by



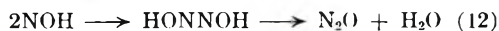
the important products at this point being formaldehyde, HCO and glyoxal. Although the relatively intense carbonyl stretching frequency bands near  $1700 \text{ cm}^{-1}$  of these combustion fragments are noticeably absent, in both the flame emission spectra and the spectra of the volatile end products of combustion, there is considerable kinetic precedence for these intermediates. They do, however, react rapidly with  $\text{NO}_2$  (Table III), and this may explain why we do not see them in the flame. Also, being relatively polar with hydrogen bonding tendencies, they would not show up clearly in the spectra of the room temperature quenched products.<sup>40</sup>

The importance of formaldehyde as a kinetic intermediate in the oxidation of hydrocarbons has been emphasized by many authors, quite recently by Scheer.<sup>41</sup> It has been found in the combustion of 18 different hydrocarbons, at temperatures of  $500\text{--}800^\circ$ .<sup>42</sup> It has in fact been suggested that

formaldehyde may be considered kinetically equivalent to a mixture of  $\text{H}_2 + \text{CO}$ .<sup>43</sup> The over-all activation energy for its oxidation is only about 21 kcal., so that this step should not lag far behind the initial break-down of the parent ester. The free radical HCO is generally considered to be unstable at normal combustion temperatures.<sup>42-44</sup> In many respects the oxidation mechanisms proposed for the oxidation of formaldehyde by  $\text{NO}_2$ <sup>45,46</sup> parallel quite closely the ordinarily proposed  $\text{O}_2$  mechanism, with  $\text{HO}_2$  in the later mechanism being replaced by HONO in the former. Scheer's mechanism for the  $\text{O}_2$ -oxidation of formaldehyde, when modified in this way, contains several features that are of particular interest. The modified mechanism would be this



Soot in the flame (see above) provides a relatively large area for the surface-catalyzed reaction 11. The nitroxyl formed in this step has a kinetic precedent,<sup>25,26,47</sup> and is used to explain the formation of nitrous oxide that is observed



To our knowledge, this is essentially the only

(43) D. W. E. Axford and R. G. W. Norrish, *Proc. Roy. Soc. (London)*, **192A**, 518 (1948).

(44) C. A. McDowell and J. H. Thomas, *Nature*, **162**, 367 (1948).

(45) J. H. Thomas, *Trans. Faraday Soc.*, **49**, 630 (1953).

(46) E. W. R. Steacie, *ref. 19*, p. 645.

(47) H. A. Taylor and C. Tanford, *J. Chem. Phys.*, **12**, 47 (1944).

(40) P. Gray, A. R. Hall and H. G. Wolfhard, *Proc. Roy. Soc. (London)*, **232**, 389 (1955).

(41) M. D. Scheer, "Fifth International Symposium on Combustion," Reinhold Publ. Corp., New York, N. Y., 1955, p. 435.

(42) E. W. Malmberg, *J. Am. Chem. Soc.*, **76**, 980 (1954).

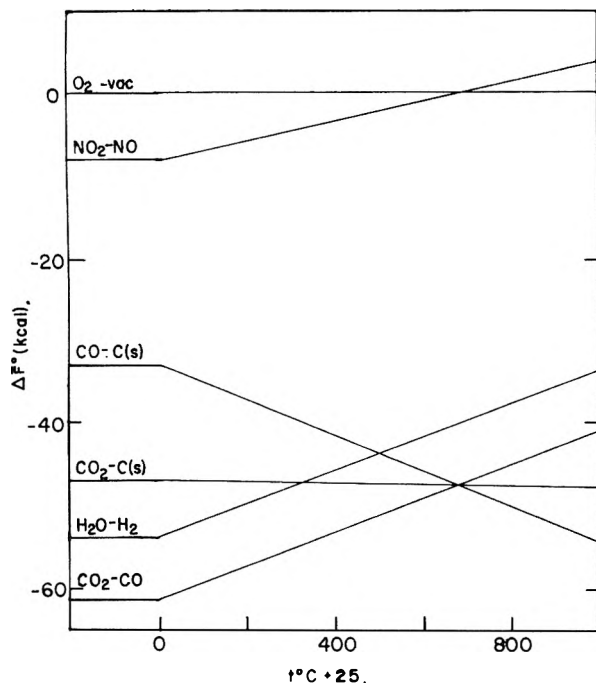


Fig. 17.—Some oxygen levels in the H-C-N-O system,  $\Delta F^\circ$  in kcal. for the reaction: oxygen-acceptor +  $\frac{1}{2}$  O<sub>2</sub> = oxygen-donor.

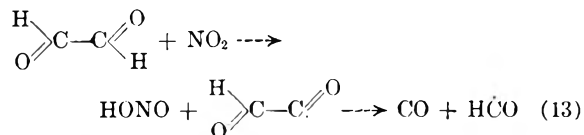
mechanism that has been suggested for the formation in the gas phase of this interesting synthetic product. The nitrous oxide itself is, of course, readily able to support combustion,<sup>48</sup> and would not be expected to build up to appreciable concentrations under normal flame conditions.

HONO, like nitrite and nitrate esters, and nitric acid, is relatively unstable with respect to cleavage of the RO-N bond<sup>29,49</sup> to give NO and OH, and, eventually, H<sub>2</sub>O.

Surface catalyzed reactions, like (11), may explain, too, why the black-body radiation temperatures in flames are often higher<sup>14</sup> than the calculated flame temperature.<sup>5a</sup>

At low temperatures, NOH presumably dimerizes to hyponitrous acid, HONNOH. This however is unstable at elevated temperatures,<sup>30</sup> and we should not expect to see it, in either the flame or the exhaust products.

The reactions of glyoxal are probably similar to those of formaldehyde. For example, initial abstraction of one of the aldehydic hydrogens by, say, NO<sub>2</sub> would lead to a sequence of reactions like



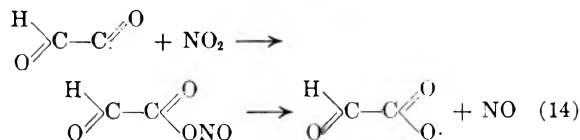
The straight thermal decomposition of glyoxal is known to produce CO, H<sub>2</sub>O, formaldehyde and carbon.<sup>50</sup> The activation energy for the reaction

(48) F. Kaufman and J. R. Kelso, *J. Chem. Phys.*, **23**, 1702 (1955); P. L. Robinson and E. J. Smith, *J. Chem. Soc.*, 3895 (1952); 1271 (1952).

(49) H. S. Johnson, L. Foering and R. J. Thompson, *THIS JOURNAL*, **57**, 390 (1953).

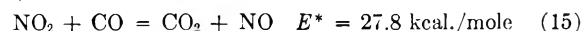
(50) E. W. R. Steacie, W. H. Hatcher and J. F. Horwood, *J. Chem. Phys.*, **3**, 291 (1935).

with NO<sub>2</sub> has been reported to be about 20 kcal./mole,<sup>20,32,51</sup> with NO, CO, CO<sub>2</sub> and H<sub>2</sub>O produced in the temperature interval of 160–210°. The mechanism suggested by Thomas<sup>51</sup> for the reaction in presence of relatively large amounts of NO<sub>2</sub> is



In the absence of large amounts of NO<sub>2</sub>, and at more elevated temperatures as in the flame radical, dismutation according to (13) probably predominates over these alternatives.

The CO produced probably reacts fairly rapidly (Table III) with NO<sub>2</sub><sup>20,52</sup>



The thermal decomposition of nitrocellulose has recently been discussed by Wolfrom, *et al.*<sup>18</sup> The formation of glyoxal by a route similar to that in nitroglycerol has been suggested; for example, initial cleavage of an O-N bond followed by a sequence of radical dismutations.

In this way, one accounts for the degradation of nitroglycerol and nitrocellulose, *via* formaldoxime, glyoxal and NO<sub>2</sub>, to NO, CO<sub>2</sub> and CO (in small amounts when NO<sub>2</sub> is present), and H<sub>2</sub>O. Hydrogen cyanide (reactions 1 and 2) and nitrous oxide (reaction 12) have also been accounted for. This leaves in Table II acetylene and ethylene, and soot to be accounted for.

If ethylene is not a synthetic product, and it seems unlikely that it is,<sup>53</sup> it must originate from the additives, or left-over solvent, and we shall not discuss it further.

The formation of soot, however, poses an interesting problem. At first sight, that we should find soot may not seem surprising inasmuch as nitrocellulose, which is the major component, is fuel rich; *i.e.*, there is insufficient oxygen present to combine with all the available carbon and hydrogen. And when allowance is made for the fact that the flame temperature is insufficient to cause much of the nitrogen present to be reduced beyond NO (the temperature being too low simply because NO is not reduced), the mixture appears still richer. But as Fig. 17 (for the construction and use of this figure, see ref. 54) shows, from a thermodynamic point of view it is hydrogen, not carbon, that is rejected first if the flame is fuel-rich. Even with nitrocellulose, with due allowance for the incomplete reduction of nitrogen, there is ample oxygen to take the carbon to CO.

The problem of carbon formation in flames has been reviewed comprehensively by Gaydon and Wolfhard.<sup>14</sup> According to their analysis, the critical parameter in a pre-mixed combustion mixture is the ratio of the number of carbon atoms present to the number of oxygen atoms,  $n_c/n_o$  and the temperature. When  $n_c/n_o$  is greater than 1, carbon should

(51) J. H. Thomas, *Trans. Faraday Soc.*, **48**, 1142 (1952).

(52) J. B. Brown and R. H. Crist, *J. Chem. Phys.*, **9**, 840 (1941).

(53) G. Porter, "Combustion Researcher and Reviews, 1955," Agardograph 9. Butterworths, London, 1955, p. 108; see also R. E. Ferguson, *Comb. and Flame Quart.*, **1**, 431 (1957).

(54) H. A. Bent, *THIS JOURNAL*, **61**, 1419 (1957).

form, above  $1000^{\circ}$ . Below  $1000^{\circ}$ , however, CO is unstable with respect to the disproportionation to  $\text{CO}_2$  and C (Fig. 17). Nevertheless, this cannot be the cause of carbon formation, even in our flames which are highly quenched, since the reaction  $2\text{CO} = \text{CO}_2 + \text{C}$  is known to be slow before  $1000^{\circ}$ .<sup>55</sup>

The mechanism of carbon formation has recently been considered by Porter,<sup>53</sup> who puts forth very cogent and persuasive thermodynamic arguments for reconsidering an acetylene mechanism of carbon formation. Porter's mechanism involved a condensation and splitting out of  $\text{H}_2$ . Several features of this mechanism are particularly attractive here. A polymerization mechanism that is tending toward thermodynamic equilibrium will, of course, be favored by high pressures, which may explain the high luminosity of our flames, compared to those of Needham and Powling<sup>6a</sup> (it was necessary to clear the bomb exit orifice of soot after every few runs). And we do see acetylene in the products. Also, black-body radiation is one of the first signs of emission detected from the flame, as one would expect if a thermal cracking mechanism operating early in the flame is responsible for the formation of the acetylene, as Porter postulates.

We note, somewhat hopefully, that a certain logical pattern appears to emerge from this discussion. Although the present account cannot pretend to completeness in a system as complex as the present one, it may be worth reiterating certain of the features of the present study. Compared to the low-pressure nitrate ester flames of previous studies, our propellant flames are noticeably sooty and luminous. Coupled with this is the fact that in the infrared the propellant flames appear to emit a nearly Planckian black-body continuum, characteristically interrupted at frequent intervals by molecular vibration-rotation bands viewed in absorption. Most if not all of these features seem to stem from the use of relatively high sustaining pressures in the cell. High pressures favor soot formation, which explains the gross spectroscopic features of the flames in the visible and infrared. The quenching of the flame by the pressurizing gas accounts for most of the complex but reproducible spectroscopic structure observed. Strong confirmation of this view is provided by the similarity of the flame spectrum to that of the quenched products of combustion. Direct detection of the elusive  $\text{NO}_2$ , possibly for the first time in the flame of a nitrate ester, suggests that such quenching may be useful in trapping, in a relatively cold "matrix," reactive fragments that might otherwise be quickly consumed by the flame. Kinetically, a simple Rice-Herzfeld free-radical type mechanism appears capable of accounting quite satisfactorily for the principal features of the thermal decomposition of nitroglycerine and nitrocellulose. In this way we are able without difficulty to account for all of the quenched products and all of the principal absorption bands of the propellant flames—with the lone, notable exception of the intense band D at  $2600\text{--}2700\text{ cm.}^{-1}$ .

**Band D.**—We can so far only speculate on the

broad, unassigned D band at  $2600\text{--}2700\text{ cm.}^{-1}$ . This is perhaps the most interesting band in the flame spectrum.

From its intensity it is tempting to conclude that this band represents a fundamental; if so, it necessarily involves the motion of a hydrogen atom. The only even moderately intense bands catalogued for this sparse region by Bellamy<sup>56</sup> are those belonging to hydrogen-bonded diketones. Were this the type of hydrogen involved, there should be present in the spectrum an even more intense band in the carbonyl region at  $1700\text{ cm.}^{-1}$ , contrary to our many observations of this region which in fact is remarkably free of any absorption (Fig. 10). Nonetheless, these facts do perhaps provide a clue to the type of hydrogen atom involved: it is not an ordinary hydrogen, such as one finds in  $\text{H}_2\text{O}$  ( $3756\text{ cm.}^{-1}$ ) or  $\text{H}_2\text{O}_2$  ( $3417$ ) or OH ( $3735$ ) or  $\text{NH}_3$  ( $3336$ ) or NH ( $3300$ ), or even CH ( $2900$ ).

In examining candidates for band D we may at the outset reject free radicals. First, no known electronically unexcited free radical has an X-H stretching frequency as low as  $2700\text{ cm.}^{-1}$ . Second and more convincing, the existence in the flame of appreciable concentrations of any free radical is almost certainly precluded by the fact that our propellant flames were thoroughly flooded with nitric oxide.<sup>57</sup> Indeed, it is perhaps worth pointing out that this is a critical deterrent in practice to realizing a completely satisfactory reduction of oxidized nitrogen in such propellant systems. The presence of nitric oxide stabilizes the system by combining with more reactive intermediates, thereby giving the flame time to expand and cool below that temperature at which nitric oxide itself is efficiently reduced.

If the species responsible for the relatively strong, broad absorption band D is not a free radical, neither, it would seem, is it a stable molecule, for this perplexing band is seen neither in the spectra of the quenched exhaust products (Figs. 15, 16), nor in the spectrum of the propellant either before or after thermal decomposition in potassium bromide pellets.<sup>31</sup>

Examining the postulated reaction mechanisms of the previous section for metastable reaction intermediates that might be lying about at appreciable concentration in a hot bath of nitric oxide, we find only one candidate, the precursor of nitrous oxide, NOH; or, possibly, HNO. Plausible theoretical grounds exist for the belief that either species might have an abnormally low hydrogen-stretching frequency. The presence of nitroxyl, as already pointed out, correlates nicely with the high soot and  $\text{CO}_2$  content of the flames, and the appearance in the exhaust gases of nitrous oxide. We note, too, from the contour of band D, that the molecule in question quite probably is not linear, and that both NOH and HNO are undoubtedly bent molecules.<sup>58</sup> In summary, it would seem by the method of Holmes<sup>59</sup> that at present the only explanation of band D is that here suggested.

(56) L. J. Bellamy, "The Infra-red Spectra of Complex Molecules," John Wiley and Sons, New York, N. Y., 1954.

(57) C. N. Hinshelwood, "The Kinetics of Chemical Change," Oxford Univ. Press, London, 1940.

(58) A. D. Walsh, *J. Chem. Soc.*, 2260 ff. (1953).

(55) Ref. 14; also, C. P. Fenimore, *J. Am. Chem. Soc.*, **69**, 3143 (1947).



**Acknowledgments.**—We should like to thank Miss Ann McHale for her assistance in many phases of this work, Mr. David Rotenberg for his

(59) R. E. Dickerson, P. J. Wheatley, P. A. Howell, W. N. Lipscomb and R. Schaeffer, *J. Chem. Phys.*, **25**, 606 (1956).

interest and helpful suggestions, and Mr. Earl Vincent for his invaluable contributions from the machine shop. The work was made possible by financial support from the Bureau of Ordnance, U. S. Navy, through contract with the University of Minnesota.

## KINETICS OF THE DECOMPOSITION OF NITRIC OXIDE IN THE RANGE 700–1800° C.

BY EDWARD L. YUAN, JOHN I. SLAUGHTER, WILLIAM E. KOERNER AND FARRINGTON DANIELS

*Contribution from the Department of Chemistry, University of Wisconsin, Madison, Wisconsin*

*Received February 18, 1959*

The decomposition of nitric oxide in packed Alundum vessels was measured by chemical and photometric analysis. Below 1100° the reaction is heterogeneous and zero order. Above 1400° and up to 1800° (the upper limit of the experimental measurements), the reaction is a simple homogeneous, bimolecular reaction. Between 1100 and 1400° both mechanisms are involved. The homogeneous second-order reaction rate is given by the expression  $k_2 = 1.9 \times 10^8 e^{-63,109/RT}$  atm.<sup>-1</sup> sec.<sup>-1</sup>

The kinetics of the reaction



were studied by German investigators half a century ago. They have been under investigation in this Laboratory for many years, particularly with reference to the fixation of atmospheric nitrogen in dual, gas-heated pebble bed furnaces packed with refractory pebbles for preheating and quick chilling<sup>1-3</sup> of the gases. A knowledge of the kinetics of the formation and decomposition of nitric oxide up to 2100° is important. More recently there has been interest in these reactions in connection with rockets and with smog. Several researches have been published including shock tube investigations at still higher temperatures, and the work in this Laboratory on the surface-catalyzed reactions from 700 to 1000° has been published.<sup>4-5</sup>

Koerner,<sup>6</sup> Slaughter<sup>7</sup> and Yuan<sup>8</sup> have measured the rate of decomposition of nitric oxide over a wide temperature range and under a variety of different experimental conditions. The work is summarized in this issue, which is honoring Dr. S. C. Lind. In these researches the nitric oxide was decomposed in a refractory tube, packed with refractory pellets and heated in an electric furnace, and the reaction was followed by chemical analysis or light absorption of the nitrogen dioxide produced. In all three investigations it was found that the decomposition is zero order and surface-catalyzed from 700° to about 1100° and homogeneous, second order at temperatures above 1400°. Between 1100 and 1400° the reaction is partly homogeneous and partly heterogeneous.

The packed reaction vessels were used to give a large heat capacity and thus retain isothermal

conditions during the exothermic decomposition. In the experiments carried out with flowing gas, the packing of refractory pebbles assured rapid attainment of the reactor temperature and ensured complete mixing and uniform gas flow across the whole area of the reaction tube. The reaction is particularly suitable for kinetic measurements by the flow method because there is no change in volume during the course of the reaction and hence no complicating factor in the residence time as the reaction proceeds.

Conclusions regarding the temperature effect and the activation energy can be in serious error if the measurements include, without proper corrections, the temperature region where both homogeneous and heterogeneous reactions occur simultaneously. In this region, the homogeneous reactions become increasingly more important at the higher temperatures.

### Preliminary Results

Koerner<sup>6</sup> carried out decomposition measurements in nitric oxide at full atmospheric pressure in a vertical, dense, Alundum tube heated with molybdenum heating coils around which purified nitrogen was passed. A packing of fine zirconia in a large steel shell provided thermal insulation. Alundum rods with 1/4 inch bore fitted snugly into each end of the Alundum tube and extended to the edge of the heated reaction zone, so that the time of entrance and exit through the indefinite temperature zones was reduced to a minimum. The hot reaction chamber, 10 inches long and 1 5/8 inches in diameter, was filled with zirconia pellets. The net space occupied by nitric oxide at atmospheric pressure was 241 ml. The temperature of the chamber was read through a window and along the bore of the inlet tube, using a calibrated optical pyrometer.

In most of the experiments a semi-flow method was used in which the hot reaction chamber was flushed out with a rapid stream of nitric oxide and then stopcocks at each end of the furnace were closed for a definite period of time, up to about a minute. Then one stopcock leading to an evacuated 2-liter bulb was opened and the reaction chamber gases were sucked into it and absorbed in a small volume of a solution of potassium hydroxide which it contained. The nitrites and nitrates were then reduced with Devarda's alloy to give ammonia which was distilled off and absorbed in a measured amount of acid solution. The amount of ammonia decomposed was determined by back titration, using a brom cresol green-methyl red indicator. The partial pressure of nitric oxide in the reaction chamber at different

(1) N. Gilbert and F. Daniels, *Ind. Eng. Chem.*, **40**, 1719 (1948).

(2) W. G. Hendrickson and F. Daniels, *ibid.*, **45**, 2613 (1953).

(3) E. D. Ermeneck, *Chem. Eng. Prog.*, **52**, 149 (1956).

(4) J. M. Fraser and F. Daniels, *THIS JOURNAL*, **62**, 215 (1958).

(5) C. S. Howard and F. Daniels, *ibid.*, **62**, 360 (1958).

(6) W. E. Koerner, Ph.D. Thesis, University of Wisconsin, 1949.

(7) J. I. Slaughter, Ph.D. Thesis, University of Wisconsin, 1953.

(8) E. L. Yuan and F. Daniels, Wright Air Development Center Report 56-536, p. 12, 1956.

times was calculated from the chemical titrations and the known volume and temperature, after making small corrections for the gas in the end capillary tubes.

In two experiments the nitric oxide was allowed to flow through continuously and the time of residence calculated from the volume of the chamber and the measured rate of flow. The results obtained by the two methods agreed closely.

The experiments were carried out at temperatures ranging from 900 to 1400°. The electric furnace was short-lived at 1400°. A typical experiment at 1200° is shown in Fig. 1. It is seen that in the course of 50 seconds, the nitric oxide changes from 1 atmosphere to about 1/4 atmosphere. It is evident that the reaction is second order as indicated by the straight line obtained by plotting the reciprocal of the partial pressure of nitric oxide against the time.

Plotting the logarithm of the specific reaction rate against the reciprocal of the absolute temperature gave a line which seemed to suggest an activation energy of about 70,000 cal. per mole at the higher temperatures and 24,500 cal. at the lower temperatures. The reaction was wall-catalyzed at the lower temperatures.

Slaughter<sup>7</sup> continued the work and built an electric furnace, heated with a coil of 1/4 inch molybdenum rod in helium, which was capable of going to 1900°. The reaction chamber of 390 ml. in the central section of a vertical Alundum tube was packed with 1/4 inch spheres of alumina. The temperature of the middle of the furnace tube was determined with a pyrometer, through a side tube. The readings were calibrated by reference to a platinum-platinum, rhodium thermocouple placed in the center of the spheres in the reaction chamber. The object of these experiments was to make measurements at temperatures well above the range where surface-catalysis could be even a minor factor.

Slaughter used a flow method with a rate of flow of 40 to 240 ml. per minute and an interstitial velocity of 0.6 to 6 cm. per second. He worked with 3% nitric oxide diluted to one atmosphere with helium, nitrogen and oxygen. It was planned to carry out the measurements under conditions prevailing in the Wisconsin process for nitrogen fixation. Another object of using nitric oxide at 0.03 atmosphere instead of 1 atmosphere was to reduce the evolution of heat and assure isothermal conditions in the flow method. This reduction of nitric oxide to 0.03 atmosphere, however, placed such a strain on the chemical analysis as to reduce the accuracy of the rate constants.

The nitric oxide, prepared from sodium nitrite and sulfuric acid with suitable purification, was allowed to stand with the diluent gas for two or three days to assure complete mixing. Samples were withdrawn from the furnace with water-cooled capillaries of stainless steel. The partial pressure of nitric oxide in the exit gases was determined by collecting the gas in an evacuated flask, sucking in 10 ml. of 30% neutral hydrogen peroxide, sucking in additional air to oxidize all the nitric oxide to nitrogen dioxide and titrating with sodium hydroxide, using brom cresol green as an indicator. The hydrogen peroxide must stand in contact with the gases for about 3 hours. The nitric oxide which decomposed into nitrogen and oxygen was indicated by the decrease in alkali titration. The partial pressure of the undecomposed nitric oxide was calculated from the titration and the known volume of the chamber.

A correction was studied<sup>7</sup> for the shrinkage in volume of the exit gases caused by the association reaction  $2\text{NO}_2 \rightleftharpoons \text{N}_2\text{O}_4$  at room temperature. Formulas were developed for this correction. The correction may be considerable at high pressures of nitric oxide, but it is negligible at pressures less than 0.03 atmosphere.

Slaughter found that at temperatures between 905 and 1047° a straight line was formed when the partial pressure of nitric oxide, starting with 0.03 atmosphere, was plotted against time out to 80 seconds. At higher temperatures, it became curved and the  $1/P_{\text{NO}}$  graph for a second-order equation was also curved—showing that the reaction is neither all zero order nor all second order. A typical experiment is recorded in Fig. 2. At still higher temperatures, the  $1/P_{\text{NO}}$  graphs became more nearly straight and the  $P_{\text{NO}}$  graphs became more curved—indicating the predominance of the homogeneous second order reaction. The activation energies obtained in this investigation appeared to be abnormally high.

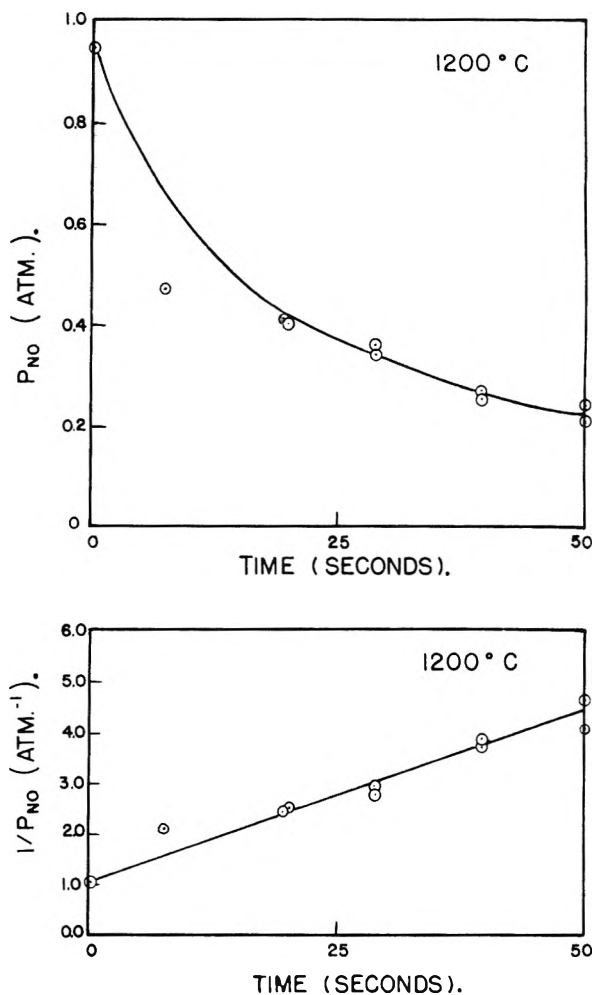


Fig. 1.—Decomposition rate of nitric oxide at 1200° measured by Koerner starting at 1 atmosphere.

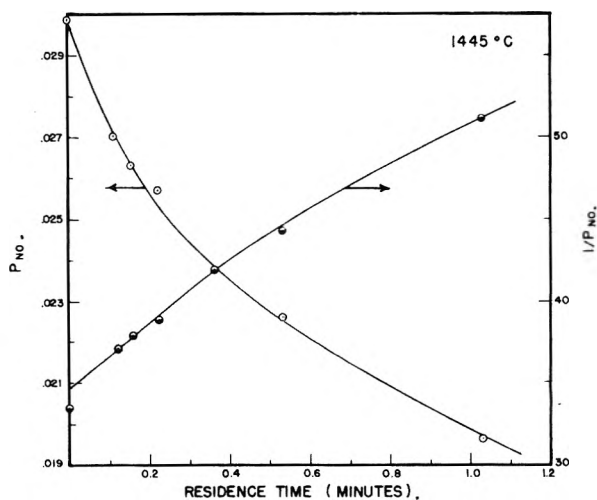


Fig. 2.—Decomposition rate of nitric oxide at 1445° expressed in atmospheres measured by Slaughter starting at 0.03 atmosphere.

### Experimental Data

Profiting by this earlier work Yuan<sup>8</sup> obtained the more accurate data which are reported here. He used a flow method with a dense Alundum tube packed with 1/4 inch Alundum spheres. He fol-

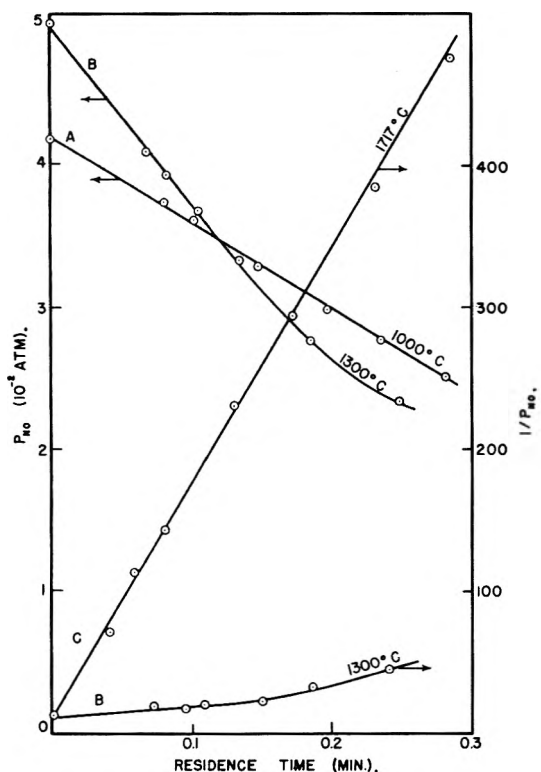


Fig. 3.—Decomposition rate of nitric oxide at various temperatures expressed in atmospheres measured by Yuan starting at about 0.04, 0.05 and 0.10 atmosphere.

lowed the course of the decomposition by measuring the amount of brown nitrogen dioxide produced. When the nitric oxide is less than half decomposed, the oxygen produced by the decomposition reacts with the remaining nitric oxide to give the nitrogen dioxide. Slaughter and R. J. Williams constructed an accurate photocell instrument with a split beam which operates a recording potentiometer using 4359Å light from a mercury lamp. It was adapted to this work. More details of its operation are given by Fraser.<sup>4</sup>

In this work from 700 to 1400°, a globar furnace manufactured by Harry W. Diertert Co. was used; from 1200 to 1600°, the molybdenum Alumund furnace<sup>7</sup> already described; and from 1400 to 1800°, a graphite furnace<sup>9</sup> constructed by Soulen was employed. Temperatures were read with a Leeds and Northrup pyrometer and checked with a thermocouple.

The rate of flow of gases was measured with a calibrated flow meter and the photometer was calibrated with mixtures of nitrogen dioxide and air. The concentrations for calibration were determined by absorbing in measured sodium hydroxide and hydrogen peroxide and titrating with standard acid, using brom cresol green as an indicator. The errors for the association reaction  $2\text{NO}_2 \rightleftharpoons \text{N}_2\text{O}_4$  were shown to be negligible as was also the possible error produced by the formation of  $\text{N}_2\text{O}_3$ <sup>10</sup> pointed out by Kaufman and Kelso.<sup>11</sup>

The concentration of nitric oxide in the inert gas was 5 to 15%, sufficiently low to avoid serious

evolution of heat and ensure isothermal conditions and yet high enough to obtain reasonably good accuracy.

As in the earlier work the decomposition of nitric oxide was found to be zero order and heterogeneous, surface catalyzed in the temperature range 700 to 1100° and homogeneous and second order at temperatures above 1400°. At temperatures between 1100 and 1400° both heterogeneous and homogeneous reactions take place simultaneously. The contribution from each depends on the area of the surface and its chemical nature, on the temperature and on the concentration. At 1 atmosphere pressure the homogeneous bimolecular reaction is faster than it is at 0.03 atmosphere and so at 0.03 atmosphere, it is necessary to go to higher temperatures than at 1 atmosphere in order to eliminate the relative effects of surface catalysis.

The rate of decomposition of the over-all reaction over the whole temperature range is

$$-\frac{dP_{\text{NO}}}{dt} = k_1 + k_2 P_{\text{NO}}^2$$

where  $k_1$  is the specific rate constant for the zero-order reaction obtained from the slope of the line  $P_{\text{NO}}$  versus time and  $k_2$  is the specific rate constant for the second-order reaction obtained from the slope of the line  $1/P_{\text{NO}}$  versus time.

Of the 67 experiments carried out at different temperatures, three typical ones are recorded in Fig. 3, where  $P_{\text{NO}} \times 10^{-2}$  atm. is plotted at the left and the reciprocals of  $P_{\text{NO}}$  are plotted at the right. The time is plotted in minutes. At 1000° the  $P_{\text{NO}}$  versus time relation gives a straight line indicating that  $k_2$  is so small that the homogeneous reaction is negligible, and that practically all the reaction goes by surface catalysis. At 1717°  $k_2$  is so much larger than  $k_1$  that the reaction is homogeneous and second order and a straight line is produced on the  $1/P_{\text{NO}}$  graph.

At 1300° with 0.05 atmosphere of nitric oxide, both the zero order heterogeneous and the bimolecular homogeneous reactions are taking place and neither graph gives a straight line.

All the data are summarized in Tables I and II, where the temperature and the diluting, inert gas are given. In all cases the walls and the packed spheres were of aluminum oxide and the nitric oxide varied from 4 to 15% by volume.

TABLE I  
SECOND-ORDER RATE CONSTANTS  
With Helium

|                                                |                    |                   |                   |      |      |      |      |
|------------------------------------------------|--------------------|-------------------|-------------------|------|------|------|------|
| Temp., °C.                                     | 1000               | 1100              | 1200              | 1300 | 1370 | 1400 | 1477 |
| $k_2$ (atm. <sup>-1</sup> sec. <sup>-1</sup> ) | 0.091 <sup>a</sup> | 0.13 <sup>a</sup> | 0.15 <sup>a</sup> | 0.25 | 0.60 | 0.75 | 3.7  |
| Temp., °C.                                     | 1527               | 1537              | 1577              | 1677 | 1697 | 1717 | 1814 |
| $k_2$ (atm. <sup>-1</sup> sec. <sup>-1</sup> ) | 3.9                | 5.0               | 6.9               | 10.5 | 17.3 | 27.3 | 56.0 |

With Nitrogen

|                                                |      |      |      |      |      |      |
|------------------------------------------------|------|------|------|------|------|------|
| Temp., °C.                                     | 1315 | 1419 | 1450 | 1505 | 1605 | 1670 |
| $k_2$ (atm. <sup>-1</sup> sec. <sup>-1</sup> ) | 0.54 | 1.6  | 2.5  | 3.6  | 5.4  | 18.8 |

<sup>a</sup> These three constants below 1300° are seriously affected by the surface catalysis.

In Fig. 4 the zero constants are plotted  $\log k_1$  versus  $10^4/T$ . At the high temperatures shown at the left of the plot, the bimolecular homogeneous reaction is introducing serious complications and at all temperatures shown, it is somewhat of a factor,

(9) J. R. Soulen, Ph.D. Thesis, University of Wisconsin, 1955.

(10) J. M. Fraser and F. Daniels, forthcoming publication.

(11) F. Kaufman and J. R. Kelso, *J. Chem. Phys.*, **23**, 1702 (1955).

TABLE II  
 ZERO-ORDER RATE CONSTANTS

| With Helium                                    |      |      |      |      |      |      |      |
|------------------------------------------------|------|------|------|------|------|------|------|
| Temp., °C.                                     | 700  | 800  | 850  | 870  | 900  | 950  | 970  |
| $k_1$ (atm. <sup>-1</sup> sec. <sup>-1</sup> ) | 0.73 | 1.0  | 1.0  | 0.95 | 1.1  | 1.1  | 1.0  |
| × 10 <sup>3</sup>                              |      |      |      |      | 0.71 |      |      |
| Temp., °C.                                     | 1000 | 1040 | 1050 | 1100 | 1150 | 1180 | 1200 |
| $k_1$ (atm. <sup>-1</sup> sec. <sup>-1</sup> ) | 1.4  | 1.1  | 1.1  | 1.1  | 1.5  | 1.5  | 1.2  |
| × 10 <sup>3</sup>                              | 1.2  |      |      | 0.97 | 1.1  |      | 1.3  |
| Temp., °C.                                     | 1240 | 1250 | 1300 | 1350 | 1400 | 1500 |      |
| $k_1$ (atm. <sup>-1</sup> sec. <sup>-1</sup> ) | 1.8  | 1.3  | 2.1  | 2.4  | 3.7  | 8.6  |      |
| × 10 <sup>3</sup>                              |      |      | 2.5  |      | 4.6  |      |      |
| With Nitrogen                                  |      |      |      |      |      |      |      |
| Temp., °C.                                     | 700  | 800  | 850  | 900  | 910  | 1000 | 1040 |
| $k_1$ (atm. <sup>-1</sup> sec. <sup>-1</sup> ) | 0.41 | 0.47 | 0.47 | 0.60 | 0.55 | 0.60 | 0.61 |
| × 10 <sup>3</sup>                              |      |      |      |      |      |      | 0.49 |
| Temp., °C.                                     | 1100 | 1110 | 1200 | 1300 |      |      |      |
| $k_1$ (atm. <sup>-1</sup> sec. <sup>-1</sup> ) | 0.57 | 0.80 | 0.67 | 1.1  |      |      |      |
| × 10 <sup>3</sup>                              | 0.51 |      | 0.75 | 1.0  |      |      |      |
| With Carbon Dioxide                            |      |      |      |      |      |      |      |
| Temp., °C.                                     | 700  | 800  | 900  | 1000 | 1100 |      |      |
| $k_1$ (atm. <sup>-1</sup> sec. <sup>-1</sup> ) | 0.23 | 0.30 | 0.33 | 0.45 | 0.45 |      |      |
| × 10 <sup>3</sup>                              |      |      |      |      |      |      |      |

becoming less at the lower temperatures. Although it is evident that the surface catalyzed reaction is affected only slightly by temperature, no conclusions can be drawn from these data regarding its energy of activation. This matter was studied later in detail<sup>4</sup> using larger surface areas and lower temperature. It was found that under the conditions prevailing in the later experiments, the activation energy for nitric oxide in helium catalyzed by Al<sub>2</sub>O<sub>3</sub> pellets of powder (not smooth spheres) was 31,600 cal. per mole.

The diluent gas affects the surface-catalyzed rate of decomposition considerably as indicated in Fig. 4. The rate is fastest in helium and slowest in carbon dioxide and intermediate in rate in the presence of nitrogen. This order is the same as that of the boiling points of the gases and it is concluded that the more condensable gases, carbon dioxide and nitrogen, are adsorbed on the catalytic surfaces, thereby reducing the effective surface and poisoning the catalyst.

In Fig. 5 the second-order graphs are shown in which log  $k_2$  is plotted against the reciprocals of the absolute temperature,  $10^4/T$ . These data are for the homogeneous, gas-phase bimolecular reaction and it is noted that there is no difference in decomposition rate with helium and with nitrogen. This fact strengthens the conclusions of the preceding paragraph that the nitrogen and carbon dioxide partially poison the catalytic surface in the heterogeneous reaction. The lowest three points corresponding to temperature below 1300° do not fall in line with the other points because the reaction is partly surface-catalyzed and the reaction abnormally fast. Under these conditions, the activation energy and the temperature effect are lower.

It is interesting that Koerner's measurements starting with higher pressures of nitric oxide and having higher reaction rates continue to give good bimolecular rate constants in competition with the surface catalyzed reaction at lower temperatures. They fit well onto the dotted line of Fig. 5.

The heat of activation for the bimolecular homogeneous decomposition of nitric oxide is 63,100 is

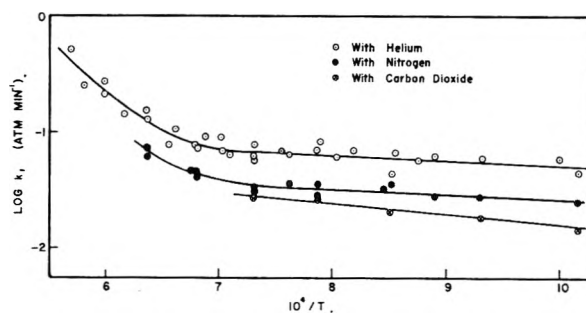


Fig. 4.—Zero-order plot.

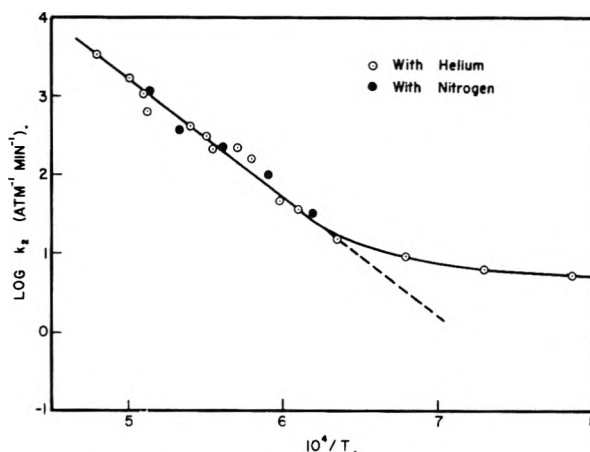


Fig. 5.—Second-order plot.

determined by least squares from these experimental data (excluding the three below 1300°). The Arrhenius equation for the specific reaction rate at different temperatures is

$$k = 1.9 \times 10^8 e^{-63,100/RT} \text{ atm.}^{-1} \text{ sec.}^{-1}$$

Different activation energies can be obtained by drawing lines through the scattered points in different temperature ranges, but the value obtained by least squares for all 17 sets of determinations is  $63.1 \pm 3.2$  kcal.

### Discussion

The data reported in this investigation are in agreement with some other published researches and the mechanisms appear to be well-established between 700 and 1800°—surface catalyzed zero order at the lower temperatures and bimolecular and homogeneous at the higher temperatures. Some of the earlier publications on this reaction were complicated by the presence of the two reactions occurring simultaneously.

The agreement of the work described here with that of Kaufman and Kelso<sup>11</sup> is excellent. Our activation energy for the homogeneous reaction of 63 kcal. is fortuitously almost within the limits of their activation energy  $63.8 \pm 0.6$  kcal., and the frequency factors are within a factor of 10. Kaufman and Kelso worked with nitric oxide at 0.065 to 0.65 atmosphere pressure in quartz flasks over the range 850 to 1178°. The present work was carried out at 0.05 to 0.15 atmosphere in packed Alundum vessels over the range 700 to 1800°.

The work described here is also in agreement with that of Wise and Frech<sup>12</sup> in finding that the reac-

(12) H. Wise and M. F. Frech, *J. Chem. Phys.*, **20**, 22, 1724 (1952).

tion at low temperatures is heterogeneous and that it is homogeneous at high temperatures and that nitrogen has a retarding effect on the heterogeneous decomposition. Wise and Frech report an activation energy for the heterogeneous reaction of 21.4 kcal. in quartz, close to that obtained with oxide catalysts in this Laboratory.<sup>4</sup> However, they report an activation energy of 78.2 kcal above 1327° for the homogeneous reaction, which is considerably higher than that described here and that reported by Kaufman and Kelso. They also report an acceleration by oxygen and an autocatalytic effect as the decomposition proceeds and oxygen is accumulated. No evidence of this oxygen effect was found in our work, but it is true that the oxygen concentrations were always low.

Vetter<sup>13</sup> studied the decomposition of nitric oxide in a flow system between 927 and 1627° and found an oxygen effect for which he proposed a chain reaction. Our results do not indicate an oxygen effect or a chain reaction in this temperature region. Vetter reports an activation energy of 75 kcal. for the bimolecular homogeneous decomposition, but Kaufman and Kelso<sup>11</sup> believe that his data at the highest temperatures where the surface effect is eliminated can give an activation energy of 61.7 kcal.

In the simplest bimolecular chemical reactions, there is some evidence that the frequency factor is equal to the number of molecules colliding. Converting the expression for  $k$  from atmospheres to moles per liter, evaluating the activation energy and calculating the frequency factor at 1727°

$$k = 3.1 \times 10^{10} \times 10^{-63,100/RT} \text{ l. mole}^{-1} \text{ sec.}^{-1}$$

The collision frequency calculated for nitric oxide at one atmosphere pressure at this temperature is about  $2.8 \times 10^{11}$  l. mole<sup>-1</sup> sec.<sup>-1</sup>. The experimentally determined frequency factor comes within a factor of about 10 of the collision frequency, indicating perhaps that not every collision between activated molecules is effective.

In simple bimolecular gas reactions, according to the Hirschfelder<sup>14</sup> approximate rule, the activation energy is roughly equal to 28% of the bonds broken. According to the older estimates for the

bond strengths of nitric oxide, the activation energy was 69 kcal. by this rule, but the presently accepted value of about 145 kcal. for the NO bond leads to an activation energy of 81 kcal. which is not in agreement with the experimental value of 63.

The results of this investigation show that as the temperature is raised above 1100 to 1400°, the decomposition goes by a different mechanism with a larger energy of activation. So it is possible that at still higher temperatures, above 1800°, another mechanism may take over with a still higher activation energy. The experimental facilities for direct measurement of the decomposition rate were severely strained to get up to 1800° and it was not possible to carry out experiments above this temperature.

Different techniques with flames and shock tubes have been used recently and they seem to indicate that at still higher temperatures, the reaction goes faster by an atom chain reaction than by the bimolecular reaction.

Zeldovich<sup>15,16</sup> suggests reactions involving atoms of oxygen and nitrogen on the basis of flame reactions above 1727°. He calculates an activation energy of  $81 \pm 10$  kcal.

Glick, Klein and Squire,<sup>17</sup> using shock tube techniques in the range 1727 to 2727° find an activation energy of  $92 \pm 5$  kcal. per mole for a mechanism involving the dissociation of oxygen into atoms.

The present researches are not able to contribute to the kinetics of the decomposition of nitric oxide at temperatures above 1800°.

**Acknowledgment.**—The authors wish to express appreciation for the support of this project for several years by the Research Committee of the University of Wisconsin with funds from the Wisconsin Alumni Research Foundation. They are glad to acknowledge also support from the Air Research and Development Command of the United States Air Force under contract No. AF 33(616)-338, and a fellowship (for W. E. K.) from E. I. du Pont de Nemours and Co.

(15) Y. B. Zeldovich, *Acta Physicochim.*, U.R.S.S., **21**, 577 (1946)

(16) Y. B. Zeldovich and I. Y. Chaplintokh, *Compt. rend. (SRSS)*, **65**, 871 (1949).

(17) H. S. Glick, J. J. Klein and W. Squire, *J. Chem. Phys.*, **27**, 850 (1957).

(13) K. Vetter, *Z. Elektrochem.*, **53**, 369, 376 (1949).

(14) J. O. Hirschfelder, *J. Chem. Phys.*, **9**, 645 (1941).

## THE KINETIC RADIATION EQUILIBRIUM OF AIR<sup>1</sup>

BY P. HARTECK AND S. DONDES

*Chemistry Department, Rensselaer Polytechnic Institute, Troy, N. Y.*

*Received February 18, 1959*

A study was made of the irradiation of nitrogen-oxygen mixtures near and at the kinetic radiation equilibrium, *i.e.*, the steady state of formation and decomposition of the constituents. Air and two to one nitrogen to oxygen mixtures showed that under proper irradiation conditions, all the oxygen is consumed to form nitrogen dioxide and nitrous oxide and, in some cases, a small surplus of nitric oxide remained. The kinetics of the nitrogen-oxygen system at the equilibrium is explained

### Introduction

Recently we have shown<sup>2</sup> that under favorable conditions, when dry air is irradiated with ionizing

radiation, most of the oxygen is consumed in the formation of nitrogen dioxide and nitrous oxide. These favorable conditions included a tempera-

(1) Work performed under U. S. Atomic Energy Commission Contract AT(30-3)-321, Task 1.

(2) P. Hardeck and S. Dondes, Second Conference on the Peaceful Uses of Atomic Energy (1958), paper No. p. 1769, in publication.

ture of about 175°, pressures of more than five atmospheres and an intensity of more than 10<sup>7</sup> Roentgen per minute. These high intensities had been achieved by using the recoil energy of the fission fragments, experimentally obtained by irradiating in a nuclear reactor, quartz vessels containing uranium-235 glass fibers of five micron diameter in contact with dry air. Based on the results of previous experiments,<sup>3</sup> and an improved knowledge of the associated kinetics,<sup>2</sup> the kinetic radiation equilibrium of dry air and other nitrogen-oxygen mixtures was reinvestigated at lower intensities (about 10<sup>6</sup> R./min.) for a total dose similar to that previously used, *i.e.*, about 5 × 10<sup>10</sup> Roentgen. By kinetic radiation equilibrium, we mean, under irradiation the steady state of formation and decomposition of constituents.

When a mixture of nitrogen and oxygen is irradiated with ionizing radiation, a complex series of reactions take place. The ionizing radiation forms ions and excites and dissociates the molecules of the gases. In pure gases, through ion recombination, additional molecules of the same species will dissociate. Under our experimental conditions, nitrogen with the highest ionization potential in the system will transfer its charge to molecules with lower ionization potentials. Thus, the nitrogen ions cannot form additional nitrogen atoms by ion recombination. This fact is important because only the nitrogen atoms can undergo reactions which form or decompose fixed nitrogen (see Table I), whereas the oxygen atoms undergo a series of reactions without changing the balance of fixed nitrogen. Fortunately, not all the reactions which occur need be considered in understanding the kinetics of the system. (Table I lists a number of reactions for which there is definitive experimental

evidence.) A more complete listing of all reactions will be presented in a future paper.

In Table I, the *G*-values are given for the dissociation processes and the rate constants (*K*-values at 300°K.) for the reactions which result from the dissociation products. It may be seen that for most of the compounds which are formed, there are several possible formation or decomposition reactions. The net result for nitrogen fixation at any instant is *dependent on temperature, pressure and radiation intensity*. However, reactions which are dominant in the early stages of irradiation may be unimportant near the equilibrium stage (*i.e.*, stationary state of the system) and *vice versa*. In Table I, reactions 3, 5, 8, 9 and 12 can be considered to be the predominant reactions when the nitrogen-oxygen system is irradiated with ionizing radiation. However, at or near equilibrium, reaction 10b predominates and under certain conditions, reaction 8d. Optimum conditions for nitrogen fixation, therefore, are difficult to determine and may be different from those conditions where the largest amount of the nitrogen oxides are in kinetic radiation equilibrium.

### Experimental

The experimental technique has previously been described.<sup>3,4</sup> Quartz vessels were filled with gas mixtures and irradiated in the Brookhaven National Laboratory reactor. In experiments 297, 298 and 299, one milligram of uranium glass fibers of 25 micron diameter and with a concentration of approximately 10% uranium-235, was placed in the reaction vessels in contact with the gas mixture. All other experiments did not have uranium bearing glass fibers. In the group of experiments using air and uranium-235, the percentage of ionizing radiation due to the fission recoil particles was 60%; that due to the N<sub>14</sub>(n,p)C<sub>14</sub> reaction, 30%; and that due to other types of ionizing radiation present in the reactor, 10%. In the group of experiments with air but in the absence of uranium, the percentage of the ionizing radiation due to the N<sub>14</sub>(n,p)C<sub>14</sub> was 75% and that due to the other types of radiation within the reactor, 25%. In the samples with the nitrogen concentration less than 78%, the contributor of the N<sub>14</sub>(n,p)C<sub>14</sub> reaction to the amount of ionizing radiation decreased proportionately to the nitrogen concentration.

The two different sets of experiments, *i.e.*, with and without the addition of a small amount of uranium-235, were performed for the following reason: We had stated in the earlier investigations,<sup>3</sup> that in the gas phase, for the same dose, the reaction rate introduced by the ionizing radiation is independent of the nature of the ionizing radiation. However, we desired to investigate this fact more fully. In our earlier experiments we had added a small amount of uranium-235 as an oxide or incorporated it in glass fibers which increased the radiation intensity by a factor of about one hundred. But the nitrogen fixation is intensity dependent since at higher radiation intensities the stationary nitric oxide concentration increases which in turn leads to an increased reaction rate for the nitrogen atoms with nitric oxide, reaction 9. Although this effect on the over-all reaction can be assessed by calculation, it seemed advisable to perform experiments with similar intensities where in one series the recoil energy is dominant, and in the other, where it is not, but in both cases, the absorbed energy per particle is about the same (see Table II). The temperature inside the reaction vessel in the group without the uranium bearing glass fibers is almost equal to the ambient temperature of 85°. The addition of the uranium bearing glass fibers to the vessels at an ambient temperature of 175°, causes a certain degree of indefiniteness in the temperature since 0.1 mg. of uranium-235 will re ease about one hundredth of a watt per cubic centimeter, which in turn will increase the temperature within the vessel by a few degrees. The fibers themselves will have a temperature of a few hundred degrees

TABLE I

#### REACTIONS MOST IMPORTANT TO THE NITROGEN FIXATION PROCESS

|                                                |                                                      |
|------------------------------------------------|------------------------------------------------------|
| (1) N <sub>2</sub> → 2N                        | <i>G</i> -value 4-5                                  |
| (2) O <sub>2</sub> → 2O                        | <i>G</i> -value 8                                    |
| (3) N + O <sub>2</sub> = NO + O                | <i>k</i> <sub>3</sub> = 10 <sup>-16±.02</sup>        |
| (4) NO <sub>2</sub> + O = NO + O <sub>2</sub>  | <i>k</i> <sub>4</sub> = 10 <sup>-12</sup>            |
| (5) 2NO + O <sub>2</sub> = 2NO <sub>2</sub>    | <i>k</i> <sub>5</sub> = 10 <sup>-37±0.2</sup>        |
| (6) 2NO ⇌ N <sub>2</sub> O <sub>4</sub>        |                                                      |
| (7) (a) NO <sub>2</sub> → NO + O               | <i>G</i> = 12                                        |
| (b) NO <sub>2</sub> → N + O + O                | <i>G</i> = 0.5                                       |
| (8) (a) N + NO <sub>2</sub> = 2NO              | <i>k</i> <sub>8a</sub> = 5 × 10 <sup>-14±0.5</sup>   |
| (b) N + NO <sub>2</sub> = N <sub>2</sub> O + O | <i>k</i> <sub>8b</sub> = 3.2 × 10 <sup>-14±0.5</sup> |
| (c) N + NO <sub>2</sub> + N <sub>2</sub> + 2O  | <i>k</i> <sub>8c</sub> = 2 × 10 <sup>-14±0.5</sup>   |

The above values, 8a,b,c are precise relative to each other

|                                                                                                    |                                               |
|----------------------------------------------------------------------------------------------------|-----------------------------------------------|
| (d) N <sub>2</sub> O <sub>4</sub> + N → NO <sub>2</sub> + 2NO                                      |                                               |
| (9) NO + N = N <sub>2</sub> + O                                                                    | <i>k</i> <sub>9</sub> = 10 <sup>-12±0.5</sup> |
| (10) (a) N <sub>2</sub> O → N <sub>2</sub> + O                                                     | <i>G</i> = 9                                  |
| (b) N <sub>2</sub> O → NO + N                                                                      | <i>G</i> = 3                                  |
| (11) NO → N + O                                                                                    | <i>G</i> = 3                                  |
| (12) <sup>a</sup> (a) NO <sup>+</sup> + e <sup>-</sup> = N + O                                     |                                               |
| (b) NO <sup>+</sup> + e <sup>-</sup> = NO + <i>hν</i>                                              |                                               |
| (c) NO + M <sup>+</sup> = NO <sup>+</sup> + M                                                      |                                               |
| (13) N <sub>2</sub> <sup>+</sup> + O <sub>2</sub> = NO <sup>+</sup> + NO (no indication)           |                                               |
| N <sub>2</sub> <sup>+</sup> + NO <sub>2</sub> = N <sub>2</sub> O + NO <sup>+</sup> (no indication) |                                               |

<sup>a</sup> These reactions are illustrative of many possible reactions involving ions depending on conditions.

(3) P. Harteck and S. Dondes, *J. Chem. Phys.*, **27**, 546 (1957).

(4) P. Harteck and S. Dondes, *ibid.*, **26**, 1727 (1957).

TABLE II IRRADIATION

| 1        | 2          | 3                              | 4                                  | 5             | 6              | 7                     | 8                                       | 9               | 10                         | 11                                 | 12                                     | 13                                   | 14                                               | 15                                                      |
|----------|------------|--------------------------------|------------------------------------|---------------|----------------|-----------------------|-----------------------------------------|-----------------|----------------------------|------------------------------------|----------------------------------------|--------------------------------------|--------------------------------------------------|---------------------------------------------------------|
| Sample # | U-235, mg. | Neutron flux $\times 10^{-12}$ | Gas                                | Pressure, mm. | Pressure, atm. | Irradiation time, hr. | Irradiation time, min. $\times 10^{-4}$ | Pile temp., °C. | Dose $R^a \times 10^{-10}$ | $R^a / \text{min.} \times 10^{-5}$ | Erg abs. $\text{cm.}^3 \times 10^{-4}$ | g. gas $\text{cm.}^3 \times 10^{-3}$ | $\Sigma \text{erg.} \text{cm.}^3 \times 10^{-9}$ | $\Sigma \text{e.v. per molecule } N_2 \text{ absorbed}$ |
| 297      | 0.1        | 0.3                            | Air                                | 1520          | 2.0            | 576                   | 3.46                                    | 175             | 2.6                        | 7.5                                | 8.1                                    | 2.4                                  | 2.7                                              | 34                                                      |
| 298      | 0.1        | .3                             | Air                                | 1520          | 2.0            | 1250                  | 7.50                                    | 175             | 5.6                        | 7.5                                | 8.1                                    | 2.4                                  | 6.0                                              | 75                                                      |
| 299      | 0.1        | .3                             | Air                                | 1520          | 2.0            | 1824                  | 11.0                                    | 175             | 8.2                        | 7.5                                | 8.1                                    | 2.4                                  | 8.9                                              | 112                                                     |
| 391      | .00        | .5                             | Air                                | 2600          | 3.42           | 307                   | 1.84                                    | 85              | 1.55                       | 8.4                                | 9.1                                    | 4.0                                  | 1.68                                             | 12.2                                                    |
| 393      | .00        | .5                             | Air                                | 2500          | 3.29           | 618                   | 3.71                                    | 85              | 3.0                        | 8.1                                | 8.8                                    | 3.9                                  | 3.25                                             | 25                                                      |
| 395      | .00        | .5                             | Air                                | 2500          | 3.29           | 933                   | 5.60                                    | 85              | 4.6                        | 8.1                                | 8.8                                    | 3.9                                  | 5.0                                              | 37.5                                                    |
| 349      | .00        | .5                             | Air                                | 10000         | 13.1           | 1140                  | 6.84                                    | 85              | 22.5                       | 33                                 | 36                                     | 15.5                                 | 24.3                                             | 46                                                      |
| 350      | .00        | .5                             | Air                                | 9000          | 11.8           | 1140                  | 6.84                                    | 85              | 20.4                       | 30                                 | 32.5                                   | 13.9                                 | 22                                               | 46                                                      |
| 351      | .00        | .5                             | Air                                | 9000          | 11.8           | 2820                  | 16.9                                    | 85              | 51.0                       | 30                                 | 32                                     | 13.9                                 | 55                                               | 117                                                     |
| 355      | .00        | .5                             | Air                                | 2100          | 2.76           | 1140                  | 6.84                                    | 85              | 4.6                        | 6.8                                | 7.3                                    | 3.1                                  | 5.0                                              | 46                                                      |
| 356      | .00        | .5                             | Air                                | 2100          | 2.76           | 1140                  | 6.84                                    | 85              | 4.6                        | 6.8                                | 7.3                                    | 3.1                                  | 5.0                                              | 46                                                      |
| 357      | .00        | .5                             | Air                                | 2300          | 3.03           | 2820                  | 16.9                                    | 85              | 12.7                       | 7.5                                | 8.1                                    | 3.6                                  | 13.7                                             | 117                                                     |
| 361      | .00        | .5                             | N <sub>2</sub> O decomposed        | 1500          | 1.97           | 1140                  | 6.84                                    | 85              | 3.0                        | 4.4                                | 4.8                                    | 2.4                                  | 3.3                                              | 42                                                      |
| 370      | .00        | .5                             | N <sub>2</sub> :O <sub>2</sub> 2:1 | 2400          | 3.16           | 1140                  | 6.84                                    | 85              | 4.8                        | 7.0                                | 7.6                                    | 3.7                                  | 5.2                                              | 42                                                      |
| 362      | .00        | .5                             | N <sub>2</sub> O decomposed        | 1500          | 1.97           | 2820                  | 16.9                                    | 85              | 7.5                        | 4.4                                | 4.8                                    | 2.4                                  | 8.1                                              | 103                                                     |
| 371      | .00        | .5                             | N <sub>2</sub> :O <sub>2</sub> 2:1 | 2400          | 3.16           | 2820                  | 16.9                                    | 85              | 12.0                       | 7.0                                | 7.5                                    | 3.8                                  | 13.0                                             | 103                                                     |
| 364      | .00        | .5                             | NO                                 | 1500          | 1.97           | 1140                  | 6.84                                    | 85              | 2.6                        | 3.7                                | 4.0                                    | 2.4                                  | 2.8                                              | 35                                                      |
| 367      | .00        | .5                             | N <sub>2</sub> :O <sub>2</sub> 1:1 | 2600          | 3.42           | 1140                  | 6.84                                    | 85              | 4.4                        | 6.5                                | 7.0                                    | 4.2                                  | 4.8                                              | 35                                                      |
| 365      | .00        | .5                             | NO                                 | 1500          | 1.97           | 2820                  | 16.9                                    | 85              | 6.4                        | 3.8                                | 4.1                                    | 2.4                                  | 6.9                                              | 87                                                      |
| 368      | .00        | .5                             | N <sub>2</sub> :O <sub>2</sub> 1:1 | 2400          | 3.16           | 2820                  | 16.9                                    | 85              | 10.2                       | 6.0                                | 6.5                                    | 3.9                                  | 11                                               | 87                                                      |

Experiments completed after manuscript submitted in which 4:1 3:2 and 1:1 mixtures of nitrogen and oxygen were irradiated for a period of 3746 hours showed no variation in the above results.

<sup>a</sup>  $2.08 \times 10^9$  ion pairs/cm.<sup>3</sup> <sup>b</sup> Less accurate method of analysis.

and it is therefore difficult to assess the "real" temperature of the system. The system may behave as if the average temperature inside the vessel would be about 25° higher than the ambient temperature.

Results

The experimental data is listed in Table II. Since the literature denotes the energy absorbed by a system in various units, we have used a number of the more common units in Table II. With large integrated doses of radiation required to reach the chemical radiation equilibrium, we have listed in row 15 of Table II, the electron volts absorbed per molecule of nitrogen. It should be noted that these values for nitrogen must be increased by about 50% for the triatomic molecules, nitrous oxide and nitrogen dioxide.

Some explanations are necessary in connection with Table II. In experiments, 297, 298 and 299, dry air was irradiated with an intensity of  $7.5 \times 10^5$  R./min., which made it possible to reach the kinetic radiation equilibrium with a dose of  $8.2 \times 10^{10}$  R. in experiment 299 within a few months. The striking result is that at the equilibrium there is practically no oxygen, only nitrogen, nitrogen dioxide and nitrous oxide. As previously shown, in this series of experiments, the small amount of uranium-235 added contributed more to the ionizing radiation, due to the fission recoil energy, than the ionizing radiation from the reactor.

In experiments 349, 350, 355 and 356, air was irradiated without the presence of uranium-235. In all these cases the kinetic radiation equilibrium had

been reached and all the oxygen had been consumed. If this result seems odd, we would like to state that in the analysis procedure the sample was immersed in liquid air after "cooling down" for a few weeks, during which time all the nitric oxide could have reacted with any oxygen present to form nitrogen dioxide. The oxides of nitrogen were condensed out with the condensate having a greenish-blue color (N<sub>2</sub>O<sub>3</sub>), indicating the presence of more nitric oxide and dinitrogen trioxide during the irradiation than oxygen. Since in the gas phase and at room temperature, the dissociation  $N_2O_3 \rightleftharpoons NO + NO_2$  lies to the right ( $k_p = \sim 0.1$ ), the nitric oxide concentration can be calculated assuming the nitric oxide concentration is equal to or slightly less than one-half the oxygen concentration. In the experiments where a substantial partial pressure of oxygen remains, the nitric oxide concentration will be small, whereas in those experiments where there is practically no oxygen at the equilibrium during the irradiation, the nitric oxide concentration will be substantial (see Table II).

In the four experiments, 361, 362, 370 and 371, the filling ratio of nitrogen to oxygen was two to one. Samples 361 and 362 were initially filled with nitrous oxide and placed in a furnace where the nitrous oxide was thermally decomposed. During the thermal decomposition, a small amount of nitrogen dioxide was formed. It will be noted that in experiments 361 and 370, not all the oxygen is consumed and the equilibrium reached. In experiments 367 and 368, the filling ratio of nitrogen to

OF N<sub>2</sub>-O<sub>2</sub> MIXTURES

| 16                                  | 17                               | 18                               | 19                        | 20                        | 21                         | 22                          | 23                                       | 24                                      | 25                                   | 26           | 27                                                | 28                         | 29                                                           |
|-------------------------------------|----------------------------------|----------------------------------|---------------------------|---------------------------|----------------------------|-----------------------------|------------------------------------------|-----------------------------------------|--------------------------------------|--------------|---------------------------------------------------|----------------------------|--------------------------------------------------------------|
| Rad./<br>min.<br>× 10 <sup>-3</sup> | Initial<br>N <sub>2</sub><br>mm. | Initial<br>O <sub>2</sub><br>mm. | Final<br>% N <sub>2</sub> | Final<br>% O <sub>2</sub> | Final<br>% NO <sub>2</sub> | Final<br>% N <sub>2</sub> O | [N <sub>2</sub> O]<br>[NO <sub>2</sub> ] | [N <sub>2</sub> O]<br>[N <sub>2</sub> ] | $G_N =$<br>60 $\frac{[N_2O]}{[N_2]}$ | [NO],<br>mm. | [NO <sub>2</sub> ]<br>[NO],<br>× 10 <sup>-2</sup> | [NO <sub>2</sub> ],<br>mm. | N <sub>2</sub> O <sub>4</sub> ⇌<br>2NO <sub>2</sub><br>α = % |
| 3.4                                 | 1185                             | 320                              | 65.5                      | 6.25                      | 12.6                       | 6.3                         | 0.50                                     | 0.096                                   | 5.75                                 | 0.5          | 3.8                                               | 192                        | 99.5                                                         |
| 3.4                                 | 1185                             | 320                              | 62.8                      | 0.55                      | 17.0                       | 6.8                         | .40                                      | .108                                    | 6.5                                  | 1.6          | 1.6                                               | 260                        | 99.5                                                         |
| 3.4                                 | 1185                             | 320                              | 62.5                      | 0.10                      | 17.4                       | 6.9                         | .39                                      | .110                                    | 6.6                                  | 2.5          | 1.1                                               | 270                        | 99.5                                                         |
| 2.3                                 | 2030                             | 545                              | 72.2                      | 10.7                      | 8.9                        | 3.98                        | .45                                      | .055                                    | 3.3                                  | 0.26         | 9.0                                               | 232                        | 89                                                           |
| 2.3                                 | 1950                             | 525                              | 67.5                      | 4.7                       | 14.7                       | 4.64                        | .313                                     | .069                                    | 4.1                                  | 0.39         | 9.5                                               | 368                        | 84                                                           |
| 2.3                                 | 1950                             | 525                              | 62.5                      | 0.00                      | 20.3                       | 5.72                        | .282                                     | .092                                    | 5.5                                  | 2.4          | 2.1                                               | 507                        | 83                                                           |
| 2.3                                 | 7800                             | 2100                             | 60.0 <sup>b</sup>         | .00                       | 17.1                       | 4.0                         | .234                                     | .067                                    | 4.0                                  | 4.0          | 4.3                                               | 1710                       | 57                                                           |
| 2.3                                 | 7000                             | 1890                             | 60.2 <sup>b</sup>         | .00                       | 17.9                       | 4.35                        | .243                                     | .072                                    | 4.3                                  | 3.9          | 4.2                                               | 1615                       | 58                                                           |
| 2.3                                 | 7000                             | 1890                             | 64.0                      | .00                       | 20.1                       | 3.9                         | .194                                     | .061                                    | 3.6                                  | 3.9          | 4.7                                               | 1810                       | 56                                                           |
| 2.3                                 | 1640                             | 441                              | 65.3                      | .00                       | 19.9                       | 5.1                         | .256                                     | .078                                    | 4.7                                  | 2.3          | 1.8                                               | 419                        | 84                                                           |
| 2.3                                 | 1640                             | 441                              | 65.3                      | .00                       | 19.9                       | 5.1                         | .256                                     | .078                                    | 4.7                                  | 2.3          | 1.8                                               | 419                        | 84                                                           |
| 2.3                                 | 1790                             | 483                              | 67.5                      | .00                       | 19.5                       | 4.5                         | .23                                      | .067                                    | 4.0                                  | 2.3          | 1.95                                              | 450                        | 82                                                           |
| 2.1                                 | 1000                             | 500                              | 48.8                      | 8.6                       | 21.4                       | 5.47                        | .255                                     | .112                                    | 6.75                                 | 0.34         | 9.5                                               | 321                        | 85                                                           |
| 2.1                                 | 1600                             | 800                              | 49.3                      | 8.7                       | 21.5                       | 4.85                        | .225                                     | .098                                    | 5.9                                  | 0.36         | 14.4                                              | 517                        | 83                                                           |
| 2.1                                 | 1000                             | 500                              | 46.1                      | 0.00                      | 31.5                       | 5.6                         | .18                                      | .12                                     | 7.2                                  | 2.4          | 1.95                                              | 473                        | 82                                                           |
| 2.1                                 | 1600                             | 800                              | 47.0                      | 0.00                      | 31.9                       | 5.2                         | .163                                     | .11                                     | 6.6                                  | 2.9          | 2.6                                               | 767                        | 75                                                           |
| 1.8                                 | 750                              | 750                              | 20.5                      | 8.6                       | 45.3                       | 4.13                        | .09                                      | .202                                    | 12.1                                 | 0.41         | 16.5                                              | 678                        | 80                                                           |
| 1.8                                 | 1300                             | 1300                             | 37.2                      | 30.4                      | 18.25                      | 3.5                         | .19                                      | .094                                    | 5.6                                  | 0.21         | 22.4                                              | 473                        | 82                                                           |
| 1.8                                 | 750                              | 750                              | 25.2                      | 6.3                       | 43.7                       | 4.8                         | .110                                     | .19                                     | 11.4                                 | 0.43         | 15.2                                              | 655                        | 80                                                           |
| 1.8                                 | 1200                             | 1200                             | 32.0                      | 19.6                      | 29.4                       | 4.1                         | .14                                      | .128                                    | 7.7                                  | 0.25         | 28                                                | 704                        | 78                                                           |

oxygen was one to one whereas in experiments 364 and 365, the vessels were filled with nitric oxide. Experiments 367, 368, 364 and 365 gave quite different results. By increasing the integrated dose, the change in the concentration of the nitrogen oxides is smaller when going from experiment 364 to 365, than from experiment 367 to 368. We therefore conclude that experiment 365 is almost at the kinetic radiation equilibrium. At a filling ratio of one to one for nitrogen and oxygen, not all the oxygen has been consumed. It could very well be possible by using lower intensities, a more favorable temperature region and higher pressures, even in a one to one filling mixture of nitrogen and oxygen, to consume all the oxygen with the formation of the oxides of nitrogen.

### Discussion

This paper is concerned with only the state near and at equilibrium of irradiated nitrogen-oxygen mixtures. In an earlier paper<sup>5</sup> preliminary results were published on the nitrogen, oxygen, nitrogen dioxide and nitrous oxide radiation equilibrium. However, those reported experiments had been done at much higher radiation intensities and predominantly in a pressure region of one atmosphere. Under the latter conditions, a relatively high stationary nitric oxide concentration was established during the radiation, which prevented the build-up of nitrogen dioxide concentrations higher than 10 to 12%.

At the kinetic radiation equilibrium the rate of formation and the rate of decomposition for each component must be equal, *i.e.*,  $\Sigma N_{(fixed)} = \text{const.}$ ;  $\Sigma N_2 = \text{const.}$ ;  $\Sigma O_2 = \text{const.}$ ;  $\Sigma N_2O = \text{const.}$ ;  $\Sigma NO_2 = \text{const.}$  Since nitrogen atoms react relatively slowly with oxygen and with only a small amount of oxygen present in most of our experiments near equilibrium conditions, the contribution of fixed nitrogen by reaction 3 can be disregarded. The nitrogen atoms will therefore react predominantly according to reaction 8 and with nitric oxide according to reaction 9. Reaction 9 is more than one order of magnitude faster than reaction 8, but since the nitrogen dioxide concentration is in some experiments more than two orders of magnitude larger than that of nitric oxide, most of the nitrogen atoms will react with nitrogen dioxide. In experiments with a high concentration of nitric oxide, the rate of reaction of nitrogen atoms with nitric oxide is of importance in determining the behavior of the system.

From our earlier experiments and by comparison with Kistiakowsky and Volpi's experiments,<sup>6</sup> the ratio of reaction 8a to 8b to 8c could be exactly determined. Note that by summing up reactions 8a, 8b and 8c, the amount of fixed nitrogen does not become radically changed, since the ratios of reaction 8a to 8b to 8c is 2.5 to 1.6 to 1.0. According to reaction 8a, 2.5 nitrogen atoms are fixed as nitric oxide; according to reaction 8b, 1.6 fixed nitrogen

(5) P. Hartek and S. Dondes, *Nucleonics*, **14**, 7, 22 (1956).

(6) G. B. Kistiakowsky and G. G. Volpi, *J. Chem. Phys.*, **27**, 1141 (1957).



molecules are converted from nitrogen dioxide to nitrous oxide; and according to reaction 8c, one fixed nitrogen molecule is destroyed. Summing up, for the 5.1 nitrogen atoms which have reacted with nitrogen dioxide, only 0.1 nitrogen dioxide molecule was consumed, or zero within the limits of error. Thus the over-all effect of the nitrogen atoms plus nitrogen dioxide reaction is negligible on the total nitrogen dioxide concentration present in the system.<sup>7</sup>

Near equilibrium reaction 3 can be neglected and with no additional fixed nitrogen as nitrogen dioxide or nitric oxide formed by reactions 8a, 8b and 8c, the only source for additional nitric oxide and nitrogen dioxide was the decomposition of nitrous oxide by ionizing radiation as we showed in an earlier system of equations.<sup>5</sup> Nitrous oxide can only be formed by reaction 8b and only that fraction 1.6/5.1 or 31% of the nitrogen atoms which react with nitrogen dioxide, will form nitrous oxide. From the stationary nitrous oxide concentration it is possible to estimate the amount of nitrogen atoms which reacted with nitrogen dioxide. Nitrogen atoms will be predominantly formed by the dissociation of nitrogen molecule ( $G_N = 8.5 \pm 0.5$ ), and additional nitrogen atoms will be formed from the dissociation of the following: nitrous oxide from reaction 10b with a  $G$ -value of 3; nitrogen dioxide from reaction 7b with a  $G$ -value of 0.5; and nitric oxide from reaction 11 with a  $G$ -value of 3. From the stationary nitrous oxide concentration, one can calculate the amount of nitrogen atoms which reacted with nitrogen dioxide. Since in most cases the nitrogen atom formation from molecular nitrogen is predominant and these nitrogen atoms primarily react with nitrogen dioxide, the following equation applies

$$2G_{(N_2)} [N_2] \times \frac{1.6}{5.1} = 1.5[N_2O]G_{N_2O} \quad (A)^8$$

where the factor

$$\frac{1.6}{5.1} = \frac{k_{8b}}{k_{8a} + k_{8b} + k_{8c}}$$

and the factor 1.5 take into consideration the larger stopping power of nitrous oxide as compared with molecular nitrogen. Equation A leads to the relation

$$2G_{(N_2)} = G_N = 60 \frac{[N_2O]}{[N_2]} \quad (B)$$

From equation B, the  $G_N$  value can be estimated. If a  $G_N$  of  $8.5 \pm 0.5$  is accepted from other experimental and theoretical considerations, the validity of equation B can be checked. From Table II, column 25, the  $G_N$  is usually found to be less than 8.5, with a few cases about half this value. If we refine our calculations, we must consider the nitrogen atoms consumed by reaction with nitric oxide (reaction 9), and from the decomposition of nitrogen dioxide (reaction 7). In experiments 364 and 365, where the nitrogen dioxide concentration is much larger than the nitrogen concentration, and where the nitric oxide concentration is so small that its reaction with nitrogen atoms can be disregarded, the uncorrected values for  $G_N$  exceed the value of

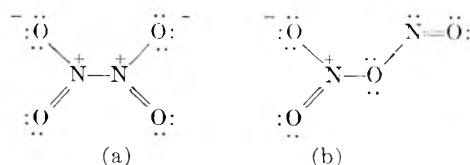
(7) For a more detailed discussion see reference 2.

(8)  $G_{N_2O}$  taken as 12.5.

8.5. By more refined calculations which take into account the nitrogen atoms formed from the nitrogen dioxide decomposition, and the  $N_2O_4 \rightleftharpoons 2NO_2$  equilibrium (see later), a fair agreement with the  $G_N$  value of 8.5 can be obtained.

In addition to the balance of nitrous oxide, the balance of nitrogen dioxide plus nitric oxide must also hold. If a considerable amount of nitrogen atoms react with nitric oxide, then the nitrogen dioxide plus nitric oxide balance would not hold, because our only source for the nitric oxide formation which has been considered, is the decomposition of nitrous oxide. In the decomposition of nitrous oxide by ionizing radiation, one-fourth is decomposed into nitric oxide and a nitrogen atom (reaction 10b) and with the  $G$ -value for the nitrous oxide decomposition of twelve, the  $G$ -value for the nitric oxide formation from the nitrous oxide decomposition is three. In a gas mixture with 5 volume % nitrous oxide, for every 100 electron volts absorbed, the nitric oxide production is  $3/2 \times G_{N_2O} \rightarrow NO + N \times 0.05 = 0.225$ . With 60% nitrogen in the mixture, for every 100 electron volts absorbed, five nitrogen atoms are formed. If only 5% of these nitrogen atoms would react with the nitric oxide, the losses of fixed nitrogen could not be balanced. But at equilibrium, where no oxygen is present, a relatively high nitric oxide concentration will build up and then more than 5% of the nitrogen atoms will react with the nitric oxide. The way out of this dilemma must be an additional reaction to form fixed nitrogen as nitrogen dioxide or nitric oxide. Up to this point we have totally disregarded ion reactions. But we would like to state that we have not found any indication that an ion reaction of the type\*:  $N_2^+ + O_2 = NO + NO^+$ , exists. Furthermore, at equilibrium, almost no oxygen is present in many cases. An ion reaction of the type:  $N_2^+ + NO_2 \rightarrow N_2O + NO^+$  is energetically possible, but if it could occur to an appreciable amount, a larger nitrous oxide concentration should be found at equilibrium. The only ion reaction we have observed was the  $NO^+$  decomposition due to ion recombination which would only increase the deficit of fixed nitrogen.

Up to this point, the reaction of nitrogen atoms with nitrogen dioxide (reaction 8a, 8b, 8c) has only been considered. Under conditions where a substantial concentration of nitrogen dioxide is present as nitrogen tetroxide, the reaction of nitrogen atoms with nitrogen tetroxide must also be considered. According to Pauling,<sup>9</sup> the structure of nitrogen tetroxide may be according to (a) or (b)



From geometric considerations according to con-

\* Author's note after submission of manuscript: However the presence of the excited  $N_2^+(B^2\Sigma_u^+)$  in addition to the other excited states of  $N_2$  had been found by emission spectroscopy using the alpha particles of Po-210 to irradiate air.

(9) L. Pauling, "The Nature of the Chemical Bond," Cornell University Press, Inc., New York, N. Y., 1945.

figurations (a) and (b), it does not seem likely that nitrogen atoms reacting with nitrogen tetroxide will give the same ratio of reaction products as shown by reactions 8a, 8b and 8c. It seems that reaction 8a will become relatively more abundant, but from energetic considerations, it is dubious whether reaction 8c will proceed at all. The reaction  $N_2O_4 + N = NO_2 + N_2 + 2O$  may not occur since the heat of formation of nitrogen tetroxide from nitrogen dioxide is 8.1 kcal. and the over-all reaction is slightly endothermic.<sup>10</sup> We conclude that under conditions where  $2NO_2 \rightleftharpoons N_2O_4$  equilibrium is not entirely shifted to the left, the nitrogen fixation becomes enhanced since the nitrogen atoms will react with the nitrogen tetroxide molecules to form  $NO_2 + 2NO$  and possibly to a minor extent  $N_2O + O$ . This seems the only method of explaining how at equilibrium a nitric oxide concentration can be built up to the extent that after waiting for a few weeks for the quantitative back reaction of  $2NO + O_2 \rightarrow 2NO_2$  to proceed, a small residual nitric oxide concentration could be observed which indicates that the nitric oxide concentration at the kinetic radiation equilibrium was somewhat larger than the oxygen concentration. In column 29 of Table II,  $\alpha$ , the degree of dissociation of nitrogen tetroxide into nitrogen dioxide, is listed. By comparing experiments 297, 298 and 299 where the ambient temperature was 175°, with experiments 391, 393 and 395, where the ambient temperature was 85°, it will be noted that the equilibrium is reached at the lower temperature with 37 electron volts absorbed per particle, whereas at 175°, the equilibrium is not reached with 34 electron volts per particle and only approached equilibrium with 75 electron volts per particle. This seems in contradiction with our earlier statements<sup>5</sup> that at higher temperatures the nitric oxide or nitrogen dioxide formation is enhanced. But this statement did hold for the earlier stages of the reaction where there was only the competition for

the nitrogen atoms between reactions 3 and 8. But at higher nitrogen dioxide concentrations, reaction 3 is without importance and at lower temperatures more nitrogen tetroxide is in equilibrium with nitrogen dioxide. This is the reason that in experiment 395, the equilibrium is reached with a smaller integrated dose than in experiment 299.

### Conclusions

1. If air is irradiated with an intensity of about  $3 \times 10^5$  rad./min. for a few months, the oxygen is consumed to an extent where there is no oxygen left, and in a few cases there is a small surplus of nitric oxide. The composition of the system at 85° is: 62.5%  $N_2$ ; 20.3%  $NO_2$ ; and 5.7%  $N_2O$ .
2. Under the same conditions, if a mixture of 2/3  $N_2$  and 1/3  $O_2$  is irradiated, all the oxygen is consumed and the composition of the system at 85° is: 46.5%  $N_2$ ; 31.5%  $NO_2$ ; and 5.5%  $N_2O$ .
3. Under the same conditions, if a mixture of 1:1  $N_2 : O_2$  is irradiated, not all the oxygen is consumed and the composition of the system at 85° is: 25%  $N_2$ ; 6.4%  $O_2$ ; 43.7%  $NO_2$ ; 0.48%  $N_2O$ .
4. In the region of the equilibrium, reaction 10b becomes the dominant nitric oxide and consequently the nitrogen dioxide producing reaction. For every 100 electron volts absorbed in the mixture, about 0.20 molecule of nitric oxide is formed.
5. Under conditions where the nitrogen tetroxide concentration has to be considered, the reactions 8a, 8b and 8c must be modified.
6. There is no indication of the occurrence of ion reactions in the nitrogen-oxygen system which form or decompose fixed nitrogen. The only exception is  $NO^+$  which has the lowest ionization potential and consumes fixed nitrogen by ion recombination and dissociation.

**Acknowledgments.**—We would like to thank Mr. R. W. Powell, Mr. J. J. Floyd, Mr. F. Reeve and Mr. M. McKenna, of the Reactor Department, Brookhaven National Laboratory, for their kind advice and cooperation in the pile experiments.

(10) Since  $NO_2 + N \rightarrow N_2 + 2O + 3 \text{ kcal.}$

# FISCHER-TROPSCH SYNTHESIS MECHANISM STUDIES. THE ADDITION OF RADIOACTIVE KETENE TO THE SYNTHESIS GAS

BY G. BLYHOLDER AND P. H. EMMETT

*Department of Chemistry, The Johns Hopkins University, Baltimore, Md.*

*Received February 19, 1959*

When methylene labeled radioactive ketene is added to the extent of 2% of the Fischer-Tropsch synthesis gas being passed over an iron catalyst at 247° and one atmosphere, the hydrocarbon products are found to have approximately a constant radioactivity per mole which is equal to the specific activity of the added ketene. When the synthesis gas with 0.25% ketene is passed over a cobalt catalyst at 185° and one atmosphere pressure the hydrocarbon products have an approximately constant activity per mole which is about one-third the specific activity of the added ketene. The results are interpreted as indicating that due to the large build in of ketene the intermediate complex in Fischer-Tropsch synthesis may resemble an adsorbed ketene molecule. A chain building mechanism is proposed in which the complex is bound to the surface by a metal-oxygen bond as well as a carbon-metal bond.

## Introduction

The kinetics and mechanism of the Fischer-Tropsch synthesis have been the subject of a considerable number of studies<sup>1-3</sup> and much conjecture. Several schemes have been advanced<sup>2</sup> for stepwise chain growth which give an isomer and carbon number distribution similar to that actually observed. It has been demonstrated<sup>4-7</sup> by radioactive tracer experiments that various oxygen containing compounds, when added in a small percentage to 1:1 H<sub>2</sub>:CO synthesis gas and passed over a reduced iron catalyst at about 235°, add into the Fischer-Tropsch synthesis products. In particular, primary alcohols having 2, 3, or 4 carbon atoms were found to yield products with a constant radioactivity per mole for hydrocarbons with a higher number of carbon atoms than the added alcohol. It was found that from 1/3 to 1/2 of the synthesis products originated from the added alcohol even though it constituted only 1 to 1.5% of the synthesis gas. It was also shown that growth of chains occurred at the carbon atom to which the OH group was attached. These experiments led to the proposal that the surface complex involved in chain building is similar to an adsorbed alcohol. It was further proposed that the C<sub>1</sub> complex is also alcoholic in nature. The apparent behavior of methyl alcohol and formaldehyde, when added to the synthesis gas, suggested that neither of these gave a C<sub>1</sub> complex identical to that formed from CO and H<sub>2</sub>.

One of the earliest mechanisms proposed for the Fischer-Tropsch synthesis involved the formation of CH<sub>2</sub> units on the surface. These were believed to polymerize to form hydrocarbons. Tracer experiments, however, do not for the most part support the idea that CH<sub>2</sub> units are formed from surface carbide and then become part of the synthesis products.

With these results in mind, it was decided to try ketene as an additive to the synthesis gas. Ketene could be expected to react in a number of ways. One of the known reactions of ketene is to split in two to form CO and methylene. Ketene labeled on only the methylene carbon was used. If the mechanism of the synthesis involves the polymerization of CH<sub>2</sub> units it might be expected that the products obtained when radioactive ketene was added to the synthesis gas would have a radioactivity per molecule which was directly proportional to the number of carbon atoms in the molecule.

If the ketene molecules break up into CO and methylene but the methylene does not take part in the synthesis then the result would probably be highly radioactive methane with the synthesis products relatively free of radioactivity.

The third principal reaction would be for ketene to act as a chain initiator in a manner analogous to alcohols. In this case the radioactivity per molecule of the synthesis products would be independent of the number of carbon atoms per molecule.

## Experimental

The ketene was made by decomposing acetone over a hot wire.<sup>8</sup> Acetone labeled with C<sup>14</sup> in the 1- or 3-position was obtained from the Isotope Specialties Company. Nitrogen gas with a flow rate maintained just large enough to keep acetone and ketene flowing smoothly through the system was used. About 35% of the acetone decomposed was converted to ketene. This efficiency was measured by bubbling the ketene bearing gas through a measured volume of 3 N sodium hydroxide solution. Ketene forms acetic acid in basic solutions. The solution was then back titrated with acid. The difference between the amounts of acid and base then was used to calculate the ketene production. The purity of the ketene was determined by running a sample of the liquid product through a vapor phase chromatography apparatus using Perkin-Elmer column D. Besides acetone the principal impurities were ethylene and a little propylene. The ethylene was removed by pumping on the sample while it was melting. The acetone and propylene were removed by distilling under vacuum from a Dry Ice trap to a liquid nitrogen trap.

A Fischer-Tropsch synthesis apparatus similar to previously described<sup>4,5</sup> ones, was used. A furnace at 350° was used to decompose any metal carbonyl formed in the carbon monoxide tank. A Deoxo unit in the hydrogen line converted oxygen to water over a catalyst, leaving the oxygen concentration less than one part per million. The catalyst was held in place in the furnace between glass wool plugs inside of a 23 mm. o.d. Pyrex tube. Down the center of this tube was a 4 mm. Pyrex tube which contained the thermocouple used to measure the furnace temperature. The

(1) H. H. Storch, N. Golumbic and R. B. Anderson, "The Fischer-Tropsch and Related Syntheses," John Wiley and Sons, Inc., New York, N. Y., 1951.

(2) R. B. Anderson, "Catalysis," Vol. 4, Chap. 1, 2, 3, Ed. by P. H. Emmett, Reinhold Publ. Corp., New York, N. Y., 1956.

(3) L. J. E. Hofer, "Catalysis," Vol. 4, Chap. 4, Ed. by P. H. Emmett, Reinhold Publ. Corp., New York, N. Y., 1956.

(4) J. T. Kummer, H. H. Podgurski, W. B. Spencer and P. H. Emmett, *J. Am. Chem. Soc.*, **73**, 564 (1951).

(5) J. T. Kummer and P. H. Emmett, *ibid.*, **75**, 5177 (1953).

(6) W. K. Hall, R. J. Kokes and P. H. Emmett, *ibid.*, **79**, 2983 (1957).

(7) R. J. Kokes, W. K. Hall and P. H. Emmett, *ibid.*, **79**, 2989 (1957).

(8) H. Gilman and A. H. Blatt, "Organic Syntheses," Coll. Vol. 1, John Wiley and Sons, Inc., New York, N. Y., 1941, p. 330.

temperature over the central 16 cm. of the furnace is within 2° of the temperature at its center (which is the maximum temperature within the furnace) when the furnace is at 300°.

The per cent. ketene contained in hydrogen bubbled through liquid ketene at -98° in the ketene bubbler is independent of the hydrogen flow rate from 50 to 200 cc./min. A flow of about 100 cc./min. was used during an actual run. The temperature of -98° was obtained with a methyl alcohol slush.

Synthesis products were analyzed on a vapor phase chromatography apparatus (Perkin-Elmer Model No. 154-B) using columns A and D. The radioactivity of the product is determined by using a conventional Geiger counter in connection with a special cell, shown in Fig. 1. The gas from the fractometer is led directly into the special cell. In the cell the reaction products are condensed on the surface cooled by liquid nitrogen. The radioactivity of any component condensed by the liquid nitrogen can be measured by the Geiger counter. Thus, as a particular component of the reaction products comes through the fractometer, it is separated, its amount and identity as determined by previous calibration are recorded, and its radioactivity is measured in the special cell. As long as there is liquid nitrogen in the cell the counting rate stays constant until a new radioactive component enters. As the new component enters the cell the counting rate increases to a new level. The difference in the two levels is then a measure of the radioactivity of the new component. The counting rate is therefore recorded as a series of increasing steps with each step representing the activity of a new component.

TABLE I

PRODUCT DISTRIBUTION OVER IRON CATALYST WITH KETENE ADDED TO SYNTHESIS GAS

|                      | Relative, moles |                             | Relative, moles |
|----------------------|-----------------|-----------------------------|-----------------|
| C <sub>3</sub>       | 1.43            | Propylene                   | 1.3             |
|                      |                 | Propane                     | 0.14            |
| C <sub>4</sub>       | 1               | Isobutane                   | .01             |
|                      |                 | Butene-1                    | .65             |
|                      |                 | Isobutylene                 |                 |
|                      |                 | <i>n</i> -Butane            |                 |
|                      |                 | Butene-2 <i>trans</i>       | .22             |
| Butene-2 <i>cis</i>  | .12             |                             |                 |
| C <sub>5</sub>       | 0.66            | 3-Methylbutene-1            | .05             |
|                      |                 | Pentene-1                   | .31             |
|                      |                 | 2-Methylbutene-1            |                 |
|                      |                 | <i>n</i> -Pentane           | .27             |
|                      |                 | Pentene-2 <i>trans</i>      |                 |
| Pentene-2 <i>cis</i> | .03             |                             |                 |
| C <sub>6</sub>       | 0.42            | Methylpentenes              | .08             |
|                      |                 | Hexene-1 + <i>n</i> -hexane | .15             |
|                      |                 | Hexene-3                    | .14             |
|                      |                 | Hexene-2                    | .05             |

TABLE II

PRODUCT DISTRIBUTION WITH COBALT CATALYST

|                | Relative, moles |                        | Relative, moles |
|----------------|-----------------|------------------------|-----------------|
| C <sub>3</sub> | 1               | Propane                | 1               |
| C <sub>4</sub> | 0.53            | Isobutylene            | 0.22            |
|                |                 | Butene-1               |                 |
| C <sub>5</sub> | .37             | <i>n</i> -Butane       | .24             |
|                |                 | <i>trans</i> -Butene-2 |                 |
|                |                 | <i>cis</i> -Butene-2   | .07             |
| C <sub>6</sub> | .34             | Pentene-1              | .10             |
|                |                 | <i>n</i> -Pentane      | .27             |

Runs were made on two catalysts. One catalyst (No. 613) is a reduced fused iron oxide. It is a singly promoted catalyst containing 1.80% SiO<sub>2</sub>, 1.60% ZrO<sub>2</sub> and 0.58% Al<sub>2</sub>O<sub>3</sub>. The furnace was charged with 50 cc. of 10 to 20

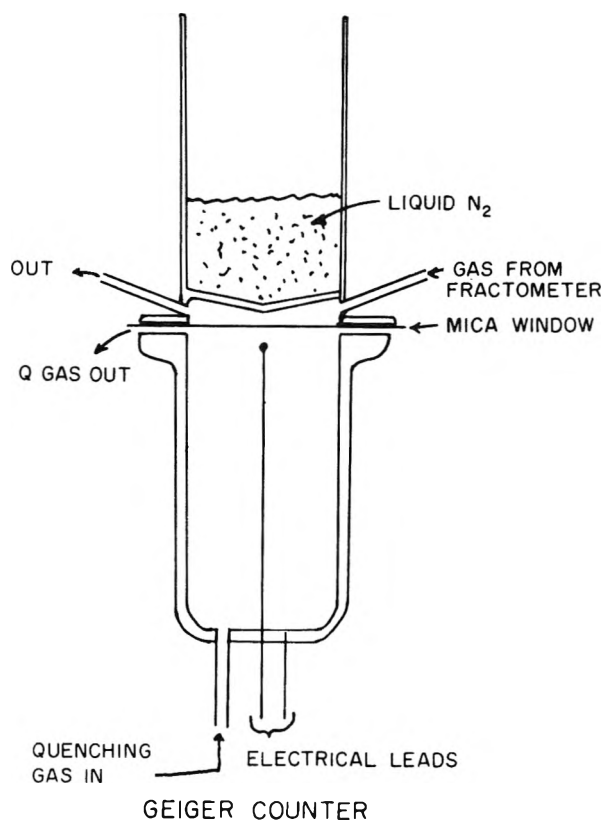


Fig. 1.—Radioactive counter cell used in conjunction with chromatographic apparatus.

mesh catalyst. After preliminary reduction at 250–450° the catalyst was reduced at 500° with H<sub>2</sub> at a space velocity of 1000 hr.<sup>-1</sup>. The ketene used in the run on the iron catalyst had an activity of 3,000 counts per minute per cc. During the run, which lasted 5 hours, the average contraction was 18% at 247°. The ketene comprised 2% of the synthesis gas. In a run on the previous day without ketene a contraction of 20% was found at 238°. On the next day a run without ketene gave a contraction of 23% at 252°.

The cobalt catalyst (No. 89EE) whose preparation is described by Anderson<sup>9</sup> and co-workers is composed of cobalt, thoria, magnesia and kieselguhr in the ratio of 100:6:12:200. The furnace was charged with 50 cc. of catalyst. After the initial reduction at 200–350° the catalyst was reduced at 400° overnight with a space velocity of H<sub>2</sub> of 1500. A run of 3.5 hours was made with 0.25% ketene added to the synthesis gas which was 2 parts H<sub>2</sub> to 1 part CO rather than the 1:1 ratio used with iron. With a synthesis gas flow of 180 cc./min. at 185° the contraction averaged 22%. Chromatographic analysis of the synthesis gas indicates that in addition to 0.25% ketene there was 0.01% butene-1 (radioactive) and that during the first 30 minutes of the run there was an average of 0.025% propylene (radioactive). After 30 minutes the amount of propylene was negligible. During the last 20 minutes of the run a small amount of radioactive acetone appeared in the synthesis gas. The impurities in the ketene were small enough to have no effect on the radioactivity of the Fischer-Tropsch products except for the butene-1 which probably increased the activity of the C<sub>4</sub> fraction somewhat.

The synthesis products were collected in a liquid nitrogen cooled trap during the run. After the run was over the trap was first warmed up to -80° and the gas evolved at this temperature was collected. Next the trap was warmed to room temperature and the gas evolved was collected. This provided convenient fractions for analysis in the vapor phase chromatographic apparatus.

## Results

In Table I is given the product distribution de-

(9) R. B. Anderson, W. K. Hall, H. Hewlett and B. Seligman, *J. Am. Chem. Soc.*, **69**, 3114 (1947).

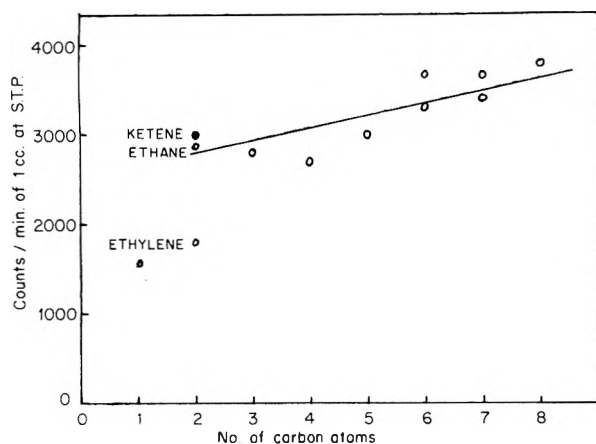


Fig. 2.—Radioactivity of hydrocarbon product with 2% radioactive ketene added to synthesis gas passed over an iron catalyst at 247° and one atmosphere pressure.

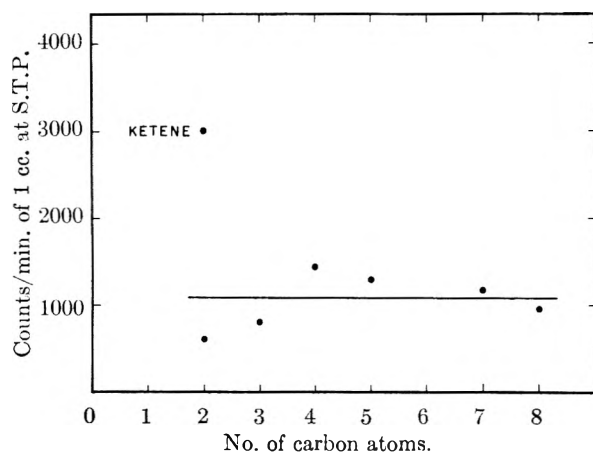


Fig. 3.—Radioactivity of hydrocarbon product with 0.25% radioactive ketene added to synthesis gas passed over a cobalt catalyst at 185° and one atmosphere pressure.

terminated by a single chromatographic analysis of the synthesis gas and products just after they left the furnace. The sample was collected with a syringe and rubber cap arrangement that allows samples to be collected during the run without disturbing the ordinary product collection apparatus. The product distribution is found to be about the same with and without ketene added. The total product distribution with respect to carbon number using an iron catalyst as given in Table I is within experimental error of that given by Weitkamp.<sup>10</sup> The product distribution using the cobalt catalyst is shown in Table II. These tables extend only from C<sub>3</sub> to C<sub>6</sub> since the column maintained in the chromatographic apparatus during a run to check the ketene content and impurities in the synthesis gas was useful for analysis over only this range.

The radioactivity of the hydrocarbon products is illustrated in Figs. 2 and 3. The radioactivity analysis was performed on the collected products after the run was completed.

Cuts corresponding to the various carbon numbers were run directly from the exit of the chromatographic column into the special cell and analyzed

(10) A. W. Weitkamp, H. S. Seelig, N. J. Bowman and W. E. Cady, *Ind. Eng. Chem.*, **45**, 343 (1953).

separately for radioactivity. For the runs over iron several points on the radioactivity *versus* carbon number curve were checked by the static method previously used and found to be in good agreement (3300 counts per minute per cc. for C<sub>4</sub> and 3800 counts per minute per cc. for C<sub>8</sub>).

#### Discussion

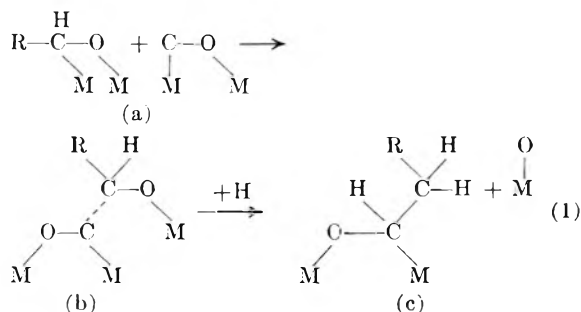
The tracer experiments clearly indicate that neither on cobalt or iron catalysts under the conditions of the present experiments do CH<sub>2</sub> groups from ketene build into the higher hydrocarbons extensively. This conclusion is evident from the approximately flat curve obtained in Figs. 2 and 3 on plotting the radioactivity of the hydrocarbons as a function of carbon number. The slight slope that actually exists could be due to experimental error or to a very slight build in of such CH<sub>2</sub> groups. Apparently ketene acts primarily to form an adsorbed complex that is capable of initiating the formation of surface chains leading to the building up of higher hydrocarbons.

The two most impressive results of the ketene experiments are the large build in obtained over iron and the fact that the build in is nearly as complete over cobalt as over iron catalysts. When radioactive ethyl, propyl or isobutyl alcohols are added as tracers over iron catalysts, at the most 1/2 to 1/3 of the hydrocarbon molecules formed come from the added alcohol; the remainder apparently come directly from CO and H<sub>2</sub>. Over cobalt catalysts the build in of the radioactive alcohols is so small that only about one hydrocarbon molecule in fifty is radioactive. In contrast to this, 2% radioactive ketene in the 1:1 H<sub>2</sub>CO mixture apparently monopolizes the surface to such an extent that practically all of the hydrocarbon molecules formed originate from a complex formed by the adsorption of ketene. The extra carbon atoms, of course, to form the C<sub>3</sub> and higher hydrocarbons come from the ordinary non-radioactive carbon monoxide in the gas mixture. Even over cobalt the ketene (in this case 0.25% in a 2:1 H<sub>2</sub>CO gas mixture) resulted in extensive incorporation into the higher hydrocarbons, one molecule in three of the hydrocarbons apparently originating from the ketene complex on the surface of the cobalt catalyst.

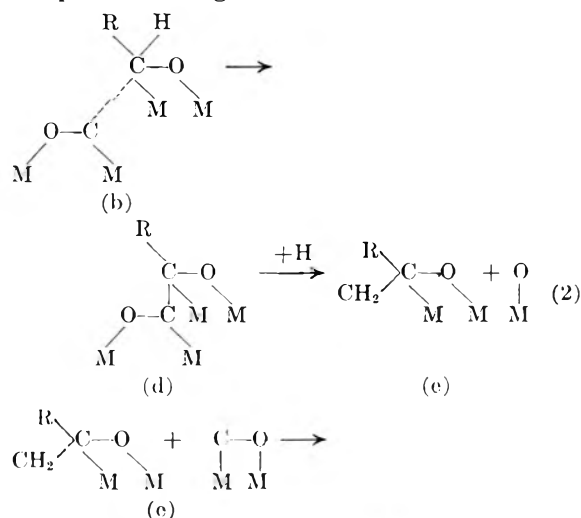
These results naturally lead to the question as to why ketene is more effective than the alcohols in acting as nuclei for the formation of the higher hydrocarbons. One possible explanation is that ketene being unsaturated is more strongly adsorbed than a saturated alcohol. The latter would have to undergo at least partial dehydrogenation before becoming adsorbed. This is an attractive hypothesis. It is consistent with the fact that ethylene is capable of forming an adsorption complex leading to higher hydrocarbons even though ethane shows no such tendency.

Another explanation of the remarkable effectiveness of adsorbed ketene in acting as nuclei for the building up of higher hydrocarbons cannot be ignored. The ketene molecule offers the possibility of being bonded to the surface not only by the carbon atoms but by the oxygen atoms. The observation of Eischens<sup>11</sup> and his co-workers to the

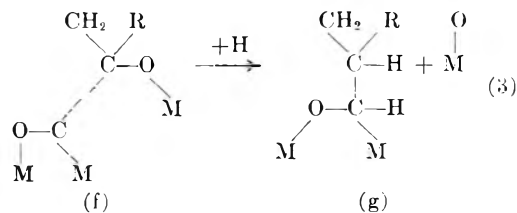
effect that  $C^{12}O^{16}$  and  $C^{13}O^{18}$  exchange oxygen atoms when adsorbed on iron at or above about  $-33^\circ$  suggests that at least some of the CO groups may be bound to the surface by both carbon and oxygen. This suggests the possibility that the intermediate complex in the Fischer-Tropsch synthesis may be held to the surface by an oxygen-metal bond as well as a carbon-metal bond. The reaction could then be formulated as



The time of addition of hydrogen to carbon is immaterial. The important point is the maintaining of the primary attachment of the complex to the surface by an oxygen-metal bond. The chain building step is the attack of the adsorbed CO, due perhaps to the unsatisfied valences of the carbon in the adsorbed CO, upon the carbon atoms of the complex. The formation of the carbon-carbon bond displaces the original carbon-oxygen bond of the complex. If, in the original complex instead of the carbon-oxygen bond being displaced, either the carbon-hydrogen or carbon-metal bond is displaced and the oxygen-carbon bond of the added CO is broken, the result is a branched chain complex. Starting with b in reaction 1



(11) R. P. Eischens and A. N. Webb, *J. Chem. Phys.*, **20**, 1048 (1952).



The by-products  $\text{CO}_2$  and  $\text{H}_2\text{O}$  of the reaction can be produced by the reduction by CO and  $\text{H}_2$  of the metal oxide produced in reactions 1, 2 and 3. The primary by-products of the reaction would then be  $\text{CO}_2$  and  $\text{H}_2\text{O}$ , the ratio depending on the relative rates of reduction by CO as compared to  $\text{H}_2$ . On cobalt catalysts since  $\text{H}_2\text{O}$  is the observed primary by-product, reduction by hydrogen is presumed to predominate. On iron catalysts the rates of reduction by both CO and  $\text{H}_2$  are apparently appreciable. With the usual assumptions reactions 1 to 3 lead to the same hydrocarbon product distribution as that given by Anderson.<sup>2</sup>

Insufficient evidence exists as yet to be certain whether the intermediate complex involves oxygen bonded directly to the surface as in reactions 1, 2 and 3 or whether the bonding is entirely through the carbon atom with the oxygen attached to the carbon as an OH group as postulated in the work with alcohols. In line with the direct oxygen bonding is the recent proposal of Burwell<sup>12</sup> that ethers may inhibit the exchange between hydrogen and hydrocarbons over nickel catalysts by virtue of being directly bonded to the surface through the oxygen. Also, the recent experiments of Gomer<sup>13</sup> with a field emission microscope show that adsorbed methyl alcohol will break an O-H bond and leave the surface as  $\text{CH}_3\text{O}^+$ . This suggests the tendency of methyl alcohol to bond to the tungsten point of the field emission apparatus at room temperature through the oxygen rather than through the carbon atom.

Further work will have to be done to decide more definitely the nature of the intermediate complex involved in the Fischer-Tropsch synthesis. The present work strongly suggests, however, that the complex formed by the adsorption of ketene on iron and cobalt catalysts is the closest approach yet found to the true  $\text{C}_2$  complex formed during the synthesis of hydrocarbons from CO and  $\text{H}_2$ .

**Acknowledgment.**—The authors gratefully acknowledge financial support for this work under a contract from the Atomic Energy Commission. The recorder used was very kindly furnished by the Leeds and Northrup Company.

(12) Private communication.

(13) Lecture at Am. Chem. Society Meeting on September 10, 1958 at Chicago.

# THE HYDROGEN-DEUTERIUM EXCHANGE ACTIVITY AND RADIATION BEHAVIOR OF SOME SILICA CATALYSTS

BY HAROLD W. KOHN AND ELLISON H. TAYLOR

*Chemistry Division, Oak Ridge National Laboratory, Oak Ridge, Tennessee  
(Operated by Union Carbide Corporation for the U. S. Atomic Energy Commission)*

*Received February 23, 1959*

Catalytic activity for  $H_2$ - $D_2$  exchange has been found in all of the types of silica examined, gel, quartz,  $\alpha$ -cristobalite, vitreous and amorphous. The activity per unit surface differs widely, being highest for quartz and vitreous silica. Since these were prepared by grinding, the high activity may have been introduced by that process. The activity observed immediately after activation declines by a factor of ten or more over ten days, and more slowly for several weeks. Irradiation with  $\gamma$ -rays or neutrons produces a dramatic increase in the activity of these silicas. The activation energy with the gel is reduced by irradiation from about 9 to about 2 kcal./mole. Quartz and vitreous silica show low activation energies even before irradiation. The enhanced activity declines with time, but at a rate indistinguishable from that of the unirradiated materials. The activity obtained by irradiation has not been equalled in an unirradiated catalyst by any activation procedure. With the low activation energies observed, only a small number of sites is needed to explain the increases in activity. Since the yields of sites are likewise small, a primary process of low probability, such as atom displacement, is suggested. The activity per displaced atom is even lower for the neutron bombardments. Within rather large uncertainties, the activity increase per unit dose is nearly equal for the different types of silica. Three silica-alumina hydrocarbon cracking catalysts behaved much like the silicas. The similarities shown by the different silicas (and silica-alumina) may mean that the local arrangement of silicon and oxygen atoms is responsible for the catalytic activity, for the only common feature of the structures is the silicon-oxygen tetrahedron.

## Introduction

Previous work from this Laboratory and elsewhere<sup>1-4</sup> has demonstrated that ionizing radiations can produce changes in the catalytic activity of a number of substances, and the possibility of advancing our knowledge of catalysis by such experiments has been suggested.<sup>1</sup> The most marked effects hitherto reported have been found with partially poisoned catalysts ( $H_2O$ -poisoned  $\gamma$ - $Al_2O_3$  for  $H_2$ - $D_2$  exchange),<sup>4</sup> and irradiation was never found to produce a more active catalyst than could be obtained by degassing at a suitable high temperature (around 500° for  $Al_2O_3$ ). Results on some other oxides ( $ThO_2$ ,  $MgO$  and  $TiO_2$ ) have also suggested that poisoning is a prerequisite for a radiation effect.<sup>5</sup> Because of the interest in finding examples in which the activity resulted from radiation-produced changes in the catalyst itself, numerous oxides known to possess some activity for hydrogen exchange have been examined for radiation effects.

Silica gel has been reported to be a feeble catalyst for the exchange<sup>6</sup> and also to participate in the decomposition by  $\gamma$ -rays of an adsorbed material.<sup>7</sup> A small double-bond isomerization activity was reported to be introduced by neutron irradiation.<sup>2</sup> These observations prompted a study of its behavior toward  $H_2$ - $D_2$  exchange after both  $\gamma$ -ray and neutron irradiation. Irradiation produced in this material an activity higher than any obtained by degassing alone, and the increase did not appear to depend on prior poisoning. Experiments were also conducted with other varieties of silica (quartz, vitreous silica,  $\alpha$ -cristobalite and Cab-o-sil), as well as with three commercial silica-alumina catalysts of different hydrocarbon cracking activities.

## Experimental

Essential data about the 8 types of catalyst used in this

study are given in Table I. Silica gel was ground and sieved between 70 and 100 mesh. A sample of  $\alpha$ -cristobalite of low surface area was prepared by heating a sample of the silica gel at 1400° for three days. Quartz, vitreous silica and high-area  $\alpha$ -cristobalite were prepared by grinding, respectively, a synthetic single crystal, a piece of laboratory silica tubing and a portion of low-area  $\alpha$ -cristobalite in a mechanical mortar and pestle, made of mullite.

Activation and activity testing were carried out in tubes (Pyrex or silica) of 35, 60 or 100 cm.<sup>3</sup> volume fitted with a stopcock and, with samples intended for reactor irradiation, with a silica break-seal. From 0.25 to 11 g. of catalyst was weighed into the tube, and the sample was activated by degassing at 400 to 700° at a final pressure of about  $10^{-5}$  mm. Thereafter it was kept under vacuum except during activity testing. The activity was measured with an approximately 50:50 mixture of  $H_2$ : $D_2$  at 20 mm. pressure. Each gas had been purified by passage through a heated palladium valve. Experiments at room temperature were kept between 24 and 26° by the controlled temperature of the laboratory. Those at elevated temperature were done in oil- or water-baths heated electrically and controlled manually, while those below room temperature were done in appropriate freezing or boiling liquids. Samples of the reacted gas were analyzed mass spectrometrically<sup>8</sup> for masses 2, 3 and 4.

Gamma irradiations were done in a 750 curie  $Co^{60}$  source. The dose rate for water in the central position, measured with a ferrous sulfate dosimeter,<sup>9</sup> was  $6 \times 10^{17}$  e.v./g. min. Most of the irradiations were done in a position where the dose rate was approximately  $1.2 \times 10^{17}$ . Reactor irradiations were carried out in the Oak Ridge Graphite Reactor at a position where the neutron flux was about  $7 \times 10^{11}$  neutrons/cm.<sup>2</sup> sec. and the gamma dose about  $7 \times 10^{15}$  e.v./g. sec. for water.<sup>10</sup>

## Results and Discussion

The most striking feature of these experiments is the production of catalytic activity in silica gel by irradiation. In the work with alumina,<sup>4</sup> the changes in activity, although quite marked under certain conditions, never brought a catalyst to a higher activity than could be achieved simply by proper degassing at an elevated temperature. Silica gel, on the other hand, appears to be only a feeble catalyst under all conditions of degassing, a typical sample

(1) E. H. Taylor and J. A. Wethington, Jr., *J. Am. Chem. Soc.*, **76**, 971 (1954).

(2) P. B. Weisz and E. W. Swegler, *J. Chem. Phys.*, **23**, 1567 (1955).

(3) E. H. Taylor and H. W. Kohn, *J. Am. Chem. Soc.*, **79**, 252 (1957).

(4) H. W. Kohn and E. H. Taylor, *THIS JOURNAL*, **63**, 500 (1959).

(5) H. W. Kohn (unpublished work).

(6) V. C. F. Holm and F. W. Blue, *Ind. Eng. Chem.*, **43**, 501 (1951).

(7) J. M. Caffrey, Jr., and A. O. Allen, *THIS JOURNAL*, **62**, 33 (1958).

(8) Analyses by Mary Gillham and W. D. Harman of the Y-12 Plant.

(9) C. J. Hochanadel and J. A. Ghormley, *J. Chem. Phys.*, **21**, 880 (1953).

(10) D. M. Richardson, A. O. Allen and J. W. Boyle, *Internl. Conf. on the Peaceful Uses of Atomic Energy*, **14**, 209 (1955).

TABLE I  
PROPERTIES OF STARTING MATERIALS

| Material                              | Surface area, m. <sup>2</sup> /g. | Level of impurities, %             |                                    |                                    | Supplier                               |
|---------------------------------------|-----------------------------------|------------------------------------|------------------------------------|------------------------------------|----------------------------------------|
|                                       |                                   | 10 <sup>-1</sup> -10 <sup>-2</sup> | 10 <sup>-2</sup> -10 <sup>-3</sup> | 10 <sup>-3</sup> -10 <sup>-4</sup> |                                        |
| Silica gel                            | 300                               | Mg                                 | Al                                 | Fe, Mo                             | Fisher Scientific Co.                  |
| α-Cristobalite                        | 6.9                               | Mg                                 | Al                                 | Fe, Mo                             |                                        |
| Cab-o-sil                             | 175-200                           | Fe, Al                             |                                    |                                    | Godfrey L. Cabot, Inc.                 |
| Vitreous silica                       | 7.9                               |                                    | Not analyzed                       |                                    |                                        |
| Quartz, synthetic                     | 6.2                               | Na                                 | Al, Ca, Fe                         | Ca, Ge, Mg                         | Cleveite Corp.                         |
| Silica-alumina cracking catalyst S-46 | 305                               |                                    | Not analyzed                       |                                    | Houdry Process Corp., Dr. S. W. Weller |
| Silica-alumina cracking catalyst S-32 | 139                               |                                    | Not analyzed                       |                                    | Houdry Process Corp., Dr. S. W. Weller |
| Silica-alumina cracking catalyst S-16 | 42                                |                                    | Not analyzed                       |                                    | Houdry Process Corp., Dr. S. W. Weller |

producing a half-time of reaction under the standard conditions of between a hundred and a thousand hours at room temperature. As little as  $1 \times 10^{19}$  e.v./g. of irradiation with  $\gamma$ -rays lowered the half-time to less than an hour. Such a half-time was never observed in degassing experiments conducted between 450 and 710°.

The details of the behavior of a typical sample of silica gel (degassed 11 days at 580°) are shown in Fig. 1, as an Arrhenius plot. The numbers near certain points indicate the time since degassing in days. At temperatures higher than 30° the data conform very well to a straight line, and the agreement between measurements made 13 days apart (points 3 and 16) is satisfactory. At 25° an aging can be observed, tending toward a value consistent with the Arrhenius plot. Experiments on another sample confirm this anomalous behavior near room temperature. This sample, also unirradiated, had a half-time at 25° of 150 hr. on one day and of 450 hr. a few days later, an obvious decline in activity. The half-time at 200° was also measured twice over this period and was 20 hr. at the beginning and 16 hr. at the end, within the expected accuracy no change. More than one process seems to be necessary to explain the anomalies, but closer specification of them is not feasible at present.

If the anomalous behavior in the 25 to 40° range is assumed not to interfere at the higher temperature, one can calculate an activation energy for the unirradiated sample of about 9 kcal./mole. The results on this sample (and on one other) after  $\gamma$ -irradiation are shown at the top of Fig. 1. These indicate activation energies of about 2 kcal./mole. The time interval within each set of measurements was kept short in order to minimize any possible effect of anomalous aging upon the slope. Since roughly the same slope was obtained several days apart and at different activity levels, as well as (after long aging) in the higher temperature range, the change in apparent activation energy on irradiating is probably real. It would be premature to base any detailed computations upon it, but it does seem to indicate that  $\gamma$ -radiation introduces a new catalytic path. If the low activation energy is taken at its face value, one does not need to postulate any large yield of new sites to explain the enhanced activity.

Some further studies of aging were carried out, with the results shown in Fig. 2. It appears that a

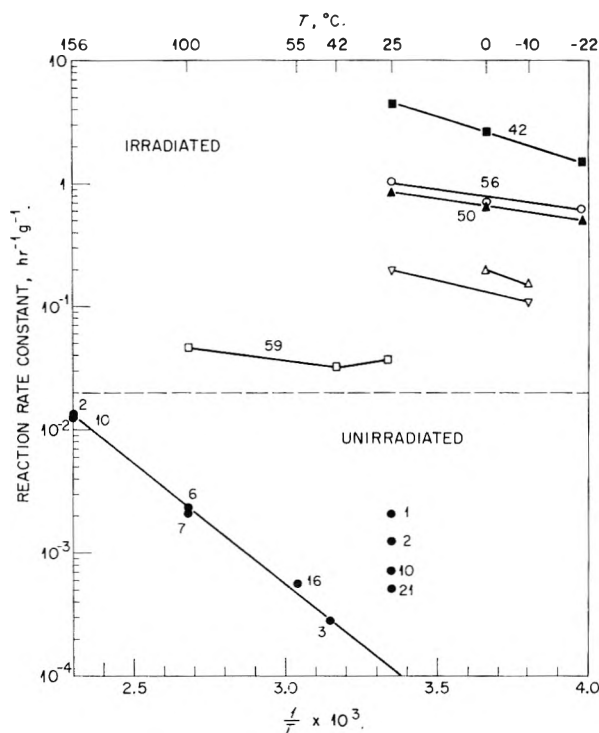


Fig. 1.—Arrhenius plot of  $H_2$ - $D_2$  exchange activity of silica gel. Sample 1: ●, not irradiated; ■, irradiated, aged 2 hours; ▲, reirradiated, aged 2 days; ○, reirradiated, aged 1 day; □, annealed 1 week. Sample 2: △, irradiated, aged 1 day; ▽, aged 2 days. Numbers refer to days elapsed since preparation.

marked, long-term decline in activity is characteristic of both unirradiated and irradiated samples of silica gel. For the first few hours after irradiation, the activity of a sample would decay with a first-order dependence, changing gradually to a dependence between 1.5 and 2.5. The activity of non-irradiated samples could not be measured in less than about a day, because of their low activity. Therefore, the decay could only be followed after a delay of at least that long. The kinetics were indistinguishable in the range where both could be measured.

This behavior of silica gel is in marked contrast to that of  $\gamma$ -alumina,<sup>4</sup> in which decay was observed in the un-irradiated catalysts only if they were not thoroughly degassed initially and were then held in the neighborhood of 200° for aging. Diffusion of wa-



TABLE II

EFFECT OF  $\gamma$ -RAYS ON  $H_2$ - $D_2$  EXCHANGE ACTIVITY OF SILICA AND SILICA-ALUMINA CATALYSTS (IRRADIATIONS AT 25°)

| Catalyst                                                 | Temp. of degassing, °C. | $k$ , first-order rate constant per unit surface before irradiation, $\text{min.}^{-1} \text{m.}^{-2}$ | Dose per unit surface, <sup>a</sup> $\text{e.v. m.}^{-2}$ | Change in $k$ from irradiation, $\text{min.}^{-1} \text{m.}^{-2}$ | Yield of ideal sites per 100 e.v. | Yield of ideal sites per displaced atom |
|----------------------------------------------------------|-------------------------|--------------------------------------------------------------------------------------------------------|-----------------------------------------------------------|-------------------------------------------------------------------|-----------------------------------|-----------------------------------------|
| At 25°                                                   |                         |                                                                                                        |                                                           |                                                                   |                                   |                                         |
| Gel 1                                                    | 450                     | $1.0 \times 10^{-8}$                                                                                   | $8.0 \times 10^{16}$                                      | $2.4 \times 10^{-5}$                                              | $1.3 \times 10^{-8}$              | $1.3 \times 10^{-3}$                    |
| Gel 2                                                    | 485                     | $1.4 \times 10^{-8}$                                                                                   | $3.6 \times 10^{16}$                                      | $1.1 \times 10^{-5}$                                              | $1.4 \times 10^{-8}$              | $1.4 \times 10^{-3}$                    |
| Gel 3                                                    | 525                     | $4.9 \times 10^{-9}$                                                                                   | $8.0 \times 10^{15}$                                      | $5.5 \times 10^{-7}$                                              | $3.1 \times 10^{-10}$             | $3.1 \times 10^{-5}$                    |
| Quartz                                                   | 500                     | $1.2 \times 10^{-4}$                                                                                   | $6.4 \times 10^{17}$                                      | $>2.1 \times 10^{-3}$                                             | $>1.6 \times 10^{-8}$             | $>1.6 \times 10^{-3}$                   |
| Vitreous                                                 | 500                     | $4.6 \times 10^{-4}$                                                                                   | $4.6 \times 10^{17}$                                      | $>9.8 \times 10^{-3}$                                             | $>9.4 \times 10^{-8}$             | $>9.4 \times 10^{-3}$                   |
| Cristobalite                                             | 550                     | $8.1 \times 10^{-6}$                                                                                   | $4.7 \times 10^{18}$                                      | $7.1 \times 10^{-3}$                                              | $6.7 \times 10^{-9}$              | $6.7 \times 10^{-4}$                    |
| Cab-o-sil                                                | 625                     | $1.1 \times 10^{-6}$                                                                                   | $2.5 \times 10^{17}$                                      | $1.9 \times 10^{-5}$                                              | $3.4 \times 10^{-10}$             | $3.4 \times 10^{-5}$                    |
| At -78°                                                  |                         |                                                                                                        |                                                           |                                                                   |                                   |                                         |
| At -196°                                                 |                         |                                                                                                        |                                                           |                                                                   |                                   |                                         |
| SiO <sub>2</sub> -Al <sub>2</sub> O <sub>3</sub><br>S-46 | 450                     | $8.8 \times 10^{-5}$                                                                                   | $3.8 \times 10^{17}$                                      | $7.3 \times 10^{-5}$                                              | $2.1 \times 10^{-7}$              | $2.1 \times 10^{-2}$                    |
| SiO <sub>2</sub> -Al <sub>2</sub> O <sub>3</sub><br>S-32 | 450                     | $2.2 \times 10^{-4}$                                                                                   | $8.3 \times 10^{17}$                                      | $1.4 \times 10^{-4}$                                              | $1.8 \times 10^{-7}$              | $1.8 \times 10^{-2}$                    |
| SiO <sub>2</sub> -Al <sub>2</sub> O <sub>3</sub><br>S-16 | 510                     | $1.7 \times 10^{-4}$                                                                                   | $2.7 \times 10^{18}$                                      | $1.6 \times 10^{-5}$                                              | $6.0 \times 10^{-9}$              | $6.0 \times 10^{-4}$                    |

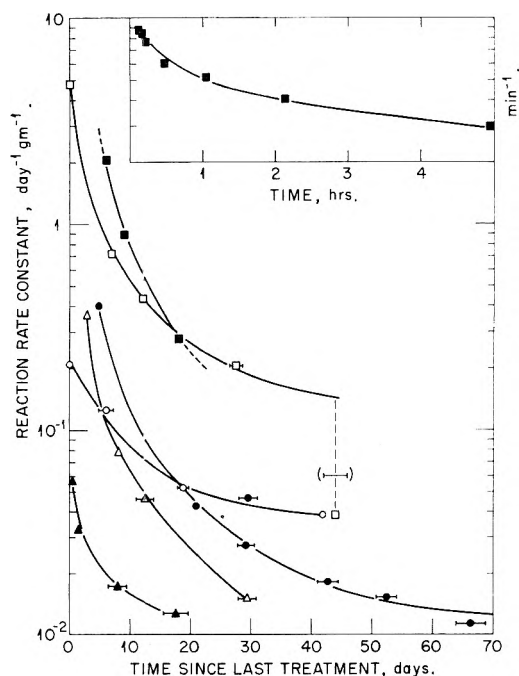
<sup>a</sup> This is the dose absorbed by the weight of catalyst presenting 1 sq. meter of surface.

Fig. 2.—Aging of silica gel catalysts. Prepared by: ■, irradiating sample degassed at 580°; □, irradiating sample degassed at 525°; ▲, degassing untreated sample at 580°; △, degassing untreated sample at 565°; ●, degassing irradiated sample at 530°; ○, degassing irradiated sample at 500°.

ter from the interior of the catalyst to the surface may be suggested as a possible reason for the aging in alumina, and this may be the case with silica gel also, since it can hardly be freed from water. It is also possible that the reactant gas, hydrogen, poisons silica gel at room temperature as it does alumina at somewhat higher temperatures.<sup>11</sup>

The unexpectedly large radiation effect with silica gel suggested a comparison with other types of silica to see whether composition or structure were

the determining influence. Quartz, vitreous silica,  $\alpha$ -cristobalite and Cab-o-sil (a commercial amorphous silica) were used. The activities are compared in Table II. The intrinsic activities of the un-irradiated materials (calculated per unit surface area) vary by a factor of about  $10^5$ . This range is what one would calculate from the activation energies, which are about 9 kcal./mole for the gel and apparently around 1 for quartz and vitreous silica. It is worth noting that the highly active samples (quartz, vitreous silica and high-area  $\alpha$ -cristobalite) were all prepared by extensive grinding which may have altered the nature of the surface as well as its extent. The effect of cold work on the catalytic activity of a metal was observed by Eckell,<sup>12</sup> and the grinding of a hard non-metal might well lead to comparable effects, perhaps through the formation of point defects, or of dislocations. There is, of course, a chemical possibility as well, that mullite (an aluminum silicate) from the mortar may be present in the ground samples. Analysis by X-ray diffraction did not reveal any mullite in the quartz, which indicates that probably no more than 1% could be present. Mullite is not thought to be highly active for the exchange, but this has not yet been experimentally verified.

Each of these other types of silica is increased in activity by irradiation with  $\gamma$ -rays, as shown in Table II. The simplest mode of comparison is to examine the ratio of the new to the old activity; this varies widely over the different materials. If the radiation is assumed to be producing new catalytic sites, rather than somehow improving those already present, then the proper mode of comparison is to calculate the additional activity introduced by the radiation. This is done in succeeding columns of Table II, which show the activity introduced per unit radiation dose, the number of catalytic sites corresponding to this and the yield of sites per 100 e.v. of absorbed energy. The number of sites is cal-

(11) S. W. Weller and S. G. Hindin, *This Journal*, **60**, 1506 (1956).(12) J. Eckell, *Z. Elektrochem.*, **39**, 433 (1933).

culated on the assumption that the first-order rate constant of one ideal site,  $k_1$ , is given by

$$k_1 = \sigma n \bar{c} \exp(-E^*/RT)/4nV$$

where  $\sigma$  = area of unit site (assumed to be  $16 \times 10^{-16}$  cm.<sup>2</sup>),  $n$  = density of molecules in gas (cm.<sup>-3</sup>),  $\bar{c}$  = average molecular velocity (assumed to be  $1.5 \times 10^5$  cm. sec.<sup>-1</sup> for H<sub>2</sub>-D<sub>2</sub> at 25°),  $E^*$  = activation energy (assumed to be 1 kcal./mole) and  $V$  = volume of gas above catalyst (cm.<sup>3</sup>). The number of sites required to give the observed reaction rate is then the increase in gross rate constant divided by the rate constant per ideal site. The calculation of the yield of sites per unit dose requires an additional assumption about the accessibility to the gas of the sites produced. For want of any information, the simplest such assumption is used, namely, that all of the sites thus produced are accessible to the gas. If some are not, then the actual yield of sites of potential catalytic utility is larger than that calculated from this assumption.

Two points are noteworthy in this comparison of different silicas. The first is that the yields are similar in all of the substances. They differ, to be sure, by a factor of over 300 in the widest pair, but the absolute initial activities vary by 10<sup>5</sup>. This suggests a picture for all of the silicas of a relatively inert matrix into which radiation can introduce similar defects at about the same rates. The higher initial activity in quartz and vitreous silica could be ascribed to a few special sites introduced during the grinding. The second observation is that the yields of such sites are low in all cases, requiring that the catalytic sites be produced by a process of rather low probability, such as atomic displacement.

The number of displacements produced by Co<sup>60</sup>  $\gamma$ -rays in silica can be estimated from theory or from measurement of some property attributable to displacements. Measurement of the paramagnetic resonance absorption of irradiated synthetic quartz indicates a yield of electron or hole trapping centers (thought to be vacancies or interstitials) of between  $6$  and  $9 \times 10^{-5}$  centers per 100 e.v.<sup>13</sup> and the yield calculated from Compton scattering is around  $1 \times 10^{-5}$  displaced atoms per 100 e.v.<sup>14</sup> The numbers of displacements required for Table II were calculated from the total dose by assuming a displacement yield of  $1 \times 10^{-5}$  per 100 e.v.

The yield of catalytically active sites per displacement thus calculated is uncertain because of the assumptions involved (activity of a unit site, displacements per 100 e.v.), but it is probably reasonable to give it some qualitative significance. The actual numbers are small ( $10^{-2}$  to  $10^{-5}$ ) and probably are not so far wrong as to raise them to unity. Most of them are around  $10^{-3}$ , indicating that only one displacement in a thousand produces an effective catalytic site.

Gamma rays produce appreciable amounts of atom displacement, but the ratio of energy transferred in this way to that transferred as electronic excitation is quite small. In view of the suggestion just made about displacements as possible precursors of catalytic sites, it was natural to study the effect of a type of radiation known to produce a large

amount of displacement. Several samples of silica and of silica-alumina were irradiated in the Oak Ridge Graphite Reactor to neutron doses between  $2.5 \times 10^{15}$  to  $2.2 \times 10^{18}$  *nv* ( $n$  = neutron density,  $v$  = average neutron velocity,  $t$  = time). These samples were so active (catalytically) that it was necessary to measure the exchange activity at  $-196^\circ$ . The results are given in Table III, where the calculation of the number of displacements is based on a yield of 3 displaced atoms per incident neutron.<sup>13</sup>

For silica gel the neutron irradiation produced a remarkable enhancement in activity, the rate constant after irradiation for an hour being about 100 times greater than that of the unirradiated material (Table II), although the measurements were done at room temperature before irradiation and at liquid nitrogen temperature after. The effect with silica-alumina, although apparent, is considerably smaller. The extra activity introduced by the bombardments may be greater than that reported in Table III, since the measurements were made (on account of the induced radioactivity) two weeks or more after removal from the reactor. The catalytic activity was disappearing at that time at a rate about equal to that of the samples irradiated with  $\gamma$ -rays and, if the similarity persists to shorter times, it can be seen from Fig. 1 that the activity immediately after removal might be considerably greater than the activity two weeks later. Therefore, the actual number of sites per displacement might be 10 to 100 times greater than that calculated from the activity measured two weeks after removal.

The calculated yields of catalytic sites per displaced atom are small, from 1/100 to 1/1000 smaller than the same figures for  $\gamma$ -rays. This may be only the result of the decay of activity before measurement in the neutron case, or it may reflect a real difference in efficiency. The displacements produced by  $\gamma$ -rays result largely in isolated interstitial-vacancy pairs, while those produced by neutrons result in more complex defects as well. The two processes would not necessarily give rise to catalytically potent defects at the same efficiency per displaced atom.

The yield does not seem to differ much between silica gel and silica-alumina, suggesting again, as in the  $\gamma$ -ray case, that a similar process is occurring.

Although an appreciable concentration of transmutations is introduced by the reactor bombardment (Table III), it is not thought that this is likely to be responsible for the large increase in catalytic activity. The elements so introduced are primarily phosphorus from the silicon and silicon from the aluminum, both by ( $n, \gamma$ ) processes followed by  $\beta$ -decay, with much smaller amounts of magnesium by ( $n, \alpha$ ) processes. Since the levels of natural impurities are much higher than those of the transmutation products, and since the elements produced are common impurities, any effect of the transmutation products is probably overwhelmed by the effect of impurities present in the original material. If the transmuted atoms were displaced by the process of formation and trapped in interstitial positions, they might exert an unusual effect, but they will probably be outweighed by the interstitials

(13) R. A. Weeks, private communication.

(14) O. E. Oen, private communication.

TABLE III  
EFFECT OF NEUTRONS ON H<sub>2</sub>-D<sub>2</sub> EXCHANGE ACTIVITY OF SILICA AND SILICA-ALUMINA CATALYSTS

| Catalyst                                                 | Neutron dose per unit surface <i>net</i> , m. <sup>-2</sup> | No. of displaced atoms per unit surface, m. <sup>-2</sup> | No. of transmuted atoms per unit surface, m. <sup>-2</sup> | Change in <i>k</i> from irradiat., min. <sup>-1</sup> m. <sup>-2</sup> | Yield of ideal sites per displaced atom |
|----------------------------------------------------------|-------------------------------------------------------------|-----------------------------------------------------------|------------------------------------------------------------|------------------------------------------------------------------------|-----------------------------------------|
|                                                          |                                                             |                                                           |                                                            |                                                                        | At -196°                                |
| Silica gel 4 <sup>a</sup>                                | 3.4 × 10 <sup>15</sup>                                      | 1.0 × 10 <sup>16</sup>                                    | 2.8 × 10 <sup>11</sup>                                     | 1.2 × 10 <sup>-4</sup>                                                 | 1.2 × 10 <sup>-7</sup>                  |
| Silica gel 2                                             | 6.1 × 10 <sup>13</sup>                                      | 1.8 × 10 <sup>14</sup>                                    | 5.0 × 10 <sup>9</sup>                                      | 9.3 × 10 <sup>-6</sup>                                                 | 5.4 × 10 <sup>-7</sup>                  |
| Silica gel 3                                             | 3.8 × 10 <sup>12</sup>                                      | 1.2 × 10 <sup>13</sup>                                    | 3.1 × 10 <sup>8</sup>                                      | 2.5 × 10 <sup>-6</sup>                                                 | 2.3 × 10 <sup>-6</sup>                  |
| SiO <sub>2</sub> -Al <sub>2</sub> O <sub>3</sub><br>S-46 | 1.6 × 10 <sup>15</sup>                                      | 4.9 × 10 <sup>15</sup>                                    | 1.2 × 10 <sup>12</sup>                                     | >1.1 × 10 <sup>-3</sup>                                                | >2.4 × 10 <sup>-6</sup>                 |
| SiO <sub>2</sub> -Al <sub>2</sub> O <sub>3</sub><br>S-32 | 3.6 × 10 <sup>15</sup>                                      | 1.1 × 10 <sup>16</sup>                                    | 2.6 × 10 <sup>12</sup>                                     | >2.4 × 10 <sup>-3</sup>                                                | >2.3 × 10 <sup>-6</sup>                 |
| SiO <sub>2</sub> -Al <sub>2</sub> O <sub>3</sub><br>S-16 | 1.2 × 10 <sup>16</sup>                                      | 3.5 × 10 <sup>16</sup>                                    | 8.5 × 10 <sup>12</sup>                                     | 3.6 × 10 <sup>-3</sup>                                                 | 1.1 × 10 <sup>-6</sup>                  |

<sup>a</sup> *k* before irradiation = 9.3 × 10<sup>-9</sup> min.<sup>-1</sup> meter<sup>-2</sup> at 25°.

produced by simple displacement, some of which will be chemically the same as some of the transmutation products.

The data have been treated and the discussion has been presented in terms of "catalytic centers," as if the activity for catalyzing the exchange resided at a discrete number of sites on the surface, and that the effect of radiation was to create new sites. It should be noted that the observations neither substantiate nor disprove this picture, and that it has been used simply as a framework for describing the results. The vacancies and interstitials might also act by lowering or raising the electron energy level in the solid and thereby altering the catalytic activity of the surface, which could be uniformly active or which could have its activity concentrated at special sites. On this picture, these

sites would not themselves be directly altered by the radiation.

The discussion has likewise, for brevity, been presented in terms of displaced atoms only and the possible role of ionization has not been described. The yield of catalytic centers per 100 e.v. of  $\gamma$ -rays is, however, about equal in the reactor and in the Co<sup>60</sup> source, and an equally plausible description could be based on removal or trapping of electrons from or in pre-existing centers. Present information does not suffice to determine which of these general mechanisms is the more probable.

**Acknowledgments.**—The authors are indebted to Dr. S. W. Weller and the Houdry Process Corporation for the samples of silica-alumina catalysts, and to Dr. P. H. Emmett for helpful discussions.

## INTENSITY AND CONCENTRATION DEPENDENCE OF SOME RADIATION-INDUCED REACTIONS IN ANTHRACENE SOLUTIONS

BY A. CHARLESBY, W. H. T. DAVISON AND D. G. LLOYD

Royal Military College of Science, Shrivenham, Swindon, Wiltshire, England  
T.I. Research Laboratories, Hinxton Hall, Saffron Walden, Essex, England

Received March 3, 1959

Dilute solutions of anthracene in hexane, cyclohexane and polysiloxanes were subjected to gamma and electron radiation, and the effect of anthracene concentration and radiation intensity on the rate of disappearance of anthracene studied. The results obtained have been compared with two alternative reaction schemes. In the case of the hydrocarbon solutions, the rate of loss of anthracene depends on  $A\sqrt{I}$ , as is to be expected from a competitive reaction between anthracene-radical and bimolecular radical-radical combination or disproportionation, where the radicals are initially distributed at random. In the case of the siloxanes, the absence of the expected radiation intensity effect implies that the radicals formed in siloxanes are removed unimolecularly in the absence of an additive. The implication of these results on current theories of the cross-linking of polymers is discussed.

### Introduction

Although radiation is known to produce both excited and ionized molecules, most of the chemical changes produced in organic systems have been ascribed to radicals. The reactions may be considerably modified by the presence of additives in low concentration, and investigations of these changes enable determination to be made of such factors as radical concentration,<sup>1</sup> reactivity constants,<sup>2</sup> energy transfer<sup>3</sup> and electron capture<sup>4</sup>

processes. Further analysis of the modified products also enables one to infer the nature of the radicals formed.<sup>5,6</sup> As the additive concentration is usually kept low (to avoid appreciable direct energy capture), it cannot significantly interfere with extremely fast reactions; the information obtained therefore relates to radicals which react slowly with one another. Using iodine<sup>1</sup> or D.P.P.H.,<sup>7</sup> it has

(1) E. N. Weber, P. F. Forsyth and R. H. Schuler, *Radiation Research*, **3**, 68 (1955).

(2) A. Charlesby and D. G. Lloyd, *Proc. Roy. Soc. (London)*, **A249**, 51 (1958).

(3) J. P. Manion and M. Burton, *THIS JOURNAL*, **56**, 560 (1952).

(4) P. J. Horner and A. J. Swallow, to be published.

(5) W. H. T. Davison, *Chem. Soc. Lond. Special Publ.* no. 9, 151 (1958).

(6) L. H. Gevantman and R. R. Williams, *THIS JOURNAL*, **56**, 569 (1952).

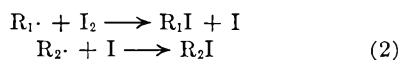
(7) A. Prevost-Bernas, *et al.*, *Disc. Faraday Soc.*, **12**, 98 (1952).

been possible in this way to measure  $G$ -values for radical production in a number of hydrocarbons, irradiated in the liquid state.

Since radicals are essentially molecules with unpaired electrons they can only disappear ultimately by reacting in pairs, either by combination or by disproportionation. From the point of view of kinetic analyses these need not be considered separately.



In the presence of a scavenger such as  $I_2$  the alternative reactions become



The relative probability of reactions 1 and 2 depends on the relative concentration of  $R\cdot$  and  $I_2$  as well as of their reactivity. The radical concentration will itself be largely determined by the radiation intensity. The rate of disappearance of additive at various initial concentrations and radiation intensities should therefore provide interesting information on the reactivities of the species involved. In fact little such information is available, most of the work being concentrated on the measurement of  $G$ -values for radical production, when the additive concentration or reactivity is sufficiently high to render negligible the combination reaction 1.

A different problem arises when molecules are irradiated in the solid state. Among the reactions occurring, crosslinking (dimerization) and degradation are prominent. The former reaction involves two molecules but the precise mechanism of the reaction has not been clearly established. One set of theories assumes that crosslinking is due to the reaction of two radicals formed independently and at random within the system. A second approach assumes that crosslinking results from the reaction of a radical with a neighboring radical formed as a result of the same primary process. Other theories again assume an ionic form of reaction. The dependence of this reaction on additive concentration and radiation intensity would be very different for these different types of reaction. For example, additive concentration and radiation intensity should play little part in the crosslinking occurring between two radicals formed by the same primary events, and in ionic reactions. In practice it is found that protection against both degradation and crosslinking is possible by relatively small amounts of additives.

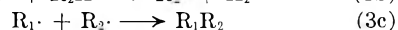
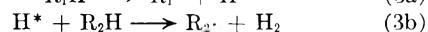
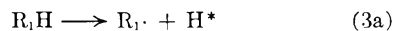
To obtain further evidence on this problem experiments were carried out in which different compounds were irradiated in the presence of a small amount of anthracene, which acted as a scavenger for the radicals produced. The anthracene concentration may be deduced readily from its ultraviolet absorption spectrum at  $375 \mu\mu$ . In these experiments the rate of disappearance of anthracene was determined as a function of its concentration and of the radiation intensity. The materials studied comprised hexane, cyclohexane<sup>2</sup> and dimethylsiloxane (silicone) polymers of varying viscosity.

The results with hexane and cyclohexane can be compared with those obtained using iodine as the

scavenger additive. Data on the effect of anthracene concentration in hexane (but not radiation intensity) have been obtained previously by Krenz.<sup>8</sup> The  $G$ -values for anthracene destruction in silicones can be compared with the  $G$ -values for crosslinking. Because of the wide range of viscosities available, their chemical similarity and the absence of complications arising from crystallinity, silicones offer a useful transition between the low molecular weight organic compounds, irradiated as liquids, and the solid high molecular weight polymers in which bodily motion of the individual molecules is largely inhibited.

### Kinetic Analysis

At low additive concentrations (A), direct energy absorption from the incident radiation can be ignored to a first approximation. Supporting evidence for this assumption is the observation that  $G(H_2)$  is unaffected by low concentrations of iodine<sup>9</sup> or anthracene.<sup>8</sup> Radicals are formed in the solvent (in these experiments hexane, cyclohexane or silicone fluid) and in the absence of additives, these may be considered to react (I) with other radicals located initially at random throughout the system, or alternatively (II) with neutral molecules or with active entities such as radicals formed only in the immediate vicinity. Since the radiation doses are low, this last form of reaction is extremely unlikely unless a single radiation event produces two adjacent radicals, as for example



where  $H^*$  is a "hot" atom which can carry out an immediate hydrogen abstraction from a neighboring molecule. If the additive is present in sufficient concentration, it may react directly with  $R_1\cdot$  and  $R_2\cdot$ . The essential difference between equations (3a, c) and (1, 2) is that in (3a, c),  $R_2\cdot$  will always be formed in the immediate vicinity of  $R_1\cdot$  and its rate of combination with  $R_1\cdot$  (equation 1) is independent of radiation intensity. We may therefore consider two distinct models for analysis. The corresponding equations in the steady state are

$$k_1I = k_2(R\cdot)^2 + k_3(R\cdot)(A) \quad (\text{Model I}) \quad (4)$$

$$k_1I = k_2'(R\cdot) + k_3(R\cdot)(A) \quad (\text{Model II}) \quad (5)$$

depending on whether radicals ( $R\cdot$ ) can disappear by the combination of two radicals, produced independently and distributed at random, or by the reaction of each initial radical within its immediate environment, independent of any further absorption of energy from primary radiation. It should be noted that equation 5 applies to any reaction mechanism where the rate of radical disappearance is first order.

In these equations  $k_1I$  represents the rate of formation of radicals by radiation of intensity  $I$ , and  $k_3(R\cdot)(A)$  their disappearance by a reaction with anthracene, whereby the latter is modified and effectively removed.  $k_1$ ,  $k_2$ ,  $k_2'$  and  $k_3$  are appropriate reactivity constants and ( $R\cdot$ ), ( $A$ ) the con-

(8) F. H. Krenz, *Nature*, **176**, 113 (1955).

(9) C. C. Schubert and R. H. Schuler, *J. Chem. Phys.*, **20**, 518 (1952).

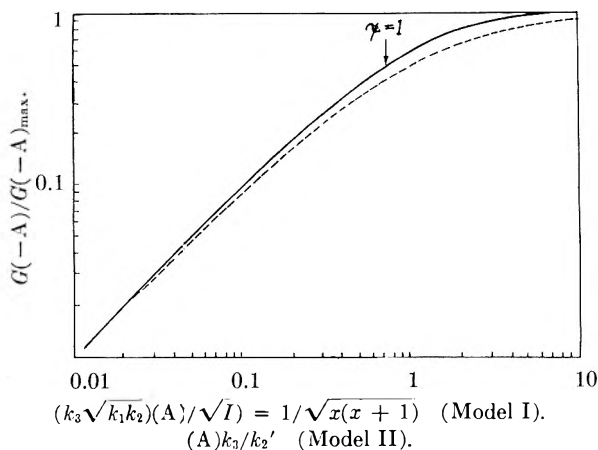


Fig. 1.—Theoretical curves showing relation between  $G(-A)$  and  $(A)/\sqrt{I}$  (model I, full line) or  $(A)$  (model II, broken line).

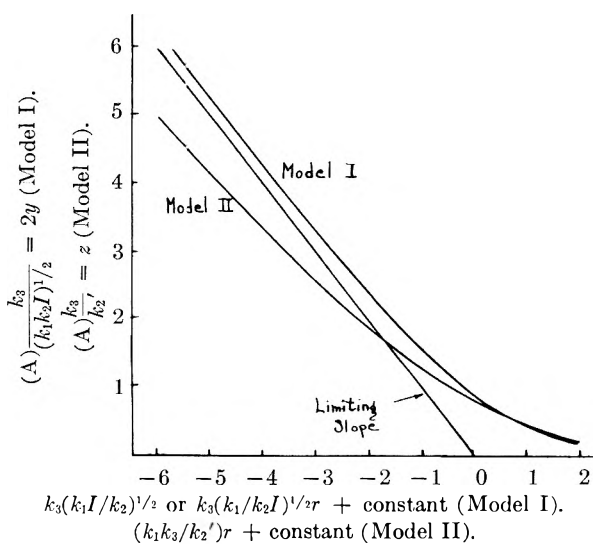


Fig. 2.—Theoretical reduction in additive concentration  $(A)$  with dose  $r$ .

centrations expressed in moles/l. Then

$$-\frac{d(A)}{dt} = k_3(R\cdot)(A) \quad (6)$$

if each radical can remove one molecule of anthracene by reacting with it in some unspecified manner. If the radical and additive molecule concentrations are expressed in moles/l., and the radiation intensity in rad/sec., an intensity  $I$  corresponds to the absorption of  $I \times 0.625 \times 10^{14}$  e.v./g. sec. or  $0.625 \times 10^{17}$  e.v./l., sec. when  $\rho$  is the density of the solution (or solvent since the additive concentration is very low). Then

$$k_1 = 0.625 \times 10^1 \rho G / 6.02 \times 10^{23} = 1.04 \times 10^{-9} \rho G \text{ moles l.}^{-1} \text{ per rad. sec.}^{-1} \quad (7)$$

where  $G$  is the  $G(R\cdot)$  value for radical formation in the solvent. The maximum rate of additive removal occurs when  $k_3(R\cdot)(A) \gg k_2(R\cdot)^2$  or  $k_2'(R\cdot)$ . Then

$$-\frac{d(A)}{dt} = k_1 I = 1.04 \times 10^{-9} \rho G I \quad (8)$$

and

$$G(-A)_{\max} = G(R\cdot) \quad (9)$$

independently of whether model (1) or (2) is applicable.

Most work on the use of radical scavengers (e.g., with iodine) has been carried out with scavenger concentrations in this range (i.e., too low for direct action or energy transfer but too high for radical-radical reaction to occur). Such work has therefore given values for  $G_{\max}(R\cdot)$  only and no information of radical concentrations or radical reactivity constants.

At lower additive concentrations differences in  $G(-A)$  should appear, the values depending on the kinetic model chosen.<sup>2,10</sup>

Model I:

$$\text{Put } x = k_2(R\cdot)/k_3(A) \quad (10)$$

$$k_1 I = k_3(A)(1+x)(R\cdot) \quad (11)$$

then

$$-\frac{d(A)}{dt} = k_3(R\cdot)(A) = \frac{k_1 I}{1+x} \quad (12)$$

$$G(-A) = \frac{G(-A)_{\max}}{1+x} = \frac{G(R\cdot)}{1+x} \quad (13)$$

while from equations 10, 11

$$(A)^2 = \frac{k_1 k_2 I}{k_3^2} \frac{1}{x(x+1)} \quad (14)$$

Equations 13 and 14 can be used jointly to give pairs of values of  $G(-A)$  and  $(A)$ . The plot obtained is shown in Fig. 1, and it is seen that  $G(-A)$  depends only on  $(A)/\sqrt{I}$ , and the reactivity constants.

$$\text{Model II: From (5) } \times (R\cdot) = \frac{k_1 I}{k_2' + k_3(A)}$$

and hence from (6)

$$-\frac{d(A)}{dt} = \frac{k_3(A)}{k_2' + k_3(A)} k_1 I \quad (15)$$

$$\text{so that } G(-A) = G(-A)_{\max} \frac{k_3(A)}{[k_2' + k_3(A)]} \quad (16)$$

This relation is also shown plotted in Fig. 1. The dependence of  $G(-A)$  on  $(A)$  is somewhat similar in the two models, but only that deduced from Model I shows any dependence on radiation intensity.

The direct relationship between  $(A)$  and dose  $r$  can be deduced for these two models.<sup>10</sup> If  $y = k_3(A)/(4k_1 I k_2)^{1/2}$  (Model I) then

$$(y^2 + 1)^{1/2} - \ln [1 + (y^2 + 1)^{1/2}] + \ln y + y = -k_3/(k_1 k_2 I)^{1/2} r + \text{constant} \quad (17)$$

while if (Model II)

$$z = k_3(A)/k_2'$$

$$z + \ln z = -(k_1 k_3/k_2') r + \text{constant} \quad (18)$$

The corresponding relationships between  $(A)$  and  $r$  are shown in Fig. 2.

At low intensities and high additive concentration both models approximate to the asymptotic values

$$2y = -k_3(k_1/k_2 I)^{1/2} r + \text{constant} \quad (\text{Model I})$$

and

$$z = -(k_1 k_3/k_2') r + \text{constant} \quad (\text{Model II})$$

and therefore in both cases

$$(A) = -k_1 r + (A_0) \quad (19)$$

(10) A. Charlesby and D. G. Lloyd, to be published.

At high intensities and low additive concentration the relations become

$$\ln(A) = -k_3(k_1/k_2I)^{1/2}r + \text{constant (Model I)} \quad (20)$$

and

$$\ln(A) = -k_3(k_1/k_2')r + \text{constant (Model II)} \quad (21)$$

It is therefore at low values of the ratio  $A/\sqrt{I}$  that the difference between the two models is most pronounced.

### Results

In the experiments, dilute de-oxygenated solutions of anthracene in hexane, cyclohexane or polydimethylsiloxane fluids of different viscosities were subjected to gamma radiation *in vacuo* from a  $\text{Co}^{60}$  source at various radiation intensities  $I$ , and to fast electrons from a 2 Mev. Van de Graaff or a 15 Mev. linear accelerator. In the latter cases the electron beam was pulsed, so that no single figure for the intensity can be given; the maximum figure for the Van de Graaff was  $10^7$  rad./sec. for periods of about 0.5 msec. and that from the linear accelerator is probably higher by an order of magnitude. The experimental details follow those described in a previous paper.<sup>2</sup> The decrease in anthracene concentration was followed by the change in ultraviolet absorption, using a Beckman DK2 ratio-recording spectrophotometer.

The  $G(-A)$  values for anthracene disappearance in hexane and in cyclohexane (using  $\text{Co}^{60}$   $\gamma$ -radiation) are shown in Fig. 3; they follow the expected dependence on  $(A)$ , and also show the dependence on  $I^{-1/2}$  predicted by Model I. The ratios  $k_3/(k_1k_2)^{1/2}$  have been chosen to obtain the best fit, but any change in their values merely shift the curves bodily along the horizontal axis in the log plot used. Also shown is the calculated curve for Model II, but at a single intensity  $I$ . Changes in  $I$  would move this curve bodily and destroy the agreement obtained.

The silicone fluids show a similar dependence of  $G(-A)$  on  $(A)$  but no dependence on  $I$  for  $\gamma$ -radiation (Fig. 4). Here the electron data are included since there is no ambiguity as to intensities. The silicone solutions therefore appear to follow Model II. The maximum values for  $G(-A)$  lie close to the  $G(R.)$  values deduced from solutions with iodine, and the  $G(\text{crosslinking})$  values.<sup>10</sup> Although there is no intensity dependence for  $\gamma$ -radiation, the values of  $G(-A)$  and  $G(-A)_{\text{max}}$  are less for electron irradiation, as are the  $G(\text{crosslinking})$  values. Thus this appears to be a real difference, although the intensity effect is much smaller, and not of the predicted character.

These  $G(-A)$  values were obtained from the slopes of  $(A)$  versus  $r$  curves. A more convincing demonstration of the differences between the solvents is obtained when  $(A)$  is plotted directly against  $r$  for different radiation intensities. At low values of  $(A)/\sqrt{I}$  both models predict a linear relation between  $\log(A)$  and dose, but in Model I the slope varies as  $I^{-1/2}$ , whereas in Model II there is no such dependence (equations 20, 21). The results show that for hexane (Fig. 5) and cyclohexane (Fig. 6)

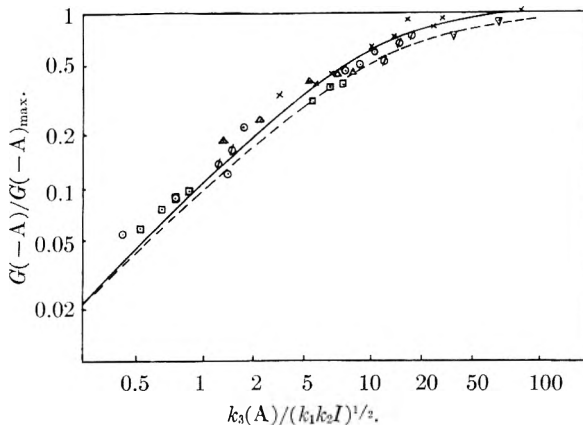


Fig. 3.—Variation of  $G(-A)$  with  $(A)$  and  $I$  in hexane and cyclohexane: —, calcd. (Model I); - - -, calcd. (model II).  $\phi$ ,  $\text{Co}^{60}\gamma$  9.9 rad./sec.;  $\square$ , 49.2 (both in hexane).  $X$ ,  $\text{Co}^{60}\gamma$  11.1 rad./sec.;  $\circ$  20.8;  $\nabla$ , 49.2;  $\triangle$  53.4 (all in cyclohexane).

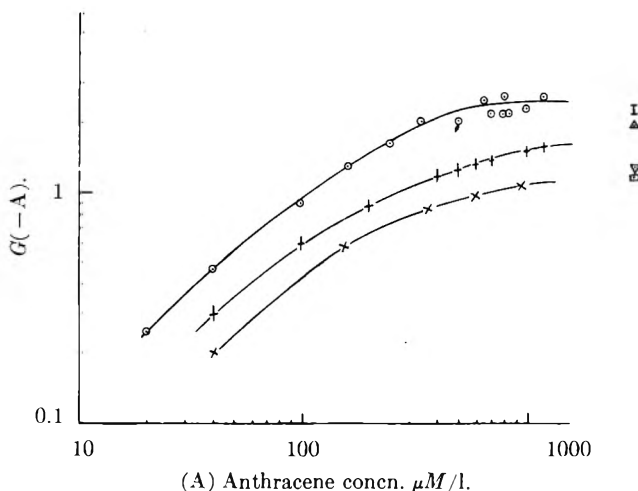


Fig. 4.—Variation of  $G(-A)$  with  $(A)$  for silicones:  $\circ$ ,  $\text{Co}^{60}\gamma$  84.2 rad./sec.;  $+$ , 2 Mev., Van de Graaff;  $X$ , 15 Mev., linear accelerator; I,  $G(R.)$ ,  $\text{Co}^{60}\gamma$  using iodine.  $G(\text{crosslinking})$ , from dose to gel:  $\Delta$ ,  $\text{Co}$ , 60 $\gamma$ ;  $\square$ , Van de Graaff;  $\nabla$  linear accelerator.

the radiation intensity factor plays an important part, whereas for two silicone fluids (Fig. 7) of viscosity 0.65 and 1000 centistokes, subjected to gamma radiation it is of no importance, over the range studied. Thus for the hexane solution the  $\log(A)/r$  slopes for  $\gamma$ -radiation at two intensities (9.9 and 49.2 rad./sec.) are in the ratio 1.8, as against a predicted ratio of  $(49.2/9.9)^{0.5} = 2.2$ . For the cyclohexane solutions, the  $\log(A)/r$  plot (Fig. 6) shows considerable divergence from linearity, but the effect of intensity follows the same pattern. The divergence is in part due to the values of  $(A)/\sqrt{I}$  being too high (and encroaching on the  $(A)/r$  linear region, eq. 19) but in part to secondary reactions. For silicones the  $\log(A)/\gamma$ -dose curves (which should show as a difference in slopes of 2.1 according to Model I), are identical to within experimental error.

The results for high intensity radiation from the Van de Graaff or linear accelerator cannot be analyzed in the same way, since the effective average intensity is unknown, and in any case steady-state

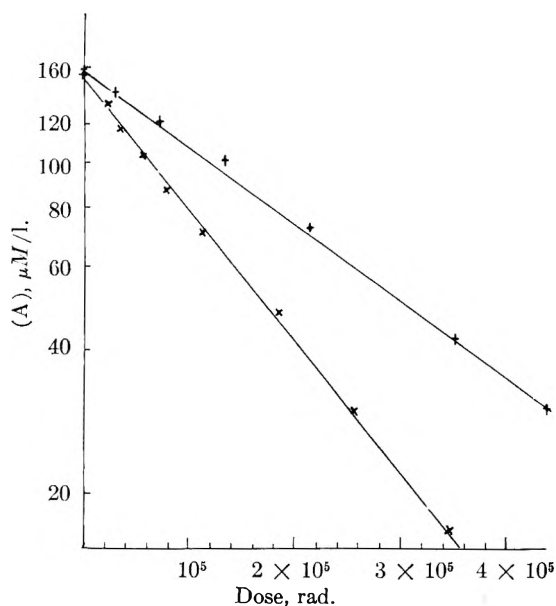


Fig. 5.—Variation of (A) with dose for anthracene-hexane mixtures at low values of (A):  $\times$ ,  $\text{Co}^{60}\gamma$ , 9.9 rad./sec.;  $+$ , 49.2 rad./sec.

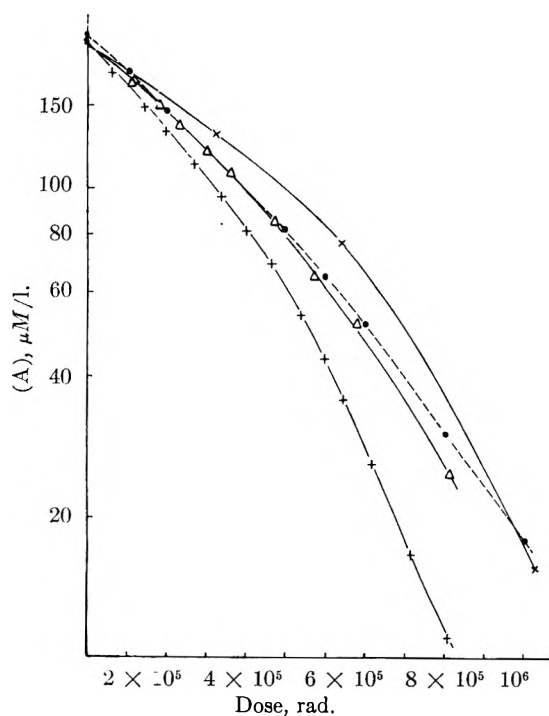


Fig. 6.—Variation of (A) with dose for anthracene-cyclohexane mixtures at low values of (A):  $+$ ,  $\text{Co}^{60}\gamma$  11.1 rad./sec.;  $\Delta$ , 20.1;  $\times$ , 53.4;  $\bullet$ , Van de Graaff (dose scale  $\times 10$ ).

conditions do not apply. However for cyclohexane the dependance of (A) on Van de Graaff dose is only one-tenth of that for 20.1 rad./sec.  $\gamma$ -radiation (pointing to a hundred-fold increase in effective intensity, *i.e.*,  $1.25 \times 10^5$  rad. min. for the Van de Graaff) whereas in silicones the Van de Graaff is half as effective as  $\gamma$ -radiation. The cause of this smaller difference is discussed below.

At higher values of (A)  $\sqrt{I}$ , the dependence of (A) on  $r$  is linear, and the intensity dependence is much less marked. This is particularly clear for cyclo-

hexane subjected to  $\gamma$ -radiation and electron radiation.<sup>2</sup>

From the observed slopes at low intensities, the following approximate values for the reactivity constants may be deduced. For hexane and cyclohexane, values of  $k_1$  ( $= 1.04 \rho G(R \cdot) \times 10^{-9}$ ) of  $5 \times 10^{-9}$  have been assumed, and for the silicones a lower value of  $3 \times 10^{-9}$ . More accurate values do not appear warranted for the present purpose. Then for hexane solutions irradiated at an intensity of 9.9 rad./sec.,  $k_3/\sqrt{k_2} = 2.9$ , and at an intensity of 49.2 rad./sec.  $k_3/\sqrt{k_2} = 3.7$ . For the cyclohexane solution irradiated at an intensity of 11.1 rad./sec.  $k_3/\sqrt{k_2} = 2$ . The latter value was also obtained by Charlesby and Lloyd from more extensive data.<sup>2</sup> For silicone fluids, for which Model II applied, the ratio  $k_3/k'_2 = 5 \times 10^3$ ; in a more detailed analysis Charlesby and Lloyd<sup>10</sup> obtained a figure of  $6.4 \times 10^3$ .

### Discussion

Although a considerable amount of attention has been paid to the use of scavengers such as iodine and D.P.P.H. as a means of measuring radical production in irradiated samples, there is little evidence in the published literature of a variation in  $G(-A)$  with additive concentration and radiation intensity under the conditions used. Krenz studied the disappearance of anthracene in irradiated hexane,<sup>8</sup> and found a dependence of  $G$ -value on anthracene concentration, but did not investigate the intensity dependence. His results can be written in the form

$$G(-A) = G(-A)_{\max} \frac{(A)}{(A) + c}$$

where  $c$  is a suitable constant. This relation is of the form predicted by Model II whereas the fuller results for anthracene-hexane mixtures described in this work agree with Model I. However, as is apparent from Fig. 1, these two models lead to somewhat similar dependance of  $G(-A)$  on (A) so that unless the measurements are carried out at different intensity levels, as in this work, they cannot be readily distinguished.

The primary purpose of the present work was to investigate this intensity dependence; the exact mechanism by which anthracene is destroyed is not therefore discussed here. Whatever the reaction it is sufficient at this stage to note the marked distinction between the behavior of anthracene in solutions of hexane and cyclohexane on the one hand, and silicones on the other. Further work seems desirable, with a simpler additive, and having a lower reactivity than iodine. The previous failure to observe a drop in  $G(-I_2)$  values at low concentrations of iodine can presumably be ascribed to the higher value for the reactivity constant  $k_3$ , which means that with iodine one is operating at an effectively higher concentration of additive.

One possible explanation for the difference between silicone fluids, and hexane or cyclohexane, is that the high viscosity of the former impedes the motion of radicals, and hence reduces the probability of two silicone radicals, formed independently, meeting to form a crosslink. However no differ-

ences are found as between 0.65 and 1000 centistoke fluids, nor has any intensity dependence been found in silicones of higher viscosity. Furthermore this explanation would result in a lower value for  $k_2$  and would not account for the observed dependence of  $G(-A)$  on  $(A)$  but not on  $I$ . It must therefore be concluded that viscosity of the solvent is not the primary cause of this difference in behavior.

The various theories which have been proposed to account for crosslinking in polymers fall into two categories, depending on whether they predict Model I or Model II behavior. If Model I is the pattern of behavior, an extremely large number of motions of each radical would be needed before it meets a partner (produced independently) to form a crosslink. Reaction with an additive, even at low concentrations, would then appear extremely probable, since the concentration of the additive is far greater than that of the radiation-induced radicals. On the other hand, with Model II, it is difficult to explain any significant effect from the additive molecules which are far apart (several hundred Ångströms at the concentrations used here); one would expect a far more rapid reaction of a radical with a neighboring molecule. One possibility is some form of energy transfer to the anthracene molecule, before radical reactions can occur. Krenz discussed the question of energy transfer in anthracene-hexane mixtures, but concluded that the prime role of anthracene at these concentration was to act as a radical acceptor. His observations that  $G(H_2)$  and  $G(CH_4)$  were unaltered by the presence of anthracene at these concentrations is evidence for the absence of energy transfer in such systems, in contrast to the classical work of Burton<sup>3</sup> with cyclohexane-benzene mixtures.

Some form of ionic reaction is another possibility. Such reactions are to be favored at low temperatures, and it would be interesting to discover whether the distinction reported here at room temperature prevails at lower temperature. Although the active entities discussed in this paper have been assumed to be radicals, there is no direct evidence for this.

Owing to the variable radiation intensity and the absence of stationary state conditions little attention has been paid here to the results obtained with the high-intensity, pulsed electron sources. For cyclohexane, the Van de Graaff appears to behave as a steady radiation source of some  $2 \times 10^3$  rad./sec. (for a nominal instantaneous intensity of about  $10^7$  rad./sec.) In silicones, where no intensity effect is observed with gammas up to about 200 rad./sec. a decreased effect (by a factor of less than 2) is obtained with the high intensity pulsed electron beam, and this decrease is also found in the maximum value  $G(-A)_{max}$ . This apparent loss in effectiveness is not due to errors in dosimetry, since the energy input was confirmed in terms of hydrogen evolution from irradiated hydrocarbons. The work of Schuler and Allen<sup>11</sup> has shown that  $G(H_2)$  is substantially independent of radiation intensity and even type of radiation, so that hydrogen evolution is

(11) R. M. Schuler and A. O. Allen, *J. Am. Chem. Soc.*, **77**, 507 (1955).

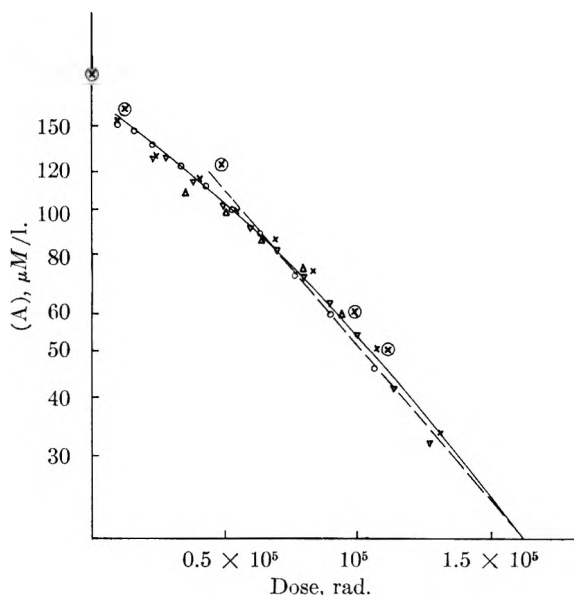


Fig. 7.—Variation of  $(A)$  with dose for anthracene-silicone mixtures at low values of  $(A)$ : ○,  $Co^{60}\gamma$  49.2 rad./sec.; ×, 11.1 (both 1000 cs.); △, 49.2; ▽, 11.1 (both 0.65 cs.); ⊗, Van de Graaff (1000 cs.) (dose scale  $\times 2$ ).

a useful method of comparing radiation intensities at widely different levels.

An explanation for the lower effectiveness of the high intensity radiation in silicones may be sought in the close proximity of ions produced from different primary tracks within a short interval of time. Recombination of ions and electrons from different tracks may then occur, before the chemical reactions from ionization and excitation within the same track have all been completed. With sufficiently low intensity  $\gamma$ -radiation, loss of ions from this interaction may be negligible. A similar argument applies to the recombination of radicals within tracks. The effect of very high intensity radiation is therefore somewhat similar to that observed with radiation of high LET, such as fast protons or  $\alpha$ -particles. This explanation is in agreement with the observation that the  $G$ -values for crosslinking (in the absence of additive) is lower for the Van de Graaff electron radiation than for radiation of lower intensity from a cobalt-60 source. The  $G$ -value is even smaller for the radiation from the linear accelerator, for which the peak radiation intensity is higher still.

Further details of this program of research are to be presented subsequently, but the present work indicates the possibility of assessing reaction mechanisms and radical lifetimes and reactions by studies of the influence of radiation intensity, additive concentration and possibly temperature on dilute liquid or solid solutions.

**Acknowledgments.**—The authors wish to acknowledge the experimental assistance of Mrs. K. E. Gibson and to record their appreciation to Professor J. Rotblat (St. Bartholomew's Hospital Medical School) for the irradiations carried out on the linear accelerator.

The Chairman of Tube Investments, Ltd., is thanked for permission to publish this paper.



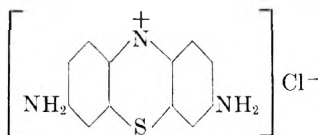
## A NOTE ON THE RADIATION INDUCED SYNTHESIS OF LAUTH'S VIOLET

BY P. BALESTIC AND M. MAGAT<sup>1</sup>*Laboratoire de Chimie Physique de la Faculté des Sciences de Paris*

Received March 20, 1959

It is established by spectroscopic and chemical evidence that  $\gamma$ -ray irradiation of aerated aqueous solutions of *p*-phenylenediamine and  $\text{H}_2\text{S}$  at  $\text{pH} > 1$  leads to a formation Lauth's Violet. Methods for isolation and purification of the dye formed are described. Some preliminary kinetic results are given.

A few years ago Loiseleur<sup>2</sup> called attention to some phenomena of radiation-induced coloration of aqueous solutions of simple organic compounds, such as *p*-diaminobenzene. Among other experiments he quoted the case of an aqueous solution of *p*-diaminobenzene, ammonium sulfide, HCl and copper sulfate at  $\text{pH} 7$  irradiated by X-rays to a total dose of some 750,000 r., which developed a strong violet color, attributed by Loiseleur to Lauth's Violet



He observed also that, in order to obtain good results, air had to be bubbled through the solution and that the reaction was suppressed if oxygen acceptors like ascorbic acid, cysteine or hydroquinone were added to the solution. No attempt was made to isolate the product or to identify it by any physical or chemical method.

Since it was to our knowledge the first case of a complicated organic synthesis induced by radiation ever mentioned, which may open new possibilities to radiation chemistry, we decided to make a thorough investigation of the kinetics of this reaction, in order to understand its mechanism.

This note summarizes some preliminary results obtained so far; they concern, on one hand, the nature of initial compounds participating in the reaction and on the other hand, the isolation, identification and dosage of the dye produced.

**Products.**—All materials except  $\text{H}_2\text{S}$  were commercial products. However it became soon apparent that reproducible results could be obtained only if all traces of impurities were carefully eliminated from *p*-diaminobenzene. To reach this objective several methods described in the literature were tried, among others the reduction by tin salts described by Weissberger and Strasser.<sup>3</sup> All the purification procedures were to be repeated several times. Ultimately a new method of purification was developed that will be described elsewhere.

$\text{H}_2\text{S}$  was prepared in the laboratory.

**Irradiation Conditions.**—Most of the irradiations were carried out at  $20^\circ$  using Co-60 sources of 600 and 100 curies, respectively. The dosimetry was done by the ferrous sulfate dosimeter of Fricke, assuming  $G(\text{Fe}^{3+}) = 15.6$  as recommended by Schuler and Allen.<sup>4</sup> The total dose was varied between 20,000 and 600,000 r., the dose rates varied between 30,000 and 150,000 r./hr. A few experiments were performed with an X-ray set under conditions approaching as closely as possible the ones used by Loiseleur.

## Results

**A. Role of Reagents.**—In a first set of experiments we have tried to establish in what form sulfur had to be present. We found that identical results were obtained if ammonium sulfide used by Loiseleur was replaced by  $\text{H}_2\text{S}$ , at initial concentrations of  $0.7 \times 10^{-2} M$  to  $1.5 \times 10^{-2} M$ . If neither  $(\text{NH}_4)_2\text{S}$  nor  $\text{H}_2\text{S}$  was added to the solution various colorations were obtained on irradiation, depending on the  $\text{pH}$ , but none of them was violet.

The importance of oxygen was verified easily, no coloration being observed even after several months, if the solution was deaerated.

**B. Influence of  $\text{pH}$ .**—In order to establish the optimum  $\text{pH}$ , we have varied the  $\text{pH}$  unit by unit between 0 and 12. We could establish the existence of two distinct domains of  $\text{pH}$  at which the violet color appeared during irradiation, the products being responsible for the coloration being different as shown by spectroscopic measurements and by the examination of their chemical properties.

(a) In neutral or slightly acid medium, the aerated mixture  $\text{C}_6\text{H}_4(\text{NH}_2)_2 \cdot 2\text{HCl}$ ,  $6.94 \times 10^{-2} M$ ;  $\text{H}_2\text{S}$ ,  $1.5 \times 10^{-2} M$ ; HCl after a dose of 400,000 r. develops a deep violet color; the solution had to be diluted in order to make the spectrochemical analysis possible. As can be seen on Fig. 1, the absorption spectrum between 4000 and 6500 Å. of the two irradiated solutions at  $\text{pH} 6.9$  and 5.9, respectively, is very different from the spectrum of Lauth's Violet. It seems hence that the violet color observed by Loiseleur under these conditions of  $\text{pH}$  is not due to Lauth's Violet as he assumed, but to an as yet unidentified compound that we presume to be a quinonic oxidation product of *p*-phenylenediamine. The same result was obtained using the irradiation conditions specified by Loiseleur.

(b) In acid medium  $\text{pH} \sim 1$  a violet coloration is observed again. The absorption spectrum of the irradiated mixture taken without dilution, shows in this case the characteristic absorption peak of Lauth's Violet, with a maximum at 6025 Å. (Fig. 1). In order to study the absorption of the compound formed in the ultraviolet region, it became necessary to isolate the dye formed because of the absorption by *p*-phenylenediamine and other compounds that may be produced.

**C. Chromatographic Separation of the Dye Formed.**—We have first investigated the chromatographic separation of a synthetic mixture of Lauth's Violet and of *p*-phenylenediamine on alumina columns. The series of eluents used—carbon tetrachloride, benzene, ether, chloroform, ethanol—showed that the diamine was eluted first,

(1) Laboratoire de Chimie Physique de la Faculté des Sciences de Paris.

(2) J. Loiseleur, *J. chim. phys.* **52**, 630 (1955).

(3) A. Weissberger and E. S. Strasser, *Z. prakt. Chem.*, **135**, 209 (1932).

(4) B. H. Schuler and A. O. Allen, *J. Chem. Phys.*, **24**, 56 (1956).

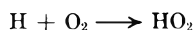
in the fraction  $\text{CCl}_4\text{-C}_6\text{H}_6$ , while the dye was eluted by a mixture  $\text{CHCl}_3 + 1\% \text{C}_2\text{H}_5\text{OH}$ . The same result was obtained with the irradiated solution.

Eventually a much simpler way was found to isolate the dye: Lauth's Violet in the base form is readily soluble in chloroform. It hence could be extracted from the aqueous solution made basic, by usual chloroform extraction. The extracted dye was further purified by chromatography on alumina. The eluate in ethanol appears to be fairly pure Lauth's Violet, presenting the two characteristic absorption peaks at 6025 and at 2700 Å. The small difference in the ultraviolet absorption is a measure of the efficiency of separation.

Experiments on synthetic mixtures show that by this procedure we recover with a good reproducibility 80% of the dye. Since Lambert-Beer law is verified the amount of the dye formed by irradiation can be determined by measuring the absorption at the maximum of the visible absorption peak directly in the eluate.

**D. Chemical Tests.**—In order to check the spectral identification of the dye formed, we have performed a series of chemical identification tests indicated by Lauth,<sup>5</sup> Koch<sup>6</sup> and Bernthsen.<sup>7</sup> For this purpose we evaporated the alcohol from the eluate and redissolved the dye in water. An addition of hydrochloric acid developed an intense azure blue coloration; an addition of sulfuric acid produced a green coloration; the addition of an alcoholic solution of NaOH led to fuchsine red, that of ammoniacal a deep violet. Finally the addition of  $\text{H}_2\text{S}$  reduced the dye to a leuco derivative, the dye being regenerated by soft oxidants. An irradiation by a light of 5460 Å. produced a red fluorescence of thionine solutions.<sup>7</sup> We satisfied ourselves that the same color changes and fluorescence were observed with a Lauth's Violet prepared by the standard chemical procedure, as stated in the literature quoted. We think to have established, with a fair degree of certainty that the dye produced by irradiation of our solutions at  $\text{pH} \sim 1$  is identical with Lauth's Violet.

**E. Kinetic Aspects.**—Only few kinetic aspects were established yet. So we find that the amount of the dye formed increased with the concentration of *p*-phenylenediamine at least in the region  $2.78 \times 10^{-1} M$  to  $3.48 \times 10^{-2} M$ . We have further established, varying the total dose, that the yield decreases with dose. This is due to the decoloration of the dye by irradiation. Strong indications are available that the role of oxygen is essentially that of a scavenger for H atoms produced by radiolysis of water through the reaction



although this point cannot be considered yet as definitely established.

Initial *G*-values, calculated on the energy absorbed by the whole solution, as high as 0.6 could be observed and it seems not impossible that this value can be yet increased by a judicious choice of concentrations of the different ingredients of the irradiated solutions.

(5) Ch. Lauth, *Bull. soc. chim. France*, **26**, 422 (1876).

(6) H. Koch, *ibid.*, **34**, 404 (1880).

(7) A. Bernthsen, *ibid.*, **43**, 563 (1885).

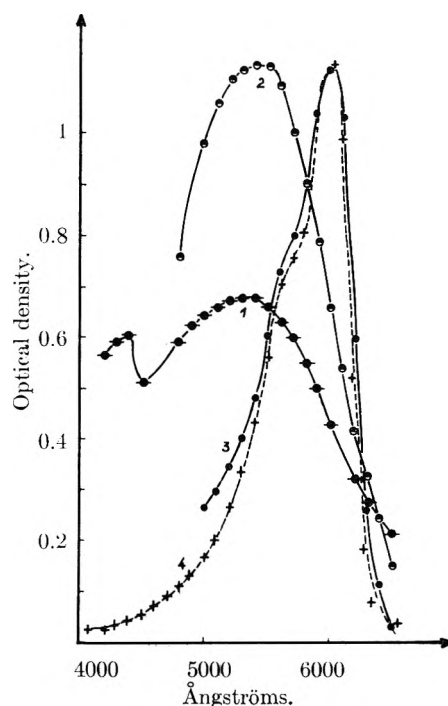


Fig. 1.—Visible absorption spectra of aerated aqueous solutions of *p*- $\text{C}_6\text{H}_4(\text{NH}_2)_2\text{HCl}$  and  $\text{H}_2\text{S}$  irradiated at different pH as compared to the spectrum of chemically prepared Lauth's Violet: (1) ●, at pH 6.9; (2) ○, at pH 5.9; (3) ●, at pH 1; (4) +, standard solution of Lauth's Violet.

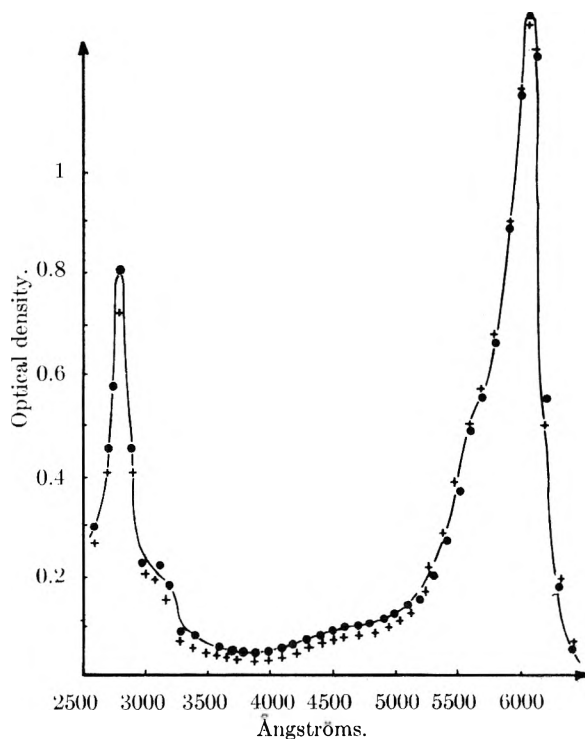


Fig. 2.—Visible and ultraviolet absorption spectra of radiation produced and chemically prepared Lauth's Violet in ethanol: (1) ●, alcoholic eluate of the radiation produced dye; (2) +, alcoholic solution of the chemically prepared Lauth's Violet.

Further kinetic work and its extension to other dye synthesis reactions indicated by Loiseleur are in progress.

### Conclusion

It seems to be established that radiation-induced synthesis of some dyes, as suggested by Loiseleur, is possible. Kinetic studies of these processes are complicated by the simultaneous radiation-induced decomposition of the dyes and by possible reactions of the dyes with H<sub>2</sub>S present leading to formation of

leuco derivatives.

The authors thank the Commissariat de l'Energie Atomique for the facilities it put at their disposal for this research and for the permission granted to publish the preliminary results.

(8) E. R. Rabinowitch and P. Epstein, *J. Am. Chem. Soc.*, **63**, 74 (1941).

## NOTES

### DIMERIC BISMUTH(I) ION, (Bi<sub>2</sub>)<sup>2+</sup> IN MOLTEN BISMUTH TRIHALIDE-BISMUTH SYSTEMS<sup>1</sup>

BY M. A. BREDIG

Contribution from the Oak Ridge National Laboratory, Chemistry  
Division, Oak Ridge, Tenn.

Received December 12, 1958

Vapor pressure measurements on the system bismuth trichloride-bismuth metal<sup>2</sup> were recently interpreted<sup>3</sup> in terms of the presence of a bismuth monochloride tetramer, (BiCl)<sub>4</sub>. However, it has now become apparent that the melting point depression observed on adding Bi to BiCl<sub>3</sub><sup>4,5</sup> is entirely incompatible with the assumption of the tetramer (or even a trimer) because a value of 2.7 kcal. would result for the heat of fusion of BiCl<sub>3</sub>, far lower than a recently determined cryoscopic value of 4.85 ± 0.10 kcal.<sup>6</sup> A still higher and probably most reliable value of 5.50 ± 0.15 kcal. has just been obtained at ORNL (A. Dworkin and M. A. Bredig), using a drop calorimeter.

It is proposed that the experimental data, especially the melting point depression<sup>4</sup> and vapor pressure measurements,<sup>2</sup> can be explained if both *dimeric* bismuth(I) chloride and *dimeric* bismuth, Bi<sub>2</sub>, are assumed to be the principal solute species at low and intermediate temperatures. Experimental depressions of the BiCl<sub>3</sub> melting point, Δ*T*, plotted against the concentration of Bi<sub>2</sub>Cl<sub>2</sub>, even at low solute concentration, in general fall nearer the line for

$$\Delta T = \frac{RT^2}{\Delta H_{\text{fusion, BiCl}_3}} \ln(1 - N_{\text{solute}})$$

than those plotted for Bi or (BiCl)<sub>4</sub> (Fig. 1). Espe-

(1) Work performed for the U. S. Atomic Energy Commission at the Oak Ridge National Laboratory, operated by the Union Carbide Corporation, Oak Ridge, Tennessee.

(2) D. Cubicciotti, F. J. Keneshea, Jr., and C. M. Kelley, *THIS JOURNAL*, **62**, 463 (1958). See also *ibid.*, **62**, 999 (1958), for the BiBr<sub>3</sub>-Bi system.

(3) John D. Corbett, *ibid.*, **62**, 1149 (1958). See also *J. Am. Chem. Soc.*, **80**, 1457 (1958).

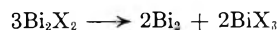
(4) S. J. Yosim, A. J. Darnell, W. Gehman and S. W. Mayer, *THIS JOURNAL*, **63**, 230 (1959). See also Abs. No. 21, 8N and No. 71, 28S, 132nd Annual Meeting, A.C.S., New York, 1957.

(5) M. A. Sokolova, G. G. Urazov and V. G. Kuznetsov, *Akad. Nauk, S.S.S.R., Inst. Gen. Inorg. Chem.*, **1**, 102 (1954).

(6) L. E. Topol and S. W. Mayer, Abstract No. 29, 14S, 134th Annual Meeting, A.C.S., Chicago, September, 1958. The formerly accepted value of 2.6 kcal. (K. K. Kelley, U. S. Bureau of Mines Bull. No. 393, 25, 1936) becomes 5.2, *i.e.*, not much different from 4.85, above, if the erroneous assumption of the presence of dimers Cu<sub>2</sub>Cl<sub>2</sub> and Fe<sub>2</sub>Cl<sub>6</sub> upon which it was based is corrected.

cially a tetramer (BiCl)<sub>4</sub> is entirely ruled out by these results. While the case against Bi atoms is not as strong, the species Bi<sub>2</sub>Cl<sub>2</sub> seems most strongly indicated, particularly if the existence of the solid (BiCl)<sub>x</sub> even above this temperature range is considered. The phase diagram, in this region, has the character of a—often nearly ideal—eutectic system of two salts, BiCl<sub>3</sub> and Bi<sub>2</sub>Cl<sub>2</sub>.

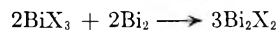
The trichloride and tribromide vapor pressures of BiX<sub>3</sub>-Bi mixtures (X = Cl or Br), measured<sup>2</sup> at approximately 300, 350 and 400°, *i.e.*, considerably above the melting points of BiX<sub>3</sub>, can also readily—within the fairly wide margin of accuracy of the measurements—be reconciled with the formation of Bi<sub>2</sub>X<sub>2</sub>. It is only necessary to assume that even at as relatively low a temperature as 300° partial decomposition of Bi<sub>2</sub>X<sub>2</sub> occurs, in accordance with the disproportionation reaction



The experimental vapor pressure data are compatible with equilibrium constants (for the *reverse* of the disproportionation reaction)

$$K = \frac{N_{\text{Bi}_2\text{X}_2}^3}{N_{\text{BiX}_3}^2 N_{\text{Bi}_2}^2}, \quad (\text{X} = \text{Cl or Br})$$

These constants were obtained in the following way: first, a plot of the final mole fraction of bismuth trihalide, *N*<sub>BiX<sub>3</sub></sub>, against *y*, the extent of the reaction



$$N_{\text{BiX}_3} = \frac{2my + 4m - 4}{my - 4 + 2m}$$

was prepared for various *m*, the initial mole fraction of bismuth metal (*m* = 0.01 to 0.40). With the relation between *y*, *m* and the equilibrium constant

$$K = \frac{N_{\text{Bi}_2\text{X}_2}^3}{N_{\text{BiX}_3}^2 N_{\text{Bi}_2}^2} = \frac{4(3my/4)^3(1 - m/2 + my/4)}{(1 - m - my/2)^2(m - my)^2}$$

curves for various constants *K* were drawn into this plot. From their intercepts with the curves for *y* vs. *N*<sub>BiX<sub>3</sub></sub>, for various *m*, those *K* were selected whose curves gave the best agreement for the *N*<sub>BiX<sub>3</sub></sub> at these intercepts with the experimental mole fractions *N*<sub>BiX<sub>3</sub></sub>, calculated from the vapor pressure measurements with the provisory assumption of activity coefficients of unity.

For BiBr<sub>3</sub>-Bi, *e.g.*, the constants are approximately 0.05 mole<sup>-1</sup> at 300° and 0.001 mole<sup>-1</sup> at 350°, and much lower at 400°. For the disproportionation reaction, this gives a Δ*H* of very roughly

+55 kcal.<sup>7</sup> These estimates reflect a relatively rapid disappearance of  $\text{Bi}_2\text{X}_2$  as a solute with increasing temperature. Table I contains an example of the possible fit between experimental and calculated  $\text{BiBr}_3$  vapor pressures. The small positive deviation from unity of the ratio of observed and calculated vapor pressures may imply a small dependence of the activity coefficient on concentration. This would be the positive deviation from Raoult's law expected with phase separation in the liquid state, however a much smaller one than proposed for the so-called "physical model,"<sup>12</sup> and rather in line with the very small one observable on plotting  $\ln(1 - N_{\text{Cd}_2\text{Cl}_2})$  vs.  $1/T$  in the somewhat analogous  $\text{CdCl}_2$ -Cd system.<sup>8</sup>

TABLE I  
ACTIVITY COEFFICIENTS OF  $\text{BiBr}_3$  AND MOLE FRACTION OF  $\text{Bi}_2\text{Br}_2$  AND  $\text{Bi}_2$  AT 300°

| Initial mole fraction $m_{\text{BiBr}_3}$ | Vapor pressure, mm.                    |                                          | Activity coefficient                      |                                                                         | Solute mole fractions        |                   |
|-------------------------------------------|----------------------------------------|------------------------------------------|-------------------------------------------|-------------------------------------------------------------------------|------------------------------|-------------------|
|                                           | Meas. <sup>a</sup><br>$p_{\text{exp}}$ | Calcd. <sup>b</sup><br>$p_{\text{calc}}$ | $p_{\text{exp}}/p_{\text{calc}}$<br>(MAB) | $p_{\text{exp}}/19.54 \cdot m_{\text{BiBr}_3}$<br>(Cubicciotti, et al.) | $N_{\text{Bi}_2\text{Br}_2}$ | $N_{\text{Bi}_2}$ |
| 1.0                                       | 19.54                                  | ...                                      | 1.000                                     | 1.000                                                                   | 0                            | 0                 |
| 0.9                                       | 18.25                                  | 18.27                                    | 1.001                                     | 1.040                                                                   | 0.034                        | 0.030             |
| .8                                        | 17.45                                  | 16.94                                    | 1.030                                     | 1.116                                                                   | .059                         | .074              |
| .7                                        | 16.30                                  | 15.49                                    | 1.052                                     | 1.193                                                                   | .079                         | .129              |
| .6                                        | 14.50                                  | 13.85                                    | 1.047                                     | 1.239                                                                   | .099                         | .192              |

<sup>a</sup> Taken from curves published in ref. 2. <sup>b</sup> From equilibrium mole fraction  $N_{\text{BiBr}_3} = K' \left( \frac{N_{\text{Bi}_2\text{Br}_2}^2}{N_{\text{Bi}_2}} \right)^{1/2}$ ;  $K' = \sqrt{0.05} = 0.22$ ;  $p_{\text{calc}} = 19.54 N_{\text{BiBr}_3}$ .

$\text{Bi}_2$  molecules, which are thought to replace  $\text{Bi}_2\text{Cl}_2$  as a solute as the temperature increases, are known to be rather stable in the gaseous state, with a heat of dissociation of 43 kcal.<sup>9</sup> This by far exceeds even the corresponding figure of 17.5 kcal. for  $\text{Na}_2$  or 11.5 for  $\text{K}_2$ , the species assumed to produce, in solutions of the alkali metals in their halides, the largest part of the observed deviations from Raoult's law for the halides.<sup>10-12</sup> At high temperature, Bi atoms also must become more and more important and are likely to be responsible for both the electronic contribution to the conductivity at low metal concentration<sup>13</sup> and the complete miscibility.<sup>4</sup>

In extending, then, previous discussions of the structure of these solutions,<sup>2-4,12</sup> the present interpretation makes an attempt to explain the variously observed deviations from Raoult's law for the solvent  $\text{BiCl}_3$  and their temperature dependence largely and specifically in terms of the dimers,  $\text{Bi}_2$  and  $\text{Bi}_2\text{X}_2$  ( $\text{X} = \text{Cl}$  or  $\text{Br}$ ), of each of two solutes, bismuth and bismuth(I) halide.<sup>14</sup> A more quantitative

(7) The entropy of the reaction, of the order of 100 e.u., or 17 e.u. per Bi, is large but not unduly so; cf. for instance the entropies of fusion for  $\text{AlCl}_3$  and  $\text{FeCl}_3$ , of 18 e.u. (U.S.N.B.S. Circular 500, 1952).

(8) A. H. W. Aten, *Z. physik. Chem.*, **73**, 578 (1910); K. Griothelm, F. Grönvold and J. Krogh-Moe, *J. Am. Chem. Soc.*, **77**, 5824 (1955).

(9) Elizabeth Brackett and Leo Brewer, UCL-3712 (1957).

(10) M. A. Bredig, J. W. Johnson and Wm. T. Smith, Jr., *J. Am. Chem. Soc.*, **77**, 307 (1955).

(11) J. W. Johnson and M. A. Bredig, *THIS JOURNAL*, **62**, 604 (1958).

(12) H. R. Bronstein and M. A. Bredig, *J. Am. Chem. Soc.*, **80**, 2077 (1958).

(13) A. H. W. Aten, *Z. physik. Chem.*, **66**, 64 (1909).

(14) An interesting new situation is indicated for  $\text{BiI}_3$ -Bi in most recent work by Cubicciotti, et al., *THIS JOURNAL*, **63**, 295 (1959);

treatment would also have to consider the cohesive force differences between the solvent and these solutes. However, even a meaningful separation of the experimentally determined partial molal free energy of mixing into partial molal entropy and enthalpy, that was attempted,<sup>2</sup> would seem to have to be based upon data considerably more accurate than available.

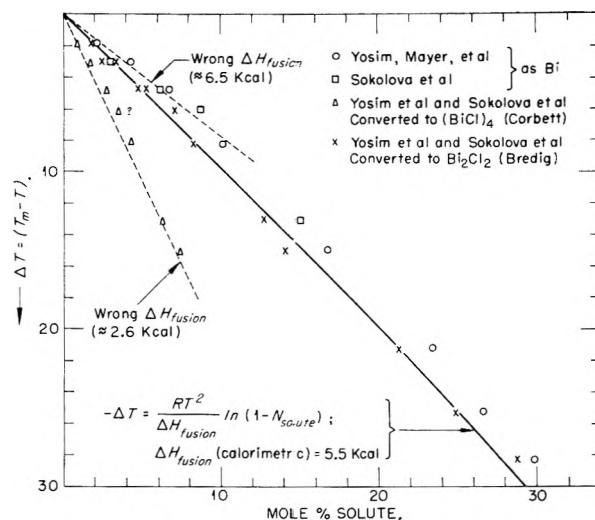


Fig. 1.—Melting point depression of bismuth trichloride on addition of bismuth. Raoult's law fit is better for solute species  $\text{Bi}_2\text{Cl}_2$  than for  $(\text{BiCl})_4$  or Bi.

The Bi(I) halide dimer proposed here is thought to contain the new diamagnetic dimeric cation  $(:\text{Bi}::\text{Bi}:)^{2+}$  or  $(\text{Bi}^{3+}(\text{e}_2^-)_2\text{Bi}^{3+})$  which would be quite analogous to the mercurous ion,  $(\text{Hg}:\text{Hg})^{2+}$ , or  $(\text{Hg}^{2+} \text{e}_2^- \text{Hg}^{2+})$ , except for two additional binding electrons ("double bond") and four (non-binding) 6s electrons.<sup>15</sup> A discussion of possible theoretical reasons for the special stability of  $(\text{Bi}_2)^{2+}$  ions and the apparent non-existence of other dimeric cations such as  $(\text{Tl}_2)^{2+}$ , or  $(\text{Pb}_2)^{2+}$  would appear premature at this time. A detailed X-ray diffraction study of solid  $\text{BiCl}$  and  $\text{BiAlCl}_4$ ,<sup>16</sup> as well as of concentrated solutions of Bi in molten  $\text{BiCl}_3$ , would be expected to supply the needed, more direct evidence for the existence of the dimeric cation  $(:\text{Bi}::\text{Bi}:)^{2+}$ .

**Acknowledgment.**—The thanks of the author are due to Drs. Corbett, Cubicciotti and Yosim for kindly furnishing manuscripts of their papers in advance of publication and to R. D. Ellison for help with the machine calculations.

here, Raoult's law was found to be valid at concentrations as high as 30 mole % of Bi as the solute.

(15) Unknown to the author until kindly pointed out to him by Dr. S. J. Yosim of Atomic International, the suggestion that the dimer  $\text{Bi}_2\text{Cl}_2$  is one of the species present in these solutions (Annual Technical Report, AEC Unclassified Programs, NAA-SR-2400, Part II, Page IV-4, dated March 15, 1958) has already replaced an earlier assumption to the contrary (NAA-SR-2124, Page 18, dated December 15, 1957).

(16) J. D. Corbett and R. K. McMullan, *J. Am. Chem. Soc.*, **78**, 2906 (1956).

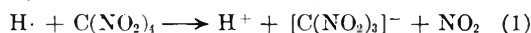
## TETRANITROMETHANE AS A RADICAL SCAVENGER IN RADIATION CHEMICAL STUDIES

By A. HENGLEIN,<sup>1</sup> J. LANGHOFF AND G. SCHMIDT

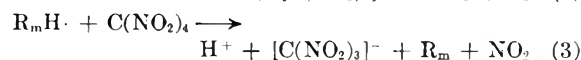
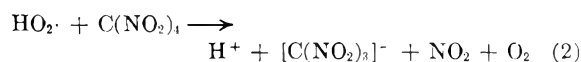
*Institute for Physical Chemistry, University of Cologne, Cologne, Germany*

*Received December 27, 1968*

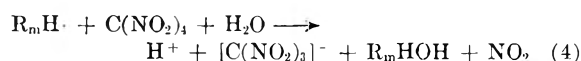
Previous studies of the radiation chemistry of tetranitromethane (TNM) in aqueous solution have shown that this substance is an effective radical scavenger when present at concentrations above  $10^{-3}$  mole/l.<sup>2</sup> Hydrogen atoms reduce this solute to give nitroform which in aqueous solutions ionizes to form the intensely colored anion  $[\text{C}(\text{NO}_2)_3]^-$  (extinction coefficient at 350  $m\mu$ ; 15,000 mole<sup>-1</sup> l. cm.<sup>-1</sup>). Since a colored material is formed from



the uncolored TNM extremely small changes in the concentration of this radical scavenger can be determined. The hydroxyl radicals formed in the radiolysis of water do not directly form nitroform from TNM. However, in the presence of an additional solute, such as hydrogen peroxide or an organic substance, OH radicals are converted by hydrogen abstraction to give  $\text{HO}_2 \cdot$  or organic radicals which in turn reduce tetranitromethane



or



Thus in aqueous systems containing reducible solutes in addition to TNM total radical yields can be measured directly. In neutral water the value of  $G$  for radical production was found to be 5.85<sup>3</sup> in agreement with other measurements of this quantity.<sup>3,4</sup>

Nitroform is also formed as the only product of the reactions of TNM in alcoholic solutions. Therefore the value of  $G$  for the formation of nitroform in the oxygen-free alcohols listed in Table I gives the 100 e.v. yields for the formation of free radicals in these compounds.

TABLE I

FORMATION OF NITROFORM IN ALCOHOLIC SOLUTIONS OF TNM ( $10^{-3}$  MOLE/L.) BY Co-60  $\gamma$ -RAYS

| Alcohol    | $G(\text{nitroform})$   |                          |
|------------|-------------------------|--------------------------|
|            | $\text{O}_2$ free soln. | $\text{O}_2$ satd. soln. |
| Methanol   | 6.6                     | 5.4                      |
| Ethanol    | 7.0                     | 6.6                      |
| 1-Propanol | 6.8                     | 6.8                      |
| 2-Propanol | 6.8                     | 6.8                      |
| 2-Butanol  | 6.2                     | 6.2                      |

Apparently the free radical yield in alcohols is somewhat higher than in water. The radical yield

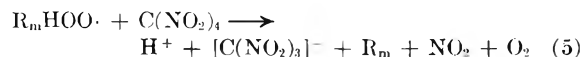
(1) Radiation Research Laboratories, Mellon Institute, Pittsburgh<sup>1</sup> Pa.

(2) A. Henglein and J. Jaspert, *Z. physik. Chem. Neue Folge*, **12**, 324 (1957).

(3) E. J. Hart, *J. Am. Chem. Soc.*, **76**, 4198 (1954).

(4) J. H. Baxendale and D. H. Smithies, *Z. physik. Chem. Neue Folge*, **7**, 242 (1956).

found for methanol is in fairly good agreement with the values of 6.1<sup>5</sup> and 6.3<sup>6</sup> found by using ferric ions as the radical detector. Dissolved oxygen has only a small influence on the yield of nitroform in methanol and ethanol and a negligible effect in the higher alcohols. It seems therefore that most of the free organic peroxy radicals also react with TNM to give nitroform



In hydrocarbons the yield for formation of nitroform is quite low since other products are formed simultaneously by the reduction of  $\text{NO}_2$  groups in TNM. In benzene  $G(\text{nitroform})$  is equal to 0.5; a brown polymer  $(\text{C}_4\text{H}_4\text{O}_2\text{N})_n$  precipitates during the irradiation. In aliphatic hydrocarbons  $G(\text{nitroform})$  is equal to 1. Here a product is formed which can be extracted with water. It has a strong absorption at 315  $m\mu$ . The dependence of this absorption on the pH shows that the product is a weak acid. The compound can be extracted from its aqueous solution using ether. Attempts to concentrate these solutions result in decomposition of the solute to nitrous gases. The same compound is formed in the radiolysis of aqueous solutions of nitroform and in the thermal reaction of dinitromethane with nitrous acid in aqueous solution. The preliminary formula of dinitroformaldoxime  $\text{C}(\text{NO}_2)_2\text{-NOH}$  is assigned to this compound.

These results show that TNM is a useful radical scavenger for studies of the radiolysis of water and alcohols. Furthermore, TNM also may find some application in other fields of the chemistry of free radicals. It may even be used for scavenging of free radicals formed in the gas phase because of its rather high vapor pressure.

(5) G. E. Adams and J. H. Baxendale, *J. Am. Chem. Soc.*, **80**, 4215 (1958).

(6) E. A. Cherniak, E. Collinson, F. S. Dainton and G. M. Meaburn, *Proc. Chem. Soc.*, 54 (1958).

## REACTIONS OF GASEOUS IONS. AMMONIUM ION FORMATION IN IONIZED AMMONIA

By LEON M. DOREMAN<sup>1</sup> AND P. C. NOBLE

*General Electric Research Laboratory, Schenectady, N. Y.*

*Received February 13, 1959*

The considerable variety of ion-molecule reactions which have now been observed and whose rates have been determined<sup>2-5</sup> consists largely of systems of organic molecules, principally the simple hydrocarbons. In the case of ionized ammonia it seemed likely, by analogy with the hydrocarbon reactions, that a hydrogen atom or proton transfer reaction would occur, forming ammonium ion in

(1) Chemistry Division, Argonne National Laboratory, Lemont, Illinois.

(2) D. P. Stevenson and D. O. Schissler, *J. Chem. Phys.*, **23**, 1353 (1955).

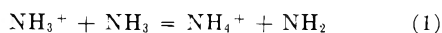
(3) D. O. Schissler and D. P. Stevenson, *ibid.*, **24**, 926 (1956).

(4) F. H. Field, J. L. Franklin and F. W. Lampe, *J. Am. Chem. Soc.*, **79**, 2419 (1957).

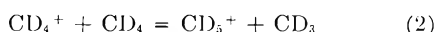
(5) G. G. Meisels, W. H. Hamill and R. R. Williams, *J. Chem. Phys.*, **25**, 790 (1956).

the gas phase. Zahlan and Burt<sup>6</sup> have recently speculated that  $\text{NH}_4^+$ , and also  $\text{N}_2\text{H}_5^+$ , might be observable in the mass spectrometer and have discussed<sup>7</sup> the role of ion-molecule reactions in the radiation chemistry of ammonia.

This note reports the results of mass spectrometric measurements which show that the reaction



does occur with high efficiency, thus confirming part of the earlier speculation.<sup>5</sup> On the other hand, no evidence was obtained for the formation of the  $\text{N}_2\text{H}_5^+$  ion. A rough estimate of the rate constant for (1) has been made by comparison, under identical mass spectrometer conditions, with the rate of the reaction



for which the rate constant previously has been reported.<sup>2</sup>

#### Experimental

The results were obtained with a General Electric analytical mass spectrometer. In these experiments the shield voltage was varied over a wide range from its normal value of 70 to 11 volts. The ion-repeller voltage, which is 8 volts under analytical conditions, was set at zero for most of the measurements and at 1 volt for the remainder. Thus most of the data were obtained with a field gradient in the source of approximately 1 v./cm. or less, an estimate which is, of course, complicated by field penetration through the various slits of the source. The emission current for all the measurements was 23 microamperes. The source was maintained at its normal temperature of 150°, except in a single experiment, the result of which must be regarded as inconclusive, when it was reduced to 50° in an attempt to obtain information about the temperature coefficient of the reaction.

Anhydrous ammonia, obtained from Matheson Co., was subjected to several bulb-to-bulb distillations over the temperature range -70 to -90°. The ammonia then was stored in a glass bulb with vacuum stopcock, from which it could be released into the mass spectrometer manifold to a predetermined pressure.

The procedure followed was to select a set of conditions of ammonia pressure, repeller voltage and shield voltage, and scan to mass 44, the masses of specific interest being 16 ( $\text{NH}_2^+$ ), 17 ( $\text{NH}_3^+$ ), 18 ( $\text{NH}_4^+$ ) and 33 ( $\text{N}_2\text{H}_5^+$ ). For comparison with the rate of reaction 2, deuteriomethane, obtained from Tracerlab, was introduced under identical conditions of repeller voltage and shield voltage and the peak heights of the product ions  $\text{CD}_5^+$  and  $\text{C}_2\text{D}_3^+$  determined.

#### Results and Discussion

The peak height for the ion of mass 18,  $\text{NH}_4^+$ , is increased very substantially by increase in pressure and decrease in repeller voltage and shield voltage. Some of the data are shown in Table I in which the observed values for the ratio mass 18/mass 17 are listed for the various conditions. The mass 18 peak height has, of course, been corrected for the  $\text{N}^{15}$  and  $\text{H}^2$  contributions from the  $\text{NH}_3^+$  ion.

That the appearance of a peak at mass 18 is due to a secondary reaction in the ion source and not to any impurity is evident from the usual criteria. Firstly the mass 18 peak height is increased with decreasing repeller field strength (decreasing repeller voltage and shield voltage). The impurity content, possibly water, is exceedingly low as is evident from the mass ratio of 0.0031 obtained under normal

(6) A. B. Zahlan and B. P. Burt, *J. Chem. Phys.*, **24**, 478 (1956).

(7) B. P. Burt and A. B. Zahlan, *ibid.*, **26**, 846 (1957).

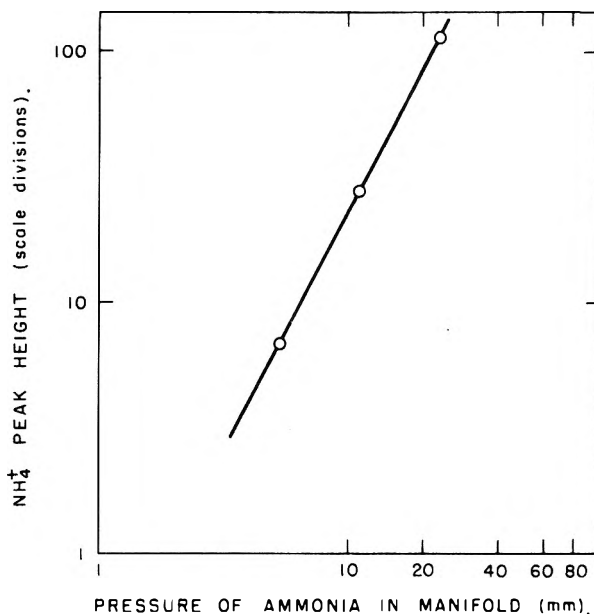


Fig. 1.—Pressure dependence of ammonium ion formation.

TABLE I  
DATA FOR  $\text{NH}_4^+$  FORMATION

| Ionization <sup>a</sup><br>gauge<br>reading<br>( $\mu$ ) | Repeller<br>voltage<br>(v.) | Shield<br>voltage<br>(v.) | Mass 18/Mass 17 |
|----------------------------------------------------------|-----------------------------|---------------------------|-----------------|
| 0.001                                                    | 8.0                         | 70                        | 0.0031          |
| .001                                                     | 0                           | 70                        | .022            |
| .009                                                     | 0                           | 70                        | .054            |
| .003                                                     | 0                           | 22.5                      | .055            |
| .03                                                      | 0                           | 15                        | .327            |
| .04                                                      | 0                           | 12                        | .857            |
| .04                                                      | 0                           | 11                        | 2.001           |

<sup>a</sup> The ionization gauge reading is not to be taken as the actual pressure in the ion source. It is merely a relative indication of the pressure increase.

analytical conditions. The reaction forming the mass 18 ion is, in fact, a homogeneous bimolecular reaction as may be seen from the second criterion that the  $\text{NH}_4^+$  peak height approaches proportionality in the square of the pressure as the extent of reaction decreases toward zero. The dependence on square of the pressure may be seen in Fig. 1 which shows data obtained at a repeller plate voltage of 1 volt. The slope of the line is 1.9.

The fact that the  $\text{NH}_4^+/\text{NH}_3^+$  peak height ratio reaches values as high as 2 is itself an indication that reaction 1 occurs with high efficiency. A rough estimate of the magnitude of the rate constant may be obtained by comparison with reaction 2, for which the rate constant is independent of temperature and has the value<sup>2</sup>  $k_2 = 1.4 \times 10^{-9}$  cm.<sup>3</sup> molec.<sup>-1</sup> sec.<sup>-1</sup>.

The comparative data for methane-*d*<sub>4</sub> and ammonia are shown in Table II in which the actual peak heights for shield voltage settings of 22.5 and 16.5 volts are listed.

An estimate of the rate constant ratio,  $k_1/k_2$ , may be obtained from the ratio

$$\frac{[\text{NH}_4^+]_0}{[\text{CD}_5^+]_0} \times \frac{[\text{CD}_4^+]_0[\text{CD}_4]}{[\text{NH}_3^+]_0[\text{NH}_3]}$$

where  $[\text{CD}_4^+]_0$  and  $[\text{NH}_3^+]_0$  are the initial ion con-

TABLE II  
COMPARATIVE DATA FOR METHANE- $d_4$  AND AMMONIA<sup>a</sup>

| Ion mass | Methane- $d_4$         |                        | Ammonia                |                        |
|----------|------------------------|------------------------|------------------------|------------------------|
|          | Shield voltage 22.5 v. | Shield voltage 16.5 v. | Shield voltage 22.5 v. | Shield voltage 16.5 v. |
| 16       |                        |                        | 6930                   | 631                    |
| 17       |                        |                        | 16900                  | 8170                   |
| 18       | 2250                   | 330                    | 2539.5                 | 2468                   |
| 20       | 3160                   | 820                    | ...                    | ...                    |
| 22       | 124.2                  | 92.4                   | ...                    | ...                    |
| 33       | ...                    | ...                    | ...                    | ...                    |
| 34       | 84.5                   | 36.1                   | ...                    | ...                    |

<sup>a</sup> Repeller voltage was set at zero for these readings.

centrations prior to reaction, taking the concentrations as being proportional to the peak heights. The actual measured sensitivities for the parent peaks of ammonia and methane- $d_4$  are 17 and 20 divisions/ $\mu$ , respectively. It is assumed that the ratios of the ion collection efficiencies  $\text{NH}_4^+/\text{NH}_3^+$  and  $\text{CD}_5^+/\text{CD}_4^+$  are equal. The fact the masses of the ions involved in reaction 1 are closely similar to those in the comparison reaction 2 is helpful in avoiding purely instrumental effects.

The two sets of data in Table II give values of 0.6 and 0.2 for the rate constant ratio, with the lower value probably being the more reliable since the instrument settings at 16.5 volts remained unchanged, rather than being reset, in taking the data. These data, then, result in the approximation  $k_1 \sim 0.5 \times 10^{-9} \text{ cm.}^3 \text{ molec.}^{-1} \text{ sec.}^{-1}$ , a value

which is, of course, significant only as an order of magnitude estimate. Reduction of the source temperature from 150 to 50° failed to show any effect. Since it is unlikely that thermal equilibrium was attained at these low pressures in the ion source, no conclusion can be reached about the temperature coefficient of the reaction.

NOTE ADDED IN PROOF.—In a recent paper V. L. Talrose and E. L. Frankevich (Treatise of the First All-Union Conference on Radiation Chemistry, page 13, Published by the Academy of Sciences of the U.S.S.R., Moscow 1958) report the observation of reaction (1) and indicate the heat of reaction to be 28 kcal./mole.

### Conclusions

The foregoing observations which show that reaction 1 does occur with high efficiency, provide a direct basis, in addition to the purely phenomenological evidence discussed by Burt and Zahlan,<sup>7</sup> for including ammonium ion formation as an important process in the radiolysis of gaseous ammonia. On the other hand, our failure to detect the  $\text{N}_2\text{H}_5^+$  ion, even though  $\text{NH}_4^+$ ,  $\text{CD}_5^+$  and  $\text{C}_2\text{D}_5^+$  were readily observable, may be taken as an indication that the reaction



also suggested by them,<sup>7</sup> has a low probability of occurrence, or that the  $\text{N}_2\text{H}_5^+$  ion formed is too unstable to be detected in a conventional analytical mass spectrometer.

# OVERPOTENTIAL ON ACTIVATED PLATINUM CATHODES IN SODIUM HYDROXIDE SOLUTIONS

BY I. A. AMMAR AND SOHEIR DARWISH

*Department of Chemistry, Faculty of Science, University of Cairo, Cairo, Egypt*

*Received May 19, 1958*

Hydrogen overpotential has been measured on platinum in 0.1 *N* sodium hydroxide at 25°. It has been found that anodic activation up to 10<sup>-2</sup> coulomb/cm.<sup>2</sup>: (i) decreases both the overpotential values and the Tafel slope; (ii) increases both the exchange current and the electron number. With the use of quantities of electricity higher than 10<sup>-2</sup> coulomb/cm.<sup>2</sup>, the direction of change of the overpotential parameters is revised.

Measurements of hydrogen overpotential on Pt in acid solutions have established the necessity of anodic activation as a means of removing surface impurities.<sup>1,2</sup> The agreement between the results obtained for activated electrodes<sup>1</sup> and those for non-activated electrodes cleaned by ultrasonication<sup>3</sup> suggests that the anomalous behavior of Tafel lines for Pt<sup>4</sup> in pure solutions may be attributed to the presence of impurities on the electrodes surface. In alkaline solutions, however, the situation is still unclear. Two Tafel line slopes (varying between 0.116 and 0.138 v. for the lower value, and between 0.220 and 0.252 v. for the higher one) have been observed in the pH range 8.2–10.9.<sup>5</sup> Above pH 10.9, one slope (0.126–0.128 v.) has been observed. In strongly alkaline solutions (above pH 12.1) it has not been possible to obtain consistent results even with the use of highly purified sodium amalgam for the solution preparation, and with extensive pre-electrolysis lasting for weeks.<sup>5</sup> In the present investigation, hydrogen overpotential is measured on activated bright Pt in 0.1 *N* NaOH at 25°, and the conditions of activation, leading to reproducible results, are discussed.

## Experimental

The experimental technique was essentially similar to that of Bockris, *et al.*<sup>1,6</sup> The cell was similar to that used by Bockris and Potter.<sup>6</sup> It was constructed of arsenic-free glass and incorporated ungreased water-sealed taps and ground glass joints. A platinized platinum electrode was used as a reference. To decrease anodic polarization, the anode was in the form of a large Pt sheet 6 cm.<sup>2</sup> in area. This electrode was far removed from the cathode compartment. The anode and cathode compartments were separated by a sintered glass disc and a tap which was kept closed during pre-electrolysis and measurements. The pre-electrolysis electrode was in the form of a Pt wire (area 0.5 cm.<sup>2</sup>) sealed to glass. A platinized Pt sheet (area 5–6 cm.<sup>2</sup>) was dipped in the solution during pre-electrolysis to adsorb impurities. The solution was vigorously agitated by pure H<sub>2</sub>. H<sub>2</sub> was purified by passing it into three furnaces containing Cu heated to 450°, then over soda lime and silica gel. Pt cathodes were cut from a spectroscopically pure Pt wire of diameter 1 mm. They were directly sealed to glass and were then cleaned with chromic acid followed by conductance water. In some experiments the bulb technique was employed.<sup>7</sup> NaOH solutions were prepared from pure crystallized NaOH (under H<sub>2</sub>) by dilution

with conductance water ( $K = 5 \times 10^{-7}$  ohm<sup>-1</sup> cm.<sup>-1</sup>) and were pre-electrolyzed in a separate cell before being transferred by H<sub>2</sub> pressure to the overpotential cell, and pre-electrolysis was again carried out at 10<sup>-2</sup> amp./cm.<sup>2</sup> for 25–30 hours. A further increase in the time of pre-electrolysis had no effect on overpotential. A successful experiment was characterized by the constancy of  $\eta$ , at a constant current density, with time and by the agreement between the "up" and "down" Tafel lines.<sup>3</sup> The electrolyte concentration was checked by titration after each experiment. The direct method of measurements was employed up to about 10<sup>-3</sup> amp./cm.<sup>2</sup> making use of a luggin capillary. Stirring had no effect on  $\eta$  at low current densities, but it decreased it at high current densities (*e.g.*, above 10<sup>-3</sup> amp./cm.<sup>2</sup>). Most of the measurements were, therefore, carried out in unstirred solutions, and only for measurements above 10<sup>-3</sup> amp./cm.<sup>2</sup> was the solution stirred. At low current densities, the current was checked by measuring the p.d. across a standard 0.1 megohm resistance. The apparent surface area was used to calculate the current density. Anodic activation was carried out at various quantities of electricity. After activation, the electrode was cathodically polarized, at the highest current density used for overpotential measurements, with H<sub>2</sub> vigorously bubbling in the solution. The electrode potential was then measured as a function of time, and the steady-state value was attained in 20–30 minutes. Following this the Tafel line was measured.

## Results

An example of the results for non-activated electrodes (sealed in air) is shown in Fig. 1 from which it is clear that the Tafel slope  $b$  is 0.26 v. It is also clear that the departure from linearity occurs at an appreciable overpotential of about 0.2 v. The "up" and "down" Tafel lines are identical, and  $\eta$  is not affected by stirring. Although the measurements at low current densities indicate a linearity between  $\eta$  and the current density up to a value of about 50 mv., yet the value of the electron number  $\lambda^9$  calculated for this electrode is about 0.2.  $\lambda$  is defined as the number of electrons necessary to complete one act of the rate-determining step and it is related to the stoichiometric number  $\nu$  by<sup>9</sup>

$$\lambda = 2/\nu$$

Neither the above value of  $\lambda$  nor the value of the Tafel slope correspond to any theory of overpotential. The mean parameters of six separate results obtained under similar conditions are given in Table I, together with the corresponding mean deviation from the mean.

Anodic activation of Pt electrodes (sealed in air) was carried out at 10<sup>-3</sup>, 10<sup>-2</sup>, 10<sup>-1</sup> and 5 × 10<sup>-1</sup> coulomb/cm.<sup>2</sup> of the electrode surface. The current was varied and the time of activation was kept constant at 2 minutes. The mean results are given in

(1) J. O'M. Bockris, I. A. Ammar and A. K. Huq, *THIS JOURNAL*, **61**, 879 (1957).

(2) E. Wicke and W. Weblus, *Z. Elektrochem.*, **56**, 159 (1952).

(3) E. Yeager, T. Oey and F. Hovorka, *THIS JOURNAL*, **87**, 268 (1953).

(4) Associated with Tafel line slopes of 0.19–0.3 v.; *cf.* J. O'M. Bockris, *Chem. Revs.*, **43**, 525 (1948).

(5) S. Schuldiner, *J. Electrochem. Soc.*, **101**, 426 (1954).

(6) J. O'M. Bockris and E. C. Potter, *J. Chem. Phys.*, **20**, 614 (1952).

(7) J. O'M. Bockris and B. Conway, *J. Sci. Instr.*, **25**, 283 (1948).

(8) Tafel lines measured from low to high current densities and *vice versa*.

(9) J. O'M. Bockris and E. C. Potter, *J. Electrochem. Soc.*, **99**, 169 (1952).



TABLE I  
PARAMETERS OF HYDROGEN EVOLUTION ON Pt ELECTRODES SEALED IN AIR

| Condition                                       | No. of expts. | $b$ (mv.)    | $i_0$ (amp./cm. <sup>2</sup> ) | $\lambda$       | $10^{-4}$ amp./cm. <sup>2</sup> | $\eta$ (mv.) at $3.16 \times 10^{-4}$ | $10^{-3}$    |
|-------------------------------------------------|---------------|--------------|--------------------------------|-----------------|---------------------------------|---------------------------------------|--------------|
| Non-activated                                   | 6             | $250 \pm 10$ | $(2.7 \pm 0.4)10^{-6}$         | $0.16 \pm 0.02$ | $385 \pm 6$                     | $508 \pm 12$                          | ...          |
| Activated at $10^{-3}$ coulomb/cm. <sup>2</sup> | 4             | $161 \pm 5$  | $(8.0 \pm 0.6)10^{-6}$         | $.24 \pm .07$   | $173 \pm 2$                     | $254 \pm 4$                           | $333 \pm 8$  |
| Activated at $10^{-2}$                          | 11            | $114 \pm 11$ | $(6.8 \pm 0.7)10^{-5}$         | $.92 \pm .18$   | $32 \pm 5$                      | $76 \pm 9$                            | $133 \pm 13$ |
| Activated at $10^{-1}$                          | 11            | $116 \pm 14$ | $(2.2 \pm 1.5)10^{-5}$         | $.56 \pm .27$   | $97 \pm 14$                     | $152 \pm 12$                          | $209 \pm 15$ |
| Activated at $5 \times 10^{-1}$                 | 6             | $127 \pm 7$  | $(1.5 \pm 1.1)10^{-5}$         | $.38 \pm .06$   | $131 \pm 22$                    | $200 \pm 10$                          | $271 \pm 3$  |

TABLE II  
PARAMETERS OF HYDROGEN EVOLUTION ON Pt ELECTRODES SEALED IN H<sub>2</sub>

| Condition                                       | No. of expts. | $b$ (mv.)    | $i_0$ (amp./cm. <sup>2</sup> ) | $\lambda$       | $10^{-4}$ amp./cm. <sup>2</sup> | $\eta$ (mv.) at $3.16 \times 10^{-4}$ | $10^{-3}$   |
|-------------------------------------------------|---------------|--------------|--------------------------------|-----------------|---------------------------------|---------------------------------------|-------------|
| Non-activated                                   | 4             | $168 \pm 10$ | $(2.1 \pm 0.2)10^{-6}$         | $0.48 \pm 0.06$ | $280 \pm 6$                     | $364 \pm 9$                           | $445 \pm 7$ |
| Activated at $10^{-2}$ coulomb/cm. <sup>2</sup> | 4             | $111 \pm 5$  | $(7.3 \pm 1.2)10^{-6}$         | $0.91 \pm 0.13$ | $128 \pm 7$                     | $183 \pm 6$                           | $239 \pm 5$ |

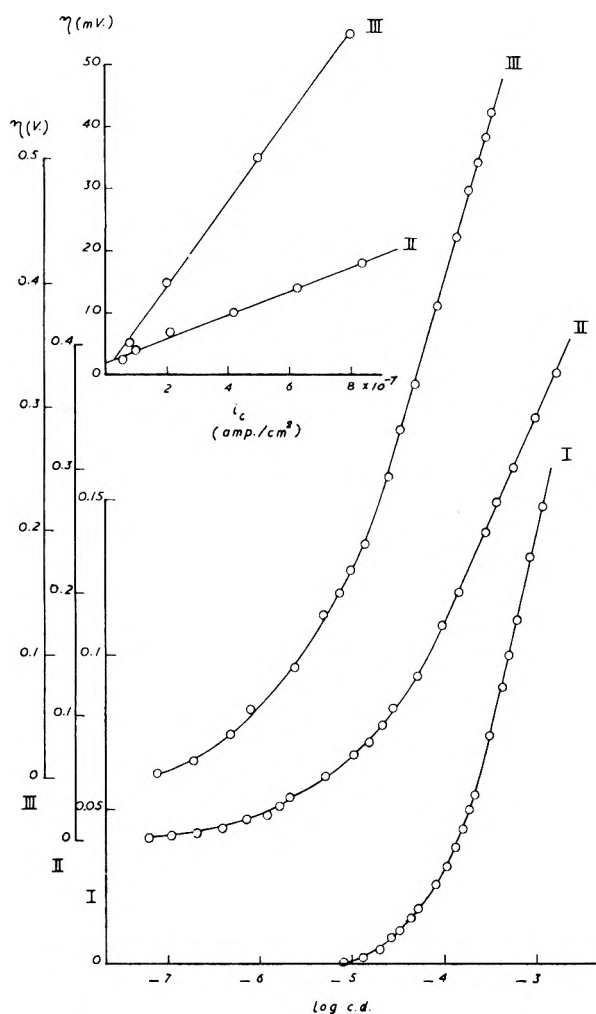


Fig. 1.—Hydrogen overpotential on Pt in 0.1 N NaOH at 25°C: I, activated at  $10^{-2}$  coulomb/cm.<sup>2</sup>; II, activated at  $10^{-3}$ ; III, non-activated.

Table I, and two examples of the results for electrodes activated at  $10^{-3}$  and  $10^{-2}$  coulomb/cm.<sup>2</sup> are shown in Fig. 1 for comparison. It is clear from this figure that the values of  $\eta$  and  $b$  for the electrode activated at  $10^{-3}$  coulomb/cm.<sup>2</sup> are smaller

than the corresponding values for the non-activated electrode, and a further decrease in  $\eta$  and  $b$  is observed for the electrode activated at  $10^{-2}$  coulomb/cm.<sup>2</sup>. Anodic activation also decreases the overpotential at which the Tafel line departs from linearity (Fig. 1). Above  $10^{-2}$  coulomb/cm.<sup>2</sup>, both  $\eta$  and  $b$  increase (Table I). The relation between the exchange current  $i_0$  and the quantity of electricity passed during activation,  $Q$ , is opposite to that between  $\eta$  and  $Q$ . The maximum value of  $\lambda$  is observed for electrodes activated at  $10^{-2}$  coulomb/cm.<sup>2</sup>. Since in alkaline solutions the rate-determining step is the discharge from water molecules<sup>6,10</sup> which is characterized by a slope of 0.118 v. at 25° and by a value of  $\lambda = 1$ , the results for electrodes activated at  $10^{-2}$  coulomb/cm.<sup>2</sup> represent the best approach of the experimental results to the theoretical requirements. No  $iR$  drop is observed in these results (*cf.* curve 1, Fig. 1), and stirring effects are negligible up to  $10^{-3}$  amp./cm.<sup>2</sup> For this reason  $iR$  correction was not necessary for the present investigation.

The mean results for electrodes sealed in H<sub>2</sub> are given in Table II which indicates that both  $\eta$  and  $b$  decrease, while  $i_0$  and  $\lambda$  increase, for activated electrodes as compared with the results for non-activated electrodes.

The effect of anodic activation on  $\eta$  may be attributed to changes in the nature of the surface such that, at low values of  $Q$ , the heat of activation for the discharge reaction is decreased with the consequent increase of the exchange current and the decrease of  $\eta$ .<sup>11</sup> This may be visualized if anodic activation cleans the electrode surface from impurities and exposes sites of adsorption for the cathodic hydrogen evolution reaction. At high values of  $Q$ , however, oxidation may take place, and the presence of oxide films increases  $\eta$ .<sup>12</sup> Although, before the measurements of  $\eta$ , the activated Pt electrode was made the cathode for 20–30 minutes at the

(10) R. Parsons and J. O'M. Bockris, *Trans. Faraday Soc.*, **47**, 914 (1951).

(11) B. Conway and J. O'M. Bockris, *Nature*, **178**, 488 (1956); *J. Chem. Phys.*, **26**, 532 (1957).

(12) A. Frumkin, *Disc. Faraday Soc.*, **1**, 57 (1947).

highest current density used for overpotential measurements (*cf.* Experimental), yet this procedure might have been incapable of reducing the surface oxide film probably produced at high values of  $Q$ .

## THE EXPERIMENTAL CHECK OF THEORIES OF THE VISCOSITIES OF SOLUTIONS<sup>1</sup>

BY WLADIMIR PHILIPPOFF AND FREDERICK H. GASKINS

*The Franklin Institute Laboratories for Research and Development, Philadelphia, Penna.*

*Received July 7, 1958*

The solutions of the synthetic polypeptide, poly- $\gamma$ -benzyl-L-glutamate (PBLG), reported by Yang<sup>2</sup> are practically monodisperse either as tightly wound  $\alpha$ -helices (similar to rigid ellipsoids) in *m*-cresol as a solvent or random coils in dichloroacetic acid. This gives the experimental possibility of testing the existing theories of the viscosities of suspensions without the disturbing influence of polydispersity. The theory for rigid ellipsoids requires a departure from the initial viscosity  $\eta_0$  at low rates of shear  $D$  with the square of either the shear stress  $\tau$  or of  $D$ , rather than linearly with  $\tau$  or  $D$ . This was confirmed for the *m*-cresol solutions of PBLG. The dichloroacetic acid solutions, however, give a linear dependence on  $\tau$ . This shows that even monodisperse solutions of random coils give a linear deviation from  $\eta_0$ . This may be the result of an "internal polydispersity" for each single coil in the sense introduced by Rouse<sup>3</sup> for the dynamic behavior of polymer solutions. The normal linear departure from  $\eta_0$  for polymer solutions is therefore very probably caused by polydispersity in a general sense.

### I. Introduction

At present two theories treating the viscosity of suspensions are applicable to solutions of high polymers: the theory of rigid ellipsoids (rods) and the one of coiled molecules. Both theories have been extensively treated; also, the dependence of the intrinsic viscosity on the molecular weight of the polymer has been tested experimentally. However, the theoretical relationships are explicitly valid for infinite dilution and usually for a rate of shear approaching zero. Until recently all polymer solutions were more or less polydisperse. This polydispersity influences the relationships derived for monodisperse solutions, but one had no way of eliminating it.

The solutions of the synthetic polypeptide (PBLG) reported by Yang (*ref.* 2) are practically monodisperse, either as rods or random coils dependent on the solvent. They give the possibility of testing experimentally the existing theories of the viscosities of suspensions without the disturbing influence of polydispersity.

The dependence of viscosity on the rate of shear (non-Newtonian viscosity) has been theoretically treated for both models. The results of the theory of rigid ellipsoids require the viscosity to be an even-powered function of the rate of shear; in other words, the decrease of viscosity from its limiting value at low rates of shear must be proportional to the square of the rate of shear  $D$ . Until now, in practically all of the investigated cases, a linear decrease of viscosity with  $D$  was found. This discrepancy could possibly have been caused by polydispersity, but it was impossible to check the validity of the theory since there were no monodisperse high polymers. The conditions for coiled molecules with regard to the non-Newtonian viscosity have not yet been calculated to make definite predictions in this respect. The PBLG gave us the experimental possibility of testing the departure of the

viscosity from the "initial" viscosity (Newtonian viscosity) at low rates of shear for both rigid rods and coils of the same material in monodisperse solutions.

The experimental check described below showed that the requirements of the theory of rigid rods are indeed fulfilled for monodisperse systems. Investigation of the monodisperse coils showed that their behavior is qualitatively different from the one of rigid rods, since the solutions of random coils give a linear deviation from  $\eta_0$ .

### II. Experimental

The material used was a synthetic polypeptide, poly- $\gamma$ -benzyl-L-glutamate (PBLG), which has been described by Yang in reference 2. We investigated several concentrations of PBLG: 0.5, 0.8 and 1.1% by weight in *m*-cresol (MC) and 0.5 and 0.82% by weight in dichloroacetic acid (DCA). All of these were measured at 25°; in addition, the 0.5% *m*-cresol solution was measured at 15 and 35°. Yang has reported these data with the exception of the data at 15 and 35°.

The viscometer used is a high pressure capillary viscometer<sup>4</sup> for which the principle of operation has been summarily described.<sup>5</sup> We could use two calibrated capillaries interchangeably at the rates of shear  $D$  required for this investigation, which ranged from 4 to about 350,000 sec.<sup>-1</sup> (a range of about 100,000 to 1) corresponding to shear stresses  $\tau$  of 6 to 65,000 dynes/cm.<sup>2</sup> (a range of 10,000 to 1). The precision of the measurements was in the mean  $\pm 1\%$  as determined by the deviation from a smoothed curve.

### III. Results

The flow curves ( $\log D$  vs.  $\log \tau$ ) have been given as Figs. 2 and 3 in Yang's paper; therefore, they will not be repeated here. In Fig. 1, we have plotted the specific viscosity

$$\eta_{sp} = \left[ \frac{t\eta_0}{t\eta_s} - 1 \right] \quad (1)$$

where  $\eta_0$  is the soln. viscosity  
 $\eta_s$  is the solvent viscosity

linearly as a function of  $\log \tau$  (in dynes/cm.<sup>2</sup>). This plot allows a large range of shearing stresses to be plotted in a limited space, but tends to

(1) Presented at the Meeting of the American Chemical Society, September, 1957, New York City.

(2) J. T. Yang, *J. Am. Chem. Soc.*, **80**, 1783 (1958).

(3) P. E. Rouse, Jr., *J. Chem. Phys.*, **21**, 1272 (1953).

(4) J. G. Brodnyan, F. H. Gaskins, W. Philippoff and E. G. Lendrat *Trans. Soc. Rheology*, **II**, in print (1958).

(5) W. Philippoff, F. H. Gaskins and J. G. Brodnyan, *J. Appl. Phys.*, **28**, 1118 (1957).

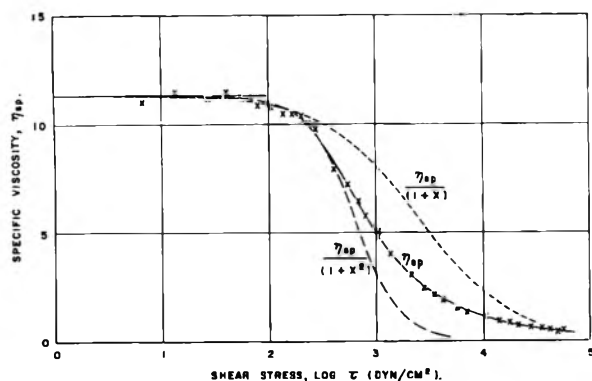


Fig. 1.—Specific viscosity vs. log shear stress for 1.1% PBLG in *m*-cresol at 25.5°.

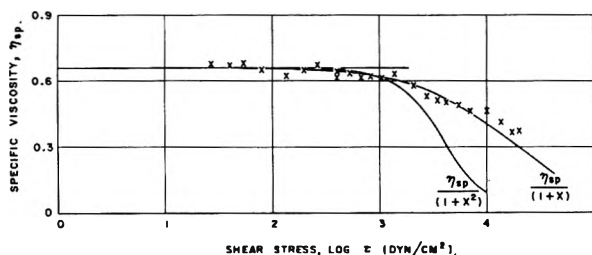


Fig. 2.—Specific viscosity vs. log shear stress for 0.5% PBLG in dichloroacetic acid at 25.5°.

magnify the errors in  $\eta_{sp}$ . The values shown are for the 1.1% PBLG in MC at 25.5°. In Fig. 2, the results similarly plotted for the 0.5% solution in DCA are shown. In Fig. 3, the measurements at different temperatures are shown for 0.5% PBLG in MC, plotting  $\eta_{sp}$  vs.  $\log D$  (in sec.<sup>-1</sup>). In the range of temperatures used (15 to 35°) the curves are distinctly separated in the entire range of  $D$  used. In Fig. 4, the latter values are plotted against  $\log \tau$ . In this case the data at the three temperatures form a narrow band around a mean curve. Beginning from about 300 dynes/cm.<sup>2</sup>, there is no detectable temperature effect in a large range of shearing stresses; below this limit a slight temperature coefficient was measured on a 0.54% solution by Yang in an Ubbelohde viscometer; i.e., the  $\eta_{sp}$  dropped slightly with increase in temperature which is a normal behavior for solutions of high polymers.

The specific viscosity data for the various solutions are listed in Table I. Here  $\eta_{sp}$  is calculated according to equation 1; however, the initial or

TABLE I  
SPECIFIC VISCOSITY DATA FOR PBLG SOLUTIONS

| Solution                      | Temp., °C. | Initial viscosity $\eta_0$ , poise | Solvent viscosity $\eta_s$ , poise | Specific viscosity, $\eta_{sp}$ |
|-------------------------------|------------|------------------------------------|------------------------------------|---------------------------------|
| 1.1% PBLG in <i>m</i> -cresol | 25.5       | 1.515                              | 0.123                              | 11.31                           |
| 0.8% PBLG in <i>m</i> -cresol | 25.5       | 0.857                              | .123                               | 5.97                            |
| 0.5% PBLG in <i>m</i> -cresol | 15.0       | .901                               | .230                               | 2.92                            |
|                               | 25.3       | .451                               | .127                               | 2.55                            |
|                               | 34.3       | .289                               | .0819                              | 2.53                            |
| 0.82% PBLG in DiClAc acid     | 25.5       | .140                               | .0630                              | 0.123                           |
| 0.50% PBLG in DiClAc acid     | 25.5       | .105                               | .0630                              | 0.660                           |

“zero-shear” viscosity of the solution is used in this case.

In Fig. 5, all the data obtained at 25° with MC and DCA have been reduced to a common curve taking the ratio of the measured (apparent) viscosity to the initial viscosity at low rates of shear plotted vs.  $\log \tau$ . Here the values form two narrow bands, one for each type of solvent; the concentration influence is very small in this plot, therefore, the results are directly applicable to  $[\eta]$ . Whereas, the flow curves for the same solutions are widely different.

#### IV. Discussion

The figures show that the solutions of PBLG have a very pronounced non-Newtonian viscosity which in all cases at low rates of shear reaches a limit: the initial viscosity. The effects are more pronounced for solutions in MC where the PBLG is present as rigid rods. In Fig. 5, the viscosity  $\eta_{sp}$  decreases by a factor of 20 in the range measured, even for the 0.5% solution where the specific viscosity was 2.5 at low rates of shear. This would also hold for  $\eta_{sp} \rightarrow 0$  or for  $[\eta]$ . The paper by Yang shows that the values of Fig. 5 replotted as the intrinsic viscosity  $[\eta]$  vs.  $\log D$  can be directly compared with the results of the theory of rigid ellipsoids calculated by Scheraga.<sup>6</sup> The coincidence is as good as could be expected and illustrates that the complicated mathematical development of the theory of rigid ellipsoids can indeed be verified when suitable systems are used. A suitable system in this sense is a suspension of monodisperse rigid rods of submicroscopic size.

In the comparison just discussed, there is no difference in the plot of  $\eta_{sp}$  either vs.  $\log D$  or vs.  $\log \tau$  since the values become reduced to infinite dilution when  $\eta_{sp} \rightarrow 0$  and shearing stress and rate of shear are proportional to each other. For any finite variable  $\eta_{sp}$ , as has been shown in Figs. 3 and 4, both plots are qualitatively different except in the region of initial viscosity ( $\eta_{sp} = \text{constant}$ ).

The results with rigid rods as seen in Figs. 1, 4 and 5 were then mathematically analyzed as to the manner in which the initial viscosity changes to the non-Newtonian viscosity. The purpose of this was to establish definitely whether the non-Newtonian behavior of monodisperse rigid rods begins as a linear or as a quadratic function of the shearing stress. To be more explicit, it has been often stated that the rate of shear  $D$  should be a series of uneven powers of the shearing stress  $\tau$  in order to be independent of the direction of flow

$$D = a_1\tau + a_2\tau^3 + a_5\tau^5 \dots \quad (2)$$

This leads to a viscosity as a function of the shear stress

$$\eta = \frac{\tau}{D} = \frac{1}{a_1 + a_3\tau^2 + a_5\tau^4 \dots} \quad (3)$$

It is however known experimentally that

$$D = a_1\tau + a_2\tau^2 + a_3\tau^3 + a_4\tau^4 \dots \quad (4)$$

which leads to a viscosity

$$\eta = \frac{1}{a_1 + a_2\tau + a_3\tau^2 + \dots} \quad (5)$$

(6) H. A. Scheraga, *J. Chem. Phys.*, **23**, 1526 (1955).

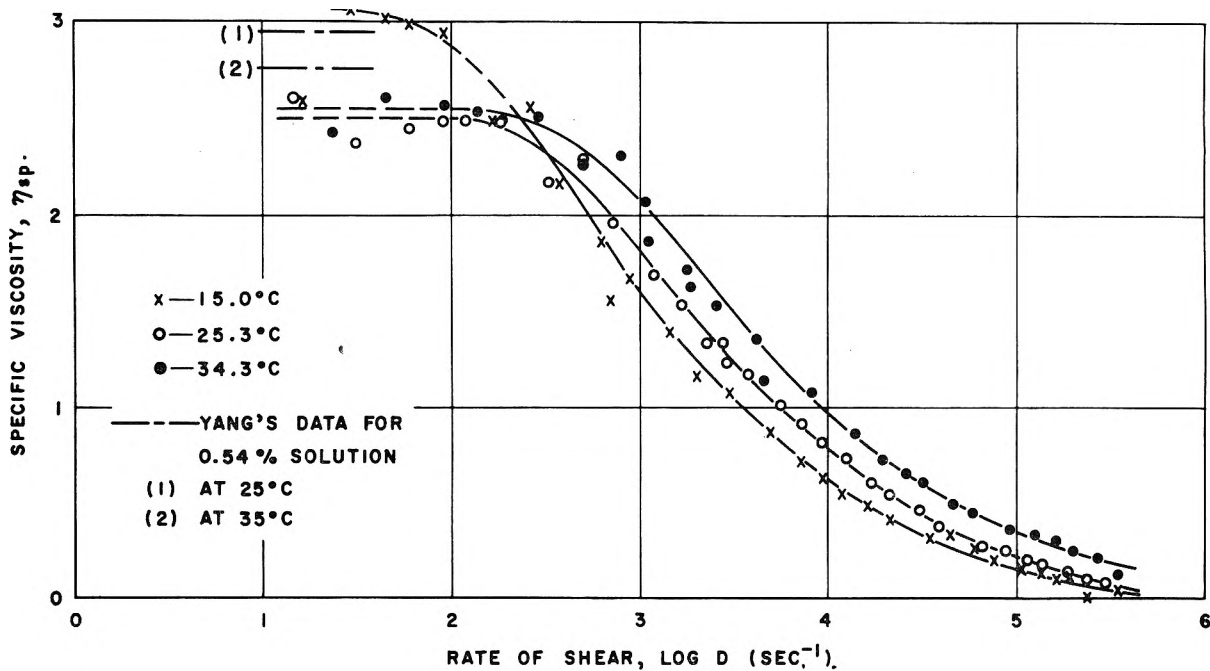


Fig. 3.—Specific viscosity vs. log rate of shear for 0.5% PBLG in *m*-cresol at several temperatures.

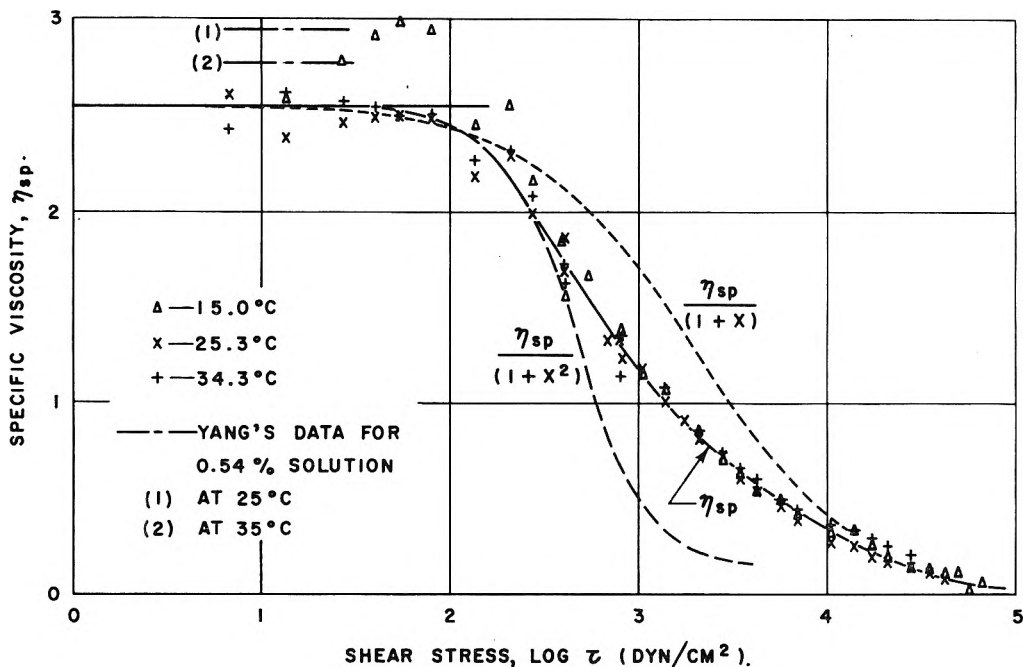


Fig. 4.—Specific viscosity vs. log shear stress for 0.5% PBLG in *m*-cresol at several temperatures.

Considering, as a first approximation, the terms with  $a_2$  and  $a_3$  only, the problem is to ascertain if  $a_2$  exists under our conditions.  $a_2$  (and  $a_4 \dots$ ) means that a change of  $+\tau$  to  $-\tau$  would give different values of  $D$ , which is not observed experimentally. This difficulty has been circumvented with no real theoretical justification by substituting the absolute value of  $\tau$  in equation 2 and 4.

In order to test these relationships, as has already been done in a previous publication,<sup>7</sup> we first discussed the form of the equations to be used. The equations shown (no. 2 to 5) apply to the absolute viscosity. However, we are more

(7) W. Philippoff and F. H. Gaskins, *J. Polymer Sci.*, **21**, 205 (1956).

interested in the increase in the viscosity due to the polymer, *i.e.*, the specific viscosity of the solution. Therefore, we graphically fitted the experimental curves to the equations

$$\eta = \frac{\eta_{sp}}{1 + x^2} \tag{6}$$

$$\eta = \frac{\eta_{sp}}{1 + x} \tag{7}$$

We have experimental data with small  $\eta_{sp}$ , where the viscosity of the solvent has a marked influence. Physically a viscosity of the solution lower than that of the solvent is not possible (or has never been observed). Therefore, it seems logical to proceed in the manner outlined above. Should we use

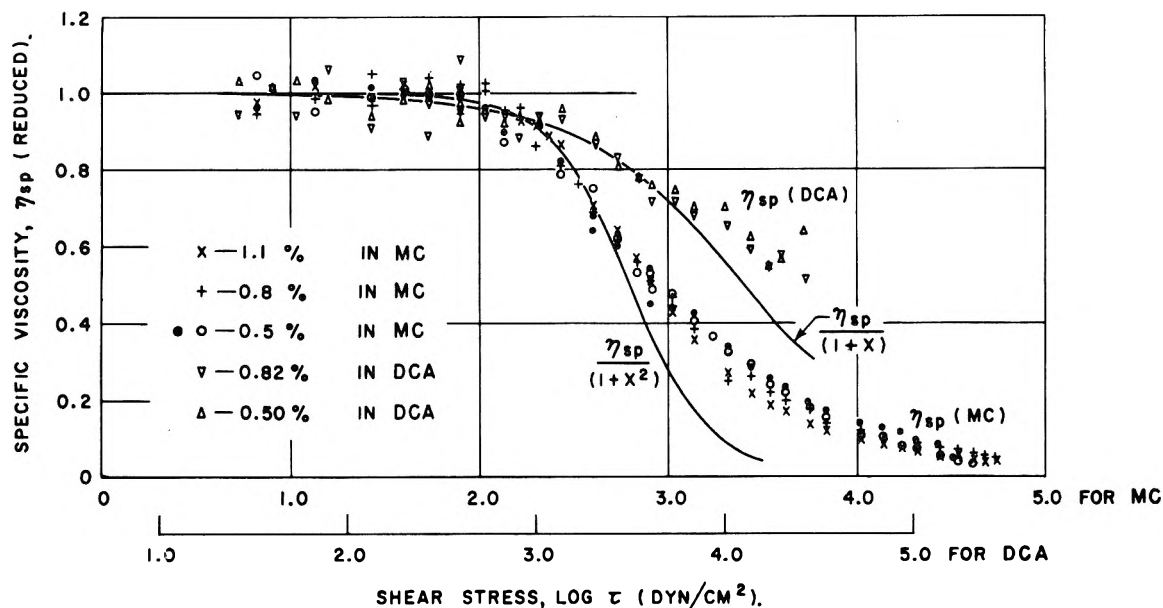


Fig. 5.—Specific viscosity vs. log shear stress for PBLG in *m*-cresol and in dichloroacetic acid at 25°.

equations 2 and 7, a drop of viscosity below that of the solvent is possible (negative  $\eta_{sp}$ ). Practically for the more viscous solution the difference within the first part of the drop in viscosities is very small. In order to evaluate the results, we introduced as  $\eta_{sp}$ , the value of the initial viscosity of the solution and shifted the curves  $[1/(1+x)]$  and  $[1/(1+x^2)]$  along the  $\log \tau$  axis until a best fit was achieved in the top part of the curve. The difference between the two curves up to about 10% viscosity decrease is exceedingly small. Therefore, the decision as to which curve fits better in this range requires enormous precision in the measurements which has not yet been achieved in the required large range of shearing stresses. However, we found that up to a value of 40% viscosity decrease the two functions deviate considerably, much in excess of the experimental scatter.

As seen in Fig. 5, the "linear" function  $[1/(1+x)]$  fits the curve of the MC solutions only up to about 8% decrease in viscosity. This is especially well seen in Fig. 1 where the linear function fits only the first 5% of viscosity decrease, in which range the two curves are indistinguishable. However, the "square" function  $[1/(1+x^2)]$  fits the curves both in Fig. 5 and in Fig. 1, up to a viscosity decrease of 40%. This means that almost a tenfold increase in coincidence is achieved by using the quadratic function. This points out that the theoretical formula, equation 1, fits the data for monodisperse rods considerably better than equation 3. We also performed a statistical analysis of the mean errors occurring in the curve fitting and got the same results as stated above.

Concerning the solutions in DCA where PBLG exists in the shape of random coils, the situation is reversed. The quadratic function is only an approximation of the first 5% of viscosity decrease where both functions are practically indistinguishable; whereas, the linear function is valid up to about 35% as seen in Figs. 5 and 2. In other

words, equation 3 is the one valid for solutions of random coils.

Due to the particular properties of the PBLG we are sure that the polydispersity with regard to the molecular weight ("polymolecularity") is not present and therefore cannot cause this marked qualitative difference. Should, however, a number of sizes and molecular weights be present, it is logical to expect that the curve for the rods as shown in Fig. 5, will be "flattened out." A similar behavior has been found experimentally for a mixture of solutions of high polymers some time ago.<sup>8</sup> The measurements with mixtures of polypeptides are entirely feasible but have not yet been made. They should give a final decision as to how the polydispersity changes the non-Newtonian viscosity decrease, particularly with regard to the constant  $a_2$ . Not having these measurements as yet, we can only consider the result as being highly probable.

The behavior of the coiled molecules can be discussed as being due to a superposition of a number of elementary mechanisms in the way suggested by Rouse (ref. 3). As has been done by Pao<sup>9</sup> this would lead to a behavior of coiled molecules even without a "polymolecularity," similar to polydisperse systems. For the dynamic behavior of solutions of coiled high polymers, this idea has been introduced by Rouse and can be termed the "internal polydispersity" of coiled molecules.

Real high polymers are neither rigid rods nor completely flexible coiled molecules; their flexibility depends on the chemical constitution. As has been mentioned the decrease of their viscosity from the initial viscosity follows equation 4 meaning that the constant  $a_2$  is present. It is very probable that this is due to the polymolecularity and/or to the

(8) W. Philippoff, *Ber. Chem. Ges.*, **70**, 827 (1937).

(9) Y. H. Pao, unpublished paper presented at APS meeting (High Polymer Physics Div.), Phila., March, 1957 (See *J. Appl. Phys.*, **28**, 591 (1957)).

"internal polydispersity" of the polymer molecule. This problem could be studied now using, for examples the recently available "monodisperse" polystyrenes and their mixtures.

**Acknowledgment.**—This work was supported by the American Viscose Corporation, Marcus Hook, Pennsylvania, whose assistance is gratefully acknowledged.

## THE DRY CARBON MONOXIDE-OXYGEN FLAME

By ROBERT WIRES, LELAND A. WATERMEIER AND ROGER A. STREHLOW

*Ballistic Research Laboratories, Aberdeen Proving Ground, Maryland*

*Received August 12, 1958*

The flame velocity, quenching distance and minimum ignition energy were determined for dry stoichiometric carbon monoxide-oxygen mixtures containing small quantities of hydrogen or deuterium at one atmosphere pressure. The amount of added hydrogen or deuterium was varied from 0.006 to 2.0%. The carbon monoxide and oxygen for making the mixtures were used only if they contained less than 10 parts per million equivalent hydrogen. The gases were dried before mixing by distillation over liquid nitrogen. The equivalent hydrogen content of each "dry" gas sample was determined by measuring either the minimum ignition energy or the burning velocity of a stoichiometric mixture prepared from the samples. Equivalent hydrogen was considered to be less than 10 p.p.m. if either the burning velocity was less than 3 cm./sec., or the minimum ignition energy was greater than 500 millijoules. Velocity data were taken in a spherical bomb using central ignition. Only the first portion (constant pressure) of the burning was used and space velocities were converted to normal burning velocities using theoretical expansion ratios. Quenching distances and ignition energy data were taken in a cell similar to that described by Lewis and von Elbe.<sup>1</sup> The data indicate that the flame properties of pure dry stoichiometric CO-O<sub>2</sub> are: flame velocity, less than 3 cm./sec.; quenching distance, greater than 0.4 cm.; and minimum ignition energy, greater than 0.5 joule. The data best fit the assumption that hydrogen atom diffusion controls the propagation process. Ignition energies and quenching distances show no effect of isotopic substitution when compared to each other and flame velocity. The data indicate that hydrogen atom diffusion and deactivation at the wall are not important to the quenching process. The behavior of the quenching data at the larger distances indicates that the CO-O<sub>2</sub> flame is much thicker than a hydrocarbon flame with the same burning velocity.

### Introduction

The carbon monoxide-oxygen flame has attracted much interest in the past. In particular, the large dependence of burning velocity on small concentrations of hydrogen-bearing compounds has led to many determinations of burning velocity as a function of hydrogen or water vapor content.<sup>2</sup> In this investigation we attempted to prepare extremely dry and pure carbon monoxide-oxygen mixtures to determine the flame behavior at the limit of zero hydrogen addition. After successfully preparing these pure gases we used them to study the effect of added hydrogen or deuterium on the burning velocity, quenching distance and minimum ignition energy of the stoichiometric flame.

**Apparatus.**—Flame properties were measured in one of two different bombs. A spherical bomb 5 inches in diameter with central ignition was used for determining the burning velocities. The flame was photographed using a repetitive spark schlieren system. Space velocities were measured from the first 2 inches of travel on these photographs and converted to burning velocities by dividing by 8.17, the theoretical expansion ratio for a stoichiometric CO-O<sub>2</sub> flame. While this ratio varies slightly with H<sub>2</sub> or D<sub>2</sub> concentration, the change is less than one-half per cent. for our concentration range. The ignition spark used in this bomb has a calculated energy ( $E = \frac{1}{2}CV^2$ ) of 1.2 joules. However, the actual energy received by the gas is much less than this because the spark was fired through a thyatron circuit for synchronization with the camera.

Minimum ignition energy and quenching distance were determined in a 3-inch bomb similar to the one described by Lewis and von Elbe.<sup>1</sup> The spark electrodes were  $\frac{1}{16}$ -inch diameter stainless steel rods with hemispherical tips. They protruded slightly from the center of the 1-inch diameter parallel glass quenching plates. The grounded electrode was mounted on a micrometer to measure plate separation when the spark occurred. The occurrence of an explosion was detected by watching through a glass window. The

apparatus was used in a conventional manner and showed good agreement with Lewis and von Elbe's data<sup>1</sup> on some selected hydrocarbon systems.

**Preparation of the Gas Samples.**—Carbon monoxide was generated by dropping formic acid into hot (160°) phosphoric acid. It was dried and purified by passing it through a water condenser, Ascarite, calcium chloride and Linde molecular sieve adsorbent. The generator and drying columns were never opened to the atmosphere except on a few occasions when it was necessary to change the drying agents because of caking. The CO was condensed and fractionally distilled over liquid nitrogen. The second of three equal fractions was saved and used in the experiments. Tank oxygen was collected with a liquid nitrogen trap and fractionally distilled by the same procedure used for CO.

Every gas sample used was tested for dryness by making a stoichiometric CO-O<sub>2</sub> mixture and sparking it in either of the bombs. In these mixtures the minimum ignition energy varied from 50 to 500 millijoules and the burning velocity from 8 to 3 cm./sec., with some mixtures not exploding. Comparison of these data with Flock and King's work,<sup>2</sup> and later with the results of our work indicates that these "dry" mixtures contained flame-propagating compounds at concentrations equivalent to a hydrogen content of 0.01 to 0.001 mole %. Those samples with the higher equivalent hydrogen content were used for preparing mixtures containing more than 0.5% H<sub>2</sub> or D<sub>2</sub>. The drier samples were used for lower H<sub>2</sub> or D<sub>2</sub> additions.

Mixtures were prepared using the method of partial pressures. The smaller additions of H<sub>2</sub> or D<sub>2</sub> were made using a thermal conductivity gauge to measure the low pressure. This gauge was calibrated against a McLeod gauge for both H<sub>2</sub> and D<sub>2</sub>. The mixtures were transferred to the explosion bombs using mercury leveling bulbs.

### Results and Discussion

The data are listed in Table I. Figure 1 shows the dependence of flame velocity,  $S$ , on the concentration of added H<sub>2</sub> or D<sub>2</sub>. The best fit straight lines are given by the equations  $S_{H_2} = 78.0(X_{H_2})^{0.40}$  and  $S_{D_2} = 62.5(X_{D_2})^{0.40}$  where  $X_{H_2}$  or  $X_{D_2}$  represents mole per cent. of added H<sub>2</sub> or D<sub>2</sub>. These equations yield an isotope effect ratio,  $S_{H_2}/S_{D_2} = 1.22 \pm 0.03$ .

(1) B. Lewis and G. von Elbe, "Combustion, Flames and Explosion of Gases," Academic Press, New York, N. Y., 1951, p. 392-425.

(2) E. F. Flock and H. K. King, N.A.C.A. Report No. 531, 1935.

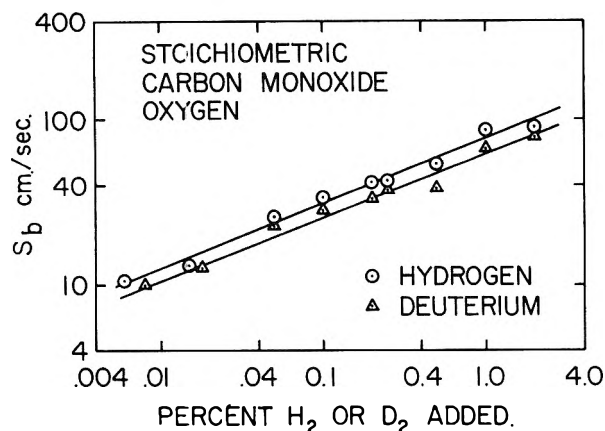


Fig. 1.—Burning velocity of the dry stoichiometric CO-O<sub>2</sub> flame with small additions of hydrogen or deuterium.

This experimental information is compared to theory by first assuming that some one mechanism completely controls the propagation process. Three general types of mechanisms are available. These are: (1) heat conduction, (2) diffusion and reaction of an active species, and (3) a controlling chemical steady state in the flame.

TABLE I  
FLAME PROPERTIES OF THE STOICHIOMETRIC CARBON MONOXIDE-OXYGEN FLAME  
(Pressure equal to one atmosphere)

| % addition          | Flame velocity, cm./sec. | Quenching distance, cm. | Min. ignition energy, mjoules |
|---------------------|--------------------------|-------------------------|-------------------------------|
| <0.001              | <3.0                     | ...                     | >500                          |
| .006 H <sub>2</sub> | 10.6                     | 0.30                    | 40                            |
| .008 D <sub>2</sub> | 9.9                      | .34                     | 54                            |
| .015 H <sub>2</sub> | 13.1                     | .29                     | 26                            |
| .018 D <sub>2</sub> | 12.7                     | .33                     | 27                            |
| .050 H <sub>2</sub> | 25.9                     | .25                     | 6.2                           |
| .050 D <sub>2</sub> | 22.8                     | .30                     | 10.5                          |
| .10 H <sub>2</sub>  | 33.7                     | .23                     | 3.2                           |
| .10 D <sub>2</sub>  | 28.8                     | .27                     | 4.6                           |
| .25 H <sub>2</sub>  | 42.7                     | .18                     | 1.25                          |
| .25 D <sub>2</sub>  | 37.0                     | .22                     | 1.90                          |
| .50 H <sub>2</sub>  | 54.3                     | .12                     | 0.60                          |
| .50 D <sub>2</sub>  | 38.3                     | .14                     | .96                           |
| 1.00 H <sub>2</sub> | 87.4                     | .11                     | .50                           |
| 1.00 D <sub>2</sub> | 66.2                     | .13                     | .70                           |
| 2.00 H <sub>2</sub> | 91.3                     | .085                    | .25                           |
| 2.00 D <sub>2</sub> | 79.5                     | .10                     | .35                           |

A simple thermal theory does not explain these results. As a matter of fact, this flame system was chosen because it lacked a thermal explanation and also because it allows one to study a chemical effect under nearly ideal conditions, namely, constant flame temperature, thermal conductivity and expansion ratio.

The consequences of forward diffusion and reaction of active species controlling flame propagation has been analyzed by Tanford and Pease.<sup>3</sup> Their theory may be simplified to consider only one active species, *i*, as rate controlling and in this form yields the velocity correlation equation

$$S \propto (k_i p_i D_i)^{0.5}$$

where *D* is the diffusion coefficient, *p* is the equilibrium partial pressure at the flame temperature, *T<sub>f</sub>*, and *k* is the reaction rate constant at some lower temperature.

Assume hydrogen atoms are the rate-controlling species and that the reaction rate constant shows no isotope effect. For equivalent concentrations of H<sub>2</sub> and D<sub>2</sub> the diffusion coefficient ratio yields  $S_{H_2}/S_{D_2} = 1.19$ . Under the same conditions,  $S_{H_2} \propto [H]^{0.5}$  and  $S_{D_2} \propto [D]^{0.5}$  where the brackets [] represent equilibrium concentrations in the flame. At the high temperature which exists in this flame the hydrogen atom concentration is not a simple function of the amount of hydrogen added to the flame because water vapor and hydroxyl radicals are also formed in quantity. From calculations for various H<sub>2</sub> additions we determined that  $[H] \propto (X_{H_2})^{0.72}$  and therefore that  $S_{H_2} \propto (X_{H_2})^{0.36}$  and  $S_{D_2} \propto (X_{D_2})^{0.36}$ . This is quite close to the experimentally observed behavior.

If diffusion and reaction of OH were considered to be the rate-controlling step the results would be as follows. From our calculations, using the zero point energy difference of OH and OD, the reaction rate constant ratio is  $k_{OH}/k_{OD} = 1.42$  at  $0.7T_f$  if identical activated complexes are formed. The temperature  $0.7T_f$  is used as an average reaction temperature in the flame front. With  $D_{OH}/D_{OD} = 1.01$  our simplified equation yields the ratio  $S_{H_2}/S_{D_2} = 1.20$ , which again agrees quite well with the experimental data. However equilibrium calculations yield  $[OH] \propto (X_{H_2})^{0.42}$  and therefore predict that  $S_{H_2} \propto (X_{H_2})^{0.21}$ . This does not agree well with the experimental results.

Gilbert and Altman<sup>4</sup> have found that the rate of flame propagation in H<sub>2</sub>-Br<sub>2</sub> flames is controlled by the steady-state molecular hydrogen concentrations in the flame zone. If this same mechanism is assumed for our system and our flame temperature is used, we find a  $k_{H_2}/k_{D_2}$  ratio of 1.36. This ratio, in turn, yields a flame velocity ratio of 1.16. The Gilbert-Altman theory further predicts the relationship  $S \propto (X_{H_2})^{0.5}$ .

Of the three mechanisms which predict the  $S_{H_2}/S_{D_2}$  found experimentally—H atom diffusion, OH radical diffusion and reaction, or a steady-state mechanism based on molecular hydrogen concentration in the flame—the H-atom diffusion mechanism alone predicts the correct concentration dependence. However the other two simplified theories predict concentration dependencies fairly close to experiment and we are therefore unable to say that only the hydrogen atom diffusion controls the flame. Friedman and Cyphers<sup>5</sup> found that their data on the wet CO-O<sub>2</sub> flame at 2010°K. could best be correlated (empirically) with the expression  $S \propto ([H] + 0.15 [OH])^{0.5}$ . This suggests a small contribution from the OH to the over-all mechanism. While Gilbert and Altman's theory fits our data fairly well it does not explain the fact that water vapor is just as effective as hydrogen in enhancing the burning velocity. A check of Fiock and King's data taken on the stoichiometric flame at one

(4) M. Gilbert and D. Altman, *ibid.*, **25**, 377 (1957).

(5) R. Friedman and J. A. Cyphers, Westinghouse Scientific Paper 60-94459-1-P2, Aug. 15, 1955.

(3) C. Tanford and R. N. Pease, *J. Chem. Phys.*, **15**, 861 (1947).

atmosphere shows that the substitution of water vapor for hydrogen at constant mole fraction of the additive does not change the burning velocity of a stoichiometric CO-O<sub>2</sub> flame. It is therefore unlikely that the first step of either H<sub>2</sub> or H<sub>2</sub>O decomposition is the rate-controlling step in the CO-O<sub>2</sub> flame since these initial decomposition rates are necessarily quite different. Furthermore McDonald's<sup>6</sup> data, taken with an 80% CO + 20% O<sub>2</sub> mixture and added H<sub>2</sub>O or D<sub>2</sub>O agrees with our data at the higher H<sub>2</sub> and D<sub>2</sub> concentrations. This suggests that the propagation velocity is relatively independent of CO-O<sub>2</sub> concentration in the stoichiometric region and agrees with the assumption that H diffusion or OH reaction controls the propagation of this flame.

A comparison of McDonald's data and ours indicated that his "dry" gas ( $S_b = 34.6$  cm./sec.) contained flame-propagating components equivalent to 0.12 mole % hydrogen. McDonald's first analysis and Scheller's<sup>7</sup> extensive theory using his data is based on the subtraction of 34.6 cm./sec. from the experimental burning velocities before comparisons are made. Since we found burning velocities as low as 3 cm./sec., an extensive re-evaluation of Scheller's theory is indicated.

Both minimum ignition energies and quenching distance show the effect of isotopic substitution (see Table I). However, when these properties are compared to each other and to the burning velocity (see Figs. 2 and 3) the isotopic effect disappears (the section of Fig. 3 above  $d = 0.25$  cm. will be discussed later). Simon and Belles<sup>8</sup> have derived an equation for quenching controlled by active particle diffusion to the wall and capture at the wall. If one assumes that diffusional loss of one active species is the main factor in quenching the flame, their equation for quenching distance reduces to the form

$$S_b d \propto D$$

where  $D$  is the diffusion coefficient of this species in the gas. Assuming hydrogen atoms to be the most important quenching species produces the theoretical ratio

$$(S_b d)_{H_2} / (S_b d)_{D_2} = D_H / D_D = 1.4$$

Since our experimental ratio is unity, hydrogen atom capture by the wall is not important in quenching this flame. The importance of hydroxyl radicals or other active species cannot be separated from the effect of thermal conductivity since their diffusion coefficient ratios are close to unity. We feel that quenching is probably a thermal process in this flame even though quenching by hydroxyl radical deactivation is not ruled out in the above discussion.

In Fig. 3 the data for the smaller quenching distances follow the relationship  $H = cd^2$  where  $c$  is a constant. This relationship is of the same form as the relationship that Lewis and von Elbe<sup>1</sup> report for a variety of hydrocarbon flames. However, the data above 0.25 cm. acts differently. Since the

(6) G. E. McDonald, "Effect of Water on the Carbon Monoxide-Oxygen Flame Velocity," NACA RM E53L08, Feb. 5, 1954.

(7) Karl Scheller, "Sixth Symposium on Combustion," Reinhold Publ. Corp., New York, N. Y., 1957, pp. 280-288.

(8) D. M. Simon and F. E. Belles, NACA Report RME51L18, March, 1952.

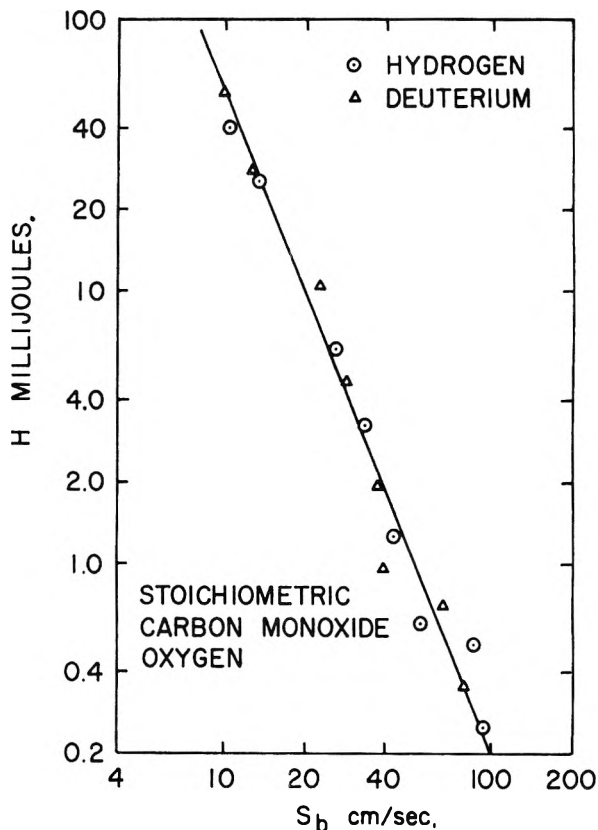


Fig. 2.—Comparison of burning velocities and minimum ignition energies for the dry stoichiometric CO-O<sub>2</sub> flame with added hydrogen or deuterium.

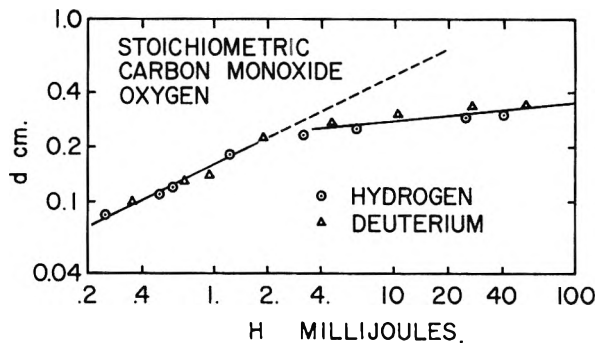


Fig. 3.—Comparison of minimum ignition energy and quenching distances for the dry stoichiometric CO-O<sub>2</sub> flame with added hydrogen or deuterium. Quenching distance determined using 1-inch diameter plates.

quenching distance in this range is less than predicted by an extension of the lower portion of the curve the plates must be less effective in quenching the flame. Therefore any additional diffusion and radical deactivation process in this low-hydrogen concentration range is ruled out since any mechanism of this type would cause an increase in quenching distance. The asymptotic nature of the data suggests that the quenching plate diameter of 1 inch was insufficient to correctly quench a CO-O<sub>2</sub> flame at separations above 0.25 cm. However we found that we could measure hydrocarbon quenching distances at least as large as 0.6 cm. with our 1-inch plates. A comparison of our data with Lewis and von Elbe's hydrocarbon data indicated that the constant  $c$  in the equation  $H = cd^2$  is five



times larger for the CO-O<sub>2</sub> flame. This explains the existence of two distinct quenching limits for the two systems if one assumes that the minimum plate diameter for effective quenching is related to the minimum ignition energy, not the quenching distance. This is probably true since the minimum ignition energy of any particular system is related to the flame thickness and, therefore, to the distance a flame must travel before it settles down to a steady state. This evidence points to the existence of a very thick flame zone in the CO-O<sub>2</sub> flame.

### Conclusions

Pure dry stoichiometric carbon monoxide-oxygen flames have been studied with added hydrogen or deuterium. The driest mixtures contain less than 10 p.p.m. of equivalent hydrogen before H<sub>2</sub> or D<sub>2</sub> addition. The data indicate that the burning

velocity of a pure dry stoichiometric CO-O<sub>2</sub> mixture is extremely low—certainly less than 3 cm./sec. We also found that other limiting values for dry mixtures were: ignition energy, greater than 0.5 joule, and quenching distance, greater than 0.4 cm. The data further indicate that the burning velocity is best correlated to hydrogen atom diffusion ahead of the flame. However, a slight contribution from an hydroxyl radical reaction in, or ahead of the flame has not been eliminated by this study. Ignition energies and quenching distances show no effect of isotopic substitution when compared to each other and flame velocity. The data indicate that hydrogen atom diffusion and deactivation at the wall is not important to the quenching process. Our data indicate that the CO-O<sub>2</sub> flame is much thicker than a hydrocarbon flame with the same burning velocity.

## CRITICAL PHENOMENA IN THE CYCLOHEXANE-ANILINE SYSTEM: EFFECT OF WATER AT DEFINITE ACTIVITY<sup>1</sup>

BY FRANK R. MEEKS, RAM GOPAL AND O. K. RICE

*Department of Chemistry, University of North Carolina, Chapel Hill, North Carolina*

*Received August 18, 1958*

Water at controlled activity has been introduced in the cyclohexane-aniline system by allowing the solution to remain in contact with a mixture of Li<sub>2</sub>SO<sub>4</sub> and Li<sub>2</sub>SO<sub>4</sub>·H<sub>2</sub>O. The critical temperature is raised about 0.3°. The shape of the coexistence curve is altered, and the flat portion at the critical temperature has largely, if not completely, disappeared.

### Introduction

Critical phenomena in the cyclohexane-aniline binary liquid system and the shape of the coexistence curve in the vicinity of the critical point have been investigated by Rowden and Rice<sup>2</sup> and Atack and Rice.<sup>3</sup> It was shown that the coexistence curve is flat and horizontal within experimental error over a range of aniline mole fraction from 0.43 to 0.465, in work for which the temperature control was 0.001°. Small amounts of water raise the separation temperature, and careful drying over calcined CaO was necessary to get reproducible results. Atack and Rice<sup>4</sup> made preliminary measurements on the effect of water, and suggested that it is negatively adsorbed at the interface. In the present work we have examined the effect of introducing water at a controlled activity, by adding a mixture of approximately equal weights of lithium sulfate monohydrate and anhydrous lithium sulfate to each sample and observing the new transition temperature. To find the actual concentration of water, further experiments on the introduction of small, known amounts of water into samples of varying composition will be necessary, and will be reported later.

(1) Work supported by the Office of Ordnance Research, U. S. Army.

(2) R. W. Rowden and O. K. Rice, "Changements de Phases," Société de Chimie Physique, Paris, 1952, p. 78; *J. Chem. Phys.*, **19**, 1123 (1951).

(3) D. Atack and O. K. Rice, *ibid.*, **22**, 382 (1954); O. K. Rice, *ibid.*, **23**, 164 (1955).

(4) D. Atack and O. K. Rice, *Disc. Faraday Soc.*, **15**, 210 (1953).

### Experimental

Aniline was purified by distillation in air, followed by vacuum distillation using a drying tube and aspirator, recrystallization and drying with CaO on a vacuum rack. Purified samples of approximately 20 cc. bearing no tinge of yellow color were stored in sealed ampoules.

National Bureau of Standards cyclohexane, Sample No. 209a-25, was used without further purification in preparation of all mixtures but two.

Baker and Adamson Reagent Grade lithium sulfate monohydrate from a single bottle was used in all the work reported here. The lithium sulfate was insoluble in the cyclohexane-aniline mixtures; evaporation of a sample which had been in contact with the salt left no residue.

Mixtures were prepared by measuring out the aniline at a known temperature into a tube with a pipet, freezing with Dry Ice-acetone, then measuring in the cyclohexane<sup>5</sup>; the opening in the top was sealed immediately with a torch. After thorough evacuation and degassing, the mixture was distilled successively into four tubes each containing several grams of freshly calcined CaO and allowed to remain on the CaO for several hours at room temperature. After distillation into a sample tube provided with a breakseal, the sample was sealed off from the drying train. A correction (of 0.001 to 0.002 mole fraction aniline) was made for evaporation of cyclohexane into the volume above the liquid.

A large, well-insulated thermostat was controlled by a specially designed thermoregulator to ±0.031°. Temperatures were measured with a platinum resistance thermometer which had been calibrated against a similar N.B.S.-calibrated thermometer. The scale appears to differ from that used by Atack and Rice<sup>3</sup> by about 0.17°, but temperature differences are of most importance. The

(5) Density, at 28°, of cyclohexane and aniline, 0.7710 and 1.0149, respectively. J. Timmermans, "Physico-Chemical Constants of Pure Organic Compounds," Elsevier Publishing Co., New York, N. Y., 1950.

bridge used had a small sensitivity to ambient temperature, but relative temperatures of different samples were controlled to about  $0.001^\circ$ , as in previous work in this Laboratory, by frequently observing several samples simultaneously.

Separation temperatures were observed for the pure systems, as described previously,<sup>3</sup> by lowering the temperature to a certain point, allowing it to remain for a half-hour, then raising the temperature to clear the opalescence in order to see if the phases had separated. The drying process was repeated until the separation temperature for the mixture remained constant from one drying to the next. The mixture was then distilled onto a 0.2–0.3 g. mixture of lithium sulfate monohydrate and anhydrous lithium sulfate, thoroughly degassed, sealed off, and the separation temperature determined. All transfers were done in a vacuum of the order of  $10^{-5}$  mm., but it was ascertained that a half hour's pumping on the monohydrate reduced its moisture content very little, and the hydrate was kept chilled as much as possible with liquid air.

In the case of the samples with the hydrate, the tubes were allowed to stand for two hours or longer at the separation temperature, rather than a half hour, before observing the separation, and many careful observations were made on each tube. The more detailed examination was dictated in part by difficulty in observing the appearance of the meniscus in the presence of the hydrate, especially for the cyclohexane-rich samples where the meniscus reappears near or at the bottom of the tube.

It is possible that the longer "settling" time allowed for the monohydrate samples, along with the more detailed investigation of single specimens, would permit the observation of differences in the separation temperatures of samples where such differences would be obscured by the shorter settling time, *i.e.*, half an hour or so. The question of settling rate is a matter which remains somewhat indeterminate at present. When tubes are left for several hours in a thermostat which can fluctuate by even  $0.001^\circ$ , however, there is no certainty that the temperature has not drifted farther downward at some time during the process than is indicated by intermittent temperature measurements on the bridge. However, the fact that many measurements were made with several tubes observed simultaneously minimizes the likelihood of "drift" error.

Sometimes there were erratic results in which either the change in temperature with addition of water was only a few hundredths of a degree, or else it was considerably larger than approximately  $0.3^\circ$ , the usual value. In either case the values followed no discernible pattern but were scattered. Aberrations of the former type might be attributable to too great a proportion of anhydrous salt in the mixture, and those of the latter to too small a proportion. In either case the sample was redried and a new mixture of hydrate and anhydrate was introduced.

Numerous samples were rejected because their pure-system separation temperatures could not be brought to a low enough value to agree with the others. This criterion of rejection was applied equally to tubes of the previous worker and to the freshly prepared tubes of the present worker. (Atack's 0.390, 0.448 and 0.457 had to be rejected because of yellowing; subsequent redistillation removed the tinge but they continued to disagree both among themselves and with other tubes. The Atack tubes of aniline mole fractions, 0.466 and 0.445 were not available.)

### Results

The results are given in Fig. 1.  $X_A$  is the mole fraction of aniline,  $T$  is the separation temperature of the pure system, and  $T'$  is the separation temperature in the presence of the hydrate.<sup>6</sup> Most

(6) The temperatures for aniline mole fractions 0.4275 and 0.4435 have been arbitrarily adjusted by subtraction of 0.027 from each  $T'$  and  $T$ ; the measured values were high due presumably to their having been prepared with a sample of cyclohexane other than the N.B.S. material. Of course these were not subject to comparison with the others, but the adjustment is felt to be justified by the fact that their temperature increments are in accord with those for other samples. The values of  $X_A$  for Atack's samples are slightly different than previously reported,<sup>3</sup> because the space above the liquid was a little greater in our tubes, and the correction for evaporation of cyclohexane was correspondingly increased. Also the correction was

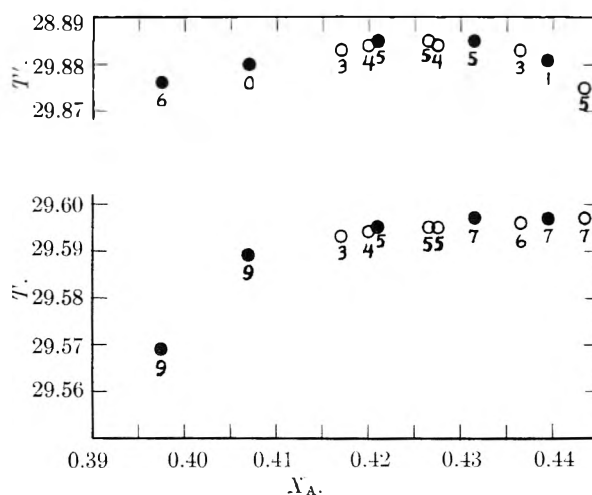


Fig. 1.—Coexistence curves (black circles, Atack's mixtures). The numbers under the circles give the last significant figure in the temperature. Thus, for the lowest point,  $T' = 29.569$ .

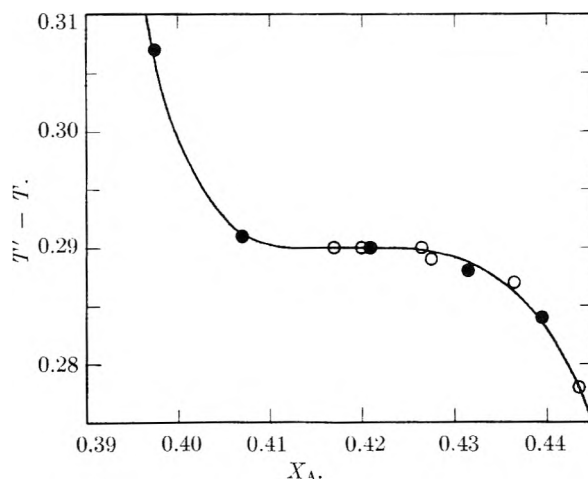


Fig. 2.—Effect of salt hydrate on transition temperature (black circles, Atack's mixtures).

striking are the shift of the critical region of the upper curve to lower aniline mole fraction and the relatively narrower mole fraction range which it covers. If there remains any flat portion at the top of the coexistence curve its presence cannot be proved by these data. It should be noted, however, that the meniscus seemed to reappear within the tube, for samples with hydrate, from aniline mole fraction 0.417 to 0.436. It seemed to appear at the top for tubes more concentrated in aniline than 0.436, and at the bottom (as far as could be discerned, considering the presence of the lithium sulfate monohydrate in the bottom of the tube) for those of aniline mole fraction less than 0.417. The change in shape of the curve produced by a small amount of water (less than  $2 \times 10^{-5}$  mole per cc. or  $2 \times 10^{-3}$  mole per mole of mixture, according to Atack and Rice<sup>4</sup>) reemphasizes the caution which is necessary in the interpretation of curves of this sort; a flat top could be missed easily on account of impurities.

In Fig. 2 we have plotted  $T' - T$  against mole inadvertently omitted by Atack and Rice<sup>3</sup> in the samples reported as mole fractions 0.4656, 0.4376 and 0.4296, and these values should be increased by about 0.0010.

fraction of aniline; this diagram brings out the fact that a given activity of water has a greater effect on the transition point the richer the system is in the substance, cyclohexane, in which water is less soluble. Since the activity of a given concentration of water is expected to be greater the richer the solution is in cyclohexane, the effect would be enhanced if one considered a given concentration rather than a given activity of water. A further thermodynamic analysis must await the completion of the experiments mentioned at the end of the Introduction.

The differences shown in Fig. 2 may be more accurate relative to each other than the individual measurements. If this is true, Fig. 2 practically eliminates the possibility of a flat top for the coexistence curve in the presence of the hydrate, for it is seen that almost all the horizontal portion of

the curve in Fig. 2 lies beyond the end of the critical region of the dry cyclohexane-aniline mixture, which occurs<sup>3</sup> at about 0.425 aniline mole fraction. If the flat portion of the coexistence curve, indicating a range of critical concentrations, is caused, when it exists, by the vanishing of the interfacial tension while the two phases are still of different composition,<sup>4</sup> addition of water at fixed activity can be expected to alter the critical temperature, for at any given temperature there will be a definite amount of adsorption at the interface, and hence a definite change in interfacial tension, corresponding to the controlled activity. But a *gradual* change in the activity of the water could not cause a *sudden* change, or vanishing, of the range of critical concentrations; this suggests, therefore, that these experiments should be repeated with a salt pair having a considerably lower aqueous tension.

## A CALORIMETRIC MEASUREMENT OF THE HEATS OF SOLUTION OF THE INERT GASES IN WATER

BY D. M. ALEXANDER<sup>1</sup>

*Contribution from the Department of Chemistry, University of Canterbury, Christchurch, New Zealand*

*Received September 2, 1958*

A microcalorimeter is described which has been used to measure heats of solution of inert gases in water. Calorimetric values in kcal./mole of the standard enthalpies of solution of neon, argon, krypton and xenon are at 25°,  $-1.4 \pm 0.4$ ,  $-2.9 \pm 0.2$ ,  $-3.8 \pm 0.2$  and  $-4.1 \pm 0.2$ , respectively.

### Introduction

The heats of solution of gases in water have in the past been calculated from the temperature variation of solubility.<sup>2</sup> In view of the experimental difficulties associated with accurate solubility measurements and the poor agreement between the results of different workers, it was thought that direct calorimetric measurements should be made of the heats of solution of the inert gases in water. No previous measurements of this sort appear to have been made with any gases apart from those of very high solubility, such as ammonia, hydrogen chloride and acetylene.

The design of the calorimeter had to be such that the temperature rises of  $10^{-4}$  to  $10^{-2}^\circ$  could be measured with some precision. Such measurements can be made by using a Paschen galvanometer and a suitable thermopile.<sup>3</sup> It was necessary also that as much gas as possible should dissolve in the shortest possible time and that the heat produced by mechanical stirring be very small. It was essential that no solution should occur before or after the mixing process, and that the quantity of gas absorbed should be measured.

### Experimental

**The Calorimeter.**—Twin Pyrex glass calorimeters were used, enclosed in an underwater air jacket. Each com-

prised a spherical bulb and cylindrical bottom bulb of equal volumes, the bottom of the top bulb and the top of the bottom bulb being connected by a narrow capillary and a ground glass joint. The top of the top bulb was connected to the top of the bottom bulb by capillary tubing and a tap.

The top bulb of one calorimeter was filled with the solvent, gas-free water and the tap closed. The bottom bulb was filled with gas, saturated with water vapor.

The top bulb of the other "blank" calorimeter was filled with a saturated solution of hydrogen in water and the bottom bulb with hydrogen saturated with water vapor. Both taps were opened together so that in both cases the liquid displaced the gas. In the first case solution occurred to the extent of about one third saturation as the water flowed from the capillary. In the "blank" calorimeter no solution occurred. The resulting difference in temperature between the bottom bulbs would then be a measure of the heat change associated with the solution of the gas, if the top bulbs were initially at the same temperature.

The top bulbs were of 100-ml. capacity and matched in volume to 0.5%. The capillaries at the bottom of each top bulb were planned to allow the top bulb to empty in a fixed time. One calorimeter took 11 min. and 25 sec. to drain, the other 11 min. and 35 sec. Three way taps were used, one side being connected to the top bulb and the other side having one stem open and the other connected to the bottom bulb and to a gas buret in a subsidiary thermostat. Glass columns in each of the bottom bulbs gave surfaces over which the water could trickle.

The bottom bulbs were 5.3 cm. in diameter and 4.3 cm. apart. Heaters were sealed into the bottom of these bulbs. Each was of 10 ohms resistance, the element being a curved coil of nichrome wire spot welded to tungsten wire leads 0.03 cm. in diameter and 3 cm. in length. These were welded to copper leads which were connected to current and potential leads. Thermostated glass capillary leads connected each calorimeter to the gas buret.

Bakelite supports held the calorimeters in an air jacket totally enclosed in a thermostat, similar to that used by Gucker, *et al.*<sup>3</sup> The thermostat bath was lagged with kapok enclosed in wood and covered with a metal plate and

(1) Chemistry Department, University of Queensland, Brisbane, Australia.

(2) (a) D. D. Eley, *Trans. Faraday Soc.*, **35**, 1281 (1939); (b) H. S. Frank and M. J. Evans, *J. Chem. Phys.*, **13**, 507 (1945).

(3) F. T. Gucker, H. B. Pickard and R. W. Planck, *J. Am. Chem. Soc.*, **61**, 459 (1939).

a similarly lagged lid. The whole thermostat was situated in a large wooden air thermostat operating at one degree below the bath temperature, to allow the calorimeters to be filled at a fixed temperature.

The thermostat was suspended by counterbalances in an angle-iron frame, so that while running, it could be raised to the fixed calorimeter assembly. The large brass plate from which the underwater jacket and stirrers were suspended was fixed by four narrow iron strips to the iron frame. The lid was also counterbalanced and moved in the frame. The regulator comprised an acetone filled copper coil, sealed to a small glass head in an external lagged box. Two stirrers driven from the same motor were mounted at the ends of the submarine jacket. A symmetrically spread bare wire was used as a heater, consuming 10-40 watts. Over a trial period of two days the bath temperature was constant to  $10^{-3}$ ° or less.

The taps were turned on by Bakelite clamps connected through Perspex spacers to brass rods. These passed through the brass plate, calorimeter cover and air thermostat roof.

The thermopile between the bottom bulbs was connected by shielded lagged leads in series with a Paschen galvanometer. It was of 40 junctions of 25 S.W.G. constantan and 41 S.W.G. copper, 4.5 cm. long, and was mounted vertically in two halves on sheets of mica 4.5 cm. high. The ends were set in nickel troughs with paraffin wax and mica insulation. These troughs were made to fit into nickel slots which were soldered on to polished nickel sleeves fitting round the bottom bulbs. The leakage modulus of the system was found to be 0.01/min. The minimum observable change in temperature across the thermopile was one micro-degree. The galvanometer could be shunted with copper resistances in an oil-bath.

**Filling Techniques.**—Gas was removed from solvent by refluxing under reduced pressure. The calorimeter was completely filled with water by evacuating it and using the vapor pressure of the heated solvent to force water into it through a cooling coil. With the calorimeter tap turned off, the bottom bulb was filled with gas by displacement of water. The caps at the bottom of each calorimeter had to be placed in position as the last drops of liquid emerged and as the gas, which was under pressure slightly above atmospheric, began to emerge. Consequently the ground glass surface of the cap was wet. Excess water was wiped off carefully and the cap sealed with wax.

The "blank" calorimeter was completely filled with a solution of hydrogen in water by displacement of hydrogen. This solution had been prepared previously at 25° in a separate vessel which was connected to the bottom of the calorimeter by a connection through which hydrogen flowed. Hydrogen was passed into the top of this vessel and allowed the solution to flow into the calorimeter.

The calorimeter tap was then turned off and the bottom bulb filled with hydrogen by displacement of this solution.

**Calorimetric Procedure.**—A series of six "blank" experiments was carried out at 25° using a saturated solution of hydrogen in each top bulb and hydrogen gas in each bottom bulb. This showed a fairly constant heat effect of  $0.0835 \pm 0.009$  cal. in one calorimeter. This resulted from an initial constant difference in temperature between the top two bulbs.

The filled calorimeters were allowed 30 hours to reach temperature equilibrium. After this time the thermopile zero was read on the galvanometer scale. There was usually a small fixed e.m.f. in the thermopile. The gas buret was then opened to the calorimeter, and a volume reading noted, using the telescope of a cathetometer.

The resultant pressure change upset the temperature equilibrium and a series of volume measurements involving smaller volume changes was made until equilibrium was restored, and were continued for about 20 minutes after this. The gas buret was shut off and the taps turned on slowly, together. As soon as the water had run through, 12 minutes after turning the taps, readings were made on the galvanometer scale and continued every three minutes for 40 minutes. It was found that the plot of the logarithm of the galvanometer deflection against time was linear. At the same time the gas buret was again connected to the calorimeter and volume measurements made. These were also continued for some time. Volume readings before and after the experiment were extrapolated to the time at which the solution process had just ended, to give the volume dissolved.

The galvanometer reading plot was extrapolated to a time three minutes after the taps had been turned on. In both cases the estimate of the time to which the extrapolation should be taken may be a few minutes in error. This error would be insignificant in the case of the volume measurements.

After equilibrium had been restored, the calorimeter was calibrated electrically. The electrical energy was judged to reproduce closely the heat of solution of the gas. Again a plot of the log of the galvanometer deflection against time was linear. This calibration was repeated. The plot was extrapolated to a time halfway through the heating period, and by comparing this deflection with that obtained in the original measurement, the heat evolved in the original measurement was calculated by proportion. By subtracting or adding the "blank" heat effect (0.0835 cal.) the heat evolved on solution of the gas at constant volume was calculated. The method of extrapolation was calculated to compensate for thermal leakage. It was found that the sensitivity of the calorimetric system sometimes changed after the system had been disassembled and reassembled, but was constant for each assembly.

Experiments were made using each of the calorimeters in turn as "blank" and it was found that results when corrected for the "blank" heat effect were the same. This was a check on the constancy of the "blank" heat effect. For the more soluble gases accuracy was limited by the poor reproducibility of electrical calibrations which differed by as much as 4%. Usually, the slope of the linear cooling plot was almost the same after a calibration as after solution of the gas. This suggests that soon after the electrical heating the same steady cooling state had been set up as existed after solution of the gas. In some cases a steeper plot was observed and these calibrations were discarded. In a series of trial calibrations it was found that for a fixed electrical energy, variation of heating period from 9 to 18 min. gave no significant variation in the galvanometer deflection, using the extrapolation methods described above.

An attempt to heat the liquid electrically as it flowed down the column failed because all the heat generated was not transmitted to the flowing liquid. The best position of the heaters, giving the correct cooling curve, was found by experiment. Before the heating period the current was passed through a dummy resistance to stabilize the current.<sup>3</sup>

TABLE I

CALORIMETRIC ENTHALPIES OF SOLUTION OF GASES IN WATER AT 25° (KCAL./MOLE)

|         |                      |                 |
|---------|----------------------|-----------------|
| Neon    | -0.9, -1.1, -2.1,    | Av. -1.4 ± 0.4  |
|         | -1.6                 |                 |
| Argon   | -2.68, -3.11, -2.84  | Av. -2.88 ± 0.2 |
| Krypton | -3.54, -3.65, -3.61, | Av. -3.78 ± 0.2 |
|         | -3.89, -3.87,        |                 |
|         | -3.96, -3.94         |                 |
| Xenon   | -4.25, -4.17, -4.16, | Av. -4.12 ± 0.2 |
|         | -4.13, -3.93         |                 |

TABLE II

COMPARISON OF CALORIMETRIC ENTHALPIES WITH THOSE DERIVED FROM VARIOUS SOLUBILITY MEASUREMENTS

|                         | (KCAL./MOLE) |       |       |       |
|-------------------------|--------------|-------|-------|-------|
|                         | Ne           | Ar    | Kr    | Xe    |
| Calorimetric            | -1.4         | -2.88 | -3.78 | -4.12 |
| Valentiner <sup>a</sup> | -1.83        | -2.74 | -3.69 | -4.29 |
| Law <sup>b</sup>        | -0.99        | -2.52 |       |       |
| Beckwith <sup>c</sup>   |              |       | -3.11 |       |
| Lannung <sup>d</sup>    | -0.81        | -2.59 |       |       |

<sup>a</sup> S. Valentiner, *Z. Physik*, 42, 253 (1927). <sup>b</sup> J. T. Law, Thesis, University of New Zealand, 1949. <sup>c</sup> J. Beckwith, Thesis, University of New Zealand, 1949. <sup>d</sup> A. Lannung, *J. Am. Chem. Soc.*, 52, 68 (1930).

### Results and Conclusions

The heat effect measured in the experiment was an integral internal energy change of solution. The internal energy change per mole of gas absorbed

was converted to an enthalpy change by the relation

$$\Delta H = \Delta U - RT$$

Each enthalpy value quoted thus represents the enthalpy change on solution of the gas at one atmosphere pressure to form a solution about one-third saturated at one atmosphere pressure.

The errors quoted in Table I are each calculated by summing the probable error of the mean of results obtained, the probable error of the blank correction, and the maximum error thought likely due to wrong extrapolation methods in correcting for heat loss.

The heats of solution calculated from solubility measurements are quoted for comparison. If it be assumed that the activity coefficients of the solutes do not change over the range of concentrations used (up to  $10^{-2} M$ ), then both the calorimetric enthalpy and the enthalpy calculated from solubility data represent the standard enthalpy of solution, or the differential enthalpy of solution per mole of gas in a solution in which the activity coefficient of the solute is that for infinite dilution and is defined as unity.

Indirect evidence indicates that this assumption is justifiable. Consideration of the heat of dilution of sucrose<sup>3</sup> and the partial molal volumes of

solutions of gases<sup>4</sup> leads to the conclusion that in the range of concentrations concerned differences between the two sets of values would be insignificant compared with experimental error.

In general, agreement with results calculated from the data of Valentiner is good, but agreement with other results poorer. Valentiner's data is smoothed from the results of earlier workers over a range of 50°, whereas the solubility data of Lannung cover a range of 23° and of Law and Beckwith cover a range of 30°. It is likely that the greater temperature range of Valentiner's solubility figures leads to an increased accuracy in the derived heat of solution. However, the absolute accuracy of solubility measurements cannot be verified by calorimetric measurements.

**Acknowledgments.**—This work was carried out at the University of Canterbury, Christchurch, New Zealand under the supervision of Professor H. N. Parton, who suggested the problem and to whom the author expresses thanks for his encouraging support. Indebtedness is expressed to the Canterbury College Council and the New Zealand University Research Fund Committee for financial support.

(4) J. Kritevsky and A. Ilinskaya, *Acta Physicochim. U.R.S.S.*, **20**, 327 (1945).

## A THERMOMETRIC METHOD FOR THERMODYNAMICS STUDIES AND MOLECULAR WEIGHT DETERMINATIONS IN SOLUTIONS<sup>1</sup>

By W. I. HIGUCHI,<sup>2</sup> M. A. SCHWARTZ, E. G. RIPPKE AND T. HIGUCHI

*School of Pharmacy, University of Wisconsin, Madison, Wisconsin*

*Received September 3, 1958*

A useful apparatus for determination of solvent activities of aqueous and non-aqueous solutions is described. The method consists essentially of determining the temperature difference of a solution and its solvent when brought into quasi vapor equilibrium in an evacuated enclosure. The theory and the basic limitations of the procedure have been explored. For aqueous systems both theory and experiments show that near thermodynamic temperature rise can be expected for even temperatures ranging below 25°. For non-aqueous systems sizable temperature rises were obtained for solvents having vapor pressures as low as that of tetralin (0.5 mm. at 25°). The method was found to be inapplicable to essentially non-volatile solvents such as hexadecane at room temperature. The inability of solvents of high volatility to attain exactly 100% of the thermodynamic rise under the imposed dynamic situation was attributed mainly to apparent liquid films present at the surfaces which retard heat transfer through them. A novel modification was achieved when heat was externally supplied to the solution to counteract its heat loss. This procedure appeared to provide essentially equilibrium data. Solvent activity and molecular weights were determined directly.

### Introduction

Thermometric determinations of molecular weights under quasi-isopiestic conditions have been carried out by several workers with systems of non-volatile solutes in various volatile solvents.<sup>3-9</sup> In the various methods used, a steady-state temperature above the ambient temperature is obtained in a partially isolated solution phase ex-

posed to the solvent vapor in air. The temperature rise of the solution caused by the vapor condensing on its surface is the basis of the determination. The activity of the solvent for the unknown solution is obtained by carrying out the experiments for a known solute.

This temperature differential is, however, ordinarily a fraction of the theoretical rise necessary to overcome the vapor pressure lowering effect of the non-volatile solute, the less than equilibrium rise being due to the proportionately large heat loss from the solution phase by convection, conduction and radiation.

The relative precision and accuracy of measurement of such dynamic systems would be expected to be less than those achieving thermodynamic rise in temperature for several reasons. The absolute

(1) Presented at the 133rd Meeting of the American Chemical Society in San Francisco, California, April 13 to 18, 1958.

(2) California Research Corporation, Richmond, Cal.

(3) R. H. Müller and H. J. Stolten, *Anal. Chem.*, **25**, 1103 (1953).

(4) B. R. Y. Iyengar, *Rec. trav. chim.*, **73**, 789 (1954).

(5) A. P. Brady, H. Huff and J. W. McBain, *THIS JOURNAL*, **55**, 305 (1951).

(6) S. B. Kulkarni, *Nature*, **171**, 219 (1953).

(7) G. B. Taylor and M. B. Hall, *Anal. Chem.*, **23**, 947 (1951).

(8) A. V. Hill, *Proc. Roy. Soc. (London)*, **127A**, 9 (1930).

(9) E. J. Baldes, *Biodynamica*, **46**, 8 (1939).

value of the temperature rise will be less. Such temperature changes as are noted, furthermore, would be susceptible to greater errors resulting from random variations in the rates of heat and mass transfer. It is apparent that a considerable improvement in the general method can be expected by making the measurements under conditions such that nearly a thermodynamic temperature differential exists between the solvent and solution phases.

In this report results of a study of such systems are presented. An apparatus which achieves near thermodynamic temperature rise is described in detail and some of the important variables of the method are discussed. The general procedure is suited to a study of thermodynamic behavior of solutions of non-volatile solutes in volatile solvents and to determination of molecular weights of organic and inorganic compounds in aqueous and volatile non-aqueous solvents.

**Apparatus.**—The setup based on the use of thermistors for detection of the temperature differential is a modification of that used by Müller and Stolten.<sup>3</sup> The special features of the present apparatus, shown in Fig. 1, are that (1) the chamber may be evacuated to remove permanent gases and hence eliminate gas phase diffusion barriers, and (2) the solvent and solution phases are continuously stirred to maximize compositional and thermal homogeneity.

Two glass cups, A, are suspended in a water jacketed glass chamber capable of being evacuated. A thermistor is mounted in each cup. An alternate arrangement involves using a vacuum jacketed cup, A', in place of one of the other plain cups. Both cups as well as the solvent reservoir, B, in the bottom of the chamber are furnished with a stirring magnet. The chamber temperature is held constant to  $\pm 0.001^\circ$  during a single measurement and to  $\pm 0.01^\circ$  over a series of experiments by means of a Sargent Thermistor regulator. Changes in ambient temperatures of  $0.01^\circ$  result in less than a 2-ohm error when closely matched thermistors are used.

The particular type of magnetic stirrer used in connection with this apparatus consisted of six fixed electromagnetic poles, two of which are shown in Fig. 1. The poles are mounted horizontally around the chamber on a common soft iron base by upright iron straps. They are activated through a commutator by a 12 volt full-wave battery charger. The magnetic poles are activated in pairs, opposite poles being activated simultaneously in such a way as to provide a horizontally revolving magnetic field of sufficient strength to spin all three stirring magnets.

Two Western Electric 14A Thermistors are connected in parallel with two  $0.100 \pm 1\%$  megohm IRC manganin wirewound resistors in a Wheatstone bridge. A 111,110 Leeds and Northrup 5 decade resistance box placed in series with one of the thermistors completes the bridge. The detectors employed are a Rubicon lamp-and-scale galvanometer with a sensitivity of 0.00065 microamp. per mm. for routine measurements and a Varian G-11 strip chart recorder for transient studies. A 0.2 megohm potentiometer is connected in series with the input to allow adjustment of the current flow to 30 microamps. The power dissipation is thus kept low and constant, eliminating heating effects due to the circuit. Under these conditions a less than one ohm change in a thermistor of about 100,000 ohms is detectable with either the recorder or the galvanometer.

**Procedure. A. Steady-state Method.**—The thermistors used in the solution cup were calibrated in a rapidly stirred bath against a Beckmann thermometer over a  $2^\circ$  range in the vicinity of the desired jacket temperature. All of the thermistor resistances were found to be about 100,000 ohms, and the temperature coefficients of resistance about 5000 ohms/ $^\circ\text{C}$ .

The experiments were performed in the following manner. Three-ml. volumes of the solvent and solutions are placed in the cups. Thirty ml. of solvent is agitated in the bottom of the chamber by means of the magnetic stirrer which also activates the magnets in the cups. Glass wool saturated

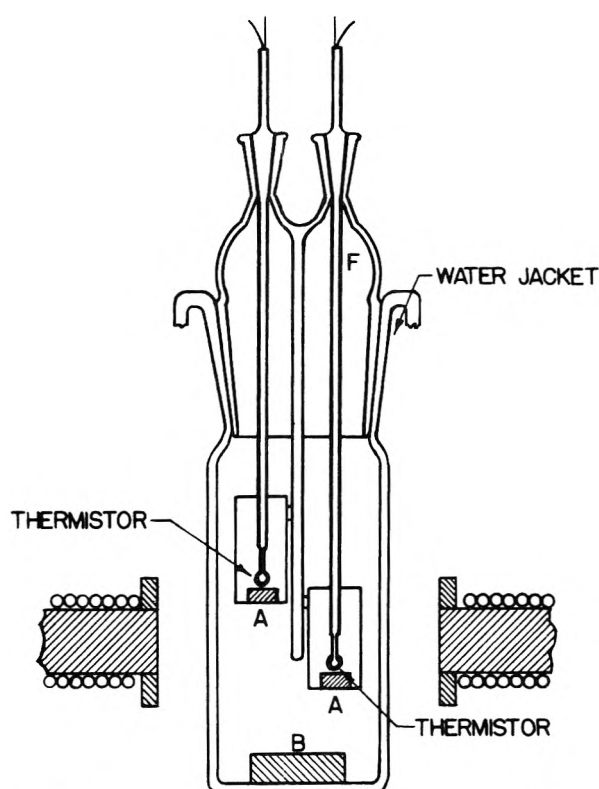


Fig. 1.—Thermometric apparatus for measuring activities of solvents in their solutions.

with the solvent is placed in the region F (see Fig. 1). The chamber is closed and evacuated. While initially there are some bubbles escaping in the cups, boiling occurs mainly in the solvent reservoir at the bottom sweeping out any remaining air from the chamber. Analyses of the solution cup before and after the runs showed negligible solvent losses due to boiling. The stopcock to the vacuum pump is closed after about 10 seconds of boiling and the system allowed to reach a steady state. The resistance change,  $\Delta R$ , necessary to return the detector to the null is recorded. The evacuation step is repeated until a constant  $\Delta R$  is obtained. Generally one or two evacuations sufficed for the volatile solvent systems (water, benzene and dioxane), while two to three were necessary in the cases of xylene and tetralin. Even small air leaks led to irreproducible results. This may be explained by postulating that an air blanket or film created by the drag on the air molecules by the condensing vapor molecules gave rise to an appreciable resistance to mass transfer.

The experiments were carried out at various concentrations up to solute mole fractions  $N_2 \sim 0.02$  for the following systems: water-urea, benzene-naphthalene, dioxane-biphenyl, xylene-naphthalene, tetralin-dibutyl phthalate and hexadecane-methyl docosanoate.<sup>10</sup> The data were fitted to the expression

$$\tau_c = KN_2 \quad (1)$$

where  $\tau_c$  is the temperature rise and  $K$  is a constant for a given solvent.

**B. Isoestic Method.**—For concentrations greater than about  $N_2 \sim 0.02$ , the rate of dilution of the solution phase was important. This effect was observable as a steady decrease in the  $\Delta R$  after the end of the transient period (Fig. 2). A 30 ohm heating coil was placed in the solution cup. The current was supplied by a storage battery and measured with a voltmeter. By adjusting the power input to such a value that no dilution was observable, it was possible to obtain an essentially thermodynamic temperature rise. This modification was particularly applicable when  $N_2$  was large.

(10) To ascertain the lower limit of the range of solvent volatility tetralin and hexadecane were tried, both at only one concentration of  $N_2 = 0.0115$  and  $N_2 = 0.0094$ , respectively.

TABLE I  
 COMPARISON WITH EQUILIBRIUM CASE AND OTHER INVESTIGATORS

| Solvent system       | $T_0$ , °C. | $K$  | $RT_0^2/\Delta H$ | % Theory | M-S <sup>b</sup> | Iyengar <sup>c</sup> |
|----------------------|-------------|------|-------------------|----------|------------------|----------------------|
| Benzene              | 26.40       | 20.5 | 22.1              | 93       | 19               | 57                   |
| Benzene <sup>a</sup> | 20.00       | 19.0 | 20.9              | 91       | ..               | ..                   |
| Dioxane              | 26.40       | 16.4 | 18.9              | 87       | ..               | 44                   |
| Water                | 26.40       | 16.2 | 17.0              | 95       | 22               | 62                   |
| Xylene <sup>a</sup>  | 20.00       | 13.7 | 16.8              | 81       | ..               | ..                   |
| Tetralin             | 26.40       | 8.9  | 14.6              | 61       | ..               | ..                   |
| Hexadecane           | 26.40       | 0    |                   | 0        |                  |                      |

<sup>a</sup> These experiments were carried out using a plain glass solution cup, and in all others a vacuum jacketed cup was used.  
<sup>b</sup> Müller and Stolten's % theory.<sup>3</sup> <sup>c</sup> Iyengar's % theory.<sup>4</sup>

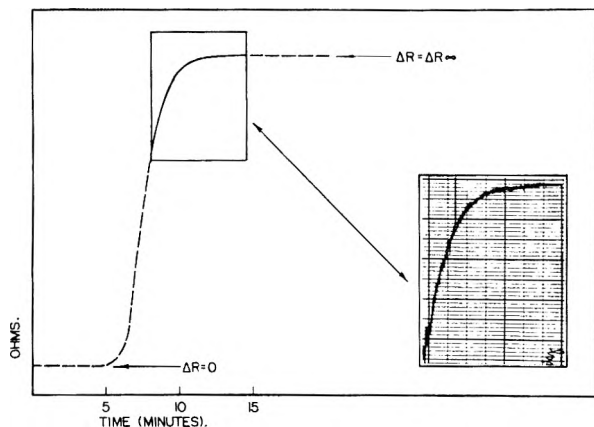


Fig. 2.—A typical recording of a differential thermal signal from the apparatus. The ordinate (ohms) corresponds to the temperature rise.

### Results and Discussion

**Steady-state Method.**—Figure 2 shows a typical recording of the output from the bridge after an evacuation. The time for attainment of steady state was 5 to 10 minutes for benzene, dioxane and water solutions, about 10 to 15 minutes for xylene solutions, and 30 to 40 minutes for tetralin. No signal was detectable with the hexadecane solution.

Straight line plots of  $\tau_c$  vs.  $N_2$  were obtained with standard deviations in  $K$  about  $0.001^\circ$ . This roughly corresponds to about a 0.5 to 1.0% uncertainty in the molecular weight determination of a 0.01 mole fraction solution. For higher concentrations the uncertainty is proportionately less. Except for tetralin where the reproducibility was about 5 ohms, different runs on the same samples were reproducible to about 2 ohms.

Table I shows experimental  $K$  values compared with the theoretical thermodynamic quantity  $RT_0^2/\Delta H$ , where  $T_0$  is the temperature of the solvent phase,  $\Delta H$  is the molar heat of vaporization, and  $R$  is the gas constant. Near thermodynamic rise was obtained for water and the more volatile organic solvents. It is clear that it is possible to obtain a temperature rise that is much greater than previously reported,<sup>3,4</sup> and that it is possible to obtain sizable signals from relatively non-volatile solvents such as tetralin.

The value of  $K = 0$  for hexadecane is tentatively attributed to insufficient evacuation although it is expected to be near zero. Solvents with vapor pressure much lower than tetralin (vapor pressure  $\sim 0.5$  mm.) are not desirable for study as the times

for steady state attainment will be inconveniently great.

The results for benzene with the jacketed and unjacketed cups indicate some improvement on the per cent. theory with the former, although not sufficiently perhaps to warrant its special construction.

Table II gives results of determinations of the molecular weights of various substances in water

 TABLE II  
 MOLECULAR WEIGHT DETERMINATIONS IN WATER

| Solute and mol. wt.  | $N_2$   | Mol. wt. (deterd.) |
|----------------------|---------|--------------------|
| Sucrose (342.30)     | 0.00634 | 340                |
| Glucose (180.16)     | .00680  | 182                |
| Phenol (94.11)       | .00900  | 567                |
| Citric Acid (192.12) | .00939  | 192                |

based on a urea-water calibration. These results were obtained with a jacket temperature variation of  $\pm 0.01^\circ$  employing an on-off regulator. Somewhat greater accuracy is indicated with the present temperature control. A slightly lower value for the apparent molecular weight of citric acid than that obtained would have perhaps been more reasonable due to some ionization of the acid ( $K_a \sim 8 \times 10^{-4}$ ). The apparently anomalous value for phenol points out a limitation of the general method. The vapor pressure of phenol in aqueous phenol solutions is great enough to counteract measurably the thermal effect of the condensing water vapor. Approximately, the situation may be described by a volatility ratio

$$r = \frac{P(\text{solute})}{N_2 P(\text{solvent})}$$

where  $P$  is the vapor pressure of the indicated component. For the phenol case  $r \sim 0.85$  and only one-sixth of the expected rise was obtained. For a naphthalene-xylene solution  $r \sim 0.03$  and the expected rise was observed in this case. Thus it appears that if  $r$  was less than about 0.03 the solute volatility could be neglected.

The theory of the method which explains the inability of the solution phase cup to achieve 100% rise has been investigated.<sup>11</sup> It was assumed that thermomolecular effects were negligible in the gas phase and  $N_2$  was small. Taking into consideration heat and mass transfer rates both inside and outside the solution phase the following approximate relation for  $\tau_c$  was obtained.

(11) Unpublished results.

$$\frac{h_c \tau_c + h_s \tau_c \left(1 + \frac{h_{cl}}{WA}\right)}{k \Delta H} = \frac{P_0 \Delta H \tau_c \left(1 + \frac{h_{cl}}{WA}\right) + \frac{P_0 M A D C_c}{\rho_s \left[\frac{AD}{s} + \frac{M}{\rho \Delta H} \left\{h_c \tau_c + h_s \tau_c \left(1 + \frac{h_{cl}}{WA}\right)\right\}\right]}{RT_0^2} + \quad (2)$$

$$\frac{P_0 M A D C_c \Delta H \tau_c \left(1 + \frac{h_{cl}}{WA}\right)}{\rho_s R T_0^2 \left[\frac{AD}{s} + \frac{M}{\rho \Delta H} \left\{h_c \tau_c + h_s \tau_c \left(1 + \frac{h_{cl}}{WA}\right)\right\}\right]}$$

Here  $h_s$  and  $h_c$  are the coefficients of heat transfer corresponding to the surface-to-environment and the solution-to-environment rates, respectively,  $t$  and  $s$  are the thicknesses of the effective liquid films for heat and mass transfer, respectively,  $W$  is the thermal conductivity of the solution,  $D$  is the diffusion coefficient of the solute in the solution,  $A$  is the surface area of the solution phase,  $M$  and  $\rho$  are the molecular weight and the liquid density of the solvent,  $C_c$  is the concentration of the solute,  $P_0$  is the equilibrium vapor pressure of the pure solvent at  $T_0$ , and  $k$  is the mass transfer coefficient which, in the absence of permanent gases in the system, is

$$k \sim \frac{\alpha A}{(2\pi M R T_0)^{1/2}}$$

with  $\alpha$  the condensation coefficient.

It may be shown easily by means of (2) and choosing suitable parameters that in the limit of very volatile solvents (benzene)  $\tau_c$  is largely determined by the rate of heat transfer through the liquid. This explains why the per cent. theoretical for water is greater than for benzene. In the limit of relatively non-volatile solvents (tetralin) the volatility becomes the determining factor.

**Isopiestic Method.**—In Table III are given results of direct solvent activity determinations with benzene–biphenyl solutions. Here  $N_1$  is the benzene mole fraction determined by evaporating the solutions to constant weight. The values are slightly lower than those determined by other investigators.<sup>12</sup> The sensitivity for these experiments was such that the temperature rise was measurable to about 0.1%. The time taken for a single determination was between 15 and 30 minutes.

TABLE III

ACTIVITY OF BENZENE IN BENZENE–BIPHENYL SOLUTIONS

| $T$<br>°C. | $N_1$       | $a$   | $a$ (lit.) <sup>12</sup> |
|------------|-------------|-------|--------------------------|
| 36.2       | 0.762 ± 0.2 | 0.766 | 0.770 ± 0.002            |
| 33.8       | 0.849 ± 0.2 | 0.849 | 0.854 ± 0.003            |

Because this method is relatively insensitive to the volatility of the solvent, it may be advantageous over the usual manometric methods for investigating systems which involve relatively non-

(12) E. A. Guggenheim, "Mixtures," Clarendon Press, Oxford, 1952, p. 236.

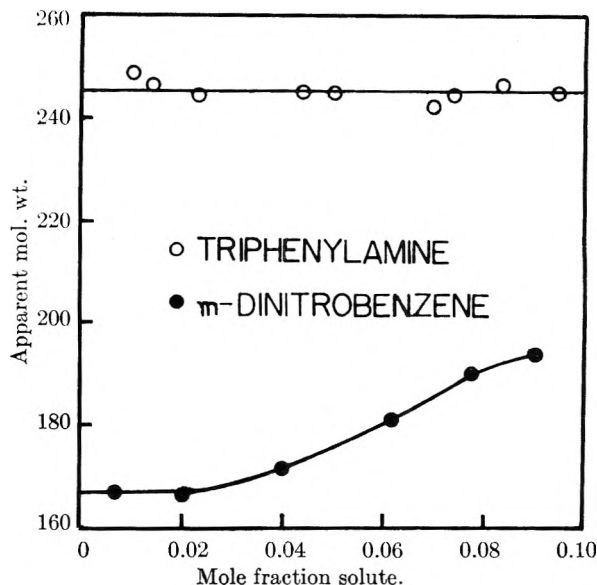


Fig. 3.—Apparent absolute molecular weight of triphenylamine and *m*-dinitrobenzene as functions of solution concentration determined under isopiestic condition.

volatile solvents such as tetralin. Also the short duration of an experiment makes the procedure well suited for studies with solutes which may normally decompose too rapidly.

When the necessary power (for isopiestic rise) was plotted against the temperature rise,  $\Delta T$ , a straight line was obtained over the entire range  $0 < \Delta T \lesssim 4^\circ$ . The data for such plots were obtained by the no dilution criterion (constant signal,  $\Delta R$ , on the recorder) for the large  $\Delta T$  values and by assuming Raoult's law at small  $\Delta T$  values. The slope of the line, which is the coefficient of sensible heat loss, was about 20 milliwatts per degree for the present apparatus.

Figure 3 shows the results of determinations of apparent molecular weight obtained by this method as a function of concentration of triphenylamine (mol. wt. 245.8) and *m*-dinitrobenzene (mol. wt. 168.11) in toluene solutions. These were obtained using a curve mentioned above of power versus  $\Delta T$ . It can be seen that triphenylamine is essentially ideal in toluene solutions whereas *m*-dinitrobenzene associates to some extent. The molecular weight at infinite dilution, obtained by extrapolation of the curve, is however the true value for *m*-dinitrobenzene.

**Acknowledgment.**—This research was supported partly under Contract DA 18-108 CML-5753 by the Directorate of Medical Research, Chemical Warfare Laboratories, Army Chemical Center, Maryland and in part by a grant from the Research Committee of the Graduate School from funds supplied by the Wisconsin Research Foundation. Mr. Schwartz would like to acknowledge financial help furnished him through the American Foundation for Pharmaceutical Education.



## THE ANION EXCHANGE OF METAL COMPLEXES.

### III. THE CADMIUM-CHLORIDE SYSTEM<sup>1-3</sup>

BY Y. MARCUS

*Contribution from the Israel Atomic Energy Commission Laboratories, Hirkirya, Tel-Aviv, Israel*

*Received September 11, 1958*

The anion-exchange method described in the previous communications was applied to a study of the cadmium-chloride complex system. The distribution of the cadmium between Dowex-1 chloride resin and the solutions was measured by the "batch" method with the aid of the tracer Cd<sup>115</sup>. Formation of mononuclear complexes up to 10<sup>-3</sup> M cadmium was confirmed. The distribution curves were determined in the range 0.04 to 9.0 M lithium chloride and 0.01 to 9.4 M hydrochloric acid. These curves coincided up to 0.2 M chloride. Above this concentration the hydrochloric acid curve is lower but both show a maximum around 4 M chloride. Construction of "ideal" distribution curves, valid for constant resin-ligand activity, made possible the evaluation of the complex system in terms of the species CdCl<sup>+</sup>, CdCl<sub>2</sub>, CdCl<sub>3</sub><sup>-</sup> and CdCl<sub>4</sub><sup>2-</sup>, with HCl forming also in hydrochloric acid. The successive formation constants found: log *k*<sub>1</sub><sup>\*</sup> = 1.95, log *k*<sub>2</sub><sup>\*</sup> = 0.55, log *k*<sub>3</sub><sup>\*</sup> = -0.15 and log *k*<sub>4</sub><sup>\*</sup> = -0.70, agree with published values. The acid dissociation constant of HCl is about unity.

#### Introduction

The cadmium-chloride system is a typical example of a divalent complex system to study by the anion-exchange method<sup>2</sup> after the univalent silver-chloride system.<sup>3</sup> It already has been studied by a variety of methods, and constants for the successive equilibria have been derived (see Table V). They may be used to check those obtained by the present method.

Anion exchange also has been applied to the cadmium chloride system. Leden<sup>4</sup> found that the anion-exchange resin Amberlite-400 absorbs cadmium, and rather better from 0.5 M sodium chloride and 0.01 M cadmium chloride than from 0.01 M cadmium chloride alone. He assumed that the species on the resin is CdCl<sub>3</sub><sup>-</sup>. Kraus, Nelson and Smith<sup>5</sup> reported that in 6 M hydrochloric acid cadmium is so strongly absorbed that it is able to displace the strongly absorbed palladium from Dowex-1 anion exchanger. Jentzsch and Frotscher<sup>6</sup> found that some anionic complex (CdCl<sub>3</sub><sup>-</sup>, CdCl<sub>4</sub><sup>2-</sup> or CdCl<sub>6</sub><sup>4-</sup>) is absorbed from hydrochloric acid solutions on the anion exchanger Wofatit L-150, and is not eluted till the acid is diluted to 0.05 M.

Fomin and co-workers<sup>7</sup> published some distribution coefficient data for potassium chloride solutions, using them to calculate ratios of activity coefficient functions, employing published complex formation constants for the cadmium chloride system. They did not, however, go the other way round and try to obtain the complex formation constants. They assumed the resin species to be RCdCl<sub>3</sub>, since in the 1-2 M potassium chloride in equilibrium with the resin this happens to be the predominant complex.

In a recent publication, Kraus and Nelson<sup>8</sup> pre-

sented a curve for the distribution of cadmium between Dowex-1 anion-exchange resin and aqueous hydrochloric acid. They maintain that cadmium is not eluted even with 0.01 M acid (although zinc is), but dilution to less than 0.001 M is necessary to remove it.

It seems from the published data that there is some lack of clarity about the species absorbed, and about the concentration of chloride necessary to remove cadmium from the resin which would imply a distribution coefficient around unity. This suggests that the cadmium-chloride system merits further investigation. The magnitude of the complex formation constants, the availability of activity data for chloride in the resin (Fig. 1 in ref. 2 and Fig. 2 in ref. 3), and finally the availability of the convenient tracer Cd<sup>115</sup> made the system attractive to investigate.

#### Experimental

Cadmium solutions were prepared by dissolving weighed amounts of cadmium metal foil containing the radioactive isotope Cd<sup>115</sup> in warm dilute hydrochloric acid, with the aid of a few drops nitric acid, precipitating the cadmium as carbonate, dissolving the latter in the stoichiometric amount of 0.002 M hydrochloric acid and boiling to remove the carbon dioxide.

Radioactivity was assayed by a dipping G.-M. counter. Cd<sup>115</sup> has two isomers, one of 54 hr. half-life, the other 43 days. The specific activity of the former is much larger than that of the latter soon after the irradiation, and as much as possible of this work was done in the lifetime of the former. Care was taken to measure the radioactivity of an aliquot of the solution which had not been contacted with the resin at the same time as an aliquot which had reached equilibrium with the resin. The distribution coefficient *D* (liter kg.<sup>-1</sup>) was calculated using the difference between the two counts, and the results were thus not affected by the decay of the Cd<sup>115</sup>.

Lithium chloride solutions containing 0.01 M hydrochloric acid were prepared. Impure commercial lithium carbonate was dissolved in hydrochloric acid, about 9 M, and the iron impurity was removed by passing the solution through a Dowex-1 anion-exchange column.<sup>9</sup> Lithium chloride was twice crystallized from the solution. Flame photometric analysis showed only lithium lines in the pure crystalline product LiCl·H<sub>2</sub>O.

Chloride was determined by titration with silver nitrate. In lithium chloride solutions the Mohr method was used and in hydrochloric acid a potentiometric method.

The anion exchanger used was Dowex-1 chloride, 10% cross-linked, of mesh size 40 to 100. It was air dried and had a capacity of 2.3 meq. per g.

Portions of solution and resin were shaken together for

(1) This work is taken from a part of a Ph.D. thesis submitted to the Hebrew University, Jerusalem, Israel, 1955. It was presented in part at the 132nd Meeting of the American Chemical Society, New York, September, 1957.

(2) Part I, Y. Marcus and C. D. Coryell, *Bull. Research Council, Israel*, **8A**, 1 (1959).

(3) Part II, Y. Marcus, *ibid.*, **8A**, 17 (1959).

(4) I. Leden, *Swensk Kem. Tidsskr.*, **64**, 147 (1952).

(5) K. A. Kraus, F. Nelson and G. W. Smith, *This Journal*, **58**, 15 (1954).

(6) D. Jentzsch and I. Frotscher, *Z. anal. Chem.*, **144**, 17 (1955).

(7) V. V. Fomin, L. N. Fedorova, V. V. Sinkovskii and M. A. Andreeva, *Zhur. Fiz. Khim.*, **29**, 2042 (1955).

(8) K. A. Kraus and F. Nelson, "Proc. Int. Conference on Peaceful Uses of Atomic Energy," Vol. 7, p. 113, 1956. This was published after the present work was completed.

(9) K. A. Kraus and G. E. Moore, *J. Am. Chem. Soc.*, **72**, 5792 (1950).

16 to 20 hr. at  $17 \pm 3^\circ$ . Relative amounts of solution and resin were chosen so as to have about half of the cadmium in the resin at equilibrium.

The error of the chloride determination was about  $\pm 0.003 M$ , which affected the accuracy only at the lowest concentrations. The average statistical error of counting was  $\pm 1.5\%$ , causing an error in the distribution coefficient of  $\pm 3\%$ , except in extreme cases, where it was larger. Possible errors in the relative amounts of resin and solution were within  $\pm 1.5\%$ . The total expected error in the distribution coefficient  $D$  is  $\pm 5\%$  for most cases.

### Results

Table I shows the effects of varying the cadmium concentration in the range  $10^{-6}$  to  $10^{-3} M$ . The relatively low specific activity of the cadmium did not allow lower concentrations to be tested. This caused rather high loading, but in no case was it higher than  $3\%$ . The results show that the distribution is unaffected by changes in the cadmium concentration. This is a strong indication that in this range, and presumably also at higher concentrations, the complexes are mononuclear.<sup>3</sup>

TABLE I

THE EFFECT OF CADMIUM CONCENTRATION ON THE ANION-EXCHANGE DISTRIBUTION IN THE CADMIUM-CHLORIDE SYSTEM

| Appr. equil. Cd concn., $10^{-4} M$ | log of Cd distr. coef. $\log D$ , l./kg. | HCl concn., $m_{HCl}$ (molarity) |
|-------------------------------------|------------------------------------------|----------------------------------|
| 0.4                                 | 2.38                                     | 0.144                            |
| 1.4                                 | 2.42                                     | .144                             |
| 7.1                                 | 2.39                                     | .144                             |
| 0.2                                 | 2.79                                     | 1.08                             |
| 0.7                                 | 2.78                                     | 1.08                             |
| 3.4                                 | 2.77                                     | 1.08                             |
| 0.3                                 | 2.25                                     | 7.00                             |
| 1.6                                 | 2.27                                     | 7.00                             |
| 8.3                                 | 2.23                                     | 7.00                             |

Table II shows the distribution of cadmium between the resin and lithium chloride solutions in the range 0.04 to 9.0  $M$ , while Table III shows the absorption from hydrochloric acid solutions in the range 0.01 to 9.4  $M$ .<sup>10</sup> The cadmium concentration was about  $10^{-4} M$  initially, ensuring low loading, and negligible consumption of chloride ions in complex formation. Values for the activity function for the chloride ligand,  $a = m_{HCl}\gamma_{\pm(HCl)}$  or  $a = m_{LiCl}\gamma_{\pm(LiCl)}$  as the case may be, in the hydrochloric acid and lithium chloride solutions, were obtained from Harned and Owen's compilation.<sup>11</sup> The results appear also in Fig. 1 as curves of  $\log D$  vs.  $\log a$ .

### Discussion

A detailed derivation and discussion of the mathematical relationship between the distribution coefficient  $D$  and the ligand activity function  $a$  is pre-

(10) Kraus and Nelson<sup>8</sup> presented a curve for the distribution of cadmium for the same nominal conditions as in the present investigation. These authors probably refer their data to "anhydrous dry" resin, not to "air dry" resin as in the present work. This would account for the constant factor of 2.5 found between their values for the distribution coefficient and those found here in the range 0.01 to 3  $M$  hydrochloric acid. This does not affect the slopes, and hence the calculated solution complexity constants. The divergencies beyond the above range could not be explained.

(11) H. S. Harned and B. B. Owen, "Physical Chemistry of Electrolyte Solutions," 2nd Ed., Reinhold Publ. Corp., New York, N. Y., 1950.

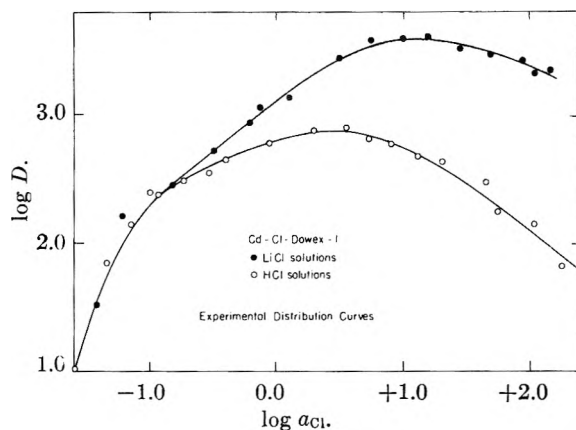


Fig. 1.—The anion exchange distribution curves ( $\log D$ ) plotted against the logarithm of the chloride activity function ( $\log a = \log m_{HCl} + \log \gamma_{\pm(HCl)}$  or  $\log a = \log m_{LiCl} + \log \gamma_{\pm(LiCl)}$ ) for the absorption of cadmium by Dowex-1 chloride from hydrochloric acid and lithium chloride solutions. Dots (LiCl) and open circles (HCl) are the experimental data, solid curves are calculated with the constants found (Table V).

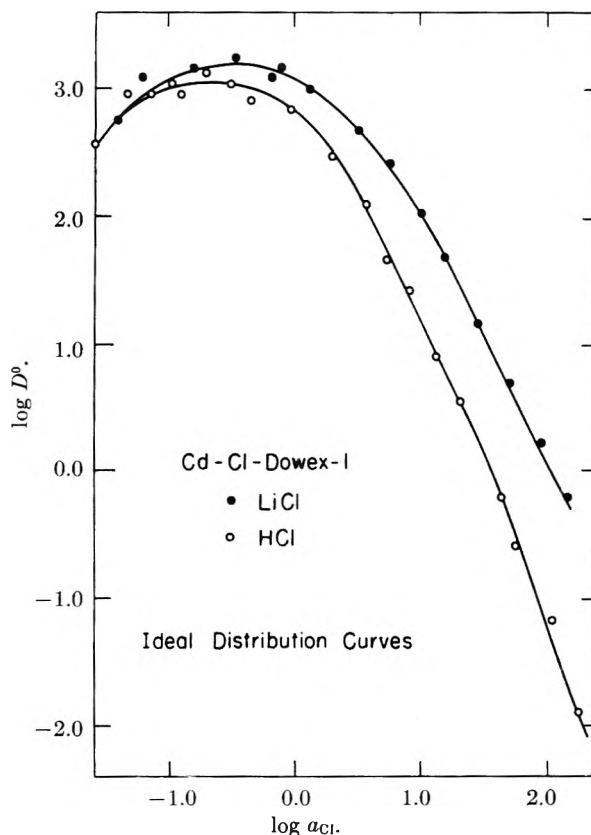


Fig. 2.—The "ideal" anion exchange distribution curves ( $\log D^0$ ), using the parameter  $p = 2$  for the predominant resin complex  $R_2CdCl_4$ , plotted against the chloride activity function ( $\log a$ ) for hydrochloric acid and lithium chloride solutions. Dots (LiCl) and open circles (HCl) were calculated from the experimental data using eq. 7, solid curves are calculated with the constants found (Table V).

sented elsewhere,<sup>2</sup> and only the main equations are given here.

Consider the complex cadmium species to be formed from the uncharged complex

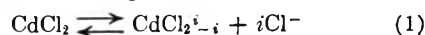


TABLE II  
 ANION EXCHANGE OF CADMIUM FROM LITHIUM CHLORIDE SOLUTIONS

| LiCl concn., $m_{\text{LiCl}}$ , $M$ | Log of Cl activity function $\log a$ | Log of Cd distribution coefficient $\log D$ (l./kg.) | LiCl concn., $m_{\text{LiCl}}$ , $M$ | Log of Cl activity function $\log a$ | Log of Cd distribution coefficient $\log D$ (l./kg.) |
|--------------------------------------|--------------------------------------|------------------------------------------------------|--------------------------------------|--------------------------------------|------------------------------------------------------|
| 0.040                                | -1.42                                | 1.52                                                 | 3.55                                 | 0.75                                 | 3.57                                                 |
| .100                                 | -1.22                                | 2.21                                                 | 4.30                                 | 1.00                                 | 3.59                                                 |
| .200                                 | -0.82                                | 2.45                                                 | 5.00                                 | 1.20                                 | 3.60                                                 |
| .400                                 | -.49                                 | 2.72                                                 | 6.00                                 | 1.45                                 | 3.51                                                 |
| .700                                 | -.21                                 | 2.94                                                 | 7.00                                 | 1.70                                 | 3.46                                                 |
| .900                                 | -.13                                 | 3.06                                                 | 8.00                                 | 1.95                                 | 3.42                                                 |
| 1.40                                 | .10                                  | 3.13                                                 | 8.50                                 | 2.05                                 | 3.32                                                 |
| 2.70                                 | .50                                  | 3.43                                                 | 9.00                                 | 2.17                                 | 3.34                                                 |

 TABLE III  
 ANION EXCHANGE OF CADMIUM FROM HYDROCHLORIC ACID SOLUTIONS

| HCl concn., $m_{\text{HCl}}$ , $M$ | Log of Cl activity function $\log a$ | Log of Cd distribution coefficient $\log D$ (l./kg.) | HCl concn., $m_{\text{HCl}}$ , $M$ | Log of Cl activity function $\log a$ | Log of Cd distribution coefficient $\log D$ (l./kg.) |
|------------------------------------|--------------------------------------|------------------------------------------------------|------------------------------------|--------------------------------------|------------------------------------------------------|
| 0.010                              | -2.0                                 | -0.3 ± 0.2                                           | 2.00                               | 0.30                                 | 2.38                                                 |
| .020                               | -1.7                                 | 0.8 ± 0.1                                            | 2.70                               | .55                                  | 2.30                                                 |
| .030                               | -1.6                                 | 1.02                                                 | 3.30                               | .73                                  | 2.31                                                 |
| .060                               | -1.34                                | 1.85                                                 | 3.90                               | .90                                  | 2.77                                                 |
| .100                               | -1.15                                | 2.15                                                 | 4.70                               | 1.11                                 | 2.67                                                 |
| .144                               | -1.00                                | 2.40                                                 | 5.40                               | 1.30                                 | 2.33                                                 |
| .170                               | -0.93                                | 2.38                                                 | 6.60                               | 1.65                                 | 2.48                                                 |
| .270                               | -.73                                 | 2.49                                                 | 7.00                               | 1.74                                 | 2.25                                                 |
| .400                               | -.53                                 | 2.55                                                 | 8.30                               | 2.03                                 | 2.15                                                 |
| .510                               | -.40                                 | 2.65                                                 | 9.40                               | 2.25                                 | 1.82                                                 |
| 1.080                              | -.05                                 | 2.78                                                 |                                    |                                      |                                                      |

where  $i$  is the charge on the complex, ranging from +2 for the hydrated, uncomplexed cadmium ion, to negative values for anionic complexes. The total concentration of cadmium will be given by

$$\Sigma m'_i = a_0' \Sigma \beta_i'^* a^{-i} \quad (2)$$

where  $a_0'$  is the thermodynamic activity of the neutral species  $\text{CdCl}_2$ , and  $\beta_i'^*$  are complexity parameters involving the thermodynamic equilibrium constants and activity coefficient functions, which are assumed independent of  $a$  (see discussion in 2).

Let the charge of the cadmium in the resin be designated by  $i = -p$ , which may be the average charge or the charge of a predominant resin species. The concentration of cadmium in the resin will be given by an expression analogous to (2)

$${}_r m'_p = {}_r a_0' {}_r \beta'^* {}_r a^p \quad (3)$$

Using the same standard state in both phases, it is easy to see that  ${}_r a'_0 = a'_0$ , and thus the distribution coefficient  $D$ , which is the ratio of the quantities given in eq. 3 and 2 will be given in logarithmic form as

$$\log D = \log ({}_r m'_p / \Sigma m'_i) = \log {}_r \beta'^* {}_r a^p + p \log {}_r a - \log \Sigma \beta_i'^* a^{-i} \quad (4)$$

The resin ligand activity function,  ${}_r a = {}_r m_{\text{MCl}_r} / \gamma_{\pm \text{MCl}_r}$ , where  $M$  is the cation  $\text{Li}^+$  or  $\text{H}^+$ , may be related to its solution analog  $a$  by the relation<sup>2, eq. 26</sup>

$$\log {}_r a = \log a + 1/2(\log {}_r m_{\text{Cl}} - \log {}_r m_{\text{M}}) \quad (5)$$

and is a measurable quantity. Calling its value  ${}_r a^0$  at  $a = 1$ , a correction function  ${}_r F_a$  is defined as

$${}_r F_a = \log {}_r a - \log {}_r a^0 \quad (6)$$

Putting  $K_r' = {}_r \beta'^* {}_r a_0^p$  we finally define a corrected or ideal distribution coefficient by

$$\log D^0 = \log D - p {}_r F_a = \log K_r' - \log \Sigma \beta_i'^* a^{-i} \quad (7)$$

**Lithium Chloride Solutions.**—Chemical considerations predict that the limiting complex in solution would be  $\text{CdCl}_2^{2-}$ . The predominant resin complex would then most likely be  $\text{R}_2\text{CdCl}_4$ , so that  $p = 2$ . Taking values of  ${}_r F_a$  from Fig. 1, ref. 2, a  $\log D^0$  vs.  $\log a$  curve was constructed, and is shown in Fig. 2. The average charge number  $i$  and the average ligand number  $\bar{n}$  were obtained from the slopes (see eqs. 31, 43 and 44c of ref. 2)

$$d \log D^0 / d \log a = \bar{i} = 2 - \bar{n} \quad (8)$$

In the range of experimental data the slope ranges from +1.5 to exactly -2.00 (from 4.5  $M$  lithium chloride onwards). This integral limiting slope is considered as justification of selecting  $p = 2$ , since other reasonable values of  $p$  would give fractional limiting slopes, which would be difficult to interpret. Bjerrum's "half-integral  $\bar{i}$ , or  $\bar{n}$ " method and Sill n's "curve fitting" method<sup>12</sup> were used to obtain the successive formation parameters  $k_i'^*$  or  $k_n^*$ , and the over-all complexity parameters  $\beta_i'^*$  or  $\beta_n^{*13}$  for the complexes  $\text{CdCl}_2^{i-}$  ( $i = 2, i-1$  and  $-2$ ) or  $\text{CdCl}_n^{2-n}$  ( $n = 1, 2, 3$  and  $4$ ) which are shown in Table IV.

**Hydrochloric Acid Solutions.**—Consider now the  $D^0$  curve for the hydrochloric acid solutions. It follows exactly the lithium chloride curve up to 0.2  $M$  chloride, but is lower thereafter. The author has shown<sup>14</sup> for the iron (III)-chloride system that differences between the distribution coefficients of iron for lithium chloride and hydrochloric acid

(12) L. G. Sill n, *Acta Chem. Scand.*, **10**, 186 (1956).

(13) The relationship of the starred parameters  $k_i'^*$ , etc., to the thermodynamic equilibrium constants is discussed elsewhere.<sup>2</sup>

(14) Y. Marcus, *Bull. Research Council Israel*, **4**, 326 (1954).

TABLE IV

THE COMPLEX FORMATION PARAMETERS FOR THE CADMIUM CHLORIDE SYSTEM IN LITHIUM CHLORIDE SOLUTIONS

| Species              | $n$ | $i$ | $\log k_n^*$    | $\log \beta_n^*$ | $\log k_i'^*$    | $\log \beta_i'^*$ |
|----------------------|-----|-----|-----------------|------------------|------------------|-------------------|
| $\text{Cd}^{2+}$     | 0   | 2   | 0.00            | 0.00             | $-1.95 \pm 0.08$ | $-2.50 \pm 0.15$  |
| $\text{CdCl}^+$      | 1   | 1   | $1.95 \pm 0.08$ | $1.95 \pm 0.08$  | $-0.55 \pm .15$  | $-0.55 \pm .15$   |
| $\text{CdCl}_2$      | 2   | 0   | $0.55 \pm .15$  | $2.50 \pm .15$   | 0.00             | 0.00              |
| $\text{CdCl}_3^-$    | 3   | -1  | $-.15 \pm .05$  | $2.35 \pm .05$   | $-.15 \pm .05$   | $-.15 \pm .05$    |
| $\text{CdCl}_4^{2-}$ | 4   | -2  | $-.70 \pm .05$  | $1.65 \pm .08$   | $-.70 \pm .05$   | $-.85 \pm .08$    |

solutions occur at concentrations above 9  $M$  chloride<sup>15</sup> and are due to chloro-acid formation. No such differences were found below 9  $M$ , and neither were they observed in the silver-chloride system, as reported by Kraus and Nelson.<sup>7</sup>

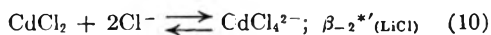
Considerable confusion has arisen concerning the interpretation of the "lithium chloride effect," which Kraus, Nelson, Clough and Carlsion have subsequently reported.<sup>16</sup> The fact is that a given metal shows different distribution coefficients for different electrolytes with the same ligand-anion at a given value of the ligand activity function  $a$ . This behavior is readily explained in a qualitative way by noting that different electrolytes give rise to different  $f_a$  functions. However, it so happens that for Dowex-1 resin chloride, lithium chloride and hydrochloric acid have virtually the same  $f_a$  functions, as may be seen by comparing the curves in Fig. 1, ref. 2, and Fig. 2, ref. 3. This consideration made Kraus and co-workers retract their former opinion that the "lithium chloride effect" is due to differences in resin and solution activities between the two systems,<sup>16</sup> in favor of chloro-acid formation.<sup>8</sup> Formation of chloro-acids of moderate strength was proposed also by Jetzsch and Frotzsch<sup>6</sup> to explain differences in absorbabilities of some metals from alkali chloride and hydrochloric acid solutions.

Recently, however, serious difficulties have arisen with this explanation, in particular in the cases of gold and gallium in concentrated chloride media.<sup>17</sup> The author feels, however, that the explanation in terms of chloro-acid formation may still be valid in many cases. It is suggested that the non-observance of a "lithium chloride effect" for silver and iron(III) below 9  $M$  chloride, and its observance for cadmium at a much lower concentration, may be interpreted in terms of non-absorbed, undissociated chloro-cadmium acid. This would be similar to the well known chloromercury acids<sup>18</sup> and species  $\text{HSnCl}_3$  postulated by Lachman and Tompkins<sup>19</sup> to explain their kinetic results. Accepting this postulated species, a parameter describing its formation can be obtained as follows.

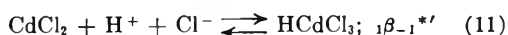
The slope of the  $D^0$  curve (Fig. 2) changes from +1.5 to -2.1. The same parameters  $\beta_2^*$ ,  $\beta_1^*$  and  $\beta_{-1}^*$  were derived for hydrochloric acid solutions as those appearing in Table IV for lithium chloride solutions. However, for slopes more negative than -1, a different  $\beta_{-2}^*$  is obtained by the curve-fitting method<sup>12</sup>:  $\log \beta_{-2}^*(\text{HCl}) = -0.07$  against  $\log \beta_{-2}^*(\text{LiCl}) = -0.85$ . Remembering that  $\beta_{-2}^*$  is the constant for the reaction



where L is the symbol for a ligand, it may be interpreted as applying to the sum of the reactions



and



The equilibrium expressions for both eq. 10 and 11

(15) Y. Marcus, paper submitted to *J. Inorg. Nuclear Chem.*

(16) K. A. Kraus, F. Nelson, F. B. Clough and R. C. Carlsion. *J. Am. Chem. Soc.*, **77**, 1391 (1955).

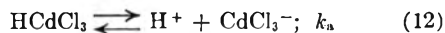
(17) K. A. Kraus, private communication, August, 1957.

(18) K. Damm and A. Weiss, *Z. Naturforsch.*, **106**, 535 (1955).

(19) S. J. Lachman and F. C. Tompkins, *Trans. Faraday Soc.*, **40**, 136 (1944).

depend inversely on the second power of the ligand function  $a$ , since  $m^2_{\text{Cl}}\gamma^2_{\pm(\text{HCl})} = m_{\text{HMCl}}\gamma^2_{\pm(\text{HCl})} = a^2$  in hydrochloric acid solutions. Subtracting  $\beta_{-2}^*(\text{LiCl})$  from  $\beta_{-2}^*(\text{HCl})$  yields the value of the equilibrium parameter for a reaction 11, the logarithm of which is  $\log \beta_{-1}^* = -0.15$ . This happens to be the same as  $\log \beta_{-1}^*$ , which means that the complex  $\text{CdCl}_2$  has in hydrochloric acid solutions equal chances to add  $\text{Cl}^-$  to give  $\text{CdCl}_3^-$  or to add  $\text{H}^+\text{Cl}^-$  to give  $\text{HCdCl}_3$ .

If one wishes to assume for hydrochloric acid of the concentrations involve (1 to 4  $M$ ) that the single ion activity coefficients for  $\text{H}^+$  and  $\text{Cl}^-$  ions are equal (thus equal to  $\gamma_{\pm(\text{HCl})}$ ) one can calculate the dissociation constant for the chloro-cadmium acid



$\log k_a = 0.00 \pm 0.25$  signifying a moderately strong acid.

The limiting slope of the  $D^0$  curve for hydrochloric acid is more negative than that expected for the limiting species  $\text{CdCl}_4^{2-}$  and  $\text{HCdCl}_3$ . This may be interpreted either as formation of further undissociated chloroacids  $\text{HCdCl}_4^-$  and  $\text{H}_2\text{CdCl}_4$ , or as a breakdown of the assumptions concerning activity coefficients. The first suggestion calls for a further parameter applying to a power of  $a$  more negative than -2. Formally, the parameter  $\beta_{-2}^*$  is the coefficient of  $a^{-3}$  in the sum in the denominator of the expression for  $D^0$  (eq. 42, ref. 2), and a value of -2.1 for  $\log \beta_{-2}^*$  makes the calculated curve fit the data. With our present meager knowledge about concentrated electrolyte solutions it seems however unwise to stress this interpretation, and the error caused by neglecting a "correction term" involving  $a^{-3}$  is not very great.

**Resin Complex Formation.**—It remains to consider the parameter  $K_r'$  which describes the interaction of  $\text{CdCl}_2$  in the resin complex, assumed to be  $\text{R}_2\text{CdCl}_4$ . The value of  $\log K_r' = 3.17 \pm 0.05$  was obtained by the curve-fitting method.<sup>12</sup> Values of the experimental and the ideal distribution coefficients  $D$  and  $D^0$  were calculated by eq. 7, utilizing this value of  $K_r'$ , the complex formation constants listed in Table IV and the values for the chloroacid formation constants given in the previous section, for both lithium chloride and hydrochloric acid solutions. The curves of  $\log D$  and  $\log D^0$  vs.  $\log a$  are shown in Figs. 1 and 2 as solid lines. They agree very well with the experimental points.

The value of  $k_r'$  thus checked may be used to calculate the equilibrium constant for the reaction



by dividing  $K_r'$  by the 2nd power of the reference state  $a^0$ . This gives  $\log K_r' - 2 \log a^0 = 3.17 - 2 \times 0.46 = 2.25$  for the logarithm of this constant. This value may be compared with the value for the corresponding reaction in the solution,  $\log \beta_{-2}^* = -0.85$ . It is seen that the resin stabilizes the cadmium complex about 1300-fold.

**Comparison with Published Constants.**—Table V gives a comparison of complex formation constants for the cadmium-chloride system obtained in the present investigation with those obtained by a

TABLE V

| COMPLEX FORMATION CONSTANTS FOR THE CADMIUM-CHLORIDE SYSTEM |                            |                        |           |           |           |           |
|-------------------------------------------------------------|----------------------------|------------------------|-----------|-----------|-----------|-----------|
| Author                                                      | Method                     | Medium                 | log $k_1$ | log $k_2$ | log $k_3$ | log $k_4$ |
| Riley <sup>20</sup>                                         | Potent. titr.              | KCl, varying           | 2.00      | 0.60      | 0.11      | 0.30      |
| Leden <sup>21</sup>                                         | Potent. titr.              | 3 M NaClO <sub>4</sub> | 1.59      | .66       | .18       |           |
| King <sup>22</sup>                                          | Solubility                 | 3 M NaClO <sub>4</sub> | 1.40      | .81       | .18       |           |
| Korshunov <sup>23</sup>                                     | Polarography               |                        |           |           | .78       | .30       |
| Vasil'ev <sup>24</sup>                                      |                            |                        | 2.18      | .43       |           |           |
| Strocchi <sup>25</sup>                                      | Polarography               | 2 M NaNO <sub>3</sub>  | 1.57      | .08       | .24       |           |
| Golub <sup>26</sup>                                         | Potentiometry              | 2.1 M KNO <sub>3</sub> | 1.77      | 1.45      | -.25      | -.05      |
| Eriksson <sup>27</sup>                                      | Polarography               | 3 M NaClO <sub>4</sub> | 1.54      | 0.52      | .40       |           |
| Vanderzee <sup>28</sup>                                     | Potentiometry              | 3 M NaClO <sub>4</sub> | 1.54      | .66       | .08       |           |
|                                                             | Extrap. to zero ionic str. |                        | 2.00      | .70       | -.58      |           |
|                                                             |                            |                        | 1.95      | .55       | -.15      | -.70      |

This work anion exchange LiCl, varying HCl, varying, in addition to above also  $\log \beta_{-1}' = -0.15$

number of authors using various different methods, ionic media and medium concentrations. Comparison is valid only if due cognizance is taken of differences in the activity coefficient functions involved.<sup>2,3</sup> It may however be pointed out that the parameters obtained by the anion-exchange method are most similar to the thermodynamic complex formation constants reported, those obtained for zero ionic strength.

Further values for comparison are:  $\log k_1$ , by conductometry and extrapolated to zero ionic strength, Righelatto<sup>29</sup> and Davies<sup>30</sup> 2.00, Harned<sup>31</sup> 1.95; Brühl,<sup>32</sup> from considerations of activity coefficients, appr. 2.5, and Turv'an<sup>33</sup> 2.30. For  $\log \beta_1$ , Knobloch<sup>34</sup> found by potentiometry in KCl solutions 2.93, while Korenman<sup>35</sup> found in HCl solutions 1.7 to 2.5. For  $\log k_3k_4 (= \log \beta_{-2}')$  Bourion<sup>36</sup> found by ebullioscopy at 100° appr. 0.0.

**Acknowledgment.**—This paper is published by the kind permission of the Director of Research, Israel Atomic Energy Commission, to whom thanks are due.

(20) H. C. Riley and V. Gallafent, *J. Chem. Soc.*, 514 (1932).

(21) I. Leden, *Z. physik. Chem.*, **188A**, 160 (1941).

(22) E. King, *J. Am. Chem. Soc.*, **71**, 319 (1949).

(23) I. A. Korshunov, N. I. Malyugina and M. O. Balabanova, *Zhur. Obshchei Khim.*, **21**, 620 (1951).

(24) A. M. Vasil'ev and V. I. Proukhina, *Zhur. Anal. Khim.*, **6**, 218 (1951).

(25) P. M. Strocchi and D. N. Hume, Abstracts 123rd Meeting Am. Chem. Soc., March 1953, p. 4P. The values quoted in Table V are those corrected for nitrate complex formation, cf. Vanderzee and Dawson.<sup>26</sup>

(26) A. M. Golub, *Ukrain. Khim. Zhur.*, **19**, 205 (1953).

(27) L. Eriksson, *Acta Chem. Scand.*, **7**, 1146 (1953).

(28) C. E. Vanderzee and H. J. Dawson, *J. Am. Chem. Soc.*, **75**, 5659 (1953).

(29) E. C. Righelatto and W. C. Davies, *Trans. Faraday Soc.*, **26**, 592 (1930).

(30) W. C. Davies, *Endeavour*, **4**, 114 (1945).

(31) H. S. Harned and M. E. Fitzgerald, *J. Am. Chem. Soc.*, **58**, 2624 (1936).

(32) L. Brühl, *Gazz. chim. ital.*, **64**, 615 (1934).

(33) Y. I. Turv'an, *Zhur. Neorg. Khim.*, **1**, 2337 (1956).

(34) W. Knobloch, *Lotos*, **78**, 110 (1930).

(35) K. M. Korenman, *Zhur. Obshchei Khim.*, **18**, 1233 (1948).

(36) F. Bourion and E. Rouyer, *Ann. Chim.*, [13] **10**, 263 (1928).

## KINETICS OF GRAPHITE OXIDATION. II

BY GEORGE BLYHOLDER<sup>1</sup> AND HENRY EYRING

*Department of Chemistry, University of Utah, Salt Lake City, Utah*

*Received September 11, 1958*

The kinetics of the oxygen-graphite reaction in the 800 to 1300° temperature range and 1 to 100  $\mu$  pressure range are investigated. Above 1000° the true surface reaction is half order with respect to oxygen and the activation energy is small. The effect of the diffusion of oxygen into the pores of the graphite sample is elucidated. Absolute rate theory together with the observed kinetics is used to develop a mechanism for the reaction.

### Introduction

In the previous paper<sup>1</sup> the reaction of oxygen with graphite in the 600 to 800° temperature range and one to one hundred  $\mu$  pressure range was presented. Here the data for this reaction from 800 to 1300° are given and discussed. The data for the two temperature ranges were taken concurrently. The division into two temperature ranges is done purely for convenience in discussing the results. In the 600 to 800° temperature range the observed reaction has a constant activation energy and is one-half order with respect to oxygen. Above 800° the plot of the log of the reaction rate versus the

inverse of the absolute temperature is no longer linear. The observed order of the reaction also changes above 800°.

### Experimental

Since all the data were gathered at the same time the apparatus is that described in the first publication.<sup>1</sup>

The graphite samples were prepared from the same batch of spectrographic electrodes manufactured by the National Carbon Company that was used for the low temperature data. The details of the sample preparation are as reported in the first paper. The geometric areas and thickness of the samples are given in Table I.

### Experimental Results

For previously stated reasons the reaction rate changes in a regular manner from one similar

(1) G. Blyholder and H. Eyring, *This Journal*, **61**, 682 (1957).

TABLE I<sup>a</sup>

| Sample | Area (cm. <sup>2</sup> ) | Thickness (cm.)    |
|--------|--------------------------|--------------------|
| 1      | 6.94                     | 0.1                |
| 2      | 1.77                     | .1                 |
| 4      | 1.4                      | .1                 |
| 9      | 1.12                     | .1                 |
| 10     | 1.32                     | .1                 |
| 11     | 1.04                     | .1                 |
| 14     | 9.88                     | $2 \times 10^{-4}$ |

<sup>a</sup> Samples which were used in both the high and low temperature range bear the same number in both publications.

run to the next. In order to obtain meaningful results, a set of conditions for a run were selected as standard. A standard run is then made between successive runs in which the conditions are varied. The results are then normalized so that all the standard runs are the same. After this adjustment the true relationship among runs at varying conditions is seen.

The temperature dependence of the reaction at an O<sub>2</sub> pressure of 26  $\mu$  is shown in Fig. 1. Samples numbered 1, 2, 9, 10 and 11 were used to obtain these data. Using samples numbered 2, 9, 10 and 11 the pressure dependence data shown in Fig. 2 were obtained. In order to place all of the pressure dependence data for one-mm. thick samples on the same graph, one rate from the data for each temperature was multiplied by a factor which would place it on the  $R = kP^{3/4}$  line in Fig. 2. All of the data for a particular temperature were then multiplied by the same factor. The results of this are the experimental points in Fig. 2. The result of a pressure dependence study on sample number 14, which had a very thin layer of graphite, is shown in Fig. 3. Due to the small amount of graphite in the thin layer of this sample the amount of graphite and consequently the rate of oxidation decreased rapidly from one run to the next on this sample. This particular set of data is therefore probably not as reliable as the rest of the data.

The results obtained by making runs with the copper oxide catalyst cold are recorded in Table II. By comparing the results of these runs with previous runs under the same conditions the amounts of carbon dioxide in the product gases can be determined. The percentage of carbon dioxide in the product gases is given in the last column of this table. These results were obtained using sample number 4.

TABLE II  
RESULTS WITH CATALYST COLD

| Rate of production of CO + CO <sub>2</sub> in $\mu/3$ min. into a 0.404 l. system at 300°K. | O <sub>2</sub> pressure, $\mu$ | Temp., °C. | % CO <sub>2</sub> |
|---------------------------------------------------------------------------------------------|--------------------------------|------------|-------------------|
| 17                                                                                          | 27                             | 804        | 3                 |
| 63                                                                                          | 27                             | 900        | 6                 |
| 149                                                                                         | 26                             | 1008       | 11                |
| 174                                                                                         | 17                             | 1107       | 22                |
| 344                                                                                         | 16                             | 1205       | 39                |
| 57                                                                                          | 28                             | 800        | 10                |

### Interpretation of Results

In the first paper it was established that, in the 600 to 800° temperature range, carbon monoxide is the primary product of the reaction of graphite with oxygen in the one to one hundred  $\mu$  pressure

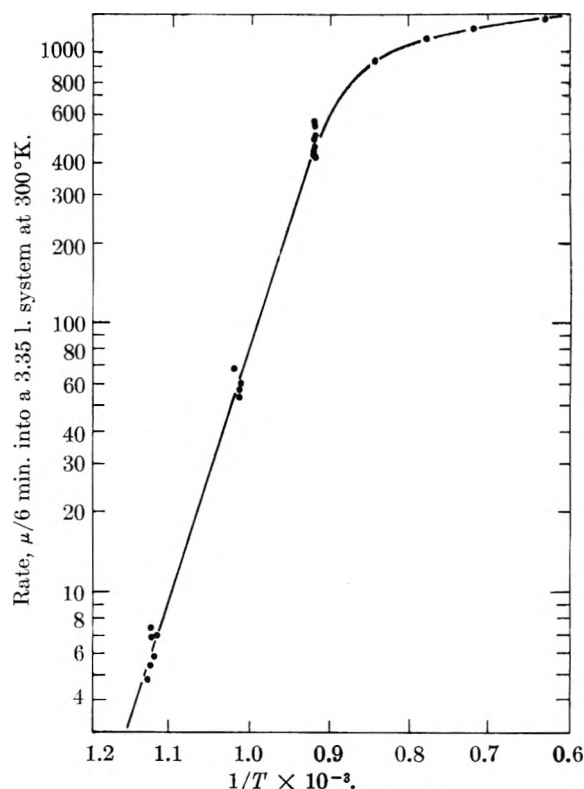
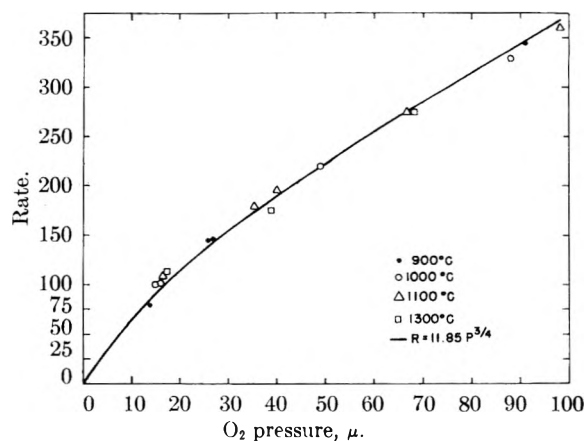
Fig. 1.—Log of rate vs.  $1/T$ .

Fig. 2.—Pressure dependence.

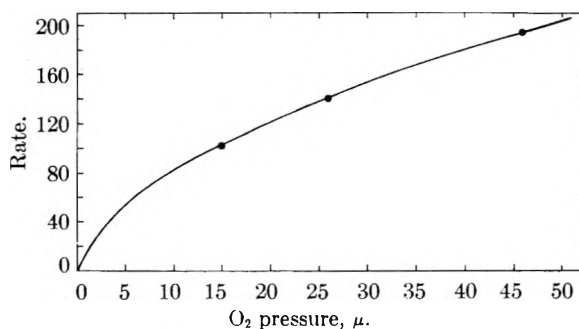
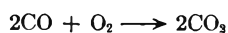


Fig. 3.—Pressure dependence of thin layer at 900°.

range. In the temperature range from 800 to 1000°, the results shown in Table II indicate that carbon monoxide is the primary product. At 1100 and 1200° the results show about 20 and 40% CO<sub>2</sub>,

respectively, in the product gas. We believe that this increase in the CO<sub>2</sub> percentage is due to the secondary reaction



The equilibrium constant for this reaction greatly favors the formation of CO<sub>2</sub>. The rate of this reaction is apparently too slow for much CO<sub>2</sub> to be observed at any but the highest temperatures studied. We shall therefore continue with the assumption, which has been demonstrated over 5/7 of the temperature range studied, that CO is the primary reaction product.

The role of pore diffusion in the reaction of oxygen with the artificial graphite used in this study was established in the first paper. Pore diffusion enters into the kinetics of a reaction of a gas with a porous solid when the reaction of the gas with the surface is fast enough that the concentration of gas in the pores of the solid is less than the concentration of gas outside the pores. This condition was demonstrated to be true in the 600 to 800° temperature range. Since the surface reaction in the 800 to 1300° temperature range is faster than in the 600 to 800 range, pore diffusion will be a factor in the reaction in the 800 to 1300° range.

The model developed by Wheeler<sup>2</sup> for the reaction of a gas in the pores of a solid will be used. One of the results of this model is that when pore diffusion affects the reaction, if the true order with respect to the gas of its reaction with the surface is  $n$ , the observed order will be  $(n + 1)/2$ . With samples  $2 \times 10^{-4}$  cm. thick, it is seen from Fig. 3 that at 900° the true surface reaction is  $1/2$  order with respect to oxygen. Using  $n = 1/2$  in the expression  $(n + 1)/2$  gives an observed order of  $3/4$  for reaction plus pore diffusion. From Fig. 2 it is seen that for samples 0.1 cm. thick the observed order of the reaction is indeed  $3/4$  at 900°. This confirms the conclusion that pore diffusion is a factor in the reaction.

Another result of Wheeler's model is that the observed activation energy for pore diffusion plus reaction will be one-half of the true activation energy for the surface reaction. This condition has been shown to be true at 800°. From Fig. 1 it is observed that above 800° the reaction rate no longer increases with the same exponential factor as the temperature is raised that it did from 600 to 800°. In the temperature range from 1100 to 1300° the activation energy has dropped to 1 kcal. per mole. Figure 2 shows that the observed order with respect to oxygen of the reaction on 0.1-cm. thick samples is  $3/4$  from 900 to 1300°. Taking pore diffusion into account, this leads to the conclusion that from 900 to 1300° the true surface reaction is  $1/2$  order with respect to oxygen.

The true surface reaction is given by the expression

$$R = KC^{1/2} \quad (1)$$

where

- $R$  = rate per unit area
- $K$  = constant
- $C$  = gas phase oxygen concn.

The rate, taking pore diffusion into consideration, is obtained from the following equation given by Wheeler.

$$\pi r^2 D \frac{d^2 C}{dx^2} = 2\pi r R \quad (2)$$

where

- $r$  = pore radius
- $D$  = diffusion coefficient
- $x$  = coordinate along pore length

Wheeler did not consider the case where  $R$  is given by equation 1. Substituting equation 1 into 2 yields

$$\pi r^2 D \frac{d^2 C}{dx^2} = 2\pi r KC^{1/2} \quad (3)$$

This is the fundamental differential equation to be solved. The boundary conditions are  $C = C_0$  at  $X = 0$  and  $dc/dx = 0$  at  $X = L$ . The latter boundary condition is found because by symmetry there is no net flow through the cross section at  $X = L$ . The reaction rate per half pore is the rate at which oxygen flows into the pore, which is  $\pi r^2 D$  times the concentration gradient at  $X = 0$ . This gives

$$R_p = \pi r^2 D \left( \frac{dc}{dx} \right)_{x=0} \quad (4)$$

where  $R_p$  is the rate per half pore. The problem is to evaluate  $(dc/dx)_{x=0}$  from equation 3.

Equation 3 may be integrated once to yield

$$\frac{dc}{dx} = \left( \frac{4}{3} \frac{2K}{rD} C^{3/2} + 2B \right)^{1/2} \quad (5)$$

where  $B$  is an integration constant. Unfortunately this equation cannot be integrated in closed form. Also the boundary conditions as given are not applicable to equations 5. Considerable simplification results from letting  $C = C_L$  at  $X = L$ , where also  $dc/dx = 0$ . With these substitutions equation 5 may be solved for  $B$  to yield

$$B = -4/3 \frac{K}{rD} C_L^{3/2} \quad (6)$$

Substituting the value for  $B$  into equation 5 gives

$$\frac{dc}{dx} = \left[ \frac{8K}{3rD} (C^{3/2} - C_L^{3/2}) \right]^{1/2}$$

At  $x = 0$  this yields

$$\left( \frac{dc}{dx} \right)_{x=0} = 2 \sqrt{\frac{2K}{3rD}} (C_0^{3/2} - C_L^{3/2})^{1/2} \quad (7)$$

where  $C_0$  is the oxygen concentration outside the solid. In the reaction from 600 to 800° it was found that a zero-order surface reaction became an observed half-order reaction when pore diffusion affected the reaction. This means that at  $X = L$ ,  $C_L = 0$  for the reaction in the 600 to 800° range. Since the surface reaction is even faster in the 800 to 1300° range, it is valid to replace  $C_L$  by 0 in equation 7. Substituting  $dc/dx_{x=0}$  from equation 7 into equation 4 yields

$$R_p = 2\pi r \sqrt{\frac{2rDK}{3}} C_0^{3/4} \quad (8)$$

Having a value for the rate per pore the total rate of the reaction may be calculated.

$$R_T = n_p R_p \quad (9)$$

(2) A. Wheeler, "Advances in Catalysis," Vol. III, Academic Press, Inc., New York, N. Y., 1951, p. 250.

where

$$R_T = \text{rate per sq. cm.-sec.}$$

$$n_p = \text{no. of pore mouths per unit area}$$

According to the model used

$$n_p = \frac{\theta'}{\pi r^2 \sqrt{2}} \quad (10)$$

where

$$\theta' = 0.4 = \text{porosity of sample}^2$$

Since the mean free path of the gas is much greater than the pore diameters, the diffusion coefficient is for molecular flow. This is given by

$$D = \frac{2r}{3} \bar{v} \quad (11)$$

where  $\bar{v}$  is the average molecular speed given by

$$\bar{v} = \sqrt{\frac{8k_B T}{\pi m}} = 2.0 \times 10^3 \sqrt{T} \quad (12)$$

in which  $m$  is the molecular mass of oxygen. Assuming a perfect gas yields

$$c_0 = 9.65 \times 10^{18} \frac{P}{T} \quad (13)$$

where  $P$  is in mm. of Hg. At  $26 \mu$  pressure and  $900^\circ$  the use of equations 10, 11, 12 and 13 in equation 9 gives

$$R_T = 5.3 \times 10^{12} \sqrt{K} \quad (14)$$

This expression for the rate taking pore diffusion into consideration may be checked by finding the value for  $K$  from a measurement of the true surface reaction and placing this value in equation 14 and comparing the result with the measured reaction rate. From Fig. 6 of the paper<sup>2</sup> on the results in the low temperature range the rate of the true surface reaction at  $900^\circ$  and  $26 \mu$  pressure is found to be  $2.7 \times 10^{13}$  molecules of  $O_2$  per  $cm.^2$ -sec. Using equation 1 this gives a  $K$  value of  $2.5 \times 10^6$ . From equation 14 the calculated rate is given by

$$R_T(\text{calcd.}) = 8.4 \times 10^{15} \text{ molecules per } cm.^2\text{-sec.}$$

From Fig. 1 the observed rate is  $6.5 \times 10^{15}$  molecules per  $cm.^2$ -sec. which is in good agreement with the calculated rate.

We now wish to inquire into the sort of kinetics necessary to obtain a half-order surface reaction. A slow step of the gas phase equilibrium dissociation of oxygen molecules into atoms followed by a fast reaction of the oxygen atoms with the surface would produce half-order kinetics. Due to the high heat of dissociation of oxygen molecules, the number of oxygen atoms in the gas phase is strongly temperature dependent. Any process depending on this as the slow step would then be strongly temperature dependent. This is clearly contradictory to the experimental evidence, so this mechanism is eliminated. We must then turn to a consideration of processes taking place on the surface.

If the adsorbed oxygen is assumed to be immobile the kinetic expressions yield only rates which are either independent of pressure or are proportional to the first power of the pressure. Since this is contradictory to the experimental results this mechanism is eliminated.

If the oxygen atoms are able to migrate on the

surface, the following expression is obtained

$$\frac{d\theta}{dt} = 2(1 - \theta)^2 P k_1 - 2k_{-1}\theta^2 - k\theta \quad (15)$$

where

$$\theta = \text{fraction of sites covered by adsorbed oxygen atoms}$$

$$k_1 = \text{rate constant for formation of surface oxide}$$

$$k_{-1} = \text{rate constant for } O_2 \text{ leaving surface}$$

$$k = \text{rate constant for oxygen atoms on the surface reacting to produce CO}$$

$$P = \text{gas phase oxygen pressure}$$

Making the steady-state assumption that  $d\theta/dt = 0$  yields

$$\theta = \frac{(4Pk_1 + k) - \sqrt{(4Pk_1 + k)^2 + 8Pk_1(2k_{-1} - 2Pk_1)}}{-2(2k_{-1} - 2Pk_1)} \quad (16)$$

In order for  $\theta$  to be real and not greater than one it is necessary that the minus sign be chosen in equation 16. In evaluating the square root, if the first of the two terms under the square root sign is allowed to dominate the second, the result is kinetics which are either zero or first order. This is contrary to experiment. If the second term under the square root sign dominates, the expression for  $\theta$  becomes

$$\theta = \sqrt{\frac{k_1 P}{k_{-1} - k_1 P}} \quad (17)$$

If now  $k_{-1} \gg k_1 P$  the result is

$$\theta = \sqrt{\frac{k_1}{k_{-1}}} P^{1/2} \quad (18)$$

The rate of production of CO is now given by

$$R = k\theta N = kN \sqrt{\frac{k_1}{k_{-1}}} P^{1/2} \quad (19)$$

where  $N$  is the number of carbon sites per  $cm.^2$  which is  $3.5 \times 10^{15}$ . This result is in accord with the experimental order of the reaction.

The rate constant  $k$  will now be considered in some detail. In order to obtain the correct pressure dependence for  $R$ , it was necessary to assume that the oxygen atoms on the surface progress from site to site on the surface rapidly enough that the distribution of oxygen atoms on sites is random despite the arrival of the oxygen atoms in pairs. In the temperature range from  $600$  to  $800^\circ$  where the reaction is zero order, it seems likely that the stable surface oxide is one in which the oxygen atom is attached to the surface by a carbonyl type bond. In the high temperature range it seems not unlikely that the oxygen atoms which are capable of rapid movement over the surface are less firmly attached to the surface than a carbonyl bond implies. For example, it may be that an oxygen atom is on the surface as a singly negatively charged ion which is attached to a carbon atom by a single bond. The movement of the oxygen atom over the surface could then be accomplished by the ion forming another single bond with an adjacent carbon atom and then breaking the bond with the original carbon atom to become an ion on a new site. Using this model an oxygen atom appears first on the surface as an oxygen ion which hops around until it forms a carbonyl type bond with a carbon atom. This carbonyl surface oxide then decomposes to produce a carbon monoxide molecule. The process



represented by the rate constant  $k$  now becomes a two-step process. Step one is the formation of a carbonyl type surface oxide. Step two is the decomposition of this oxide to give CO. If  $\beta$  is the fraction of the oxygen atoms on the surface which have carbonyl type bonds with the surface, we have

$$\frac{d\beta}{dt} = k_2(1 - \beta) - k_{-2}\beta - k_3\beta \quad (20)$$

where

- $k_2$  = rate of formation of carbonyl type oxide
- $k_{-2}$  = rate of reverse of process for  $k_2$
- $k_3$  = rate of decomposition of carbonyl type oxide to carbon monoxide

Making the steady-state assumption that  $d\beta/dt = 0$ , the equation (21) is obtained

$$\beta = \frac{k_2}{k_2 + k_{-2} + k_3} \quad (21)$$

In equation 26,  $k$  may now be replaced by  $k_3\beta$ , so that

$$R = k_3 N \beta \sqrt{\frac{k_1}{k_{-1}}} P^{1/2} \quad (22)$$

There are three different expressions for  $R$  depending on which term in the denominator of equation 21 dominates the others.

If  $k_3$  dominates  $k_2$  and  $k_{-2}$ , the result is that  $\beta = k_2/k_3$  with  $\beta \ll 1$ . The rate is given by

$$R = k_2 N \sqrt{\frac{k_1}{k_{-1}}} P^{1/2} \quad (23)$$

In this case the carbonyl surface oxide decomposes as soon as it is formed to give a carbon monoxide molecule.

Since there is a fairly detailed model in each of the three cases, the absolute rate theory of Eyring<sup>4</sup> may be used together with the measured activation energies to calculate rates for each of the three cases. The calculated rates then may be compared with the experimental rate to determine which model best fits the data. In general a rate constant  $k'$  is given by

$$k' = \kappa \frac{k_B T}{h} \frac{f_{\pm}}{f_i} e^{-E^{\circ}/RGT}$$

where

- $\kappa$  = transmission coefficient
- $k_B$  = Boltzmann constant
- $T$  = temperature, °K.
- $h$  = Planck constant
- $f_{\pm}$  = partition function for activated complex
- $f_i$  = partition function for reactants
- $E^{\circ}$  = activation energy, cal. per mole at absolute zero
- $R$  = gas constant, cal. per mole-deg.

It will be assumed that the transmission coefficient is the same for passage in both directions over the potential barrier since the activated complex is also the same for passage in either direction. Vibrational partition functions are assumed to make a negligible contribution. These assumptions yield

$$\frac{k_1}{k_{-1}} = \frac{(f_0)^2}{f_{O_2G}} e^{-(E^{\circ}_1 - E^{\circ}_{-1})/RT} \quad (24)$$

where

- $f_0$  = partition function for mobile oxygen atoms on surface

$f_{O_2G}$  = partition function for gas phase oxygen molecule  
 $f_{O_2G} = (f_{tr})^2(f_{rot})^2 = 3.2 \times 10^{22}$  at 1600°K.

where

- $f_{tr}$  = translational partition function
- $f_{rot}$  = rotational partition function

In addition

$$k_2 = \kappa_2 \frac{kT}{h} \frac{f_2^{\pm}}{f_0} e^{-E^{\circ}_2/RT} \quad (25)$$

Since  $f_2^{\pm}$  involves only vibrational partition functions it is assumed to be one.

In the use of equations 24 and 25 to evaluate equation 23  $f_0$  disappears from the final expression for  $R$ . The final result using the experimental activation energy at 1600°K. is

$$H_2\kappa = 6.4 \times 10^{12} P^{1/2} \quad (26)$$

In this expression for  $R$  the value of the transmission coefficient  $\kappa_2$  must be considered. For the model of oxygen on the surface that has been proposed the transmission coefficient  $\kappa_2$  is for the reaction of a singly negatively charged oxygen atom with one bond with a surface carbon atom undergoing an electronic rearrangement to become an oxygen atom attached to the surface carbon atom by a carbonyl type bond. Thus both the initial and final states have their own potential energy surface. Therefore the reaction must involve a transition from one potential energy surface to another. For reactions involving a transition from one potential surface to another the transmission coefficient may be expected<sup>5</sup> to be small. A value for  $\kappa_2$  of  $10^{-6}$  would not be unreasonable.

The experimental reaction rate may be evaluated from Fig. 1. At 1600° K. and 26  $\mu$

$$R_T = 2.8 \times 10^{16} \text{ molecules } O_2/\text{cm.}^2\text{-sec.} \quad (27)$$

By use of an equation like (18) but evaluated at 1600°K. and 26  $\mu$  pressure, the true surface reaction is evaluated as

$$R = 3.1 \times 10^7 P^{1/2} \text{ molecules } O_2/\text{cm.}^2\text{-sec.} \quad (28)$$

or  $R = 6.2 \times 10^7 P^{1/2} \text{ molecules } CO/\text{cm.}^2\text{-sec.}$

This experimental rate may be compared to equation 26 where the pressure, as also in equation 28, is expressed as molecules per cm.<sup>3</sup>. The calculated rates for the cases where  $k_2$  and  $k_{-2}$  dominate the denominator of equation 21 do not agree with the experimental data. However, the case considered with a reasonable value of the transmission coefficient fits the data quite well. It is thus concluded that the rate-determining step in the oxygen-graphite reaction above 1000° in the 1 to 100  $\mu$  pressure range involves the transition of an oxygen atom in a semi-mobile state on the surface to a carbonyl-like structure which quickly decomposes to yield a CO molecule.

**Acknowledgment.**—The authors gratefully acknowledge the California Research Corporation for a fellowship which supported George Blyholder during much of this work and the United States Air Force for support under contract No. AF 33(038)20839.

(3) S. Glasstone, K. J. Laidler and H. Eyring, "The Theory of Rate Processes," McGraw-Hill Book Co., Inc., New York, N. Y., 1941.

# CALORIMETRIC DETERMINATION OF THE SURFACE ENTHALPY OF POTASSIUM CHLORIDE<sup>1</sup>

By P. BALK<sup>2</sup> AND G. C. BENSON

*Division of Pure Chemistry, National Research Council, Ottawa, Canada*

*Received October 14, 1958*

Heats of solution of KCl in water at 25° have been measured for powders with specific areas ranging from 0 to 60 m.<sup>2</sup> g.<sup>-1</sup>. The data yield a value of 252 erg cm.<sup>-2</sup> for the surface enthalpy at 25°. Comparison is made with other experimental information and with the values obtained in theoretical calculations. It appears that the experimental surface enthalpy is considerably higher than predicted by theory for the {100} face; possible explanations of this discrepancy are considered.

## I. Introduction

A knowledge of the force field and crystal structure in the surface regions of a solid is of importance in any fundamental consideration of physical and chemical phenomena occurring in or near the solid surface. Some information about this force field and the surface structure can be obtained from the experimental measurement of thermodynamic properties of the substance as a function of the specific surface area combined with the development of a consistent theoretical model.

The alkali halides seem to provide a very suitable class of materials for surface studies. Their simple lattice structures have been the subject of numerous theoretical investigations and a great deal of progress has been made in formulating models which lead to an understanding of their bulk properties. Since the early calculations of surface energies by Madelung<sup>3</sup> and by Born and Stern<sup>4</sup> nearly forty years ago, the surface properties of the alkali halides have also received considerable theoretical attention. However, in this case the applicability of the proposed models has yet to be established due to a lack of reliable experimental data.

The measurement of surface thermodynamic properties of solids is generally difficult because inherently it involves a study of small differences between relatively large quantities. Until recently this was particularly true in the case of the alkali halides due to the fact that these materials had not been prepared in a suitably fine state of subdivision to make the surface contributions significant. In the past five years a method for preparing alkali halide powders with surface areas as high as 60 m.<sup>2</sup> g.<sup>-1</sup> has been developed and a study of the surface properties of these materials is now more feasible.

Jura and Garland<sup>5</sup> have pointed out that in simple cases all the surface thermodynamic properties of a crystalline solid can be obtained from a knowledge of the surface heat capacity as a function of temperature, together with a value of the surface enthalpy at a single temperature. In the case of the alkali halides some experimental work has been done on the heat capacity of small particles of NaCl<sup>6,7</sup> but no definite value could be as-

sociated, in a strict thermodynamic sense, with the surface. The other quantity referred to by Jura and Garland, the surface enthalpy, can be obtained most directly from experimental determinations, in a suitable solvent, of heats of solution of powders having different specific surface areas. This approach was first used for alkali halides by Lipsett, Johnson and Maass,<sup>8</sup> and has been adopted in a number of succeeding investigations.<sup>9-15</sup> In all cases the alkali halide studied was again NaCl. However, it appears that the surface enthalpy of this compound determined experimentally at 25° and corrected approximately to 0°K., is much higher than the values predicted for the {100} face of the crystal by simple theoretical models. Accordingly it is of some interest to obtain experimental results for other alkali halides and to attempt a similar comparison with theory.

In the present paper a value of the surface enthalpy of KCl at 25° is reported. The next section contains some details of the experimental procedure. This is followed by a presentation of the results of a number of heat of solution determinations on KCl with areas from 0 to 60 m.<sup>2</sup> g.<sup>-1</sup>. In the last section the new value for the surface enthalpy, deduced from these data, is discussed in relation to other available experimental information and to the predictions of various theoretical models.

## II. Experimental

Samples with high specific surface areas were prepared by electrostatic precipitation of KCl smokes. The apparatus for producing these aerosols differs somewhat from that used in this Laboratory in an investigation of the surface enthalpy of NaCl<sup>15</sup> and will be described briefly by reference to Fig. 1. The hemi-spherical Pyrex dome and platinum crucible are similar to the assembly used by Thompson, Rose and Morrison,<sup>16</sup> but the baffle in the latter has been omitted. The carrier gas is introduced through two quartz tubes A and B. One of these (A) ends in a slit orifice which directs

(1) Issued as N.R.C. No. 5114. Paper presented in part at the "Symposium on Energetics of Surfaces and Interfaces" sponsored by the Division of Colloid Chemistry, 134th National Meeting of the American Chemical Society, Chicago, Ill., September 9, 1958.

(2) National Research Council of Canada Postdoctorate Fellow 1956-1958.

(3) E. Madelung, *Phys. Z.*, **20**, 494 (1919).

(4) M. Born and O. Stern, *Physik-math. Kl. Sitzber. preuss. Akad. Wiss.*, **48**, 901 (1919).

(5) G. Jura and C. W. Garland, *J. Am. Chem. Soc.*, **74**, 6033 (1952).

(6) D. Patterson, J. A. Morrison and F. W. Thompson, *Can. J. Chem.*, **33**, 240 (1955).

(7) J. A. Morrison and D. Patterson, *Trans. Faraday Soc.*, **52**, 764 (1956).

(8) S. G. Lipsett, F. M. Johnson and O. Maass, *J. Am. Chem. Soc.*, **49**, 925 (1927).

(9) S. G. Lipsett, F. M. Johnson and O. Maass, *ibid.*, **49**, 1940 (1927).

(10) S. G. Lipsett, F. M. Johnson and O. Maass, *ibid.*, **50**, 2701 (1928).

(11) G. E. Boyd and W. D. Harkins, *ibid.*, **64**, 1190 (1942).

(12) J. E. Wertz, private communication mentioned in ref. 13.

(13) G. C. Benson and G. W. Benson, *Can. J. Chem.*, **33**, 232 (1955).

(14) E. Hutchinson and K. E. Manchester, *Rev. Sci. Instr.*, **26**, 364 (1955).

(15) G. C. Benson, H. P. Schreiber and F. van Zeggeren, *Can. J. Chem.*, **34**, 1553 (1956).

(16) F. W. Thompson, G. S. Rose and J. A. Morrison, *J. Sci. Instr.*, **32**, 325 (1955).

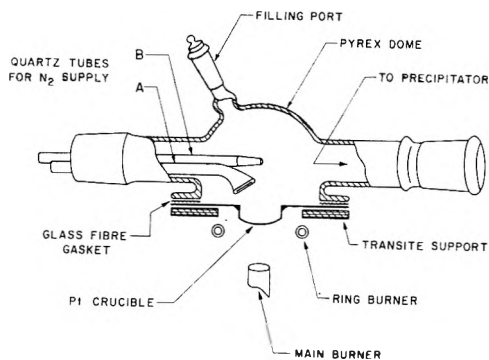


Fig. 1.—Diagram of salt evaporation apparatus.

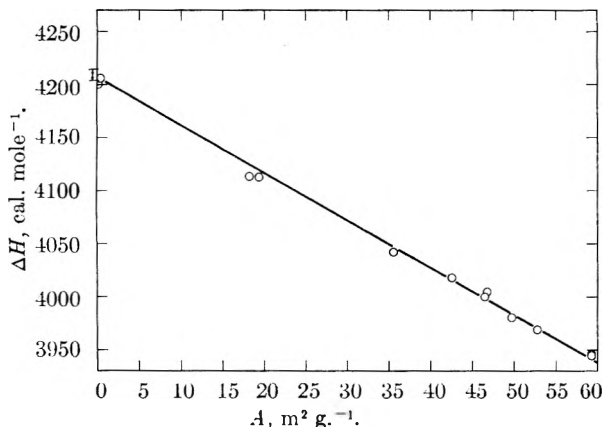


Fig. 2.—Plot of heat of solution ( $\Delta H$ , cal. mole<sup>-1</sup>) at 25° as a function of the specific area ( $A$ , m<sup>2</sup> g<sup>-1</sup>) for KCl powders dissolved in water to form a 0.2 *m* solution.

the gas over the surface of the molten potassium chloride with a high relative velocity. The second tube (B) provides an auxiliary gas stream which assists in carrying the smoke out of the dome. With this apparatus it was possible to obtain materials with specific surface areas in the range 15 to 60 m<sup>2</sup> g<sup>-1</sup>, employing flow rates much smaller than those indicated by Young and Morrison<sup>17</sup> and by van Zeggeren, Schreiber and Benson.<sup>18</sup> Cylinders of commercial dry nitrogen (99.7% purity) were used as a source of carrier gas and a total flow rate of 14 l. min<sup>-1</sup> at room temperature and atmospheric pressure was adopted. The temperature of the bottom of the crucible, measured with an optical pyrometer, was in the range 890 to 950°. Samples with different specific surfaces were produced by altering the crucible temperature and by varying the relative flows of gas through A and B keeping the total constant. In general lower temperatures and higher relative flow rates in tube A were used to produce the higher specific surface materials. The dimensions of the electrostatic precipitator were the same as those given in reference 18. All samples were collected with 7.5 kv. (60 cycles/sec.) between the central wire and the outer shim.

Recently attention has been drawn to the possible occurrence of nitrate in salt powders prepared by electrostatic precipitation.<sup>18</sup> In the present investigation a careful check was kept on the nitrate content of the KCl samples. The analysis for nitrate was carried out with a photoelectric colorimeter and was based on the reaction with brucine in sulfuric acid.<sup>19</sup> In all cases the nitrate content (stated as weight per cent. potassium nitrate) was less than 0.015%. All the samples of "fine" KCl were pure white powders and no indication of non-stoichiometry was observed in pH measurements on aqueous solutions prepared from them.

Electron photomicrographs were taken of a variety of samples of different specific surface areas, as used in the

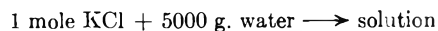
present work. The little crystals were in all cases approximately spherical in shape and although there was a definite tendency to develop flat sides, very few pure cubes could be detected. In view of the failure to find cubic-shaped particles the original form of the evaporation apparatus was restored (see ref. 16). This did not lead to any significant change in the particle shape of the product. After obtaining these results it seemed interesting to check on the shape of NaCl particles produced in this apparatus. The electron micrographs for this material turned out to be similar to those of KCl.

The calorimetric equipment was essentially the same as that used in the previous work on NaCl<sup>13,16</sup> and has been described in detail by Benson and Benson.<sup>20</sup> However, the mechanism for breaking the sample bulb was modified slightly to allow tipping of the calorimeter vessel before the reaction period. This change has been explained elsewhere in connection with the description of another calorimeter.<sup>21</sup> The experimental techniques for handling the fine KCl, measurement of the surface area by low temperature nitrogen adsorption and determination of the heat of solution in conductivity water at 25° were the same as in reference 15.

A number of heat of solution experiments were carried out with "coarse" (zero area) KCl. Analytical reagent grade material which had been recrystallized three times from conductivity water and dried by heating under vacuum was used for this purpose.

### III. Results

The final concentrations in the heat of solution determinations for both "coarse" and "fine" material were in the range 0.1 to 0.2 molal. The heats of dilution given by Lange and Leighton<sup>22</sup> were used to correct all the heats of solution to a standard concentration of 0.2 *m*. The results are shown in Fig. 2 where the  $\Delta H$  in defined calories (1 defined calorie = 4.1840 absolute joules) for the process



at 25.00° is plotted against the BET area  $A$  of the salt in m<sup>2</sup> g<sup>-1</sup> (based on 16.2 Å<sup>2</sup> for the area occupied by the nitrogen molecule).

The twelve open points (there are two nearly coincident results at 59.3 m<sup>2</sup> g<sup>-1</sup>) were obtained in "fine" salt experiments. Of these the ten in the range 15–60 m<sup>2</sup> g<sup>-1</sup> represent work with samples made directly by precipitation of smokes in eight independent preparations. The material used for the two points at low area was obtained by sintering high area material through exposure to water vapor followed by heating to 200° under vacuum.

The results of nine runs on "coarse" salt all fall in the range 4205.7 to 4214.4 cal. mole<sup>-1</sup> indicated on the ordinate axis. The mean of these results is 4209.6 cal. mole<sup>-1</sup> with a probable error of 2.8 cal. mole<sup>-1</sup>.

The solid line plotted in Fig. 2 was obtained by a least square treatment of the combined data for "coarse" and "fine" salt. The equation of this line is

$$\Delta H = 4207.4 - 4.486A$$

The probable error of the intercept is 1.0 cal. mole<sup>-1</sup> and of the slope 0.033 cal. mole<sup>-1</sup> (m<sup>2</sup> g<sup>-1</sup>)<sup>-1</sup>.

### IV. Discussion

Interpolation at  $m = 0.2$  in the table of thermochemical data for aqueous KCl solutions at 25°

(17) D. M. Young and J. A. Morrison, *J. Sci. Instr.*, **31**, 90 (1954).

(18) F. van Zeggeren, H. P. Schreiber and G. C. Benson, *Can. J. Chem.*, **34**, 1501 (1956).

(19) A.S.T.M. Standards, Pt. 7, American Society for Testing Materials, Baltimore, 1955, p. 1419.

(20) G. C. Benson and G. W. Benson, *Rev. Sci. Instr.*, **26**, 477 (1955).

(21) G. C. Benson, E. D. Goddard and C. A. J. Hoeve, *ibid.*, **27**, 725 (1956).

(22) E. Lange and P. A. Leighton, *Z. Elektrochem.*, **34**, 566 (1928).

TABLE I  
SUMMARY OF EXPERIMENTAL AND THEORETICAL DATA ON THE SURFACE ENERGY OF KCl AND NaCl

|      | Surface enthalpy, erg. cm. <sup>-2</sup> |               | Theoretical surface energy at 0°K., erg cm. <sup>-2</sup> |                                |                        | Quantum mechanical [100] face undistorted | Surface tension of the liquid, dyne cm. <sup>-1</sup> 0°K. (extrapolated) |
|------|------------------------------------------|---------------|-----------------------------------------------------------|--------------------------------|------------------------|-------------------------------------------|---------------------------------------------------------------------------|
|      | 25° (exptl.)                             | 0°K. (estmd.) | {100} face undistorted                                    | Classical {100} face distorted | {110} face undistorted |                                           |                                                                           |
| KCl  | 252                                      | 239           | 163                                                       | 131                            | 352                    | 184                                       | 173                                                                       |
| NaCl | 276                                      | 262           | 188                                                       | 124                            | 445                    | 187                                       | 190                                                                       |

compiled by the National Bureau of Standards<sup>23</sup> leads to a value of  $\Delta H = 4204$  cal. mole<sup>-1</sup> for the solution process. The agreement between this result and the intercept of the least square line is quite reasonable in view of the heterogeneity of the data on which the N.B.S. table for KCl is based. Further evidence that the N.B.S. values for KCl are too low has been reported recently by Gunn.<sup>24</sup> Using the heats of dilution of reference 22 a value of  $\Delta H = 4210.2$  cal. mole<sup>-1</sup> at  $m = 0.2$  can be derived from Gunn's data.

The surface enthalpy of KCl at 25° obtained from the slope of the line in Fig. 2 is 252 erg cm.<sup>-2</sup> with a probable error of 2 erg cm.<sup>-2</sup>. Comparison of this result with other experimental and theoretical data available in the literature can only be made rather indirectly. For solids at ordinary pressures it is customary to neglect the variation of the surface Gibbs free energy with pressure and to identify the surface enthalpy with the surface energy. Most theoretical models used for calculating the surface energies of the alkali halides pertain to 0°K., whereas measurements of enthalpy are carried out for the material at 25° and specific heat data are needed to obtain the value at 0°K. Implicit in this approach is the assumption that each separate crystalline particle is in a state of thermodynamic equilibrium.

In attempting a comparison between experiment and theory it is of interest to consider the corresponding information for NaCl at the same time. The data are summarized in Table I. Column 2 contains the experimental values of the surface enthalpy of KCl and NaCl.<sup>15</sup> The correction to 0°K. in the next column involves a rather uncertain estimate of the quantity

$$\int_0^{298} C_s dT$$

where  $C_s$  is the surface heat capacity. For NaCl<sup>16,7</sup> an upper limit of the value of this integral appears to be 10 to 20 erg cm.<sup>-2</sup> or 3.5 to 7.0% of the surface enthalpy at 25°. In the case of another crystal with the same type of lattice structure, magnesium oxide, Jura and Garland<sup>5</sup> obtained a value of 50 erg cm.<sup>-2</sup>, *i.e.*, a 4.6% correction. A value of 5% has been adopted for both salts in calculating the figures in column 3.

The theoretical estimates for the energy of the {100} faces (columns 4 and 7), which occur predominantly in macrocrystals of NaCl and KCl, were obtained in classical<sup>25,26</sup> and quantum me-

chanical<sup>27</sup> considerations of the problem, respectively. In the classical treatment the model was essentially the same as used by Huggins and Mayer<sup>28</sup> for calculating the cohesive energies of the alkali halides. The energy of interaction between ions was taken to be a sum of electrostatic, van der Waals and repulsive terms. In the quantum mechanical calculation there were no terms corresponding to the van der Waals interactions but contributions from exchange, overlap of the charge distributions and many-body forces were included. In both calculations it is assumed that the relative positions and the states of polarization of the ions in the surface regions of the crystal are the same as those of ions far in the interior. It is likely, however, that the surface regions are distorted; corrections due to this effect have been estimated recently<sup>29</sup> and the resulting values for the surface energy are given in column 5. In the quantum mechanical calculation<sup>27</sup> the neglect of distortion effects compensates in part for the omission of terms corresponding to the van der Waals interaction.

From a comparison between the theoretical figures for the energy of the {100} faces and the experimental values it is apparent that there is lack of agreement for KCl as well as for NaCl. This divergence, combined with the information obtained from the electron micrographs, might be interpreted by supposing that the crystals are not in a state of thermodynamic equilibrium at 25° but that their surfaces are partly made up of {110} faces. The surface energies for the {110} face have only been calculated classically<sup>25,26</sup> and are given in column 6; computations on the surface distortion of these faces are in progress, but values are not yet available. Assuming the distortion energy to be equal for the {100} and {110} faces the experimental results would imply that on both the KCl and the NaCl crystals roughly 55% {110} face is present. Moreover, it is not impossible that the material investigated experimentally may contain other non-equilibrium structures frozen in from the preparation at elevated temperatures. The work presented in this paper and in references 13 and 15 indicates that the contribution from the {110} face and other non-equilibrium structures, if important, must be statistically reproducible and proportional to the specific surface area.

The possibility that higher index faces are present on the crystals used in this work is rather surprising in view of the fact that some authors<sup>30-32</sup>

(23) "Selected values of chemical thermodynamic properties," Circular of the National Bureau of Standards, 500, U. S. Government Printing Office, Washington, D. C., 1952, p. 487.

(24) S. R. Gunn, *Rev. Sci. Instr.*, **29**, 377 (1958).

(25) R. Shuttleworth, *Proc. Phys. Soc. (London)*, **A62**, 167 (1949).

(26) F. van Zeggeren and G. C. Benson, *J. Chem. Phys.*, **26**, 1077 (1957).

(27) F. van Zeggeren and G. C. Benson, *Can. J. Phys.*, **34**, 985 (1956).

(28) M. L. Huggins and J. E. Mayer, *J. Chem. Phys.*, **1**, 643 (1933).

(29) G. C. Benson, P. Balk and P. White, *Ibid.*, in press.

(30) A. G. Keenan and J. M. Holmes, *THIS JOURNAL*, **53**, 1309 (1949).

(31) A. Craig and R. McIntosh, *Can. J. Chem.*, **30**, 448 (1952).

have reported predominantly cubic-shaped particles prepared by essentially the same procedure, volatilization of the molten salt in a stream of dry carrier gas. It should be mentioned, however, that in one of the papers referred to above<sup>31</sup> there is evidence that at high surface areas departures from the cubic shape do occur. The only explanation that can be offered for these conflicting observations is that the crystal shape obtained may depend rather critically on certain geometrical and operational conditions in the apparatus which are not fully understood at present.

For the sake of completeness it should be pointed out that the accuracy of the experimental value of the surface enthalpy is to a large extent dependent on the reliability of the method used for measuring the surface area of the samples. However there is considerable evidence, which has been reviewed by Emmett,<sup>33</sup> that the BET method provides a fairly trustworthy value of the surface area in the case of non-porous solids, and it seems very unlikely that

(32) L. G. Harrison, J. A. Morrison and G. S. Rose, *THIS JOURNAL*, **61**, 1314 (1957).

(33) P. H. Emmett, "Catalysis," Vol. I, Reinhold Publ. Corp., New York, N. Y., 1954, see Chapter 2.

the inaccuracy in this value could be large enough to alter the results in a significant way.

At 0°K. the surface enthalpy and the surface Gibbs free energy become equal; also the surface tension of a liquid is numerically equal to the surface Gibbs free energy. Thus surface tensions for molten salts, extrapolated to 0°K., have sometimes been compared with surface energies calculated for the solid state. The entries in column 8 were obtained by extrapolation to 0°K. of surface tension data measured by Jaeger<sup>34</sup> for the molten salts over a range of temperature above their melting points. It should be noted that these extrapolations are very long and even if accepted there is still considerable ambiguity in such comparisons since the difference in the surface Gibbs free energy which may be expected in passing from the liquid to the solid state is unknown.

**Acknowledgment.**—The authors wish to thank Dr. J. R. Colvin of the Division of Applied Biology of the National Research Council for his co-operation in obtaining the electron micrographs, and Mr. P. D'Arcy for assistance with the calorimetric measurements.

(34) F. M. Jaeger, *Z. anorg. Chem.*, **101**, 1 (1917).

## THE SOLIDIFICATION KINETICS OF BENZENE

BY J. B. HUDSON, W. B. HILLIG AND R. M. STRONG<sup>1</sup>

*General Electric Research Laboratory, Schenectady, New York*

*Received October 18, 1968*

The solidification kinetics of benzene were investigated as well as the effects of small amounts of impurities, heat transfer and growth anisotropy on these growth kinetics. Measurements were made at various undercoolings between 0.01 and 1.5° using zone-refined benzene vacuum sublimed into drawn glass capillaries, and data taken to determine the relationship between the growth velocity  $u$  and the undercooling  $\Delta T$ . The observed dependence of  $u$  on  $\Delta T$  is given by  $u = (1.08 \pm 0.08) \times 10^{-1}(\Delta T)^{(1.64 \pm 0.06)}$  cm./sec. The zone-melting process used could refine benzene to a triple point of 5.527° as compared with the highest literature value of 5.525°. Small amounts of dissolved impurity were found to cause deviations from the above growth law which were shown to be due to their effect on the melting point of the sample. Heat transfer effects were shown to be negligible. There was no observable growth anisotropy. The form of the growth law indicates that growth proceeds by the addition of new material to the crystal only at steps caused by the intersection of one or more screw dislocations with the crystal surface. This mechanism, proposed by Hillig and Turnbull, has been shown to apply to a number of other substances.

Solidification of a pure molten substance is fundamentally an interface controlled reaction. Accordingly the factors determining the growth rate can be expected to include: (1) the driving force for the reaction, *i.e.*, the difference in free energy between the solid and liquid states; (2) the mobility of the liquid molecules at the interface; (3) the roughness or perfection of the crystal interface; (4) the appropriate surface free energy; (5) the crystallographic orientation of the advancing interface; (6) molecular shape and dimensions; (7) the effect of foreign substances at the growing surface; and (8) heat flow considerations.

Three distinct freezing mechanisms have been proposed, each leading to a different dependence of the growth rate  $u$  upon the undercooling  $\Delta T$ . The earliest model was proposed by Wilson<sup>2</sup> and later made more explicit by Frenkel.<sup>3</sup> It assumes

that the rate-controlling process is the molecular rearrangement of the disordered liquid molecules which can occur anywhere at the interface. This corresponds to growth on a molecularly rough surface and at small undercoolings results in the relationship  $u = C_1\Delta T$ , where  $C_1$  is a non-arbitrary constant calculable from independently known physical constants of the system.

The second mechanism assumes: (1) the interface is molecularly smooth, *i.e.*, perfectly planar; (2) that growth can only occur if there are steps of molecular height on such a perfect surface; (3) that the lateral growth of such a step is a rapid process. The controlling step is the nucleation of a new step, in the form of a pillbox of unimolecular height. The energy barrier for this process arises from the energy that must be expended to form new surface. The growth law for this case is

$$u = C_2(\exp - C_3/\Delta T)$$

In the Volmer and Marder<sup>4</sup> treatment,  $C_2$  is a

(1) Department of Chemistry, Rensselaer Polytechnic Institute, Troy, New York.

(2) H. A. Wilson, *Phil. Mag.*, **50**, 238 (1900).

(3) J. Frenkel, *Physik. Z. Sowjetunion*, **1**, 498 (1932).

(4) M. I. Volmer and M. Marder, *Z. physik. Chem.*, **A164**, 97 (1931).

constant to be empirically determined. However, according to Kaischew and Stranski,<sup>5</sup>  $C_2$  is itself a function of  $\Delta T$ , one that is more slowly varying than the exponential term.

The third mechanism, that proposed by Hillig and Turnbull,<sup>6</sup> assumes that because of lattice imperfections a situation intermediate between the two above cases exists, *i.e.*, the surface can be considered to be partially rough, and that growth occurs at these sites of roughness. In particular, they assume that screw dislocations<sup>7</sup> intersect the surface and produce steps of one or more molecular diameters in height. These steps are pinned to the center of the lattice disturbance, and hence during growth these steps wind themselves into spirals. For a single dislocation the spacing between spiral turns is inversely proportional to  $\Delta T$ , leading to the growth law

$$u = C_4 \Delta T^2$$

where  $C_4$  is a non-arbitrary constant involving the surface free energy, which may or may not be known. This relationship neglects the interaction between dislocations and heat flow effects both of which act in the direction of making  $u$  a somewhat less sensitive function of  $\Delta T$ .

Experience on a limited number of substances shows that the growth kinetics can generally be described adequately by the equation

$$u = C_5 \Delta T^{1.7 \pm 0.1}$$

where  $C_5$  and the exact exponent of  $\Delta T$  are functions of the substance (and orientation presumably).<sup>6</sup> This  $\Delta T$  dependence approximates most closely the theoretical one based upon the screw dislocation model. Comparison of experimental constants  $C_5$  with the predicted ones  $C_4$  based on this model shows varying agreements. Substances having molecular shapes of low symmetry and/or existing as associated liquids in the molten state are in best agreement, whereas the observed growth rate constant for the highly symmetrical  $P_4$  molecule and for tin metal is about 3 orders of magnitude greater than predicted.

In order to distinguish between the various growth mechanisms, it is necessary to know the experimental limiting growth law at small undercoolings. Of course, the substance must be free from any impurities which may influence the interface kinetics. Very little information on growth kinetics is available subject to the above restrictions. Therefore, it was the purpose of this investigation to provide such measurements under conditions in which the effects of heat flow can be minimized. A substance which has a known crystal structure and a well-defined molecular shape and which forms a non-associated melt was needed. Benzene was selected as a suitable material not only because of its convenient melting point and its availability in fairly high purity, but also because of packing of the flat hexagonal molecules in the

solid is such that all crystal planes might be sufficiently rough for the Wilson-Frenkel mechanism to occur. In order to eliminate kinetically active impurities, a method of purification involving solidification was adopted.

### Experimental

**Materials and Apparatus.**—The benzene used was Phillips Research Grade Benzene initially 99.93% pure and further purified by vacuum sublimation and zone refining as described below.

Refining of the sample was carried out in a vacuum system which included two cold fingers to allow successive sublimations in a degassing process, a vertical tube in which zone melting was carried out, and a manifold on which the capillaries for containing the sample were pulled. The refining tube was cooled with a denatured alcohol refrigerant pumped through the surrounding vacuum-jacketed tube. Refrigerant temperature was maintained near 0°. Four stages of purification were obtained by using four separate resistance heaters in series. Current to the heaters was regulated by a Variac, and the heaters were lowered at a rate of 2 cm. per hour.

Kinetic measurements were made in a refrigerated constant temperature-bath capable of controlling temperature during the course of the measurements to  $\pm 0.001^\circ$ . This bath was regulated with a Princo "Magneset" thermoregulator which was used to provide a high-low type current control to a 250 watt infrared lamp which served as a heat source. Temperature in the bath was measured with a Beckmann thermometer which had been calibrated against a Bureau of Standards Certified platinum resistance thermometer. Sample tubes were held either in a Lucite rack capable of holding five tubes at a time or at large undercoolings in a holder set into the bottom of the bath through which growth could be nucleated from outside.

The capillaries for containing the samples were about 30 cm. long, 0.5 to 1.0 mm. inside diameter, and 0.2 to 0.3 mm. wall thickness. Silver capillaries, used for comparative heat transfer measurements, were made by soldering a section of silver capillary tubing to two pieces of drawn glass capillary and attached to the vacuum system for filling. A few capillaries were made with bends in them such that the growing crystal had to traverse a 90° bend of 5 mm. radius. These were for determining any growth anisotropy.

**Purification and Sample Preparation.**—The purification system described above was initially evacuated, flamed out to a residual pressure of less than 0.01  $\mu$  and filled with dry nitrogen. The benzene was run into the system through a silica gel filter and then frozen with liquid nitrogen. The opening through which the benzene was admitted then was sealed and the system pumped down to below one micron pressure.

Dissolved gases were removed by four sublimations between the two cold fingers, the first two with liquid nitrogen in the finger, the last two using a Dry Ice-acetone mixture. Pumping was continued throughout the first sublimation and recommended at the conclusion of each succeeding one. After this degassing process, the benzene was melted and condensed into the refining tube, where it was again frozen.

The zone melting was then begun. After each pass of the heater, all residual vapor in the system was frozen out with liquid nitrogen onto one of the cold fingers and isolated from the rest of the system. The top inch of the solid benzene column was melted and a sample condensed into one of the attached capillaries. The sample was frozen in liquid nitrogen to a predetermined level and all residual benzene vapor in the system frozen out on the other cold finger with liquid nitrogen.

The sample tube then was sealed off. Before the next refining pass was started all material frozen out in the sampling process was pumped out of the system. As expected, the rate of purification dropped off rapidly from one pass to the next, and after four passes a point was reached where no further purification could be observed.

The procedure detailed above was evolved to eliminate the problem of contamination of the sample with impurities formed through pyrolysis of benzene vapor in the course of sealing off the sample tubes. When the refining process was first attempted, the sample was simply evaporated into a capillary and the capillary sealed off with a torch. As a result, there was an uncontrolled accumulation of pyrolysis

(5) R. Kaischew and I. N. Stranski, *ibid.*, **A170**, 295 (1934).

(6) W. B. Hillig and D. Turnbull, *J. Chem. Phys.*, **24**, 914 (1956).

(7) A screw dislocation is a type of lattice defect in which parallel crystallographic planes are joined together forming a single topological surface in the manner of a spiral ramp. A density of about  $10^8$  to  $10^{10}$  of such dislocations per sq. cm. have been found for metals and LiF, for example.

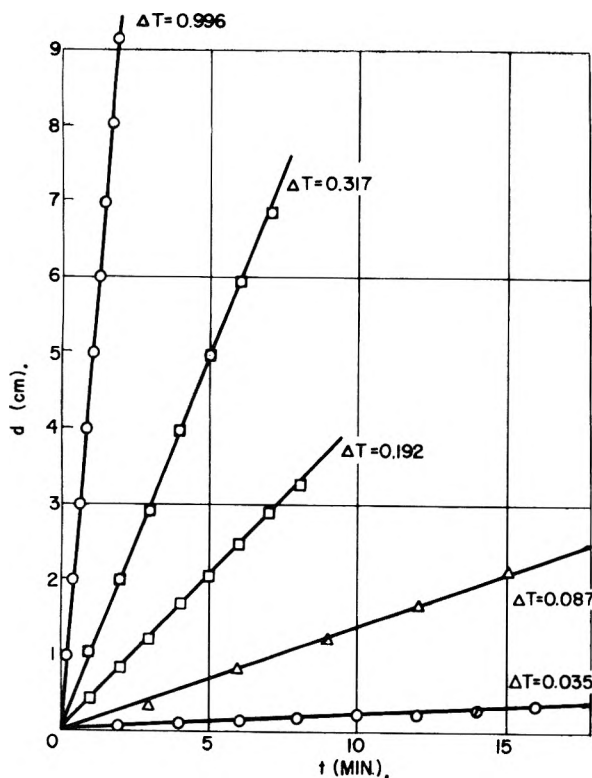


Fig. 1.—Distance vs. time for one tube at various undercoolings.

products and each successive sample was less pure than the preceding one had been as the amount of impurity added by pyrolysis was greater than that removed by the zone melting.

Less thorough purifications of benzene by zone refining have been reported by Rock<sup>8</sup> and by Wolf and Deutsch.<sup>9</sup> The effectiveness of zone refining in removing the impurities present in the benzene used in the present work was demonstrated in the observation of a similar process in the course of kinetic measurements; it was observed that in the course of repeated melting and freezing in a capillary the melting point of the benzene in which pyrolysis had occurred rose by as much as 0.02°.

**Kinetic Measurements.**—The melting point of each sample was taken to be the highest temperature at which no visible melting occurred in 15 minutes.

Depending on the undercooling, two slightly different procedures were used in measuring the kinetics. At undercoolings less than half a degree the sample tubes were set in a lucite rack, five at a time, and freezing nucleated by immersion in liquid nitrogen. The rack was then placed in the bath to a depth of about eight cm. until all tubes had frozen to the same height, that of the water surface. The rack was then lowered and measurements begun. At larger undercoolings only one tube was measured at a time. It was placed in a holder in the bottom of the bath and freezing nucleated by applying Dry Ice to the holder. Measurements were begun immediately after nucleation. In all cases the position of the leading edge was the point measured.

For all tubes measurements were begun at 1.0 to 1.5° undercooling and  $\Delta T$  decreased by approximately one third after each run until the value 0.01° was reached. Observations were made at time or distance intervals such that ten to twelve points could be taken within the length of the tube or within one hour whichever took less time.

Measurements in silver capillaries were made by observing the growth velocity in the glass sections as usual, and for the silver sections noting the time in and time out of this section and its length. Measurements in bent capillaries were made similarly to those in straight glass tubes but with a special cathetometer stand which measured distances both horizontally and vertically.

(8) H. Rock, *Naturwiss.*, **43**, 81 (1956).

(9) H. C. Wolf and H. P. Deutsch, *ibid.*, **41**, 425 (1954).

With the system used it was possible to measure distance to  $\pm 0.5$  mm. temperature to  $\pm 0.001^\circ$ , and time to  $\pm 1.0\%$  of the time interval used. The time and distance error is not cumulative, as each point was measured with reference to zero time and the height at zero time.

## Results

**Purification.**—Initially the amount of impurity added by pyrolysis of the benzene during the sealing-off operation exceeded the amount removed by the zone melting. When this difficulty had been overcome through use of the procedure described above, it was possible to bring the sample benzene to a degree of purity corresponding to a triple point of  $5.527 \pm 0.001^\circ$ . This point was reached after three or four passes of the heater, and additional zone melting effected no further improvement. The degassed starting material had a triple point of  $5.523 \pm 0.002^\circ$ . These values are to be compared with the highest literature value for the triple point of  $5.525^\circ$ .<sup>10</sup>

**Kinetic Measurements.**—The data from each kinetic run were used to make a plot of distance vs. time of the type shown in Fig. 1. The crystallization velocity is the slope of this curve. For all samples at undercoolings over 0.1°, these distance vs. time plots were linear. Below 0.1° undercooling, especially for less pure samples the velocity tended to decrease with time. A plot showing this effect is given in Fig. 2. Data for three tubes of varying purity, all at the same bath temperature, are given. The dotted curve is the extrapolated zero-time slope, which was used to determine the velocity in such cases. Justification for this procedure is given below.

When the velocity in a given tube had been obtained for at least seven different undercoolings, a plot was made of  $\log u$  vs.  $\Delta T$ , both corrected for impurity effects as discussed later. In all cases this plot was a straight line. This linearity can be seen in Fig. 3 which is the log-log plot for one of the tubes measured.

The equation of the line of the form  $u = A\Delta T^n$  was calculated for each tube measured. Results of this calculation are shown in Table I. The average of all tubes gives for a rate equation

$$u = (1.08 \pm 0.08) \times 10^{-1}(\Delta T)^{1.64 \pm 0.06} \text{ cm./sec.} \quad (1)$$

where the limits of error shown are the greatest observed departures from the average value given.

TABLE I  
SUMMARY OF GROWTH LAW CONSTANTS FOR ALL TUBES

| Tube no. <sup>a</sup> | M.p.,<br>°C. | No. of<br>meas. | n           | A, cm./sec.   |
|-----------------------|--------------|-----------------|-------------|---------------|
| Initial sample        | 5.484        | 13              | 1.69        | 0.116         |
| 0 pass, 6/12/57       | 5.513        | 7               | 1.58        | .106          |
| 0 pass, 8/22/57       | 5.527        | 32              | 1.64        | .105          |
| 1 pass, 9/6/57        | 5.507        | 7               | 1.56        | .102          |
| 2 pass, 9/9/57        | 5.516        | 14              | 1.69        | .107          |
| 3 pass, 9/11/57       | 5.523        | 15              | 1.70        | .116          |
| 4 pass, B9/17/57      | 5.523        | 10              | 1.64        | .111          |
| 1 pass, B10/11/57     | 5.526        | 7               | 1.69        | .101          |
| 0 pass, 10/9/57       | 5.522        | 7               | 1.60        | .105          |
| Av.                   |              |                 | 1.64 ± 0.06 | 0.108 ± 0.008 |

<sup>a</sup> Tube number designation—number of passes and date sealed off. The four tubes 1 pass 9/6/57—4 pass-3 9/17/57 form a series of consecutive passes.

(10) G. D. Oliver, M. Eaton and H. M. Huffman, *J. Am. Chem. Soc.*, **70**, 1502 (1948).

The measurements made in silver capillaries when plotted in the same manner, give the rate law for growth in silver

$$u_{Ag} = 1.91 \times 10^{-1} (\Delta T)^{1.64} \text{cm./sec.} \quad (2)$$

The growth in the glass sections followed the same law as did the all-glass capillaries.

Two tubes identical except for the fact that one contained air at atmospheric pressure over the benzene and the other contained only benzene vapor over the liquid, showed a difference in melting point of  $0.034^\circ$ . The melting point change due to this pressure difference calculated from the Clausius-Clapeyron equation is  $0.034^\circ$ .

### Discussion of Results

**Validity of the Dislocation Mechanism.**—The observed growth law for benzene is of the form  $u = A(\Delta T)^n$  with  $n$  approximately 1.7. This is the same as for all other substances measured which apparently freeze by the dislocation mechanism.<sup>6</sup> The observed value of  $A$  agrees with the theoretical one to within an order of magnitude.

The form of the dependence on undercooling at once rules out the possibility of growth by a two-dimensional nucleation mechanism, which would require a dependence of velocity on undercooling of the form  $\log u = -K/\Delta T$ . Likewise, any mechanism based on heat transfer is ruled out by the only slight dependence of the velocity on heat conductivity of the capillary material used.

**Impurity Effects.**—The melting point lowering caused by dissolved impurities is the source of two effects noted in the course of this work. The first of these is seen when growth in several tubes of varying purity is observed at one bath temperature. The purer samples have higher melting points and thus are at a greater effective  $\Delta T$  and show correspondingly greater growth rates than less pure samples. This effect can be seen in Fig. 2. In the calculation of the crystallization velocity, allowance was made for this effect by measuring the melting point of each sample tube used, rather than calculating  $\Delta T$ 's from a standard literature value of the melting point.

This effect may be used to calculate the melting point of an unknown sample from the known melting point of a previously measured sample. The ratio of the velocities in the two tubes should be equal to the ratio of their undercoolings raised to the 1.65 power. This relationship has been tested on pairs of the samples used in this work and has predicted the unknown melting point to within  $0.005^\circ$ .

At undercoolings less than  $0.10^\circ$  a second impurity effect appeared, *viz.*, a time dependence of the growth velocity. This effect arose from the partial rejection of impurities at the solid-liquid interface as freezing progressed. This rejection caused an accumulation of impurity at the interface which in turn decreased the undercooling as time passed and thus decreased the velocity. In order to correct for the ambiguity in the velocity in these cases, the initial slope of the  $d$  vs.  $t$  curve was used to determine the velocity, as this is the point at which the melting point was measured.

The progressive redistribution of impurities in this process is the source of another error, as the

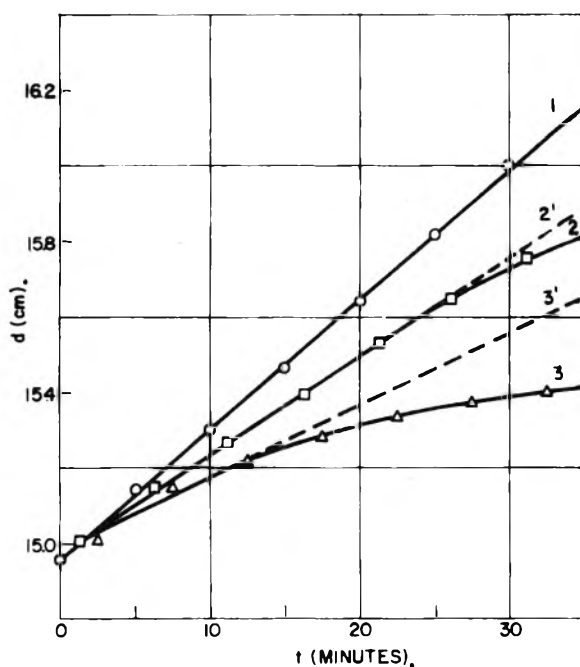


Fig. 2.—Distance vs. time for three tubes at  $T_B = 5.489^\circ$ : tube (1), m.p.  $5.525^\circ$ ; (2),  $5.523^\circ$ ; (3),  $5.512^\circ$ .

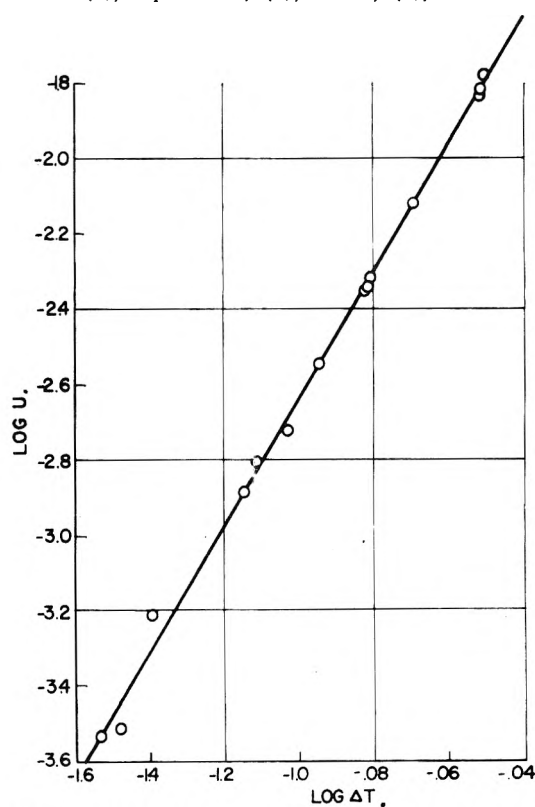


Fig. 3.— $\log U$  vs.  $\log \Delta T$  for one tube;  $n = 1.70$ ;  $A = 0.116$ .

melting point will be changing with each freezing and melting cycle, and thus an undercooling calculated from a melting point measured at the end of a series of measurements will be somewhat in error. Practically, by starting measurements at large undercoolings and progressively decreasing them, and then measuring the melting point after the last kinetic run, the errors due to this effect are negligible.



**Heat Transfer Effects.**—Heat transfer effects account for two experimentally observed phenomena. The first is the more rapid growth in silver capillaries than in glass. Throughout this work it has been assumed implicitly that the temperature of the solid-liquid interface is the same as that of the bath. This would be the case only if heat transfer from the interface to the bath were perfect. Actually this is not the case, and  $T_i$ , the temperature of the interface at the capillary wall (where the growth front was measured), will be somewhat above the bath temperature,  $T_B$ . The magnitude of this difference will be proportional to the thermal conductivity of the capillary used. Thus the silver capillary with a thermal conductivity about one thousand times as great as that of glass would be expected to minimize the difference ( $T_i - T_B$ ) and thus permit a greater growth velocity at a given bath temperature than is observed in glass. That the observed difference in growth velocity is so small compared to the difference in the thermal conductivities indicates that the original supposition ( $T_i = T_B$ ) is a good approximation.

The observed conical shape of the interface and the change of this shape with increasing undercooling may also be explained in terms of restricted heat flow. At an infinitesimal undercooling the velocity  $u$  and hence the heat produced  $Q$  would be very nearly zero; in the absence of any growth anisotropy, a planar interface should result. As the undercooling is increased slightly,  $u$  and correspondingly  $Q$  become finite and increase as  $\Delta T^{1.65}$ . The driving force for heat transfer, however, increases only as the first power of  $\Delta T$ . Thus, in order to dispose of the increasing amount of heat liberated the area for heat transfer, in this case the area of the interface, must increase. Since heat transfer is most efficient at the capillary wall, where the resistance to heat transfer is least, a conical interface develops, extending into the solid to a depth such that the area available for heat transfer is sufficient to carry away all the heat liberated. As the undercooling is further increased still more area is required, and the depth of the cone increases correspondingly.

**Anisotropy Measurements.**—On the basis of observations made on other materials, it was thought that the growth of benzene might be anisotropic, with one crystallographic direction showing a larger growth velocity than any other. If this were the case, then this direction would invariably be oriented along the long axis of the

tube as growth proceeds, for, of all the nuclei formed upon nucleation, those having this orientation would, through their greater growth velocity, outstrip all nuclei of less favorable orientation.

Optical measurements were made on the benzene crystals grown, using polarized light to determine the orientation of the major crystallographic axes within the tube. These measurements showed the orientation to be random, and thus no favored orientation for growth exists in benzene. A check on these results was made by observing the growth of a benzene single crystal around a  $90^\circ$  bend of small radius.

If growth were anisotropic, then one would expect that when the growth front reached the bend and the fast growth direction was blocked by the tube wall, either the growth rate would decrease as a less favorable orientation became rate controlling or a new, favorably oriented crystal would be nucleated. Careful observations of crystals as they grew around bends of 5 mm. radius showed that the crystal maintains constant growth velocity and unchanged orientation as it grows around the bend.

**Summary.**—In conclusion, it may be stated that the growth rate of benzene in glass capillaries can be represented by the formula

$$u = (1.08 \pm 0.08) \times 10^{-1}(\Delta T)^{1.64 \pm 0.06} \text{ cm./sec.} \quad (3)$$

for undercoolings ranging from  $0.01$  to  $1.5^\circ$ . Undercoolings outside these limits were not investigated. This growth rate relationship supports the dislocation theory of crystal growth in pure liquids.

Benzene can be purified to some extent by zone melting, provided sufficient care is taken to eliminate contamination by pyrolysis of the sample.

The only noticeable effects of impurities on the growth law stated above can be explained in terms of the melting point lowering caused by dissolved impurity. When corrections were made for these effects, the kinetic law above was obeyed for all samples tested within the limits of error stated above, and the variation in results from tube to tube showed no relation to the purity of the sample.

There is no favored crystallographic direction for growth. The orientation of the crystal within the capillary is random.

**Acknowledgments.**—Conversations with many members of the Metallurgy and Ceramics Research Department staff were valuable to the authors. This report is based on a thesis submitted to Rensselaer Polytechnic Institute in partial fulfillment of the M.S. degree requirements for one of the authors.

ISOTOPIC EXCHANGE BETWEEN ETHERS AND DEUTERIUM ON METALLIC CATALYSTS<sup>1</sup>

BY JOAN M. FORREST, ROBERT L. BURWELL, JR., AND BENJAMIN K. C. SHIM

*Contribution from the Department of Chemistry, Northwestern University, Evanston, Illinois*

Received August 21, 1958

The oxygen atom of an ether blocks the propagation of the isotopic exchange reaction between an ether and deuterium on a rhodium, a palladium and a nickel catalyst. For example, in one period of residence on the surface, the most exchanged product of propyl ether is  $C_3D_7CC_3H_7$ . A large part of the rhodium surface is covered with ether adsorbed at the oxygen atom. This species does not lead to exchange and much reduces the rate of exchange of the ether. The presence of an ether markedly reduces the rate of exchange of alkanes introduced with or just after an ether. Sweeping the catalyst with hydrogen at reaction temperatures (usually 150°) restores the original rate of alkane exchange. The presence of an ether alters the shape of the isotopic distribution pattern of heptane and probably that of cyclopentane. Isotopic distribution patterns are reported for propyl, isopropyl, ethyl butyl, methyl amyl and methyl *sec*-butyl ether, tetrahydrofuran and dioxane.

This Laboratory recently has studied isotopic exchange between deuterium and a variety of hydrocarbons on metallic catalysts.<sup>2-5</sup> Extension of these studies to ethers appeared of general interest with one aspect being of particular interest. All hydrogen atoms in normal alkanes and methyl-alkanes are subject to isotopic exchange with deuterium in one period of adsorption on a metallic catalyst. However, a *gem*-dimethyl group serves as a block to the propagation of the exchange reaction.<sup>2,3,5</sup> For example, with 3,3-dimethylpentane, the most exchanged species which is formed in one adsorption period is  $C_2D_5C(CH_3)_2C_2H_5$ ; whereas with 3-methylhexane, the most exchanged species is  $C_7D_{16}$ . It appeared of particular interest to discover whether an oxygen atom in an ether would also serve as a block, *i.e.*, would but one of the two alkyl groups in an ether be subject to exchange?

This paper reports the results of the isotopic exchange of several ethers on rhodium, nickel and palladium catalysts.

## Experimental

Catalysts were crushed and sieved to 20-40 mesh: 0.5% rhodium on alumina pellets (Baker and Co., Inc.), nickel-kieselguhr (Harshaw Chemical Company) and 3.3% palladium on  $\gamma$ -alumina.<sup>6</sup> Catalysts were pretreated with hydrogen or deuterium at 350° for 10 to 20 hours.

Ethers, obtained from commercial sources or prepared by the Williamson reaction, were carefully fractionated and, in the work with rhodium catalysts, checked for purity by gas chromatography.

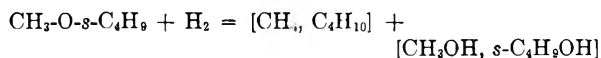
In the catalytic experiments, mixtures of ether vapor and deuterium or hydrogen were prepared by passing the gas through a thermostated saturator containing ether. General procedures resembled those previously used.<sup>2-5</sup>

## Results

**Hydrogenolysis.**—Isotopic exchange between deuterium and alkanes occurs at temperatures well below those at which hydrogenolysis commences. However, as will appear, isotopic exchange of ethers requires distinctly higher temperatures than that of hydrocarbons. Since virtually nothing is

known about hydrogenolysis of aliphatic ethers,<sup>6</sup> we had to investigate this in a preliminary way. We employed hydrogen to ether ratios of about 2 and ether flow rates of about 0.005 to 0.01 mole per cc. of catalyst per hour.

With nickel-kieselguhr, propyl ether exhibits no detectable hydrogenolysis at 205°. At 252°, the condensate shows carbonyl but not hydroxyl absorption in the infrared. The off-gas contains methane, ethane and propane. Methyl *sec*-butyl ether undergoes detectable hydrogenolysis at temperatures of 112° and higher. At this temperature, hydroxyl absorption predominates in the infrared. At 179°, the major condensable products are methanol, *sec*-butyl alcohol and methyl ethyl ketone as determined by differential infrared absorption against synthetic mixtures. The last compound appeared to be the major product but none amounted to more than 2%. The initial reaction is probably



The alcohols may then dehydrogenate. In the presence of one-half atmosphere of hydrogen, the ratio of methyl ethyl ketone to *sec*-butyl alcohol would reach 1.0 at about 180°.<sup>7</sup>

With palladium-alumina, detectable cleavage of methyl *sec*-butyl ether occurs at about the same temperature as with nickel-kieselguhr.

When the rhodium-alumina experiments were run, gas chromatography had become available. Ethyl ether exhibited no hydrogenolysis at 150° but traces of products (about 0.1% hydrogenolysis) were observed at 200°. The products of exchange of the other ethers studied on rhodium were all chromatographed. No signs of hydrogenolysis exceeding 0.1% at 150° were seen except with isopropyl ether in which case the total degree of hydrogenolysis was about 1%.

**Isotopic Exchange.**—Exchange experiments on rhodium were run at a mole ratio of deuterium to ether of 3.0. On the other catalysts the ratio was about 2. All experiments on rhodium were run on one sample of 0.5 g. of catalyst. The catalyst was occasionally retreated with hydrogen at 350°. As tested by the exchange reaction between 2-methyl-

(1) This work was sponsored by the Office of Ordnance Research, United States Army.

(2) R. L. Burwell, Jr., and W. S. Briggs, *J. Am. Chem. Soc.*, **74**, 5096 (1952).

(3) H. C. Rowlinson, R. L. Burwell, Jr., and R. H. Tuxworth, *This Journal*, **59**, 225 (1955).

(4) R. L. Burwell, Jr., and R. H. Tuxworth, *ibid.*, **60**, 1043 (1956).

(5) R. L. Burwell, Jr., B. K. C. Shim and H. C. Rowlinson, *J. Am. Chem. Soc.*, **79**, 5142 (1957).

(6) R. L. Burwell, Jr., *Chem. Revs.*, **54**, 676 (1954).

(7) H. J. Kolb and R. L. Burwell, Jr., *J. Am. Chem. Soc.*, **67**, 1084 (1945).

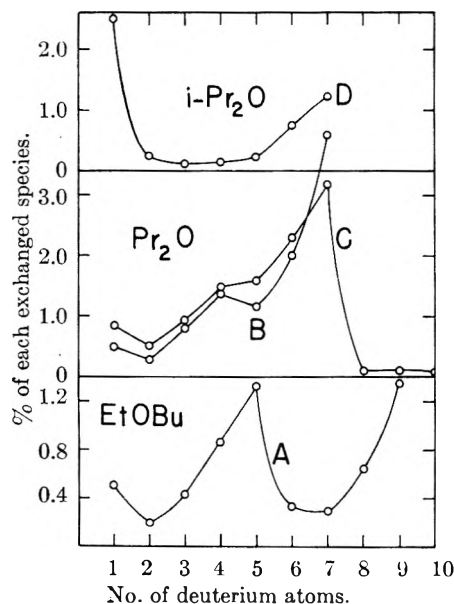


Fig. 1.—Isotopic exchange of ethers with deuterium on rhodium. Conditions of the runs are given in Table I.

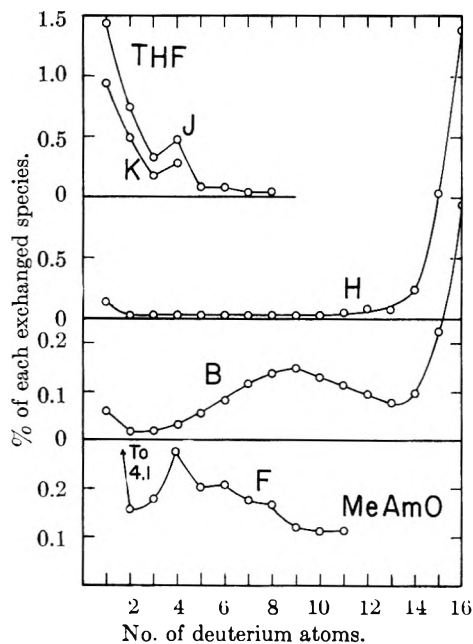


Fig. 2.—Isotopic exchange on rhodium. Conditions are given in Table I. Curves J and K are tetrahydrofuran, B and H are heptane.

pentane and deuterium at 150°, there was little change in the activity of the reactivated catalyst over a period of six months. Results of isotopic exchange runs are given in Figs. 1 and 2 and Table I.

Mass spectrographic analyses of the products of exchange on rhodium were obtained on a Consolidated mass spectrometer at the Institute of Gas Technology, Chicago. Those on the nickel and palladium catalysts were obtained on a Westinghouse instrument in the Department of Chemical Engineering at Northwestern University. In allowing for a carbonium ion peak one unit below the parent peak, it was assumed that probabilities of loss of a hydrogen or of a deuterium atom are pro-

TABLE I  
ISOTOPIC EXCHANGE ON THE RHODIUM-ALUMINA CATALYST

| Run | Compound                       | Temp., °C.         | Flow rate <sup>a</sup> | Ex-change, <sup>b</sup> % |
|-----|--------------------------------|--------------------|------------------------|---------------------------|
| A   | Ethyl butyl ether              | 120                | 10                     | 6.4                       |
| E   | Ethyl butyl ether              | 150                | 10                     | 12.9                      |
| C   | Propyl ether                   | 150                | 10                     | 11.4                      |
| D   | Isopropyl ether                | 150                | 25                     | 5.2                       |
| F   | Methyl amyl ether              | 150                | 10                     | 5.8                       |
| B   | Propyl ether + heptane         | 150 <sup>c</sup>   | 10                     | 10.9<br>1.9               |
| G   | Heptane <sup>d</sup>           | 150                | 15 <sup>e</sup>        | 2.6                       |
| H   | Heptane                        | 100                | 20                     | 4.3                       |
| I   | Heptane <sup>f</sup>           | 150                | 10                     | 69.0                      |
| J   | Tetrahydrofuran                | 150                | 2.5                    | 3.2                       |
| K   | Tetrahydrofuran + cyclopentane | 150 <sup>c,d</sup> | 5                      | 2.0<br>1.7                |
| L   | Cyclopentane                   | 75                 | 25                     | 40.0                      |
| M   | Cyclopentane                   | 100                | 25                     | 87.5                      |
| N   | Dioxane                        | 150                | 2.5                    | 5.0                       |

<sup>a</sup> In cc. of deuterium per minute. The mole ratio of deuterium to compound was 3.0. <sup>b</sup> % of molecules with any degree of deuterium introduction. <sup>c</sup> Temperature of saturator and the ratio of ether:hydrocarbon in the saturator so adjusted that ether:hydrocarbon:deuterium was about 1:1:6 in vapor stream. <sup>d</sup> Followed immediately upon preceding run. <sup>e</sup> D<sub>2</sub>:heptane about 6.0. <sup>f</sup> Despite extensive isotopic dilution, the isotopic distribution pattern was clearly of the type of run H.

portional to their numbers in the particular exchanged species with the probability of loss of deuterium being 0.75 that of hydrogen. While this procedure cannot be exactly correct, it would introduce no substantial error into the analysis except for ethyl butyl ether, methyl amyl ether and tetrahydrofuran for which the carbonium ion peaks are 22, 23 and 92% of the parents. Even here, any change in the shapes of the isotopic distribution patterns would be minor.

Two mixtures of ether and hydrocarbon were passed over the rhodium catalyst with deuterium and then separated into the two components for analysis. A mixture of propyl ether and heptane was separated by extraction of the ether with sulfuric acid at 0°. The sulfuric acid layer was diluted and the ether swept from it into a cold trap by a stream of air (run B). Tetrahydrofuran was removed from cyclopentane by extraction with water. The ether was recovered by saturating the aqueous extract with potassium carbonate. Any residual ether was removed from the cyclopentane by a final extraction with 85% phosphoric acid.

### Discussion

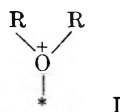
On the rhodium catalyst, as shown in Fig. 1, the exchange reaction cannot propagate past the ether oxygen atom. In run C with propyl ether, the concentration of exchanged species reaches a maximum at C<sub>6</sub>H<sub>7</sub>D<sub>7</sub>O which corresponds to C<sub>3</sub>D<sub>7</sub>OC<sub>3</sub>H<sub>7</sub>. The small concentrations of more highly exchanged species are about those to be expected from adsorption and exchange of a molecule which has already exchanged once. Similar results were obtained with isopropyl ether, run D. Run A with ethyl butyl ether exhibits two maxima, one at d<sub>8</sub> and the other at d<sub>9</sub> corresponding to the species, C<sub>2</sub>D<sub>5</sub>OC<sub>4</sub>H<sub>9</sub> and C<sub>2</sub>H<sub>5</sub>OC<sub>4</sub>D<sub>9</sub>.

Isotopic exchange between propyl ether and deuterium on nickel-kieselguhr at 205° also demonstrates that the exchange reaction cannot propagate across the oxygen atom. However, the concentrations of the exchanged species declined steadily from C<sub>6</sub>H<sub>13</sub>DO to C<sub>6</sub>H<sub>7</sub>D<sub>7</sub>O in a fashion which seems characteristic of this catalyst.<sup>2-4</sup> Exchange of methyl *sec*-butyl ether was analyzed at mass 73 because of the weakness of the parent peak. This species is (CH<sub>3</sub>-O=CHCH<sub>2</sub>CH<sub>3</sub>)<sup>+</sup>. On both nickel-kieselguhr at 143° and palladium-alumina at 104°, the most exchanged species corresponded to (CH<sub>3</sub>-O=CD<sub>2</sub>CD<sub>3</sub>)<sup>+</sup>.

Thus, the exchange patterns of R-O-R and  $\begin{matrix} \text{CH}_3 \\ | \\ \text{R}-\text{C}-\text{R} \\ | \\ \text{CH}_3 \end{matrix}$  are similar and the oxygen atom of an ether and a *gem*-dimethyl group both block propagation of the exchange reaction. However, although the latter group has no large effect upon the rate of the exchange reaction, the ethers exchange very much more slowly than the analogous alkanes. Does this marked reduction in the rate of exchange result from a reduced rate of cleavage of the carbon-hydrogen bonds in ethers or from the surface of the catalyst being largely covered with strongly adsorbed ether?

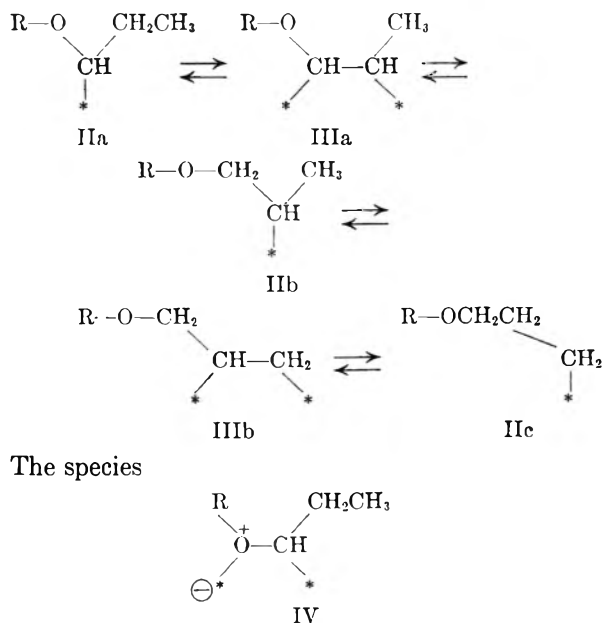
If a stream of 2-methylpentane and deuterium is substituted for one of propyl ether and deuterium, the first sample of alkane examined exhibits much less exchange than would be observed on a freshly activated catalyst. However, if hydrogen is passed over the catalyst for one hour before alkane is introduced, nearly normal exchange of the alkane is observed. Thus, ether seems to act as a temporary poison for the exchange of alkanes.<sup>8</sup> Dioxane is a much stronger poison. Immediately after its use, exchange of 2-methylpentane is almost completely inhibited. However, passage of hydrogen over the catalyst at the same temperature (150°) for 35 hours restores the activity to that of a freshly reactivated catalyst. Tetrahydrofuran resembles dioxane but is probably removed somewhat faster. Immediately after its use in a run like run J of Table I, the exchange of 2-methylpentane was largely inhibited. Passage of hydrogen for three hours largely, but not completely, restored its activity for exchange of 2-methylpentane.

Thus, ethers are strongly adsorbed on the surface of the rhodium catalyst and reduce the access of alkanes to the surface. The following mechanism is suggested: the strong adsorption of ethers involves a dative bond between the oxygen atom and the surface



Exchange of the ether proceeds as with alkanes by alternation between mono- and diadsorbed species,<sup>5,9</sup> for example, with propyl ether

(8) This behavior is reminiscent of the detoxification experiments of Maxted, in particular, removal of diethyl sulfide as a poison on platinum by flushing with inert gas. E. B. Maxted and M. Josephs, *J. Chem. Soc.*, 264 (1956).

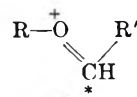


and its analogs are forbidden since they would permit isotopic exchange to propagate across the ether oxygen atom. Similarly, species I cannot proceed to species II or III, return to I and desorb. Apparently, species II is formed directly from the gas phase (or from a van der Waals layer). Thus, ether poisons its own exchange as well as that of alkane.

Exchange of methyl amyl ether is shown in Fig. 2, run F. One might expect that maxima at  $d_3$  and  $d_{11}$  would be observed analogous to the results with ethyl butyl ether, run A, Fig. 1. Although no exchange is observed beyond  $d_{11}$ , no discontinuity follows  $d_3$ . But, in the mechanism above, the CH<sub>3</sub>O- group cannot be converted to the CD<sub>2</sub>O- group. Initial adsorption as \*-CH<sub>2</sub>OR can only lead to CDH<sub>2</sub>OR since species III cannot form. This result is analogous to that with neopentane which gives (CH<sub>3</sub>)<sub>3</sub>CCH<sub>2</sub>D as the primary product of isotopic exchange.<sup>3,10</sup> Neopentane exchanges much more slowly than other pentanes and methane exchanges much more slowly than ethane and ethane than propane.<sup>11</sup> Reactions of organic molecules which proceed much more slowly at primary positions are characteristic of reactions in which some positive charge is transferred to the carbon atom. This suggests that monoadsorbed alkane may be somewhat polarized



If so, adsorption adjacent to the oxygen atom of ethers would be favored because of stabilization by some contribution of the following form to the resonance hybrid



(9) J. R. Anderson and C. Kemball, *Proc. Roy. Soc. (London)*, **223A**, 361 (1954).

(10) C. Kemball, *Trans. Faraday Soc.*, **50**, 1344 (1954).

Thus, the large value of  $d_1$  in methyl amyl ether may result from considerable contributions of  $\text{CH}_2\text{-DOC}_5\text{H}_{11}$ . The concentration of  $d_1$  was also very large in the exchange of methyl *sec*-butyl ether on nickel-kieselguhr and palladium-alumina.

Although we made no attempt to measure exact rates of exchange, the data indicate that ethyl butyl ether, propyl ether and isopropyl ether exchange at about the same rate at  $150^\circ$ ; dioxane, about 0.1 and tetrahydrofuran, about 0.07 times as fast.

The slowness of exchange of dioxane and its rather strong poisoning action suggests that the inhibitory species I may be held at both oxygen atoms.<sup>12</sup> Also, the strength of binding in species I should reflect the basicity of the ether. As an estimate of this, it would be interesting to study the degree of inhibition of the exchange of reference alkanes in the presence of a series of ethers.

We have performed two experiments somewhat related to this. In one, a mixture of deuterium and ethyl butyl ether and its alkane analog, heptane, was passed over the rhodium catalyst (run B, Table I). The condensed ether and heptane were separated and analyzed by mass spectroscopy. The exchange pattern of the ether was like that of ether run alone (compare runs B and C in Fig. 1), and the rate of exchange of the ether was little affected by heptane. Heptane exchanged about one-sixth as fast as the ether. The ether-heptane-deuterium mixture was then replaced by heptane-deuterium (run G). As shown in Table I, the rate of exchange of heptane was about twice that in the mixture when one makes allowance for the increase in flow rate but only one-thirtieth that of heptane on a freshly reactivated catalyst (run I). Thus, the ether decreases the rate of exchange of heptane by about a factor of sixty.

The distribution pattern of exchanged tetrahydrofuran which is shown in Fig. 2, run J, exhibits a marked break between  $d_4$  and  $d_6$  and resembles that of its analog, 1,1-dimethylcyclopentane on palladium-alumina (Fig. 2 of ref. 5) although the concentrations of species  $d_5$  to  $d_8$  are smaller with tetrahydrofuran. The surface-carbon bonds in diadsorbed tetrahydrofuran (species III) must be *cis*. Thus, alternation between II and III can only exchange one side of the tetrahydrofuran ring. The problem is similar to that with cyclopentane<sup>5,13</sup> but on our catalyst at  $150^\circ$ , the probability of that species which leads from one side of the cyclopentane ring to the other side<sup>5</sup> is low.

In the exchange patterns of dioxane at  $150^\circ$ , only traces of species  $d_6$  and up were observed; again, the oxygen atom acts as a barrier to propagation of the exchange reaction. The concentrations of the less deuterated species in run N were:  $d_1$ , 3.64%;  $d_2$ , 0.48%;  $d_3$ , 0.18;  $d_4$ , 0.65. One might expect dioxane to resemble cyclohexane.<sup>5</sup> It has been pro-

posed that diadsorbed alkane, species III, must be in the eclipsed conformation.<sup>5</sup> If true, species III in dioxane would involve *cis* carbon-surface bonds. As with cyclopentane, some other species is required to reach that species III which involves removal of the other two hydrogen atoms on the same ethylene group and a discontinuity should separate  $d_2$  and  $d_3$ . It is not clear whether the observed pattern represents this situation.

Run J with tetrahydrofuran alone was followed immediately by one in which a mixture of this ether with cyclopentane was employed (run K). The rate of exchange of tetrahydrofuran was little altered and the shape of its isotopic distribution pattern was nearly identical to that in run J as shown in Fig. 2. The concentrations of species  $d_6$  to  $d_8$  are not shown for run K but they are in the same proportion to those in run J as are the concentrations of  $d_1$  to  $d_4$ . Thus, a large fraction of  $d_5$  to  $d_8$  is the product of one residence on the surface and not the result of two successive periods of residence. Only a tenth as many molecules of cyclopentane exchanged in run K as did molecules of the ether. Yet cyclopentane exchanges so rapidly on a reactivated catalyst that we could not make measurements at  $150^\circ$ . Extrapolation of run L and M to  $150^\circ$  suggests that tetrahydrofuran depresses the rate of exchange of cyclopentane by a factor of at least 1000.

In the isotopic exchange pattern of cyclopentane, run in mixture with tetrahydrofuran (run K) the concentrations of all species save the most extensively deuterated are low; that of  $d_9$  is 0.030% and that of  $d_{10}$ , 0.073%. All others add to but 0.07%. No discontinuity separates  $d_5$  and  $d_6$ . At  $75^\circ$ , cyclopentane run alone gives a very different pattern (run L). The concentration of  $d_1$ - $d_5$  is much greater than  $d_6$ - $d_{10}$  and the discontinuity between  $d_5$  and  $d_6$  is large. Cyclopentane exchanges so rapidly that exchange patterns at  $100^\circ$  and up are too close to equilibrium to be interpretable. It seems unlikely that the pattern could alter so drastically between  $75$  and  $150^\circ$  although this cannot be excluded. It seems more likely that the presence of tetrahydrofuran exerts a marked effect upon the exchange pattern.

With cyclohexane at  $100^\circ$ , an evaporated rhodium film gives a pattern much like that of cyclopentane on the reactivated rhodium-alumina catalyst, but, of course, the discontinuity separates  $d_6$  and  $d_7$ .<sup>5</sup> However a poisoned film gave a pattern much like that of cyclopentane in mixture with tetrahydrofuran: no discontinuity and prevalence of extensively exchanged species.

The exchange pattern of heptane in the mixture with propyl ether is B in Fig. 2. The pattern of the run with heptane alone which followed immediately resembled this except for an increase in the value of  $d_{15}$  by a factor of 1.2 and of  $d_{16}$  by 2.0. In heptane run alone at  $100^\circ$  on a freshly reactivated catalyst (run H, Fig. 2), the exchanged species are almost entirely either  $d_{15}$  or  $d_{16}$  and the maximum at  $d_9$  observed in runs B and G is entirely absent. The pattern at  $150^\circ$  is similar to that of run H. Thus, there is no doubt that the presence of propyl

(11) K. Morikawa, N. R. Trenner and H. S. Taylor, *J. Am. Chem. Soc.*, **59**, 1103 (1937).

(12) Strong adsorption of dioxane may be rather general. Its introduction into the mass spectrometer resulted in the release of considerable material from the walls of the instrument and once introduced, dioxane pumps out very slowly.

(13) J. R. Anderson and C. Kamball, *Proc. Roy. Soc. (London)*, **226A**, 472 (1954).

ether causes a marked change in the heptane pattern.

We have too few results of this type to attempt a detailed interpretation but three effects may be instanced as of possible importance: steric, electronic and that resulting from heterogeneity of the catalyst surface. As an example of a possible steric effect, if the surface is largely covered by propyl ether, the heptane pattern may be influenced by restrictions upon rotations about carbon-carbon bonds in species II. In the extreme, this might make one set of secondary hydrogen atoms (one per carbon atom) more exchangeable than the other. More than one type of electronic effect is possible.

A high concentration of species I would considerably affect the structure of the d-band of the catalyst. The mere effect of species I in charging the metal negatively or the presence of the surface dipoles in species I might affect the degree or even the direction of polarization of species such as II. Finally, the ether might poison the more active sites or crystallographic planes and transfer activity to sites or planes which ordinarily make little contribution to exchange. We believe that investigation of the effect of a more strongly adsorbed molecule upon the exchange pattern of another molecule provides a hitherto unexploited source of information about the nature of chemisorbed species.

## NOTES

### THE SOLUBILITY OF BENZENE IN WATER

By D. M. ALEXANDER

Chemistry Department, University of Queensland, Brisbane, Australia

Received September 2, 1958

The solubilities in water of a series of aromatic hydrocarbons, including benzene, have been determined by Bohon and Claussen<sup>1</sup> at temperatures between 0 and 43°. These authors have calculated heats of solution for the solution of one mole of liquid hydrocarbon in water. Herington<sup>2</sup> has used their results and combined them with vapor pressure values for the pure hydrocarbons to calculate the free energy change for the solution of one mole of hydrocarbon vapor at 1 mm. pressure to form a solution of unit mole fraction. He finds a plot of this free energy change against temperature to be linear, which means that the derived heat of solution is constant over the temperature range. This is unexpected since  $\Delta C_p$  values for all gases in water are known to be large.

For benzene Glew and Robertson<sup>3</sup> using the same data and the same standard states calculate for  $\Delta C_p$  a value of 78 cal./deg. mole. Similar high values are calculated for other aromatic hydrocarbons. Examination of the plot referred to above does reveal a slight curvature larger than could be accounted for by experimental error. However, it was thought that a measurement of the solubility of benzene over an extended temperature range would greatly decrease the uncertainty in this  $\Delta C_p$  value.

#### Experimental

Analar benzene was shaken with mercury and purified according to the method of Mair, *et al.*<sup>4</sup> The method of solubility measurement was based on that of Bohon and Claussen.<sup>1</sup> The flask used for preparing the saturated solutions was not fitted with taps but with two glass U tubes containing mercury so that the solution should not come

into contact with tap grease. It was filled with water, a little benzene and a little mercury to allow better stirring. Saturation was attained after 24 hours gentle shaking and it was found that constant solubility results were obtained when the solution had stood for five hours after this. However at each temperature further shaking periods were allowed and at least one long period of standing of about 24 hours to ensure saturation and complete separation of the two phases.

Samples were collected in a calibrated dilution flask filled with mercury and a known volume of water. The saturated solution was forced out of the solution flask by a head of mercury and collected over mercury in the dilution flask at the temperature of the experiment. The volume of the diluted solution was observed when it had reached room temperature. This solution was transferred to a 1 cm. quartz absorption cell again by displacement of mercury, to prevent evaporation of benzene from the solution.

The optical densities were determined with a Beckman model D.U. ultraviolet spectrophotometer at a number of peaks in the benzene spectrum and compared with the optical densities of a series of standard solutions of benzene in water.

#### Results and Discussion

The results agree well with those of Bohon and Claussen.<sup>1</sup>  $\Delta G^0$  values were calculated for the change

benzene vapor (fugacity = 1 mm.)  $\longrightarrow$   
soln. of benzene in water (M.F. = 1, hypothetical)

Values for the vapor pressure of benzene<sup>5</sup> were converted to fugacities by using published values of the second virial coefficient.<sup>6</sup> The vapor pressure of benzene above a saturated solution of water in benzene was calculated by Raoult's law. This involved an extrapolation to other temperatures of the results of Joris and Taylor<sup>7</sup> for the solubility of water in benzene.

The values of  $\Delta G^0$ , the standard free energy of solution, may be represented by the equation

$$\Delta G^0 = -29389 + 541.273T - 169.000T \log T$$

where  $T$  is the absolute temperature. Values of  $\Delta G^0$  calculated from this equation are given in column 4 of Table I. The value of  $\Delta C_p$  corresponding

(1) R. L. Bohon and W. F. Claussen, *J. Am. Chem. Soc.*, **73**, 1571 (1951).

(2) E. F. G. Herington, *ibid.*, **73**, 5883 (1951).

(3) D. N. Glew and R. E. Robertson, *This Journal*, **60**, 332 (1956).

(4) B. J. Mair, D. J. Termini, C. B. Willingham and F. D. Rossini, *J. Research Natl. Bur. Standards*, **37**, 229 (1946).

(5) A. F. Forziati, W. R. Norris and F. D. Rossini, *ibid.*, **43**, 555 (1949).

(6) P. G. Francis, M. L. McGlashen, S. D. Hamann and W. J. McManamey, *J. Chem. Phys.*, **20**, 1341 (1952).

(7) G. G. Joris and H. S. Taylor, *ibid.*, **16**, 45 (1948).

to this equation is 73 cal./deg. mole. It is estimated that the error in  $c$ , the concentration, could be  $\pm 0.5\%$ , in each  $\Delta G^0$  value  $\pm 0.1\%$  and in the  $\Delta C_p$  value  $\pm 5$  cal./deg. mole.

TABLE I  
SOLUBILITY OF BENZENE IN WATER

| $t$ ,<br>°C. | $c$ ,<br>g./l.    | $\Delta G^0$ , cal./mole |        |
|--------------|-------------------|--------------------------|--------|
|              |                   | Obsd.                    | Calcd. |
| 0.8          | 1.84 <sup>a</sup> | 6037                     | 6032   |
| 9.4          | 1.79              | 6496                     | 6500   |
| 16.8         | 1.77              | 6893                     | 6894   |
| 24.0         | 1.80              | 7259                     | 7259   |
| 31.0         | 1.83              | 7606                     | 7603   |
| 38.0         | 1.92              | 7936                     | 7936   |
| 44.7         | 2.03              | 8240                     | 8242   |
| 51.5         | 2.14              | 8544                     | 8542   |
| 58.8         | 2.34              | 8856                     | 8854   |
| 65.4         | 2.57              | 9121                     | 9120   |

<sup>a</sup> In some experiments at 0.8° benzene (m.p. 5.5°) was present as the supercooled liquid. This figure refers to these experiments. In others solid benzene was present and its solubility found to be 1.71 g./l. at this temperature.

### THE TIME LAG IN DIFFUSION. III

BY H. O. POLLAK AND H. L. FRISCH

Bell Telephone Laboratories, Incorporated, Murray Hill, New Jersey  
Received November 29, 1958

This note is concerned with deriving a sufficient condition that the reduced time lag<sup>1,2</sup> for the (one-dimensional) diffusion of a species through a membrane (with fixed surface concentrations  $c$  and 0, respectively, and initially free of the diffusing species) under the concentration dependent diffusion coefficient  $\mathfrak{D}(c)$  is a non-decreasing function of  $c$ .

The reduced time lag  $F(c)$  has been shown to be<sup>2</sup>

$$F(c) = \frac{\int_0^c w \mathfrak{D}(w) \int_w^c \mathfrak{D}(u) du dw}{c \left( \int_0^c \mathfrak{D}(u) du \right)^2} \quad (1)$$

Integration by parts shows this to equal

$$F(c) = \frac{1}{2c} \frac{\int_0^c \left( \int_w^c \mathfrak{D}(u) du \right)^2 dw}{\left( \int_0^c \mathfrak{D}(u) du \right)^2} \quad (2)$$

Setting

$$\varphi(w) = \int_0^w \mathfrak{D}(u) du$$

and

$$w = xc$$

we find that (2) becomes

$$F(c) = \frac{1}{2} \int_0^1 \left[ 1 - \frac{\varphi(xc)}{\varphi(c)} \right]^2 dx \quad (3)$$

Our aim is to test whether  $F'(c) \geq 0$ . This will certainly be true if  $F(c_1) > F(c_0)$  if  $c_1 > c_0$ . Thus if it should be the case that

$$1 - \frac{\varphi(xc_1)}{\varphi(c_1)} \geq 1 - \frac{\varphi(xc_0)}{\varphi(c_0)} \quad (4)$$

(1) H. L. Frisch, *THIS JOURNAL*, **61**, 93 (1957).

(2) H. L. Frisch, *ibid.*, **62**, 401 (1958); the nomenclature and definitions used throughout this paper are in accord with those of reference 1, 2.

for  $c_1 > c_0$  and  $0 \leq x \leq 1$ , then  $F'(c)$  would be positive for all  $c$ . (4) is equivalent to

$$\frac{\varphi(c_0)}{\varphi(xc_0)} \leq \frac{\varphi(c_1)}{\varphi(xc_1)}$$

or, if  $c_0 = e^{s_0}$ ,  $c_1 = e^{s_1}$ ,  $x = e^{-u}$ , and

$$\ln \varphi(e^y) = g(y) \quad (5)$$

to

$$g(s_0) - g(s_0 - u) \leq g(s_1) - g(s_1 - u) \quad (6)$$

for any  $s_0 < s_1$  and  $u > 0$ . But (6) is equivalent to  $g'(y)$  being an increasing function, i.e.,  $g$  is convex. We have thus proved the following theorem: If

$$\ln \int_0^{e^y} \mathfrak{D}(u) du = g(y) \quad (7)$$

is a convex function of  $y$ , then  $F'(c) \geq 0$  for all positive  $c$ .

The physical importance of this result stems from the fact that if  $F'(c) \geq 0$  and

$$\lim_{c \rightarrow 0} \mathfrak{D}(c) = D_0, \text{ a constant}$$

then the inequality stated by equation 15 of reference 2 can be replaced by the stronger

$$\frac{1}{6} \leq F(c) \leq \frac{1}{2} \quad (8)$$

This is true for example if  $D(c)$  is a polynomial (or infinite series) with positive coefficients  $b_j$

$$\mathfrak{D}(c) = \sum_{j=0}^n b_j c^j$$

Then

$$\exp[g(y)] = e^y \sum_{j=0}^n \frac{b_j}{j+1} e^{jy}$$

and

$$g''(y) = \frac{\sum_{j=0}^n \frac{b_j}{j+1} e^{jy} \sum_{j=0}^n \frac{j^2 b_j}{j+1} e^{jy} - \left( \sum_{j=0}^n \frac{j b_j}{j+1} e^{jy} \right)^2}{\left( \sum_{j=0}^n \frac{b_j}{j+1} e^{jy} \right)^2} \geq 0$$

since the numerator by the Schwarz inequality is non-negative.

### ADSORPTION OF CETYLPYRIDINIUM CHLORIDE ON GLASS

BY A. E. WESTWELL AND E. W. ANACKER

Chemistry Department, Montana State College, Bozeman, Montana  
Received October 28, 1958

In a recent light scattering study<sup>1</sup> of cetylpyridinium chloride (CPC)-sodium chloride-water mixtures, two breaks in the scattering curve at low surfactant concentrations were found. This is illustrated in Fig. 1. The usual behavior at low surfactant concentrations is indicated by the broken line. Since all solutions had been filtered through fritted glass prior to the light scattering measurements, adsorption of CPC on the filter was suggested<sup>2</sup> as a possible explanation of the observed departure from

(1) E. W. Anacker, *THIS JOURNAL*, **62**, 41 (1958).

(2) By referee of 1.

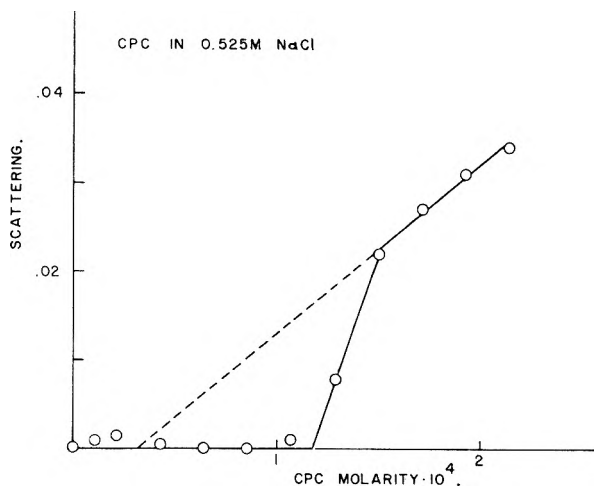


Fig. 1.—Scattering of dilute cetylpyridinium chloride solutions 0.525 mo.ar in NaCl.

until blue litmus was not affected by the filtrate. Two hours usually were required for the rinsing.

### Results and Discussion

In Fig. 2 are shown the results of experiments in which  $9.3 \times 10^{-5}$  molar CPC solutions (0.00 to 0.50 molar in NaCl) were filtered through the fritted glass. Absorbances are plotted relative to a zero value for water. Although the absorbance of water is only slightly changed by the addition of NaCl, the absorbance of a CPC solution may be changed appreciably. This can be seen through a comparison of the heights of the short horizontal lines representing the absorbances of the unfiltered solutions. Apparently the addition of NaCl beyond the 0.25 molar level is of little effect.

The number of moles of CPC adsorbed on the fritted glass may be estimated from  $(A'/A)(V/1000)(c)$ .  $A'$  is the area between an absorbance curve and the horizontal line corresponding to the

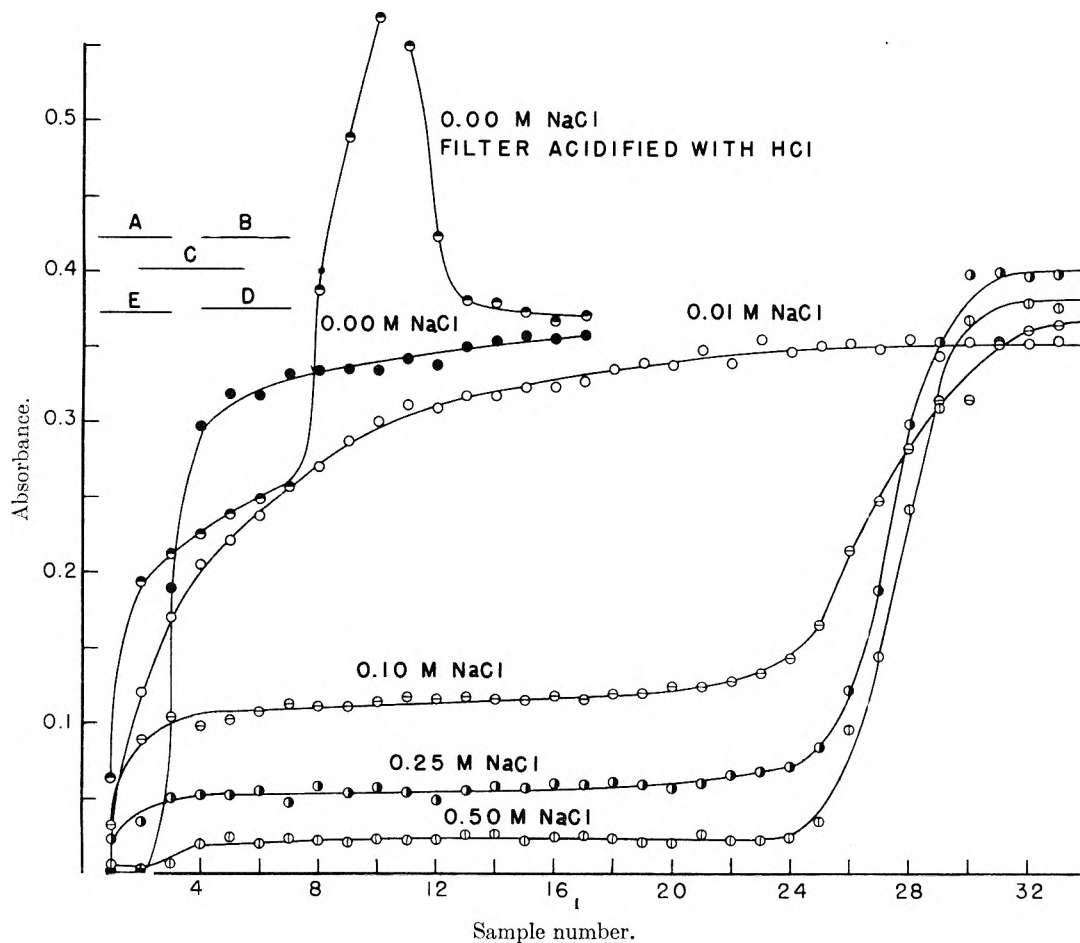


Fig. 2.—Ultraviolet absorption ( $260 \text{ m}\mu$ ) of solutions, originally  $9.3 \times 10^{-5}$  molar in cetylpyridinium chloride and 0.00 to 0.50 molar in NaCl, after passage through an ultrafine, fritted Pyrex glass funnel. A, B, C, D and E indicate absorbances of the unfiltered cetylpyridinium chloride solutions 0.50, 0.25, 0.10, 0.01 and 0.00 molar in NaCl, respectively.

expected behavior. This suggestion has now been explored.

### Experimental

CPC solutions containing varying amounts of NaCl were filtered through an ultrafine, fritted Pyrex glass funnel. The adsorption of CPC on the fritted glass disk was followed by the spectrophotometric analysis ( $260 \text{ m}\mu$ ) of small filtrate fractions emerging from the funnel. Before each run the funnel was cleaned with hot concentrated sulfuric, nitric and hydrochloric acids and rinsed with hot distilled water

absorbance of the solution placed on the fritted glass,  $A$  is the area between the horizontal line just referred to and the sample number axis,  $V$  is the volume of the solution in cc. passed through the filter, and  $c$  is its CPC molarity. Implicit in this expression is the assumption that there is no adsorption of NaCl on the filter. That this may not be the case is suggested by the apparent leveling



off of the absorbance curves (sample numbers 30 to 34) at heights lower than those corresponding to the unfiltered solutions. A correction for adsorption of NaCl on the filter should be made in an accurate determination of the amount of CPC adsorbed. However, we do not feel that our data warrant such a sophisticated treatment as this. According to the above expression  $1.1 \times 10^{-5}$  mole of CPC<sup>3</sup> is adsorbed by the fritted glass from 150 cc. (34 samples) of  $9.3 \times 10^{-5}$  molar CPC in 0.50 molar NaCl.

In one experiment the fritted glass funnel was cleaned with concentrated sulfuric and nitric acids and then washed with distilled water as before. Approximately 80 cc. of 12 *N* hydrochloric acid was then filtered through the fritted glass. Following this a  $9.3 \times 10^{-5}$  molar solution of CPC was slowly passed through the filter. The absorbance curve in Fig. 2 for this run shows a maximum well above the absorbance level of the unfiltered solution. Since the addition of HCl to CPC-H<sub>2</sub>O mixtures did not appreciably affect the ultraviolet absorption of these mixtures, it was concluded that concentration of the CPC had taken place.

The failure of scattering intensities at very small CPC concentrations in the presence of NaCl to lie along the extrapolated (broken) line in Fig. 1 can be explained as follows. Since solutions were filtered in order of increasing concentration, the adsorption of CPC on the filter removed a relatively high fraction of the surfactant present in the first few solutions. The measured scattering intensities therefore corresponded to lower CPC concentrations than those for which they were plotted. After the filter became saturated, solutions came through unchanged in concentration and the measured scattering intensities were plotted correctly. The extrapolation of the upper linear portion of the scattering curve to the concentration axis represents the correct critical micelle concentration.

In working with cationic surfactants at low concentrations, one should either reverse the order of filtration (start with the most concentrated solution) or pass large quantities of the dilute solutions through the filter before collecting samples for turbidity measurements.

**Acknowledgment.**—This research was supported by a grant from the Petroleum Research Fund administered by the American Chemical Society. Grateful acknowledgment is hereby made to the donors of this fund.

(3) According to Drake and Ritter,<sup>4</sup> the surface area of fritted glass, ultrafine porosity, is 0.69 m.<sup>2</sup>/g. Since our fritted glass disk weighed 3.3 g., it presumably had a surface area of  $2.4 \times 10^{20}$  Å.<sup>2</sup> If  $1.1 \times 10^{-5}$  mole of CPC occupies this area, each CPC molecule holds title to 36 Å.<sup>2</sup> on the average.

(4) L. C. Drake and H. L. Ritter, *Ind. Eng. Chem., Anal. Ed.*, **17**, 787 (1945).

## A USEFUL ADSORPTION ISOTHERM

BY O. REDLICH AND D. L. PETERSON

Shell Development Company, Emeryville, California

Received December 20, 1968

Freundlich's adsorption isotherm is well known to give an excellent representation of many data

for moderate partial pressures or concentrations. It is not a reasonable relation, however, for dilute vapors or solutions, notwithstanding some recent contentions.<sup>1</sup> For low concentrations Langmuir's equation is sound and well confirmed. Strangely enough, combinations<sup>2</sup> of the two relations approach Freundlich's equation as a limit for low concentrations and Langmuir's for high ones.

As expected, we found that a relation with the *opposite* kind of limits represents some data on Molecular Sieves quite well. The amount  $q$  of a normal paraffin adsorbed on Molecular Sieves (Linde Type 5A) is given as a function of the partial pressure  $p$  of the adsorbate by the relation

$$q = Ap/(1 + Bp^g) \quad (1)$$

containing the three empirical coefficients  $A$ ,  $B$ ,  $g$ . The value of the exponent  $g$  lies between 0 and 1. At high pressures the relation becomes

$$q = (A/B)p^{1-g} \quad (2)$$

and at low pressures

$$q = Ap \quad (3)$$

in accord with the low pressure limit of Langmuir's equation. An example is shown in Fig. 1. The

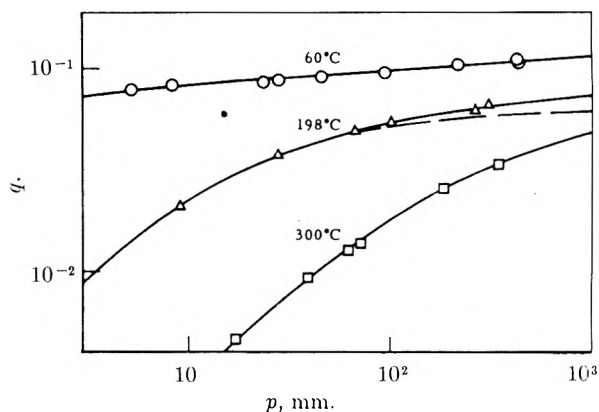


Fig. 1.—Adsorption isotherms of *n*-pentane on molecular sieves (type 5A). The broken line represents a Langmuir isotherm; Freundlich's equation is represented in this diagram by any straight line.

coefficients can be suitably expressed as functions of the temperature and the carbon number of the paraffin.

In analogy with Langmuir's equation for mixtures, the relation

$$q_i = A_i p_i / (1 + \sum_j B_j p_j^{g_j}) \quad (4)$$

has been found to be useful for mixtures of adsorbable substances. According to this relation, the separation factor

$$\beta = q_i p_r / q_r p_i = A_i / A_r \quad (5)$$

is independent of the concentration.

This relation is believed to be applicable to a large class of adsorptions, far beyond the field of Molecular Sieves.

(1) A. E. Hirschler and T. S. Mertes, *Ind. Eng. Chem.*, **47**, 193 (1955). Also in "Chemistry of Petroleum Hydrocarbons," Vol. 1, Reinhold Publ. Corp., New York, N. Y., 1954, p. 155.

(2) R. Sips, *J. Chem. Phys.*, **16**, 490 (1948); **18**, 1024 (1950). Cf. T. Vermeulen in "Advances in Chemical Engineering," Vol. 2, Academic Press, Inc., New York, N. Y., 1958, p. 147.

## RAPID FLOW TITRATION AND THE RATE OF THE ACID EXPANSION OF BOVINE SERUM ALBUMIN<sup>1,2</sup>

BY REX E. LOVRIEN<sup>3</sup> AND CHARLES TANFORD

Department of Chemistry, State University of Iowa, Iowa City, Iowa

Received December 3, 1958

Bovine serum albumin (BSA) and hemoglobin undergo superficially similar configurational changes in acid solutions. Both reactions involve an expansion of the protein molecule and a steepening of the titration curve, so that protons are bound far more readily than an extension of the neutral part of the titration curve would lead one to expect. Both reactions, moreover, are reversible. The major reported difference between them lies in the reaction rate, that for hemoglobin being measurably slow, while that for BSA has been found to be instantaneous by all methods of measurement used so far, none of which, however, has included measurements made less than one minute after preparation of a solution of given composition. Viscosity and titration data reported from this Laboratory generally were obtained about 10 to 15 minutes after preparation of a solution.

This note reports a titration curve of BSA, each point of which was obtained within one second of the time of mixing of the protein with appropriate amounts of acid. The apparatus used is similar to that of Steinhardt and Zaiser,<sup>4</sup> except that it employed a bulb type glass electrode (Beckman Instruments, Inc., electrode type 40285) in a chamber illustrated by Fig. 1. Junction with a salt bridge leading to a saturated calomel electrode was made through a very fine capillary, as shown in Fig. 1.

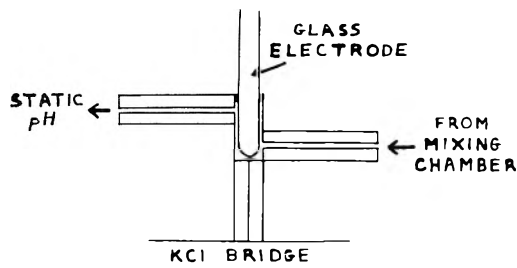


Fig. 1.—Glass electrode chamber for flow titration.

The apparatus was tested by repeating Steinhardt and Zaiser's rapid titration of ferrihemoglobin,<sup>5</sup> with the results shown in Fig. 2. The results are seen to deviate from those of Steinhardt and Zaiser in the direction to be expected from the fact that our measurements were made roughly one second after mixing of a solution, whereas Steinhardt and Zaiser's were three second measurements.

The results obtained with BSA are shown in Fig. 3. There is no difference at all between the titra-

(1) This work was supported by research grant G-1805 from the National Science Foundation, and by research grant RG-2350 from the National Institutes of Health, U. S. Public Health Service.

(2) Presented at the 133rd meeting of the American Chemical Society, San Francisco, April, 1958

(3) Abstracted from the Ph.D. thesis of Rex E. Lovrien, State University of Iowa, 1958.

(4) J. Steinhardt and E. M. Zaiser, *J. Biol. Chem.* **190**, 197 (1951).

(5) J. Steinhardt and E. M. Zaiser, *J. Am. Chem. Soc.*, **75**, 1599 (1953).

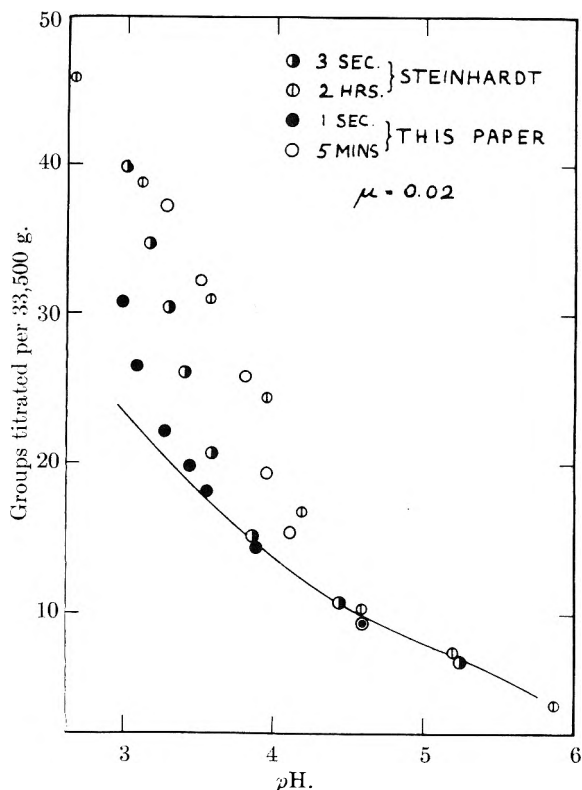


Fig. 2.—Flow titration for ferrihemoglobin, ionic strength 0.02, 25°. The calculated curve is based on parameters which fit the titration curve of the native protein.

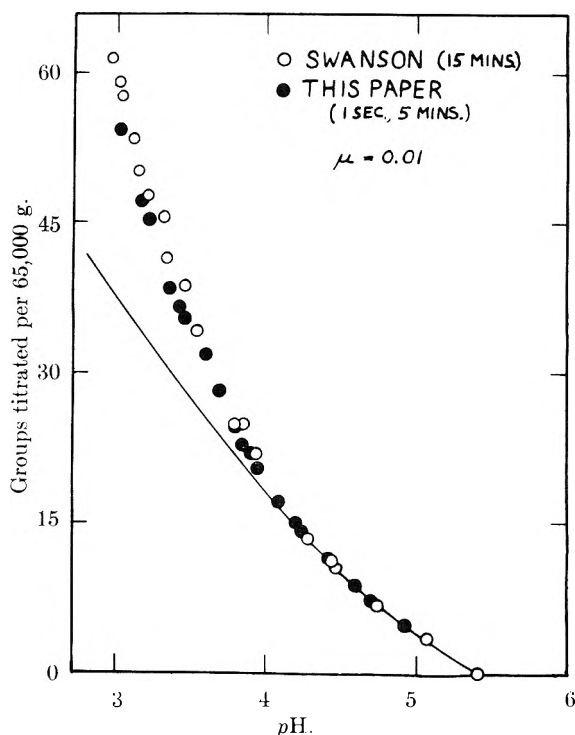


Fig. 3.—Flow titration for BSA, ionic strength 0.01, 25°. Similar data were obtained at higher ionic strengths. No distinction is made between "static" (*i.e.*, 5 minute) and flow data because identical pH values were obtained for every solution. The calculated curve is again based on the properties of the native, unexpanded protein.

tion curve measured within one second of mixing and that determined in the usual way after a lapse

of several minutes. The barely detectable difference between the titration curves here obtained and the corresponding curve published earlier<sup>6</sup> is not significant since the relative amounts of acid and protein, calculated, as they are here, from rates of flow of two separate solutions, must be subject to a considerable experimental error.

It must be concluded that the configurational change of BSA is a very fast reaction, with a half-life considerably less than one second. This conclusion is quite independent of the mechanism assumed,<sup>7</sup> since, over the pH range of interest, the expansion of the molecule, which is primarily responsible for the steepness of the titration curve, must be the *final* step in any assumed sequence of reactions.

It should be noted that the present considerations do not, of course, give any information about the very slow reactions, such as aggregation, of which BSA which has previously undergone expansion is capable.

(6) C. Tanford, S. A. Swanson and W. S. Shore, *ibid.*, **77**, 6414 (1955).

(7) For example, K. Aoki and J. F. Foster, *ibid.*, **79**, 3385, 3393 (1957).

## A PHOTOELECTRIC METHOD FOR OBSERVING SEDIMENTATION AT LOW CONCENTRATION<sup>1</sup>

By D. A. I. GORING<sup>2</sup> AND CAROL CHEPESWICK BRYSON

Received November 17, 1958

In the ultracentrifuge, certain naturally occurring polyelectrolytes probably sediment as networks at concentrations above about 0.2%.<sup>3,4</sup> The sedimentation constant  $s$  is dependent on concentration but not on molecular weight. At lower concentrations the network breaks up and molecules sediment separately. It is under these conditions that dispersion in  $s$  most readily occurs. Schlieren or interferometric methods are insensitive at such low values of concentration. Recently an ultraviolet absorption technique has been used with nucleic acid.<sup>5</sup> Many macromolecules (*e.g.*, polysaccharides) do not absorb in the ultraviolet.

The present note describes a simple modification of a Spinco Model E ultracentrifuge which permits sedimentation to be observed by means of the absorption of visible light. The macromolecule under study was sodium carrageenate, the sodium salt of a polygalactose sulfate prepared from the seaweed, *Chondrus crispus*. Color was introduced by the adsorption of a small quantity of a basic dye on to the molecule. The various uncertainties of photographic analysis were avoided by

(1) Contribution from the Atlantic Regional Laboratory, National Research Council, Halifax, N.S. This work was done three years ago. At the time it was felt that publication should await further study. Since a certain amount of interest has been shown in the technique this brief account has been submitted.

(2) Pulp and Paper Research Institute of Canada, Montreal, Que.

(3) D. A. I. Goring and C. Chepeswick, *J. Colloid Sci.*, **10**, 440 (1955).

(4) J. H. Fessler and A. G. Ogston, *Trans. Faraday Soc.*, **47**, 667 (1951).

(5) K. V. Shooter and J. A. V. Butler, *ibid.*, **52**, 734 (1956).

scanning the image during the run with a phototube connected to a suitable recorder.

The ultracentrifuge was modified as follows. The cylindrical lens and schlieren bar were removed. The image of the cell was scanned by a 1 mm.  $\times$  22 mm. slit cut in the standard Spinco plate holder. The side panel of the machine was removed. A hole was cut in the back of the plate guide exposing 6.8 cm. of the back of the plate holder. A phototube in a light-tight box was mounted on the plate holder behind the slit. The scanning time was increased from about 7 to 22 sec. by cutting the drive-rod and inserting a 3 to 1 reducing gear box. The longer scanning time was necessary because of the lag in the recorder.

The necessary photoelectric sensitivity was obtained by use of an IP21 photomultiplier with 90 v. per dynode stage and 45 v. between the ninth dynode and the anode. The anode was grounded across a precision variable resistor (10,000 or 100,000 ohm Helipot) and the potential generated was measured on a Bristol recording millivoltmeter. Uniform illumination of the cell was difficult. This was tested by scanning the cell at the end of each run when the sedimentation was assumed complete. With a non-absorbing liquid in the cell a fairly constant response of the photomultiplier could be obtained by adjusting the lateral alignment of the lamp housing of the centrifuge.

The principal objective of the dye-mixing procedure was to make a polyelectrolyte-dye complex in which the molecular dispersion was essentially unchanged from that of the original polyelectrolyte. This was achieved by using only enough dye molecules to combine with about  $1/10$  of the  $-\text{OSO}_3^-$  groups on the carrageenate. The procedure evolved after much trial and error was to mix equal portions of solutions of sodium carrageenate (200 p.p.m.) in water and crystal violet (24 p.p.m.) in aqueous  $\text{Na}_2\text{HPO}_4$  (200 p.p.m.). The dye-phosphate solution was added dropwise to the carrageenate with vigorous stirring.

The dye-carrageenate solution was then centrifuged at 51,000 r.p.m. The image was scanned at intervals of five minutes over a period of 2-3 hours. Three pictures from a typical chart are shown in Fig. 1. The top, meniscus and

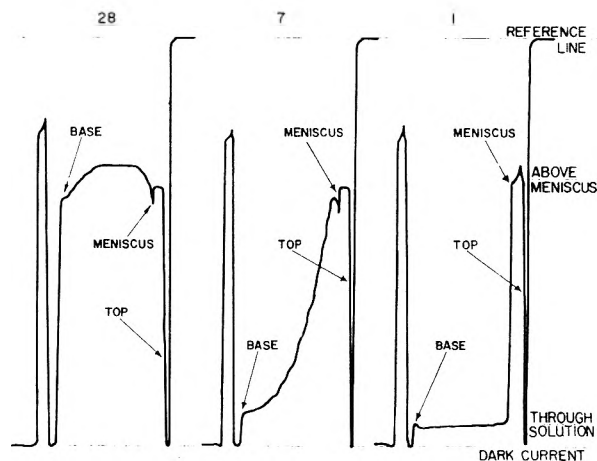


Fig. 1.—Recorder charts obtained from the first, seventh and final scan of image. Vertical distances are proportional to the output of the photomultiplier.

base of the cell are clearly defined by vertical marks of the pen. Some residual unevenness of illumination is shown in the final scan (No. 28) where the light intensity through the liquid is slightly greater than that through the air above the meniscus. The optical density at any particular level in the cell was obtained by assuming that the ordinate at that level in the final scan corresponded to 100% transmission.

The above data were obtained at a concentration of 100 p.p.m. carrageenate. It was possible, however, to make measurements down to 10 p.p.m. of the polyelectrolyte, such concentrations being inaccessible by conventional methods.

The authors wish to thank Dr. J. W. Lorimer for help in preparing the manuscript.

## PHYSICAL CHEMIST

(Inorganic)

Expanding aluminum producer presents unique opportunity for challenging work in the research phase of its Alumina Division. Join this comprehensive program studying applications in adsorption, catalysis, abrasion, pigment, surface coating, salt production and many other fields. Prefer younger men with advanced degrees but limited experience. Write immediately giving details on age, education, experience, and salary required.

**General Employment Manager  
Reynolds Metals Company  
Richmond, Virginia**

## PYROGRAPHITE SCIENTISTS

Establishment of Raytheon's new Pyrographite Program has resulted in several attractive openings for qualified men:

- Ph.D. or advanced degree in physical chemistry or solid-state physics. Will initiate a mechanism study of gas-solid reactions in high temperatures.
- Ph.D. or advanced degree in chemical engineering, metallurgy or physical chemistry. Will conduct high temperature process studies on a group of interesting materials for missile and commercial applications.
- BS or MS in mechanical or chemical engineering, physical chemistry or ceramics. Will conduct measurements at elevated temperatures of various thermal, mechanical and electrical properties of new refractory materials.

**You will enjoy the many advantages of living in the suburban Boston area. Modern benefits. Please send detailed resume to:**

W. S. Crowell, Jr.  
Raytheon Company  
Gore Building  
Waltham, Massachusetts

## Handling and Uses of the Alkali Metals

Number 19 in  
Advances in Chemistry Series

Introductory Remarks  
Recovery of Lithium from Complex Silicates  
Some Practical Aspects of Handling Lithium Metal  
Uses of Lithium Metal  
Lithium and Other Alkali Metal Polymerization Catalysts  
Binary System Sodium-Lithium  
Sodium Handling at Argonne National Laboratory  
Sodium Handling Equipment  
Recleaning Sodium Heat Transfer Systems  
Corrosion Resistance of Metals and Alloys to Sodium and Lithium  
Evaluation of the Sodium-Water Reaction in Heat Transfer Systems

Manufacture, Handling, and Uses of Sodium Hydride  
Sodium Peroxide Production Story  
Preparation of Sodium Superoxide  
Preparation of Metal Powders by Sodium Reduction  
Present and Potential Uses of Sodium in Metallurgy  
Reactions of Sodium with Organic Compounds  
Determination of Sodium Monoxide in Sodium  
Manufacture of Potassium and Sodium-Potassium Alloys  
Manufacture and Use of Potassium Superoxide

184 pages—paper bound—\$4.75 per copy

**Order from:**

**Special Issues Sales  
American Chemical Society**

1155 Sixteenth Street, N.W., Washington 6, D.C.

1957 EDITION

# American Chemical Society

## DIRECTORY of GRADUATE RESEARCH

-----

### INCLUDES:

Faculties, Publications, and Doctoral Theses in Departments of Chemistry, Biochemistry, and Chemical Engineering at United States Universities

-----

- ▶ All institutions which offer Ph.D. in chemistry, biochemistry, or chemical engineering
  - ▶ Instructional staff of each institution
  - ▶ Research reported at each institution for past two years
  - ▶ Alphabetical index of 2,878 faculty members and their affiliation; alphabetical index of 236 schools
- 

The ACS Directory of Graduate Research is the only U. S. Directory of its kind. The 3rd edition, prepared by the ACS Committee on Professional Training, now includes all schools and departments (with five exceptions where data were received too late for inclusion) concerned primarily with chemistry, biochemistry, or chemical engineering, known to offer the Ph.D. degree.

-----

The Directory is an excellent indication not only of research reported during the last two years at these institutions but also of research done prior to that time. Each faculty member reports publications for 1956-57; where these have not totaled 10 papers, some articles prior to 1956 are reported. This volume fully describes the breadth of research interest of each member of the instructional staff.

-----

Because of the indexing system, access to information is straightforward and easy—the work of a moment to find the listing you need. Invaluable to anyone interested in academic or industrial scientific research and to those responsible for counseling students about graduate research.

-----

Paper bound.....634 pages.....\$3.50

ORDER FROM

Special Issues Sales

**AMERICAN CHEMICAL SOCIETY**  
1155-16th STREET, N.W.  
WASHINGTON, D. C.

2127  
13. 20